

american society for mass spectrometry

30th

ANNUAL CONFERENCE ON MASS SPECTROMETRY AND ALLIED TOPICS

ABSTRACTS

June 6–11, 1982
Honolulu

sponsored in cooperation with

THE AUSTRALIAN AND NEW ZEALAND SOCIETY
FOR MASS SPECTROMETRY
THE JAPANESE SOCIETY FOR
MEDICAL MASS SPECTROMETRY
THE MASS SPECTROSCOPY SOCIETY OF JAPAN

474 pages

TABLE OF CONTENTS

1. INTRODUCTION iii

2. BOARD OF DIRECTORS iv

3. CORPORATE MEMBERS iv

4. PROCEEDINGS OF THE THIRTIETH ANNUAL CONFERENCE vi

5. INDEX OF AUTHORS 874

6. MINUTES OF THE ANNUAL BUSINESS MEETING 886

7. ASTM E-14: Minutes of the Business Meeting 888

8. ASMS COMMITTEE REPORTS

- ASTM Committee D-2 890
- Qualitative Organic Techniques 894
- Biomedical applications 895
- Fundamentals 896
- Education 897
- Quantitative Organic Analysis 898
- High Temperature and Inorganic Solids 899
- Isotope Ratio Measurements 900
- Nomenclature 901

9. ASMS WORKSHOP REPORTS

- Orphaned Instruments 910
- Quantitative Mixture Analysis 913
- Ion Optics for Extraction of Secondary Ions from Surfaces 914
- Hardware and Software for Intercomputer Communication . . 915
- Good Laboratory Practices 917
- Resolution in MS/MS 918
- Standard Operating Conditions for Triple Quadrupoles While Acquiring Library MS/MS Spectra 920
- Collision-Induced Decompositions: Internal Energy Effects 922
- FAB: Where Are We Now? 923
- Quantitative Quadrupole 924
- Laser Mass Spectrometry for the Production and Measurement of Inorganic Ions 925

10. OFFICERS: ASTM COMMITTEE E-14 and ASMS 927

11. PARTICIPANTS, 30th ANNUAL CONFERENCE 928

PRINTED IN U.S.A.

INTRODUCTION

This "Bound Volume", which appears annually, is the official record of the American Society for Mass Spectrometry, containing not only the abstracts of papers presented at the conference, but also reports of workshops and of standing and ad hoc committees, special reports as appropriate, minutes of the annual business meeting and other matters of interest to the membership.

I would like to extend my thanks to all contributors for their cooperation in adhering to the space limitations and time contraints, and I am especially grateful to the committee and workshop chairpersons who managed to prepare and deliver their reports despite the short time available since the conference. I wish to express appreciation to Mr. Robert Meltzer and ASTM, who once again have handled the printing and distribution and done so with their usual efficiency.

The warmest expression of gratitude is due Mrs. Judith Watson of the ASMS office in East Lansing. In her cheerful and efficient manner, she has done the bulk of the work and has so made the job of the Editor an incredibly easy one.

F. W. Lampe, Editor

ACKNOWLEDGEMENTS

The Board of Directors of ASMS gratefully acknowledges:

The participation of the cooperating societies and particularly the efforts of Dr. Peter J. Derrick (The Australian and New Zealand Society for Mass Spectrometry), Dr. Isamu Matsumoto (The Japanese Society for Medical Mass Spectrometry), and Dr. Makoto Suzuki (The Mass Spectroscopy Society of Japan).

The financial support of the following Corporate Members for their one-time contributions for this meeting.

- The Colorado Group (in Memory of Glenn Kerfoot)
- Extranuclear Laboratories
- Hewlett Packard
- KRATOS Analytical Instruments
- Nicolet Instruments
- Phrasor Scientific
- Scientific Glass Engineering
- Sciex

CITATION NOTICE

This volume contains the abstracts of papers presented at the Thirtieth Annual Conference on Mass Spectrometry and Allied Topics, held in Honolulu, Hawaii, June 6-11, 1982. It is intended that this volume be distributed only to members of ASMS and conference registrants and, therefore, it is not to be considered a publication. It is requested that any reference to individual abstracts in this volume be cited in the following form:

> "Author(s); Presented at the 30th Annual Conference on Mass Spectrometry and Allied Topics, Honolulu, Hawaii, June 6-11, 1982."

AMERICAN SOCIETY FOR MASS SPECTROMETRY

BOARD OF DIRECTORS

President
Burnaby Munson
Department of Chemistry
University of Delaware
Newark, DE 19711

Vice President for Programs
Catherine C. Fenselau
Department of Pharmacology
Johns Hopkins University
725 North Wolfe Street
Baltimore, MD 21205

Vice President for Arrangements
Keith R. Compson
KRATOS Analytical Instruments
24 Booker Street
Westwood, NJ 07675

Secretary
Terrence R. Ashe
Exxon Research and Engineering Co.
Post Office Box 121
Linden, NJ 07036

Treasurer
Margaret A. Frisch
IBM, Thomas J. Watson Research Center
Box 218
Yorktown Heights, NY 10598

Chairman, ASTM Committee E-14
Thomas Aczel
Exxon Research and Engineering Co.
Post Office Box 4255
Baytown, TX 77520

Member at Large
Fred W. Lampe
Department of Chemistry
Pennsylvania State University
University Park, PA 16802

Member at Large
J. Throck Watson
Department of Biochemistry
Michigan State University
East Lansing, MI 48824

Past President
James A. McCloskey
Department of Medicinal Chemistry
University of Utah
Salt Lake City, UT 84112

SOCIETY OFFICE
Judith A. Watson
Post Office Box 1508
East Lansing, MI 48823
517/337-2548

The American Society for Mass Spectrometry is grateful to the Corporate Members for their support.

BALZERS
8 Sagamore Park Road
Hudson, NH 03051

R. J. BRUNFELDT Co.
Post Office Box 3636
Bartlesville, OK 74003

CAMBRIDGE ISOTOPE LABORATORIES
141 Magazine Street
Cambridge, MA 02139

COLORADO GROUP
490 Orchard Street
Golden, CO 80401

CVC PRODUCTS, Inc.
Post Office Box 1886
Rochester, NY 14853

EXTRANUCLEAR LABORATORIES
Post Office Box 11512
Pittsburgh, PA 15238

FINNIGAN CORPORATION
355 River Oaks Parkway
San Jose, CA 95134

FINNIGAN INSTITUTE
11 Triangle Park Drive
Cincinnati, OH 45246

GALILEO ELECTRO-OPTICS
Galileo Park
Sturbridge, MA 01518

HEWLETT PACKARD
1601 California Avenue
Palo Alto, CA 94304

INFICON LEYBOLD-HERAEUS
6500 Fly Road
East Syracuse, NY 13057

JEOL, Ltd/USA
235 Birchwood Avenue
Cranford, NJ 07016

KOR ISOTOPES
56 Rogers Street
Cambridge, MA 02142

KRATOS ANALYTICAL INSTRUMENTS
24 Booker Street
Westwood, NJ 07675

MASSPEC, Inc.
275 Turkey Creek
Bartlesville, OK 74003

MEAD COMPUCHEM
Post Office Box 12652
Research Triangle Park, NC

MERCK & CO. ISOTOPES
899 Pointe Claire
Dorval, Quebec H9R 4P7

NICOLET INSTRUMENTS
5225 Verona Road
Madison, WI 53711

NIH/EPA CHEMICAL INFORMATION SYSTEMS
7215 York Road
Baltimore, MD 21212

NUCLIDE CORPORATION
642 East College Avenue
State College, PA 16801

PERNICKA CORPORATION
450 East Middlefield Road
Mountainview, CA 94043

PHRASOR SCIENTIFIC
1536 Highland Avenue
Duarte, CA 91010

QUANTA-RAY
1250 Charleston Road
Mountainview, CA 94043

RDS NERMAG
3064 Scott Blvd.
Santa Clara, CA 95050

SCIEX
55 Glencameron Road
Thornhill, Ontario L3T 1P2

SCIENTIFIC GLASS ENGINEERING
2007 Kramer Lane
Austin, TX 78758

SHRADER ANALYTICAL LABORATORIES
3450 Lovett Avenue
Detroit, MI 48210

The Technology Shop
Post Office Box 443
Weston, MA 02193

TEKNIVENT CORPORATION
10774 Trenton Avenue
St. Louis, MO 63132

TMS ANALYTICAL SERVICES, Inc.
Post Office Box 13
Evansville, IN 47701

UTI
325 North Mathilda Avenue
Sunnyvale, CA 94086

VACUMETRICS, Inc.
2261 Palma Drive
Ventura, CA 93003

VG INSTRUMENTS
300 Broad Street
Stamford, CT 06901

VG ISOTOPES
300 Broad Street
Stamford, CT 06901

JOHN WILEY AND SON
605 Third Avenue
New York, NY 10158

PROCEEDINGS OF THE THIRTIETH ANNUAL CONFERENCE

MOA — **Instrumental Techniques**

THE MEASUREMENT OF TRANSPORT PARAMETERS OF ATMOSPHERIC GASES IN AN EPOXY RESIN BY PRECISION ABRASION MASS 1
*GRAYSON, M A AND WOLF, C J

ELEMENTAL ANALYSIS BY COMBINED MICROWAVE PLASMA-GC/MS 3
*HEPPNER, R A

MS/MS BY TIME-RESOLVED MAGNETIC DISPERSION MASS SPECTROMETRY 5
*STULTS, J T, ENKE, C G, HOLLAND, J F, PINKSTON, J D, ALLISON, J AND WATSON, J T

AN AUTOMATIC, PRECISION CALIBRATOR FOR AN EIGHT COMPONENT RESIDUAL GAS ANALYSER 7
*CLARK, J S, FARR, F L, WALLACE, W D AND CRIDDLE, M J

SPATIAL DISTRIBUTION OF PRIMARY IONS IN CHEMICAL IONIZATION AND NI-63 ATMOSPHERIC PRESSURE IONIZATION 9
*FUJII, T, HOPSON, W AND MEISELS, G G

BENZENE PYROLYSIS AND SOOT FORMATION AT HIGH TEMPERATURES 11
*UDSETH, H AND SMITH, R D

INTRODUCTORY LECTURE: Isotopic Effects in Fragmentation 13
*DERRICK, P J

MOB — **Symposium: Ions and Light**

PHOTODISSOCIATION OF IONS IN DOUBLE-FOCUSING MASS SPECTROMETERS 14
*HARRIS, F M AND BEYNON, J H

STATE SELECTED ION-MOLECULE REACTIONS BY A TESICO TECHNIQUE 18
*TANAKA, K, KATO, T AND KOYANO, I

VIBRATIONAL STATE DYNAMICS OF GAS PHASE ION-MOLECULE REACTIONS BY INFRARED CHEMILUMINESCENCE AND LASER 22
BIERBAUM, V M

A PHOTODISSOCIATION STUDY OF THE HALOGEN IONS CL2+, BR2+, AND I2+ AT 3 CM-1 RESOLUTION 24
SMITH, D L, MCLOUGHLIN, R G AND *MORRISON, J D

RESONANCE, AUTOIONIZATION AND KINETIC EFFECTS IN PHOTOIONIZATION 25
*PARR, A C AND ROSENSTOCK, H M

Quantitation of Xenobiotic and Endogenous Compounds

MEASUREMENT OF TETRAHYDROCANNABINOL IN BODY FLUIDS AND TISSUES USING METASTABLE ION MONITORING 28
*HARVEY, D J, LEUSCHNER, J T AND PATON, W D

SULFUR-CONTAINING METABOLITES OF POLYCHLORINATED BIPHENYLS IN PATIENTS WITH "YUSHO" 30
*HARAGUCHI, K, KUROKI, H AND MASUDA, Y

DETERMINATION OF FORMALDEHYDE IN BIOLOGICAL TISSUES BY GAS CHROMATOGRAPHY MASS SPECTROMETRY 32
HECK, H A, *WHITE, E L AND SCHMITZ, M C

STUDIES ON DNA BASE ANALYSIS BY GC/MS 34
*CRAIN, P F AND MCCLOSKEY, J A

MAXIMIZING PRECISION AND ACCURACY IN QUANTITATION OF SERUM TESTOSTERONE 36
PATTERSON, D G, *HOLLER, J S AND BAIRD, M A

ASSESSMENT OF CORTISOL IN HUMAN SERUM PROPOSED DEFINITIVE & REFERENCE METHOD 38
*JONCKHEERE, J A, LAMBERT, W E AND DE LEENHEER, A P

DETECTION AND QUANTITATION OF CAMP IN PLANT TISSUES BY A STABLE ISOTOPE DILUTION GC/MS/MID ASSAY 40
JOHNSON, L P, *MACLEOD, J K, LETHAM, D S AND PARKER, C W

METABOLISM OF L-THREO-3, 4-DIHYDROXYPHENYLSERINE IN PATIENTS WITH DEGENERATIVE DISEASES OF THE CENTRAL 41
*SUZUKI, T, HIGA, S, SAKODA, S, HAYASHI, A, KONDO, T AND NARABAYASHI, H

QUANTITATION OF IMIPRAMINE AND IMIPRAMINE-D4 IN BLOOD PLASMA BY GC/FIMS 43
*BUTTRILL, S E, YOUNG, S E AND ALKALAY, D

MS/MS IN PHARMACOKINETIC STUDIES 45
*SENN, M AND ENDELE, R

MOD — **Organic Desorption Techniques**

CHARACTERISTICS OF A CESIUM ION SIMS SOURCE FOR STUDIES OF BIOLOGICAL SUBSTANCES OF INTERMEDIATE 47
ABERTH, W, WALLS, F, STRAUB, K AND *BURLINGAME, A L

SOME FUNDAMENTAL ASPECTS OF FAST ATOM BOMBARDMENT MASS SPECTROMETRY 49
*BONE, W M, HUNT, D F AND MARASCO, J

ANALYSIS OF THE OPERATION OF THE FACS (FAST ATOM CAPILLARITRON SOURCE) 51
*PEREL, J AND MAHONEY, J F

ORGANIC SIMS STUDIES WITH A FACS SOURCE 53
*WILLIAMS, P AND ADAMS, D

HIGH FIELD SURFACE CHEMISTRY ON A VOLCANO TYPE FIELD IONIZATION SOURCE 55
*FLEMING, R H AND JOHN, G A

MULTIPLY CHARGED IONS IN ELECTROHYDRODYNAMIC IONIZATION MS 57
*CHAN, K W AND COOK, K D

SPECULATIONS ON THE MECHANISM OF THERMOSPRAY AND OTHER SOFT IONIZATION TECHNIQUES 59
*VESTAL, M L

THE SURFACE IONIZATION SPECTRA OF RESIDUALS AND VOLATILE ORGANIC COMPOUNDS ON RE FILAMENTS 60
*CHATFIELD, D A

ROLE OF SAMPLE MELTING POINT AND SAMPLE VAPOR PRESSURE IN ONSET OF FIELD DESORPTION 62
*WOOD, G W AND RAMANA, D V

MOE — **Ion Molecule Reactions**

THE GAS PHASE CHEMISTRY OF METAL-IONS WITH MULTI-FUNCTIONAL ORGANIC MOLECULES 64
HUANG, S K, LOMBARSKI, M, MCELVANY, S, RADECKI, B, TSARBOPOLOUS, A AND *ALLISON, J

ION CHEMISTRY IN THE ATMOSPHERE OF TITAN 67
*HUNTRESS, W T AND ANICICH, V G

ELECTRON AFFINITY MEASUREMENTS USING EQUILIBRIUM ELECTRON TRANSFER REACTIONS 68
FUKUDA, E K AND *MCIVER, R T

DIPOLE STABILIZED ANIONS 70
*BARTMESS, J E AND CALDWELL, G

UNIMOLECULAR AND BIMOLECULAR REACTIONS IN THE C4H6+ SYSTEM EXPERIMENT AND THEORY 71
JARROLD, M F, KEMPER, P R, BASS, L M, VAN KOPPEN, P AND BOWERS, M T

STUDIES OF THE AMMONIUM RADICAL BY NEUTRALIZED ION-BEAM SPECTROSCOPY 72
*GELLENE, G I AND PORTER, R F

REACTIONS OF VIBRATIONALLY EXCITED IONS WITH NEUTRALS IN A FLOW DRIFT SYSTEM 74
*FERGUSON, M D, FERGUSON, E E, FAHEY, D, BOHRINGER, H AND FEHSENFELD, F

TEMPERATURE DEPENDENCE OF ION MOLECULE REACTIONS 76
MAGNERA, T F, SENSHARMA, D K AND *KEBARLE, P

ION-MOLECULE REACTIONS AND STRUCTURES OF HYDROCARBON IONS RELEVANT IN COMBUSTION 77
BRILL, F W AND *EYLER, J R

FLOWING AFTERGLOW AND SELECTED ION FLOW TUBE STUDIES OF THE REACTIONS OF H2N-, HO-, AND HO18- WITH N2O, 78
*BIERBAUM, V M, GRABOWSKI, J J AND DEPUY, C H

NO2+ ION FORMED BY THE N3+ +O2 REACTION 80
*MATSUOKA, S, NAKAMURA, H AND TAMURA, T

MOF — **Instrument Design**

GAS DYNAMICS AND DESIGN CONSIDERATIONS FOR INTRODUCING FAST ELUTING GAS CHROMATOGRAPHIC PEAKS FROM CAPILLARY 82
*GOODLEY, P C AND HAMBURGEN, W R

CAPILLARY COLUMN SUPERCRITICAL FLUID CHROMATOGRAPHY-MASS SPECTROMETRY 84
*SMITH, R D AND FJELDSTED, J

A STUDY OF THE DISSOCIATION PHENOMENA IN ELECTROSTATIC AND QUADRUPOLE COLLISION CHAMBERS IN AN API-MS/MS 86
*CALDECOURT, V, TOU, J AND ZAKETT, D

TRAJECTORIES, ENERGIES, AND SPATIAL AND ANGULAR APERTURES IN AN RF QUADRUPOLE APPLICATION TO 88
SIEGEL, M W

APPLICATION OF PERFECT FOCUSING MASS SPECTROMETER TO ATOMIC COLLISION EXPERIMENTS 90
*ARIKAWA, T AND KANAZAWA, K

EFFECT OF MAGNETIC FIELD INHOMOGENEITY ON EXACT MASS DETERMINATION IN ICR SPECTROMETRY 92
*SCHUCH, D, CHUNG, K M AND HARTMAN, H

AN ELONGATED TRAPPED ION CELL FOR FOURIER TRANSFORM MASS SPECTROMETRY WITH A SUPERCONDUCTING MAGNET 93
*HUNTER, R L AND MCIVER, R T

INEXPENSIVE MODIFICATION OF A KRATOS MS-50 FOR FAB 95
SHADOFF, L A AND *ZAKETT, D

TIME RESOLVED PHOTOIONIZATION MASS SPECTROMETRY IN THE MILLISECOND RANGE 96
*LIFSHITZ, C, GOLDENBERG, M, MALINOVICH, Y
AND PERES, M

MPA — **Xenobiotic Metabolism; Liquid Chromatography Mass Spectrometry; Fragmentation Mechanisms**

GCMS CHARACTERIZATION OF VALPROIC ACID METABOLITES IN HUMAN SERUM AND URINE 98
ACHEAMPONG, A A, *ABBOTT, F S AND BURTON, R R

CHEMICAL IONIZATION MASS SPECTRAL IDENTIFICATION OF THE ANTHELMINTHIC AGENT MEBENDAZOLE AND ITS 100
*KENNISH, J M

STUDY OF DIBUCAINE METABOLISM IDENTIFICATION OF URINARY METABOLITES IN RAT, RABBIT AND MAN 102
*IGARASHI, K, KASUYA, F AND FUKUI, M

CRUISE MISSILE FUEL INHALATION KINETICS AND METABOLITE IDENTIFICATION BY GC/MS 104
INMAN, R C, *YU, K O AND KELLER, W C

EFFECTS OF DEUTERIUM AND CHLORINE SUBSTITUTION ON THE METABOLISM OF CHLOROETHANES 106
*THOMPSON, J A AND HO, B

METABOLIC PATHWAY OF DIISOPROPYLNAPHTHALENE IN CARP 108
*KOJIMA, H AND YOSHIDA, T

15

IMINOCYCLOPHOSPHAMIDE, A NEW METABOLITE OF CYCLOPHOSPHAMIDE 110
*LEHMAN, J P AND COLVIN, O M

A STUDY OF SENSITIVITY VS ION SOURCE TEMPERATURE FOR DIRECT LIQUID INTRODUCTION LC-MS 112
*DUBAY, G R AND CADIZ, M

SAMPLE DETECTION USING LIQUID CHROMATOGRAPH/MASS SPECTROMETER INTERFACE WITH STATIONARY CONCENTRATOR 115
LO, H H AND *SIEGEL, M W

DESIGN AND PERFORMANCE OF LC-MS SYSTEMS USING THE THERMOSPRAY TECHNIQUE 117
BLAKLEY, C R AND *VESTAL, M L

PERFORMANCE CHARACTERISTICS OF THE THERMOSPRAY LC-MS INTERFACE 118
*YERGEY, A L, VESTAL, M L AND BLAKLEY, C R

A STUDY ON TECHNIQUES FOR MICRO-HPLC/MS 120
*TAKEUCHI, T, MATSUOKA, K AND ISHII, D

MASS SPECTROMETRIC ANALYSIS OF 1, 3, 5, 7-TETRANITRO-1, 3, 5, 7- TETRAZACYCLOOCTANE (HMX) 122
*MONCUR, J G AND SHARP, T E

CHARACTERIZATION OF POLYMERS AND POLYMERIC COMPONENTS BY LC/MS USING DIRECT LIQUID INLET (DLI) INTERFACE 124
*CANADA, D C AND ZINGG, D S

APPLICATIONS OF A DIRECT LC/MS SYSTEM UTILIZING AN INSULATED DROPLET DRIFT ZONE FOR SOLVENT EVAPORATION 125
DEVANT, G, HARDY, M, DEDIEU, M, BOUNINE, J P
AND *ARPINO, P J

MS CHARACTERIZATION OF LEUKOTRIENE HYDROXY FATTY ACIDS 127
*HARPER, T AND MURPHY, R C

MASS SPECTROMETRIC FRAGMENTATION PATHWAYS OF 1, 8-NONADIYNE 129
*ROBBINS, R C AND FOSTER, N G

MASS SPECTROMETRY OF NICOTINE AND SOME STRUCTURAL ISOMERS 131
*MAGIN, D F, EINOLF, W N AND SECOR, H

AB INITIO MO STUDY OF THE FRAGMENTATION OF N-BUTANE 133
TAKEUCHI, T, *YAMAMOTO, M AND NISHIMOTO, K

CID MIKE SPECTROMETRY OF EPIMERIC STEROID ALCOHOLS 135
LAUBER, R, STEINAUER, R, *SCHLUNEGGER, U P, DAN, P
AND *ZARETSKII, Z V

ENERGY RELEASE FROM C4H8O2+, BUTANOIC ACID AND RELATED IONS 137
MCADOO, D J AND *HUDSON, C E

CHARACTERISTICS OF SOME NOVEL GLUCURONIDES BY FAB 139
YELLE, L AND FENSELAU, C C

MPB — ***Direct Exposure Chemical Ionization; Quantitation and Bioavailability; Stable Isotopes in Metabolism Studies***

NCI QUANTITATIVE ANALYSIS USING VARIOUS ELECTRON ENERGY MODERATING GASES 141
*GREGOR, I K AND GUILHAUS, M

DESORPTION CHEMICAL IONIZATION MASS SPECTROMETRY OF BENZYL ETHERS DERIVATIVES OF 3-HYDROXY STEROIDS USING 143
HIRANO, Y, DJERASSI, C AND *TECON, P

NOVEL-IONIZATION AND SAMPLE INTRODUCTION TECHNIQUES FOR THE ANALYSIS OF THERMALLY-LABILE AND NON-VOLATILE 145
*KENYON, C N AND GOODLEY, P C

FACILE IONIZATION INDUCED BY AMMONIUM SALTS LOW & HIGH RESOLUTION MASS SPECTRA OF NON VOLATILE, 147
*PRAMANIK, B N, BARTNER, P, GIRIJAVALLABHAN, V, GANGULY, A K, BOSE, A K AND PRAKASH, O

D/CI MASS SPECTROMETRY IN THE STRUCTURE ELUCIDATION OF GUANIDINO COMPOUNDS 149
*ALDERWEIRELDT, F C, ESMANS, E L, MARESCAU, B AND LOWENTHAL, A

MASS SPECTROMETRY OF IRIDOID GLYCOSIDES 151
*FRAISSE, D, BECCHI, M, RAYNAUD, J AND TABET, J C

THE DESORPTIVE CHEMICAL IONIZATION MASS SPECTROMETRIC STUDIES OF NOGALAMYCIN ANALOGUES 153
*DUHOLKE, W K AND ZOUTENDAM, P H

IN-BEAM EI AND MIKE STUDIES ON N-ALKYLPYRIDINIUM SALTS 155
*OHASHI, M, BARRON, R P AND BENSON, W R

DIRECT EXPOSURE CHEMICAL IONIZATION MASS SPECTROMETRY OF INTACT PHOSPHOLIPIDS 157
HATCH, F

SIMULTANEOUS DETERMINATION OF THE INTRAVENOUS AND ORAL PHARMACOKINETICS OF TIMOLOL 159
*CARLIN, J R, ROGERS, J D, DAVIES, R O, FERGUSON, R K AND VANDENHEUVEL, W J

PHARMACOKINETIC STUDIES OF ORAL AND SUPOSITORIAL ADMINISTERED METYRAPONE AND ITS EFFECTS ON THE 11- 161
*ICHIMURA, K, CHIBA, K, SAITO, K, NOZAKI, Y AND KATO, K

DETERMINATION OF ALBUTEROL IN PLASMA BY GAS CHROMATOGRAPHY/ CHEMICAL IONIZATION MASS SPECTROMETRY 163
WEISBERGER, M AND *POWELL, M L

CONFIDENCE LIMITS FOR THE GAS CHROMATOGRAPHIC/ISOTOPE DILUTION MASS SPECTROMETRIC DETERMINATION OF 165
MOLER, G F, DELONGCHAMP, R R, KORFMACHER, W A AND *MITCHUM, R K

GLC-CHEMICAL IONIZATION SELECTED ION MONITORING ASSAY FOR GLYCEROL FORMAL IN ANIMAL TISSUES 167
*WALKER, R W, BAYLIS, F P, BROWN, J E, MINSKER, D H, ROBERTSON, R T AND VANDENHEUVEL, W J

THE DETERMINATION OF PICOGRAM QUANTITIES OF TRACAZOLATE (ICI 136,753) BY CAPILLARY GC/MS/SIM 169
*MONSON, K R, NEILSON, K L AND MALBICA, J O

QUANTITATION OF DICLOFENAC SODIUM IN HUMAN PLASMA BY GC/MS 171
*HASHIMOTO, Y, IRIE, T, YAMASHITA, K, ISHIBASHI, M AND MIYAZAKI, H

TRICLOSAN QUANTITATION WITH GC/MS 172
*ALKALAY, D, THOMPSON, T A, GOODBLATT, R S, BORMAN, C H AND VOLK, J

QUANTITATION OF GLUCOSE, BILE ACIDS AND VITAMIN D3 IN CHILDREN BY ISOTOPE DILUTION MASS SPECTROMETRY 173
DAN, P, GELFAND, M J, TSANG, R C, HEUBI, J E, SPERLING, M A AND NORMAN, E J

GCMS QUANTITATION OF GAMMA-AMINOBUTYRIC ACID IN BIOLOGICAL SPECIMENS 174
*NORMAN, E J, WEE, E L AND ZIMMERMAN, E F

ADRENOLEUKODYSTROPHY ORIGIN OF ABNORMAL FATTY ACIDS DETERMINED BY ISOTOPE INCORPORATION IN PLASMA AND 175
MOSER, H W, MOSER, A B, KISHIMOTO, Y, FENSELAU, C AND *PALLANTE, S L

DETERMINATION OF BODY WATER VOLUME BY DEUTERIUM ISOTOPE DILUTION MEASUREMENT BY CIMS 177
BENCSATH, F A, BRADLOW, H L AND *FIELD, F H

USE OF 13CO2 BREATH ANALYSIS AS AN AID IN ELUCIDATING ROUTES OF DRUG METABOLISM 178
*SCHOELLER, D A, KOTAKE, A N, LAMBERT, G H AND BAKER, A L

METABOLISM OF (2H)PREGNENOLONE IN TESTIS 180
*SHIMIZU, K

LUNG TOXICITY AND METABOLISM OF DEUTERIUM LABELED BUTYLATED HYDROXYTOLUENE 181
*YAMAMOTO, K, TAJIMA, K AND MIZUTANI, T

DYNAMIC PARAMETERS OF GLYCINE METABOLISM DURING PREGNANCY, DETERMINED BY STABLE ISOTOPE(15N) AND GC/MS 183
*LAPIDOT, A, AMIR, J, HOD, M, REISNER, S R AND OVADIA, Y

TOA — **Food Chain Contamination; Residue Analysis**

DETECTION OF GLUCURONIDE CONJUGATES OF XENOBIOTICS BY DIRECT-INSERTION MASS SPECTROMETRY 185
*KALMAN, D AND EATON, D

ANALYSIS OF CHLORINATED PHENOL ACETATES BY GC/MS 187
YERT, L W, CLINE, R E AND *HOLLER, J S

ANALYSIS OF COMPOUNDS FROM NIAGARA FALLS DUMP SITES USING NCI GC/MS 188
KAMINSKY, R AND *HITES, R A

MASS SPECTRAL INDENTIFICATION OF HALOGENATED ORGANIC COMPOUNDS FROM SEDIMENTS NEAR HAZARDOUS WASTE DISPOSAL 190
PROCTOR, B L

APPLICATIONS OF GAS CHROMATOGRAPHY-NEGATIVE ION CHEMICAL IONIZATION MASS SPECTROMETRY IN CONFIRMATORY 192
STOUT, S J

GC AND SOLID PROBE MASS SPECTROMETRIC CONFIRMATORY ASSAYS FOR ARPRINOCID IN POULTRY TISSUES 194
TWAY, P C

QUANTITATIVE DETERMINATION OF POLYCHLORINATED DIPHENYL ETHERS IN FISH BY HIGH RESOLUTION GC-MS 196
*LAU, P Y AND NEWSOME, W H

CAPILLARY GC/MS PROFILING OF XENOBIOTIC CHEMICALS IN BIOFLUIDS IN EI AND NCI MODES 197
DEKANAL, J, KIRLEW, P, TANG, S Y AND *DOUGHERTY, R C

CHLORINATED COMPOUNDS IN "YUSHO" PATIENTS' BLOOD IN TAIWAN 198
KASHIMOTO, T, *MIYATA, H, FUKUSHIMA, S, KUNITA, N, TUNG, T C, HSU, S T, CHANG, C J, TANG, S Y, OHI, G AND YAMAMOTO, S

TOB — **Symposium: Cluster Ions**

RECENT FLOWING AFTERGLOW STUDIES OF CLUSTER ION REACTIONS 200
FERGUSON, E E

TEMPERATURE DEPENDENCE OF THIRD BODY ION CLUSTERING REACTIONS 204
LAU, Y K, IKUTA, S, MAGNERA, F AND *KEBARLE, P

DISSOCIATION OF METASTABLE CLUSTER IONS 205
STEPHAN, K, MARK, T D, *FUTRELL, J H AND CASTLEMAN, A W

CLUSTER IONS UNDERSTANDING TRANSITIONS FROM THE GASEOUS TO THE CONDENSED STATE 209
CASTLEMAN, A W AND *KEESEE, R G

CLUSTER IONS FROM BOMBARDMENT OF LOW-TEMPERATURE SOLIDS 212
ORTH, R G, JONKMAN, H T, STULIK, D AND *MICHL, J

TOC — **Respiratory Gas Analysis; Xenobiotic Metabolism**

A NEW DEVELOPMENT OF RESPIRATORY MASS SPECTROMETER AND COMPUTER SYSTEM FOR THE STUDY OF LUNG AND CIRCULATORY 216
*NISHI, I, TOMIZAWA, G AND TATSUTA, L

USE OF A QUADRUPOLE MS FOR PRECISION GAS SOLUBILITY MEASUREMENTS IN BLOOD 218
*CRIDDLE, M J, CLARK, J S AND HARRIS, T R

NON-INVASIVE MEASUREMENT OF OXYGEN AND CARBON DIOXIDE CONTENTS OF PULMONARY BLOOD 220
*CLARK, J S, CRIDDLE, M J, FARR, F L AND HARRIS, T H

CARBON ISOTOPIC COMPOSITION OF THE UNITED STATES & JAPANESE DIETS 222
*SCHOELLER, D A, KORALEWSKI, C AND NAKAMURA, K

TANDEM MS STUDIES OF DRUG ACTION AND METABOLISM 224
*YOST, R A, BROTHERTON, H O AND PERCHALSKI, R J

14

IDENTIFICATION OF HUMAN URINARY METABOLITES OF BUPROPION 226
*CHANDRASURIN, P, SCHROEDER, D H, HINTON, M L, EISEMAN, J L AND BRENT, D A

MASS SPECTRAL AND CHROMATOGRAPHIC STUDIES ON DETORUBICIN AND DOXORUBICIN 227
*ROBOZ, J, SUZUKI, R, SILIDES, D, GREAVES, J, WEIL, M AND HOLLAND, J F

METABOLISM OF ENDO-DICYCLOPENTADIENE BY IMMOBILIZED CYTOCHROME P-450 228
*VAN BREEMEN, R B AND FENSELAU, C C

TOD — **Applications of Organic FAB and SIMS**

DETERMINATION OF PRIMARY STRUCTURE IN OLIGOPEPTIDES BY SECONDARY ION MS 229
*WESTMORE, J B, BEAVIS, R, ENS, W AND STANDING, K G

FAB IN SPECIALIZED ANALYSIS OF PROTEINS AND PEPTIDES 231
*CAPRIOLI, R M, SMITH, L A AND BECKNER, C F

FABMS IN PROTEIN SEQUENCING APPLICATION TO MACROMOMYCIN AND NEOCARZINOSTATIN 232
*GIBSON, B W AND BIEMANN, K

FAB SPECTROMETRY OF STEROID CONJUGATES 234
*LIEHR, J G, BECKNER, C F, BALLATORE, A M AND CAPRIOLI, R M

MEASUREMENT OF BILE ACIDS 3-, 7-, 12- MONO SULFATES BY FAB/MS 236
GOTO, J, NAMBARA, T, *ITAGAKI, Y, HIGUCHI, T AND NAITO, Y

ANALYSIS OF STEROID AND VITAMIN D GLUCURONIDES AND SULFATES BY FAB- AND EI-MS 238
*JARDINE, I, SCANLAN, G F, MATTOX, V R AND KUMAR, R

THE APPLICATION OF FAB SPECTRA FOR STRUCTURE ELUCIDATION 240
STRADLING, R S, MOORE, L E, TAYLOR, L C, WAKEFIELD, C J AND COMPSON, K R

FAB AND FIELD DESORPTION MS OF NUCLEOSIDE AND NUCLEOTIDE ADDUCTS OF CHEMICAL CARCINOGENS 242
*MITCHUM, R K, EVANS, F E, KADLUBAR, F F, FREEMAN, J P AND ROACH, D

THE ROLE OF FAB IN THE SOLUTION OF DIFFICULT MASS SPECTRAL PROBLEMS 243
*COSTELLO, C E, VAN LANGENHOVE, A, MARTIN, S A AND BIEMANN, K

ANALYSIS OF MIXTURES BY HPLC AND FAB 246
*KEMP, T R, LEWIS, I A AND BILL, J C

FAST ATOM BOMBARDMENT MASS SPECTROMETRY USING A MAT CH5 DF MASS SPECTROMETER 247
*BACZYNSKYJ, L AND NIELSEN, J W

TOE — **Studies of Cluster Ions**

ION-MOLECULE REACTIONS OF METAL IONS WITH FUNCTIONALIZED ORGANIC MOLECULES CATIONIZED SPECIES 248
CASTRO, M. ADAMS, T. ANDERSON, D J AND *RUSSELL, D H

GAS-PHASE BASICITIES FROM METASTABLE PROTON-BOUND DIMER DISSOCIATION 248
*AUE, D H, PEDLEY, M, WEBB, H M AND BOWERS, M T

PROTON-BOUND DIMER FROM UNIMOLECULAR DISSOCIATION OF A MOLECULAR ION A PHOTOIONIZATION STUDY OF METHYL 249
BIERMANN, H W AND *MORTON, T H

ELUCIDATION OF CLUSTER ION STRUCTURES BY SECONDARY ION MASS SPECTROMETRY 251
*CAMPANA, J E, BARLAK, T M, DUNLAP, B I, WYATT, J R, DECORPO, J J AND COLTON, R J

GAS PHASE REACTIONS OF IRON CARBONYL RADICAL ANION METAL CLUSTERS 253
*WRONKA, J, WEDDLE, G AND RIDGE, D P

THERMOCHEMICAL DETERMINATIONS FROM WEAKLY BONDED CLUSTER IONS METAL ION AFFINITIES FROM METAL BOUND 255
*MCLUCKEY, S A AND COOKS, R G

BIMOLECULAR PRODUCTION AND THERMOCHEMISTRY OF GAS PHASE IONS SOLVATED BY A SINGLE SOLVENT MOLECULE BY 257
LARSON, J W AND *MCMAHON, T B

MS/MS FOR INVESTIGATION OF THE STRUCTURE OF ION-MOLECULE REACTION INTERMEDIATE COMPLEXES 258
*GROENEWOLD, G S, *LAY, J O AND GROSS, M L

STRUCTURES AND FRAGMENTATIONS OF PROTONATED BENZENES 260
*ICHIKAWA, H, NAKAJIMA, Y AND HARRISON, A G

TOF — **Biochemistry**

POLYPEPTIDE SEQUENCING BY EXOPEPTIDASE DIGESTION IN COMBINATION WITH FIELD DESORPTION AND FAST ATOM 262
*PRZYBYLSKI, M, VAN DEN BROEK, R AND TSUGITA, A

MASS SPECTROMETRY OF BRADYKININ 263
NEUMANN, G M AND *DERRICK, P J

MEASUREMENT OF BRAIN NEUROPEPTIDES AT THE PART PER BILLION LEVEL WITH FDMS 264
DESIDERIO, D M

IN-BEAM ELECTRON IONIZATION MASS SPECTRA OF OLIGOSACCHARIDES AND RELATED COMPOUNDS 266
*OHASHI, M AND TSUJIMOTO, K

BEER AND PYROLYSIS/MASS SPECTROMETRY 268
*DURFEE, S L, TSAO, R, VOORHEES, K J, RUOCCO, J J AND MOORE, S E

FAB AND DIRECT CHEMICAL IONIZATION MASS SPECTRAL STUDIES OF PHORBOL ESTER TUMOR PROMOTERS 270
*CARR, S A, REINHOLD, V N AND COSTELLO, C E

THE ISOLATION AND IDENTIFICATION OF NUCLEOSIDE DIALDEHYDES BY GC/MS 272
*SOLSTEN, R T AND SCHRAM, K H

NEW METHOD OF ADRENAL STEROID MEASUREMENT -11-DEOXY-CORTISOL- IN HUMAN PLASMA BY GC/MS 274
*NOZAKI, Y, KATO, K, ICHIMURA, K, CHIBA, K AND SAITO, K

A NEW DERIVATIVE FOR THE STUDY OF ALDOSTERONE AND ITS METABOLITES BY MASS SPECTROMETRY 276
REINHOLD, V N

MASS SPECTROMETRY APPROACHES TO QUANTITATIVE TRIGLYCERIDE ANALYSIS 278
*SANDERS, R A

TPA — **Instrument Design: Analysers; Structure Elucidation; Disease Profiling; Organic SIMS and FAB Applications**

GC-FT/MS INTERFACING CONSIDERATIONS 280
*KINSINGER, J, GHADERI, S, HEIN, R, HANNA, A AND MARRA, J

DEVELOPMENTS IN MAGNET TECHNOLOGY AND DATA SYSTEM CONTROL OF THE MS80 MASS SPECTROMETER 282
DENNE, D R, *STRADLING, R S, WAKEFIELD, C J, MOORE, L E, ADAMS, J M AND GRIFFITH, R S

A NEW TYPE OF DOUBLE-FOCUSING MASS SPECTROMETER (DF-MS) 284
*TAKEDA, T, SHIMADZE, K, SHIRATSUCHI, K AND KUBODERA, T

A NEW FAST SCANNING HIGH FIELD MAGNETIC ANALYSER 286
*BILL, J C, GREEN, B N AND BROOKS, P W

EXPERIMENTAL AND COMPUTER-SIMULATED ION TRANSMISSION IN A TRIPLE QUADRUPOLE MASS SPECTROMETER 288
*STILLWELL, R N, CARROLL, D I, NOWLIN, J G AND HORNING, E C

ACCURATE MASS DIFFERENCE MEASUREMENTS COMBINED WITH HIGH SENSITIVITY USING THE CHEMICAL RESOLUTION OF A 290
*DAWSON, P H

DEVELOPMENT OF A DATA SYSTEM CONTROLLED NEUTRAL LOSS CALIBRATION PROCEDURE FOR A TRIPLE STAGE QUADRUPOLE 292
STEINER, U, KIRBY, H, SOKOLOW, S AND *SLAYBACK, J

CONSTRUCTION OF A REVOLVING STAND FOR CLEANING ION SOURCE AND RODS OF QUADRUPOLE MASS SPECTROMETER 294
GIANG, B Y

ION TRANSMISSION THROUGH REALISTIC FRINGE FIELDS OF A QUADRUPOLE MS 296
*MINTZ, D M

FIELD DESORPTION MASS SPECTROMETRY OF BIOLOGICALLY ACTIVE GLYCOSIDES FROM THREE KINDS OF ASTEROIDEA 298
*KOMORI, T, ITAKURA, Y, SAKAMOTO, K, TAGUCHI, S AND MAETANI, I

IDENTIFICATION OF M-PHENOXYBENZALDEHYDE RELATED MINORS IN PAY-OFF (FLUCYTHRINATE) INSECTICIDE BY GAS 300
*CARDACIOTTO, S J, CHANG, T, MILLEN, W G AND THOMSON, M L

STRUCTURAL CHARACTERIZATION OF COMPLEX AMINOGLYCOSIDE ANTIBIOTICS BY EMITTER CHEMICAL IONIZATION MASS 302
*TAKEDA, N, HARADA, K I, SUZUKI, M AND TATEMATSU, A

GAS CHROMATOGRAPHIC-MASS SPECTROMETRIC PROFILE OF AMINE METABOLITES IN URINE OF PATIENTS WITH CHRONIC 304
*OHKI, T, SAITO, A, YAMANAKA, N, OHTA, K, NIWA, T AND MAEDA, K

RAPID AND RELIABLE DIAGNOSIS OF TYROSINEMIA BY GC/MS 306
*SHINKA, T, KUHARA, T AND MATSUMOTO, I

GC/MS ANALYSIS OF LACTIC ACIDOSIS PREVIOUSLY DIAGNOSED AS MAPLE SYRUP URINE DISEASE 308
*MATSUMOTO, I AND KUHARA, T

QUANTITATIVE DETERMINATION OF DEHYDROEPIANDROSTERONE SULPHATE IN PLASMA USING STABLE ISOTOPE DILUTION AND 310
GASKELL, S J, BROWNSEY, B G, BROOKS, P W AND *GREEN, B N

ANALYSIS OF CONJUGATED STEROIDS BY GC AND FAB/MS 312
*SHACKLETON, C H, ROITMAN, E AND STRAUB, K

STRUCTURAL CHARACTERIZATION OF NATURALLY OCCURRING OLIGOSACCHARIDES BY MATRIX-ASSISTED MOLECULAR SIMS 314
*SUZUKI, M, HARADA, K I, TATEMATSU, A AND KAMBARA, H

CHARACTERIZATION OF PROTECTED OLIGONUCLEOTIDES BY SECONDARY ION MS 316
*STANDING, K G, BEAVIS, R, ENS, W, WESTMORE, J B AND NEMER, M J

THE COMPOSITIONAL PROFILES OF MELAMINE RESINS USING FD AND FAB MASS SPECTROMETRY 318
CHANG, T T

APPLICATIONS OF THE FAB TECHNIQUE TO SULFONIC ACID AND THEIR SALTS COMPARED TO OTHER SENSITIVE SUBSTANCES 320
*RAPP, U, HOHN, M, PESCH, R AND DOBBERSTEIN, P

FAB ANALYSIS OF TRANSITION METAL COMPLEXES USING 18-CROWN-6 AS THE MATRIX 321
*MINARD, R D AND GEOFFROY, G L

FAST ATOM BOMBARDMENT MS/MS FOR STRUCTURAL AND MIXTURE ANALYSIS 323
*CROW, F W, TOMER, K B AND GROSS, M L

SURFACE ANALYSIS OF ORGANIC ADSORBATES ON CARBON PARTICLES 325
*ROSS, M M AND COLTON, R J

SIGNAL-TO-NOISE RATIO IN ICR MASS SPECTROMETRY 326
*LEDFORD, E B AND REMPEL, D

TWO COLOR PYROMETRY FOR ISOTOPE RATIO MEASUREMENTS 328
*DELMORE, J E, RANKIN, R A AND BUTTARS, L W

TRACE LEVEL MEASUREMENT OF IODINE-129 BY NEGATIVE SURFACE IONIZATION MASS SPECTROMETRY 329
*STOFFELS, J J

ISOTOPIC DETECTION OF 129I BY MULTIPHOTON IONIZATION 330
*LUBMAN, D M AND ZARE, R N

ISOTOPE-RATIO MEASUREMENTS USING THE RIBERMAG R-10-10 QUADRUPOLE GCMS 332
JUDSON, C M

DESIGN PRINCIPLES AND APPLICATIONS OF MULTIPLE COLLECTORS IN THERMAL IONIZATION ISOTOPE RATIO 334
*HABFAST, K, RACHE, H AND WEBER, M

REMOVAL OF THE DYNAMIC RANGE LIMITATION IMPOSED BY THE USE OF COUNTING MODE IN RESPIRATORY GAS ANALYSIS 335
*CLARK, J S, CRIDDLE, M J AND FARR, F L

CALIBRATION STABILITY OF THE ELECTRO-OPTICAL ION DETECTOR 337
*BRITTEN, R A

COMPUTER-ASSISTED CONTROL AND DATA ACQUISITION FOR AN MS702 SSMS 339
*RANKIN, P C

A SIMPLE AND INEXPENSIVE CONVERSION OF THE ELECTRONIC SUPPLIES IN AN AEI 702 SPARK SOURCE MASS SPECTROGRAPH 341
*DUGGER, D L AND MAKLAE, G

A MASS SPECTROMETRIC TECHNIQUE FOR MEASURING THE ACTIVATION ENERGIES OF THE PERMEATION OF ALKALI METALS 343
*DUGGER, D L AND RHODES, W H

A QUANTITATIVE MASS SPECTROMETER FOR HYDROCARBON ANALYSIS 345
*STORY, M, LASER, B AND HABFAST, K

MOLECULAR BEAM MASS SPECTROMETRIC STUDY OF THE COMBUSTION OF SINGLE COAL PARTICLES 347
*GREENE, F T AND O'DONNELL, J E

RESULTS WITH AN AUTOMATED MULTI-SAMPLE INTRODUCTION SYSTEM FOR EI/CI, DCI, AND FAB IONIZATION 348
*BRUNNEE, C, KAUFMANN, H, MICHELSEN, H, PESCH, R AND RAPP, U

QUALITY CONTROL OF GLAS AND HERMETICALLY SEALED SEMICONDUCTOR PACKAGES BY GAS ANALYSIS 350
*KOPRIO, J AND ROSELIUS, H

ANALYSIS OF AEROSOL PARTICLES BY MASS SPECTROMETRY 352
*SINHA, M P AND FRIEDLANDER, S K

CALIBRATION OF A MASS SPECTROMETER FOR ANALYSIS OF ULTRAMICRO GAS SAMPLES USING A DYNAMIC METHOD OF 354
*GRAVEN, W M AND GILMARTIN, D E

ANALYSIS OF AEROSPACE ADHESIVES AND PREPREG FABRICS 356
*MONCUR, J G, CAMPA, A B AND PINOLI, P C

AN INVESTIGATION OF THE REPRODUCIBILITY OF RESULTS AND DETECTION LIMITS OF AN AUTOMATIC GC/MS/DS METHOD FOR 358
*RYAN, P A, WARBURTON, G A, TAYLOR, K T AND MOORE, L E

CHARACTERIZATION OF HEADSPACE VAPORS OF ABUSED ALKYL NITRITES 360
ALLEY, C C, *HOLLER, J S AND LITTLE, J A

CI-MASS FRAGMENTOGRAPHIC ANALYSIS OF METHAMPHETAMINE AND AMPHETAMINE IN HUMAN AUTOPSY TISSUES AFTER ACUTE 362
*KOJIMA, T, UNE, I AND YASHIKI, M

GC/MS ANALYSIS OF N-ALKYLATED BARBITURATES 364
*CALLERY, P S, NAYAR, M S, LESLIE, J, STOGNIEW, M AND ANDREWS, P A

DETECTION OF WAKE AMINES FROM BODY FLUIDS AND TISSUES BY GC/MS ON MEDICOLEGAL ASPECTS 365
*NAGATA, T AND KAGEURA, M

PCP N-OXIDE, A POTENTIAL METABOLITE OF PHENCYCLIDINE 367
*HALLSTROM, G AND CHO, A K

SELECTED ION MONITORING (SIM) OF T-BUTYLSILYL DERIVATIVES OF AMOXAPINE AND ITS 7-OH- AND 8-OH- 369
*HURST, H E AND RODGERS, G C

NEGATIVE ION MASS SPECTROMETRY OF PERFLUOROACYLATED OPIATES 371
*HARA, K AND BRANDENBERGER, H

WOA — **Symposium: Isotopes and Metabolic Kinetics**

ANALYSIS OF FATTY ACID SYNTHESIS REGULATION BY MASS FRAGMENTOGRAPHY 373
*SEYAMA, Y, OTSUKA, H, KAWAGUCHI, A, OKUDA, S AND YAMAKAWA, T

GC/MS DETERMINATION OF STABLE ISOTOPES OF SELENIUM AND CHROMIUM USED IN HUMAN METABOLIC STUDIES 377
*VEILLON, C, REAMER, D C, LEVANDER, O A AND SWANSON, C A

STUDY ON METABOLISM OF PHENYLALANINE, TYROSINE AND TRYPTOPHANE AND RELATED COMPOUNDS USING DEUTERATED 378
*NARUSE, H, HAYASHI, T, SUZUKI, E, MATSUDA, I AND TAKAHASHI, R

THE STUDY OF CARBOHYDRATE METABOLISM WITH STABLE ISOTOPES 382
*TSERNG, K Y AND KALHAN, S C

MODELING TECHNIQUES ESTABLISH FEASIBILITY OF MINERAL METABOLISM STUDIES 383
*IRVING, C S, YERGEY, A L, HACHEY, D L AND KLEIN, P D

WOB — **Organic and Inorganic SIMS and FAB**

ORGANIC SIMS CHARACTERIZATION OF POLYMERIC SYSTEMS 386
MAGEE, C W, *HARRINGTON, W L, GALE, P J AND BENTZ, B L

SECONDARY ION MASS SPECTROMETRY APPLICATIONS TO BIOMOLECULES 388
*BUSCH, K L AND COOKS, R G

INTERLABORATORY STUDIES OF FAB-MASS SPECTROMETRY OF SELECTED BIOMOLECULES 390
*MURPHY, R C AND CLAY, K L

STRUCTURAL STUDIES ON BIOPOLYMERS BY FAB 392
*WILLIAMS, D H, BRADLEY, C V, MAGGIO, J, SANTIKARN, S AND SMITH, D H

SURFACE ANALYSIS OF POLYMERS AND OTHER SOLID MATERIALS BY FAB MS 393
*LATTIMER, R P, PAUSCH, J B AND HANSEN, G E

RELATIVE YIELDS OF POSITIVE IONS SPUTTERED FROM SEVERAL SILICIDES 395
SATKIEWICZ, F G

MASS DISCRIMINATION EFFECTS IN SIMS 397
*OKANO, J AND NISHIMURA, H

QUANTITATIVE SIMS ANALYSIS OF TRITIUM PERMEATION BARRIER OXIDE FILMS GROWN ON LASER MODIFIED INCOLOY 399
*CHRISTIE, W H AND EBY, R E

SIMS CHARACTERIZATION OF INORGANIC COMPOUNDS 401
*SPARROW, G R

WOC — **Ion Cyclotron Resonance Mass Spectrometry; Ion Molecule Reactions**

SIGNALS, NOISE, SENSITIVITY AND RESOLUTION IN ICR SPECTROSCOPY 403
*COMISAROW, M B

FOURIER TRANSFORM ICR SPECTROMETER USING HIGH FIELD SUPER CONDUCTING MAGNET 404
KELLERHALS, H AND *WANCZEK, K P

FOURIER TRANSFORM MASS SPECTROMETRY A NEW APPROACH TO MS/MS 407
*GHADERI, S, SPENCER, R B, HEIN, R E AND MARRA, J

DATA TREATMENT OF DISCRETE FOURIER SPECTRA 409
GIANCASPRO, C AND *COMISAROW, M B

COMPLEX ORGANIC MIXTURE ANALYSIS USING COMBINED CAPILLARY GC-FTIR-FTMS 410
WHITE, R L, GISS, G N AND WILKINS, C L

THE EXTENT OF PYROLYSIS IN A ICR MASS SPECTROMETER 412
BOAND, G, HOURIET, R AND *GAUMANN, T

FOURIER TRANSFORM MS OF MID TO HIGH MASS MOLECULES 414
*GHADERI, S, GROSS, M L AND WILKINS, C L

COLLISION INDUCED DISSOCIATION IN A FOURIER TRANSFORM MS 416
*CODY, R B AND FREISER, B S

NEGATIVE ION FORMATION BY ATTACHMENT OF ELECTRON TO RADICALS 417
*INQUE, M

WOD — **Stable Isotopes in Metabolism Studies**

QUANTITATIVE ANALYSIS OF NUTRITIONAL TRACE METALS ENRICHMENT USING A GCMS SYSTEM 419
*FENNESEY, P V, CHRISTIE, D, FAVIER, A, STAGE, A AND HAMBIDGE, K M

DETERMINATION OF STABLE METAL ISOTOPES IN MICROLITER VOLUMES OF SOLUTIONS BY INDUCTIVELY COUPLED 421
*HOUK, R S AND THOMPSON, J J

STUDIES ON THE MECHANISM OF -OXIDATION OF FATTY ACIDS IN BACTERIA USING 18O2 422
*YANO, I, YABUUCHI, E AND KISHIMOTO, Y

THE STUDY OF NITROGEN METABOLISM IN MARINE ALGAE AND HIGHER PLANTS USING DIRECT ANALYSIS OF 15N 424
*SUMMONS, R E, OSMOND, C B AND WOO, K C

NITROGEN CYCLING IN HIBERNATING BEARS 426
WOLFE, R R, NELSON, R A, *WOLFE, M H AND ROGERS, L

THE USE OF STABLE ISOTOPES TO STUDY ENDOGENOUS NITRATE-NITRITE FORMATION IN HUMANS 427
WAGNER, D A, *WISHNOK, J S AND TANNENBAUM, S R

BIOSYNTHETIC STUDIES OF MYCOLIC ACIDS IN NOCARDIA USING 13C STABLE ISOTOPES 429
*TOMIYASU, I, TORIYAMA, S AND YANO, I

INTRODUCTORY LECTURE: What You Always Wanted to Know about Collision Theory and Were Afraid to Ask 431
BOWERS, M T

WOE — ***Symposium; Nuclear Safeguards; High Temperature and Inorganics***

MASS SPECTROMETRIC MEASUREMENTS FOR NUCLEAR SAFEGUARDS 432
*CARTER, J A, SMITH, D H AND WALKER, R L

THE USE OF MASS SPECTROMETRY FOR SAFEGUARDS AT AN OPERATING REPROCESSING FACILITY 434
*FILBY, E E, WEBB, G W, RANKIN, R A, DELMORE, J E AND EMEL, W A

SIMULTANEOUS CONCENTRATION & ISOTOPIC URANIUM ANALYSIS OF LOW LEVEL DISCARDS BY ISOTOPE DILUTION MASS 436
CASABONA, L

SAFEGUARDS MEASUREMENTS CAPABILITIES AS OBSERVED BY THE SALE PROGRAM 437
*CRAWFORD, D W, CONNOLLY, V E AND MORAN, B W

THE CURRENT STATUS AND FUTURE ROLE OF NBS ISOTOPIC STANDARDS FOR NUCLEAR ENERGY 440
GARNER, E L, GILLS, T E AND *MOORE, L J

15

DETERMINATION OF REMOTE ACCOUNTABILITY TANK CONTENTS BY ISOTOPE DILUTION MASS SPECTROMETRY 441
*PERRIN, R E, ROKOP, D J AND FRANK, D J

High Temperature and Inorganics

AN ON-LINE, AUTOMATED GAS INLET SYSTEM FOR A FIELD MASS SPECTROMETER 442
*NEWTON, J C, CRAWFORD, R W, FRIESEN, R D AND SMITH, C F

MASS SPECTROMETRIC STUDIES OF GASEOUS URANIUM CHLORIDE SPECIES 444
*HILDENBRAND, D L AND LAU, K H

FORMATION OF METAL ATOM-CLUSTERS AND MEASUREMENT OF IONIZATION POTENTIALS 445
*SAITO, Y, YAMAUCHI, K, NODA, T AND MIHAMA, K

PLASMA SOURCE MS OF INORGANIC SAMPLES USING A MICROMASS 12-12S QUADRUPOLE MASS ANALYZER 447
DATE, A R, GRAY, A L, SMITH, C AND *TURNER, P J

MASS SPECTROMETRY AS A ROUTE TO VERY ACCURATE THERMOCHEMICAL DATA 449
STORMS, E

NEGATIVE IONS FROM CAF2-AL2O3 MIXTURES 451
*KATO, E AND SHIOKAWA, T

VAPOR PRESSURE MEASUREMENT OF CESIUM IODIDE AND OXIDES BY HIGH TEMPERATURE MASS SPECTROSCOPY 453
*YAMAWAKI, M, HIRAI, M, NAGASAKI, M AND KANNO, M

WOF — **Ion Molecule Reactions; Negative Ion Chemical Ionization**

ION-MOLECULE REACTIONS OF PH3 IMPLICATIONS FOR INTERSTELLAR DETECTION OF PHOSPHORUS CONTAINING 455
*THORNE, L R, ANICICH, V G AND HUNTRESS, W T

DISTINGUISHING BETWEEN POSITIONAL INTERCHANGE AND RANDOMIZATION OF DEUTERIUM LABEL A KINETIC ANALYSIS 456
BIERMAN, H W AND *MORTON, T H

LEWIS ACID-BASE REACTIONS OF BORATE AND BORINATE ESTERS 457
*BARTMESS, J E AND KIPLINGER, J

MECHANISM FOR THE REACTION OF 2,3,7,8-TETRACHLORODIBENZO-P-DIOXIN WITH OXYGEN UNDER N MS CONDITIONS 458
*MITCHUM, R K, KORFMACHER, W A AND ALTHAUS, J R

NEGATIVE ION CHEMICAL IONIZATION MASS SPECTROMETRY APPLICATIONS TO PROSTAGLANDIN AND DRUG ANALYSIS 460
*SWEETMAN, B J, LEVIN, F, WATSON, M, UETRECHT, J AND OATES, J A

ENHANCED SENSITIVITY AND SELECTIVITY FOR DETECTION OF NITROAROMATIC COMPOUNDS USING NEGATIVE CHEMICAL 461
*NISHIOKA, M G, PETERSON, B A AND HIDY, B J

MEDICAL AND BIOCHEMICAL APPLICATION OF NEGATIVE ION CHEMICAL IONIZATION MS - ULTRA-MICRO ANALYSIS OF 462
*HAYASHI, T, NARUSE, H, IIDA, Y AND DAISHIMA, S

DERIVATIVES FOR ELECTRON CAPTURE NCI: ANALYSIS OF GAMMA-AMINOBUTYRIC ACID AND METABOLITES OF BIOGENIC 464
*FAULL, K F, MARTIN, J AND BARCHAS, J D

MOLECULAR ADDUCT NEGATIVE ION FORMATION BY TRIFLUOROACETYLATED NUCLEOSIDES 466
*FINNEY, R W, HUGHES, H, NOWLIN, J AND HORNING, E C

NEGATIVE ION MS BY LOW PRESSURE CHEMICAL IONIZATION AND ITS COMBINATION WITH CONVENTIONAL POSITIVE ION MS 468
BRANDENBERGER, H

WOG — **Isotope Ratios**

LASER PHOTOIONIZATION MASS SPECTROSCOPY FOR ISOTOPIC AND ELEMENTAL ANALYSIS 470
*NOGAR, N S AND MILLER, C M

PULSED GLOW DISCHARGE IONIZATION SOURCE FOR ELEMENTAL ANALYSIS 472
*SAVICKAS, P J AND HARRISON, W W

GLOW DISCHARGE MASS SPECTROMETRY OF THE LANTHANIDE ELEMENTS 473
*KEEFE, R B, POMPLIANO, D L AND HARRISON, W W

SPARK SOURCE MASS SPECTROMETRIC ANALYSIS OF GALLIUM ARSENIDE FOR TRACE LEVELS OF OXYGEN AND CARBON USING 475
*WALTERS, D C, LOOK, D C AND TIERNAN, T O

THE DETERMINATION OF MICROGRAM QUANTITIES OF SULFUR BY THERMAL IONIZATION MASS SPECTROMETRY 477
PAULSEN, P J AND *KELLEY, W R

IMPROVED PRECISION & ANALYSIS TIMES BY THERMAL IONISATION MS 478
*TURNER, P J AND CANTLE, J E

HIGH PRECISION GAS ANALYSIS MS AT HIGH AND LOW RESOLUTION 480
*ELLIOTT, R M, WRIGHT, B AND CANTLE, J E

ISOTOPIC ANALYSIS WITH THE LASER MICROPROBE MASS ANALYZER(LAMMA) 482
*SIMONS, D S

TELLURIUM ANOMALIES IN THE METEORITE ABEE? 484
*SMITH, C L AND DE LAETER, J R

ISOTOPIC ANALYSIS OF NANOGRAM AMOUNTS OF TELLURIUM AND PALLADIUM IN TERRESTRIAL ROCKS 486
*ROSMAN, K J, LOSS, R D AND LAETER, J R

STERIC HINDRANCE OF HYDROGEN BONDING: THERMOCHEMISTRY OF INTERACTIONS IN ALKYLPYRIDINES 488
*SIECK, L W AND MEOT-NER, M

CONDENSATION REACTIONS OF HYDROCARBON IONS WITH ACETYLENE AND HYDROGEN CYANIDE 490
*ANICICH, V G, BLAKE, G A, HUNTRESS, W T AND MCEWAN, M J

KINETICS AND DEACTIVATION BY NEUTRAL NON-POLAR BATH GASES OF (C4H9)+ AND (C4H8)2+ IONS FORMED IN ISOBUTENE 491
NAGASE, K AND *HERMAN, J A

DETECTION OF THE NEUTRAL PRODUCTS OF ION-MOLECULE REACTIONS 493
*FRANCL, T J, KEECH, J R AND MCIVER, R T

COMBINED DRIFT-TUBE AND BEAM LUMINESCENCE STUDY OF THE CHARGE TRANSFER REACTION OF HE+ WITH XE IN THE ENERGY 495
HOWORKA, F, KUEN, I, VILLENGER, H, LINDINGER, W AND *FUTRELL, J H

ENERGETICS OF NEGATIVE MOLECULAR IONS FORMED IN HIGH TEMPERATURE ENVIRONMENTS 498
*WU, R L AND TIERNAN, T O

GAS PHASE BASICITIES OF METHYL, PHENYL PHOSPHINES 500
*IKUTA, S AND KEBARLE, P

CHARGE STRIPPING OF HYDROCARBON POSITIVE IONS 501
HERBERT, C G, PROCTOR, C J, RABRENOVIC, M, *HARRIS, F M AND BEYNON, J H

IONIZATION ENERGIES AND ENTROPIES OF CYCLOALKANES. KINETICS OF INTRINSICALLY FAST CHARGE-TRANSFER PROCESS 503
*SIECK, L W AND MAUTNER, M

PHOTOIONIZATION MASS SPECTROMETRY OF NH2OH: HEATS OF FORMATION OF HNO+ AND NOH+ 504
KUTINA, R E, GOODMAN, G L AND *BERKOWITZ, J

ENERGY TRANSFER IN THE HIGH ENERGY COLLISION AL ACTIVATION OF CH4+ 506
CROW, F W, TOMER, K R, GROSS, M AND *FUTRELL, J H

ENERGY DEPOSITION IN GAS PHASE IONS· ANGLE RESOLVED MASS SPECTROMETRY AND OTHER TECHNIGUES 507
MCLUCKEY, S A AND *COOKS, R G

A STUDY OF THE STRUCTURES OF DECOMPOSING AND NON-DECOMPOSING (C6H5O)+ IONS 509
*SAKURAI, H, TATEMATSU, A AND NAKATA, H

MASS SPECTROMETRY/MASS SPECTROMETRY STUDIES OF RING-OPENED VS CYCLIC IONS 511
*MILLER, D L, *DASS, C AND GROSS, M L

A STUDY OF THE MECHANISM OF THE LOW ENERGY COLLISION INDUCED DISSOCIATION OF C6H6+ USING A TRIPLE 513
*DAWSON, P H AND SUN, W F

ADVANTAGES OF MS/MS FOR ANALYSIS OF PYRROLIZIDINE ALKALOIDS 515
*HADDON, W F, MAOLYNEUX, R J AND KERSHAW, P

A NEW INSTRUMENT FOR THE ANALYTICAL APPLICATION OF MS-MS 516
BATEMAN, R H, *GREEN, B N AND SMITH, D C

APPLICATION OF AN AUTOMATIC GC-MS-DS SYSTEM TO THE ROUTINE QUALITY CONTROL OF PHARMACEUTICAL PRODUCTS 518
*RYAN, P A, WARBURTON, G A, TAYLOR, K T AND MOORE, L E

IDENTIFICATION OF AFLATOXINS BY QUADRUPOLE MS/MS 520
*PLATTNER, R D, BENNETT, G A, STUBBLEFIELD, R D AND SLAYBACK, J R

ADDUCT ION FORMATION IN A COLLISION CELL OF THE TANDEM QUADRUPOLE MS 522
*CARROLL, D I, NOWLIN, J G, STILLWELL, R N AND HORNING, E C

ON THE USE OF TRIPLE-QUADRUPOLE MS/MS FOR PEAK IDENTIFICATION IN COMPLEX INORGANIC SIMS SPECTRA 523
*MAGEE, C W, GALE, P J, BENTZ, B L AND SHABONOWITZ, J

STUDIES IN GC-CI MS 526
FENG, T M, RUDEWICZ, P AND MUNSON, B

WPB — **Instrument Design: Ionization; Laser Absorption and Desorption; Fast Atom Bombardment; Secondary Ion Mass Spectrometry**

A VERY HIGH YIELD ELECTRON IMPACT ION SOURCE FOR ANALYTICAL MASS SPECTROMETRY 527
*KOONTZ, S L AND DENTON, M B

ION OPTICAL PROPERTIES OF ELECTRON-BEAM-GUIDING ION SOURCE AND ITS APPLICATION TO MASS ANALYZER 529
*KISHI, T AND TAKAGI, T

EHD ION SOURCE WITH A RESERVOIR AND EMITTER TIP HEATED BY ELECTRON BOMBARDMENT 531
*OKUTANI, T, YAGI, K, NODA, T, TAMURA, H, OKANO, H AND WATANABE, H

ATMOSPHERIC PRESSURE PLASMA (ICP OR MIP)/MS FOR ELEMENTAL ANALYSIS 533
*DOUGLAS, D J, QUAN, E S AND SMITH, R G

CHARACTERISTICS OF A VOLCANO STYLE FIELD IONIZATION SOURCE AND A HIGH RESOLUTION (MS-9) MASS SPECTROMETER 534
*YOUNG, S E AND BUTTRILL, S E

LIQUID IONIZATION FIELD DESORPTION MASS SPECTROMETRY - EFFECT OF ELECTRIC FIELD ON A SAMPLE PROBE 536
*TSUCHIYA, M, NONAKA, T AND TAIRA, T

A FISSION FRAGMENT IONIZATION STUDY OF CHLOROPHYLL 538
CHAIT, B T AND *FIELD, F H

DISCHARGE IONIZATION SECONDARY ION MASS SPECTROMETRY (DISIMS) 539
*STAFFORD, G C AND BRADFORD, D C

PLASMA DISCHARGE MASS SPECTROMETRY FOR INORGANIC TRACE ANALYSIS 541
*CANTLE, J E, TURNER, P J, HALL, E AND KAY, R

DESIGN OF FAST ATOM GUNS AND ION SOURCES FOR FABMS 543
*HOGG, A M

RELEASE OF SECONDARY IONS UNDER VARYING FAB CONDITIONS 545
*GIESSMANN, U AND BAROFSKY, D F

A UNIQUE FAST ATOM SOURCE FOR MASS SPECTROMETRY APPLICATIONS 546
*MAHONEY, J F, GOEBEL, D M, PEREL, J AND FORRESTER, A T

A NEW MINIATURE "ON-SOURCE" FAB GUN 548
RUDAT, M A

FAB/FD/FI SOURCE FOR THE COMPACT GC/MS AND ITS PERFORMANCE 550
NAITO, Y, KUNIHIRO, F, KANMEI, Y, *KUBOTA, E AND NAITO, M

MODIFICATION OF AN HP 5985B GC/MS FOR MOLECULAR SIMS 552
MAGEE, C W, HARRINGTON, W L AND *GALE, P J

A SIMPLE METHOD FOR OBTAINING SIMS (FAB) SPECTRA OF ORGANICS 554
MCEWEN, C N

MOLECULAR ION DISTRIBUTIONS OF MIDDLE MOLECULES 556
*YERGEY, J, HANSEN, G, HELLER, D, FENSELAU, C AND COTTER, R

MASS CALIBRATION IN FABMS AN EVALUATION OF CALIBRATION COMPOUNDS SUITABLE FOR ACCURATE MASS 558
*VAN LANGENHOVE, A, COSTELLO, C E, CHEN, H F, BILLER, J E AND BIEMANN, K

HIGH RESOLUTION AND ACCURATE MASS MEASUREMENTS USING FAB 560
*HELLER, D, HANSEN, G, YERGEY, J, COTTER, R J AND FENSELAU, C

APPROACHES TO ACCURATE MASS DETERMINATION IN FABMS 562
*OCCOLOWITZ, J L

FAB AS AN IONIZATION TECHNIQUE: SENSITIVITY AND APPLICABILITY STUDIES 564
*HEMLING, M E, COOK, J C, RINEHART, K L AND OLSON, K L

CHEMICAL FACTORS INFLUENCING FAB MASS SPECTROMETRY 566
*BONE, W M, HUNT, D F AND MARASCO, J

OPTIMIZATION OF EXPERIMENTAL PROCEDURES FOR FABMS 567
*MARTIN, S A, COSTELLO, C E AND BIEMANN, K

KINETICS OF ION FORMATION FROM INORGANIC AND ORGANIC SALTS BY PULSED LASER IRRADIATION 569
*KRUEGER, F R, SCHUELER, B AND JOST, B

LC-MS SYSTEM EMPLOYING THERMOSPRAY SAMPLE WITH BELT TRANSPORT AND LASER DESORPTION 570
*HARDIN, E D AND VESTAL, M L

LASER DESORPTION MASS SPECTROMETRY 571
*COTTER, R J AND VANBREEMEN, R B

DESIGN AND TESTING OF A NEW ION SOURCE FOR DIRECT INJECTION LC/MS 603
*ARPINO, P J, BOUNINE, J P, DEDIEU, M AND DEVANT, G

MASS SPECTRA OF POLAR ORGANIC COMPOUNDS IN AQUEOUS SOLUTIONS INTRODUCED INTO AN INDUCTIVELY COUPLED 605
*HOUK, R S AND OLIVARES, J A

NUCLEOSIDE ANALYSIS BY COMBINED LC-MS 606
*EDMONDS, C G, PANG, H, MCCLOSKEY, J A, BLAKLEY, C R AND VESTAL, M L

LC-MS OF NUCLEOSIDES USING A COMMERCIALLY AVAILABLE DLI-PROBE 608
*ESMANS, E L, LUYTEN, Y AND ALDERWEIRELDT, F C

APPLICATIONS OF MICRO LC/MS TO THE DETERMINATION OF DRUG RESIDUES FOUND IN EQUINE PLASMA AND URINE 610
*HENION, J D, ECKERS, C AND MAYLIN, G A

THE DETERMINATION OF STEROIDS AND RELATED COMPOUNDS BY MICRO LC/MS 612
*ECKERS, C, SKRABALAK, D AND HENION, J D

HIGH-PRESSURE MASS SPECTROMETRY OF SOME LC-MS LIQUID REAGENTS 614
*YINON, J AND COHEN, A

APPROACHES TO ON-LINE ION-PAIR EXTRACTION AND DERIVATIZATION FOR HIGH PERFORMANCE LIQUID 616
*VOUROS, P, LANKMAYR, E P, HAYES, M J, KARGER, B L AND MCGUIRE, J M

ROD — **Laser techniques and Applications**

PHOTOIONIZATION MASS SPECTROMETRIC STUDY OF CH3SH, CD3SH AND CH3SD 617
KUTINA, R E, EDWARDS, A K, GOODMAN, G L AND *BERKOWITZ, J

252CF-PDMS OF PHOTOACTIVATED AL3O3 FILMS 619
JACOBS, D AND *MACFARLANE, R D

THE EFFECT OF SOURCE TEMPERATURE ON THE PHOTODISSOCIATION OF POSITIVE MOLECULAR IONS 620
*HARRIS, F M, GRIFFITHS, I W, MUKHTAR, E S AND BEYNON, J H

ION FRAGMENTATION KINETICS AS A PROBE OF MULTIPHOTON IONIZATION 622
*RIDER, D M, DURANT, J, ANDERSON, S AND ZARE, R N

PHOTOFRAGMENT SPECTROSCOPY STUDIES. ENERGY PARTITIONING AND ION STRUCTURE 622
KRAILLER, R E, MCLAURIN, A E AND *RUSSELL, D H

MULTIPHOTON IONIZATION-POTENTIAL AND LIMITATIONS 623
HUDGENS, J W, DIGIUSEPPE, T G, DUIGNAN, M AND *WYATT, J R

ANALYTICAL MULTIPHOTON IONIZATION STUDIES OF IRON-CONTAINING COMPOUNDS 625
*HARRISON, W W, RIDER, D M AND ZARE, R N

MIXTURE ANALYSIS BY MULTIPHOTON IONIZATION MASS SPECTROMETRY 573
*RIDER, D M, DURANT, J, ANDERSON, S AND ZARE, R N

MASS SPECTROMETRY OF AROMATIC MOLECULES WITH RESONANCE ENHANCED MULTIPHOTON IONIZATION 574
*LUBMAN, D M AND KRONICK, M N

ROA — Symposium. **Molecular Ion Emission/Desorption from Surfaces**

THE (252CF-PDMS, SIMS, LD, FAB) OF THIN FILMS OF BIOMOLECULES. CONDENSED STATE CHEMISTRY IN THE HIGH 576
MACFARLANE, R D

SPUTTERING OF ORGANIC MOLECULES 577
MAGEE, C W

SECONDARY ION MASS SPECTROMETRY OF ORGANIC COMPOUNDS 581
BENNINGHOVEN, A

LASER DESORPTION, SECONDARY ION MASS SPECTROMETRY, AND OTHER FORMS OF DESORPTION IONIZATION. PHENOMENA AND 585
*COOKS, R G AND BUSCH, K L

ROB — Symposium: **Isotopes in Geochemistry and Geochronology**

ISOTOPE ANALYSIS OF NOBLE GASES AND SOME APPLICATIONS IN THE EARTH SCIENCES 589
*HEBEDA, E H

URANIUM-LEAD MINERAL GEOCHRONOLOGY 591
*BAADSGAARD, H

PRECISE URANIUM-LEAD AGES USING ZIRCONS 592
*KROGH, T E

URANIUM-LEAD AGES WITHIN SINGLE ZIRCONS USING A SENSITIVE HIGH RESOLUTION ION MICROSCOPE 593
*COMPSTON, W, WILLIAMS, I S AND CLEMENT, S W

ARCHEAN GEOCHRONOLOGY OF INDIA 596
BASU, A R

ROC — ***Liquid Chromatography Mass Spectrometry***

QUANTITATIVE TRACE ANALYSIS BY REVERSED-PHASE LC/MS EMPLOYING CONTINUOUS SAMPLE PRE-CONCENTRATION 597
CHRISTENSEN, R G, HERTZ, H S, MEISELMAN, S AND WHITE, E

ION EVAPORATION/MASS SPECTROMETRY OF LABILE COMPOUNDS - ANALYSIS BY MS/MS AND LC/MS 599
*THOMSON, B A, IRIBARNE, J V AND DZIEDZIC, P J

APPLICATION OF DIRECTLY COUPLED LC/MS USING A NEW VACUUM NEBULIZING INTERFACE INCORPORATED WITH A 601
*TSUGE, S, MATSUMOTO, K, YOSHIDA, H, OHTA, K AND HIRATA, Y

DETERMINATION OF TRACE AMOUNTS OF AMINES IN WATER WITH 2,4-DINITROPHENYLAMINE DERIVATIVES BY GC/CHEM 658
*KOGA, M, AKIYAMA, T AND SHINOHARA, R

PARTS-PER-TRILLION ANALYSIS OF SEMIVOLATILE PRIORITY POLLUTANTS BY CLOSED LOOP STRIPPING GC/MS 660
*TRUSSEL, A R AND CLARK, R R

ANALYSIS OF CHLORHEXIDINE IN WASTE WATER USING AN EXTRELUT COLUMN, ON-COLUMN METHYLATION AND MASS 662
*MATSUSHIMA, H AND SAKURAI, N

QUALITY CONTROL PROTOCOL FOR THE FUSED SILICA CAPILLARY COLUMN GC/MS DETERMINATION OF SEMIVOLATILE 664
*LOPEZ-AVILA, V AND SAUTER, A D

ANALYSIS OF ORGANIC POLLUTANTS IN ENVIRONMENTAL SAMPLES BY GC/MS INCLUDING POSITIVE/NEGATIVE EI/CI 664
*LAO, R C, THOMAS, R S AND LOCKWOOD, J

RPA — **Chemical Ionization; Combustion; Environmental Contamination; Fuel Analysis; High Temperature Inorganic Applications; Inorganic SIMS**

NEGATIVE (CC14) AND POSITIVE (NH3) CHEMICAL IONIZATION OF THE EXPLOSIVE HEXANITROSTIBENE 665
*YELTON, R D

AMMONIA CHEMICAL IONIZATION OF THE EXPLOSIVES PENTAERYTHRITOLTETRANITRATE AND DIPENTAERYTHRITOL 667
*YELTON, R D

ASPECTS OF SINGLET OXYGEN CHEMISTRY IN CHEMICAL IONIZATION MASS SPECTROMETRY 669
*LANE, D C AND MCGUIRE, J M

CONFORMATIONAL EFFECTS IN THE AMMONIA CHEMICAL IONIZATION MASS SPECTROMETRY OF CYCLIC ALCOHOLS 671
WINKLER, F J, GULACAR, F O AND *BUCHS, A

QUANTITATIVE ANALYSIS OF VITAMINS BY MASS SPECTROMETRY 673
*FRAISSE, D J, MAQUIN, F AND BOURGEOIS, C E

CHARACTERIZATION OF GLUCURONIDES BY AMMONIA CHEMICAL IONIZATION MASS SPECTROMETRY (CI-MS) USING LINKED 675
*HASHIMOTO, Y, ISHIBASHI, M, MIYAZAKI, H, NOZIMA, K, YAMAUCHI, E AND AOYAMA, T

CHEMICAL IONIZATION MASS SPECTROMETRY OF BIFUNCTIONAL COMPOUNDS 676
*NAKATA, H, KONISHI, H, TAKEDA, N, SUZUKI, M AND TATEMATSU, A

POSITIVE AND NEGATIVE ION HYDROGEN CHEMICAL IONIZATION OF PORPHYRINS AND METALLOPROPHYRINS BY QUADRUPOLE 678
*SUNDARAMAN, P, GALLEGOS, E J, SLAYBACK, J R, JOHNSTON, M AND BAKER, E W

THE DETECTION OF SULFUR AND NITROGEN OXIDES IN THE ATMOSPHERE BY API/MS 678
*BENOIT, F M

HIGH PRESSURE LIQUID CARBON DIOXIDE EXTRACTION OF TETRACHLORODIBENZO- P-DIOXINS (TCDDS) 679
*DEROOS, F L, AICHELE, D G, TABOR, J E AND LARSON, M

15

LASER DESORPTION TLC/CI MASS SPECTROMETRY 627
*RAMALEY, L, VAUGHAN, M A, JAMIESON, W D AND BURNETT, N H

LASER DESORPTION FOURIER TRANSFORM MASS SPECTROMETRY 628
*MCCRERY, D A, LEDFORD, E B AND GROSS, M L

MS ELUCIDATION OF CHEMICAL BEHAVIOR ON COPPER-COPPER OXIDE CATALYSTS 630
*WOOD, G M, UPCHURCH, B T, HOYT, R F, PAULIN, P A, HOLMES, R A AND WILDNER, E L

ROE — **Symposium: Analysis of Industrial Polymers**

DIRECT ANALYSIS OF INDUSTRIAL POLYMERS BY MS - AN INTRODUCTION 631
*LATTIMER, R P

SOME SUBSTRATE TEMPERATURE EFFECTS ON MOLECULAR IONS SPUTTERED FROM POLYMERIC LIQUID SURFACES 633
*LIGON, W V AND DORN, S B

FIELD DESORPTION OF POLYMERS 635
CRAIG, A G, MCCRAE, C E AND *DERRICK, P J

THE APPLICATION OF FIELD DESORPTION MASS SPECTROMETRY TO QUANTITATION AND STRUCTURAL ELUCIDATION OF PHENOLIC 636
HERMAN, G, SKOTNICKI, P AND *WESTON, A F

HIGH-RESOLUTION HIGH-SENSITIVITY MASS SPECTROMETERS FOR HIGH MASS ANALYSIS 640
*MATSUDA, H

HIGH MOLECULAR WEIGHT MASS SPECTROMETRY 644
*BEUHLER, R J AND FRIEDMAN, L

PROBING ION-POLYMER INTERACTIONS BY ELECTROHYDRODYNAMIC IONIZATION MASS SPECTROMETRY 645
CHAN, K W AND *COOK, K D

ROF — **Water Analysis by Capillary GCMS**

USING THE MASS SPECTROMETER AS A CHLORINE-SELECTIVE DETECTOR 648
LABROSSE, J AND *ANDEREGG, R J

CAPILLARY GC/MS AND CAPILLARY GC/FID PROTOCOL FOR THE IDENTIFICATION AND CHARACTERIZATION OF 650
*HUGHES, S M, MITROSKY, S AND BROOKS, J J

COMBINED FUSED SILICA CAPILLARY COLUMN GAS CHROMATOGRAPHY/MASS SPECTROMETRY IN ENVIRONMENTAL 653
*SIEVERS, R E, BARKLEY, R M, HUTTE, R S, WILLIAMS, E J, CONDITT, M K AND HAWTHORNE, S B

PRECISION AND ACCURACY OF MEASUREMENTS AT HIGH RESOLUTION WITH A FAST SCANNING MAGNET AND A CAPILLARY 655
*BUDDE, W L, EICHELBERGER, J W AND DONNELLY, J P

TRACE WATER ANALYSIS IN GASES USING THE IPC-200 656
*FREES, L C, HOLKEBOER, D H AND FARDEN, J

MASS SPECTRAL CHARACTERIZATION OF DIESEL ENGINE PARTICULATE EMISSION EXTRACTS 681
*NISHIOKA, M G, DEROOS, F L AND PETERSON, B A

GC/MS ANALYSIS OF THE BIODEGRADATION PRODUCTS OF 4-CHLOROBIPHENYL BY GRAM NEGATIVE MICROORGANISMS 682
*MASSEL, R, MESSIERI, F AND SYLVESTRE, M

PENTACYCLIC TERPANES IN A 420-MILLION-YEAR-OLD (SILURIAN) BITUMEN 684
ANDERS, D E AND *KING, J D

A NEW TECHNIQUE FOR DETERMINING PETROLEUM STERANE DISTRIBUTIONS USING SELECTIVE METASTABLE ION 686
*STRADLING, R S AND ZUMBERGE, J E

ELUCIDATION OF CHEMICAL CHARACTERISTICS OF COAL FROM PYROLYSIS MASS SPECTRAL PATTERNS 687
*HARPER, A M, POPE, D L, METCALF, G S
AND MEUZELAAR, H L

CLASS ASSIGNMENT OF UNKNOWN COAL LIQUID CONSTITUENTS BY COMPUTERIZED PATTERN RECOGNITION TECHNIQUES 689
*METCALF, G S, MCCLENNEN, W H, HARPER, A M,
MEUZELAAR, H L AND HILL, G R

PYROLYSIS GC/MS OF SPECIFICALLY TREATED COALS 691
*GLISH, G L, MCBAY, E H, RAINEY, W T, LARSEN, J W
AND LIOTTA, R

ON THE INTERPRETATION OF THE MASS SPECTRA OF MIXTURES 693
*STAUFFER, J L, LARSEN, D J, NORWOOD, K C
AND LEVINS, P L

SECONDARY ION MS OF FROZEN SOLUTIONS OF INORGANIC SALTS 695
*STULIK, D, ORTH, R G AND MICHL, J

MASS SPECTROMETRY OF VIC-DIOXIMATE COMPLEXES OF NICKEL, PALLADIUM AND PLATINUM 696
*WESTMORE, J B AND FUNG, D

A MOLECULAR BEAM/MASS SPECTROMETER SYSTEM FOR DYNAMIC PYROLYSIS STUDIES 698
*MILNE, T A AND SOLTYS, M N

PHOTOELECTRON SPECTRA OF GAS-PHASE LANTHANIDE TRIHALIDES 700
RUSCIC, B M, GOODMAN, G L AND *BERKOWITZ, J

ANALYSIS OF CORRECTION FACTORS USED FOR MOLECULAR BEAM MS 702
*STEVENSON, D A AND KISKER, D W

ATOMIC METAL ION CHEMICAL IONIZATION USING FOURIER TRANSFORM MS 704
CODY, R B, BURNIER, R C, BYRD, G D, JACOBSON, D B
AND *FREISER, B S

HOW TO MAKE THE DS-50/55 SYSTEM ACTUALLY WORK 705
TERWILLIGER, D T

PRIORITY POLLUTANT PROGRAMS FOR THE VG-2050 DATA SYSTEM 707
SHRADER, S

GEOCHEMICAL DATA PROCESSING WITH THE DS-50 DATA SYSTEM 709
*KING, J D

PLTIO - A NEW INTERPRETIVE PROGRAM FOR HEWLETT PACKARD GC/MS DATA SYSTEMS 711
*SCHOENGOLD, D M

EXTENSIONS TO AN INCOS DATA SYSTEM 713
*JAMIESON, W D AND LEWIS, E

PERFORMANCE OPTIMIZATION OF HP 5985A MASS SPECTROMETER VIA OPERATOR INTERACTION 715
*MUSSELMAN, B D, DAVENPORT, M J AND HOLLAND, J F

LINKING AN INCOS DATA SYSTEM TO ANOTHER MINICOMPUTER 717
*JAMIESON, W D, DYER, E W AND MASON, F G

EXPANSION OF THE INCOS LIBRARY SEARCH 719
*SLIVON, L E AND AICHELE, D G

DCI, IN BEAM EI, AND LINKED SCAN B/E, STUDIES ON -(L--AMINOADIPYL)- PEPTIDES PRECURSORS OF THE PENICILLIN 720
ADLINGTON, R M AND ALPIN, R T

CHARACTERIZATION OF LIPOXYGENASE METABOLITES OF ARACHIDONIC AND LINOLEIC ACID BY GC/MS 722
*CLAEYS, M, COENE, M C AND VAN HOVE, C

PEPTIDE SEQUENCING AND AMINO ACID MIXTURE ANALYSIS BY GCMS KETOACID ESTER FORMATION IN ONE PROCEDURAL STEP 724
*METRAL, C J, JAYASIMHULU, K, KORNEL, A AND DAY, R A

DIFFERENTIATION BETWEEN LEUCINE AND ISOLEUCINE IN PEPTIDES BY -C=X DERIVATIVES 726
*DAY, R A, METRAL, C J AND JAYASIMHULU, K

FAB AND DIRECT CHEMICAL IONIZATION MASS SPECTROMETRIC ANALYSIS OF GLYCOSPHINGOLIPIDS 728
*CARR, S A AND REINHOLD, V N

STRUCTURAL STUDIES OF CARBOHYDRATE OLIGOMERS BY FAB AND DIRECT CHEMICAL IONIZATION MS 730
*REINHOLD, V N AND CARR, S A

FD/MS ANALYSIS OF HIGHLY UNSATURATED MYCOLIC ACIDS AND THEIR TREHALOSE ESTERS 732
*SHIZUKUISHI, S, AKIMORI, N, TOMIYASU, I AND YANO, I

ANALYSIS OF N-ACETYLNEURAMINIC ACID AND ITS DERIVATIVES BY GC/MS 734
MINEO, S, NUMATA, M AND *METORI, K

GC/MS OF THE MOLECULAR SPECIES OF DEUTERATED NATURAL GLYCEROPHOSPHOLIPIDS 736
*SAITO, K, SATOUCHI, K AND GAMO, M

DEUTERATED TRIMETHYLANILINIUM HYDROXIDE, PREPARATION AND UTILITY FOR ON COLUMN PERMETHYLATION OF MODIFIED
*SCHRAM, K H, TEECE, R G AND SLOWIKOWSKI, D 738

DETERMINATION OF 18O-LABELLING IN NUCLEOSIDE -PHOSPHATES
*KRICK, T P, WALSETH, T F, EIDE, S J AND GOLDBERG, N D 740

CHARACTERIZATION OF PURINE AND PYRIMIDINE BASES AS THEIR N, O-PERKALKYL AND TRIFLUOROACETYL/N, O-PERKALKYL
GELIJKENS, C F, *SMITH, D L AND MCCLOSKEY, J A 742

IDENTIFICATION OF N4-DIMETHYL-5-METHYL-2'-DEOXYCYTIDINE FOLLOWING THE YLCARBAMYL CHLORIDE WITH THYMIDINE
*SOLOMON, J J, SEGAL, A, MATE, U AND VAN DUUREN, B L 744

A STUDY OF THE UNUSUAL CHEMICAL REACTIVITY OF 7, 8, 9, 10- TETRAHYDROBENZO(A)PYRENE DERIVATIVES AT
*ROLLER, P P AND YANG, S K 745

FOA — **MSMS and Fragmentation Mechanisms**

MASS SPECTROMETRIC STUDIES IN STRUCTURAL AND STEREOCHEMICAL PROBLEMS OF 1-OXACEPHEMS
*NAKAGAWA, Y AND IKENISHI, Y 746

CALCULATED ANGULAR DISTRIBUTIONS OF FRAGMENT IONS FROM POLYATOMIC ION COLLISIONS
*TODD, P J AND WARMACK, R J 748

IONIC DECOMPOSITION MAPS
MASON, R S, FARNCOMBE, M J AND *JENNINGS, K R 750

A STUDY OF THE FRAGMENTATION BEHAVIOR OF ANISOLE BY THRESHOLD PHOTOELECTRON COINCIDENT PHOTOION (TPE-CPI)
GILMAN, J P, DAS, P R, *FUJII, T AND MEISELS, G G 751

STRUCTURES AND FRAGMENTATION MECHANISMS OF THE IONS OF ETHANOL BY TRIPLE QUADRUPOLE MS
*LATVEN, R K, MCFARLAND, M B AND ENKE, C G 753

THE DIECKMANN CONDENSATION & RELATED REACTIONS IN THE MASS SPECTROMETER
*BURINSKY, D J AND COOKS, R G 755

MS/MS OF OXIDATIVE INSERTION REACTIONS
MCEWEN, C N 757

DIFFERENTIATION OF POSITIONAL ISOMERS WITH COLLISION ACTIVATED REACTIONS IN A TRIPLE QUADRUPOLE MASS
*CHAKEL, J A AND ENKE, C G 758

SURVEY OF THE ENERGY DEPENDENCE OF THE COLLISIONALLY ACTIVATED DECOMPOSITION (CAD) SPECTRA OF ORGANIC SALTS
*ZAKETT, D AND TOU, J C 759

METASTABLE PEAK SHAPES AND THE PARTITION OF INTERNAL ENERGY IN THE REACTION (C2H5O)+ (CHO)+ + CH4
DONCHI, K F, RUMPF, B A AND *DERRICK, P J 761

FOB — **Symposium: Characterization of Shale Oils (Co-Sponsored by ASTM)**

MASS SPECTROMETRIC ANALYSIS OF SELECTED DISTILLATE FRACTIONS FROM SHALE OIL 762
*WEBER, J H, HEPPNER, R A AND GUFFEY, F D

OPTIMUM GC/MS/C CONFIGURATION FOR THE ANALYSIS OF PARAHO SHALE OIL <400F 766
GALLEGOS, E J

GC/MS COMPARISON OF SELECTED KETONES, NITRILES, AND ALKYL AROMATICS IN GREEN RIVER AND RUNDLE SHALE OILS 769
PANCIROV, R J AND ASHE, T R

COMBINED GC/MS ANALYSIS OF SELECTED SULFUR COMPOUNDS IN OIL SHALE RETORT GASES 770
*GUFFEY, F D AND BLANTON, W E

APPLICATION OF MASS SPECTROMETRY TO PETROLEUM EXPLORATION 770
*SEIFERT, W K, MOLDOWAN, J M AND GALLEGOS, E J

MASS SPECTRAL CHARACTERIZATION OF THE ACID AND BASE FRACTIONS FROM AN EASTERN AND WESTERN SHALE OIL 771
GREENWOOD, G

PYROLYSIS-MASS SPECTROMETRY STUDIES OF OIL SHALE AND OIL SHALE KEROGENS 773
MEUZELAAR, H L, HARPER, A M, *FUTRELL, J H AND LARTER, S

FIELD IONIZATION MS ANALYSIS OF SATURATES IN SHALE OIL 774
*SCHEPPELE, S E, GRINDSTAFF, Q G AND GRIZZLE, P L

AN EVALUATION OF TRIPLE QUADRUPOLE MS/MS FOR ON-LINE GAS ANALYSIS OF TRACE SULFUR CONTAINING SPECIES FROM 776
*WONG, C M, CRAWFORD, R W AND YOST, R A

FOC — **Structure Elucidation**

STRUCTURAL AND STEREOCHEMICAL INFORMATION FROM TANDEM MS 777
*CHENG, M T, BARBALAS, M P, PEGUES, R F, PROCTOR, C J, TURECEK, F AND MCLAFFERTY, F W

DIMETHYL ETHER. A VERSATILE REAGENT GAS FOR ORGANIC FUNCTIONAL GROUP RECOGNITION BY CHEMICAL IONIZATION 778
KEOUGH, T

DERIVATIVES FOR THE STRUCTURAL DETERMINATION OF BRANCHED, UNSATURATED AND CYCLOPROPYL LONG-CHAIN 780
*HARVEY, D J

FRAGMENTATION OF 3-DEAZAURIDINE AND SELECTED DERIVATIVES 782
*SCHRAM, K H

NEGATIVE ION CHEMICAL IONIZATION MASS SPECTROMETRY OF PYRROLIZIDINE ALKALOIDS 784
*DREIFUSS, P A, CARESS, E A, BRUMLEY, W C AND SPHON, J A

STRUCTURAL DETERMINATION OF ECDYSTEROIDS AND BRASSINOSTEROIDS BY MASS SPECTROMETRY 786
*IKEKAWA, N, TAKATSUTO, S AND IKEDA, T

COMPUTER-AIDED INTERPRETATION OF MASS SPECTRA 788
*BACZYNSKYJ, L AND DUCHAMP, D J

PREPARATION OF PEPTIDES LABELLED WITH DEUTERIUM ON THE PHENYLALANINE AND TYROSINE AROMATIC RINGS 789
*FAULL, K F AND BARCHAS, J D

FOD — **Applications of MSMS**

MATRIX EFFECTS IN DIRECT MIXTURE ANALYSIS BY MS/MS 791
*DAVIDSON, W R, THOMSON, B A, SHUSHAN, B I AND FULFORD, J E

TLC/MS/MS OF DRUGS IN BIOLOGICAL SAMPLES 792
*HENION, J D AND THOMSON, B A

MS/MS OF ENZYME CLEAVAGE PRODUCTS 794
*KALEY, R G AND WEINGARTEN, H I

'SOFT COLLISION' GC/MS/MS AS A PROBE INTO THE STEREOCHEMISTRY OF SUGAR SUBUNITS IN COMPLEX NATURAL 796
*RICHTER, W J AND BLUM, W

CHARACTERIZATION OF ORGANICS IN COAL LIQUIDS AND DEISEL PARTICULATES BY MS/MS 798
*LI, Z M, CIUPEK, J C, WOOD, K V AND COOKS, R G

A COMPREHENSIVE ANALYTICAL SCHEME FOR THE ANALYSIS OF ORGANICS IN ENVIRONMENTAL MATRICES BY MS/MS 800
HUNT, D F, *SHABANOWTIZ, J, HARVEY, T M AND COATES, M

A MICRO COMPUTER CONTROLLED TANDEM QUADRUPOLE MASS SPECTROMETER USING A DIRECT INSERTION PROBE FOR 802
*VOYKSNER, R D, HASS, J R AND BURSEY, M M

TANDEM MASS SPECTROMETRY WITH IMPROVED MASS RANGE 804
*PROCTOR, C J, AMSTER, I J, BALDWIN, M A, BARBALAS, M P, MCLAFFERTY, F W AND YALOW, R S

HIGH PRESSURE COLLISIONAL ACTIVATION 805
BLOM, K F AND MUNSON, B

FOE — **Synfuels and Combustion**

IDENTIFICATION OF SULFUR COMPOUNDS IN A GASOLINE BY GAS CHROMATOGRAPHY QUADRUPOLE MASS SPECTROMETER 807
GUIEZE, , *DEVANT, G AND LOYAUX,

AN IMPROVED METHOD FOR CALCULATING COMPOUND TYPES IN HYDROCARBON MIXTURES 807
*BOCKHOFF, F M AND ASAMOTO, B

FIELD DESOPTION-HIGH MASS SPECTRAL ANALYSIS OF COAL LIQUEFACTION BOTTOMS AND PETROLEUM RESIDS 808
ACZEL, T AND LARAMEE, J A

HIGH PERFORMANCE MS IN THE OPTIMIZATION OF COAL LIQUEFACTION PROCESSES COAL LIQUEFACTION MATERIALS 810
*WILSON, B W, CHESS, E K AND GROSS, M L

SCREENING AVIATION FUELS FOR THIOPHENES USING TRIPLE QUADRUPOLE MASS SPECTROMETRY 812
*MYERHOLTZ, C A AND ENKE, C G

GC/MS AND MS/MS STUDIES OF DIESEL EXHAUST EMISSIONS FROM CHEMICALLY DEFINED FUELS 814
*HENDERSON, T R, SUN, J D AND CLARK, C R

CAPILLARY COLUMN GC - LOW RESOLUTION MS TECHNIQUES FOR MONITORING TOXIC ORGANIC COMPOUNDS IN COMBUSTION 816
*TIERNAN, T O, GARRETT, J H, SOLCH, J G, VANNESS, G F AND TAYLOR, M L

GCMS NALYSIS OF POLAR COMPONENTS IN THE OIL PRODUCTS AND WASTE WATER EFFLUENT FROM THE GFETC SLAGGING FIXED 818
*OLSON, E S, DIEHL, J W AND MILLER, D J

FOF — **Disease Profiling**

URINARY METABOLIC PROFILES OF AROMATIC AMINO ACIDS METABOLIC DISORDERS 819
SHINKA, T, MATSUMOTO, I, AOYAMA, T, HIGUCHI, T, NOJIMA, K AND *LIN, Y Y

AMMONIA METABOLISM OF A PATIENT WITH ORNITHINE TRANSCARBAMYLASE DEFICIENCY DETECTED BY 15N TRACER 822
*YABUUCHI, H, KODAMA, H, SAMUKAWA, K, NOSE, O AND OKADA, S

STUDIES OF HYPERTENSIVE RAT URINARY ORGANIC ACIDS USING CAPILLARY GC/MS 824
*HAYASHI, A AND MORITA, M

METABOLIC PROFILING OF DIABETIC KETOACIDOSIS USING GC-MS 826
*NIWA, T, MAEDA, K, OHKI, T AND SHIBATA, M

IDENTIFICATION AND METABOLISM OF 3-ETHYL-3-HYDROXYGLUTARIC ACID IN URINE OF PATIENTS 828
*KUHARA, T, MATSUMOTO, I, SHINKA, T AND MATSUO, M

QUANTITATIVE URINARY STEROIDS OF HYPERANDROGENIC WOMEN BY FINNIGAN OWA 1020 GAS CHROMATOGRAPHY-SPECTROMETRY 830
*LIN, S N, AO, J, CAPRIOLI, R M, RODRIQUEZ, L J, SMITH, K D AND STEINBERGER, E

QUANTITATION AND IDENTIFICATION OF URINARY STEROID HORMONES IN PRECOCIUS PUBERTY 831
*PIKE, A W, FENNESEY, P V AND MOYNIHAN, C

-KETO AND -HYDROXY ACID EXCRETION IN AN ERROR OF FATTY ACID CATABOLISM 832
*MAMER, O A, MONTGOMERY, J A, MILLER, J AND COLLE, E

THE NIH/EPA MASS SPECTRAL DATABASE AND SEARCH SYSTEM 833
*MARTINSEN, D P, HELLER, S R, BUDDE, W L, MILNE, W A AND OLDHAM, R G

PERSONAL MASS SPECTRAL DATABASE IN FLOPPY DISK SYSTEM 835
KOYAMA, Y, TAZAWA, T AND *MAEDA, K

REAL-TIME PBM MATCHING OF UNKNOWN MASS SPECTRA ON A GC/MS/COM SYSTEM 837
*MUN, I K, STAUFFER, D B, STAEDELI, W, GUO, C J, MCLAFFERTY, F W, PETERSON, D W AND SERUM, J W

A RAPID AND RELIABLE PROGRAM FOR THE DETERMINATION OF TARGET COMPOUNDS IN GC/MS DATA FILES 838
*RYAN, P W AND COLBY, B N

COMPUTERIZED LABORATORY MANAGEMENT SYSTEM FOR ENHANCED QUALITY CONTROL AND SAMPLE TRACKING IN VOLUME ORIENTED 839
*RUSSELL, J W AND FULTON, K H

A DATA BASE MANAGEMENT SYSTEM FOR MS/MS AND OTHER MULTIDIMENSIONAL INSTRUMENTS 841
*CRAWFORD, R W, WONG, C M, BRAND, H R, GREGG, H R, HOFFMAN, P A AND ENKE, C G

PORTABLE, REMOTELY OPERATED, COMPUTER CONTROLLED, QUADRUPOLE MASS SPECTROMETER FOR FIELD USE 843
*FRIESEN, R D, NEWTON, J C AND SMITH, C F

A VERSATILE SOFTWARE CONTROL SYSTEM FOR A TRIPLE QUADRUPOLE MASS SPECTROMETER 845
*MYERHOLTZ, C A AND ENKE, C G

MICROCOMPUTER-BASED DATA ACQUISITION SYSTEM FOR ION CYCLOTRON RESONANCE MASS SPECTROMETRY 847
BUCKLEY, T J AND *EYLER, J R

INVESTIGATING THE USES OF A COMMODORE PET MICROCOMPUTER IN CONVENTIONAL ION CYCLOTRON RESONANCE 848
*MCELVANY, S AND ALLISON, J

ANALYSIS OF MALEIC ANHYDRIDE IN DIETS OF RODENTS BY GC/MS 850
*WHITE, E L, HECK, H A AND CHEPLEN, J M

THE RAPID SCREENING OF FOOD PRODUCTS FOR MYCOTOXINS BY MS/MS 851
*DAVIDSON, W R, TANNER, S D, NGO, A AND GREENHALGH, R

CONFIRMATION OF VOLATILE NITROSAMINES IN MEAT FOOD PRODUCTS BY GAS CHROMATOGRAPHY/MEDIUM RESOLUTION MASS 852
SUN, T

MS ANALYSIS OF THE LINKAGE OF PESTICIDE RESIDUES AND HUMUS CONSTITUENTS 854
*MINARD, R D, BOLLAG, J M AND LIU, S Y

IDENTIFICATION OF TRIFLUOROMETHYLBENZENE DERIVATIVES BY NEGATIVE ION CHEMICAL IONIZATION MASS SPECTROMETRY 855
PROCTOR, B L

NEGATIVE ION CHEMICAL IONIZATION MASS SPECTROMETRY OF PHENOLIC PRIORITY POLLUTANT COMPOUNDS 857
*BAYER, C W AND LOWE, L E

LONG TERM RESPONSE AND RETENTION TIME PRECISION OF COMBINED ACID AND BASE/NEUTRAL FRACTION PRIORITY 858
*COLBY, B N, RYAN, P W AND WILKINSON, J E

STUDIES OF AQUEOUS SOLUTION OF GLUTARALDEHYDE BY CAPILLARY GAS CHROMATOGRAPHY-MASS SPECTROMETRY 859
MASADA, Y, *HASHIMOTO, K, SUMIDA, Y, TASHIMA, T, SATHO, N, SHIZUKUISHI, K AND MOCHIKI, A

MS DETERMINATION OF TRACE ORGANIC COMPOUNDS IN AQUEOUS WASTES ASSOCIATED WITH ENERGY PRODUCTION 861
*HILPERT, L R, RICHIE, K L AND HERTZ, H S

GAS CHROMATOGRAPHY-FIELD IONIZATION MASS SPECTROMETRY (GC-FIMS) 863
*FLEMING, R H, BUTRILL, S E, SMITH, J H AND HARPER, J C

DRY INJECTOR REGAINS SENSITIVITY AND MAINTAINS SEPARATION FOR CAPILLARY GCMS ANALYSIS 865
*ALLEN, R H, PIKE, A AND FENNESEY, P V

A CHEMICAL REACTION CAPILLARY GC/MS INTERFACE 866
*ABRAMSON, F P AND MARKEY, S P

THE INTEGRATED GC PROBE: A NEW ANALYTICAL TOOL FOR HIGH BOILING COMPOUNDS AND MS/MS 868
RUDAT, M A

GC/MS AND GC/FT-IR, A COMPARISON 869
*GALLAHER, K L AND BERLEC, D

MODIFICATIONS OF AUTOMATED REVERSE LIBRARY SEARCHING ALGORITHMS (MSSMET) BASED ON EXPERIMENTAL OBSERVATIONS 871
*HOLLAND, J F, WESTOVER, L, VRBANAC, J, PINKSTON, J D AND SWEELEY, C C

CHARACTERIZATION OF POLYAROMATIC NITROGEN BASES IN CRUDE OIL 873
SCHMITTER, J M, DORBON, M, DERYCKE, G, IGNIATIADIS, I AND *ARPINO, P J

THE DETERMINATION OF THE TRANSPORT PROPERTIES OF ATMOSPHERIC GASES IN AN EPOXY RESIN BY PRECISION ABRASION MASS SPECTROMETRY*

Michael A. Grayson and Clarence J. Wolf
McDonnell Douglas Research Laboratories
St. Louis, MO 63166

The transport properties, i.e., solubility and diffusion, of the atmospheric gases in epoxy resins are of immediate interest because of their increased use as structural components of high-performance aerospace systems. Two compounds, water and oxygen, are of particular importance because of their effect on the physical properties of epoxy resins and their high chemical reactivity. The transport properties of both of these compounds were investigated by precision abrasion mass spectroscopy (PAMS)[1] of resin coupons exposed to a controlled temperature and humidity environment.

The resin, Ciba Geigy MY-720 (which is approximately 70% tetraglycidyldiaminodiphenyl methane) and Ciba Geigy Eporal (primarily diaminodiphenyl sulfone) was cast in silicone molds in the form of rectangular plates 3 x 10 x 20 mm according to the method described by Fanter.[2] Test coupons were exposed to controlled thermal (35°, 50°, 65°, and 80°C) and humid (0% RH, 100% RH, or immersed in water) environments for time periods ranging from 6 to 7000 h.

The distribution profiles of the compounds of interest were determined by measuring a characteristic ion during abrasion. In this study, the ions monitored were: m/e 17, 28, 32, and 44 for water vapor (m/e 18 was usually saturated), nitrogen, oxygen, and carbon dioxide, respectively.

The distribution profiles from at least three holes in a single sample were averaged and used to calculate a single data point. A typical distribution profile (averaged about the midpoint of the sample) is shown in Figure 1. The dotted line shows the half-profile for one environmental exposure condition measured by PAMS, while the solid line represents the theoretical half-profile determined by a least-squares analysis of the measured profile.

A summary of the transport properties of water in the epoxy resin exposed to 100% RH and immersed in water is given in Table 1.

The activation energies for the diffusion of water are 49.4 kJ/mol and 49.8 kJ/mol for immersed samples and samples exposed to 100% RH respectively. The diffusion process is similar for samples exposed to 100% RH and immersed in water. However, there is a significant difference in the equilibrium concentration of water in the resin exposed to the two different environments. Gravimetric data recorded during these experiments confirms this observation, i.e., samples immersed in water gain more weight than those exposed to a 100% RH environment. Samples immersed or suspended in 100% RH atmosphere continue to sorb water slowly after apparent saturation. The PAMS data show a flat or saturation profile even though the resin continues to sorb water at a rate corresponding to less than 0.1% per 1000 h exposure.

In all resins investigated, the distribution profiles of water had a large signal-to-noise ratio; however, in many cases, the distribution profiles of oxygen were low, had poor signal/noise ratios, and, in some cases, were nonexistent. Nevertheless, several observations were made:

- Oxygen was present only in samples exposed to a wet environment;
- The distribution profile of oxygen in wet samples was similar to the water distribution profile;
- Samples immersed in water contained as much oxygen as those exposed to air with 100% RH.

In a completely dry resin sample, i.e., containing less than 0.01 wt% water, the solubility and diffusion of oxygen is essentially zero as illustrated in Figure 2 where the oxygen profiles in a wet (containing 4.1 wt% H_2O) and a dry (< 0.01 wt% H_2O) resin are shown. The wet sample was aged in a humid atmosphere (100% RH at 65°C) for 7000 h, while the dry sample was aged for the same time interval in a completely dry atmosphere at 65°C. The same phenomenon was observed at all temperatures, and it appears that for any measurable amount of oxygen to diffuse into this resin, water must be present. At 65°C, the diffusion coefficient and solubility of oxygen in the resin are 2×10^{-12} m^2/s and 10^{-3} $g(O_2)/g(resin)/10^5$ Pa O_2 respectively.

The solubility of both nitrogen and carbon dioxide is less than 10^{-4} g/g of resin and exhibited a distribution profile equivalent to that of the background.

*This work was conducted under the McDonnell Douglas Independent Research and Development program.

The data indicate that both oxygen and water dissolve in and diffuse through the MY720/Eporal resin system. The transport of water can be analyzed successfully in terms of Fickian diffusion until the sample is nearly saturated. The solubility and diffusion of oxygen are closely coupled with the transport of water.

References

1. *M. A. Grayson, E. A. Theby, and K. O. Lippold, Rev. Sci. Instrum. 52, 1521 (1981).*
2. *D. L. Fanter, Rev. Sci. Instrum. 49, 1005 (1978).*

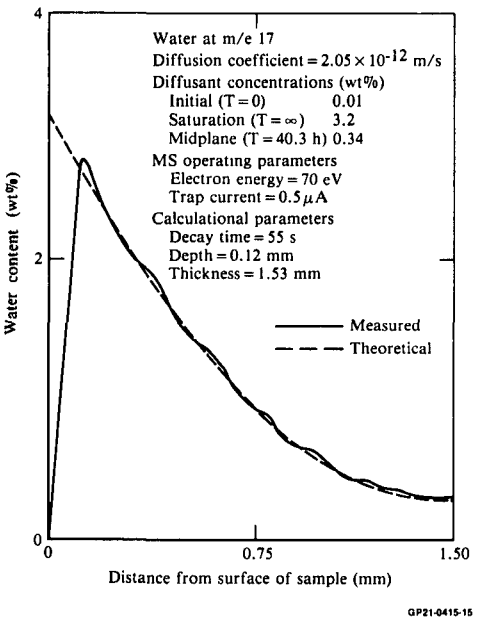


Fig. 1 Comparison of the measured and theoretical moisture distribution profiles after 40.3 h exposure to 100% RH at 65°C.

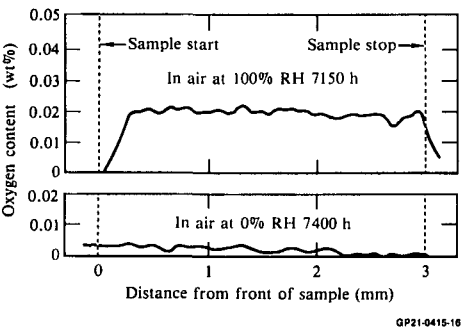


Fig. 2 Oxygen distribution profiles in "wet" and "dry" samples.

Table 1. Transport properties of water in an epoxy resin.

Temperature (°C)	Diffusion coefficient (10^{-12} m²/s)		Equilibrium content (wt%)		Solubility g(H_2O)/g(resin)	
	Immersed	100% RH	Immersed	100% RH	Immersed	100% RH
35	0.31	0.31	5.8	5.4	1.0	1.0
50	0.75	0.72	5.4	5.1	0.44	0.42
65	1.7	1.9	4.5	3.5	0.18	0.14
80	3.8	3.5	4.5	3.5	0.10	0.07

ELEMENTAL ANALYSIS BY COMBINED MICROWAVE PLASMA-GC/MS

R.A. Heppner; Laramie Energy Technology Center; Department of Energy; Laramie, Wyoming 82071

The microwave plasma device described here makes it possible to use a mass spectrometer as an element selective detector for atomic species typically found in organic compounds. The device has been used as a specific detector for C, O, N, S, and Cl atoms; other species could probably also be detected. Utilization of the device requires very little modification to existing mass spectrometer or GC/MS systems.

The process whereby specific elemental detection can be accomplished is as follows:

1. Material from a GC (or other device) is directed into a specially designed plasma interface unit (see figure 1) where it is exposed to the extremely high temperature of the plasma. The discharge is contained by a quartz tube 2cm in diameter and 30cm long. Buffer gas (helium and hydrogen have been used) flows through the tube at 1-10 cm^3/sec at a pressure of 1-20 kPa. A fused silica line leads sample material directly into the discharge; a similar line, connected to a piece of 3mm diameter quartz tubing samples the species produced in the discharge. Microwave power of approximately 100 Watts at 2.45 GHz is used.

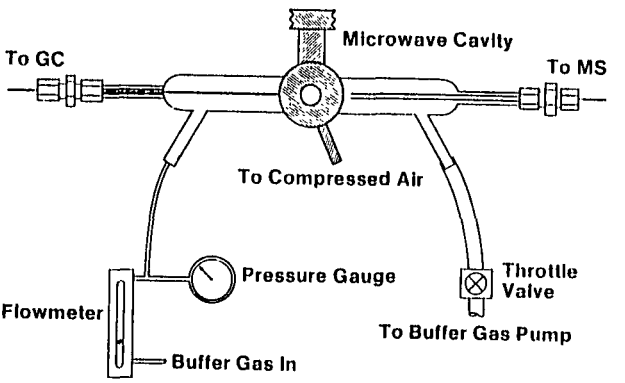


Figure 1. Microwave Plasma Interface Unit.

2. During collisions with the energetic ions and electrons present in the discharge, sample molecules are dissociated into their atomic species. These recombine among themselves and with hydrogen in the buffer gas to form very simple compounds (their molecular weights are typically less than 40 amu).

3. A sample of the compounds produced by the plasma discharge is admitted to a mass spectrometer and quantitatively analyzed using a mass spectral matrix analysis method.[1]

4. With the results from the matrix analysis, simple calculations are done to determine the relative amounts of each element present in the original sample material.

It is interesting to note that the molecular structure of the original sample material has very little influence over the species produced by the plasma. The species produced depend only upon the elements present in the original sample molecules. For instance, toluene and hexane are very different structurally, but as figure 2 shows, the mass spectra of the compounds produced in the discharge for hexane and toluene are very similar. The produced compounds are methane, acetylene, and ethene.

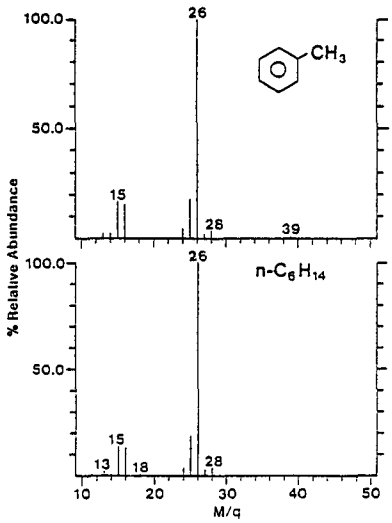


Figure 2. Results of the application of the microwave discharge to toluene and hexane.

Figure 3 shows the results obtained when C/O ratios are measured for a series of oxygen containing compounds using the plasma technique. A number of different compound types were used to obtain the data: alcohols, ketones, aldehydes, and acids. Compounds were chosen which had chain and ring types of structures. The line in figure 3 indicates the desired relation between measured and actual C/O ratios. Note that the data points fall very close to the line except for the measurements made at large C/O ratios, where it is believed that the quantitative measurement of methane gas from the plasma is in error. Similar results have been obtained for the measurement of C/N ratios.

The plasma technique described here utilizes 0.05 to 5 microliter sample size, and the response is linear over this range. Work is in progress to determine the optimum operating conditions for the plasma and to extend the application of this technique to solid samples.

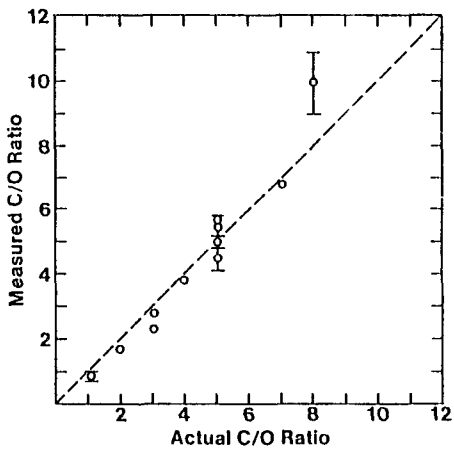


Figure 3. Measurement of C/O ratio for oxygen containing compounds.

References

[1]Fausett, Donald W. and Weber, James H., "Mass Spectral Pattern Recognition via Techniques of Mathematical Programming", Anal. Chem. 50, 722-731 (1978).

MS/MS BY TIME-RESOLVED MAGNETIC DISPERSION MASS SPECTROMETRY

J.T. Stults, C.G. Enke, J.F. Holland, J.D. Pinkston, J. Allison, and J.T. Watson

NIH/MSU Mass Spectrometry Facility
Michigan State University
East Lansing, Michigan 48824

Tandem mass spectrometry (MS/MS) has become a popular tool for mixture analysis and structure elucidation. However, acquiring the large amount of information that can be obtained with this technique requires large samples and considerable analysis time. A new technique, time-resolved magnetic dispersion mass spectrometry, now provides the capability for acquiring the complete MS/MS data field in a much shorter time, perhaps on the time scale of a chromatographic peak.

With reference to Figure 1, a brief pulse of ions formed in the ion source can be accelerated to constant energy. Ion velocity is inversely related to the square root of the mass. The ions are allowed to undergo dissociation, either by high energy collisionally induced or metastable decomposition, in the field-free region between the source and magnetic sector. Subsequent dispersion by a magnetic field separates ions according to momentum. The detection electronics are linked to the source pulse so that ion flight times, and thus velocities, are also measured.

In the dissociation process, there is relatively little change in velocity between the parent and daughter so a daughter ion has essentially the same flight time as its parent. As a result, time-of-flight measurements of a daughter ion indicate the mass of the parent ion. However, due to the change in mass, there is a change in ion momentum upon fragmentation. A magnetic sector can be used to separate daughter ions of various momenta from their parents.

Daughter ion mass is given by equation (1), derived by replacing velocity with flight time (ℓ/t) in the basic magnetic sector equation.

$$m/z = Bt\ (er/\ell) \qquad (1)$$

Note that ion mass assignment can be based on the product of B and t, independent of ion energy. Any energy spread among ions of a given mass will manifest itself as different values of B and t but with the Bt product constant.

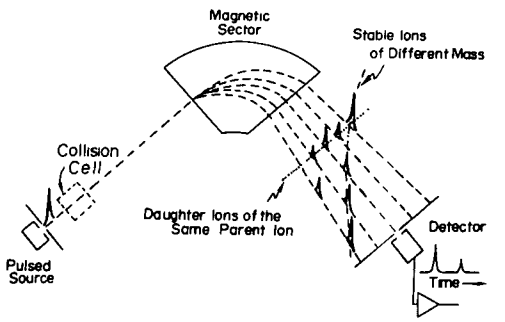
Figure 2 shows the MS/MS data field in terms of B and t. With a time sampling technique, as employed in conventional time-of-flight instruments, only a single arrival time or 'time slice' is sampled for each pulse of the ion source. This sampled arrival time can be slowly changed during subsequent pulses of the source to cover all arrival times. By varying both B and t in different ways, the various types of MS/MS scans can be obtained as outlined below.

The values of B and t which would give a spectrum containing only stable ions (those that undergo no dissociation after leaving the ion source) appear as a diagonal line. If B and t were scanned in concert along this line, a conventional mass spectrum (free of metastables) would be obtained. For a daughter ion scan, the arrival time is held constant and the magnetic field is scanned such that different momenta are examined. A parent ion scan involves holding the product Bt constant while scanning B and t in a linked fashion to move along the constant Bt curve.

These individual scans would be unnecessary if all arrival times could be sampled for each source pulse. This measurement technique, called time-array detection (TAD), will be implemented with an integrating transient recorder under development in our lab. With TAD it should be possible, in a single scan of the magnet (a few seconds), to obtain the full MS/MS data field from which can be extracted all daughters of all parents. This will greatly enhance the utility of MS/MS as a chromatographic detector.

Preliminary data have been taken with an LKB 9000, modified for ion beam pulsing and time-resolved detection, as a demonstration of the time-resolved magnetic dispersion mass

spectrometer. As an example, a metastable decomposition of benzonitrile, 103^{+}--76^{+} + HCN, was examined. On an oscilloscope, ions of mass 103 were observed at the calibrated magnetic field strength for that mass with a flight time of 14.1 μs. At the magnetic field strength (momentum) corresponding to stable ions of mass 56, the mass 56 ions were observed at 10.6 μs, and a second peak was also observed at 14.1 μs at this same momentum. The values of B and t indicated the second peak corresponded to ions of mass 76. The flight time indicated that they were daughter ions of mass 103. Note that 56 is the 'apparent mass' for this metastable ion, i.e., $76^2/103 = 56$, but that through time-resolved detection, it is clearly identified as a daughter of mass 56 from a parent of mass 103.



Time-Resolved Magnetic Dispersion Mass Spectrometer

Figure 1

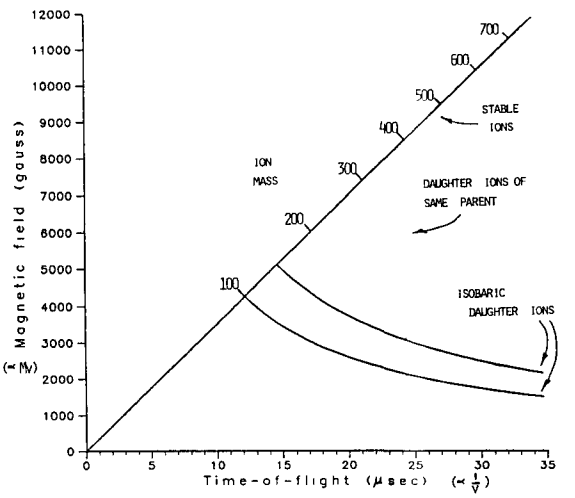


Figure 2

AN AUTOMATIC, PRECISION CALIBRATOR FOR AN EIGHT COMPONENT RESIDUAL GAS ANALYZER; J. S. Clark, F. L. Farr, W. D. Wallace, M. J. Criddle; Primary Children's Medical Center, Salt Lake City, Utah 84103.

As a residual gas analyzer, the mass spectrometer offers the advantages of high sensitivity and dynamic range, and unsurpassed frequency response, with multiple gas analysis capability. If these specifications are pushed to their technical limits, compromises occur in other specifications such as linearity, stability, and spectral interference. These compromises can quickly produce unacceptably cumbersome calibration requirements for achieving acceptable quantitative measurements. Added to the problem is the difficulty of obtaining reliably accurate mixtures of calibration gases, as the number of gas components increases.

This paper describes an automatic, precision calibrator for an eight component residual gas analyzer. The calibrator employs an accurate flow proportioning method for combining eight gases with variable compositions under microprocessor control. A self balancing principle for calibration is employed which uses the mass spectrometer as a comparator. The mass spectrometer first measures an unknown gas mixture, recording the response to each gas component in memory of the controlling microprocessor. The input to the M.S. is then directed to the gas mixer which is controlled by the same processor. The processor then adjusts the gas fraction of each gas mixer component until the M.S. response to the output of the gas mixer equals the M.S. response to the unknown sample.

The principle of operation of the gas mixer is illustrated in Figure 1. (For simplicity of presentation, only three gases are shown. The concept applies to mixing any number of gases). Input gases are delivered to an isobaric regulator system, which forces each gas to a common pressure at the input of its central valve. By appropriate sequencing of the valve operations, each gas flows independently through the common orifice restrictor in time sequence between the other two gases. A particular time averaged mixture is determined by the relative time each valve is open relative to the other two. The accuracy gas pressure method is determined by the accuracy of valve timing, the precision of relative gas pressure regulation of the isobaric regulator, the establishment of common gas temperature, and the invariance of relative resistance to flow through the common orifice of each gas with respect to each of the others.

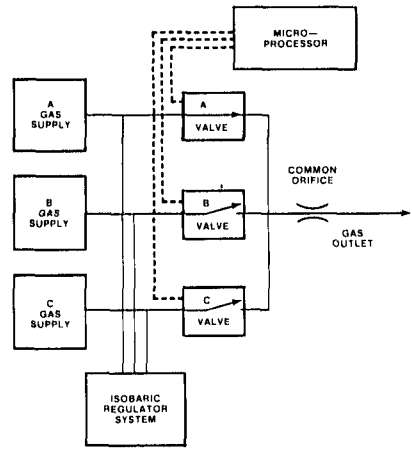


Figure 1. Simplified diagram of gas mixing apparatus.

The isobaric regulation system contains a back-pressure regulator. Equal pressures of the gases at the input of the solenoid valves are maintained by the connections to the common pressure of the back-pressure regulator. This regulator bleeds all flow into the system above 25 psig to exhaust. In initial setup, flow of each gas into the system is adjusted by its cylinder pressure regulator so the flow through its input orifice exceeds (10-20%) flow in the common orifice when its solenoid valve is open. This assures a sufficient bulk flow of each gas toward the reservoir and prevents contamination due to back diffusion of gases at the solenoid valve inputs.

A feature which adds to the accuracy of the method is the removal of flow dependence on outlet pressure. This is accomplished by maintaining choked flow conditions within the common orifice. This flow condition exists when the upstream absolute pressure is at least twice downstream absolute pressure.

The equations used for timing the gas control valves assumes that the ratios of flow through the common orifice for each gas relative to each of the other gases are constant. The accuracy to which the flow ratios are known determines the ultimate accuracy of method. For ideal gases and a mathematically perfect orifice, the flow ratio for gas (i) relative to gas (j) is given by

$$Rij = \frac{MWj}{Mwi}$$

where Rij = Fi/Fj, F is gas flow, and MW is the molecular weight of the gas. This equation also assumes identical input pressure and temperature for each gas at the orifice as well as choked flow conditions.

However, with real gases and physical orifices, the viscosity of each gas also contributes some degree to the orifice resistance. The viscosity component of the total resistance is influenced by the geometry of the orifice. Small geometrical differences from orifice to orifice which occur in their manufacture produce a difference in the relative amount of the viscosity vs. density resistance components of the common orifice. Therefore, to achieve the maximum gas mixing accuracy by the method, an independent calibration must be made to determine the flow ratios (Rs) of the common orifice. Once a calibration is made, recalibration should be unnecessary because the common orifice geometry is fixed.

The gas fraction of any one gas (Xj) in a mixture of n gases is the volume of the gas (Vj) divided by the total volume of gases in the composition $\Sigma i=1^{n}Vi$. This volume of gas can be expressed as the flow of that gas (Fj) multiplied by its time of flow (Tj).

$$Xj = \frac{Vj}{\sum_{i=1}^{n} Vi} = \frac{FjTj}{\sum_{i=1}^{n} FiTi} \qquad (1)$$

We can reference all subsequent gas flows to gas number one and define this ratio as Rj. This makes R=1. In addition, we define the period (P) to be the sum of the time of all gases.

$$Rj = Fj/Fi \qquad (2)$$

$$P = \sum_{i=1}^{n} Ti \qquad (3)$$

We can now substitute expression 2 into 1 and obtain

$$Xj = \frac{RjTj}{\sum_{i=1}^{n} RiTi} \qquad (4)$$

Using expression 4 in expansion form and substituting the expansion form of (3) for the case when j=1 in expression 4, we can write the system of equations shown in Chart I. This linear system of n first-order polynominal equations in n unknowns of T. This system is solved by the Gaussian elimination algorithm microprocessor.

Chart I

$$\begin{array}{llll}
T_1 + T_2 & + T_3 & + \cdots T_n & = P \\
X_2T_1 + R_2(X_2-1)T_2 & + R_2X_2T_3 & + \cdots R_nX_2T_n & = 0 \\
X_3T_1 + R_3X_3T_2 & + R_3(X_3-1)T_3 & + \cdots R_nX_3T_n & = 0 \\
\vdots \quad \vdots & \vdots & \vdots & \vdots \\
X_nT_1 + R_2X_nT_2 & + R_3X_nT_3 & + \cdots R_n(X_n-1)T_n & = 0
\end{array}$$

Accuracy Evaluation

Gas mixer accuracy was checked using three gas component mixers produces for use as calibrators for blood gas analyzers (1). The gas mixer output was checked by balancing against six primary standard mixtures of O_2 and CO_2, using a gas chromatograph (HP5880A) as the gas sensor. The results are given in Table 1. The gas mixer GC comparisons are seen to be within ±0.05% absolute over the total range as indicated for each gas.

Table I. CO_2 and O_2 Gas Mixer Accuracy Comparison by Gas Chromatography [a]

CO_2			O_2		
thumb-wheel %	gas chromatograph results		thumb-wheel %	gas chromatograph results	
	mean	std dev		mean	std dev
2.00	1.94	0 027	4.00	4 05	0.036
3.00	2.96	0.027	7 00	7 06	0.045
5.00	4.97	0.027	12.00	12.03	0.033
7.00	6.98	0.031	20.00	20.02	0.036
10.00	9.98	0.037	50.00	50.04	0.045
20.00	20 05	0 056			

[a] Number of data points were 42 for each gas percentage

REFERENCES

(1) Wallace, W.D., Clark, J.S., and Cutler, C.A. "Common Orifice Flow for Precision Gas Mixing". Analytical Chemistry (53):2313-2318 (1981)

INITIAL SPATIAL DISTRIBUTION OF REACTANT IONS IN CHEMICAL IONIZATION AND Ni-63 API SOURCES.

Toshihiro Fujii*, Wendy Hopson and G.G. Meisels, Dept. of Chemistry, University of Nebraska, Lincoln, Nebraska 68588-0304.

Electrons of energies ranging from 100 to 500 eV are widely used for the production of reactant ions in chemical ionization (CI) sources. However, the spatial distribution of these ions and the incident electron's penetration into the CI source are virtually unknown, although this information is important to the design of CI sources, to the optimization of their performance and to a better understanding of their characteristics. Recently Meisels et al. reported a method (1) for investigating the spatial ionizing and energy-loss properties of electrons in the 100 to 1000 eV energy range. It is based upon the drift properties of ions under specific conditions which allow correlation of the time required for an ion to drift out of the source with its point of formation by the electron beam.

We report here an application of this method to electron penetration measurements in CH_4 and i-C_4H_{10} in order to determine the spatial distributions of reactant ions produced by 100 to 600 eV electrons under typical CI conditions. Measurements for N_2 were made to allow an estimation of the range of ^{63}Ni beta rays in atmospheric pressure ionization (API) sources.

Experimental. The specially designed ion source has been described previously (2). It features the placement of the electron entrance aperture coaxial with the ion exit slit, the use of two drift guard rings to establish a uniform electric field within the source whose drift region is 2.29 cm and a pulsed electron gun.

Spatial Distribution of Reactant Ion Formation. When the electron entrance aperture is coaxial with the ion exit slit, the residence time distribution (RTD) depends on the distance which the ionizing electrons travel into the source. Figure 1 (points) shows the experimental RTD's of CH_5^+ in 0.5 Torr CH_4 at electron energies of 20 eV and 320 eV, demonstrating the dependence on energy. [5] The solid curve through the narrow distribution in Fig. 1 was drawn using the diffusion coefficient as the only adustable parameter to the theoretical expression for the RTD of the ions originating from a point source.

When the drift properties of the ion are known, residence times may be related to the point of ion formation or distance from the electron gun. Assumed initial ion density distributions are convoluted with RTD's calculated for onset of points of origin, until a best fit, represented by the curve for the distribution at 320 eV is obtained (Fig. 1). This yields n(z), the spatial distributions of CH_5^+ formation. Figure 2 presents n(z), normalized at the origin, for 120 and 320 eV electrons in 0.5 Torr methane.

Electron Range vs Electron Energy. The formation of primary positive ions occurs within less than 10^{-7} sec of the electron pulse. At sufficiently high source pressures, such as those under which CI sources operates, the reaction time to form reactant ion is on the order of 2×10^{-7} sec. Therefore, n(x) is proportionate to di/dx, the linear ionization rate (the number of ion pairs, di, formed per unit pathlength, dx), where x is the distance of penetration into the source. Integration of the linear ionization rate to a specified upper limit, such as 97%, of the total ionization gives R_{97}^I, the range within which 97% of the ionization occurs. This ionization range differs somewhat from the normal definition of range as the distance to which 97% of the electrons penetrate. Figure 3 shows R_{97}^I in $\mu g/cm^2$ for CH_4 as a function of electron energy. As expected, the range is independent of pressure and temperature when expressed in these units. Figure 3 also shows that the ionization range is almost linear with electron energy between 100 and 600 eV.

Chemical Ionization Sensitivity. Figure 4 shows the product of the pressure and the ionization range as a function of electron energy for CH_4 and i-C_4H_{10}, two reagent gases often used in CI sources. In CH_4, electron energies of at least 500 eV are required to cause reactant ion formation 1 cm from the electron entrance aperture when the CI source is operated at 1 Torr. The electron energy must be about three times higher in i-C_4H_{10} than in other gases to achieve the same electron penetration; presumably this is one requirement of equivalent sensitivity. If source performance has been optimized for methane, Figure 4 permits the selection of electron energy for isobutane at which the initial spatial distribution of reactant ions is approximately the same.

^{63}Ni-beta Range in API Sources. The beta emitter, ^{63}Ni, is now widely used as an ionizer for several sensitive analytical instruments such as the ECD in gas chromatography and API mass spectrometry. Although the energy distribution of ^{63}Ni betas has been measured accurately, the range characteristics of electrons in N_2 at atmospheric pressure, valuable in the design of sources for APIMS or ECDGC, are not known well.

We have extrapolated the electron ionization range up to the maximum energy of ^{63}Ni beta ray in nitrogen by using the generally accepted range-energy relationship (3) that range increases as the 1.75 power of energy between 500 to 5000 eV and as E^2 at higher energies. Thus the range for 67 KeV electrons, the maximum energy of ^{63}Ni beta rays, was calculated to be 10.5 cm in 1 atm nitrogen. This may be compared with the value of 7.9 cm estimated by Ayala et al. (4). They used an empirical range-energy relationship (5) which assumes that the product of density and range is constant regardless of the substance.

The resulting range curve is folded into the energy distribution of beta rays from ^{63}Ni obtained for carrier-free ^{63}Ni deposited on a saturation thickness of platinum foil (6). Figure 5 is the result of that convolution process; the dashed line in that figure is based on the estimates of Ayala et al. The

agreement between our estimates and those of Ayala et al. is very good, particularly considering the uncertainties involved.

Acknowledgments: We thank the Department of Energy for support under contract number AT(11-1)-2567.

References: *National Institute for Environmental Studies, P.O. Yatabe, Tsukbaraki, Ibaraki 300-21 Japan. (1) G.G. Meisels and A.J. Illies, Anal. Chem., **53**, 2162 (1981). (2) A.J. Illies and G.G. Meisels, Anal. Chem., **52**, 326 (1980). (3) M. Burton and J.L. Magee, "Advances in Radiation Chemistry"; Wiley-Interscience; New York (1969). (4) J.A. Ayala and W.E. Wentworth, J. Chromtogr., **1**, 195 (1980). (5) L. Katz and A.S. Penfold, Rev. Mod. Phys., **28**, 28 (1952). (6) J.L. Preiss, R.W. Fink and B.L. Robinson, J. Inorg. Mol. Chem., **4**, 233 (1957).

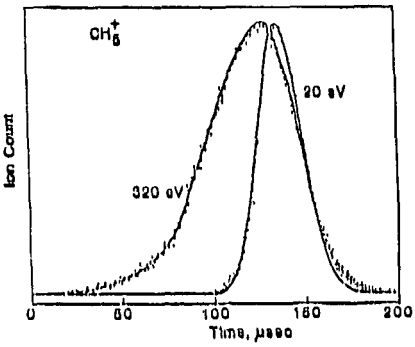


Fig. 1: Experimental residence time distribution for CH_5^+ in CH_4

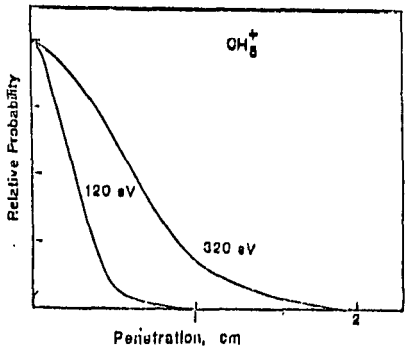


Fig. 2: The spatial ionization distribution to show the point of reactant ion formation along the electron beam.

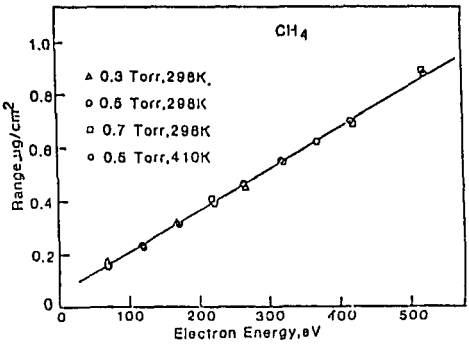


Fig. 3: Electron ranges in CH_4 at three different pressures and two different temperatures.

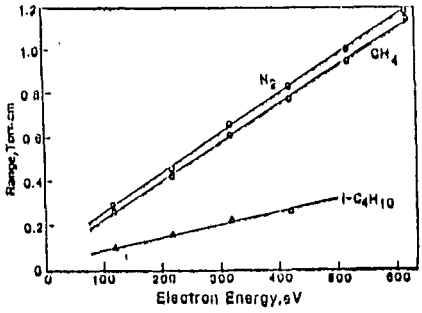


Fig. 4: Electron range for CH_4, $i\text{-}C_4H_{10}$ and N_2 as a function of electron energy.

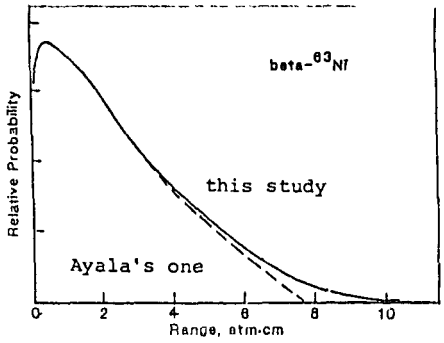


Fig. 5: Calculated range distribution of Ni-63 betas in N_2.

BENZENE PYROLYSIS AND SOOT FORMATION AT HIGH TEMPERATURES[a]

Smith, R. D., Johnson, A. L., and Udseth, H.

Physical Sciences Department, Pacific Northwest Laboratory[b]
Richland, Washington 99352, USA

The chemistry of aromatic hydrocarbon compounds at high temperatures is of continuing interest due to its role in the production of synthetic fuels, in various liquefaction and pyrolysis processes, and in the formation of polycyclic aromatic pollutants and soot in these and in ultimate usage (i.e., combustion). We have studied the high temperature pyrolysis of benzene by monitoring the gas phase species flowing from a Knudsen reaction cell using modulated molecular beam mass spectrometry and constructed a "wall-less" reactor to clarify the role played by heterogeneous effects. The pyrolysis in a tungsten Knudsen cell was studied at temperatures up to 1900°C and pressures to 5 torr. At low pressures, hydrogen and carbonaceous deposits (soot) on the reaction cell wall were the dominant products. Carbon deposition is most efficient at low pressures; carbon deposition increases with pressure, but the percent of total carbon deposited decreases as gas phase reactions become important. Figure 1 shows the carbon distribution between soot, benzene and other gas phase products. In (a) we have results characteristic of the higher pressures used where gas phase products are seen early at less than 800°C and significant soot formation does not occur until 1200°C. From there on, soot formation is rapid and by 1600°C it accounts for 80% of the carbon, and benzene has been completely pyrolized. Figures (b) and (c) show results typical of the low pressure experiments. Gas phase products are not produced until 1200°C where soot formation has begun. Soot formation is then rapid and continues out to 1600°C. At the lowest pressures used (10^{-3} torr) no gas phase carbon products were detected. The disappearance of benzene at the low pressure limit was found to have an apparent activation energy of 82 ± 5 kcal/mole; the measured activation energy is too low for H atom loss from benzene which may dominate under homogeneous pyrolysis conditions. The rate of carbon formation was determined indirectly from the difference between carbon flow into the reactor and products leaving the reactor, and good agreement was noted for carbon recovered from the reactor for extended experiments at 1600°C. At higher pressures, where gas phase reactions dominate, C_2H_2, C_4H_2, $C_{12}H_{10}$, $C_{12}H_8$, H_2 and carbon were the major products. Figure 2 shows the major gas phase products as a mole percent of the total gas phase carbon for an experiment carried out at a pressure of 1 torr in a reaction cell with a 0.4 mm diameter orifice. Benzene, C_2H_2 and C_4H_2 were the major products at all temperatures, accounting for over 90% of the gas phase carbon, with C_2H_2 going to 75% of the gas phase carbon at 1600°C. The results suggest that carbon formation occurs through a C_6H_x (x = 4, 5 or 6) intermediate species (which is not phenyl radical or benzyne) and which is efficiently removed by surface collisions and, hence, cannot be detected in Knudsen reactors. On the basis of these results, and examination of the gas phase products, it is suggested that a C_6H_6 excited species (possibly the first triplet state) is an intermediate to both soot formation and gas phase products under conditions allowing many wall collisions. Thus, it appears that the mechanisms of benzene pyrolysis may be strongly dependent upon the presence of surfaces. In order to establish the reaction mechanism under homogeneous conditions, a fast flow reactor was interfaced to the modulated molecular beam mass spectrometer and species injected into the high temperature flow in such a manner as to approximate a "wall-less" reactor. Figure 3 shows a schematic of this apparatus. This apparatus allows the observation of decomposition products of benzene molecules injected into a hot (up to 1900°C) inert gas stream. These experiments will be described and the mechanism for benzene pyrolysis will be presented.

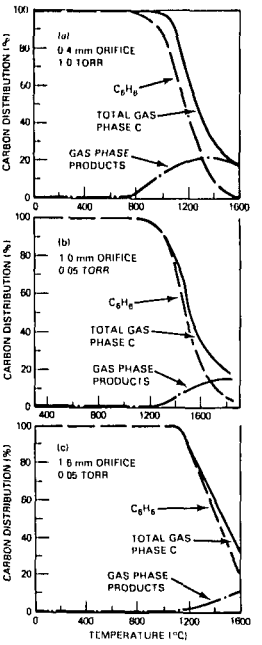


FIGURE 1

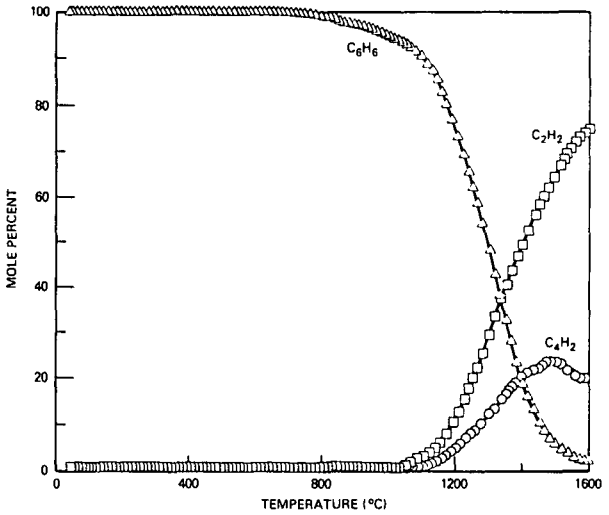


FIGURE 2

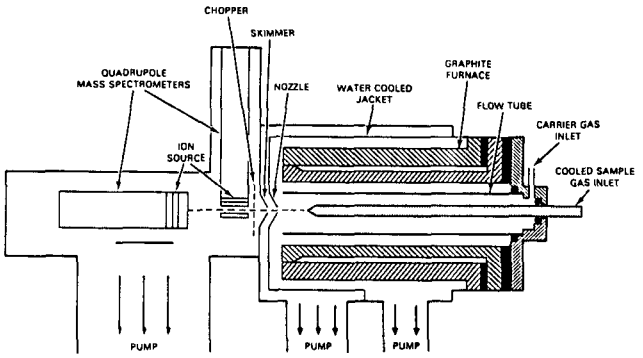


FIGURE 3

a) Prepared for the U.S. Department of Energy under Contract DE-AC06-76RLO 1830.
b) Operated by Battelle Memorial Institute.

ISOTOPIC EFFECTS IN FRAGMENTATION

Peter J. Derrick

School of Chemistry, The University of New South Wales
P.O. Box 1 Kensington, NSW 2033
Australia

Isotopic effects in unimolecular fragmentation of ions (i.e. isotopic effects upon ion abundances) stem from kinetic isotope effects (i.e. effects of isotopic substitution on rate constants for fragmentation) and from effects of isotopic substitution on ionization probabilities and hence internal energy contents. These two factors are difficult to separate in the case of intermolecular isotope effects upon ion abundances. Intramolecular isotope effects upon ion abundances reflect kinetic isotope effects.

Intramolecular kinetic isotope effects are closely constrained by the Teller-Redlich product rule and by the zero point energy rule. They provide information on the detailed properties of transition states.

The full text of this presentation will appear in a forthcoming issue of Mass Spectrometry Reviews.

PHOTODISSOCIATION OF IONS IN DOUBLE-FOCUSING MASS SPECTROMETERS.

F.M.Harris and J.H.Beynon.

Royal Society Research Unit, University College of Swansea, Singleton Park, Swansea SA2 8PP, U.K.

Several experimental techniques are in use at Swansea to study the dissociation of ions. With metastable ions, various ionic lifetimes corresponding to times between entering and leaving the field-free regions of double-focusing mass spectrometers are sampled with the result that the ranges of internal energies of the fragmenting ions are relatively small. Stable ions i.e. those having insufficient internal energies to dissociate between source and detector can be excited in the field-free regions. A technique which has been extensively used at Swansea and elsewhere is that of collisional excitation in which the internal energy of the ions is raised at the expense of their translational energy. The ions gain, however, a range of energies extending from virtually zero to several tens of electron volts. Collisional excitation gives rise, for example, to quite high energy processes such as charge stripping which may require energies of the order of 20 eV. Evidence exists, however, that the average deposition of energy is much lower than this, for example 1-2 eV for 8 keV ions.

The fact that collisions give ions a range of energies which is not known precisely and which can only be coarsely controlled led to the development at Swansea of methods in which excitation of ions is induced with photons of known energy. The radiation is provided by an argon-ion laser which is capable of emitting light of eleven individual wavelengths. Photoexcitation can thus be changed in a controlled fashion with the photoexcitation at each step being known accurately.

Prior to the work reported here, studies of the photodissociation of organic ions had been carried out using conventional as well as laser-light sources coupled to ICR spectrometers (for a review, see reference [1]). In our work double-focusing mass spectrometers are used these being modified so that laser radiation can be introduced into suitable field-free regions. The ions, of course, pass only once through the interaction region ensuring that photoexcited ions undergo no ion-molecule reactions at the low pressures of the systems. Ion densities too are sufficiently low to ensure negligible ion-ion interactions. Thus in these experiments, dissociation of photoexcited ions takes place in a collision-free environment.

One considerable advantage of working with ions having high translational energies such as those usually used in double-focusing mass spectrometers is that amplification of the translational energy released in a dissociation reaction takes place in the laboratory frame of reference [2]. Thus experiments in such spectrometers makes it possible to measure this important quantity with high accuracy and, as will be seen later, to see how it depends on the photoexcitation energy.

Two double-focusing mass spectrometers have been modified [3,4] at Swansea for studies of photodissociation of ions. The first, referred to as the Varian spectrometer because its major components were supplied by Varian MAT, is of conventional geometry, i.e. the electric sector precedes the magnetic sector. It has been modified to allow radiation from the argon-ion laser to pass into the source housing via a quartz window, through a hole in the repeller plate, through the source and into the first field-free region. Ions which are photoexcited and dissociate in this region give photofragment ions which are

transmitted through the electric sector by scanning the voltages applied to its plates. The other spectrometer which has been modified is the ZAB-2F having reversed geometry. Mass-selected ions are irradiated in the second field-free region by radiation which enters the spectrometer via a modified magnet flight tube to which is attached a quartz window. Photofragment ions are transmitted to the detector by scanning the voltages applied to the electric sector plates. In both systems two mirrors are used to steer the laser beam and two lenses to focus it. Both spectrometers have the same photofragment-ion detection system; the laser beam is mechanically chopped at 2.4 kHz and the pulsed ion currents arriving in phase with the chopping frequency are detected and measured using a lock-in amplifier. This system has the useful feature that it measures only the fragment-ion currents which result from dissociation of photoexcited ions. The fragment ions from dissociation of metastable ions are not recorded by it.

The Varian spectrometer was used initially to explore how readily a wide variety of ions absorb radiation in the wavelength range of light from the argon-ion laser (514.5 - 357 nm). It was also used to establish the various investigative techniques which can be performed with the photoexcitation facility. However, most of the detailed work has been done on the ZAB-2F since it has the capability of introducing ions of one pre-selected species into the interaction region which simplifies the fragment-ion spectra obtained.

A main line of study has been that of the dependence of the relative rates of competing photodissociation reactions on photoexcitation energy. For some ions, e.g. those of the nitrosubstituted aromatics, the main metastable reaction is a low-energy process involving the loss of $NO^{\cdot}$. However, when the ions are photoexcited by photons having energies in the range 2.41 - 3.47 eV the dominant photodissociation reaction is one involving the loss of $NO_2^{\cdot}$. A more interesting ion is that of n-butylbenzene which when photoexcited by 2.41 eV photons gives fragment ions 91^+ and 92^+ in approximately equal abundances. As the photoexcitation energy is increased the reaction giving 91^+ becomes increasingly dominant over that giving 92^+ until at 3.47 eV photoexcitation energy the 91^+ ions are 6.9 times more abundant than the 92^+ ions. These results are a consequence of the changes in the relative values of the rate coefficients for each dissociation reaction as the total internal energy of the photoexcited parent ions increases. Since changes in photoexcitation energy are accurately known in this type of experiment it was thought worthwhile to analyse the data mathematically in an attempt to derive the equations for the rates of the reactions as a function of the internal energy of the ions.

The analytical procedure can be illustrated by considering the case of an ion M^+ which can dissociate via two competing reactions to give fragment ions A^+ and B^+. If the reactions have critical energies E_A and E_B it can be shown that the number of M^+ ions arriving at any point in the field-free region, t seconds after the ions' formation, is dN(E)K where

$$K = \exp\left\{-\left[k_A(E-E_A) + k_B(E-E_B)\right]t\right\} \qquad (1)$$

The terms $k_A(E-E_A)$ and $k_B(E-E_B)$ are the rate constants respectively for the reactions giving A^+ and B^+, and dN(E) is the number of parent ions created at t=o having internal energies between E and E+dE.

If photon absorption occurs for a fraction f(E) of the ions passing this point, it can be shown that the number of ions that will fragment to form A^+ in the second field-free region as the result of photodissociation is

$$\int_0^{E_{max}} \frac{dN(E)\ f(E)\ k_A\ (\varepsilon+E-E_A)}{k_A(\varepsilon+E-E_A) + k_B(\varepsilon+E-E_B)}\ K(1-M) \qquad (2)$$

where

$$M = \exp\left\{-[k_A\ (\epsilon+E-E_A) + k_B\ (\epsilon+E-E_B)]\ [t_2-t_1]\right\},$$

ϵ = photon energy

and t_2 = time at which the ions leave the field-free region.

The total number of ions available for the 'normal' metastable ion dissociation in the field-free region is reduced, however, when the laser light is on, due to the effective removal of a fraction f(E) of these ions from the beam. The reduction is

$$\int_{E_A}^{E_{max}} \frac{dN(E)\ f(E)\ k_A(E-E_A)}{k_A(E-E_A) + k_B(E-E_B)} \quad [K - L] \qquad (3)$$

where

$$L = \exp\left\{-[k_A(E-E_A) + k_B(E-E_B)]\ t_2\right\}$$

The total effect of the laser light on the A^+ fragment-ion current can then be obtained by subtracting expression (3) from (2). A similar procedure is followed to calculate the B^+ fragment-ion yield.

One of the main problems in the analysis is that the initial energy distribution dN(E) is unknown. A reasonable estimate of its approximate form can be made from the photoelectron spectrum of n-butylbenzene. The uncertainty may, however, not be quite as critical as would appear at first sight. The distribution changes markedly during the lifetime of the ions and at the second field-free region of the ZAB it has changed so much that the initial form chosen does not appear to be too critical. Another problem is whether or not f(E) should be treated as a constant. Again the photoelectron spectrum helps. It exhibits a wide peak of overlapping bands extending from ~1.7 eV to 8.3 eV above the ionization energy which means that ions reaching the second field-free region all have a good if not exactly equal chance of absorbing radiation in the energy range of 2.41 - 3.47 eV used in the present work.

In the analysis, the well-known rate equation $k(E) = \nu[(E-E_c)/E]^{s-1}$ derived from simple QET was used. In it, ν is a frequency factor, E_c the critical energy for the reaction being considered and s the effective number of oscillators. The results of the analysis show that the rate equations for the formation of 91^+ and 92^+ are respectively

$$k(E) = 3\times10^{13}\left(\frac{E-2.6}{E}\right)^{17}$$

and

$$k(E) = 6\times10^{9}\left(\frac{E-1.4}{E}\right)^{17}$$

This procedure can be applied to two or more competing reactions which show measurable relative rate changes with photoexcitation in the output range of the argon-ion laser.

Another major study carried out using the laser and the ZAB spectrometer has been of the dependence on the photoexcitation energy of the average translational energy released, $\overline{T}$, when an ion dissociates. As mentioned earlier, $\overline{T}$ can be measured with high accuracy on the ZAB spectrometer. The molecular ions of ten species of alkylbenzenes were studied [5] and found to give a linear dependence of $\overline{T}$ on ϵ, the photon energy. Further, differing dissociation reactions from the same ionic species show differing gradients in the $\overline{T}$ versus ϵ graphs. Various statistical theories have been examined and used to calculate $\overline{T}$ as a

function of ϵ. On comparison with experimental data it is found that each theory predicts lower values of $\overline{T}$ at given values of ϵ and that the gradients of the calculated $\overline{T}$ versus ϵ graphs are smaller than those obtained from the experimental data.

Previous work done with ICR spectrometers have made use of photoabsorption studies to distinguish isomeric ions. In the work at Swansea we have made use of measurements of $\overline{T}$ to distinguish the isomeric ions of the Xylenes. These have been difficult if not impossible to distinguish by other techniques in mass spectrometry. The results showed that the dependence of $\overline{T}$ on ϵ was distinctly dependent on the isomeric ion under investigation.[6].

The results from the investigations into competitive reactions and the release of translational energy have in many cases been found to be sensitively dependent on the photoexcitation energy. Even for changes in ϵ as low as 0.1 eV the changes in the measured data have been significant. With these in mind, recent work has been concerned with detecting changes in the internal energy of ions before they enter the interaction region. In these experiments the photoexcitation energy was kept constant and the total internal energy of the photoexcited ions changed by changing the internal energy distribution of the ions with which the photons interact. In the experiments so far, this has been done by changing the temperature of the source. The results obtained for a variety of ions indicate that a change in source temperature of 100°C changes the average internal energy of the ions which reach the second field-free region of the ZAB by between 0.2 and 0.3 eV. A detailed account of this work is given in another paper at the Conference.

In other recent work, the laser has been recoupled to the Varian spectrometer and photodissociation of ions within the ion chamber studied. The ions, after being generated by electron ionization, move slowly to the exit aperture of the chamber prior to being accelerated through the full potential applied to the source. The number density of ions in the chamber is high and the interaction rate is at least an order of magnitude higher than that in the field-free region where the ions have several kiloelectron volts of translational energy. A further advantage is that photofragment ions generated in the chamber are, when they leave the chamber, accelerated through the full potential of the source and can be recorded by scanning the magnetic field as is done to obtain a normal mass spectrum. Because of the fact that the laser beam is chopped and the photofragment ions are detected using a phase-sensitive detector, only the spectrum of the photofragment ions is recorded. Photofragment-ion peaks are thus well separated because the full resolution of the double-focusing mass spectrometer is operative when photodissociation is done this way. Large negative signals were recorded by the lock-in amplifier at the molecular-ion mass positions of several of the samples studied. These represent the depletion of the molecular ions due to photodissociation and are thus a measure of the photoabsorption cross sections of the ions provided the assumption is made that all the photoexcited ions dissociate. Because of the high photon-ion interaction rate obtained using this technique, measurements of relative photoabsorption cross sections and their dependence on laser-light wavelength are readily made with high accuracy.

References

1. R.C.Dunbar, Gas Phase Ion Chemistry, 2, 181 (1979).
2. R.G.Cooks, J.H.Beynon, R.M.Caprioli and G.R.Lester, Metastable Ions, Elsevier, Amsterdam (1973).
3. F.M.Harris, E.S.Mukhtar, I.W.Griffiths and J.H.Beynon, Proc.Roy.Soc. A.374, 461 (1981).
4. E.S.Mukhtar, I.W.Griffiths, F.M.Harris and J.H.Beynon, Int.J.Mass Spectrom. and Ion Phys. 37, 159 (1981).
5. E.S.Mukhtar, I.W.Griffiths, R.E.March, F.M.Harris and J.H.Beynon, Int.J.Mass Spectrom. and Ion Phys. 41, 61 (1981).
6. E.S.Mukhtar, I.W.Griffiths, F.M.Harris and J.H.Beynon, Org.Mass Spectrom. 16, 51 (1981).

STATE SELECTED ION - MOLECULE REACTIONS BY A TESICO TECHNIQUE

Kenichiro Tanaka, Tatsuhisa Kato, and Inosuke Koyano

Institute for Molecular Science
Myodaiji, Okazaki, 444 Japan

INTRODUCTION

A number of investigations of ion-molecule reactions have been carried out with ions produced by photoionization. Some of these utilized the strong advantage of photoionization in the ability to prepare the reactant ions with known distribution of internal states, in an attempt to investigate the roles of internal energy of the reactant ions. Although these studies yielded a considerable amount of information on this interesting subject, the techniques employed in these experiments remained indirect and thus the information obtained is either qualitative or quantitative only with considerable uncertainties. Since the cross sections for individual internal states are at best deduced from the observation of overall reactions of reactants in more than one internal states, sizable errors are introduced into the quantitative results obtained, owing to the uncertainties in the knowledge of relative population in these states.

In order to overcome these drawbacks and obtain state selected reaction cross sections amenable to theoretical examination, we have developed a technique which utilizes threshold electron - secondary ion coincidence (TESICO).[1] The coincidence technique was first successfully applied to bimolecular processes by Baer and co-workers[2] in the studies of collision induced dissociation of molecular ions and charge-transfer reactions. The TESICO technique extends this to bimolecular chemical (rearrangement) reactions. The present paper reports a brief description of the technique and its recent application to the reaction of $O_2^+(X^2\Pi_g,v\,;\,a^4\Pi_u,v)$ with H_2.

EXPERIMENTAL

The TESICO technique and the apparatus have been described in detail elsewhere[1] and are given here only briefly. The technique as applied to the present system is illustrated schematically in Fig. 1. The reactant O_2^+ ions and the corresponding photoelectrons are produced in the ionization chamber by photoionization of O_2 at the threshold wavelength for each internal state of interest. Reactions take place in the reaction chamber which contains H_2 as a target molecule. The mass analyzed product O_2H^+ and H_2^+ ions, as well as unreacted O_2^+ ions, are counted in coincidence with the threshold (zero kinetic energy) electrons using a time-to-amplitude converter (TAC) and a multichannel analyzer (MCA). The basic data obtained are thus coincidence time-of-flight spectra of particular ions. When the wavelength of the

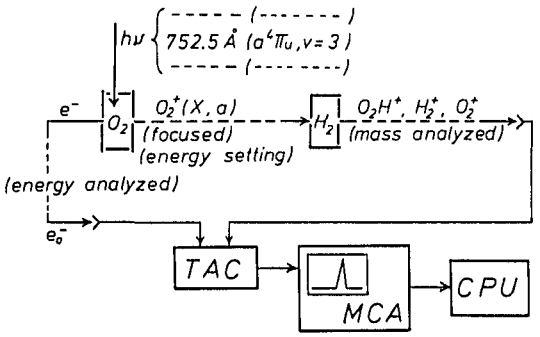


Fig. 1. Schematic drawing for the TESICO technique.

incident radiation corresponds to the threshold energy of the i-th internal state of O_2^+, the ions produced are $O_2^+(i)$, $O_2^+(i-1)$, $\cdots$, $O_2^+(0)$, among which only $O_2^+(i)$ gives threshold electrons. Thus, although all of the above ions may react with H_2 to produce O_2H^+ and H_2^+, we can observe the reaction of $O_2^+(i)$ selectively by measuring O_2^+, O_2H^+, and H_2^+ in coincidence with threshold electrons. The state selected cross sections $\sigma(i)$ are determined directly from the coincidence intensity ratios of the reactant and product ions $[O_2H^+(i) / O_2^+(i)$ and $H_2^+(i) / O_2^+(i)]$.

STATE SELECTED REACTIONS OF O_2^+ WITH H_2

The wide applicability of the TESICO technique in studying state selected ion-molecule reactions has been demonstrated in the vibrational state selection in the $H_2^+ + H_2$[1], $H_2^+ + Ar$[3], and $N_2^+ + Ar$[4] reactions, and in the spin-orbit state selection in the $Ar^+ + H_2$[5] and $Ar^+ + N_2 / CO$[6] reactions. In the present work we have applied this technique to the vibronic state selection of O_2^+ ions in the reactions

$$O_2^+ + H_2 \rightarrow O_2H^+ + H, \quad \Delta H = +41 \text{ kcal·mol}^{-1} \qquad (1)$$

$$\rightarrow H_2^+ + O_2, \quad \Delta H = +78 \text{ kcal·mol}^{-1}. \qquad (2)$$

Reaction (1) has previously been studied by Ajello et al.[7] with respect to the internal states of the reactant ions, while there seem to be no previous studies on Reaction (2). Ajello et al. confirmed, in a photoionization efficiency study of a mixture of hydrogen and oxygen, the formation of O_2H^+ from the $O_2^+(a^4\Pi_u) + H_2$ reaction, while failing to recognize the same product from the reaction of $O_2^+(X^2\Pi_g)$. In the present study, we have selected the higher vibrational states ($v = 19$ and 20) of $O_2^+(X^2\Pi_g)$ and the vibrational states $v = 0 - 8$ of $O_2^+(a^4\Pi_u)$, and determined the individual cross sections for all these states, both for Reactions (1) and (2).

Experimental results obtained at the collision energy of 0.25 eV are summarized in Fig. 2. Figure 2 reveals, for the first time and in a clear form,

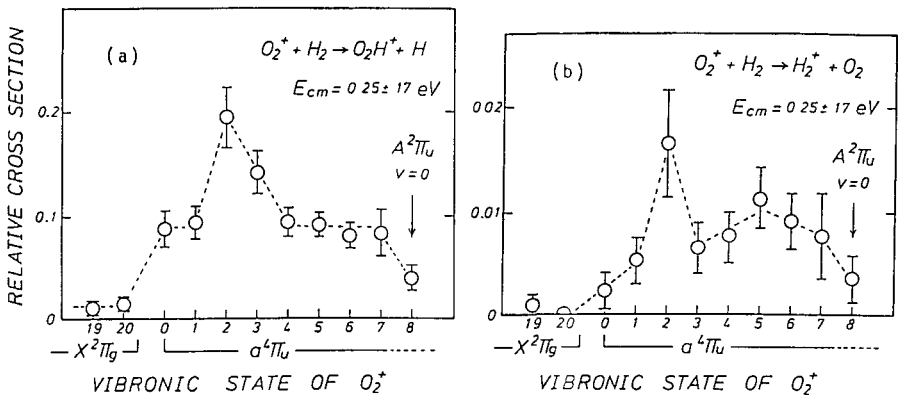


Fig. 2. State selected reaction cross sections for 11 vibrational states of $O_2^+(X^2\Pi_g)$ and $O_2^+(a^4\Pi_u)$. (a) Reaction (1), (b) Reaction (2)

that the cross sections of Reactions (1) and (2) exhibit marvelous quantum number dependence in the regions studied. The important features found are as follows :

i) The v = 19 and 20 states of $X^2\Pi_g$ have a small but significant cross section for Reaction (1).

ii) An order of magnitude increase in the cross section of Reaction (1) is observed in going from v = 20 of $X^2\Pi_g$ to v = 0 of $a^4\Pi_u$ state.

iii) The cross sections for the $a^4\Pi_u$ state, for both Reactions (1) and (2), show interesting v - dependence, having a peak at v = 2.

iv) The cross sections for Reaction (2) show almost the same v - dependence as that for Reaction (1), but the values of the cross sections are roughly an order of magnitude smaller than those for Reaction (1)

Both Reactions (1) and (2) are endoergic for the ground state O_2^+ ions, and are exoergic for vibrationally excited [$v \geq 9$ for Reaction (1), $v \geq 17$ for Reaction (2)] or electronically excited $a^4\Pi_u$ states. Since the collision energy used is much lower than the reaction endoergicity, the features i) and ii) show that Reaction (1) indeed proceeds in the $X^2\Pi_g$ state at collision energy below the translational threshold, provided sufficient vibrational energy is supplied. Furthermore, these features show that a form of electronic energy is required to enhance this reaction considerably.

From previous experiments, it is known that Reaction (1) with $O_2^+(X^2\Pi_g)$ proceeds via a long lived complex at low collision energies ($\leq$ 5 eV),[8,9] whereas with $O_2^+(a^4\Pi_u)$ via a direct (stripping) mechanism even at low collision energies.[9] The considerably larger cross sections for $O_2^+(a^4\Pi_u)$ than those for $O_2^+(X^2\Pi_g)$ observed in the present study may indirectly support these mechanisms. We have also performed two kinds of experiment on the isotope effect

in the reaction $O_2^+ + HD \rightarrow O_2H^+ / O_2D^+ + D / H$. One is a measurement of the intensity ratio O_2D^+ / O_2H^+ at two wavelengths, 956.1 and 584.2 Å, without state selection. At 956.1 Å, O_2^+ are produced only in the $X^2\Pi_g$ ($v \leq 4$) states, while at 584.2 Å a mixture of the $X^2\Pi_g$ and $a^4\Pi_u$ states is produced. The results obtained at the collision energy of 2.5 eV show that the ratios O_2D^+ / O_2H^+ are much larger than unity (~ 7) for 956.1 Å but smaller than unity (~ 0.7) for 584.2 Å, indicating different mechanisms operating in the reactions with the $X^2\Pi_g$ and $a^4\Pi_u$ states. The other experiment is a measurement of the state selected cross sections for the production of O_2D^+ (σ_D) and O_2H^+ (σ_H). For the $v = 0 - 4$ of $O_2^+(a^4\Pi_u)$, σ_D and σ_H show exactly the same variation with vibrational quantum number. The ratio of the cross sections σ_D / σ_H is almost constant throughout $v = 0 - 4$, and its values are slightly smaller than unity. These are consistent with the expectation from a direct reaction mechanism.

The cross section ratios σ_D / σ_H for the $v = 19$ and 20 states of $O_2^+(X^2\Pi_g)$, on the other hand, appear to be smaller than unity. This result is of particular interest because the complex mechanism predicts the ratio to be considerably larger than unity. Thus, the result obtained may indicate that the mechanism of the $X^2\Pi_g$ reaction changes from complex to direct ones when a sufficient energy is supplied in the form of reactant vibration, just as it does when a sufficient translational energy (≥ 5 eV, cm) is supplied.[8]

As to the most interesting feature iii) mentioned above, we do not have any definitive explanation at present. The similarity in the v - dependence of the cross sections between Reactions (1) and (2) certainly indicates that these two (reaction) channels are intimately related to each other in the dynamical behavior. However, the interpretation of the enhanced cross sections at $v = 2$ of $a^4\Pi_u$ simply in terms of energy defects and the Franck - Condon factors is found to fail in the present reaction system. The whole interpretation of the present experimental results awaits future development in the studies of the potential energy surfaces and reaction dynamics.

REFERENCES

[1] K. Tanaka and I. Koyano, J. Chem. Phys. 69, 3422 (1978); I. Koyano and K. Tanaka, ibid. 72, 4858 (1980).
[2] T. Baer, L. Squires and A. S. Werner, Chem. Phys. 6, 325 (1974); L. Squires and T. Baer, J. Chem. Phys. 65, 4001 (1976); ibid. 68, 4901 (1978).
[3] K. Tanaka, T. Kato and I. Koyano, J. Chem. Phys. 75, 4941 (1981).
[4] T. Kato, K. Tanaka and I. Koyano, J. Chem. Phys. 77, No.2 (1982) in press.
[5] K. Tanaka, J. Durup, T. Kato and I. Koyano, J. Chem. Phys. 74, 5561 (1981).
[6] T. Kato, K. Tanaka and I. Koyano, J. Chem. Phys. 77, No.1 (1982) in press.
[7] J. M. Ajello, W. T. Huntress, A. L. Lane, P. R. LeBreton and A. D. Williamson, J. Chem. Phys. 60, 1211 (1974).
[8] M. H. Chiang, E. A. Gislason, B. H. Mahan, C. W. Tsao and A. S. Werner, J. Phys. Chem. 75, 1426 (1971).
[9] G. Bosse, A. Ding and A. Henglein, Ber. Bunsenges. Phys. Chem. 75, 413 (1971).

VIBRATIONAL STATE DYNAMICS OF GAS PHASE ION-MOLECULE REACTIONS BY INFRARED CHEMILUMINESCENCE AND LASER INDUCED FLUORESCENCE

Veronica M. Bierbaum
Department of Chemistry, University of Colorado, and
Joint Institute for Laboratory Astrophysics, Boulder, Colorado 80309

Infrared chemiluminescence and laser induced fluorescence are powerful and complementary techniques for the study of the dynamics of ion-molecule reactions. We have coupled these techniques with a flowing afterglow apparatus to probe the vibrational product state distribution of ion-molecule reactions and to examine collisional excitation and relaxation processes for diatomic ions. Nascent vibrational state distributions are obtained for the HF product of the proton transfer reactions,

$$F^- + HX \rightarrow HF(v) + X^-, \; X = Cl, Br \text{ and } I. \quad (1)$$

The product states are measured by low resolution infrared chemiluminescence spectra obtained with a Ge:Cu infrared detector and circular variable filters. The ion-molecule processes channel a substantial fraction of their exothermicity into product vibration. In spite of the deep attractive wells of the F^- + HX potential energy surface, the extent of vibrational excitation in these reactions is very similar to, although slightly smaller than that of the corresponding neutral reactions. This suggests that the kinematic effect of the mass combination (transfer of a light particle between two heavy particles) dominates over the influence of the shape of the potential energy surface in determining the vibrational state distribution of the products.

The reaction of N^+ with O_2 is known to generate both NO^+ and O_2^+ but the disposition of the reaction exothermicity is not fully characterized:

$$N^+ + O_2 \rightarrow NO^+ + O(^3P) \quad (2)$$
$$\rightarrow NO^+ + O(^1D) \quad (3)$$
$$\rightarrow NO^+ + O(^1S) \quad (4)$$
$$\rightarrow O_2^+ + N(^4S) \quad (5)$$
$$\rightarrow O_2^+ + N(^2D) \quad (6)$$

We have observed infrared chemiluminescence both from $NO^+(v)$ formed in the reaction of N^+ with O_2 as well as from NO(v) generated in a secondary reaction

$$N(^2D) + O_2 \rightarrow NO + O \quad (7)$$

Our preliminary results indicate that reactions (4) and (6) are the dominant channels.

There is currently little information on vibrational and rotational excitation and relaxation of ions by collisions. Laser induced fluorescence allows direct monitoring of individual vibrational and rotational states and their dependence on added

collision gases. Using a flow-drift apparatus coupled with laser induced fluorescence we have studied N_2^+ in helium at fields between 0 and 22 Td. We find that the rotational excitation is described by a single temperature that is in agreement with theory (L. A. Viehland, S. L. Lin and E. A. Mason, Chem. Phys. 54, 341 (1981)). The rotational excitation and relaxation processes appear to be very rapid.

ACKNOWLEDGMENT

The author gratefully acknowledges the support of the Air Force Office of Scientific Research and the collaboration of her colleagues, S. R. Leone, G. B. Ellison, T. S. Zwier, J. C. Weisshaar, M. A. Smith, C. E. Hamilton and M. A. Duncan.

MOB 4 A PHOTODISSOCIATION STUDY OF THE HALOGEN IONS Cl_2^+, Br_2^+ AND I_2^+ AT 3 cm^{-1} RESOLUTION. D.L. Smith, R.G. McLoughlin and J.D. Morrison. Department of Physical Chemistry, La Trobe University, Bundoora, Victoria 3083, Australia.

The diatomic halogen ions are observed to undergo both predissociation and direct dissociation. The predissociation is attributed to interaction of the $\tilde{B}^2\Sigma g^+$ state with a higher energy state of the same symmetry. Predissociating levels of the $\tilde{B}^2\Sigma g^+$ state are populated as a result of photoinduced transitions from the metastable $\tilde{A}^2\pi u$ state. The lifetime of the $\tilde{A}^2\pi u$ state is unusually long considering that this state can relax via an optically allowed transition to the $\tilde{X}^2\pi g$ ground state, a transition which has been observed in the fluorescence spectrum of Cl_2^+[1] and Br_2^+[2].

1. F.P. Huberman, J. Molec. Spectrosc., 20 (1966) 29.

2. P.R.V. Haranath and P.T. Rao, Indian J. Phys., 29 (1955) 205.

RESONANCE, AUTOIONIZATION AND KINETIC EFFECTS IN PHOTOIONIZATION

Albert C. Parr and Henry M. Rosenstock
Center for Radiation Research
National Bureau of Standards
Washington, DC 20234

Resonance phenomena in molecular photoionization have recently received considerable attention. A number of studies of the effects of shape resonances and autoionization on vibrationally resolved asymmetry parameters and vibrational transition probabilities have been carried out.[1] The measurement of vibrationally resolved photoelectron spectra with polarized light, as a function of wavelength and angle has produced a wealth of new information on the effects of autoionization and shape resonance on photoionization. As an example, CO_2 was studied in detail in the wavelength region around 750Å.[2] This region of the spectrum has a large resonance in the photoionization cross section.[3] The results of this study show that autoionization produces vibrational transitions which are Franck-Condon forbidden, including excitation of bending modes in the linear CO_2^+ ground state. The non-Franck-Condon transitions can amount to as much as 40% of the total vibrational intensity.

Another example is the shape resonance in N_2.[4] This shape resonance arises from the centrifugal barrier encountered by the outgoing photoelectron. It is particularly important for the higher angular momentum components of the outgoing electron wavefunction. The effect of the resonance is to produce strong electron-nuclear interaction which leads to a breakdown of Born-Oppenheimer approximation and, consequently, the Franck-Condon principle. The result is that the vibrational transition probabilities and asymmetry parameter can become perturbed over several eV. Figure 1 shows the vibrationally resolved branching ratios for N_2 in the 20 to 40 eV region. The dots are our data and the solid line is a calculated curve by Dehmer and Dill.[5]

The use of variable delay time threshold photoelectron photoion coincidence experiments will be discussed using iodobenzene as an example.[6] Autoionization is shown to play an important part in the formation of excited ionic states, particularly in the Franck-Condon gap regions not accessible by direct ionization. By using several different coincidence systems, ion source residence times can be varied from about one to 57 microseconds, and breakdown curves determined (see Fig. 2). As a result, the fragmentation rate energy dependence can be determined over a range

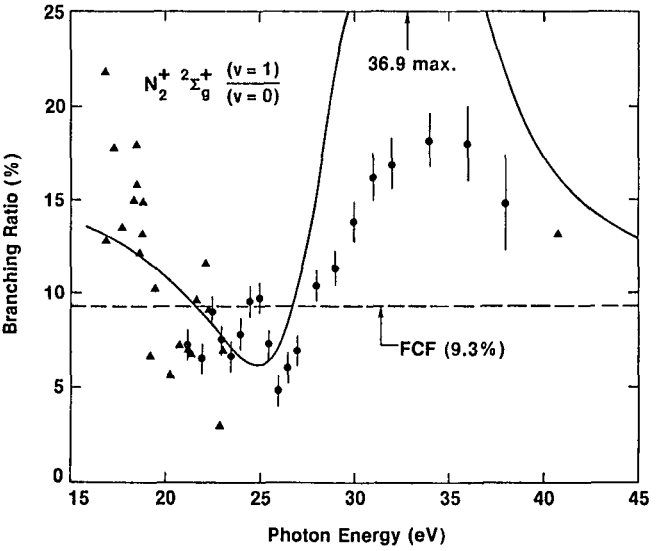


Figure 1 Branching ratios as a function of photon energy for production of ν=0, 1 levels of $N_2^+ X\ ^2\Sigma_g^+$ by photoionization of N_2. ● results of triply differential photoelectron spectroscopy, ref. 4. ▲ Data from Gardner and Samson. (J. Electron Spectros. 13, 7 (1978) Theory of Dill, Dehmer and Wallace (Ref. 5). The Franck-Condon factor is 9.3% as calculated by D.C. Albritton, 1979 (private communication).

of more than three orders of magnitude. Individual breakdown curves can each be analyzed statistically to give sections of this rate energy dependence. These lead to a consistent set of accurate kinetic parameters for the fragmentation process. The threshold energy for the process,

$$C_6H_5I + h\nu \rightarrow C_6H_5^+ + I$$

is 11.010 $\pm$ .01 eV. This gives a derived heat of formation for the $C_6H_5^+$ ion of 1133 $\pm$5 Kj/mol, in excellent agreement with earlier studies on C_6H_5Cl and C_6H_5Br.[7]

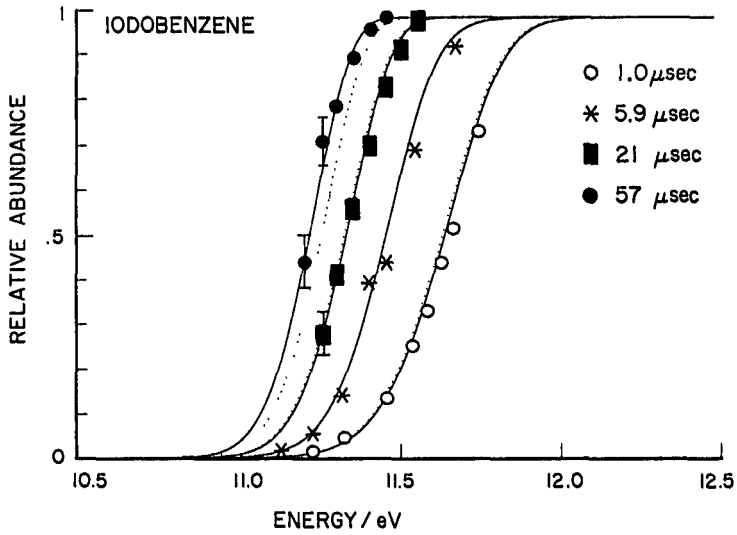


Figure 2 Iodobenzene breakdown curve (only fragment ions shown) at four different ion source residence times. The long time curves, at 21 and 57 μs, were determined at the University of Basel using fixed wavelength (58.4 nm) variable electron energy coincidence analysis. The short time curves 1 and 5.9 μs were determined at NBS using threshold photoelectron photonion coincidence techniques (————) individual best statistical fits, (· · · · ·) global fit to the entire data set.

Acknowledgements: This work has been supported in part by the Office of Naval Research and the Department of Energy.

References

1. R.P. Madden and A.C. Parr, Appl. Optics 21, 179 (1982). (see references therein).

2. A.C. Parr, D.L. Ederer, J.L. Dehmer and D.M.P. Holland, J. Chem. Phys. to be published.

3. K.E. McCulloh. J. Chem. Phys. 59, 4250 (1973).

4. J.B. West, A.C. Parr, B.E. Cole, D.L. Ederer, R. Stockbauer and J.L. Dehmer, J. Phys. B: Atom. Molec. Phys. 13, L105 (1980).

5. D. Dill, J.L. Dehmer, S. Wallace, Phys. Rev. Letts. 43, 1005 (1979).

6. J. Dannacher, H.M. Rosenstock, R. Buff, A.C. Parr, R.L. Stockbauer, R. Bombach, and J.P. Stadelmann. Submitted to Chemical Physics.

7. H.M. Rosenstock, R.L. Stockbauer and A.C. Parr, J. Chem. Phys. 73, 773 (1980).

MEASUREMENT OF Δ^9-TETRAHYDROCANNABINOL IN BODY FLUIDS AND TISSUES USING METASTABLE ION MONITORING: PHARMACOKINETICS IN RABBITS AND MICE

D.J. HARVEY, J.T.A. LEUSCHNER, W.D.M. PATON

University Department of Pharmacology,
South Parks Road,
Oxford, OX1 3QT, U.K.

Δ^9-Tetrahydrocannabinol (Δ^9-THC), the major psychoactive principle of marihuana is difficult to measure in body fluids and plasma because of the low levels normally found during intoxication. This is the result both of the drug's high activity and lipid solubility, the latter property causing a rapid drop in peak plasma levels as the result of uptake of the drug by tissues. Most available methods for quantitation, principally radioimmunoassay, GC/MS, and electron capture GLC[1,2] only allow quantitation to the 0.1-1.0 ng/ml range in plasma and to the low ng range in tissues. This is the consequence, in the case of GLC and GC/MS methods, of the presence of co-extracted biological material, mainly lipids. Extensive clean-up stages are thus a feature of most existing assays but even with these methods it is difficult to detect the drug for more than a few hours after administration.

We have recently developed a GC/MS method for the quantitation of Δ^9-THC in plasma in which metastable ion monitoring was used to filter out much of the "biological noise".[3,4] [1",1",2",2"-$^2H_4$]-cannabinol ([1",1",2",2"-$^2H_4$]CBN) was used as the internal standard; this and Δ^9-THC were extracted from plasma with hexane, methylated with diazomethane to remove fatty acids from the metastable ion chromatogram, and converted into trimethylsilyl (TMS) derivatives by reaction with N,O-bis(trimethylsilyl)trifluoroacetamide. Measurements were conducted with a V.G. Micromass 70/70F double-focussing mass spectrometer interfaced via a glass jet separator to a Varian 2440 gas chromatograph containing a 2 m x 2 mm (ID) glass column packed with 3% SE-30 on 100-120 mesh Gas Chrom Q. The spectrometer was tuned to the $[M\text{-}CH_3]^+$ fragment ion at m/z 371 and the accelerating voltage was raised from 4.0 kV to 4.16 kV in order to focus the metastable ion arising from the M^+ (m/z 386) to $[M\text{-}CH_3]^+$ (m/z 371) transition. Other operating conditions were: GLC column oven, 220°; injector, separator and ion source temperatures, 300, 300 and 260° respectively; electron energy, 70 eV; trap current, 1 mA. The sensitivity of the assay was such that Δ^9-THC could be measured to the 5 pg/ml level with an analysis time of 1 hour.

The method has now been used to investigate the pharmacokinetics of the drug in both rabbits and mice and to study the accumulation of the drug in tissues. Female New Zealand white rabbits (2.5-3 kg) were treated intravenously (marginal ear vein) with a solution of Δ^9-THC in Tween-80 and isotonic saline at doses of 1.0 and 0.1 mg/kg. Blood samples were collected from the other marginal ear vein at intervals until the drug could no longer be detected in plasma. Four weeks after this point the animals were again injected with the same dose of the drug daily for either 8 or 22 days and samples were collected as above starting immediately after the last dose. For tissue analysis, 4 animals were treated with a single dose of Δ^9-THC (1.0 mg/kg) and 4 with 8 doses as above and individual animals were killed at various times after administration. Tissues were removed for THC analysis. Male Charles River CD-1 mice (23-25 g) were treated with Δ^9-THC in Tween-80 and isotonic saline at 10 mg/kg via the tail vein and groups of 4 mice were killed at various times after drug administration for measurement of plasma and tissue levels of the drug.

THC could be measured for 8 days after the 1 mg/kg dose in rabbits and for 26 days after the 22 day treatment (Fig. 1). Plasma kinetics were examined by least squares non-linear regression analysis by computer (NONLIN). The plasma curve in rabbits could be described by up to 5 exponentials depending on the rabbit and quality of data at the early time points. The terminal (elimination) phase which appeared after about 2 days ranged from 34.16 to 59.30 hours with a mean of 46.75 hours (n = 5) after a single dose and from 77.94 to 120.02 hours with a mean of 94.63 hours (n = 5) after the 8-day treatment.

Brain levels were also measured using this technique and found to be 10-50 times the plasma levels, expressed as weight of THC, per wet weight of tissue. The levels declined in parallel with the plasma concentration. For other tissues, the method had to be modified to remove large amounts of lipid that were co-extracted with hexane. This was done by chromatographing the hexane extract on a 5 g column of Sephadex LH-20 in chloroform

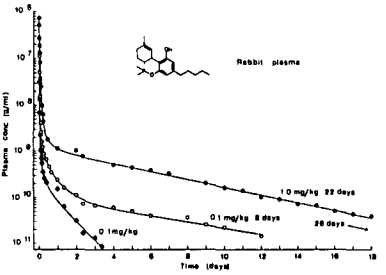


Figure 1. Plasma concentrations of Δ^9-THC in rabbit plasma after three different doses.

and collecting the 18-30 ml fraction. This was then derivatized as above. Fat samples had to be chromatographed twice on the Sephadex column to reduce the lipid levels sufficiently. Measurements of Δ^9-THC were made in lung, spleen, heart, peritoneal fat and renal fat with similar results to those obtained from brain being obtained for lung and spleen. Drug concentrations in heart were somewhat higher at about 100 fold the plasma level, but the main concentration was found in fat where the levels were 10^3-10^4 times those found in plasma. Calculations of clearance values and studies on the metabolism of Δ^9-THC show that even though metabolism is extensive the major factor governing elimination of the drug from the body is slow release from the tissues. Similar results were obtained from the mice where drug levels in plasma could be monitored for up to 72 hours.

It has been proposed that one of the major sites of action for Δ^9-THC is the cell membrane. Levels of the drug were thus measured in erythrocyte membranes obtained from groups of 4 mice killed at various times after drug administration (10 mg/kg) as described above. Membrane samples weighing only a few mg were isolated by the method of Hanahan and Ekholm[5] (1975) and the Δ^9-THC was measured using the method described above for plasma. THC concentrations again paralleled the plasma levels, falling from 6.06 ng/mg membrane protein at 15 min to 0.29 ng/mg protein at 10 hours. This corresponded to plasma values of 3.17 to 0.061 ng/ml over the same time period.

Finally, the method was used to measure THC concentrations in rabbit ocular fluids in connection with the drug's action on glaucoma and in CSF. Although the drug could only just be detected in the latter fluid, levels in aqueous humor were found to be in the 1-10 ng/ml range in samples collected from 0-3 hours after injection.

Acknowledgements

We thank the Medical Research Council for support under a Programme Research Grant and the Wellcome Trust for additional financial support.

References

1. R.E. Willette (Editor) Cannabinoid Assays in Humans, Res. Monogr. Ser. No. 7, NIDA, Rockville, MD, 1976.

2. J.A. Vinson (Editor) Cannabinoid Assays in Physiological Fluids, ACS Symposium Ser. No. 98, American Chemical Society, New York, 1979.

3. D.J. Harvey, J.T.A. Leuschner and W.D.M. Paton, J. Chromatogr., 202, 83 (1980).

4. D.J. Harvey, J.T.A. Leuschner and W.D.M. Paton, Proc. 29th Annual Conference, American Society for Mass Spec. Allied Topics, Minneapolis, May 24-29, 1981, pp. 535-536.

5. D.J. Hanahan and J.E. Ekholm, Methods in Enzymol., 31, 168 (1974).

SULFUR-CONTAINING METABOLITES OF POLYCHLORINATED BIPHENYLS IN PATIENTS WITH "YUSHO"

Koichi Haraguchi, Hiroaki Kuroki and Yoshito Masuda
Daiichi College of Pharmaceutical Sciences
22-1 Tamagawa-Cho, Minami-Ku, Fukuoka, 815, Japan

Polychlorinated biphenyls (PCBs) are known to be very persistent and accumulative environmental pollutants. A serious outbreak of PCB poisoning called Yusho was experienced in western Japan in 1968. It was caused by the injestion of the rice oil which had been contaminated with Kanechlor 400, a commercial preparation of PCBs in Japan, in its production process. To clarify the metabolic fate of PCBs in the patients with Yusho and to understand how the metabolites affect the etiology of Yusho, the tissues of the patients were analyzed for sulfur-containing metabolites of PCBs.

Fatty materials of the liver, lung and mesentery adipose tissue were saponified with 2 N NaOH-ethanol solution and then extracted with n-hexane after dilution with a double volume of water. The n-hexane extract was concentrated to a small volume and chromatographed on a column of silica gel eluting successively with n-hexane, 10 % diethyl ether in n-hexane, and 50 % diethyl ether in n-hexane. The first eluate was analyzed for PCBs by gas chromatography with electron capture detection (GC-ECD). The second and third eluates were further cleaned up by the partition between n-hexane and conc. sulfuric acid and the high pressure liquid chromatography on a μ-Bondapak C-18 reversed-phase column eluting with 70 % acetonitril in water. The eluates corresponding nearly to the retention times of authentic 4-methylthio-2,5,2',5'-tetra-CB and 4-methylsulfone-2,5,2',5'-tetra-CB were collected separately. Both the eluates were respectively diluted with water and extracted with n-hexane. The n-hexane extract was concentrated to a small volume and subjected to GC-ECD, gas chromatography-mass spectrometry (GC/MS), and mass fragmentography (MF).

Fig. 1 shows GC-ECD of the methylthio-PCB fractions from the liver, lung and adipose tissue of a Yusho patient. One of the GC peaks was identical with that of 4-methylthio-2,5,2',5'-tetra-CB in its retention time. The fractions were also determined by GC/MS (Fig. 2) and MF, indicating the presence of methylthio-PCBs in the tissues.

Fig. 3 shows GC-ECD of the methylsulfone-PCB fractions from the liver, lung and adipose tissue of a Yusho patient. One of the large GC peaks was identical with that of 4-methylsulfone-2,5,2',5'-tetra-CB in its retention time. GC/MS and MF of the fractions (Fig. 2 and 4) confirmed the presence of methylsulfone-PCBs having 3 to 6 chlorine atoms in the tissues.

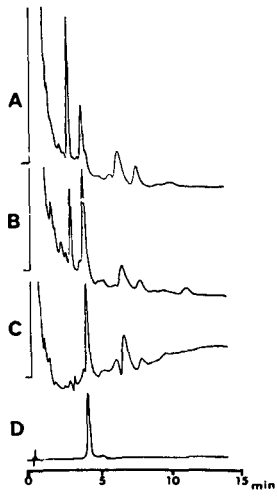


Fig. 1 GC-ECD of methylthio-PCB fractions from the tissues of a Yusho patient
A: Liver, B: Lung, C: Adipose tissue, D: 4-Methylthio-2,5,2',5'-tetra-CB

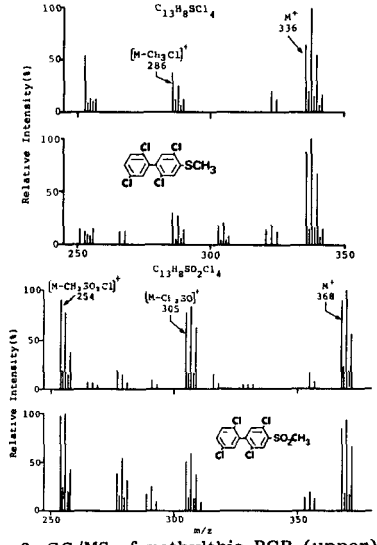


Fig. 2 GC/MS of methylthio-PCB (upper) and methylsulfone-PCB (lower) fractions from Yusho patients and of authentic samples

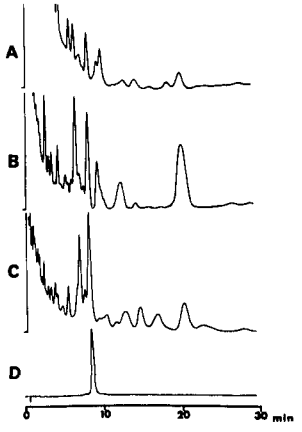


Fig. 3 GC-ECD of methylsulfone-PCB fractions from the tissues of a Yusho patient
A: Adipose tissue, B: Liver, C: Lung,
D: 4-Methylsulfone-2,5,2',5'-tetra-CB

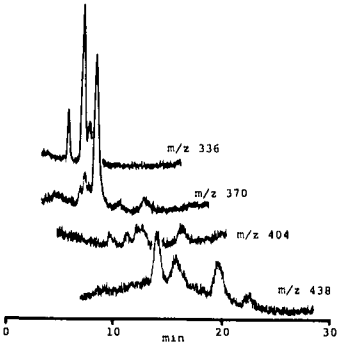


Fig. 4 MF of methylsulfone-PCB fraction from the lung of a Yusho patient

The levels of sulfur-containig metabolites of PCBs in the tissues were quantified by GC-ECD and are listed in Table 1. The concentrations of methylthio-PCBs in the liver, lung and adipose tissue of Yusho patients were 0.1 – 0.5, 0.2 – 1.4 and 0.5 – 1.0 ppb, respectively, and those of methylsulfone-PCBs were 0.3 – 0.7, 1.0 – 2.5 and 0.7 – 1.0 ppb, respectively, whereas the levels of PCBs in these tissues were estimated to be 28 – 100, 18 – 66 and 880 – 2200 ppb, respectively. The ratios of methylthio- and methylsulfone-PCBs to PCBs in Yusho patients were, therefore, 1 – 2 % in the liver, 4 – 8 % in the lung and 0.1 – 0.2 % in the adipose tissue, indicating these sulfur-containing metabolites were relatively accumulative in the lung and liver than in the adipose tissue. The metabolite levels of control patients were approximately 1/10 of those of the Yusho patients.

Table 1 Levels of PCBs and methylthio- and methylsulfone-PCBs in the tissues of Yusho patients

Case		Tissue	Sample weight (g)	Concentration (ppb) of PCBs	MeS-PCBs	$MeSO_2$-PCBs	MeS- + $MeSO_2$-PCBs / PCBs (%)
Yusho patient	1	Liver	33.5	45	0.5	0.4	2.0
		Lung	8.8	66	1.4	1.1	3.8
		Adipose	14.0	880	0.5	0.7	0.1
		Liver	34.0	100	0.5	0.7	1.2
"	2	Lung	32.0	18	0.4	1.0	7.7
		Adipose	12.6	2200	1.0	0.8	0.1
		Liver	57.9	28	0.1	0.3	1.4
"	3	Lung	57.1	56	0.2	2.5	4.8
		Adipose	14.1	970	1.0	1.0	0.2
Control patient	4	Liver	86.5	9	nd	0.05	0.6
		Lung	85.2	7	0.07	0.2	3.9
		Adipose	54.7	160	nd	0.2	0.1
		Liver	74.7	56	nd	0.04	0.07
"	5	Lung	61.6	18	0.05	0.9	5.2
		Adipose	61.7	180	nd	0.05	0.03

nd : Not detected (less than 0.01 ppb)

DETERMINATION OF FORMALDEHYDE IN BIOLOGICAL TISSUES BY GAS CHROMATOGRAPHY MASS SPECTROMETRY

H. d'A. Heck, E. L. White, and M. C. Schmitz

Department of Biochemical Toxicology
Chemical Industry Institute of Toxicology
P. O. Box 12137
Research Triangle Park, NC 27709

Formaldehyde (CH_2O) is a respiratory tract irritant, a mutagen in some prokaryotic and eukaryotic test systems, and a nasal carcinogen in Fischer-344 rats when the animals are exposed to 14.3 ppm of the airborne chemical, 6 h/day, 5 days/week, for as long as two years. CH_2O is also a normal product of metabolism, required for the biosynthesis of purines, thymine, and certain amino acids, and it is released in oxidative N-, O-, and S-demethylations catalyzed by mixed function oxidases. The analytical method described here was developed to meet the need for a sensitive assay for CH_2O in biological tissues that could be used in studies of CH_2O distribution after inhalation exposure.

An outline of the procedure used to analyze CH_2O in tissues is shown in Fig. 1.

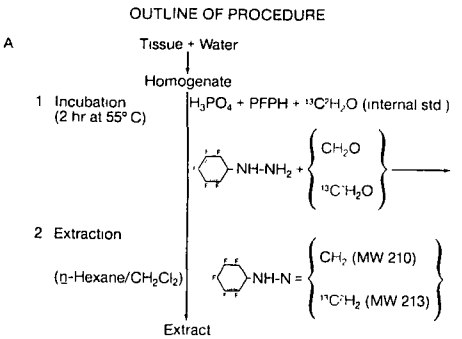


Fig. 1. Analytical method for CH_2O in tissues.

Tissue samples are homogenized in water, mixed with pentafluorophenylhydrazine (PFPH), an internal standard ($^{13}C^2H_2O$), and dilute phosphoric acid to lower the pH to approximately 1.5. The samples are incubated at 55° C for 2 h to form the pentafluorophenylhydrazones of CH_2O (PFPH(CH_2)) and of $^{13}C^2H_2O$ (PFPH($^{13}C^2H_2$)) *in situ*. The derivatives are extracted and analyzed by GCMS using selected ion monitoring at the molecular ions of PFPH(CH_2) (*m/z* 210) and PFPH($^{13}C^2H_2$) (*m/z* 213). Ionization is by electron impact (70 eV) (Fig. 2).

A selected ion recording of an extract from liver of a control (unexposed) rat is shown in Fig. 3. Interferences from impurities in the tissue sample are negligible. A significant amount of endogenous CH_2O was found in liver and in other tissues, including lung, testes, brain, plasma, and nasal mucosa. Concentrations ranged from approximately 0.05 to 0.5 μmole/g wet weight.

Since as much as 99% of the CH_2O in tissues may be bound to nucleophiles,[1] the analytical method was evaluated using solutions that contained high concentrations of glutathione or tetrahydrofolate, both of which bind CH_2O reversibly. Binding of CH_2O to these compounds did not affect the analytical result.[2] Hence, it is concluded that the method measures total CH_2O, both free and reversibly bound.

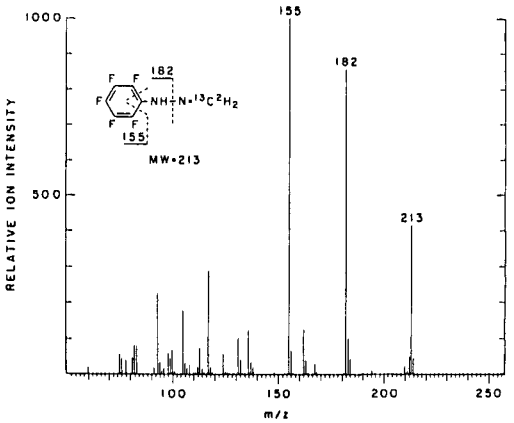


Fig 2 Electron impact mass spectrum of PFPH($^{13}C^{2}H_2$)

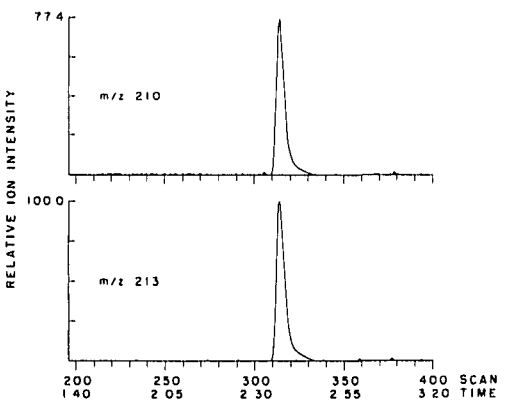


Fig 3. Elution of PFPH(CH_2) and PFPH($^{13}C^{2}H_2$) from an SP-2250 capillary column after extraction from liver

When rats were exposed to 15 ppm of airborne CH_2O for 6 h, no increase in the CH_2O concentration of the nasal mucosa was detected. In contrast, methyl chloride exposure (3000 ppm for 6 h) significantly increased the concentration of CH_2O in liver, testes, and brain.[2] Formaldehyde appears to be a metabolite of CH_3Cl, and moreover, CH_3Cl depletes glutathione.[2] Since the latter is a required cofactor of formaldehyde dehydrogenase, these results suggest that the increased tissue concentrations of CH_2O after CH_3Cl exposure may be due in part to a slower rate of CH_2O oxidation. Formaldehyde exposure does not affect its own metabolism in the nasal mucosa.[1]

1. H. d'A. Heck and M. C. Schmitz, Toxicol. Appl. Pharmacol., submitted.

2. D. E. Dodd, J. S. Bus, and C. S. Barrow, Toxicol. Appl. Pharmacol., 62, 228 (1982).

STUDIES ON DNA BASE ANALYSIS BY GC/MS

P. F. Crain and J. A. McCloskey
Departments of Medicinal Chemistry and Biochemistry
University of Utah
Salt Lake City, Utah 84112

Many DNAs typically contain low levels of the modified base 5-methylcytosine (m^5cyt), ranging from 1-2 in 5386 bases (phage ØX-174) to upwards of 10% in higher plants. In the case of higher organisms, the role of base modification of DNA is largely unknown. Shortcomings of widely-used methods for quantitative analysis of 5-methylcytosine have necessitated the development of more sensitive, specific, and accurate methods for measuring very low levels of m^5cyt in order to probe its biological role. To this end we are developing a stable isotope dilution-based GC/MS assay for 5-methylcytosine in submicrogram amounts of DNA.

5-(Methyl-$\underline{d}_3$)cytosine was selected as an appropriate internal standard/carrier, and its synthesis is outlined in Figure 1[1]. 5-(Methyl-$\underline{d}_3$)uracil

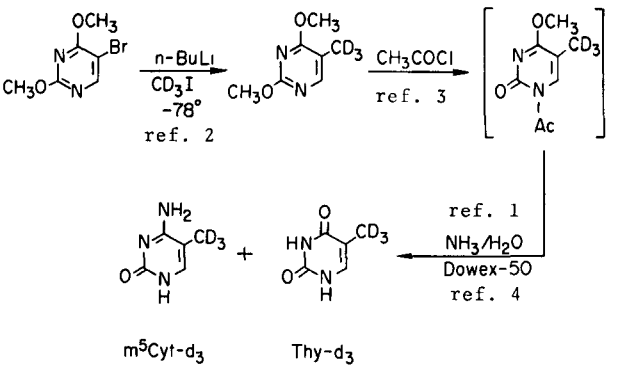


Figure 1. Scheme for synthesis of 5-(methyl-$\underline{d}_3$)cytosine and thymine-$\underline{d}_3$.

(thymine-$\underline{d}_3$) is a by-product of the final reaction step, and this compound can be used to determine the amount of thymine in the DNA. The level of 5-methylcytosine can then be expressed relative to the amount of thymine in the DNA.

Gas chromatography/mass spectrometry of the bases released from DNA by acid hydrolysis is performed using the bis(t-butyldimethylsilyl) derivatives. These derivatives can be formed in good yield by heating the bases for 45 min at 130 deg in a mixture of pyridine/N-methyl-N-t-butyldimethylsilyltrifluoroacetamide (1:1). These derivatives offer an enhancement in sensitivity for selected ion monitoring of about a factor of two, compared with the more widely-used TMS derivatives. Standard curves are constructed in the usual fashion; mixtures of labeled and unlabeled bases are subjected to sham acid digestion before derivatization and analysis. The standard curves exhibit linearity over greater than two orders of magnitude (Figure 2), which is sufficient for analysis because amounts of thymine and 5-methylcytosine expected are usually approximately known prior to analysis.

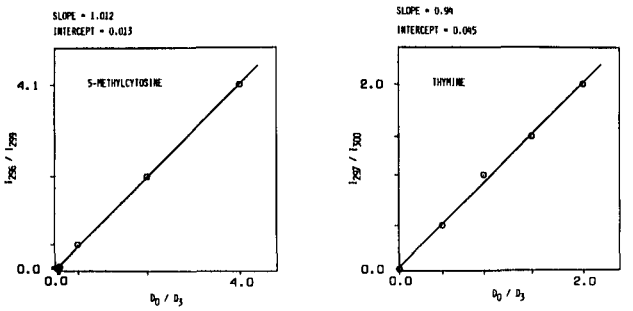


Fig. 2. Standard curves for analysis of 5-methylcytosine and thymine in DNA.

For the analysis of m^5cyt and thy in a DNA sample, 1-2 µg of DNA are dried into a tube made from 4mm i.d. glass tubing. Appropriate amounts of the deuterated internal standards are added and the mixture is dried. Acid digestion is accomplished with trifluoroacetic acid for 1 hr at 180°. After the acid is removed, the digest is derivatized as previously described. GC/MS (LKB 9000S, 6' 4% OV-11) is performed monitoring the M - 57 ion (corresponding to loss of t-butyl radical from M) of m^5cyt (m/z 296) and thy (m/z 297), and their deuterated analogues (m/z 299 and 300, respectively).

DNAs measured for 5-methylcytosine content were from calf thymus (Fig. 3a), for which our determination (1.60 % ± 0.08) is in good agreement with literature values[5]; pBR322 (expected to contain a maximum of 12 m^5cyt residues in 8724 bases[6]), for which we have measured values ranging from 11.1 to 11.4 residues (Fig. 3b); and ØX-174 (1-2 residues in 5386 bases[7]), for which we have obtained values in the range 1.4-1.7 5-methylcytosines per DNA molecule.

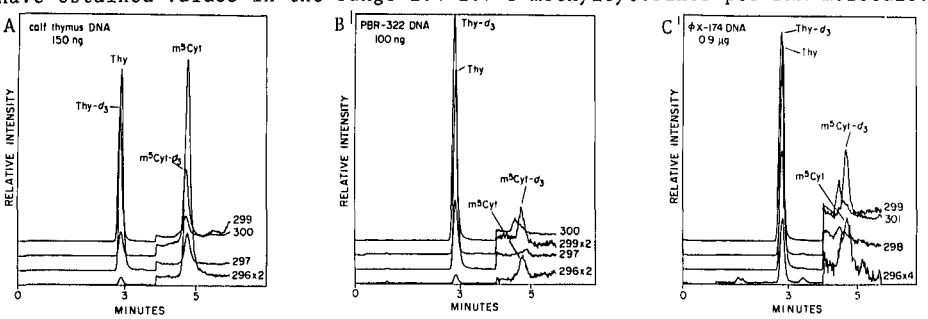


Figure 3. Selected ion recordings of selected DNAs.

Submicrogram amounts of DNA can be analyzed, and the accuracy of measurement is sufficient for biological applications. Substantial enhancement in sensitivity can be obtained with glass capillary GC/MS and this approach is currently under investigation in our laboratory.

References

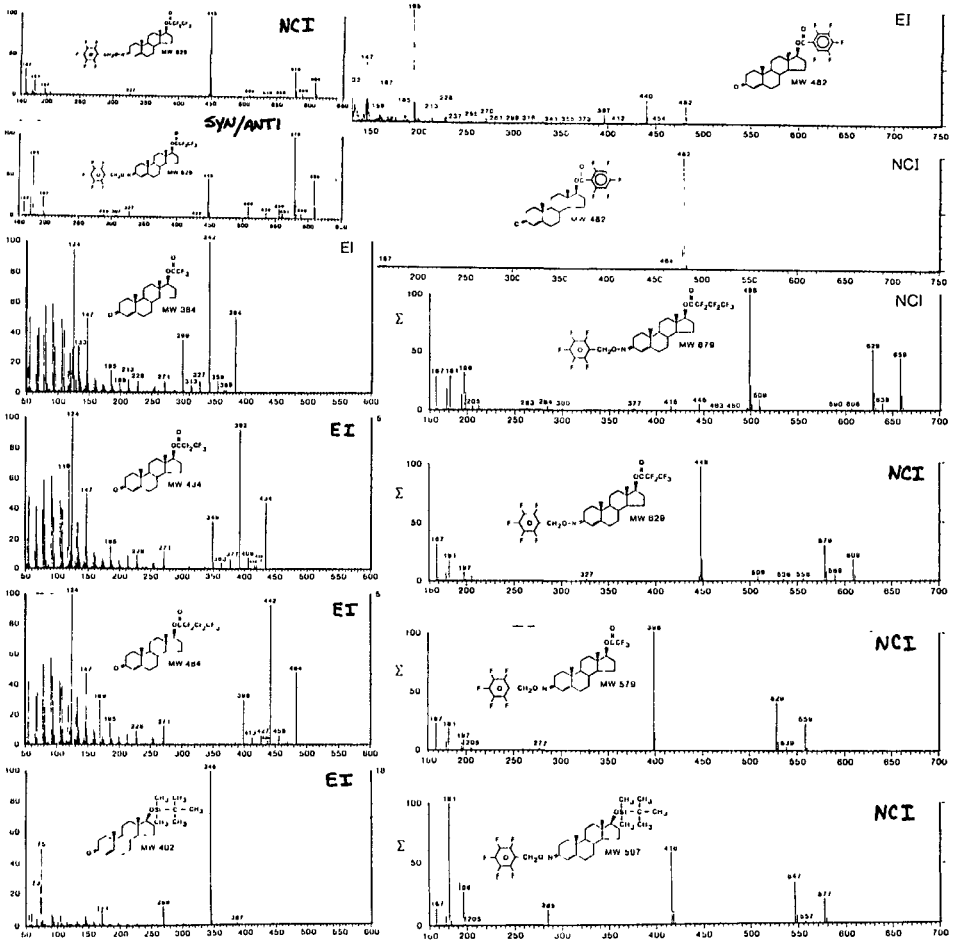
1. Ballweg, H., Tetrahedron Lett., 2171-2173 (1968).
2. Ulbricht, T. L. V., Tetrahedron 6, 225-231 (1959).
3. Prystasz, M., in Nucleic Acid Chemistry. Improved and New Synthetic Procedures and Techniques, L. B. Townsend and R. S. Tipson, eds., Wiley-Interscience, N. Y., 1978, pp 78-79.
4. Singhal, R. P., Arch. Biochem. Biophys. 152, 800-810 (1972).
5. Shapiro, H. S., in Handbook of Biochemistry and Molecular Biology, vol. II, 3rd Ed., G. D. Fasman, ed., CRC Press, Cleveland, 1976, p. 272.
6. Sutcliffe, J. G., Nucleic ACids Res. 5, 2721-2728 (1978).
7. Hattman, S. H., et al, J. Virol. 32, 845-851 (1979).

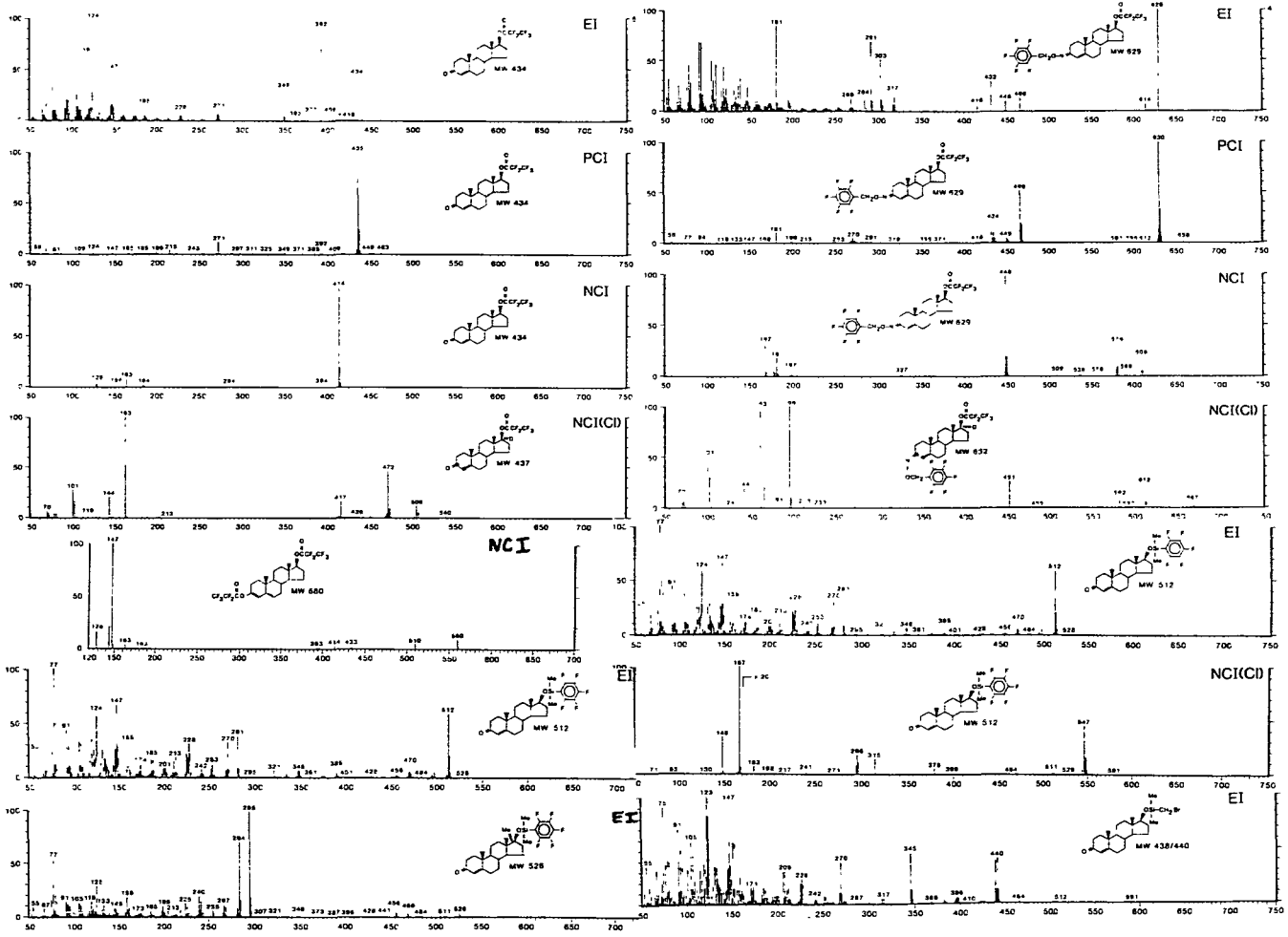
MAXIMIZING PRECISION AND ACCURACY IN QUANTITATION OF SERUM TESTOSTERONE

D.G. Patterson, J.S. Holler, M.A. Baird. Clinical Chemistry Division, Center for Environmental Health, Centers for Disease Control, Public Health Service, U.S. Department of Health and Human Services, Atlanta, Georgia 30333.

The analysis of serum testosterone with the very high precision and accuracy required for a definitive method necessitates the selection of the best derivative for the quantitation. This derivative must provide the ions which maximize sensitivity and, at the same time, preserve the specificity of the analysis. In addition, the isotopically labeled internal standard must be examined to insure the integrity of the isotope, both in the chemical derivatization and in the mass spectral fragmentation process.

A series of 18 different derivatives of testosterone have been examined by electron impact (EI), positive-ion chemical ionization (PCI), and negative-ion chemical ionization (NCI). Derivatives of three different isotopically labeled testosterones have also been examined by EI, NCI, and PCI. The mechanisms for the major fragmentations of the various derivatives under EI, PCI, and NCI conditions have been elucidated. The strategy for choosing the best derivative and determining the appropriate ions for monitoring to maximize precision of the quantitative analysis has been devised.




EI
MW 434
PCI
MW 434
NCI
MW 434
NCI(CI)
MW 437
NCI
MW 680
EI
MW 512
EI
MW 526
EI
MW 629
PCI
MW 629
NCI
MW 629
NCI(CI)
MW 632
EI
MW 512
NCI(CI)
MW 512
EI
MW 438/440

ASSESSMENT OF CORTISOL IN HUMAN SERUM: PROPOSED DEFINITIVE AND REFERENCE METHOD.

J.A. Jonckheere, W.E. Lambert and A.P. De Leenheer
Laboratoria voor Medische Biochemie en voor Klinische Analyse, Rijksuniversiteit Gent, Harelbekestraat 72, B-9000 GENT, BELGIUM

INTRODUCTION

The need for the establishment of definitive and reference methodologies in clinical chemistry is widely recognized. In the field of steroids, isotope dilution mass spectrometry (IDMS) has been put forward on many occasions as technique for reference methodologies. Only the study group at the U.S. National Bureau of Standards (NBS) published a method for total cholesterol of sufficient low imprecision to be regarded as definitive method (1). The present work envisaged the assessment of cortisol in human serum by means of IDMS as candidate definitive method and by HPLC as candidate reference method.

HUMAN SERUM SAMPLES

All samples used in this study were provided by the Community Bureau of Reference (BCR European Community), and were selected randomly from the froozen serum pool. For the IDMS method 1.00 mL samples were weighted and the relative density used for the result expression in weight/volume. The sampling of 200 µL for the HPLC method was done by a conditioned semi-automatic pipette.

CALIBRATION STANDARDS

IDMS: Two stock solutions were prepared by weighing appropriate amounts of NBS Cortisol SRM 921 and ethanol. Calibration standards were prepared from these stock solutions to surround closely the anticipated concentration in the human serum pool.

HPLC: From the stock solutions aliquots were taken, and diluted to contain 42.04, 84.08 and 168.15 ng cortisol/mL, in the solvent used for HPLC.

INTERNAL STANDARD

IDMS: An equal amount of 4-^{14}C labeled cortisol was added by a semi-automatic pipette of 200 µL, to provide a nearly 1:1 ratio in the measurement.

HPLC:To increase the specificity of the internal standardisation, two internal standards were added. The samples were spiked with 40 µL of the HPLC solvent containing 6α-methylprednisolone and 19-nor-testosterone at 1.15 and 1.32 ng/µl, respectively.

EXTRACTION

For both methods, after addition of 0.1 N NaOH, the steroid was extracted with dichloromethane. After a washing with water, the organic layer was taken to dryness under a nitrogen stream. Recovery values yielded 104 ± 3.6% (n = 8). After reconstitution in 100 µL chromatographic eluent, HPLC samples were ready for injection.

PREPARATION FOR GAS CHROMATOGRAPHY

The dry residue is treated with a methoxylamine solution in pyridine for 30 min at 60 °C. After removal of excess reagent trisilylimidazole was added and after heating at 100 °C for 60 min, the di-methoxime-trimethylsilyl-derivative was formed. Subsequent gel chromatography on Lipidex 5000 was used to remove excess silylating agent and further purification of the extract. After reduction to 100 µL, a 1-µL aliquot was injected.

INSTRUMENTATION AND QUANTITATION

IDMS: A HP5992B GC/MS instrument was equipped with a 25 m SE30 fused silica open tubular column (0.32 mm ID) operated isothermally at 280 °C. An all-glass moving needle injection system and a single stage jet separator were used to connect the column. Peak heights of the chromatographic eluent at m/z 605 and 607 were used for the ratio determination.

HPLC:In a HP1081B HPLC instrument a 15 x 0.32 cm ID column, packed with 5 µ RSIL C18 HL, was installed and eluted with a mixture of methanol:water (57.5:42.5, v/v) at 40°C at a flow rate of 0.7 mL/min. The column effluent was monitored at 254 nm. Quantitation was performed by peak height ratio measurement.

MEASUREMENT STAGES

IDMS: The first run consisted of the measurement of 6 bracketing standards and 6 serum samples analysed in duplicate in alternating sequence. On four different occasions 3 bracketing standards and 2 serum samples were analysed in duplicate. Cortisol levels in samples were obtained by linear interpolation on the daily standard curve, constructed by the method of least squares.

HPLC: During the first day, 6 samples and the 3 standards, measured in triplicate were ran. On another occasion the measurement was repeated for 6 other samples and standards. The last run consisted of 4 samples and 3 standards. Cortisol levels in samples were retrieved from a linear standard curve obtained by weighted least squares regression.

RESULTS

An analysis of variance (ANOVA) was carried out to evaluate the consistency of both measurement processes. This ANOVA compares the sum of squares within-run (SS_i) and between-run (SS_e) to decide wether all results are consistent and a grand mean can be calculated. Complete details on both methodologies are submitted for publication (2)(3).

IDMS

RUN NUMBER	MEAN (ng/mL)	SAMPLES	S.D.(ng/mL)
1	90.7675	12	0.13336
2	90.7625	4	0.56234
3	90.5425	4	0.50042
4	90.9825	4	0.23768
5	90.9475	4	0.46850
GRAND MEAN (G.M.) :	90.7911	28	
F-TEST :	$(SS_e/(5-1)) / (SS_i/(28-5))$	= 1.05887	p = 0.60
C.V.% :	$100(SS_e+SS_i)/ (G.M. (n-1))$	= 0.38067	

HPLC

RUN NUMBER	MEAN (ng/mL)	SAMPLES	S.D.(ng/mL)
1	89.75992	6	1.85866
2	89.71272	6	1.30622
3	91.22153	4	0.90141
GRAND MEAN :	90.10762	16	
F-TEST :	1.52461	p=0.75	
C.V.% :	1.69197		

This work was supported through N.F.S.R. bursaries to J.J. and W.L. and F.G.W.O. contract nr. 3.0011.81

(1).A. Cohen, H.S. Hertz, J. Mandel, R.C. Paule, R. Schaffer, L.T. Sniegoski, T. Sun, M.J. Welch and E. White V, Clin. Chem.,26,854 (1980).
(2).J.A.A. Jonckheere and A.P. De Leenheer, submitted for publication in Biomed. Mass Spectrom..
(3).W.E. Lambert, J-P.M. De Slypere, J.A. Jonckheere, A. Vermeulen and A.P. De Leenheer, submitted for publication in Clin. Chem..

Detection and Quantitation of cAMP in Plant Tissues by a Stable Isotope Dilution GC/MS/MID Assay.

L.P. Johnson, J.K. MacLeod, D.S. Letham* and C.W. Parker*

Research Schools of Chemistry and *Biological Sciences,
Australian National University, Canberra, A.C.T., 2600
Australia.

We have designed a stable isotope dilution assay in which picomole quantities of adenosine 3':5'-cyclic monophosphate (cAMP) can be determined with high precision and selectivity by GC/MS/MID.[1] Using synthetic [2,8-$^{2}H_{2}$,6-^{15}N]-cAMP as the internal standard, the $[M-CH_3]^+$ fragment ions of the tri-TMS derivatives of endogenous cAMP (*m/z* 530) and the internal standard (*m/z* 533) were monitored. The sensitivity of the assay as judged from the lower limit of detection of the mass spectrometer was ∿3 pmol. A comparison of cAMP levels in samples of rat liver and human urine determined by the GC/MS/MID assay, protein-binding assay and radioimmunoassay (RIA) showed correlation for the three assay methods to within 10% variation. The intra-assay coefficients of variation of the GC/MS assay for the rat liver and urine samples were 5.3% and 6% respectively.

This method has now been applied to the analysis of plant tissue to determine whether cAMP is present in plants.[2] The biochemical assay procedures developed for the quantitation of cAMP in animal tissues (RIA, protein-binding, etc.) are very unreliable when applied to plant tissue. We have detected the presence and measured the levels of cAMP in sterile tobacco callus tissue cultures, bean seedlings and immature kernels of sweet corn at levels ranging from 70 to 126 pmol/g fresh weight. Within the limits of detection of the method, no cAMP was found in young lemon leaves. A radioimmunoassay for cAMP carried out in parallel with the GC/MS assay gave values which were several times higher than the latter and decreased with increasing purity of the plant extract. Because there were a number of compounds present in column and TLC purified plant extracts which contained ions at the *m/z* values used for monitoring cAMP (but differing in retention times on GC), a HPLC system was devised to remove these. The HPLC system also permitted separation of 3:5-cAMP from any 2:3-cAMP which could also conceivably be present in the plant and which would interfere with the quantitation.

1. L.P. Johnson, J.K. MacLeod, R.E. Summons and N.H. Hunt, Anal. Biochem., 106, 285 (1980)

2. L.P. Johnson, J.K. MacLeod, C.W. Parker, D.S. Letham and N.H. Hunt, Planta, 152, 195 (1981)

METABOLISM OF L-THREO-3,4-DIHYDROXYPHENYLSERINE IN PATIENTS WITH DEGENERATIVE DISEASES OF THE CENTRAL NERVOUS SYSTEM

T. Suzuki, S. Higa, S. Sakoda, A. Hayashi,
S. Kishimoto, T. Kondo°, and H. Narabayashi°
The Third Department of Internal Medicine, Osaka University Hospital, Fukushima-ku, Osaka 553, Japan and °Department of Neurology, Juntendo University Hospital, Bunkyo-ku, Tokyo 113, Japan

To investigate the use of L-threo-3,4-dihydroxyphenylserine(L-threo-DOPS), an immediate precursor amino acid of (-)-norepinephrine(NE), as a therapeutic agent for degenerative diseases of the central nervous system, especially Parkinson's disease, we studied the metabolism of L-threo-DOPS with and without peripheral decarboxylase inhibitors(DCI) such as benserazide and carbidopa, by administering the drug orally to patients with the disorders.

NE in biological fluids was isolated by boric acid gel and assayed by selected ion monitoring(1). L-threo-DOPS and 3,4-dihydroxymandelic acid were eluted from the boric acid gel column with 4 ml of 10 % sorbitol before elution of NE, and were determined by high performance liquid chromatography(2).

As shown in Fig. 1, a single dose of 300 mg of L-threo-DOPS was well absorbed in 18 patients with various degenerative diseases of the central nervous system (8 had Parkinson's disease, 2 had Shy-Drager syndrome, 7 had spinocerebellar degenerations, and 1 had pure akinesia), giving maximum concentrations 3-4 h after dosage. It also induced sustained elevation of plasma NE levels with a peak at 4 h. 20 % of the dose was recovered unchanged in the urine within 12 h. L-threo-DOPS in combination with DCI produced higher plasma concentrations of L-threo-DOPS and suppressed increase in NE concentrations in plasma(Fig.2). Further, measurable amounts of DL-threo-DOPS were detected in cerebrospinal fluid during repeated administration of DL-threo-DOPS with DCI, although changes in NE concentrations were variable.

These findings suggest that L-threo-DOPS with DCI can be applied to the treatment of degenerative diseases of the central nervous system. We have very recently reported that DL-threo-DOPS with DCI alleviated the freezing phenomena in the parkinsonian patients(3).

References

1. Yoshida, J., Yoshino, K., Matsunaga, T., Higa, S., Suzuki, T., Hayashi, A. and Yamamura, Y., Biomed. Mass Spectrom. 7, 396-398 (1980).
2. Suzuki, T., Higa, S., Sakoda, S., Ueji, M., Hayashi, A. and Yamamura, Y., Proc. Jap. Soc. Med. Mass Spectrom. 5, 173-176 (1980).
3. Narabayashi, H., Kondo, T., Hayashi, A., Suzuki, T. and Nagatsu, T., Proc. Japan Acad. 57 (B), 351-354 (1981).

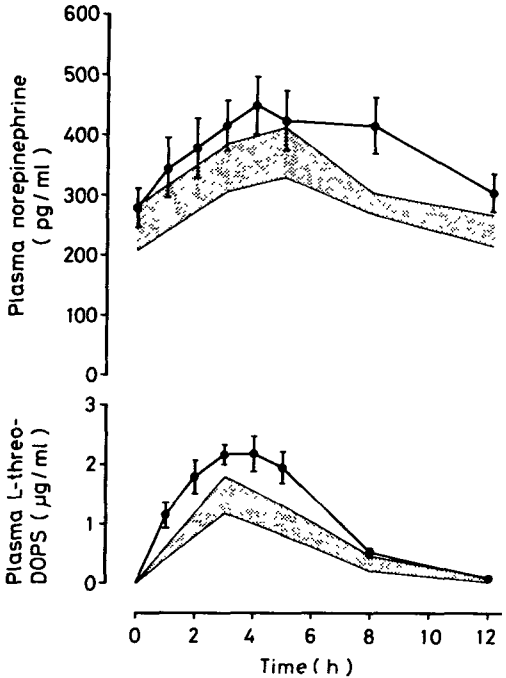


Fig. 1. Time course of plasma L-threo-DOPS and norepinephrine concentrations in 18 patients with degenerative diseases of the central nervous system after a single 300 mg oral dose of L-threo-DOPS. Vertical bars indicate the SEM. The shaded area denotes the range of normal.

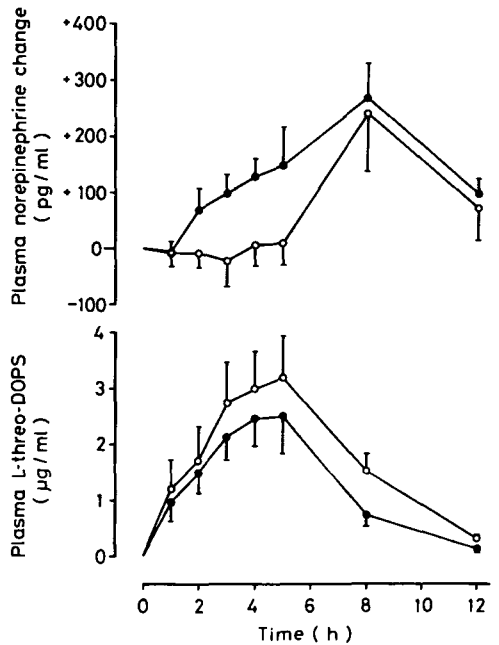


Fig. 2. Time course of plasma L-threo-DOPS concentrations and of change in plasma norepinephrine in 8 patients with Parkinson's disease after a single 300 mg oral dose of L-threo-DOPS alone(dark circles) and combined with 60 mg of carbidopa(open circles).

QUANTITATION OF IMIPRAMINE AND IMIPRAMINE-d4 IN BLOOD PLASMA BY GC/FIMS

by

S. E. Buttrill, Jr. and S. E. Young

SRI International

Menlo Park, CA 94025

and

David Alkalay

Ciba-Geigy

Ardsley, NY 10502

Introduction

This paper describes a method for quantitating simultaneously imipramine (IP) and imipramine labeled with four deteriums (IP-d4) in human blood plasma. The method was developed as part of a comparison of the bioavailabilities of two impramine preparations. In the first of two legs of the bioavailability study, human subjects are given the first dosage form (IP) together with an equal amount of IP-d4 dissolved in water. The ratio of the plasma level of IP to that of IP-d4 is the bioavailability of a dosage form relative to the completely dissolved (optimally bioavailable) IP-d4. During the second leg of the study, the subjects received the second dosage form. By always comparing the bioavailability of the imipramine dosage form to the IP-d4, both the intra and inter-subject variabilities can be eliminated. Using only a few human subjects, the relative bioavailabilities of the two dosage forms can be determined with high precision.

Sample Extractions

Human blood plasma samples (4 ml) were spiked with 50 ng/ml of IP-d8, which was used as the internal standard for the subsoquent GC/FIMS analysis. The plasma was extracted three times with hexane: isoamyl alcohol (95:5, V:V). The combined organic phases were extracted into 0.05 N HCl which was then washed once with hexane. The aqueous phase was made basic with 1.5 ml of 1.5 M sodium carbonate and the imprimines extracted into hexane. The hexane fraction is again extracted into 0.05 N HCl and then back again into hexane. All glassware used was silanized to reduce surface losses.

GC/FIMS Instrumentation

The GC/FIMS instrument used in the study is described in paper FPA 24 of this meeting. A two meter, 3 mm, glass column packed with 3% Dexil-300 was used. The hexane extract was dried under high purity nitrogen and taken up into about 10 microliters of hexane saturated with methanol. About 6-7 microliters was injected onto the column at 220°C isothermal. The molecular ions were monitored at m/z 280, 284, and 288. It was found that the IP-d8 elutes

about 5-6 seconds sooner than the unlabeled IP under these conditions. In order to achieve the desired precision for this study, it was necessary to modify the computer program used to calculate peak areas to take into account the difference in the retention times of the 3 imiprimines.

GC/FIMS Instrument Precision

Standard solutions of the imiprimines in hexane were prepared for use in monitoring the performance of the GC/FIMS instrument during the course of this study. In all cases the concentration of IP-d8 was 50 ng/µl. One solution contained 10 ng/µl of both IP and IP-d4 and a second contained 1.0 ng/µl of IP and IP-d4. One µl injections of these solutions were made repeatedly during the entire course of this study. At the 10 ng level the coefficients of variation for IP and IP-d4 were 3.8% and 4.4% respectively for 32 injections. At the 1.0 ng level, the coefficients of variation were 4.3% and 7.2% respectively. The results for these standard samples show the precision of the GC/FIMS instrument alone independent of any variability introduced from the preparation and extraction of the human blood plasma samples. Factors which affect the instrument precision include the reproducibility of the GC peak shapes, GC column memory, the long term chemical background, and the accuracy of the computer programs used to locate GC peaks, calculate peak areas, and substract background.

Precision of Quantitation From Blood Plasma

During the course of the human subject study, a number of calibration curve samples were prepared and analyzed together with the unknowns. Over a 30 day period, 14 samples were run which contained 1 ng/ml of both IP and IP-d4. The absolute concentrations found were within 5% of the expected values, and the ratio of the IP-d4 to the IP was within 2% of the expected value. The coefficient of variation for the IP measurement was 8.8% and that for IP-d4 was 7.9%. The higher coefficients of variation for the samples measured from blood plasma reflect the additional random errors introduced in the sample preparation and extraction process. These are principally minor errors in volumetric measurements of the plasma and the standard solution of IP-d8 used as the internal standard.

MS/MS IN PHARMACOKINETIC STUDIES

M. SENN and R. ENDELE, CHEM. RES. DIVISION, BOEHRINGER MANNHEIM GMBH,
6800 MANNHEIM, WEST GERMANY

Introduction

The analysis of drugs and metabolites in a biological matrix using Tandem mass spectrometers is a still emerging technique. The determinations are more complex than the well established and accepted GC/MS analysis.

In this paper we present some results of the MS/MS multiple reaction monitoring technique in the determination of drugs and metabolites in serum and urine.

Experimental

The mass spectrometer used was a Finnigan TSQ (Triple Stage Quadrupole) in positive and negative chemical ionization operated in the multiple reaction monitoring mode controlled by an Incos data system. The target gas was nitrogen at a pressure of approx. 4mTorr. The Finnigan standard GC equipped with a wide bore capillary column was used. The Injection mode for compound 1a (Fig. 2) was on-column.

Work up procedures:

The sample preparation and derivatization of Metipranolol with trifluoroacetic anhydride is described elsewhere (1).

Isosorbide-5-nitratoglucuronide:
Urine, diluted with methanol (1:10), is evaporated to dryness after addition of internal standard (p-nitrophenyl glucuronide), esterified (methanol HCl), again evaporated, taken up in methylene chloride and centrifuged. Aliquots are derivatized with HMDS and TMCS in pyridine, evaporated, taken up again in methylene chloride and injected into a wide bore capillary column by an on-column injection technique. This sample preparation and the on-column injection is necessary to suppress thermal and/or catalytic decomposition.

Isosorbide-glucuronide:
Urine is diluted with methanol, evaporated and silylated (with HMDS and TMCS in pyridine). The silylation mixture is directly injected on a fused silica GC-column using standard injection technique at a temperature of 280°C.

Results and Discussion:

The measurement of drugs in the low level concentration range using a Triple Quadrupole mass spectrometer depends among other instrument-parameters mainly on the optimized parent daughter conversion: the decomposition of the primary ion in the collision process is influenced by the collision energy which can be easily varied by changing the Q-1/Q-2 rod offset voltage. The parent daughter conversion in dependance of the collision energy is illustrated in Fig. 1. At the top the formula for deacetylmetipranolol (R = H), and the GC-derivative R = $COCF_3$ is given. The most abundant ion in the CI spectrum is 308 representing the aliphatic portion of the molecule. Mass 308 decomposes in the soft collision experiment to 266 by loss of C_3H_6 and to 152 by double elimination of C_3H_6 and trifluoroacetic acid. In the diagram the Q-1/Q-2 offset voltage is plotted against the relative intensities of the ions 308, 266 and 152.

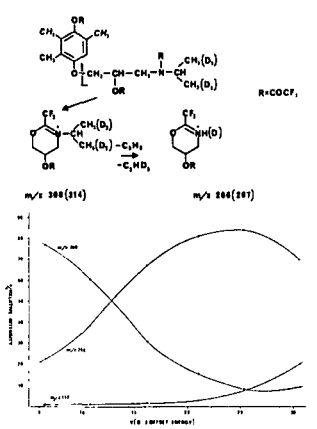


Fig. 1

By raising the collision energy the abundance of the daughter ion 266 increases to a maximum at approx. 25 volts, whereas the precurser decreases. At higher energies the ion at mass 152 becomes more intense. The optimized parent daughter ratio is relevant for the detection limit of any assay. For deacetylmetipranolol the detection limit (0.1 ng/ml) was enhanced by one order of magnitude compared to the GC/MS assay (1). The attained precision of better than 5 % coefficient of variation means that data of the quality required for pharmacokinetic evaluation can be furnished.

Isosorbide-5-mononitrate (IS-5-MN, Formula given in Fig. 2) is the main metabolite of Isosorbide-dinitrate and has now been introduced into therapy. IS-5-MN is metabolized mainly to its 2-glucuronide (compound 1)

and to isosorbide glucuronide (compound 2). The GC-derivatives 1a and 2a are prepared for the quantitative assays. p-nitrophenyl glucuronide serves as internal standard.

Different chemical and mass spectroscopic properties of the conjugates made it necessary to develop a separate specific assay for compound 1 and compound 2. The work up procedure for the nitrato-conjugate discriminates against isosorbide glucuronide.

Ammonia chemical ionization of 1a leads to a mass spectrum with the base peak at m/z 570, resulting from ammonia attachment to the molecular ion minus NO_2 plus one hydrogen. This type of hydrolytic reaction is not uncommon when studying organic nitrates. Collision activation of m/z 570 produces daughter ions characteristic of glucuronic methyl-ester: m/z 407, 317 and 275. In the soft collision experiment of the quasimolecular ion of the internal standard ($M + NH_4$ = 563) the same daughter ions are dominant.

For the quantitative assay the instrument is optimized to the 570→317 transmission. A standard curve in urine has been constructed by ratioing the 317 ions. The response is linear from 10 ng to 25 pg of sample amount injected, the coefficient of variation was 2 % (n = 7, 0.5 ng). GC-on column injection was necessary to prevent decomposition of the nitrato-glucuronide in the injector.

The thermal instability of the nitrato-group was utilized to develop a method to determine the sum of compound 1 and 2 as their persilyl-derivatives with a minimum of sample preparation. The TMS-derivative of compound 1 is quantitatively converted to the derivative of compound 2 in the GC-injector.

Negative CI with methylene chloride as reactant gas gives a base peak at m/z 609 (M-TMS). m/z 609 decomposes mainly to the ion at 447 by a one step process: M-(TMSOTMS).

In Fig. 3 a MID recording of blank urine containing the standard - only mass 609 is shown - is compared to the same blank urine sample in the multiple reaction monitoring (MRM) mode by scanning the daughter ion 447. The third trace represents an urine sample spiked with 500 pg isosorbide conjugate (standard not shown).

The main features and advantages of GC/MS/MS like very high sensitivity, selectivity and specificity, open up possibilities of being able to analyse very low concentrations of drugs and metabolites in a biological matrix with excellent precision and in many cases with a minimum of sample work up.

The instrument price and the complexity of the system will hopefully not slow the development of MS/MS analysis.

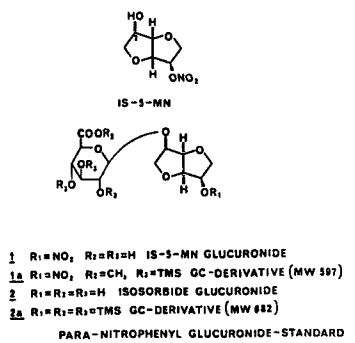


Fig. 2

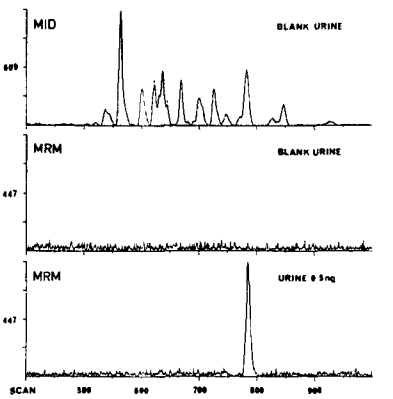


Fig. 3

References:

(1) R. Endele, M. Senn and U. Abshagen, J.Chromatogr. 227, 187 (1982)

SECONDARY ION MASS SPECTROMETRY OF BIO-ORGANIC COMPOUNDS OBTAINED USING A CESIUM ION PRIMARY BEAM AND A LIQUID TARGET MATRIX

William Aberth, Fred Walls, Kenneth M. Straub and A.L. Burlingame
Mass Spectrometry Resource, Dept. of Pharmaceutical Chemistry
University of California, San Francisco, CA 94143

The development of "soft" ionization techniques for mass spectrometry which have the ability to produce gas phase molecular ions without prior evaporation of the sample is in the process of revolutionizing our ability to detect, identify, and characterize the structures of thermally and chemically labile substances.

Recently, Barber, Surman and co-workers reported on the development of "fast atom bombardment" (FAB), where the sample is supported in a glycerol or related viscous fluid matrix and bombarded with a fast (6-8 keV) neutral argon beam (1,2). The mass spectra of a wide variety of polar, biologically relevant molecules up to 3,500 daltons were shown, with signal-to-noise ratios equivalent to those observed in conventional electron impact mass spectra. Clear and impressive results using FABMS have since been reported on such research problems as peptide sequencing, oligosaccharide analysis, bile salt analysis, and the structural characterization of polar, thermally labile substances including nucleotides, sulfate esters, and polypeptide antibiotics.

However, in the initial publications describing FABMS, the developers of the technique reported that the need for a neutral primary beam was prompted by the observation that charged primary beams resulted in surface charging of the sample and subsequent loss of the secondary ion beam, and that there was difficulty steering a charged primary beam into the high voltage ion source region of modern sector instruments.

In this work we use a Cs^+ primary ion beam with a liquid matrix SIMS source. This ion source also permits concurrent use of a commercial 8 keV Xe^0 FAB gun (Kratos, Inc.) for comparative purposes (see Fig. 1). The primary Cs^+ ion gun produces a 6 keV Cs^+ beam focused to a spot size of between 1 and 2 mm diameter at the target surface. The Cs^+ ions are produced by evaporation from a surface coated with cesium alumina silicate. Beam intensity can be independently controlled by varying the temperature of the evaporation surface. A Cs^+ current of about 1μA, produced at a temperature of 1,000°C, was generally used. The ion gun incorporates an extractor plate and Einzel lens for primary beam focusing. The entire structure is 3.4 cm long and is mounted within the mass spectrometer source housing. Samples were prepared by either dissolving or making a slurry of the solid in glycerol.

Figure 2 shows the positive ion SIMS spectra of the undecapeptide met-lys-bradykinin. This example is included since the FAB spectrum of this compound has been reported in the literature by others (3). It is evident that there is little difference between the fragmentation patterns of the FAB and SIMS spectra. We have compared spectra obtained with our Cs^+ primary gun and the Xe FAB gun for a wide variety of bio-organic compounds including other model peptides over the mass range 1000-2900 d, nucleotides, nucleosides, phospholipids, and steroid conjugates (see paper TPA 22) and have obtained essentially identical results.

This result demonstrates that the use of a neutral atom beam as the primary sputtering source does not have any inherent advantage over the use of a charged beam. The similar yields in secondary ion current and the observation that retuning of the ion source focusing controls is not required when switching between the two modes of operation, show that charging of the sample matrix by the primary ion beam is not significant. The consistent difference between the two techniques is that the Cs^+ gun produces about 3X more secondary ion signal than the Xe^0 gun. With adequate attention to source design, the use of a primary ion beam with a liquid matrix target may result in superior performance for structural studies of biological substances in magnetic sector instruments. In light of these results, the use of the term FAB to describe the state of the sample and its matrix on the electrode surface (viscous liquid as opposed to solid) is misleading. SIMS is the established, preferred acronym for describing the phenomenological process of sputter ionization. For the particular application to liquid matrix targets, it would be more appropriate to modify the term SIMS to specify that target, i.e., LIQUID-SIMS.

This work was supported by NIH Grant RR01614 and the negative ion source was made available by a grant from the University of California, San Francisco, Academic Senate.

References

1. Barber, M.; Bardoli, R.S.; Elliott, G.J.; Sedgwick, R.D.; Tyler, A.N. J. Chem. Soc. Chem. Commun. 1981, 325.
2. Surman, D.J.; Vickerman, J.C. J. Chem. Res. (S) 1981, 170; ibid., J. Chem. Soc. Chem. Commun. 1981, 324.
3. Barber, M.; Bordoli, R.J.; Sedgwick, R.D.; Tyler, A.N.; Whally, E.T. Biomed. Mass Spectrom. 1981, 8, 337.

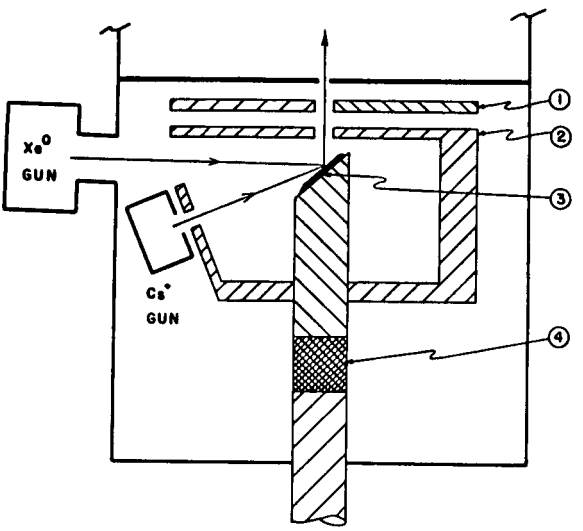


Fig. 1. Schematic of source mounting of FAB (Xe^0) and SIMS (Cs^+) primary ion guns. (1) Beam centering plates; (2) source block; (3) sample target; (4) direct insertion probe.

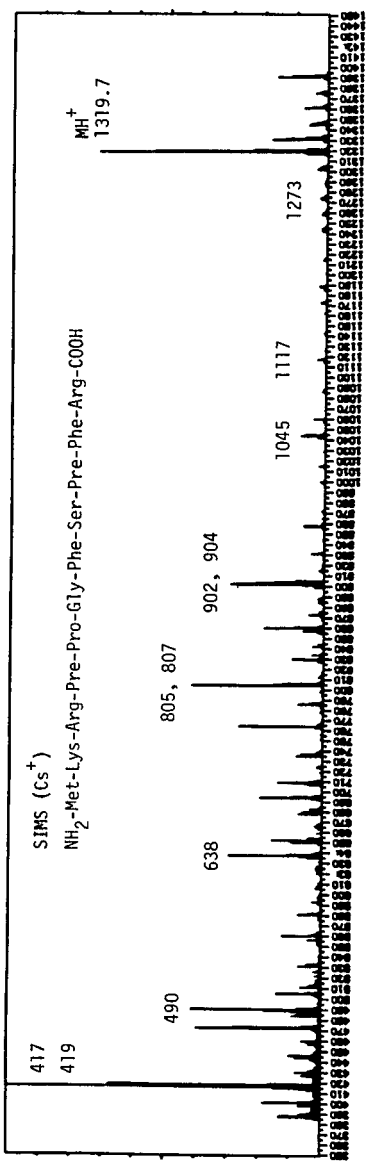


Fig. 2. SIMS (positive ion) spectrum of met-lys-bradykinin (Met-Lys-Arg-Pro-Pro-Gly-Phe-Ser-Pro-Phe-Arg). Major sequence ions are labeled.

SOME FUNDAMENTAL ASPECTS OF FAST ATOM BOMBARDMENT MASS SPECTROMETRY

W.M. Bone, D.F. Hunt, J.M. Marasco; Department of Chemistry, University of Virginia, Charlottesville, Virginia 22901

The recent development of FAB-MS has allowed investigators to record mass spectra of previously intactable compounds. Interest to date has centered largely on utilizing the technique to solve specific structural problems of bio-chemical importance. Indeed FAB-MS is well suited for these problems but as an analytical technique it has grown so quickly that many of the more fundamental aspects have been overlooked. These fundamental aspects may be either physical or chemical in nature.

The physical aspects we have considered include temperature profiles of sample and glyceral ions; molecular ion intensity as a function of primary beam current density and energy; as well as some comparisons of ions and neutrals as the primary beam and different gases.

Figure 1 illustrates the temperature dependence of some positive ions including the glycerol monomer, dimer and trimer as well as a peptide sample. At about 25°C the sample ion intensity is maximized and the glycerol peaks are small but increase rapidly with temperature.

Figure 2 is a plot of the protonated molecular ion current obtained from a peptide as the primary beam current density is varied at three different energies. It may be expected that the lines plotted would be parallel with higher energy beams yielding greater ion current. This is generally the case but the lines do cross at low current densities probably because the primary beam is misaligned. If the current density could be further increased the sample ion current may reach at maximum which would level off depending on the nature of the sample and its concentration in the glycerol. The effect would probably occur at current densities $>10^{15}$ part./cm^2sec.

Other experiments indicate that ionization takes place primarily in the liquid phase (glycerol) and that the molecular ion intensity is greatly dependent on the sample concentration in the glycerol. This concentration effect is important when trying to quantitate FAB results and care should be taken to transfer known amounts of glycerol to the probe tip reproducibly. Figure 3 illustrates the concentration effect.

The chemical factors influencing FAB-MS data are concerned mainly with the acidity or basicity of the sample relative to glycerol and are considered in more detail elsewhere.

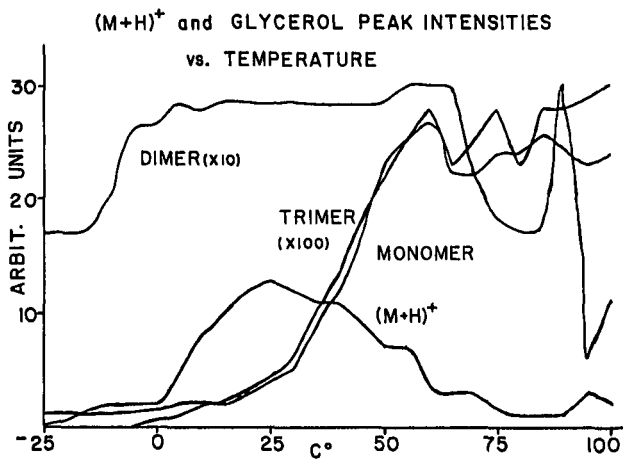


Figure 1

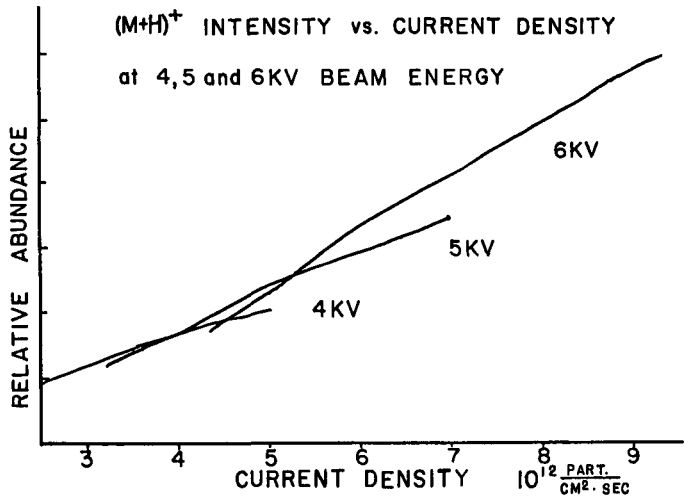


Figure 2

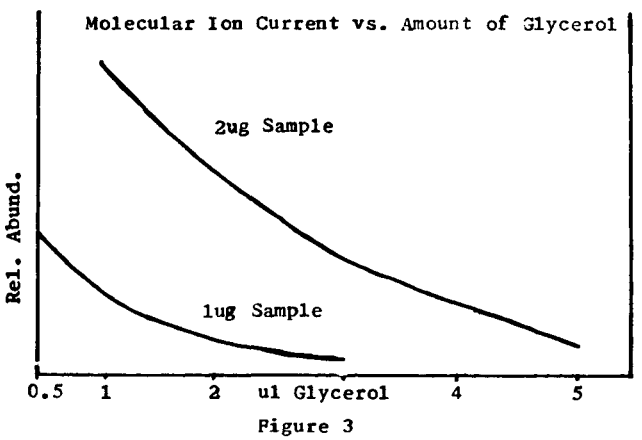


Figure 3

ANALYSIS OF THE OPERATION OF THE FACS

(Fast Atom Capillaritron Source)

Julius Perel and John F. Mahoney

Phrasor Scientific, Inc., Duarte, CA 91010

Sputtering, known for well over 100 years, is a process in which solid or liquid surfaces bombarded by energetic ions, emit atoms of the surface material. The technique was used to erode surfaces, then later used to coat other surfaces with the emitted atoms. It was then discovered that a small fraction, perhaps 1%, of the emitted particles were electrically charged. By bombarding a solid surface with ions (primary) and directing the secondary ions coming off the surface into a mass spectrometer, analysis of the surface composition was accomplished. This technique, secondary ion mass spectroscopy (SIMS) was used in depth profile and in diffusion studies. Fast Atom Bombardment (FAB) was also found to produce sputtering and secondary ions, but was particularly useful when high electric fields at the target, made of insulating material, charged up during ion bombardment or when the target required high voltage as in magnetic sector mass spectrometers. FAB was found to soft-ionize organic and inorganic samples dissolved in a liquid matrix. This allowed for the introduction of nonvolatile and thermally fragile molecules into a mass spectrometer. It only required that the sample molecules diffuse to the vicinity of the surface and sputter as an ion when bombarded by fast atoms or ions. A source capable of generating a beam of fast atoms and fast ions is described here.

Fast atoms are produced by first generating ions that are accelerated through an electric field, then neutralized by capturing electrons. Early fast atom sources employed an ion accelerator to produce a fast ion beam which would then be directed through a charge transfer cell containing a gas. The emerging beam generally contained fast ions and atoms.

The Capillaritron Ion Source produces ions in a plasma at the exit end of a fine capillary nozzle[1,2] as shown in Fig. 1. The plasma is generated when high voltage (> 1kV) is applied to the nozzle and sufficient gas passes through the nozzle. For a standard nozzle whose channel diameter is 25 microns, a flow rate of about one SCCM is achieved when the gas pressure in the plenum is about 300 torr[3]. Fig. 2 shows that under this condition, the calculated gas pressure at the nozzle tip is approximately 80 torr with the pressure dropping to about one torr at a distance of one nozzle diameter (125 micron) downstream. The pressure drops beyond this to a background pressure of about 10^{-5} torr within 2cm. Assuming 10kV applied to the nozzle, also illustrated in Fig. 2, the potential drops to half the nozzle voltage 2 nozzle diameters downstream. In 10 diameters, it drops to 15% and down to tens of volts at 200 diameters (2.5cm).

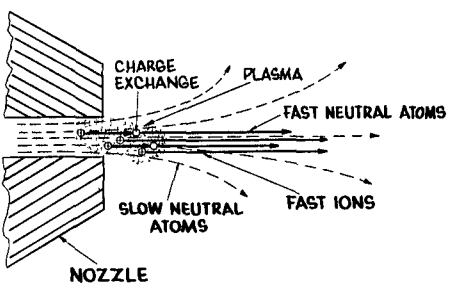


Fig. 1 Particle Interaction In the Plasma at the Nozzle Tip

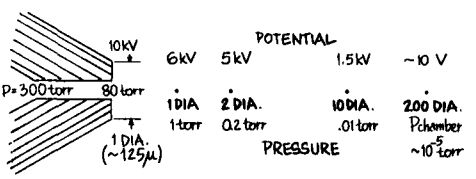


Fig. 2 Potential Falloff and Pressure Decrease Along Beam Axis

Some ions generated in the plasma and accelerated away from the nozzle will undergo charge transfer collisions as shown in Fig. 3. The collision can occur with distances of several Å existing between the fast ion and thermal atom at closest approach. Virtually no momentum transfer occurs and the fast particle travels on undeflected. Only the electron is transferred from the thermal atom to the fast ion resulting in a fast atom and thermal ion. The newly formed ion is then accelerated by the existing electric field. The energy (velocity) achieved by each ion (or fast atom) is determined by the difference in potential between the place that the ion first forms and the place of neutralization. Because of the charge transfer collision, the resulting fast atom and the new ion will share the full energy (10keV) if these particles do not undergo another charge transfer. When charge transfer occurs at distances of centimeters downstream, the newly formed ions can have energies of tens of electron volts which is appropriate for direct analysis in quadrupole mass spectrometers.

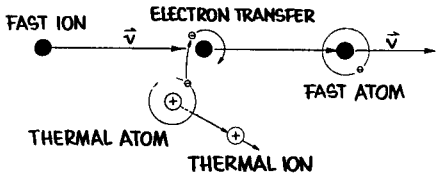


Fig. 3 Charge Transfer Collision Between Fast Ion and Thermal Atom

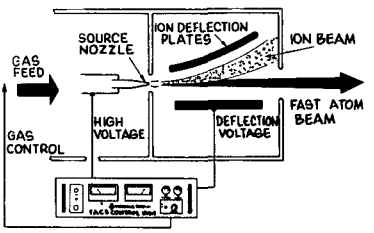


Fig. 4 Operation of the Fast Atom Capillaritron Source

The emerging beam contains ions, having a distribution of energies ranging from a few eV to the entire energy, a similar distribution of fast atoms, and thermal atoms.[4] Downstream about 1cm, the beam is primarily ions and fast atoms. If the ions are deflected out as shown in Fig. 4, the beam is then composed of just fast atoms. Measurements are made using a Calorimeter/Faraday cup probe to simultaneously determine the power deposited and the current collected.[5] These measurements show that the ion beam power and fast atom beam power are approximately equal.

REFERENCES

1. J.F.Mahoney, J.Perel and A.T.Forrester, Appl.Phys.Lett., 38, 320 (1981).

2. J.Perel, J.F.Mahoney, B.E.Kalensher and A.T.Forrester, AIAA-81-0747, 15th Inter. Electric. Propul Conf., Las Vegas, NV (21-23 April 1981).

3. B.E.Kalensher and J.Perel, J.of Appl.Phys. 53, 2904 (1982).

4. D.M.Goebel, J.Perel, J.F.Mahoney and A.T.Forrester, "Characteristics of the Capillaritron Ion Source", submitted to J. Appl. Phys. (1982).

5. J.F.Mahoney, D.M.Goebel, J.Perel and A.T.Forrester, "A Unique Fast Atom Source for Mass Spectrometry Applications", accepted by Biomed. Mass Spectrom.

Organic SIMS Studies with a Capillaritron Ion Source

Peter Williams and Daniel M. Adams
Department of Chemistry
Arizona State University
Tempe, Arizona 85287

We have successfully coupled a new type of ion/neutral source, the Capillaritron <1> to a MAT 312 instrument for organic SIMS studies. By miniaturizing the source, we have succeeded in mounting the entire Capillaritron source assembly within the 312 source housing, allowing us to bombard a sample surface which is normal to the ion-optical axis of the mass spectrometer. This arrangement gives significantly improved transmission over the angled probe arrangements dictated by external mounting of the source. We report here some details of the performance of this arrangement, and a comparison with the performance of a state-of-the-art inorganic SIMS instrument (Cameca IMS 3f) which indicates the room for improvement in organic applications.

As initially delivered, the Capillaritron was flange-mounted, and was mounted on the GC inlet of the 312. This arrangement dictated the use of an angled sample probe (at 45° to both the beam and the ion-optic axis of the 312). NaI-doped glycerol sample techniques were used, as reported in this meeting by Barber et al last year. Using as a test compound an antineoplastic agent, phyllanthostatin I, which had only been run with extreme difficulty by FD, the SIMS technique gave a clearly distinguishable (parent + Na) peak.

Although a large number of compounds were run successfully, it was clear that the use of an angled probe severely limited sensitivity. Therefore, we have miniaturized the source as shown in Fig. 1, to the extent that it can be mounted inside the source housing of the 312, allowing us to sputter a sample probe whose surface is normal to the ion-optic axis. The use of a moderate extraction field in the sample region improved the transmission by a factor of 10. Although the optics are by no means fully optimized, we feel that the capability to extract ions normal to the sample surface will ultimately allow secondary ion transmissions comparable to those achieved in state-of-the-art inorganic SIMS, where the Cameca IMS 3f can achieve a transmission on the order of 10% at low resolving power.

Performance of the Capillaritron source has been highly satisfactory. The source operates routinely at ~ 10μA emission at 8 kV applied voltage. A novel feature of the source is that feed gas is supplied through a leak valve on the 312 gas inlet line, and transported to the high voltage nozzle via flexible fused silica tubing. A few feet of this tubing eliminates the possibility of discharges in the gas feed line. (The present size of the source is largely dictated by the Swagelok coupling used to connect the glass capillary to the nozzle.) We do not suppress the ion component of the beam, but allow both ions and neutrals to strike the sample. Retaining the ion component gives rise to no problems with sample charging, so long as the glycerol is appropriately doped, and can be an advantage: gas-phase species can be ionized quite efficiently by ion impact, and PFK, for example, introduced as a gas, gives a calibration spectrum very similar to the EI spectrum. Nozzle erosion has not been a problem; due to the instant on-off capabilities of the source, it can be switched off at all times when data is not being acquired. We have operated with a single nozzle for over 1 month with no signs of degradation. The pressure in the sample chamber with the source operating is rather high ~ 1×10^{-4} torr, but this does not appear to degrade the mass spectrometer performance noticeably.

We have attempted to compare the performance of our system directly with that of the Cameca instrument by sputtering a silicon sample ion-implanted with boron. This sample had previously been characterized by a wide variety of inorganic SIMS systems. The characteristic variation of the boron concentration with depth allows a depth scale, and therefore a sputtering rate, to be established. The performance of the 312/Capillaritron system is compared with that of the Cameca IMS 3f in Table I. Clearly, there is much room for improvement, although the gram sensitivity of the technique is already impressively high.

Reference:

1. "Capillaritron: A New, Versatile Ion Source," J. F. Mahoney, J. Perel and A. T. Forrester, Appl. Phys. Lett., 38, (1981) 320.

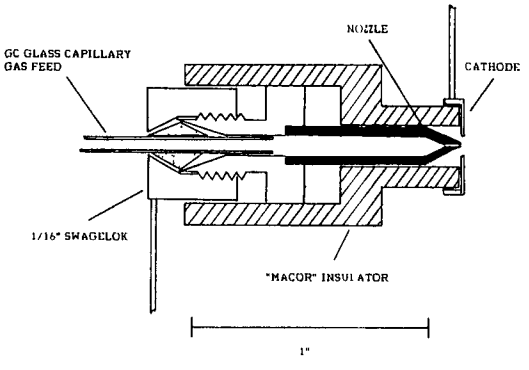
Table I

Comparison of 312/Capillaritron with Cameca IMS 3f: analysis of boron-implanted silicon sample

	312/Capillaritron	Cameca IMS 3f
Sputter rate (Si)	< 0.25 Å/s	2 Å/s
Current density	25 $\mu A/cm^2$	250 $\mu A/cm^2$
B^+ count rate	< 1000 c/s	5×10^6 c/s
Analysed area	0.25 cm^2	2×10^{-4} cm^2
Est. transmission	2×10^{-7}	10^{-1}

Figure 1

Miniaturized Capillaritron Ion/Neutral Source



HIGH FIELD SURFACE CHEMISTRY ON A VOLCANO TYPE FIELD IONIZATION SOURCE

R. H. Fleming and G. A. St. John

SRI International
333 Ravenswood
Menlo Park, CA 94025

Field ionization (FI) produces only molecular ions for the vast majority of compounds. The mechanism for the field ionization appears to involve adsorption of sample, ionization, and field desorption of the ions. Evidence for this process involves the enhancement of ionization efficiency of many classes of compounds in the presence of aromatic materials such as benzene. In addition other (usually small) peaks are observed in FI mass spectra. These peaks arise from association and fragmentation reactions which occur largely (if not exclusively) on the surfaces of anodes. Thus, a rich chemistry involving many different processes occurs on surfaces in the presence of high electric fields. We have studied these processes using a volcano type FI source.

Aromatic substances have long been known to activate FI emitters causing them to produce ions more efficiently. One mechanism for enhancement of ionization efficiency involves production of pointed carbon dendrites from the aromatic compound. The electric field is higher in the region of the pointed tips and sample molecules are more easily ionized. This does not appear to be the sole mechanism of benzene enhancement of volcano ionization efficiency.

For alkane samples we observe an ionization enhancement of 2-3 times in the presence of a 1:1 ratio of benzene or toluene. The enhancement is prompt, occurring in about ten seconds whereas dendrite formation usually requires longer times (1-2 hr). The enhancement is also observed with benzene-d_6, but no deuterium containing ions appear except $C_6D_6^+$. Thus carbon dendrite formation would require all of the deuterium to leave as neutral atoms or molecules, an unlikely event in an ion source. In scanning electron micrographs, carbon dendrites are sometimes observed. However, sources with no apparent dendrites are often functionally indistinguishable from sources with dendrites. These observations are consistent with a FI mechanism that involves adsorption of sample on the emitter. The benzene activation must work by changing the nature of the surface and not exclusively by providing regions of higher electric field at the tips of dendrites.

Several association reactions are observed which must also occur on the volcano surface. Basic substances are often protonated even though the system pressure is far too low to allow ion-molecule reactions. The source of the protons is apparently volcano adsorbed water. Water itself is observed as a variable mixture of H_2O^+ and H_3O^+. The H_3O^+ ion represents from 8% to 100% of the total depending on mass spectrometer operating conditions. The basic substance diisopropyl methylphosphonate is always 100% protonated and even benzene has been observed to be 1% protonated in a high resolution FI mass spectrum in which $C_6H_7^+$ can be separated from $^{13}C^{12}C_5H_6^+$.

The volcano itself is constructed of copper. Ions of Cu^+, $Cu(H_2O)^+$, and $Cu(H_2O)_2^+$ have been observed at low intensity and in the presence of large benzene samples, small signals from $Cu(C_6H_6)^+$ and $Cu(C_6H_6)_2^+$ are observed. These ions also apparently arise from reactions of water or benzene with copper or copper ions on the surface of the volcano.

Even fragmentation reactions may occur on the surface. Although FI usually gives only molecular ions, some quaternary carbon-containing compounds do produce daughter ions. For example isooctane has m/z 57 ($C_4H_9^+$) as its base peak. In a fragmentation of isooctane ion ($C_8H_{18}^+$) along its flight path, $C_4H_9^+$ will get about one half of the energy and C_4H_9 neutral will get the other half. Since the volcano is typically adjusted to 15 V and the quadrupole housing is at ground, an ion cannot even enter the analyzer if it loses 15 eV or more. The time required for $C_8H_{18}^+$ to reach 30 eV is 17 ps in an electric field of 5×10^6 V/cm. The distance travelled in this time is 600 Å. Any loss of C_4H_9 after the 17 ps "window" would involve loss of more than 15 eV and leave the $C_4H_9^+$ with too little energy to be analyzed. Thus fragmentation must either occur on the surface or in the narrow 17 ps time "window".

In conclusion, enhancement of the ion forming capability of a volcano type FI source occurs by chemical modification of the volcano surface rather than exclusively by deposition of dendritic tips. To be influenced by the surface, the sample must be first adsorbed and then ionized and desorbed. Similarly, association reactions must be preceeded by adsorption of sample. Fragmentation reactions also have a high probability of occurring on the surface. By extension it appears that simple field ionization without enhancement or surface reactions probably also occurs by sample adsorption followed by ionization and desorption.

MULTIPLY CHARGED IONS IN ELECTROHYDRODYNAMIC IONIZATION MASS SPECTROMETRY. KELVIN W.S. CHAN and KELSEY D. COOK*, School of Chemical Sciences and Materials Research Laboratory, University of Illinois, Urbana, IL 61801.

While multiply charged ions are not often observed in most conventional mass spectrometric techniques, ions as highly charged as triply positive [1] and doubly negative[2] have been sampled directly from glycerol solution by Electrohydrodynamic Ionization Mass Spectrometry (EHMS)[3]. These ions are formed in solution via electrolytic dissociation of salts or ion attachment by polar analytes. The pre-formed ions are then extracted into the gaseous phase by an electrostatic field. Thus, the EH process is a sampling phenomenon rather than an ionization technique.

Because the EHMS experiment relies on low energy solution phase chemistry for ionization, it is accompanied by apparently negligible internal energy deposition. To illustrate this, a series of diquaternary ammonium diiodides (diquat, MI_2) (Table 1) was studied. These salts can dissociate in solution to form $(MI)^+$ and $(M)^{2+}$ ions. Because there are two localized charge centers in these ions, an intramolecular coulombic repulsion force exists. During mass spectrometric ionization and sampling, additional energy is imparted to these ions. If the total of these energies exceeds the activation energy for the charge separation reaction (fragmentation), doubly charged ions will not be observed. This has reportedly been the case for other ionization mechanisms. For example, published secondary ion mass spectra[4] of these diquats contained large ammounts of fragment ions while the molecular dications were of relatively low abundance or absent. By contrast, in the EH mass spectra of these salts, intact molecular ions were always detected. For example, Figure 1 showed the positive ion EH mass spectrum of diquat 3. This mass spectrum, as well as other EH mass spectra of the diquats studied, contained mainly singly and doubly charged molecular species, confirming that the amount of internal energy deposited in the EH process was relatively small.

Because molecular ions are always sampled, in order to ascertain the analytical utility of the EH sampling process, it is important to determine if the ions detected are representative of those in solution. Thus a study of the sampling efficiency of EHMS for ions of different charges and structures was undertaken.

To compare the sampling efficiency for various ions, a selectivity ratio, S, was used. S for component A over B, S(A/B), is defined as:

$$S(A/B) = \frac{\Sigma I_A/\Sigma I_B}{\text{moles A/moles B}}$$

where I_A and I_B are the intensities of ions of component A and B respectively. S=1 indicates equal efficiency for the two components. Table 2 showed the S(A/B) for several systems containing equal concentration of two components. For a system containing ions of similar charge and structure (ferrous and ruthenious trisbipyridine complexes), the sampling efficiencies were similar (S≈1). However, S for doubly over singly charged ions (such as Mg^{2+} and Na^+, $(CH_3)_3N^+-(CH_2)_5-N^+(CH_3)_3$ and $(CH_3)_4N^+$) were very small, suggesting the sampling efficiencies were quite different. The ions detected were solvated to some degree. These solvated ions can undergo metastable decomposition (desolvation) in the first field free region of the spectrometer. The resulting metastable ions can be detected by decreasing the voltage of the electrostatic analyzer. S^* calculated from these desolvated metastable ions were higher than their respective S (Table 2) This observation indicated that the higher charged ions were heavily solvated. The stronger interaction with solvent impeded the efficiency of EH sampling of these multiply charged ions. From these results, it can be concluded that the EH sampling efficiencies for ions of similar charge and structure are similar. However, the EH sampling process is greatly dependent on the charge and structure of the ions and efficiences for ions dissimilar in these properties may vary greatly.

ACKNOWLEDGEMENT

This work is partially funded jointly by the National Science Foundation and the Army Research Office, under grant number NSF-DMR-80-24632. The Materials Research Laboratory is supported in part by NSF grant DMR-80-20250.

REFERENCES

1. S.-T. F. Lai, K. W. Chan, and K. D. Cook, Macromolecules 13, 953 (1980).
2. S.-T. F. Lai and C. A. Evans, Jr., Org. Mass Spectrom. 13, 733 (1978).
3. B. P. Stimpson and C. A. Evans, Jr., J. Electrostatics 5, 411 (1978).
4. T. M. Ryan, R. J. Day, and R. G. Cooks, Anal. Chem. 52, 2054 (1980).

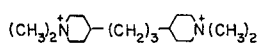
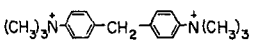
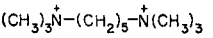
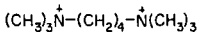
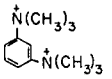
Diquaternary ammonium ions	
1	
2	
3	
4	
5	

Table 1: The series of diquaternary ammonium diiodides studied.

Components	S(A/B)	S* (A/B)
A: $Ru(bipyridine)_3^{2+}$ B: $Fe(bipyridine)_3^{2+}$	1.2	---
A: Mg^{2+} B: Na^+	0.0	0.1
A: Diquat 3 B: $(CH_3)_4N^+$	0.1	2.4

Table 2: Selectivity ratios, S(A/B), of the three systems containing equal concentration of the two components.

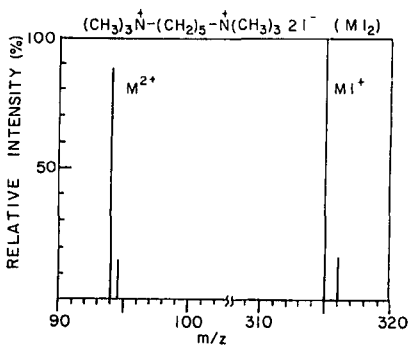


Figure 1: Positive ion EH mass spectrum of diquat 3 (0.1 mole%) with NaI (6.3 mole%) in glycerol (100.0 mole %)

MOD 8 SPECULATIONS ON THE MECHANISM OF THERMOSPRAY AND OTHER SOFT IONIZATION TECHNIQUES; M.L. VESTAL; Dept. of Chem., Univ. of Houston, Houston, TX 77004

Recently we reported that molecular ions were produced when aqueous solutions containing nonvolatile solutes were rapidly vaporized as the result of forcing the liquid through a narrow heated capillary.[1] This "thermospray" process produces mass spectra for many nonvolatile molecules which are similar to those obtained by field desorption and other soft ionization techniques. We have recently conducted a series of studies aimed at elucidating the mechanisms involved in this apparently new ionization process. While these studies are not fully completed, preliminary results suggest that the mechanism is dominated by the spray electrification processes characterized many years ago by Loeb and coworkers.[2] The most important mechanism appears to be symmetrical charging produced by statistical distribution of positive and negative ions among the droplets produced by spraying a liquid containing solvated ions. True spray electrification produced by sudden disruption of the electrical double layer at the gas-liquid interface may also be involved. Field desorption of molecular ions from charged micro particles or droplets may be involved in producing the ions observed in the mass spectrometer. Evidence for these mechanisms will be presented along with a discussion of the implications for other soft ionization techniques which may involve production of ions by disruption of liquid surfaces such as field desorption, FAB, laser desorption, and rapid thermal desorption.

[1] C.R. Blakley, J.J. Carmody, and M.L. Vestal, JACS,102,5931, (1980).

[2] Leonard B. Loeb, Static Electrification, Springer-Verlag, Berlin (1958).

THE SURFACE IONIZATION SPECTRA OF RESIDUALS AND VOLATILE ORGANIC COMPOUNDS ON Re FILAMENTS BY TOFMS

Dale A. Chatfield
Department of Chemistry, San Diego State University, San Diego, CA 92182

Numerous papers regarding ionization processes in mass spectrometry have appeared in the last few years under the names thermal, surface, pyrolysis, and desorption. Of these techniques, surface ionization (SI) has generally been regarded as a highly energetic process that produces little, if any, structural information about organic molecules. Herein, the term SI is meant to define the ionization process of N_o to N_+ described by the Saha-Langmuir equation, shown in Eq. 1. In this expression, g_+ and g_o are the

$$\frac{N_+}{N_o} = \frac{g_+}{g_o} \exp [(\Theta - IP)/kT] \qquad (1)$$

statistical weights of N_+ and N_o, Θ the work function of the metal surface at which ionization occurs at temperature T, and k is the Boltzmann constant. This equation has been uniformly applied to the ionization of metals with low ionization potentials (IP) by Zandberg and associates (1) with success using oxidized W, but its application to organic species has been very limited. One difficulty that has been addressed but not completely resolved has been the question of thermal equilibrium that Eq. 1 assumes between N_+, N_o and the heated metal surface.

In this investigation, the mass spectra of residual organic species and select organic compounds are reported at 1150 and 1400 K on oxidized Re filaments. A time of flight mass spectrometer (TOFMS) has been modified for this task by removal of the conventional electron ionization source and mounting a 10 mm long x 2 mm wide x 0.02 mm thick zone refined Re filament coplanar to the ion source optics. To improve resolution, special circuitry has been constructed to gate both the back plate and the draw-out lens and apply a bias voltage to the Re filament. Turbo pumps, heaters and a liquid nitrogen cold trap have been included to reduce residual organic vapors. Samples of organic compounds are introduced to the TOFMS via a capillary column gas-liquid chromatograph (GLC).

The background spectrum of residuals contained a predominance of Na^+, K^+ and organic fragment ions between m/e 57 and 300. Upon prolonged heating, above 1000 K, the intensities of the organic species reduced dramatically, but Na^+, K^+ and intense doublets at 256-58 and 288-90 persisted. The intensity of these ions dropped to very low levels upon 20 hrs. of heating. The intensity of the latter doublets, tentatively assigned as $KReO_2^+$ or $NaReO_3^+$ (m/e 256-58) and $KReO_4^+$ (m/e 288-90), was dependent upon temperature, alkali metal ion intensities, and surface treatment with oxygen. Prolonged heating of the filament at 1400 K and 10^{-7} torr resulted in the loss of Na^+ and K^+ from the spectrum, apparently due to a depletion of these metals from the surface of the filament. The Re oxide layer was altered as well in the heating process. The doublet peaks were observed to reappear only when alkali metal ions reappeared in the spectrum and oxygen was present at the Re surface. Addition of organic vapors resulted in a decrease in the intensity of all ions in the spectrum, but their intensities could be restored by heating to >1000 K with 2×10^{-5} torr air for several minutes.

The ions appearing in the mass spectrum between m/e 57 and 300 appear to be organic in nature. Addition of $^{18}O_2$ to the source chamber did not alter the observed masses of the ions below m/e 150, so it is assumed that they are entirely hydrocarbon in nature. Predominant ions appeared at m/e 57, 69, 77, 83, 87, 99, 111, 121, 129, 151, 180 and 195. Due to the limited resolution of

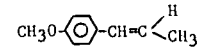
the instrument in its present configuration, there may be an uncertainty of ± 1 dalton in the mass assignments of the higher mass peaks. Upon prolonged heating of the Re filament above 1200 K and the ion source region to 200°C, the intensities of these ions reduced to an acceptable level, with Na^+, K^+ and 57 being the only ions present. Because of significant noise levels present at lower filament temperatures all but two studies were carried out at higher temperatures.

A summary of the predominant ions that were present in the mass spectra of select organic compounds is listed in Table I. These results are generally in agreement with the observations by Zandberg (2) but not with those reported by Davis (3). Zandberg reported that aniline forms an intense molecular ion and pyridine a protonated species. However, the major fragment ion from t-butanol was m/e 60, and the t-butyl cation reported earlier was less intense. In general, the aliphatic hydrocarbons cleave to form fragment ions only, but the aromatic compounds produce M^+ and $(M + H)^+$ ions with little, if any, fragmentation. Of these aromatic compounds, only the SI spectrum of anethole contained an $(M-CH_3)^+$ ion of approximately 25% of the protonated molecular ion intensity. Unlike the spectra reported by Davis, no $(M-H)^+$ ions were observed. This difference may be attributable to the much higher filament temperatures used in these experiments. It should be added that the elution of the organic compound under study from the GLC and the resultant appearance of ions was preceded by a sudden rise in the intensities of Na^+ and K^+ in the mass spectrum. This phenomenon was observed to some extent for all organic compounds, but elution of CH_2Cl_2 resulted in a many-fold increase in alkali metal ion intensity. During the appearance of m/e values attributed to the organic compounds, the Na^+ and K^+ intensities decreased, and remained so for a period of several minutes thereafter.

Several preliminary experiments were conducted at lower filament temperatures for t-butanol and aniline. At 1200 K an intense peak at m/e 132 was observed for aniline, which is believed to be the cation $(M + K)^+$. Similarly, a peak appearing at the m/e ratio of the potassium adduct of t-butanol (m/e 113) was observed. However, due to the substantial background intensities that were also present, these findings need to be confirmed in other experiments wherein the background spectra are improved. However, it should be noted that the ions at m/e 132 and 113 from aniline and t-butanol, respectively, did not appear when the K^+ ion was absent from the mass spectrum.

1. E. Ya Zandberg, Zh. Tekh. Fiz., 44, 1809 (1974).
2. E. Ya Zandberg and U. Kh. Rasulev, Russian Academy of Science report No. 729, 1981.
3. W.D. Davis, 21st Ann. Conf. Mass Spectrom. and Allied Topics, San Francisco, CA 1973, paper Q1.

Table I. Surface Ionization Mass Spectra of Select Organic Compounds at 1200°K

Compound	m/e	Ion(s)
t-Butanol	57, 60	$(CH_3)_3C^+$, C_3H_8O
2,2,3-Trimethyl pentane	57	$(CH_3)_3C^+$
Benzene	78	M^+
Fluorobenzene	96	M^+
Bromobenzene	156-59	M^+, $(M + H)^+$
Phenol	95	$(M + H)^+$
Aniline	93	M^+
Anethole 	149,133	$(M + H)^+$, $(M-CH_3)^+$
Pyridine	80	$(M + H)^+$
$CHCl_3$	82-86	CCl_2^+

ROLE OF SAMPLE MELTING POINT AND SAMPLE VAPOR PRESSURE IN ONSET OF FIELD DESORPTION

Gordon W. Wood and Devalla V. Ramana
Department of Chemistry, University of Windsor
Windsor, ON, Canada, N9B 3P4

A recent publication (1) demonstrated for a series of metal powders a close relationship between FDMS onset temperature and sample vapor pressure. Further, desorption onset was apparently unrelated to melting points, since ions were first detected considerably below the melting point for three of four metals, and significantly above the melting point in the fourth example.

We have conducted some preliminary FDMS experiments on a series of long-chain fatty acid homologues in an attempt to evaluate the relative importance of melting and vaporization in the onset of FD for organic compounds. For these well-characterized compounds the relation of boiling point (here expressed for $p = 10^{-6}$ Torr) to carbon number is a smooth curve while the melting points change in a series of steps (Fig. 1). Source temperatures used were either above ($85^{o}C$) or below ($52^{o}C$) the temperature ranges thus defined and they appear as dashed lines in the figure.

Our data show that for these fatty acids $D_{\frac{1}{2}}$ (anode current in mA at which the sample is one-half desorbed) approximates the boiling point curve more closely than the melting point curve (Fig. 2). The slope of the experimental points suggests that the effective pressure in the source may be somewhat higher than the arbitrarily chosen 10^{-6} Torr.

That melting of the sample also has an important effect on desorption is shown in Fig. 3 where desorption profiles taken above melting ($85^{o}C$) and below melting ($52^{o}C$) are compared.

Experiments designed to clarify and broaden these findings are in progress.

1. Okuyama, F.; Shen, G.-H. Int. J. Mass Spectrom. Ion Phys. 1981, 39, 327-337.

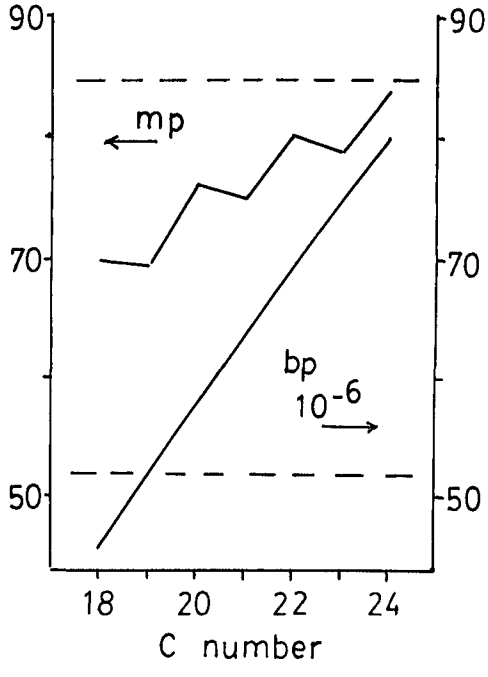


Fig. 1

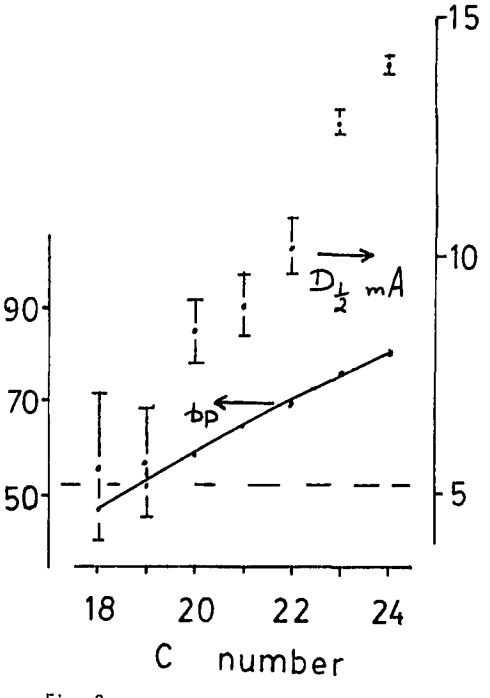


Fig. 2

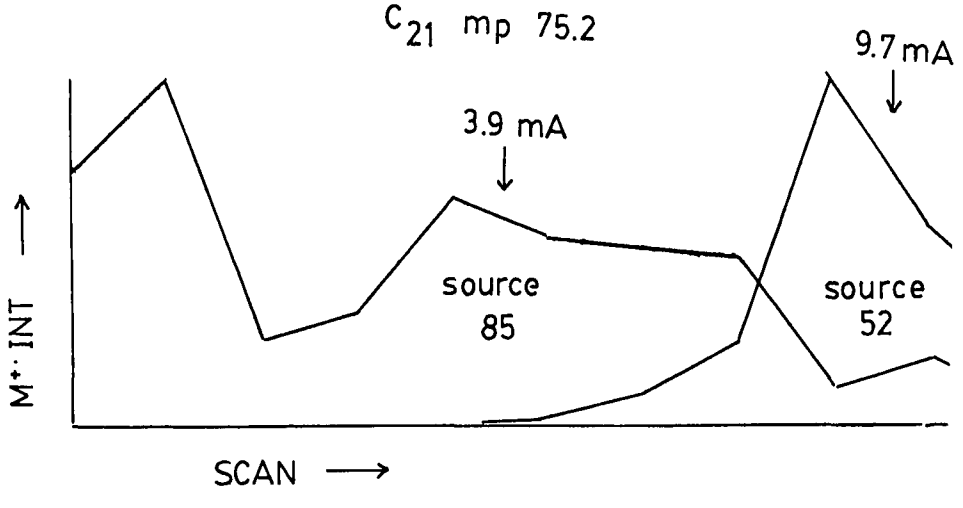


Fig. 3.

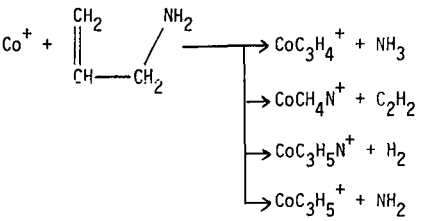
THE GAS PHASE CHEMISTRY OF METAL IONS WITH MULTI-FUNCTIONAL ORGANIC MOLECULES;
Huang, S.K.; Lombarski, M.; McElvany, S.; Radecki, B.D.; Tsarbopoulos, A.; and
Allison, J., Michigan State University, Chemistry Department, East Lansing, MI
48824

Transition metal (+1) ions react in the gas phase with a number of polar compounds by the general process[1]

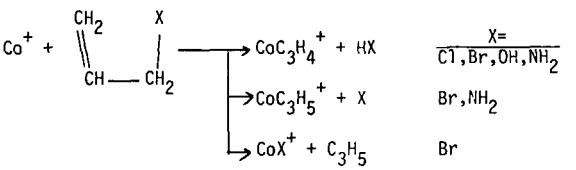
$$Co^+ + R\text{-}X \longrightarrow Co(R\text{-}H)^+ + HX \qquad (1)$$

that is, by a metal insertion, β-hydrogen atom shift mechanism.[2] Reactions of this type do not occur for simple amines, however, presumably because of the weakness of the $Co^+\text{-}NH_2$ bond which makes the insertion step thermodynamically unfavored. We place an upper limit on this bondstrength, $D(Co^+\text{-}NH_2) < 19$ kcal/mole.[3]

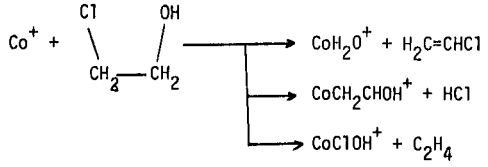
We have been studying the chemistry of metal- and metal-containing ions with a number of types of bifunctional molecules, in order to determine if metals will exhibit a preference for one functional group over another. In connection with our work with saturated amines, we find that allylamine does show evidence for metal insertion into C-N bonds.



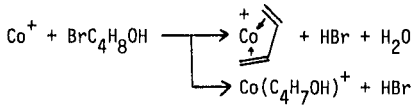
Apparently, the unusually strong bond between C_3H_5 (allyl group) and Co^+ makes insertion into the $C\text{-}NH_2$ bond favorable for this amine. For the bifunctional compounds where one group is an olefinic group, the metal appears to preferentially interact with halogen and alcohol groups over C=C double bonds.



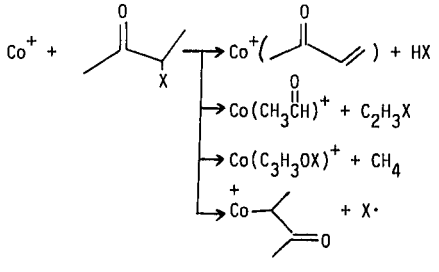
When two functional groups are on adjacent C atoms in an organic molecule, Co^+ can interact with either or both at the same time, e.g.



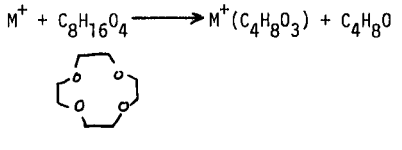
Apparently the Co^+ can react with such molecules via a five-membered ring intermediate. If, however, the functional groups are farther apart, the metal must "choose" which site is preferred. 1,4-bifunctional butanes such as this shown here, indicate that the interaction between Co^+ and halogens is stronger than between the metal and the alcohol functionality.



Substituted ketones contrast with the above result. Halogenated ketones form products typical for ketones (insertion into R-COR' bonds) and typical for halides (insertion into C-X bonds).



Finally, the recent interest in the interactions of metal ions with crown ethers in solution has prompted us to study the chemistry of gas phase metal ions with cyclic and straight chain polyethers. We find that metal ions such as Fe^+ and Cr^+ react with crown ethers and fragment the molecule.



We do however, find that metal-crown complexes can be formed in the gas phase by reactions such as

$$Cr(CO)_2^+ + C_8H_{16}O_4 \qquad Cr(C_8H_{16}O_4)^+ + 2CO$$

(Note - we don't see Fe^+-crown complexes). We estimate the interaction energy to be $D(Cr^+\text{-}C_8H_{16}O_4) = 77 \pm 11$ kcal/mole. (Compare this to $D(Cr^+\text{-}CO) = 26.6$ kcal/mole.)

References

1. J. Allison, D.P. Ridge, J. Amer. Chem. Soc., 101, 4998 (1979).
2. J. Allison, D.P. Ridge, J. Amer. Chem. Soc., 98, 7445 (1976).
3. B.D. Radecki, J. Allison, to appear in J. Amer. Chem. Soc.

MOE 2 ION CHEMISTRY IN THE ATMOSPHERE OF TITAN;
W. T. Huntress, Jr. and V. G. Anicich, Jet Propulsion Laboratory, California Institute of Technology, Pasadena, CA 91109.

The Voyager 1 investigation of Titan, Saturn's largest moon, revealed the presence of a complex, organically rich atmosphere containing a thick, orange-red cloud layer covering the entire satellite. The atmosphere is composed principally of N_2 containing 2% CH_4 with quantities of C_2H_2, C_2H_4, C_2H_6, C_3H_4, C_4H_2, HCN, C_2N_2 and HC_2CN in the parts-per-thousand range. Ion chemistry is initiated in Titan's upper atmosphere by solar ultraviolet photoionization and in the lower atmosphere by galactic cosmic rays. Laboratory work on ion-molecule reactions in mixtures of the species identified in Titan's atmosphere are being conducted using ion-cyclotron resonance techniques at JPL. The laboratory data base is being used to construct a model of Titan's upper atmospheric chemistry in collaboration with M. Allen and Y. Yung at the Caltech campus. The results of the laboratory and modeling work have so far revealed that ion chemistry may be important for the production of ammonia, higher-order hydrocarbons and unsaturated nitriles in Titan's atmosphere. Some of the haze layers observed in the upper atmosphere of Titan may be nucleated by the formation of large acetylenic and cyanoacetylenic polymer ions.

Electron Affinity Measurements Using Equilibrium Electron Transfer Reactions

Elaine K. Fukuda and Robert T. McIver, Jr.

Department of Chemistry
University of California
Irvine, California 92717

One of the fundamental properties of a negative ion is the lowest energy required to remove an electron. This energy is called the electron affinity (EA) and is equal to ΔE for the process $M^- = M + e$, where both the ion and the neutral are gaseous species in their ground states and the electron has zero kinetic and potential energy. Recently we have observed several exothermic electron transfer reactions which indicate that the electron affinities of nitrobenzene and SO_2 are considerably greater than is currently believed. The reactions were studied by pulsed ion cyclotron resonance (ICR) spectroscopy using a trapped ion analyzer cell to store the ions for several hundred milliseconds.[1] In addition equilbrium constants for ion-molecule reactions of the type

$$M^- + SO_2 = SO_2^- + M \qquad (1)$$

have been measured to get precise values ($\pm$ 0.01 eV) for the free energy change and relative electron affinities.

A pulsed ICR time plot of ion abundance *vs.* reaction time is shown in Fig. 1. Nitrobenzene was first added to a partial pressure of 4×10^{-6} torr, and then SO_2 was added to a partial pressure of 2×10^{-7} torr. The abundance of m/z 123^- increases rapidly at first and then decays as the abundance of m/z 64^- increases, eventually reaching a steady state condition. These data suggest that reaction 2 is exothermic and that the electron affinity of SO_2 is greater than that for nitrobenzene.

$$C_6H_5NO_2^- + SO_2 = SO_2^- + C_6H_5NO_2 \qquad (2)$$

The equilibrium constant for reaction 2 can be calculated and therefore the free energy change. The data shown in Fig. 1 give $\Delta G^\circ = -3.2 \pm 0.2$ kcal/mol. Figure 2 shows the results (ΔG°, kcal/mole) for several other equilibrium electron transfer reactions. Each reported value is the average of at least 3 experiments. Multiple overlaps were used to insure internal consistency of the data.

A second series of experiments have been performed to establish a reference point for the relative scale. An important one is the exothermic reaction of t-butoxide with nitrobenzene, which indicates that the electron affinity of nitrobenzene is greater than that for the *t*-butoxy radical (1.90 eV). Additional work in our laboratory has established that there is a gap of about 5 $\pm$ 2 kcal/mole between the electron affinity of nitrobenzene and the *t*-butoxy radical.[2] Assuming a value of 1.90 $\pm$ 0.01 eV for the electron affinity of $(CH_3)_3CO$ and applying a small correction for the estimated entropy change for the reaction the pulsed ICR data yield: $EA(C_6H_5NO_2) = 2.1 \pm 0.1$ eV and $EA(SO_2) = 2.2 \pm 0.1$ eV.

Previous work supports a value around 1.1 eV for the electron affinity of SO_2, considerably lower than our pulsed ICR value of 2.2 $\pm$ 0.1 eV.[3] Chemical evidence in support of the pulsed ICR value for $EA(SO_2)$ is shown in Table I. In all the cases for

which data are available, the electron affinity of a compound containing sulfur is greater than the homologous compound containing oxygen. If 1.1 eV were the correct electron affinity for SO_2, it would be lower than that for O_3, in striking reversal of the trend. In contrast, the pulsed ICR value of 2.2 eV is right in line with the trend.

If one assumes that the pulsed ICR electron affinity values are correct, a low value obtained by photoelectron spectroscopy and photodetachment may be explained by detachment from hot ions in the beam or a metastable electronic state of SO_2. Low values obtained by the endothermic electron transfer and cesium collisional ionization experiments imply that there is a large activation energy barrier for these reactions and the products are formed in excited states.

[1] R.T. McIver, Jr., Rev. Sci. Instrum., 49, 111 (1978)

[2] work to be published

[3] B.K. Janousek and J.I. Brauman, in "Gas Phase Ion Chemistry," M.T. Bowers ed., Vol. 2, Chapter 10 (1979)

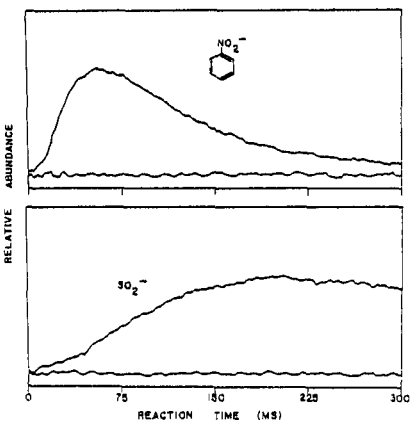


Figure 1. Pulsed ICR time plots of $C_6H_5NO_2^-$ and SO_2^-.

Comparison of Electron Affinities for Various *Oxygen and Sulfur Compounds*

Compound	Electron Affinity (eV)
O	1.462
S	2.0772
OH	1.83
SH	2.28
CH_3O	1.59
CH_3S	1.88
$(CH_3)_3CO$	1.90
$(CH_3)_3CS$	2.06
O_2	0.4
SO	1.126
S_2	1.663
C_6H_5O	< 2.36
C_6H_5S	< 2.47
O_3	2.0
SO_2	1.1 (lit.) or 2.2 (this work)

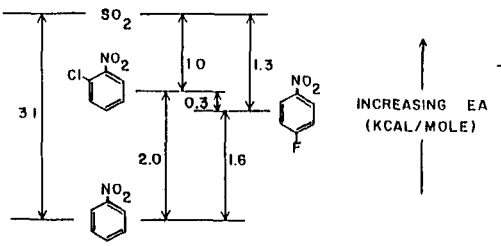


Figure 2. Results of equilibrium electron transfer reactions

DIPOLE STABILIZED ANIONS. John E. Bartmess, Gary Caldwell, and Melvin D. Rozeboom, Department of Chemistry, Indiana University, Bloomington, Indiana 47405, U.S.A.

Using ICR spectrometry, the stability of a variety of anions, stabilized not by direct resonance but by through space polar effects, has been measured. Both the acyl proton of DMF and the N-methyl site are more acidic than NH_3; the occurrance of side-reactions such as the Riveros reaction 1 and hydrolysis prevent assignment of a lower limit.

$$HO^- + HCONMe_2 \rightarrow HO^-\cdots HNMe_2 + CO \qquad (1)$$

Tetramethylurea readily hydrolyses to $Me_2NCO_2^-$ on attack of HO^-. Amides with larger N-alkyl groups undergo elimination to give $RCONR'^-$ with NH_2^-, HO^-, and various alkoxides. Formamidines $tBuN{=}CHNR_2$ have similar chemistry to the analogous formamides. Cycloheptenones are 10 kcal/mole more acidic than expected for a propene-type functionality indicated a transannular stabilization of the allyl anion by the carbonyl dipole. Similarly, 3-keto alcohols are at least 6 kcal/mole more acidic than predicted by linear free energy relationships.

MOE 5 UNIMOLECULAR AND BIMOLECULAR REACTIONS IN THE $C_4H_6^+$ SYSTEM: EXPERIMENT AND THEORY; Martin F. Jarrold, Paul R. Kemper, Lewis M. Bass, Petra A.M. van Koppen and Michael T. Bowers, Dept. of Chemistry, Univ. of Calif., Santa Barbara, CA. 93106.

A considerable amount of data exists in the literature on the $C_4H_6^+$ system. These include absolute unimolecular rate constants and product distributions as a function of internal energy measured by photoion-photoelectron coincidence and extensive metastable studies. A scattering of bimolecular data is also available. We have recently remeasured the absolute rate constants and branching ratios of the bimolecular reactions originating from $C_2H_4^+/C_2H_2$ and $C_2H_2^{+\cdot}/C_2H_4$ entrance channels. Deuterated reagents have also been used and the extent of scrambling in the various reaction channels determined. Kinetic energy distributions and relative metastable intensity ratios have recently been measured by us as well. All the data is analysed using the recently developed (1) Transition state switching model formalism of statistical rate theory. A detailed comparison between experiment and theory will be presented.

---

1. W.J. Chesnavich, L. Bass, T. Su and M.T. Bowers, J. Chem. Phys. 74, 228 (1981)

STUDIES OF THE AMMONIUM RADICAL BY NEUTRALIZED ION-BEAM SPECTROSCOPY

Gregory I. Gellene and Richard F. Porter
Department of Chemistry, Cornell University, Ithaca, NY 14853

Neutralized ion-beam spectroscopy is a technique for studying molecules formed in an electron capture process:

$$\underset{\text{(fast)}}{RH^+} + \underset{\text{(slow)}}{M(g)} \rightarrow \underset{\text{(fast)}}{RH} + \underset{\text{(slow)}}{M^+} \qquad (1)$$

The state of the radical products may be characterized as dissociative, predissociative, or stable. Dissociative states ($\tau < 10^{-13}$s) are identified by structureless broadening of the beam profile due to the components of the fragments velocity normal to the center of mass velocity vector. Alternatively, the profile of a stable state ($\tau > 10^{-5}$s) is characterized by a spacial distribution typical of the primary ion beam. The most interesting profiles are those which arise from predissociative states ($10^{-12} < \tau < 10^{-6}$s). Although the vast majority of these states will fragment prior to detection (transit time is 10^{-6} to 10^{-7}s), the broadened beam profiles will contain structure reflecting the presence of a predissociative barrier. In some cases this structure can provide information on barrier parameters which describe the potential along the dissociation coordinate.

This technique is illustrated by a study of the ground state potential of the ammonium radical produced in a fast electron capture process:

$$NH_4^+ \; Na(g) \rightarrow NH_4 + Na^+ \qquad (2)$$

Scattering profiles for heavy (NH_3) and light (H) dissociation products were obtained from beam measurements with 5-16 keV NH_4^+ ions. From these measurements the ionization potential of 4.73 ± 0.06 eV for NH_4 is calculated if rotational energy is neglected. The energy level diagram in Figure 1 shows the relative stability of the isotopically substituted ammonium radicals with respect to their dissociation products. Loss of deuterium atoms from isotopically mixed radicals, although energetically allowed, was not observed. This preferential loss of H atoms is consistent with a tunneling dissociation mechanism involving a predissociative barrier. The ND_4 radical has unusual stability with dissociation life-times for stable and unstable states differing by at least two orders of magnitude ($\tau > 20$ μs and $\tau < 150$ ns, respectively). The ground state of ND_4 lies close to or below its dissociation limit while the height of the dissociation barrier is between 0.33 and 0.40 eV above the fragmentation products of ND_3 and D. Whether the observed stability is thermodynamic or only kinetic cannot be determined from these results.

The magnitude of the zero point lowerings for deuterium substituted ammonium radicals parallels the scaling observed for the zero point lowerings for methane molecules (Figure 1). Regardless of the exact zero point spacings, the methane scaling demonstrates that the minimum in the radical electronic potential will lie approximately 0.2 eV below that of its dissociation products. The stabilities of CH_3NH_3 and CH_3ND_3 radicals have also been investigated and the conclusions about the ground state stability of the methylammonium radical are qualitatively similar to those for the ammonium radical. These results suggest that a barrier to dissociation is a general feature of the ammonium radical potential.

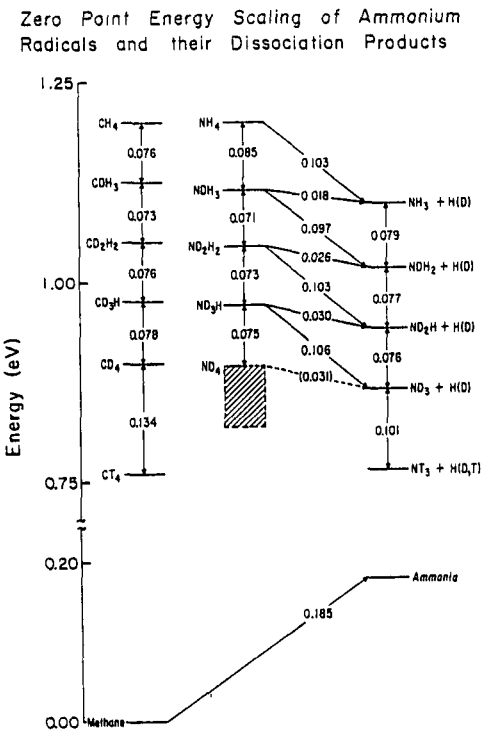


Figure 1. Energy scaling of isotopically substituted ammonium radicals with respect to their dissociation products.

REACTIONS OF VIBRATIONALLY EXCITED IONS WITH NEUTRALS IN A FLOW-DRIFT SYSTEM

M. Durup-Ferguson*, E.E. Ferguson, D.W. Fahey, H. Böhringer+ and F.C. Fehsenfeld

A study of several charge transfer reactions between diatomic and triatomic ions with neutrals is reported as a function of kinetic and vibrational excitation energy of the ions. The reactions include the charge transfer reactions $SO_2^+ + NO$, $CO_2^+ + O_2$, $CO_2^+ + NO$, $N_2O^+ + NO$ and the rearrangement reaction $O_2^+ + CH_4$.

The kinetic energy of the ions can be varied from thermal to $\sim$ 1 eV in a drift tube by varying the applied electric field and pressure of the buffer gas. For each ion-neutral center of mass kinetic energy the ion-buffer center of mass kinetic energy depends on the mass of the buffer gas leading to greater vibrational and rotational excitation in the heavier buffer.

All the reactions studied here exhibit the same behavior of the rate constants as a function of the kinetic energy: a decrease, followed by an increase, and an enhancement in the heavier buffer as regard to He. Two enhancement mechanisms may be involved: one operating in the low energy regime dominated by the collision complex and one operating in the higher energy regime dominated by a direct mechanism. By adding vibration relaxing molecules to the buffer, we have shown that in no case does the He buffer produce vibrational excitation of the ions in contrast to Ar and Ne. In every case the addition of a small percentage of the parent molecules of the ions gives (more likely by charge transfer) a considerable vibrational deexcitation.

Considering the total energy of the reacting ions, i.e. kinetic and vibrational energy, the studied reactions belong to three catagories.

1st: In the reaction $H_2O^+ + NO \rightarrow NO^+ + H_2O$, the addition of 3 kT (where T is the ion-buffer collision temperature), to the kinetic energy coordinate of the Ne buffer rate constant data brings the data into agreement with the He buffer rate constant data. This suggests that the ion vibrational energy qualitatively plays the same role as the translational energy in the reaction.

2nd: In the reaction $SO_2^+ + NO \rightarrow NO^+ + SO_2$, the rate constant data can be brought into agreement as above by the addition of $\frac{3}{2}$ kT to the kinetic energy coordinate in the Ar buffer data. This suggests that only the ion bending mode is efficient in enhancing the rate constant, presumably in a direct process. The rate constants for specific bending-mode vibrational states can be calculated by a fit to the rate constant data. The results are $k_{(v=1)} = 2.4\ k_{(v=0)}$ and $k_{(v>1)} = 3.6\ k_{(v=0)}$ for kinetic energy values between 0.04 eV and 0.4 eV.

3rd: The charge transfer reactions $CO_2^+ + O_2$, $CO_2^+ + NO$, and $N_2O^+ + NO$ involving linear ions exhibit a higher enhancement than due to four vibrational degrees of freedom. In this case, 8 kT would have to be added to the kinetic energy coordinate in order to fit Ar or Ne buffer constants with He ones.

A speculative explanation could be that due to the degeneracy of the bending vibration in linear ions a coupling of the vibration angular momentum with the orbiting angular momentum would enhance a larger lifetime of the intermediate complex and therefore the rate constant.

In the case of $O_2^+ + CH_4 \rightarrow$ products, the rate constant is also enhanced in Ar as

compared to He buffer. A crude analysis indicates that O_2^+ in the first several vibrational states reacts with CH_4 about fifteen times faster than ground state O_2^+. This enhancement is significantly quenched by the addition of O_2, which vibrationally relaxes O_2^+ by charge-transfer. An analysis of this process leads to the conclusion that O_2^+ (v=1) ions are vibrationally relaxed in about 1% of their collisions in Ar at 0.3 eV collision energy. O_2 quenching experiments in N_2 buffer show that N_2 also quenches O_2^+ (v) in 2-3% of the collisions at kinetic energies below 0.5 eV. The helium deexcitation efficiency is much less than 0.1% for O_2^+ (v) in the low energy (<0.13 eV) range.

The Flow Drift experiments open up a new technique for the study of vibrational excitation and deexcitation of ions at low energy as well as the dependence of ion-molecule reaction rate constants on vibrational excitation.

*Permanent Address: Laboratoire de Résonance Electronique et Ionique
Université de Paris Sud
91405 Orsay, France

+Permanent Address: Max-Planck-Institut für Kernphysik
Heidelberg, Germany

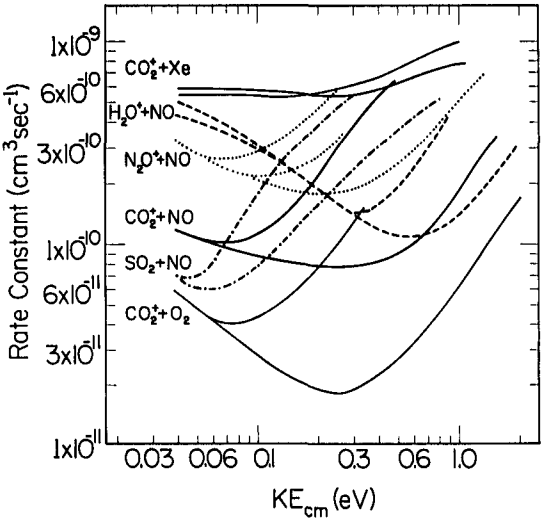
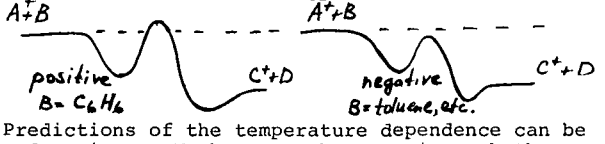


Figure 1. Rate constants for charge transfer reactions as a function of mean kinetic energy. Data are shown for each reaction for He and Ar buffer gases except for H_2O^+ + NO where the buffers are He and Ne and for N_2O^+ + NO where the buffers are He, Ne, and Ar.

MOE 8 ...TEMPERATURE DEPENDENCE OF ION MOLECULE REACTIONS. T.F. Magnera, D. K. SenSharma and P. Kebarle, Chemistry Department, University of Alberta, Edmonton, Canada T6G 2G2

The reactions $Me_2Cl^+ + B = MeB^+ + MeCl$ proceed at lower then orbiting rates for several Bases B. The temperature dependence for B = benzene was positive, while the temperature dependence for toluene, isopropylbenzene, Me_2O, Et_2O was negative. These results can be explained with the assumption that the reaction coordinate has a substantial internal energy barrier as shown.



Predictions of the temperature dependence can be made using RRKM theory. The question, whether hydride transfers with negative temperature dependence, have internal barriers was explored. Calculations for the reaction: iso-$C_3H_7^+$ + iso-C_4H_{10} = C_3H_8 + tert-$C_4H_9^+$ did not give a good fit to the experimental temperature dependence of Mautner and Field, if the assumption was made that the transition state occurs on top of an internal barrier. A good fit could be obtained by assuming that the transition state occurs at the Langevin complex. The inefficiency at high temperature is due to reactants with high rotational quantum numbers. The centrifugal barrier for these cases occurs at a distance between the two reactants which is small. At this small distance each reactant can not rotate freely as is required for the loose complex that leads to unit collision efficiency.

MOE 9 ION-MOLECULE REACTIONS AND STRUCTURES OF HYDROCARBON IONS RELEVANT IN COMBUSTION; F. W. Brill and J. R. Eyler, Department of Chemistry, University of Florida, Gainesville, FL 32611

We have undertaken a series of experiments to study the reactivities, structures, and thermochemistry of hydrocarbon ions which may be important (D. B. Olson and H. F. Calcote, Proc., 8th Symp. (Int'l.) on Combustion, The Combustion Institute, 1981, p. 453) in soot nucleation. Initial investigations used ion cyclotron resonance (icr) mass spectrometry to monitor sequential ion-molecule reactions in acetylene, involving ions such as $C_4H_2^+$, $C_4H_3^+$, $C_6H_4^+$ and $C_6H_5^+$ (F. W. Brill and J. R. Eyler, J. Phys. Chem., 1981, 85, 1091). We have also used icr, collision-induced decomposition (cid) techniques in a ZAB-2F mass spectrometer, and reactive scattering in a triple quadrupole mass spectrometer to study the structures of a number of $C_3H_x^+$, $C_5H_x^+$, and $C_6H_x^+$ ions. Rates of ion-molecule reactions involving these ions and a number of flame neutrals, and results of structure differentiation studies involving these ions will be presented. Implications for soot formation will be discussed.

FLOWING AFTERGLOW AND SELECTED ION FLOW TUBE STUDIES OF THE REACTIONS OF H_2N^-, H_2P^-, HO^- AND $H^{18}O^-$ WITH N_2O, CO_2, SO_2, CS_2 AND OCS

Veronica M. Bierbaum, Charles H. DePuy, Joseph J. Grabowski and David Richard Anderson

Department of Chemistry, University of Colorado, Boulder, Colorado 80309

We have employed the flowing afterglow and SIFT techniques to synthesize a variety of novel anions of nitrogen, phosphorous and sulfur and to probe the mechanism of their formation. Amide reacts readily with nitrous oxide, carbon dioxide, carbon disulfide and sulfur dioxide to form, respectively, N_3^-, OCN^-, SCN^- and OSN^-.

$$H_2N^- + N_2O \rightarrow N\text{-}N\text{-}N^- + H_2O \qquad k = 3.0 \times 10^{-10}$$

$$H_2N^- + CO_2 \rightarrow O\text{-}C\text{-}N^- + H_2O \qquad k = 1.1 \times 10^{-9}$$

$$H_2N^- + CS_2 \rightarrow S\text{-}C\text{-}N^- + H_2S \qquad k = 1.8 \times 10^{-9}$$

$$\rightarrow HS^- + SCNH$$

$$H_2N^- + SO_2 \rightarrow O\text{-}S\text{-}N^- + H_2O \qquad k = 3.0 \times 10^{-9}$$

$$\rightarrow SO_2^- + H_2N$$

We picture the reaction proceeding in the following manner:

$$H_2N^- + CO_2 \rightarrow \left[H_2N\text{-}\underset{\underset{O^-}{|}}{C}\text{=}O\right]$$

$$\downarrow$$

$$^-N\text{-}C\text{-}O + H_2O \rightarrow \left[HN\text{-}\underset{\underset{OH^-}{|}}{C}\text{=}O\right]$$

The anion and neutral are attracted by ion-dipole forces into a complex which can redissociate, be stabilized by collision, or as represented above, undergo further reaction. Proton transfer from nitrogen to oxygen followed by loss of hydroxide generates a new complex; proton abstraction by HO^- with dissociation of the complex forms the cyanate ion and water. In the reaction of amide with carbon disulfide, this final proton transfer step does not proceed to completion and HS^- is observed as a product in addition to SCN^-. In the reaction of amide with sulfur dioxide, electron transfer is the dominant channel since the electron affinity of SO_2 exceeds that of H_2N.

In an attempt to explore competitive intramolecular proton transfer to sulfur versus oxygen, we examined the reaction of amide with carbon oxysulfide.

$$H_2N^- + SCO \rightarrow O\text{-}C\text{-}N^- + H_2S$$

$$\rightarrow HS^- + OCNH \qquad K = 1.9 \times 10^{-9}$$

$$\rightarrow H_2NS^- + CO$$

The first two channels, formation of OCN^- and HS^- are in direct analogy to the reaction of CS_2, and proceed by initial proton transfer to sulfur.

$$\nearrow \left[\underset{\underset{OH}{|}}{H\bar{N}C}\text{=}S\right] \rightarrow \left[HNCS\right]\left[HO^-\right] \rightarrow NCS^- + H_2O$$

$$\left[\underset{\underset{O^-}{|}}{H_2NC}\text{=}S\right] \quad \downdownarrows$$

$$\searrow \left[\underset{\underset{O}{|}}{H\bar{N}C}\text{-}SH\right] \rightarrow \left[HNCO\right]\left[HS^-\right] \rightarrow HS^- + HNCO$$

$$\rightarrow NCO^- + H_2S$$

Lack of production of SCN^- indicates that one of the steps in this mechanism, either proton transfer to oxygen or rearrangement to HNCS and HO^-, is unfavorable. The third pathway in the reaction of amide with OCS generates the interesting species H_2NS^-. Carbon oxysulfide similarly serves as a sulfur atom donor to a variety of negative ions, generating a series of novel sulfur-containing products:

$$(CH_3)_2N^- + SCO \rightarrow (CH_3)_2NS^- + CO$$

$$C_6H_5^- + SCO \rightarrow C_6H_5S^- + CO$$

$$CH_2{=}CHCH_2^- + SCO \rightarrow CH_2{=}CHCH_2S^- + CO$$

$$N{\equiv}CCH_2^- + SCO \rightarrow N{\equiv}CCH_2S^- + CO$$

The reactions of phosphide show many similarities to those of amide:

$$H_2P^- + N_2O \rightarrow N{=}N{-}P^- + H_2O \qquad k = 2.3 \times 10^{-12}$$

$$\rightarrow H_2PO^- + N_2$$

$$H_2P^- + CO_2 \rightarrow H_2PCO_2^- \qquad k < 1.0 \times 10^{-12}$$

$$H_2P^- + CS_2 \rightarrow S{=}C{=}P^- + H_2S \qquad k = 1.4 \times 10^{-10}$$

$$\rightarrow PS^- + H_2CS$$

$$H_2P^- + SO_2 \rightarrow O{=}S{=}P^- + H_2O \qquad k = 2.9 \times 10^{-11}$$

$$\rightarrow SO_2^- + H_2P$$

$$\rightarrow PO_2^- + H_2S$$

$$H_2P^- + SCO \rightarrow O{=}C{=}P^- + H_2S \qquad k = 3.2 \times 10^{-11}$$

$$\rightarrow H_2PS^- + CO$$

The most striking differences include a) the considerably decreased reactivity of H_2P^- relative to H_2N^-; b) formation of only adduct in the reaction of phosphide with carbon dioxide; c) existence of new product channels which generate H_2PO^-, PS^- and PO_2^-.

The reactions of hydroxide with nitrous oxide, carbon dioxide and sulfur dioxide proceed only by simple association. However, a mechanism similar to that exhibited by amide or phosphide (i.e., association with intramolecular proton transfer) would be hidden unless labeled hydroxide were employed:

$$^{\cdot}OH^- + CO_2 \rightleftharpoons \left[H^{\cdot}O{-}\underset{\underset{O^-}{|}}{C}{=}O\right] \overset{M}{\rightleftharpoons} HCO_2O^{\cdot -}$$

$$\downarrow$$

$$\left[^{-}{}^{\cdot}O{-}\underset{\underset{OH}{|}}{C}{=}O\right] \rightarrow \left[^{\cdot}O{-}C{=}O \;\; OH^-\right] \rightarrow OH^- + {}^{\cdot}OCO$$

Using our newly constructed selected ion flow tube we injected $H^{18}O^-$ from the mixture of ions resulting from electron impact on H_2O^{18}/H_2O^{16}. Upon addition of N_2O, CO_2 or SO_2 we observed facile production of unlabeled hydroxide:

$$^{18}OH^- + N_2O \rightarrow OH^- + N_2O^{18} \qquad k = 1.2 \times 10^{-11}$$

$$^{18}OH^- + CO_2 \rightarrow OH^- + {}^{18}OCO \qquad k = 5.7 \times 10^{-10}$$

$$^{18}OH^- + SO_2 \rightarrow OH^- + {}^{18}OSO \qquad k = 1.2 \times 10^{-9}$$

This observation confirms that intramolecular proton transfer within the reaction complex occurs on timescales much shorter than required for collisional stabilization of the adduct.

NO_2^+ ION FORMED BY THE $N_3^+ + O_2$ REACTION

S. MATSUOKA, H. NAKAMURA and T. TAMURA (Nucl. Eng. Res. Laboratory, Univ. of Tokyo, Tokai-mura, Ibaraki-ken, JAPAN)

INTRODUCTION

In a relatively high pressure N_2-O_2(trace) gas system, N_3^+ and N_4^+ are formed as pseudo-primary ions by electron impact, discharge, or irradiation. The ion N_3^+ reacts with O_2 as follows:

$$N_3^+ + O_2 \xrightarrow{k_1} \begin{cases} NO^+ + N_2 + O & (1a) \\ NO_2^+ + N_2 & (1b) \end{cases}$$

Recently we found that the NO_2^+ ion thus formed further changes to NO^+ ion.[1] That is,

$$NO_2^+ + \cdots \xrightarrow{k_2} NO^+ + \cdots \qquad (2)$$

Here we report that the NO_2^+ ion formed by Reaction (1b) has a different reactivity from that of nitrogen dioxide cation $(O\text{-}N\text{-}O)^+$ and also report a reliable product ion ratio of Reaction (1), $NO_2^+/NO^+(=r)$, for which much conflicting values were reported so far.

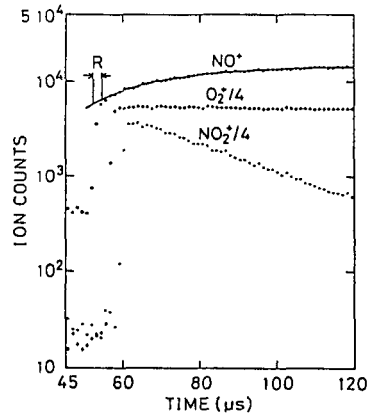


FIG. 1. Time-dependence curves of product ion intensities for N_2-O_2(1050 ppm) gas at 303 K.

EXPERIMENTAL

Experiments were performed using a time-resolved atmospheric pressure ionization mass spectrometer (TRAPI).[1,2] Its details are described elsewhere[1] and a brief summary will be given here. Repetitive x-ray pulses generate ions uniformly in the gas flowing through the reactor. Part of them issuing out into the vacuum chamber through a pinhole aperture is mass-analyzed by a quadrupole mass spectrometer and then pulse-counted by a detection system forming a mass spectrum of ions and time-dependence curves of mass-selected ion intensities. Time-resolution of time-dependence curves is 1-2 μs. Dose per x-ray pulse is 34 mR which generates 6.4×10^7 ions/cm^3 in nitrogen gas (STP).

RESULTS AND DISCUSSION

A. Reactivity of NO_2^+

Figure 1 shows semilog plots of O_2^+, NO^+, and NO_2^+ counts vs time obtained for N_2-O_2(1050 ppm) gas at 303 K and 760 Torr. As O_2^+ ion formed by the reaction of N_4^+ with O_2 is stable in this gas system, its intensity shows little decrease with time. On the other hand the NO_2^+ intensity decreases by Reaction (2) and the reaction rate constant k_2 can be determined from the decay slope of NO_2^+ in Fig. 1. The values of k_2 (s^{-1}) at various temperatures and for various concentrations of nitrogen and oxygen are given in Fig. 2 in Arrhenius plots. Oxygen contents from 95 to 4550 ppm (total pressure = 760 Torr) and nitrogen pressure from 760 to 1110 Torr (oxygen content = 1050 ppm) do not affect k_2 value. Temperature, however, significantly affect k_2 value, giving

$$k_2 = 5.6 \times 10^7 \exp(-4500/RT)\ s^{-1}$$

In addition to the bare ions the ion clusters with nitrogen molecules are also observed. The degree of clustering is significantly influenced by temperature and pressure of the gas.

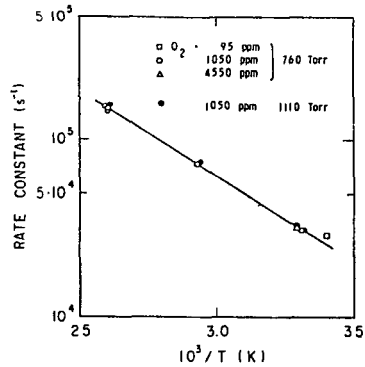


FIG. 2. Arrhenius plots of k_2 value for various oxygen and nitrogen concentrations.

However, identical time-dependence curves in form are obtained whether ions have nitrogen clusters or not.

Figure 3 represents semilog plots of O_2^+, NO^+, NO_2^+, $C_3H_7^+$, $C_4H_{10}^+$, and $C_4H_9^+$ counts vs time obtained for N_2-O_2(1050 ppm)-n-C_4H_{10}(0.94 ppm) gas at 303 K and 760 Torr. These curves show that the O_2^+ and NO_2^+ ions react with the added n-butane producing $C_4H_{10}^+$ and $C_3H_7^+$. The reaction rate constants are obtained from their decay slopes as 1.5×10^{-9} and 1.0×10^{-9} cm^3 s^{-1}, respectively. This value for NO_2^+ is nearly one order of magnitude larger than the reported value[3] for the hydride transfer reaction between nitrogen dioxide cation and n-butane. In the calculation of rate constants about 20% correction for the presence of unbidden water has been made whose quantity can be evaluated from the decrease of NO^+ intensity due to the reaction, $NO^+ + H_2O(+N_2) \rightarrow NO^+ \cdot H_2O(+N_2)$.

The above results, with a usual consideration that excess energy of NO_2^+ given by Reaction (1b) would be promptly relaxed in nitrogen gas at atmospheric pressure, show that NO_2^+ has a different isomeric form from that of nitrogen dioxide cation $(O\text{-}N\text{-}O)^+$. Reaction (2) is considered to be a unimolecular decomposition.

B. Measurement of $NO_2^+/NO^+(=r)$

The time-dependence curve of NO^+ intensity is given by the following equation.

$$[NO^+] = \frac{[N_3^+]_0}{1+r}\left[\left\{1 + r - (1 - \frac{k_2 r}{k_1[O_2]-k_2})\exp(-k_1[O_2]t)\right\} - \frac{k_1[O_2]r}{k_1[O_2]-k_2}\exp(-k_2 t)\right] \quad (3)$$

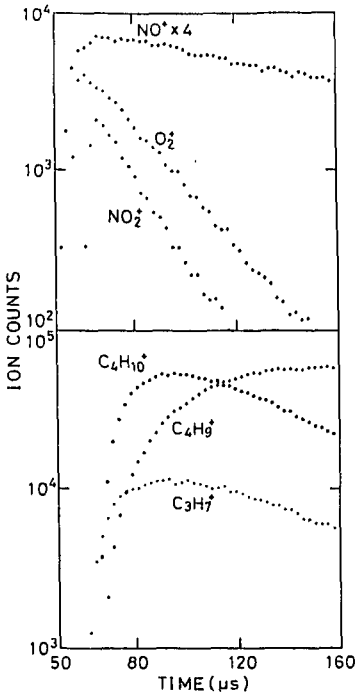


FIG. 3. Time-dependence curves of product ion intensities for N_2-O_2(1050 ppm)-n-butane(0.94 ppm) gas at 303 K.

The solid line given by Eq.(3) with $\exp(-k_1[O_2]t)=0$ is drawn in Fig. 1 to fit the experimental points in the region where $\exp(-k_1[O_2]t)$ term diminishes. If the "effective starting point", i.e. t=0 point, on the solid line is determined, the ratio r can readily be obtained. This point can be determined within 3 μs uncertainty in the figure (R in Fig. 1), the uncertainty arising from the resolving time of TRAPI and a necessary time for Reaction (1) to be completed. The ratio measured in this study is 1.72 ± 0.2, the error being due to the uncertainty of the "effective starting point". On the other hand Smith et al. obtained the ratio of 0.43 at a pressure of 0.65 Torr (He = 0.45 and N_2 = 0.20 Torr) in a selected ion flow tube method (SIFT)[4] and McCrumb and Warneck the ratio of 1.33 at N_2=3.4 Torr in a drift-tube mass spectrometer (DTMS)[5]. In a SIFT technique the product ions are detected after ~100 μs of their formation. Thus part of NO_2^+ ion would be converted to NO^+ by Reaction (2) even at a pressure of 0.65 Torr. In a DTMS this period should be much shorter than in a SIFT, giving the measured ratio closer to our value.

The ratio r showed a slight decrease with increasing temperature. This, however, might be due to Reaction (2) occurring outside the reactor near the pinhole aperture.

References

1. S. Matsuoka, H. Nakamura, and T. Tamura, J. Chem. Phys. 75, 681 (1981).
2. Y. Ikezoe, S. Shimizu, S. Sato, S. Matsuoka, H. Nakamura, and T. Tamura, Radn. Phys. Chem. in press.
3. P. Ausloos and S.G. Lias, Int. J. Chem. Kinet. 10, 657 (1978).
4. D. Smith, N.G. Adams, and T.M. Miller, J. Chem. Phys. 69, 308 (1978).
5. J.L. McCrumb and P. Warneck, J. Chem. Phys. 66, 5416 (1977).

GAS DYNAMICS AND DESIGN CONSIDERATIONS FOR INTRODUCING FAST ELUTING GAS CHROMATOGRAPHIC PEAKS FROM CAPILLARY COLUMNS INTO A VACUUM SYSTEM

Paul C. Goodley and William R. Hamburgen, Hewlett-Packard Company, 1601 California Avenue, Palo Alto, California 94304

Recent developments in separation science using small bore fused silica capillary columns for gas chromatography have brought about the need for a closer examination of the effects of gas dynamics on sample introduction into the mass spectrometer vacuum system. Current GC capillary columns having an inner diameter of 0.2 mm produce peak widths of 300 to 600 milliseconds at half-height. More recent developments using smaller microbore tubing of 40 to 100 μm capillary columns (1-3) have shown peaks to be in the 30 to 100 msec. range at half-height. These fast eluting peaks have revealed peak shape and yield deficiencies which can also cause losses in GC column resolution prior to the MS detector which compromises the original efficiency capabilities of the column design.

Three important design considerations for interfacing a GC to an MS are: (1) thermal, (2) chemical reactivity, and (3) gas dynamics. The gas dynamics are examined in this paper. Figure 1 depicts the test system used to acquire the data. It consisted of a low dead-volume sampling valve (Figure 2) coupled to an atmospheric split device (4-6) (Figure 3) which was coupled to a turbomolecular vacuum pump. The valve was actuated pneumatically and injected a 0.2 μL volume of nitrogen gas into a helium stream. The detection of the injected nitrogen peak was accomplished by taking advantage of the differences in response of the nude Bayard-Alpert ion gauge tube to each of the gases. The vacuum system pump-out time constant for the 225 cc volume was calculated to be four milliseconds. The reproducibility of the total system was measured by using an HP 3390 Integrator to integrate the area under the peak of the injected volume of nitrogen gas, which showed less than a 1% standard deviation for 200 samples. The detector signal from the B-A gauge was fed into an FET high gain amplifier and into an analog-to-digital converter for the data acquisition. The data was acquired at 1.22 kHz or 820 microseconds for each data point yielding 2000 data points for each experiment.

The effects of various gas interface design parameters on the peak shape were examined by comparing the ratios of the width of front half of the peak to the width of the rear half at various heights ranging from 13.4 to 88.2% of maximum height (Figure 4). For an ideal symetrical peak these ratios would be unity. Figure 5 depicts the effects of varying the end-to-end spacing of the column to the vacuum line in the gas interface. Degradation of peak shape was pronounced with increasing end-to-end spacing when reverse scavenge gas flow was used. Conversely, peak shape was relatively insensitive to spacing when forward direction scavenge gas flow was used.

An important observation not illustrated by a figure in this paper was the effect of the scavenge sleeve diameter on peak shape. The peak shape improved as the clearance between the sleeve and the coupled lines was reduced. In addition, lower scavenge gas flow improves the peak shape and yield, however, zero flow appears to cause degradation of peak shape. Most of this degradation is likely due to the disruption of laminar flow along the sleeve walls, especially when shear forces are induced by fluid flow in opposite directions.

These experiments indicate optimum peak shape and chromatography can be obtained using gas interface couplings by: (1) using close fitting scavenge sleeves, (2) close end-to-end spacing, and (3) low forward scavenge gas flow.

Extension of this experiment for the comparison between direct coupling and open split gas coupling would require a fast acting sampling valve with a closing transit time of 10 msec.

1. Bertsch, W., Private Communication (1981).
2. Stark, T., Private Communication (1982).
3. Yang, F. J. and S. P. Cram, Pittsburgh Conference on Analytical Chemistry #115 (1981).
4. Henneberg, D., U. Henrichs, and G. Schomburg, Chromatographia 8: 449-451 (1975).
5. Henneberg, D., U. Henrichs, J. Husmann, and G. Schomburg, J. Chromatog. 167: 139-147 (1978).
6. Kenyon, C. and P. C. Goodley presented at 29th Annual Conference on Mass Spectrometry and Allied Topics, Minneapolis, Minnesota, May (1981).

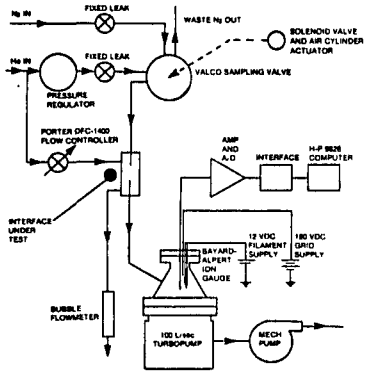


Figure 1.

TEST SYSTEM CONFIGURATION

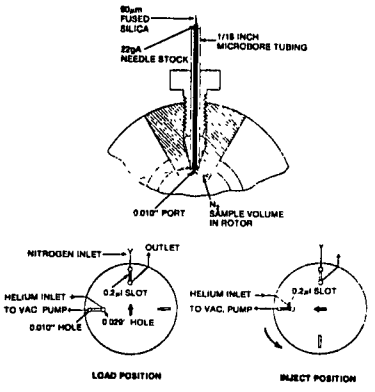


Figure 2.

LOW DEAD VOLUME SAMPLING VALVE

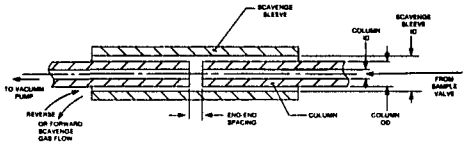


Figure 3.

GAS INTERFACE

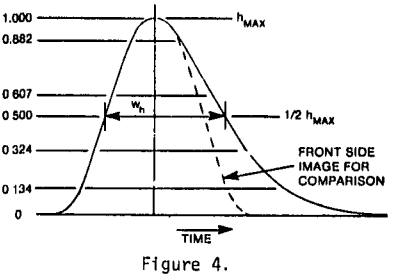


Figure 4.

POISSON DISTRIBUTION

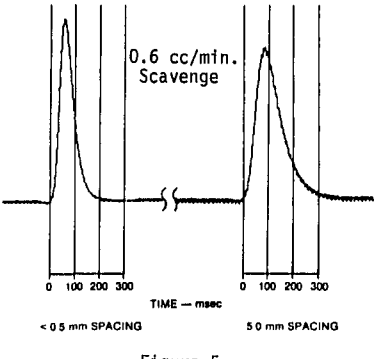


Figure 5.

EFFECT OF END TO END SPACING REVERSE SCAVENGE GAS FLOW

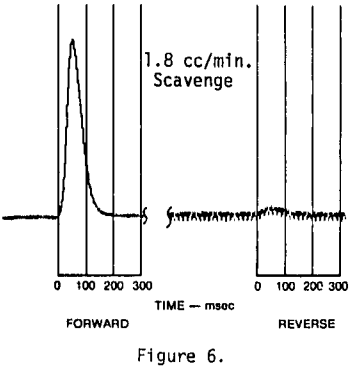


Figure 6.

EFFECT OF FORWARD AND REVERSE SCAVENGE GAS FLOW AT 5mm END TO END SPACING

CAPILLARY COLUMN SUPERCRITICAL FLUID CHROMATOGRAPHY-MASS SPECTROMETRY[a]

Richard D. Smith*, John C. Fjeldsted[b] and Milton L. Lee[b]

Chemical Methods and Kinetics Section
Physical Sciences Department
Pacific Northwest Laboratory
Richland, WA 99352

The analysis of complex mixtures of biochemical, environmental, synthetic fuels, and similar substances is hindered by the molecular weight range and selectivity of present analytical instrumentation. Liquid chromatography can be used to separate higher molecular weight and less volatile compounds. However, the chromatographic resolution of liquid chromatography is much less than with modern capillary column GC; the solvating capability of the mobile phase is often insufficient for large compounds containing several functional groups; and a sensitive and selective detector is required. Modern high performance liquid chromatography (HPLC) is rapidly approaching the practical limits on the number of effective theoretical plates; additional limitations arise from the lack of sufficiently sensitive or selective detectors. The ideal detector for HPLC is the mass spectrometer due to its inherent sensitivity and selectivity. However, interfacing these instruments is a difficult task and is limiting due to fundamental incompatibilities in liquid flow rate, and solvent evaporation or removal.

The use of capillary column supercritical fluid chromatography (SFC) offers the solution to these problems. The potential advantages of SFC accrue from the nature of the supercritical fluid. In SFC the mobile phase is maintained at a temperature somewhat above its critical point. The density of the supercritical phase is typically several hundred times greater than that of the gas, but significantly less than that of the liquid. Thus, the properties are intermediate between those of a gas and those of a liquid. The shorter intermolecular distances result in increased molecular interactions manifested by an increase in the solubilizing power of the mobile phase for the solute. This results in the capability of a much wider range of applications than available to GC, including the chromatography of very high molecular weight compounds (>3000). The mild thermal conditions (determined by the choice of SFC mobile phase) allow the application of SFC to thermally labile compounds. Additionally, since the solvating capability of the mobile phase is dependent upon pressure, one has the capability for accurate control of this parameter. Thus in SFC one can use pressure programming in a manner analogous to temperature programming in GC. Another advantage of SFC is the substantially lower partition ratios observed relative to GC, resulting in the ability to chromatograph large molecules with reasonable retention times.

A prototype capillary SFC-MS instrument has been developed at Battelle-Northwest to investigate the range of SFC applications. Figure 1 gives a schematic illustration of the instrumentation.

Figure 2 illustrates the application of the capillary SFC-MS to a mixture of five polycyclic aromatic hydrocarbon compounds in methylene chloride. The separation used a 0.2-mm x 20-m column and n-pentane as the mobile phase. The SFC pressure program used 15 minutes at 20 atm followed by a pressure increase of 0.8 atm/min to 40 atm. The injected mixture contained a nominal 40 ng of naphthalene, anthracene, pyrene, benzo[a]pyrene and coronene. The results show the mixture is easily separated and demonstrated results comparable to conventional HPLC separations. The application to an 800 average molecular weight polystyrene sample is illustrated in Figure 3. These results show that each polystyrene oligomer is clearly resolved and detected by the mass spectrometer. These results demonstrate the efficient detection of essentially nonvolatile molecules. In addition, numerous thermally labile compounds have been successfully analyzed in our laboratory using carbon dioxide as the supercritical fluid.

In summary, a capillary column SFC-MS has been developed and tested, and initial results suggest that excellent separations and sensitivities are possible with appropriate method development. The SFC-MS interface designed in this work resembles the direct liquid injection technique used for LC-MS with three major differences: 1) optimum separations are obtained by maintaining constant temperature conditions to as close to the ion source as possible, 2) the SFC-MS interface avoids liquid-gas phase transitions during injection into the ion source, and 3) the pressure restrictor size is the major factor in determining mobile phase flow rate. Advantages of the capillary SFC DFI mass spectrometer interface accrue due to the low flow rates, high mobile phase volatility, and the capability for mixed CI reagents.

Additionally, the SFC-MS interface seems to allow more efficient detection of nonvolatile or thermally labile compounds than in LC-MS and appears to be much less likely to suffer from plugging of the DFI probe orifice. Finally, a capillary column SFC-MS interface can be adapted to most GC-MS instruments with only slight modification.

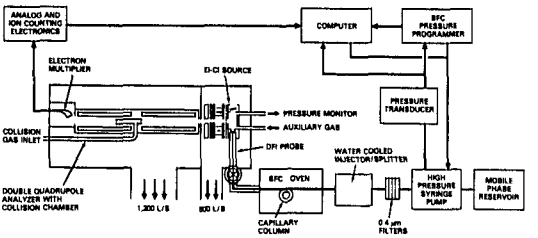


Figure 1
Overall schematic illustration of the capillary column SFC-MS developed in this work.

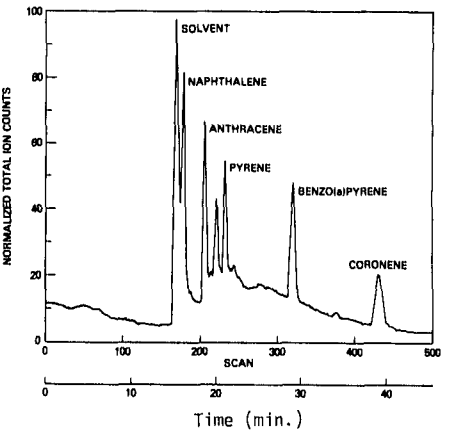


Figure 2
Total reconstructed ion chromatograph for a SFC-MS analysis of a mixture of five polycyclic chromatic hydrocarbon compounds and associated impurities.

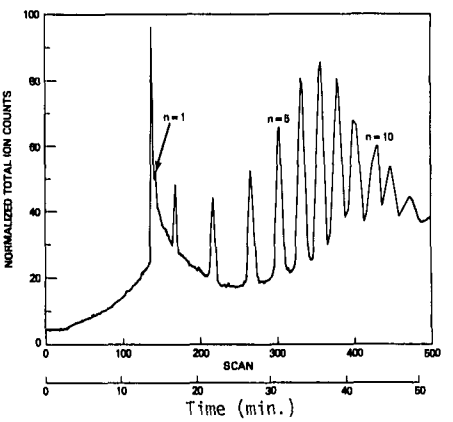


Figure 3
Total ion chromatogram for the SFC-MS analysis of a polystyrene sample having an average molecular weight of 800. The chromatogram shows the first twelve oligomers which have molecular weights of 104 n + 58.

a) Prepared for the U.S. Department of Energy under Contract DE-AC06-76RLO 1830.
b) Department of Chemistry, Brigham Young University, Provo, UT 84602

A STUDY OF THE DISSOCIATION PHENOMENA IN ELECTROSTATIC AND QUADRUPOLE COLLISION CHAMBERS IN AN API-MS/MS SYSTEM

V. Caldecourt, J. Tou and D. Zakett
Analytical Laboratory, Michigan Division
Dow Chemical Company, Midland, MI 48640

In Dow's atmospheric pressure ionization tandem section quadrupole mass spectrometer (API-MS/MS) (1), there are two collision chambers, an electrostatic focused declustering chamber and a quadrupole focused collision chamber. Both chambers perform similar functions but with significantly different characteristics.

The energy spread in the ion beam of the m/z 112 ions from chlorobenzene traversing the declustering chamber is seen to be small from the retarding potential curve I, obtained by plotting the electron multiplier current as a function of the field axis potential of the first quadrupole, Q1, in Figure 1. Curve II is a similar plot for the electron multiplier current as a function of the field axis potential of Q2. The energy spread has increased 4-5 fold, apparently because of the RF fields in Q1, and has become large enough to affect the peak shape in a Q3 spectrum. These measurements were made without collision gas added.

From the retarding potential data taken on Q3 with a nominal axial energy of 100 ev it can be seen in Figure 2 that the range of energies encountered upon collisionally activated decomposition in Q2 is very large. The parent ion shows an energy spread similar to that seen in Figure 1. Another part of this energy spread can be explained by the partitioning of the energy of the parent ion (2) between the fragment ions and the neutrals. However, the energy distribution curves for the fragment ions extend nearly to the source potential (V_B) for m/z 51 and past the source potential for m/z 77 indicating that part of the collisionally activated dissociation took place between Q1 and Q2 where the axial ion energy was low. Such a wide energy spread will cause considerable deterioration of the peak shape and resolution in spectra generated by Q3. At lower axial energies, e.g. 20 ev, the energy spread will again be approximately equal to the axial energy and will still be a significant problem.

The declustering chamber shows excellent efficiency at converting the molecular ions to the two major fragments with increasing applied potential in the data presented in Figure 3. Figure 4 shows similar data for the fragmentation produced in the quadrupole collision cell where the conversion of molecular ions appears less efficient. Possibly this is caused by a combination of mass discrimination and scattering losses.

Fragmentation in the quadrupole collision cell is also a function of the RF voltage. This effect is most apparent at low nominal axial ion energies. In Figure 5, the intensity of the molecular ions and major fragments is plotted as a function of RF voltage when the nominal axial ion energy is 5 ev. The increase in the percent yield of the fragments at m/z 51 and 77 are shown in Figure 6. Since previous theoretical work (3) indicates that the RF fields in the quadrupoles would not contribute significantly to the axial ion energy, it is suspected that this effect is caused by the fringing RF fields at the quadrupole ends.

References

(1) V. Caldecourt, D. Zakett, J. Tou, 29th Annual Conference of the American Society for Mass Spectrometry, May 24-29, 1981 pg. 668
(2) P. H. Dawson and D. J. Douglas, 29th Annual Conference of the American Society for Mass Spectrometry, May 24-29, 1981 pg. 116
(3) R. A. Yost, C. G. Enke, D. C. McGilvery, D. Smith, J. P. Morrison, Int. J. Mass Spectrom. Ion Physics, 30 127 (1979)

Figure 1.

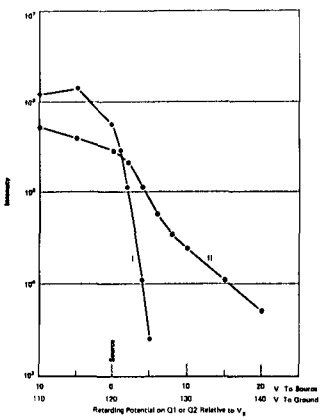


Figure 2.

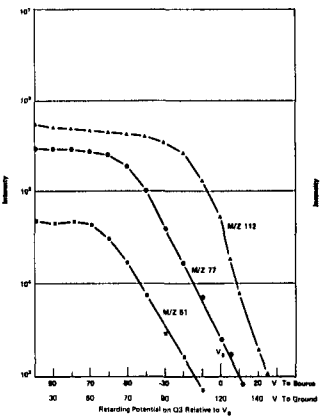


Figure 3.

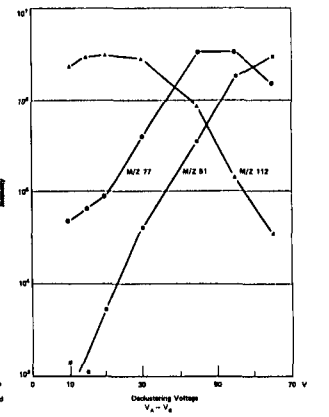


Figure 4.

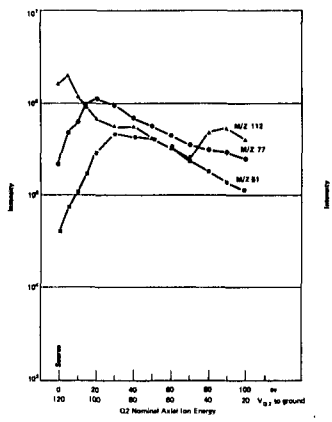


Figure 5.

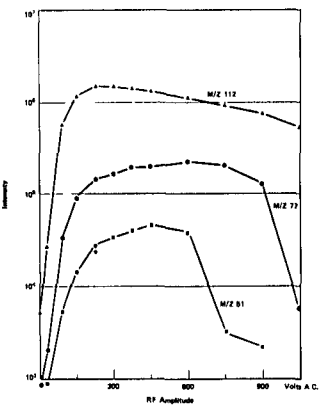
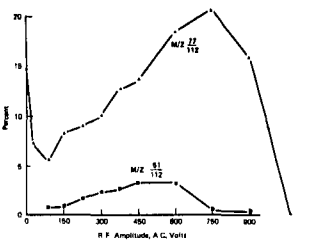


Figure 6.



TRAJECTORIES, ENERGIES, AND SPATIAL AND ANGULAR APERTURES IN AN RF QUADRUPOLE: APPLICATION TO QUADRUPOLE MS/MS. M.W. Siegel, Extranuclear Laboratories, Inc., PO Box 11512, Pittsburgh, PA 15238.

A convenient dimensionless form of the equations of motion of a singly charged ion in a quadrupole mass filter is

$$\ddot{x} = +0.3504\ (M/m)(\cos\phi + \alpha)x$$
$$\ddot{y} = -0.3504\ (M/m)(\cos\phi + \alpha)y \qquad (1)$$

where x and y are dimensionless spatial coordinates in which the quadrupole inscribed radius R_o is unity, m is the ion mass, M is the ion mass to which the instrument is set, α is the ratio of DC to RF voltage, $\phi = 2\pi ft$ where f is the RF frequency, and the dots signify differentiation with respect to ϕ. This work considers the special case $\alpha = 0$, corresponding to an RF-only quadrupole, viz., the middle quadrupole in a triple quadrupole MS/MS instrument. However, the computational techniques discussed easily carry over to the general case of a normal RF-DC quadrupole mass filter. In this special case, since $\ddot{y}(\phi) = \ddot{x}(\pi+\phi)$, only half the computation is required.

It follows from equations (1) that the dimensionless positions and velocities at any phase ϕ are linear functions of the initial conditions x(0) and $v(0) \equiv \dot{x}(0)$:

$$x(\phi) = F00(\phi)x(0) + F01(\phi)v(0)$$
$$v(\phi) = F10(\phi)x(0) + F11(\phi)v(0) \quad \text{or} \quad \vec{u}(\phi) = \underset{\sim}{F}(\phi)\vec{u}(0) \qquad (2)$$

The matrix elements $F00(\phi)$, etc., characterize all the trajectories for a given M/m, independent of R_o, f, and the explicit value of m. The matrix elements are easily found by numerically integrating the equations of motion (1) for two particular initial conditions, $\vec{u1} = (1,0)$ and $\vec{u2} = (0,1)$. Clearly $\underset{\sim}{F}(2\pi n) = \underset{\sim}{F}(2\pi)^n$, so integration over one RF cycle fully determines the motion for all ϕ. This integration over two trajectories and one RF cycle for one initial phase also characterizes the motion for all initial phases ϕ_o, since for $\phi_o \neq 0$ it is straightforward to translate the actual initial conditions $\vec{u}(\phi_o)$ backward by ϕ_o, then forward by $(\phi + \phi_o)$. Thus for any initial position, velocity and phase

$$\vec{u}(\phi+\phi_o) = \underset{\sim}{F}((\phi+\phi_o)\,\mathrm{MOD}\,2\pi)\ \underset{\sim}{F}(2\pi)^{(\phi+\phi_o)\,\mathrm{DIV}\,2\pi}\ \underset{\sim}{F}(\phi_o)^{-1}\vec{u}(\phi_o) \qquad (3)$$

where A MOD B is the remainder of A divided by B, and A DIV B is the integer part of A divided by B.

The maximum speed that an ion can have anywhere on its trajectory and still never run into a pole at x=1 is the speed acquired after one-quarter RF cycle by an ion with initial conditions $\vec{u}(\phi_o=\pi) = (1,0)$:

$$v_{max} = -(F10(3\pi/2)F00^{-1}(\pi) + F11(3\pi/2)F10^{-1}(\pi)) \qquad (4)$$

The maximum kinetic energy associated with the transverse motion is then

$$W^T_{max} = \frac{1}{2}\, m(2\pi f\, v_{max} R_o)^2 \qquad (5)$$

Since 1 amu $(cm/sec)^2 = 1.036 \times 10^{-12}$ eV, to an excellent approximation W^T_{max} is in eV when m is in amu, f in MHz, and R_o in cm. This energy is typically the same order of magnitude as the beam energy, so it is significant, but not so large as to change the low energy character of triple quadrupole MS/MS collisions. Using the computational technique outlined above, it is straightforward to find the acceptance in initial phase space (x,v): on a grid of spatial extent corresponding to the entrance aperture diameter and velocity extent corresponding to $\pm v_{max}$, and initial phase ϕ_o between 0 and 2π, equation 3 is applied for successive values of ϕ to determine those initial conditions for which x never exceeds 1.

The solid angle accepted at a point (x,y) in the entrance plane of the quadrupole is then determined by the product of the accepted x-velocity range at x and the accepted y-velocity range at y, averaged over initial RF phase. As mentioned above, the y-acceptance at any ϕ_o is just the x-acceptance at $(\phi_o + \pi)$. Two additional symmetries reduce the number of calculations actually required. First, the acceptances have point symmetry about (0,0), and the second the acceptance for $(2\pi - \phi_o)$ is the acceptance for ϕ_o mirrored across the velocity axis. Thus it is necessary to calculate the acceptance only over either one phase space quadrant for ϕ_o = 0 to 2π, or over two phase space quadrants for ϕ_o = 0 to π.

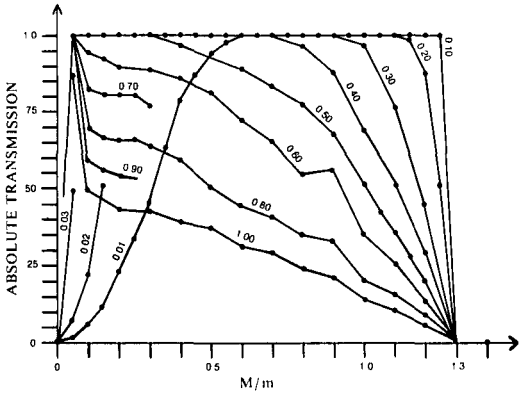
To obtain a realistic measure of the practical transmission, as contrasted to the acceptance (which describes only the quadrupole, without reference to any property of the ion beam), it is necessary to examine the spatial and angular properties of the ion beam in the entrance aperture. According to the brightness theorem, the product of the beam radius, its angular divergence, and the square root of its energy is constant. Relating these three quantities in the ionizer to their corresponding values in the quadrupole entrance,

$$R_i A_i W_i^{\frac{1}{2}} = R_e A_e W_e^{\frac{1}{2}} \tag{6}$$

where R, A, and W denote radius, angle and kinetic energy respectively, and subscripts i and e denote ionizer and quadrupole entrance positions respectively. It follows that the dimensionless transverse velocity in the entrance aperture is limited to

$$v_{entr} = (R_i/R_e)A_i(2W_i/m)^{\frac{1}{2}}/2\pi f R_o \tag{7}$$

with A in radians, W_i in eV, m in amu, f in MHz, and R_i, R_e, and R_o in cm. For realistic values of R_e/R_o, i.e., a few tenths, v_{entr} is less than v_{max}, so there is no transmission loss due to solid angle limitations. However, this is not always so, in which case the transmission is obtained by multiplying the acceptance by $(v_{max}/v_{entr})^2$.



RF quadrupole transmission vs. M/m parameterized by the ratio of quadrupole entrance aperture radius R_e to quadrupole inscribed radius R_o. Fixed parameters were

R_o = 0.416 cm,

f = 1.2 MHz,

R_i = 0.5 R_o,

A_i = π/12 radians (30°),

W_i = 0.025 eV (thermal energy)

m = 100 amu

APPLICATION OF PERFECT FOCUSING MASS SPECTROMETER TO ATOMIC COLLISION EXPERIMENTS

Tatsuo ARIKAWA, Ken-ichi KANAZAWA and Seiji TSURUBUCHI

Department of Applied Physics, Faculty of Technology,
Tokyo University of Agriculture and Technology,
Naka-machi 2-24-16, Koganei-shi, Tokyo 184, Japan

The perfect focusing mass spectrometer[1] has been constructed, and preliminary tests concerning both perfect energy focusing and perfect angular focusing (4π focusing) properties have been performed by locating a small alkali - ion source at the source point. Luminosities more than 93 % were obtained at energies tested from 100 eV down to 100 meV. Such a focusing property can be realized by the superposition of a three dimensional electrostatic quadrupole field: $\Phi = \Phi_0 (- x^2 - y^2 + 2z^2)$ with a uniform magnetic field: $\vec{H} = (0, 0, H)$[2-4] Due to those perfect focusing properties, this mass spectrometer is completely free from any chromatic aberrations, and hence, in principle, the mass resolution can be made infinity while keeping the lumonosity almost 100 %[5,7] The cross sectional view of the perfect focusing mass spectrometer is shown in Fig. 1.

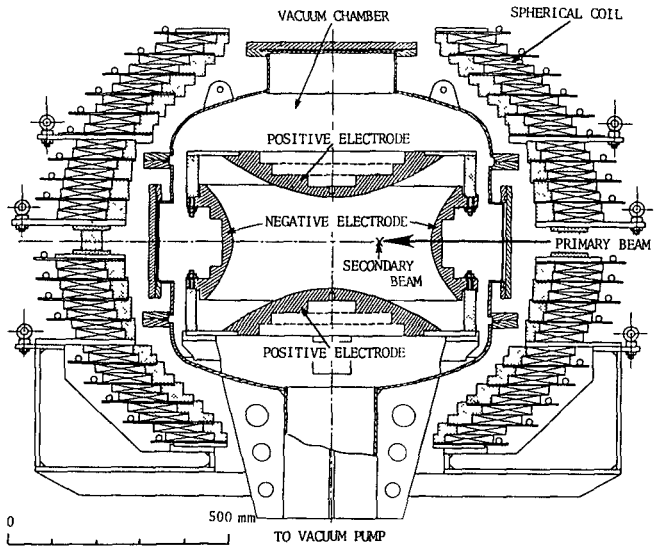


Fig.1: Cross sectional view of the perfect focusing mass spectrometer. In the test experiment, the ion source was inserted to the scattering point along zero-potential line-ruled surface so as not to disturb the electric field.

The most advantageous feature of the perfect focusing mass spectrometer is obtained when applied to an atomic collision experiment. If a crossed-beam experiment is performed inside the spectrometer, all ionic products which are formed at the collision center are focused to their respective focusing point with 100 % efficiency. Some typical trajectories of ions are shown in Fig.2, where only such ions as scattered upward with an angle of 25° with respect to the z

axis are presented. Other ions scattered differently are also focused to the same focusing point, provided that their charge-to-mass ratios are identical. Therefore, the absolute total cross sections can be obtained even in the crossed-beam geometry. Especially it is convenient for the measurement of branching ratio of each reaction channel such as chemi-ionization, in which Penning ionization, dissociative ionization, associative ionization and rearrangement ionization are included. Preliminary experiments were carried out for the collisions of metastable $He^*(2^1S, 2^3S)$ on CH_4. Though the data are at present relative, almost all peaks except C^+ peak were observed.

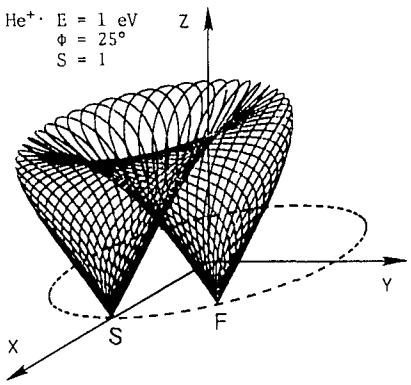


Fig.2: A part of perfect mass-focusing trajectories. $\phi = 25°$, $0 \leqq \theta < 360°$.

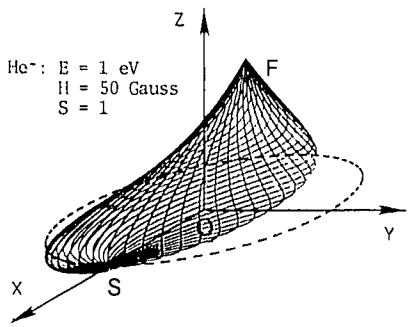


Fig.3: Typical perfect energy-focusing trajectories.

The measurement of the differential cross sections is also possible, because the perfect focusing mass spectrometer is based on the principle of the conformal mapping, where one-to-one correspondence between scattered angle at the collision point and the focusing angle at the detector point holds exactly[5]. There is no need to scan the position of the detector as is normally done in a conventional crossed-beam apparatus. Angular dependence of dissociative ionization of CH_4 by electron impact near the threshold was measured. Results were in good agreement with the recent elaborate data of Mathur[8].

Further advantage of the perfect focusing mass spectrometer is that the perfect energy analysis can be made only by changing the polarity of the electric field. In this geometry, the focusing property in the z axis fails. However, the perfect focusing still remains on the x-y plane. Therefore, all those ions whose velocities in the z component are identical can be focused at certain point F as shown in Fig.3. This implies the energy analysis as well as the mass analysis can be done simultaneously for both signs of ions.

REFERENCES:
1) T. Arikawa: Japan. J. Appl. Phys., 2 (1963) 420.
2) T. Arikawa et.al.: J. Phys. Soc. Japan, 17 (1962) 711.
3) T. Arikawa: Mass Spectroscopy Japan, 19 (1971) 1.
4) T. Arikawa: ibid., 19 (1971)166.
5) T. Arikawa, K.Kanazawa and S.Tsurubuchi; Abstract of papers,XII ICPEAC,1981, p.1157.
6) K. Kanazawa, S.Tsurubuchi and T.Arikawa: Mass Spectroscopy Japan,29 (1981) 61.
7) T. Arikawa, K.Kanazawa and S.Tsurubuchi: Atomic Collision Research Jpn., 7 (1981) 159.
8) D. Mathur: J. Phys. B: Atom. Molec. Phys., 13 (1980) 4703.

Effects of Magnetic Field Inhomogeneity on Exact Mass Determination in ICR Spectrometry

D. Schuch, K.-M. Chung and H. Hartmann

Institute of Physical and Theoretical Chemistry
University of Frankfurt, Robert-Mayer-Str. 11, 6 Frankfurt/M., FRG

Recently, in the ICR spectrometry an increasing interest exists in the development of ICR spectrometers utilizing superconducting solenoid magnets with magnetic field strength up to 80-100 kG which extend the measurable mass range into the region of higher masses. On the other hand, due to such high magnetic field strength, inhomogeneities which are growing proportional to field strength increasingly affect the accuracy of measurements. Therefore, magnets with highest possible homogeneous field are the aim of technical development. It shall be investigated in this work up to which extent it is necessary to improve the homogeneity of solenoid magnets used in ICR spectrometers by the aid of expensive technology in order to achieve a still measurable effect with respect to exact mass determination. For this purpose, the change of cyclotron frequency due to magnetic field inhomogeneity will be calculated and the resulting difference between measured and actual masses determined. As the inhomogeneity of a solenoid depends on all three space coordinates, classically the motion of an ion under the influence of this inhomogeneous field is described by a system of three coupled non-linear differential equations which should be solved at most numerically. Therefore, we use a different method regarding the quantum mechanical Schrödinger equation of this problem calculating the contributions due to inhomogeneity perturbation theoretically with the aid of a wave packet formalism. The relation between shift of cyclotron frequency and experimental parameters is given and the order of magnitude of the perturbation is estimated for limiting conditions. It is shown that even in the most unfavourable case the influence of magnetic field inhomogeneity is negligibly small.

An Elongated Trapped Ion Cell for Fourier Transform Mass Spectrometry with a Superconducting Magnet

Richard L. Hunter and Robert T. McIver, Jr.
Department of Chemistry
University of California
Irvine, California 92717

In recent years ion cyclotron resonance spectrometers have developed into high performance mass spectrometers featuring very high mass resolution and rapid scanning. One of the major factors that has contributed to this development is the design of improved analyzer cells. In 1965 Wobschall described a cell for measuring ion-molecule collision cross-sections. In 1967 a three-section drift cell was designed for use in the Varian Assoc. Syrotron mass spectrometer. Both these cells had separate regions for formation and detection of ions and suffered from low mass resolution and a mass range limit of about m/z 200. In 1970 McIver introduced a trapped ion analyzer cell having one region for ion formation, chemistry, and detection by operating in a pulsed mode.[1] Comisarow has described a modified trapped ion cell of cubic geometry which is applicable to Fourier transform ICR experiments.[2] Trapped ion cells store ions for several seconds at low pressure, permit high resolution and the study of a wide variety of ion-molecule reations.

Our interest in developing a new trapped ion analyzer cell was to improve its dynamic range and and mass measurement accuracy for high molecular weight ions. We have recently done experiments with an elongated trapped ion cell which consists of six flat electrodes arranged to form a box with inside dimensions 3.2 x 3.2 x 15.2 cm. The cell operates best with a ground potential on the upper, lower, and end plates, and for positive ions about +1 volts on the trapping plates. The cell is housed in a stainless steel vacuum chamber pumped with a 150 ℓ/s ion pump to a base pressure near 10^{-10} torr. The vacuum chamber can be easily inserted and removed from a 3.4 T superconducting solenoid magnet.

Figure 1(a) shows a plot of 0.1 V equipotential lines for conventional and cubic trapped ion cells. Since there is a potential of 0.5V in the center of these cells, ions occupy a thin wafer in the center and undergo harmonic oscillation between the trapping plates at about 20 kHz. To avoid space charge effects with these cells, the number of ions should be kept below about 3×10^5.[3] Figure 1(b) is a plot of the equipotentials in the elongated cell. Since the trapping plates are farther apart the potential in the center of this cell is only about 1.2 mV and ions can occupy a much larger region of the cell. Figure 2 shows a plot of the ICR signal intensity for m/z 78 ions as a function of the number of ions in the elongated cell. Linear detection sensitivity is observed if the number of ions in the cell is kept below about 2×10^7 ions. It appears that the elongated cell will hold far more ions than conventional trapped cells.

Another important feature of the elongated cell is that the resonance frequency is quite insensitive to changes in the cell dc voltages. This is illustrated in Fig. 3 where resonance shifts in a trapped ion cell are compared with those observed in an elongated cell. For m/z 78 ions the apparent resonance can be shifted by more than a mass unit. This problem is even more pronounced at higher masses since this shift increases as the square of the mass to charge ratio. In the elongated cell a shift of only .002 u is observed for a change in trapping potential of over 7 volts. Accurate mass measurement is

much easier in an elongated cell because the shift due to cell dc voltages is much smaller.

From these observations, we conclude that an elongated trapped ion cell used with a superconducting magnet is the method of choice for experiments requiring accurate mass measurements at high molecular weights.

[1] R.T. McIver, Jr. in Lecture Notes in Chemistry: Ion Cyclotron Resonance Spectrometry, H. Hartmann and K.-P. Wanczek, eds., Springer-Verlag, Berlin, 1978, pp. 97-135.

[2] M.B. Comisarow, Int. J. Mass Spectrom. Ion Phys., 37, 251 (1980).

[3] R.T. McIver, Jr., R.L. Hunter, E.B. Ledford, Jr., M.J. Locke, and T.J. Francl, Int. J. Mass Spectrom. Ion. Phys., 39, 65 (1981)

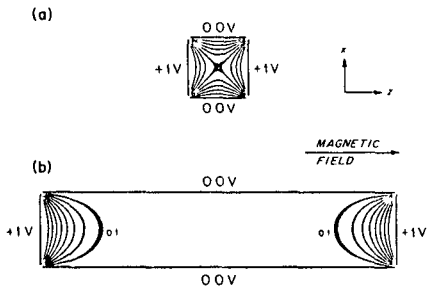


Figure 1. Equipotentials in (a) conventional trapped ion cell and (b) an elongated trapped ion cell are spaced by 0.1 V.

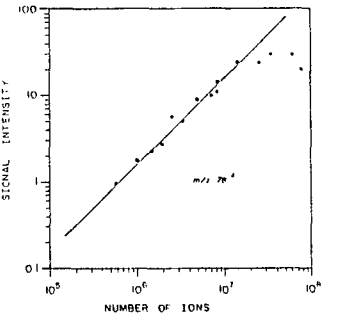


Figure 2. The elongated trapped cell has an ion capacity almost 100 times that of conventional trapped cells.

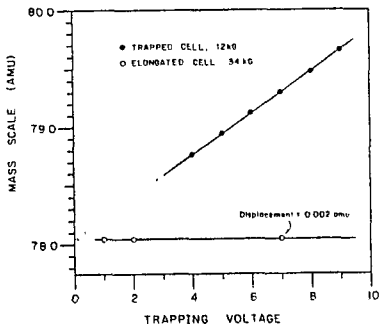


Figure 3. Conventional trapped cells exhibit large resonance shifts due to the applied trapping voltages. The shift is almost negligible in the elongated trapped cell.

MOF 9 INEXPENSIVE MODIFICATION OF A KRATOS MS-50 FOR FAST ATOM BOMBARDMENT (FAB); L. A. Shadoff and D. Zakett, Dow Chemical Company, Midland, MI 48640

A Kratos MS-50 mass spectrometer has been inexpensively modified to allow FAB ionization. Modifications to the instrument include the construction of a simple probe for sample introduction, very minor changes to the standard electron impact ion source, and an adaptor flange to mount the ion tech atom gun on the upper left ion source housing port. The sample for FAB is introduced through the standard solid probe inlet and is intersected by the atom beam in the region of the source exit slit. Both the solid probe axis and atom beam path are oriented within the instruments Y-Z plane of analysis.

Alkali sulfate salts dissolved in concentrated sulfuric acid have been found suitable for use as a mass calibration material and allows routine computerized data acquisition.

The instrumental modifications and mass calibration procedure will be discussed.

Time Resolved Photoionization Mass Spectrometry in the Millisecond Range

by

C. Lifshitz, M. Goldenberg, Y. Malinovich and M. Peres
Department of Physical Chemistry, The Hebrew University of Jerusalem
Jerusalem 91904, Israel

A photoionization mass spectrometer operating in a time resolved manner, from the microsecond to the millisecond range, has been constructed. The central part of the instrument (Fig. 1) is a Cylindrical Ion Trap (CIT) of the type used previously[1] in conjunction with electron impact experiments. The Hinteregger VUV light source is pulsed and the photoions produced are trapped in the CIT. They are ejected into the quadrupole mass filter by a drawout pulse, following a variable delay time, and counted only during the ejection pulse. Typical operating conditions are as follows: The RF potential applied to the cylindrical barrel electrode is 0.5 MHz($\Omega/2\pi$) and $\sim$1000V peak to peak; the cylindrical electrode is biased by a +20V DC potential. The planar end-cap electrodes are earthed and ions are ejected after a pre-determined storage time by means of a -30V pulse (width 20-50 μs) applied from a pulse generator PGB to the end-cap nearest the mass filter. The entrance and exit slits of the monochromator are 500 μm and 600 μm respectively giving an effective resolution of 5.0Å.

The CIT stores photoions as is shown in Fig. 2. The TPIMS combines good energy resolution with time resolution. It is employed for: (a) Time resolved appearance energy measurements for ionic fragmentations which are characterized by large 'kinetic shifts', i.e. whose rate-energy dependence is a very slowly rising function of the excess energy above threshold; (b) Measurements of reaction rate coefficients for ion-molecule reactions involving ions in well defined internal energy states.

1. R.E. Mather, R.M. Waldren, J.F.J. Todd and R.E. March, Int. J. Mass Spectrom. Ion Phys. 33 (1980) 201.

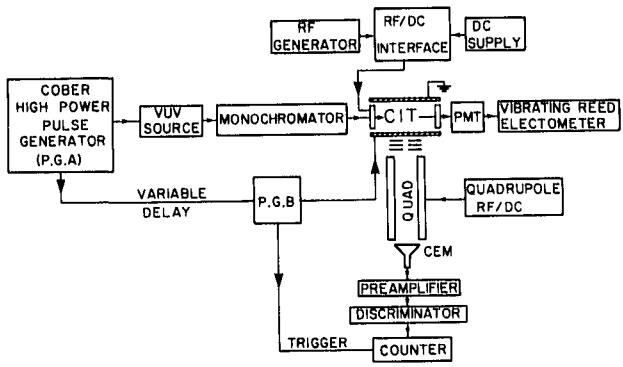


Figure 1: Time-resolved photoionization mass spectrometer (TPIMS). The VUV source is a Hinteregger hydrogen discharge lamp; the monochromator is a McPherson Model 225 1-m, normal incidence instrument and the quadrupole mass spectrometer is a EAI QUAD 1110. The dimensions of the cylindrical ion trap (CIT) are (see ref. 1): r_1 = 2 cm and z_1 = 1.5 cm. PMT-photomultiplier; CEM-Channeltron Electron Multiplier; PG-Pulse Generator.

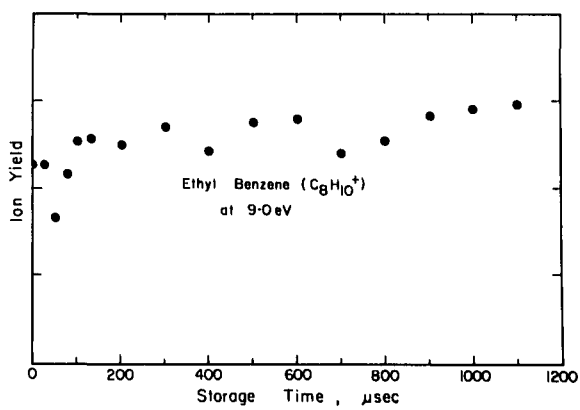


Figure 2: Ion intensity as function of storage time (μsec) at a sample gas pressure $\lesssim 10^{-5}$ torr.

GCMS CHARACTERIZATION OF VALPROIC ACID METABOLITES IN HUMAN SERUM AND URINE.

Andrew A. Acheampong, Frank S. Abbott and Roland R. Burton. Faculty of Pharmaceutical Sciences, University of British Columbia, Vancouver, British Columbia, Canada, V6T 1W5

Valproic acid (dipropylacetic acid, VPA) is an antiepileptic drug which is effective in absence seizures. VPA is extensively metabolized in humans[1] and there are indications that VPA metabolites may contribute to the anticonvulsant activity[2]. Metabolites may explain the late onset of therapeutic effect and carry-over effects of VPA observed in some clinical and animal studies. Interest in VPA metabolites has also been stimulated by the potential hepatotoxicity of VPA. A complete metabolite pattern of VPA is needed to assess the relative importance of each metabolic pathway.

Identification of metabolites of VPA is hampered by the chemical lability of the metabolites and the structural similarity of the metabolites to some endogenous fatty acids[1]. Recently, a diunsaturated metabolite of unknown structure was identified in patient's serum[3]. To enhance the certainty in identification of some of the metabolites, we decided to carry out appropriate stable-isotope labelling studies to confirm reported metabolites and to identify any trace new metabolites.

Di-(3-$^2H_3$-propyl)acetic acid (VPA-$^2H_6$) was synthesized for use in this study. VPA-$^2H_6$ (600 mg) was given orally to a healthy volunteer who was at steady state serum concentrations of unlabelled VPA. This experiment was part of a study of VPA steady state kinetics. Following the VPA-$^2H_6$ dose, blood and urine samples were collected at various times over an interval of 12 hr. Serum samples (0-11 hr after labelled dose) were acidified to pH 2, extracted twice with ethyl acetate and centrifuged each time. The combined ethyl acetate layers were dried and concentrated with dry N_2. The extracts were derivatized with diazomethane or N-methyl-N-trimethylsilyltrifluoroacetamide or t-butyldimethylchlorosilane. Urine samples were adjusted to pH 13 and heated at 90°C for 1 hr to effect hydrolysis of conjugates. The urine was acidified and extracted three times with ethyl acetate. The combined ethyl acetate was dried over sodium sulfate and then concentrated under vacuum. The concentrated urine extract was derivatized as for serum extract. Analysis of derivatized extracts was performed with a Varian MAT 111 GCMS (EI) connected on line to a Varian 620L computer and using either a 3% OV-17 or 3% Dexsil 300 column and temperature programming (80-280° at 8°/min).

The total ion chromatograms of derivatized extracts contained many peaks. Resolution of GC peaks on the 6 m long packed column was sufficient to obtain mass spectra of compounds. Diagnostic ion doublets resulting from the unlabelled and labelled substance were present in the mass spectra of metabolites. Since concentrations of unlabelled VPA and metabolites were at pseudo-steady state before the VPA-$^2H_6$ dose, the ratio of unlabelled ions and their corresponding labelled ions varied from 2:1 to 8:1.

In the serum extract, 3-heptanone (decarboxylated product of 2-propyl-3-ketopentanoic acid), 2-propyl-3-pentenoic acid, 2-propyl-2-pentenoic acid, 2-propyl-4-hydroxypentanoic acid lactone and 2-propyl-5-hydroxypentanoic acid lactone were identified. A new metabolite 2-propyl-4-ketopentanoic acid (4-keto VPA) was identified in serum and urine extracts. In the mass spectrum of 4-keto VPA-($^2H_0$+$^2H_6$) ion doublets appeared at m/z 43, 46 ($CH_3C{=}O$, $C^2H_3C{=}O)^+$, m/z 115, 118 ($M{-}CH_3COCH_2)^+$ and m/z 130, 133 $(M-42)^+$.

Two isomers of a diunsaturated VPA metabolite were identified in serum and urine extracts. The presence of a molecular ion doublet m/z 154, 160 in the mass spectrum of the GC peak corresponding to the methyl ester of the major diene VPA isomer of longer retention time proves that the double bonds are not located at the terminal positions of the propyl chains. Two possible structures are 2,4-heptadiene-4-carboxylic acid and 2,5-heptadiene-4-carboxylic acid.

Three dicarboxylic acids were confirmed as VPA metabolites in the urine extract. These were 2-propylglutaric acid, 2-propylsuccinic acid and, propylmalonic acid. The mass spectrum of the GC peak corresponding to the dimethylester of 2-propylsuccinic acid-($^2H_0$+$^2H_3$) had characteristic ion doublets at m/z 114, 117 $(M-74)^+$, 115, 118 $(M-73)^+$, and 157, 160 $(M-31)^+$. In the mass spectrum of the di-tertiarybutyldimethylsilyl derivative of 2-propylsuccinic acid-($^2H_0$+$^2H_3$) the characteristic M^+-57 ion doublet occurred at m/z 331, 334. The mass spectrum of the dimethyl ester of 2-propylmalonic acid ($^2H_0$+$^2H_3$) had ion doublets at m/z 143, 146 $(M-31)^+$ and a base peak at m/z 132 $(M-42)^+$. The mass spectrum of

the di-tertiarybutyldimethylsilyl derivative of 2-propylmalonic acid ($^2H_0$+$^2H_3$) had a characteristic ion doublet at m/z 317, 320 $(M-57)^+$ and other ion doublets at m/z 298, 292 $(M-57-CO)^+$ and m/z 273, 276 $(M-57-CO_2)^+$.

The identification of VPA metabolites using VPA-$^2H_6$ as tracer was also verified by superimposing labelled and unlabelled peaks from the mass chromatograms and by comparing the retention times and mass spectra of isolated components in the extracts to those of synthesized reference compounds.

References

1. R. Gugler and G.E. von Unruh, Clin. Pharmacokinet., 5, 67 (1980).

2. H. Nau and W. Loscher, J. Pharmacol. Exp. Ther., 220, 654 (1982).

3. W. Kochen and H. Scheffner, In Antiepileptic Therapy: Advances in Drug Monitoring, ed. by S.I. Johannessen, P.L. Morselli, C.E. Pippenger, A. Richens, D. Schmidt and H. Meinardi, p. 111-117, Raven Press, New York, 1980.

Chemical Ionization Mass Spectral Identification of the Anthelminthic Agent Mebendazole and its Metabolites; J.M. Kennish; Chemistry Department, University of Alaska, Anchorage, 3221 Providence Drive, Anchorage, Alaska 99508

Alveolar hydated disease (AHD), caused by the larval stage of a taeniide cestode (tape worm), *Echinococcus multilocularis*, is one of the most lethal of all helminthic infections in man. This cestode is limited geographically to the northern hemisphere, where it is endemic in Alaska, some regions in Canada, Central Europe, Siberia and northern Japan. In 1964 it was introduced into the continuous forty-eight states and subsequently has become widely established in central North America.

The etiologic agent occurs in natural hosts such as foxes and small rodents. Dogs and cats may replace foxes as the final host of this cestode, particularly in rural villages, providing a potentially important source of infection for man through contacts with animal excrement. In AHD caused by *Echinococcus multilocularis*, the primary site of infection is the liver. The histological character of the lesion as well as the clinical course of the disease are such that it may be mistaken for hepatic carcinoma.

Hydatid disease has remained one of the few helminthic diseases for which there is no effective chemotherapy. Surgery has been the only curative treatment but extensive AHD is inoperative. The critical need for nonsurgical treatment of AHD has existed for a long time; only recently has a drug showing promise of controlling the disease become available. Mebendazole (methyl-5-benzoyl-2-benzimidazole carbamate), a compound of the benzimidizole group, has been shown to be unusually effective against larval cestodes *in vivo*. The drug apparently acts by interfering with the uptake of glucose by the cestodes. Inhibition of glucose uptake appears to lead to endogenous depletion of glycogen stored in the parasite.

Studies with animals infected with *Echinococcus multilocularis* have shown that mebendazole greatly inhibits larval proliferation but does not kill all larval tissues. In animals and in humans the drug is poorly adsorbed from the stomach resulting in low blood concentrations utilizing current chemical dosing techniques it is apparent that repeated and prolonged treatment may be necessary and long-term follow-up of the individually treated patients will be necessary before cure can be confidently predicted.

Favorable response has been observed in patients whose administered dose consistently achieves plasma concentrations in the range of 90-100 ng/ml. However, large inter and intra individual variations in drug absorption, metabolism, and excretion have been observed (1). These variations can be reduced by dosing with food but it appears that monitoring plasma levels during long-term therapy is necessary. As a result a pharmacokinetic study has been established to measure the therapeutic efficiency of Mebendazole in Alaskan Eskimos infected with *Echinococcus multilocularis* (2). The plasma concentrations were monitored in seven patients utilizing the high performance liquid chromatographic (HPLC) assay of Allan *et al* (3).

Mass spectrometry has been helpful in identifying and characterizing mebendazole and its metabolites. The compounds were isolated by HPLC and analyzed by electron impact and methane chemical ionization mass spectrometry utilizing the direct probe. The major ions of the mass spectra of mebendazole and its metabolites are shown in table 1.

TABLE 1

Mass Spectra of Mebendazole and its Metabolites

Methyl-5-Benzimidazole Carbamate	
EI	295(75), 218(100), 186(91), 105(55), 77(64)
CI	324(34), 297(44), 296(100), 295(23), 119(23), 105(44)
2-Amino-5-Benzoylbenzimdazole	
EI	237(45), 160(100), 132(25), 105(37), 77(24)
CI	266(24), 238(100), 105(40)
2-Amino-5-(α-hydroxybenzyl)-Benzimidazole	
EI	239(34), 160(26), 134(100), 105(48), 77(22)
CI	240(61), 239(39), 238(77), 222(64), 162(100), 134(91), 105(24)
Methyl-5-(α-hydroxybenzyl)-2-Benzimidazole Carbamate	
EI	297(51), 192(69), 160(91), 105(100), 77(46)
CI	298(77), 297(52), 280(100), 220(77), 192(93), 107(26), 105(21)

1. Braithwaite, P.A., Roberts, M.S., Allan, R.J. and Watson, T.R., Clinical Pharmacokinetics of High Dose Mebendazole in Patients Treated for Cystic Hydatid Disease, Eur. J. Chem. Pharm. Submitted (1982).

2. Kennish, J.M., Schallock, M. and Wilson, J.F., Plasma Kinetics of the Anthelminthic Agent Mebendazole in Alaskan Eskimos Infected with *Echinococcus Multilocularis*, Proceedings of the 32nd Alaska Science Conference, Fairbanks, AK 1981.

3. Allan, R.J., Goodman, H.T. and Watson, T.R., Two High Performance Liquid Chromatographic Determinations for Mebendazole and Its Metabolites in Human Plasma Using a Rapid Sep Pak C18 Extraction, J. Chromatogr, 183, 311 (1980).

STUDY OF DIBUCAINE METABOLISM : IDENTIFICATION OF URINARY METABOLITES IN RAT, RABBIT AND MAN

Kazuo Igarashi, Fumiyo Kasuya and Miyoshi Fukui

Faculty of Pharmaceutical Sciences, Kobegakuin University., Kobe 673, Japan

Dibucaine, 2-butoxy-N-(2-diethylaminoethyl)cinchoninamide, has been used as a local anesthetic since 1930, but the drug metabolism has not been studied in detail. This is probably related to the lack of sensitive and selective methods of detection and determination of the compounds in biological fluids. Recently, T.Kuhara et al(1976) and T.Shinohara et al (1977) have reported the six metabolites of dibucaine in animals urine using GC-MS. In addition, T.Shinohara et al(1979) indicated that the urinary excretion of these metabolites including the unchanged drug was determined by HPLC, and was accounting for less than several per cent of the administered dose. Therefore, the major portion of its metabolites have not been identified. The present report describes the further isolation and identification of the urinary metabolites including four new metabolites in rat, rabbit and man.

The urine samples collected for 24 hours after drug administration were passed through a column of Amberlite XAD-2 resin. The metabolites were eluted with MeOH. After evaporation of MeOH, the residue was dissolved in a small volume of water, and extracted with methylene chloride at pH 9. The solvent was evaporated, and the residue was redissolved in MeOH to subject to preparative TLC. The metabolites visualized under UV light or by spraing with Dragendorff reagent were scraped off and eluted with MeOH. The structure of these isolated metabolites was identified by comparison of the gas chromatographic and mass spectral properties with those of authentic compounds. The mass spectra were obtained with a HITACHI model M-60 GC-MS instrument at 20 eV with 100 μAmp ionization current. GC column was used a 1 m x 2 mm glass column packed with 2% OV-101 on Chromosorb W/HP(100-120 mesh). The column temperature was held at 260°C.

Total eleven metabolites including unchanged dibucaine were detected in three species by TLC and GC methods. Six metabolites were found in rat, rabbit and man, respectively. The predominant metabolite differed in each species: M-10 and M-5 in rat, M-6 and M-4 in rabbit, and M-8 and M-4 in man, respectively. Six of these eleven metabolites were the same as the known compounds, and four were unknown metabolites. This unknown metabolites M-2 and M-6 were found only in rabbit urine, and M-3 and M-8 only in human

urine. The structures of these isolated metabolites were determined by GC-MS. The mass spectra of these metabolites were identical to those of authentic compounds. These metabolites were found to be 2',3'-dihydroxybutoxy product(diol,M-6), 2-hydroxyethoxy product(M-8), and their N-de-ethyl products(M-2 and M-3), respectively. Moreover, to clarify the produced process of these new type metabolites, the synthesized 2'-hydroxybutoxy compound(ω-1-OH, M-10) was administered to rabbit or man. In this experiment, the major urinary metabolite was M-6 in rabbit, and M-8 in man, respectively. These findings suggest that the diol and 2-hydroxyethoxy product are formed via ω-1-OH product which was commonly found in all three species. In addition, the position of hydroxy group on aromatic ring of M-5, which was found in rat urine, was examined by hydrolysis in 6N-HCl for 2hr at 130°C. The result of this experiment showed that M-5 was 6-hydroxy product.

On the basis of these data, seven metabolic pathways on dibucaine metabolism could be confirmed in the species studied as shown in Fig.1. Of these metabolic pathways, the process giving rise to the diol product or the 2-hydroxyethoxy product via ω-1 hydroxylation of the alkyl side chain has not been observed in other drug metabolism. In addition, total amounts of these metabolites including unchanged dibucaine were accounted for approximately 10% of the administered dose after 24 hours, and also there were species difference in the dibucaine metabolism.

1. T.Kuhara, T.Okuda, Y.Inoue and I.Matsumoto : Proc. Jap. Soc. Med. Mass Spectrum., 1 62-66 (1976).
2. T.Shinohara and A.Momose : The 97th Annual Meeting of Pharmaceutical Society of Japan, Tokyo, April, 1977.
3. T.Shinohara and A.Momose : The 99th Annual Meeting of Pharmaceutical Society of Japan, Sapporo, August, 1979.

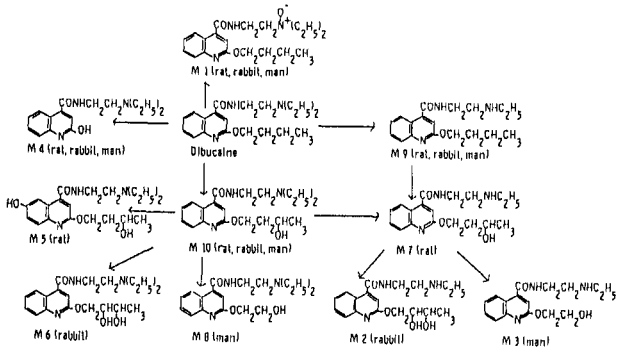


Fig.1 POSTULATED METABOLIC PATHWAY OF DIBUCAINE

CRUISE MISSILE FUEL INHALATION KINETICS AND METABOLITE IDENTIFICATION BY GC/MS. Roger C. Inman, Kyung O. Yu and William C. Keller. Toxic Hazards Division, Air Force Aerospace Medical Research Laboratory, Wright-Patterson Air Force Base, Ohio.

Specially synthesized high density liquid fuels have been developed by the United States Air Force and Navy for use in cruise missile systems. These fuels have increased the range of the missiles about 15% over that which could be achieved with conventional fuels. This new generation fuel will upon occasion be involved in accidental environmental contamination, short-term high concentration exposure of humans and animals, and low concentration occupational exposure. This work seeks to develop the analytical techniques required to response appropriately to these exposures.

One of the major components of cruise missile fuels is called JP-10, the exo-isomer of 2,3,3a,4,5,6,7,7a-octahydro-4,7-methanoindene (Figure 1) which should be over 98.5% (pure) to be used as fuel. The endoisomer comes as the impurity.

A mixture of air and JP-10 was introduced into the inhalation chamber (66 ℓ) through a gas-washing bottle at a rate of 10 ℓ/min. The JP-10 concentration in the chamber was determined by G.C. with an automated gas sampling valve every 4 or 5 minutes.

Rats with tail artery catheters were exposed to 600 ppm JP-10 for 6 hrs in the chamber. The catheter was extended from the exposure chamber through sealed ports that allowed sampling without interrupting the inhalation exposure. Periodic blood samples were taken from each rat through this catheter. No symptoms of toxicity were observed at 600 ppm concentration. 0.2 ml of blood was extracted with 0.15 ml hexane and 1 μℓ of the hexane layer was injected into the G.C. The G.C. area was compared to a known standard. A STD curve was obtained by adding a known amount of JP-10 to fresh rat blood. The following figure shows the concentration of JP-10 in blood vs. time. Blood samples were taken every 10 min. during the 1st hour, every 15 min during the 2nd hour and then every 30 min. during the next 4 hrs. JP-10 levels were plateaued after 90 min. of continuous inhalation exposure (Figure 2). JP-10 blood samples were identified by GC/MS.

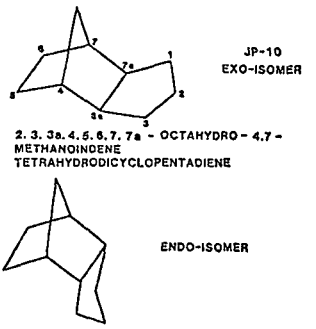


FIGURE 1

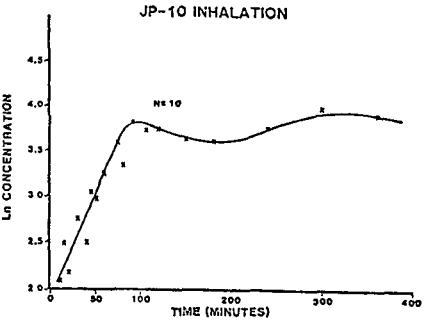


FIGURE 2

After the 6 hr exposure the rats were placed in the metabolic cages for 12 hrs for urine collection. Pooled urine was treated with the enzyme ß-glucuronidase with aryl sulfatase (Calbiochem, LaJolla, CA) at 37°C for 16 hrs. After the enzyme RX, it was poured into the Clin Elut (Analytichem International, Harbor City, CA) and then extracted with hexane. The hexane was concentrated and 1 µℓ was injected into the GC/MS. The major metabolite of JP-10 is 5-hydroxy exo-JP-10 (Figure 3). There are distinctly different fragmentation patterns between 1-hydroxy and 5-hydroxy-exo-JP-10. We compared them with synthetic samples. The TMS-O-derivatives (Figure 4) were prepared by treating hydroxy compounds with silylating agents. Possible structure assignments of the major peaks are shown in the following two spectra.

In conclusion we reported a kinetic study of JP-10 and its metabolite, 5-hydroxy exo-JP-10 and its TMS-O-derivatives.

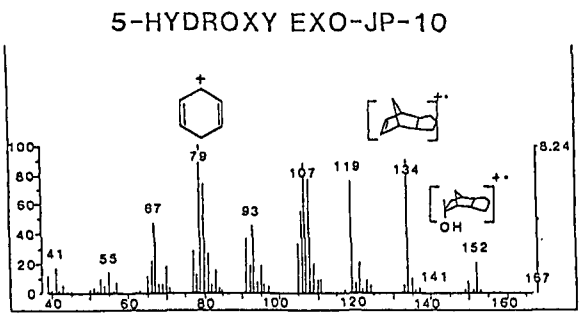


FIGURE 3

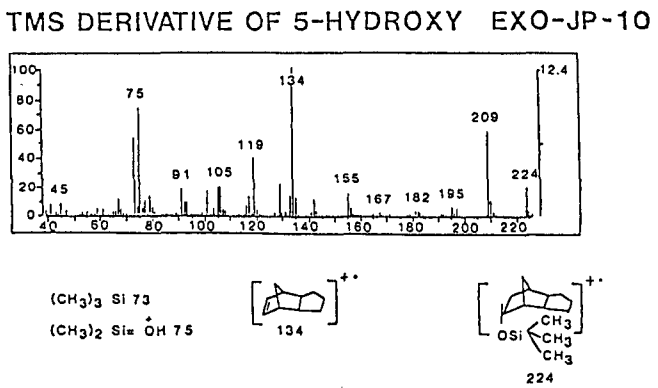


FIGURE 4

Effects of Deuterium and Chlorine Substitution on the Metabolism of Chloroethanes

John A. Thompson and Bert Ho
School of Pharmacy
University of Colorado
Boulder, Colorado 80309

The wide-spread use of polychloroethanes and the known or suspected toxicities of many of these compounds have led to interest in their metabolism and in relationships between metabolism and toxicity. Early work by Van Dyke and coworkers (1,2) established the role of hepatic cytochrome P-450 in the release of ^{36}Cl from labeled polychloroethanes in the presence of O_2. As preliminary work to detailed investigations of metabolite formation, we have studied relationships between chlorine and deuterium substitution and the extent of NADPH-dependent degradation of substrates in rat liver microsomes. The results allow predictions to be made regarding the mechanisms of oxidative and reductive metabolism.

To facilitate the analyses of polychloroethanes and volatile metabolites from in vitro studies, purge/trap techniques were developed to isolate and concentrate volatiles from microsomal incubates on short columns of Tenax GC. The compounds were then thermally desorbed from the traps, concentrated at the head of a GC column and analyzed by GC/MS techniques. A special apparatus was designed to permit incubation and purging to be performed in the same air-tight vessel. Very high recoveries (>95%) were demonstrated for several halogenated hydrocarbons with boiling points in the range 4-187°C. With the aid of 1-chlorobutane as the internal standard, the NADPH-dependent disappearance of all eight polychloroethanes was quantitated in incubations containing microsomes from phenobarbital-treated rats. In the presence of oxygen, 1,1,2,2-tetrachloroethane was metabolized at a rate of 15 nmoles/mg protein/20 min. The relative rates of metabolism of the other polychloroethanes are shown in table 1.

Table 1

Relative Rates of Metabolism of Polychloroethanes

	Aerobic (%)	Anaerobic (%)
CH_2ClCH_2Cl	4	4
$CHCl_2CH_3$	36	4
$CHCl_2CH_2Cl$	62	10
CCl_3CH_3	16	10
$CHCl_2CHCl_2$	100	22
CCl_3CH_2Cl	18	89
CCl_3CHCl_2	33	95
CCl_3CCl_3	22	100

Effects of deuterium substitution on rates of oxidative metabolism were measured by using 1:1 mixtures of labeled and unlabeled substrates and quantitating the amounts of each substrate consumed by GC/MS. The ions monitored and the kinetic isotope effects are listed in table 2.

Table 2

Kinetic Isotope Effects on Oxidative Metabolism

Deuterated Substrate	Ions Monitored (m/z)	k^H/k^D
$CDCl_2CH_3$	83/84	1.9
$CHCl_2CD_3$	65/68	1.0
$CDCl_2CH_2Cl$	132/133	2.0
$CHCl_2CD_2Cl$	97/103	1.0
$CDCl_2CDCl_2$	83/84	2.9

The relationships between chlorine substitution and relative rates of enzymatic degradation demonstrate that in the presence of oxygen, the most reactive compounds contain a dichloromethyl group. Increasing the chlorine substitution at the other position decreases C-H bond strength at the $-CHCl_2$ group (3). This correlates (except for pentachloroethane) with the order of increasing oxidative reactivity. These results are consistent with a mechanism involving initial enzymatic attack at the C-H bond to form an unstable dihalohydrin which can decompose by loss of HCl to yield various metabolites.

Those substrates most susceptible to enzymatic attack under anaerobic conditions (table 1) have a trichloromethyl group and at least one chlorine at carbon-2. These observations are consistent with a reduction pathway involving the donation of an electron from cytochrome P-450 to the substrate followed by C-Cl bond cleavage to form an intermediate carbon-free radical and a chloride ion.

Acknowledgement

This work was supported by grant ES 02069 from the National Institute of Environmental Health Sciences.

References

1. R.A. Van Dyke and C.G. Wineman, Biochem. Pharmacol. 20, 463 (1971).
2. R.A. Van Dyke and A.J. Gandolfi, Mol. Pharmacol. 11, 809 (1975).
3. G. Loew, J. Trudell and H. Motulsky, Mol. Pharmacol. 9, 152 (1973).

Metabolic pathway of 2,6-Diisopropylnaphthalene in carp

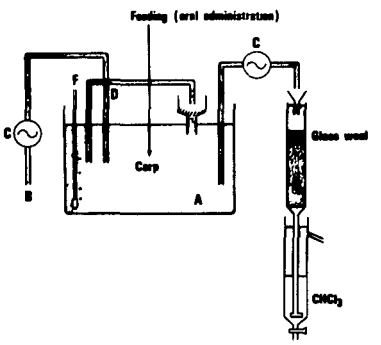
H.KOJIMA and T.YOSHIDA: Dept. of Marine Environmental Science and Technology., Tokyo University of Fisheries

Diisopropylnaphthalene (DIPN) has been widely used for a solvent of carbonless paper as a chemical substitute for polychlorinated biephenyls (PCBs). In order to clarify the environmental fate of this compound, its metabolites has been studied from ecotoxicological viewpoints, and the compounds have been identified either as a metabolite in carp (Cyprinus carpio) or as microbial metabolites. Characterization of in vivo and in vitro metabolites of 2,6-DIPN in carp was studied.

In vivo experiment was carried out to identify its metabolites in carp, which were administered 2% 2,6-DIPN supplemented fish pellets daily for 10 days. The aquarium water was combined and evaporated to dryness. The residues were chromatographed on silica gel in a column and purified further by preparative TLC. Used for the in vitro studies was a carp hepatopancreas homogenate(33% in 0.25M sucrose solution),which was incubated with 5μM 2,6-DIPN in the presense of cofactors (NADP,NADPH,G-6-P) at 37°C for 20 minutes. The reaction was ceased by addition of ethanol and the centrifuged supernatant was evaporated to dryness. The residue was purified by preparative TLC. Structural identification of in vivo and in vitro metabolites were performed by UV, IR, NMR and MS spectral analyses.

Since these metabolites showed UV-absorption at 275 nm which did not shift by adding 1N KOH/EtOH, the naphthalene ring skeleton itself apparenly remained unchanged and these compounds were evidently derived from 2,6-DIPN. Thus, the structural modification from 2,6-DIPN took place at the alkyl substituent. Both of the TMS ethers of M-I and -II showed the molecular ion m/z 300 in the MS spectra, indicating to be monohydroxy derivatives of 2,6-DIPN. The former, however, gave a fragment ion peak [m/z 211(M^+-OTMS)], whereas the latter showed an ion m/z 197(M^+-CH_2OTMS). Their structures were assigned by the NMR spectra, M-I being a tertiary carbinol(δ1.66, 6H, s) and M-II being a primary alcohol(δ3.78, 2H, d). From these results, 2,6-DIPN metabolites were clearly shown to be formed by two types of oxidation at the isopropyl group,i,e, at the methine position and at the methyl group.

The molecular ion m/z 388 of the TMS ethers of M-III and -IV suggested the dihydroxy derivatives of 2,6-DIPN. M-III was



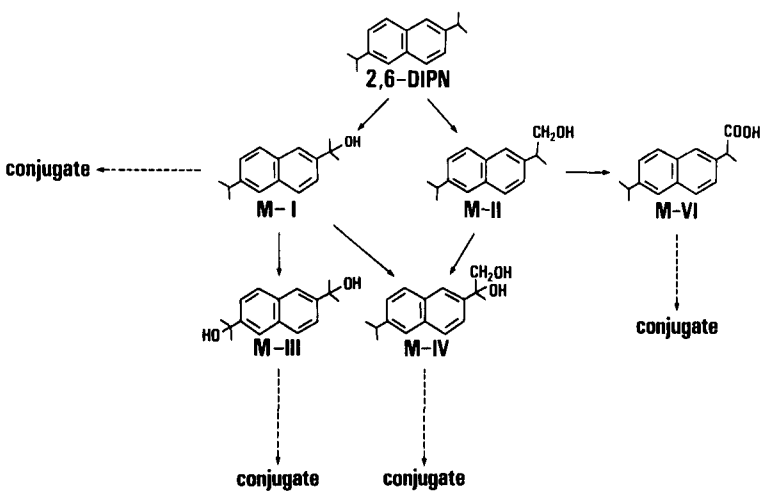
A. Test Aquarium
B. Dechorinated tap water
C Perista pump
D. Recycling system
Water/glass wool filter
E. Amberlite XAD-2 column
F. Aeration

Fig.1 Experimental apparatus in vivo

characterized by its fragment ion peaks [m/z 299(M^+-OTMS), 209(M^+-2OTMS+H)], suggesting two tertiary hydroxyl groups. The fragment ion peak [m/z 285(M^+-CH_2OTMS), 43($C_3H_7^+$)] appearing in M-IV suggested the presence of a primary alcohol and an isopropyl group and M-IV was determined to be a primary and tertiary glycol structure (δ1.62, 3H, s; δ3.78, 2H, dd) after D_2O addition. The MS, NMR spectra and IR data of M-VI implies the presence of charasteristic carboxyl group(m/z 197(M^+-COOH), max 1710 cm^{-1}, δ6.0,broad).

M-I, -II and -IV were also detected in the in vitro studies, showing possible enzymatic oxidation of 2,6-DIPN. The reaction velocities of M-I, -II and -IV formation from varing concentrations of 2,6-DIPN were also determined. The Km value to produce M-I was much higher than that of M-II, and Vmax of two reactions were also different. This fact suggests that these reactions were processed by different enzymes in hepatopanceras of carp.

Summarized results and the possible metabolic pathway of 2,6-DIPN in carp, based on metabolites identified are postulated. Idetification of the possible conjugated metabolites is still in progress.



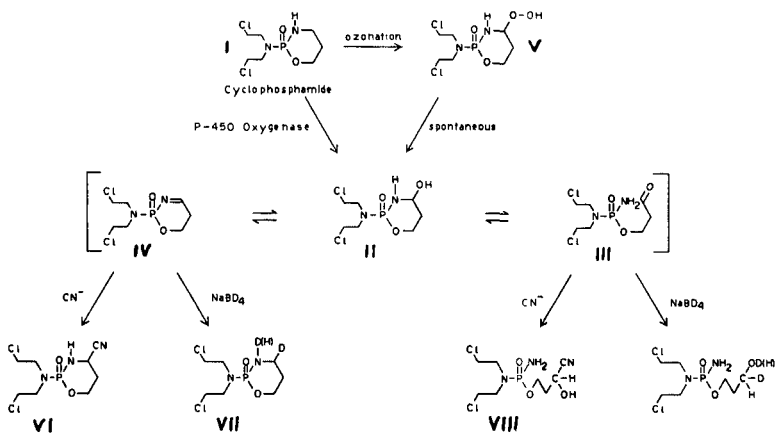
Estimated metabolic pathway of 2,6-DIPN in carp

IMINOCYCLOPHOSPHAMIDE, A NEW METABOLITE OF CYCLOPHOSPHAMIDE

James P. Lehman and O. Michael Colvin
The Johns Hopkins Oncology Center, Baltimore, MD 21205

The metabolic activation of cyclophosphamide (I) to an effective antitumor agent comprises an unusual combination of chemical and enzymatic transformations. The primary event is oxygenation by hepatic P-450 oxygenases to 4-hydroxycyclophosphamide (II). This is in tautomeric equilibrium with aldophosphamide (III), which decomposes spontaneously to the alkylating agent phosphoramide mustard and acrolein. Although phosphoramide mustard is viewed as the ultimate intracellular alkylating agent, it does not appear to be suitable for intercellular transport.

Considerable precedent exists, both from mechanistic studies of drug metabolism and from physical organic chemistry studies of carbinolamine chemistry for the existence of imines in equilibrium with carbinolamines. We have postulated the formation of iminocyclophosphamide (IV) as a result of the enzymatic activation of cyclophosphamide. We report here the characterization of cyano, deutero, and ^{18}O derivatives of this activated metabolite, iminocyclophosphamide.



There are two routes to 4-hydroxycyclophosphamide (II), either by enzymatic oxygenation of cyclophosphamide (I) by P-450 oxygenases or by the spontaneous decomposition of 4-hydroperoxycyclophosphamide (V). Cyclophosphamide, NADPH, and NaCN were incubated with an immobilized hepatic microsomal enzyme system containing P-450 oxygenase activity which was described earlier (1). The resulting 4-cyanocyclophosphamide was recovered by solvent extraction and purified by TLC. Its mass spectrum and chromatographic characteristics were identical to those of authentic chemically synthesized 4-cyanocyclophosphamide and those of the compound which was prepared by decomposing 4-hydroperoxycyclophosphamide (V) in the presence of NaCN.

4-Deuterocyclophosphamide (VII) was generated by decomposing 4-hydroperoxycyclophosphamide in the presence of NaB^2H_4. The product was recovered by solvent extraction and purified by HPLC. The isobutane CI mass spectrum demonstrated the incorporation of one ^2H, the amide hydrogen having been exchanged by the reagent gas ions. The electron impact mass spectrum showed a mixture of mono- and dideutero species, the amide hydrogen apparently having been partially exchanged with water in the reaction mixture. The position of the deuterium was confirmed by NMR spectrometry.

When 4-hydroperoxycyclophosphamide was decomposed in 60 % enriched $H_2{}^{18}O$ and the cyanohydrin (VIII) of aldophosphamide (III) was generated by the addition of $NaHSO_3$ and NaCN, the cyanohydrin recovered by solvent extraction was found to contain 59.5 % ^{18}O by analysis of its molecular ion. This incorporation of ^{18}O is consistent with the intermediacy of iminocyclophosphamide (IV) in equilibrium with 4-hydroxycyclophosphamide (II) and aldophosphamide (III).

The delicate balance between tumor toxicity and general toxicity which uniquely characterizes cyclophosphamide among therapeutic mustards may be sustained in part by chemical (non-enzymatic) transformations. The reactive imine metabolite would play a significant role in chemical aspects of cyclophosphamide metabolism and disposition in vivo. Furthermore, the chemical transformations associated with the imine/hydroxy/aldehyde equilibrium are most readily interpretable in terms of the known chemistry of imines. The identification of a central role for iminocyclophosphamide in cyclophosphamide metabolism also may suggest new approaches to the design of antitumor agents.

1. J. P. Lehman, L. Ferrin, C. Fenselau, and G. S. Yost, Drug Metab. Disp. 9, 15 (1981)

A STUDY OF SENSITIVITY VS. ION SOURCE TEMPERATURE FOR DIRECT LIQUID INTRODUCTION LC-MS.

G.R. Dubay, M.Cadiz, Analytical Res. and Dev., Bristol-Myers Pharm. Res. & Dev., Syracuse, New York 13201

Many compounds of biological interest including the penicillens and cephlosporins are not stable enough for separation by GLC analysis. HPLC can be used to conveniently separate them but frequently ore structure specific analysis is required. Mass spectrometry can be used to provide mass specific data after the sample is isolated but some questions are raised about the integrity of the sample during work up. In-line HPLC has been developing to supply a rapid mass specific analysis for important compounds.(1) Since the samples analyzed in-line questions of sample integrity are overcome. To maximize the sensitivity of this technique we have studied the effects of ion source temperature for direct liquid introduction(DLI)-MS.

In this work ion source temperature was found to strongly affect the response of two analogous compounds in the temperature range from 200 to 350.(2) In DLI-MS the solvent vaporizes and yields the chemical ionization gas used for analysis. The methanol-water mixture (2:3) used here produced a series of cluster ions which react with compounds eluting from the column to give the protonated molecular ions. The effect of temperature on the protonation reaction and sensitivity of analysis can be understood through an investigation of the effects of ion source temperature on cluster ion formation.(3)

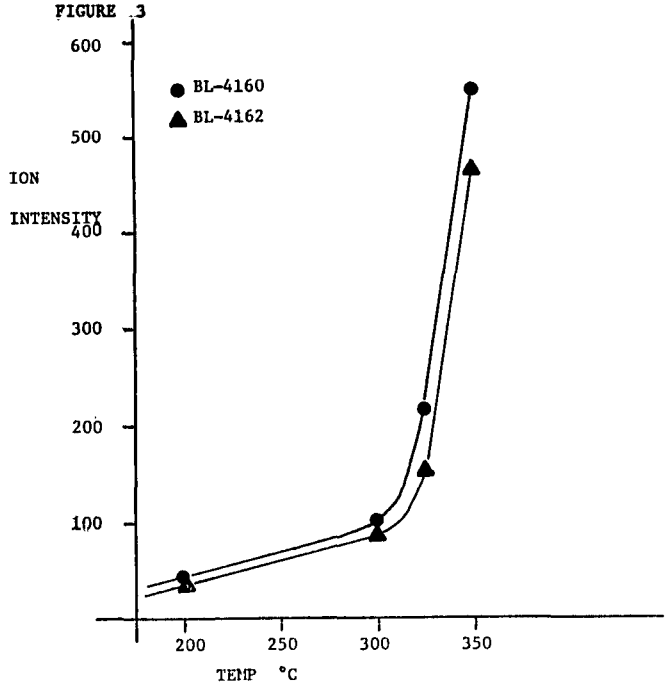
Cluster ions of the form (n·CH3OH+H)+ are formed by the CH_3OH-H_2O mixture and it was thought that the average value of n is dependent on the ion source temperature. The degree of aggregation is important because large cluster ions stabilize the charge well and do not react as rapidly. Conversely, smaller cluster ions are higher in energy and would react more rapidly to give proton transfer which produces protonated molecular ions. The temperature at which the greatest number of small cluster ions are produced should yield the most intense spectra from DLI-MS. Thus, the relationship of ion source temperature and the degree of clustering was studied before the sensitivity of DLI-MS response was related to ion source temperature.

It was observed that there is a strong correlation between ion source temperature and the degree of ion clustering. As temperature was increased the amount of clustering decreases. A ratio of m/z=65 to m/z=97, which represent the (n·CH_3OH+H)+ ion where n=2 and =3, can be used to show how the smaller cluster ion increases in relative abundance as temperature is increased (Figure 1). The curve in Figure 1 shows that from 142 to 280 the relative abundance of the n=2 cluster ion grows steadily but above 280 the relative abundance increases very rapidly with no maximum observed. It was also found that the total number of cluster ions in the source was steadily increasing as the temperature was increased.

The smallest cluster ion observed at m/z is the n=1 ion which has low abundances at temperatures below 280. As the temperature rises above 280 a rapid increase in the n=1 cluster ion is observed. By comparing the relative ratio of m/z=33 and =97 for the n=1 and =3 cluster ions the effects of temperature on the abundance of cluster ions can be seen (Figure 2). The same relationship is seen as present in Figure 1, the relative abundance of the smaller cluster ion increases rapidly above 280 until the maximum temperature is reached. Though not shown in the figures, the total abundance of the n=1 and n=2 cluster ions increased until the maximum temperature was reached. Thus, as the ion source temperature was increased the reactant gas plasma contained more cluster ions, and the reactivity of the cluster ions formed was higher.

Our hypothesis was that as the number and reactivity of ions in the source increased the sensitivity of DLI-MS would increase. Thus, it was expected that the sensitivity of DLI-MS would increase when the reactivity of the reactant gas plasma was increased. This was observed as the ion source temperature was increased. Concomitantly, there was an increase observed in the production of protonated molecular ions.(Figure 3) Both BL-4162 and BL-4160 showed increased response when the temperature was raised from 200 to 290, and above 300 the yielded of protonated molecular ions rapidly increased. This rise was at the same temperature at which the abundance of the n=1 ion increases rapidly as does the n=2, and the n=1 ion is the most reactive component of the reactant gas plasma.

FIGURE 3



In summary, it was observed that for $CH_3OH:H_2O$ during DLI-MS large cluster ions are prominent below a ion source temperature of 280. Above this temperature the smaller more reactive cluster ions dominate the ion plasma and enhance sensitivity. A temperature at which the abundance of n=1 and =2 cluster ions can be maximized probably exists but it is not attainabe with the HP-5985B. At this temperature a maximum sesitivity would be achieved.

1. Recent review in J.Chromatography, 1982, 251(2), p.91-225
2. J. Henion, 29th Annual Conference on Mass Spectrometry and Allied Topics, May 24-29, Minneapolis, Minnesota, oral communication concerning the effects of temperature though not studied.
3. Similar effects have been observed for $CH_3CN:H_2O$ but experiments incomplete.

FIGURE 1

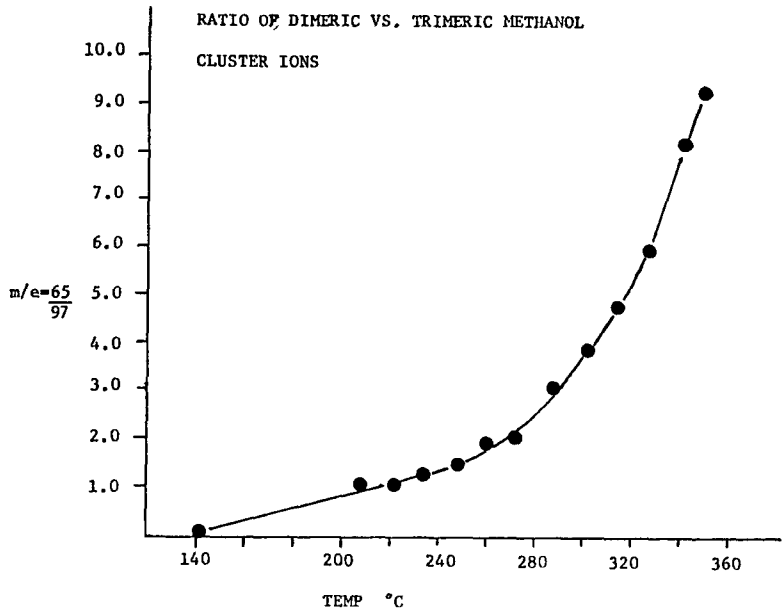
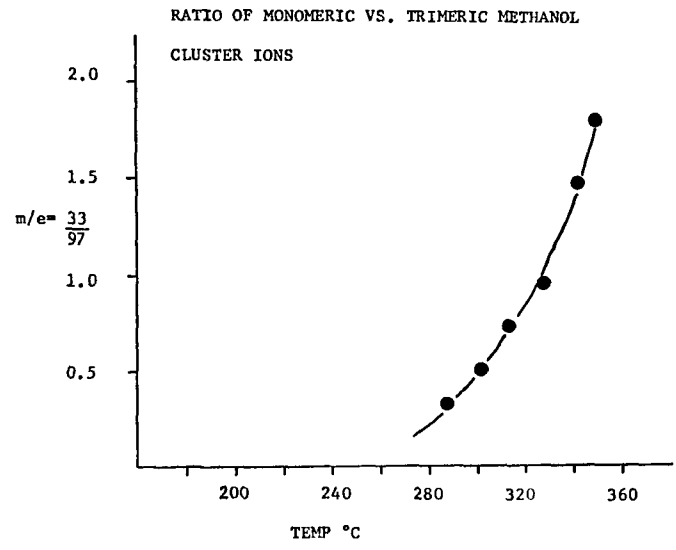


FIGURE 2



SAMPLE DETECTION USING LIQUID CHROMATOGRAPH/MASS SPECTROMETER INTERFACE WITH STATIONARY CONCENTRATOR. H.H. Lo and M.W. Siegel, Extranuclear Laboratories, Inc., P.O. Box 11512, Pittsburgh, PA 15238 U.S.A.

A liquid chromatograph/mass spectrometer (LC/MS) interface based on the NBS design[1] has been constructed, and preliminary results have been obtained. The interface, which contains no moving parts, continuously concentrates the effluent stream by vaporizing the solvent as it flows down a tapered wire which is heated by passing electric current through it. This vertical wire is intersected by a horizontal wire confined, except at the intersection, in a stainless-steel capillary tube through which the concentrated solution is delivered and volatilized into the ion source of a MS. Normal-phase solvents such as hexane, can be concentrated sufficiently that the entire residual flow is delivered to the MS; however, with reversed-phase solvents such as water, a modest split occurs at the intersection.

The temperatures of the concentrator are 50°C at the top and 45°C at the intersection when the solvent used is CH_3OH/50% H_2O flowing at 1 mL/min and the heating power is 22 W. The power needed for normal-phase operation with hexane/3% CH_3OH flowing at 1 mL/min is only about 5.4 W.

Using positive-ion chemical ionization (PCI) technique, benzophenone was detected both in normal (hexane/3% CH_3OH, column: silica/10) and reversed (CH_3OH/30% H_2O or CH_3CN/40% H_2O, column: C18/10) phases with a sensitivity of the order of 1 ng under the selected ion monitoring (SIM) mode. In the present work, the reagent gases were the mobile-phase solvents used. Figure 1 shows the strip-chart recording of the UV response at 254 nm and the SIM at 183 amu of 100 ng benzophenone. Methyl p-hydroxybenzoate (methylparaben) was also observed using PCI in reversed phase with a similar sensitivity.

A compound containing methyl, ethyl and propyl parabens was analyzed using both PCI and NCI (negative-ion CI) in reversed phase. The LC flow rate was 0.7 mL/min and the solvent was CH_3CN/40% H_2O. In Fig. 2 the lower trace represents the PCI response of SIM at 153, 167 and 181 amu for parabens which contain 200 ng of methylparaben; the upper trace is the UV response of parabens. The result obtained using NCI is almost identical to that using PCI, except that the negative ions observed are at 151, 165 and 179 amu. The mass chromatogram can be reconstructed from a full-spectrum scanning and the result obtained using PCI is shown in Fig. 3. In this case the amount of paraben injected was 6 times that under SIM mode shown in Fig. 2.

[1] R.G. Christensen, H.S. Hertz, S. Meiselman, and E. White V, Anal. Chem. 53, 171 (1981).

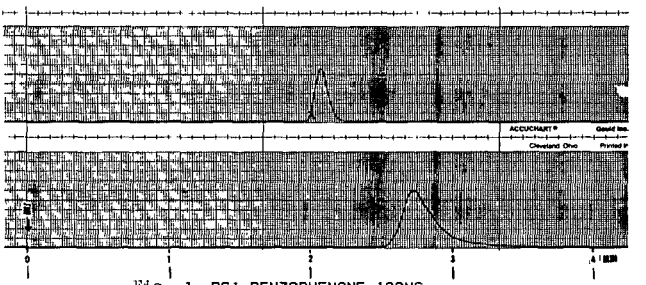


Fig. 1 PCI BENZOPHENONE 100NG
COLUMN: SILICA A/10
1ML/MIN HEXANE/3%MEOH
UV(AT 254NM):UPPER TRACE
MS(SIM MODE):LOWER TRACE

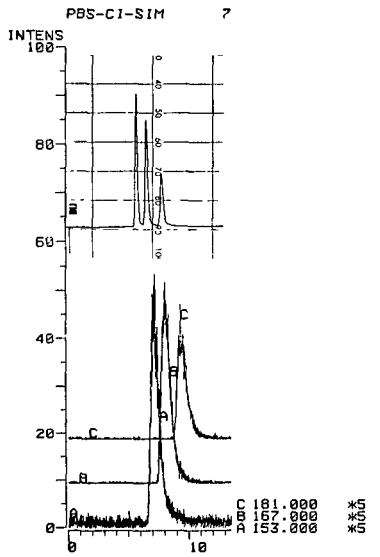


Fig. 2 PCI PARABENS 1UL(A=200NG)
.7ML/MIN 40/60 H20/MECN
SOURCE 225C
UV(AT 254NM):UPPER TRACE
MS(SIM MODE):LOWER TRACE

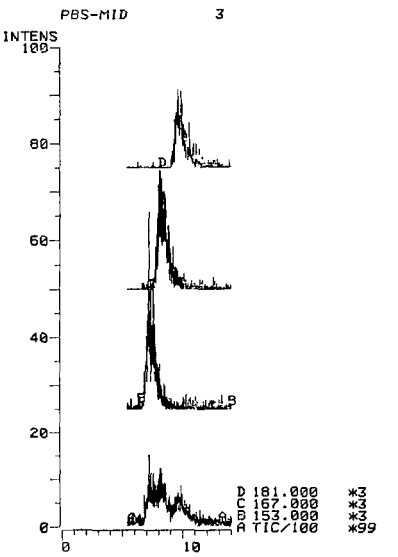


Fig. 3 PCI PARABENS 6UL(B=1.2UG)
.7ML/MIN 40/60 H20/MECN
SOURCE 225C
MASS CHROMATOGRAM
PBS-CI-3

MPA 11 DESIGN AND PERFORMANCE OF LC-MS SYSTEMS USE-

ING THE THERMOSPRAY TECHNIQUE: C.R. BLAKLEY and M.L. VESTAL: Dept. of Chem., Univ. of Houston, Houston, TX 77004

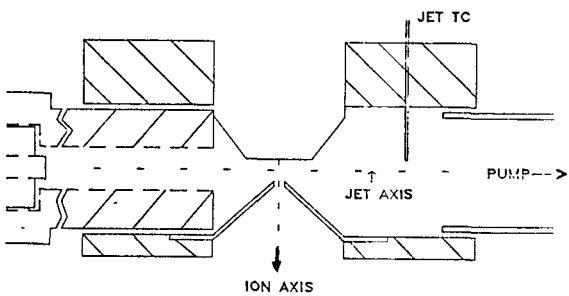
The latest version of the thermospray LC-MS interface has been installed on a Biospect quadrupole mass spectrometer. This interface requires only minor modification of the commercial instrument with a single mechanical vacuum pump required in addition to the pumping system normally used for CI operation. It appears that this LC interface can readily be adapted to other quadrupole mass spectrometers. LC effluents are thermosprayed directly into the ion source and the excess vapor pumped away by the added mechanical vacuum pump which is directly coupled to the ion source through a port opposite the electrically heated thermospray vaporizer. This system provides stable vaporization and ionization at flow rates up to 1 ml/min of aqueous mobile phoase. When used with mobile phases containing significant concentrations of ions in solution (ca. 10^{-4}-10^{-1}M) no external ionizing source is required to achieve detection of many nonvolatile solutes at the subnanogram level. When used with weakly ionized mobile phases, an additional source of gas phase ions is required to obtain comparable sensitivity. Both a conventional electron gun and a radioactive Ni-63 source have been used. Data on the performance of this system for analysis of mixtures of biological and environmental samples by on-line, high-speed, reversed phase LC-MS are presented.

PERFORMANCE CHARACTERISTICS OF THE THERMOSPRAY LC-MS INTERFACE. A.L. Yergey, M.L. Vestal, C.R. Blakley, D.J. Liberato, NICHD, NIH, Bethesda, MD 20205, Dept. of Chemistry, U. of Houston, Houston, TX 77004, Dept. of Pharmacology, Johns Hopkins Medical School, Baltimore, MD

The thermospray LC-MS interface can be used with a wide range of aqueous and non-aqueous solvents including volatile buffers. The interface uses 100% of the HPLC eluent at flow rates ranging from 0.5 to 1.2 ml/min, and, when buffered solvents are present, requires no ionization source other than the buffer itself (1). In this work we report the optimum operating conditions for several solvent compositions at a variety of flow rates for both positive and negative ions. We present positive and negative ion mass spectra of a variety of normally intractable compounds which are indicative of the potential of the interface.

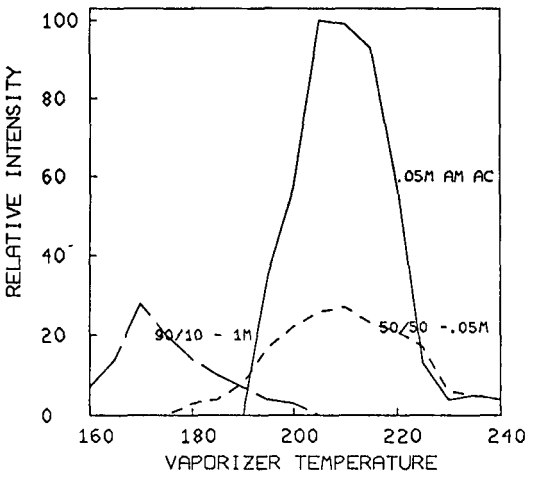
Apparatus - A BIOSPECT quadrupole mass spectrometer with an extensively modified source was coupled to an Hewlett Packard Model 1048-A HPLC through a Valco high pressure injection valve (HP series) equipped with a 25 ml injection loop.

A schematic of the ion source configuration presently in use is shown in Fig. 1.



Solvent from the HPLC (0.8-1.2 ml/min) is pumped through an approximately 0.1 mm orifice brazed into the nozzle shown at the left of the Figure. The nozzle is approximately 2.5 cm away from the ion axis, and the spray formed at the nozzle tip is conducted to the sampling region through a 0.3 cm I.D. tube. The cone through which ions leave the source is about 0.08 cm off the jet axis and about 0.15 cm away from the copper tip projecting into the vapor stream from the rear of the source. Optimum operating conditions for solute response in 0.05 M ammonium acetate (AmAc) flowing at 1.2 ml/min are vaporizer temperature 240°C, and source temperature 265°C which result in a jet temperature of about 165°C.

Solvent Ions - Figure 2 shows total solvent ion current for three solvent systems,



0.05 M AmAc, 50/50:MeOH/.05 M AmAc and 90/10:MeOH/1 M AmAc. Note that the maximum solvent ion response is at a temperature about 20°C lower than that stated for solute ion response. This phenomenon appears to be a general one. It was necessary to increase the buffer concentration to 1 M AmAc in the 90 MeOH/10 AmAC solvent mixture so that sufficient ions were available for solute ionization. The principal ions in each of the solvent systems are summarized in Table I.

Principal Solvent Ions

	Ions (m/z)
.05 M AmAc	$NH_3.NH_4^+$-(35), $H_2O.NH_4^+$-(36), $(H_2O)_2.NH_4^+$-(54), $(CH_3COOH.NH_3.NH_4-18)^+$-(77), $CH_3COOH.NH_4^+$-(78)
50/50:MeOH/.05 M AmAc	$CH_3.NH_4^+$-(50), $CH_3OH.H_2O.NH_4^+$-(68), $(CH_3OH)_2.NH_4^+$-(82)
90/10:MeOH/1 M AmAc	$CH_3OH.NH_4^+$-(50), $(CH_3OH_2)_2.NH_4^+$-(82)

The largest ion in each solvent system are m/z 77, 50 and 50 respectively.

Solute Response - The response of three solutes, choline chloride, glycyl-glycine and tetra-n-butyl ammonium iodide (TBAI) was determined as a function of solvent composition at the flow rates shown in Fig. 2, using repeated injections of 9 nm for the first two materials and 3 nmole for the third. The mass filter was scanned over a 500 amu window in 4 sec. The maximum response for each solute was obtained at temperatures approximately 20 °C above the solvent ion maximum with TBAI and gly-gly giving about 10-times less responsive. The intensities of these responses were such that a conservative estimate of the limit of detection for these materials is 3-5 pmoles. Mass spectra were obtained for a variety of materials including 15-HPETE, Δ-9-THC, tetrapeptides, glucuronides, melatonin, and several antibiotics.

(1) C.R. Blakley and M.L. Vestal. 29th Annual Conference on Mass Spectrometry and Allied Topics, May 24-29, 1981. Minneapolis, Minnesota, Proceedings, p. 275.

A Study On Techniques For Micro-HPLC/MS

Toyohide Takeuchi*, Kiyonari Matsuoka and Daido Ishii
Department of Applied Chemistry
Faculty of Engineering
Nagoya University
Chikusa-ku, Nagoya-shi, 464 JAPAN

Micro techniques for off-line coupling of a micro-high-performance liquid chromatograph(micro-HPLC) and a mass spectrometer(MS), EMD-05A (ESCO) were examined.

In previous work[1], direct coupling of ultra-micro-HPLC and MS(JMS-D300, JEOL) was examined, in which flow-rate of the LC mobile phase was only 0.83μl/min, keeping the pressure in the ion source less than 10^{-6} torr. In the present work, off-line coupling was examined since direct introduction of LC effluent at 0.2μl/min into MS(EMD-05A) led to the increase of the pressure(higher than 10^{-5}torr). Some parameters which affect the mass detection were examined.

The interface employed in this work is illustrated in Fig.1. The micro sampling tube is composed of a stainless-steel tube with semicircular cross-section(0.27mm I.D., 0.51mm O.D. and 19cm length), on which sample solution is placed. The solvent was vaporized prior to detection and the micro sampling tube was settled in the interface as shown in Fig.1. After the interface was vacuumized, the sampling tube was mechanically inserted into a heated stainless-steel tubing(0.90mm I.D., 1.26mm O.D. and 26cm length). Solutes vaporized in the heating pipe entered into the ion source with the stream of nitrogen and ionized in the EI mode. Temperature of the heating pipe was adjusted by altering the applied voltage. Unfortunately, exact temperature was failed to be measured.

Breezing of nitrogen into MS effectively reduced the tailing of a peak and oxidation of compounds. Flow-rate of nitrogen was regurated by pass-

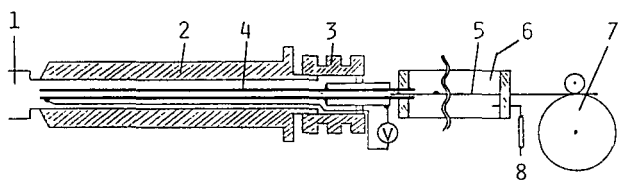


Fig.1 Schematic diagram of the interface
1. Ion source, 2. Probe, 3. Swage lock,
4. Heating pipe, 5. Micro sampling tube,
6. Galss tube, 7. Moving machine,
8. Nitrogen

ing it through a micro packed column(0.5mm I.D.), e.g., 40μl/min in the case of a 10-cm column packed with 10-μm silica gel.

Response was strongly dependent on moving speed of the micro sampling tube. The larger the moving speed, the higher peak was observed. Peak width was independent of the moving speed, being around 20sec. The optimum speed was ca. 6cm/min.

Fig.2 shows the TIM profile of pyrene obtained by this technique. Each peak corresponds to 500ng of pyrene placed at intervals of 3cm.

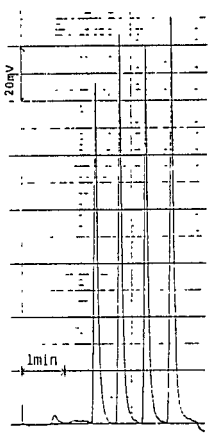


Fig.3 shows mass spectra of 50ng of pyrene and background. The molecular ion (m/e=202) is abundant.

This technique was applicable to aromatic hydrocarbons, some components in a cold medicine and phthalates. Non-volatile compounds such as sugars could not be detected by this method.

Reference

1. T. Takeuchi, D. Ishii, A. Saito and T. Ohki, J. High Resolut. Chromatogr. Chromatogr. Commun., 5(1982)91.

Fig.2 TIM profile of pyrene
Sample:each 500ng of pyrene at intervals of 3cm
Moving speed:6cm/min
Analyzer pressure:6×10^{-6}torr
TIM:150-500

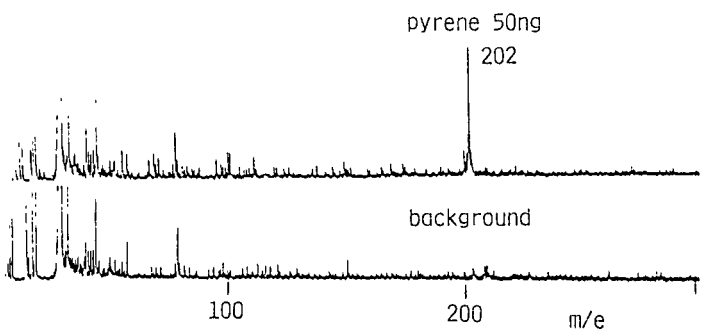


Fig. 3 Mass spectra of pyrene and background

MASS SPECTROMETRIC ANALYSIS AND THERMAL DECOMPOSITION STUDY OF 1,3,5,7-tetranitro-1,3,5,7-tetraazacyclooctane (HMX)

J.G. Moncur, T.E. Sharp, Lockheed Missiles & Space Co., Palo Alto, CA 94304

HMX, a cyclic nitramine is used as an explosive and as a propellant for solid fuel rockets. Many methods have been described for introducing HMX into mass spectrometers(1-4). In the present study, liquid chromatography mass spectrometry (LC/MS) and direct chemical ionization (DCI), proved successful in yielding adduct ions characteristic to the molecular weight of HMX. However, in-beam electron impact and gas chromatographic introduction were unsuccessful for HMX molecular ion production. An instrument schematic is shown in Figure which depicts the hardware used herein (a Finnigan Model 4021 GC/MS).

Direct chemical ionization of HMX was conducted using an ammonia plasma in positive and negative ion mode (Figure 2) with desorption from a stainless steel solid probe extender tip (5) which is heated via rheostat voltage control. (See figures for specific experimental details.) Ionization in positive ion mode yielded adduct ions with HMX at m/z 314 and 331 for addition of $(NH_4)^+$ and $(NH_3NH_4)^+$ reactant ions, (Figure 3). Ionization in negative ion mode produced a small repsonse at m/z 342 which was probably from addition of $(NO_2)^-$ or $(N_2H_2O)^-$ to HMX, and a weaker m/z 296 ion from electron capture via $(NH_3)^-$ or $(NH_3NH_4)^-$, (Figure 4). LC/MS introduction with an acetone/water carrier/plasma ionization yielded ions at m/z 355 and 339 for adduct formation with protonated acetone and acylium ions, (Figure 5). Figure 6 is a spectrum of the acetone/water plasma in positive ion mode (i.e. acylium ions, protonated acetone, and protonated acetone dimer). The LC/MS interface utilized was patterned after the early work of Takeuchi, et al (6), and performance may have been limited by the large gap (8 inches) between the jet nebulizer (an SGE glass jet separator) and the ion source of the mass spectrometer. In later work of Takeuchi, Tsuge (7), et al, many improvements to this type of interface have been reported.

Thermal decomposition studies (8) of HMX were conducted at 350°C in a crude thermal reactor (Figure 1) with a small exit near an open ion source with 20eV electron impact ionization to yield adducts and fragments with m/z 28 through 889, (Figure 7). The evolution of m/z 30, 44, 297, 593, 889 ions are plotted as a function of time in Figure 8. Most of the high mass peaks arise from (a) positively charged adduct compounds (e.g. protonated monomer - m/z 297, dimer - 593, and trimer - m/z 889; and ionized NO and NO_2 plus monomeric HMX - m/z 326 , 342), and (b) positively charged fragment compounds (e.g. loss of neutral methylene nitramine groups from protonated monomeric, dimeric, and trimeric HMX to form m/z 815, 741, 667, 519, 445, 371, and 223). When the experiment was repeated with the filament off, no ions were detected. Note that the association to HMX molecules to yield $(M+H)^+$, $(M+NO_2)^+$, and $(M+CH_3N_2O_3)^+$ ions has been reported to result from a high gas phase concentration of HMX in a CI ion source (3).

In the present work, the complex reactions which HMX undergoes at the elevated temperatures and pressures of the thermal reactor may be pertinent to the actual use of HMX in propellants and expolsives. A possible mechanism which partially explains how HMX decomposes to form adduct and fragment compounds with molecular weights 28 - 889 is that the explosion occured in the pressurized thermal reactor by free radical reactions (e.g. pyrolysis) and the reaction products were expelled by the burst of the explosion into the high vacuum region of the ion source. These thermally produced radicals/neutrals were then presumably ionized by the 20eV electrons in the ion source and were detected with minimal electron-induced fragmentation.

An alternate explanation is that a significant portion of the HMX molecules may have been expelled from the reactor in sufficiently high concentration to allow ionization by ion-molecule reactions in the open ion source, (as in chemical ionization (3)). In fact, the Finnigan Model 4021 ion source is only moderately open when run in "Vent" mode, and the electron beam is fairly close to the reactor outlet. Both of these design factors favor the second hypothesis (ion-molecule reactions in the open ion source). However, if the reactor was positioned close to a completely open EI ion source with an off axis electron beam, the presence of protonated monomers, dimers, and trimers would substantially favor the first hypothesis (formation of free radicals/neutrals by thermal process followed by electron impact ionization).

References

1.P. Vouros, B.A. Peterson, L. Colwell, B.L. Karger, H. Harris, Anal.Chem.,V.49,N.7(1977)1039.
2.J. Yinon, S.Zitrin, "The Analysis of Explosives", Pergamon Press, 1981.
3.R.C. Spreen, B. Munson, 29th Annual Conf. on Mass Spectrometry and Allied Topics(1981)583.
4.R.D. Voyksner, Y. Tondeur, C.E. Parker, J.D. Henion, J. Yinon, ibid, (1981)297.
5.R.P. Barron, Biomed. Mass Spec., 5, 10, (1978) 578.
6.T. Takeuchi, Y. Hirata, Y. Okumura, Anal.Chem., V.50, N.4, (1978) 659.
7.Y. Yoshida, H. Yoshida, S. Tsuge, T. Takeuchi, K. Mochizuki, HRC&CC, 3, (1980), 17.
8.M. Farber, R.D. Srivastava, Chem.Phy.Let., V.80, N.2, (1981), 345.

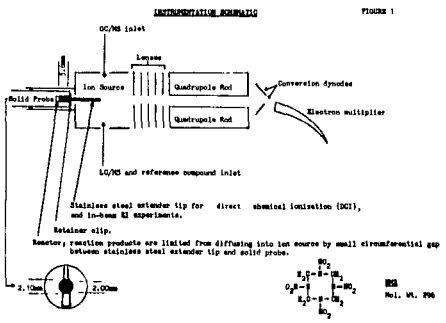


FIGURE 1

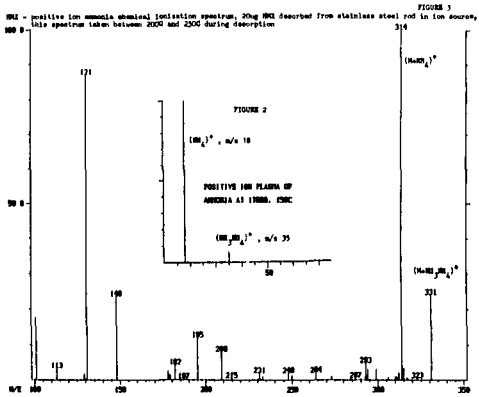


FIGURE 3

HMX - positive ion ammonia chemical ionisation spectrum, 20ng HMX described from stainless steel rod in ion source, this spectrum taken between 200C and 250C during desorption

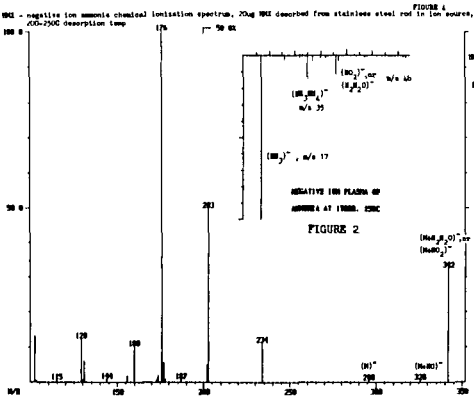


FIGURE 4

HMX - negative ion ammonia chemical ionisation spectrum, 20ng HMX described from stainless steel rod in ion source, 200-250C desorption temp

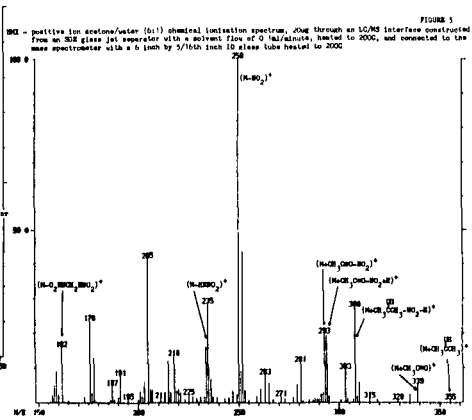


FIGURE 5

HMX - positive ion acetone/water (6:1) chemical ionisation spectrum, 20ng through an LC/MS interface constructed from an SSX glass jet separator with a solvent flow of 0 ml/minute, heated to 200C, and connected to the mass spectrometer with a 6 inch by 5/16th inch ID glass tube heated to 200C

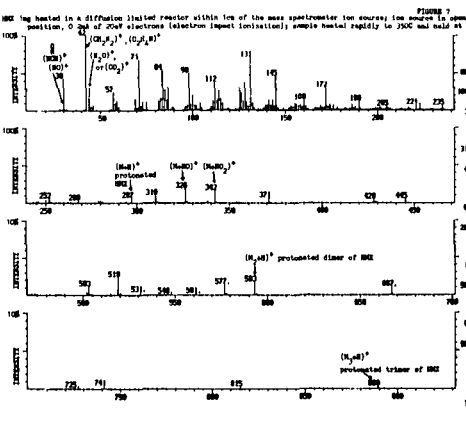


FIGURE 7

HMX 1mg heated in a diffusion limited reactor within 1cm of the mass spectrometer ion source; ion source in open position, 0.2mA of 70eV electrons (electron impact ionisation); sample heated rapidly to 350C and held at 350C

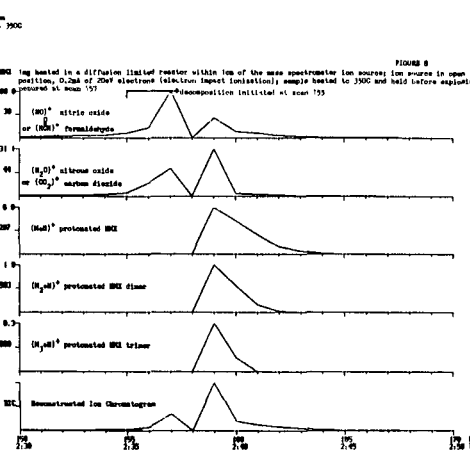


FIGURE 8

CHARACTERIZATION OF POLYMERS AND POLYMERIC COMPONENTS BY LC/MS USING DIRECT LIQUID INLET (DLI) INTERFACE*

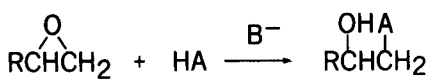
D. C. Canada and D. S. Zingg

Union Carbide Corporation, Nuclear Division
Oak Ridge, Tennessee

The identification of "non-volatile" organic components in complex matrices is one of the most difficult problems facing the analytical chemist. This paper reports on the application of DLI LC/MS techniques to the identification and characterization of "non-volatile" polymeric ethers. Oligomers of polyphenyl ethers, esterified polyethlene glycols, polysilyl ethers, and the diglycidyl ether of Bisphenol A (DGEBA) have been characterized by these methods. In addition to the expected molecular weight information, some of these polymeric ethers have enough excess internal energy to fragment after ionization supplying useful structural information.

This work was done with a Hewlett-Packard 5985B mass spectrometer interfaced to a Hewlett-Packard 1084B liquid chromatograph. An unmodified, 1/2-in. O.D. DLI interface was employed for sample addition. CH_3CN/H_2O solvent mixtures were used to affect separation of individual oligomers on reverse-phase (RP-8) LC columns.

Since organic molecules tend to redistribute their excess internal energy in a random manner among the active degrees of freedom of the molecular ion, little fragmentation is expected of these larger components by CI methods. In fact, it was observed that polyphenyl ethers and esterified polyethylene glycols react with the CH_3CN/H_2O CI reagent gases by simple proton addition with little further fragmentation. As expected, the Brønsted acids thus formed have insufficient excess internal energy to undergo further cleavage or rearrangement. Contrary to the above suppositions, polysilyl ethers fragment rather easily under these conditions perhaps due to the relatively weak Si-O bond. Molecular ion information is absent in the mass spectra of the silyl ethers examined and rearrangement processes make the interpretation of the mass spectral data difficult. Components associated with DGEBA were found to have sufficient excess internal energy to fragment by simple cleavage at the benzylic carbon under these conditions. These components are usually the result of reaction with the epoxy functional group. In general, base catalyzed nucleophilic attack occurs preferentially on the least substituted epoxy carbon, i.e.,



DGEBA impurities have been predicted from this rule of orientation and 13 components tentatively identified by DLI LC/MS. Polymeric isomers may be inferred from the LC/MS data. For example, one might assume the formation of minor components by counter addition to the normal base catalyzed epoxy cleavage process. One of these suspected isomers was found corresponding to a $DGEBA_{(n=1)}$ isomer. The presence of a 341^+ ion in the mass spectrum of the suspected counter addition product further supports the tentative isomer identification.

*Prepared for the U.S. Department of Energy under U.S. Government Contract W-7405 eng 26.

APPLICATIONS OF A DIRECT LC/MS SYSTEM UTILIZING A SPECIAL DESOLVATION CHAMBER.

M. Dedieu (1), G. Devant (1),C. Juin (1), M. Hardy (1), J.P. Bounine (2), P.J. Arpino (3), G. Guiochon(3).

(1) Nermag Corp.,49 quai du Halage, F-92500 Rueil-Malmaison, France.
(2) Rhône Poulenc Recherches, Centre Nicolas Grillet, F-94400 Vitry,France.
(3) Ecole Polytechnique, laboratoire CAP, F-91128 Palaiseau, France.

A simple and inexpensive modification to a LC/MS interface fitted with a direct liquid introduction (DLI) nebulizer has been installed on our quadrupole mass spectrometer. The device (fig.1) is placed between a conventional DLI nebulizer and the CI source block. Solute ions which resisted previous LC/MS investigations are now amenable to the technique.

The DLI probe was described previously[1] and utilizes a similar nickel diaphragm with a ca 2 µm pinhole orifice as the nebulizer. It was used without modifications, but no cooling water was circulated through the DLI probe. The LC/MS interface was operated in the split mode, nebulizing 10 µl/min of a 50/50 (v:v) acetonitrile- water solution, buffered at PH 5 by a volatile trimethylamine-formic acid buffer.

The new droplet transfer line comprizes a blackened copper radiator, a heated desolvation chamber, and an alumina insulating spacer. The assembly is permanently screwed to the CI source block.

The radiator (3 cm OD) fits around the end of the desolvation chamber to which the tip of the DLI probe butts tightly during a LC/MS run. It keeps the diaphragm in the DLI probe tip at ca 60°C when the drift cone in the desolvation chamber is at high temperatures; the nebulization by the diaphragm would otherwise be unstable. The radiator replaces the cooling water through the DLI probe.

The desolvation chamber is a stainless steel block (15 mm x 46 mm), machined to accomodate a cartridge heater and the droplet drift zone. The shape of the drift zone is sharply converging at the entrance, then diverging at a low angle in the remaining portion. The droplets from the nebulizer are concentrated and accelerated to sonic velocities during their flight through this nozzle.[2] A different geometry has been also tried(see paper ROC4).

The alumina spacer acts as a thermal barrier between the desolvation chamber and the CI source, so that both zones can be held at different temperatures. Typically, the temperatures of the chamber and the CI source block are 200°C and 150°C, respectively.

The device has been in use for several months and has proved to be effective for handling non volatile molecules, including vitamin B12. In this example, 50 ng of vitamin B12 were injected into the CI source. The negative ion spectrum (fig.2) shows an abundant ion at m/z 1353, corresponding to (M-H). Fragments at lower masses are not abundant, and this suggests that our ionizing conditions are extremely soft.

1) Arpino,P.J.;Krien,P.;Vajta,S.;Devant,G. J.Chromatogr.1981,203,117.
2) Dedieu,M.;Juin,C.;Arpino,P.J.;Bounine,J.P.;Guiochon,G. J. Chromatogr. 1982,251,203.

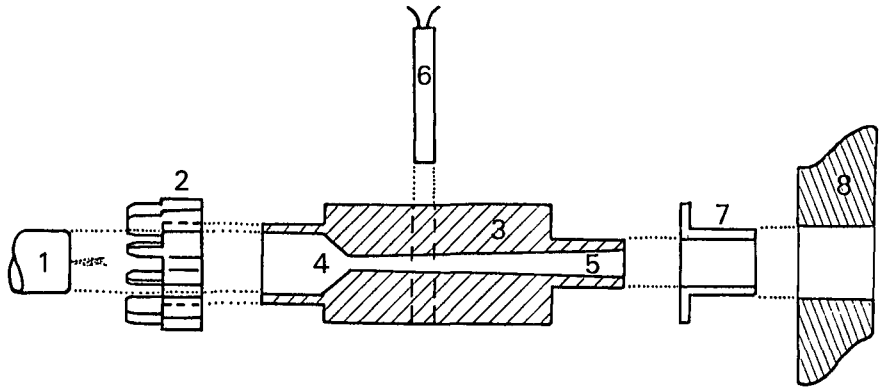


figure 1: Schematic diagram of the LC/MS transfer line of droplets. (1) Vespel end of the DLI probe, (2) blackened copper radiator, (3) stainless steel desolvation chamber, (4) pre-evaporation zone, (5) heated divergent cone, (6) 30W electrical heater, (7) Alumina insulator, (8) CI source block.

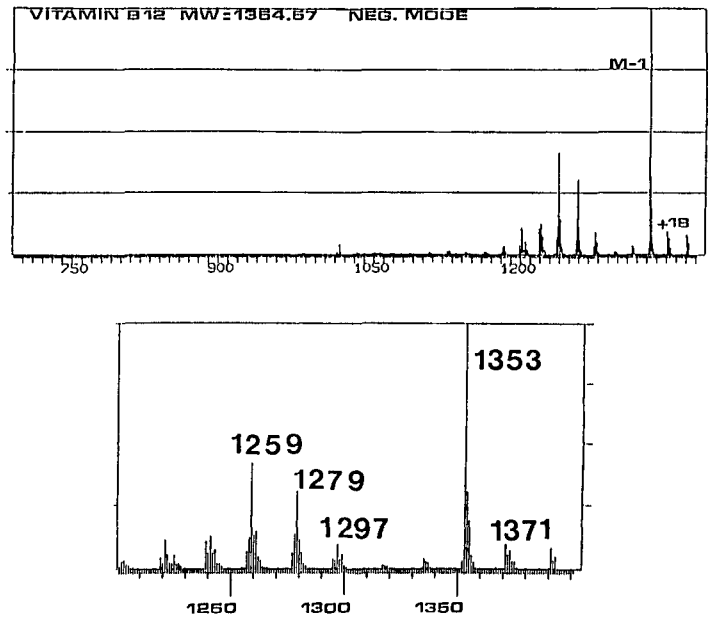


figure 2: Negative ion mass spectrum of vitamin B 12 under the new DLI LC/MS conditions. The spectrum was recorded during the injection of 50 ng of sample into the CI source.

Mass Spectrometric Characterization of Leukotriene Hydroxy Fatty Acids. Timothy W. Harper and R.C. Murphy, Department of Pharmacology, University of Colorado School of Medicine, Denver, Colorado 80262.

A novel class of lipoxygenase derived metabolites of arachidonic acid has recently been isolated from a variety of biological sources. These compounds, termed leukotrienes, are derived from a triene expoxide intermediate (viz., LTA_4) and include a hydroxy fatty acid class (e.g., LTB_4) and a peptidolipid class (e.g., LTC_4) (1,2). LTB_4, recently identified as 5(S), 12(R), dihydroxy, 6,8,10,14 cis, trans, trans, cis eicosatetraenoate is a potent chemokinetic and chemotactic factor and may be involved in inflammation as well as hypersensitivity reactions (3). Two relatively inactive LTB_4 isomers have also been isolated and identified as 5(S), 12(R) and 5(S), 12(S), dihydroxy, 6,8,10,14, trans, trans, trans, cis eicosatetraenoate (Δ^6-trans LTB_4) (2).

Methyl ester, trimethylsilyl ether derivatives of the three 5,12 dihydroxyeicosatetraenoates yield electron impact mass spectra which are essentially identical. Several of the major ions were tentatively identified by earlier workers, although positive identification of fragmentation pathways for these compounds has proved difficult due to extensive rearrangements and limited availability of material for study (2). The recent availability of synthetic LTA_4 and the use of isotopically labeled variants of LTB_4 has permitted tentative identification of several fragmentation pathways of these compounds (5).

LTB_4 and the two Δ^6-trans LTB_4 isomers were isolated from mouse mastocytoma cells (5). Δ^6-trans LTB_4 isomers were also prepared by acid catalyzed hydration of synthetic LTA_4 epoxides for isotopic labeling studies. 12,14,15 (D_3) LTA_4, 8,10 (D_2) LTA_4, and 8,10,12,14,15 (D_5) LTA_4 were synthesized and kindly supplied by Y. Girard and J. Rokach of Merck-Frosst Canada, Inc. Hydration of LTA_4 with $H_2{}^{18}O$/HCl incorporated ^{18}O at the 12 position. Reaction of LTA_4 with methanol/HCl yielded 5-hydroxy, 12-methoxy eicosatetraenoate.

Methyl esters were formed by methylation with diazomethane/ether. Trimethylsilation was performed by addition of bis(trimethylsilyl) trifluoroacetamide/acetonitrile. T-butyldimethylsilyl derivatives were prepared by addition of t-butyldimethylsilyl chloride and imidazole/dimethylformamide and warming to 60°C for 45 minutes, followed by addition of water and extraction with dichloromethane.

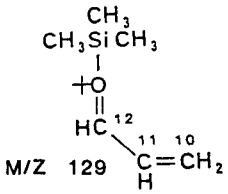
Oxygen-18 was incorporated into the carboxyl group by hydrolysis of LTB_4 methyl ester with porcine liver esterase in $H_2{}^{18}O$. Isotopic labeling of the methyl ester portion was accomplished by methylation with CD_2N_2. D_9-TMS derivatives were prepared with D_9 N,O-bis (trimethylsilyl) acetamide.

Gas chromatography-mass spectrometry was performed using a Finnigan 9500 gas chromatograph with a glass 2.5 mm X 1.2 m 3% OV 101/Gaschrom Q column interfaced to a Finnigan 3200 quadrupole mass spectrometer. The gc column was temperature programmed from 200° C to 270°C at 4°/min. Mass spectra were recorded under electron impact with 70eV ionizing energy. High resolution data was obtained by peak matching on a VG Micromass 7070H mass spectrometer.

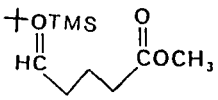
Three major ions in the mass spectrum of Δ^6-trans LTB_4 methyl ester, trimethylsilyl ether, m/z 129, 203, and 217, were identified by high resolution mass spectrometry and by comparison of spectra of various labeled Δ^6-trans LTB_4 derivatives. M/z 129 and m/z 217 were each shifted by one AMU in the 8,10 (D_2) species, by one AMU in the 12,14,15 species, and by 2 AMU in the 8,10,12,14,15 species. M/z 203 was unchanged in the spectra of all three deuterated species. Oxygen-18 labeling of the carboxyl group resulted in a clear shift of m/z 203 to m/z 205 and 207. The oxygen-18 carboxyl labeled species also yielded strong ions at m/z 129 and m/z 217 with less intense ions at m/z 131 and 219. Spectra of deuterium labeled methyl esters-TMS esters revealed a shift of m/z 203 to 205 whereas m/z 129 and 217 were unchanged. Incorporation of oxygen-18 at the 12 position shifted m/z 217 to 219, did not alter m/z 203, and yielded both a strong m/z 129 and a less intense ion at m/z 131.

Replacement of the 12-OTMS with $-OCH_3$ shifted m/z 217 to 159 but did not change m/z 129 and 203. The 5,12, D_9 TMS derivative exhibited ions at m/z 129 and 138, and at m/z 203 and 212, whereas m/z 217 was shifted to 235. Replacement of the 5 and 12 OTMS group with -OTBDMS shifted m/z 129 to 171, m/z 203 to 245 and m/z 217 to 301. High resolution measurements of ions at nominal masses 129,203, and 217 yielded exact masses of 129.07312, 203.11030, and 217.10706 which correspond to elemental compositions of $C_6H_{13}OSi$, $C_9H_{19}O_3Si$, and $C_9H_{21}O_2Si_2$, respectively.

M/z 129, is the base peak in the 5,12 dihydroxy eicosatetraenoat methyl ester, TMS ether mass spectrum and is also a prominent ion in spectra of other hydroxy fatty acids. Under high resolution, the ion at nominal mass 129 is seen to consist of one major and two minor ions. The more intense m/z 129 ion contains one TMS group, no methyl ester hydrogens or carboxyl oxygens, one hydrogen atom from positions 8 or 10 and one hydrogen atom from positions 12,14, or 15. Presence of the 12-oxygen is indicated as is the presence of the 5-TMS. The major m/z 129 ion is, therefore, assigned the structure below.



M/Z 129

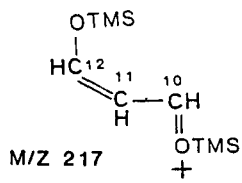


M/Z 203

M/z 203 was tentatively identified by Borgeat and Samuelsson as M-(111+180) and $CH_3OOC(CH_2)_3CHOTMS$ (5). High resolution studies indicate the presence of one major ion plus one minor ion at the same nominal mass. The more intense ion appears to contain one TMS group, the carboxyl oxygens and methyl ester hydrogens, but not the 12-oxygen or any hydrogen atoms from positions 8,10,12,14, or 15. Based on these data, m/z 203 is assigned the above structure.

M/z 217, tentatively identified by Borgeat and Samuelsson as $TMSO(CH)_3OTMS$, is somewhat unusual in that it contains both the 5 and the 12 TMS groups, the 12-oxygen, one hydrogen from position 8 or 10, and one hydrogen from positions 12,14, or 15. The m/z 217 ion does not contain either the methyl ester hydrogens, or the carboxyl oxygens. High resolution data support the assigned elemental composition of m/z 217.

A proposed mechanism for formation of m/z 217 involves cleavage α to the 12-OTMS (between carbons 12 and 13). Charge induced double bond migration from Δ^{10} to Δ^{11} and attack of the 5-oxygen at carbon-10 leads to formation of a 7 membered ring. Cleavage of the 5 carbon-oxygen bond and the 9-10 carbon-carbon bond with ring closure between carbons 5 and 9 leads to formation of the observed m/z 217 rearrangement ion.



M/Z 217

Acknowledgements:

This work was supported in part by a grant from the National Institutes of Health (HL25785).

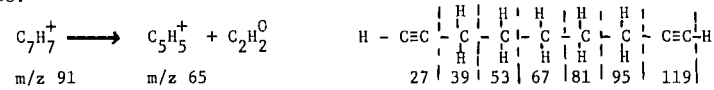
References:

1. Samuelsson, B, Borgeat, P., Hammarstrom, S. and Murphy, R.C. (1979) Prostaglandins 17, 785-787.
2. Borgeat, P. and Samuelsson, B. (1979) J. Biol. Chem. 254, 2643-2646.
3. Ford-Hutchinson, A.W., Bray, M.A., Doig, M.V., Shipley, M.E. and SMith, M.J.H. (1980) Nature 286, 265-265.
4. Rokach, J., Girard, Y., Guidon, Y., Atkinson, J., Larue, M., Young, R., Masson, P and Holme, G. (1980) Tetrahedron Lett. 21, 1485-1488.
5. Murphy, R.C. and Mathews W.R. In Methods in ENzymology: Prostaglandins and Arachidonate Metabolism (ed. Lands & Smith), in press.

MASS SPECTROSCOPIC FRAGMENTATION PATHWAYS OF 1,8-NONADIYNE,
ROBBINS, R.C., AND FOSTER, N.G.; Department of Chemistry
TEXAS WOMAN'S UNIVERSITY, DENTON, TEXAS 76204

The mass spectral behavior of alkadiynes have been reported and discussed (1-7). Clevage of the bonds beta to the triple bond was observed to make important contributions to these spectra. None of this work involved carbon-13 labelling. Deuterium labelled alkynes and diynes showed the proclivity of deutrium scrambling. 1,5 hexadiyne has been reported to undergo time dependent conversion to a cyclic form and hence the spectrum exhibits both linear and cyclic fragmentation patterns (8). The peculiarities of alpha-omega diyne behavior in the mass was noted in passing in a program to obtain reference mass spectra for exhaust gas component identifications by the United States Bureau of Mines, (7) Bartlesville, Oklahoma.

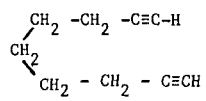
The mass spectra of these terminal diynes contain some peaks that are hard to explain by classical fragmentation pathways. For diynes of length greater than six carbons the mass spectra contain an intense ion at mass 91 and also ions at 65, 64, 54, 53, 51. This pattern resembles that followed by fragmentation of tropylium ion, rather than by expressly linear processes. Other than a hydrogen atom adjacent to a terminal carbon-carbon triple bond, alpha cleavage was found to be a minor process by earlier workers.



In the case of 1,8 nonadiyne, (mol. wt. 120) it must lose two carbons plus some hydrogen to produce an ion of m/z 91. One way this may occur is by head to tail interaction or self-solvation.

Intramolecular charge-exchange or charge-resonance complexes in gaseous ions have been proposed by earlier workers, (9,10) but the proposed interaction of the alpha-omega alkadiynes was not considered in the work of others with diynes.

Conformation of the molecule at the time of ionization may be an important factor (12). Shown in Figure 1 are selected model arrangements illustrating close approach of the terminal pi bonds as well as more linear forms in which the interaction would be extremely weak. For the linear form m/z could be pictured to form by alpha cleavage to the triple bond as shown with the concurrent ejection or rearrangement of four hydrogens. If the U-shaped configuration is ionized then an energetically easier pathway to m/z 91 can be visualized. The ejection of a neutral C_2H_4 (or a C_2H_5 in concerted fashion) can occur.



Only bonds beta or gamma to the triple bond would have been cleaved and with the remaking of a C-C bond and rearrangement of hydrogens to the 2 and 8 carbon atoms, the very stable $C_7H_7^+$ ion would be produced.

To study these possibilities C-13 labelling in the 1,2,8,9 positions and in the 3,7 positions was selected because of the relative ease of synthesis.

The 1,2,8,9-C-13-1,8-nonadiyne was synthesized by bubbling 99.9% atom pure 1,2-C-13-ethyne into a solution of sodium in liquid ammonia at -33°C and to the resulting solution was added 1,5-dibromopentane. The solution was stirred until the ammonia evaporated. The salts were extracted with ether and filtered. The ether was rotovaped off and the crude product purified by G.C. The 3,7-C-13-1,8-nonadiyne was prepared similarly this time using unlabelled ethyne and adding 1,5-C-13-1,5-dibromopentane. Subsequent treatment was the same.

Examination of the mass spectra of the two different labelled compounds shows the expected $(M-1)^+$ ion to be stronger than the $(M)^+$ ion. The ion at m/z 91 of the unlabelled species is formed mostly by the extrusion of carbon atoms 4,5, and 6 with attendent hydrogens. A fraction of the ion must be formed by inclusion of only one of the carbon-13

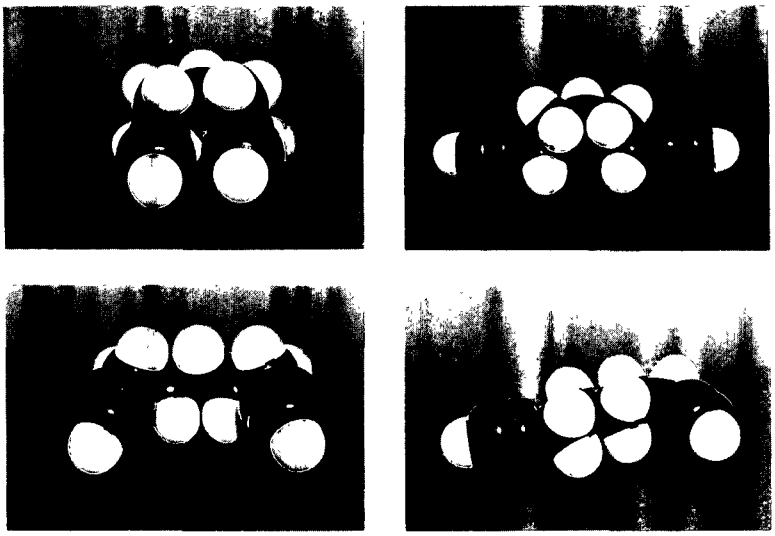


FIG. I.

atoms in the 3,7-compound as reflected by the m/z 92 peak. The tetra-labelled compound shows even less of an intensity at m/z's 93 and 94. Some linear processes are occurring to produce the ions in the 77-84 region of the three molecules in question. An ion at m/z 105 shows with moderate intensity in the unlabelled molecule. Corresponding ions at m/z 109 and 107 for the tetra and di-labelled molecules supports an unusual mechanism, that is the terminal carbons are not involved, but rather a methylene or (methyl) group appears to be being lost from the center of the chain with the charge remaining on the two ends which must be held together by interaction of the two terminal pi bonds. Metastable processes in which one or two hydrogens are lost are apparent in all of the spectra.

The doubly charged ions in all of the spectra indicate an interesting small scale process of the molecular ion (or the M-1) proceeding to strip off hydrogens and forming a very stable ion at m/z 115 in the unlabelled molecule. The labelled compounds do likewise with the doubly charged ions appearing at m/z 58.5 instead of at 57.5. Further calculation of the contributions of the various ions to the various processes will be made as will examination by MS/MS to show the processes occurring for various fragment ions as well as for the metastable processes.

1,2) Polykova, A.A., Khmel-Nitskii, R.A., and Petrov, A.A., Zh. Obschch. Kim., 34, 1484, 3296 (1964).
3) Beynon, J.H., "Mass Spectrometry and its Applications to Organic Chemistry", p.271, Elsevier, Amsterdam, (1960).
4) Beynon, J.H., Saudners, R.A., and Williams, A.E., "The Mass Spectra of Organic Molecules," p.107. Amer. Elsevier, New York. (1968).
5) Dolejsek, Hanuš, V., and Vokač, K.,"Adv. in Mass Spectrometry", p. 503 (W.L. Mead.Ed) Inst. of Petrol, London, 1966.
6) Woodgate, P.D., Mayer, K.K. and Djerassi, C., J. Am. Chem. Soc. 94, Part 3, 3115 (1972).
7) U.S.B.M. Report of Investigations #6854, R.F. Kendall and B.H. Eccleston, 1966.
8) Lifeshitz, C. and Gefen, S., Int. J. Mass. Spectrom. Ion Phys., 35, 31 (1980).
9) Winstein, S. and Lossing, F.P., J. Am. Chem. Soc., 86, 4485 (1964)
10) Meyerson, S., Hart, H., and Leitch, L.C., ibid. 90, 3419 (1968).
11) Meyerson, S. and Leitch, L.C. ibid. 93, 2244 (1971).
12) Winnik, M.A., Chemical Reviews, 81, #5, 491 (1981).

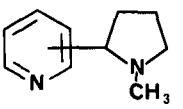
MASS SPECTROMETRY OF NICOTINE AND SOME STRUCTURAL ISOMERS.

by

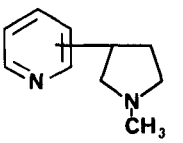
D. F. Magin, W. N. Einolf, and H. V. Secor
Philip Morris Research Center
P. O. Box 26583
Richmond, Virginia 23261

Low resolution mass spectrometry, precise mass measurements, and metastable ion studies have pinpointed three major factors influencing the fragmentation of nicotines (I) and isonicotines (II):

a) the presence of an aromatic ring system: b) the position of attachment of the aromatic ring to the pyrrolidine ring; and, c) whether the pyrrolidine ring is attached to a carbon adjacent to the pyridine nitrogen.



(I) Nicotines
(2,3, or 4, 2')



(II) Isonicotines
(2,3, or 4, 3')

The m/z 84 ion is characteristic of the nicotines, those compounds which have *the pyridine ring attached at the 2'-position of the pyrrolidine ring. For the iso-*nicotines, where the substitution on the pyrrolidine ring is at the 3'-position, m/z 57 is the characteristic peak. In addition, a large peak at m/z 106 is indicative of those compounds where substitution on the pyridine ring is at the 2-position, regardless of the point of attachment on the pyrrolidine ring.

Fragmentation patterns and explanations of fragmentation mechanisms are detailed, which are consistent with the observed behavior of a series of nicotines and isonicotines.

The mass spectra obtained on a MAT 112S instrument at an accelerating voltage of 820V, ionizing energy of 80 eV, and resolution of 350 are shown below. Samples were introduced into the ion source at a source temperature of 135°C using a direct insertion probe.

FIGURE 2A

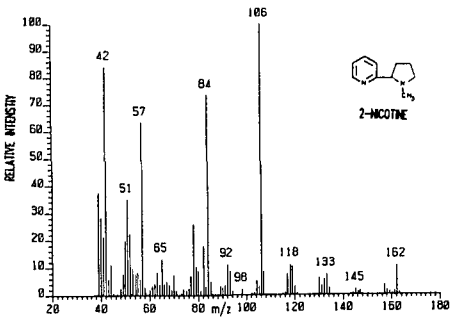


FIGURE 3A

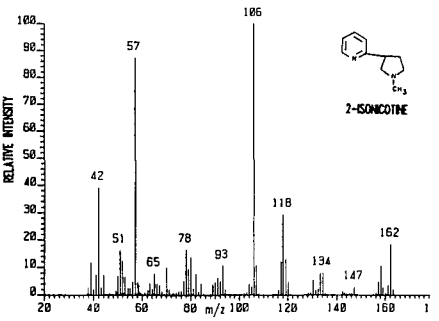


FIGURE 2B

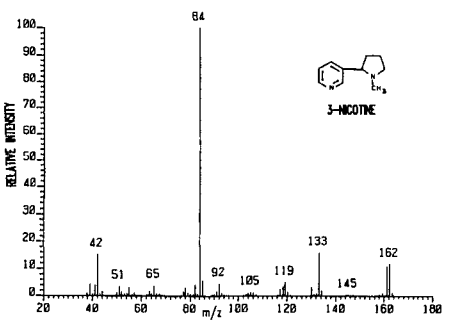


FIGURE 3B

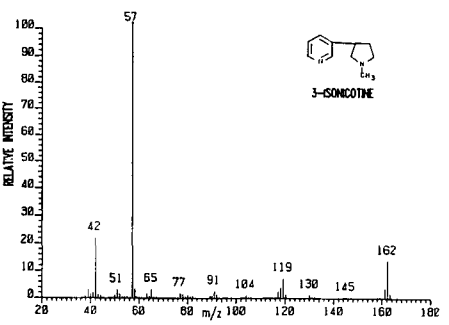


FIGURE 2C

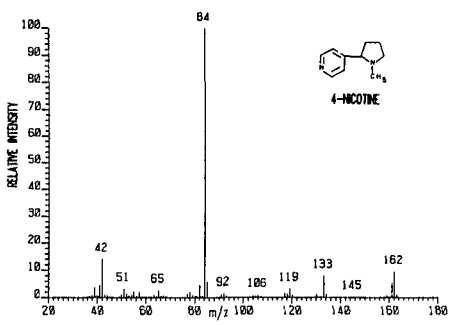
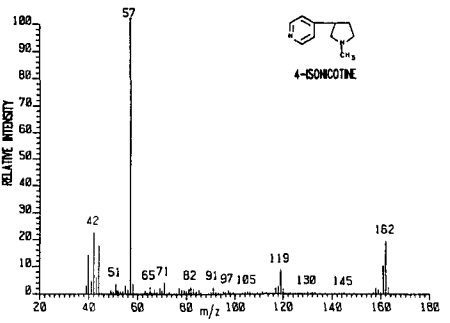


FIGURE 3C



THEORETICAL STUDY OF ELECTRON IMPACT MASS SPECTROMETRY. I. AB INITIO MO STUDY OF THE FRAGMENTATION OF N-BUTANE

TAKEUCHI, T., YAMAMOTO, M., and NISHIMOTO, K.*
Faculty of Science, Nara Women's University, Nara 630, JAPAN and Faculty of Science, Osaka-City University, Sumiyoshi-ku, Osaka 558, JAPAN*

The purpose of our work is to explain theoretically the fragmentation mechanism of organic compounds. In the present study the fragmentation mechanism of n-butane by the low energy electron bombardment has been studied by means of the ab initio MO method.

CALCULATION

Geometry —— Optimized geometries of possible n-butane cation conformers, reaction intermediates and fragments have been calculated with the STO-3G minimal basis set using the gradient technique. The energies have been calculated by the 4-31G basis set using geometries from the STO-3G method.

Potential Curve —— In the calculation of potential curve, we have made the following assumptions. We draw the potential curve against the C-C bond distance. At the initial stage of reaction, the change of a C-C bond distance is very small, so that the other geometry parameters such as the C-H bond distances, the other C-C bond distances and bond angles are assumed to be unchanged. When the C-C bond distance becomes larger than 2.0Å, we have done geometry optimization with the STO-3G minimal basis set at a given C-C bond distance. For the comparison the energy has been calculated with the 4-31G basis set. In the present study, we have assumed the following four fragmentation schemes;

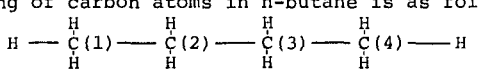
Scheme I ; $n\text{-}C_4H_{10}^{+\cdot *} \rightarrow \underset{\text{I-1}}{CH_3CH_2CH_2\text{---}CH_3}^{+\cdot} \rightarrow \underset{\text{I-2}}{CH_3CH_2CH_2^+} + \underset{\text{I-3}}{\cdot CH_3}$

Scheme II ; $n\text{-}C_4H_{10}^{+\cdot *} \rightarrow \underset{\text{II-1}}{CH_3CH_2\text{---}CH_2CH_3}^{+\cdot} \rightarrow \underset{\text{II-2}}{CH_3CH_2^+} + \underset{\text{II-3}}{\cdot CH_2CH_3}$

Scheme III ; $n\text{-}C_4H_{10}^{+\cdot *} \rightarrow \underset{\text{III-1}}{\begin{matrix} CH_3\text{---}CH_2\text{---}CH_3 \\ \diagdown\ \ \diagup \\ \ \ CH_2 \end{matrix}}^{+\cdot} \rightarrow \underset{\text{III-2}}{\begin{matrix} CH_3\text{---}CH_2 \\ \diagdown\ \ \diagup \\ \ \ CH_2 \end{matrix}}^{+} + \underset{\text{I-3}}{\cdot CH_3}$

Scheme III'; $n\text{-}C_4H_{10}^{+\cdot *} \rightarrow \underset{\text{III'-1}}{\begin{matrix} CH_3 & CH_2\text{---}CH_3 \\ \diagdown & \diagup \\ CH\cdots H & \end{matrix}}^{+\cdot} \rightarrow \underset{\text{III'-2}}{\begin{matrix} CH_3 & CH_3 \\ \diagdown & \diagup \\ CH & \end{matrix}}^{+} + \underset{\text{I-3}}{\cdot CH_3}$

where $n\text{-}C_4H_{10}^{+\cdot *}$ means the molecular cation at the Franck-Condon state. The numbering of carbon atoms in n-butane is as follows;



Calculations have been carried out using IMSPAK program.

RESULTS AND DISCUSSION

Possible Reaction Paths —— Energy variations due to the C-C bond lengthening have been calculated for Schemes I and II. They are shown in Fig. 1. From this figure, the course of reaction at each schemes is expected as follows.

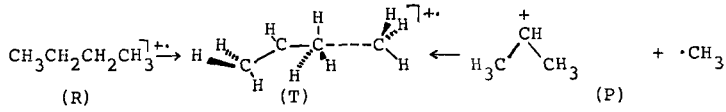
Scheme I (simple bond scission). When the C(3)-C(4) bond distance is largely lengthened by the electron bombardment, $C_3H_7^+ + \cdot CH_3$ fragmentation occurs via the reaction intermediate I-1. At the low energy bombardment this scheme produces molecular cation I-1 (see Fig.1).

Scheme II (simple bond scission). When the C(2)-C(3) bond distance is lengthened or the C(3)-C(4) bond distance is slightly lengthened by the electron bombardment, $C_4H_{10}^{+\cdot}$ goes to stable molecular cation II-1. Therefore, at the low energy bombardment Scheme II fragmentation occurs. This scheme brings to produce molecular cation II-1 (see Fig.1).

In order to explain the experimental data that the $C_1 + C_3$ fragmentation occurs at the low energy, we must consider the other type of the reaction scheme.

Schemes III and III' (fragmentation with bending mode control). Since the $C_1 + C_3$ fragmentation has occurred overwhelmingly and 2-propyl cation has

been calculated to be the most stable $C_3H_7^+$ species, one can expect that the reaction proceeds via the three-membered ring formation and 2,3-H-shift. There are two possible Schemes III and III'. However, the preliminary calculation for these schemes shows that III'-1 is more stable than III-1. Therefore, we have examined Scheme III'. Scheme III will be responsible for $CH_4 + C_3H_6^{+\cdot}$ fragmentation. At first, we calculated the energy variation starting from the molecular cation changing bond distances and bond angles ((R) → (T)). Then we obtained the left hand side



curve in Fig.2. Next, we have calculated the energy variation starting from the isolated $(CH_3)_2\dot{C}H + \cdot CH_3$ system (P) to transient structure (T) ((P) → (T)). At each R(C(3)-C(4)) the geometry has been optimized. Then we have obtained the right hand side curve in Fig.2. There is rather high energy barrier. In the left hand side of the barrier the geometry is that of $CH_3\overset{+}{C}H_2CH_2\text{---}\dot{C}H_3$. In the contract with this geometry of the right hand side of this barrier is that of $CH_3\overset{+}{C}HCH_3\text{---}\dot{C}H_3$. Therefore, the proton tunneling at this energy barrier is expected.

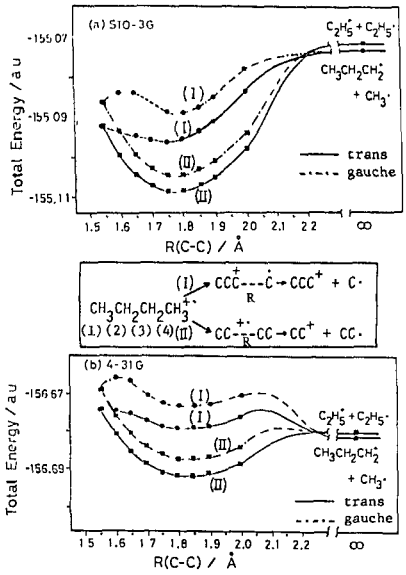


Fig. 1 Calculated Potential Curve for Fragmentation with Stretching Mode Control.

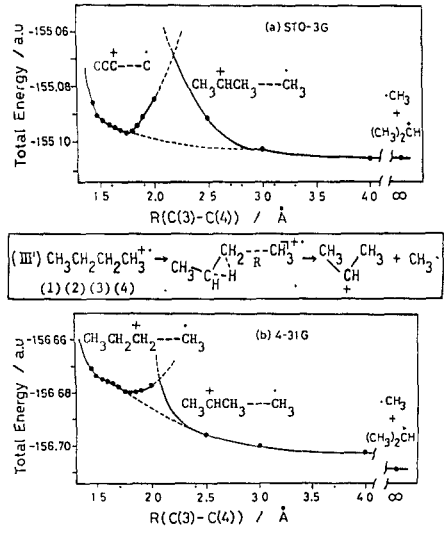


Fig. 2 Calculated Potential Curve for Fragmentation with Bending Mode Control.

PROPOSED FRAGMENTATION PROCESS OF N-BUTANE

Electron impact initially makes the molecular cation at the Franck-Condon state. Then 2,3-H-shift occurs. At the same time the terminal C-C bond is weakened and a proton tunneling occurs. Finally 2-propyl cation and methyl radical are produced.

CID MIKE SPECTROMETRY OF EPIMERIC STEROID ALCOHOLS

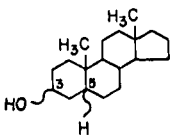
R. Lauber, R. Steinauer and U.P. Schlunegger, Institute of Organic Chemistry University of Berne, CH-3012 Bern, Switzerland, and P. Dan and Z.V.I. Zaretskii, Isotope Department, The Weizmann Institute of Science, Rehovot 76100, Israel.

Recently we have shown[1] that in epimeric steroid alcohols, differing in both configuration of hydroxyls and the mode of the rings A/B junction, the large quantity of translational energy releases upon the loss of angular $\cdot CH_3$ from $(M-H_2O)^{+\cdot}$ ions, suggesting that rate determining isomerisation of $(M-H_2O)^{+\cdot}$ ions occurs, prior to $\cdot CH_3$ loss and formation of the $(M-H_2O-CH_3)^+$ ions. To prove this suggestion and to compare the structures of the $(M-H_2O-CH_3)^+$ ions formed from epimeric hydroxy androstanes, the collision induced decomposition mass-analyzed kinetic energy (CID MIKE) spectra of epimeric cis and trans-A/B 3-hydroxy-,17-hydroxy- and 3-hydroxy-17-keto-androstanes as well as respective cholestanes (Fig.1), were studied, using a modified MAT CH-5DF reversed geometry mass spectrometer. It was demonstrated that while CID MIKE spectra of both molecular and $(M-H_2O)^{+\cdot}$ ions in epimers are distinctly different, those of $(M-H_2O-CH_3)^+$ ions are nearly identical between androstane stereoisomers differing in configuration of hydroxyls and in the mode of rings A/B junction. These results demonstrate that structurally identical $(M-H_2O-CH_3)^+$ ions are formed from configurationally different steroid alcohols of androstane series (Fig.2). On the other hand, contrary to epimeric 3-hydroxy androstanes, the CID MIKE spectra (and the respective structures) of $(M-H_2O-CH_3)^+$ ions in case of 3-hydroxy cholestane epimers are different. The isomerisation mechanism preceding the loss of $\cdot CH_3$ from $(M-H_2O)^{+\cdot}$ ion will be discussed.

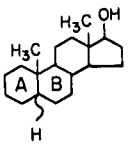
References

[1] Z.V.I. Zaretskii and P. Dan, Presented at 29th Annual Conference on Mass Spectrometry and Allied Topics; Minneapolis, MN, May 24-29, 1981.

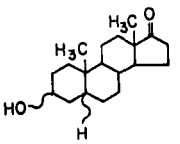
Compounds Used in the Study



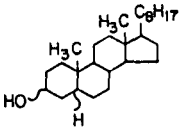
1 5α,3β
2 5α,3α
3 5β,3β
4 5β,3α



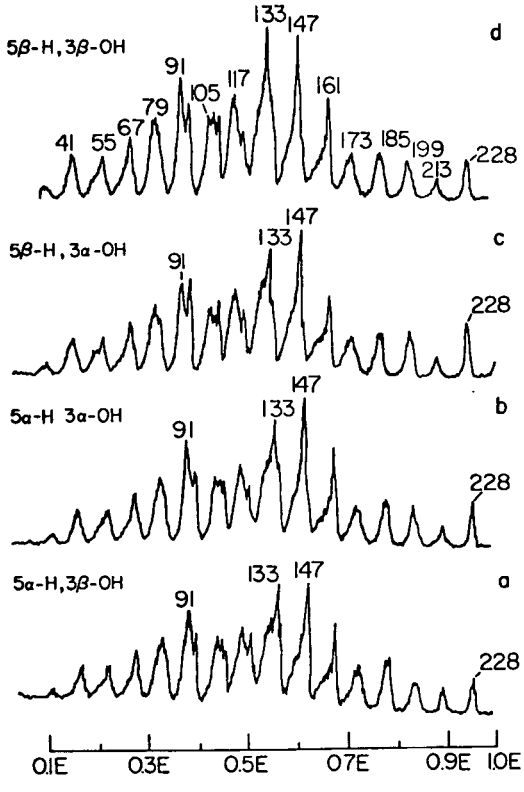
5 5α
6 5β



7 5α,3β
8 5α,3α
9 5β,3β
10 5β,3α



11 5α,3β
12 5α,3α
13 5β,3β
14 5β,3α



CID MIKES of m/z 243 $[M-H_2O-CH_3]^+$ ions in 5α- and 5β-Androstan- 3-ols

ENERGY RELEASE FROM $C_4H_8O_2^+$ BUTANOIC ACID AND RELATED IONS

Charles E. Hudson and David J. McAdoo
Marine Biomedical Institute, University of
Texas Medical Branch, Galveston, Texas 77550

It was reported in 1978 that the metastable loss of ethylene from ionized butanoic acid (1) occurs with considerable exchange between the γ,β and carboxyl hydrogens. The loss of methyl containing the γ carbon occurs without such exchange however.[1] It was later found that the ratio of methyl to ethylene loss for 1 depended upon the source of the ion. Butanoic acid ions derived from esters show a smaller proportion of ethylene loss than directly ionized butanoic acid, but correspondingly labeled acids and esters give the same isotopic pattern of methyl and ethylene losses. The collisional activation (CA) spectra of the ester derived ions showed more methyl and less ethylene loss than the CA spectrum of directly ionized butanoic acid.[2] The following conclusions were drawn: (1) Loss of CH_3 and C_2H_4 occur from different population of ions. (2) Ions losing methyl have rearranged irreversibly while ions losing ethylene isomerize reversibly. (3) The proportion of such rearranged ions depends upon the source of butanoic acid ions. (4) The nature of the rearrangements are independent of whether the ion is derived from an acid or an ester.

We have measured the translational energy released in the fragmentations to see if this quantity also depends on the precursor. The data in Table 1 and 2 were collected at different times and under different conditions or resolution, presumably giving rise to the differences between the two sets of data.

Table 1

Precursor	$I(C_2H_4)/I(CH_3)$	$T\frac{1}{2}(CH_3)$ (meV)	$T\frac{1}{2}(C_2H_4)$ (meV)
$CH_3CH_2CH_2CO_2H$	0.17	18.7	3.2
$CH_3CH_2CH_2CO_2CD_2CH_3$	0.02	24.4	9.4

Table 2

Precursor	Ion	$I(-C_2H_4)/I(-CH_3)$	$T\frac{1}{2}(-CH_3)$	$T\frac{1}{2}(-C_2H_4)$
$CH_3CH_2CH_2CO_2H$	$CH_3CH_2CH_2CO_2\overset{+}{H}\cdot$	.32	12.3	3.6
$CH_3CH_2CH_2CO_2CH(CH_3)_2$	$CH_3CH_2CH_2CO_2\overset{+}{H}\cdot$	.08	15.8	7.6
$(CH_3)_3CCH(CH_3)CH_2CO_2H$	$CH_3\dot{C}HCH_2CO_2H_2^+$	.02	20.1	12.8
$(CH_3CH_2)CDCO_2H$	$CH_3CH_2\dot{C}DCO_2H_2^+$	.01	17.8	10.3
$CH_3CH_2C(CH_3)_2CO_2H$	$(CH_3)_2\dot{C}CO_2H_2$	.007	31.7	15.3
$CH_3CH_2CH_2CO_2CH(CH_3)CD_3$	$CH_3CH_2CH_2CO_2H^{+\cdot}$	0.12	19.6	----

The energies released from ions derived from esters are larger than the energies released from directly ionized butanoic acid. We attribute this difference to a competition due to another reaction of the ester ion.

$$CH_3CH_2CH_2CO_2CD_2CH_3^{+\cdot} \rightarrow \dot{C}H_2C(=\overset{+}{O}H)OCD_2CH_3$$

Since 2 is more stable than 1, it will be formed to the exclusion of 1 except at energies considerably above the threshold for forming 1. This raises the energy content of 1 derived from esters and consequently the energy released. More of the higher energy butanoic ions isomerize to structures which lose methyl upon metastable decomposition.

Table 2 also shows that various isomers of 1 release more energy in their metastable fragmentations than 1 does. This may also be due to suppressions of higher energy competing reactions.

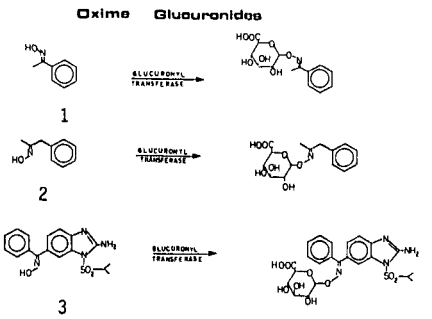
CHARACTERIZATION OF SOME NOVEL GLUCURONIDES BY FAST ATOM BOMBARDEMENT AND ELECTRON IMPACT MASS SPECTROMETRY

Lauren M. Yelle and Catherine Fenselau

The Johns Hopkins School of Medicine, Baltimore, MD 21205

Oxime groups occur in many xenobiotics, either in the parent compound or in biotransformed species from primary amine-containing drugs. Glucuronidation has been reported to be a pathway for elimination of these types of molecules. Carbinolamines are postulated to be intermediates in metabolic N-demethylation reactions. Conjugation as glucuronides is believed to be a pathway for detoxification of these reactive species. We have synthesized the glucuronides three oximes and two carbinolamines in vitro, using immobilized microsomal rabbit liver enzymes. The metabolites obtained were analyzed by both positive and negative FAB mass spectrometry as well as EI mass spectrometry.

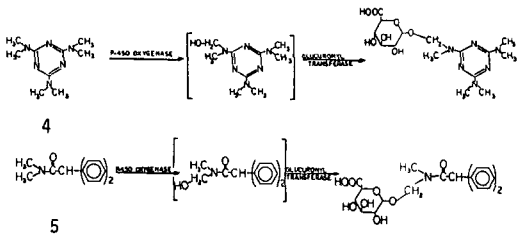
The synthesis of the three oxime glucuronides is shown below. Acetophenone oxime (1) was chosen as a model oxime; amphetamine oxime (2) is a known metabolite of amphetamine; and enviroxime (3) is an antiviral agent currently undergoing clinical trials.



The mass spectral analyses of these glucuronides yielded strong molecular ion species in both positive and negative FAB. In the positive ion mode, loss of glucuronic acid to give the protonated aglycon was observed in each case. No other useful fragmentation was obtained. The EI spectra of the TMS derivatives of these glucuronides gave weak molecular ions, however, intense fragment ions provided the information necessary to determine the site of conjugation.

The compounds diphenamide and hexamethylmelamine were chosen for the synthesis of carbinolamine glucuronides, which is illustrated below. Hexamethylmelamine (4) is a cytotoxic anti-cancer agent and diphenamid (5) is an herbicide. Both these molecules have been reported to be metabolized to an intermediate carbinolamine.

Carbinolamine Glucuronides



4

5

The FAB spectra of these carbinolamine glucuronides gave results similar to those obtained for the oxime glucuronides - namely, strong molecular ion species, yet little useful fragmentation. In positive FAB, the loss of glucuronic acid to give the protonated aglycon was observed, and in negative ion mode loss of the neutral aglycon to yield glucuronic acid was typical. The EI spectra of the TMSderivatives produced no molecular ion species, but the characteristic fragmentation confirmed the site of conjugation, which was especially important in the case of diphenamid.

NCI QUANTITATIVE ANALYSIS WITH VARIOUS ELECTRON ENERGY MODERATING GASES.

I.K. Gregor and M. Guilhaus, Chemistry School, University of New South Wales, Kensington, N.S.W., 2033, Australia.

A necessary prerequisite for quantitative analysis by the use of electron attachment negative chemical ionisation (NCI) conditions is to select the gas best suited to function in the dual role of electron energy moderator as well as collisional stabilisation medium for excited molecular negative ions. Thus, a quantitative and comparative study has been made of the effect exerted by the gases N_2, CH_4, i-C_4H_{10}, He, Ne, Ar, Kr, Xe on the instrumental sensitivity exhibited for specific electron attachment reactions carried out under NCI conditions, where ion source gas pressures, gas plasma temperatures and sample heating rates have all been monitored and controlled.

Sensitivity data (C/μg) have been obtained on a VG MM-16F mass spectrometer equipped with an EI/CI ion source by the application of selected and integrating ion current procedures which allowed the quantity of charge arriving at the first dynode of the electron multiplier to be measured during the evaporation of 100 ng. samples of selected organic and metal-organic compounds into the ion source. The most comprehensive data sets were obtained for the analytes anthraquinone and bis(diethyldithiocarbamato)nickel(II) for which long lived molecular negative ions are formed upon gas phase electron attachment under NCI conditions. Our results may be summarised as follows:

1. The maximum ratio of charge collected per μg of sample introduced into the ion source (C/μg) increased with the size of the gas atom/molecule. This trend showed an almost linear relationship for the rare gas series for which atomic sizes can be assigned in terms of their Lennard-Jones radii.
2. Under the ion source conditions employed, maximum C/μg values were obtained when gas densities were in the range 0.05 - 1.7 x 10^{-7} g cm^{-3}. Significantly, heavier gases displayed narrower pressure regions over which the C/μg values were maximised.
3. The relative ability of the gases to provide the highest C/μg levels could be ranked as follows:

   $$He < Ne << N_2 < Ar \approx CH_4 < Kr < Xe < i\text{-}C_4H_{10}$$

4. For analytical purposes, being mindful of the pressures required for optimum instrumental sensitivity, source contamination deficiencies, availability *etc.*, the electron energy moderating/collisional stabilising gases of greatest utility appear to be CH_4, Ar, N_2.

Detection limits have been determined for a selection of underivatised and derivatised organic and metal-organic analytes. Some typical results are given in the following Table:

Analyte	Derivative	m/z	Temp.(°C)	Detection Limit (g) [1]
Anthraquinone	underivatised	208	240	1×10^{-11}
Cr	$Cr(dpm)_3$ [2]	601	170	1×10^{-12}
Co	$Co(dpm)_3$	608	170	1.6×10^{-13}
Ni	$Ni(Et_2.dtc)_2$ [3,4]	354	240	1.0×10^{-12}
Malathion	$Ni(Me_2.dtp)_2$ [5]	372	160	2.0×10^{-9}
Ethion	$Ni(Et_2.dtp)_2$ [5]	428	160	1.0×10^{-9}

[1] The detection limit was taken as the lowest amount of analyte introduced into the ion source which gave rise to an integrated ion current evaporation profile, monitored at the stated m/z, which was easily distinguishable from the signal given by the pure solvent residue, under the same instrumental conditions. Dished vespel rods were used for in-beam sample introduction; CH_4 was the electron energy moderating gas with an ion source pressure of 0.10 Torr.

[2] dpm = $[Me_3C.\ CO.CH.CO.\ CMe_3]^-$

[3] $Et_2.dtc = [S_2.CN.Et_2]^-$

[4] For metal-organic compounds, probe tip surfaces substantially influence attainable detection limits, particularly for in-beam sample introduction. For this analyte, surfaces provided by the following materials are ranked in descending order of performance: vespel rods, silanised/SE-30 coated silica cups, uncoated silica cups, Pt DCI filament wire.

[5] $Me_2dtp = [(MeO)_2.P.S_2]^-$; $Et_2dtp = [(EtO)_2.P.S_2]^-$

DESORPTION CHEMICAL IONIZATION (DCI) MASS SPECTROMETRY OF BENZYL ETHER DERIVATIVES OF 3-HYDROXYSTEROIDS WITH AMMONIA, METHANE AND ISOBUTANE

Yutaka HIRANO and Carl DJERASSI
Dept. of Chemistry, Stanford University, STANFORD, CA 94305

Pierre TECON
NERMAG Inc., Scott Bvd., SANTA CLARA, CA 95050

Introduction

Pursuing our investigations of DCI spectra of steroids derivatives, we were surprised to observe several species in the DCI spectra of benzyl ether derivatives of 3-hydroxy steroids which were not formed in their ester counterparts (Ref. 1).

Fast and unequivocal structure confirmation of steroidal ethers is essential because these compounds are widely encountered as intermediates in our syntheses where the benzyl ether is used to protect hydroxyl functions.

In the detailed discussion of the main species appearing in the DCI spectra of ester derivatives, we defined and rationalized the Adduct ion A^+, the Protonated molecular ion P^+, the Substitution ion S^+, the Molecular ion $M^{+\cdot}$ and the Elimination ions E_1^+ and $E_2^{+\cdot}$ (Ref. 1,2).

In addition to the above, the DCI spectra of benzyl ether derivatives of 3-hydroxy steroids display the following species:

T^+ $(W-CH_3)^+$	X^+ $(Y^*NH_3)^+$
V^+ $(E_1-CH_4)^+$ or $(E_2-CH_3)^+$	Y^+ $(MH'-RH'')^+$
$W^{+\cdot}$ $(MH-OR)^{+\cdot}$	Z^+ $(M-H-ROH)^+$ or $(Y-H_2O)^+$

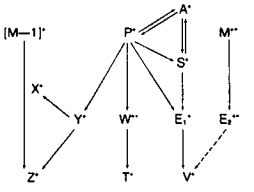
The compounds analyzed were: 3α-5α-H benzyl ether cholestanol
3β-5α-H benzyl ether cholestanol
3α-Δ^5 benzyl ether cholesterol
3β-Δ^5 benzyl ether cholesterol

The reagent gases used were NH_3, ND_3, CH_4, CD_4 and isobutane.

Discussion

The following Scheme shows the processes observed and rationalize the results.

THE CHEMISTRY OF DCI-PRODUCED SPECIES



The following comments can be made:

- as found for the ester derivatives (Ref. 1), the Substitution ion $S^+ = (M\text{-}OR+NH_3)^+$ is observed only when a double bond is present in the nucleus (Δ^5 in the present case).

- the fragmentation of the Δ^5 benzyl ether derivatives differs from that of the saturated analogs: indeed, the cholesterol derivatives fragment via $W^{+\cdot}$, which then decomposes by losing a methyl group to give T^+, whereas the cholestanol derivatives rearrange to Y^+ and then form the X^+ adduct or decompose to Z^+.

- species A^+, P^+, $M^{+\cdot}$, S^+, E_1^+ and $E_2^{+\cdot}$ appear in the benzyl ether derivatives spectra similar to the ester analogs. The intensity of $E_2^{+\cdot}$ is significantly lower however.

- as reported previously, selective stabilization of P^+ (probably through the double bond) in the 3α configuration, allowing the differenciation of epimers is also occuring with these samples.

The complete results are being submitted for publication.

Experimental

The DCI spectra were obtained on a RIBERMAG R10-10 quadrupole mass spectrometer equipped with the standard DCI system, and using the SADR data system.

The detailed experimental conditions have been reported in Ref. 1.

References

1) Pierre Tecon, Yutaka Hirano and Carl Djerassi, Org. Mass Spectrom 1982, in press

2) Pierre Tecon, Yutaka Hirano and Carl Djerassi, paper presented at the "29th Annual Conf. on Mass Spectrometry and Allied Topics, Minneapolis, MN 1981"

NOVEL-IONIZATION AND SAMPLE INTRODUCTION TECHNIQUES FOR THE ANALYSIS OF THERMALLY-LABILE AND NON-VOLATILE COMPOUNDS BY A QUADRUPOLE MASS SPECTROMETER.

Christine N. Kenyon and Paul C. Goodley, Hewlett-Packard Company, 1601 California Avenue, Palo Alto, California 94304.

Recently a number of techniques have been employed for the mass spectrometric analysis of thermally-labile and/or non-volatile compounds. Field desorption (FD), fast atom of fast ion bombardment (FAB or FIB), secondary ion mass spectrometry (SIMS), desorption chemical ionization (DCI), and coupled liquid chromatography-mass spectrometry (LC/MS) are among the most commonly used of these techniques. Direct Liquid Inlet LC/MS (DLI LC/MS), FAB, and DCI have been successfully implemented on a single Hewlett-Packard 5995B GC/MS/DS. The results obtained for the analysis of thermally-labile and non-volatile compounds of biochemical importance using these three techniques are compared in this paper.

The DLI LC/MS has been previously described in (1,2). The FAB system consisted of a Phrasor Scientific Company Fast Atom Capillaritron Source (FACS) and Controller supplied in a kit for retrofitting to the 5985B[3,4,5]. A diagram of the FACS source installed on the instrument is shown in Figure 1. The DCI system consisted of a Vacumetrics DCI probe and programmer.

The analysis of complex mixtures of peptides by mass spectrometry has in the past involved their derivatization prior to GC/MS. DLI LC/MS spectra show that the endorphin leucine-enkephalin can be sequenced by this technique and that complimentary information is obtained by comparison of positive and negative ion results. A strong $(M + 1)^+$ or $(M - 1)^-$ as well as abundant diagnostic fragment ions occur in both modes of operation.

Nucleosides and nucleotides are also difficult to analyze by mass spectrometry using classical techniques of mass spectrometry. Either DCI or FAB can often be used for the analysis of these compounds. As an example, the mass spectra of adenosine-5' - monophosphate (AMP) by both positive and negative ion DLI LC/MS and positive ion FAB have been obtained. The positive and negative ion DLI LC/MS spectra are shown in Figure 2 and the positive ion FAB spectrum of AMP is shown in Figure 3. The quasimolecular ion is quite strong in both the FAB spectrum and in the DLI LC/MS spectra of AMP. The DCI spectra of 2' -O-methyladenosine shows a base peak of $(M + 1)^+$ or $(M - 1)^-$ in positive (ammonia-methane) or negative (nitrous oxide-methane) ion DCI. However, the results of the DCI analysis of AMP showed that this technique is not useful for the analysis of this nucleotide.

Vitamin D_3 and its metabolites are measured in the diagnosis and monitoring of therapeutic regimens related to calcium absorption. These compounds are commonly separated by HPLC and can be determined by mass spectrometry using FAB or DLI LC/MS[6,7]. The use of the technique of DCI in either positive or negative ion mode of operation is illustrated by the positive and negative ion DCI spectra of the metabolie 24,24-dihydroxyvitamin D_3 (Figure 4). In both spectra, the quasimolecular ion is the base peak allowing the easy and sensitive measurement of this compound.

Ethidium bromide is a dye which inhibits synthesis of nucleic acids and proteins by intercalating between nucleic acid base pairs. It is a quaternary ammonium salt which is non-volatile and is thermally decomposed during electron impact ionization. This compound has been analyzed by DCI yielding reproducible spectra which show strong molecular ion information in both positive (ammonia-methane) and negative (nitrous oxide-methane) ion modes. The spectra obtained are shown in Figure 5.

Sugar phosphates decompose using most sample introduction techniques. FAB, however, can be used to obtain mass spectra of mannose-1-phosphate as the dicyclohexylammonium salt. The positive ion FAB mass spectrum of this compound shows strong ions for $(M + H + salt)^+$ at m/z 360, $(M-PO2)^+$, and (cyclohexylamine + H)+.

Thus, DLI LC/MS, FAB, and DCI can be utilized on a single quadrupole mass spectrometer to analyze labile and non-volatile compounds of biochemical importance. DLI LC/MS is the only one of these methods which combines chromatographic separation with mass spectrometric analysis.

1. A. Melera, Adv. Mass Spectrom. 8B:1597 (1980).
2. C. N. Kenyon, A. Melera, and F. Erni, J. Anal. Toxicol. 5:216 (1981).
3. B. Kalensher and J. Perel, J. Applied Physics (in press).
4. J. Mahoney, D. Gorbel, J. Perel, T. Forrester, Biomedical Mass Spectrometry (in press).
5. R. A. Kerr, Science 216,166 (1982).
6. J. O. Whitney, Personal Communication
7. C. N. Kenyon, P. C. Goodley, D. J. Dixon, J. O. Whitney, K. Faull, and J. A. Barchas, Manuscript in preparation.

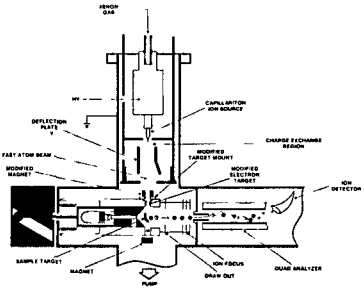


Figure 1. Phrasor FACS gun interfaced to an HP 5985B GC/MS.

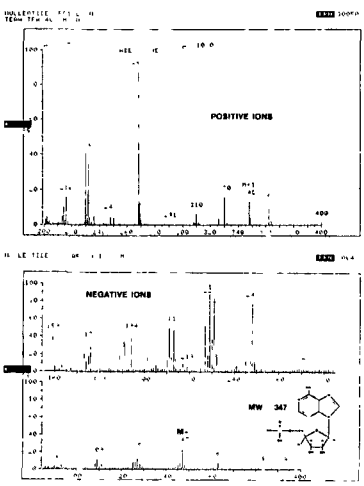


Figure 2. DLI LC/MS mass spectra of AMP.

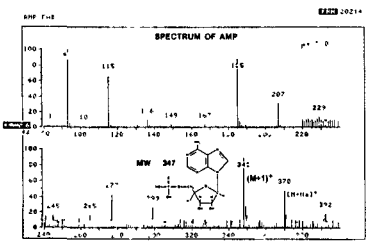


Figure 3. Positive ion FAB. Courtesy of Dr. Kym Faull, Stanford University.

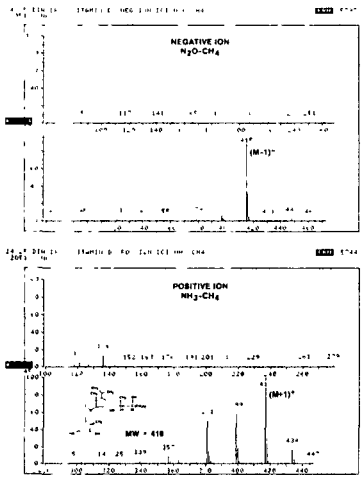


Figure 4. DCI spectra of 24,25-dihydroxy-vitamin D_3.

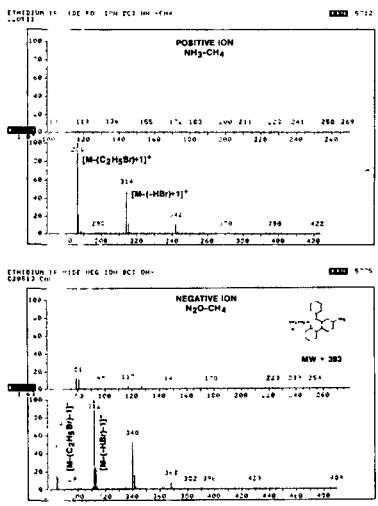


Figure 5. DCI mass spectra of ethidium bromide.

FACILE IONIZATION INDUCED BY AMMONIUM SALTS: LOW AND HIGH RESOLUTION MASS SPECTRA OF NON VOLATILE, MULTIFUNCTIONAL, BIOACTIVE COMPOUNDS.

B.N. Pramanik, P. Bartner, V. Girijavallabhan, A.K. Ganguly, Schering Corp., Bloomfield, N.J. 07003. A.K. Bose and Om Prakash, Stevens Institute of Technology, Hoboken, N.J. 07030

Many biologically active compounds are nonvolatile and/or thermolabile and fail to give satisfactory mass spectra under electron impact conditions. We report here a simple technique for obtaining meaningful spectra from many such compounds using a direct probe in commercially available, low resolution or high resolution, electron impact mass spectrometers (EIMS). Unlike other techniques (field desorption, plasma desorption, laser desorption, flash desorption, fast atom bombardment, "in beam", etc.) our method does not require any modification of the conventional spectrometer or addition of expensive accessories.

This technique is based on our previous observation[1,2] that the addition of ammonium salts (NH_4X) to a solid sample in a chemical ionization mass spectrometer produces abundant $(M+H)^+$ and/or $(M+NH_4)^+$ ions as well as $(M+X)^-$ and $(M-1)^-$ ions.

We extended the ammonium chloride technique to electron impact mass spectrometry and observed that ionization of sample compounds is remarkably facilitated (as shown by increase in the ion current in the higher molecular weight region of the spectrum, see Fig. 1). Our technique for EI mass spectrometry involves using a conventional solid probe while adding a trace of ammonium chloride as a solid (or a solution of ammonium iodide in methanol) to a solid sample which may even be in the form of a salt.

To obtain some insight into the ionization enhancement in the presence of ammonium chloride we have studied the spectra of penicillin G in detail. Under electron impact conditions, the potassium or sodium salt of penicillin G produces fragment ions which are much smaller than the whole molecule and therefore do not provide much structural information. Being thermolabile, even free penicillanic acid gave a poor spectrum-a weak molecular ion was seen very briefly.

By using the ammonium salt addition technique we observed much improved spectra: the molecular ion M^+ of the free acid corresponding to the salt was observed as the highest molecular weight peak (see fig. 2). That the observed molecular ion at m/z 334 was not $(M + NH_4^+ - H_2O)$ was established easily: the position of this peak remains unchanged upon the substitution of $^{15}NH_4Cl$ for NH_4Cl; also, the exact elemental composition of the ion at m/z 334 was found to correspond to the free acid of penicillin G.

The sodium salt of methicillin displayed $(M-CO_2H)^+$ as the heaviest ion but the potassium salt of oxacillin produced a fairly stable M^+ corresponding to the free acid. The base peak in the case of these antibiotics and the higher molecular weight fragment ions provided useful structural information.

The sodium salt of Sch 29482 a penem antibiotic
displayed stable molecular ion at m/z 275 (free acid).
The elemental composition of the ion at m/z 275 and the fragments were determined by high resolution mass spectrometry.

In our experiments the probe temperature was low ($<300^0$) and the probe was not in the "in beam" configuration. When the temperature of the probe was allowed to rise to about 300^0C, the spectra of the sodium salt of bile acids showed some unusual features. The $(RCO_2Na)^+$ ion was the heaviest ion observed although briefly in the case of the sodium salt of the bile acid (sodiumlithocholate) as well as the glycine conjugate (glycolithocholate). It should be noted that the heaviest ions were not cationized species $(RCO_2H + Na)^+$ but the molecular ion corresponding to the sodium salt $(RCO_2Na)^+$ under study.

To gain information on the role of ammonium salts for enhancing ionization, we have studied the EI mass spectra of NH_4Cl, ND_4Cl, and $^{15}NH_4Cl$. Exact masses were measured by high resolution techniques.

The most abundant ions are $(NH_3)^+$ and $(HCl)^+$ indicating that much of the NH_4Cl undergoes decomposition to $NH_3(g)$ and the HCl(g) which get ionized under electron impact conditions. It is noteworthy that Cl^+ and $(NH_2)^+$ are formed in substantial abundance although Cl^- and $(NH_2)^-$ correspond to the preferred, lower-energy, electronic configuration.

The formation of significant quantities of high energy and presumably unstable Cl^+ and $(NH_2)^+$ ions from NH_4Cl raises the distinct possibility of ionization of some of the sample molecules to M^+ by electron tranfer[3] to these ions.

Whatever be the exact mechanism(s) of ionization, it is our observation that ammonium salts facilitate the ionization of nonvolatile/thermally unstable compounds and produce improved spectra in a standard EI mass spectrometer. Most of the ions are stable enough to permit high resolution measurements to obtain exact elemental composition of the ions, thus providing valuable structural information.

Thus, in case of sucrose which shows under standard EIMS conditions only fragment ions of m/z <300, the heaviest stable ion corresponded to the molecular ion at m/z 342. The spectrum was stable enough to permit exact mass determination of several major fragments using high resolution accessories. Additional structural information was obtained by re-recording the spectrum after substituting ND_4Cl for NH_4Cl and taking note of the extent of deuteration.

In summary, the ammonium chloride addition technique facilitates the recording of EI type spectra (not proton or cation adduct type CI spectra) and permits the determination of the exact mass of the molecular ion and/or high molecular weight fragments.

References

(1) Bose, A.K.; Fujiwara, H.; Pramanik, B.N.; Lazaro, E.; Spillert,, C.R. Anal. Biochem. 1978, 89, 284.

(2) Bose, A.K.; Pramanik, B.; Tabei, K.; Bates, A.D. Presented at 28th Annual Conference on Mass Spectrometry and Allied Topics, New York, N.Y., May 25-30, 1980.

(3) McLafferty, F.W., Interpretation of Mass Spectra; University Science Books, Mill Valley, California, 1980, p. 92.

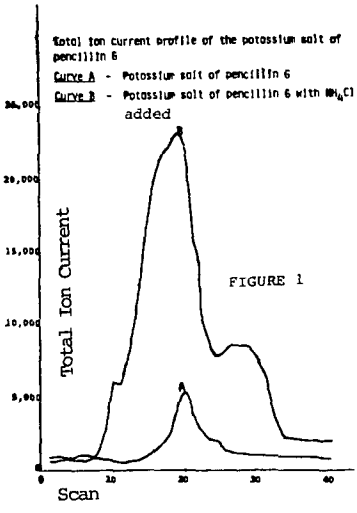


FIGURE 1

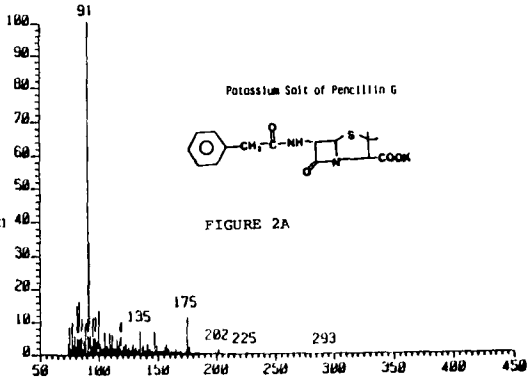


FIGURE 2A

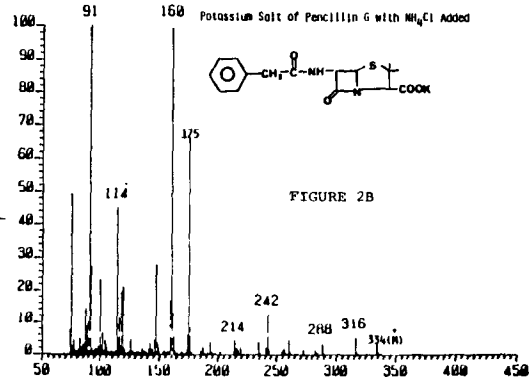


FIGURE 2B

D/CI MASS SPECTROMETRY IN THE STRUCTURE ELUCIDATION OF GUANIDINO COMPOUNDS.

F.C.ALDERWEIRELDT, E.L.ESMANS, B.MARESCAU, A/LOWENTHAL
University of Antwerp (RUCA-UIA)
Groenenborgerlaan 171
B2020 Antwerp BELGIUM

Y.ROBIN
Laboratoire de Biochemie Marine
de l'Ecole Pratiques des Hautes Etudes
Place Marcelin Berthelot
75321 Paris FRANCE

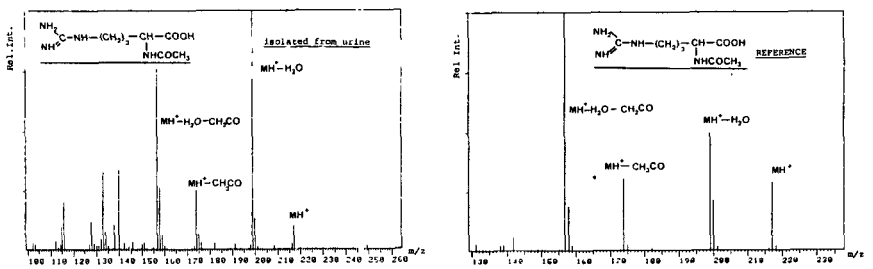
In order to elucidate the structure of different natural guanidino compounds by GC-MS, a double derivatization procedure is neccesary. Generally this is done by converting the guanidino function into a pyrimidyl ring by treating the molecule with acetyl acetone[1]. Other polar functions such as carboxyl groups, have to esterified or trimethylsilylated. A choice between the latter procedures is made with regard to the structure of other functionalities present in the molecule.

In order to investigate wether desorption/chemical ionization (D/C.I.) mass spectrometry eventually could be used as a complementary technique to GC-MS, (giving rapid molecular weight information and eventually avoiding a particular derivatization procedure) the D/C.I. mass spectra of 21 biologically important guanidino compounds were recorded with ammonia as the reagent gas. (Table 1.)

	$(MH)^+$	$(MH)^+-H_2O$	$(MH)^+-2H_2O$	$(MH)^+-NH_3$
1. $RNHCH_2CH(NH_2)COOH$		129(100)		130(18)
2. $RNH(CH_2)_4CH(NH_2)COOH$	189(100)			172(13)
3. $RNHO(CH_2)_2CH(NH_2)COOH$	177(100)			
4. $RNH(CH_2)_2CH(NH_2)COOH$		143(8)		
5. $RNH(CH_2)_2CH(NH_2)COOH$	175(20)	157(22)		
6. $RNHCH_2CH(CH_3)COOH$		128(100)		
7. $RNH(CH_2)_2COOH$	132(100)	114(71)		
8. $RN(CH_3)CH_2COOH$	132(87)	114(100)		
9. $RNH(CH_2)_5COOH$	174(100)	156(5)		
10. $RNH(CH_2)_4COOH$	160(100)	142(47)		
11. $RNHCH(C_2H_5)COOH$		128(100)		
12. $RNH(CH_2)_3COOH$	146(2)	128(100)		
13. $RNHCH_2COOH$	118(100)	100(85)		
14. $RNHCH(CH_2CH_2COOH)COOH$		172(100)	154(12)	
15. $RNHCH(CH_2COOH)COOH$		158(100)		
16. $RNHCH_2CH(OH)CH_2COOH$	162(19)	144(12)	126(100)	
17. $RNH(CH_2)_3CH(OH)COOH$	176(6)		140(35)	
18. $RNH(CH_2)_3COCOOH$		156(100)		
19. $RNH(CH_2)_3CONH_2$				128(100)
20. $RNH(CH_2)_2SO_3H$	168(19)			
21. $RNHCH(CH_2Phe)COOH$	208(100)	199(66)		

R= $NH_2-\overset{\overset{H}{|}}{C}-$
$\quad\quad\quad

Some diagnostic peaks are summarized in Table 1.
The mass spectra were recorded on a Ribermag 10-10 quadrupole mass spectrometer equipped with a Sidar data system. The compounds were dissolved in water and 1-2 µg of product was placed upon a 60µmtungsten wire by means of a microsyringe.For most compounds studied,protonated molecular ions $(M+H)^+$ were observed at a *b.e.t.* of approximately 300 mA. From the results in Table 1,it is obvious that molecular weight assignment,using the highest m/z-value is not so straightforward,unless reference spectra are available.
From the urine of patients suffering from hyperarginineamia a guanidino positive compound was isolated by liquid chromatography on a Dowex 50-X-8 resin using a 0.04M Pyridine/HCOOH (pH=4) solution as eluant. The solvent was removed by lyophylisation and extra purification was done by semi-preparative HPLC on a LiChrosorb 10-NH_2-column with a 0.01M NH_4OOCH(A)/ CH_3CN(B) eluant(78%B→50%B in 10 min.) A D/C.I. spectrum was taken and the product could be identified as N-α-acetylarginine by comparison with the reference spectrum.(Fig.1 and 2)



Figs.1-2
The structure of an unknown guanidino compound isolated from sea-anemonea. is been investigated. A structure is proposed and will be discussed.

ACKNOWLEDGEMENTS.
We thank the NFWO for financial support and Mr.W.Van Dongen for the HPLC-analysis.

REFERENCES.
1. B.Marescau,J.Pintens,A.Löwenthal,E.Esmans,F.C.Alderweireldt,Journ.Clin. Chem.Clin.Biochem.,19,61(1981)
2. B.Marescau,A.Löwenthal,E.Esmans,Y.Luyten,F.Alderweireldt,Journ.Chrom., 224,185(1981)

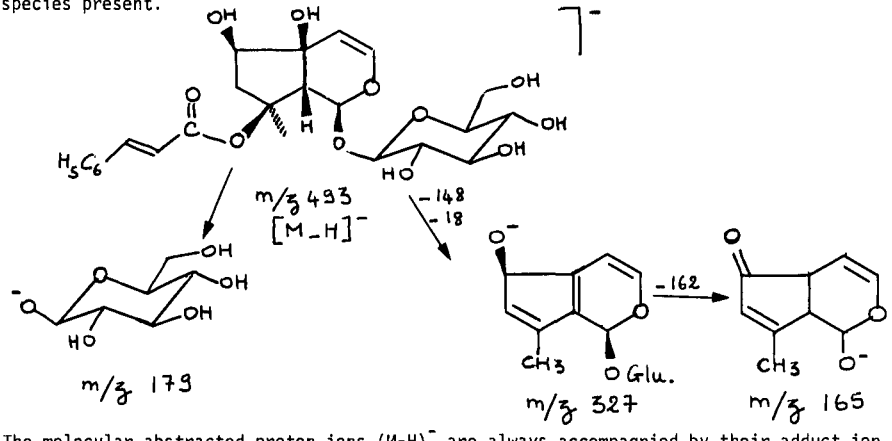
oooooooooooooooo

MASS SPECTROMETRY OF IRIDOID GLYCOSIDES

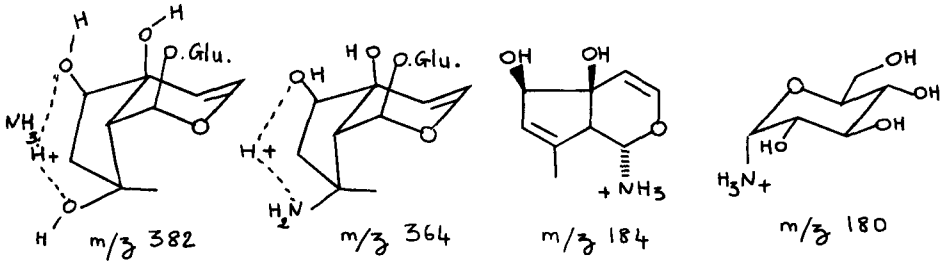
M. BECCHI,[++] D. FRAISSE,[+] C. LIGNAC,[+] J. RAYNAUD,[+++] and J.C. TABET[+]

\+ Centre de Spcectrometrie de masse SCA-CNRS
BP 22 - 69390 VERNAISON - FRANCE
++ Sarsyntex - BP 100 - 33701 MERIGNAC - FRANCE
+++ Laboratoire de Botanique - Faculté de Pharmacie
69373 LYON - FRANCE

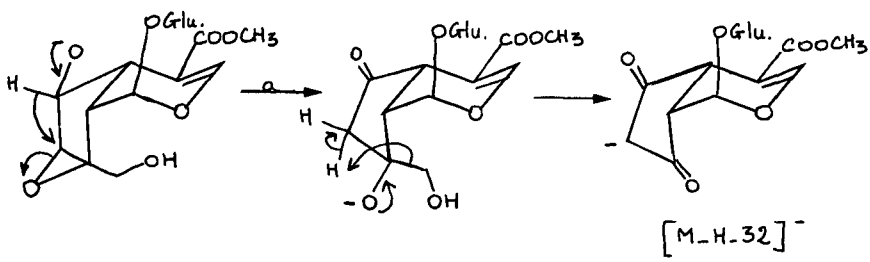
Thermally labile and especially polar compounds often require chemical derivatisation to make them volatile enough to permit mass spectrometry analysis. However this strategy is limited by three main drawbacks a) structural modification b) sample contamination and c) an important increase of the compound molecular weight.
New soft ionisation techniques developed in the past ten years offer an attractive alternative to derivatisation. In this work we report the analysis of iridoid and secoiridoid glycosides (Shanzhiside methyl ester, Aucubine, 8-O- Acetyl harpagide, Harpagoside, Oleuropeine, Loganic acid, Loganine, Verbenaline, Picroside I, Picroside II and Asperuloside) using chemical ionisation, desorption chemical ionisation (1) and fast atom bombardment (2) techniques.
Such naturally occuring compounds are of interest due to their use as important precursors in prostaglandin synthesis (3-4).
Electron impact and positive chemical ionisation spectra of these compounds do not show molecular ions and often contain little structural information.
Although PCI mass spectra of peracetylated derivatives usually exhibit a molecular or pseudo ion peak, derivatisation and extensive sample cleanup are required.
Negative chemical ionisation with OH^- as reagent ion give mass spectra with small molecular abstracted proton ions, however fragment ions often give valuable structural informations. $(M-H-Glucose)^-$ and $(M-H-Aglycon)^-$ formed competitively (schema 1) are the most important species present.



The molecular abstracted proton ions $(M-H)^-$ are always accompagnied by their adduct ion $(M+N_2O-H)^-$ of comparable intensity. The use of Cl^- as reagent ion increases the chance of observing the pseudo-molecular ion $(M+Cl)^-$; the intensity of $(M+Cl)^-$ peak is often as higher as 100 % but can also be of small abundance depending on the compound. Although the use of DCI, an other alternative technique is no more satisfactory than previously techniques in the negative ion mode with OH^-. Positive DCI (NH_4^+) spectra always show the adduct ion $(M+NH_4)^+$ in contrast with PCI (NH_4^+). In addition the DCI (NH_4^+) spectra of these compounds are characterized by the presence of even mass ions resulting from nucleophilic substitution reactions, i.e., substitution of hydroxyl groups by amino groups (NH_2^-) in the source in contradiction with what has been sometimes reported in the litterature (1).
As shown by early work (5-6) such ion-molecule reactions can lead to the following ions, for example the adduction. $(M+NH_4)^+$ of 8-O- Acetyl Harpagide (schema 2).



The use of ND_3 confirms that these reactions are probably bimolecular in certain cases and do not produce isobaric ions $M^{+\circ}$ by charge exchange. Additional evidence indicates that under favorable stereochemical condition the aglycon moiety can loose H_2O through transfert of the proton of NH_3^+. If the $(M+NH_4)^+$ ion is sufficiently stable, stereochemical effects appear to play major role in directing the loss of H_2O. In spite of all these possibilities it's still difficult to distinguish certain position of isomers such as shanzhiside methyl ester and 8-O- acetyl harpagide. Fast atom bombardment (FAB) spectra often permit to differantiate such isomers and MIKE ou MIKE/CID spectra provide better information. Positive ion FAB mass spectra show mainly adduct ions $(M+93)^+$ $(M+K)^+$ and $(M+Na)^+$; $(M+H)^+$ ions are sometimes of low abundance and $(2M+H)^+$ ions are also observed in some cases.
Principal losses result from the elimination of the heteroside either from $(M+93)^+$ or $(MH)^+$, f llowed by loss of H_2O as confirmed by MIKE spectra of MH^+. In the negative ion mode the mass spectra are mainly characterized by the presence of $(M-H)^-$ and $(M-H-Glucose)^-$ and sometimes $(M-H+92)^-$. The stereochemistry of the molecules is very important in directing fragmentation pathways.
In general peaks corresponding to the free acids are observed with esters. All these reactions certainly require transfert of H^- induced by the lone pair of electrons of the alcoxyde oxygen (schema 3)



In conclusion iridoid and secoiridoid glycosides can be studied using soft ionisation and desorption techniques. DCI and FAB mass spectra are complementary but the FAB technique providesmore valuable information as MIKE and MIKE/CID spectra are available.

(1) K. Hostettmann, J. Doumas, M. Hardy, Hel. Chim. Acta, 64, 297-303 (1981).

(2) M. Barber, R.S. Bordoli, R.D. Sedgwick, A.N. Tyler, J. chem. Soc., Chem. Commun 325 (1981)

(3) M. Naruto, K. Ohno, N. Naruse, H. Takeuchi, Tetrahedron letters, 251-254 (1979)

(4) W. Berkowitz, I. Sasson, P.S. Sampothkumas, J. Hrabef, S. Choudhry, D. Pierce Tetrahedron letters, 1641-1644 (1979).

(5) J. Basrard, D. Do Khac Manh, M. Fetizon, D. Fraisse, J.C. Tabet, J.C.S. Perkin II 1591 (1981).

(6) A. David, D. Fraisse, S. Scanzi, J.C. Tabet, Tetrahedron (under Press 1982).

THE DESORPTION CHEMICAL IONIZATION MASS SPECTROMETRIC STUDIES OF NOGALAMYCIN ANALOGUES

Wayne K. Duholke and Paul H. Zoutendam
Control Research and Development Laboratories
The Upjohn Company, Kalamazoo, MI 49001

The anthracycline antibiotic, nogalamycin, and many of the nogalamycin analogues (1) are active against gram-positive microorganisms and exhibit potential as antitumor agents (2). Desorption chemical ionization (DCI) was investigated for its value in aiding the characterization of these analogues. The electron impact spectra were useful in characterizing the glucopyranose portion of the molecules. The corresponding chemical ionization and DCI spectra show more strongly the ions arising from nogalose.

The iso-butane DCI mass spectrum of nogalamycin is typical of this group of compounds (Figure 1). A strong $(M + H)^+$ ion is obtained with considerable fragmentation. Most of the nogalamycin analogues will dissociate at varying rates to nogarene and/or nogalarene if exposed to heat. This dissociation results from the dehydration of the A ring. For example, the iso-butane DCI mass spectrum of 7-(R)-O-methylnogarol (Figure 2) gives ample $(M + H)^+$ but also includes a strong ion at m/z 492, which corresponds to the spectrum for nogarene (Figure 3). Similarly, the iso-butane DCI mass spectrum of 7-(S)-O-methylnogalarol (Figure 4) gives a strong ion at m/z 550 corresponding to nogalarene (Figure 5).

DCI was found to give protonated molecular ions for these labile compounds where electron impact and chemical ionization mass spectra did not give molecular weight information. In the DCI mass spectra, structurally significant fragment ions were observed which will be useful in elucidating the structures of analogues that have not been previously characterized.

References:

1. Paul F. Wiley, et al, J. Org. Chem 44, 4030 (1979).

2. G. L. Neil, S. L. Kuentzel and J. P. McGovren, Cancer Treat. Rep., 63, 1971 (1979).

Figure 1

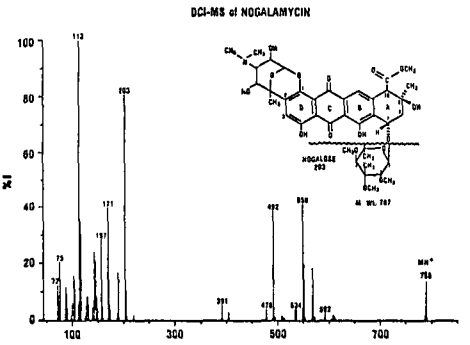


Figure 2

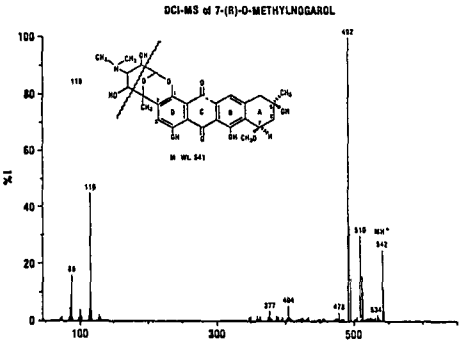


Figure 3

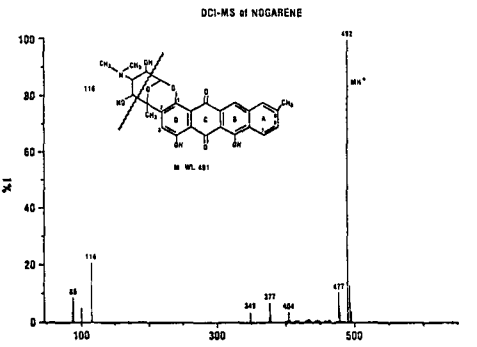


Figure 4

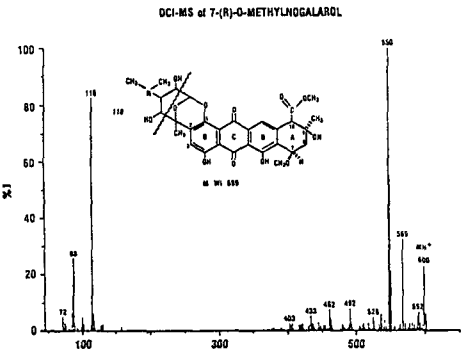
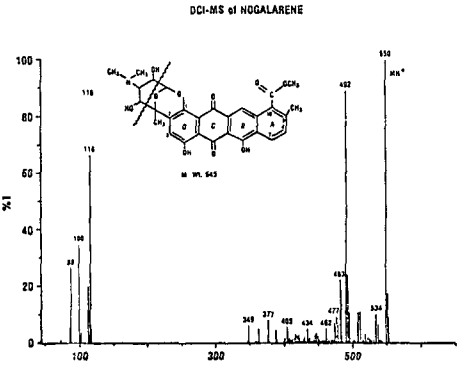


Figure 5



IN-BEAM EI AND MIKE STUDIES ON N-ALKYLPYRIDINIUM SALTS

Mamoru OHASHI, Robert P. BARRON, and Walter R. BENSON
Division of Drug Chemistry, Food & Drug Administration
Washington, D. C. 20204

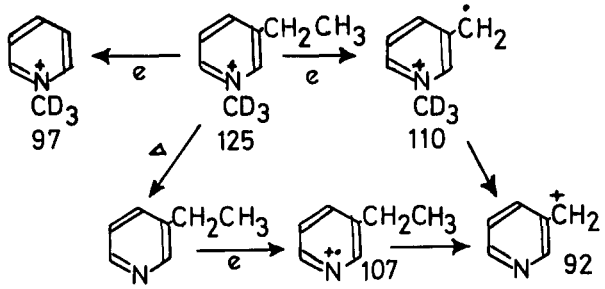
Historically, the interpretation of mass spectra of N-alkylpyridinium halides has been based on the formation, and subsequent ionization, of volatile thermal decomposition products.(1) In the cases of 2- and 4-alkyl substituted N-methyl pyridines, hydrogen halide elimination during vaporization, or on the hot ion source surfaces, is a dominant thermal process prior to electron ionization (EI). With an alkyl substituent in the 3-position, however, demethylation becomes so pronounced that other thermal processes such as hydrogen halide elimination or the reduction of the pyridinium ring are suppressed. We have successfully applied in-beam EI and MIKES techniques to elucidate the fragmentation pathways involving the intact molecular cations of tetraalkyl quaternary ammonium salts.(2) This paper, as an extension of that work, deals with the application of both techniques to determine the electron-ionization induced fragmentation of N-alkylpyridinium cations.

In accord with previous results by conventional EI techniques, the in-beam EI MS of 1-methyl-2-ethyl- (1) and 1-methyl-4-ethylpyridinium iodide (2) and their 1-trideuteromethyl analogues exhibit only [cation-H] and [cation-2H] peaks in their molecular weight regions. These processes can best be rationalized by the EI induced fragmentation of the corresponding methines produced thermally prior to electron impact.

The conventional EI mass spectrum of 1-methyl-3-ethylpyridinium iodide (3) exhibits peaks at m/z 142 (MeI), 128 (HI), 127 (I), 107 (cation-Me) and 92 (cation-2Me). No peak at m/e 122, corresponding to the cation, is observed. On the other hand, the in-beam EI mass spectrum of 3, shown in Fig. 1, exhibits abundant peaks at m/z 122 (cation), m/z 107 (cation-Me) and m/z 92 (cation-2Me). The mass chromatogram of peaks at m/z 92, 107, 122 and 142 clearly indicate major portions of the m/z 107 and 92 ions are not derived from the cation at m/z 122 but from the thermal decomposition product, M-MeI.

The in-beam EI mass spectrum of the N-trideuteromethyl analogue (4), shown in Fig. 2, exhibits [cation-CD_3] at m/z 107 and [cation-Me] at m/z 110, as well as the cation at m/z 125 and [cation-Me-CD_3]at m/z 92. The mass chromatogram of the ions at m/z 145 (CD_3I), 125, 110, 107 and 92, shown in Fig. 3, clearly indicate the peaks at m/z 125 and 110 arise from different reactions than those of m/z 145, 107 and 92.

The MIKE spectrum (Fig. 4a) of the cation of 4 at m/z 125, confirming the loss of methyl from the ethyl group as opposed to the N-methyl, indicates this process is the major fragmentation upon electron impact of the cation. The loss of the N-methyl group is attributed to thermal decomposition prior to electron impact. High voltage scanning ion kinetic energy (IKE) spectra established that the [cation-Me-CD_3] at m/e 92 is derived from two processes: (i) EI induced successive losses of the C-methyl and N-methyl groups from the cation, and (ii) EI induced fragmentation of 3-ethylpyridine produced by the thermal decomposition of the cation prior to electron impact.(3) The fragmentation pathways of 1-trideuteromethyl-3-ethylpyridinium cation are summarized in the following scheme.



1) R. Salsman and G. van Binst, Org. Mass Spectrom., 8, 357 (1974); E. Larsen, H. Egsgaard and H. Holmen, ibid., 13, 417 (1978).
2) M. Ohashi, R. P. Barron and W. R. Benson, J. Am. Chem. Soc., 103, 3943 (1981).
3) K. Biemann, Mass Spectrometry, McGraw-Hill, New York, 1962, p. 135.

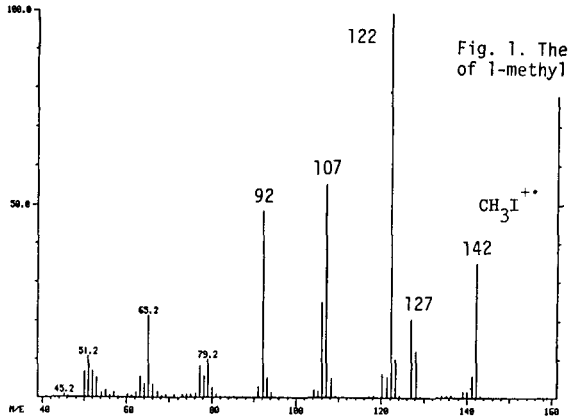


Fig. 1. The in-beam EI mass spectrum of 1-methyl-3-ethylpyridinium iodide(3).

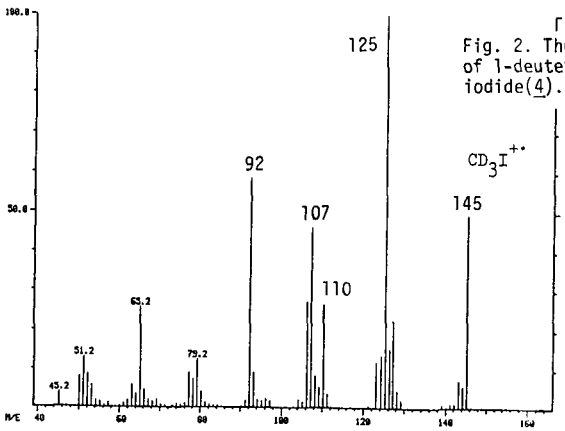


Fig. 2. The in-beam EI mass spectrum of 1-deuteromethyl-3-ethylpyridinium iodide(4).

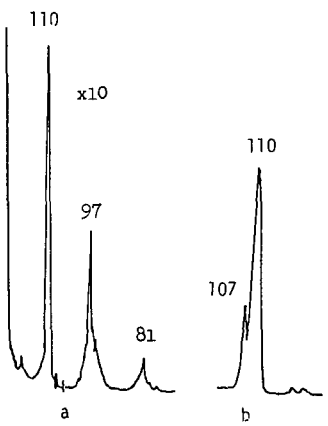


Fig. 4.
a) The MIKE spectrum of 4(m/z 125).
b) The HV scanning IKE spectrum of m/z 92.

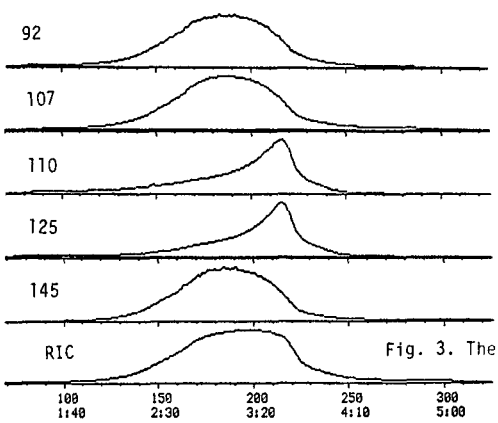


Fig. 3. The mass chromatogram of (4).

"DIRECT EXPOSURE CHEMICAL IONIZATION MASS SPECTROMETRY OF INTACT PHOSPHOLIPIDS", Frank W. Hatch, Boehringer Ingelheim, Ltd., Research and Development, P. O. Box 368, Ridgefield, CT 06877

Structure elucidation and analysis of naturally occurring phospholipids by mass spectrometry has been an area of active research. In 1971 Klein reported the 70 ev electron impact spectra for several phosphatidylcholine and fragmentation patterns for these compounds [1]. In general, fragmentation was extensive and no molecular ions were observed. Field desorption mass spectrometry of phospholipid type compounds has been studied by G. W. Wood et al[2,3]. Intense $(M+H)^+$ ions were observed but FDMS was not found suitable for positional isomer differentiation. The isobutane chemical ionization mass spectrum of dioleoyl phosphatidylcholine was reported by R. Foltz[4]. The spectrum exhibited a strong $(M+H)^+$ ion but no experimental details were reported.

In light of these previous results we have investigated the use of "direct exposure" CIMS techniques. Several CI reagent gas systems were employed to obtain structural information and to distinguish between thermal and ionization processes. Complete structure elucidation, including the differentiation of the α and β positional isomers of palmitoyl-oleoyl-phosphatidylcholine, could be carried out by a combination of positive ion and negative ion CIMS techniques.

All experiments were carried out on a Finnigan 4023 GC/MS/DS system using the standard EI/CI source and a modified tight CI source. The modified source allowed source pressures approxiamtely 5 times the standard source pressure to be achieved with comparable analyzer pressures. Samples were introduced for direct exposure CIMS experiments as described by Horning et al[5]. The source temperature was 280° C to 300° C.

RESULTS

Both isobutane and ammonia reagent gases provide $(M+H)^+$ ions of sufficient intensity for molecular weight determination of 1-palmitoyl-2-oleoyl-phosphatidylcholine. The isobutane spectrum of this compound exhibits three major ions at m/z 577, m/z 339 and m/z 313. These fragment ions clearly define the two acid residues but not their relative chain position. The ammonia CI spectrum exhibits an increase in high mass ions relative to the isobutane system; however, the fragments indicative of the acid residues are lost. Assignment of major fragments, m/z 718 and m/z 612, are not readily apparent. The isomeric palmitoyl-oleoyl-phosphatidylcholines give essentially identical isobutane and ammonia CI mass spectra.

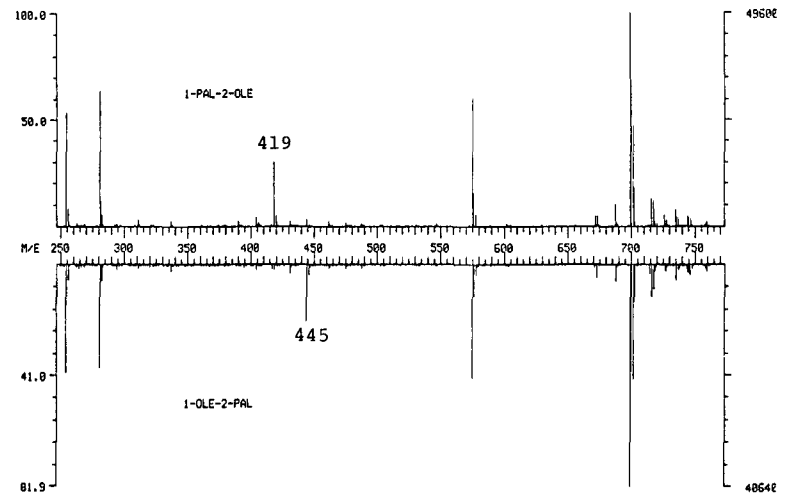
The negative ion CIMS with methane and ammonia moderating gases provides a method of distinguishing these two positional isomers, Figure I. The spectrum of each compound contains a unique ion at m/z 445 or m/z 419. The molecular weight region provides little information. The base peak ion cluster at m/z 699 to m/z 701 corresponds to the loss of trimethylamine from the parent compound; however, thermal processes may also be occurring which complicates structural assignments.

The methane/pyridine chemical ionization mass spectrum of 1-palmitoyl-2-oleoyl-phosphatidylcholine at 2.2 torr and 300° C is given in Figure II. The intense ion at m/z 780 corresponds to the addition of $C_5H_6N^+$ to a neutral decomposition product of molecular weight 700

Thermal decomposition of the phosphatidylcholine by a Hofmann elimination reaction produces an olefin and loss of trimethylamine. Thermal decomposition can also occur at the phosphoryl linkage to produce an additional alcohol or an olefin, molecular weight 594 and 576, respectively.

In light of the competing thermal and ionization processes, the major ions in the positive ion ammonia CI mass spectrum and negative ion CI mass spectrum may be tentatively assigned for 1-palmitoyl-2-oleoyl-phosphatidylcholine. The ammonia CI mass spectrum contains predominantly NH_4^+ adduct ions of thermally induced neutrals along with the $(M+H)^+$ parent ion and major fragment ion at m/z 577. The negative ion chemical ionization mass spectrum most likely results from dissociative electron attachment to the olefinic Hofmann degradation product. Ions at m/z 281 and m/z 255 characterize the acid residues. The hypothesized formation of a 6-membered ring species for the ions of m/z 575 and m/z 419 can account for the selective loss of the 2-position acid moeity and therefore allows the differentiation of these α/β isomeric compounds.

Figure I. Negative Ion CIMS of Isomeric Phosphatidylcholine



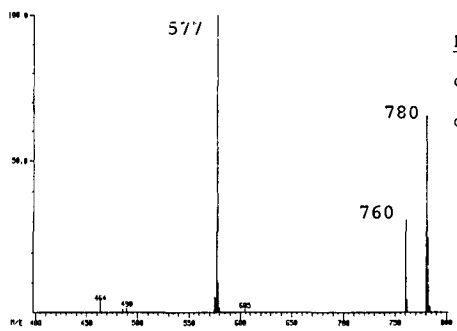
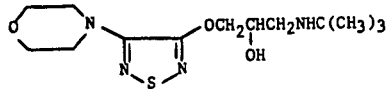


Figure II. CH_4/Pyridine CIMS of 1-Pal-2-Ole-phosphatidylcholine

1. Klein R. A., J. Lipid Research, 1971, 12, 123 (and later papers)
2. Wood G. W. et al, Biomed. Mass Spectrometry, 1976, 3, 172
3. Wood G. W. et al, Chemistry and Physics of Lipids, 1977, 18, 316
4. Foltz R. L., Lloydia, 1972, 35, 35, 344
5. Horning E. C. et al, Anal. Chemistry, 1981, 53, 2007

SIMULTANEOUS DETERMINATION OF THE INTRAVENOUS AND ORAL PHARMACOKINETICS OF TIMOLOL. J.R. Carlin*, J.D. Rogers**, R.O.Davis**, R.K. Ferguson***, and W.J.A. VandenHeuvel*. Merck Sharp & Dohme Research Laboratories, *Rahway, NJ 07065; **West Point, PA 19486; ***Thomas Jefferson University Hospital, Philadelphia, PA 19107

The pharmacokinetics of timolol maleate or BLOCADREN, [S-(-)-1-(tert.-butylamino)-3-[(4-morpholino-1,2,5-thiadiazol-3-yl)oxy]-2-propanol•H maleate],



have been determined by use of stable isotopes. Quantification of timolol and its $^{13}C_3$-analog $RCH_2NHC(^{13}CH_3)_3$ in human plasma and urine was carried out by using a selected ion monitoring procedure[1]. The method employs a C_{18} Sep-Pak for isolation of the drug-containing fraction, capillary column GLC of the TMSi derivatives of the compounds of interest and the internal standard $RCH_2NHC(C^2H_3)_3$ and detection via selected ion monitoring. Analyses are carried out on a Finnigan Model 3200 GLC-MS (equipped with a 6110 computer system) in the electron impact ionization mode. The mass spectrometer is operated by using the following conditions; ionizing potential, 70eV; emission current, 0.8 mA; electron multiplier, 1200 v. The ions monitored for quantification (m/z 86 from timolol and 89 and 95 from the $^{13}C_3$- and $^2H_9$-analogs, respectively) arise from the sidechains of the three compounds [e.g., $CH_2\overset{+}{N}HC(CH_3)_3$ for m/z 86]. The auto peak search routine which is part of the data system was used to measure peak intensity. Concentrations of each species of timolol in plasma and urine samples were determined by comparison of each observed intensity ratio (I_{86}/I_{95} and I_{89}/I_{95}) with standard curves. Repeatability assays were carried out (N=5) by use of two pools of human control plasma fortified at the 1.0 and 10.0 ng/ml level with a 1:1 mixture of timolol and its $^{13}C_3$-labeled analog. The CV% values averaged 2.5 — no significant difference was expressed by either species of drug. The method offers the selectivity and sensitivity (<1.0 ng/ml) necessary to quantify timolol levels throughout a pharmacokinetic study.

Three healthy subjects were each given three oral doses of unlabeled timolol maleate (5, 15, and 45 mg of drug in solution); simultaneously, each received (via infusion) an intravenous dose containing 4 mg of $^{13}C_3$-labeled timolol maleate in saline. Blood and urine samples were collected prior to treatment and at timed intervals for up to 12 and 72 h post dose, respectively. Simultaneous dosing offers the advantage of determining the kinetics of drug disposition at the same time the absorption process is under study. Knowledge of these factors is important in the rational use of drugs. Assuming that the intravenous route is permitted, then the absolute bioavailability of other parenteral or enteral routes can be determined in a single experiment. Oral bioavailability was based on AUC ratios which had been corrected for differences in plasma clearance and dose. Results from this study indicated the pharmacokinetics of timolol were linear over the dose ranges investigated and the bioavailability of the drug exhibited significant intersubject variation (.34-.70).

The results of the plasma analyses were illustrated via plasma concentration-time curves. A representative plot showing drug levels for both species of timolol is presented below. After oral dosing, the drug was rapidly absorbed and reached a peak plasma concentration in 30 to 45 min. The $T_{1/2}$ found for both forms of the drug averaged 2.9 $\mp$ 0.1 h. The data also showed that the $T_{1/2}$ was not affected by increases in the amount of drug dosed orally up to the 45 mg level. The volume of distribution for timolol is ~1 L/kg. Analysis of urine data (expressed as percent of dose) showed that an average of 25% of the i.v. dose was excreted unchanged in 72 h, whereas recovery of the oral dose varied from 6 to 20%. Renal clearance estimates suggest that these differences stem from variations in the nonrenal clearance of the drug.

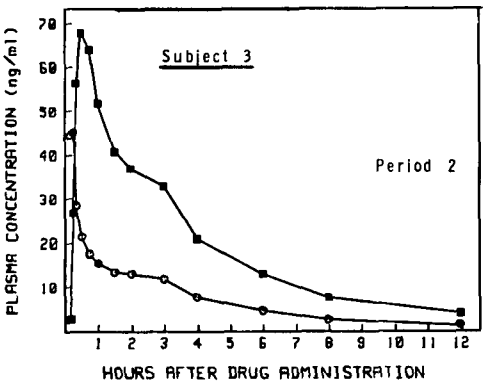
1/ J.R. Carlin, R.W. Walker, R.O. Davies, R.K. Ferguson and W.J.A. VandenHeuvel, J. Pharm. Sci., 69, 111 (1980).

Plasma Concentration-Time Curves After Simultaneous Oral and I.V. Doses

Key:

15 mg Timolol (Oral) ■——■

4 mg $^{13}C_3$-Timolol (I.V.) O——O



PHARMACOKINETIC STUDIES OF THE ORAL AND RECTAL ADMINISTRATINS OF METYRAPONE AND ITS EFFECT ON THE 11-ß-HYDROXYLASE IN MAN :Kazuyoshi Ichimura[1],Kazuyoshi Chiba[1],Kazuki Saito,[2] Yutaka Nozaki[1],Kiyohiko Kato[1]Department of Pediatrics[1]and Laboratory of GC/MS[2]School of Medicine,Keio University.Department of Pediatrics,Yamanashi Medical college[3]

SUMMARY:

Metyrapone(M) and reduced metyrapone(RM),a major metabolite of M in vivo,inhibit activity of 11-ß-hydroxylase which converts 11-deoxycortisol and deoxycorticosterone to cortisol and corticosterone. M and RM are known as drugs for endocrinological examination of hypothalamic-pituitary-adrenal axis. A method for the measurement of M and RM in serum with GC/MS is reported. Concentrations of M and RM in serum obtained with this method were pharmacokinetically analyzed by one-compartment open system model.

INTRODUCTION:

Objects of this report are as follows:

1) A quantitative analysis of the serum M and RM concentrations.
2) The age-related kinetic studies of M after the oral and rectal M-administrations.
3) A study of the relationship between the serum concentrations of M and/or RM,and the inhibition of 11-ß-hydroxylase.

METHODS:

The conditions of GC/MS were as follows:
Electron ionization.Glass column;ϕ 2 mm,length 1 m, 3% OV-17 on chromosorb W-HP (80-100 mesh). Injection port temperature;270°C. Column temperature;220°C. Ionization voltage ;70eV. Accelerating voltage;3kV. GC/MS;JMS-D300,JMA-2000,JGC-20K. Sililating;TMS(TMCS: TMSI:BSTFA=3:1:3).
Procedure of measurement was shown in Fig(1).
The areas of mass fragmentgram,which were measured at m/z 106 for M,m/z 180 for TMS-derivative of RM and m/z 136 for internal standard (Thonzyramine hydrochloride),were used for the caluculation of M and RM (Fig.2).
The pharmacokinetic study of M was analyzed by one-compartment open system model(reference 1).
$\frac{Sx100}{S + F}$ and $\frac{DOCx100}{DOC + B}$ were used as index od inhibition of 11-ß-hydroxylase.
*S:11-deoxycortisol,F:cortisol,DOC:deoxycorticosterone,B:corticosterone.
The comparison of potencies of M and RM was analyzed,by using AKAIKEŚ INFORMATION CRITERION(AIC) (reference 2,3).

RESULTS:

Sililation of hydroxyl group of RM prevented the tailing of RM.
The extraction of M and RM from serum was found to yield to 90 ± 5 % for M,85 ± 6 % for RM.
The coefficients of variation in between-assays and within-assays of accuracy and precision were less than 8.4 %.
The artificial time course data calculated by using the one-compartment open system model equation were conforming well to serum concentration-time course data for M and RM(Fig.3).
The logarithmic values of the serum M + RM concentrations highly related to indices of inhibition of 11-ß-hydroxylase of the glucocorticoid-pathway and mineralocorticoid-pathway in children.

CONCLUSIONS:

The method of measurement for M and RM was simple,sensitive,specific and highly reproducible.
Metabolism of M after absorption of M through alimentary tract in children was similar in all groups.
The inhibition of 11-ß-hydroxylase related to serum concentrations of total metyrapone (M + RM) (Fig.4).
RM was nealy same effective as M on 11-ß-hydroxylase in children.
The sensitivity to M and RM was higher than in the mineralocorticoid-pathway than in the glucocorticoid-pathway.

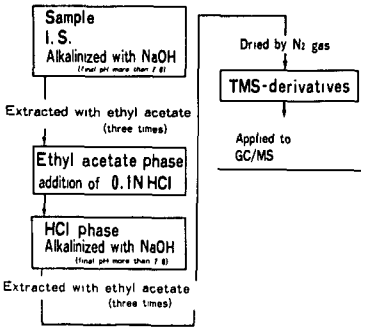


Fig.1. Analytical procedure of metyrapone and reduced metyrapone by GC/MS. GC/MS: gas chromatography mass spectrometry

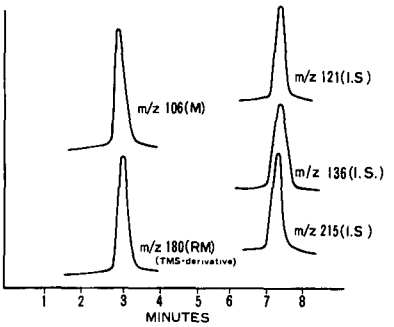


Fig.2. Typical mass fragmentogram of M,RM (TMS-derivative) and I.S.

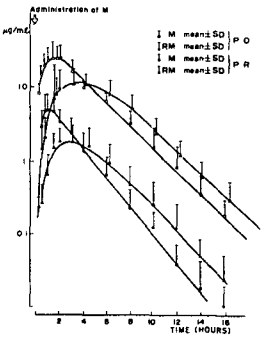


Fig.3. The serum metyrapone(M)and reduced metyrapone(RM)concentrations after oral or rectal administration of M(50mg/kg)

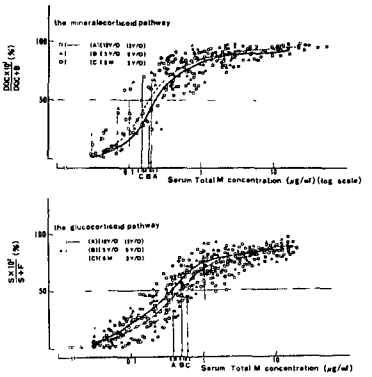


Fig.4. Concentration-effect curves for Total M(metyrapone+reduced metyrapone)on the 11-β-hydroxylase in the various age-groups
The relations are expressed as inhibitory index against the Total M concentrations

REFARENCES:

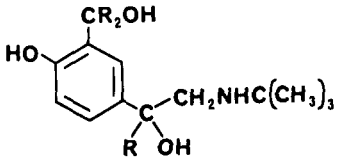
1) Gibaldi,M. and Perrier,D. : Pharmacokinetics Drugs and the Pharmaceutical Science. Vol.1., Macel Dekker Inc.,N.Y.,1975,293-296.

2)Akaike,H.: Information theory and extension of maximum likelihood principle.In Petrov,B.N. and Csaki,F.(eds),Second International Symposium on Information Theory,Akademiai Kiado, Budapest,1973,267-281.

3) Ozaki,T.and Tong,h.: On the fitting of non-stationary autoregressive models in time series analysis. Proc.of 8th Hawaii Int.Conf. on system science,1975.

DETERMINATION OF ALBUTEROL IN PLASMA BY GAS CHROMATOGRAPHY-CHEMICAL IONIZATION MASS SPECTROMETRY: Miryam Weisberger and Mark L. Powell, Schering Corporation, Bloomfield, New Jersey 07003

Albuterol, 2-tert-butylamino-1-[4'-hydroxy-3'(hydroxymethyl)-phenyl]-1-ethanol (I), is a ß-adrenergic bronchodilator used widely as a therapeutic agent for the treatment of bronchial asthma. The drug has been shown to be extensively metabolized by man (1,2). Based on the results of studies using radiolabeled albuterol, it was calculated that the peak plasma concentration following a 4 mg oral dose was likely to be about 20 ng/ml (1,3). Because of the specificity and sensitivity requirements for clinical bioavailability/ pharmacokinetic studies, a quantitative method was recently developed for the determination of albuterol in plasma samples in the sub-nanogram range using gas chromatography-chemical ionization mass spectrometry. This method is more sensitive than previously published methods (3) and it affords more rapid sample processing.



I Albuterol R = H
II Albuterol-d_3 R = ^2H

Albuterol (I) and trideuterio albuterol (II) (stable isotope internal standard) were extracted from plasma into ethyl acetate at pH 11.0, with average recoveries of 89% at albuterol concentrations ranging from 0.25 ng/ml to 25 ng/ml. After conversion to their TMS derivatives, gas chromatographic separations were achieved using a 6' x 2 mm glass column packed with 3% OV-1 on 80/100 Supelcoport, with helium being used as the carrier gas at a flow rate of 20 ml/min.

Selected ion monitoring of the MH^+ ions (ammonia was used as chemical ionization reagent gas) of the protio and deuterio compounds as their TMS derivatives (m/z 456 and 459, respectively; Figure 1) gave ion ratios which were converted to plasma concentrations using standard curves. A typical selected ion current profile for a plasma sample containing albuterol and albuterol-d_3 is shown in Figure 2. All chromatograms were free of any endogenous interfering peaks (Figure 3).

Figure 1. A. Ammonia C.I. mass spectrum of TMS-albuterol B. Ammonia C.I. mass spectrum of TMS-albuterol-d_3.

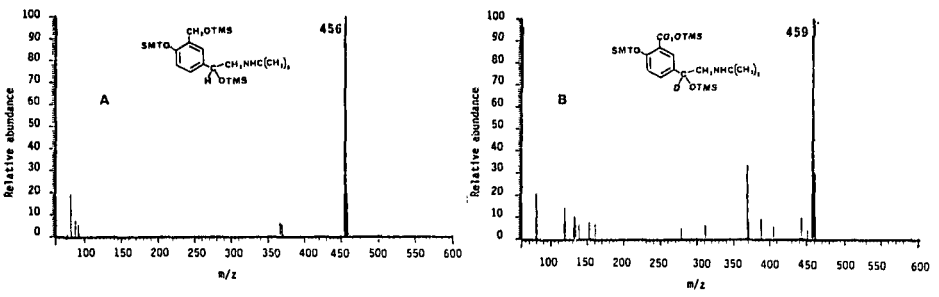


Figure 2. Selected ion current profile from the analysis of a 2 ml control plasma sample containing 25 ng/ml of albuterol (m/z 456) and 50 ng/ml of albuterol-d_3 (m/z 459).

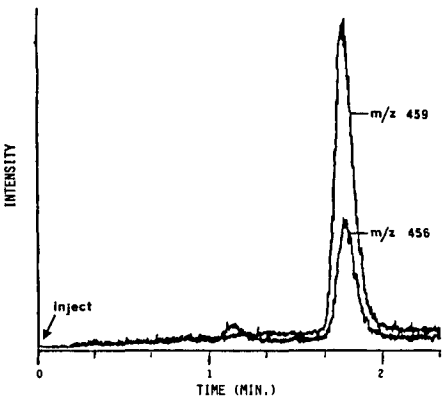
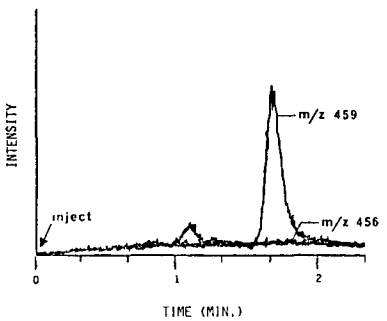


Figure 3. Selected ion current profile from the analysis of a 2 ml control plasma sample containing 50 ng/ml of albuterol-d_3 (m/z 459).



Linearity was demonstrated for albuterol concentrations ranging from 0.25 ng/ml to 25 ng/ml. The limit of quantitation is at least 0.25 ng/ml (coefficient of variation <5%). The assay precision and accuracy, in terms of percent error, are both <20% at 0.25 ng/ml of albuterol. The method is rapid, specific and sensitive enough for use in clinical pharmacokinetic, absorption and bioavailability studies employing therapeutic doses of albuterol.

References

1. Evans, M.E., Walker, S.R., Brittain, R.T. and Paterson, J.W., Xenobiotica, 3, 113 (1973).

2. Lin, C., Li, Y., McGlotten, J., Morton, J.B. and Symchowicz, S., Drug Metab. and Dispos., 5, 234 (1977).

3. Martin, L.E., Rees, Janet and Tanner, R.J.N., Biomed. Mass Spectrom., 3, 184 (1976).

CONFIDENCE LIMITS FOR THE ISOTOPE DILUTION/GAS CHROMATOGRAPHIC-MASS SPECTROMETRIC DETERMINATION OF 2,3,7,8-TETRACHLORODIBENZO-p-DIOXIN IN ENVIRONMENTAL SAMPLES

G.F. Moler, R.R. Delongchamp, W.A. Korfmacher,
B.A. Pearce, and R.K. Mitchum

Department of Health and Human Services
Food and Drug Administration
National Center for Toxicological Research
Jefferson, Arkansas 72079

2,3,7,8-Tetrachlorodibenzo-p-dioxin (TCDD) is a toxic by-product produced during the manufacture of 2,4,5-trichlorophenol, a precursor used in the synthesis of the herbicides 2,4,5-trichlorophenoxyacetic acid and (2,3,5-T) 2,4,5-trichlorophenoxypropionic acid (Silvex). Due to the extreme toxicity of TCDD and the fact that it has entered the environment and continues to enter the environment (mainly through the application of 2,4,5-T and Silvex), analytical chemists have had to address the problems encountered in the determination of TCDD at very low concentrations, generally in the low part-per-trillion (ppt) range.

The need for high specificity, in addition to sensitivity, has led to the use of *isotope dilution/gas chromatographic-mass spectrometric (ID/GC-MS) methodology.* The goal of ever-lowering the detection limit of TCDD has led to ID/GC-MS methodology producing a current detection limit of less than 1.0 ppt. But one aspect of the ID/GC-MS determination of TCDD that has been largely neglected has been the computation of valid confidence limits for the levels of TCDD reportedly found in the environmental samples. Most authors have not reported confidence limits at all; others report limits based on the standard deviation of the repetitive quantitation of the environmental sample, a method which ignores errors inherent in the formulation of standard curves.

An investigation was begun with the purpose of developing a method to compute statistically valid confidence limits for the ID/GC-MS determination of TCDD, to identify and quantitate all significant sources of variance in the analysis of environmental samples for TCDD, and to implement the quantitation procedures on a GC-MS-interfaced computer.

Sources of Variance

Significant sources of variance in the reported concentration of TCDD in samples were found to be:

1) weighing the standards;
2) weighing the environmental sample;
3) spiking the environmental sample; and
4) peak quantitation and ID/GC-MS linear regression.

The magnitudes of the relative contributions of the four sources of variance depended upon the environmental sample size, the weights of the standards used, precisions of the standard and sample balances, and the ID/GC-MS regression method used. In most cases the ID/GC-MS regression was by far the most significant source of variance.

Regression Methods

ID/GC-MS least-squares linear regressions examined included the replicate measurement method and the SSD method. The accuracies of the methods were determined with the use of computer simulations and with ID/GC-MS data.

The replicate measurement method uses replicate injections for all standards and samples and the common formula for the sample variance (s^2). It was found that this method produced fairly accurate confidence limits if a large (≥ 5) number of injections were made for each sample.

The SSD (Squared Successive Differences) method uses a newly-developed procedure to estimate the variance of the area of a single chromatography peak. This method was found to produce more accurate confidence limits than the replicate measurement method and did not suffer from the practical limitation of the replicate measurement method (the need for replicate injections).

Implementation

A statistical analysis software package which incorporated all four significant sources of variance in the ID/GC-MS determination of TCDD was implemented on a Finnigan INCOS 2300 Data System. This package consisted of two programs written in FORTRAN IV: STANDARD and UNKNOWN. STANDARD created an SSD ID/GC-MS standard curve, stored curve

parameters in a disk file, and produced a written report. UNKNOWN determined if TCDD was present in a sample, calculated a detection limit for every injection, and produced 95% confidence limits for any TCDD found.

Implementation of such a validated software package by most or all laboratories performing the ID/GC-MS determination of TCDD would greatly aid in the consistency and acceptance of the reported concentrations of TCDD found in environmental samples.

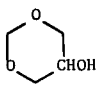
GLC - CHEMICAL IONIZATION SELECTED ION MONITORING ASSAY FOR GLYCEROL FORMAL IN ANIMAL TISSUES

R. W. Walker,* F. P. Baylis,* J. E. Brown,* D. H. Minsker,**
R. T. Robertson** and W. J. A. VandenHeuvel*

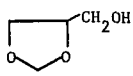
Merck Sharp & Dohme Research Laboratories
*Rahway, NJ 07065
**West Point, PA 19486

Although numerous studies aimed at detecting submicrogram quantities of drugs in the tissues of food-producing animals are carried out routinely in the development of new animal health drugs, little attention is usually given to the tissue concentration of the components of the dosing vehicle. Glycerol formal, a mixture of the cyclic condensation products of glycerol and formaldehyde, has been used as a non-aqueous solvent in parenterally administered products (Spiegel and Noseworthy, 1963) such as TRIVETRIN (ABPI Compendium, 1978) and OXYTETRACYCLINE (U.S. Patent, 1973) apparently with no reported toxic effects. Aliverti and coworkers (1980) recently reported that in the rat, glycerol formal induces embryo and fetal toxicity and is also teratogenic [leading to cardiovascular defects and mishapen (wavy) ribs]. As glycerol formal is a component of several injectable formulations presently under investigation in our laboratories, the paper by Aliverti et al. (1980) prompted us to develop and apply a sensitive and specific assay for measuring any residues of glycerol formal in animal tissue and to subject this solvent to teratogenicity studies.

Combined gas-liquid chromatography (GLC)-mass spectrometry with selected ion monitoring is an often-employed approach for quantifying compounds of biological interest at the parts per billion level (Carlin et al., 1980; Garland and Powell, 1981; Suhre et al., 1981). Initial experiments using electron impact ionization mass spectrometry as a detection approach for glycerol formal were not encouraging (e.g., no characteristic ions of high intensity were produced), but chemical ionization (isobutane reagent gas) appeared to offer a potentially suitable method for detection and quantification of glycerol formal. The chemical ionization mass spectrum of glycerol formal is dominated by its pseudomolecular ion (MH^+) of m/z 105; by monitoring the MH^+ ion a detection limit of 1 ng injected on-column was found.

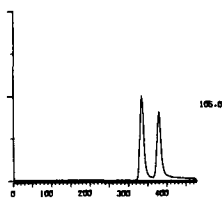


5-hydroxy-1,3-dioxane
~60%



4-hydroxymethyl-1,3-dioxolane
~40%

Glycerol formal is a 60/40 mixture of two isomeric compounds, 5-hydroxy-1,3-dioxane and 4-hydroxymethyl-1,3-dioxolane. These isomers are not separated by a Carbowax packed column, but are separated by a 20 m methyl silicone fused silica capillary column with a peak height (m/z 105) response ratio of 57/43. Thus the two condensation products possess similar mass spectrometric ionization yields and a packed column with no isomer separation can be used with confidence to determine total glycerol formal residue levels.



Use of a mass spectrometric-based detection assay system offers the opportunity for utilizing a heavy isotope-labeled analog of the compound of interest as internal standard (Carlin et al., 1980; Suhre et al., 1981). Dideutero glycerol formal was prepared from glycerol and paraformaldehyde-d_2. The chemical ionization mass spectrum of this compound showed the expected base peak at m/z 107.

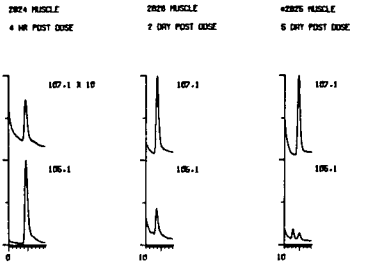
The isolation procedure developed for this assay involves partitioning of the extracted glycerol formal between water and methylene chloride at different volume ratios, exploiting the K_D CH_2Cl_2/H_2O (0.13) of glycerol formal in this halogenated solvent. Experiments with control tissues (fat, kidney, liver, muscle) and control tissues spiked with glycerol formal have demonstrated an overall lower assay sensitivity limit of 0.02-0.04 ppm using a 2 g tissue sample and monitoring the ions of m/z 105 and 107.

All analyses were carried out using a Finnigan 3200 GLC-quadrupole MS instrument with a 6110 computer system. Operation was in the chemical ionization mode utilizing selected ion monitoring. MH^+ ions for glycerol formal (m/z 105) and the glycerol formal-d_2 internal standard (m/z 107) were monitored and peak height intensities obtained via computer printout. The mass spectrometric operating conditions were as follows: chemical ionization with isobutane reagent gas (0.6 torr), amplifier gain of 10^{-9} amp/volt, electron multiplier setting of 1200 volts, electron energy of 140 electron volts, and emission current of 0.8 milliamps. The GLC operating conditions included: 1.2 m x 3 mm I.D. glass U-tube packed with 0.2% Carbowax 1500 on 80/100 Carbopack C (Supelco), isobutane carrier gas (10 ml/min), column oven 140°, glycerol formal retention time of ~2 min. The m/z 105 to m/z 107 peak height (intensity) ratios of a series of isolates obtained from spiked control tissue were subjected to linear regression analysis to generate equations for calculating ppm values. These samples contained different amounts of glycerol formal (0.1 to 0.5 μg) and 1 μg of internal standard. Isolates from tissues were examined and the I_{105}/I_{107} ratios at the retention time of interest obtained via computer printout. The concentration of glycerol formal in the samples was determined from peak height intensity ratio values by using the slope and intercept values from the regression analyses.

Assays for glycerol formal were carried out in four animal studies involving cattle, horses, and swine. No glycerol formal was found in tissues from barrows and gilts obtained at slaughter one day post dose.

The highest residue of glycerol formal in a cattle study was found in the 4 h post dose muscle injection site tissue (22.5 ppm) which rapidly decreased to 0.08 ppm after 5 days post dose.

Plasma samples were collected during a single animal steer residue study and subsequently assayed for glycerol formal. The amount observed was greatest soon after administration (~9 ppm at 0.5 h) and dropped below the lower limit of sensitivity between 8 and 24 h post dose. The apparent T 1/2 was ~3.5 h.



Assay of the plasma isolates using selected ion monitoring with capillary column GLC demonstrate that the 5-hydroxy-1,3-dioxane disappears at a slower rate than does the 4-hydroxymethyl-1,3-dioxolane (apparent T 1/2 value of ~3.8 and ~0.6 h respectively), presumably because of a slower rate of excretion and/or metabolism.

The maximum glycerol formal residue found in an edible tissue at 5 d post dose is ~0.1 ppm, whereas a treatment-related increase in occurence of teratology (wavy ribs) in rats requires 150 mg of glycerol formal per kg. Thus a 70 kg person consuming 500 g of the residue-containing tissue would be exposed to ~0.7 μg of glycerol formal per kg, 0.0005% of the teratogenic dose in the rat.

Literature Cited

ABPI Compendium of Data Sheets for Veterinary Products, Pharmid Publications, Ltd., London, 1978, 422.

Aliverti, V., Bonanomi, L., Giavini, E., Leone, V. G. and Mariani, L. Toxicol. Appld. Pharmacol., 1980, 56, 93-100.

Carlin, J. R., Walker, R. W., Davies, R. O., Ferguson, R. T. and VandenHeuvel, W. J. A., J. Pharm. Sci., 1980, 69, 1111-1115.

Garland, W. A. and Powell, M. L., J. Chromatog. Sci., 1981, 19, 392-434.

Greenbaum, S. B., Schaaf, K. H. and Klein, H. C., U.S. Patent, 1973, 3,712,949.

Spiegel, A. J. and Noseworthy, M. M., J. Pharm. Sci., 1963, 52, 917-927.

Suhre, F. B., Simpson, R. M. and Shafer, J. W., J. Agric. Food Chem., 1981, 29, 727-729.

THE DETERMINATION OF PICOGRAM QUANTITIES OF TRACAZOLATE (ICI 136,753) BY CAPILLARY GC/MS/SIM. K.R.Monson, K.L.Neilson, and J.O.Malbica, Stuart Pharmaceuticals, Div. of ICI Americas Inc., Wilmington, DE 19897

OBJECTIVE

(1) Develop a GC/MS assay capable of detecting picogram quantities of tracazolate (Figure 1) utilizing deuterated tracazolate (Figure 2) as the internal standard.

(2) Apply the method to the determination of tracazolate in rat blood following an 80 mg/kg oral dose and to the study of in vitro rat gut absorption.

INTRODUCTION

Tracazolate, 4-N-butylamino-1-ethyl-6-methyl-H-pyrazolo (3,4-b) pyridine-5-carboxylic acid ethyl ester is currently under evaluation in Phase 1 clinical trials as an anxiolytic drug. The compound was found during preclinical in vivo studies in dog and rodents to be extensively metabolized. Similarly, the in vitro everted rat intestine model for evaluating intestinal absorption showed 80% of the compound was found to be metabolized as it traversed the intestinal cell towards the serosal side during a two hour incubation period[1].

PROCEDURE

(A) Rat Whole Blood Levels of Tracazolate

The cranial vena cava of a rat was cannulated via the jugular vein to allow for repetitive sampling over a 48-hour period following a single 80 mg/kg oral dose. The samples were processed according to the procedure outlined in Figure 3.

(B) In-Vitro Everted Rat Gut Preparation

The procedure used is a modification of the method of Crane and Wilson[2]. The segment of gut used in the study was obtained from the jejunum. The mucosal side was exposed to tracazolate at a concentration of 6 mcg/ml. The sampling process, proceeded for 60 minutes, at which time the samples were processed according to Figure 3.

(C) Instrumental

The method utilized splitless injection on a Finnigan 4000 GC/MS with a 30 meter x 0.25 mm Durabond DB-1 (0.25μfilm thickness) connected directly to the source. The Incos 2300 data system with the MID program was used to monitor the ions m/e 304 and 309.

RESULTS AND DISCUSSION

Reconstructed GC/MS ion chromatograms using selected ion monitoring of extracts from whole blood, and whole blood spiked at 10.0 ng/ml tracazolate-d_5 and 1 ng/ml tracazolate are shown in Figure 4. Similar chromatograms were obtained when plasma was substituted for whole blood. The limit of detection for the assay is 100 pg/ml based on a minimum response of three times the background ion current for m/e 304.1

The blood level profile of tracazolate in rat following a single 80 mg/kg oral dose is shown in Figure 5. The inherent sensitivity and specificity of the assay precludes the requirement of large sample volumes for assay. Multiple sampling of a cannulated rat eliminates the inter-individual variation in absorption.

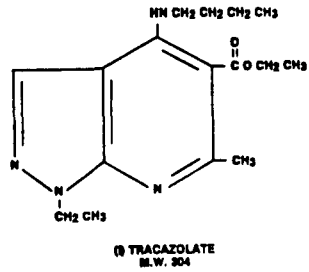
The absorption of tracazolate by the in vitro everted rat gut model as measured by GC/MS shows bi-phasic characteristics as shown in Figure 6. Extrapolation of the initial portion of the curve to the time axis indicates a lag time of less than five minutes. Clearance of the compound was not determined due to the exponential nature of the curve.

CONCLUSIONS AND COMMENTS

A sensitive and specific quantitative GC/MS method employing selected ion monitoring has been developed which is capable of detecting 200-500 pg/ml tracazolate in plasma or whole blood. This method has been applied to the determination of blood levels of tracazolate in a dosed cannulated rat where sample size is a restriction. The method has also been utilized to study the in-vitro absorption of tracazolate by the everted rat gut.

REFERENCES

(1) Personal Communication, Dr. N. H. Lee and Ms. J. Morse, Stuart Pharmaceuticals, Division of ICI Americas, Wilm. DE.
(2) R. K. Crane and T. H. Wilson, J. Appl. Physiol., 12:145 (1958)



(I) TRACAZOLATE
M.W. 304

Figure 1

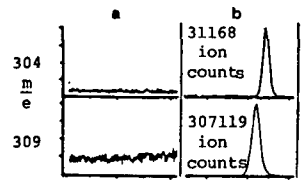
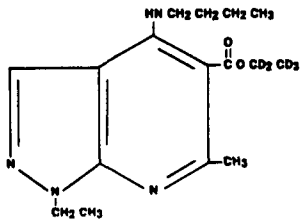


Figure 4



(II) TRACAZOLATE - d_5
M.W. 309

Figure 2

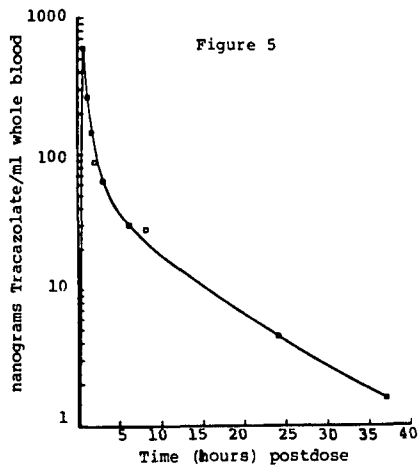
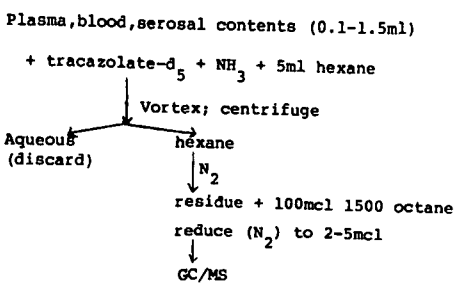


Figure 5

Figure 3



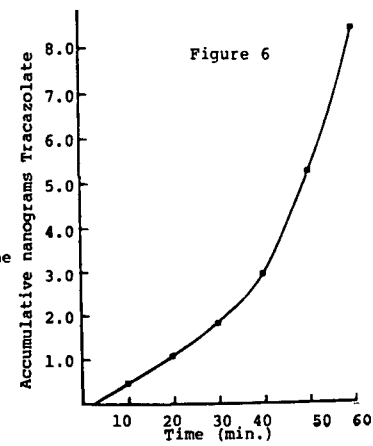


Figure 6

MPB 16 QUANTITATION OF DICLOFENAC SODIUM IN HUMAN PLASMA BY GAS CHROMATOGRAPHY-MASS SPECTROMETRY, Y. HASHIMOTO, T. IRIE, K. YAMASHITA, M. ISHIBASHI and H. MIYAZAKI, Res. Lab. Pharm. Div., Nippon Kayaku Co., 3-31 Shimo, Kita-ku, Tokyo 115, JAPAN

A specific and accurate method for the determination of diclofenac sodium in human plasma was developed by gas chromatography-mass spectrometry using [$^{2}H_{6}$] variant as an internal standard. Diclofenac sodium was derivatized to its methyl ester by treating with HCl-methanol. This diclofenac methyl ester gave a single, well-shaped gas chromatographic peak, suggesting that this esterification proceeded smoothly without the formation of by-product. EI-mass spectrum of this methyl ester gave a molecular ion as a prominent peak, which was confirmed by the presence of the doublet ion at m/z 309 and 311 due to the characteristic intensity of chlorine atom. The quantitation limit of diclofenac methyl ester by this present method was 5 ng/ml plasma when monitored the molecular ion of m/z 309, being sufficient to determine the plasma levels of diclofenac sodium. When administrated 25 mg of diclofenac sodium to 10 volunteers, the average of the plasma levels reached maximum of 460 ± 90 ng/ml at 1 hour after administration and declined with half-life of approximately 1 hour.

TRICLOSAN QUANTITATION WITH GAS CHROMATOGRAPHY/MASS SPECTROMETRY

D. Alkalay, T. A. Thompson, H. S. Goodblatt,
C. H. Borman, and J. Volk

Research and Development Department, Pharmaceuticals Division,
Ciba-Geigy Corporation, Ardsley, NY 10502.

Triclosan, 2',4,4'-trichloro-2-hydroxydiphenyl ether, is a broad spectrum germicidal agent used frequently as a component of skin cleaning formulations. Dermal applications may result in percutaneous drug absorption. This procedure was developed as a specific and sensitive method with a wide linear range and the capability to be used for drug determinations in plasma and in urine.

The method relies on the use of a bromo-analog of triclosan as the internal standard, on a simple extraction with hexane at a pH of 2.2, on derivatization of the phenols with acetic anhydride/pyridine, and on the combined use of gas chromatography with electron impact mass spectrometry and computerized data handling (Finnigan model 3300 GC/MS equipped with model 6100 data system). The derivatization improves the gas chromatographic properties of triclosan and its bromo-analog by converting them into the respective acetates. The latter, under EI conditions (70 eV), lose the acetyl group and the selected ion monitoring is done at m/z 288 and 334, which are the molecular ions of triclosan and its bromo-analog, respectively.

The method is specific, accurate, and precise. It permits triclosan determinations in biological fluids at concentrations ranging from 5 to 10,000 ng/ml. The procedure is suitable for routine analyses and has sufficient sensitivity to permit monitoring human plasma levels in subjects using regularly skin cleaners containing triclosan.

QUANTITATION OF GLUCOSE, BILE ACIDS AND VITAMIN D_3 IN CHILDREN BY ISOTOPE DILUTION - MASS SPECTROMETRY. P. Dan, M.J. Gelfand, R.C. Tsang, J.E. Heubi, M.A. Sperling, M.I. Sperling. P.M. Clemons, E.J. Norman.
Dept. of Medicine (Hematology-Oncology), Radiology (Radioisotope Laboratory) and Pediatrics. University of Cincinnati, Cincinnati, Ohio 45267

Mass fragmentography of glucose with D-Glucose-6,6-d_2 as a tracer was performed. The method involves conversion of glucose into glucofuranose cyclic 1,2:3,5-bis (butylboronate) -6-acetate, followed by quantitation using packed column GC/MS with monitoring of selected ions. The ions that were monitored are $(M-57)^+$ at M/Z 297 (unlabeled) and M/Z 299 (labeled). Kinetics of glucose metabolism were studied in children with growth hormone deficiency, before and during a Hyperinsulinemic-Euglycemic Clamp.

Mass fragmentographic determination of bile acids, using dideuterated chenodeoxycholate as internal standard and packed column GC/MS was performed. A derivatization has been done where the carboxyl groups were methylated and the hydroxyl groups acetylated. The ions that were monitored for quantitation are: $(M-2x60)^+$ at M/Z 370 (unlabeled chenodeoxycholate) and M/Z 372 (labeled chenodeoxycholate). Proper abundant ions for other bile acids will be chosen. The changes in the total amount of individual bile acids in children with growth hormone deficiency and partial hypopituitarism were calculated according to Duane's method[1].

A mass fragmentographic method for Vitamin D_3 analysis in the serum pool was developed. Vitamin D_2 is used as internal standard[2]. The vitamins were converted into heptafluorobutyryl derivatives or into TMS derivatives. According to this study, TMS derivatives are better suited for mass fragmentographic assays than HFB derivatives.

Mass spectral identification and quantitation was accomplished using a Finnigan 3200 electron impact quadropole mass spectrometer interfaced with a glass jet separator to a Finnigan 9500 gas chromatograph. The system is equipped with a Teknivent Data System.

1. Duane WC, Alder RD and Bennion LJ, J. Lipid Res., 16, 155, 1975.

2. DeLeenherr AP and Cruyl AAM, in "Quantitative Mass Spectrometry in Life Science", Elsevier Press, p. 165, 1977.

GCMS QUANTITATION OF GAMMA-AMINOBUTYRIC ACID IN BIOLOGICAL SPECIMENS.

EJ Norman, EL Wee and EF Zimmerman. Department of Medicine (Hematology-Oncology), Children's Hospital Research Foundation (Cell Biology), University of Cincinnati, Cincinnati, Ohio 45267

Gamma-aminobutyric acid (GABA) is a suspected inhibitory neurotransmitter found in millimolar concentrations in mammalian central nervous systems.[1] Decreased levels of brain GABA are found in patients with Huntington's Chorea[2]. GABA may also play a role in palate reorientation since it inhibits shelf elevation in embryo culture[3].

A gas chromatrography mass spectrometry selected ion monitoring procedure was used for quantitation using 2,2-$^2H_2$-GABA as an internal standard. The previously unreported derivative of N-heptafluorobutyl-GABA-cyclohexyl[4] ester was prepared. Mouse embryo tissue of 5 bodies, 5 brains or 35 palate pairs were homogenized in 1 ml, and 0.1 ml of d. H_2O, respectively. Small aliquots were removed for protein determination by Lowry's[5] method. Four times the volume of 100% alcohol was added. To 0.5 ml of the homogenates 100 ng of [2,2-$^2H_2$] GABA was added as an internal standard. Samples were centrifuged at 9500 RPM for 30 minutes and the supernatant was evaporated to dryness.

GABA was esterified[4] and reacted with 200 µl of ethyl acetate and 100 µl of heptafluorobutyl anhydride at 80°C for 15 minutes. The sample was evaporated to dryness with nitrogen at 80°C and dissolved in 200 µl of methanol.

Quantitation was accomplished with a Finnigan 3200 electron impact mass spectrometer interfaced to a Teknivent data system. A Finnigan 9500 gas chromatograph with a 3% OV-17 packed column was used for isothermal (1-4 µl) injections at 185°C. M/Z 282 (GABA) and M/Z 284 (GABA-d_2) were monitored for quantitating ions while M/Z 254, 299 (GABA) and M/Z 256, 301 (GABA - d_2) were confirming ions. Methane negative ion mass spectrometry of these derivatives gave intense high mass ions of m/z 380, 361 (GABA) and M/Z 382, 363 (GABA-d_2). Quantitation was obtained using a standard curve prepared with the samples.

A sensitive, specific mass spectrometric method for the quantitation of GABA in biological specimens has been shown. The HFB-GABA-cyclohexyl derivatives give increased GC retention times and mass spectra with abundant high mass ions.

This procedure allows rapid quantitation of GABA with a minimum of sample clean up. Although three ions were monitored without major interference for both GABA and GABA-d_2 capillary column separation or MSMS would probably give improved accuracy and specificity in quantitating low levels of GABA in complex biological specimens.

Preliminary work with negative ion mass spectrometry indicates that these derivatives give approximately 40 times increased sensitivity over electron impact mass spectrometry.

Acknowledgements:

We thank Jeanne Wolfe and Ms. Kathy Geiger for technical assistance and Dr. Quentin V. Thomas, Finnigan Institute, Cincinnati, Ohio, for negative ion mass spectra.

1. Colby BN and McCaman MW, Biomed. Mass. Spectrom. 5, 215 (1978).

2. Stahl WL and Swanson PD, Neurology 24, 813 (1974).

3. Zimmerman EF, Wee EL, Monaghan K and Norman EJ, Teratology 23, 71A (1981).

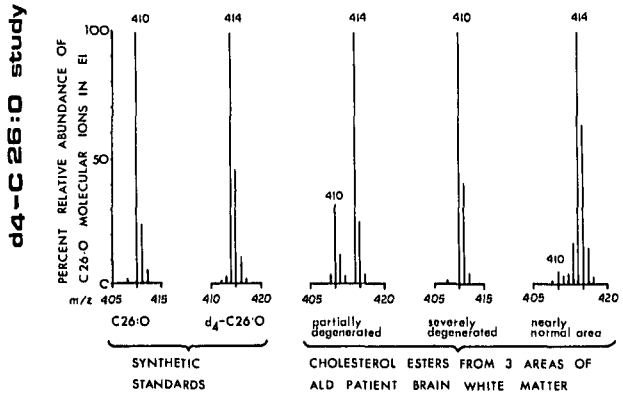
4. Norman EJ, Berry HK, and Denton MD, Biomed. Mass Spectrom. 6, 546 (1979).

ADRENOLEUKODYSTROPHY: THE ORIGIN OF ABNORMAL FATTY ACIDS DETERMINED BY ISOTOPE INCORPORATION IN PLASMA AND TISSUES. Hugo W. Moser, Ann B. Moser, Yasuo Kishimoto and Sharon L. Pallante. John F. Kennedy Institute, Dept. of Neurology and the Department of Pharmacology, Johns Hopkins School of Medicine, Baltimore, Maryland 21205

Adrenoleukosystrophy (ALD), also known as bronzed schilder's disease, is an X-linked hereditary neurological disorder associated with progressive demyelination of cerebral white matter, pigmentation of the skin and adrenal insufficiency. It is usually diagnosed in boys 4-8 years old, resulting in a vegetative state in 1 year and death in 2-4 years. As its toxicity is almost certainly due to the accumulation of long chain fatty acids in the brain, urgency necessitates the determination of the origin of these abnormal acids (whether endogenous or, as is true for the phytanic acid in Refsum's Syndrome, of exogenous origin and therefore susceptible to dietary control).

One patient was given (3,3,5,5-$^{2}H_4$) Hexacosanoic acid (C26:0) labelled with the deuterium at the C-2 position orally, while 2 patients received D_2O. Analysis of plasma and post mortem brain and liver tissue was done by gas chromatography mass spectrometry/ selected ion monitoring utilizing chemical ionization with isobutane. Lipid fractions analyzed included total lipids, cholesterol esters, sphingomyelin, cerebrosides and glycerophospholipids. The molecular ion regions of both palmitate (C16:0) and C26:0 fatty acid methyl esters were monitored and compared with synthetic standards and samples from normal tissue in order to determine isotope enrichment. The relative importance of each pathway can thus be assessed and possible nutritional therapy planned.

A terminal patient with adrenoleukodystrophy (ALD) was given 10 mg by mouth of (3,3,5,5,-d_4) hexacosanoic acid (C 26:0) daily for 100 days until autopsy. Cholesterol esters were isolated from 3 areas of progressive demyelination in brain white matter and methylated. GCMS analysis indicated the incorporation of the d_4-C 26:0 was highest in the area of mildest involvement, suggestive of significant exogenous origin.



Deuterium Inc. by D_2O:

ALD patient was given 10→20 mls of D_2O/day 1st week, then 50 ml/day July 18 until death Dec. 22 (2.5% of total H_2O intake). Urine analysis showed a 1% deuterium level equil. by August.

Sample Preparation: Method:

Plasma, Myelin & tissue --- Folch et al., JBC, 226, 497 (1957)
Myelin & "Floating Lipid"--- Autilio et al., J. Neuroch. 11, 17 (1964)

Sample Preparation, cont'd. Method:

Glycerophospholipids	---	Eichberg et al., JBC 248, 3615 (1973)
Sphingomyelin	---	Vance & Sweeley, J. Lipid Res. 8, 621 (1967)
Cerebrosides	---	Yahara et al., J. Neuroch. 34(3), 694 (1980)

All fatty acids were converted to methyl esters by use of methanolic HCl. All samples were processed at the Kennedy Inst. and analyzed on an HP GC with SP2100 capillary column for the % of each fatty acid (C15:0-- C32:0) in the mixture. Special attention was paid to increases in C24:0 and C26:0 fatty acids. Deuterium incorporation, in the C16:0, C18:0, and the elevated C24:0 and C26:0 fatty acids, was evaluated in the Mass Spec. Center-Pharmacology Department on a DuPont DP-102 GC/MS/DS using an OV-101 packed column and SIM on the same samples. Incorporation of the deuterium from the D_2O in the body water would indicate that there is also significant endogenous synthesis of the abnormal long chain fatty acids.

d_2O study

MOLE % DEUTERIUM INCORPORATION

	C16:0	C18:0	C24:0	C26:0
ALD PATIENT				
CHOLESTEROL ESTER				
LIVER	17.46			16.32
FLOATING LIPID	6.6 ±.2	8.2 ±.4	9.2 ± 2	10.6 ±.1
MYELIN	6.03			5.34
TOTAL LIPIDS				
PLASMA	15.7			24.3 ±.8
LIVER	15.5 ±.2			20.6 ± 1
WHITE MATTER	18.27±.04			
SPHINGOMYELIN				
LIVER	15.4±.05			24.55
FRONTAL WHITE	9.8 ±.5			
FRONT. WHITE+GRAY	16.3±.1			16.7 ±.9
PLASMA 6/27 EARLY	12.54			-
8/15 MID	15.4 ±.3			14.77
9/5 LATE	16.6 ±.15			15.5± .2
9/12 LATE	16.21			14.6 ±.15
MYELIN	4.35			5.79
GLYCEROPHOSPHOLIPID				
PLASMA 6/6 PRE D_2O	0	0	0.2± 2	.87
8/8 D_2O	18.44	20.5 ±.2	20.7 ±.4	23 ±.5
9/12 D_2O	19.9±.04	21.9 ±.1	21.5±.11	25.24
12/15 D_2O	19.7± 5	23.5± 3	23.6± 8	26.39
AMN PATIENT				
SPHINGOMYELIN				
PLASMA EARLY D_2O	0			4.2± 6
MID D_2O	0			8.1± 5
LATE D_2O	0			8.2±.05

Dietary restriction alone did not have a demonstrable beneficial effect in ALD. This is probably due to the fact that in ALD the very long chain fatty acids are of endogenous and dietary origin both, and suggests that endogenous sources are more significant. Enzymatic studies indicate that the basic defect in ALD is the impaired capacity to degrade very long chain fatty acids -- possibly in the peroxisomes. Exact definition of the defect, and study of its co-factor requirements may provide additional therapeutic leads. Other therapeutic approaches such as bone marrow transplants are being considered.

DETERMINATION OF BODY WATER VOLUME BY DEUTERIUM ISOTOPE DILUTION MEASUREMENT BY CIMS: F.A. Bencsath, H.L. Bradlow, F.H. Field, Rockefeller University, 1230 York Avenue, New York, N.Y. 10021

A deuterium isotope dilution procedure is used to determine total body water in human steroid metabolism studies. We have developed two CIMS methods to determine deuterium concentration in water in the range 0-0.60% D_2O. One of these utilizes the batch inlet system, methane reagent gas, and the peak matching device of a magnetic sector mass spectrometer. The second one utilizes the directly coupled gas chromatograph of a quadrupole MS and computer control for ion selection and data processing. In this method the water itself serves as reagent gas. The deuterium concentration is calculated from the ratio of the ion intensities at m/z = 20 (DH_2O^+) and 19 (H_3O^+).

Both methods give linear calibration curves. The second one is faster because less effort is needed to eliminate memory effects and because of extensive computer assistance. In the past three years these methods have been used successfully to determine body water volumes of approximately 300 subjects.

USE OF $^{13}CO_2$ BREATH ANALYSIS AS AN AID IN ELUCIDATING ROUTES OF DRUG METABOLISM

D.A. Schoeller, A.N. Kotake, G.H. Lambert, and A.L. Baker
Departments of Medicine and Pharmacology, The University of Chicago and
Department of Pediatrics, Michael Reese Hospital

Carbon dioxide is an often overlooked product of drug metabolism that can be measured in breath following the administration of appropriately labeled drugs. The time course and quantity of the expired CO_2 can aid in the elucidation and quantitation of drug metabolism. The use of a CO_2 breath test for the study of drug metabolism requires that the drug be labeled with ^{13}C or ^{14}C, and that the rate of cleavage of the labeled group from the drug be slower than the subsequent oxidation of the labeled carbon to bicarbonate and its excretion as CO_2. Because both of these requirements can be met by caffeine, we have chosen caffeine to illustrate the use of CO_2 breath analysis in the study of drug metabolism.

The complexity of caffeine metabolism is evident from the large number of urinary metabolites that have been identified by previous investigators (1,2). The metabolites include at least 5 di- and mono-methylxanthines, and at least as many di- and mono-methyluric acids. Thus, caffeine metabolism involves both N-demethylation and ring hydroxylation. Based on the absence of trimethyluric acid in the urine and the relative absence of 3 methylated metabolites, others have postulated the simplified metabolic scheme in Fig. 1a to account for the major metabolites.

Despite the number of studies, it has been difficult to quantitate the relative rates of demethylation at each of the 3 methyl positions and to determine the sequence of the various demethylation reactions and ring hydroxylation. The difficulty results from the large number of metabolites and the limitation of urinary profile analysis imposed by the lack of time resolution.

METHODS: The subjects were males between 20 and 35 y/o who were in good health, and who had no history of liver diseases. Subjects did not ingest caffeine for 36 to 48 h and fasted for 8 to 15 h before the test. Caffeine labeled with ^{14}C in all three (1,3,7-) methyl positions (TRI-CAF) or caffeine labeled with ^{13}C in one of the methyl positions (1-,3-, or 7-CAF) was dissolved in 20 ml of water and administered orally. The subjects remained seated throughout the 8 h breath collection period. Breath $^{14}CO_2$ was collected in 2 mmoles of Hyamine hydroxide and the ^{14}C content determined by scintillation spectrometry (3). Breath $^{13}CO_2$ was collected in a 3 L plastic bag, a 50 mL aliquot was removed, the CO_2 was purified cryogenically, and the excess $^{13}CO_2$ content was determined by isotope ratio mass spectrometry (4). The caffeine dose was 1, 3, or 5 mg/kg body weight for the TRI-CAF (2 uCi ^{14}C) dose response study, and for the monolabeled caffeine studies.

RESULTS and DISCUSSION: The absolute instantaneous rates of CO_2 excretion at 2 h after TRI-CAF administration increased almost linearly between the doses of 1 and 3 mg/kg, but did not increase between 3 and 5 mg/kg (Table 1). It is unlikely that

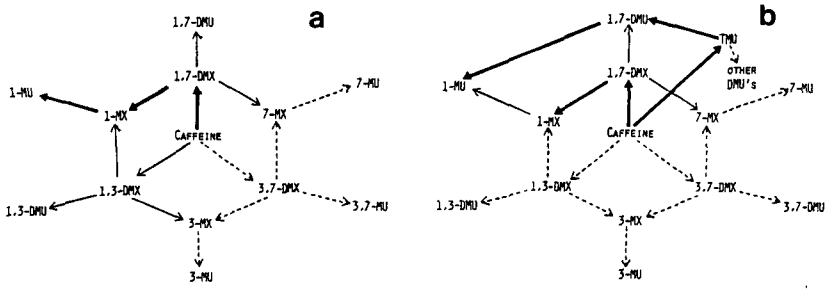


Figure 1. a. Currently accepted scheme of caffeine metabolism in humans.
b. Proposed scheme suggested by the current work. Major pathways are indicated by dark lines, minor pathways dashed lines. DMX: dimethylxanthine, MX: methylxanthine, TMU: trimethyluric acid, DMU: dimethyluric acid, and MU: methyluric acid.

Table 1. Dose response of the excretion of $^{14}CO_2$ at 2 h after the administration of (1,3,7-trimethyl ^{14}C) caffeine.

	$^{14}CO_2$ excretion rate	
	nonsmokers (n=4)	smokers (n=5)
mg/kg	umol/kg/h	umol/kg/h
1	0.24±0.02[a]	0.40±0.06
3	0.48±0.05	1.03±0.15
5	0.53±0.10	1.15±0.10

[a]mean ± SE

the saturation in the rate of CO_2 excretion resulted from a saturation in caffeine absorption because plasma caffeine levels are equivalent after oral and i.v. administration of 7 mg/kg caffeine. Neither is it likely that the saturation occurs in any process after N-demethylation as 2 to 3 fold greater rates of CO_2 production are observed from the in vivo N-demethylation of aminopyrine (3). Thus, we conclude that caffeine N-demethylation is saturated above doses of 3 mg/kg. Because caffeine clearance is not saturated at these low doses, it appears that ring hydroxylation is the major route of caffeine clearance from blood. This hypothesis requires that trimethyluric acid be further metabolized via N-demethylation before excretion because little of the ring hydroxylation product trimethyluric acid is excreted in the urine (1).

Figure 2 summarizes the $^{13}CO_2$ excretion profiles following the administration of the monolabeled caffeines to a nonsmoker and a smoker. During the first 2 h of the breath test, the ratios of the cummulative $^{13}CO_2$ excretions from 1-, 3-, and 7-CAF were 7:80:13 respectively. Thus, over 80% of the primary demethylation of caffeine and trimethyluric acid occurs at the 3 position. The excretion of $^{13}CO_2$ from 7-CAF reached a maximum at 7 h after administration, well after serum caffeine levels had fallen below peak levels. Thus, the substrate for 7-demethylation must be a metabolite of caffeine, possibly 1,7-dimethyluric acid, 1,7-demethylxanthine, or trimethyluric acid.

The use of labeled CO_2 analysis in breath complements traditional methods of drug analysis and aids in the elucidation of the routes of caffeine metabolism as summarized in Fig. 1b. Like urinary profiling, the breath test is noninvasive, but because breath is a continuous excretion product, it provides better time course data.

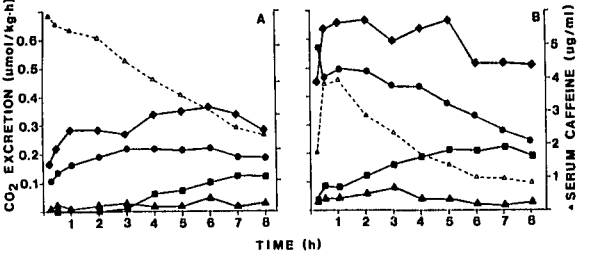


Figure 2. Time course of $^{13}CO_2$ excretion following the administration of 3 mg/kg of the various labeled caffeines to a nonsmoker (A), and a smoker (B). (◆) TRI-CAF, (▲) 1-CAF, (●) 3-CAF, (■) 7-CAF, and (△) serum caffeine concentration.

Work was supported by NIH grants AM 26678 and AM 22220. This work is presented in detail in a paper accepted by the Journal of Pharmacology and Therapeutics.

1. H.H. Cornish and P.A. Christman. J Biol Chem 228:315-323, 1957.
2. A. Aldridge, J.V. Aranda, and A.H. Neims. Clin Pharmacol Ther 25:447-453, 1979.
3. J.F. Schneider, D.A. Schoeller, B. Nemchausky, et al. Clin Chim Acta 84:153-162, 1978.
4. D.A. Schoeller and P.D. Klein. Biomed Mass Spectrom 5:29-31, 1978.

MPB 23 METABOLISM OF [^{2}H]PREGNENOLONE IN TESTIS; K. Shimizu; Institute of Steroid Research, Tottori University School of Medicine, Yonago, Japan.

The side chain cleavage mechanism in C_{19} steroid formation from pregnenolone was studied by incubating [^{2}H]pregnenolone with boar testis microsomal fraction. After incubation of [17α-^{2}H]pregnenolone in the presence of NADPH under an $^{18}O_2$ atmosphere, the following metabolites labeled with ^{2}H or ^{18}O (or both) were identified: 16α-[16-^{18}O, 17α-^{2}H]hydroxypregnenolone, 17α-[17-^{18}O]hydroxypregnenolone, [17-^{18}O]dehydroepiandrosterone, 5-[17β-^{2}H, 17-^{18}O]androstene-3β,17α-diol, 5-[17-^{18}O]androstene-3β,17β-diol and 5,16-[17-^{2}H]androstadien-3β-ol. Among the metabolites isolated from incubation of [16α-^{2}H]pregnenolone, the ^{2}H atom was retained in 17α-hydroxypregnenolone, dehydroepiandrosterone, 5-androstene-3β,17α-diol and 5-androstene-3β,17β-diol, while the ^{2}H atom was missing in 16α-hydroxypregnenolone and 5,16-androstadien-3β-ol. After incubation of [16β-^{2}H]pregnenolone the ^{2}H atom was retained in all above-mentioned metabolites.

These results and metabolism time study indicate that there are three mechanisms of side chain cleavage in C_{19} steroid formation in boar testis microsomal fraction. One path involves 17α-hydroxylation with loss of the 17α-hydrogen, followed by removal of the side chain to give dehydroepiandrosterone. The second path is a reaction in which 17α-hydroxylation from molecular oxygen, rearrangement of the 17α-hydrogen to the 17β-position, and removal of the side chain, occur at the same time to give 5-androstene-3β,17α-diol. The third path gives 5,16-androstadien-3β-ol retaining the 17α-hydrogen after removal of the side chain and the 16α-hydrogen.

LUNG TOXICITY AND METABOLISM OF DEUTERIUM LABELED BUTYLATED HYDROXYTOLUENE

K. Yamamoto, K. Tajima, and T. Mizutani°

School of Pharmacy, Hokuriku University, Kanazawa 920-11, Japan and

°Department of Food Science, Kyoto Prefectural University, Kyoto 606, Japan

Butylated hydroxytoluene (BHT), an antioxidant widely used as a food preservative, produces lung damage in mice (1). The conversion of BHT to unidentified reactive metabolites by microsomal enzymes was suggested by Kehrer and Witschi (2). In a previous paper (3), we proposed that BHT-quinone methide (BHT-QM) (Fig. 1) as an active metabolite may be responsible for the lung damage. To provide further evidence for this concept, we examined the effects of deuteration in the 4-methyl group of BHT on the lung toxicity and metabolism in mice.

Deuterated compounds, BHT-d_3 (98% D), BHT-SØBr-d_2 (96% D), and BHT-OH-d_3 (97% D) (Fig. 2) were synthesized by unambiguous methods. The mass spectra of BHT-SØBr, BHT-OH, and their deuterated analogs are shown in Fig. 3. Lung toxic doses of either BHT or BHT-d_3 were administered ip to male ddY mice and lung damage was assessed by determining wet and dry lung weights after 4 days. An equimolar mixture of BHT and BHT-d_3 was incubated with 9,000g supernatant fraction of mouse liver in the presence of an NADPH generating system. BHT-QM, an unstable metabolite, was trapped with p-bromobenzenethiol (BrØSH) and analyzed as BHT-SØBr by ECD-GC and GC/MS on an OV-1 column at 240°C. There found no isotope effect on the trapping reaction of BHT-QM. BHT-OH was directly analyzed at 130°C. To investigate the isotope effect on metabolic rate, the selected ion monitoring was operated on masses 221 and 219 for BHT-SØBr and 239 and 236 for BHT-OH. Mass spectrometer conditions were as follows: ionizing voltage of 22 eV, total emission current of 300 μA, accelerating voltage of 3 kV. In each case of BHT-SØBr and BHT-OH, the relative peak height of the selected ions was proportional to the molar ratio of the deuterated to undeuterated compounds (Fig. 4). An equimolar mixture (3,000 mg/kg) of BHT and BHT-d_3 was administered ip to mice. The lungs and livers were excised after 4 hr and homogenized. Determination of BHT-QM and BHT-OH were carried out as described for the *in vitro* study.

The lung damaging effect of BHT-d_3 was significantly lower than that of BHT (Fig. 5). Table 1 shows that the *in vitro* rate of BHT-QM formation was slowed in BHT-d_3. On the other hand, the rate of metabolism to BHT-OH slightly increased with deuterium labeling. As shown in Table 2, there observed similar isotope effects of deuteration on the *in vivo* metabolic rate of BHT. Although the isotope effects of deuteration were somewhat small, the lower rate of BHT-QM formation corresponds to the lower toxicity of deuterated BHT. These observations are consistent with BHT-QM being a lung toxic metabolite.

References

1. A.A. Marino and J.T. Mitchell, Proc. Soc. Exp. Biol. Med. 140, 122 (1972).
2. J.P. Kehrer and H. Witschi, Toxicol. Appl. Pharmacol. 53, 333 (1980).
3. T. Mizutani, I. Ishida, K. Yamamoto, and K. Tajima, Toxicol. Appl. Pharmacol. 62, 273 (1982).

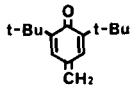
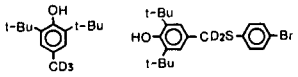


Fig. 1. BHT-QM



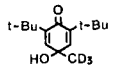


Fig. 2. Deuterium-Labeled BHT and Its Derivatives

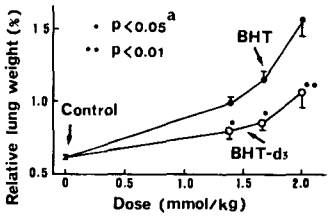


Fig. 5. Effects of BHT and BHT-d_3 on Relative Lung Weight in Mice a) compared with BHT.

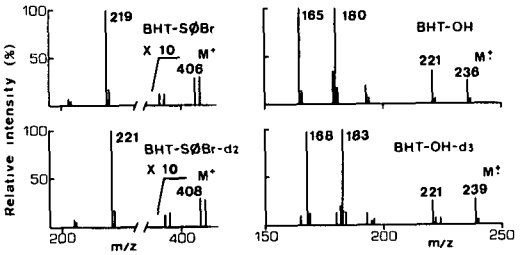


Fig. 3. Mass Spectra of BHT-SØBr, BHT-OH, and Their Deuterated Analogs

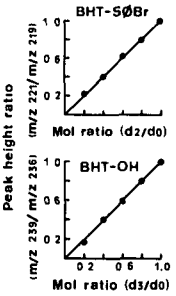


Fig. 4. Standard Curves for BHT-SØBr and BHT-OH

Table 1. Ratio of Deuterated to Undeuterated Metabolites after Incubation of BHT and BHT-d_3 Mixture (1:1) with Liver 9,000g Sup. Fractions

Incubation time (min)	BHT-QM (d_2/d_0)[a]	BHT-OH (d_3/d_0)
10	0.81 ± 0.09	1.26 ± 0.08
25	0.86 ± 0.02	1.17 ± 0.04

a) BHT-QM was determined after being converted to BHT-SØBr.

Table 2. Ratio of Deuterated to Undeuterated Metabolites 4 hr after ip Administration of BHT and BHT-d_3 Mixture (1:1)

Tissue	BHT-QM (d_2/d_0)[a]	BHT-OH (d_3/d_0)
Lung	0.66 ± 0.03	1.38 ± 0.17
Liver	0.85 ± 0.01	1.25 ± 0.07

a) See note a to Table 1.

GLYCINE METABOLISM DURING PREGNANCY,DETERMINED BY STABLE ISOTOPE [^{15}N] AND GC-MS;

A. Lapidot*, J. Amir, S.R. Reisner, L. Feldman, M. Hod, Y. Ovadia; *Isotope Research, Weizmann Institute of Science, Rehovot and Neonatal and Obstetric Departments, Beilinson Medical Center, Petah Tikva, Israel

The nitrogen supply for the growing fetus is the circulating maternal free-amino acids (1). Very little is known about their dynamic transport and metabolism in the intact body. Their uptake by the gravid uterus or by the umbilical circulation seems to be unrelated to maternal blood concentration.

The techniques currently available for studying maternal-fetal exchange processes are for the most part, invasive and the risks for both mother and fetus makes them unsuitable for human research. The use of animals to investigate unknown aspects of human function creates obvious aspects difficulties of interpretation of the data in terms of the validity to human situation.

Restrictions in the use of radioactive tracers in healthy humans have prompted us to develop a convenient non-invasive stable isotope and GC-MS technique to determine the nitrogen - 15 enrichment of plasma amino acids. The method is capable to measure the rate of uptake and the pools of extracellular amino acids in whole body. The technique was applied to several human studies including newborn infants during the neonatal period (2-6).

This study reports dynamic aspects of glycine metabolism in healthy and diabetic pregnant women throughout gestation. The study was also designed to measure transplacental flux of the isotope labeled amino acid to the amniotic fluid and to the fetus. Thus it was of interest to compare the rate of uptake of the labeled amino acid and the pool size of the measured amino acid (a) in pregnant women of different gestational age under the same experimental condition as normal healthy women; (b) to determine whether fetal uptake of amino acid via the umbilical circulation is detectable by the isotopic methodology used in this study; and (c) to compare the uptake and the pool size of amino acids when maternal metabolism is impaired, as in diabetic pregnancy.

RESULT AND DISCUSSION

Diagnosis or interpretation of changes in amino acid concentration or pattern in terms of particular component is limited, as changes in concentration are not sensitive indicators because the fluxes into and out of the free pools are much greater than the pool sizes. Changes in concentrations of intermediates give little information on changes in fluxes of metabolites. In conclusion static measurements of pool sizes reveal fragmentary information about dynamic changes in the components of inflow or outflow, but point out the fact that some changes has occurred which therefore ought to be investigated. The metabolic changes in normal pregnancy provide milestones for what to expect and when, in the management of diabetes in pregnancy. This study describes for the first time in vivo dynamic measurements in human pregnancy that might explain maternal adaptation to the new phsiological condition.

Pool sizes, turnover rate constants and fluxes of glycine were determined in healthy women and diabetic patients. Single doses of ^{15}N glycine (>90%, 50-100 µmoles/kg body wt.) were administered intravenously. Blood samples (1-3 ml) were collected before and at five minute intervals for 60 min. after injection. Plasma samples, obtained after plasma proteins removal and delipidization were determined for their ^{15}N-glycine isotopic enrichment values, measured as mol % excess as previously described (4). Briefly, the n-trifluoro n-butyl esters of glycine were prepared and analyzed by EI, GCMS (Finnigan models 1015 and 4000 quadrupole mass spectrometer). The fragment selected by MID was m/e 126,127,128 (2). We have previously demonstrated that linear isotope disappearance curves, carried within the first hour following the administration of the labeled amino acid describe undirectional irreversible flux of glycine through a single compartment(3). The isotope enrichment of the labeled compounds is expressed by: $I_t = [W/(A+W)] \exp(kt) \times 100$. The turnover rate constant of glycine in the pool $k(hr^{-1})$, is obtained from the slope of the curve (Fig. 1). The pool size,A(µmole/100g. body wt) is $A = d \times [(I_d/I_o) - 1]$, where d is the dose of labeled glycine (µmole/100g. body wt), I_d is the isotope enrichment of the administered glycine, and I_o is the isotope enrichment of plasma glycine extrapolated to time zero. The errors in the slope and intercept were calculated and depicted by joint confidence region maps, (see Fig. 2). This powerful and accurate method for visually evaluating the significance

of differences in pool sizes, rate constants and fluxes, in a population of humans or individual human in different metabolic or pathological states has been used (3-6).

No significant changes of glycine pool sizes or turnover rate constants were observed in the group of the first trimester pregnant women in comparison with the control women(4); pool sizes of 8.3-9 μmoles/kg body wt. and turnover rate constants of 2.6-3.2 h^{-1} were found. During the second and third trimesters of pregnancy only pool size values decreased (3.3-6.8 μmoles/kg body wt.), whereas turnover rate constants did not change significantly.

A comparison study has been done on non-insulin and insulin dependent patients during the third trimester of pregnancy. Significant differences accompanied with high turnover rate constant (5.1-5.3 h^{-1}) in the insulin dependent patients were noted.

Extremely low pool sizes (1.0 and 1.7 μmoles/kg body wt_1) accompanied with significantly high turnover rate constants (4.13 and 5.09 h^{-1}) were found in two juvenile onset (insuline-dependent) diabetic patients. Increased rate of maternal-fetus transport of glycine has been determined from the ^{15}N-glycine enrichments of the umbilical cord and amniotic fluid.

These results revealed undoubtedly that monitoring the rate of disappearance of plasma amino acid and pool sizes of extra-cellular pools is a very sensitive probe for determining abnormal amino acid metabolism in diabetic pregnancy.

Variation of Glycine Dynamic Parameters in Healthy Pregnant Women

Group	Pool(1) (mean)	T.R.C.(2) (mean)	Flux(3) (mean)
1st trimester	9.0±2	3.4±0.3	30.±6.1
2nd trimester	4.5±1.7	3.4±0.3	15.0±5.8
3rd trimester	4.5±2.1	3.3±0.4	14.6±7.8

(1) μmoles/100g body wt; (2) Turnover rate constant (hr^{-1}); (3) μmoles hr^{-1}/100g body wt.

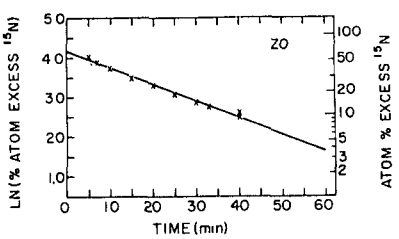


Fig. 1. ^{15}N-glycine enrichment curve; an example of a study in non-insulin pregnant woman

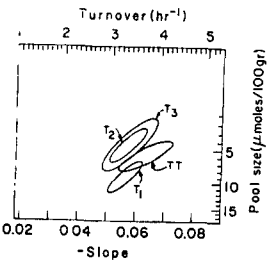


Fig. 2. Joint confidence region maps (slopes intercepts); a summary of glycine dynamic parameters during the three trimesters.

1. J.A. Lemons, Seminars in Perinatology, 3, 177 (1979).
2. C.S. Irving, I. Nissim and A. Lapidot, Biomed. Mass Spectrom, 5, 177 (1978).
3. I. Nissim and A. Lapidot, Am. J. Physiol. 237,E418 (1979).
4. A. Lapidot and I. Nissim, Metabolism, 29, 230 (1980).
5. A. Lapidot and I. Nissim, In: Advances in Mass Spectrometry, Quayle, A. Ed., Hdyden, London, 1142-1154 (1980).
6. J. Amir, S.H. Reisner and A. Lapidot, Pediatr. Res., 14, 1238-1244 (1980).

DETECTION OF GLUCURONIDE CONJUGATES OF XENOBIOTICS BY DIRECT-INSERTION MASS SPECTROMETRY

David Kalman and David Eaton; Department of Environmental Health, University of Washington, Seattle, Washington, 98195

Environmental toxicants are in many instances greatly concentrated in biological compartments such as bile or liver tissue. Biological transformation such as conjugation of these agents prior to excretion confers water solubility, which may be exploited to separate the conjugated material from other components of the sample. Mass spectrometry of such materials has been accomplished by hydrolysis or by chemical derivatization followed by GC/MS or direct insertion MS, but the conjugated species itself is typically too nonvolatile to detect by conventional direct insertions MS. Desorbtion chemical ionization (DCI) using a prototype platinum wire DCI probe designed by Vacumetrics for the Finnigan 4023 GC/MS system has been used to obtain positive and negative ion spectra of phenol glucuronide conjugates and conjugated naphthols.

The mass spectra were obtained by pulsed positive-negative ion chemical ionization (PPNICI) using two reagent gas systems: methane and 3:1 methane/nitrous oxide, both at an inlet pressure of 4×10^{-5} torr. The spectra obtained in either system varied with time during the course of the desorbtion, reflecting the simultaneous processes of desorbtion and pyrolysis, as other authors have noted. Variation of source temperature as well as rate and degree of probe heating could be used to maximize the detection of molecular species and large fragment ions. The predominant processes observed were protonation and cleavage of the sugar moiety for positive CI, and resonance electron capture, deprotonation, dehydration, and cleavage of the glycosidic bond for negative C.I. In all cases, negative ion chemical ionization produced spectra with much higher ion intensities for molecular ions and dehydrated molecular ions than did positive ion C.I.. In many instances, the two spectra were complementary, with the negative ion spectrum revealing the molecular ion or deprotonated molecular ion, and the positive ion spectrum revealing the aglycon structure. Figure 1 shows a typical example, 1-naphthyl β-D-glucuronide. Tables 1 and 2 summarize the spectra for the compounds studied.

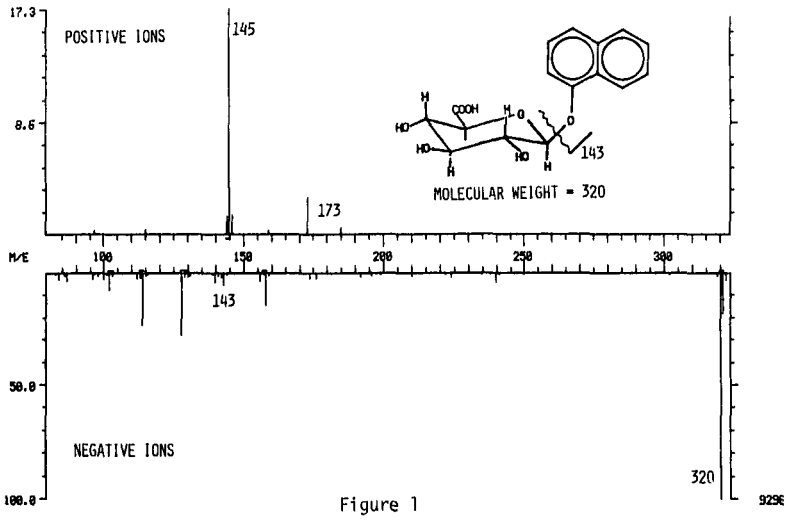


Figure 1

COMPOUND	MW	RELATIVE INTENSITY:			(GLUCURONIC ACID FRAGMENTS)		
		MH^+	ROH_2^+	OTHER	177	159	131
PHENYL-GLUC	270	-	70		53	100	2
o-AMINO-PHENYL-GLUC	285	29	100		-	-	-
p-NITRO-PHENYL-GLUC	315	-	100		1	16	7
1-NAPHTHYL-GLUC	320	-	100	$(ROH+29)^+-17$	-	-	-
8-HYDROXY-QUINOLINE-GLUC	321	-	100	$(ROH+29)^+-18$	-	-	-
1-NAPHTHYL-BISULFATE	224	32	48	$(MH-H_2O)^+-49$	$(H_3SO_4)^+$ - 100		
2-NAPHTHYL-β-GLUCOPYRAN-OSIDE	306	3	100		-	-	-
GLUCURONIC ACID	194				5	100	33

M = INTACT GLUCURONIDE MOLECULE : R = AGLYCON MOIETY

TABLE 1 - METHANE POSITIVE ION C.I. - SUMMARY

COMPOUND	MW	RELATIVE INTENSITY:					(GLUCURONIC FRAGMENTS)		
		$(M\cdot)^-$	$(M-H)^-$	$(ROH\cdot)^-$	$(RO)^-$	OTHER	176	158	114
PHENYL-GLUC	270	14	100	-	2		19	19	24
o-AMINO-PHENYL-GLUC	285	12	80	-	15	$(M-2H_2O)=19$	13	21	100
p-NITRO-PHENYL-GLUC	315	37	8	100	62	$(M-OH)=68$	10	3	6
1-NAPHTHYL-GLUC	320	100	1	-	5		2	14	24
8-HYDROXY-QUINOLINE-GLUC	321	100	2	2	-	$(M-H_2O)=13$	48	16	64
1-NAPHTHYL-BISULFATE	224	17	100	-	-	$(M-H_2O)=33$			
2-NAPHTHYL-β-GLUCOPYRAN-OSIDE	306	2	10	58	29	$(2M-H)^-$			
GLUCURONIC ACID	194	1	3				100	51	83

M = INTACT GLUCURONIDE MOLECULE : R = AGLYCON MOIETY

TABLE 2 - METHANE NEGATIVE ION C.I. - SUMMARY

The use of nitrous oxide/methane reagent gas has been reported to produce good negative ion chemical ionization spectra for glucuronides of natural products. The population of hydroxide ions in the ion source was observed to produce only minor changes in the spectra. This may be attributed to the relative efficiency of resonance electron capture for the compounds studied, and to the tendency to dehydration exhibited by the glucuronide moiety.

ANALYSIS OF CHLORINATED PHENOL ACETATES BY GAS CHROMATOGRAPHY/MASS SPECTROMETRY

L.W. Yert, R.E. Cline, and J.S. Holler

Clinical Chemistry Division, Center for Environmental Health, Centers for Disease Control, Public Health Service, U.S. Department of Health and Human Services, Atlanta, Georgia 30333

Chlorinated phenols are an important class of industrial chemicals, forming the basis for many commercial products. The large volume of this class of compounds, coupled with the types of applications, has resulted in widespread environmental contamination. Since many of the isomers are toxic, appropriate analytical procedures should be available to monitor exposure to these compounds. Humans are exposed to numerous sources of chlorinated phenols which occur as an impurity in techanical-grade phenol derivatives. Free chlorinated phenols may be formed by the degradation of industrial products in the environment and the chlorination of drinking water.

Urine is the most readily obtainable body fluid for monitoring human exposure. Sample preparation includes treatment with sulfuric acid and heat to hydrolyze phenolic conjugates, followed by extraction and acetylation to form a suitable derivative. In this study, all isomers and congeners of chlorinated phenols were examined for gas chromatographic and mass spectral behavior. A rugged column system for separating a number of the derivatives is 3% OV-101 on Ultrabond 20M. Complete separation of all isomers is obtained on the special column 5% SP1200, 1.75% Bentone 34. Since complete separation of all chlorinated phenol derivatives is attainable, these compounds could be routinely monitored by using gas chromatography with electron capture detection.

The electron impact mass spectrometry of these compounds is simple and straightforward. With adequate chromatography, this technique readily characterizes phenol derivatives. A molecular ion is observed for all derivatives with an intensity 5-15% of the base peak. In all cases, the base peak in the spectrum is due to loss of the acetyl protecting group ($M-COCH_2$). Few other significant fragment ions are observed in the spectrum; when present, these other ions are usually less than 25% of the base peak. Individual isomers of a given level of halogenation cannot be distinguished by the electron impact mass spectrum alone; therefore, gas chromatographic retention time is an important component in the analytical characterization.

Use of trade names is for identification only and does not constitute endorsement by the Public Health Service or by the U.S. Department of Health and Human Services.

ANALYSIS OF COMPOUNDS FROM NIAGARA FALLS DUMP SITES USING NCI GC/MS

Ray Kaminsky and Ronald A. Hites
School of Public and Environmental Affairs
and Department of Chemistry
Indiana University
400 East Seventh Street
Bloomington, Indiana 47405

Lake Ontario has an area of 19,000 km^2 and an average depth of 84 m; thus, it ranks about tenth in the world in size and volume. More than 6.5 million people who live on its shore and in its drainage basin drink water from this lake. Twenty-six billion m^3 of water and 4.8 million tons of fine grain sediment enter the lake each year from the Niagara River. This large sediment contribution is particularly significant because it carries organic compounds into the lake. Even though the Niagara River has been burdened by extensive dumping of wastes near its shores, very little information existed on these organic compounds. Thus, we identified many such compounds entering the Niagara River from the chemical dump sites along its shores (1). This study is an examination of the fate of these compounds in the sediment of Lake Ontario.

Methods. Sediment samples from Lake Ontario were taken mainly in the Niagara Basin where much of the suspended particles from the Niagara River tend to accumulate. Several studies have shown that sediment eminating from the Niagara River also tends to be transported eastward along the south shore. Thus, some of our samples were from this area. Sediment samples were collected in October 1980 with a Shepex sampler on board the CSS LIMNOS, and they were immediately frozen in solvent-washed glass jars with foil-lined caps.

Each sample was thawed for not more than 48 hours prior to analysis, loaded into glass-wool-packed glass extraction thimbles for extraction in a soxhlet apparatus, and extracted for 24 hours with isopropanol followed by a second 24 hour extraction with dichloromethane. The sediments were then air dried and weighed. Analyses were carried out using GC/MS in the electron impact (EI) and negative chemical ionization (NCI) modes. A Hewlett Packard 5985 GC/MS system modified to bring the column (a J & W fused silica 30 m DB-5) directly into the ion source was used.

Results. Organic compounds identified in Lake Ontario sediment are shown in Table 1. Of particular interest are the two fluorine-containing compounds: dichloro(trifluoro-methyl)-benzophenone and dichloro(trifluoromethyl)-difluorodiphenylmethane. These two compounds are found only in a Hooker Chemical dump site along the Niagara, and thus, unlike the more widely produced chlorobenzenes and toluenes, provide conclusive evidence that compounds entering the lake from this source accumulate to detectable levels. This occurs despite the dilution which takes place due to the high average flow (7000 m^3/sec) of water in the Niagara. The data given in Table 1 also indicate that such compounds may be transported a considerable distance from their point of introduction into the lake. In this case, one of the fluorinated compounds was observed more than 50 km from the mouth of the Niagara.

Most of the compounds we observed entering the Niagara River have been detected in the sediments of Lake Ontario. The primary exceptions appear to be those compounds possessing three chlorines or less, especially if their abundance at the Niagara River sites were low to begin with. Such compounds would not be present in sufficient quantities to be detected by EI, and NCI lacks the sensitivity to respond to these lesser halogenated molecules. On the other hand, NCI detected what appear to be very small quantities of certain compounds similar to those entering the river but differing by being more highly chlorinated. For example, mono-, di-, and trichlorophenanthrene were detected in the Niagara River but not in the lake; however, just the opposite appears to be the case for tetra-, penta-, and hexachlorophenanthrene.

One group of compounds was commonly found in the lake but was conspicuous for its absence in the Niagara dumpsites: the chlorinated styrenes. For confirmation, the penta-through octachlorostyrenes were synthesized by chlorination of dichlorostyrene. Insufficient quantities of these compounds were present in the lake to obtain EI spectra, but NCI data confirmed their presence. Several of the by-products of our synthesized chlorostyrenes were detected in at least 3 of the lake sites, thus lending additional confidence to our identification of these compounds.

Although hexa- and heptachlorostyrene have not previously been reported in the Great Lakes, their presence, along with octachlorostyrene, is not surprising given the previous findings of octachlorostyrene in fish from Lake Ontario (2). Although we may presume that their presence in the sediment led to their ultimate accumulation in the fish, why these compounds are present in the lake in the first place is not yet clear. While chlorinated styrenes are not known to be commercially produced, they may be by-products of some other industrial process. The presence, however, of the by-products from the chlorostyrene synthesis suggests that the chlorinated styrenes were not accidentally produced. Their finding remains a mystery which we are continuing to investigate.

The chlorinated naphthalenes are probably halowaxes. Each halowax is a mixture of variously chlorinated naphthalenes. The quantity of each chlorinated homolog in a mixture of halowaxes is, therefore, difficult to determine. We know, however, that their quantities are small enough to be detected only with NCI, and the tetra- through octachloronaphthalenes are generally present. These compounds were once widely employed in a great variety of uses similar to those of PCB's. Although they are no longer being manufactured in the United States, their persistence in the environment would be expected in view of their great stability. Although their entry into Lake Ontario may have been from a variety of sources, it may be significant that their only domestic source was upstream from the lake in Pennsylvania.

Acknowledgement. We thank the U.S. EPA for support (Grant No. 808961) and Dr. Klaus L. E. Kaiser of the Canada Centre for Inland Waters for samples.

References.

1. V. A. Elder, B. L. Proctor, and R. A. Hites, Environ. Sci. Tech., 15, 1237 (1981).
2. D. W. Kuehl et al., J. Great Lakes Res., 7, 330 (1981).

TABLE I

	SITE NUMBER												
	15	18	20	21	22	23	24	25	34	36	38	39	40
Chlorobenzenes													
3 Cl	Tr	9	9	1.0	15	80	ND	10	ND	4.7	Tr	71	Tr
4 Cl	14	49	36	2.5	13	47	11	15	ND	12	ND	88	Tr
5 Cl	22	23	24	2.0	4.3	14	5.6	21	Tr	16	Tr	32	ND
6 Cl	89	52	58	7.7	17	47	51	47	10	65	ND	57	7.6
Chlorotoluenes													
3 Cl	ND	ND	ND	ND	1.5	Tr	Tr	Tr	ND	ND	ND	ND	ND
5 Cl	21	12	28	26	7.2	28	11	13	ND	29	ND	6.5	3.8
Chlorostyrenes													
6 Cl	ND	ND	12	ND	5.9	ND	ND	ND	ND	ND	ND	7.5	ND
7 Cl	13	Tr	18	ND	5.6	ND	8.8	ND	ND	0.1	ND	12	ND
8 Cl	16	0.3	49	ND	12	2.2	22	1.5	ND	0.3	Tr	33	ND
Mirex	20	37	17	ND	ND	Tr	62	8.2	ND	16	ND	33	ND
Dichloro(trifluoromethyl)-αα-difluorodiphenylmethane			0.4		0.8							0.6	
Dichloro(trifluoromethyl)-benzophenone			1.1		1.4							ND	
Tetrachloroethylene			Tr	Tr	Tr								
Hexachlorobutadiene			Tr	Tr	8.7			Tr					
Chlorodibenzofurans													
6 Cl		+			+	+	+			+		+	
7 Cl								+		+			
8 Cl	+		+							+			
Chlorophenanthrenes													
4 Cl										+			
5 Cl	+	+	+		+	+		+		+		+	
6 Cl	+		+		+	+		+		+		+	
Chloropyrenes													
9 Cl			+									+	
10 Cl		+	+					+					
Chloronaphthalenes	+	+	+		+	+	+	+		+		+	
PCB's	+	+	+	+	+	+	+	+		+		+	

Tr = Detected but not quantified due to low abundance
ND = Not detected
+ = Detected but not quantified due to lack of standard

MASS SPECTRAL IDENTIFICATION OF HALOGENATED ORGANIC COMPOUNDS FROM SEDIMENTS AND GROUNDWATER NEAR HAZARDOUS WASTE DISPOSAL SITES, Bertha L. Proctor, University of Texas at Dallas, Richardson, Texas 75080

Methane pulse positive pulse negative chemical ionization mass spectrometry coupled with fused silica capillary column gas chromatographic techniques were used to analyze crude extracts of sediments and groundwater receiving leachate from several hazardous waste disposal sites. This method was extremely useful in the identification of organic compounds and substantially reduced sample preparation time.

Negative ion chemical ionization (NCI) mass spectrometry aids in the characterization of complex mixtures by lowering the detection limits for compounds with electron withdrawing groups (1) provides some structural information (2) and reduces background (unresolved complex organic mixture common to electron impact). Positive chemical ionization (PCI) usually provides molecular weight confirmation and fragmentation patterns for a broader range of organic compounds, allowing for some interpretation of mass spectra.

STUDY AREA

Sediments from the Niagara River and two tributaries near Niagara Falls, New York and three groundwater samples near a disposal site east of Houston, Texas were selected for analyses.

The 102nd Street Bay of the Niagara River receives runoff from 5 waste disposal sites including the Love Canal, Griffin Park, Hooker 102nd Street, Olin site and a municipal dump

Gill Creek, Niagara Falls, New York flows through an industrial complex and receives a variety of waste from surface runoff and unauthorized dumping

Bloody Run Creek Niagara Falls, New York, receives runoff from the Hyde Park Disposal area which contains over 80,000 tons of organic waste (Table I).

The Sykes Farm located near Crosby, Texas was an unauthorized disposal site for approximately 15 years. There are no records of the types or amount of material dumped into the five sand pits or left in metal drums on the surface. Groundwater samples from three recently installed monitoring wells were collected for analysis.

INSTRUMENTATION CONDITIONS

A. Mass Spectrometer		B. Gas Chromatograph	
Source Temperature	180C	Injector	On Column
Source Pressure	0.1 Torr	Column	30M SE-54 Fused Silica
Reagent Gas	CH_4	Temperature Program	50C(3min)-10C/min-280
Mass Range	50-500 amu		(10min)

RESULTS

Table 2 contains a partial listing of organic compounds identified by pulse positive pulse negative chemical ionization mass spectrometry. Figures 1 and 2 show mass spectra of two compounds identified by this method. In conclusion pulse positive pulse negative chemical ionization mass spectrometry may be preferable to electron impact mass spectrometry for initial screening of complex samples. This method allows identification of numerous compounds and decreases sample preparation time. Unfortunately this method also produces less fragmentation information for the interpretation of mass spectra and requires longer time to tune the instrument initially.

TABLE I: HYDE PARK LAND FILL

Type of Waste

C-56 der.	5600 tons
Organic phosphates	4400 tons
BTC	1700 tons
Chlorinations	9300 tons
BTF Der.	8500 tons
TCP	3300 tons
BHC	2000 tons
Chlorobenzenes, Toluenes	18000 tons
Benzyl chloride	3400 tons
Sulfides	11500 tons
Misc.	13500 tons
TOTAL	80200 tons

TABLE II: COMPOUNDS IDENTIFIED

Chlorobenzenes	(1-6 Cl)
Chlorotoluenes	(2-5 Cl)
Phenols	(1-5 Cl)
PAH's	
BHC	
Mirex	
Benzyl Alcohols	(1-3 Cl)
Benzoic Acids	(1-5 Cl)
Benzamides	(1-4 Cl)
Phenothiazene	
Benzotrifluoride der.	

1. Budzikiewicz, H. Angew.Chem.Int.Ed.Engl. 20, 624-637 1981
2. Dougherty, R.C. Anal.Chem. 53 #4 625-636 1981

Figure 1

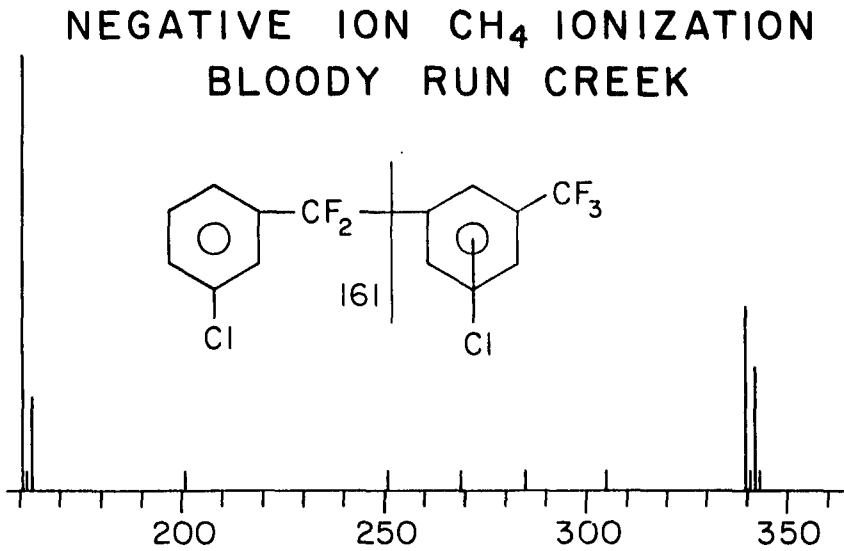
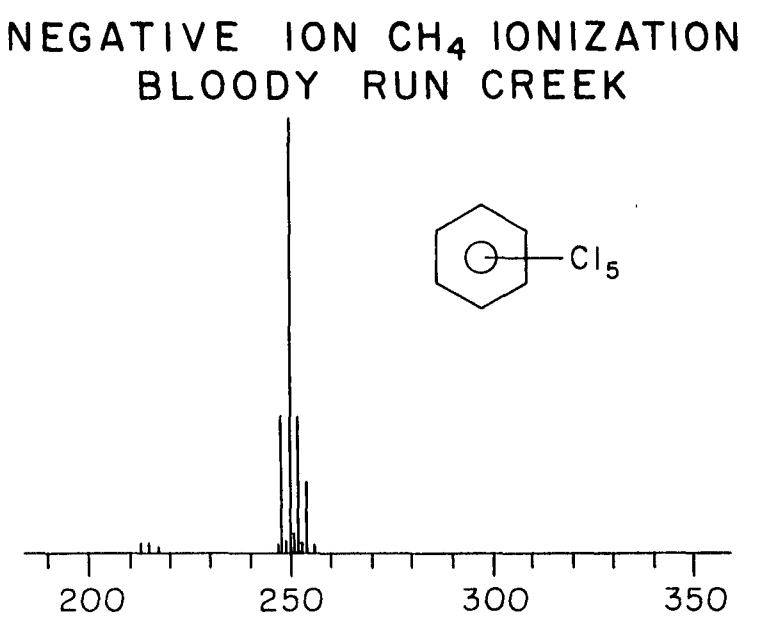


Figure 2



APPLICATIONS OF GAS CHROMATOGRAPHY-NEGATIVE ION CHEMICAL IONIZATION MASS SPECTROMETRY IN CONFIRMATORY PROCEDURES FOR PESTICIDE RESIDUES

S. J. Stout

American Cyanamid Company, Agricultural Research Division, P. O. Box 400, Princeton, New Jersey 08540

Both the advantages and limitations of gas chromatography-negative ion chemical ionization mass spectrometry (GC-NICI) arise from the technique's close similarity to gas chromatography using a conventional electron capture detector (GC-ECD). The specificity of both techniques arises from the wide range of response factors from different compound classes. However, the fact that almost every compound, with the possible exception of the aliphatic hydrocarbons, has some electron capture response is the reason the ECD has the reputation of being the least specific of the specific detectors for pesticide residue analysis. Moreover, while good ECD response means good NICI response, it does not guarantee sufficient negative ion mass spectral data for confirmatory purposes.

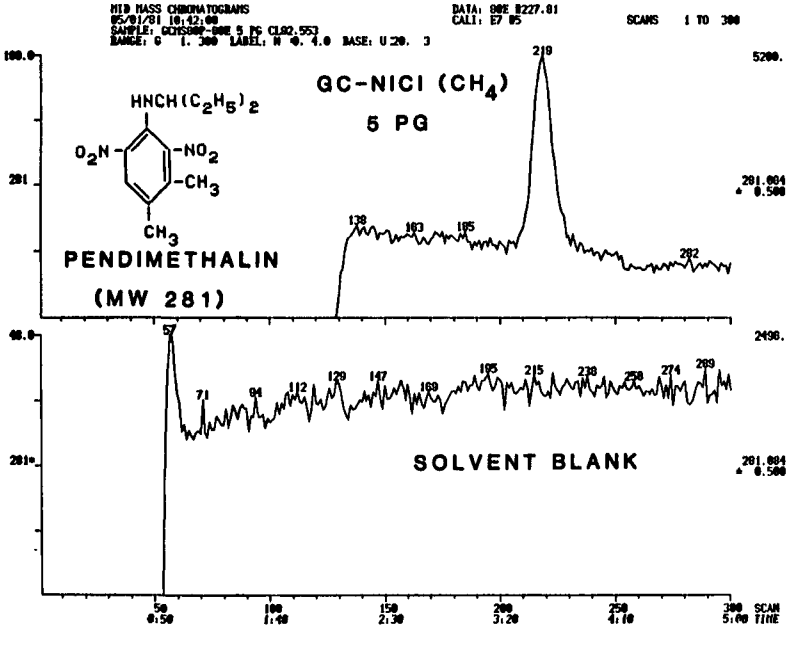
The most obvious applications of GC-NICI for confirmatory procedures in pesticide residue analysis are straightforward extensions of GC-ECD methods of analysis as illustrated in the GC-NICI analysis of pendimethalin, a dinitroaniline herbicide, at the pg level. As might be expected, the dinitroaniline has tremendous EC response and is routinely monitored by GC-ECD. The NICI (CH_4) mass spectrum is dominated by the $M^{-\cdot}$ at m/z 281^-. There is also an NO_2^- ion of about 20% relative intensity. The chromatogram shown in Figure 1 is from selected ion monitoring of the m/z 281^- ion. As shown, 5 pg is readily detected and the hallowed atto-mole region of analysis is probably attainable; but I thought it more useful to illustrate the type of response one can get with relatively little effort. Actually, in the case of pendimethalin, being able to do sub-pg analysis is somewhat academic because the GC-ECD analysis uses a standard injection of 100 pg for the analysis of pendimethalin at 0.05 ppm in the commodity being analyzed. At the 100 pg level, we routinely run the instrument in the full scan mode to look for any potential coeluting interferences under the pendimethalin peak.

The use of GC-NICI as a confirmatory technique to complement a gas chromatographic method using a flame photometric detector (GC-FPD) is illustrated in the analysis of fosthietan, an organophosphate pesticide, in corn tissues. While organophosphate pesticides show good EC response, they usually generate ions indicative of only the phosphate moiety which would be inadequate information for a confirmatory technique. Consequently, GC-NICI alone wasn't expected to be adequate for the confirmatory analysis of fosthietan. However, fosthietan generates an $M^{-\cdot}$ at m/z 241^- and several fragment ions useful for confirmatory purposes. The PICI (CH_4) spectrum of fosthietan shows an $(M + H)^+$ ion and two fragment ions useful for confirmatory purposes, but the PICI response to fosthietan is 50-fold less than the NICI response.

While several control and fortified corn tissue samples previously analyzed by GC-FPD were analyzed successfully by GC-NICI, a comparison of the GC-FPD and the GC-NICI analyses illustrates an earlier statement about the ECD being the least specific of the specific detectors for pesticide residue analysis. While GC-FPD of the corn tissue extracts shows two early eluting peaks well resolved from the fosthietan peak, full scan analysis in GC-NICI shows at least 10 peaks having greater response than the fosthietan peak. Several of these elute close to the fosthietan peak and there is a smaller peak which nearly coelutes with the analyte. It is unlikely that GC-ECD alone could be used to analyze these extracts. The specificity of GC-ECD must be augmented by the mass specificity of NICI to facilitate the analyses of these extracts.

The final application of GC-NICI I would like to present is the development of a GC-MS confirmatory method of analysis for sulfamethazine in cattle tissues. Sulfamethazine is routinely monitored by GC-ECD and, consequently, would be expected to have excellent response in GC-NICI. As expected, this is the case. However, the NICI (CH_4) mass spectrum of sulfamethazine characterizes only the sulfonic acid portion of the sulfonamide. This sulfonic acid moiety is common to many sulfonamides from which sulfamethazine is to be distinguished. Consequently, the NICI data is not adequate by itself for a confirmatory procedure. I believe this example illustrates a point made earlier that while good EC response means good NICI response, it does not guarantee the analytical utility of the NICI mass spectral data. The PICI (CH_4) mass spectrum of sulfamethazine shows an $(M + H)^+$ ion at m/z 293^+ and fragment ions characteristic of the amine functionality. This data is satisfactory for a confirmatory method of analysis; however, the PICI response is 100-fold less than the NICI response. While NICI alone cannot be used for the confirmatory analysis of sulfamethazine, it does offer a means to check the quantitative data from PICI analyses and does provide additional confirmatory data which complements the PICI data.

To summarize, I would like to say that we have had extremely good success in using GC-NICI as a confirmatory technique for pesticide residue analysis. As I hope this presentation has illustrated, sometimes the applications can be straightforward extensions of GC-ECD methods of analysis; sometimes applications work where you suspect they might not; and sometimes, unfortunately, you don't get the data really required for confirmation.

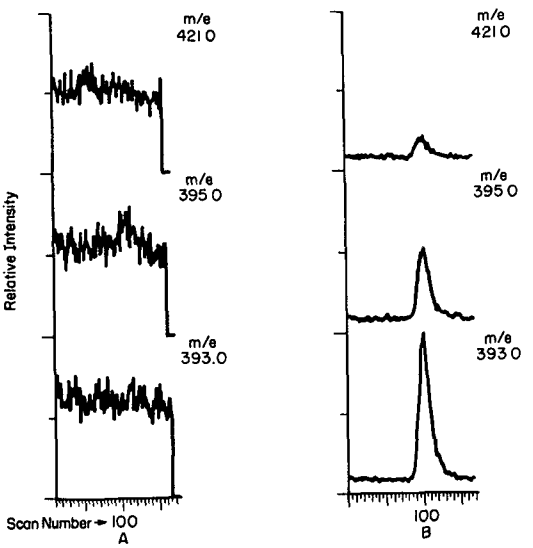


GC AND SOLID PROBE MASS SPECTROMETRIC CONFIRMATORY ASSAYS FOR ARPRINOCID IN POULTRY TISSUES. Patricia C. Tway. Merck Sharp & Dohme Research Laboratories, P. O. Box 2000, Rahway, NJ 07065.

Arprinocid [6-amino-9-(2-chloro-6-fluorobenzyl)purine] is a coccidiostat which is used prophylactically in broiler chickens. The residue levels of arprinocid and its metabolites in animal tissues are monitored routinely by an HPLC assay with fluorescence detection. For a drug to be approved by the Food and Drug Administration, a confirmatory tissue assay must also be developed. This assay must meet the same requirements of sensitivity, reproducibility, and specificity as the routine tissue assay and must, if at all possible, give some structural information to confirm the suspected drug residue.

Metabolism work has shown that most of the drug-related residue in chicken tissues at the withdrawal time is covalently bonded to macromolecular constituents of the tissue and is not solvent extractable, but that this residue can be released as 2-chloro-6-fluorobenzylamine by acid hydrolysis of the tissue homogenate.[1] The dansyl derivative of 2-chloro-6-fluorobenzylamine is then formed to eliminate losses due to the volatility of the underivatized amine during sample cleanup, and also to utilize the fluorescence properties of this derivative as a sensitive HPLC detection system.

Two mass spectrometric confirmatory assays have been developed for arprinocid and its metabolites based on confirming the presence of the dansyl derivative of 2-chloro-6-fluorobenzylamine in a tissue extract. The primary assay is a quantitative GC/MS assay utilizing methane chemical ionization and multiple ion detection monitoring the pseudo-molecular ion $(M+1)^+$, its chlorine isotope peak $(M+3)^+$, and the $(M+29)^+$ peak.[2] This assay was developed on a Finnigan 3200 using a 3% SP-2100 GC column for the separation. Figure 1 shows multiple ion detection chromatograms of chicken liver samples, (A) nonmedicated and (B) spiked at 0.25 ppm.



This assay has a sensitivity of 0.04 ppm, a limit of detection of 0.01 ppm, and recoveries average 76%. The method of addition is used for quantitation because the compound has different response factors in the presence and absence of tissue components.

In the course of further work on an assay for arprinocid and its metabolites in other sample matrices (i.e. urine), a shorter qualitative rather than quantitative confirmatory assay was desired. A second method was therefore developed using the LC belt interface on a Finnigan 4000 as a solid probe, and methane chemical ionization to examine the tissue residue samples. The dichloro analog of arprinocid was used as an internal standard to allow semi-quantitative assay results; the $(M+1)^+$ ion (m/e 393) of the dansyl derivative of fluorochlorobenzylamine was compared to the $(M+1)^+$ ion (m/e 409) of the dansyl derivative of dichlorobenzylamine. Linear standard curves with a correlation coefficient of .996 were obtained. Recoveries from spiked samples range from 75-95%.

The possibility of false positives in this assay because of the lack of a chromatographic cleanup before mass spectrometric detection was eliminated by monitoring three fragment ions as well as the molecular ion to supply additional structural confirmation. The fingerprint of the fragmentation pattern clearly showed either a drug related residue or tissue interferences in the sample. The solid probe assay is much faster (~ one sample/minute) than the GC/MS assay and is used routinely to confirm residues that are positive by the fluorescence assay.

---

1. J. R. Carlin, A. Rosegay, F. J. Wolf, T. A. Jacob, Agricultural and Food Chemistry 30, 253 (1982).

2. P. C. Tway, J. S. Wood, Jr., G. V. Downing, Agricultural and Food Chemistry 27, 753 (1979).

TOA 7 QUANTITATIVE DETERMINATION OF POLY-CHLORINATED DIPHENYL ETHERS IN FISH BY HIGH RESOLUTION GC-MS; P.-Y. Lau and W.H. Newsome; Food Research Division, Health Protection Branch, Health and Welfare Canada, Tunney's Pasture, Ottawa, Ontario, CANADA K1A 0L2.

Chlorinated diphenyl ethers (PCDPE's), which occur as impurities in chlorinated phenol (PCP) preparations, have been shown to be converted to dibenzofurans by UV irradiation as well as to dibenzofurans and dibenzo-p-dioxins by pyrolysis.

During the course of our Lake Ontario Fish survey, 6 dioxin-contaminated fish samples were analyzed for tetra- to deca-chlorodiphenyl ethers. The analytical procedure involved extraction with acetone:hexane (2:1), Florisil chromatography and final cleanup by reversed phase HPLC. Congeners and isomers were separated on a 30-m chemically bonded SE-54 (DB-5) fused silica column and quantitated by medium resolution multiple ion detection on the molecular ion cluster (M, M+2, M+4 ions) of each congener. The concentration of each isomer was calculated based on a specific isomer standard: 2,3,4,2',3',4'- for hexa-CDPE's; 2,4,5,2',3',4',5'- for hepta-CDPE's; 2,4,5,2',3',4',5',6'- for octa-CDPE's and 2,3,4,5,2',3',4',5',6'- for nona-CDPE's.

Following our extraction and cleanup scheme, only higher congeners (hexa-, 0.2-6 ppb; hepta-, 0.8-64 ppb; octa-, 0.4-5 ppb; nona-, 0.7-15 ppb) were found. Correlations of PCDPE's, TCDD and PCB's with one another, and with the fat content, will be discussed.

CAPILLARY GC/MS PROFILING OF XENOBIOTIC CHEMICALS IN BIOFLUIDS IN EI AND NCI MODES

John de Kanel, S.-Y. Tang and Ralph C. Dougherty
Department of Chemistry
Florida State University
Tallahassee, FL 32306

Previous work has suggested that the apparent decline in male fertility in the Western World as judged by declining average sperm counts may be in part related to ambient exposure to xenobiotic chemicals[1]. By examining all of the reports that are available in world literature on sperm counts in humans we have found that the average sperm count was stable in the period 1929 to 1960 with the average being 112 million cells/ml. The period subsequent to 1950 average sperm counts have been declining at a rate of approximately 1.9 million cells per ml for data obtained in the continental United States. In an attempt to address possible causitive factors for this decline we have obtained seminal plasma samples from volunteer donors by recruiting donors through an ad in an university newspaper.

For a group of 52 males we have found the average sperm count to be 58.5 million cells per ml. This value is consistent with predictions for the mean sperm count in the continental United States based on linear regression analysis of all of the reports available on nonselected male populations for the past 30 years[2].

Samples have been cleaned up by desolving a 2 ml aliquot in 50 ml of 10% sulfuric acid followed by extraction of the acidic solution with hexane diethyl ether. The extracts were reduced in volumn and subjected to high resolution size separation chromatography using tetrahydrofuran as a solvent with styragel as the solid phase. The low molecular weight fraction contains virtually all of the lipophilic xenobiotic chemicals, free fatty acids, alkanes and even carbon aldehydes which appeared because of acid hydrolysis of the plasmalogens in the sample.

The low molecular weight fraction was examined by isobutane negative chemical ionization mass spectrometry with sample introduction through a 30 M fused silica capillary coated with DB-5 methyl/phenyl silicone polymer (Finnigan 4510). The limit of detection for compounds like polychlorobiphenyls using this method appears to be at least one order of magnitude higher than the limit of detection using direct probe introduction into an AEI-MS 902 mass spectrometer.

Virtually all of the samples examined contained significant quantities of phthalate esters, which are known to be testicular toxins at high doses[3]. Other compounds detected included tetrachloroacetone, polychlorophenols, polychlorobenzenes and butylated hydroxytoluene and hydroxyanisole.

Examination of the electron impact gc mass spectra of the same samples gave profiles for the low molecular weight lipophilic components of the extract. In these extracts there appears to be a relationship between the ratio of plasmalogen derived aldehydes to free fatty acids and the sperm count for the individual samples. At this time the number of samples examined is not large enough to assess the statistical significance of this finding.

References

1. R.C. Dougherty, M.J. Whitaker, S.-Y. Tang, R. Bottcher, M. Keller and D.W. Kuehl, in "Environmental Health Chemistry", J.D. McKinney, ed., Ann Arbor Science Publishers, Ann Arbor, MI, 1980, pp 263-277.

2. R.C. Dougherty, J. de Kanel and S.-Y. Tang, to be published.

3. T.J.B. Gray, I.R. Rowland, D.M.D. Foster and S.D. Gangolli, Toxicol. Letters 11, 141-147 (1982).

Chlorinated Compounds in Taiwanese "Yusho" patients' blood

T. Kashimoto, H. Miyata, S. Fukushima, N. Kunita, T.C. Tung°, S.T. Hsu°, C.J. Chang°, S.Y. Tang°, G. Ohi°° and S. Yamamoto°°; Osaka Prefectural Institute of Public Health, 1-3-69, Nakamichi, Higashinari-Ku, Osaka 537, Japan, °College of Medicine, National Taiwan University, 1 Jen-Ai Road, Taiwan and °°Faculty of Medicine, University of Tokyo, 7-3-1, Hongo, Bunkyo-Ku, Tokyo 113, Japan

In 1979, an outbreak of "Yusho", characterized by acne, pigmentation of the skin, and nervous and gastrointestinal disorders, occurred in Central Taiwan. It was caused by the intake of toxic oil and affected about 2,000 people before 1981. The rice oil was found to be contaminated with PCBs, PCQs (polychloroquaterphenyls) (substances perhaps equally toxic as PCBs), and PCDFs (polychloroquaterphenyls) (compounds approximately hundreds of times more toxic than PCBs). However, the toxic oil had not only about ten times fewer contaminations of these compounds but also roughly 5 times lower ratios of PCQs or PCDFs to PCBs in comparison with those found in the contaminated oil which caused the Japanese Yusho outbreak in 1968.

One year after the outbreak, all people who had ingested the toxic oil had high blood levels of PCBs, PCQs and PCDFs, on the average 42, 8.6 and 0.076 ppb, respectively. According to the degree of severity of the clinical signs of patients, their blood levels of these compounds increased as shown in Table 1. This tendency towards increasingly severe symptons was especially clear as the amount of PCDF in the blood level was raised.

There was a sex difference at the component ratios of PCB congeners retained in the blood of patients with Yusho as represented in Fig. 1. The male blood contained fewer amounts of relatively eliminable PCB congeners such as peak No. 9 and 15 components in ECD-GC chromatogram on 2% OV-1 column (2 m x 2.2 mm) and larger amounts of bioaccumulative congeners such as peak No. 18 through 25 components in comparison with the female blood. This result indicates that males might have stronger capacity to metabolize PCB.

Compares with the original oil, the limited PCDF congeners were detected in the blood samples (Fig. 2). Peak No. 1, 2 and 3 components shown in the upper chromatogram were identified as 2,3,7,8-tetra, 1,2,4,7,8-penta and 2,3,4,7,8-pentachlorodibenzofuran congeners,

Table 1. PCB, PCQ and PCDF levels (Mean ±S.D.) in the blood of Taiwanese patients with Yusho

Degree of severity of clinical signs	No. of sample	Blood concentration (ppb)		
		PCB	PCQ	PCDF
None	5	12 ± 6	1.7 ± 1.1	0.024 ± 0.018
Slight	24	38 ± 13	7.9 ± 3.7	0.062 ± 0.024
Moderate	14	43 ± 11	8.2 ± 3.5	0.079 ± 0.030
Heavy	24	49 ± 20	11.0 ± 5.2	0.100 ± 0.040
	Total No.		Average	
	67	42 ± 17	8.6 ± 4.8	0.076 ± 0.038

respectively, by the coincidences the retention times of those peaks with those of authentic compounds on 20 m capillary, OV-17 packed and SE-52 packed columns, respectively. Peak No. 4 component was speculated to be 1,2,3,6,7,8-hexachlorinated isomer. These identified isomers have been reported to be high toxic compounds, toxicologically hundreds to thousands times higher than PCBs (1).

After consideration of this result and our biological study in which PCDFs could bring similar clinical signs of Yusho in monkeys (2), PCDFs might be major pathogenic substances in the development of Yusho.

(1) Moore, J.A. (1979) Comparative Toxicity of Three Halogenated Dibenzofurans in Guinea Pigs, Mice and Rhesus Monkeys. Annals NY Acad Sci. W.J. Nicolson and J.A. Moore, EDs., pp. 151-163.

(2) Hori, S. et al. Effect of Polychlorinated Diphenyls and Polychlorinated Quaterphenyls in Cynomolgus Monkey (*macaca fascicularis*). Toxicology (in press)

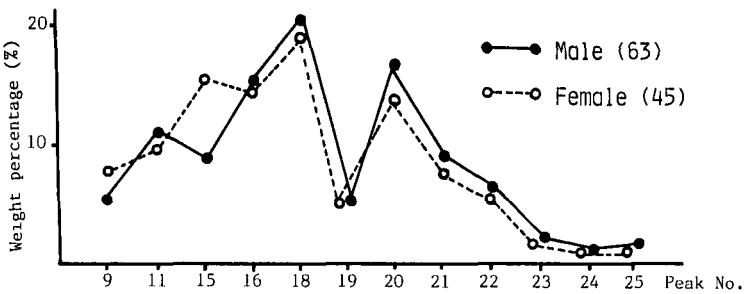


Fig. 1. The component ratio of PCB retained in the bloods of Taiwanese patients with Yusho

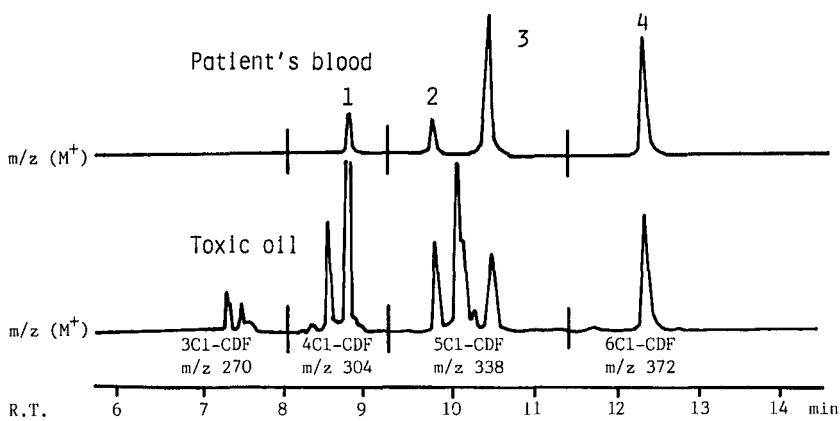


Fig. 2. GC-MS fragmentograms of PCDF in the toxic oil and the blood of patients with Yusho in Taiwan

Recent Flowing Afterglow Studies of Cluster Ion Reactions

Eldon E. Ferguson
NOAA, Aeronomy Laboratory
Boulder, Colorado 80303

The other four papers of this symposium deal with production and loss mechanisms of cluster ions, an area of extensive and continuing research. This paper concentrates on the reactivity of cluster ions, an area in which very little research has been done. The most extensive previous investigation involved measurement of rate constants for several dozen hydrated negative ion-neutral reactions.[1] Our research in this field has been motivated by our interest in atmospheric ion chemistry. Our primary goal has been to understand the ion composition of the atmosphere. At all altitudes below $\sim$ 80 km in the earth's atmosphere, cluster ions play a dominant role in the ion chemistry. The first atmospheric positive ion composition measurements at altitudes below 80 km were reported in 1965, obtained by means of rocket borne mass spectrometers. The dominant ions observed were proton hydrates, $H^+(H_2O)_n$, subsequently shown to be initiated by cluster ion reactions $NO^+(H_2O)_3 + H_2O \rightarrow H^+(H_2O)_3 + HNO_2$ and $O_2^+(H_2O) + H_2O \rightarrow H_3O^+ + OH + O_2$. The first negative ion reaction measurements below 80 km were reported in 1971 and cluster ions were again found to be dominant, including hydrated NO_3^-, CO_3^- and HCO_3^- ions among others. The negative ion chemistry is still not satisfactorily understood and many puzzles remain. In recent years the first stratospheric ion composition measurements have been carried out by means of balloon borne mass spectrometers. Again cluster ions are found to be dominant, with the positive ions involving acetonitrile and the negative ions sulfuric acid. These in situ measurements provide the incentive for additional laboratory studies of cluster ion production and loss mechanisms. Currently the first tropospheric ion measurements are being carried out (by Arnold and his colleagues at Heidelberg) and as these results become available additional new laboratory data will be required for their elucidation. In addition to the challenge of explaining the observed atmospheric abundance of cluster ions these ions play an important role as extremely sensitive monitors of certain critical atmospheric trace neutral species. The ambient ion composition serves as a passive chemical ionization mass spectrometric analytical probe of trace neutral species. The ion measurements for example have provided the first measurements of neutral CH_3CN and H_2SO_4 concentrations

in the stratosphere. It remains to be seen what trace species will be revealed when tropospheric ion composition measurements become available but analytical sensitivities as great as one part in 10^{16} can be anticipated.

There is also a possibility that ion reactions may play an important role in atmospheric chemistry, either acting as sources or sinks for certain trace species. For this reason we have been investigating a new class of ion catalyzed reactions occurring in cluster ions in which the central ion plays no "chemical" role, i.e. does not form chemical bonds.

One example we have studied[2] is the reaction

$$Na^+ \cdot O_3 + NO \rightarrow NO_2 + O_2 + Na^+ \qquad (1)$$

for which the rate constant is enhanced by a factor of greater than 10^3 over the reaction between unclustered O_3 and NO. A similar enhancement is found for O_3 clustered to Li^+ and a somewhat lower enhancement when K^+ is the cluster ion.

The reaction

$$Li^+ \cdot N_2O_5 + NO \rightarrow Li^+ \cdot N_2O_4 + NO_2 \qquad (2)$$

occurs with a rate constant 1.2(-11) $cm^3 s^{-1}$ whereas the unclustered N_2O_5 reaction rate constant with NO is less than 1(-20) $cm^3 s^{-1}$. Reaction (2) is 50 times slower when Li^+ is replaced by Na^+ and too slow to measure when the ion is K^+, $<5(-14)$ cm^3 s^{-1}. The cluster ion reactions (1) and (2) were found to have no significant temperature dependence. A likely explanation for this reactivity enhancement is the very obvious one in which the neutral reactants are attracted toward the ion-clustered reactants by the electrostatic forces and provided with kinetic energy to overcome the activation energy barrier.

We have attempted to measure an enhancement in the reaction

$$N_2O_5 + H_2O \rightarrow 2HNO_3 \qquad (3)$$

when the H_2O is clustered to various ions,

$H^+(H_2O)_n$, $CH_4CN^+(H_2O)_n$, $CH_4CN^+(CH_3CN)_n(H_2O)_m$ and $NO_3^-(H_2O)_n^3$. These ions occur in the natural stratosphere and if reactions such as

$$X^+(H_2O) + N_2O_5 \rightarrow X^+(HNO_3) + HNO_3 \qquad (4)$$

occurred with large reaction probabilities this could be of great importance in the stratospheric odd nitrogen chemistry and consequently in the stratospheric ozone balance. This is because HNO_3 is a relatively stable sink for NO_x while N_2O_5 is not. Reaction (3) is unmeasurably slow in the gas phase. It is an extremely rapid heterogeneous surface reaction which suggested to us that it might well occur on ion clusters, the

ion clusters playing the role of a surface. What we have found[3] is that the ions $H^+(H_2O)_n$ react with N_2O_5 with rate constants k(n) = 1.1(-9)(1), 8.0(-10)(2), 4.5(-11)(3), <4(-12)(4), <7(-12)(5) and <1(-11)(6), i.e. hydration beyond n=3 effectively quenches reaction. It is also found that CH_4CN^+ and $CH_4CN^+(H_2O)$ react with N_2O_5, k = 8.3(-10) and 4.1(-10) $cm^3\ s^{-1}$ respectively but that $CH_4CN^+(H_2O)_n$ with n = 2, 3 and 4 and $CH_4CN^+(CH_3CN)(H_2O)_n$ with n = 1 and 2 do not efficiently react with N_2O_5, the rate constants all being less than 10^{-12} $cm^3\ s^{-1}$. It is only the non-reactive hydrates which have sufficient stratospheric concentrations to be potentially important for reaction (4) and so ion catalyzed conversion of N_2O_5 to HNO_3 does not appear to be atmospherically important. In the case of negative ions, $NO_3^-(H_2O)_n$ with n = 1 and 2 do not react with N_2O_5, k < 10^{-11} $cm^3\ s^{-1}$.

Although no ground level atmospheric ion compositions have been determined, the question of the nature of the ions is of some interest. In particular the negative ions have been reported to be biologically active and have been assumed to be hydrated O_2^- (super-oxide) ions. We have recently studied reactions of these ions, using a cooled flowing afterglow system with a relatively high pressure ion source region to produce hydrated $O_2^-(H_2O)_n$ up to n = 5.[4] It is found that $O_2^-(H_2O)_n$ with n up to 4 reacts rapidly with O_3 and SO_2, and $O_2^-(H_2O)_n$ with n up to 5 reacts rapidly with NO. All of these species are sufficiently abundant even in a pristine atmosphere to assure a negligible concentration of ambient $O_2^-(H_2O)_n$ ions. Of greatest chemical interest is the reaction of hydrated O_2^- with O_3, which is determined to be electron transfer from isotopic O_2 studies. The electron transfer from O_2^- to O_3 is uninhibited by hydration up to n = 4. Thus there is an efficient reaction process, involving the concerted transfer of an electron and three water molecules in the reaction

$$O_2^-(H_2O)_4 + O_3 \rightarrow O_3^-(H_2O)_3 + O_2 + H_2O \qquad (5)$$

with $k_5 \sim 4.6(-10)$ $cm^3\ s^{-1}$. This almost certainly occurs in a long lived complex. The resonant charge-transfer of $^{1818}O_2^-$ with $^{1616}O_2$, is found to occur with $\sim 1/2$ the collision rate constant (as expected) but the charge-transfer reaction is sharply inhibited by hydration of the ion. The ion SiO_3^- has been found to be exceedingly stable. It does not react with O, O_3, NO, NO_2, CO, CO_2 or Cl_2.[5] On this basis we speculate that the cluster ions $SiO_3^-(SiO_2)_m(MgO)_n$ may occur in the atmosphere around 85 km as a consequence of meteor ablation and subsequent electron attachment to small neutral agglomerates.

This might account for some otherwise unexplained heavy ions near 87 km but is highly speculative pending the acquiring of high resolution mass spectra in this altitude region.

1. F.C. Fehsenfeld and E.E. Ferguson, J. Chem. Phys. 61, 3181 (1974).
2. B.R. Rowe, A.A. Viggiano, F.C. Fehsenfeld, D.W. Fahey and E.E. Ferguson, J. Chem. Phys. 76, 742 (1982).
3. H. Böhringer, D. W. Fahey, F. C. Fehsenfeld, and E.E. Ferguson, unpublished results.
4. D.W. Fahey, H. Böhringer, F.C. Fehsenfeld, and E.E. Ferguson, J. Chem. Phys. 76, 1799 (1982).
5. A.A. Viggiano, F. Arnold, D.W. Fahey, F.C. Fehsenfeld, and E.E. Ferguson, Planetary and Space Sci., in press.

TOB 2 TEMPERATURE DEPENDENCE OF THIRD BODY ION CLUSTERING REACTIONS. Y. K. Lau, S. Ikuta, T. F. Magnera and P. Kebarle, Chemistry Department University of Alberta, Edmonton, Canada T6G 2G2.

The kinetics and temperature dependence of the clustering rate constants for the reactions:

(1) $H_3O^+(H_2O)_{n-1} + H_2O + M = H_3O^+(H_2O)_n + M$

(2) $Cl^-(H_2O)_{n-1} + H_2O + M = Cl^-(H_2O)_n + M$

were determined for n=1 to n=5. Preliminary data for the hydration of F^- are also available. The rate constants fit the equation $k_n = aT^{-b}$. For a series involving a given ion, it is found that both a and b increase with n. Values of b as high as b = 14 are encountered for n=4 and n=5. This leads to the surprizing result that, for these cases, most of the large negative temperature dependence of the equilibrium constant $K_{n-1,n} = k_n/k_{-n}$ is due to the negative temperature dependence of the forward clustering rate constant k_n and not to a large positive temperature of k_{-n}.

The log k_n vs log T plots for a given series form a specific pattern which to a certain extent reflects the pattern of the equilibrium constants. The rate constants $k_n(Cl^-)$ are considerably smaller than the $k_n(H_3O^+)$ for small n. However as n increases, the plots begin to look more alike. The experimental results are compared with predictions of RRK and RRKM theory.

DISSOCIATION OF METASTABLE CLUSTER IONS

K. Stephan, T. D. Märk

Kernphysik u. Gaselektronik, Institut f. Experimentalphysik
Leopold Franzens Universität, A 6020 Innsbruck, Austria

J. H. Futrell

Dept. Chemistry, University Utah, Salt Lake City, Utah 84112, USA

A.W. Castleman, Jr.

Dept. Chemistry, University Colorado, Boulder, Colorado 80309, USA

Introduction

Recently, there has been an increased interest in information on the formation and properties of neutral and ionized clusters. This is due in part to the fact that these studies provide basic information on cluster species and also because of the many applications in atmospheric+interphase physics and condensed state physics /1-3/.

Properties of gas phase clusters are investigated by a variety of methods, ranging from high pressure mass spectrometry to nozzle expansion. Supersonic expansion is e.g. generally used to produce beams of vibrationally and rotationally cooled Van der Waals molecules which are then probed by electron impact ionization, photoionization or Penning ionization in combination with mass spectrometry /1-6/. A problem of particular current interest concerning these experimental techniques of cluster detection is fragmentation of clusters occurring either in the ionization process or after ion formation by decomposition of ionic species in the analyzing system. Therefore, this topic is of great importance for the interpretation of mass spectra. Moreover, the investigation of unimolecular and/or collision induced dissociation of cluster ions offers the unique advantage of generating series of molecular ions having different numbers of degrees of freedom, complexity and size, but having similar chemical properties. This allows, in principle, further insight into the fragmentation process within the frame of the quasi-equilibrium-theory.

Stace and Shukla /7-9/ were the first to report the observation of metastable dissociation of cluster ions (CO_2 and acetone) produced by electron impact ionization. Sunner and Kebarle /1o/ have recently reported studies on the unimolecular dissociation of $K^+\cdot(H_2O)_n$, $H^+\cdot(H_2O)_2$ and $(C_6H_6)_2^+$ ion clusters in the vacuum of the analyzer of a temperature controlled high pressure mass spectrometer apparatus. Independently, we have investigated the occurrence of unimolecular dissociation of cluster ions in Ar, N_2, CO_2 and NH_3 produced by electron impact /5,11-16/. The important objective of our work was (1) to clearly distinguish cluster ions which decay by collision induced dissociation from those which decompose by metastable dissociation, (2) to detect experimental parameters in cluster production which might influence the production of metastable cluster ions and (3) to provide some guidance

for the theoretical description of metastable cluster ion decomposition.

EXPERIMENTAL

The electron impact -molecular beam-ion source and the mass spectrometer used have been described previously /5,11-16, 17-19/. Hence, only the salient features of the experiment will be discussed. Neutral clusters are produced by expanding typically a mixture of 100 to 500 Torr of the species to be clustered seeded with 1000 to 2000 Torr He through a 10 μ nozzle. The stagnation chamber and the nozzle can be cooled to temperatures ~ 105 K in order to obtain a sufficient amount of cluster signal and measurements were made at temperatures up to 300 K.

The molecular beam containing the neutral clusters is crossed at right angles by an electron beam of variable energy. Ions produced by electron impact ionization are extracted at right angles from the ionization regime by a weak electric field penetrating into the collision chamber. Special deflection plates in the ion optics between ion source and mass spectrometer serve to sweep the ion beam across the mass spectrometer entrance slit, thus allowing to distinguish between ions formed by cluster ionization and background ions with the same m/ze /19/.

Ions passing the mass spectrometer entrance slit are analyzed in a reversed Nier-Johnson geometry doubly focussing mass spectrometer according to their dissociation channels by decoupling the acceleration, deflection and magnetic field /2o,21/. This method allows the direct analysis of specific dissociation processes occurring in the field free region between the earth slit of the ion source and the entrance of the magnetic sector field.

Prior to the investigation of cluster ions, we checked the reliability of the apparatus and technique by studying the metastable dissociation of NO_2 /22/ and of propane /11,13,14/. Results obtained corrobated and extended previous measurements.

Results and Discussion

By measuring the pressure dependence of the unimolecular decomposition rate it is possible to distinguish between metastable (M) and collision induced (CID) dissociations. Fig. 1 shows as an example, that for the processes $Ar_3^+ \rightarrow Ar_2^+$ and $Ar_3^+ \rightarrow Ar^+$ both the product ion signals Ar_2^+ and Ar^+ and the precursor ion signal Ar_3^+ are affected by the gas pressure in the field free region. In order to allow for the change of precursor ion signal with pressure, the ratio of daughter ion (i_d) to precursor ion (i_p) signal is also shown in Fig. 1. Extrapolation of these curves to zero pressure yields the rate for metastable dissociation (zero-pressure intercept), whereas the cross section for collision induced dissociation may be obtained from the slope of the respective dependences /2o,23/.

Applying this technique the following unimolecular reactions were investigated quantitatively (the observed dissociation mechanism is given in parenthesis):

(1) $NH_3^+ \rightarrow NH_2^+ + H$ (CID)

(2) $(NH_3)_2^+ \rightarrow NH_4^+ + NH_2$ (CID + M)

(3)	$(NH_3)_2^+ \rightarrow NH_3^+ + NH_3$	(CID)
(4)	$(NH_3)_2H^+ \rightarrow NH_4^+ + NH_3$	(CID)
(5)	$(NH_3)_3^+ \rightarrow (NH_3)_2H^+ + NH_2$	(CID + M)
(6)	$(NH_3)_3H^+ \rightarrow (NH_4^+) + 2\ NH_3$	(CID)
(7)	$(NH_3)_3H^+ \rightarrow (NH_3)_2H^+ + NH_3$	(CID + M)
(8)	$(CO_2)_2^+ \rightarrow CO_2^+ + CO_2$	(CID)
(9)	$Ar_3^{+*} \rightarrow Ar_2^+ + Ar$	(CID + M)
	$\rightarrow Ar^+ + 2Ar$	(CID + M)
(10)	$ArN_2^+ \rightarrow Ar^+ + N_2$	(CID + M)
	$\rightarrow N_2^+ + Ar$	(CID + M)
(11)	$ArN_4^+ \rightarrow N_4^+ + Ar$	(CID + M)
	$\rightarrow ArN_2^+ + N_2$	(CID + M)
(12)	$Ar_2N_2^+ \rightarrow ArN_2^+ + Ar$	(CID + M)
	$\rightarrow Ar^+ + ArN_2$	(CID + M)
(13)	$N_4^+ \rightarrow N_2^+ + N_2$	(CID + M)

In addition we have studied the electron energy dependence of the ratio i_d/i_p of reaction (9) and (1o). It was found that in the energy regime accessible to our experiment (20 to 180 eV) the ion current ratio does not change within $\pm$ 10%. Moreover, we have recently also started to investigate the dependence of the metastable decomposition rate as a function of the stagnation gas temperature /16/. It was found that the unimolecular dissociation rate for $Ar_3^{+*} \rightarrow Ar_2^+$ changes dramatically with stagnation gas temperature (see Fig. ?). This is likely due to the fact, that the neutral state distribution before ionization is strongly affected by the stagnation gas (and nozzle) temperature. This in turn leads to a distribution of states in the ionic cluster (after electron impact ionization) also depending on temperature (see also Ref. 1o).

Hence, in summary from the present studies it may be concluded that small cluster ions may be described by a simple pseudo-oscillator (e.g., pseudo-diatomic, triatomic, etc.) model. According to this model, the energization of these clusters by electron impact or collision will result in prompt dissociation. The lifetime may be about one oscillation for the dimer, and somewhat longer for the trimer, etc. In the present work simple dissociations described by process (3),(4),(6) and (8) are observed to be exclusively collision induced. On the other hand we have also observed metastable decay for small cluster ions, e.g. for Ar_3^+, ArN_2^+ and N_4^+. In this case (forbidden) predissociation and /or tunneling might be invoked as a likely mechanism of this metastability.

The observation of metastable decay for the rearrangement processes (2) and (5) and the dissociation reaction (7) suggests that in this case energy exchange within a statistical ensemble of strongly-coupled oscillators might control the decomposition kinetics of these species (QET theory). Molecular complexity, the availability of rearrangement coupling decomposition channels, and the strength of bonding in the cluster are relevant factors which affect the transition from short-lifetime to long-lifetime cluster ions.

Acknowledgments

Work partially supported by the Österreichischer Fonds zur Förderung der wissenschaftlichen Forschung under Projekt S-18/05 and S-18/08.

References

/1/ Proc. 8th Int. Symposium on Moleculear Beams, Cannes (1981)
/2/ Proc. 2nd Int. Meeting Small Particles and Inorganic clusters, Lausanne (198o), see Surface Science 1o6 (1981)
/3/ NATO Adv. Study Inst. "Impact of Cluster Physics in Material Science and Technology", Cap d'Agde (1982)
/4/ A.W. Castleman, Jr., Contr. Symp. Atomic Surface Phys. (W. Lindinger et al.,Ed) 3 (1982)1
/5/ T.D. Märk, K. Stephan, H. Helm, J.H. Futrell, E. Mark, K.I. Peterson, A.W. Castleman, Jr., N. Djuric and A. Stamatovic, Contr. Symp. Atomic Surface Phys. (W. Lindinger et al., Ed.) 3 (1982) 7
/6/ H. Haberland, personal communication, 1982
/7/ A.J. Stace and A.K. Shukla, Int. J. Mass Spectrom. Ion Phys., 36 (198o) 119
/8/ A.J. Stace and A.K. Shukla, Chem. Phys. Lett., 85 (1982) 157
/9/ A.J. Stace and A.K. Shukla, J. Phys. Chem., 86 (1982) 865
/10/ J. Sunner and P. Kebarle, J. Phys. Chem., 85 (1981) 327
/11/ J.H. Futrell, K. Stephan, A.W. Castleman, Jr., and T.D. Märk, Proc. 8th Int. Symp. Molecular Beams, Cannes (1981) 262
/12/ K. Stephan and T.D. Märk, Chem. Phys. Lett., 87 (1982) 226
/13/ J.H. Futrell, K. Stephan, and T.D. Märk, J.Chem. Phys., in print, June 1, 1982
/14/ K. Stephan, T.D. Märk, J.H. Futrell and A.W. Castleman, Jr., Vacuum TAIP, in press
/15/ K. Stephan, T.D. Märk, E. Märk, A. Stamatovic, N. Djuric, and A.W. Castleman, Jr., Beitr. Plasmaphysik, in print
/16/ K. Stephan and T.D. Märk, Chem. Phys. Lett., in print
/17/ H. Helm, K. Stephan and T.D. Märk, Phys. Rev., A 19 (1979) 2154
/18/ K. Stephan, H. Helm and T.D. Märk, J. Chem. Phys., 73 (198o) 3763
/19/ H. Helm, K. Stephan, T.D. Märk and D.L. Huestis, J. Chem. Phys., 74 (1981) 3844
/2o/ R.G. Cooks, J.H. Beynon, R.M. Caprioli, and G.R. Lester, Metastable ions (Elsevier, Amsterdam, 1973)
/21/ K. Levsen, Fundamental aspects of organic mass spectrometry (Weinheim, New York, 1978)
/22/ E. Märk, T.D. Märk, Y.B. Kim and K. Stephan, J. Chem. Phys., 75 (1981) 4446
/23/ For this technique see e.g. A.J. Lorquet, J. Momigny and H. Wankenne, J. Chem. Phys., 67 (197o) 64

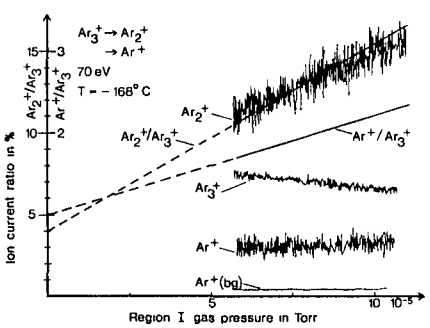


Fig.1

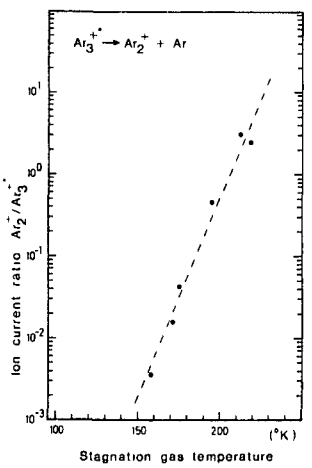


Fig.2

"Cluster ions: Understanding transitions from the gaseous to the condensed state," A.W Castleman, Jr. and R.G. Keesee, 152 Davey Laboratory, Dept. of Chemistry, The Pennsylvania State University, University Park, PA 16802

Introduction

During recent years, there has been growing interest in studies of the formation and properties of small gas-phase complexes comprised of molecules attached to ions. One reason is recognition that research on the properties of ion clusters is valuable in obtaining a more complete understanding of the forces between ions and neutral molecules. Particularly revealing in this regard are the results of systematic studies of the bonding of various ligands including protic and aprotic polar molecules, and non-polar molecules, attached to a variety of different atomic and molecular ions [1]. Other basic areas to which work on ion clusters have a bearing include the field of interphase physics which is concerned with elucidating the molecular details responsible for phase transitions (nucleation phenomena) [2], the development of surfaces, and ultimately solvation phenomenon [3-4] and the formation of the condensed state. In addition, ion complexes are formed in the ionizers of mass spectrometers, in combustion reactions, are believed to be present in interstellar media under certain conditions, and are ubiquitous throughout the earth's atmosphere [5,6]. For these reasons, work on ion clusters has been of interest to researchers in a variety of related fields. Two approaches used in our laboratory to understand gas to condensed phase transitions through investigation of cluster ions will be discussed. The first involves the direct determination of the thermodynamic properties of cluster ions and the second concerns the study of cluster ions produced from neutral clusters via electron impact.

Studies of the Thermodynamic Properties of Ion-Molecule Complexes

Using a high pressure mass spectrometric technique, enthalpy and entropy values are obtained for the clustering of successive molecules by determining the slope and intercept of a van't Hoff plot of the equilibrium constant for each step as a function of the inverse of the temperature. Unlike the majority of nucleation experiments conducted with cloud chambers or supersonic jets, with our high pressure mass spectrometric technique it is possible to obtain information on the initial clustering reactions leading to vapor nucleation.

Among the systems studied thus far have been the clustering of various molecules onto cations of the alkali metals, alkali earths, and several of the transition metals [7]. Anionic species have included the atomic halides and a number of molecular ions, among them CO_3^-, HCO_3^-, NO_2^-, NO_3^-, and SO_3^- [8]. Clustering molecules have been chosen for their interest as solvents, for their binding properties, and for their atmospheric significance. In addition to elucidating details of the early stages of nucleation, the determination of thermodynamic quantities contributes to a more complete understanding of cluster bonding and structure [8]. The gas phase clustering results in many instances corroborate properties observed for ions solvated in liquids; for instance Ag^+ and Cu^+ exhibit particularly stable diligand gas phase complexes. The effect of molecular structure of ions during the early stages of clustering is also evident in the experimental results. CNDO energy minimization calculations on the hydration of NO_2^-, NO_3^- and HCO_3^- qualitatively reproduce these results [8]. Also, charge delocalization is found to have a significant adverse effect on the favorability of further clustering. Work on the simultaneous clustering of ions by two different types of molecules is now in progress to better understand the role of the mutual interaction of solvent molecules.

The results of the present studies have led to an understanding of factors controlling the strength of the bonding of various neutrals to ions both with regard to the role of the ion and of the neutral. The results show that the strength of the bonding of the ions with the three neutrals CO_2, H_2O, and SO_2 is consistent with the inequality

$$OH^->F^-,O^->O_2^->NO_2^->Cl^->NO_3^->CO_3^->SO_4^-\approx SO_3^-\approx Br^->I^- \qquad (1)$$

This relationship appears to parallel the order of the gas phase basicity of the negative ions where the strongest bases exhibit the largest bond dissociation energies (see Reference 8).

Another interesting comparison is that of the relative bond dissociation energies, $D(A^-–B)$ for a given ion, with the different ligands SO_2, H_2O, and CO_2. In the case of large ions, the order of bonding correlates mainly with the dipole moments of the neutrals, while the polarizabilities are the main factors for small ions.

Neutral Clusters and the Changing Properties of Electrolyte-like Species Upon Clustering

In order to establish the applicability of the data for single ions in interpreting the solvation of neutral electrolytes, we have undertaken an extensive study of cluster distributions and changing dipole moment of systems which can form charge-transfer complexes. A variety of systems were chosen for investigation in order to compare the behavior of ones which can form charge transfer complexes with others which display simple hydrogen bondings such as water, ammonia, methanol, and ethanol.

The results of the cluster distribution measurements strongly suggest that solvation of the nitric acid begins at very small cluster sizes [9]. Careful experiments employing both a hexapole and quadrupole electrostatic focusing technique have failed to reveal large dipole moment changes in clusters beyond the second hydration step. This finding is interpreted as suggesting that the nitric acid water clusters readily form a mobile proton upon solvation which leads to a complex having a dipole moment averaging to zero during the observational time required by passage time through the electrostatic focusing field. This interpretation is further supported by studies of water clusters [10].

In expansion experiments made with D_2O/H_2O isotopes, a rather interesting observation was also made. Each successively larger cluster ranging from the trimer to the thirteen-mer was found to be enriched in the heavier isotope by approximately 26 per cent over the preceding cluster. The distributions measured in the ionizer were subjected to analysis by way of comparison to an expected statistical distribution in terms of the deuterium to hydrogen ratios. Instead of the expected binomial distribution of isotopic peaks, a pronounced shift to the heavier deuterium isotope was observed in each clustering step. The shift was found to be cumulative and did not have any apparent trend with increasing size. Good agreement in determined enrichment values for experiments with different starting compositions suggested that the enrichment is consistent with a single mechanism. The trend is well described by a unimolecular decomposition controlled model involving a density of states factor and the difference in the zero-point energies between species containing identical numbers of clustered water molecules, but varying isotopic composition [11]. Evidently there is a close connection between understanding the unimolecular breakup of small clusters and cluster distributions produced under cluster generating conditions.

Acknowledgements

Support of DOE under Grant #DE-AC02-78EV04778, NASA under Grant #NSG-2248, the Atmospheric Sciences Section of NSF under Grant #ATM 79-13801, and the ARO under Grant #DAAG29-79-C-0133 is gratefully acknowledged.

References

(1) A.W. Castleman, Jr., P.M. Holland and R.G. Keesee, "Ion Association Processes and Ion Clustering: Elucidating Transitions from the Gaseous to the Condensed Phase," *Radiat. Phys. Chem.*, (in press)

(2) (a) A.W. Castleman, Jr. in: *Advances in Colloid & Interface Science "Nucleation"* A. Zettlemoyer, Ed., Elsevier Press, Oxford, **10**, 1979, p. 73; (b) P.M. Holland and A.W. Castleman, Jr., "The Thomson Equation Revisited in Light of Ion Clustering Experiments" *J. Phys. Chem* (submitted); (c) A.W. Castleman, Jr., B.D. Kay, V. Hermann, P.M. Holland and T.D. Märk, *Surf. Sci.*, **106**, 179 (1981); (d) K.I. Peterson, P.M. Holland, R.G. Keesee, N. Lee, T.D. Märk

and A.W. Castleman, Jr., *Surf. Sci*, **106**, 136 (1981); (e) A.W. Castleman, Jr., P.M. Holland, B.D. Kay, R.G. Keesee, T.D. Märk, K.I. Peterson, F.J. Schelling and B.L. Upschulte, *J. Vac. Sci Technol.*, **18**, 586 (1981)

(3) P. Kebarle, *Modern Aspects Electrochem*, **9**, 1 (1974)

(4) (a) A.W. Castleman, Jr. in: *Kinetics of Ion-Molecule Reactions*, P. Ausloos, Ed., Plenum, New York, 1979, p. 295; (b) A.W. Castleman, Jr. and R.G. Keesee in: *Electron and Ion Swarms*, L.G. Christophorou, Ed, Pergamon, New York, 1981, p. 189

(5) (a) E.E. Ferguson, F.C. Fehsenfeld and D.L Albritton in: *Gas Phase Ion Chemistry*, M.T. Bowers, Ed., Academic Press, New York, 1979, p. 45; (b) D. Smith and N.G. Adams in: *Topics in Current Chemistry*, **89**, Springer-Verlag, Berlin, 1980

(6) (a) A.W. Castleman, Jr. and R.G. Keesee in: *The Stratospheric Aerosol Layer*, Vol. 28, R.C. Whitten, Ed., Springer-Verlag, Berlin, 1982, p. 69; (b) A.W. Castleman, Jr., *J. Aerosol Sci.*, **13**, 73 (1982); (c) A.W. Castleman, Jr., "Neutral and charged clusters in the atmosphere--their importance and potential role in heterogeneous catalysis," *J. Geophys, Res.* (in press); (d) R.G. Keesee, N. Lee and A.W. Castleman, Jr., *J. Geophys. Res*, **84**, 3719 (1979); (e) A.W. Castleman, Jr. and R.G. Keesee in: *Annual Review of Earth and Planetary Sciences, 9, Annual Reviews, Inc., Palo Alto, 1981, p. 227; (f) A W Castleman, Jr., Space Sci. Rev.*, **15**, 547 (1974); (g) A.W. Castleman, Jr., *Astrophys. Space Sci.*, **65**, 337 (1979); (h) A.W. Castleman, Jr. in: *Atmospheric Water Vapor*, A. Deepak, T.D. Wilkerson and L.H. Ruhnke, Eds., Academic Press, 1980, p. 599

(7) (a) P.M. Holland and A.W. Castleman, Jr., *J. Chem. Phys.*, **76**, 4195 (1982); (b) A.W. Castleman, Jr., P.M. Holland, D.M. Lindsay and K.I. Peterson, *J. Am. Chem. Soc*, **100**, 6039 (1978); (c) A.W. Castleman, Jr., *Chem Phys. Lett.*, **53**, 560 (1978); (d) I N. Tang, M.S. Lian and A W. Castleman, Jr., *J. Chem. Phys*, **65**, 4022 (1976)

(8) (a) R.G. Keesee, N. Lee and A.W. Castleman, Jr., *J Chem Phys*, **73**, 2195 (1980); (b) N. Lee, R.G. Keesee and A.W. Castleman, Jr., *J Chem. Phys.*, **72**, 1089 (1980); (c) R.G. Keesee, N. Lee and A.W. Castleman, Jr., *J. Am. Chem Soc.*, **101**, 2599 (1979)

(9) B.D. Kay, V. Hermann and A.W. Castleman, Jr., *Chem Phys. Lett.*, **80**, 469 (1981)

(10) V. Hermann, B.D. Kay and A.W. Castleman, Jr., "Evidence for the Existence of Structures in Gas-Phase Homomolecular Clusters of Water," *Chem. Phys.* (submitted)

(11) B.D. Kay, "Dynamics, Energetics, and Structure of Hydrogen Bonded Clusters: Elucidating the Transition from the Gaseous to the Condensed Phase," Ph.D. Thesis, Dept. of Chemistry, University of Colorado, 1981

ION CLUSTERS FROM LOW-TEMPERATURE SOLIDS

Robert G. Orth, Harry T. Jonkman, Dusan Stulik, and Josef Michl; Department of Chemistry, University of Utah, Salt Lake City, Utah 84112

Some time ago we became interested in the application of secondary ion mass spectrometry (SIMS) in matrix-isolation spectroscopy. We found that primary ion bombardment of argon matrices held at 15-20 K ejected ions characteristic of molecules present in high dilution within the matrix.[1] For instance, methane in argon (1:500) bombarded with He^+ ions of 1 keV energy yielded easily detectable peaks at m/e 16, 15, 14, 13, and 12 as well as peaks at 20, 40, and 80. In doing these experiments, we soon noticed that heavier primary ions, particularly those of higher energy, produce considerable quantities of the latter type of secondary ions, and in particular, of cluster ions due to the matrix material (Figure 1). In the present lecture, I shall concentrate exclusively on these cluster ions.

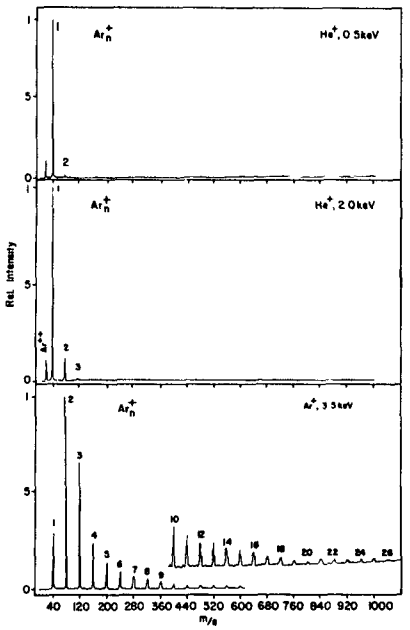


Figure 1. Positive SIMS of solid argon matrix (18 K) with He^+ as the primary ion at impacting energies of 0.5 keV and 2.0 keV, and Ar^+ as the impacting ion at an energy of 3.5 keV.

The formation of large cluster ions, both positive and negative, from low-temperature solids composed of small molecules appears to be the rule rather than the exception,[1-7] and it is conceivable that ion bombardment of gases solidified at low temperatures will turn out to be a useful way of producing large clusters for further study. The charge-carrying species generally is one derived from the molecule of the solid in a way which produces a particularly stable cation or anion. This charge carrier is then surrounded by several molecules representing "solvating units". For some solids the solvating unit is identical with the molecule of the solid. An example of such a behavior is given in Figure 2, showing the positive and negative cluster ions formed upon bombardment of solid CO_2. Here, the prevalent carrier of positive charge is the O_2^+ ion, and the prevalent carrier of the

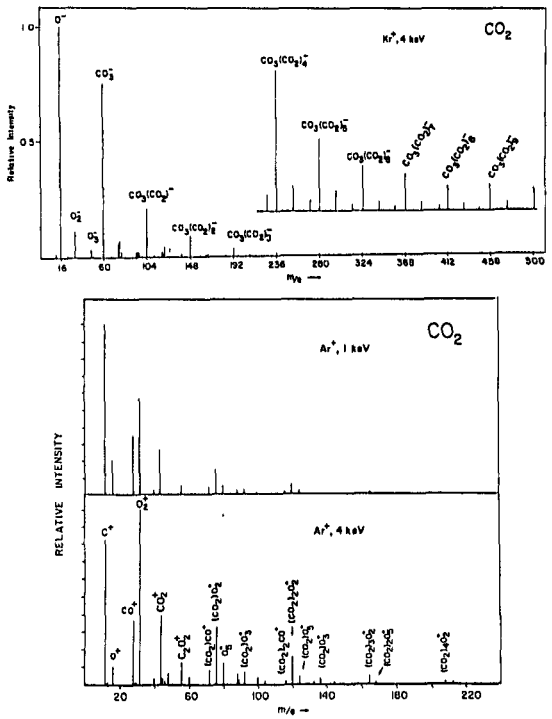


Figure 2. Negative (top) and positive (bottom) SIMS of solid CO_2 (18 K). Reproduced from ref. 5.

negative charge the CO_3^- ion;[5] the solvating unit is CO_2. In other solids, the nature of the solvating unit is different from the molecules of which the solid matrix is composed. Perhaps the most dramatic example of the situation which we have observed so far is the case of solid NO, which produces few negative cluster ions, but a very prominent series of positive cluster ions containing NO^+ as the charge carrier, and several molecules of N_2O_3 as solvating units.[4,6] Figure 3 shows the SIMS of solid NO under the conditions conducive to the production of large cluster ions (heavy and energetic primary ion) and contrasts it with the spectrum obtained under conditions leading to few or no cluster ions (light primary ion). Other nitrogen oxides also produce transformed solvating units.[4,6] For instance, positive SIMS of solid N_2O_4 contains the cluster series $NO^+(N_2O_3)_n(N_2O_4)_m$ and negative SIMS of solid N_2O_4 contains the intense cluster series $NO_3^-(N_2O_3)_n(N_2O_4)_m$. It is interesting to note that the relative oxygen content of the clusters is not simply correlated with the stoichiometry of the solid matrix: the relative abundance of the N_2O_4 solvating unit increases in the order solid NO, solid N_2O_3, solid N_2O, and solid N_2O_4. A survey of the observed solvating units for SIMS of various small-molecule solids is given in Table 1.

It should be pointed out that our assignments of the stoichiometric solvating unit are based only on the m/e ratios observed in SIMS and have not yet been confirmed by other experiments, such as collision-induced dissociation. Nothing is known about the internal structure of the solvating units, although one might suspect that it is identical with the internal structure of the ordinary molecules of identical atomic composition.

The clusters observed in this work have a lower average energy than the parent ion and fragment ions also observed in the secondary ion spectra. The secondary ion energy distribution is narrower for the cluster ions and peaks at lower energies. The distribution is

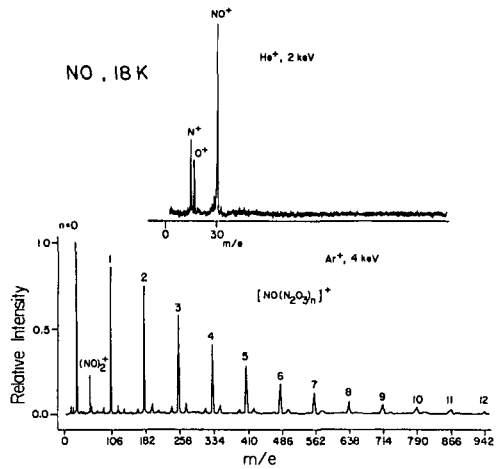


Figure 3. Positive SIMS of solid NO (18 K). Reproduced from ref. 4.

particularly narrow for negative cluster ions. It is possible that at least some of these ions are formed by attachment of electrons originating in the flood gun, which is used to neutralize the surface charge, to small neutral pieces of the molecular solid sputtered by the bombardment.

Table 1

Solvating units observed in clusters produced by ion bombardment of low-temperature molecular solids

SOLID	SOLVATING UNIT IN CLUSTER	SOLID	SOLVATING UNIT IN CLUSTER
Ar	Ar	N_2O	N_2O_3, N_2O_4
Kr	Kr	NO	N_2O_3
Xe	Xe	N_2O_3	N_2O_3, N_2O_4
N_2	N_2	N_2O_4	N_2O_3, N_2O_4
CO	CO	O_2	O_3
CO_2	CO_2		

The composition and size of the clusters indicates that a large number of chemical transformations are triggered by the impact of the primary ion on these solids. Measurements on virgin surfaces indicate that this is not a result of cumulative damage to the surface by a primary ion bombardment. Rather, the large number of, say, N_2O_3 molecules which are present in a cluster formed upon bombardment of solid NO all originate in the impact of a single primary ion. The chemical processes involved appear to be highly specific. Certainly the nature of the secondary ion spectra is highly sensitive to the chemical composition of the solid and not only to its stoichiometry. For instance, the SIMS of a 1:1 solid mixture of N_2 and O_2 is entirely different from the spectrum of solid NO.

A hypothesis for the nature of the processes involved in the formation of the large cluster ions observed in these experiments, which is compatible with all of the observations made so far, can be formulated (Figure 4). The initial impact of an energetic

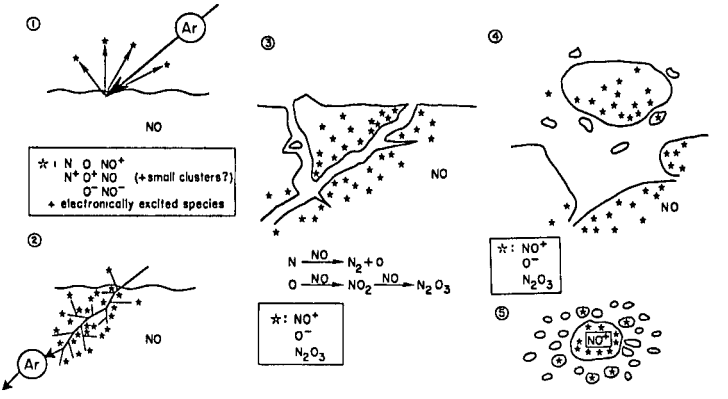


Figure 4. A hypothesis accounting for the SIMS of solid NO. The postulated sequence of events is indicated by the circled numbers from the initial impact (1) to the production of a $NO^+(N_2O_3)_n$ cluster ion (5).

primary ion on the surface of the molecular solid produces a batch of molecular and fragment ions at a variety of velocities from the top molecular layer. Further events depend on the size of the primary ion. If it is small (He^+), it will penetrate deep into the solid and the density of the deposited energy will be relatively small. If it is heavy (Ar^+), it will be stopped relatively soon and all of its energy will be deposited in a relatively short damage track produced, increasing the probability that relatively large pieces of the solid will be ejected. The nature of the damage in the solid will be somewhat similar to that known from radiation chemistry: fragments, ionized species, and electronically excited species will be produced. For instance, in solid NO, one can expect the formation of N, N^+, O, O^+, O^-, NO^+, NO^- in their ground and various electronically excited states. These original damage centers will be rapidly transformed by chemical reactions with excess NO in their surroundings. Reactions such as: $N + NO \rightarrow N_2 + O$, $O + NO \rightarrow NO_2$, $NO_2 + NO \rightarrow N_2O_3$, and analogous processes involving charged species will produce a considerable number of molecules of N_2O_3 in the damage track. The positive charges will be scavenged to yield NO^+, the negative charges will reside on species such as O^- and NO_3^-. If a piece of the solid is lifted from its surface, presumably with considerable mixing of its components, and if it contains a charge so that it can be observed in our experiments, it will most likely initially contain a large number of the original molecules of the solid NO and some of the products of the damage caused in the solid by the impact, i.e. primarily N_2O_3. This piece of low-temperature solid will stabilize itself by losing its most volatile components by evaporation. It is likely that these will be molecules held least firmly to the central charge, i.e. molecules with the lowest dipole moment and polarizability. In the case of solid NO, molecules of N_2O_3 should hold onto the central charge far better than molecules of NO, and this provides an explanation for the observed composition of the cluster ions. Similar arguments can account for the nature of other transformed solvating units observed in the molecular solids which we have investigated so far (e.g., ozone solvating units from solid oxygen). However, at this time the hypothesis is pure speculation and much additional experimental work will be required to support it more firmly.

Acknowledgement. This work was supported by an NSF grant (CHE 78-27094).

References

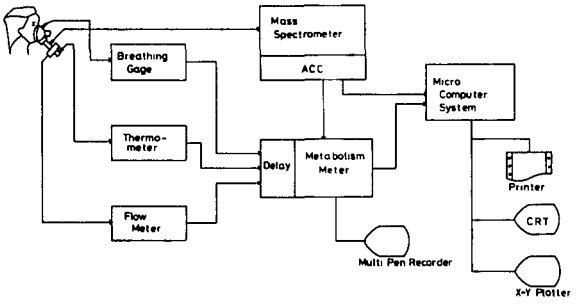
1. H.T. Jonkman and J. Michl, J.C.S. Chem. Commun. 751 (1978).
2. R.G. Orth, H.T. Jonkman, D.H. Powell, and J. Michl, J.Am.Chem.Soc. 103, 6026 (1981).
3. H.T. Jonkman and J. Michl, J.Am.Chem.Soc. 103, 733 (1981).
4. R.G. Orth, H.T. Jonkman, and J. Michl, J.Am.Chem.Soc., in press (1982).
5. R.G. Orth, H.T. Jonkman, and J. Michl, Int. J. Mass Spectrom.Ion Phys., in press (1982).
6. R.G. Orth, H.T. Jonkman, and J. Michl, J. Am. Chem. Soc. 103, 1564 (1981).
7. R.G. Orth, H.T. Jonkman, and J. Michl, submitted for publication.

DEVELOPMENT OF RESPIRATORY MASS SPECTROMETER AND COMPUTER SYSTEM FOR THE STUDY OF LUNG AND CIRCULATORY SYSTEM FUNCTION

I. NISHI, G. TOMIZAWA, Faculty of Science and Technology, Science University of Tokyo, Noda, Japan and L. TATSUTA, Faculty of Economics, The Dokkyo University, Soka, Japan

A new measuring system for the study of lung and circuratory system has been developed. The system consits of a respiratory mass spectrometer, a pneumotachometer, a thermometer(to detect the expired gas temperature), a heart rate meter, a respiratory rate checker and a microcomputer with its I/O units. The block diagram of the system is illustrated in Fig. 1. The mask used has been specially made to combine the pneumotachometer and the breath rate meter. Only the expired gas is sampled from down stream just out side of the exit valve of the mask.

Fig. 1



The principle of the measuring method for the fundamental factors is expressed by the following formulas. These formulas are deduced under the condition that the expired N_2 content is equal to the inspired N_2 content. This condition may be valid in the steady state of the respiration.

$$V_E(STPS) = \frac{P_B - PH_2O(tr)}{P_B - 47} \cdot \frac{310}{273 + tr} \int_0^T v_{E(t-t_D)}dt \qquad \text{---------- (1)}$$

$$VO_2(STPD) = \frac{P_B - PH_2O(tr)}{760} \cdot \frac{273}{273 + tr} \int_0^T \left(\frac{FO_{2I}}{FN_{2I}} \cdot FN_{2E} - FO_{2E}\right) v_E(t-t_D)dt \qquad \text{---------- (2)}$$

$$VCO_2(STPD) = \frac{P_B - PH_2O(tr)}{760} \cdot \frac{273}{273 + tr} \int_0^T (FCO_{2E} - FCO_{2I})\, v_E(t-t_D)dt \qquad \text{---------- (3)}$$

$$R = \dot{V}CO_2/\dot{V}O_2 \qquad \text{---------- (4)}$$

$$\dot{V}_E(\ell/min) = VO_2 \cdot \frac{60}{T} \qquad T = \sum_i^n T_i \qquad \text{---------- (5)}$$

where V_E, VO_2, VCO_2, are total air expired , O_2 consumed, CO_2 produced respectively, P_B, $PH_2O(tr)$ are Barometic pressure and the suturated water vapour pressure at temperature tr. v_E is expiring flow rate. t_D is delay time. FO_{2I} and FO_{2E} are the inspired and expired O_2 concentrations. T_i is the i-th breathing period.

The calculation for each breath is made by an analogue processor and the result is transmitted to the digital computer to perform further processing.

The physiological factors to be measured are as follows.

(1) FCO_2, FO_2, FN_2, FAr, P_ACO_2, P_AN_2, v, RR, H.R

(2) $\dot{V}_E$, $\dot{V}O_2$, $\dot{V}CO_2$, $\dot{V}N_2$, $\dot{V}_E/W$, $\dot{V}CO_2/W$, $\dot{V}O_2/W$, $\dot{V}O_2/H.R$, $\dot{V}O_2/A$, $\dot{V}_{AE}$, $\dot{V}_D$, FRC, V.C

(3) $R(=\dot{V}CO_2/\dot{V}O_2)$, $\dot{V}O_2/\dot{V}_E$, $\dot{V}CO_2/\dot{V}_E$, $\dot{V}_E/CO_2$

(4) E, E/A, E/W, BMR, RMR

These factors are printed out in the breath by breath mode , at 10, 30, 60 seconds intervals. After the real time measurement the results are rearranged on the X-Y plotter by using the memorized data. The examples are illustrated in Fig. 2 and Fig. 3. Several different programs have been developed according to the applications.

In Fig.2, the load is 5 minutes 150 watt ergometer repeated exercise followed by 5 minutes rest interval. In Fig.3 the load is stepping-wise. The measurement was made at 10 second interval. In the both figure, symbols a,b,c,d,e,f,g express $\dot{V}O_2/\dot{V}_E$, R(RQ), HR,RR, $\dot{V}O_2$, $\dot{V}CO_2$ and $\dot{V}_E$ respectively. These factors were drawn by different colors in the original figures. The changing patterns of the measured factors depend on the physiological state of the lung and circulatory system and the metabolic state of the tissues concerned. Therefor the pattern of the measured results tells us the physiological state and the metabolic response of the body.

With applying the present method, more accurate and higher dimentional physiological measurement will be easily and less invasively attained.

The difference of the measurements between the present method and the Daglas Bag method is proved to be within ±3% for up to 100 ℓ/min of $\dot{V}_E$ under the steady state condition. For the transit period, where the alveolar gas concentrations are changing, the changing rates of the alveolar partial gas contents($-V_{LA}\ dF^O{}_{2E}/dt$, $V_{LA}\ dF^{CO}{}_{2E}/dt$) should be taken into consideration to determine the true alveolar gas exchange.

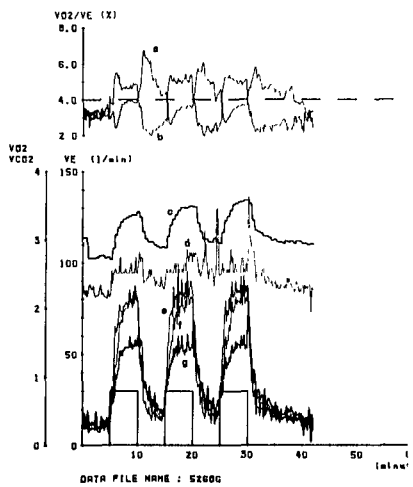


Fig. 2

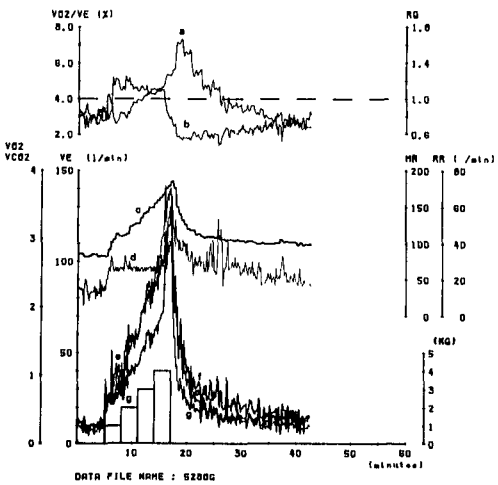


Fig. 3

USE OF A QUADRAPOLE MS FOR PRECISION GAS SOLUBILITY MEASUREMENTS IN BLOOD: M. J Criddle, J. S. Clark, T. R. Harris; Primary Children's Medical Center, Salt Lake City, Utah 84103.

Accurate knowledge of blood gas solubility for several inert gases is required for measurement of the pulmonary parameters described in our companion paper (1). Variations in solubility values among individuals and variations in solubility values with time for a given individual suggest the need for a practical apparatus capable of making accurate, serial solubility measurements on individual patients, using the same gas analyzer (mass spectrometer) used for patient monitoring. This need particularly applies to infants in respiratory distress who are receiving constant lipid infusion which can significantly influence the blood : gas partition for many gases.

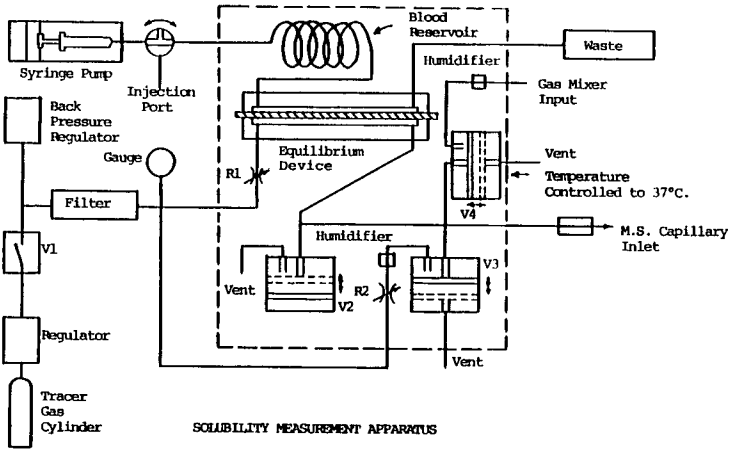
A practical solubility apparatus has been designed utilizing an equilibrium device and the principle of continuous flow proportioning of an inert gas mixture with a blood sample. The equilibrium device establishes gas partial pressure equilibrium and maintains separation between the gas mixture and the blood, permitting direct measurement of the equilibrated gas by the mass spectrometer. By mass balance, the blood gas solubility (λ) is given by:

$$\lambda j = \left(\frac{FIj}{Fj} - 1\right)\left(\frac{\text{Gas Flow}}{\text{Blood Flow}}\right)$$

where Fj and FIj are the equilibration and initial gas fractions of the jth component of the gas mixture.

Referring to the figure, the blood section consists of the syringe pump, injection port, blood reservoir, equilibrium device and waste. One-half cc of blood is manually placed into the blood reservoir through the injection port. The blood flow rate is held constant by the Harvard syringe pump. Gas flow through the equilibrium device is held constant by input pressure control and by the adjustable orifice R1. Input pressure to the orifice is controlled by the back pressure regulator. This flow is greater than the mass spectrometer gas consumption which allows the surplus gas to vent to atmosphere through V2. This design maintains a constant system pressure without contamination. Sampling of the gas mixture prior to equilibration is accomplished by switching V3. This is done without disturbing the flow or pressure in the equilibrium device.

Calibration of the mass spectrometer is provided by an eleven component gas mixer. The calibration gas enters the system through valve V4, again without disturbing the equilibrium device. The self-balancing principle of calibration is employed as described in a companion paper (2). All gases are humidified. The temperature of the system is maintained at 37°C.



SOLUBILITY MEASUREMENT APPARATUS

Care has been taken to minimize variations of all parameters which effect the equilibrium gas concentrations. Blood flow, gas flow, system pressure, temperature and humidity are tightly controlled. At present, the system accuracy is limited by the stability of the mass spectrometer. The use of the eleven component gas mixing calibration system overcomes the non linearities of the mass spectrometer when its characteristics are constant between measurement and calibration. Mass spectrometer drift is corrected to some degree by insoluble inert gas data which is affected by drift but unaffected by the equilibrium process. The mass spectrometer serves the function of a nulling sensor. However, this doesn't overcome the noise and non proportional drift which appears to be the limiting factors in system performance.

The above limitations to measurement accuracy are greatly influenced by the blood sample volume restrictions imposed by the physician. Reducing sample volume forces a proportional decrease in blood and gas flows due to time constant constraints of the equilibrium device. The gas flow reduction also forces an equal reduction in M.S. gas inlet flow, increasing the time constant of the gas analysis. These influences create intervals between measurements and calibration which are essentially inversely proportional to sample volume. This problem necessitates a compromise between the desired sample volume restriction and the desired accuracy specification. This compromise can be significantly reduced by a stable M.S.

The mass spectrometer system is described in the companion paper (3). The capillary for use with the solubility device has a smaller ID than the patient inlet tube to accommodate the lower gas consumption requirement of the solubility device.

REFERENCES

(1) Clark, J.S., Criddle, M.J., Farr, F.L., Harris, T.H., Non-Invasive Measurement of Mixed Venous Oxygen and Carbon Dioxide Contents. 1982 Conference on Mass Spectrometry and Allied Topics, sponsored by American Society for Mass Spectrometry.

(2) Clark, J.S., Farr, F.L., Wallace, W.D., Criddle, M.J., An Automatic, Precision Calibrator for an Eight Component Residual Gas Analyser. 1982 Conference on Mass Spectometry and Allied Topics, sponsored by American Society for Mass Spectrometry.

(3) Clark, J.S., Criddle, M.J., Farr, F.L., Removal of the Dynamic Range Limitation Imposed by the use of Counting Mode in Respiratory Gas Analysis. 1982 Conference on Mass Spectrometry and Allied Topics, sponsored by American Society for Mass Spectrometry.

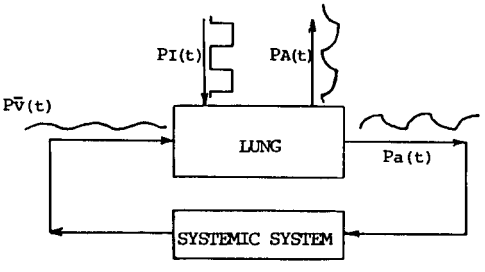
NON-INVASIVE MEASUREMENT OF MIXED VENOUS OXYGEN AND CARBON DIOXIDE CONTENTS; J. S. Clark, M. J. Criddle, F. L. Farr, T. R. Harris; Primary Children's Medical Center, Salt Lake City, Utah 84103.

In recent years, monitoring of the oxygen contents of blood supplying the lung and blood leaving the lung has become a major therapeutic guide in the management of adult patients in many intensive care units. Obtaining the pulmonary arterial oxygen data requires the insertion of a catheter into the pulmonary artery by way of the right heart. Such a highly invasive procedure is normally considered unacceptable for a sick newborn because of the risks, due not only to infant size and sensitivity to manipulation, but also due to the risks of cerebral damage. The cerebral threat is from catheter generated clots which could by-pass the protection normally offered by the lung because of shunting through fetal pathways. The objective of this paper is to present an outline of methodology for non-invasive monitoring of pulmonary arterial gas contents and other gas exchange parameters which utilize mass spectrometry technology.

Our method for determination of pulmonary arterial gas contents depends on 1) measurement of pulmonary blood flow ($\dot{Q}$) by an inert gas technique, and 2) knowledge of the relationship of alveolar gas concentrations and the blood as it leaves the lung.

While inert gas techniques have been applied successfully to the measurement of $\dot{Q}$ for cooperating subjects with fairly uniform lungs, the methods breakdown for 1) sick patients who can't tolerate rebreathing, or 2) non cooperative patients, or 3) subjects with significantly non uniform lungs.

Our method for measurement of $\dot{Q}$ overcomes these limitations. The problems associated with rebreathing and patient cooperation have been eliminated by providing inert gas delivery in the form of a continuous square wave as shown in the figure. The $\dot{Q}$ information is



contained solely in time varying data which is un-influenced by $P\bar{v}(t)$ to the extent that $P\bar{v}(t)$ is constant over a cycle period. The systemic system acts as a filter to the input function Pa(t), producing significantly less interference from the effects of venous return for a given cycle period than is found in the rebreathing method. The new method thus provides the opportunity for a continuous measurement of blood flow without interference with normal gas exchange.

The non homogeniety of the lung is dealt with by using a multiple compartment model, each compartment being characterized by a specific ratio of ventilation/perfusion ($\dot{V}/\dot{Q}$). A mix of five inert gases of differing blood solubilities is used to determine the relative ventilation ($\dot{V}i/\dot{V}$) of each compartment similar to that of Wagner et al (1). This is accomplished by solving the following linear set of 5 equations and 5 unknowns, obtained by applying mass balance to each compartment, for each gas.

$$\frac{PEj}{PIj} = \sum_{i=1}^{5} Aij \, \dot{V}i/\dot{V} \quad ,j = 1,5 \qquad (1)$$

where PEj/PIj is the ratio of the expired to inspired concentration of the jth gas, $\dot{V}i$ is the ventilation of the ith compartment, and

$$Aij = \frac{Pij}{PIj} = \frac{1}{1 + \lambda j(\dot{Q}/\dot{V})i} \qquad (2)$$

where Pij is the pressure of the jth gas in the ith compartment, and the ratios $(\dot{Q}/\dot{V})i$ are chosen such that the solution vector to equation 1 has all positive elements.

The relationship between alveolar physiologic gas concentration and gas concentration of blood leaving the lung is often determined by gas-blood solubilities and the assumption that chemical equilibrium is achieved between the alveolar gas and the blood. This assumption has been demonstrated to be invalid for O_2 for some patient classes (2). Evidence which questions CO_2 equilibrium - particularly in infants - has also been presented (3).

In our method, the questionable equilibrium assumption, Pai = PAi, for the physiologic gases is replaced by the constraint equations

$$PaO_{2i} = PAO_{2i}\left(1 - e^{\frac{-DO_2}{\lambda i\dot{Q}i}}\right) \qquad (3)$$

$$PaCO_{2i} = PAO_{2i}\left(1 - e^{\frac{-DCO_2}{\lambda i\dot{Q}i}}\right) \qquad (4)$$

Data for determining the two diffusion parameters DO_2 and DCO_2 is provided by the addition of physiologic isotopes $^{18}O_2$ and $^{13}CO_2$ to the inert gases. The constants are obtained from the following two equations, obtained from equations 1-4.

$$\frac{PE^{18}O_2}{PI^{18}O_2} = \sum_{i=1}^{5} \left(\frac{1}{1 + \lambda iO_2(\dot{V}/\dot{Q})i\left(1 - e^{\frac{-DO_2}{\lambda i\dot{Q}i}}\right)}\right) \frac{\dot{V}i}{\dot{V}} \qquad (5)$$

$$\frac{PE^{13}CO_2}{PI^{13}CO_2} = \sum_{i=1}^{5} \left(\frac{1}{1 + \lambda iCO_2(\dot{V}/\dot{Q})i\left(1 - e^{\frac{-DCO_2}{\lambda i\dot{Q}i}}\right)}\right) \frac{\dot{V}i}{\dot{V}} \qquad (6)$$

With DO_2 and DCO_2 determined, a complete set of model parameters are available for calculating the mixed venous contents of oxygen and carbon dioxide - our stated goal. Additionally, the gas contents of blood leaving the lung and pulmonary blood flow are determined non-invasively.

REFERENCES

(1) Wagner, P.D., Saltzman, H.A., West, J.B. Measurement of Continuous Distributions of Ventilation/Perfusion Ratios: Theory. J. Appl. Physiol. 36(5):588-599 (1974)

(2) Wagner, P.D. Ventilation-Perfusion Inequality & Gas Exchange During Exercise in Lung Disease. Muscular Exercise and the Lung pgs. 345-356 (1977)

(3) Holland, R.A.B., Edited by C. Bauer. Kinetics of CO_2 Uptake by Red Cells. Biophys. and Phys. of Carbon Dioxide Pgs. 299-205 (1980)

CARBON ISOTOPIC COMPOSITION OF THE UNITED STATES AND JAPANESE DIETS

D.A. Schoeller, C. Koralewski, Dept. of Medicine, Univ. of Chicago, Chicago, IL. 60637
K. Nakamura, Sankyo Co. Ltd., Tokyo, Japan, and
J. Santrock, Indiana University, Bloomington, IN.

Breath tests have been used to monitor the in vivo oxidation of ^{13}C labeled substrates by measuring the excretion of excess $^{13}CO_2$. In general, the excess $^{13}CO_2$ is determined relative to the $^{13}C/^{12}C$ ratio of a breath CO_2 sample collected before the labeled substrate is administered. Thus, it is assumed that neither the physiological effect of the substrate nor any other aspect of the test protocol changes the $^{13}C/^{12}C$ ratio of endogenous CO_2, and that any change in the ratio is due only to the oxidation of the label in the exogenous substrate. However, experience indicates that the $^{13}C/^{12}C$ ratio of endogenous CO_2 is not constant under all conditions. In order to better understand the source of variation in the endogenous $^{13}C/^{12}C$ ratio, we determined the isotopic composition of dietary carbon and related this to the isotopic composition of protein, carbohydrate, and fat in human plasma. Finally, the isotopic compositions of these three metabolic fuels were compared with the isotopic composition of breath CO_2 in resting and exercising subjects.

METHODS: Per capita dietary intake was obtained from literature for both the United States and Japan (1,2). The foods were divided into 11 classes (meats, poultry, fish, dairy, cereals, fruits, vegetables, potatoes, legumes, oils, and sugar) and the per capita intake of carbon as protein, carbohydrate, or fat was calculated for each group. Three to six samples of foods from each group were purchased in local markets in metropolitan Chicago and Tokyo. Fat and protein fractions from animal products were separated by extraction of the former with chloroform:methanol (2:1) and were analyzed separately. Plant products were not pretreated except for freeze-drying.

Heparinized blood and breath samples were collected from health laboratory personnel in Chicago and Tokyo. Fat was extracted from 2 ml of plasma by two equal volume washes with chloroform:methanol (2:1) and the solvent was removed by evaporation. Proteins were precipitated from the lipid free plasma with 0.8 ml of saturated $Ba(OH)_2$ and 0.8 ml of 10% and $ZnSO_4$ and freeze dried. The lipid free, deproteinized plasma was passed through a mixed bed strong acid/strong base ion exchange column (Rexyn™ 300, Fisher), leaving glucose as the major component remaining in solution. The glucose solution was freeze-dried.

One to 3 mg of each dried sample was combusted at 825°C over 1 g of CuO_2 and 0.05 g of silver wire in an evacuated, sealed quartz tube. The resulting CO_2 was cryogenically purified in vacuum and isotopically analyzed on a Nuclide 3-60 ratio mass spectrometer. The results were expressed relative to Pee Dee Belemnite limestone in units of "per mil":

$$\delta^{13}C_{PDB} = \frac{(^{13}C/^{12}C)_{sample} - (^{13}C/^{12}C)_{PDB}}{(^{13}C/^{12}C)_{PDB}} \times 1000$$

RESULTS and DISCUSSION: The differences between the isotopic compositions of the macronutrients in the American and Japanese diets were similar (Table 1). Proteins were the most enriched in ^{13}C, carbohydrates were depleted in ^{13}C by 1 to 2°/oo, and fats were depleted by 5 to 6°/oo relative to protein. The two diets, however, were isotopically distinct, as the American diet was enriched by 4°/oo relative to the Japanese diet. The ^{13}C enrichment in the American diet reflected greater use of cane sugar and corn fed animal products. Both cane sugar and corn are C_4 plants and are about 15°/oo enriched in ^{13}C relative to the more common C_3 plants (3).

The carbon isotopic compositions of the plasma proteins, carbohydrates, and fats in 9 Chicago residents and 6 Tokyo residents were generally similar to the dietary estimates (Table 1). The influence of diet on the isotopic composition of tissue has been previously demonstrated by Lacroix (4), and DeNero and Epstein (5). The nearly perfect match between the predicted and measured isotopic compositions in the American subjects probably indicates that very little mixing occurs between the carbon of the three macronutrients. The large difference between the predicted and measured carbon isotopic composition of fat in the Japanese subjects cannot be explained at this time but it is speculated that it may be due to the synthesis of fat from carbohydrate, as the Japanese diet is high in carbohydrates.

Table 1. Carbon isotopic composition of dietary macronutrients and plasma components in the United States and Japan.

	Isotopic Composition, $\delta^{13}C_{PDB}$, ‰			
	United States		Japan	
	Diet	Plasma	Diet	Plasma
Protein	-17.9	-18.1 (0.7)[a]	-21.1	-19.3 (0.2)[b]
Carbohydrate	-19.1	-19.6 (1.9)	-22.8	-21.1 (0.8)
Fat	-22.3	-21.6 (0.9)	-26.5	-23.1 (0.1)
Post absorptive CO_2				
predicted	-20.4	-20.4	-24.3	-21.9
measured		-20.9 (1.3)		-24.4 (1.2)

[a]standard deviation, n=9; [b]standard deviation, n=9.

The isotopic composition of expired CO_2 was predicted assuming that the average 70 kg subject produces about 110 ml/min of CO_2 from carbohydrates, 85 ml/min of CO_2 from fat, and 5 ml/min of CO_2 from protein (6). The values predicted from the diet agree very well with the measured values (Table 1). The values predicted from the measured isotopic compositions of the plasma macronutrients do not agree for the Japanese subjects.

Because of the isotopic differences between carbohydrates and fat, it would be expected that any change in the relative rates of carbohydrate and fat oxidation would change the isotopic composition of breath CO_2. To illustrate this effect, we measured the isotopic composition of two trained American subjects during a 90 min, 12 mile run (Figure 1). After the first 10 min of exercise, the CO_2 was depleted in ^{13}C relative to the start, thereafter, the expired CO_2 was enriched in ^{13}C. The ^{13}C enrichment during the latter portion of the run is consistent with the increased carbohydrate utilization that has been demonstrated by respiratory gas analysis (6). The depletion of ^{13}C during the first 10 min of the run may result from an isotope effect, or it may represent fat utilization.

The carbon isotope composition of breath CO_2 reflects the isotopic composition of the metabolic fuels. These in turn are controlled by the diet. Thus, changes in diet or metabolic fuel utilization can alter the isotopic composition of expired CO_2. These changes will produce systematic errors in the analysis of $^{13}CO_2$ breath test data unless they are properly controlled or unless appropriate baseline corrections are made.

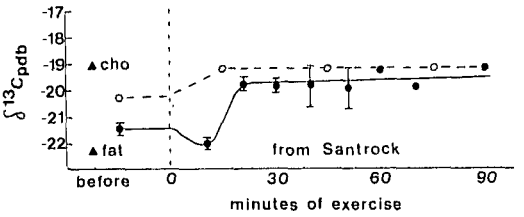


Figure 1. Effect of exercise on the isotope composition of expired CO_2. Solid circles are measured values from two subjects during a 12 mile run. Open circles are values predicted from fuel utilization data of Ravussin et al (6).

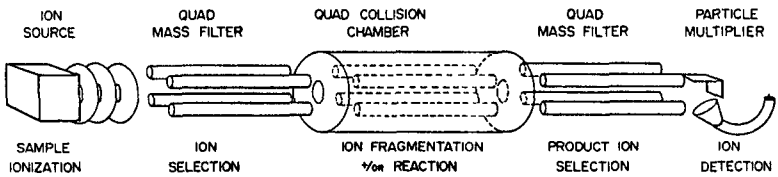
The authors thank R. Derouin for the isotopic analysis. This work was supported by NIH grant AM 26678.

1. Consumption of principle foods, In: Information Please Almanac, Atlas and Yearbook, Simon and Schuster, N.Y. 1981, p. 91.
2. Asahi Nenkan, Tokyo, p. 361, 1980.
3. M.H. O'Leary, Phytochemistry, 20:553, 1981.
4. M. Lacroix, In: Isotope Ratios as Pollutant Source and Behavior Indicators IAEA, Vienna, 1975, p. 343.
5. P. DeNiro and S. Epstein, Geochim. Cosmochim. Acta. 42:495, 1978.
6. E. Ravussin, P. Pahud, A. Dorner, et al. Pflugers, Arch. 382:197, 1979.

TANDEM MASS SPECTROMETRY FOR STUDIES OF DRUG ACTION AND METABOLISM.

R. A. Yost, H. O. Brotherton and R. J. Perchalski, University of Florida, Department of Chemistry, Gainesville, FL 32611, USA

The selectivity and sensitivity required for trace analysis of drugs in physiological samples are usually provided by chromatography or combined chromatography/mass spectrometry (GC/MS). Screening procedures that include chromatographic separations can involve lengthy sample preparation in addition to the significant amount of time required by the separations themselves. We are currently developing rapid, sensitive techniques based on tandem mass spectrometry (MS/MS) which should eliminate the need for chromatographic separation as well as greatly reduce the amount of sample preparation required. The new MS/MS techniques (1) replace the chromatographic separation with a mass spectrometric separation and allow simultaneous analysis of a number of drugs at the part per billion level. The Triple Quadrupole Mass Spectrometer consists of, in series, a dual chemical ionization/electron impact (CI/EI) sample ionization source, a quadrupole mass filter, an RF-only quadrupole that can be pressurized with a collision gas, a second quadrupole mass filter, and an electron multiplier. The sample is introduced into the inoization source in a glass vial on a direct insertion probe.



Three major applications of this technique will be discussed: (1) rapid screening for illegal drugs in racing animals; (2) sub-part-per-billion analysis of chlorinated compounds in human blood and urine; and (3) pharmacological studies involving localization, pharmacokinetics, and metabolism of antiepileptic drugs. Improved methods for the identification and quantification of drugs in physiological fluids are needed in order to control the use of drugs in racing animals. We are developing procedures which should allow these analyses to be performed much more rapidly than current methods with detection limits at the part per billion level. Several approaches to this problem are being considered, including the direct analysis of drugs in blood serum, the use of simple acidic and basic extractions, and deproteination of the blood serum. The direct analysis allows a rapid identification at concentrations greater than about 10 parts per million, but quantitation appears impractical due to the protein binding of most drugs and the thermal decomposition of the proteins in the blood serum at high temperatures. Both the extraction and deproteination procedures allow the detection and quantitation of the drugs at the part per billion level. Some of the most common drugs and their metabolites are being studied. These include phenylbutazone, procaine and its metabolite para-amino-benzoic acid, caffeine, theobromine, theophylline, and aspirin (the latter three having the same nominal molecular weight). A 1 µl sample of the solution containing the drug(s) of interest is placed in the tip of a direct insertion probe which is then inserted into the ionizer and heated rapidly to about 300°C. The MS/MS daughter spectra of the selected molecular ions produced by positive or negative CI are then collected.

Techniques for trace analysis of hexaclorobenzene and trichlorophenol in human serum and urine are also being developed. Hexane extracts are injected into a 40 cm packed microbore or capillary GC column, with detection by negative CI/selected reaction monitoring using one fragmentation for each compound. Detection limits in the high part per trillion range are possible at a rate of 2-3 samples/minute.

In addition to these studies, we are developing methods for pharmacokinetic and pharmacologic investigations that will allow: (1) determination of regional distributions of drugs, metabolites and biomolecules in target organs; (2) determination of the time-course of drug uptake into and release from target organs; and (3) determination of structures of all metabolites of a particular drug that are present in plasma from parent drug fragmentation patterns. The first of these will give information that can be used to formulate a mechanism of action of a particular drug by association of drug location with proximal changes in biomolecule concentration and function of surrounding anatomical structures; the second and

third will give valuable data that can be used to establish dosage regimens, therapeutic monitoring schedules and identify metabolites that may also have pharmacologic activity. Currently, we are concentrating our efforts on the antiepileptic drugs, including phenobarbital, phenytoin, carbamazipine, ethosuximide valproic acid and diazepam. These drugs are determined in small (10-15 mg) samples of rat brain tissue after homogenization and extraction. After chronic or acute dosing, depending on the type of information sought, the brain is sectioned by a microsurgical technique that allows clean separation of various brain regions, such as: sensorimotor cortex, cerebellar gray and white matter, visual cortex, hippocampus, corpus callosum and basal ganglia. The tandem quadrupole makes it possible to assay each sample for any or all drugs simultaneously by solids probe in as little as 2-3 minutes and by use of a short GC column in as little as 20 seconds.

Pharmacokinetic studies can be performed without disruption of a drug regimen by substituting for a single dose the stable-isotope labeled drug. The first stage of mass separation in MS/MS provides a rapid way to monitor the time-dependent concentrations of both the labeled and unlabeled drugs as well as metabolites. This technique has been employed to determine the half-life, under steady state conditions, of antiepileptic drugs such as phenytoin.

Structural elucidation of metabolites by MS/MS is possible for many drugs by analysis of single plasma extract (2). Since metabolites that are not present in plasma are not generally bioavailable, this determination gives a good indication of drug byproducts that may have pharmacological activity. The steps involve: (1) determination of the CI and daughter spectra of the parent drugs, in order to identify characteristic fragment structures (daughter ions and neutral losses) which wolud be present in metabolites; (2) selection of one or more of these daughter ions or losses; (3) determination of a parent spectrum for the selected daughter ions or neutrals in a plasma sample in order to identify all metabolite parent ions which yield the characteristic fragment structures; and (4) determination of daughter spectra for each parent to permit elucidation of the complete metabolite structure. Since metabolites are degradation or addition products of parent drugs, this method can be applied generally.

(1) R. A. Yost, C. G. Enke, Anal. Chem., 1979, 51, 1251A-1264A.

(2) R. J. Perchalski, R. A. Yost, to appear in Anal. Chem., July 1982.

TOC 6 IDENTIFICATION OF HUMAN URINARY METABOLITES OF BUPROPION; PISAL CHANDRASURIN, DAVID H. SCHROEDER, MELVIN L. HINTON, JULIE L. EISEMAN, and DAVID A. BRENT; Wellcome Research Laboratories, Research Triangle Park, North Carolina 27709

Metabolites of bupropion hydrochloride (Wellbutrin®; 2-tert-butylamino-3'-chloropropiophenone hydrochloride), an antidepressant, were identified in human urine. The drug was labeled with carbon-14 in the carbonyl moiety. Several radioactive fractions from urine were obtained using HPLC and further described by their retention times as determined by gas chromatography using an FID detector in series with $^{14}CO_2$ detector. By using GC/MS on EI and CI modes, five metabolites of the drug were identified. The metabolites were the isomeric aminoalcohol reduction products of bupropion, glucuronides of these aminoalcohols, hydroxy-t-butyl derivatives of the aminoalcohol and the parent aminoketone and m-chlorohippuric acid. The mass spectra of these metabolites matched the mass spectra and the GC retention times of the corresponding synthetic compounds.

MASS SPECTRAL AND CHROMATOGRAPHIC STUDIES ON DETORUBICIN AND DOXORUBICIN.

John Roboz, Robert Suzuki, Demetra Silides, John Greaves, Marise Weil, and James F. Holland. Dept. Neoplastic Diseases, Mount Sinai School of Medicine, New York, N.Y. 10029, and Service D'Oncologie, Hopital Salpetriere, Paris, France.

Detorubicin, DET (13-diethoxyacetyl ester of doxorubicin) has clinically been shown to be a promising antileukemic drug (Jacquillat, Weil, et al., Cancer Treatment Report, 63, 889 1979). DET has been considered a pro-drug for doxorubicin, DOX (adriamycin) but having its own distinct pharmacologic and therapeutic properties (Campeneere et al., Cancer Treatment Reports, 63, 861 1979). We assume that DET persists in biological fluids for a limited time period as the esterified anthracycline. This might explain the unique pharmacologic properties attributed to it. Based on stability experiments, we propose to administer DET in 0.001 N HCl to prevent hydrolysis to DOX. Also, collected blood is kept (after immediate centrifugation) in a final concentration of 0.05 N HCl. For HPLC analysis DET and DOX are extracted with chloroform-methanol (4:1). For MS analysis the aglycone is utilized after hydrolysis of the extract with 0.01 N HCl (60°C, 30 min). Mass spectra (accurate masses, high resolution) of the aglycones of DET and DOX were obtained for the underivatized compounds using DCI with either CH_4 or NH_3 as the reagent gases and for DET using a belt type HPLC interface. Spectra of TMS derivatives were obtained with both EI and CI using direct probe and DCI. Ions suitable for high resolution selected ion monitoring were selected, exact masses were determined, and chemical compositions established. For SIM of DET and DOX in serum, after separation by reverse phase HPLC, we utilized the M^+ ions when DCI was used for the underivatized compounds. The $M-2H_2O$ ions were used with the HPLC interface. The EI mode gave the most satisfactory results when the HPLC belt was used for DET as the underivatized compound. TMS derivatives were best monitored as $M-CH_3$ ions using the direct probe (EI or CI), or as $M-CH_3$-TMS ions when DCI was used. The EI fragmentation pattern revealed characteristic fragmentation corresponding to the successive degradation of the side chain and the elimination of water from the ring structure. The technique permits the study of the intrinsic activities of DET prior to its partial in vivo conversion to DOX, and also the detection of the aglycones as possible metabolites of DET.

Supported by Grant CA-15936 from the National Cancer Institute and by the T.G. Martell Memorial Foundation for Leukemia Research. Work performed as part of the French-American Cooperation Program.

METABOLISM OF ENDO-DICYCLOPENTADIENE BY IMMOBILIZED CYTOCHROME P-450.

Richard B. van Breemen and Catherine C. Fenselau. Department of Pharmacology and Experimental Therapeutics, The Johns Hopkins University School of Medicine, 725 N. Wolfe St., Baltimore, MD 21205.

endo-Dicyclopentadiene, a widely used industrial intermediate, was incubated with rabbit liver cytochrome P-450 which had been immobilized on beaded Sepharose. Chemical derivatizations and deuterium labelling coupled with GC/MS analysis were used to characterize the metabolites. The structures of the two primary metabolites were identified as the monoepoxides of endo-dicyclopentadiene: endo-4-oxatetracyclo $6.2.1.0^{2,7}.0^{3,5}$ undec-9-ene (1) and endo-9-oxatetracyclo $5.3.1.0^{2,6}.0^{8,10}$undec-3-ene (2). Confirmation was made by comparison with material synthesized in the laboratory by peracetic acid oxidation of endo-dicyclopentadiene.

DETERMINATION OF PRIMARY STRUCTURE IN OLIGOPEPTIDES BY SECONDARY ION MASS SPECTROMETRY

J. B. WESTMORE

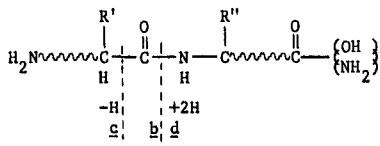
Department of Chemistry

WERNER ENS and KENNETH G. STANDING

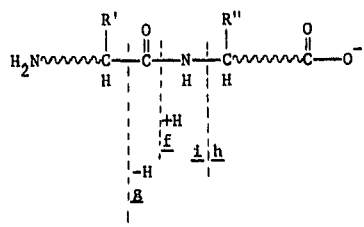
Department of Physics
University of Manitoba
Winnipeg, Manitoba R3T 2N2
Canada

Positive and negative secondary ion mass spectra obtained by bombardment of thin films of underivatized oligopeptides with a pulsed beam of Cs^+ ions of energy 5 - 15 keV were recorded using a time-of-flight mass spectrometer (1). Many of the secondary ions are metastable. Prominent features in the spectra are ions characteristic of the intact molecule and ions diagnostic of the amino acid composition of the peptide. Also observed are ions identifying the sequence of amino acids in the peptide, as shown below. Oligopeptides studied included leucine-enkephalin (Tyr-Gly-Gly-Phe-Leu), MW 555, (2), methionine-enkephalin (Tyr-Gly-Gly-Phe-Met), MW 573, (2), and [D-Ala^2]-met-enkephalinamide, (Tyr-Ala-Gly-Phe-Met-NH_2), MW 586, together with the larger peptides bradykinin (Arg-Pro-Pro-Gly-Phe-Ser-Pro-Phe-Arg), MW 1059. substance P octapeptide (Pro-Gln-Gln-Phe-Phe-Gly-Leu-Met-NH_2), 966, and substance P (Arg-Pro-Lys-Pro-Gln-Gln-Phe-Phe-Gly-Leu-Met-NH_2), MW 1347. Representative positive and negative secondary ion spectra are shown for bradykinin. The positive ion spectrum can be compared with spectra obtained for this molecule by fast atom bombardment (3) and field desorption (4).

SEQUENCE IONS IN POSITIVE SPECTRA:

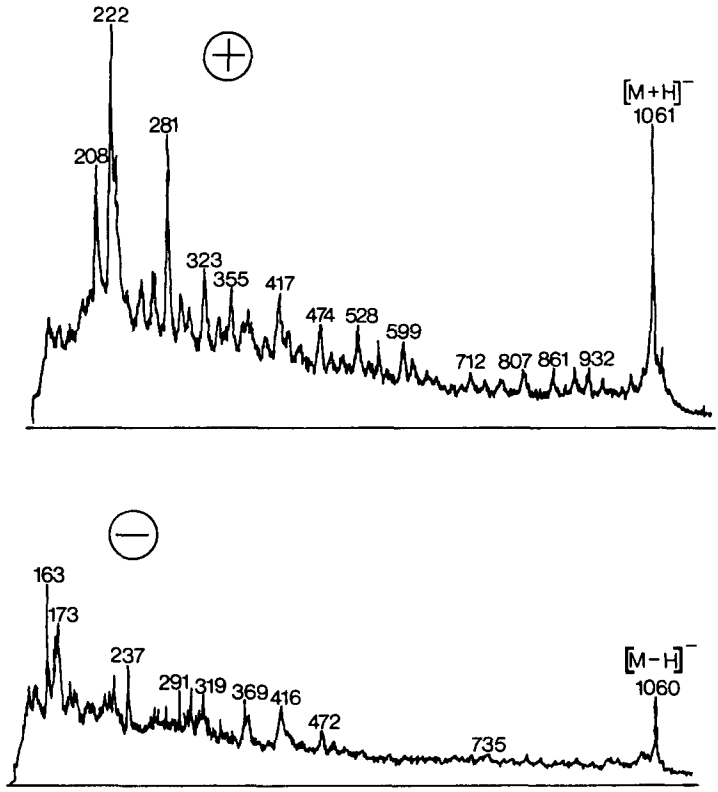


SEQUENCE IONS IN NEGATIVE SPECTRA:



H-Arg-Pro-Pro-Gly-Phe-Ser-Pro-Phe-Arg-OH

BRADYKININ (MW 1060.2)



(1). B. T. Chait and K. G. Standing, Int. J. Mass Spectrom. Ion Phys. 40, 185 (1981)
(2). J. B. Westmore, W. Ens and K. G. Standing, Biomed. Mass Spectrom. 9, 119 (1982)
(3). M. Barber, R. S. Bordoli, R. D. Sedgwick, A. N. Tyler and E. T. Whalley, Biomed. Mass Spectrom. 8, 337 (1981)
(4). S. Asante-Poku, G. W. Wood and D. E. Schmidt, Biomed. Mass Spectrom. 2, 121 (1975)

Fast Atom Bombardment in Specialized Analysis of Proteins and Peptides

Richard M. Caprioli, Laurence A. Smith and Carl F. Beckner

Analytical Chemistry Center and Department of Biochemistry and Molecular Biology, University of Texas Medical School at Houston, Houston, Texas 77030

Fast atom bombardment mass spectrometry has been used to analyze specific structural aspects of peptides and proteins, including N-terminal determination of proteins using dansyl chloride and real-time monitoring of proteolytic hydrolyses of peptides.

FAB mass spectrometry was used to identify and quantitate the dansyl amino acids from several proteins, including bovine serum albumin, bromelain, pepsin, trypsin, ribonuclease A, and bacteriophage P-22 tail protein (1). The amino acid sequence of the bacteriophage P-22 tail protein is not known, but its DNA sequence has been determined (2). Our analysis indicated that threonine is the N-terminal residue. This is the amino acid in position 2 in the sequence predicted from the DNA sequence. Signal-to-noise measurements were made with standard dansyl amino acids. The dansyl amino acids were found to have a linear response at concentrations less than approximately 5nmole/μl. At higher concentrations, little or no increase in signal was seen, which is consistent with the fact that FAB is a surface phenomenon. The responses of the dansyl amino acids were quantitated using dansyl aminobutyric acid as an internal standard, with a lower limit of detection of approximately 0.1nmole.

Real-time monitoring of proteolytic hydrolyses were performed using several enzymes, including trypsin, dipeptidyl aminopeptidase I, and carboxypeptidase Y. It was found that enzymatic activity could be maintained for up to twenty minutes when exposure times to the atom beam were at 30 sec. intervals. Activity is lost at this point due to drying of the sample matrix on the probe. This method was used to follow the complete hydrolyses of (val^4) angiotensin III, a heptapeptide, by carboxypeptidase Y (3). In the latter case, an ion at m/z 918 $(M+H)^+$ for (val^4) angiotensin III (arg-val-tyr-val-his-pro-phe) could be seen. After approximately 13 minutes into the reaction the most intense ion was that at m/z 771 corresponding to the species which would be produced on formation of a peptide which had lost the C-terminal phenylalanine. After 18 minutes, m/z 918 had further decreased in intensity, m/z 771 increased, and ions at m/z 674 (peptide minus phe, pro) and m/z 536 (peptide minus phe, pro, his) also appeared although of lesser intensity. After 30 hrs of hydrolysis outside the instrument, an aliquot subjected to FAB showed $(M+H)^+$ ions for amino acids with all of the other peptide fragments observed earlier now not detectable.

1. Carl F. Beckner and Richard M. Caprioli, Biomed. Mass Spectrom., submitted.

2. R.T. Sauer, W. Krovatin, A.R. Peteete and P.B. Berget, Biochem. J., in press.

3. Laurence A. Smith and Richard M. Caprioli, Biomed. Mass Spectrom., submitted.

FABMS IN PROTEIN SEQUENCING: APPLICATION TO MACROMOMYCIN, NEOCARZINOSTATIN AND DNA-GENERATED PROTEIN SEQUENCES

B.W. Gibson and K. Biemann

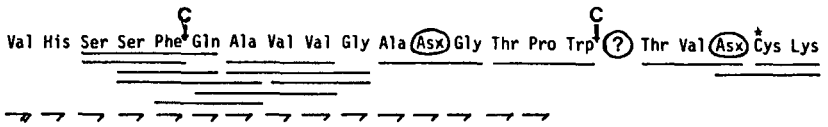
Department of Chemistry
Massachusetts Institute of Technology
Cambridge, MA 02139

Recently we completed the determination of the primary structure of macromomycin (MCR) (1) and modified the sequence of neocarzinostatin (NCS) (2), two related antitumor proteins, using a combination of Edman degradation, GCMS and FABMS. The latter technique, FABMS, proved to be a particularly powerful and sensitive method for solving many and often intractable problems encountered in the sequencing of these two proteins.

We applied FABMS to the study of MCR at a time when the structure was near completion. The FABMS experiments were performed on either intact or specific enzyme hydrolyzates of the tryptic peptides of MCR. The resulting spectra gave the protonated and sodium cationized molecular ion clusters for the various underivatized peptides in the complex mixture and, in the case of pure peptides, limited sequence ions. We then compared the molecular weights of the peptides expected from our proposed or tentative sequences with those observed. This allowed us to rapidly confirm or disprove sequences, identify and correct gaps in the sequence, and make the remaining amide and acid assignments.

The third tryptic fragment from S-carboxymethyl MCR, T-3, provides a good example of this strategy. GCMS experiments had identified various peptides (underlining) and Edman degradation (indicated by →) had twice gone 15 cycles. Together they left two Asx residues unassigned and the possibility of a gap between Trp and the C-terminal five amino acids:

MCR T-3



We hydrolyzed T-3 with α-chymotrypsin (c) since there existed two primary cleavage sites for this enzyme, Phe and Trp. The FABMS spectrum of this complex hydrolyzate (Fig.1) indicated three abundant molecular ion clusters and a less abundant cluster that was subsequently identified as originating from cleavage at a secondary site. The identifications of the three major peptides with molecular weights of 575, 678, and 1099 resulted in the following assignments:

Val His Ser Ser Phe (575) Gln Ala Val Val Gly Ala Asp Gly Thr Pro Trp (1099)

Gly Thr Val Asn Cys Lys (678)

The peptides of MW 575 and 1099 were easily identified as the first two chymotryptic peptides. The latter valine requires that Asx is Asp in the undecapeptide. The third peptide MW 678 was identified as the C-terminal chymotryptic peptide containing a previously unidentified glycine which was consistent with homology considerations between MCR and NCS, and with the assignment of Asx as Asn. Thus, from one single FABMS experiment we were able to make two amide/acid assignments, place a missing amino acid, and confirm the general correctness of the T-3 tryptic peptide.

Neocarzinostatin presented a somewhat different problem. A sequence had been previously published but was thought to be incorrect in light of its comparison to the homologous MCR (3). We used FABMS to rapidly pinpoint the regions of error by carrying out a set of similar experiments on the tryptic peptides of NCS. We found major discrepancies in the largest tryptic fragment that showed that an error in the ordering of the sequenced secondary chymotryptic peptides had occurred. In addition, three missing and five misidentified amino acids were discovered and corrected. The final modifications to the sequence of NCS were made by a combination of FABMS and GCMS experiments that concentrated on these regions.

These results demonstrated the utility of FABMS for checking the correctness of protein structures and it was of interest to explore the utility of this approach to the testing and verification of the amino acid sequence of large proteins deduced from the DNA sequence of the corresponding structural gene (4). Digestion of the proteins (∿10 nmol) with trypsin should give a mixture of peptides the molecular weights of which would be calculated based on the proposed amino acid sequence and the specificity of this enzyme which cleaves after lysine and arginine. Agreement with the molecular weights found upon FABMS of the mixture

would confirm the structure, disagreement would point at the regions where the DNA sequence must be in error.

Initial results using S-carboxymethyl bovine serum albumin (BSA, MW 66,000) as a model protein showed only 15-20 peptides, a coverage of only 20%. However, when we fractionated the tryptic hydrolyzate into 5 fractions by HPLC, we identified a much larger number of peptides (∿50), covering about 55% of the sequence. Fig. 2 shows a small part of these data.

We are now in the process of applying this technique to proteins whose corresponding DNA is being sequenced. In the case of peptides that are identified but do not fit the predicted protein sequence, we are developing a strategy which reveals the insertion/deletion errors or base misidentifications in the DNA sequence.

REFERENCES

1. Samy, T.S.A., Hahm, K.-S., Modest, E.J., Lampman, G.W., Keutman, K.T., Umezawa, H., Herlihy, W.C., Gibson, B.W., Carr, S.A. and Biemann, K., J. Biol. Chem., in press.
2. Gibson, B.W., Herlihy, W.C., Hahm, K.-S., Meienhofer, J., Samy, T.S.A., and Biemann, K., Manuscript in preparation.
3. Meienhofer, J., Maeda, H., Glaser, C.B., Czomboz, J., and Kuromizo, K., Science 178, 875-876 (1972).
4. Biemann, K., Proceedings of the Japanese Society for Medical Mass Spectrometry, 6, 21-32 (1981).

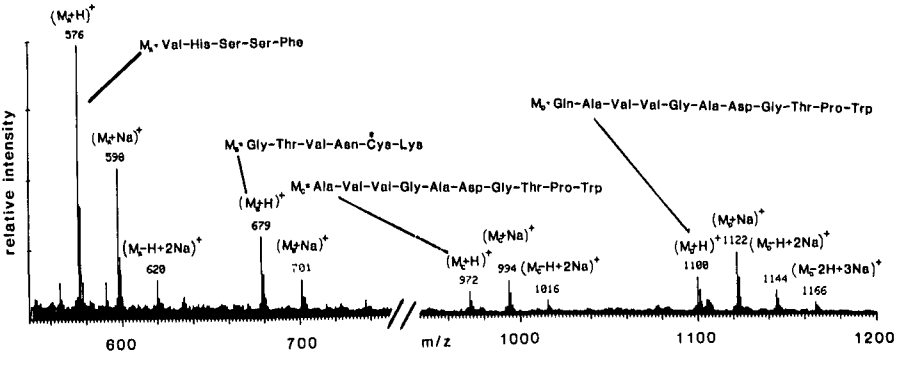


Figure 1. FABMS of an α-chymotryptic digest of MCR T-3.

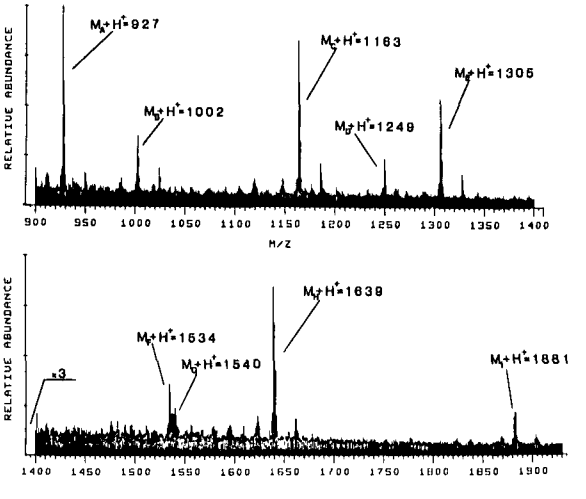


Figure 2. FABMS (region 900-1960) of HPLC Fraction 3 of tryptic digest of S-carboxymethylated BSA.

FAB Spectrometry of Steroid Conjugates

Joachim G. Liehr, Carl F. Beckner, Annie M. Ballatore

and Richard M. Caprioli

Analytical Chemistry Center and Department of Biochemistry

and Molecular Biology, University of Texas Medical School

at Houston, Houston, Texas 77030

Most steroids in plasma, bile, urine, or feces are present in a conjugated form. Conjugating groups on steroid hormones usually are glucuronic and/or sulfuric acid. Most bile acids are conjugated with glycine or taurine. Due to the polar character of these conjugating groups structural analysis of steroids is usually carried out after enzymatic or non-enzymatic hydrolysis. To test the applicability of FAB-MS to the analysis of intact, underivatized steroid conjugates, a series of bile salts and estrogen glucuronides or sulfates were analyzed by this novel technique. The FAB mass spectra of 13 estrogen (DES, estrone, estradiol, estriol) glucuronides and/or sulfates[1] and of six glycine or taurine conjugates of common bile acids[2,3] were all characterized by abundant molecular species. Protonated molecular ions and/or $[M+alkali]^+$ ions of high intensity were prominent and allowed an unambiguous deduction of the molecular weight of the sample. Even in FAB spectra of doubly conjugated estrogens, of dipotassium estradiol-17β 3-sulfate 17-(β-D-glucuronide) and of dipotassium estradiol-17β 3-(β-D-glucuronide) 17-sulfate, $[M+K]^+$ ions, m/z 643, were found to be base peaks when sample concentrations were sufficiently high on the insertion probe. Fragment ions were of low intensity or absent. The nature of the alkali component in the steroid conjugate salt was readily determined. When sample concentrations in the glycerol/water or glycerol/DMSO solvent were low, ionization of glycerol or glycerol oligomers would result in intense ions: m/z 115 $[M(glycerol)+Na]^+$; m/z 131 $[M(glycerol)+K]^+$; m/z 185 $[2M(glycerol)+H]^+$; m/z 207 $[2M(glycerol)+Na]^+$; m/z 223 $[2M(glycerol)+K]^+$.

The FAB spectral information obtained using commercially available steroid conjugates was utilized in the characterization of modified bile salts synthesized to study hepatic bile acid transport in vivo. N-cholyl derivatives of L-leucine, L-alanine, D-alanine, β-alanine, L-proline and γ-aminobutyric acid were prepared and these synthetic bile conjugates were characterized by EI and FAB mass spectra[2]. As seen with naturally occurring bile salts, FAB spectra of the synthetic conjugates featured ions formed by attachment of a proton or an alkali ion to the bile salt to give intense $[M+H]^+$, $[M+Na]^+$, or $[M+K]^+$ ions, which then showed little fragmentation.

In the course of syntheses of modified bile conjugates, FAB spectrometry was used to identify the reaction products obtained in the conversion of bile salts. For instance, the product of oxidation of sodium tauro-3α, 12α-dihydroxy-7-oxo-5β-cholanate (Fig. 1) was expected to be sodium tauro-3α, 12α-dihydroxy-7-oximino-5β-cholanate, but traditional methods of analysis (EIMS, ^{1}H-NMR, IR, UV) did not provide adequate structural information. The FAB spectrum of the reaction product (Fig. 2) showed that the product was mainly the expected 7-oximino derivative. Both compounds, the 7-keto and the 7-oximino bile salt were characterized by an $[M+H]^+$ and by an $[M+Na]^+$ ion formed by attachment to the neutral salt molecule (Fig. 1 and 2).

This work was supported in part by grants from the National Institute of Health (Grant Nr. 5 R01 AM 21504 and Grant Nr. 1 R01 CA 27539).

1. Joachim G. Liehr, Carl F. Beckner, Annie M. Ballatore and Richard M. Caprioli. Fast atom bombardment mass spectrometry of estrogen glucuronides and sulfates. Accepted for publication by STEROIDS.

2. Annie M. Ballatore, Carl F. Beckner, Richard M. Caprioli, Neville E. Hoffman and Joachim G. Liehr. Synthesis and Spectroscopic analysis of modified bile salts. Submitted for publication by Chemistry and Physics of Lipids.

3. J.O. Whitney, S. Lewis, K.M. Straub, F.C. Walls, A.L. Burlingame and M.M. Thaler. Quantitative and qualitative analysis of intact conjugated bile salts in human bile using radial compression HPLC, field desorption and fast atom bombardment mass spectrometry. Abstracts, 29th Annual Conf. Mass Spectrom. Allied Topics, May 24, 1981, Minneapolis, MN, p. 729.

Figure 1:

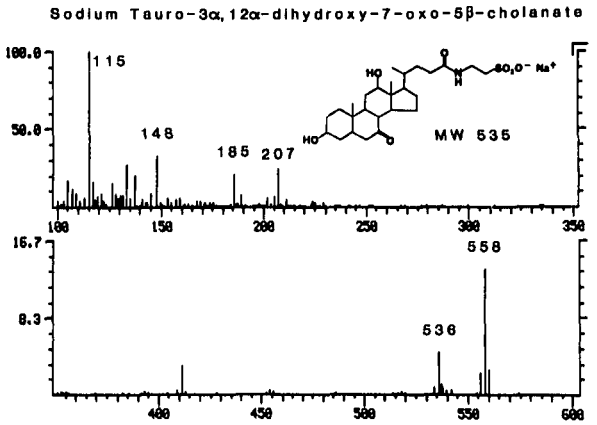
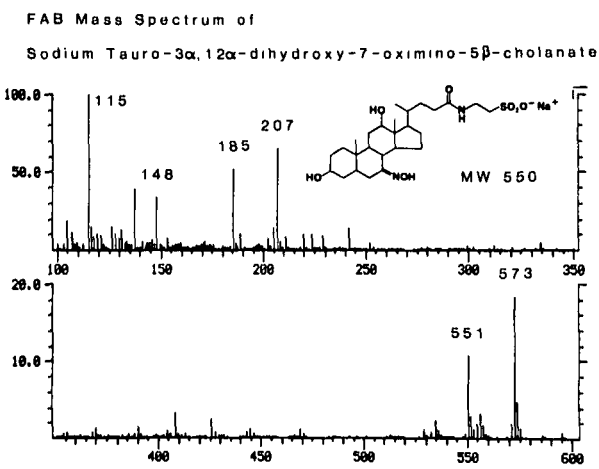


Figure 2:



MEASUREMENT OF BILE ACID 3-, 7-, 12-MONO SULFATES BY FAST ATOM BOMBARDMENT MASS SPECTROMETRY

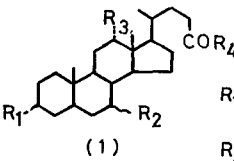
Y. Itagaki, T. Higuchi and Y. Naito
JEOL Ltd., Akishima, Tokyo 196 Japan

J. Goto and T. Nambara
Pharmaceutical Institute, Tohoku University, Sendai, Japan

Recently, HPLC has been applied to the separation of bile acid 3-sulfates.[1] The peaks obtained by HPLC, however, are sometimes difficult to assign. To assist in the identification of these HPLC peaks, the conventional FD ionization method has been available as a mass spectrometric technique.

But for these bile acid sulfates, the FD method is not effective due to the degradation of sulfates. The newly developed Fast Atom Bombardment (FAB) method has been attracting wide attention as an easier ionization method than FD. We have developed a FAB/FD combination source for the JMS-DX300 compact double focusing mass spectrometer. The fast atom beam energy used is 6 keV and beam diameter is approx. 2 mm. The FAB target is inserted and set in the ionization chamber by the standard FD probe. This FAB target does not require exact adjustment of its position and/or angle because a neutral beam is steerable.

In total 30 bile acid 3-, 7-, 12-sulfates (1) have been synthesized and submitted to positive and negative FAB measurements.



(1)

$R_{1,2,3}$ = OH or OSO_3H

R_4 = OH, glycine, taurine

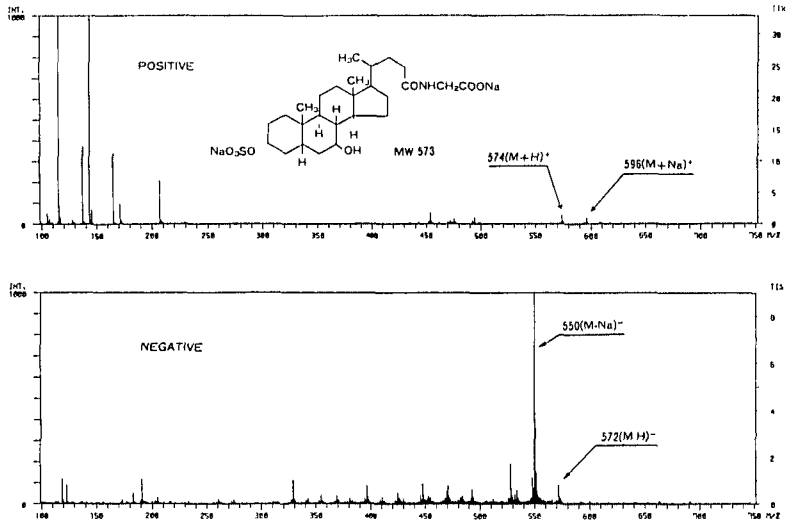
To confirm the fragmentation path way, metastable ions (B/E and B^2/E scan) were also studied.

It was found that the presence of sodium salt and other alkaline metals, which sometime give rise to disturbing ions in the FD method can be entirely ignored in FAB. All the compounds were measured as they were in the form of sodium salts.

The positive and negative ion spectra of glycoursodeoxycholic acid 3-sulfate are shown in Fig. 1. The $[M+H]^+$ and $[M+Na]^+$ ions are observed at m/z 574 and m/z 596 for the positive ion FAB spectrum. The loss of $NaHSO_4$ from the $[M+H]^+$ and $[M+Na]^+$ gave rise to m/z 454 and m/z 476, respectively.

Characteristic peaks m/z 143 and m/z 165 at lower mass region are assigned as Na_2HSO_4 and Na_3SO_4 ions. On the other hand, m/z 572 $[M-H]^-$ and m/z 550 $[M-Na]^-$ ions are observed in the negative FAB spectrum. The ion m/z 119 which corresponds to $NaSO_4^-$ ion was also found. Generally, the $[M-Na]^-$ ion was very strong, most of the bile acids gave $[M-Na]^-$ ion as base peaks.

Positive and negative FAB were confirmed to be effective techniques for identification of sulfates of bile acids and their glycine or taurine conjugates.



Positive and Negative Ion FAB Spectrum of sodium glycoursodeoxycholic acid3-sulfate

Reference:

1) J. Goto, H. Kato, Y. Saruta and T. Nambara: J. of Chromatogr., 226, 13 (1981).

ANALYSIS OF STEROID AND VITAMIN D GLUCURONIDES AND SULFATES BY FAB- AND EI-MS

Ian Jardine, Gale F. Scanlan, Vernon R. Mattox and Rajiv Kumar
Mayo Foundation, Rochester, Minnesota 55905.

We are involved in the synthesis, isolation, structural elucidation and function of glucuronide and sulfate conjugates of steroids and vitamin D. These conjugates are synthesized by conventional methods or are isolated from the bile of rats, for example, after administration of radiolabeled vitamin D or its active metabolites. We have investigated FAB-MS for the analysis of these conjugates and have found that this technique is an extremely useful complementary tool to EI-MS for their analysis.

When the free acid of steroid glucuronides was examined by positive ion FAB-MS, a protonated molecular ion was clearly identifiable for the simpler steroid glucuronides examined (e.g., Fig. 1a; the large "G" represents the glucuronide moiety; ions clearly associated with aglycone fragments are marked in Figs. 1a, 3 and 4 with an asterisk). However, as the complexity of the aglycone increased with the addition of hydroxyl groups, the intensity of the $[M + H]^+$ ion was low or absent. It was then necessary to add sodium ions (e.g., sodium acetate) to the sample on the probe to generate MNa^+ and/or $[M - H + 2Na]^+$ ions for molecular weight information (e.g., Fig. 1b). However, whereas the positive FAB spectra of all free acids examined produced characteristic and useful aglycone fragmentation (e.g., Fig. 1a), addition of sodium acetate eliminated such fragments (e.g., Fig. 1b). The negative ion FAB-MS of all steroid and vitamin D glucuronides examined revealed intense $[M - H]^-$ ions with minimal or zero fragmentation (e.g., Fig. 2).

Of considerable interest was the observation that the positive ion FAB spectra of the methyl esters of glucuronide-steroid conjugates gave very useful spectra. Thus, the molecular weight is clearly revealed as MNa^+, particularly if some sodium acetate is added to the sample, but useful fragmentation is still retained (e.g., the spectrum of the methyl ester of a diglucuronide; Fig 3). In general, ammonium salts of glucuronides (or sulfates) did not reveal MNH_4^+ ions but rather MNa^+, which were usually small unless enhanced by Na ion addition. Barium ($\frac{1}{2}Ba^{++}$) salts of steroid glucuronides did not give useful positive ion spectra.

The negative ion spectra of steroid and vitamin D sulfate conjugates clearly reveal $[M-H]^-$ ions with little fragmentation (e.g., Fig. 4a). The positive ion spectra consist predominantly of $[M + Na]^+$ or $[M + K]^+$ ions, with an ion of low intensity associated with the aglycone fragment (e.g., Fig 4b).

We isolated a glucuronide conjugate of 1,25-dihydroxy-vitamin D_3 from rat bile.[1] Positive ion FAB-MS of 2 µg of isolated material revealed an ion that is consistent with a natriated sodium salt of this glucuronide (Fig. 5). Following methylation of the carboxylic acid group and formation of trimethylsilyl ethers of the hydroxyl groups using 2 µg of isolated material, the fragmentation pattern of the product was compatible with that of a monoglucuronide of 1,25-dihydroxyvitamin D_3 (Fig. 6). The intact metabolite was treated with β-glucuronidase and the resulting aglycon gave a mass spectrum consistent with 1,25-dihydroxyvitamin D_3. *The mass spectra do not allow unequivocal location of the* glucuronide moiety to a particular hydroxyl group, but the fragmentation pattern of Fig. 6 suggests that conjugation at the 1 or 3 position is more likely. For example, m/z 131, which could result from cleavage between C-24 and C-25 on the side chain to give $(CH_3)_2 C = Si(CH_3)_3^+$ is prominent, but not as intense as would be expected for such a fragmentation.

[1] R. D. Litwiller, V. R. Mattox, I. Jardine and R. Kumar, J. Biol. Chem., in press, 1982.

Fig. 1a

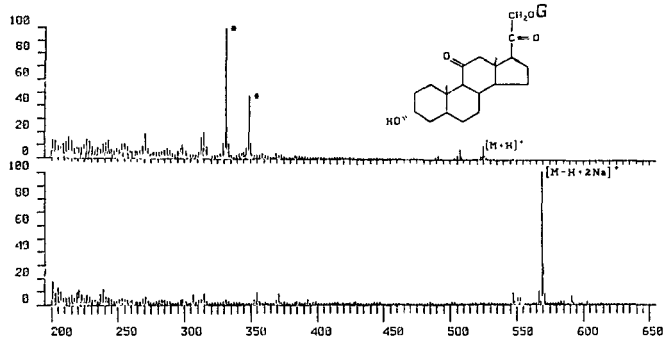


Fig. 1b

Fig. 2

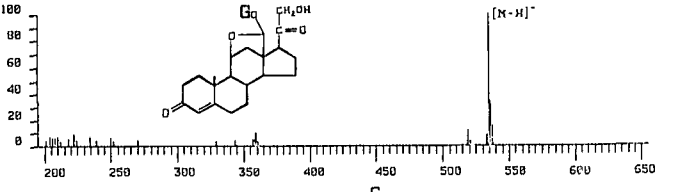


Fig. 3

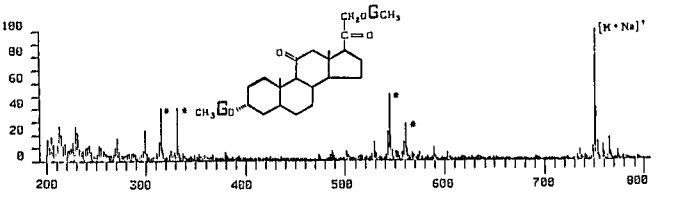


Fig. 4b

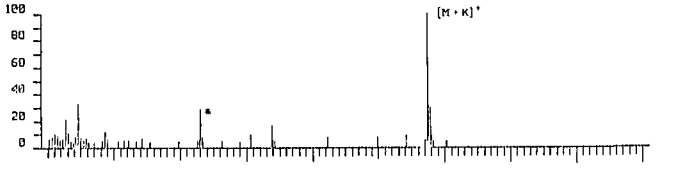


Fig. 4a

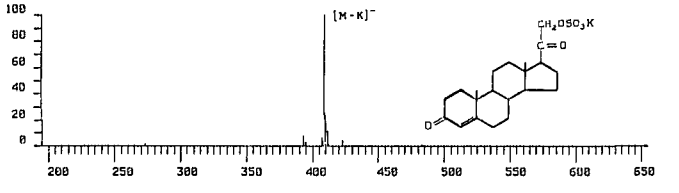


Fig. 5

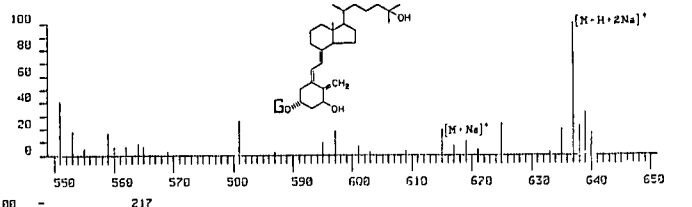
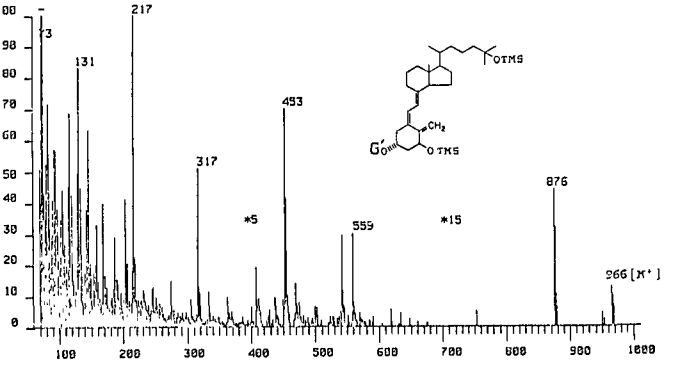


Fig. 6



THE APPLICATION OF FAB SPECTRA FOR STRUCTURE ELUCIDATION

Stradling R.S., Moore L.E., Taylor L.C.E., Wakefield C.J., Compson K.R.
Kratos Analytical Instruments, Barton Dock Road, Urmston,
Manchester M31 2LD, England

The development of Fast Atom Bombardment Mass Spectrometry has lead to analytical information on a wide range of compounds. Spectra produced often exhibit a great deal of structural information, and as an aid to interpretation the techniques of peak matching and metastable scanning can be used. The linked B/E scan is used to follow the unimolecular decomposition products of a selected parent ion. The FAB spectrum of Met Enkephalin shows all the necessary fragment ions to confirm the peptide sequence. In addition linked scanning confirms that these sequence ions also arise by unimolecular decomposition of the $(M + H)^+$ molecular ion, Figure 1. Further B/E scans from sequence ion fragments identifies subsequent products from these daughter ions. For example the loss of CO from the $(Tyr\text{-}Gly\text{-}Gly\text{-}Phe)^+$ ion to give a peak at 397 is confirmed. Additionally the $(Tyr\text{-}Gly\text{-}Gly)^+$ ion is shown to arise from the same parent ion, Figure 2. The negative ion linked scan reveals peaks at 409, 352, 295 due to $(Gly\text{-}Gly\text{-}Phe\text{-}Met)^-$, $(Gly\text{-}Phe\text{-}Met)^-$, $(Phe\text{-}Met)^-$ respectively.

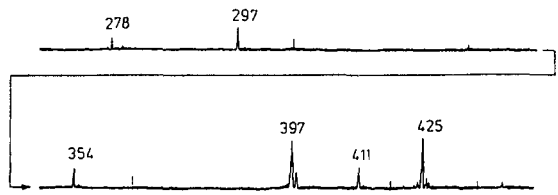


Figure (1) MET ENKEPHALIN B/E FROM $(M+H)^+$

The normal FAB spectrum of Eledoisin peptide (Lys-Phe-Ile-Gly-Leu-Met) gives an intense MH^+ ion at m/z 707, Figure 3. Accurate mass measurement against a sample of KI in glycerol at 9000 resolving power produced an answer accurate to 2.6 ppm. The intensity of the m/z 723 peak is found to increase with time and when mass measured against the MH^+ peak a mass difference of 15.994939 was found. This differs from the mass of oxygen by 1.5 ppm and indicates that oxidation of the peptide is occurring with the formation of a sulphone.

The B/E scan from the MH^+ ion produces the anticipated sequence ions, moreover the daughter ion peaks formed by decomposition of the sulphone (m/z 723) also gives the same sequence ion peaks. Differences do occur at the high mass end of the spectrum reflecting modification of the methionine residue.

A series of linked scans of Antiamoebin I, Table 1, illustrates how the amino acid sequence can be determined, particularly at the low mass end of the spectrum where background signal level may be high.

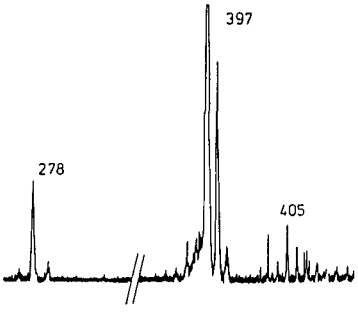


Figure (2) MET ENKEPHALIN SCAN FROM 425

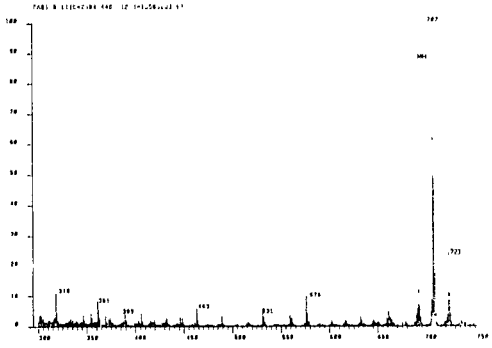


Figure (3) FAB CLEDOGIN PEPTIDE MH+707

• AMPIAMPHILIN I M wt 1669 (B/E SCAN)

PARENT I'N	DAUGHTER I'N	LOSS OF
1670	1432	• PRO-PHE *
1422	1317	AIB
"	1224	HYP-AIB *
1224	884	HYP-GLN-IVA
884	799	AIB
"	714	AIB-AIB
"	601	LEU-AIB-AIB
"	544	GLY-LEU-AIB-AIB
601	544	GLY
"	445	IVA-GLY
"	360	AIB-IVA-GLY *
544	445	IVA
"	360	AIB-IVA
360	275	AIB *
275	190	AIB *

Thus * establishes the sequence ions

Table (1)

FAST ATOM BOMBARDMENT AND FIELD DESORPTION MASS SPECTROMETRY OF NUCLEOSIDE AND NUCLEOTIDE ADDUCTS OF CHEMICAL CARCINOGENS, R. K. Mitchum, F. E. Evans, J. P. Freeman and D. Roach, Food and Drug Administration, National Center for Toxicological Research, Jefferson, AR 72079.

The mass spectral characterization of nucleoside phosphates and nucleoside adducts of chemical carcinogens has traditionally been approached by derivatization of the adduct via either persilylation or methylation producing a volatile derivative which can be characterized via either electron impact or chemical ionization techniques. Direct inbeam insertion has provided another useful technique but suffers from the same shortcomings as electron impact or chemical ionization. The lack of suitable molecular weight information renders these techniques of little value for the analysis of the title compounds.

Fast atom bombardment (FAB) represents a new ionization technique that has been shown to be suitable for the analysis of highly polar compounds. In contrast, field desorption (FD) mass spectrometry has proven to only have limited utility for the characterization of many highly polar compounds and when successful produces weak and transient ion currents.

The experiments reported here were performed on a Varian-MAT CH_5-DF modified for FAB with an Ion Tech neutral beam gun. The neutral gun was mounted perpendicular to the ion trajectory. The sample introduction was via the FD probe using a suitably constructed target. Glycerol was used as the matrix and xenon was used as the neutral beam source. The FD spectra were obtained with a Kratos MS-50.

The FAB mass spectrum of the nucleoside 2-deoxyguanosine is characterized by both the protonated molecular ion as well as cleavage of the sugar moiety. The FAB spectrum of 2-deoxyguanosine-5'-monophosphate disodium salt, however, shows no fragmentation and is comprised of protonated molecular ions and $(M + Na)^+$, $(M-1+2Na)^+$ and $(M-2+3Na)^+$ corresponding to the Na cluster of the free acid and the respective sodium salts. The FAB spectrum of N-acetyl-N-2-fluorenyl-5'-8-aminodeoxyguanosine the adduct of the carcinogen, N-acetyl 2-aminofluorene exhibits a protonated molecular ion at m/z 568 as well as products corresponding to cleavage of the sugar. Conversely the FD mass spectrum exhibits no molecular ion and only ions corresponding to cleavage at the sugar and fragmentation of the fluorene moiety.

The FAB mass specturm of the dinucleosides deoxyguanylyl-(3'-5')-deoxycytidine and deoxycytidylyl-(3'-5')-deoxyquanosine both exhibit protonated molecular ions. The N-acetylflourenyl derivative of deoxyguanylyl-(3'-5')-deoxycytidine produces a protonated molecular ion at m/z 778 and the corresponding $(M+Na)^+$ ion.

In conclusion the positive ion xenon fast atom bombardment induced mass spectrum of nucleosides, nucleotides, dinucleosides as well as their derivatives prepared from the carcinogen N-acetyl-2-aminofluorene all form protonated molecular ions or if analyzed as the salt the corresponding sodium cluster ion.

THE ROLE OF FAB IN THE SOLUTION OF DIFFICULT MASS SPECTRAL PROBLEMS

C.E. Costello, A.M. Van Langenhove, S.A. Martin and K. Biemann

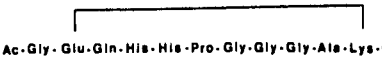
Department of Chemistry
Massachusetts Institute of Technology
Cambridge, MA 02139

FABMS is already taking its place as an effective new approach to structural problems, even though the phenomenon is not yet well understood and the experimental techniques are still evolving rapidly. We have had the opportunity to apply this tool to the characterization of a number of natural and synthetic samples. The results obtained for four problems are discussed here as illustrations of the types of information contributed by FABMS experiments.

The peptide 1 below and its cyclized analog 2 were synthesized by J.D. Young and G.R. Matsueda of the Cellular and Molecular Research Laboratory, Massachusetts General Hospital (MGH) with the goal of using 2 as an antigen to prepare antibodies to the γ-γ dimer chains of fibrin. It was necessary to demonstrate that compound 1 had the proper amino acid sequence and molecular weight, and that the cyclization to 2 had been successfully accomplished. The (+) FAB mass spectra of the two samples clearly showed both these points. In the spectrum of 1 the expected $(M+H)^+$ ion was detected at m/z 1172, the base peak of the spectrum. The complete sequence could be read from either end of the peptide, by observation of the series corresponding to cleavage of the NH-C_α bond with charge retention on the N-terminal portion and of the CO-NH bond with charge retention on the C-terminal portion. Both of these cleavages are accompanied by hydrogen migration to the fragment which retains the charge. The mass spectrum of 2 also had the $(M+H)^+$ ion as its base peak (m/z 1154), but sequence information was suppressed within the cyclic portion of the molecule. Therefore the points of cyclization were defined.

Ac-Gly-Glu-Gln-His-His-Pro-Gly-Gly-Gly-Ala-Lys-Gly-amide

1



Ac-Gly-Glu-Gln-His-His-Pro-Gly-Gly-Gly-Ala-Lys-Gly-amide

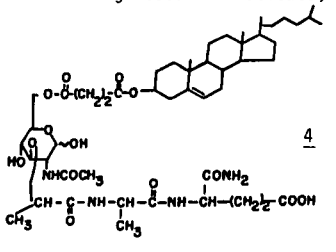
2

The synthesis of β-MSH (β-melanocyte-stimulating hormone) 3 by D. Carr and M. Rosenblatt of the Endocrine Unit, MGH, was designed to aid in the immunoassay of β-lipoprotein. Some question arose as to whether the proper peptide had been prepared, or a compound which had a higher molecular weight due to incorporation of a blocking group such as trifluoroacetyl had resulted. Figure 1 shows the portion of the (+) FABMS in the molecular ion region. This result indicated that a compound of the desired molecular weight had been prepared. A trypsin digest was carried out as a quick check on the sequence. Table 1 shows the molecular weights of fragments to be expected as a result of the activity of trypsin on this peptide. Figure 2 shows the m/z 650-750 region of the (+)FABMS, which includes the protonated and sodium cationized molecular ions of the trypsin fragments A, B, and C. It could thus be concluded that the appropriate molecular weight peptide had been prepared and that the sequence seemed correct.

3 H_2N-Asp-Glu-Gly-Pro-Tyr-Arg-Met-Glu-His-Phe-Arg-Trp-Gly-Ser-Pro-Pro-Lys-Asp-COOH

beta-MSH MW 2202

For compounds in two research projects which involve muramyl peptides, FABMS has been able to provide structural detail on the basis of mass spectral fragmentation and mass shifts observed after derivatization. The compound 4 was synthesized by C.M. Gupta of the Central Drug Research Institute, Lucknow, India, as one of a series of immunostimulants. The (+)FAB mass spectrum has a base peak corresponding to $(M+H)^+$ and a peak of nearly equal abundance corresponding to loss of water from the protonated molecular ion. Ions corresponding to other fragmentation pathways were of only very low abundance. The (-)FAB mass spectrum, however, had much higher overall signal intensity and many diagnostic fragments were observed, as shown in Figure 3. This spectrum confirmed the proposed structure and indicates that FABMS will be useful for detailed structural analysis of these compounds. Thirty micrograms of another muramyl peptide, called Factor S because it induces sleep in humans and other mammals, was isolated from 5000 liters of

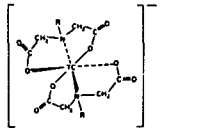


4

human urine, by J.R. Pappenheimer and M.L. Karnovsky of the Harvard Medical School. In one (+)FABMS experiment with this sample, the ions at m/z 922 and 940 were observed and were postulated to the $(M+H)^+$ and $(M+H)^+-H_2O$ as in the spectrum of 4. In order to determine the number of free carboxyl groups in this compound, dilute HCl in methanol was added to the sample in the glycerol matrix. Figure 4A and B shows the molecular ion region before and after esterification. The m/z 922 and 940 peaks shifted to m/z 950 and 968 respectively, indicating the presence of two free acid groups in the molecule.

FABMS has also been used to determine the number of ligands and the oxidation state of technetium in the radiopharmaceutical Tc-HIDA, an important radioimaging agent. After use of a Sep-Pak® to concentrate the tin and technetium complexes present in the eluate from the Technetium 99m generator, and HPLC to separate the Tc and Sn complexes from each other, the (+)FABMS of the HPLC peak showing radioactivity was obtained. The low resolution scan is shown in Figure 5. Exact mass measurement of the peak at m/z 685 by peak matching with the $(glycerol_7+H)^+$ cluster at m/z 645 at a resolution of $M/\Delta M = 10{,}000$ gave the exact mass shown, corresponding to the elemental composition $C_{28}H_{34}N_4O_{10}Tc$, indicating that the complex contained two ligands and had a net charge of -1, 5, requiring the addition of two protons to form the species observed.

These examples typify the results obtained in FABMS experiments when an attempt is made to select the most suitable conditions for the measurement by choice of extracting positive or negative ions, and simple steps to purify and/or derivatize the sample so that the analyst can assure that the type of information needed to answer the questions posed will result.



Partial chemical structure of Tc-HIDA Sodium bis [N-(2,6-dimethyl-phenylcarbamoylmethyl)iminodiacetato] technetate (III).

5

FABMS: SYNTHETIC HORMONE

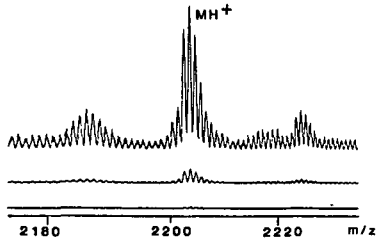


FIGURE 1

SYNTHETIC HORMONE MW CONFIRMATION BY FABMS SCAN OF TRYPSIN DIGEST

TRYPSIN FRAGMENT	MW	SYMBOL
$C_{31}H_{45}N_9O_{12}$	735	A
$C_{31}H_{46}N_{10}O_8S$	718	B
$C_{32}H_{46}N_8O_8$	670	C
$C_4H_7NO_4$	133	D
	(2256)	
- 3 H_2O	- 54	
HORMONE MW	2202	

TABLE 1

FABMS: TRYPSIN DIGEST OF SYNTHETIC HORMONE

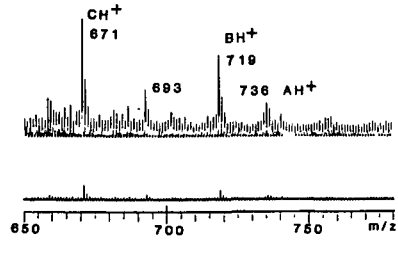


FIGURE 2

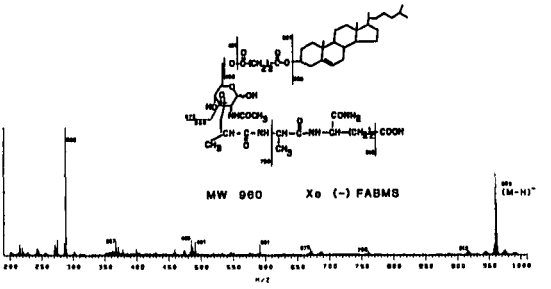


FIGURE 3

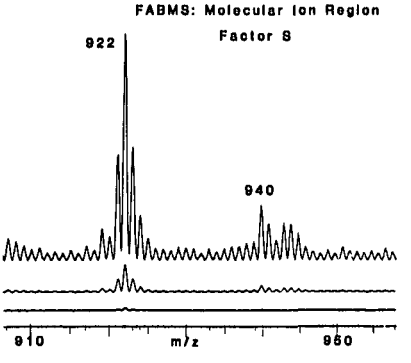


FIGURE 4A

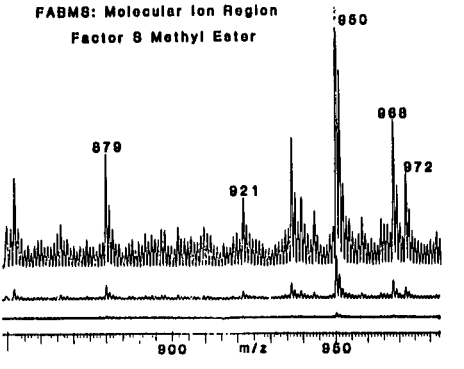


FIGURE 4B

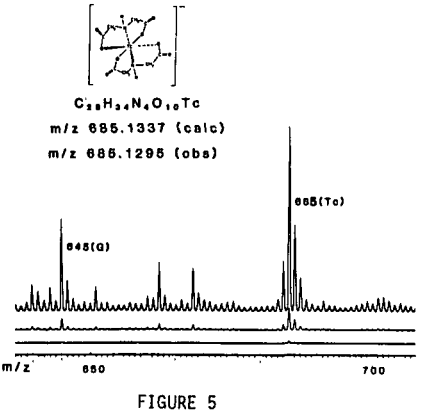


FIGURE 5

TOD 10 ANALYSIS OF MIXTURES BY HPLC AND FAB. T.R. Kemp, I.A. Lewis, J.C. Bill, VG Analytical Limited Tudor Road, Altrincham Cheshire, England.

The most recent ionisation method to be applied in mass spectrometry, fast atom bombardment (FAB), has extended the technique into new areas, particularly in biochemistry and pharmacology. Large polar molecular of biological significance can now be ionized intact without the need for chemical modification. The technique has been applied successfully in many areas, including peptides, glycolipids metalloporphyrins and oligo-saccharides. In many cases, however, the compound of interest is present in admixture with related compounds, and the current technology demands extensive sample preparation prior to admission to the mass spectrometer.

High performance liquid chromatography (HPLC) has all the attributes necessary to provide rapid separation of the active components from these mixtures. Not only can the technique cope with the size and polarity of the compounds under examination, but it also provides the sample in a form which is convenient for direct admission to the FAB source.

Examples of the application of the separative powers of HPLC and the analytical power of FAB mass spectrometry to the analysis of mixtures of compounds of pharmacological importance will be presented.

FAST ATOM BOMBARDMENT (FAB) MASS SPECTROMETRY USING A MAT CH5 DF MASS SPECTROMETER;
L. Baczynskyj and J. W. Nielsen, Physical and Analytical Chemistry Research, The Upjohn Company, Kalamazoo, MI 49001

An ion gun (purchased from Ion Tech.) has been adapted to our MAT CH5 double-focussing mass spectrometer. The connecting tube which houses the ion gun is 3.75" long and has the appropriate flanges at each end. Using the E.I./F.I./F.D. combination ion source, samples are introduced into the ionization region via the F.D. probe. The emitter holder has been outfitted with a stainless steel or copper plate. The sample under investigation is deposited on this plate in solution or suspension in glycerol. Argon or Xenon gas is used to produce the Fast Atoms.

The mass scale is routinely calibrated up to mass 1,500 in the E.I. mode using the UPACS II data system. The FAB mass spectra of all the compounds run so far had a molecular weight of less than 1,500. The spectra were acquired and processed using our computer system. Full mass spectra from mass 12 to 1,500 are obtained and the peaks due to glycerol can be subtracted whenever this is required. In this manner the mass spectra of Ficellomycin (M.W. 312), Penicillin O Na^+ salt (M.W. 352), Prostacyclin Na^+ salt (M.W. 374), Feldamycin (M.W. 407), Prostaglandin $F_{2\alpha}$·THAM salt (M.W. 475), Hydrocortisone Hemisuccinate Na^+ salt (M.W. 484), Pactamycin (M.W. 558), Erythromycin (M.W. 733) and Zorbamycin (M.W. 1411) were recorded. High resolution mass measurements by the peak matching technique of the pseudo-molecular ion and the major fragment ion of Erythromycin gave the following results: 734.4695 Found, 734.4690 Theory for $C_{37}H_{68}N_1O_{13}$; 158.1170 Found, 158.1181 Theory for $C_8H_{16}N_1O_2$. From these measurements it appears that the accuracy of the mass determinations are similar to those obtained by electron impact. Mass-analyzed Ion Kinetic Energy Spectra (MIKES) were obtained on the pseudo-molecular ion of Ficellomycin and Feldamycin. The determination of the peak centers was done manually.

In general, the FAB ionization technique is as easy and as reproducible as the electron impact ionization mode. However, the lack of a convenient mass marker for peak matching and the limited peak matching range (10%) make it somewhat difficult to use. Also the scanning is limited to 1,500 daltons using our computer system. So far we have run more than 100 samples with the FAB technique and found it as an excellent addition to our other techniques on hand.

TOE 1 GAS-PHASE BASICITIES FROM METASTABLE PROTON-BOUND DIMER DISSOCIATION; Donald H. Aue, Michael Pedley, Hugh M. Webb, and Michael T. Bowers, Department of Chemistry, University of California, Santa Barbara, CA 93106.

The relative gas-phase basicities of a large number of amines, pyridines, and other bases have been determined in equilibrium proton-transfer reactions (1) and compared with the ratios of products AH^+ and BH^+ from the

$$AH^+ + B \rightleftharpoons BH^+ + A \quad (1)$$

$$[AHB^+]^* \longrightarrow BH^+ + A \quad (2)$$

$$[AHB^+]^* \longrightarrow AH^+ + B \quad (3)$$

metastable proton bound dimer $[AHB^+]^*$ in reactions (2) and (3)* studied in a VG ZAB-2F mass spectrometer. The ratios of AH^+ to BH^+ in these experiments are correlated quantitatively with the relative gas-phase basicities of A and B within 0.5 to 1.0 kcal/mole. This metastable technique is uniquely useful when applied to heterocyclic bases and amino acids, where equilibrium proton-transfer measurements are not readily applicable because of low sample volatility or slow proton transfer.

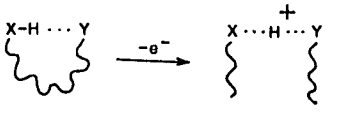
*S. A. McLuckey, D. Cameron, and R. G. Cooks, J. Am. Chem. Soc., 103, 1313 (1981).

TOE 2 ION-MOLECULE REACTIONS OF METAL IONS WITH FUNCTIONALIZED ORGANIC MOLECULES: CATIONIZED SPECIES, M. Castro, T. Adams, D.-J. Anderson and D.H. Russell, Dept. of Chem., Texas A&M Univ., College Station, TX. 77843.

Metals ions bound to organic species are frequently observed in mass spectra produced by surface-ionization of organics, e.g., laser desorption, SIMS, etc. These so-called "cationized" species could potentially provide important structural information on large molecules as well as insight into the mechanism(s) of surface ionization. Cationized organics can also be formed by gas phase ion-molecule reactions of metal ions with functionalized organic neutrals. We are presently using gas phase ion molecule reactions, using fourier transform mass spectrometry (FTMS) techniques, to model cationized species. The studies include model systems incorporating carboxylic acids, amines, and alcohols as neutral reagents and a wide variety of metal ions. The chemistry of these systems and mechanistic information will be presented.

PROTON-BOUND DIMER FROM UNIMOLECULAR DISSOCIATION OF A MOLECULAR ION. A PHOTOIONIZATION STUDY OF METHYL CELLOSOLVE. H. W. Biermann and Thomas Hellman Morton, Department of Chemistry, University of California, Riverside, California 92521

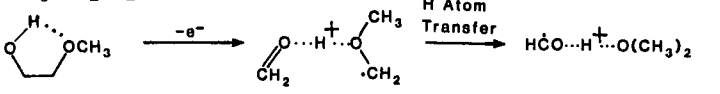
We have been interested in the formation of cluster ions from the unimolecular decomposition of molecules at low pressures following ionization.[1-4] One possibility for such a reaction is represented in reaction 1. Can removal of an electron from an internally hydrogen-bonded neutral lead to formation of a proton-bound dimer? Simple cleavage of the chain in the molecular ion should lead to such a species, provided that an internal proton bridge has been formed beforehand.

(1) 

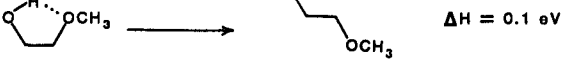
We have studied the photoionization mass spectra of methyl cellosolve, $CH_3OCH_2CH_2OH$, in order to probe whether reaction 1 takes place. Methyl cellosolve was chosen because microwave studies of the neutral molecule show that it is internally hydrogen bonded to a large extent.[5] The major ionic product from low energy photoionization at 10^{-7} Torr is protonated dimethyl ether, as shown in reaction 2. The assigned structure of this fragment ion has been confirmed by Cody and Freiser, using CID of the m/z 47 peak from electron impact ionization of methyl cellosolve in an FT-MS.[6]

(2) $$CH_3OCH_2CH_2OH \xrightarrow{\text{Photoionization}} \underset{\text{m/z 47}}{(CH_3)_2OH^+} + CHO\cdot$$

The products of reaction 2 certainly look like the products of decomposition of a cluster ion. Reaction 3 shows how such a cluster ion — formyl radical strongly hydrogen bonded to dimethyl ether — could be produced unimolecularly. As required by the depicted mechanism, photoionization of $CH_3OCH_2CD_2OH$ and of $CH_3OCH_2CH_2OD$ produce m/z 48.

(3) 

How can we demonstrate the intervention of the proton-bridged intermediates drawn in reaction 3? One way is to disrupt the internal hydrogen bond of the neutral prior to ionization. Without this hydrogen bond, cleavage of the chain should lead to formation of $CH_3OCH_2^+$ (m/z 45) instead. How can we disrupt the hydrogen bond of the neutral parent? Brown has shown that internal hydrogen bonding causes the first two ionization potentials of methoxy alcohols (the I. P.'s of the symmetric and antisymmetric combinations of oxygen lone pairs) to be approximately 0.4 eV closer together than they are in the absence of hydrogen bonding.[7] Since disruption of this hydrogen bond is only 0.1 eV endothermic,[8] long lived autoionizing electronic states of highly excited neutral methyl cellosolve should preferentially ionize via a non-hydrogen-bonded isomer, as implied by the thermodynamics of reaction 4.

(4) 

Adiabatic I.P. = 9.5 eV Adiabatic I.P. ≈ 9.3 eV

Figure 1 shows the ion yields from photoionization of methyl cellosolve at its adiabatic I. P. (9.5 eV from UV-PES[9]) and at its first vertical I. P. (10.2 eV). At the adiabatic I. P., the proportion of m/z 45 relative to m/z 47 is greater than at the vertical I. P., consistent with our prediction. Note that the total ion current at the adiabatic IP is not much lower than at the vertical I. P. — this is due to the fact that, at lower energies, many of the ionizations are taking place from long lived autoionizing states of the neutral parent ("optical metastables", to use Maccoll's terminology[10]). At the first vertical I. P., the proportion of vertical ionizations increases, and the m/z 47:m/z 45 ratio increases from 1.6 at 9.5 eV to 2.4 at 10.2 eV. We rule out alternative explanations by noting that, as the ionizing energy is further increased, the m/z 47:m/z 45 ratio decreases again; at 11.6-11.8 eV ionizing energy, the ratio drops to 0.44.

Acknowledgment. The support of the Committee on Research of the University of California, Riverside, Academic Senate and of the donors of the Petroleum Research Fund, administered by the American Chemical Society, are gratefully acknowledged.

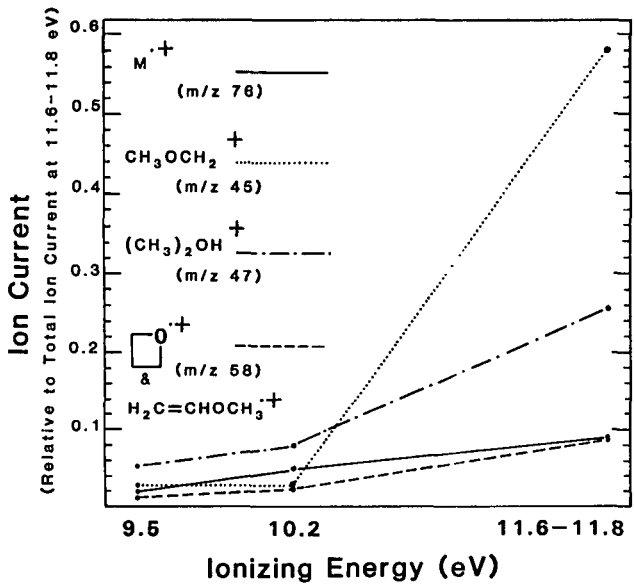


Figure 1. Ion yields (normalized to constant photon flux) from photoionization of methyl cellosolve using an oxygen resonance lamp (9.5 eV), a hydrogen resonance lamp (Lyman α, 10.2 eV), and an argon resonance lamp (11.6-11.8 eV).

REFERENCES

1. T.H. Morton, J. Am. Chem. Soc. 102, 1596-1602 (1980).

2. D.G. Hall, and T.H. Morton, J. Am. Chem. Soc. 102, 5686-5688 (1980).

3. W.P. Freeman, H.W. Biermann, and T.H. Morton, J. Am. Chem. Soc. 104, 2307-2308 (1982).

4. T.H. Morton, Tetrahedron Reports, in press.

5. P. Buckley and M. Brochu, Can. J. Chem. 50, 1149-1156 (1971); W. Caminati and E.B. Wilson, J. Mol. Spectrosc. 81, 356-372 (1980).

6. R.D. Cody and B.S. Freiser, personal communication, cited in ref. 4.

7. R.S. Brown, Can. J. Chem. 54, 1929-1937 (1976).

8. L.P. Kuhn and R.A. Wires, J. Am. Chem. Soc. 86, 2161-2165 (1964).

9. We are grateful to J. C. Schultz for recording the He(I) PES spectrum on the Caltech photoelectron spectrometer.

10. A. Maccoll, Org. Mass Spectrom. 17, 1-9 (1982).

ELUCIDATION OF CLUSTER ION STRUCTURES BY SECONDARY ION MASS SPECTROMETRY

Joseph E. Campana, Thomas M. Barlak, Brett I. Dunlap, Jeffrey R. Wyatt
James J. DeCorpo and Richard J. Colton
Naval Research Laboratory, Washington, D.C. 20375

Secondary Ion Mass Spectrometry (SIMS) by ion and neutral bombardment of alkali halides (MX) results in cluster ions of the form $[M(MX)_n]^+$ and $[X(MX)_n]^-$. We have recently reported the SIMS spectra of the alkali iodides[1-3] (MI) using a SIMS instrument with exceptional high-mass capabilities.[4] The high-performance instrumental capabilities of the SIMS instrument allowed the first observation of noteworthy anomolies in the ion intensities at high-mass values in the positive ion SIMS spectra (argon ion bombardment) of CsI(n=19), RbI (n=16), KI (n=11), and NaI (n=22), where n is the largest cluster ion species observed.

The characteristic features of the mass spectra previously reported[1-3] are the following: (1) the plot of the log ion intensity vs log n decreased linearly; (2) the n=13 species was equal to or more intense than the n=12 species; (3) the n=14 and 15 species were dramatically absent or of decreased intensity relative to the n=13 and 16 species; additionally, in the spectra of NaI and KI, (4) the n=22 species was equal to or more intense than the n=21 species; and (5) ions were not observed beyond the n=22 species. These striking features in the SIMS spectra led us to postulate that the increased stability of the n=13 cluster ion (containing 27 atomic species) indicated by its ion intensity enhancement relative to its neighbors (n=12, 14, 15), could be attributed to the symmetrically stable 3x3x3 "cubic-like" structure (where the numbers refer to the number of atoms on a side of a parallelipiped). Likewise, the ion intensity enhancement observed at n=22 (cluster ion containing 45 atomic species) was explained by a 3x3x5 "cubic-like" structure.

Increasing the mass of the primary particle usually results in an increase in the sputter and secondary ion yields. The ion intensity distribution for CsI under xenon ion bombardment is shown in Figure 1. Mass-resolved cesium iodide cluster ions were observed to n=70 or m/z 18,320. Ion intensity enhancements and corresponding anomolous n-regions were also observed corresponding to the 3x3x5 (n=37) and 5x5x5 (n=62) structures.

We have extended the SIMS results to the sodium halides (NaX) where experimental evidence is presented for ionic radii effects on the stability of specific cluster ions.[5] The SIMS positive ion cluster ion intensities for NaX (X=F,^{35}Cl,^{79}Br,I) are summarized in Figure 2. The ion intensity anomalies previously associated with "cubic-like" structures are present for all the sodium halides. It can be seen that the stability of the 3x3x1 (n=4) structure is more stable for cluster ions with smaller interatomic separation.

The principle conclusion drawn from our results and hypothesis is that one type of stable configuration for certain small alkali halide cluster species produced by sputter-emission mechanisms is the closed-packed, "cubic-like" geometry. Furthermore, the postulated "cubic-like" structures are intrinsic to the bulk crystal structure.

We have recently interpreted these SIMS results by a simple bond-breaking model or more appropriately a crystal-cleaving picture, which involves cluster-ion surface energies. Specifically, let β be the probability that a given bond is broken and $(1-\beta)$ that probability that it is not broken. In the simple cubic structure each atom is bonded to six nearest neighbors; thus, within this model, each such linear configuration occurs with probability

$$P_N(\text{linear}) = \beta^{4N+2}\,(1-\beta)^{N-1}, \qquad (1)$$

where N is the number of atoms in the configuration. For a 27-atom linear array (n=13) we have

$$P_{27}(\text{linear}) = \beta^{110}\,(1-\beta)^{26}. \qquad (2)$$

At the other extreme is the 27 atom 3x3x3 cubic geometry. It occurs with probability

$$P_{27}(\text{cube}) = \beta^{54}\,(1-\beta)^{54} \qquad (3)$$

Therefore, in the small β limit the cubic structure is β^{-66} more probable than the linear structure. For ionic crystals, the nearest neighbor description of bonding is somewhat inappropriate because of long-range electrostatic interactions. A crystal-cleaving picture, involving surface energies, is more appropriate. We have computed the surface energies of two 27-atom bcc clusters. The first is a 3x3x3 bcc cluster having six (110) planes and the second is the same except with the ion at one corner is removed and placed at the center of a nonadjacent face (all other charge signs reversed). Although, the latter structure is more spherical, its total energy is 1.04 greater than the former. The cluster size distribution (number of clusters vs number of atoms) resulting from the simple nearest neighbor bond-breaking model of SIMS has been studied for one- and two-dimensional and Bethe lattices.[6] In two-dimensional lattices, anomolies in the distribution can occur as a function of the probability of breaking any bond. The anomolies differentiate between square, honeycomb and triangular lattices. Theoretical cluster distributions based on Bethe lattices of coordination number 6 and 8, corresponding to the simple cubic and bcc salts respectively, are in excellent agreement with postive and negative ion CsI and NaI data.

These latter experimental data have been obtained on a state-of-the-art commercial instrument (V. G. Instruments) with a high-field magnet which has allowed the observation of mass-resolved CsI cluster ions (to n=99) exceeding m/z 25,000.[7]

References

1. J. E. Campana, T. M. Barlak, R. J. Colton, J. J. DeCorpo, J. R. Wyatt, and B. I. Dunlap, Phys. Rev. Letters 1981, 47, 1046-1049.
2. T. M. Barlak, J. E. Campana, R. J. Colton, J. J. DeCorpo, and J. R. Wyatt, J. Phys. Chem. 1981, 85, 3840-3844.
3. T. M. Barlak, J. R. Wyatt, R. J. Colton, J. J. DeCorpo, and J. E. Campana, J. Amer. Chem. Soc., 1982, 104, 1211-1215.
4. R. J. Colton, J. E. Campana, T. M. Barlak, J. J. DeCorpo, and J. R. Wyatt, Rev. Sci. Instrum., 1980, 51, 1685-1689.
5. T. M. Barlak, J. E. Campana, J. R. Wyatt, J. J. DeCorpo, R. J. Colton, submitted for publication.
6. B. I. Dunlap, submitted for publication
7. J. E. Campana, R. J. Colton, J. R. Wyatt, R. H. Bateman and B. N. Green, in preparation.

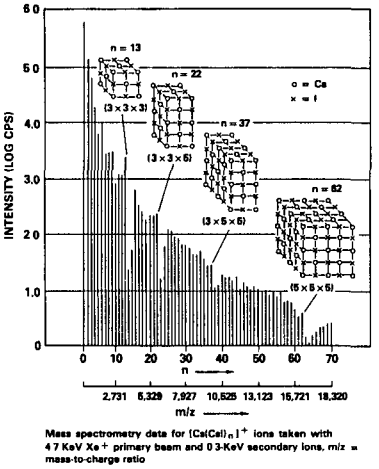


Figure 1

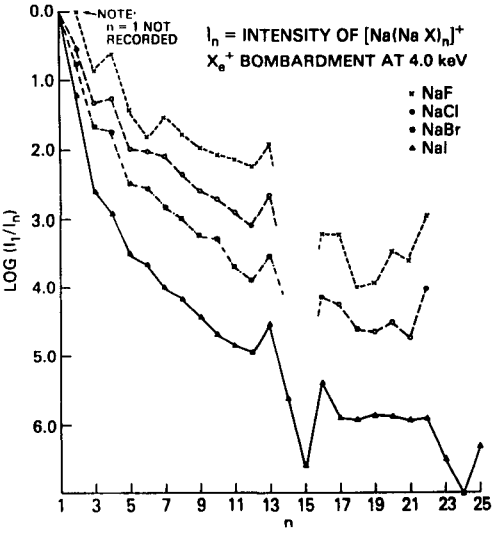


Figure 2

Gas Phase Reactions of

Iron Carbonyl Radical Anion Metal Clusters

John Wronka and D. P. Ridge
Chemistry Department, University of Delaware
Newark, Delaware 19711

Positive ions formed by electron impact on $Fe(CO)_5$ are known to undergo extensive clustering reactions with $Fe(CO)_5$ forming ions containing 2,3 and 4 iron atoms[1]. Only one clustering reaction has been reported of negative ions in $Fe(CO)_5$[1,2]:

$$Fe(CO)_3^- + Fe(CO)_5 \longrightarrow Fe_2(CO)_6^- + 2CO \qquad (1)$$

$Fe(CO)_4^-$ which is formed by electron attachment to $Fe(CO)_5$ has been reported to be unreactive with $Fe(CO)_5$[1,2]. If $Fe(CO)_5$ is reduced chemically in condensed phase, however, $Fe_2(CO)_8^-$, $Fe_3(CO)_{11}^-$, $Fe_3(CO)_{12}^-$ and $Fe_4(CO)_{13}^-$ are formed and have been identified by ESR[3]. Using the continuous trapped ion cyclotron resonance technique it is possible to observe $Fe_2(CO)_8^-$ and $Fe_4(CO)_{13}^-$ and several other cluster ions formed by negative ion molecule reactions in $Fe(CO)_5$.

The trapped ion technique used and the double resonance techniques used are essentially those described in the literature[4-7] The major reaction pathways are:

$$Fe(CO)_4^- \xrightarrow[-CO]{} Fe_2(CO)_8^- \qquad (2)$$

$$Fe(CO)_3^- \xrightarrow[-2CO]{} (Fe_2(CO)_6^-)^* \begin{cases} \xrightarrow{M} Fe_2(CO)_6^- \\ \xrightarrow[-CO]{k_{uni}} Fe_2(CO)_5^- \end{cases} \qquad (3)$$

$$Fe_2(CO)_6^- \xrightarrow[-CO]{} Fe_3(CO)_{10}^- \xrightarrow[-2CO]{} Fe_4(CO)_{13}^- \qquad (4)$$

$$Fe_2(CO)_5^- \xrightarrow[-CO]{} Fe_3(CO)_9^- \xrightarrow[-2CO]{} Fe_4(CO)_{12}^- \qquad (5)$$

Some ions which do not appear in this scheme may be generated by collision induced decomposition and then the subsequent chemistry of the ion formed may be examined. Most of the ions lose one or more CO ligands when subjected to cyclotron heating. A summary of the overall rate constants for reaction of some of the ions are given in Table I. The reactivity of the ions increases with electron deficiency. The electron deficiency is the number of electrons required in order for all iron atoms to have 18 valence electrons. The deficiences were determined assuming only

single metal-metal bonds.

A simple steady state treatment of the scheme in reaction (3) gives a value of $k_{uni} \cong 5\ s^{-1}$ assuming "strong" collisions.

Table 1

Relative Rate Constants

Ion	Electron Deficiency	Relative Rate
$Fe(CO)_3^-$	3	1100 ± 100
$Fe(CO)_4^-$	1	(1)
$Fe_2(CO)_5^-$	7	530 ± 100
$Fe_2(CO)_6^-$	5	20 ± 5
$Fe_2(CO)_7^-$	3	< 3
$Fe_2(CO)_8^-$	1	< 0.1
$Fe_4(CO)_{13}^-$	1	< 1

References:

1. M. S. Foster and J. L. Beauchamp, J. Amer. Chem. Soc., 97, 4808 (1975).
2. R. C. Dunbar, J. F. Ennever, and J. P. Fakler, Jr., Inorg. Chem., 12, 2734 (1973).
3. P. J. Krusic, J. San Filippo, Jr., B. Hutchinson, R. L. Hance, and L. M. Daniels, J. Am. Chem. Soc. 1981, 103, 2129.
4. R. L. Hunter and R. T. McIver, Jr., Anal. Chem., 51, 699 (1979).
5. C. Caldwell and J. Bartmess, presented at 29th Meeting of ASMS in Minneapolis, 1981.
6. J. Wronka and D. P. Ridge, Rev. Sci. Inst., 53, 491 (1982).
7. J. Wronka and D. P. Ridge, Int. J. Mass Spec. and Ion Phys., in press.

THERMOCHEMICAL DETERMINATIONS FROM WEAKLY BONDED CLUSTER IONS. METAL ION AFFINITIES FROM METAL BOUND DIMER IONS

S.A. McLuckey and R.G. Cooks
Department of Chemistry
Purdue University
West Lafayette, Indiana 47907

The methodology previously demonstrated for ranking proton affinities through the dissociation kinetics of proton bound dimer ions (1) has been extended to ranking metal cation affinities from the fragmentations of metal containing clusters. Metal bound cluster ions containing two ligands L_1 and L_2 bonded to a central metal ion M^+ are formed by laser irradiation of a metal foil or salt in the presence of a mixture of L_1 and L_2 in a combination Chemical Ionization/Laser Desorption ion source. Ions corresponding to the mass of $L_1ML_2^+$ are selected and subjected to high energy collisional activation. The fragment ions resulting from the dissociation of the cluster are monitored by a second stage of mass analysis. In those cases where a loosely bound metal centered cluster is formed, the most abundant fragment ions observed correspond to the mono-solvated metal ion as indicated below:

$$(L_1\text{---}M\text{---}L_2)^+ \xrightarrow{k_1} (L_1\text{---}M)^+ + L_2$$
$$(L_1\text{---}M\text{---}L_2)^+ \xrightarrow{k_2} L_1 + (M\text{---}L_2)^+$$

The relative rates k_1 and k_2 of the competitive fragmentation pathways, as reflected by the fragment ion abundances, indicate the relative metal ion affinities of L_1 and L_2. For example, Figure 1 shows the fragment ion spectrum obtained from collisional activation of sodium ion bound to ethanol and isopropanol. The relative fragment ion abundances show ethanol to be more easily lost from the complex than isopropanol and hence has a lower sodium ion affinity. Table I shows the rates for methanol loss relative to loss of L from metal containing clusters of the form $(MeOH)M(L)^+$ for $M=Ag^+$, Cu^+, and Na^+. These rates indicate the trends in metal ion affinities of several small alcohols.

TABLE I

M \ L	MeOH	EtOH	n-PrOH	i-PrOH	n-BuOH	t-BuOH
Ag^+	1	2.9	4.9	6.2	9.4	15.8
Cu^+	1	4.8	10.5	11.2	20.4	
Nu^+	1	3.0	5.1	7.7	13.2	15.0

In some cases fragment ion spectra indicate a rearranged precursor ion structure. For example, the ion formed by the attachment of two methanol molecules to sodium ion fragments to give primarily Na^+ attached to dimethyl ether with lesser abundances of $(Na+H_2O)^+$ and $(Na+CH_3OH)^+$ (Figure 2) in an analogous fashion to the fragmentation of $H^+ + 2CH_3OH$ which gives predominantly protonated dimethylether. In cases where fragmentations other than the simple losses of L_1 and L_2 are dominant, a ranking of relative cation affinities is precluded.

The method can be used to investigate the site of metal attachment in polyfunctional molecules. For example, it has been shown that Ag^+ bonds predominantly to the external double bond in 4-vinylcyclohexene and that it interacts with just one olefin in 1,3-butadiene.

Generalizations of the kinetic method in three further ways are in hand. (i) Affinities for negatively charged ions are being measured, e.g. hydride affinities of organoboranes. (ii) Ionization energies and other enthalpies of radicals are being examined. (iii) Affinities for polyatomic species such as carbenium ions, benzoyl ions, etc. are being attempted. In each case, generation of the appropriate cluster ion is the pivotal requirement.

(1) S.A. McLuckey, D. Cameron and R.G. Cooks, J. Amer. Chem. Soc., 103, 1313, 1981.

Figure 1

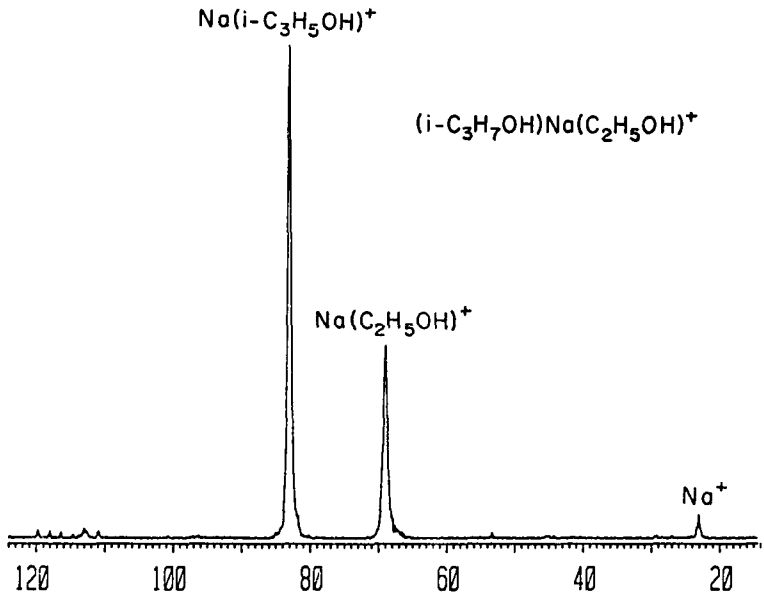
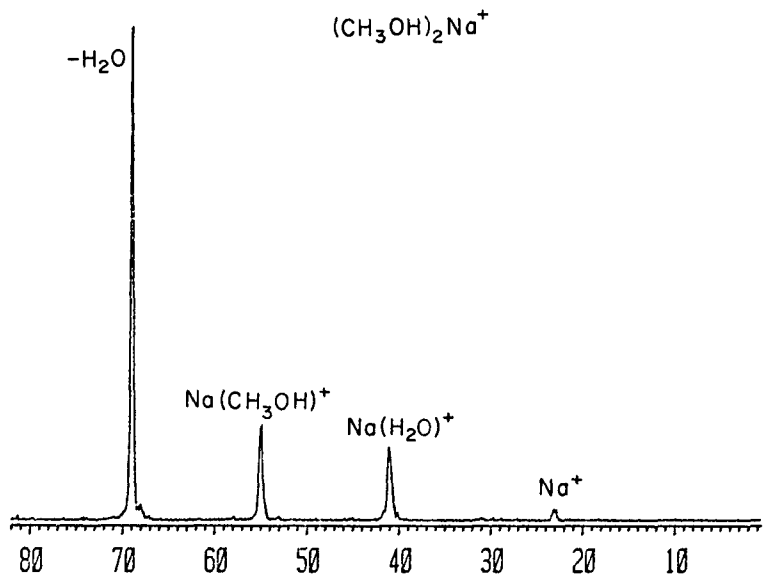


Figure 2



BIMOLECULAR PRODUCTION AND THERMOCHEMISTRY OF GAS PHASE IONS SOLVATED BY A SINGLET SOLVENT MOLECULE BY ION CYCLOTRON RESONANCE SOLVENT EXCHANGE EQUILIBRIA MEASUREMENTS.

J. W. Larson and T. B. McMahon
Department of Chemistry
University of New Brunswick
Fredericton, NB, Canada
E3B 6E2

Using ion cyclotron resonance trapped ion techniques and fast bimolecular processes involving the gas phase ion chemistry of $(CHF_2)_2O$, proton bound dimers of nearly 30 oxygen n-donor bases have been generated. In mixtures of two oxygen n-donor bases and $(CHF_2)_2O$, base exchange equilibria have been examined and thermochemistry of the processes obtained. Results reveal a remarkable constancy of hydrogen bond energies of 30.8 $\pm$ 2 kcal $mole^{-1}$ in symmetric proton bound dimers regardless of functional group involved or gas phase basicity. Exceptions to the constant hydrogen bond energy can be explained in terms of either inhibition of resonance by "solvation", relief or ring strain, or steric crowding. In unsymmetric proton bound dimers, the strength of the hydrogen bond is shown to be directly related to the difference in proton affinity of the two bases involved. In the few cases where data from other techniques is available, excellent agreement is obtained.

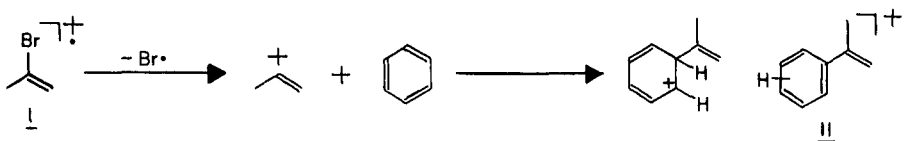
In negative ion systems bimolecular fluoride exchange equilibria between molecules bearing labile protons have been examined and accurate hydrogen bond energies between fluoride ion and proton acids obtained. Included in the systems examined is FHF^-, postulated to have the strongest known hydrogen bond.

MS/MS FOR THE INVESTIGATION OF THE STRUCTURE OF ION-MOLECULE REACTION INTERMEDIATE COMPLEXES, G.S. Groenewold, J.O. Lay and M.L. Gross, Department of Chemistry, University of Nebraska, Lincoln, NE.

The combination of a chemical ionization (CI) source and a mass spectrometer capable of MS/MS is a powerful tool for the determination of ion-molecule complex structures. This technique is analogous to a laboratory synthesis in that the CI source functions as a reaction vessel, MS 1 carries out product separation and MS 2 provides a structurally characteristic mass spectrum of the ion-molecule adduct. In our laboratory, ion-molecule reactions are run at a source pressure of 1 torr. Product ion selection at high mass resolution is performed using the first two sectors of a Kratos MS50TA mass spectrometer (1). The product is then characterized using collision induced dissociation (CID) and a scan of the third sector of the triple analyzer. The structure of the ion-molecule adduct is assigned by comparison with CID scans of appropriate model compounds. In this paper, we describe the reactions of $C_3H_5^+$ plus benzene, 1,3-butadiene‡ plus butadiene and [1,3-butadiene plus methyl vinyl ether]‡.

$C_3H_5^+$ + Benzene

C_3H_5 cations from a variety of sources react with neutral benzene to yield a pressure stabilized C_9H_{11} cation. The structure of these adducts, and hence of the original C_3H_5 cations, may be determined by comparing their spectra with CID spectra of protonated C_9H_{10} model compounds. For example, the ion-molecule complex resulting from the reaction of $C_3H_5^+$ (from 2-propenyl bromide, I) and benzene gives a CID spectrum which is nearly identical to that of protonated α-methyl styrene (II). This is strong evidence supporting the chemistry described in Scheme 1. This technique allows unequivocable differentiation of the 2-propenyl and allyl cations (2), and suggests the existance of a third, unique 1-propenyl type isomer. This conclusion is supported by pulsed ICR studies, which show that each of the three C_3H_5 cations has a unique rate constant for the reaction with benzene. These experiments demonstrate that the derivatization of cations using ion-molecule reactions can be a powerful tool for distinguishing isomeric cations which otherwise give similar CID spectra.



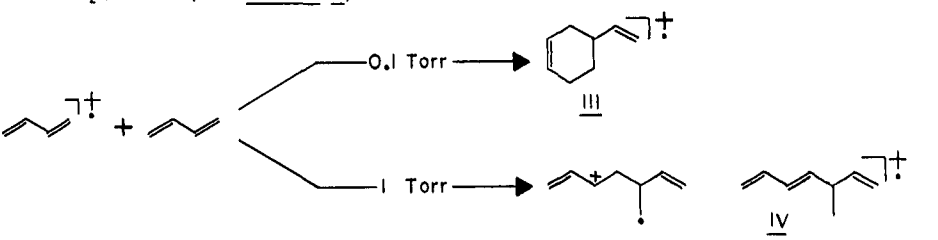
I II

Scheme 1

1,3-Butadiene‡ + Butadiene

1,3-Butadiene radical cation reacts with butadiene neutral to yield an ion-molecule complex with the composition C_8H_{12}. The CID spectrum of the pressure stabilized $C_8H_{12}^{\ddagger}$ can be observed to change dramatically, depending on the pressure in the source. At a pressure of approximately 0.1 torr, the losses of $\cdot CH_3$, $\cdot C_2H_5$ and C_3H_6 together account for greater than 50% of the total ion current (TIC) in the CID spectrum. 4-Vinylcyclohexene(III) is the only one of 14 isomeric model C_8H_{12} compounds to exhibit this characteristic. In contrast to the result at 0.1 torr, the CID spectrum of the butadiene ion-molecule complex formed and stabilized at about 1 torr is dominated by the loss of $\cdot CH_3$, which alone accounts for greater than 50% of the TIC. This spectrum is similar to that of an acyclic model compound, 5-methyl-1,3,6-heptatriene(IV).

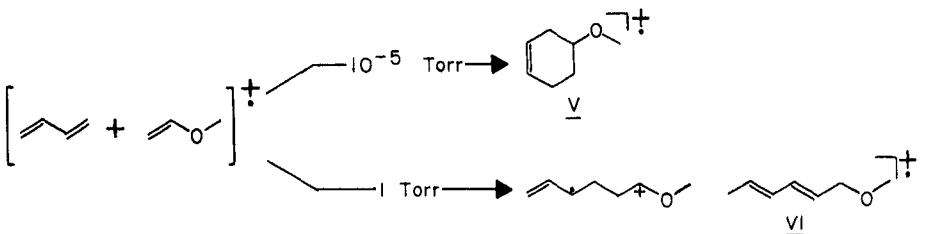
These results are best interpreted in terms of a less probable cycloadduct which dominates the CID spectrum at lower pressure (that is, limited collisional stabilization) because it has a greater ability to accomodate energy relative to the acyclic structure. The more probable acyclic structure is observed when extensive collisional stabilization is available (high pressure) and the ability to accomodate energy becomes less important (see Scheme 2).



Scheme 2

[1,3-Butadiene + Methyl Vinyl Ether]$^{+}$

A 1:1 mixture of 1,3-butadiene and methyl vinyl ether undergoes an ion-molecule reaction to yield a stable $C_7H_{12}O$ cation at a pressure of 1 torr. The CID spectrum of the complex shows that the loss of CH_3OH accounts for less that 5% of the TIC, in sharp contrast to the CID spectrum of the [4+2] cycloadduct (4-methoxycyclohexene, V) in which the loss of CH_3OH accounts for greater than 50% of the TIC. The CID spectrum of the complex is very similar to that of 1-methoxy-2,4-hexadiene (VI), which suggests that the complex has an acyclic structure when formed at a pressure of 1 torr. These results differ from the ICR work of Nibbering, who concluded that at pressures of approximately 10^{-5} torr a cycloaddition was occurring (3). The chemistry presented in Scheme 3 may be analogous to that of the butadiene plus butadiene system, where a cycloadduct is observed at low pressure and an acyclic adduct dominates at higher pressure.



Scheme 3

References

(1). Gross, M.L., Chess, E.K., Lyon, P.A., Crow, F.W., Evans, S. and Tudge, H., Int. J. Mass Spectrom. Ion Phys., in press.

(2). Bowers, M.T., Shuying, L., Kemper, P., Stradling, R., Webb, H., Aue, D.H., Gilbert, J.R. and Jennings, K.R., J. Amer. Chem. Soc., 1980, 102, 4830-2.

(3). van Doorn, R., Nibbering, N.M.M., Ferrer-Correia, A.J.V. and Jennings, K.R., Org. Mass Spectrom., 1978, 13, 729-32.

STRUCTURES AND FRAGMENTATIONS OF PROTONATED BENZENES

H. Ichikawa and Y. Nakajima
Hoshi College of Pharmacy, Shinagawa, Tokyo, Japan

A. G. Harrison
Department of Chemistry, University of Toronto, Toronto, Ont., Canada

One of the prominent fragmentations in CI mass spectrometry of the derivatives of benzene is the elimination of functional group carring a hydrogen atom and leaving phenyl ion.[1] According to the observations so far, this reaction occurs predominantly in benzene, phenol, toluene, aniline, chrolobenzene, and fluorobenzene but not in benzaldehyde and benzonitrile. In the latter cases, they only give the intense peaks of the MH^+ ion. The difference of behavior must be caused by inherent characteristics of the MH^+ ion. It is also observed from deuterium CI experiment[2] that in chlorobenzene a considerable amount of D-H scrambling is observed while in fluorobenzene such a scrambling reaction does not take place. We have studied these and related problems using MO theories.

We adopted MINDO/3 method for MO theoretical calculation. Since, although it is not very often, MINDO/3 is known to give errorneous results mainly because of underestimation of core repulsion, we also used non-empirical STO-3G method[3] to check the unreasonable or doubtful results of MINDO/3.

Table I shows the relative abundance of phenyl ion and the E_{AB} values.[4] A positive values of difference shows that protonation makes the C-X bond (where X is the substituent) weaker than that in the neutral state while a negative value means that it becomes stronger. Except the case of toluene, the difference of E_{AB} value can explain the ease or difficulty of cleavage of the C-X bond. The negative values of difference in benzaldehyde and benzonitrile are due to electron flow to the substituent caused by enhanced power of electron withdrawal of the substituent. This may be the reason for the absence of phenyl ion. The negative value in toluene can be explained by the result that the methyl-protonated toluene is essentially an adduct of benzyl ion and a hydrogen molecule. Unlike other benzenes fragmentation of protonated toluene is found to start from ipso-protonation indicating the reason of disagreement.

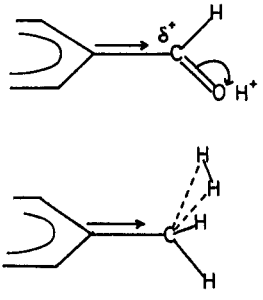
The potential energy (PE) curves of hydrogen migration in protonated chlorobenzene and fluorobenzene are shown in Figure 1. Comparing the internal energy given by protonation (ca. 80 kcal/mol by H_2 CI), the difference of PE between various protonation in chlorobenzene is small enough to allow easy interconversion between ring- and Cl-protonations. On the other hand, in fluorobenzene there is much difference of PE depending on the position of protonation. The PE of F-protonation is exceptionally high. Another interesting thing is that there are two minima of PE during the dissociation of the C-X bond suggesting formation of some kinds of adducts. High PE of F-protonation indicates that there may be a PE barrier that may prohibit the proton migration. At the protonation by H_3^+, most of F-protonated species are considered to fall down to the adducts, rather than going to the benzene ring. Therefore, it is very probale that there are two kinds of protonated fluorobenzene, ring-protonated species and the adduct which are kept isolated. The adduct actually undergoes fragmentation.

1 H. W. Leung and A. G. Harrison, Can. J. Chem., 54, 3439 (1976); J. Am. Chem. Soc., 101, 3168 (1979).
2 To be published.
3 We used the program HONDO5, QCPE No. 403, Indiana Univ. (1979).
4 H. Fischer and H. Kollmar, Theoret. Chim. Acta, 16, 163 (1970).

Table I. The Ion Abundances of $C_6H_5^+$ and the E_{AB} Values between C_1 and X Before and After Protonation

X	Ion abnd.[a]	C_6H_5-X	C_6H_5-XH^+	Diff.
OH	14	-17.693	-12.223	5.470
NH_2	8	-20.174	-13.969	6.205
Cl	70	-10.951	-5.519	5.432
F	24	-14.044	-5.476	8.568
CH_3	5	-15.979	-18.250	-2.271
CHO	0	-16.571	-19.346	-2.775
CN	0	-16.254	-16.760	-0.506

[a] % of total additive intensities in H_2CI.



Possible reason for negative value of difference.

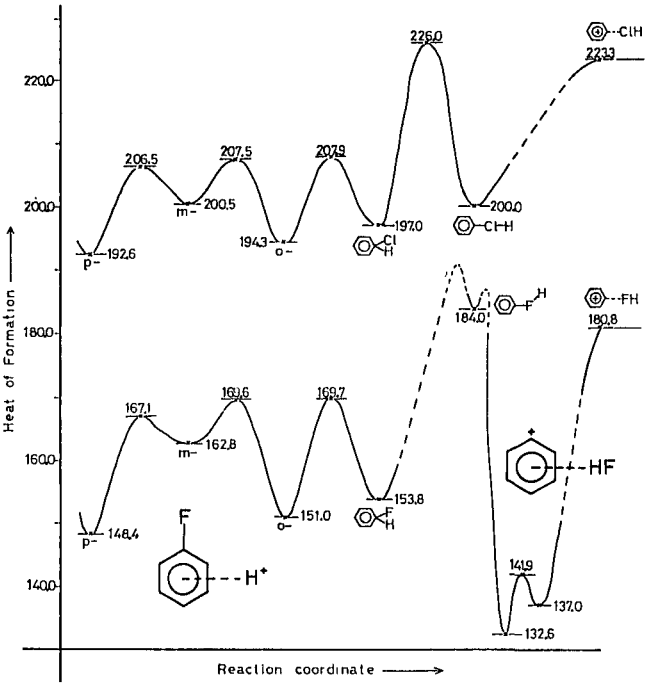


Figure 1. Potential energy curves of hydrogen migration in protonated chlorobenzene and fluorobenzene.

TOF 1 POLYPEPTIDE SEQUENCING BY EXOPEPTIDASE DIGESTION IN COMBINATION WITH FIELD DESORPTION AND FAST-ATOM-BOMBARDMENT MASS SPECTROMETRY; M. Przybylski, R.van den Broek and A. Tsugita, Institut für Org.Chemie der Universität, D-6500 Mainz und European Molecular Biology Laboratory, D-6900 Heidelberg, West Germany

Both field desorption (FD) and fast-atom-bombardment (FAB) mass spectrometry yield abundant molecular or quasi-molecular ions of underivatized peptides but direct derivation of sequence data from fragment ions appears to be limited so far. Digestion with exopeptidases is a classical sequencing method which has been limited in its application, e.g. because of inhomogeneous kinetics and the problem of determining repetitive amino acid residues. The typical kinetic feature of exopeptidase digestion which should match the possibility of mixture analysis by FD and FAB spectra prompted our interest in using these combinations for peptide sequencing. In a model study, complete sequence data were obtained for several biological peptides, e.g. bradykinins and tryptic/chymotryptic fragments of glucagon, by direct FD mass spectral analysis of sub-nmol aliquots taken after partial digestion with aminopeptidase M and carboxypeptidase A/B, or of aliquot mixtures (1). The use of pyridinium or ammonium acetate buffers, precise programming of the emitter current and accumulation of the complete desorption profile by a data system were essential preconditions for FD mass spectrometry to produce homogeneous sets of MH^+ ions up to ca. m/e 2,000. First comparative studies by FAB mass spectrometry indicated advantages above ca. m/e 1,500 but in several cases did not yield unequivocal sequence data in the lower mass range due to matrix and/or fragment ions.Combination of exopeptidase digestion from either terminus with FD and FAB mass spectrometry has recently been successfully applied to molecular weight and sequence determinations of several CNBr fragments from T4 phage 23 protein, and subunits of T4 phage ligase. The certainty of this combined approach appears to be particularly advantageous. (1)A.Tsugita,R.v.d.Broek,M.Przybylski,FEBS-Lett.,in press.

MASS SPECTROMETRY OF BRADYKININ

Gregory M. Neumann and Peter J. Derrick,

School of Chemistry, The University of New South Wales,
P.O. Box 1 Kensington, NSW 2033,
Australia

The nonapeptide bradykinin gives a field desorption mass spectrum which persists for hours[1]. *Collisional activation spectra are reported for the following ions in the field desorption mass spectrum: m/z 254, m/z 419, m/z 572, m/z 807, m/z 1061* $(M+H)^+$, *m/z 415, m/z 542* $(M+H+Na)^{2+}$ *amd m/z 531* $(M+2H)^{2+}$. *The collisional activation spectra of m/z 254, m/z 419 and m/z 807 are consistent with these ions being either N-terminal or C-terminal sequence ions i.e. related in direct manner to the structure of the original peptide. The collisional activation spectrum of m/z 572 suggests that this may be an N-terminal amide ion.*

The doubly charged ions m/z 415, m/z 542 and m/z 531 suffer charge loss and expulsion of an H atom during collisional activation[1]. *In the case of m/z 531* $(M+2H)^+$, *the process with helium collision gas would be represented:*

$$(M + 2H)^{2+} + He \rightarrow (M + H)^+ + H^{\cdot} + He^+.$$

The singly charged ions so formed subsequently decompose.

The collisional activation spectrum of the psuedomolecular ion $(M+H)^+$ *is remarkable in that there is one salient fragment peak. It is proposed that this predominance of one fragmentation pathway is a consequence of the psuedomolecular ion* $(M+H)^+$ *formed by field desorption having one preferred conformation in the gas phase. This preferred conformation would be associated with a preferred primary structure, in the sense that the additional proton would be located at a particular site* (Pro^3). *The position of the proton, it is proposed, is in general a factor directing the fragmentation of the psuedomolecular ion of a peptide.*

1. *For a fuller account, see G.M. Neumann and P.J. Derrick in "Tandem Mass Spectrometry", ed. F.W. McLafferty, John Wiley and Sons Inc., New York, 1982.*

MEASUREMENT OF BRAIN NEUROPEPTIDES AT THE PART PER BILLION LEVEL WITH RP-HPLC AND FDMS

D.M. Desiderio[1,2], S. Yamada[2], M. Kai[2], F.S. Tanzer[3], and G. Fridland[2]
Department of Neurology,[1]
Charles B. Stout Neuroscience Mass Spectrometry Laboratory,[2] and
Department of Oral Diagnosis[3]
University of Tennessee Center for Health Sciences
800 Madison Avenue, Memphis, Tennessee 38163

Data is reported on an off-line combination of RP-HPLC and FDMS measurement of an opioid-related pentapeptide, leucine-enkephalin (YGGFL) in several brain regions and in tooth pulp. This study is part of a larger program examining the molecular basis for pain mechanisms, mapping of various pain-related neuropeptides (beta-endorphin, met-enkephalin, leu-enkephalin, dynorphin, bradykinin, and substance P) in several brain regions. Part of this study extends into a study of larger precursors and smaller metabolites known to occur in biologic tissues and fluids.

Four brain regions were mapped for leu-enkephalin concentrations. Tissue extracts from caudate nucleus (1), hypothalamus (2), thalamus (3), and spinal cord (4) were analyzed for leu-enkephalin concentration. Canine tooth pulp extracts were also analyzed for met-enkephalin (5). Data from this study are presented in the table.

TABLE 1
Endogenous Amounts of Leucine Enkephalin in Various Brain Regions Measured by FDMS and RIA
(ng LE g^{-1} wet weight tissue)

TISSUE	FDMS	RIA*
Caudate Nucleus	423, 351, 272, 453 375 (375 ± 70)	520(6), 200(7), 64(8), 14(9) (200 ± 228)
Hypothalamus	268, 240, 225 (244 ± 22)	
Spinal Cord	70	
Thalamus	52	
Tooth Pulp	3000 (ME)	

*Based on 10% protein in brain tissue.

Reproducibility of this combination of RP-HPLC and FDMS measurement are indicated in the table. For example, for caudate nucleus tissue extracts, 375 ± 70 (n = 5) ng leu-enkephalin g^{-1} wet weight tissue was quantified (10). These data indicate a coefficient of variation of 19%. Hypothalamus extracts yielded 244± 22 ng leu-enkephalin g^{-1} wet weight tissue, corresponding to a coefficient of variation of 9% (n = 3). The righthand column in Table 1 collects the four known RIA measurements of leu-enkephalin in caudate nucleus tissue. Spinal cord contains 70 ng LE, thalamus 52 LE, and tooth pulp 3,000 ng ME g^{-1} wet weight tissue. It is significant to note that up to now, using manual measurements and a higher homolog internal standard, 50 parts per billion of neuropeptide can be quantified in a structurally unambiguous manner by the combination of RP-HPLC and FDMS (11).

The study for quantifying leu-enkephalin in spinal cord tissue addressed another question (4). Up to now, one biologic tissue extract was divided into two equal parts, and one-half was spiked with the peptide being measured (for example, 200 ng LE g^{-1} tissue) and the other left unspiked. Comparing integrated ion currents of $(M+H)^+$ of the peptide plus internal standard yielded data in the table. Another experiment was designed to test if that type of single-spike analytic method is the most statistically significant approach to that measurement. Towards that end, a series of samples with stepwise increases of spiking was measured to determine straight-line statistics. Data from that experiment

indicate that our previous method of using only one pair of spiked versus unspiked samples is sufficient for determination of neuropeptides in brain extracts at the part per billion (pmol) level. The spiking level, however, was found to be optimal between 400-1,000 ng g^{-1} tissue compared to the previously utilized 200 ng g^{-1} tissue. FDMS measurement of spinal cord tissue extracts yielded a value of 70 ng of LE g^{-1} of tissue while RIA yielded 95 ng of LE g^{-1} of tissue. There are several ways to rationalize this difference observed between FDMS and RIA: the difference in the various laboratories' methods of handling tissue; rapidity with which tissue is obtained; rapidity with which temperature is lowered to inhibit enzymatic and/or chemical interconversion of peptides; antibody specificity and cross-reactivity of the RIA measurement; total molecular specificity of the FDMS measurement; "emotional state" of the animal at the time of death; and other unknown factors.

We have developed an Apple II-based microprocessor interface for the Finnigan (Varian) MAT 731 mass spectrometer. The microprocessor functions in three modes: (a) drive emitter heating current in software programmable rates; (b) integrate ion currents from the sample of interest and internal standard, then calculate the ratio of the two ion currents; (c) integrate multiple low resolution scans which is very useful for FD-CA-B/E (12) mass spectral scans.

Techniques under development include fast atom bombardment (FAB) mass spectrometry, FAB-CA-B/E scanning (13) to obtain amino acid sequence data.

Conclusions

This experimental program indicates chemically underivatized neuropeptides are reproducibly quantified at the part per billion level from biologic tissue extracts and fluids.

This work supported by NIH GM NS 26666 and 28611.

References

1. D.M. Desiderio, S. Yamada, F.S. Tanzer, J. Horton, J. Trimble, J. Chromatogr. 217, 437 (1981).
2. S. Yamada, D.M. Desiderio, Anal. Biochem., submitted.
3. D.M. Desiderio, S. Yamada, in Advances in Chromatography, A. Zlatkis, Ed., Univ. Houston, 1982, p. 85.
4. D.M. Desiderio and S. Yamada, Biomed. Mass Spectrom., submitted.
5. F.S. Tanzer, D.M. Desiderio, and S. Yamada, in Peptides, D.H.Rich & E. Gross, Eds., Pierce Chem. Co., Rockford, ILL, 1981, p. 761.
6. I. Lindberg, and J. Dahl, J. Neurochem. 36, 506 (1981).
7. A. Dupont, J. Lepine, P. Langelier, Y. Merand, D. Rouleau, H. Vaudry, C. Gros, and N. Barden, Reg. Peptides 1, 43 (1980).
8. M. Kubek, and J.F. Wilber, Neurosci. Lett. 18, 155 (1980).
9. P,C, Emson, A. Arregui, V. Clement-Jones, B.E.B. Sandberg, and M. Rossor, Brain Res. 199, 147 (1980).
10. D.M. Desiderio in Handbook of Use of HPLC for Separation of Amino Acids, Peptides, and Proteins, W.S. Hancock, Ed., CRC Press, Boca Raten, FL, in press.
11. D.M. Desiderio, in Advances in Chromatography, Vol. 22, J.C. Giddings and P. Brown, Eds, Marcel Dekker, in preparation.
12. D.M. Desiderio, S. Yamada, J.Z. Sabbatini, F.S. Tanzer, Biomed. Mass Spectrom. 8, 10 (1981).
13. D.M. Desiderio and I. Katakuse, manuscript in preparation.

IN-BEAM ELECTRON IONIZATION MASS SPECTRA OF OLIGOSACCHARIDES AND RELATED COMPOUNDS

Mamoru OHASHI and Kazuo TSUJIMOTO
Department of Materials Science, The University of Electro-Communications
Chofu, Tokyo 182, Japan

Recently in-beam techniques have ttracted considerable interest in mass spectral studies of nonvolatile and thermally labile compounds(1). We have investigated the in-beam EI mass spectrometry of amino acids, peptides, aminosugars, alcohols, and quaternary ammonium salts(2). Now we wish to report the characteristics of in-beam EI spectra of several oligosaccharides.

Instrumentation In-beam EI and the conventional EI mass spectra were both obtained with a Hitachi RMU-6M single focusing mass spectrometer modified with an in-beam/direct inlet source. Ionizing voltage 20 eV, accelerating voltage 3.2 KV, chamber temp 200°C were employed. The sample heater was set at an appropriate temperature(200-400°C) before insertion of the samples.

Monosaccharides All the in-beam EI spectra of hexoaldopyranoses, hexoketofuranoses, pentoaldofuranoses exhibit a series of peaks corresponding to successive losses of H_2O from the $[2M+1-H_2O]^+$ ion in addition to the prominent $[M+1]^+$ and $[M+1-H_2O]^+$ peaks. The higher the temperature of the sample heater was, the more abundant the $[M+1]^+$ ion was. Figure 1a shows the in-beam EI mass spectrum of glucose as a typical example.

Disaccharides Figure 1b shows the in-beam EI spectrum of sucrose which strongly resembles to that obtained by in-beam CI or flash desorption EI. Spectral features in the m/z 181-343 region are quite similar to those of glucose. Again a series of peaks derived from successive losses of H_2O from the $[2M+1-H_2O]^+$ ion at m/z 667 are observed together with the abundant $[M+1]^+$ and $[M+1-H_2O]^+$ ions. The presence of ions derived from these dimer ions suggests that ionization took place in cluster or associated molecules near the surface of the probe.

Tri- and Tetrasaccharides Maltose and aminocyclitol antibiotics up to the trisaccharide level like kanamycins easily gave the $[M+1]^+$ peaks in their in-beam EI spectra. However, in-beam EI spectrum of a tetrasaccharide stachyose did not give the $[M+1]^+$ peak, but the $[M+1-H_2O]^+$ peak was observed,instead, at m/z 649 as the highest mass number. The in-beam EI spectra of two hydrolytic products of a bacterial antibiotics glysperin(3), N-alanyltetrasaccharide(I, R=Ala) and its dealanyl derivative(II, R=H), both gave the corresponding $[M+1]^+$ peaks as well as their sequence-determining fragments. A comparison of these two spectra makes it possible to deduce the sequence of the four sugar moieies in glysperin as shown in Scheme 1.

Figure 1a

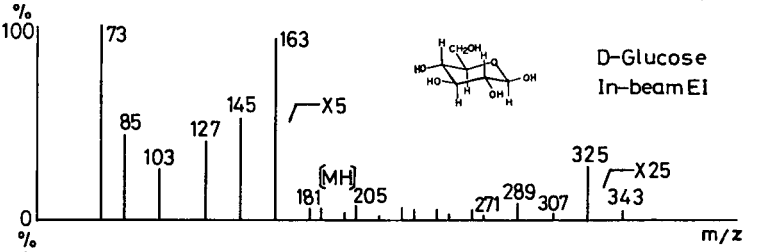
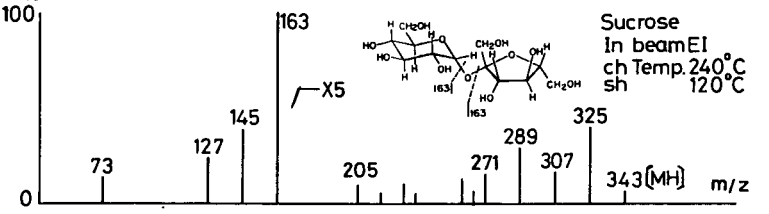


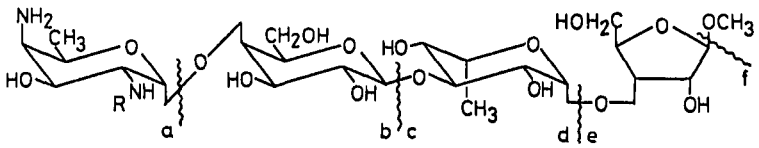
Figure 1b



Pentasaccharides In the in-beam EI mass spectra of viridopentaoses(IIIA, B, C)(4), the $[M+1]^+$ ion was detected within a few seconds after the sample was brought precisely in contact with the ionizing electron beam at a high temperature(i.e. the sample heater and the chamber were heated at 390°C and 240°C respectively before insertion of the samples). Lifetimes of the $[M+1]^+$ peaks were less than 2 s. Rapid repeated scannings around the molecular ion regions were effective for the detection of the $[M+1]^+$ peaks. Immediately after the insertion of the sample, the repeated scanning(1 s/a scan for 100 u) was started, then within several scans the $[M+1]^+$ peak appeared at least once in the chart. The sequence-determining peaks are shown in Scheme 2.

Scheme 1

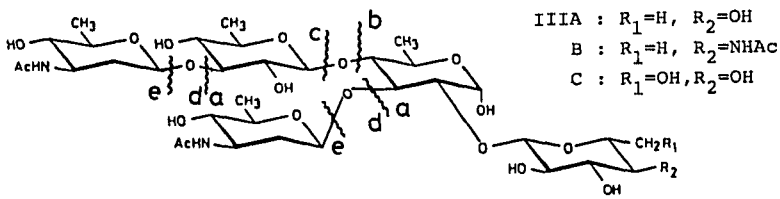
In-beam EI Spectra of Hydrolytic Products of Glysperin



	M+1	a	b	c	d	e	f
I R=COCH(NH$_2$)CH$_3$	688(1.4)	215(5)	378(1)	309(5)	523(1)	163(10)	656(1)
II R=H	617(21)	145(100)	307(4)	309(2)	453(5)	163(8)	585(2)

Scheme 2

In-beam EI Spectra of Viridopentaoses



IIIA : R_1=H, R_2=OH
B : R_1=H, R_2=NHAc
C : R_1=OH, R_2=OH

	M+1	MH-H_2O	MH-2H_2O	a	b	c	d	e
IIIA	799	780	763	610	464	318	188	172
B	840	822	804	651	505	318	188	172
C	815	797	778	626	480	318	188	172

References
(1) R. J. Cotter, Anal. Chem., 52, 1589A(1980).
(2) M. Ohashi, K.Tsujimoto, S. Tamura, N.Nakayama, Y. Okumura, A. Sakurai, Biomed. Mass Spectrom., 7 153(1980) and references cited therein; M. Ohashi, R. P. Barron, W. R. Benson, J. Am. Chem. Soc., 103, 3943(1981).
(3) T. Tsuno, M. Konishi, T. Naito, H. Kawaguchi, J. Antibiotics, 34, 390(1981).
(4) K. Harada, S. Ito, M. Suzuki, Tetrahedron Lett., 41, 3665(1979).

BEER AND PYROLYSIS/MASS SPECTROMETRY

S.L. Durfee, R. Tsao, and K.J. Voorhees
Department of Chemistry and Geochemistry
Colorado School of Mines
Golden, Colorado 80401

J.J. Ruocco and S.E. Moore
Adolph Coors Co.
Golden, Colorado 80401

Beer is composed of a complex mixture of biopolymers plus lower molecular weight compounds. Although gas chromatography has been used to analyze the materials less than Cs, no attempt has been made to characterize the biopolymers and correlate the chemical information with the various taste and physical properties of the beer.

Five major premium and super premium beers have been investigated to determine chemical changes which occur during shelf life aging. Reference numbers have been used for the different beers rather than brand name. Bottles of each beer were exposed to 37°C for 7 days. After this period, samples of the heat treated beer along with identical refrigerated samples were investigated by pyrolysis/mass spectrometry pattern recognition procedures (Py-MS). Eight microliters of each sample were coated onto a 510°C Curie-point wire. Pyrolysis of the remaining solids was done using an Extranuclear SpectrEL Py-MS system. Pyrolysis time was 5 seconds and rise time 100ms. 25 spectra were summed together for each pyrolysis mass spectrum. Pattern recognition including principal component/factor analysis, distance calculations, and non-linear mapping was done using the ARTHUR package (1).

Figure 1 shows a non-linear map of five of the refrigerated super premium beers. The map suggests that the beers were chemically different. Blind taste panel results confirmed significantly different taste properties for the five samples. Similar Py-MS and taste panel results were also observed for the premium beers. Comparison of the Py-MS data from the heat treated and refrigerated sample showed most beers were modified when exposed to heat. Figure 2 shows the non-linear map for the super premium treated and untreated samples. The taste panel categorized the flavor changes in these samples as drastic.

Each individual pair has been investigated separately using principal component/factor analysis. The goal of this approach was to determine changes occurring in the actual chemical constituents. Figure 3 shows a plot of principal component 1 plotted against 2 for beer number 1. This particular plot was chosen because factors 1 and 2 differentiated between the heated and refrigerated samples. An even better separation could be obtained using these factors by rotating the factor axis. After performing a rotation of factor 2 by +140° toward factor 1, the factor spectrum shown in Figure 4 was obtained. Three important chemical classes are shown in the spectrum. First, a series of peaks for polysaccarides was observed. In addition, m/z 61 probably associated with a glycerine based compound, and two characteristic peptide peaks (m/z 97 and 99) were also observed. Other factor combinations provided similar information for other homologous series. Future work for this project will include a detailed analysis of the peaks by Py-MS/MS and their correlation to the biochemistry of the observed processes.

1. D.L. Duewer, K.R. Koskinen, and B.R. Kowalski, Laboratory for Chemometrics, University of Washington.

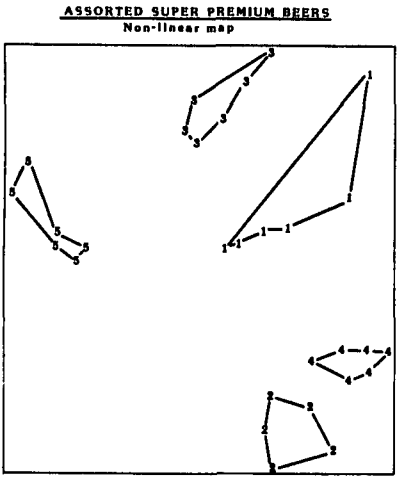


Figure 1.

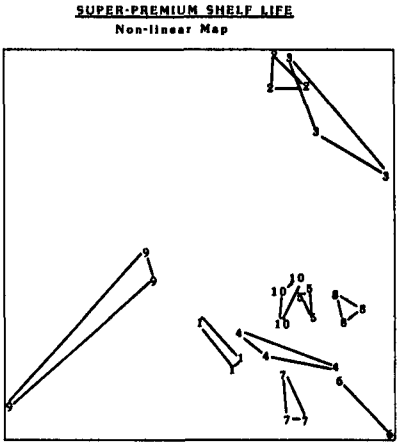


Figure 2.

Legend
(Figs. 1 and 2)

Ref.	Heat.
1	6
2	7
3	8
4	9
5	10

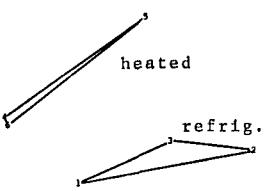


Figure 3. Factor 1 plotted against 2 for Beer 1

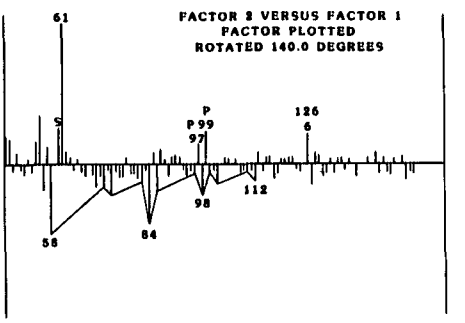


Figure 4.

FAST ATOM BOMBARDMENT AND DIRECT CHEMICAL IONIZATION MASS SPECTRAL STUDIES OF PHORBOL ESTER TUMOR PROMOTERS. Steven A. Carr and Vernon N. Reinhold, Dept. of Biol. Chem., Harvard Medical School, Boston, MA 02115, and Catherine E. Costello, Dept. of Chem., Massachusetts Institute of Technology, Cambridge, MA 02139.

Esters of the tetracyclic diterpene phorbol and related diterpene derivatives constitute one of the most potent classes of tumor promoters yet investigated[1]. The molecular modes of action of these phorbol esters are under active investigation to elucidate the relationship between structure and several diverse physiological responses. One central but as yet unanswered question is whether the phorbol esters interact at specific cell surface receptors or via nonspecific binding with the cell membrane. The high potency of these compounds (nanomolar concentration range) and the observation that minor changes in structure can markedly affect activity strongly suggest that specific receptors exist.

The structural determination of phorbol esters is analytically challenging because isomers differing only in the locations of chemically labile acyl substituents must be distinguished, often on very limited amounts of sample. We have previously shown that FD and direct chemical ionization (DCI) from polyimide coated wires[2] using NH_3 as the reagent gas provide both molecular weight and useful structural information on phorbol esters. The NH_3-DCI approach is quite sensitive, requiring 0.1 to 0.3 μg for a complete mass spectrum, and as little as 3ng for selected detection of the protonated or ammonia cationized molecular ion[3].

In the present work we have studied the nature of the fragment ions produced under NH_3-DCI conditions using isotopically labeled reagent gases, and in addition, evaluated the utility of fast atom bombardment (FAB) MS for the structural analysis of these compounds. We have found that DCI, FAB and FD can all be used to differentiate isomers of the phorbol esters in which the acyl groups on C12 and C13 are reversed, since ions arising from selective cleavage of the substituent at C12 are prominent in these ionization modes. In addition, we have used DCI and FAB MS to help guide the synthesis of a phorbol ester photoaffinity label and affinity column which are being used by P. Blumberg (NIH) to characterize potential receptors.

The NH_3-DCI mass spectra of the phorbal esters are usually dominated by the $(M+NH_4)^+$ adduct ion (Fig. 1). When nitrogen is present in either of the acyl substituents a prominent $(M+H)^+$ appears which is due to the increased Bronsted basicity of the molecule. The most prominent high mass fragment corresponds to the loss of the substituent R12 (as the acid, (R12+H)), from $(M+H)^+$. The analogous fragment arising from loss of R13 is generally very weak, if present. However, a prominent fragment corresponding to $(R13+NH_4)^+$ is usually present (Fig. 1). Ions due to the loss of protecting groups from $(M+H)^+$ are also observed (e.g., $((MH-Boc)+H)^+$ = m/z 576, Fig. 1). The presence of a trityl group on C20 causes a shift in the base peak to m/z 243 $(C(phenyl)_3^+)$.

The use of $^{15}NH_3$ and N^2H_3 as the reagent gases greatly facilitates the assignment of molecular and fragment structure. For example, the cluster of even mass fragment ions at m/z 364, 346 and 328 (Fig. 1) are, surprisingly, all ammonia adducts. These clusters may correspond to the 12,13 epoxide rearrangement ions resulting from the loss of both R12 and R13, one group as the acid and the other as the acylium.

Phorbol esters ionized by FAB exhibit intense protonated and cationized molecular ions as well as glycerol attachment ions. Fragmentation is entirely analogous to that observed by NH_3-DCI. Approximately 10-30 fold more material is required for FAB in order to achieve results which are comparable to the NH_3-DCI data. FAB proved better suited and more reproducible than NH_3-DCI for highly polar phorbol ester derivatives, and when salts or other contaminants were present. For example, the phorbol-biotinyl affinity column substrate yielded a poor NH_3-DCI mass spectrum, with most ions a consequence of pyrolysis. In contrast, excellent results were obtained by FAB (Fig. 2).

Compounds used in this study were furnished by P. Blumberg, NIH. This work is supported by grant No. 5 PO1 GM 26625 from the National Institutes of Health.

[1]Blumberg, P. (1980) CRC Critical Rev. Toxicology 8, 153-197.

[2]Reinhold, V.N. and Carr, S.A. (1982) Anal. Chem. 54, 499-503.

[3]Costello, C.E., Schkuta, A., Biemann, K. and Reinhold, V.N. (1981) 29th Annual Conf. on Mass Spec. and Allied Topics, Minneapolis, Minn., pp 588-589.

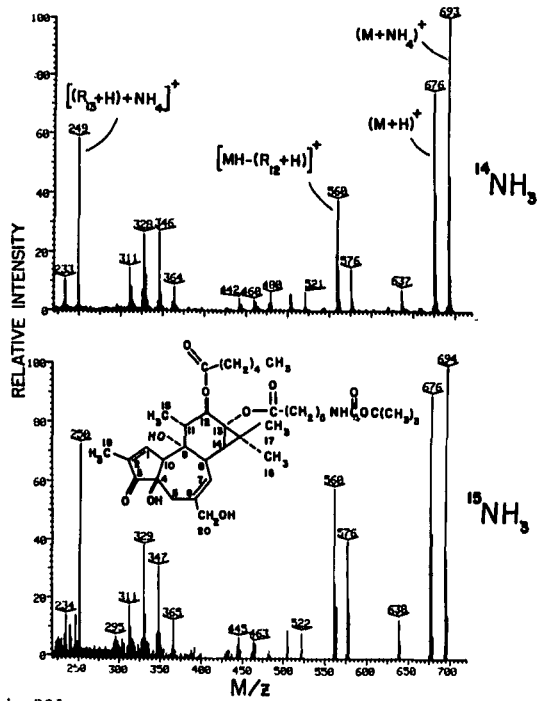


Fig. 1. Ammonia-DCI mass spectra of Phorbol-13-Boc-Aminohexanoate-12-Hexanoate using a) $^{14}NH_3$, and, b) $^{15}NH_3$ as the reagent gas.

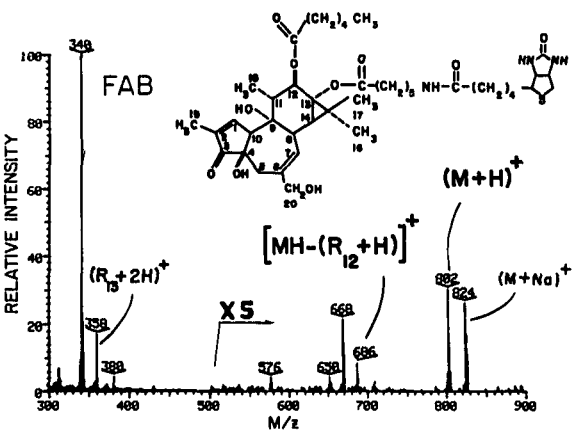
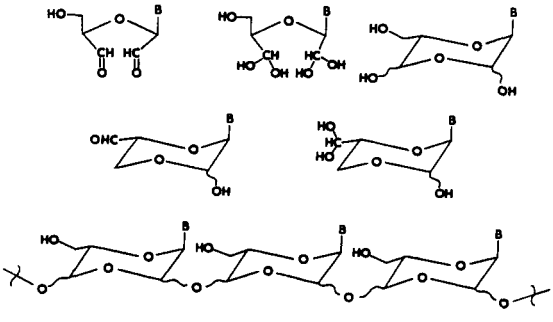


Fig. 2. FAB mass spectrum of Phorbol-13-N-Biotinyl-ϵ-Aminohexanoate-12-hexanoate.

THE ISOLATION AND IDENTIFICATION OF NUCLEOSIDE DIALDEHYDES BY GC-MS, R. Thomas Solsten and Karl H. Schram, Department of Pharmaceutical Sciences, College of Pharmacy, University of Arizona, Tucson, AZ 85721.

The dialdehyde analogs of several nucleosides have been shown to possess antitumor activity and have undergone clinical trials.[1,2] However, their mechanism of action or the active species has yet to be reported. In aqueous solution, the dialdehydes can exist as intra- and inter-molecular hydrates and hemi-acetals which are shown in Figure 1.

Figure 1



1. B = Adenine
2. B = Hypoxanthine
3. B = 5-Uracil

Formation of the trimethylsilyl derivatives of 1-3 permits the gas chromatographic separation of the major components in this mixture. We have found that on-column thermal degradation of the polymer occurs giving rise to the monomeric nucleosides. The structures shown in Figure 1 have been assigned by employing low and high resolution mass spectrometry. In addition, the TMS-d_9 derivatives and ^{18}Oxygen labeled hydrates were prepared to aid in the structure elucidation.

Shown in Figures 2 and 3 are the two major components formed as intra-molecular hemi-acetals of adenosine dialdehyde. Notable differences in the fragmentation of the sugar residue permits discrimination of these isomers. Degradation of the acetal linked polymer produces the two nucleosides shown in Figures 4 and 5. The internal residues give rise to the species with a molecular ion at m/z 409, while the terminal residue is responsible for the nucleoside with a molecular ion at m/z 481. These structures are consistent with the results of the isotopic labeling and the elemental compositions for the major fragments were confirmed by high resolution mass spectrometry.

Figure 2

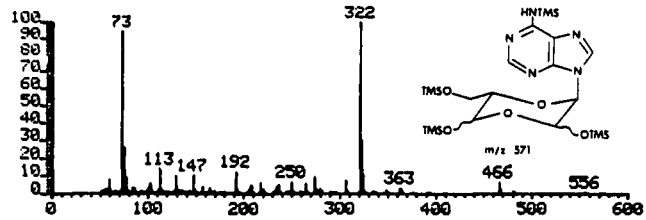


Figure 3

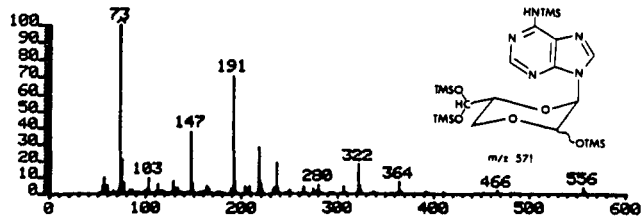


Figure 4

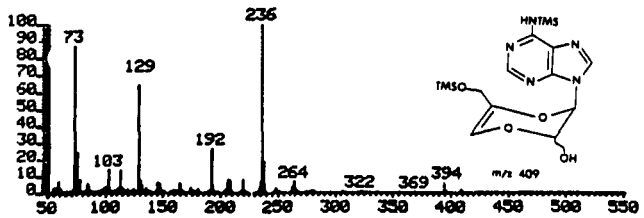
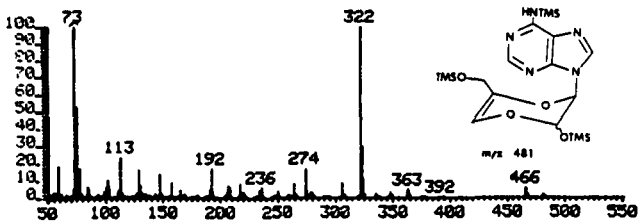


Figure 5



1. W. Dvonch, et al., Cancer Research 26, 2386 (1966).

2. J.J. Kinahan, et al., Cancer Research 40, 498 (1980).

NEW METHOD OF ADRENAL STEROID MEASUREMENT- 11 deoxycortisol- - IN HUMAN PLASMA

NOZAKI,Y.[1], KATOH,K.[1], ICHIMURA,K.[2], CHIBA,K.[2], and SAITO,K.[2]
1) Yamanashi medical college,Dept of Pediat.,Yamanashi.Japan.
2) Schoöl of medicine,KEIO univ.,Tokyo,Japan.

11β-hydroxylase is well known as the enzyme locating only in the adrenal grand in human. 11-deoxycortisol(S) is the key steroid in the diagnosis of some adrenal disorders such as 11β-hydroxylase deficiency and some types of adrenal tumors. However,some difficulties were still known about the method of plasma S measurement employed untill now,especially in clinical use,because of their poor sensitivities,large cross-reactivities and long assay-times.

Materials and methods were as follows; Reagents,analytical grade, obtaind from Sigma chemical co.,Pierce chemical co.(USA),and Gas-chromato co.(Japan), Antisera from Teikokuzoki co.(Japan),and Gas-chromatography-mass spectrometry (GC/MS) of JGC 20K for GC,JMS D300 for MS and JMS 2000 for recorder,eqquiped with 1m glass colomn,2mmI.D.,packed with 1% OV-1 on Gas-Chrom Q,80-100 mesh were used. Column temperature programmed from 230°C to 280°C at the rate of 6°C/min,290°C at injected port,180°C of ion source chamber,Ionizing voltage of 70 eV,Ionizing current of 300μA,Accelating voltage of 3KV,and flow rate of helium as the carrier gas of 40 ml/min were used. About radioimmunoassay measurement(RIA),methylene chloride($MeCl_2$)-extraction,microcolumn(7mmI.D. 60mm length)-chromatography at 25°C,and solvent system($MeCl_2$: methanol:ethanol =97:2:1) were employed to purify the samples.Then RIA was done. About GC/MS measurement,extraction,cyclization with n-butylboronic acid,the formation of o-methyloxime derivatives(MO) and the formation of trimethylsilyl ether(TMS) were described in Table 1. 5α-cholestane(m/z 372) was used for internal standard (IS). Plasma sampling was drawn before and after metyrapone test.

Results

S and IS were equally extracted completely with $MeCl_2$ and/or ethyl acetate. GC/MS characteristics of trimethylsilyl oximes of S (Fig 1) showed 8 min.of retention.times and ions mass at 548(M),517,458,445,and 427 which results were indistinguishable from o-trimethylsilyl oximes of corticosterone(Fig 2), 21-deoxycortisol and 18-OH-deoxycorticosterone.[3] GC of n-butylboronic S and n-butylboronic oximes of S showed clear single peak,which were impling the cyclization were done considerably. Ions mass at 412(M),244(M-168) of n-butyl-boronic S were corresponding to the ions mass at 470(M),273(M-197) of n-butyl-boronic oximes of S,in Fig 1,which arised by the partial D ring cleavege.[3] This n-butylboronic oximes of S was intact to the coventional silylating reagents. The working curve(Fig 3) showed good lineality. Accuracy and precision were less than 12 % of coefficients of variations between 1 ng/ml to 970 ng/ml. Sensitivity was 0.1 ng/tube.The data with this method indicated good correlationship ($r=0.98, p<0.01$) with the data obtained from RIA with Sephadex LH 20-chromatography,mentioned above.

Clinical application(Fig 4)

After single oral metyrapone test(50 mg/kg),more than 6mcg/ml increase of plasma S were detected in all normal subjects,but not in all ACTH-deficients with pituitary dwarfism. This finding suggest this single test is as useful as 3 days-ordinary method,when cut-off point is setted on 6 mcg/ml increase after 50 mg/kg single oral metyrapone administration.

Conclusion

Cyclization of S with n-butylboronic acid,accompaning with o-methyloximes derivatives is showed useful in the plasma S measurement by GC/MS. This assay system overcomes the known method in it's speed,cost and accuracy.

Reference

1) Kalmar,K.E.(1979) Journal of lipid Research,20,729-739
2) Begue.R.J.,Dumas.M.,Moriniere.M.,Nivois.C.,and Padieu.P.(1979) Biomedical mass spectrometry.6,479-481

GC/MS ; Japan Electric-Optics Laboratory co.,Japan

Table 1 Procedure of serum 11-deoxycortisol measurement

Standard serums pretreated with charcol were added to the purified 11-deoxycortisol (final concentrations of 11-deoxycortisol of 3ng/ml to 300ng/ml)

↓

Standard serums and samples (1~5ml) were divided in equal three parts

↓

Then internal standards (5α cholestene of 1μg or 10ng or 100ng) were added to each sample

↓

Extraction with Methylene chloride (5~15ml) was done

↓

Dryness with N_2 gas of each sample extracted

↓

Ethyl acetate (50μl~500μl) was added to each sample

↓

n-buthylboronic acid (10μg~100μg) were added to each sample

↓

Incubation for 5 to 10 minutes at room temperature

↓

Dryness with N_2 gas

↓

O methylhydroxylamine (10-100μg) was added with pyridine (100 500μl)

↓

Incubation for 2 to 24 hrs at 60°C

↓

Dryness with N_2 gas

↓

TMCS BSTFA TMSI (1 3 3)(10-50μl) or HMDS (0.1~0.5ml) with trace TMCS dissolved in pyridine pyridine were added

↓

Incubation for 5 to 10 minutes at room temperature

↓

Dryness with N_2 gas

↓

Apply to GC/MS after resolution of Ethyl acetate (50~500μl)

↓

Apply to GC/MS

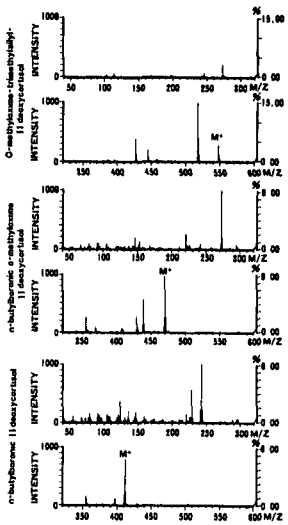
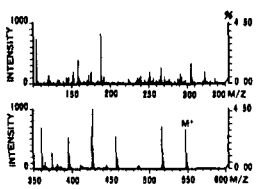
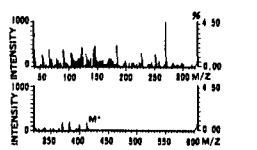


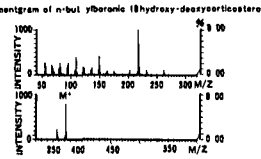
Fig 1 Fragmentgram of several forms of 11deoxycortisol



a) Fragmentgram of O-methyloxime trimethylsilyl corticosterone



b) Fragmentgram of n-but ylboronic 18hydroxy-deoxycorticosterone



c) Fragmentgram of 5α cholestene

Fig 2 Several fragmentgrams with some relations to this assay system

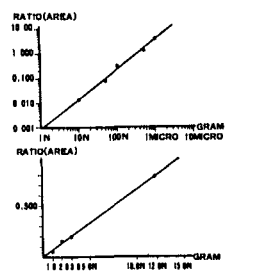


Fig 3

Working curve (relative) of n-but ylboronic O-methyloxime 11-deoxycortisol

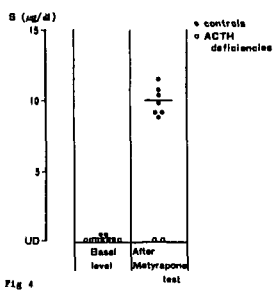


Fig 4

Serum S changes after Metyrapone (30mg/kg p.o.) test

METHYL BORONATION FOR THE STUDY OF ALDOSTERONE AND ITS METABOLITES BY GC/MS

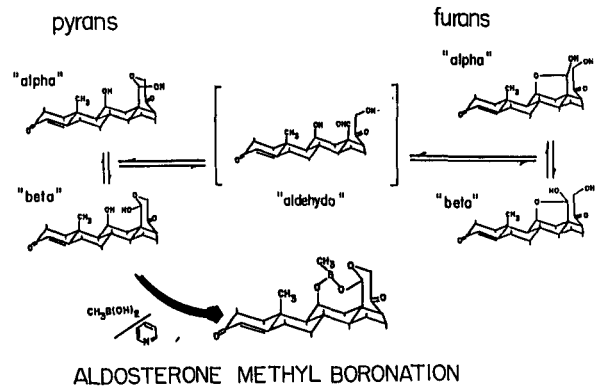
Vernon N. Reinhold
Department of Biological Chemistry (LHRRB)
Harvard University Medical School
Boston, MA 02115

Over the years, aldosterone, an important mineral corticoid hormone, has posed considerable problems in its quantification and structural determination. These difficulties stem from the C-18 aldehydic group and its intramolecular reactivity with proximal nucleophiles to produce a series of isomeric acetals and their anomers. This underlying problem of isomeric heterogeneity seriously compromises attempts to assign structure to aldosterone metabolic products. Gas-liquid chromatography (GLC), when used to resolve these products, requires sample derivatization to overcome the problem of metabolite polarity. Most derivatization procedures exacerbate the problem further by inducing their own added heterogeneity (methoximes, syn/anti) or give rise to a more equal distribution of all possible anomers and isomers. Investigators using earlier chromatographic procedures were unaware of this problem which, with current capillary column technology and direct mass spectral coupling, becomes a more obvious problem. Many published accounts have appeared discussing aldosterone isomeric structures, and although the current analytical picture is unclear, our preliminary GLC/MS studies suggest all products can be accounted for by considering the two anomeric components of a pyran and furan equilibrium (Scheme 1). The distribution and concentration of these products varies greatly between solvents and may be considered a consequence of solvent and sample dipole-dipole interactions (anomeric effect). Methyl boronic acid derivatization, which forms boronate esters between proximal nucleophiles, traps one of these anomeric components to make a single structural entity, the 11,18-(2-methyl dioxaborepane)-aldosterone derivative (Scheme 1). We have studied this product by GLC/EIMS (Fig. 1), GLC/CIMS, and high resolution EIMS (Table 1). Further structural characterization by IR and NMR are being pursued. With a more simplified GLC pattern, resulting from the methyl boronation of HPLC purified aldosterone metabolic fractions, structural assignment problems are now at a more manageable analytical level and these investigations are continuing.

TABLE 1

HIGH RESOLUTION RESULTS FROM THE METHYL BORONATE DERIVATIVE OF ALDOSTERONE

Determined Mass	Calculated Mass	Diff. (mmu)	Composition
111.06062	111.06173	-1.1	$C_5H_8O_2{}^{11}B_1$
175.09238	175.09303	-0.7	$C_{10}H_{12}O_2{}^{11}B_1$
194.11252	194.11141	1.1	$C_{10}H_{15}O_3{}^{11}B_1$
323.18227	323.18186	0.4	$C_{20}H_{24}O_3{}^{11}B_1$
338.20530	338.20533	0.0	$C_{21}H_{27}O_3{}^{11}B_1$
356.21325	356.21591	-2.7	$C_{21}H_{29}O_4{}^{11}B_1$
384.21005	384.21080	-0.8	$C_{22}H_{29}O_5{}^{11}B_1$



Scheme 1.) Proposed equilibrium between furan and pyran anomers leading to methyl boronate trapping of β-pyran isomer to the 2-methyl dioxaborepane derivative.

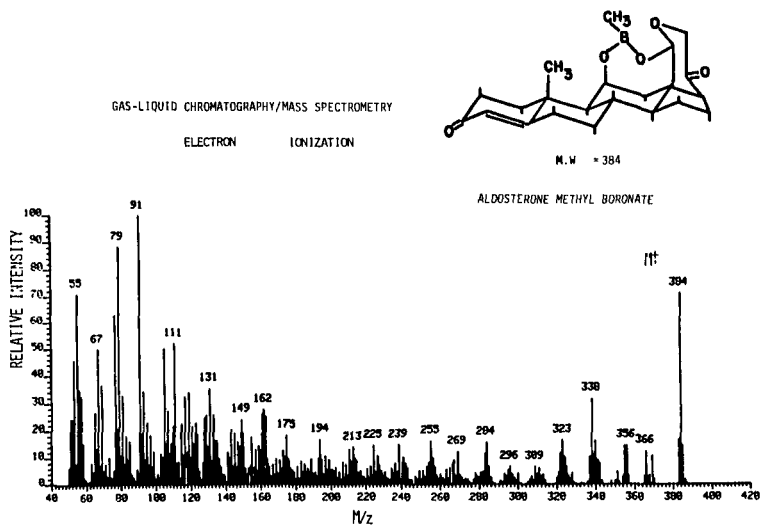


Figure 1.) Electron ionization of the single GLC peak obtained following methyl boronic acid derivatization.

MASS SPECTROMETRY APPROACHES TO QUANTITATIVE TRIGLYCERIDE ANALYSIS. R. A. Sanders, The Procter & Gamble Company, 6071 Center Hill Road, Cincinnati, Ohio 45224.

Introduction

Gas chromatographic (GC) methods have long been used to characterize the triglyceride composition of products containing fats and oils. One such method (carbon number profile or CNP) separates the intact triglycerides according to their molecular weight. However, the chromatographic resolution of the CNP method, even with capillary columns, does not permit a complete separation of species differing only in the number of carbon-carbon double bonds or species differing only in the fatty acid arrangement on the glycerol backbone. This work describes two quantitative mass spectrometry methods developed to overcome these limitations. The first method, called molecular weight profile or MWP, is analogous to a high resolution carbon number profile. Whereas CNP measures nominally five or six distinct triglyceride components in a typical vegetable oil, MWP measures 16-20 components due to its ability to distinguish between species differing only in the degree of carbon-carbon unsaturation. This method is applied to the fat mixture introduced from the direct insertion probe with no sample preparation, and uses ammonia chemical ionization. The data system collects scans continuously during sample distillation, and sums the ion intensities for the entire run for each component. The second method measures the relative amounts of positional isomers (e.g. glycerol-1,3-oleate-2-palmitate or OPO and glycerol-1-palmitate-2,3-oleate or POO) when such isomer pairs have been previously separated from the triglyceride mixture. This method employs electron ionization and ion monitoring as the sample is introduced via the direct insertion probe. Both methods can be implemented with an approximate precision of 5% rsd.

Experimental

MWP Method: A Kratos MS-30 with a combination EI/CI source was used effectively in either dual beam or single beam modes. The MS-30 was calibrated over the mass range 717-931 Daltons by introducing perfluorokerosene through a batch inlet at 150°C. The ion source temperature was 250°C. The pressure in the ion chamber was not measured (pressure outside the cell in the source vacuum chamber was approximately 5×10^{-5} torr). Under these conditions the ratio of m/z 18 to m/z 35 was 3:1. The repeller potential was set (reproducibly) near zero volts. The static resolution (10% valley) was 3000 and the scan rate was 10 s/decade.

Under these conditions molar response factors varied as a function of degree of unsaturation from 1.0 for trisaturates to 0.85 for species with three double bonds based on triplicate analyses of a standard five-component, triglyceride mixture. These response factors were included in the calculations, and the standard mixture was analyzed along with samples in order to insure day-to-day reproducibility of response. The signal for a particular component included the sum of intensities at $(P+18)^+$ and $(P+19)^+$ since the species containing a single ^{13}C constitute a significant portion (35-40%) of the total ionization from each component. When two components differ in molecular weight by only two Daltons, the higher weight species can have a significant contribution from the two-^{13}C species of the lower weight component. Accordingly, an appropriate correction was made to the intensity measured at the higher molecular weight based on the two-^{13}C response of components in the standard mixture.

Samples consisted of approximately 3.5 µg of vegetable oil. The solids probe was heated ballistically to 350°C while repetitively scanning the magnetic field. The signals for each component, summed over isotopes and corrected as described above, were normalized such that the sum over all components in the weight range 717-931 Daltons was 100%.

Positional Isomer Method: A Hewlett-Packard 5995B mass spectrometer was used in the electron impact mode (70 eV) with a source temperature of 300°C. The solids probe was heated from ambient to 350°C at 50°C/minute. Ions monitored were the $(P-RCO_2CH_2)^+$ ions which form readily from loss of the fatty acid from the 1 or 3 position, but less readily from the 2 position. Despite the fact that all these ions are present at low relative abundances [the major electron impact fragment ions in this mass region correspond to $(P-RCO_2)$], adequate ion intensities result in the ion monitoring mode from 1-10 µg of sample. Isomer pairs for which methods were developed include the 1,3 and 1,2 isomers of distearate-palmitate (StStP and StPSt), dioleate-palmitate (OOP and OPO), and dipalmitate-oleate (PPO and POP). Additionally, a method for measuring the relative amounts of glycerol-1-stearate-2-palmitate-3-

oleate (SPO) and glycerol-1-palmitate-2-stearate-3-oleate (PSO) was developed. Calibration curves were determined as illustrated by the OOP/OPO system where the $(P\text{-}RCO_2CH_2)^+$ ion intensities are I_{563} and I_{589}. The ratio $R=I_{589}/I_{589}+I_{563}$ was plotted versus percent OOP. R varies by approximately an order of magnitude from pure OPO to pure OOP which was typical for all cases studied.

Samples free of triglycerides except for the isomers of interest were prepared from vegetable oil by argentation TLC and HPLC methods not described here. Purity was checked by the molecular weight profile method previously described.

Results and Discussion

Molecular weight profile results for a typical vegetable oil analyzed are shown in Table I where the weight percentages of triglyceride components from duplicate analyses are listed. All symbols were previously defined except L and Ln which indicate linoleic and linolenic acid moieties, respectively. The accuracy of the method is difficult to judge due to the lack of any technique which can provide comparable results. One approach, however, is to sum the results within each carbon number and compare the results to those obtained by the chromatographic CNP method. Additionally, MWP results may be used to calculate the fatty acid composition for comparison with chromatographic results. These comparisons were made, and the excellent agreement gives confidence that the accuracy, as well as the precision of this method, is reliable. A typical positional isomer calibration curve is shown in Figure 1 for five OPO/OOP standard mixtures. Near linearity of these plots was observed, though consideration of the signal expression demonstrates that perfect linearity is expected only if the sum of the two ions monitored is the same for both isomeric components. Since the positional isomer method can give severely distorted results if other triglyceride components (e.g. POP or PPO) are present, it is essential to check the purity of chromatographic isolates by the molecular weight profile or other comparable method.

MOLECULAR WEIGHT PROFILE RESULTS ON PALM OIL

MW	WT % RUN 1	WT % RUN 2	CARBON #, # D.B.	ISOMERS
778	—	0.6	46:0	PPM,PMP
804	1.7	2.0	48:1	POM,PMO,OPM
806	4.7	4.9	48:0	PPP
830	13.4	11.8	50:2	PPL,PLP
832	35.4	37.3	50:1	PPO,POP
854	2.9	2.7	52:4	PLL,LPL,POLn,OPLn, PLnO
856	7.0	6.2	52:3	PLO,POL,OPL,PStLn, StPLn,PLnSt
858	19.7	19.1	52:2	POO,OPO,StPL,StLP, LStP
860	8.6	6.8	52:1	PStO,StPO,POSt
862	—	0.4	52:0	PStSt,StPSt
882	1.6	1.4	54:4	StPLn,OStLn,StLnO, StLL,LStL,LOO,OLO
884	3.1	2.9	54:3	OOO,StOL,StLO,OStL, StStLn,StLnSt
886	1.5	1.9	54:2	StOO,OStO,StStL, StLSt
888	0.5	0.6	54:1	StStO,StOSt
890	—	0.1	54:0	StStSt

Table I

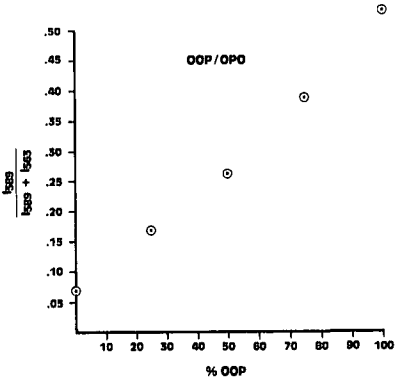


Figure 1

GC-FT/MS: INTERFACE CONSIDERATIONS

J. Kinsinger, S. Ghaderi, R. Hein, A. Hanna and J. Marra
Nicolet Analytical Instruments; Madison, WI 53711

With the advent of high resolution fused silica capillary columns, the need for rapid acquisition mass spectrometers has increased. The Fourier transform mass spectrometer has several advantages over conventional scanning instruments for use as a GC/MS instrument. A broad band (wide mass range) acquisition can be completed in 5 to 10 milliseconds. Data can be averaged as it is being acquired increasing the signal to noise. All ions are detected simultaneously thus eliminating problems of changing sample concentration during a scan. The ability to acquire high resolution mass spectral data can also be utilized.

The need for low pressure to obtain high resolution mass spectra represents the major limitation to optimal performance of both systems.

The use of an open split interface has enabled us to take advantage of the features of the FT/MS instrument while readily overcoming the limitations.

We used a Nicolet FT/MS-1000 mass spectrometer with an H-P 5880 gas chromatograph. The SGE open split unit was mounted in a separate temperature-controlled oven adjacent to the GC oven. Fused silica tubing from SGE was used for the one meter long transfer line. GC columns used were 12 to 15 meter nonpolar fused silica columns.

The size of the fused silica transfer tubing was used to establish the desired operating pressure in the mass spectrometer. Table 1 illustrates the operating pressures obtained with various tubing diameters. Mass spectral information can be obtained at all operating pressures, only the maximum obtainable resolution changes. As the open split unit operates at atmospheric pressure, changes in column flow due to temperature programming do not affect the pressure in the mass spectrometer.

The advantages of simultaneous ion detection can be illustrated by the data in Table 2 taken from the chromatogram shown in Figure 1. The first GC peak, a compound called CN (alpha-chloroacetophenone), has the mass spectrum shown in Figure 2. As shown in Table 2, the first, middle and last mass spectra across the GC peak all have similar mass spectral intensities. Rapidly eluting GC components are not a problem for FT/MS instruments.

High resolution data has been obtained on GC components. We have recorded the molecular ion of anisole (m/z 108) with a resolution of 20,000.

The combined features of rapid acquisition and simultaneous ion detection make the Fourier transform mass spectrometer an ideal GC-MS instrument.

TABLE 1
Vacuum Chamber Pressure versus Transfer Line Size.

Diameter of Fused Silica Transfer Tubing (mm)	Operating Pressure (torr)
0.025	2x10-6
0.050	5x10-6
0.075	2x10-7
0.100	1x10-6

TABLE 2

Relative Mass Spectral Intensities Across a GC Peak

Spectrum no.	m/z 50	m/z 51	m/z 77	m/z 105
1	16.9	36.0	29.8	100
4	15.9	36.7	30.1	100
6	23.0	45.2	36.1	100

Conditions: mass range–47 to 300 amu
acquisition time–22.5 msec.
no. of acquisitions averaged–50
pressure–1x10–6 torr

Figure 1

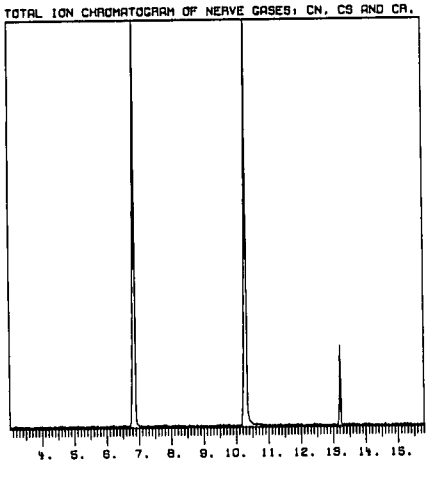
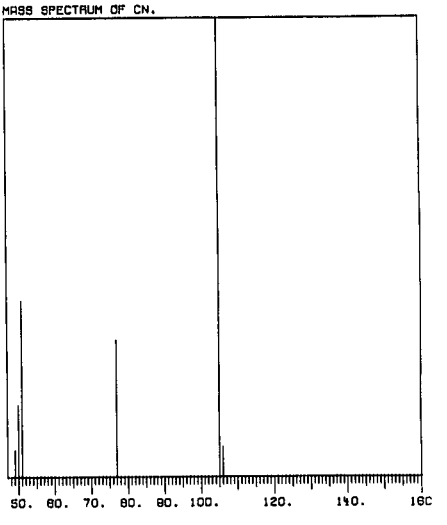


Figure 2



DEVELOPMENTS IN ION OPTICS AND ELECTRONIC CONTROL OF THE KRATOS MS80

Denne D.R., Stradling R.S., Warburton G.A., Taylor L.C.E.
Kratos Analytical Instruments, Barton Dock Road, Urmston
Manchester M31 2LD, England

Recent developments in ionization techniques have made possible the mass spectrometry of classes of compounds that have not previously yielded useful spectra. Many high molecular weight compounds can now be ionized and consequently there is a need to extend the mass range of current mass spectrometers.

Coincidental with the developments in ionization techniques, improvements in gas chromatography have created a need for greater simplicity in the operation of GC-MS instruments.

The only practical method of extending mass range is by increasing the radius of the magnet. However, using conventional technology, the overall size of the instrument (and therefore its cost) would need to be significantly greater in order to maintain the double focussing condition with the existing electrostatic analyser. The longer path length would also create difficulties in maintaining sensitivity and resolution.

A theoretical computer model of the ion optics of a double focussing mass spectrometer has been developed. This uses the program of Matsuda, Matsuo and Wallnik (TRIO) but with additions to take account of fringing fields and the effect of hexapoles. This program has been linked to other programs that allow practical magnets to be constructed and it is now possible to consider more complex concepts in magnet design such as the use of inhomogeneous fields.

It has been found that a segmented inhomogeneous field makes possible an increased magnet radius without a significant change to the size of the instrument.

The use of segmented inhomogeneous fields is totally new to mass spectrometry. In addition to more than doubling the mass range without an increase instrument size, focussing in the 'Z' plane (parallel to the beam defining slits) is also permitted.

These design concepts have been incorporated into a new magnet for the MS80 mass spectrometer. Known as the MS80RF, this instrument has a mass range of 2,400, compared with the standard instrument which has a mass range of 1,000. The sensitivity and resolution (25,000) specifications have been maintained.

The pole faces of the magnet are fully laminated and this has given the instrument a scan speed capability of better than 0.1 seconds per decade with a correspondingly fast reset. This performance faithfully reproduces the chromatograms of the highest resolution capillary columns.

An important feature of this instrument is its application to alternate CI/EI (ACE) scanning in which the performance of the magnet must be matched by the speed with which the source can switch between ionization modes. The chromatogram below shows a complete cycle time (EI - reset - CI - reset) of only 1.4 seconds. (Figure 1).

In order to simplify the operation of the MS80 most functions of the mass spectrometer and integrated data system are now operated through the Autoconsole keyboard thus replacing the major portion of the previous controls and providing a marked advance in speed and simplicity of operation. Important new instrumental functions such as keyboard selection of masses, magnetic peak switching and automatic peak matching are now standard on the Autoconsole version of MS80. Data system control permits selection of major instrument parameters such as resolution, electron current, scan rate, narrow scan width and bandwidth.

The various modes of operation of the mass spectrometer including EI, CI, ACE, positive and negative ions, are also controlled in this manner. Focussing is simplified by a peak selection and display facility, featuring a continuously updated report of intensity and resolution.

Routine experiments can be catered for by recalling the appropriate set of previously established multiple command sequences required for a particular analysis. Alternatively the operator can use a simple interactive prompting procedure.

The system operates by means of a series of menus which establish the parameters for each operation, for example, instrument setup, tuning, data acquisition, etc. As an example the illustration (Figure 2) shows the menu for peak focus.

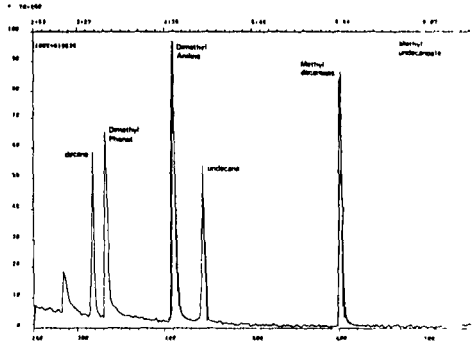


Figure (1) MS80 RF ACE GC run showing total cycle time of 14 seconds

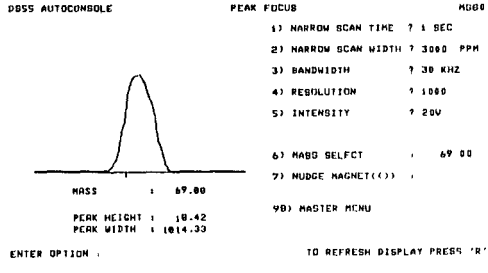


Figure (2) PEAK AT M/Z 69 IN THE EI SPECTRUM OF PFK AT A RESOLUTION OF 1000

A NEW TYPE OF DOUBLE-FOCUSING MASS SPECTROMETER

TAKEDA, T., SHIMADZU, K., SHIRATSUCHI, K. AND KUBODERA, T.
SHIMADZU CORP., R/D ENGINEERING DEPT., KYOTO, JAPAN

1 INTRODUCTION

In the field of GC/MS analyses, accuracy of measurements has been increased by making use of a double-focusing mass spectrometer(DF/MS) together with techniques of high resolution mode. In addition, combined scanning of the electric field and the magnetic field is used for the purpose of obtaining the collision induced dissociation spectra(CID). Thus needs for DF/MS are on the increase.

We have designed a new type of DF/MS, a reversed geometry type(R-DF/MS)[1]. The instrument has been tested and is continuing from several points of view. Tentative results are reported as follows.

2 THEORY

A series of reports[2),3)] are refered to for the design of the instrument. According to the theory, the final image(X_f) can be calculated by using transfer matrices.

In this work 12x12 matrices were used for calculating the second order aberration coefficients. The following equations hold.

$$[X_f]=(D3)\cdot(Eo)\cdot(E)\cdot(Ei)\cdot(D2)\cdot(Mo)\cdot(M)\cdot(Mi)\cdot[Xo] \quad (1)$$
$$=(A)\cdot[Xo]$$

where the transfer matrices (D),(M) and (E) represent those of field free regions, the magnetic field and the troidal electric field, respectively. Suffixes i and o of M and E denote the fringing fields at the entrane and exit boundaries of the fields.

[Xo] and X are the vectors composed of 12 elements: Xo, αo, βo and so on. Image width X_f in the median plane is written as follows.

$$X_f=Ax\cdot Xo+A_\alpha\cdot\alpha o+A_\delta\cdot\delta o+\triangle \quad (2)$$

$$\triangle=Am(|A_{\alpha\alpha}\cdot(\alpha o)^2|+|A_{\alpha\delta}\cdot(\alpha o\delta o|+|A_{\delta\delta}\cdot\delta o^2|+|A_{yy}\cdot(Yo/Am)^2|+|A_{y\beta}\cdot(Yo/Am)\beta o|+|A_{\beta\beta}\cdot\beta o^2|) \quad (3)$$

where Ax represents the image magnification, $A_\alpha=A_\delta=0$ from the double-focusing condition. αo and βo represent the divergent angles in the median and vertical planes; δo and Yo represent the energy spread of the ion beam and the

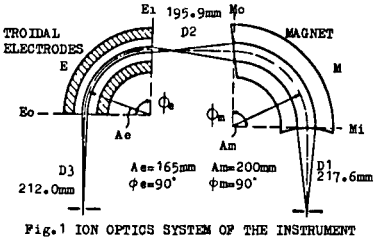


Fig.1 ION OPTICS SYSTEM OF THE INSTRUMENT

TABLE 1, CALCULATED VALUES OF PARAMETERS

First Order Parameters		Second Order Aberration Coefficients		Third Order Aberration Coefficients			
Ax	1.51	$A_{\alpha\alpha}$	-0.003	$A_{\alpha\alpha\alpha}$	15.4	$A_{\alpha\beta\beta}$	-20.4
Ar	1.57	$A_{\alpha\delta}$	-0.007	$A_{\alpha\alpha\delta}$	-48.2	$A_{\delta yy}$	0.96
Ay	-0.18	$A_{\delta\delta}$	0.704	$A_{\alpha\delta\delta}$	57.1	$A_{\delta y\beta}$	9.5
As	0.65	A_{yy}	-0.007	$A_{\delta\delta\delta}$	-27.7	$A_{\delta\beta\beta}$	20.0
		$A_{y\beta}$	0.005	$A_{\alpha yy}$	-2.4		
		$A_{\beta\beta}$	-0.309	$A_{\alpha y\beta}$	-13.3		

THIRD ORDER ABERRATION COEFFICIENTS ARE CALCULATED BY COMPUT R PROGRAM TRIO.[4)]

half-height of the ion source slit respectively. Δ represents the aberration due to the second order aberration coefficients. These are functions of ϕm, ϕe,Ae,D1,D2,D3 and so on.(see Fig.1) Calculations have been done in order to minimize the absolute values of $A_{\alpha\alpha}$~$A_{\beta\beta}$, by using a newly developed computer program. The results of the calculation are shown in Fig.1 and Table 1.

3 EXPERIMENTS

Experiments have been done from various points of view. Tentative results are shown in the followings.

A: Resolution has been tested. Tentative result without α slit is shown in Fig. 2.



Fig.2 RESOLUTION

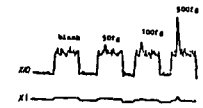


Fig.3 SENSITIVITY
S.I.M.;H.C.B.
M/Z 284

B: Sensitivity has been tested by making use of the single ion monitoring at resolution of 1,000. Detection with high sensitivity of 50 fg of hexachlorobenzen was obtained in the GC/MS mode. The result are shown in Fig. 3.

C: APPLICATION

PCB's in the air were analysed by means of mass fragmentography(M.F.). Impurities can be removed as the resolution increases.(Fig. 4)

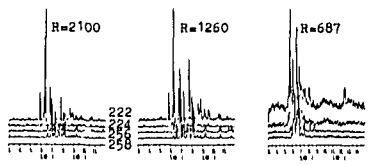


Fig 4 MASS FRAGMENTOGRAM OF PCB IN THE AIR(~Pg)

Bile acid was analysed by making of the solventless capillary column(SE 30:20m). This analysis was done by means of mass chromatography(M.C.). (Fig. 5)

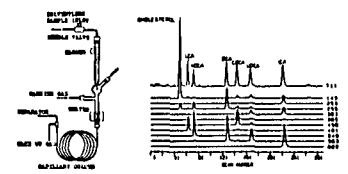


Fig. 5 ANALYSIS WITH CAPILLARY COLUMN: MASS CHROMATOGRAM OF O-ETHYL ESTER, O-DIMETHYL-SILYL ESTER
(BY COURTESY OF J. TAMAGAWA AND F. HARATAKE)

4 RESULTS AND DISCUSSION

This instrument has the following features. Reversed geometry type of DF/MS has the advantage of yielding mass analysed ion kinetic energy spectrum(MIKES). Bright ion optics system is attained by making use of the troidal electrodes. The focusing property in the vertical direction is excellent, as the image magnification is about 1/6. (Fig. 6)

cation is about 1/6. (Fig. 6)

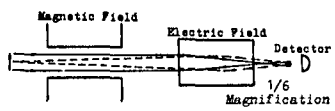


Fig. 6 Focussing Property Of The Vertical Direction

REFERENCE

1 T.Takeda and T. Kubodera, Mass Spectrsc.(Japan) in printing
2 H. Matsuda and H. Wollnik, Nucl. Instr. Meth.,77,283(1970)
3 T. Matsuo, H. Matsuda and H. Wollnik, Nucl. Instr. Meth., 103,515(1972)
4 T. Matsuo, H. Matsuda, Y. Fujita and H. Wollnik, Mass Spectrsc. 24,19(1976)

A NEW FAST SCANNING MAGNETIC ANALYSER. BILL J.C., GREEN B.N. and BROOKS P.W.
VG Analytical Limited, Altrincham, Cheshire. England.

INTRODUCTION

The successful application of the fast atom bombardment (FAB) ionization technique to an ever-increasing range of compounds, has provided further impetus to the development of instruments with increased mass range. Previously, such instruments have been either based on a magnetic analyzer with relatively slow scan rate, thus having only a limited application in other areas of mass spectrometry (e.g. GC/MS and DCI) or, they have used other types of analyzer (e.g. time of flight) which have limited resolution. Since the introduction of laminated magnet technology to mass spectrometry, and with careful design of high saturation induction pole tips, it is now possible to construct magnetic analyzers capable of significantly higher field strengths (i.e. mass range) whilst retaining the fast scanning properties of an analyzer suitable for capillary column GC/MS applications and without compromise of the accurate mass measurement capability of the instrument.

HIGH MASS PERFORMANCE

By combining high saturation induction pole tips with the already developed fully laminated magnet core on the VG ZAB, the maximum magnetic field has been increased from about 1.9 T to nearly 2.4 T. This has resulted in the maximum mass at the full ion energy of 8 kV being increased from 2000 to over 3000.

At reduced ion energy, the mass range of the ZAB HF is increased significantly above 3000. Clusters of cesium iodide have been observed up to $Cs_{99}I_{98}$ (25,594 daltons) by operating at 1 kV ion energy. In this laboratory, the largest organic molecule, so far ionised intact by FAB, is bovine insulin. In Figure 1 is shown the result of summing 6 positive ion scans, each of 10 seconds duration, over the mass range 5725-5745. These were recorded at 4 kV ion energy from a single introduction of insulin dissolved in thioglycerol. The potassium iodide cluster $K_{35}I_{34}$ (5678.49 daltons) was used to calibrate the mass scale. The calculated mass of the $(M+H)^+$ ion of bovine insulin assuming the molecular compositon $C_{254}H_{377}N_{65}O_{75}S_6$ is 5730.61.

SCANNING PERFORMANCE

By fully laminating the yoke of the magnet, the eddy current limit to scan rate has been essentially eliminated. The ultimate scan rate of the new magnet, when operating with a coil configuration giving 1000 mass range at 8kV ion energy is approximately $10(M)^{\frac{1}{2}}$ mS/decade. Thus, below m/z 600, field controlled scans may be carried out down to 300 mS/decade.

Figure 2 shows a reconstructed Total Ion Chromatogram from an analysis of a mixture of methyl esters, during which the instrument was repetitively scanned from m/z 500 to m/z 25 at 300 mS/decade and at a resolution of 1000. Also shown is the spectrum from about 10 ng of methyl palmitate injected on the column.

A further advantage of the laminated magnet construction is that the change of focus which occurs as the scan rate is increased with solid core magnets, is minimised. Hence it is practicable to scan down to 1 sec/decade at a resolution of 5000. This resolution is sufficient to separate reference peaks from sample peaks in most cases. Also, the cycle time is fast enough for most GC applications.

An assessment of the mass measurement accuracy achieved at 1sec/decade and 5000 resolution was carried out by measuring 27 perchlorobutadiene (PCB) peaks over the mass range 94-266 using PFK as the internal reference and gave an average RMS error of 5.3 ppm on single scan data. For this test, the PCB and PFK were introduced into the septum inlet system.

Similar accuracies were obtained with a mixture of esters introduced via the GC. A partial listing of the elemental composition calculations of the full spectrum of methyl palmitate is shown in Figure 3.

Conclusion

A high field magnet has been constructed, with little or no compromise of scan rate performance resulting from laminated yoke technology, or mass measurement performance.

Figure 1

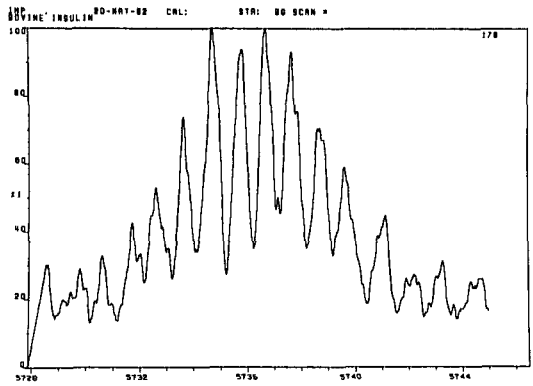


Figure 2

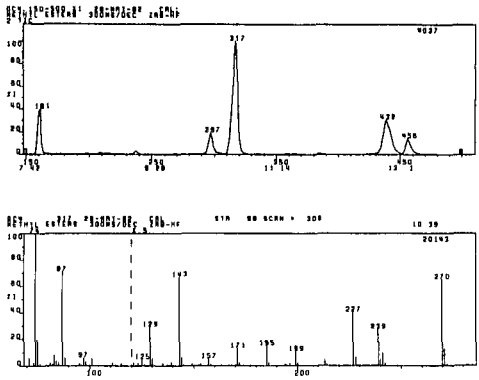


Figure 3

M4.251 RT 0: 9:35 20-MAY-82 TIC:538 AUTO-GRIN=1 1. 1
BASE INT.=1535 B/G SCAN=247 STATUS:1

M/E		C	H	D 16	PPM	ACC.MASS	%HT MOD
271	*	17	34	2	-3.7	271.2592	5.86
270		17	34	2	-4.1	270.2559	29.19
	*	17	33	2	12.5	270 2514	
242		15	30	2	-6.9	242.2246	1.97
	*	15	29	2	11.7	242.2201	
241		15	29	2	13.9	241.2167	4.30
240	*	16	31	1	2 2	240 2408	3.52
239		16	31	1	0.8	239.2375	16.16
228	*	14	27	2	1.3	228.2044	3.84
227		14	27	2	-5.6	227.2011	18.24
	*	14	26	2	14.2	227.1966	
213		13	25	2	5.6	213.1854	1.82
						207.0297	1 04
200	*	12	23	2	1.7	200.1731	1 04
199		12	23	2	-2.4	199.1698	5.15

EXPERIMENTAL AND COMPUTER-SIMULATED ION TRANSMISSION IN A TRIPLE-QUADRUPOLE MASS SPECTROMETER.

R. N. Stillwell, D. I. Carroll, J. G. Nowlin and E. C. Horning.
Institute for Lipid Research, Baylor College of Medicine, Houston TX 77030.

A triple-quadrupole mass spectrometer for collision-induced dissociation studies and high-sensitivity analyses was constructed with an ion source and lenses designed with the aid of computer modeling.

Electrostatic field calculation. The geometry and potentials of the cylindrically-symmetrical electrodes are specified to the program CFIELD. Inter-electrode potentials are set initially to the potential of the nearest electrode, and refined by stepwise successive over-relaxation by repeatedly applying the formula:

$$V_0 \leftarrow V_0 + C_f \cdot (V_0' - V_0)$$

where:

$$V_0' = (V_1+V_2+V_3+V_4)/4.0 + (V_3-V_1)\cdot h/(8r)$$

h is the mesh interval; r is the distance from the center. C_f is the over-relaxation factor, which decreases towards 1 as the relaxation proceeds.

Ion path calculation. The initial positions and velocities of the ions to be traced are supplied to the program KLEMP, together with the electrostatic field calculated by CFIELD. The ion paths are calculated by numeric integration of the Newtonian equations of motion:

$$\frac{d^2z}{dt^2} = -\frac{e}{m}\cdot\frac{\partial V}{\partial z} \qquad \frac{d^2r}{dt^2} = -\frac{e}{m}\cdot\frac{\partial V}{\partial r}$$

by an algorithm described by Klemperer (O. Klemperer and M. E. Barnett, Electron Optics, 3rd edition, 1971). Electrostatic potentials and the partial derivatives between grid points are calculated by bicubic interpolation.

Plotting. Field contours and cross sections are plotted by bicubic interpolation. Ion paths are plotted as calculated by KLEMP. Other plots can be generated to show the rate of convergence of relaxation, the kinetic and potential energies of ions, etc.

Implementation. All programs are written in Flecs-Fortran except for the central calculations in CFIELD and KLEMP, which are coded in assembler for speed. They run on a PDP11/45 under IAS. A complete simulation takes from 15 to 90 minutes (elapsed), depending primarily on the complexity of the plot desired and the system load.

Experimental. A Finnigan 1015 source and lens of known characteristics was modeled first. Best ion transmission in the model correlated approximately with optimal focusing potential in the actual source. The effect of converting this source from a repeller-plate to an extractor design was modeled. As expected, the extractor gave better ion focusing. The design of the source makes it difficult to do the actual conversion.

Various lens configurations were then modeled. The lens shown in the figures was chosen since it gives excellent ion transmission for thermal ions and plenty of pumping area for separating neutrals. A triple-quadrupole mass spectrometer was built with three of these lenses. In the instrument as built, ion transmission through the second lens (between Q1 and Q2) was measured as a function of lens voltages. Maximum transmission occurred just before the central element reached the cutoff potential of 20V, as predicted by the model. Sensitivity of the instrument is good. In order to determine sensitivity, Q1 was set to pass m/z 211 (MH^+ of benzil) and Q3 was set to pass m/z 105 ($C_6H_5CO^+$). Samples of benzil injected through the GC inlet gave linear response with good signal/noise down to the low pg range.

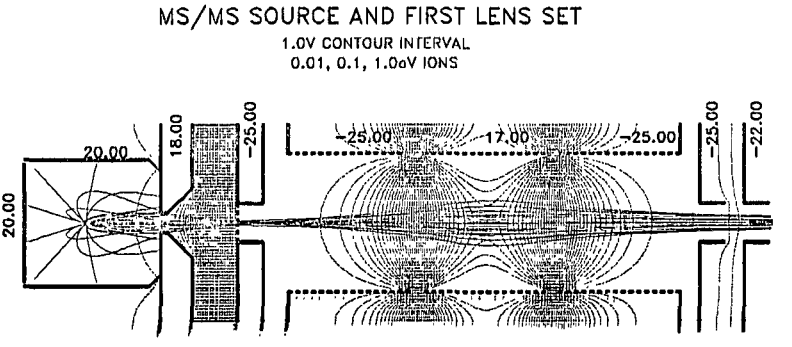


Figure 1. Ion source and lens of triple quadrupole mass spectrometer. Two other similar lenses are between Q1 and Q2 and between Q2 and Q3.

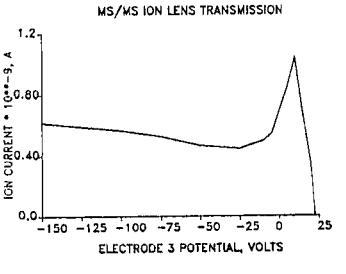


Figure 2. Ion transmission of second lens

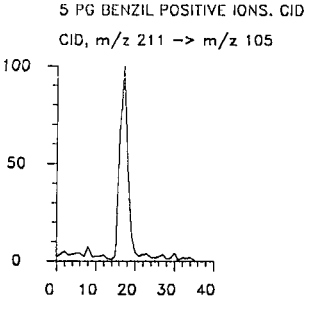


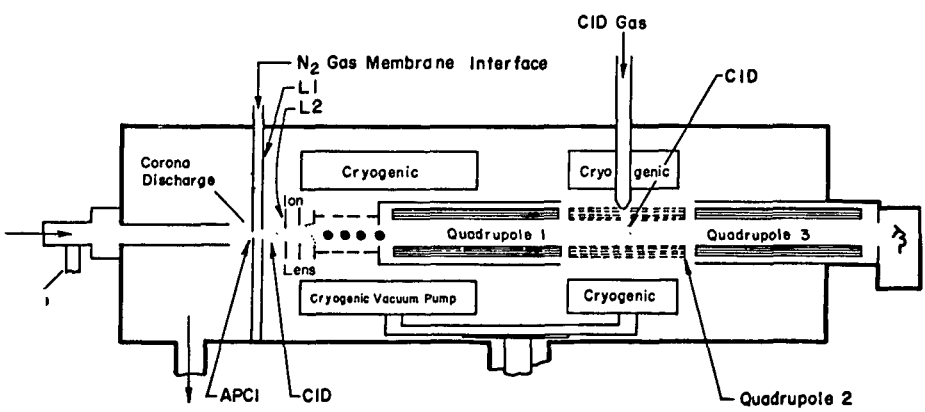
Figure 3. Response of the mass spectrometer to 5pg of benzil through the GC inlet.

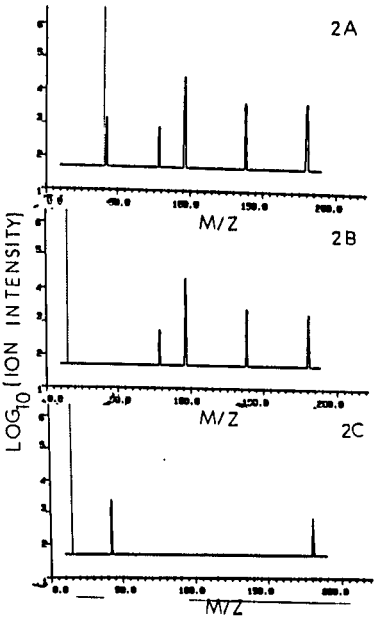
ACCURATE MASS DIFFERENCE MEASUREMENTS COMBINED WITH HIGH SENSITIVITY USING THE CHEMICAL RESOLUTION OF A TRIPLE QUADRUPOLE; P.H. Dawson, Division of Physics, National Research Council of Canada, Ottawa, Ontario, K1A 0R6

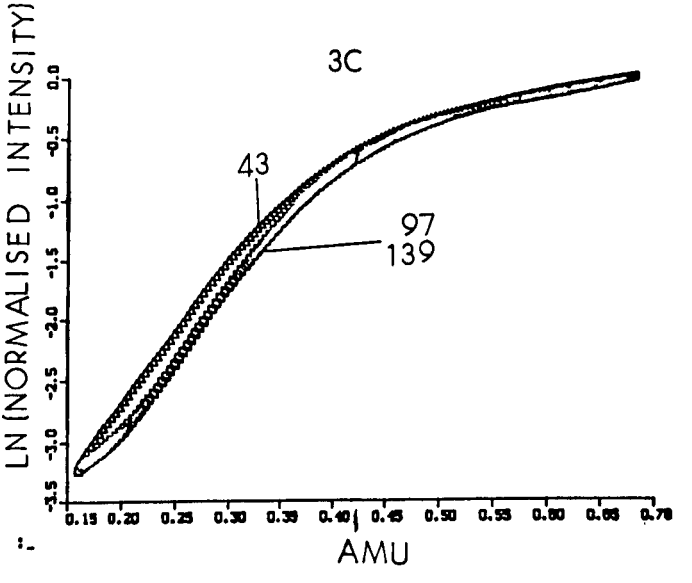
Triple quadrupoles use the first analyser to separate parent ions according to their nominal M/Z. These ions are fragmented by collisions in the second quadrupole and the characteristic daughter ions are analysed in the third quadrupole. Total transmission can be very high in a well designed system and most parent ions can be efficiently fragmented. The MS/MS technique is widely used in the analysis of complex mixtures. However, some additional information may be necessary to distinguish parents of the same nominal mass, particularly if library fragmentation spectra are not available. This paper will demonstrate the ability to distinguish and measure small mass differences in parents which have different characteristic daughters. Several examples will be shown using spectra obtained with a slightly modified TAGA 6000 triple quadrupole. The chemical resolution of the CID process permits accurate measurements without interference between the species. (In effect, one achieves a high resolution separation of the overlapping peaks.) One advantage over the more conventional physical achievement of high mass resolution is that measurements can be made with wide peaks corresponding to high ion transmission and with one species far in excess of the other. The only requirement is that the two parents have similar energy distributions so that they give identical peak shapes and small peak shifts can be accurately observed. The technique can be used (a) to distinguish, in a complex spectrum, which daughter ions are associated together and which arise from different parents and to measure the mass difference between the parents, or (b) to accurately determine the mass of a parent ion by adding a reference compound.

The accompanying example illustrates the identification of the protonated parent of 3:4 dimethoxyacetophenone (M/Z = 181.086) in the presence of that of di-isopropylmethylphosphonate (M/Z = 181.099). With a laboratory collision energy of 17 eV and an argon target, the CID spectrum of the "unknown" mixture is as shown in fig. 1. At this collision energy, di-isopropylmethylphosphonate H^+ does not give a daughter at M/Z = 43 (fig. 2 shows a reference spectrum). The presence of 3:4 dimethoxyacetophenone H^+ is suspected since it produces largely M/Z = 43 (fig. 3 shows a reference spectrum) but the CID spectrum is not informative. A measurement of the mass difference $\delta M = 0.013$ (or 1 part in 14000) can be used for confirmation.

The third quadrupole was used to alternately monitor the M/Z = 139, 97 and 43 daughters while scanning the leading edge of the M/Z = 181 parent with the first quadrupole in steps of 1/64 amu. Figure 4 shows the smoothed, interpolated and normalised data for the three peaks. The 139 and 97 peaks arise from the same parent and are exactly coincident. The parent giving the 43 peak is laterally displaced. An automated matching technique indicated $\delta M = 0.020 \pm 0.008$ confirming 3:4 dimethoxyacetophenone H^+ as the parent. Present accuracy is limited by the step size in scanning the parent peak to about 1 part in 25000.




2A
2B
2C
M/Z
M/Z
M/Z
LOG_{10} (ION INTENSITY)


3C
43
97
139
LN (NORMALISED INTENSITY)
AMU

DEVELOPMENT OF A DATA SYSTEM CONTROLLED NEUTRAL LOSS CALIBRATION PROCEDURE FOR A TRIPLE STAGE QUADRUPOLE MS/MS INSTRUMENT

Steiner, U., Kirby, H., Sokolow, S., Finnigan MAT, San Jose, CA.

A neutral loss (NL) spectrum on a triple stage quadrupole (TSQ)* is obtained by scanning quadrupole Q1 and quadrupole Q3 at the same time and rate but with a fixed mass offset. The results are spectra which represent ions that have lost a common mass. To satisfy scan speed and system integration we used the following hardware:

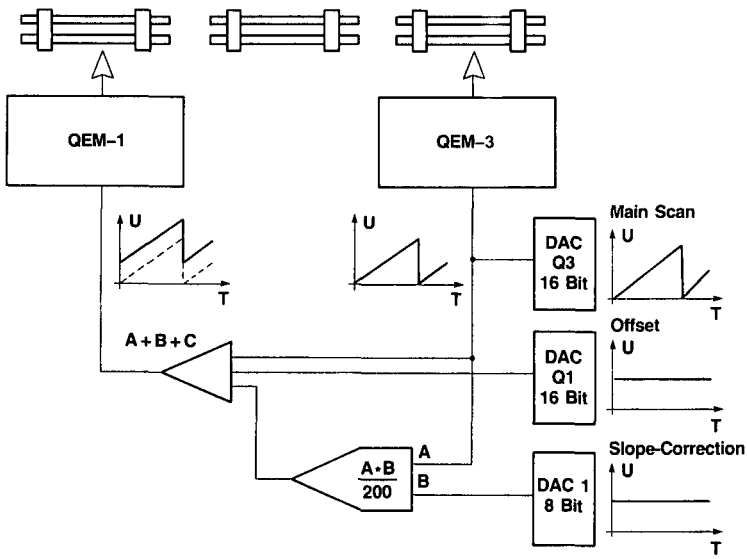


Figure 1

A digital ramp generator scans DAC Q3 (16BIT) which drives quadrupole Q3, DAC Q1 (16BIT) is used to select the mass difference between Q1 and Q3. By reversing its polarity a neutral gain spectrum can be obtained. To compensate for the different gains in the quadrupole electronic modules (QEM) a slope correction DAC has been added.

For the calibration of the DACs, a new program NLDGN (Neutral Loss Diagnostic) was developed. It's main functions are:

- Creation of a calibration table for setting the offset mass on DAC Q1.
- Minimizing the slope error by optimizing the setting on the slope correction DAC.
- Display of maximum mass error for a selected offset and a given scan range.

* Trademark

We developed the following calibration sequence:

1. Acquisition of a three dimensional data map of calibration compound by scanning the offset (DAC Q1) and incrementing Q3 once per scan. In order to collect sufficient ions, Q2 and Q3 are in RF only mode.
2. Standard calibration of scan file by using a reference table and the corresponding offset on Q3.
3. Calculation of slope error for a given neutral loss by reading through all calibration tables and comparing the DAC steps to each other.
4. Correcting the slope by sending an updated value to the slope correction hardware.
5. If the slope error is greater than 0.1u repeat sequence starting at Step #1.
6. Create a calibration table for the neutral loss offset by altering the offset mass; calculate the best offset value and add that value to the calibration file.
7. Display of maximum mass error between Q1 and Q3.

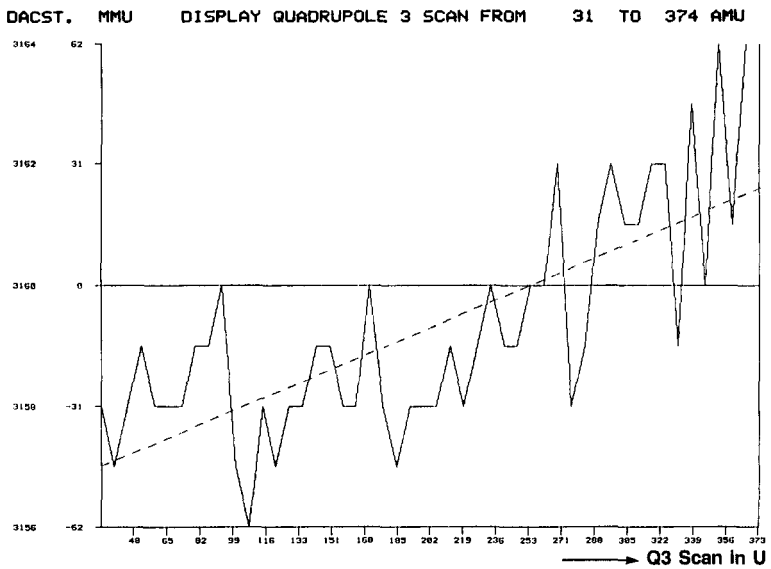


Figure 2

In this example the offset was 50u and Q3 would scan from 30 to 400u. The mass difference between the two scans is in this case plus or minus 62mnu.

CONCLUSION AND RESULTS:

Once the automatic calibration is completed (it takes about 10 min.) the user simply selects a scan range and an offset mass to define a neutral loss spectrum. As with any operation mode, (Q1MS, Q3MS, parent and daughter) a neutral loss can be used within an experiment or with multiple selected ion monitoring. The scan speed limitation is only given by the RF/DC drivers which is 1000u in 0.1 sec. The stability of the whole system allows the calibration to be valid over more than two weeks.

CONSTRUCTION OF A REVOLVING STAND FOR CLEANING ION SOURCE AND RODS OF QUADRUPOLE MASS SPECTROMETER

Benjamin Y. Giang

de Guigne Technical Center, Stauffer Chemical Company, Richmond, CA 94804

Maintaining a clean ion source is essential for the optimum operation of a mass spectrometer.[1] This report describes the design and the construction of a revolving stand for cleaning the ion source of quadrupole mass spectrometers. The stand as described can be constructed in any carpentry shop.

The design for the ion source stand is shown in Figure 1. It consists of the stand box, the lazy susan turntable bearing and the base. The dimensions of each of the parts is described in the table below.

Dimensions of the Parts

Description	Length in Inches	(Centimeters)	Width in Inches	(cm)	Quantity
Top of Stand Box	8.75	(20.3)	9.25	(23.5)	1
Side Pieces of Stand Box	6.75	(17.2)	9.25	(23.5)	2
Bottom of Stand Box	6.5	(16.5)	9.25	(23.5)	1
Back of Stand Box	6.5	(16.5)	6	(15.2)	1
Base of Stand	11.5	(29.2)	9.25	(23.5)	1
Lazy Susan Turntable Bearing	6	(15.2)	6	(15.2)	1

The various parts for the stand box are assembled with glue and nails. After assembling, the box should resemble the top portion of Figure 1. The turntable bearing is fastened to the bottom of the stand box and the base with screws. The finished product should be a stand box rotating the top of a base board. The stand has been very useful to our laboratory.

[1] Finnigan Spectra 1975, 5(1), 5.

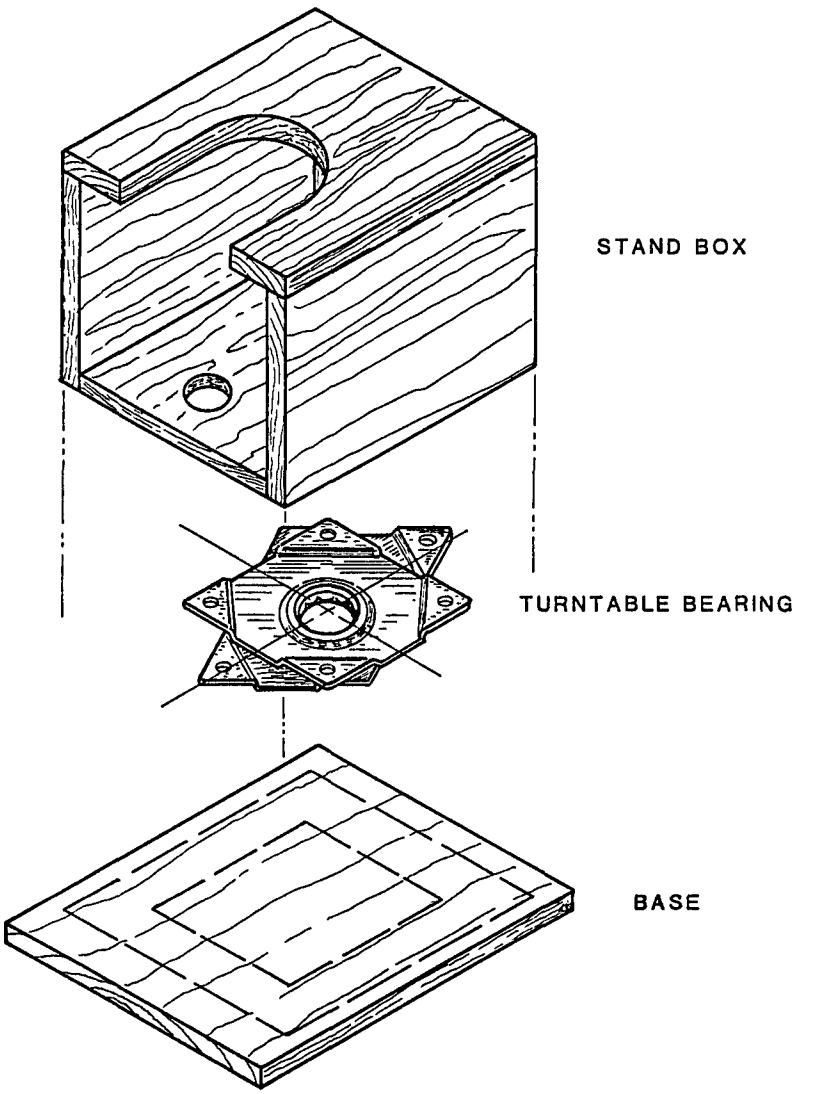


FIGURE 1. Assembly of the Stand-Box, the Turntable bearing, and the Base into the Rotatable Stand for Source Cleaning.

ION TRANSMISSION THROUGH REALISTIC FRINGE FIELDS OF A QUADRUPOLE MASS SPECTROMETER

Donald M. Mintz

Finnigan MAT, 355 River Oaks Parkway, San Jose, CA 95134

The influence of fringing fields of a quadrupole mass spectrometer and cylindrical lenses has been studied theoretically only in the most approximate of ways to date because of the lack of knowledge of an exact potential. One previous assumption has the potential turning on linearly from 0 to the value in the device center over some range. By this treatment, range is merely a parameter and is not tied directly to the physical dimensions of the device. Furthermore, the linear fringe field potential cannot satisfy Laplace's equation, which would require gradients in the potential off axis beyond those given us by the purely hyperbolic potential.

This study begins with an exact calculation of the three dimensional potential by solving Laplace's equation using the method of successive overrelaxation on a potential grid. The problem must be treated three dimensionally because of the difference in azimuthal symmetry of a source exit lens and the quadrupole field. Several source-quadrupole geometries were examined, including those of Finnigan's model 4000 and 4500 mass spectrometers. For the sake of simplicity, and without loss of generality, the quadrupole field was assumed to be hyperbolic, even though those instruments have round rod quadrupoles. Because of the extensive symmetry which remains, a calculation need only treat a wedge-shaped 1/8th of the device. The geometry of a sample 4000 fringe field is shown in Figure 1.

A second step was to plot the axial variation of potential for different radial cuts. Sample axial potential profiles are shown in Figure 2. For calculations of ion transmission in such fringe fields, it was judged too cumbersome to calculate electric forces by numerical interpolation of derivatives on such a large potential grid. Instead, it seemed more worthwhile to find an analytical function which might give us the required potential variation and be amenable to parameterization. Such a functional form is;

$$V(x,y,z) = \left[\frac{x^2-y^2}{R_0^2}\right] \cdot \left(1 - \beta \frac{\alpha}{\exp(cz+d)+\exp(-cz-d)}\right)$$

where α, β, c, and d are parameters and R_0 is the inscribed radius of the mass filter. The optimal values of α are 4 and 2.3 for the 4000 and 4500 entrance geometries, respectively. Corresponding values of d are 1.317 and 0.541. The functions β and c are parameterized to give the required off-axis variation and dependence on L_{90}, the distance over which the potential close to the device axis rises to 90% of its value in the device center. In turn, β, c, and L_{90} may be express in terms of a "shift", an axial displacement of the quadrupole with respect to its normal position abutting the source.

Results are shown in Figure 3. Transmission is higher than that predicted by simple models of fringe field potential which don't incorporate the full off-axis potential variation. Still, the results displayed here show an optimum transmission for fringe field lengths L_{90} in the range 1.5-2 cycles of RF, in agreement with those simple fringe field models. For fringe fields shorter than this, the transmission falls slightly, but not to zero. On the other hand, for fringe fields appreciably longer than 1.5-2 cycles, transmission can fall to zero. Control of L_{90} through varying the source-quadrupole "shift" permits a limited range of adjustment of L_{90}. In contrast, the fringe field length varies inversely as the square root of the axial ion energy, which permits substantial control. Indeed, for m/z 400 ions, transmission in Figure 3 optimizes for approximately 2 eV axial energy. That the m/z 400 transmission generally optimizes at 5-10 eV ion energy when a Finnigan model 4000 or 4500 source is clean probably indicates that source extraction is a more important factor in overall mass spectrometer performance.

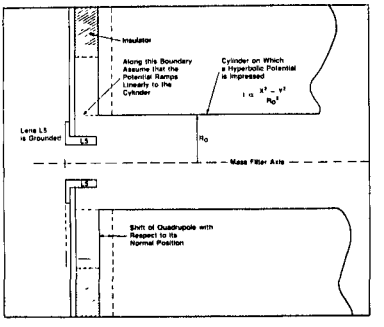


Figure 1. 4000 Entrance Geometry

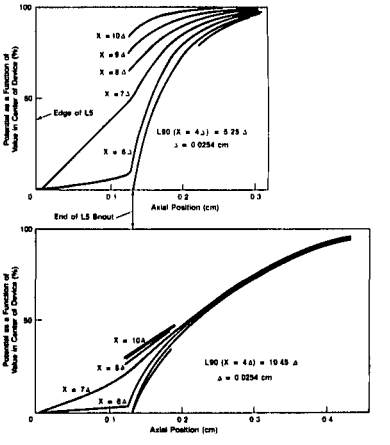
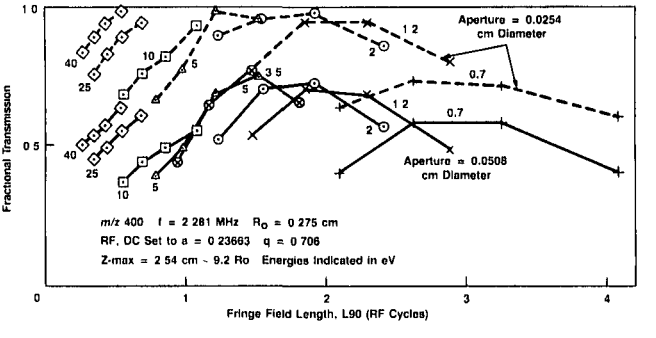


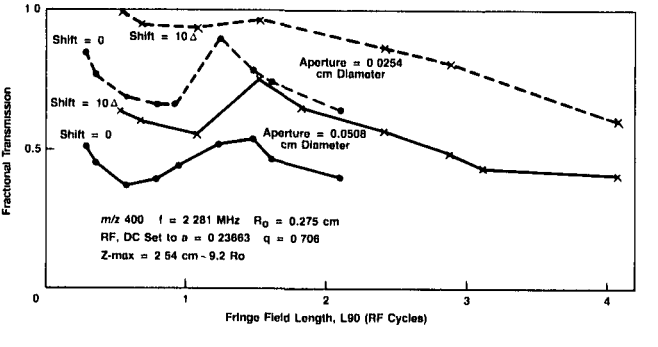
Figure 2. Axial potential profiles at different radii, taken along the X axis, where the potential varies the most. Top: shift=0. Bottom: shift=10Δ.

Figure 3a, 3b. Ion transmission through 4000 fringe fields and the indicated entrance entrance aperture. 3a) lines represent single energies and four different entrance geometries. 3b) lines for each entrance geometry (shift). Same data as 3a.

3a)



3b)



FIELD DESORPTION MASS SPECTROMETRY OF BIOLOGICALLY ACTIVE GLYCOSIDES FROM THREE SPECIES OF ASTEROIDEA INVERTEBRATES

T. Komori, Y. Itakura, K. Sakamoto, S. Taguchi and I. Maetani

Faculty of Pharmaceutical Sciences, Kyushu University, Maedashi 3-1-1, Higashi-ku, Fukuoka, 812, Japan

Oligoglycosides sulfates from starfish are well known toxic components against coral reefs, snail and bivalves, etc., and have attracted considerable attention. These polar glycosides as an almost inseparable mixture possessing much the same related structure. As for the isolation of genuine glycosides in a pure form, new methods for separation have been established in our laboratory

We applied field desorption mass (FDMS) spectrometry to elucidate the structure of unstable 20-hydroxy-cholesten-23-one type glycosides isolated from three species of Asteroidea invertebrates (Acanthaster planci L., Astropecten latespinosus Meissner and Luidia maculata Müller et Troschel). For this purpose, two pregnene-type glycosides, one cholesten-23-one type glycoside, two 20-hydroxy-cholesten-23-one type glycosides and a reference genuine sapogenin, 6,20-dihydroxy-23-oxo-5α-cholest-9(11)-en-3β-ol were examined. Fast atome bombardment mass (FAB-MS) spectrometry of genuine glycoside, 3-O-sodiumsulfate of 20-hydroxy-cholesten-23-one type glycoside, was also done.

The FDMS spectra were recorded on a JEOL D-300/JMA 2000 system (combined EI/FI/FD ion source). The spectra were partly produced on a JEOL DX-300/JMA-3500 system. FAB-MS spectra were recorded JEOL DX-300/FAB FD ion source-data system JMA-3500. ^{13}C-NMR spectra were recorded on a JEOL FX-100 spectrometer.

20-Hydroxy-cholesten-23-one type glycosides produced an intense ion peak provided by proton-induced retro aldol type fragmentation of β-hydroxy-carbonyl function in the side chain, but a weak M + Na ion peak. A terminal sugar unit was subsequently removed from the above intense ion by proton attack at the glycosidic linkage. The FDMS spectra, in conjunction with ^{13}C-NMR results, corroborate the 20-hydroxy-23-carbonyl structure in these glycosides. In the spectra of the sulfate of a pregnene type glycoside-permethylate,

an intense ion due to proton-induced solvolysis type fragmentation [M+Na+H-(SO_3Na) or M+H-SO_3] was found, as a base peak. In the spectra of cholestenone- and pregnene type glycosides, the M + Na ion is a base peak and the fragments due to proton-induced cleavages of glycosidic bonds have also been citation (1 - 5).

FAB-MS spectrometry of the genuine glycoside sulfate is a useful aid for determination of molecular size and of the structure of both aglycone and sugar moiety.

References

(1) Schulten, H.-R., Komori, T., Nohara, T., Higuchi, R., and Kawasaki, T.: Tetrahedron, 34, 1003 (1978)

(2) Komori, T., Kawamura, M., Miyahara, K., Kawasaki, T., Tanaka, O., Yahara, S., and Schulten, H.-R.: Z. Naturforsch, 34C, 1094 (1979)

(3) Komori, T., Maetani, I., Okamura, N., Kawasaki, T., Nohara, T., and Schulten, H.-R.: Liebigs Ann. Chem., 1981, 683.

(4) Komori, T., Sanechika, Y., Ito, Y., Matsuo, J., Nohara, T., Kawasaki, T., and Schulten, H.-R.: Liebigs Ann. Chem., 1980,1979.

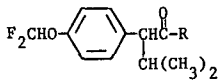
(5) Komori, T., and Kawasaki, T.: JEOL News, 18A, 39 (1982).

IDENTIFICATION OF M-PHENOXYBENZALDEHYDE RELATED MINORS IN PAY-OFF* (FLUCYTHRINATE) INSECTICIDE BY GAS CHROMATOGRAPHY LOW AND HIGH RESOLUTION CHEMICAL IONIZATION AND ELECTRON IMPACT MASS SPECTROMETRY

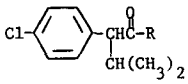
S. J. Cardaciotto, T. Chang, W. G. Millen, M. L. Thomson

American Cyanamid Company, Agricultural Research Division, Process and Analytical Research, P.O. Box 400, Princeton, New Jersey 08540

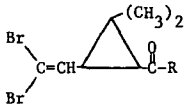
Gas chromatography-chemical ionization (GC-CI) and electron impact (EI) mass spectrometry were utilized to identify the m-phenoxybenzaldehyde related minors in PAY-OFF* and has led to understanding the effect of the aldehyde composition on its quality. The aldehyde is an expensive raw material which is used in the manufacture of flucythrinate (PAY-OFF*) and other pyrethroid insecticides such as fenvalerate and decamethrin.



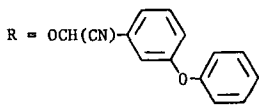
Flucythrinate



Fenvalerate

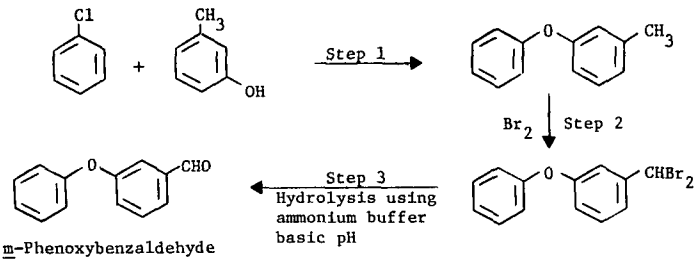


Decamethrin



Several minor components were identified and structural assignments were developed based on the mass spectral data generated from low resolution CI analyses and EI and CI exact mass measurements. Mechanisms were proposed for the formation of each of the minor components consistent with a synthetic pathway for the aldehyde.

Proposed Reaction Pathway to m-Phenoxybenzaldehyde



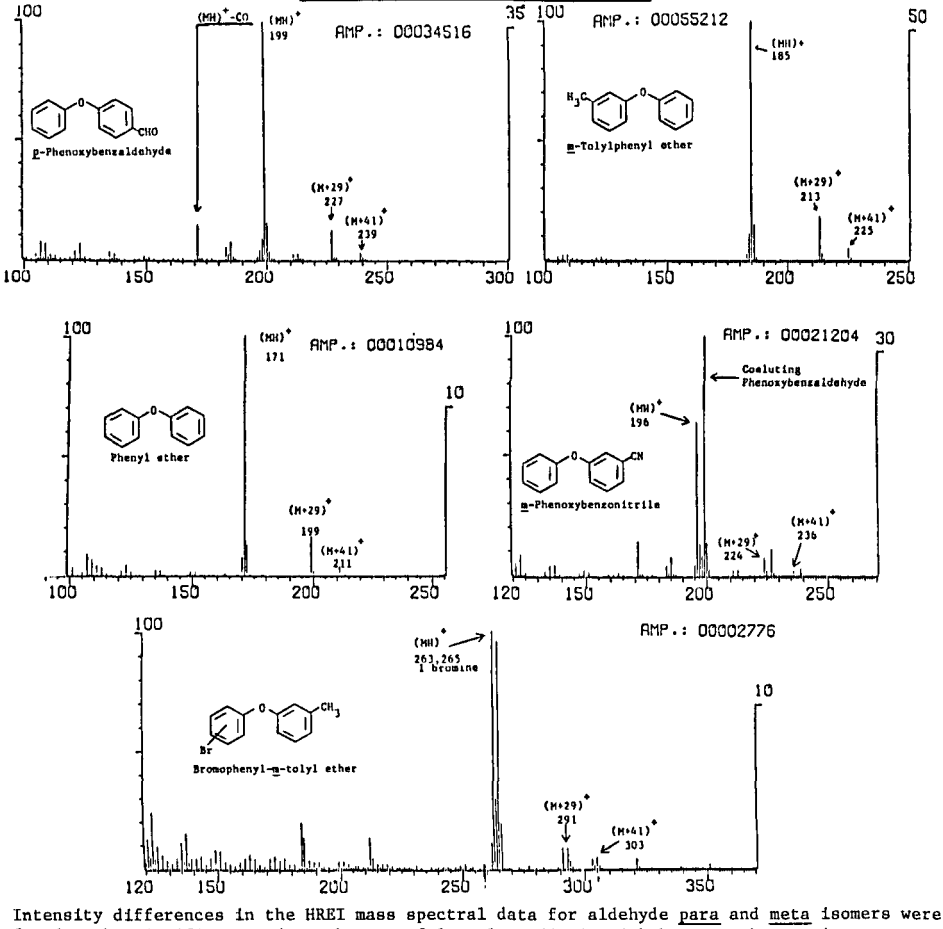
m-Phenoxybenzaldehyde

By-Products of m-Phenoxybenzaldehyde and Source of Formation

p-Phenoxybenzaldehyde	Step 1 - p-Cresol impurity in m-Cresol
m-Tolylphenyl ether	Step 1 - Residual Step 1 product
Phenyl ether	Step 1 - Phenol impurity in m-Cresol
m-Phenoxybenzonitrile	Step 2 - Reaction of ammonia and a benzotribromide by-product
Bromophenyl-m-tolyl ether	Step 2 - Ring brominated by-product

* Trademark of American Cyanamid Company

Methane Chemical Ionization Spectra



Intensity differences in the HREI mass spectral data for aldehyde para and meta isomers were found to be significant and may be a useful tool to distinguish between the two isomers.

High Resolution Electron Impact Ionization of para- and meta-Phenoxybenzaldehyde

Molecular Formula	Ion	Measured Mass (Δ, mmu) para	Measured Mass (Δ, mmu) meta	Relative Intensity (%) para	Relative Intensity (%) meta
$C_{13}H_{10}O_2$	$M^{+\cdot}$	198.0676 (-0.5)	198.0680 (0.0)	100	100
$C_{13}H_9O_2$	M-H	197.0597 (-0.6)	197.0587 (-1.5)	99	38
$C_{12}H_{10}O$	M-CO	170.0713 (-1.9)	170.0693 (-3.8)	2	5
$C_{12}H_9O$	M-H-CO	169.0645 (-0.9)	169.0647 (-0.6)	7	28
$C_{11}H_9$	M-H-2(CO)	141.0700 (0.4)	141.0704 (0.0)	16	21

STRUCTURAL CHARACTERIZATION OF COMPLEX AMINOGLYCOSIDE ANTIBIOTICS BY EMITTER CHEMICAL IONIZATION MASS SPECTROMETRY

Naohito TAKEDA, Ken-ichi HARADA, Makoto SUZUKI and Akira TATEMATSU
Faculty of Pharmacy, Meijo University, Nagoya 468, JAPAN

The application of emitter chemical ionization (desorption CI) technique to the analysis for thermally labile or highly involatile substances is rapidly expanding.[1] We have recently demonstrated the utilities of the technique for molecular weight determination and structural characterization of aminoglycoside antibiotics, mainly kanamycin A, B and C.[2] However, the major problems with this technique are that the thermal decompositions exceeding the production of the ions indicative of the molecular weight (e.g. MH^+) are often observed, particularly in applying to the more thermally unstable / involatile compounds. There are two interesting publications concerning the problems : one by Carroll et al., who used amine adduct formation with pyridine / isobutane mixed reagent gases,[3] and another by Reinhold and Carr, who used polyimide - coated wires.[4]

We have now used a 10 turn - coiled wire rather than a linear one, where more effective sample heating will be expected. Further, we have covered the coiled wire surface with silicon microneedles by the activation with silane gas (SiH_4 5% + Ar 95%),[5] as required. In order to explore the practical values of this technique with the coiled silicon - activated wires, various types of complex aminoglycoside antibiotics ; neomycin B, destomycin C, fortimicin A etc., have been determined by isobutane and ammonia as the reagent gases.

In all emitter (desorption) CI mass spectra examined, MH^+ ions and various types of structurally informative fragment ions were observed with both reagent gases. The application to the silicon - activated wires had generally led to the enhancement of the relative intensities of MH^+ ions in comparison with the naked wires. As a typical instance, desorption CI(NH_3) mass spectrum of neomycin B is shown in Fig. 1. A number of structurally

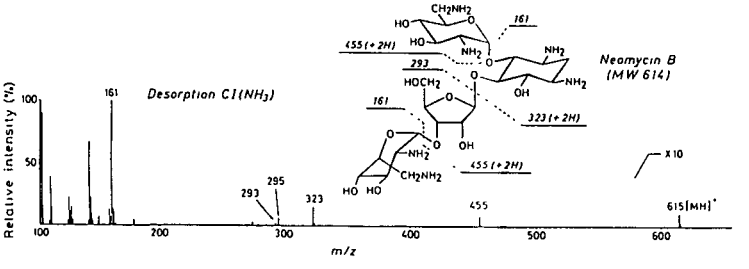


Fig. 1

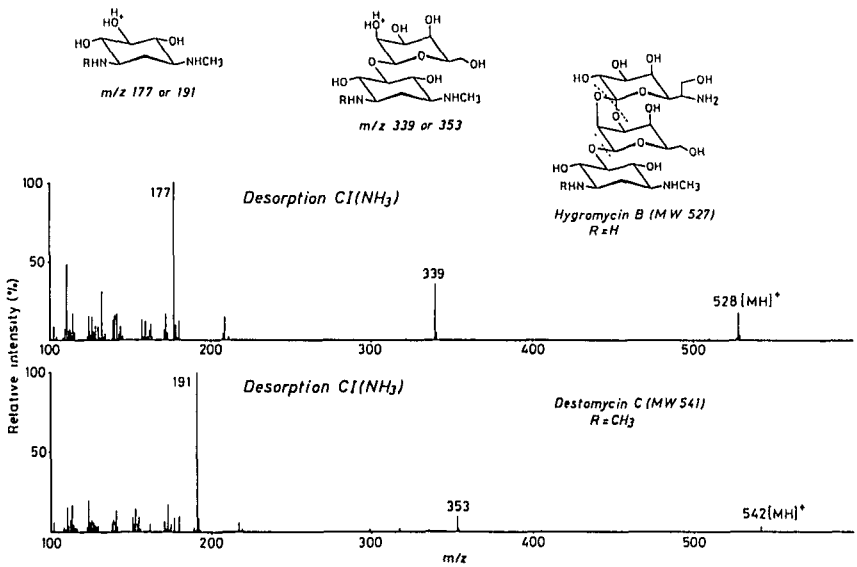
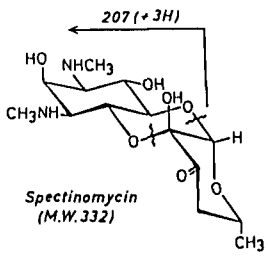


Fig. 2



informative ions attributed to the cleavages of glycosidic linkages are clearly observed. On the other hand, interesting glycosidic fragmentations are observed in the mass spectra of hygromycin B and destomycin C, where in addition to MH^+ ions (m/z 528 and 542), aminocyclitol- (m/z 177 and 191) and pseudodisaccharide - derived ions (m/z 339 and 353) offer further recognition for structural characterization of this series of antibiotics (Fig. 2). Similar two bonds - fission was also observed in the mass spectrum of spectinomycin.

References

1) R. J. Cotter; Anal. Chem., 52, 1589A (1980).

2) N. Takeda, K. I. Harada, M. Suzuki, A. Tatematsu and T. Kubodera; J. Antibiotics, 34, 617 (1981); Org. Mass Spectrom., 17 (1982) in press.

3) D. I. Carroll, J. G. Nowlin, R. N. Stillwell and E. C. Horning; Anal. Chem., 53, 2007 (1981).

4) V. N. Reinhold and S. A. Carr; Anal. Chem., 54, 499 (1982).

5) T. Matsuo, H. Matsuda and I. Katakuse; Anal. Chem., 51, 69 (1979).

GAS CHROMATOGRAPHIC - MASS SPECTROMETRIC PROFILE OF AMINE METABOLITES IN URINE OF PATIENTS WITH CHRONIC DISEASE; OHKI,T, SAITO,A, YAMANAKA, N, OHTA,K, NIWA,T AND MAEDA,K; The Bio-Dynamics Research Institute, 1-3-2, Tamamizu-cho, Mizuho-ku, Nagoya 467, Japan

INTRODUCTION

Recently, GC/MS has been used to screen a number of metabolites in blood or urine. However, very few studies have been devoted to the application of the profiling amine analysis to clinical diagnosis, since the amine levels were very low. A profiling analysis of all the amines, including phenolic and aliphatic amines, has not been attempted, except in our previous study(1). It is important to analyze the urinary amines which are the intermediate metabolites of amino acids and possess biogenic activity.

The present study was undertaken to screen simultaneously phenolic amines and aliphatic amines in uremic urine using GC/MS.

MATERIALS AND METHODS

URINE SAMPLES

Twenty-four-hr urine samples were collected in containers containing 50 ml of 3 N HCl and stored at -20 °C until analyzed.

SAMPLE PREPARATION

As an internal standard, 40 nmoles of N-3-aminopropyl-1,3-diaminopropane was added to 5 ml of urine. To hydrolyze the conjugated amines, 5 ml of conc. HCl was added to the samples and heated at 100 °C for 16 hr. The sample was evaporated to dryness and dissolved in phosphate buffer including 0.7 moles of NaCl(2), and applied to Dowex 50W X-8 column. After washing with 50 ml of phosphate buffer and 30 ml of 1 N HCl, the absorbed amines were eluted with 100 ml of 6 N HCl. The eluate was evaporated to dryness with a rotary evaporator. 200 µl of anhydrous ethyl acetate and 200 µl of pentafluoropropionic anhydride were added to the dry residue, and the amines were acylated at 70 °C for 15 min. The sample was dried with a stream of nitrogen and redissolved in 100 µl of ethyl acetate. Two µl of this solution was subjected to GC/MS.

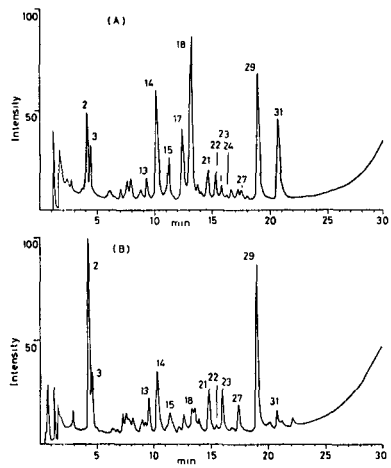


Fig. 1 Gas chromatogram of the urinary amines of (A) a normal subject and (B) a patient with renal failure. Column: 3% OV1(2m x 2mm), Temperature: 75-260 °C at 6 °C/min.

RESULTS AND DISCUSSION

Figure 1 shows chromatogram of amines in the urine of a normal subject and a patient with renal failure. Peaks were identified as follows: 2, methylguanidine; 3, guanidine; 14, putrescine; 17, cadaverine; 18, p-tyramine; 22, dopamine; 24, 3-methoxytyramine; 29, N-3-aminopropyl-1,3-diaminopropane(internal standard); 31, spermidine. These amines were identified by comparison with mass spectra and retention times of authentic compounds.

Table I
Urinary excretion of 7 amines in normal subjects and uremic patients.

	Control(n=9)	Uremia(n=7)
Putrescine	17.52 ± 8.65	2.80 ± 1.08
Cadaverine	2.74 ± 3.07	0.68 ± 0.53
Spermidine	7.51 ± 1.98	0.93 ± 0.45
p-Tyramine	12.05 ± 9.23	2.89 ± 2.28
Dopamine	3.75 ± 1.67	0.71 ± 0.75
3-Methoxytyramine	1.35 ± 0.89	0.28 ± 0.19
Methylguanidine	26.4 ± 10.2	49.2 ± 25.0

μmoles/24 h.

Table I shows the urinary excretion of 7 amines in normal subjects and uremic patients. The levels of methylguanidine in urine of uremic patients were increased in comparison with that of normal urine, whereas those of other amines were decreased one-fifth. In patients with renal failure, many metabolites which are normally excreted in the urine are retained in the blood, causing various uremic symptons. Methylguanidine is noted to be one of the uremic toxins. It is also known that the levels of polyamines and tyramine are elevated in blood of uremic patients. The present finding that only the levels of methylguanidine was increased in uremic urine is very striking. It is considered that the increase of polyamine and tyramine in uremic blood results from decreased excretion, whereas increase of methylguanidine results from increased production.

In patients with pheochromocytoma or neuroblastoma, metabolic disorders of catecholamie have been reported by many investigators. The present procedure for simultaneous quantitation of polyamines and phenolic amines such as 3-methoxytyramine and dopamine may be useful to study these disease.

REFERENCES

1. T.Ohki et al., J. chromatogr., 228(1982)51.
2. H.Inoue et al., Anal. Biochem., 56(1973)408.

RAPID AND RELIABLE DIAGNOSIS OF HYPERTYROSINEMIA BY GC/MS

T. Shinka, T. Kuhara and I. Matsumoto
Research Institute of Medical Mass Spectrometry
Kurume University School of Medicine, Kurume, Fukuoka 830, Japan

Hypertyrosinemia is caused by a deficiency of cytosol tyrosine aminotransferase, hepatic 4-hydroxyphenylpyruvate oxidase or fumarylacetoacetase. These diseases are generally known as tyrosinosis. In addition, hepatic dysfunction also elicits hypertyrosinemia. Attempts have been made to distinguish between tyrosinosis and hepatic dysfunction and further to discriminate among the above-mentioned three types of tyrosinosis using gas chromatography-mass spectrometry-computer (GC-MS-COM) system.

Urine samples were frozen immediately after collection and stored at -20°C until analysis. Tyrosine catabolites were extracted with diethylether, and trimethylsilylated with BSTFA (bis-trimethylsilyl-trifluoroacetamide). Amino acids were separated from urine by cation exchange (resin Bio Rad AG 50W X 12) and trimethylsilylated with BSTFA and acetonitrile. Organic acids and amino acids were separated by gas chromatography on a 2m glass column packed with 3% OV-17 on Gas Chrom Q. Oven temperature was maintained at 80°C for 2 min, and then raised to 290°C at a ratio of 6°C/min. Mass spectra were measured repetitively every 5 seconds, stored in a memory disc and treated by a data processing system.

Fifteen urine samples of hypertyrosinemia patients were analyzed. In the organic acid fraction, markedly increased excretion of 4-hydroxyphenyllactate (HPLA), 4-hydroxyphenylpyruvate(HPPA) and 4-hydroxyphenylacetate(HPAA) was observed in both tyrosinosis and acute liver disease patients. However, tyrosine catabolites were not significantly elevated in the case of chronic liver disease. The ratio of HPLA/HPPA in tyrosinosis was between 2 and 4 (Table 1). In acute liver desease, it exceeded 10 and a large amount of lactate was detected. In the amino acid fraction, marked hyperaminoaciduria, caused especially by tyrosine(24-186 times), glycine(9-30 times), serine(8-53 times), threonine(17-772 times) and sometimes methionine, were observed in most cases. Only in the case of patient T.I., who had been diagnosed to suffer from tyrosine aminotransferase deficiency, tyrosinuria was observed and hyperaminoaciduria was not.

These data clearly indicate that it is possible to distinguish between tyrosinosis and liver dysfunction by an inspection of urinary HPLA and HPPA. Discrimination between three types of tyrosinosis(1) by comparison of each HPLA/HPPA ratio is difficult. However, in the case of transitory tyrosinemia

of the newborn, ascribed to immaturity of enzymes in the degradation of tyrosine, tyrosine and its metabolites are remarkably reduced within 4-5 weeks after birth. Therefore, it is possible to distinguish this type of tyrosinemia from the other two by analyses of urines at different ages. Our data also suggest that an examination of urinary amino acids is very useful to discriminate tyrosinosis. In the case of tyrosinemia without hepatorenal dysfunction, like tyrosine aminotransferase deficiency, there is no abnormal excretion of amino acids except tyrosine. On the other hand, there is a marked hyperaminoaciduria, especially caused by glycogenic amino acids, in tyrosinemia with hepatorenal dysfunction, like in fumarylacetoacetase or HPPA oxidase deficiency. This phenomenon was found in transitory tyrosinemia, too. Grenier(2) reported that α_1-fetoprotein combined with tyrosine determination was very useful for diagnosis of hepatic tyrosinemia because it was increased in serum in a large percentage of these patients. α_1-Fetoprotein presumably originates from fetal liver, regenerated liver or hepatoma. It seems, therefore, that the abnormal excretion of the above-mentioned glycogenic amino acids in tyrosinosis is suspected to be caused by liver dysfunction or immaturity of liver, and probably reflects the synthetic methionine metabolism under these liver conditions. In this way, it is possible to make an accurate diagnosis of tyrosinosis by GC-MS-COM analysis.

References

1) S. Halvoren, Neonatal Screening for Inborn Errors of Metabolism, edited by H. Bickel, et al., Spriger-Verlage, New York, pp.45-57, 1980

2) A. Grenier, L. Belanger and C. Laberge, Clin. Chem. 22, 1001-1004 (1976)

Table 1. Urinary excretion of tyrosine and its metabolites

Patient	Age	HPAA	HPLA	HPPA	Tyr	HPLA/HPPA	Other
Normal		0 70	<0 02	N.D	0 03		
R K	1m	2 45	50 95	19 83	0 24	2 6	Ser Thr
R A	1m	5 58	38 65	12 41	0 24	3 1	Gly Ser Thr Orn Lys Cit His
K M	1m	1 30	45 50	15 30	0.03	3 0	Gly Ser Thr Orn Cit
S K	1m	4.55	60 79	24 77	1 19	3.3	Gly Ser Thr
H.I	1m	6 61	37 93	19 83	6 33	1 9	Gly Ser Thr Lys
M.R	1m	6 84	61.24	23 39	5 19	2.6	Gly Ser Thr Orn Lys
S N	2m	6 47	39 02	14 61	0.40	2 6	Gly Ser
T.N	1m	12 06	101 54	31 63	0 06	3 2	Ser Thr
T U	1m	14.87	110.64	21 74	0 60	5 1	Gly Ser Thr Pro Hypro
T I	4y	10.06	29 67	6 39	1 01	3 5	
O.O	6m	15 45	93 78	37 47	1,59	2 5	Gly Ser Thr
T F	3m	10 90	27 77	21 73	1 99	1 3	Gly Ser
T K	2y	3 20	48 60	7 50	2.82	6 2	Ser Thr Lys His Met
S H	3w	15 56	64 60	2 90	2 17	22 3	Gly Ser Thr
M N	1m	2 70	242 00	23 00	0 47	10 5	Lys His
Indian Childhood Cirrhosis			0 1-2 63		0 62-4 71		

Values expressed relative to IS peak area

GC/MS ANALYSIS OF URINARY METABOLITES OF A PATIENT WITH LACTIC ACIDOSIS DUE TO E3 DEFICIENCY PREVIOUSLY DIAGNOSED AS MAPLE SYRUP URINE DISEASE

I. Matsumoto and T. Kuhara
Research Institute of Medical Mass Spectrometry
Kurume University School of Medicine, Kurume, Fukuoka 830, Japan

Dihydrolipoyl dehydrogenase(E3) deficiency was first described in 1976 by Haworth et al. and later by Robinson et al.(1). Chronic lactic acidosis, hypoglycemia upon fasting, and progressive neurological deterioration are characteristic of this disorder. E3 is a component of the pyruvate, 2-oxoglutarate and branched-chain keto acid dehydrogenase complexes. Elevated levels of serum and urinary lactic acid, 2-oxoglutaric acid and alanine have been found in patients with E3 deficiency. Plasma levels of branched-chain amino acids and the urinary level of 2-hydroxyisovaleric acid had been significantly elevated. There are no reports, however, on detailed investigations of the urinary acidic metabolites excreted by patients with E3 deficiency. We report here GC/MS studies on the urinary metabolic profiles of a patient with E3 deficiency. The patient had originally been suspected to have maple syrup urine disease(MSUD) by mass screening using the Gathrie test.

A boy, the first child of unrelated Japanese parents, was born at term. On the third day of life, it was noted that the patient's blood leucine was above 5mg/dl by the Gathrie test. However, he appeared well until four months of age when he experienced the first severe clinical episode. At the age of seven months he was admitted to Kurume University Medical Center. Developmental retardation and severe metabolic acidosis were observed.

Urine specimens were stored at -20°C until use. The use of creatinine as a reference point for the measurement of urinary organic acids has been recommended by Jellum et al. Urine samples equivalent to 0.5 mg of creatinine were adjusted to pH 1.0, spiked with 20 μg of n-heptadecanoic acid as an internal standard and extracted with diethyl ether. The organic acids were trimethylsilylated and analyzed using GC/MS/COM. GC/MS conditions were described in a previous paper(2).

Massive urinary excretion of lactic acid and 2-oxoglutaric acid were observed. Significantly elevated levels of 2-ethylhydracrylic acid, 2-hydroxyisovaleric acid, 2-hydroxyisocaproic acid and 2-oxoisocaproic acid were also demonstrated. After branched-chain amino acid restriction, urinary branched-chain 2-oxo- and 2-hydroxy acids were almost disappeared and 2-oxoglutaric acid level was slightly lowered. The latter observation indicates

that 2-oxoglutarate dehydrogenase complex exhibits inhibition by branched-chain keto acids as demonstrated in highly purified pig heart 2-oxoglutarate dehydrogenase complex(3). The urinary excretion of lactate, however, did not decrease after branched-chain amino acid restriction. In an acute period, the patient was slightly ketoacidotic and excreted larger amounts of lactic acid and 2-oxoglutaric acid than in a static period. In E3 deficiency, oxidative decarboxylation of pyruvic acid is decreased, due to decreased E3 activity of pyruvate dehydrogenase complex. This decrease in pyruvate oxidation may be enhanced by the inactivation of pyruvate dehydrogenase caused by increase in the acetyl CoA/CoASH ratio(4).

It is shown that, prior to confirmatory enzyme studies, patients with E3 deficiency who were suspected to have intermittent MSUD or chronic lactic acidosis can be rapidly identified by GC/MS analysis of urinary acids. This identification may also permit the choice of a suitable diet, high in carbohydrate, which is recommended for this disease but not for MSUD, and inapplicable to pyruvate dehydrogenase deficiency, another chronic lactic acidosis.

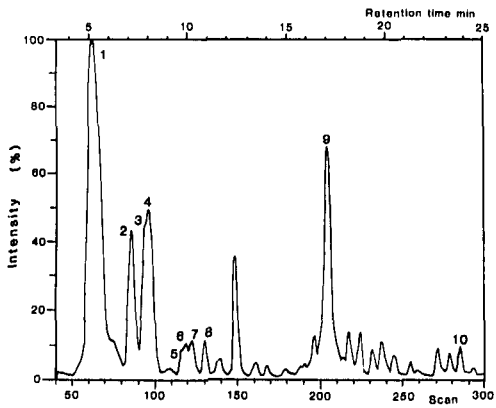


Fig. 1. TIM chromatogram of TMS derivatives of acids from the urine, taken on admission when the patient was experiencing clinical episodes. 1. lactic, 2. 2-hydroxybutyric, 3. 2-hydroxy-isovaleric, 4. 3-hydroxybutyric, 5. 2-hydroxyisocaproic & 2-ethylhydracrylic, 6. acetoacetic (isomer 1), 7. 2-oxoisocaproic, 8. acetoacetic(isomer 2), 9. 2-oxoglutaric, 10. heptadecanoic acid (IS)

References

1. B. H. Robinson, J. Taylor, S. G. Kahler & H. N. Kirkman, Eur. J. Pediatr., 136, 35-39 (1981)
2. T. Kuhara & I. Matsumoto, Biomed. Mass Spectrom., 7, 424-428 (1980)
3. T. Kanzaki, T. Hayakawa, M. Hamada, Y. Fukuyoshi & M. Koike, J. Biol. Chem., 244, 1183-1187 (1969)
4. R. G. Hansford, J. Biol. Chem., 251, 5483-5489 (1976)

QUANTITATIVE DETERMINATION OF DEHYDROEPIANDROSTERONE SULPHATE USING STABLE ISOTOPE DILUTION AND FAST ATOM BOMBARDMENT MASS SPECTROMETRY

Simon J. Gaskell, Brian G. Brownsey, Tenovus Institute for Cancer Research, Welsh National School of Medicine, Cardiff, CF4 4XX, U.K.

Paul. W. Brooks, Brian N. Green, V.G. Analytical Ltd., Tudor Road, Altrincham, Cheshire, WA14 5RZ, U.K.

Steroid sulphates have not hitherto been amenable to direct mass spectrometric analysis. Analyses have generally involved chromatographic isolation of sulphate conjugates and enzymic hydrolysis or solvolysis to yield the parent steroids which are derivatised prior to GC-MS analysis. Fast atom bombardment (FAB) mass spectrometry has been shown to be an effective technique in the analysis of polar and involatile compounds which resist other forms of mass spectrometric analysis (1). In this paper we report the application of FAB MS to the study of steroid sulphates, including preliminary data on quantitative determinations.

All analyses were carried out on VG 70-70E or ZAB instruments, at a resolution of 500-1000 (10% valley). Xenon comprised the fast atom beam. The sample target was coated with glycerol (0.3 µL) before application of sample in methanol solution.

Negative ion spectra of dehydroepiandrosterone sulphate (DHAS), sodium salt and other steroid sulphates were obtained with good reproducibility and high sensitivity; full spectra were recorded with as little as 12 ng sample. The major feature was the steroid sulphate anion (A^-:m/z 367 for the example of DHAS); other peaks (other than those attributable to glycerol background) were attributed to dimeric species (m/z 757, $|2A + Na|^-$) and glycerol adduct ions (m/z 459, $|A + glyc|^-$; m/z 481, $|A - H + glyc + Na|^-$).

An identical spectrum was obtained from the isomeric steroid, testosterone sulphate. Detection of daughter ions derived from fragmentation of the parent ion beam, of m/z 367, in the first and second field-free regions of the ZAB spectrometer (using a B/E linked scan and mass-analysed ion kinetic energy (MIKE) spectrometry, respectively) permitted the differentiation of the two steroids. Thus, the MIKE spectrum of DHAS (m/z 367) included a peak attributable to loss of C_3H_5O by D-ring fragmentation. An ion associated with loss of 124 mass units (A/B ring fragment) was observed only in the MIKE spectrum of testosterone sulphate; the same feature was observed in the spectrum of daughter ions obtained by B/E linked scan.

Much reduced sensitivity was obtained during analyses of DHAS in biological extracts. Suppression of ion yield by coextracted material was minimised by the use of a highly selective isolation procedure incorporating immunoadsorption with a solid-phase coupled anti-DHAS serum. For quantitative analyses, $|7,7\text{-}^2H_2|$DHAS, prepared as previously described (2), was used as internal standard. A standard curve was derived from analyses of mixtures of DHAS (100-800 ng) and internal standard (500 ng) by repetitive

scanning across a narrow mass range; excellent linearity was obtained ($r = 0.998$) but the non-zero intercept indicated significant interference from a glycerol background ion of m/z 367 ($|4M-H|^-$). The interference became severe during analyses of biological extracts.

Conversion of analyte and internal standard to pentafluorobenzyloxime derivatives was achieved by reaction with a pyridine solution (10 mg/mL) of O-pentafluorobenzyl hydroxylamine hydrochloride for 30 min at 20°. After evaporation of solvent, water was added and the steroid sulphates extracted with diethyl ether/ethanol (4/1). Quantification was subsequently achieved by repetitive scanning across a narrow mass range to detect m/z 562 and 564, corresponding to the derivatised steroid sulphate anions. A satisfactory standard curve was obtained following analyses of standards. Analyses of extracts of various volumes of plasma gave consistent quantitative data though precision was generally poor, apparently due to variable ion suppression effects.

While further study is evidently required to improve isolation procedures (to reduce suppression of ion yield) and enhance analytical selectivity, it is clear that FAB mass spectrometry is a valuable technique for both qualitative and quantitative analyses of steroid sulphates.

References

1. Barber M, Bordoli R S, Sedgewick R D, Tyler A N, J Chem Soc Chem Commun 1981 : 325-327.
2. Finlay E M H, Morton M S, Gaskell S J, Steroids 1982; 39 : 63-71.

Acknowledgement

Work at the Tenovus Institute is generously supported by the Tenovus Organisation.

ANALYSIS OF CONJUGATED STEROIDS BY LIQUID MATRIX SECONDARY ION MASS SPECTROMETRY (INCLUDING FABMS) AND BY GAS CHROMATOGRAPHY

C.H.L. Shackleton, E. Roitman and K. Straub
Biomedical Mass Spectrometry Resource, Dept. of Pharmaceutical Chemistry
University of California, San Francisco, CA 94143

Terminal products of steroid metabolism are excreted in urine conjugated with glucuronic or sulfuric acid. Conventional methodology for the identification and quantification of conjugated steroids requires enzymatic or chemical hydrolysis of the conjugates prior to analysis. These lengthy methods give excellent "profiles" of excreted and circulating steroids but continuing attention is needed to seek ways to make conjugated steroid methodology less labor intensive and more applicable to routine analysis.

We have been studying the direct analysis of steroid conjugates by gas chromatography raphy and by secondary ion mass spectrometry (including FAB).

1. Gas Chromatography. Protection of steroid glucuronides for gas chromatographic analysis is relatively straightforward. The carboxylic acid is conveniently protected by methylation and the remaining carbonyl and hydroxyl groups can be stabilized by methyloxime formation and trimethylsilylation by procedures developed for free steroids. The key to steroid glucuronide analysis by gas chromatography is the use of capillary columns stable at high temperature since the most complex steroid glucuronides (e.g., cortol) elute at around 320-330° from 25 meter OV-1 columns. All the steroid glucuronides we have investigated so far give single peaks but the "response factor" (peak height against height of C_{36} and C_{44} alkanes used as internal standards) is occasionally low (25%), particularly for steroids with dihydroxyacetone side-chains (e.g., tetrahydrocortisone, tetrahydrocortisol). An example of a steroid profile produced by this technique is shown in Fig. 1.

2. Secondary Ion Mass Spectrometry. The techniques utilized relied on analysis of secondary ions obtained by bombarding a steroid conjugate sample placed in a liquid matrix (glycerol) with neutral atoms (Xe^0, FAB) or cesium ions (Cs^+, SIMS). The design and operation of the SIMS source have been published in these proceedings (Aberth et al., abstract no. MOD2). In our experience, the spectra produced by using neutral or charged beams are identical and both techniques will be referred to as SIMS.

Steroid glucuronides and monosulfates. The SIMS spectra of all steroid glucuronide and monosulfate sodium salts are essentially similar and a typical example (pregnanolone glucuronide) is illustrated in Fig. 2. The positive ion spectrum is dominated by an ion of mass equivalent to $[M + 2Na]^+$ (M equivalent to mass of free acid) although ions of mass corresponding to $[M + Na]^+$ and $[M + 3Na]^+$ are also significant. In the negative ion spectrum the base peak has a mass equivalent to $[M - H]^-$ with a smaller peak at an m/z value corresponding to $[MNa - H]^-$.

Steroid disulfates. Fig. 3 shows the negative ion mass spectrum of the sodium salt of pregnanediol-3,20-disulfate. This spectrum was dominated by an ion at m/z 501 equivalent to $[MNa - H]^-$. Useful ions above m/z 400 were not obtained in the positive ion spectrum.

Urine samples. The relative simplicity of negative ion SIMS spectra encouraged us to attempt analysis of steroid conjugate mixtures. (a) Sulfate fraction of infant urine. Gas chromatographic and GC/MS analysis had shown that the dominant steroids in this sample were 16α-hydroxy-DHA, 16-oxo-androstenediol and 16α-hydroxypregnenolone. The negative ion mass spectrum was therefore appropriate (Fig. 4). The major peak was at m/z 411 which represents $[M - H^-]$ of 16α-hydroxypregnenolone and the subsidiary peak at m/z 383 represents $[M - H]^-$ for the isomeric compounds 16α-hydroxy-DHA and 16-oxo-androstenediol. (b) Glucuronides from adult urine. The spectrum illustrated in Fig. 5 shows peaks for androsterone + etiocholanolone (m/z 465, $[M - H]^-$), their 11-oxo-derivatives (m/z 479), their 11β-hydroxy-derivatives (m/z,,481), the tetrahydrocorticosterones (m/z 525), tetrahydrocortisone (m/z 539), the tetrahydrocortisols and cortolones (m/z 541).

Conclusion. Both gas chromatography and SIMS can be used for the analysis of intact glucuronides. The latter technique, particularly in the negative ion mode, probably has the greatest potential since derivative formation is not required. We have examined profiles obtained from urine of patients with several of the inborn errors of steroid synthesis (e.g., 21-hydroxylase defect, 17α-hydroxylase defect and 3β-hydroxysteroid dehydrogenase defect) and have found that all can be distinguished solely on the basis of a negative SIMS spectrum. Since neutral or ion primary beam guns can be readily placed on existing magnetic sector or quadrupole instruments, it is probable that this technique will become increasingly useful in clinical steroid analysis.

This work was supported by NIH Grant RR01614 and the negative ion source was made available by a grant from the University of California, San Francisco, Academic Senate.

Fig 1

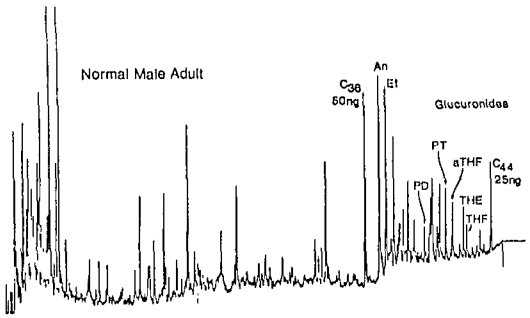


Fig 2

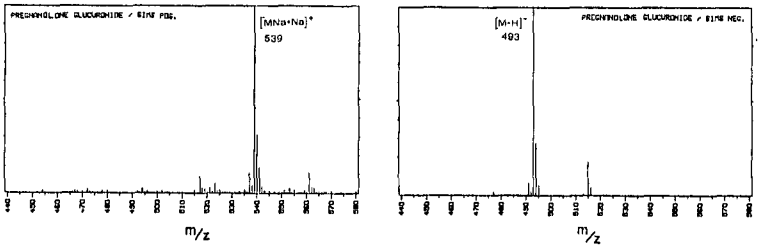


Fig 3

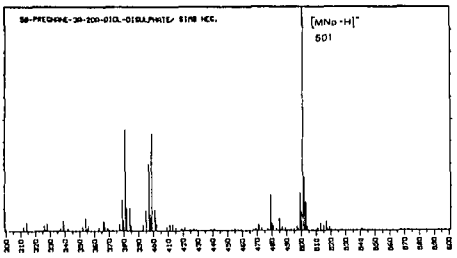


Fig 4.

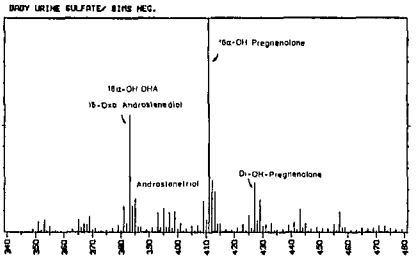
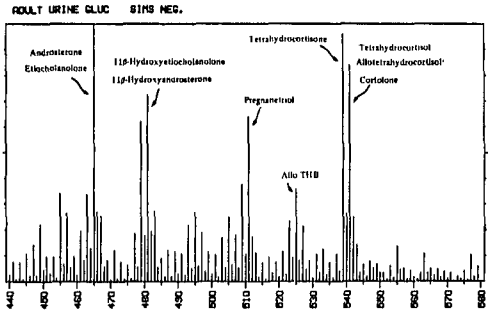


Fig. 5



STRUCTURAL CHARACTERIZATION OF NATURALLY OCCURRING OLIGOSACCHARIDES BY MATRIX-ASSISTED MOLECULAR SIMS

Makoto SUZUKI, Ken-ichi HARADA, Akira TATEMATSU and Hideki KAMBARA*
Faculty of Pharmacy, Meijo University, Tempaku, Nagoya 468, JAPAN
*Central Research Laboratory, Hitachi Ltd., Kokubunji, Tokyo 185, JAPAN

The molecular secondary ion (SI) mass spectra of several naturally occurring oligosaccharides, raffinose (1), stachyose (2), γ-cyclodextrine (3), amikacin (4) and viridopentaoses (5A, 5B, 5C)[1] are investigated with or without matrices.

The molecular ion species observed in SI mass spectra of 1 and 2 without matrix (dry surface) are $[M+Na]^+$, $[M+K]^+$ and $[M+Ag]^+$, and fragment ions due to glycosidic bond cleavages are accompanied by sodiation or argentation.[2] In glycerol matrix-assisted SI mass spectra of 1 and 2, protonated molecule $[MH^+]$ appears together with $[M+Na]^+$ and prtonated type fragment ions derived from di-, and trisaccharide moities are definitely observed. These sequence ions provide significant information for their structural characterization.

When basic matrices such as 3-amino-1,2-propanol, ethanolamine, di- and triethanolamine are used, adduct ions appear in their mass spectra, resulting from the reaction of substrate with the protonated amines.[3] In the case of γ-cyclodextrine (3) with diethanolamine (DEA), the adduct ion $[M+DEAH]^+$ is observed at m/z 1402 (Fig. 1).[3] Because these adduct ions are considerably stable, no fragment ion can be recognized in the spectra of oligosaccharides, except for matrix derived ions.

However, an aminoglycoside antibiotic, amikacin (4) produces specific sequence ions with protonated and sodiated molecules, in both cases of glycerol and diethanolamine matrix.[3]

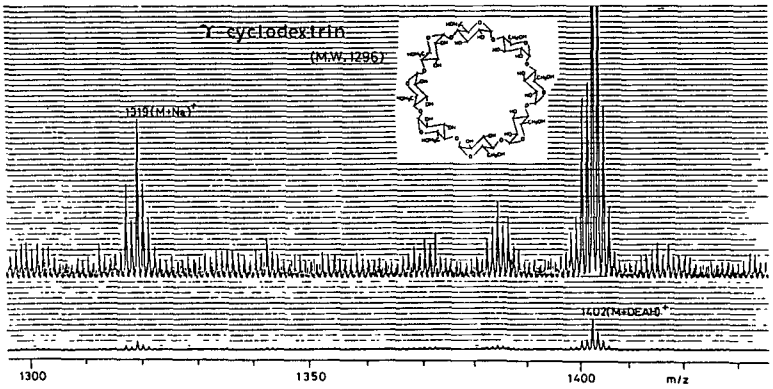


Fig. 1 Secondary ion mass spectrum of γ-cyclodextrin (3) with diethanolamine

Besides, viridopentaoses (5A, 5B, 5C), basic hetero-oligosaccharides derived from antibiotic Sporaviridin[4] gave quite suggestive results. Namely, SI mass spectra of this series with glycerol matrix are analogous to those of 1 and 2, however, only amino-sugar containing fragments as sequence ions are clearly recognized.[5]

As an example, SI mass spectra of viridopentaose B (5B) are shown in Fig. 2, and we can observe clear molecular ion species, $[MH^+]$, $[M+Na]^+$ and $[M+DEAH]^+$, and amino-sugar containing sequence ions in the case of diethanolamine matrix.[5] These adduct ion formation and regular fragmentation from protonated molecule suggest that the behavior of SI mass spectra seems to be very close to those of CI mass spectra using basic reagent gas such as ammonia or trimethylamine.

As menthioned above, the effective use of matrix in molecular SIMS will be powerful technique for the structural characterization of involatile and/or thermally unstable polar natural compounds.

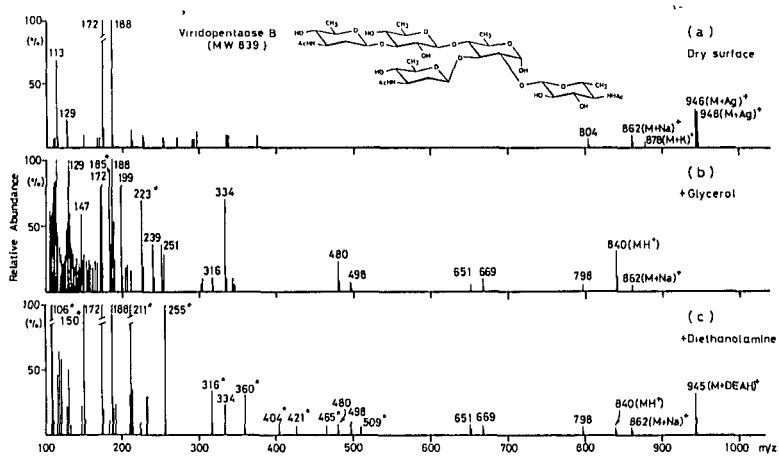


Fig. 2 Secondary ion mass spectra of viridopentaose B (5B)
[* Matrix derived ions]

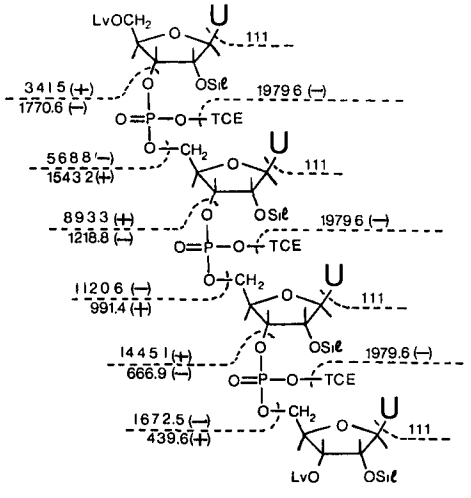
References

1) K. I. Harada, S. Itō, M. Suzuki, Tetrahedron Letters, 23, in press (1982).
2) H. Kambara, S. Hishida, Org. Mass Spectrom., 16, 167 (1981); Anal. Chem., 53, 2340 (1981).
3) K. I. Harada, M. Suzuki, H. Kambara, Org. Mass Spectrom., 17, in press (1982).
4) T. Okuda, Y. Itō, T. Yamaguchi, T. Furumai, M. Suzuki, M. Tsuruoka, J. Antibiotics, Ser. A, 19, 85 (1966).
5) K. I. Harada, M. Suzuki, H. Kambara, Tetrahedron Letters, 23, in press (1982).

CHARACTERIZATION OF PROTECTED OLIGONUCLEOTIDES BY SECONDARY ION MASS SPECTROMETRY

K.G.STANDING R. Beavis, W. Ens, Physics Department, University of Manitoba; J.B. WESTMORE, Chemistry Department, University of Manitoba, Winnipeg,Canada R3T 2N2;
K.K. OGILVIE and M.J. Nemer, Chemistry Department, McGill University, Montreal, Canada H3A 2K6

We have recently reported positive and negative secondary ion mass spectra for eight fully protected diribonucleoside monophosphates [1]. The measurements have now been extended to tri-, tetra-, and pentaribonucleotides with molecular masses up to~3000 u. The spectra, produced by 10 to 25 keV Cs+ ions, were examined in a time-of-flight mass spectrometer [2]. Many diagnostically useful ions which enable determination of the molecular weight, identification of the protecting groups present, identification of the nucleobases present and determination of the base sequence,are observed. They include those characteristic of the intact molecule, e.g. [M+H]+ , [M+Na]+ , [M-H]- and [M+Cl]-, and fragment ions formed by fission of bonds involving the phosphate linkages. These are carbocations involving the 3′ or 5′ carbons of the ribose units in the positive ion spectra, and phosphate diester anions in the negative ion spectra. The secondary ion spectra of these protected oligonucleotides are very similar to those obtained for related compounds by fission fragment bombardment [3], but they show considerably more fragmentation than the field desorption spectra of protected mono- and dinucleotides [4]. The structure of a tetranucleotide and its protecting groups are shown in figure 1. The time-of-flight spectra for this compound are shown in figure 2. The peaks labelled M′ correspond to a trinucleotide impurity with the same structure as the tetranucleotide but with an OH group in the 3′ position instead of a levulinyl (Lv) protecting group.



Mol. Wt.
2112.0

MMT = $CH_3OC_6H_4-C(C_6H_5)_2$

Siℓ = t.$BuMe_2Si$

Lv = $CH_3COCH_2CH_2CO$

TCE = $CCℓ_3CH_2$

Bz = C_6H_5CO

FIGURE 1
Fully protected tetranucleotide.

REFERENCES

1. W.Ens, K.G. Standing, J.B. Westmore, K.K. Ogilvie and M.J. Nemer, Anal. Chem. 54 960 (1982).
2. B.T. Chait and K.G. Standing, Int. J. Mass Spectrom. Ion Phys. 40 ,185 (1981).
3. C.J. McNeal, K.K. Ogilvie, N.Y. Theriault and M.J. Nemer, J. Am. Chem. Soc., 104 , 972, 976, 981 (1982).
4. H.M. Schiedel and H.-R. Schulten, Z. Naturforsch. 36b , 967 (1981).

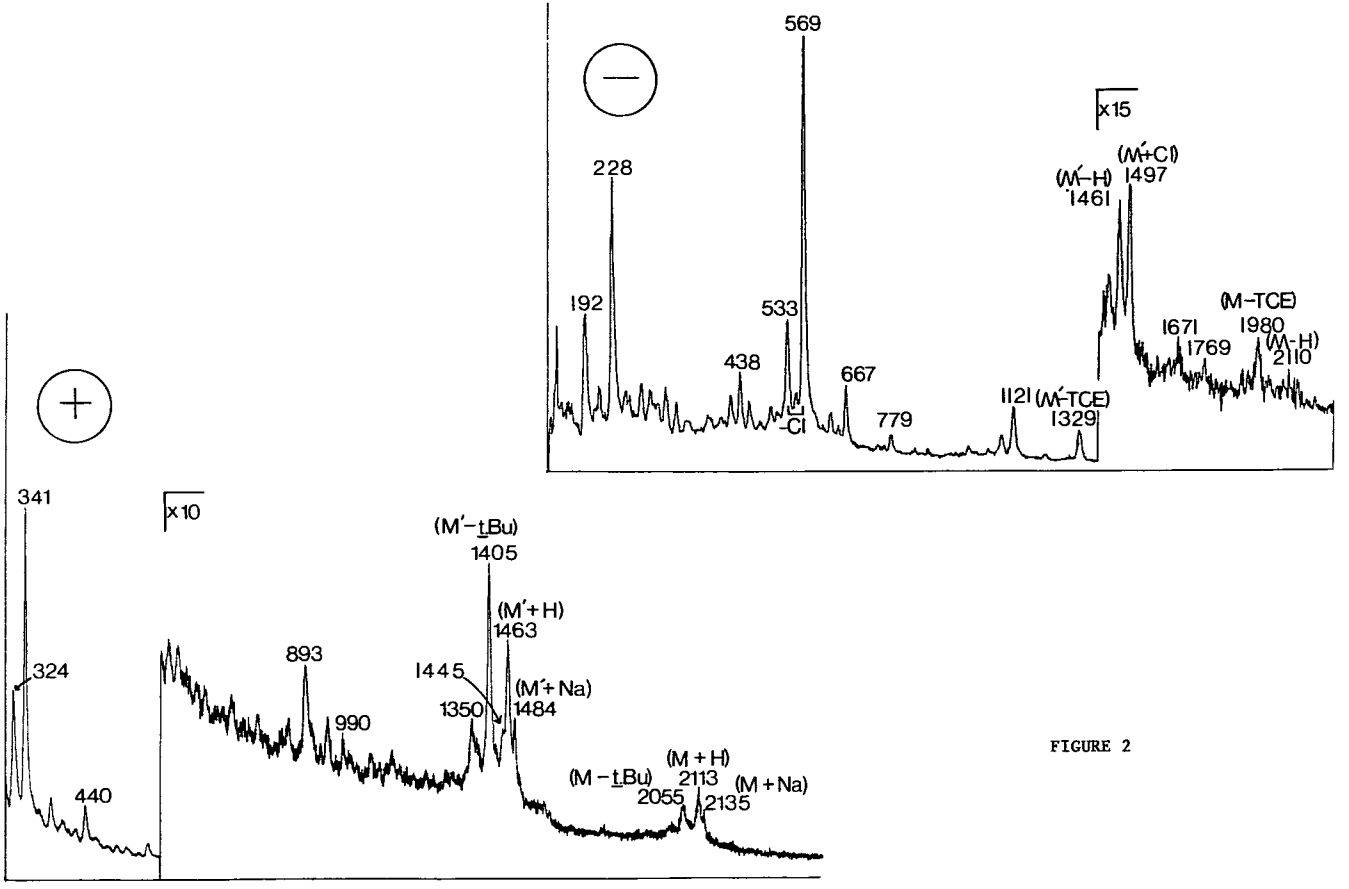

569
228
192
533
438
667
779
1121
(M´-TCE)
1329
(M´-H)
1461
(M´+Cl)
1497
1671
1769
(M-TCE)
1980
(M-H)
2110
-Cl
x15
341
324
440
x10
893
990
(M´-tBu)
1405
(M´+H)
1463
1445
1350
(M´+Na)
1484
(M-tBu)
2055
(M+H)
2113
(M+Na)
2135

FIGURE 2

THE COMPOSITIONAL PROFILES OF MELAMINE RESINS USING FD AND FAB MASS SPECTROMETRY

Ted T. Chang
American Cyanamid Company, Stamford, Conn. 06904

A knowledge of the chemical composition of low molecular weight melamine resins, e.g., CYMEL® 300 resin, is important because of their extensive use as cross-linking agents for polymers containing various functional groups, especially in surface coatings. These resins are complex mixtures of monomeric and oligomeric products resulting from the reaction of melamine with various amounts of formaldehyde and an alcohol, usually methanol. A typical monomeric specie is hexamethoxymethyl melamine, referred to as MF_6Me_6, i.e., the reaction product of one mole of melamine (M) and six moles each of formaldehyde (F) and methanol (Me).

Complete characterization of these resins is a difficult analytical problem. Current analytical procedures (chemical, NMR, IR, etc.) do not provide the complete composition. Conventional mass spectrometric techniques, i.e., EI and CI, are not applicable because these resins are thermally unstable. However, FD and FAB were successfully used to provide unique compositional profiles of these resins.

FD produced well-defined spectra at low emitter currents with distinct molecular ions. The following emitter currents were used: 0-5 mA for the monomeric fraction, 6-12 mA for the dimeric fraction and 10-15 mA for the higher oligomeric fractions. The signals for the monomeric and dimeric fractions were intense, stable and reproducible. A single dipping of the emitter into a 10% solution of sample in methanol frequently provided signals lasting 10-15 minutes, allowing ample time for peak-matching, collision activation, etc. Signals from the higher oligomeric fractions were less persistent.

Because the FD spectra consisted of intense molecular ions with little fragmentation, interpretation was greatly facilitated. In a typical resin, ten monomeric components were identified including the major component, MF_6Me_6, and lesser amounts of, e.g., MF_6Me_5, MF_5Me_5 and MF_7Me_6. The latter component is of interest because it contains the substituent $-CH_2OCH_2OCH_3$, which was previously suspected but not proved.

The FD spectrum of the dimeric fraction showed the presence of two bridging units, $-CH_2-$ and $-CH_2OCH_2-$, corresponding to $Me_5F_5M-CH_2-MF_5Me_5$ (MW 704) and $Me_5F_5M-CH_2OCH_2-MF_5Me_5$ (MW 734), respectively. The trimeric and tetrameric fractions showed the presence of various combinations of the same two bridging units observed in dimeric fractions. The $-CH_2-$ bridging was predominant for all the oligomeric fractions.

FAB spectra gave $(M-H)^+$ and $(M-H-CH_2O)^+$ as major fragment ions and weak molecular ions. Although the FAB spectra were more complex than the FD spectra, they provided a more complete compositional profile because all fractions from monomer through tetramer were observed simultaneously in a single spectrum.

Exact mass measurements were obtained for FD by peak-matching the FD peak versus an EI peak of an appropriate reference compound (either PFK or FOMBLIN oil*) by alternately displaying these peaks on an oscilloscope. The FD resolution was 6-8 K and the measured exact mass was within 10 ppm of the theoretical.

* product of Montecatini-Edison

The conclusions were as follows:

(1) Both FD and FAB produced mass spectra of melamine resins without thermal degradation;

(2) FD spectra showed intense molecular ions with little fragmentation;

(3) FAB spectra gave weak molecular ions and intense ions of $(M-H)^+$ and $(M-H-CH_2O)^+$;

(4) FD is a better technique for identifying the components in each fraction and for obtaining their distributional profile;

(5) FAB is more suited for the simultaneous examination of all fractions; and

(6) Both $-CH_2-$ and $-CH_2OCH_2-$ are present as bridging units for oligomerization, with the $-CH_2-$ unit predominating.

APPLICATIONS OF THE FAB TECHNIQUE TO SULFONIC ACID AND THEIR SALTS COMPARED TO OTHER SENSITIVE SUBSTANCES.

R. Pesch, U. Rapp, M. Höhn and P. Dobberstein,
Finnigan MAT GmbH, Barkhausenstr. 2, D-2800 Bremen, W. Germany

The overwhelming power of the FAB technique to ionize intractable compounds has been documented throughout the last year especially in the analysis of peptides, antibiotics and other biologically relevant compounds.

The analysis of sulfonic acids is of high interest because these compounds are important synthetic products especially in dye chemistry. With FD or DCI some results could be obtained but both methods failed to be generally applicable. Especially the DCI technique showed some promising results on free acids but failed with their salts.

The FAB technique turned out to be well suited for the analysis of even complicated and labile sulfonic acids. The so-called "letter acids" and some other related compounds were investigated under positive and negative ionization conditions to gain some systematic material on highly substituted naphthaline sulfonic acids. As one would expect and is shown in earlier investigations there are indications that aromatic amino groups, as present in a variety of dyestuff synthetic products tend to suppress molecular ions.

The comparison between the spectra of positive and negative ions shows that in many cases the negative ion spectra yield the analytically more interesting results because they are more unambigious.

Another class of compounds which attracts attention is the group of folic acid derivatives, of which the pteridines are naturally occuring. Up to now they have been very difficult to analyze by mass spectrometry in general. Examples will be shown to different behaviour under FAB conditions, where e.g. a tetrahhydrofolic acid yields excellent results, and the folic acid derivative itself shows a very poor spectrum.

FAB ANALYSIS OF TRANSITION METAL COMPLEXES USING 18-CROWN-6 AS THE MATRIX

Robert D. Minard and G. L. Geoffroy, Department of Chemistry,
Penn State University, University Park, PA 16802.

INTRODUCTION: We have had reasonable success running pure carbonyl cluster organometallic compounds by electron impact. However, as carbonyl groups are replaced by triphenylphosphine (-PPh_3), diphenyl phosphito (-PPh_2-) and chloro groups, volatility of the organometallic compounds decrease and useable mass spectra could not be obtained. Thus, we were anxious to try FAB ionization on these compounds.

We suspected (and have obtained experimental proof) that Glycerol would be unsuitable as a matrix and therefore searched for a less reactive aprotic matrix. Gordon Hansen at the Middle Atlantic Mass Spectrometry Facility suggested a polyether such as tetraglyme [$CH_3O(CH_2CH_2O)_4CH_3$]. This gave encouraging results but evaporates quite rapidly in high vacuum and spectra fade quickly. Therefore, we tried 18-crown-6 [$(CH_2CH_2O)_6$] which is a solid with a melting point of 39-40°C. By adding about 10% tetraglyme the melting point of 18-crown-6 is depressed so that it remains liquid at room temperature. Using this mixture as the matrix allowed the FAB mass spectra of a number of organometallic compounds to be obtained and in almost all cases molecular weight information was observed. Selected examples are shown below.

RESULTS: All spectra were run on a KRATOS MS 9/50 mass spectrometer with extended range magnet. Scans were taken at 30 to 100 secs/decade and mass assignments checked using a calibrated Hall probe mass marker. Oscillographic recording was used since arcing would shut down the data system. Approximately 20-30 µl of the ether matrix mixture was used with 10 to 100 µgs of sample. Positive FAB spectra of some selected organometallic compounds are shown in figures 1-4.

CONCLUSIONS:

1). 18-crown-6 is a useful aprotic matrix for producing FAB Spectra of many organometallic compounds.

2). These spectra often contain a mixture of overlapping radical cation and protonated molecular ions giving molecular weight information but difficult-to-interpret isotope patterns. These molecular ions are often weak and require maximum signal amplification for their detection.

3). These spectra contain structurally significant fragmentations such as stepwise loss of all carbonyls, chloro, phenyl, triphenylphosphine and other coordinating groups.

4). Using 18-crown-6, FAB Spectra can be obtained for up to 10 minutes, depending on the compound. Normally the best spectra are obtained in the first minute. Initially clear matrix solutions often come out black after atom bombardment indicating chemical reactions are occurring on the probe tip.

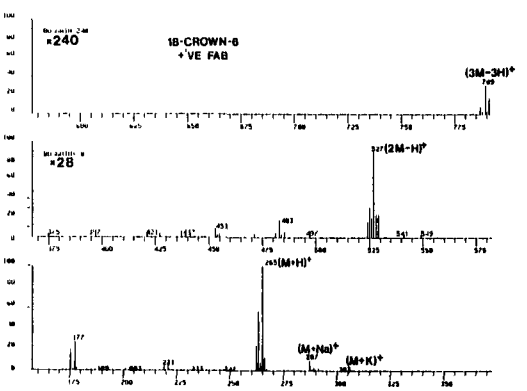


Figure 1: Positive FAB spectrum of 18-crown-6 matrix.

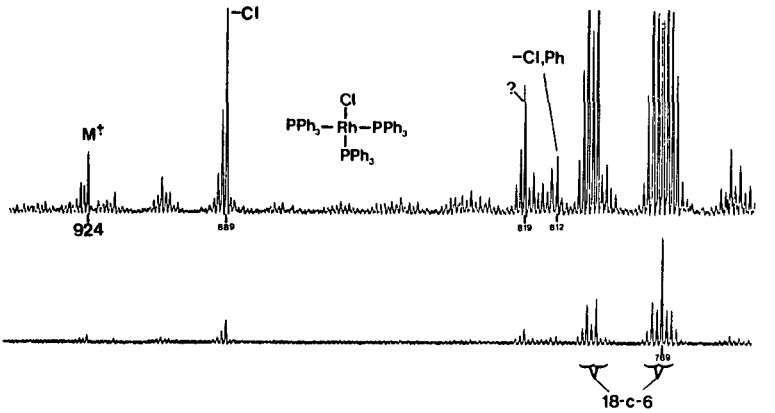


Figure 1

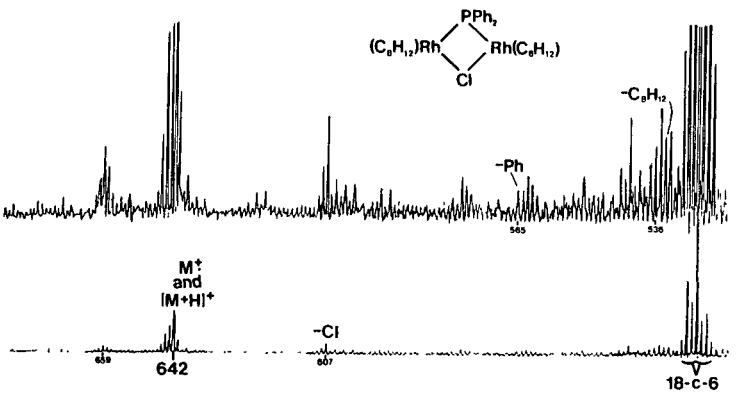


Figure 2

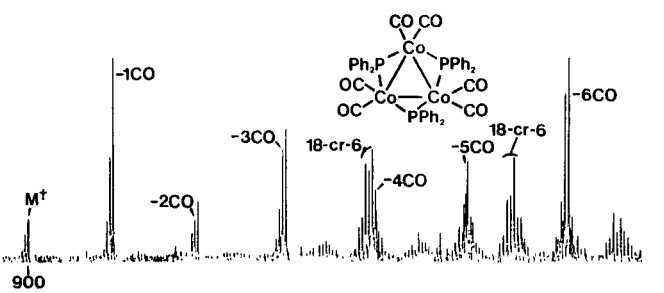


Figure 3

TPA 28 FAST ATOM BOMBARDMENT MS/MS FOR STRUCTURAL AND MIXTURE ANALYSIS, F. W. Crow, K. B. Tomer and M. L. Gross, Midwest Center for Mass Spectrometry, Department of Chemistry, University of Nebraska, Lincoln, NE 68588.

The objective of this work was to study amino acid containing material using fast atom bombardment and MS/MS on a triple sector mass spectrometer. The protocol used in these studies was: 1) obtain the low resolution FAB mass spectrum; 2) peak match the molecular ion species to obtain elemental composition and; 3) obtain structural information by a) CID of molecular ion species and/or major fragment ions (MS/MS) and b) CID multiple reaction monitoring (MS/MS/MS).

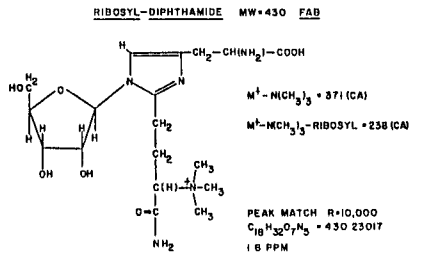


Figure 1.

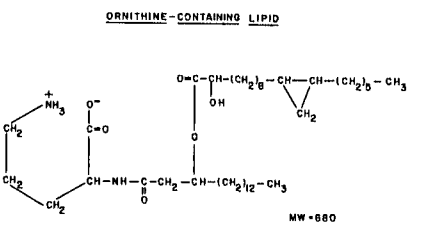


Figure 2.

The first project (with J. W. Bodley, University of Minnesota) was to confirm the proposed structure of a novel amino acid, diphthamide, as its riboside. The only known function of the amino acid is to act as a receptor for ribosylation by diphtheria toxin. This process gives rise to the toxicity of diptheria toxin. The structure, Figure 1, was confirmed by peak matching and the CID spectrum of the protonated molecular ion.

The second problem (with H. Knoche, University of Nebraska) was the confirmation of the structure of an ornithine containing lipid, Figure 2, isolated from thiobacillus thioxidans. This lipid material was found to consist of two homologs differing by a methylene group. The atomic compositions were confirmed by FAB/high resolution peak matching. Collisional activation indicated that the additional methylene group is located on the fatty acid moiety of the lipid.

The third project was to identify the amino acid sequence of HC-Toxin, which is a host specific toxin produced by Helminthosporium carbonum. There are three possible configurations of the four amino acids, Figure 3. The FAB mass spectrum shows a major fragmentation at m/z 240. This ion is formed by loss of the epoxyketoamino acid fragment from the ring-opened MH^+ ion and contains two alanine and one proline residues. Thus, the further fragmentation of this ion will define the sequence of the three residues. The possible structures of this ion arising from the three possible structures of the parent tetrapeptide along with their expected fragmentations are shown in Scheme 1. The ions of m/z 143 and 72 were not observed in the FAB spectrum while m/z 169 and 70 were found. This indicates that structure 3 is the correct sequence.

Two further experiments were formed to corroborate this observation. The CID spectrum of m/z 240 was taken, Figure 4, and m/z 169, 141 and 70 were observed in accord with the assignment of structure 3. To ensure that the ions observed in the CID spectrum arise from sequential losses, the CID spectrum of m/z 169 produced uniquely from m/z 240 was taken. This was accomplished by selecting m/z 169 produced by collisional activation of m/z 240 in a collision cell located after the source but before MS-I and taking its CID spectrum using MS-II. This result, an MS/MS/MS spectrum, compares favorably with the CID spectrum of

m/z 169 formed in the FAB source (see Figures 5A and 5B). This confirms that the CID spectrum of m/z 169 is indeed representative of an ionic fragment of m/z 240 and not of another unanticipated precursor.

Thus, we propose that the normal spectrum produced by FAB ionization, and more importantly, the specific decomposition spectra produced by collisional activation are in accord with structure III and not structure I.

Acknowledgment: This work was supported by the Midwest Center for Mass Spectrometry, a National Science Foundation Regional Instrumentation Facility (Grant No. CHE78-18572).

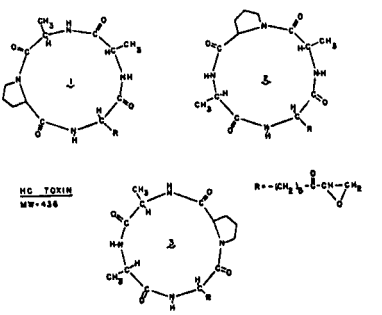


Figure 3.
Possible Structures of HC Toxin

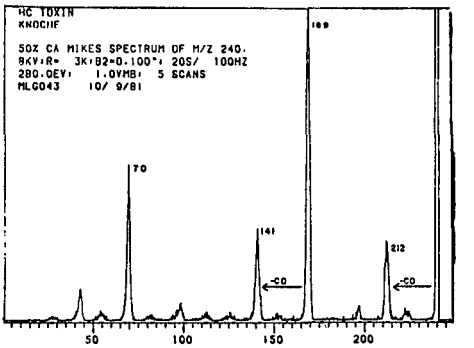


Figure 4.

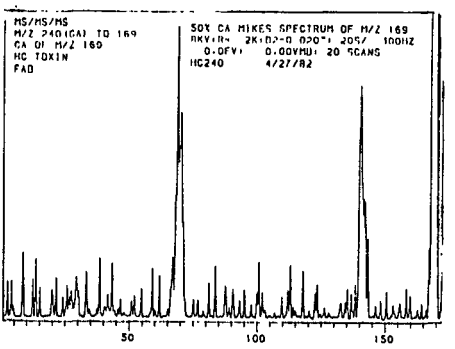


Figure 5A.
MS/MS/MS spectrum of m/z 169 formed from m/z 240

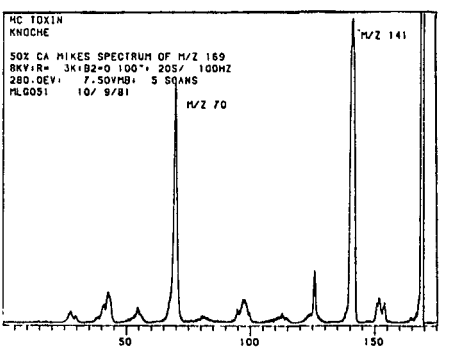


Figure 5B.
CA spectrum of m/z 169

Surface Analysis of Organic Adsorbates on Carbon Particles, Mark M. Ross, Richard J. Colton, Naval Research Laboratory, Chemistry Division, Washington, DC 20375.

Carbonaceous particulate matter is generated by numerous sources such as coal- or oil-burning furnaces and plants and diesel engines. Certain organic compounds such as polycyclic aromatic compounds (PAC), which are products of incomplete combustion, have been shown to adsorb on the surface of carbon particles. Many of these substances have adverse biological effects since they are known to be carcinogenic, mutagenic, etc.. In other areas of industry, activated carbon surfaces are used to scavenge organic pollutants from air and water. With these applications in mind, we began to investigate methods to directly analyze various organic compounds, such as benzene, substituted benzenes, napthalene, acenaphthene, phenanthrene, and pyrene, on carbon particles. We report here the use of secondary ion mass spectrometry (SIMS) and thermal desorption/gas chromatography/mass spectrometry for such analyses.

First, a double-focusing SIMS instrument, employing a 10^{-7}-10^{-8} A/cm^2 Ar^+ ion beam, is used to detect organics of varying molecular weight which are adsorbed on activated carbon and subsequently burnished onto silver. Intense and long-lived (>30 min for 1 μg of sample) molecular ion emission, both M^+ and $(Ag+M)^+$, is observed for the PACs used (e.g. naphthalene to pyrene). The detection limit is determined to be approximately 2 ng, or 1 μg phenanthrene/ 50 mg carbon. Using a series of methyl-substituted benzenes, we determined that an adsorption energy of >10 kcal/mole for the compound on carbon is necessary to hold the sample molecules on the surface of the carbon for SIMS analysis. This adsorption permits, for the first time, the study of volatile compounds without prior sample freezing.

Second, a CAMECA IMS-300 ion microscope is used to analyze organic compounds using dynamic beam conditions, >10^{-5} A/cm^2. The CAMECA results are compared with those of the more static experiments using the double-focusing instrument. Initially, we found that no molecular ion emission could be detected for organic compounds on metal (Ag or In) surfaces using the CAMECA. Subsequently, a liquid gallium matrix was used and intense M^+ ions are observed for 10-40 μg of phenanthrene, anthracene, flouranthene, and pyrene. The molecular ion signal is initially very high and then decays to a steady-state level which can last for more than 30 minutes with 20 μg of the organic. Detection of the particular compound seems dependent upon molecular weight of the sample and upon establishing a steady-state migration of sample molecules across the gallium surface to the primary ion beam. The self-renewing liquid gallium surface appears promising for dynamic SIMS applications and has certain advantages over other mobile matrices such as glycerol.

Finally, organic compounds are desorbed from carbon particles onto a fused-silica capillary column for FID or MS detection. Thermal desorption produced peak profiles which are always broad. So far, the desorption experiment was successful only with relatively large concentrations of the organic sample (e.g. 0.1 mg/200 mg carbon). Improvements are currently being made in the efficiency of transfer of evolved species from the carbon surface to the head of the column.

TPA 30 THEORY OF SIGNAL-TO-NOISE FOR ICR MASS SPECTRMETRY, E.B. Ledford, Jr. and Donald L. Rempel, Chemistry Department, B-25 Hamilton, Univ. of Nebraska, Lincoln NE 68588

The generation and processing of ion resonance signals from a capacitance bridge detector has been the subject of theoretical studies (1). The objective of this study is to quantitatively compare the theory of the capacitance bridge detector and ICR analyser cell with experimental performance, and to derive a theory for the propagation of noise through the signal processing chain used to construct mass spectra.

The present experiments concern peak heights obtained in a standard pulsed ICR experiment. An rf burst excitation lasting two milliseconds was used to stimulate ion resonance signals. The resulting power absorption transient was passed to a mixer/integrator circuit which computes in analog fashion one point on the Fourier transform of the ion response. Peak profiles were generated by means of a narrow magnetic field sweep. Peak height as a function of experimental parameters was measured and compared to theory. The theoretical peak height expression is

$$V_{INT} = \frac{NqV_{EX}AV_{REF}T_0^2}{4T_{INT}BL^2C_TV_M}$$

in which V_{int} =integrator output on resonance; N = number of ions; q = unit charge; A = amplifier gain; V_{ref} = mixer reference rf level base-to-peak; V_{ex} = excitation rf level base-to-peak; T_0 = integration time; B = magnetic field strength; L^{ex} = cell height; C_T = total bridge capacitance; V_m = mixer gain constant. Peak heights plotted v.s. rf level, pressure, and electron beam current were straight lines with zero intercepts. Data from these plots were pooled to form a comparison between theory and experiment (Figure 1). In all experiments peak heights are one tenth the value expected on the basis of theory. Unless a systematic error in the measurement of experimental parameters can be found to account for the discrepancy between theory and experiment, the results suggest that not all ions trapped in the analyser cell contribute to resonance signals.

One problem encountered in this experiment was the discovery of coulombic ion loss from the analyser cell. This loss mechanism does not appear to involve ion-molecule collisions and is highly dependent upon applied trap voltage. Estimates of the number of ions trapped in the cell can be corrupted under conditions of coulombic ion loss. In all attempts at quantitative comparison of experimental and theoretical peak heights, conditions were chosen in which no symptoms of coulombic ion loss were apparent.

With regard to noise, the following theoretical expression for the uncertainty (standard deveiation) in the peak height (equation 1) has been derived:

$$\sigma_{V_{INT}} = \frac{AV_{REF}T_0^{1/2}}{T_{INT}V_M}\left\{\overline{N_A^2} + \frac{1}{(W_EC_T)^2}\left[\overline{I_A^2} + \frac{4kT_M}{R}\right]\right\}^{1/2}$$

in which $\sigma_{V_{int}}$ = standard deviation in V_{int}; $\overline{N_A^2}$ = amplifier noise voltage density, input referred; w_E = mixer reference frequency; k = Boltzmann's constant; T_m = temperature; and $\overline{I_A^2}$ = amplifier noise current density, input referred. Experimental tests of this expression are in progress.

Future work will include more extensive comparison of theory and experiment, and will involve analyser cells of various geometries. In addition, a new tool will be used to provide insight into the operation of the ICR analyser cell: impulse excitation of ion resonance. According to theory, a Dirac-delta impulse applied to the analyser cell should give rise to a Lorentzian peak having the following peak height:

$$V_{INT} = \frac{NqAV_{REF}(V_{EX}T)}{4T_{INT}BL^2C_TV_M\zeta}$$

in which T = 1 second; V_{ex} = weight of Dirac-delta impulse; ζ = damping constant for exponential decay of ion resonance signals. While an ideal Dirac-delta impulse excitation cannot be constructed, an approximation can be. A pulse 1 us wide with amplitude variable

from 0-300 Volt has been produced and applied to an ICR analyser cell. Strong resonance signals from benzene are observed with a pulse amplitude of 40 Volts at a magnetic field strength of 0.78 Tesla. More extensive characterization of the impulse response is in progress.

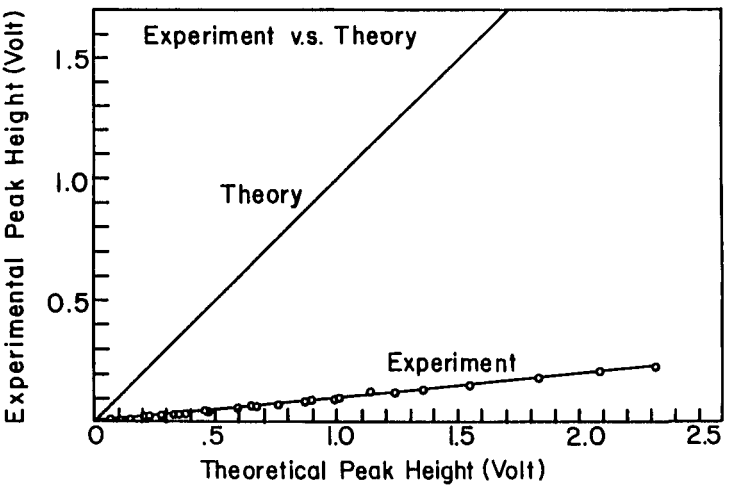


FIGURE 1. Comparison of experimental and theoretical peak heights for a standard pulsed ICR experiment. Solid line represents agreement between theory and experiment. Experimental line is derived by pooling data from plots of peak height v.s. rf level, pressure, and electron beam intensity. Experimental peak heights are one tenth of theoretical values. Unless a systematic error in the computation of theoretical peak heights can be found, the result suggests that only 10% of the ions trapped in a conventional ICR analyser cell contribute to resonance signals.

REFERENCE

1. R.T. McIver, Jr., E.B. Ledford, Jr., and Richard L. Hunter. "Theory for detection of ion cyclotron resonance signals," J. Chem. Phys. 72, 2535 (1980).

TWO COLOR PYROMETRY FOR ISOTOPE RATIO MEASUREMENTS: J. E. Delmore, R. A. Rankin, L. W. Buttars, Idaho National Engineering Laboratory/EXXON Nuclear Idaho Co., Idaho Falls, Idaho 83401

An automatic two color pyrometer for monitoring ionizing filament temperature has been installed on a Nuclide mass spectrometer used for measuring isotope ratios. The pyrometer is permanently mounted outside the source housing and monitors the temperature through a sapphire window. The most accurate isotope ratio measurements are made when the temperature is set by pyrometry, to account for variations in filament material. The two color pyrometer has the following advantages over the manual pyrometer it replaced: 1) A slight clouding of the window has less effect on the measurement. 2) A reading can be taken without operator intervention. 3) Computer interfacing is easy. 4) Resolution is improved from 5-15^{0} to 1-2^{0}. 5) The temperature is easily monitored for the duration of the analysis, allowing the detection of any instabilities. 6) The color perception of the operator does not influence the measurement. A single, experienced operator performed uranium system calibrations using both pyrometers. The same levels of accuracy and precision were obtained in both cases, but the two color pyrometer being more convenient and more adaptable to automation. The accuracy and precision obtained were substantially better than can be obtained from adjusting the center filament temperatures with either filament current on Re signal instensity.

MEASUREMENT OF IODINE-129 AT THE FEMTOGRAM LEVEL BY NEGATIVE SURFACE IONIZATION MASS SPECTROMETRY

J. J. Stoffels
Pacific Northwest Laboratory
Richland, WA 99352

OBJECTIVE

Develop a mass spectrometric method for measuring trace level iodine-129 in environmental samples.

INTRODUCTION

The best sensitivity for measurement of environmental iodine-129 has been provided by neutron activation analysis. However, the neutron activation method lacks precision for trace levels of iodine-129, involves a lengthy analytical procedure and requires a high-flux source of neutrons. The mass spectrometric method being developed is expected to improve all these areas of iodine-129 measurement technology.

INSTRUMENTATION

- Ion Source
  - Triple-filament surface ionization.
  - Lanthanum hexaboride ionizer, ϕ = 2.7 eV
    LaB_6 powder in a methanol suspension is deposited on a rhenium filament by electrophoresis and sintered in vacuum.
  - I^- ion current: 10^{-10} - 10^{-9} A at 1000°C from 100 ng of sodium iodide.
- Mass Analyzer
  - Three stage: two 12-inch, 90° magnetic sectors and one 12-inch, 90° electric sector.
  - Abundance sensitivity: better than 10^{-11} for negative ions in the iodine mass region.
- Ion Detector (under development)
  - Ion/electron/scintillation converter for pulse counting negative and positive ions.
  - Insertable Faraday collector for measuring ion currents $>10^{-13}$ A.

PRELIMINARY RESULTS

- Measurement Sensitivity: 10^7 atoms (2×10^{-15} g) of ^{129}I gives an ion signal which is twice the mass spectrometer background.
- Isotope Ratio Capability: $1/10^8$ limited by interfering hydrocarbon background.
- Sample Utilization: ~1% (1 ion collected/100 atoms of sample).

FUTURE WORK

- Develop physical and chemical procedures for separating iodine from environmental samples in a form suitable for mass spectrometric analysis.
- Reduce hydrocarbon background interference to permit measurement of $^{129}I/^{127}I$ ratios greater than 10^{-8}.

Isotopic Detection of ^{129}I by Multiphoton Ionization

David M. Lubman and Richard N. Zare
Quanta-Ray, Inc.
Mountain View, CA 94043

The problem of monitoring ultralow levels of various radioisotopes in the environment is of current interest. In particular, ^{129}I with a half-life of 17 million years, can be used as a tracer of radioactive contamination in the environment over an extended period of time. ^{129}I is produced as a major product ($\sim$1%) in the fission process and soon mixes with the natural isotope, ^{127}I, in the environment. Thus, monitoring ^{129}I can be accomplished through the detection of the mixed molecule $^{127}I^{129}I$. The sensitivity desired for analyzing these gaseous samples is on the order of 10^7 atoms/cc of ^{127}I; i.e. an isotope detection ratio of $1:10^8$. The present method of analysis is based upon neutron activation. This method is extremely time consuming and cannot be used for real-time measurements. In addition, it requires chemical removal of contaminants which otherwise result in a radioactive background which limits the discrimination achievable with this technique.

In this presentation, we demonstrate an I_2 detection scheme using two-color laser multiphoton ionization in which the two beams of differing wavelengths overlap in space. The two wavelengths were a green beam (λ=640-530 nm) obtained by pumping various dyes in a Quanta-Ray Nd:YAG pumped dye laser which was overlapped by the UV 3rd harmonic (λ=355 nm) of the same Nd:YAG system. The samples were analyzed in pyrex ionization cells which contained a pair of electrodes $\sim$1 cm apart. In figure 1 the ionization spectra of $^{127}I_2$ and a 1:20 mixture of $^{127}I^{129}I$:$^{127}I_2$ are quite different as expected. Because the spectrum of $^{127}I^{129}I$ differs from that of $^{127}I_2$ by the isotope shift, it is possible to excite selectively one isotopic molecule in the presence of the other. A two-color scheme is preferable to a one-color scheme because it can provide additional selectivity of the wanted isotope. We have demonstrated by correct choice of wavelengths a detection ratio of ^{129}I:^{127}I of $2\text{-}3:10^4$ in an ionization cell. In a vacuum system using a quadrupole mass spectrometer we should in principle be able to discriminate $^{127}I^{129}I$ from $^{127}I_2$ in an abundance ratio on the order of $1:10^8$ or better with our selective laser source. Under molecular beam conditions we were able to detect $^{127}I_2$ at the base pressure of the chamber, i.e. 2×18^{-8} Torr or 1.5×10^8 molecules/cc. The theoretical limit of detection based upon the magnitude of the signal obtained is on the order of 10^4-10^5 molecules/cc.

The mechanism of this laser ionization scheme was investigated in order to optimize its analytical potential. The I_2 ionization signal was found to depend on a combination of both colored beams. If one of the beams was blocked the signal disappeared completely. Thus, I_2 can be uniquely discriminated from background organics. The ionization signal as a function of the green wavelength was found to be completely different from the B state fluorescence. The lifetime of this state was found to be at least 10x that of the B state, so that the B state is not the resonant state involved. In addition, a delay experiment showed that absorption of a green photon preceded the UV photon. If the green wavelength was held constant and the UV beam was scanned another state with discrete structure was observed. Thus two real resonant states are involved in the ionization

process. By changing either the green or UV wavelength an almost unlimited number of possible combinations are available for maximizing isotopic discrimination and minimizing background. We have just explored a rather restricted number of these combinations.

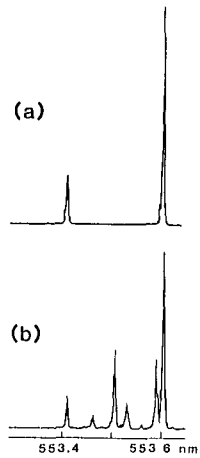


fig. 1
Two-color MPI spectrum of (a) $^{127}I_2$ and (b) a 1:20 mixture of $^{127}I^{129}I$:$^{127}I_2$

ISOTOPE RATIO MEASUREMENTS USING THE RIBERMAG R-10-10 QUADRUPOLE GCMS; Charles M. Judson, Mass Spectrometry Laboratory, Malott Hall, University of Kansas, Lawrence, KS, 66045.

The Mass Spectrometry Laboratory at the University of Kansas frequently performs isotope ratio measurements for quantitation by isotope dilution, and for studies of reaction mechanisms. The method used is GCMS analysis by measurement of molecular ions or characteristic fragment ions. The specific procedures used are: (a) intensities are measured at the tops of the mass peaks; (b) data are accumulated by a digital data system; and (c) mass peak intensities are integrated across the GC peaks, and ratios of the integrals are calculated. The instrument used for these measurements is a Ribermag R-10-10 quadrupole mass spectrometer (manufactured by Nermag, S.A.), used with a Girdel gas chromatograph and a Ribermag data system.

With samples from complex mixtures, the precision and accuracy of isotope ratio measurements is generally limited by the failure of the gas chromatograph to separate the impurities, unless high resolution or MS/MS instrumentation is available. The work reported in this paper is concerned, however, with the limitations to precision obtainable in the absence of impurities, representing the ultimate precision obtainable with this instrumentation. Most of these measurements were made by injection to an SE-30 packed GC column of 2 microliters of a solution with approximately 1% of normal nitrobenzene, and a slightly lower concentration of D-5 nitrobenzene. These conditions were selected to obtain high integrated ion intensities and thereby to minimize variations due to random arrival rates. It was ultimately found, as noted below, that it was better to use more dilute solutions with a capillary column.

The Ribermag instrument can be adjusted to give a reasonably smooth and sufficiently flat peak top by operation at a somewhat reduced ion energy, with a negligible sacrifice in sensitivity. The peak shape can also be adjusted for symmetry by trimming the voltages applied to the deflector electrodes located at the multiplier entrance. Measurements were made with resolution adjusted to provide a peak width at half-height of 1/2 amu.

To avoid any possibility of variations due to modulation at 60 cycles, measurements were generally made with 17 millisecond measurement times. However, no improvement in precision due to use of 17 millisecond measurement times was experimentally demonstrated.

Mass peaks can be measured with this instrument in three different ways; (1) by stepping to a single predetermined point on the top of each mass peak; (2) by measuring successive points across a small region at the top of each mass peak, finding the point of maximum intensity, and recording the maximum intensity and the exact mass at which that maximum was found; or (3) measuring successive points across the top of each mass peak, recording the exact mass for the maximum intensity as in (2), but recording the average intensity for the peaks measured. The best precision is obtained by methods (2) and (3). We have not experimentally found a difference in the precision obtainable by methods (2) and (3). We believe that method (3), recording average values, should be used for measurements of low concentrations because a larger number of ion arrivals are measured. Method (1), single peak top measurements, will sometimes, but not always, give precision equal to that obtained by methods (2) and (3).

The zero value of the amplifier-digitizer system is adjusted so that a finite background is measured when no ions are being collected. This avoids the possibile errors that would arise if, in adjusting the background to zero, the background were actually adjusted to a small negative value.

Except for measurements at very low ion current intensities, amplifier range and multiplier voltage are selected so that the intensity of the largest mass peak, measured at the top of the GC peak is at least 50% of the saturation level of the digitizer. This minimizes the error caused by digitization at discrete levels. For low ion current intensities, this procedure can be used but will not provide any improvement in signal/noise.

In the present experiment we are measuring ratios that are near to unity. For ratios that are not near to unity, the measurement time should be adjusted to measure the less intense peak for a longer time. The data system accomodates to this selection of different measurement times to keep the same dynamic range for both ions.

Background subtraction can be made by assuming (1) a constant background equal to the background preceding the GC peak, or (2) an average value for the background preceding and following the GC peak. When the background is a peak tail and not a contribution from an interfering constituent, the initial background should be used. If this initial background is noisy, an average value of this initial background should be used, but not an average of the initial and final backgrounds.

Using 1% solutions of nitrobenzene injected to an SE-30 packed column, the ion chromatograms deviate from ideal. In addition to the expected isotopic fractionation, there are significant peak tails, and the two isotopic peaks have different shapes. This condition provides a good test for the effect of non-ideal chromatography on the procedures required for precise isotope ratio measurements.

We encountered one requirement for precise isotope ratio measurements which appears not to have always been recognized, and which is accentuated in the case of non-ideal peak shapes. This requirement is that the end-point for the integration of the GC peak must be taken consistently and must include the major part of the tail of the GC peak. In this case with 1% solutions injected to a packed column, the calculated isotope ratios, plotted against the ratio of the final intensity to the intensity at the top of the GC peak, do not extrapolate to a definite value. There is not an absolute correct ratio. As we add more and more measurements that are ratios of two small numbers, we eventually increase the error by adding more points. However, precision can be evaluated, and ratios of ratios can be calculated, by integrating to a specified final intensity, for example to 1% of the intensity at the GC peak.

Using this procedure, we made single ratio measurements with 6 to 50 measurements/half-width of the GC peak. No trend of measured ratios with increasing number of measurements/GC peak was found, within a precision of 0.5%. We then measured the precision for three repeated injections using 20 and 50 measurements/half-width of the GC peak. We were able to repeatably obtain a standard deviation of about 0.15% with 50 measurements/half-width, but always had a larger deviation with 20 measurements/half-width. These results appear to be consistent with the calculations of Mathews and Hayes (Analytical Chemistry, 48, 1375,1976). In any specific case of non-ideal chromatography, the number of measurements/GC peak required for a specified precision should be experimentally evaluated for the GC conditions to be used.

Using more dilute solutions, and injecting with a moving-rod injector into a capillary SE-54 column, isotopic peaks having reasonably identical peak shapes were obtained. Variation with the end-point of the integration was then a much lesser problem, and the ratio calculated with a final intensity of 1% of the peak intensity is very close to the ratio extrapolated for a final intensity of zero. Time has not permitted measurements under these conditions of the variation in measured ratios with the number of measurements/GC peak, or of standard deviations for repeated measurements. However, it can be expected that the required number of measurements/GC peak will be reduced, and that the precision for a specified number of measurements/GC peak will be improved.

Conclusion. A standard deviation of 0.15% has been consistently obtained for three successive measurements of isotope ratios for nitrobenzene and d-5 nitrobenzene with injection to a packed column at concentrations that gave high ion current intensities, but also non-ideal chromatograph peaks. The precautions required to obtain this precision have been described above. More nearly ideal chromatograph peaks can be obtained using more dilute solutions injected to a capillary column with integrated ion currents that are still greater than 10^8 measured ions/GC peak. We expect to obtain substantially better than 0.1% standard deviation with these improved chromatographic conditions.

TPB 5 DESIGN PRINCIPLES AND APPLICATIONS OF MULTIPLE COLLECTORS IN THERMAL IONIZATION ISOTOPE RATIO DETERMINATIONS; K. Habfast, H. Rache, and M. Weber, Finnigan MAT GmbH, Bremen, Germany

In thermal ionization mass spectrometry, complete automation - sample heating, data collection, data evaluation - has considerably enhanced precision and sample throughput in isotope ratio measurements.

Further improvements can be expected by simultaneous recording of all ion beams of interest by a multiple collector.

The design of a multiple collector which produces not only precise, but also accurate results, however, is not trivial.

We will present our current state of the art concerning the design of collectors and collector sets, channel gain calibration devices and data evaluation methods (algorithms) to ensure accurate results. Moreover we will discuss the use of multiple collectors for the isotope analysis of sub-nanogram samples.

REMOVAL OF THE DYNAMIC RANGE LIMITATION IMPOSED BY THE USE OF COUNTING MODE IN RESPIRATORY GAS ANALYSIS; Clark, J.S., Criddle, M.J., and Farr, F.L.; Primary Children's Medical Center, Salt Lake City, Utah 84103.

The methodology as described in our companion paper (1), for non-invasive measurement of pulmonary blood flow and the physiologic gas contents of arterial and mixed venous blood, imposes some new challenges for the analysis of the respiratory gases. The requirements of the gas analyzer include 1) simultaneous measurement of eleven gas components, 2) a frequency response capability for following the expired gas concentration profiles for infants with respiratory rates up to 100/min., and 3) a peak-to-peak dynamic range capability of 10^6. The first two requirements indicate the need for a mass spectrometer with peak stepping capability which pushes the state of the art. Adding the dynamic range specification to the first two requirements presents even a greater challenge to existing technology. For instance, in analog mode, dynamic range of this magnitude is normally obtained through combinations of adjustments of the multiplier voltage and the electrometer gain. However, this approach is incompatible with the rapid peak stepping requirements of the mass spectrometer. In counting mode, dynamic range is again obtained at the sacrifice of frequency response for the gas components of lower concentration. This paper presents our approach to a solution to this problem.

Our basic approach has been to operate in the counting mode with a M.S. sensitivity high enough to provide the count rate needed for achieving an adequate signal-to-noise ratio for gases in the lowest concentration bracket. The count rate, is adjusted to the same order of magnitude for all monitored peaks by controlling the electric field between the mass resolution element and the electron multiplier. Our method is illustrated in figure 1.

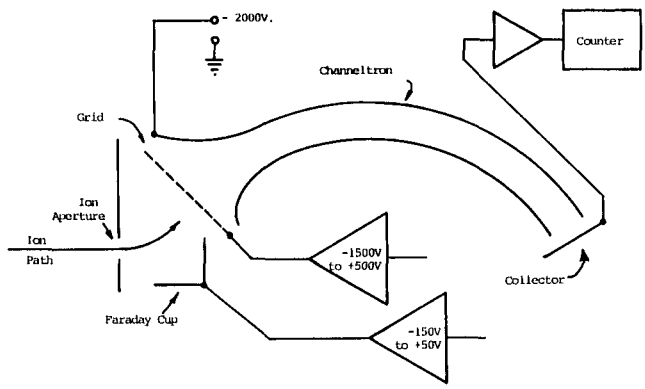


Figure 1.

The electric field in front of the electron multiplier (Channeltron) is controlled by a fine stainless steel grid placed 2 mm in front of the horn of the Channeltron. The grid potential is controlled by a high voltage amplifier (KEPCO OPS 2000 B), which is biased to provide an output between +500 and -1500 volts. The amount of attenuation desired for each peak is predetermined and added to the set of parameters used by the mass spectrometer controller. The attenuation of ion current as a function of grid voltage is shown in Figure 2.

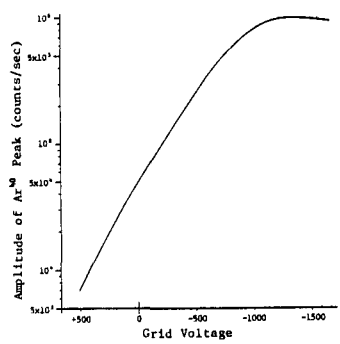


Figure 2.

One particular advantage of counting mode we have sought to retain is the theoretical (Gaussian) signal-to-noise ratio. The effect of attenuation signal-to-noise has been found to be quite modest. The decrease is less than a factor of 2 for an attenuation of 10^4. However, there is an accompanying distortion in peak shape that has necessitated the addition of Faraday cup voltage control for its elimination. This is accomplished by another amplifier having a range of +50 to -150 volts. Thus an additional predetermined parameter is added to the microprocessor control set, which is also tailored to each peak.

The M.S. system, shown in figure 3, has a UTI Controller, RF Generator, and a sensitive quadrapole analyzer. In counting mode, the mass spectrometer microprocessor (Z-80) starts and stops the counter and reads the number of counts. The counts are sent to the system microprocessor for data reduction, storage and display. The µP sets the DAC levels which interface to the mass spectrometer. The 16-bit DAC provides 0-10 volts signal which is used by the controller to set the amplitude of the RF, which determines the mass peak. This signal is also summed with the signal from a 12-bit DAC and used to set the DC potential of the rods. The RF/DC ratio determines the resolution. The µP also sets the levels of the 12-bit DAC's which control the high voltage amplifiers which drive the faraday cup and the grid.

A blanking feature has been added to the system to prevent saturation of the multiplier while crossing larger peaks. While this could have been accomplished by either grid control or the resolution control, we chose the resolution control because it has the faster time constant and adds little to the total settling time of the system. (Resolution control, by the microprocessor, on a peak to peak basis exists because of the need to maximize the signal-to-noise for all the gases). An analog protect circuit has also been added to the system as further protection against multiplier saturation. The analog output of the discriminator is filtered and sent to a comparator circuit which controls the multiplier high voltage supply.

At this time we have not measured the effects of this attenuation method on linearity. Linearity deficiencies of the system are corrected automatically by the self-balancing method described in our companion paper (2).

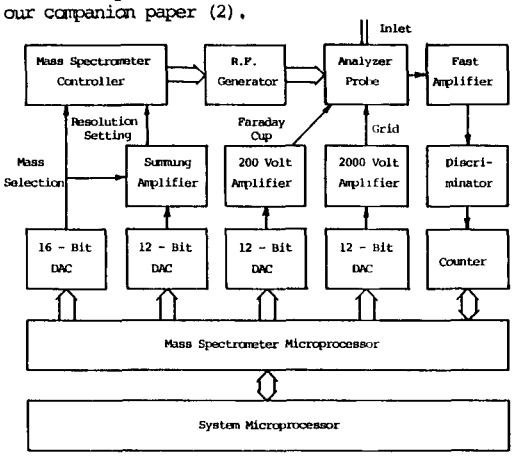


Figure 3.

REFERENCES

(1) Clark, J.S., Criddle, M.J., Farr, F.L., Harris, T.R. Non-Invasive Measurement of Mixed Venous Oxygen and Carbon Dioxide Contents. 1982 Conference on Mass Spectrometry and Allied Topics, Sponsored by American Society for Mass Spectrometry.

(2) Clark, J.S., Farr, F.L., Wallace, W.D., Criddle, M.J. An Automatic, Precision Calibrator for an Eight Component Residual Gas Analyzer. 1982 Conference on Mass Spectrometry and Allied Topics, Sponsored by American Society for Mass Spectrometry.

CALIBRATION STABILITY OF THE ELECTRO-OPTICAL ION DETECTOR

by R. A. Britten and C. E. Giffin
Jet Propulsion Laboratory; Pasadena, CA 91001

The Electro-Optical Ion Detector (EOID) has been described in several prior papers at ASMS. Sometimes referred to as a "high sensitivity electronic photoplate," the EOID gives an instrument sensitivity which is two to three orders of magnitude greater than that provided by conventional scanning or photoplate instruments.

Unlike most other MS detectors, the EOID must be calibrated. This calibration is necessary because the EOID consists of several discrete components, none of which can be manufactured with complete lateral uniformity. In a prior paper (1) the authors have proposed doing a (relative) sensitivity calibration on EOID's by using a slow magnetic scan to sweep mass spectral peaks over ranges of adjacent detector elements. A magnetic scan was proposed in order to avoid changing any operating parameters in the ion source and to avoid changing ion impact energies at the detector.

Hedfjall and Ryhage(2) have reported an EOID calibration effort using methodology similar to what we proposed except that it involved an electric rather a magnetic scan. "The (ion) intensity," they say, "is compensated for decreasing accelerating voltage." They do not elaborate on just how this compensation is done.

Results from Hedfjall and Ryhage's work are presented in figure 1. One result seen there is a sensitivity drift of ± 5% in just 48 minutes. They infer (incorrectly, in our view) that this drift came from the EOID and conclude that "the EOID cannot yet advantageously be used for qualitative or quantitative GC/MS analysis."

At our laboratory EOID calibration work has been done using magnetic scans. Some results of this work are summarized in figures 2-5. Figure 2 shows the short term intensity fluctuations (noise) on unswept peaks of various heights. Figure 3 shows the results of sweeping a mass 162 peak (from PFK) over a range of adjacent detector elements (pixels). Figure 4 shows the consistency with which this pattern can be duplicated over time. The duplication is as good as can be expected in view of the observed noise levels. Figure 5 shows observed gain variations as a function of time. The upward slope of this graph shows that EOID sensitivity calibrations do fade with time, but the time period over which this happens is of the order of several weeks.

If one thinks in terms of the usual random walk model, drifts of the sort reported by Hedfjall and Ryhage (± 5% in 48 minutes) ought to lead to near chaos over a period of three or four weeks. From the present work it is evident that this simply does not happen. The instability noted by Hedfjall and Ryhage must have come from some source other than the EOID.

The authors of the present paper were mistaken in thinking that a magnetic scan could provide adequate coverage for complete EOID calibration. The magnetic scan technique is easy to implement and good for demonstrating stability, but it works well only over a very limited range. If, as in our case, the EOID is placed in the collector plane of a Mattauch-Herzog spectrometer, then it lies in the fringing field of a magnet. During a magnetic scan, this fringing field changes; and electron trajectories within the EOID are altered. These altered electron trajectories shift the effective alignment of the channel electron multiplier array with respect to the other EOID components. Once this alignment shift becomes much larger than half a pixel width, the detector being calibrated is no longer the same as the detector being used. Our data show clear evidence of such misalignment with magnetic scans as low as 3%.

Only electric scanning can give the sort of broad sweeps necessary go achieve overlaps and do the sort of bootstrapping necessary to calibrate a broad mass range detector (see figure 6). Figure 7 shows the results of an overlap and bootstrap operation involving three separate mass spectral peaks. Though it may not be obvious from the picture, the three traces track quite well.

With current technology some EOID components cannot be manufactured with physical dimensions much greater than an inch. To get broader coverage in the detector plane it is necessary to place several of these components side by side. As reported previously, mass scale irregularities can occur at these junctions; so it is necessary to calibrate the mass scale.

The EOID mass calibration procedure has been described previously (1). It involves correcting for known geometric artifacts at component junctions and then using key index peaks in a reference spectrum as a basis for quadratic interpolation. Calibrations done in this way (figure 8) are found to be stable over several months (figure 9). Small daily changes (resulting from changing E and B fields in the spectrometer) are corrected with a simple multiplicative factor.

CONCLUSION

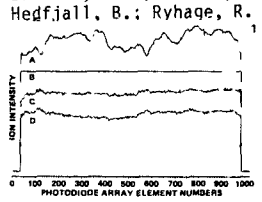
The EOID is a high sensitivity detector very useful in certain applications, but it needs to be calibrated. A one-point update on the mass scale takes about two minutes and is usually adequate for general purposes. A complete reworking of the mass scale takes about half an hour. The relative sensitivity calibration procedure is still under development. Once it is refined, a complete reworking of the relative sensitivity values will probably require about half an hour per photodiode array.

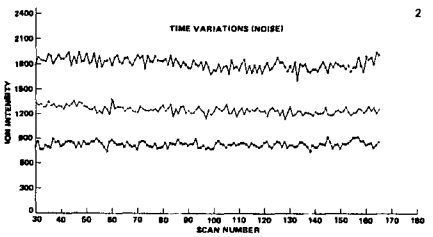
Despite what has been said in one published report, EOID's are remarkably stable devices. Once they are calibrated, they do not need to be calibrated again for weeks or possibly even months.

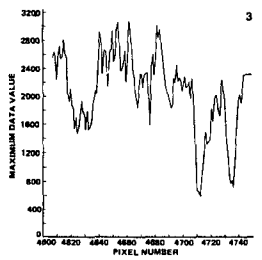
---

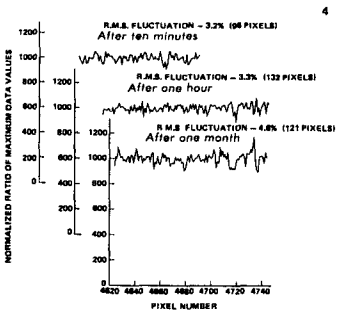
(1) Britten, R.A.; Giffin, C.E. 28th ASMS Conference (New York); paper TPMP4.

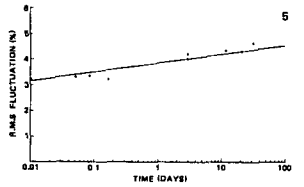
(2) Hedfjall, B.; Ryhage, R. Anal. Chem. 1981, 53, 1641-44.

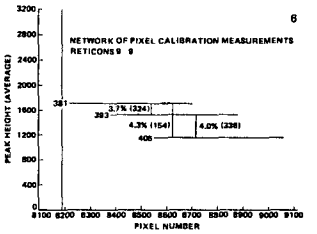


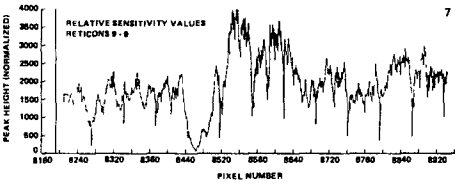


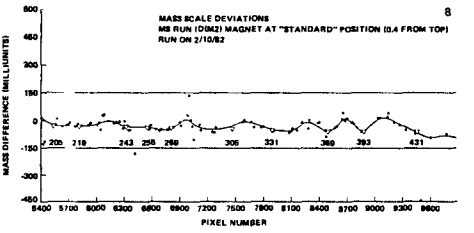


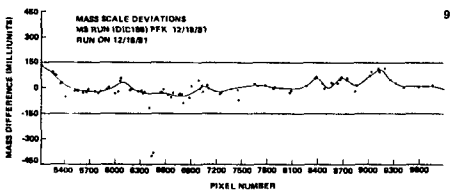












COMPUTER-ASSISTED CONTROL AND DATA ACQUISITION FOR AN MS702 SSMS

Peter C. Rankin

Soil Bureau, Lower Hutt, New Zealand

INTRODUCTION

The normal operation for the electrical detection of ions in a MS702 spark source mass spectrometer is for two signals to be taken from the spectrometer and ratioed. One signal (Total Ion Current) is a fraction of the total ion intensity of the undispersed ion beam and is a measure of the ion intensity produced by sparking. The other signal (Electron Multiplier) is a measure of the intensity of the individual m/e ions separated by the magnetic field. The production of ions from a sparked sample (particularly a pressed powdered sample/graphite mixture) is erratic and the Total Ion Current signal has to be used as a reference to compensate for the fluctuating ion production. This permits meaningful Electron Multiplier signals to be measured. Thus, in electrical detection, one measures the ion intensity of a particular m/e as the ratio

$$\frac{\text{ion electron multiplier signal}}{\text{total ion current signal}}$$

The practical limitation to electrical detection is that the measurement of a specific m/e ion is essentially instantaneous and the measured intensity could be erroneous due to the erratic ion formation in the spark. Only small amounts of sample are consumed during sparking and sample/graphite inhomogeneity gives rise to unreproducible ion intensities. Thus, from a magnetic scan using electrical ion detection, one can not be assured that the measured ion intensity is proportional to isotopic abundance and concentration in the sparked sample. What is missing is the integrating characteristics of the photo-emulsion detector. The experience at Soil Bureau with the MS702, electrical detection and magnet scanning has demonstrated that electrical detection as supplied is not a practical ion detection system for quantitative trace element analysis of geological or soil samples. Peak switching necessary to electrical detection is an attempt to overcome the lack of integrating with magnet scanning but factors such as magnet instability, and hysterisis still result in practical problems.

The solution to the problem was to employ the well recognised technique of improving spectral signal-to-noise ratio by adding and storing of repetitive scans. The availability of low cost microprocessor based computers opened up the possibility to log the SSMS data directly into the computer and to carry out automatic processing of the acquired information. Micro-processors were used to acquire data from a magnetic scan of the spectrum of a sparked sample and to add this to data acquired from preceding magnetic scans. The approach of accumulating repetitive scan data is not new and has been reported by Harrison (1974) and De Ceuninck (1978) both of whom used multiple-channel scan analysers as their recording devices. Their approach illustrated the viability of collecting and adding successive spark source mass spectral data.

FEATURES OF THE SYSTEM

1. Two PACE (National Semiconductor) CPU's were chosen because of uniformity of instructions and power supplies, and flexibility of communication between them by means of flag lines and testable condition lines. This communication was by a double handshake technique.

2. An early decision was made to dedicate one CPU exclusively to the task of controlling magnet cycling. A completely un-interruptable magnet scan cycle was considered essential to obtaining reproducible magnetic field changes and it also ensured that unforeseen problems in a multi-interrupt environment would not arise to perturb magnet cycling or interfere with signal sampling.

3. The SLAVE microprocessor system produces a series of voltage steps with time from its DAC output. These are amplified to a maximum value of 60 V and applied to the existing magnet current control circuit. The steps occur at a rate dependent on the mass range being scanned and the resolution required by the operator, but in any event they occur at a high enough rate that the magnet inductance smooths them.

4. In early trials it was discovered that the magnet system is sufficiently nonlinear and hysteretic that a formal relationship between magnet current and field for any range and rate of scanning would be difficult to specify. The solution chosen was to allow the choice of various scan 'regimes' (A regime has a fixed top field and bottom field between which the field is scanned, and a fixed rate at which it is scanned). The system is then calibrated for that regime by analysing a known sample, and identifying four peaks evenly spaced across the scan range. A cubic relationship is established and from which any data channel can have a mass accurately assigned to it. The m/e's used to calibrate the normal scan regime used for soil/rock trace element analyses were Au-197, Lu-175, C_{11}-132 and Rh-103.

5. The cycling of the magnet was as follows:

(i) decreasing field at a rate determined by entered parameters of 'top mass', 'bottom mass' and number of data channels/mass. Spectral data was collected only on a decreasing field.

(ii) increasing field at twice the rate of the decreasing field.

(iii) a static 10 second hold once the increasing field had reached 'top mass' and before the decreasing field portion of the cycle re-starts.

6. Every 20 milliseconds data from the Total Ion Monitor and Electron Multiplier were recorded by 2 sample and hold circuits. Because the ion beam composition fluctuates so much during sparking it is essential there be no time skew between the sampling the two analog inputs. The use of sample/hold devices ensures that the two analog values input to the master microprocessor are sampled at an exact time with respect to the magnet field.

7. Auto-ranging of both digitised input signals is needed because of the large dynamic ranges of the inputs. This arises because of the facility to vary the gain of the electron multiplier by several orders of magnitude. The auto-ranging is accomplished by reed relay controlled gain switching in a 2-pass procedure. One digitiser (ADC) services both sample and hold circuits and the 2-pass auto-ranging procedure takes 2 milliseconds per sample and hold.

8. Each spectrum can be represented by up to 6000 data points.

9. The digitised spectrum is processed to determine peak heights, peak areas and ratios of peak data with respect to an internal standard (Lu-175).

10. Spectral Alignment. A signal accumulating technique to improve signal/noise ratios depends on having a reproducible scan so that the contents of the same channels are added after successive scans. In spite of confidence in the reproducibility of the computer controlled magnetic scan of the MS702 a software procedure of spectral alignment prior to addition of data was developed. The graphite powder used to mix with geological or soil samples was doped with the internal standard Lutetium (m/e175) plus the mono-isotopic elements Gold (m/e197) and Rhodium (m/e103). Before the addition of successive scan data these peaks would be aligned with respect to specified channels which had been determined from the magnet calibration scan (see 4 above). After alignment the data from the newly acquired scan and the accumulated data would be added. The assumption was made that any instrumental drift would cause spectra shift in one direction only. Thus, misalignment of the reference peaks could be detected by the software averaged for each reference peak and a correction applied. A more sophisticated correction procedure would be required if instrumental drift produced a stretch or squeeze type of change to the spectral data in relation to channel number.

A Simple and Inexpensive Conversion of the Electronic Supplies in an AEI 702 Spark Source Mass Spectrograph

Donald L. Dugger and Greg Maklae
GTE Laboratories, Inc., Waltham, MA. 02254.

Although in recent years the Spark Source Mass Spectrograph has experienced very little activity in the way of new developments, it remains a very useful and important analytical tool for many applications. Most of the instruments in the field were built using tube-type circuitry, and it is almost impossible to buy a new instrument since they are no longer being manufactured. Therefore, it is important to maintain those in the field in order to assure that the technique will remain available to those who have need of its analytical capability. This has become an increasingly difficult problem in recent years for a couple of reasons. First, update conversions to solid-state circuitry from various sources tend to be prohibitively expensive. Second, the difficulty in maintaining the original supplies, which at this point in time tend to be extremely unreliable and fall short of the stability needed to achieve maximum resolution and sensitivity in the instrument. In addition, either replacement parts are very expensive and hard to get, or they are no longer available.

In our particular laboratory we were constantly having problems with the magnet power supply, especially shorting at the base of the U19 tubes. In addition, when the supply was operating it no longer met specs. Also troublesome were at least two of the 250 volt power supplies as well as the 2 KV supply. Although these supplies did meet specs when operating, one or more units would usually go down any time the instrument was powered down either accidentally or on purpose. After considering the alternatives, it was decided to replace on an individual basis all troublesome circuits.

The three 250 volt supplies were replaced with units purchased from Adtech (Model #APS 250-.1). These supplies and the 2 KV supplies (Hewlett-Packard, Model #6521A, two supplies connected in series) were the first to be replaced. The small supplies were mounted on sheet metal in the drawer originally occupied by the tube circuits. The 2 KV supplies were mounted on a rack adjacent to the main frame of the instrument. All of these supplies plus the -85 volt and suppressor supplies were attached electrically to the appropriate connectors on the drawer for distribution to other circuits. This means the 2 KV is still routed through the constant temperature oil bath, etc. The magnet supply was purchased from Kepco, Model #HB 525(m). In contrast to the other supplies, the output from this unit, which is mounted in the adjacent rack, is connected directly to the magnet coils at the junction boxes located on top of each coil. This means it bypasses the constant temperature oil bath, range selector switch, and front panel meter. The magnet setting is controlled by either the front panel controls on the supply, or can be programmed externally through connections in the rear.

The success of these replacements has been determined by comparing electronic stability measurements of each supply with previously obtained measurements. In the original A.E.I. manual for the 702 Spark Source these were given in ppm values. In all cases, the stability of the current supplies has been found to be equal to or better than the originals (250 volt: 175 ppm vs 80 ppm; 2 KV: 40 ppm vs 15 ppm; and magnet: 150 ppm vs 12 ppm).

The replacement was quick and simple and the total cost for equipment based on 1979-1981 prices was under $5000. Mass spectra obtained using the photoplate detector is excellent.

A Mass Spectrometric Technique for Measuring the Activation Energies of the Permeation of Alkali Metals through Operating high pressure Sodium Lamp Envelopes

Donald L. Dugger and William H. Rhodes,
GTE Laboratories, Inc., Waltham, MA. 02254

A Quadrupole mass spectrometer has been used to detect the permeation of sodium and potassium through the alumina arc tube of high pressure sodium lamps. Commercially available 150 watt lamps were operated adjacent to a quadrupole ion source within a high vacuum chamber. These lamps were operated over a wattage range of 50 to 260 watts corresponding to wall temperatures of 1070° to 1310°K. These operating conditions increased the internal alkali pressure giving a variable driving force to the permeation process. The work presented concerns a description of the instrumentation and methodology for accumulating and reducing data to characterize the nature of the activation energy of the permeation process.

The mass spectrometer employed is an E.A.I. Quad 1110A. It is mounted in an ion pumped stainless steel vacuum chamber. Typical operating pressures were $5x10^{-9}$ to $5x10^{-8}$ Torr. The lamp envelopes used in this study were standard commercially available 150 watt alumina arc tubes which were lit using a Variac, and isolation transformer, and a variable linear reactor (choke). The lamps were biased at -70 Vdc with respect to the quadrupole.

A MINC 11/23 computer system with 64K memory, RT11 Operating system, RX02 floppies, and a Decwriter III printer was used to scan the quadrupole and acquire data from the electron multiplier output. Fortran IV was used for all programming. Software has not yet been written to reduce the data on this system. Therefore, the reduction and Arrhenius plots were performed on an X-Y recorder on a second computer which was previously used when data were being recorded and measured by hand. This system is

composed of an Hewlett-Packard 21MX M-Series computer with 32K memory, 7900A disc drive, Zeta Plotter Model 100, and a Tektronics 4631 hard copy unit. Programs were written using a combination of HP Basic and Fortran IV.

The quadrupole was scanned 3 to 5 times at each temperature setting and the raw data stored on a floppy disc. This data was processed using peak detect software and averaged. The averaged results and corresponding temperatures were printed on the line printer. At present, the intensities of the alkali metals in millivolts and the temperatures are entered manually into the second computer for processing.

The log of intensity when plotted versus the reciprocal of the absolute temperature resulted in a straight line, whose slope is the activation energy of the variable driving force permeation process. Typical reproducibility of the procedure yields the following values: 189 kcal/mole for seven runs for sodium with a standard deviation of ±11, and 168 kcal/mole for four runs for potassium with a standard deviation of ±8. The kinetics and mechanisms of this process are still under investigation, and will become clearer when constant alkali pressure experiments are completed.

Several problems have been encountered in this work including heat generated by the lamp at high wattages which causes outgassing and interference with the potassium measurement. Also troublesome is the problem of achieving equilibrium which may effect the reproducibility of the measurements. And lastly, the sodium and potassium emitting from the lamp, which is only a few millimeters from the ion source, causes some problems with shorting of the ion source ceramics after several runs.

A QUANTITATIVE MASS SPECTROMETER FOR HYDROCARBON ANALYSIS; M. Story, Finnigan MAT Corporation, 355 River Oaks Parkway, San Jose, CA 95134; B. Laser, K. Habfast, Finnigan MAT GmbH, Bremen, Germany

INTRODUCTION

The field of quantitative hydrocarbon mixture and type analysis by mass spectrometry requires a spectrometer with high precision and long term stability capabilities. Mass spectrometer design for the last 15 years has concentrated on high resolution, GC coupling, and isotope ratio measurements. It is only in the field of isotope ratio measurements that emphasis has been placed on long term reproducibility and accuracy.
A new spectrometer has been designed utilizing technology from isotope ratio mass spectrometry especially for use in hydrocarbon compound and type analysis. The instrument is a single focussing magnetic sector type, with a 23 cm radius and 26.5 entrance angle, stigmatic focussing in the z direction, a resolving power equivalent to a 46 cm radius system and very high ion transmission. The ion source is of special design for stable fragmentation patterns, high sensitivity and long term operation. Faraday cup detection with metastable suppression is utilized.
Software has been written for the INCOS Data System to do type and structure analysis as well as compound analysis from batch inlet samples.

HYDROCARBON TYPE AND STRUCTURE ANALYSIS BY MASS SPECTROMETRY

A set of weight vectors is determined [1] from a large group of pure compounds typically found in gasoline. These vectors are then utilized with pattern separation techniques to determine hydrocarbon types and structural features of the average molecule. Figure 1 is an output of such an analysis.

MIXTURE ANALYSIS BY MULTIPLE REGRESSION TECHNIQUES

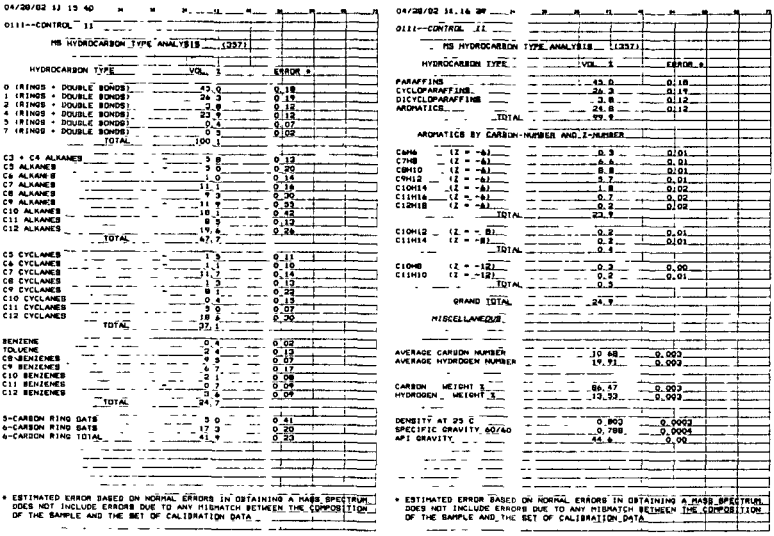
The program "MULT" is an INCOS program that separates a mass spectrum of a mixture by multiple regression techniques [2] [3] into a list of compounds and their concentrations. The program utilizes a library of 1000 compounds and narrows this to a subset of 100 compounds that most likely fit the unknown. Then all compounds in the library are added to the unknown one at a time. By a stepwise linear regression technique, if an improvement in the fit of the analysis is accomplished by adding the compound it is left in, if no improvement or a negative concentration is realized the entry is eliminated from the candidates.
An example of such an analysis is shown in Figure 2.

LABORATORY QUALITY CONTROL PROGRAMS

Software programs have been written to allow the analyst to follow the sensitivity, mass spectral fragmentation and analysis of standard mixtures as a function of time. See Figure 3.

SPECTROMETER PERFORMANCE

In order to perform reliable quantitative mixture analysis the spectrometer must meet certain requirements. The peaks should be flat topped for precise height measurement. The ion source must have a linear sensitivity response versus pressure and it must also exhibit long term fragmentation stability. Fragmentation stability is shown in Figure 4.



04/28/82 11 15 40

0111--CONTROL 11

MS HYDROCARBON TYPE ANALYSIS (337)

HYDROCARBON TYPE	VOL %	ERROR *
0 (RINGS + DOUBLE BONDS)	45.0	0.18
1 (RINGS + DOUBLE BONDS)	26.3	0.19
2 (RINGS + DOUBLE BONDS)	7.8	0.12
3 (RINGS + DOUBLE BONDS)	20.9	0.13
4 (RINGS + DOUBLE BONDS)	0.4	0.07
5 (RINGS + DOUBLE BONDS)	0.5	0.02
TOTAL	100.1	
C2 + C4 ALKANES	3.8	0.12
C3 ALKANES	3.0	0.20
C6 ALKANES	1.0	0.14
C7 ALKANES	11.1	0.19
C8 ALKANES	9.3	0.30
C9 ALKANES	11.9	0.32
C10 ALKANES	10.1	0.42
C11 ALKANES	8.9	0.13
C12 ALKANES	19.6	0.28
TOTAL	47.7	
C5 CYCLANES	1.3	0.11
C6 CYCLANES	1.1	0.10
C7 CYCLANES	11.7	0.14
C8 CYCLANES	1.3	0.13
C9 CYCLANES	0.1	0.22
C10 CYCLANES	0.4	0.13
C11 CYCLANES	3.0	0.07
C12 CYCLANES	18.6	0.30
TOTAL	37.1	
BENZENE	0.4	0.02
TOLUENE	2.4	0.13
C8 BENZENES	9.5	0.07
C9 BENZENES	6.7	0.17
C10 BENZENES	2.1	0.08
C11 BENZENES	0.7	0.06
C12 BENZENES	3.6	0.09
TOTAL	24.7	
5-CARBON RING DATS	5.0	0.41
6-CARBON RING DATS	17.3	0.20
4-CARBON RING TOTAL	41.9	0.23

* ESTIMATED ERROR BASED ON NORMAL ERRORS IN OBTAINING A MASS SPECTRUM DOES NOT INCLUDE ERRORS DUE TO ANY MISMATCH BETWEEN THE COMPOSITION OF THE SAMPLE AND THE SET OF CALIBRATION DATA

04/28/82 14.14 29

0111--CONTROL 11

MS HYDROCARBON TYPE ANALYSIS (337)

HYDROCARBON TYPE	VOL %	ERROR *
PARAFFINS	45.0	0.18
CYCLOPARAFFINS	29.3	0.19
DICYCLOPARAFFINS	3.8	0.12
AROMATICS	24.0	0.12
TOTAL	99.9	

AROMATICS BY CARBON-NUMBER AND Z-NUMBER

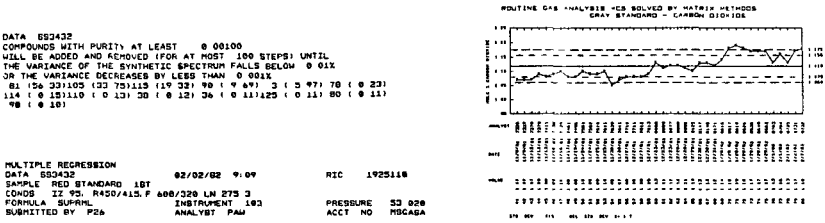
C6H6 (Z = -6)	0.3	0.01	
C7H8 (Z = -8)	6.8	0.01	
C8H10 (Z = -8)	8.8	0.01	
C9H12 (Z = -6)	5.7	0.01	
C10H14 (Z = -8)	1.8	0.02	
C11H16 (Z = -10)	0.7	0.02	
C12H18 (Z = -12)	0.2	0.02	
TOTAL	23.9		
C10H12 (Z = -10)	0.2	0.01	
C11H14 (Z = -12)	0.2	0.01	
TOTAL	0.4		
C10H8 (Z = -12)	0.3	0.00	
C11H10 (Z = -12)	0.2	0.01	
TOTAL	0.3		
GRAND TOTAL	24.7		

MISCELLANEOUS

AVERAGE CARBON NUMBER	10.68	0.003
AVERAGE HYDROGEN NUMBER	19.91	0.003
CARBON WEIGHT %	86.47	0.003
HYDROGEN WEIGHT %	13.53	0.003
DENSITY AT 25 C	0.800	0.0002
SPECIFIC GRAVITY 60/60	0.798	0.0004
API GRAVITY	44.6	0.00

* ESTIMATED ERROR BASED ON NORMAL ERRORS IN OBTAINING A MASS SPECTRUM DOES NOT INCLUDE ERRORS DUE TO ANY MISMATCH BETWEEN THE COMPOSITION OF THE SAMPLE AND THE SET OF CALIBRATION DATA

FIGURE 1



DATA SS3432
COMPOUNDS WITH PURITY AT LEAST 0 00100
WILL BE ADDED AND REMOVED (FOR AT MOST 100 STEPS) UNTIL
THE VARIANCE OF THE SYNTHETIC SPECTRUM FALLS BELOW 0 01%
OR THE VARIANCE DECREASES BY LESS THAN 0 001%
81 (56 33)105 (33 75)115 (19 32) 98 (9 69) 3 (5 97) 78 (0 23)
114 (0 15)110 (0 13) 30 (0 12) 36 (0 11)125 (0 11) 80 (0 11)
78 (0 10)

MULTIPLE REGRESSION
DATA SS3432 02/02/82 9:09 RIC 1925118
SAMPLE RED STANDARD 1BT
CONDS IZ 90: R450/415.F 600/320 LN 275 3
FORMULA SUPRHL INSTRUMENT 103 PRESSURE 53 020
SUBMITTED BY P2a ANALYST PAW ACCT NO MSCASA

SEARCH TOL 0 0010 F-FAC (IN) 4 00 F-FAC (OUT) 2 00
TARGET ERROR 0 01% DIMIN RETURNS 0 001%
VARIANCE ACHIEVED= 0 10%

COMPOUNDS	PARTIAL PRESSURES	ERRORS
3 1,3 BUTADIENE	2.53	0 3%
36 ARGON	0 01	0 3%
78 ETHANE	3 27	0 7%
80 ETHYL CHLORIDE	0 02	0 6%
81 ETHYLENE	17 19	0 8%
98 HYDROGEN	6 94	0 4%
98 METHYL CHLORIDE	0 01	0 3%
105 METHANE	15 29	0 4%
110 OXYGEN	0 03	0 5%
111 PENTANE	0 01	0 2%
14 PROPANE	0 04	0 5%
.15 PROPYLENE	6 67	0 4%
125 WATER	0 02	0 3%
TOTAL	52 84	

FIGURE 2

FIGURE 3

DAY	MASSES / INTENSITY RATIO				
	58 / 15	43 / 58	43 / 26	43 / 15	43 / 29
1	4.477	8.221	20.10	36.80	2.530
2	4.482	8.220	20.10	36.80	2.529
3	4.486	8.215	20.10	36.81	2.529
4	4.480	8.206	20.09	36.75	2.530
5	4.481	8.205	20.09	36.80	2.530
6	4.480	8.199	20.07	36.74	2.530
8	4.479	8.197	20.08	36.72	2.535
10	4.480	8.167	19.95	36.60	2.535
12	4.472	8.166	19.92	36.55	2.535
14	4.462	8.159	19.85	36.42	2.535
MEAN	4.478	8.1955	20.036	36.699	2.532
SD	0.0060	0.023	0.093	0.1328	0.0027
RSD	0.0014	0.0028	0.0046	0.0036	0.0011

FIGURE 4

1) D.D. Tunnicliff and P.A. Wadsworth, Anal. Chem., 45, 12 (1973)
2) D.D. Tunnicliff and P.A. Wadsworth, Anal. Chem., 37, 1082 (1965)
3) M.W. Weiss and S. Sokolow, 28th Annual Conference ASMS., New York City, N.Y., (1980)

MOLECULAR BEAM MASS SPECTROMETRIC STUDY OF THE COMBUSTION OF SINGLE COAL PARTICLES *

Frank T. Greene and J. Eugene O'Donnell
MIDWEST RESEARCH INSTITUTE
Kansas City, Missouri 64112

Molecular beam mass spectrometry is being used to study the pyrolysis and combustion of single coal particles. A selected coal particle was contained in a selected atmosphere and heated by CW CO_2 radiation having a peak flux of 1000 W/cm^2. Complete spectra for m/e from 10 to 100 amu, integrated over the irradiation times, were obtained using a time-averaging phase sensitive detection technique. Irradiations were carried out in both air and inert gases at atmospheric pressure. Major species observed included C_1, C_2, C_3 and aromatic hydrocarbons as well as combustion products. The time dependent behavior of selected pairs of major species was followed simultaneously using a dual mass spectrometer molecular beam sampling system. Apparent anomalies indicate that mass transport and/or gas dynamic effects may be important.

* Work supported by U.S. Department of Energy, Pittsburgh Energy Technology Center under Contract No. DE-AC22-81 PC40274.

RESULTS WITH AN AUTOMATED MULTI-SAMPLE INTRODUCTION SYSTEM FOR EI/CI, DCI, AND FAB IONIZATION

C. Brunnée, H. Kaufmann, H. Michelsen, R. Pesch, U. Rapp,
Finnigan MAT GmbH, Bremen, Germany

A microprocessor-controlled direct insertion probe has been designed and tested (Fig. 1). With this device up to 46 crucibles, DCI filaments or FAB sample holders can be stored in a turret magazine and introduced sequentially into the source of the mass spectrometer (Fig. 2). The analysis procedure: background control - sample introduction - heating of the sample (EI/CI, DCI)- recording of the spectra - sample sequencing - is fully automated for unattended (overnight) operation.

Because of low heat capacity and effective direct water cooling the crucibles for EI/CI ionization have a temperature response of only a few seconds (Fig. 3). The evaporation is either controlled by temperature programming or by maintaining a constant total ion current (TIC). The TIC together with the thermogram recording provides a fast overview about the sample characteristics as well as the quality of the sample preparation. The TIC control also allows the application of fractional distillation for mixture analyses. Untreated analgesic pills (Fig. 4) and other drugs (Fig. 5) have been analyzed by this technique. Overlapping spectra have been separated by the computer program ACLEAN and the obtained spectra have been compared with library spectra.

TIC-controlled pyrolysis of technical or natural polymers has been conducted with this system. The analysis provided extensive information on sample structure and on low boiling fractions like stabilizers and plasticizers.

Automated analyses of thermally labile compounds have been performed using DCI probe tips. These tips can be inserted into the magazine instead of the normal EI/CI crucibles.

The magazine also accepts FAB sample holders. Fig. 6 shows a typical result. The system can be used for the analysis of fractions collected from a high pressure liquid chromatograph.

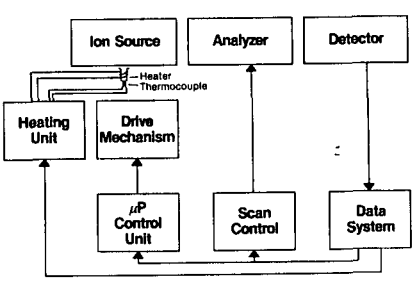


Fig. 1 Block Diagram

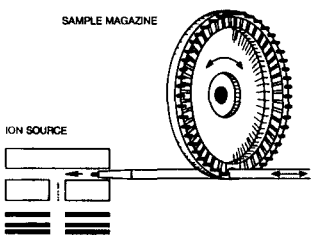


Fig. 2 Schematics

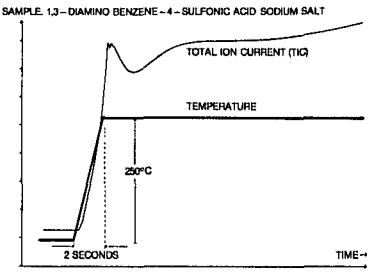


Fig. 3 Rapid temperature-controlled heating of crucible (EI)

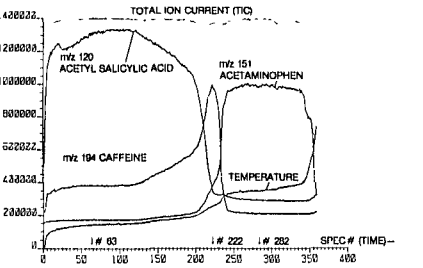
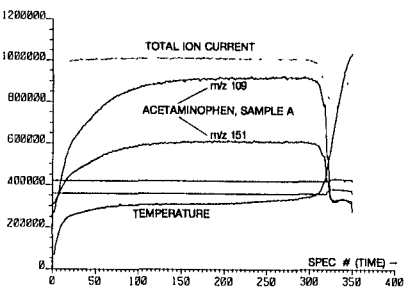


Fig. 4 Analysis of an untreated analgesic pill by TIC-controlled fractionation



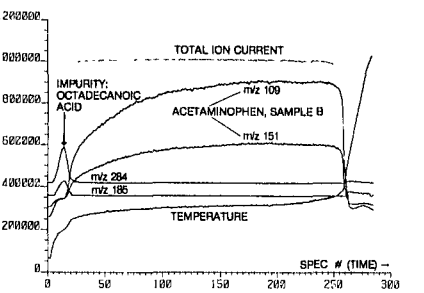


Fig. 5 Analysis of two Tylenol tablets (aspirin type drug), sample B containing impurity octadecanoic acid

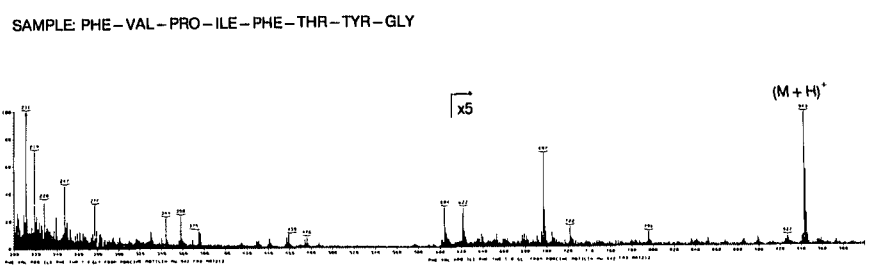


Fig. 6 Typical FAB spectrum of peptide

QUALITY CONTROL OF GLASS AND HERMETICALLY SEALED SEMICONDUCTOR PACKAGES

Koprio J. A., Balzers AG, Principality of Liechtenstein
Roselius H., Balzers, Hudson N.H., U.S.A.

THE PROBLEM

The analysis of small amounts of sealed gases is an analytical task which is encountered more and more frequently in industrial laboratories for quality control and trouble shooting purposes. Some examples occur in the glass manufacturing industry to trace the origin of undesired gas inclusions in glass and more recently in the quality control of hermetically sealed integrated circuit packages. Other applications of small gas volume analysis include leak detection and integrity tests of filling gas of electrical components and other sealed volumes.
In these various applications the emphasis is placed on different aspects, however there are some common requirements to all of them:

- o sample conditioning and preparation under high-vacuum or UHV conditions (removal of adsorbed gases and especially H_2O from the surface of a package).
- o high sensitivity of the gas detector.
- o fast response time of detector and sampling system.
- o low detection limits.
- o fail-proof handling and efficient through-put of samples.
- o fast data aquisition.
- o acceptable turn around time for result evaluation.

A SOLUTION

General Description

A sample, representative of a batch or a series of products is mechanically opened with a piercing device inside a heated vacuum system. The expanding gases are being analyzed with a quadrupole mass spectrometer while pumping them directly through the ion source of the analyzer. The quadrupole power supply is linked to a computer which controls the fast data aquisition and evaluation. In order to achieve a good time resolution in the analysis of the piercing and pump down process a computer controlled peak jumping method has been adapted.
This dynamic sampling method, which is in contrast to the more common batch inlet, has the advantage of a shorter residence time of the gas inside a heated expansion volume, thus reducing the possibilities of surface catalyzed reactions which can impede the detection of surface sensitive compounds (e.g. H_2O, O_2, SO_2 etc.)
The system is also equipped with a calibration and conditioning option, which allows the expansion of a defined quantity of gas into the sampling recipient, thus enabling the user to calibrate the system with a gas of known composition under the same experimental condition (temperature, surface area) as present during the analysis.

THE HARDWARE

As a gas detector, a quadrupole mass spectrometer is used (BALZERS QMG 511) which has the intrinsic virtues of fast response time and high sensitivity. Those properties can only be taken advantage of to their full extent when combined with an ion source which is optimized for the same characteristics.

A BALZERS gas-tight axial ion source incorporates these properties and has the additional advantages of high dynamic range (linearity of ion current vs. pressure) as well as a filament situated in a zone of high pumping speed (at lower pressure than found in the ionizing area thus reducing the possibilities of sample pyrolysis and prolonging the standing time of the filament). The quadrupole is housed in a recipient pumped by a turbomolecular pump TPU 330 roughing pump combination and is kept at a typical pressure of 10^{-9} mbar. The transfer line between the analyzer recipient and the sample preparation recipient is kept as short as possible in order to reduce the possibilities of surface adsorption. The sampling recipient itself contains two valves: one for pumping of the recipient (by a turbomolecular pump e.g. TPU 040) and the other one leading over the transfer line to the quadrupole mass spectrometer. The piercing device consists of a mechanically actuated and bellows sealed metal pin which is driven into the sample. The loading part is equipped, optionally, with a calibration system which allows the expansion of a minute quantity of calibration gas into the piercing recipient. An automatic data aquisition for calibration purposes is possible by using pneumatically driven valves which are actuated by the process interface QPI 512. This unit is connected through the I/O print to the quadrupole data bus which in turn is linked through the buffer and linetransceiver to the DEC - PDP 11 series computer.

THE SOFTWARE

The application software is running under the DEC RT-11 operating system and is based on the "QMG-Basic" and the "Multiple Ion Monitoring" Software Packages (BALZERS Software).
The application program loads the parameters such as selected masses, sensitivities dwell time per amu etc. into the master program. Under these preselected conditions the background spectrum is measured and upon an externally applied START command the measurement is started. (Piercing of the sample).

The data are stored in the memory and after completion of the measurement the background is subtracted. In a special subroutine the break time is determined. Now a table of ion currents vs. time can optionally be printed out. In the data evaluation routine the time dependence of the various ion currents can be plotted out and the cursors set for the extrapolation routine which a) extrapolates the ion current back to break time t= 0 or b) extrapolates the data forward to the point in time where the level of the ion current drops back below the level of twice the background signal. The time integrated signal summed over the measured values plus the extrapolated values is used in this method for the quantitation of the signals. With the method described above it is possible to analyzer samples down to $,5 \cdot 10^{-9}$ l volume (STP). For the larger samples such as I.C. packages the detection limit for the gases of interest are below $5 \cdot 10^{-5}$.

ANALYSIS OF AEROSOL PARTICLES BY MASS SPECTROMETRY

M. P. Sinha, D. A. Chatfield*,
Jet Propulsion Laboratory, California Institute of Technology, Pasadena, Ca. 91109
R. M. Platz, V. L. Vilker, S. K. Friedlander
University of California, Los Angeles, Ca. 90024

A method for the chemical analysis of single aerosol particles in the inhalable size range, on a continuous real time basis is being developed in our laboratory. It uses the technique of mass spectrometry. A beam of aerosol particles is generated for the introduction of the aerosol sample into the ion-source region of the mass spectrometer where it is volatilized and ionized for its subsequent mass separation and detection. In our earlier work[1], the particles were thermally volatilized after their impaction on a hot rhenium filament. The ensuing vapor was then ionized by the conventional method of electron bombardment. The method was found to be useful for the analysis of individual particles of organic as well as inorganic nature. It, however, suffers from complexities stemming from the mass fragmentation of the parent molecules. In order to alleviate this problem, a somewhat softer method of ionization is presently being investigated. It uses a high energy Nd-YAG laser. This paper describes some of the preliminary results of laser ionization-mass spectrometry of aerosol particles.

The details of the experimental arrangement have been described elsewhere.[2] A beam of particles is generated by a free jet expansion of aerosol through a capillary and skimmer system. The beam is led into the modified ion-optics region of a quadrupole mass spectrometer (UTI-100C) where it is zapped by a Nd-YAG laser pulse for its volatilization and ionization. The laser set-up is shown schematically in Figure 1. He-Ne laers are used for the synchronization of the particle with YAG laser pulse. For the efficient synchronization, one needs to sense the arrival of the particle upstream of the ion source of the mass spectrometer and to know its velocity. Velocity distributions of the different size aerosol particles were determined using the technique of laser light scattering. Beams of monodisperse particles were produced from a vibrating orifice aerosol generator. Two CW He-Ne lasers I, II, were located at a known distance of separation at right angles to the particle beam. The laser light pulses scattered by a particle passing through the lasers I and II were monitored by the photomultipliers I and II, respectively. The particle time-of-flight between the two laser beams was measured by counting the pulses from a 4 MHz-clock. The count was initiated by the start pulse from the PMT I and stopped by the pulse from PMT II. The digital count was then converted to an analog voltage and the velocity distribution determined by measuring the pulse height distribution. Figure 2 shows the plot of velocity vs. diameter for different size aerosol particles. The error bars indicate one standard deviation (less than 5% of the most probable velocity.) The narrow distribution facilitates the synchronization of the particle and the YAG laser pulse in the source region of the mass spectrometer.

The YAG laser provides ~1 Joule of energy per pulse at a repetition rate of less than 20 per second, the pulse width being about 120 μsec. In this free running mode of the laser, the synchronization of the focused laser pulse with the particle was relatively easier. The scattered pulse from the sensing He-Ne laser I provided the trigger signal for the high energy YAG laser. A suitable delay was introduced in the trigger line to account for the flight time of the particles between laser I and the YAG location. The spread in the velocity of the aerosol particles did not introduce any complication because of the rather large YAG laser pulse width (~120 μsec). Figure 3 shows the mass spectrometer signal for K+ resulting from a 1.8 μm diameter potassium biphthalate particle when it is hit by a YAG laser pulse. The upper trace shows the trigger signal from PMT I, followed by the YAG laser pulse as seen by this PMT. The lower trace is the signal from the quadrupole mass spectrometer manually set at 39 amu. Manual operation of the mass spectrometer is necessary because of the extremely fast generation of the ions by the laser pulse. No signal from the organic counterpart of the salt could be detected. The mean power density of the laser pulse was about $\sim 10^5$ W cm^{-2}. This power density is believed to be low for the ionization of organic molecules.

---

*Permanent Address: State University of California, San Diego, Ca. 92182

We report here on our first observation of the ions from the individual aerosol particles in a beam produced by laser ionization. The power densities of the laser pulse need to be increased for the general application of this method. This can be accomplished by Q-switching the Nd-YAG laser. This, however, makes the synchronization of the laser pulse with the particle very crucial. Work with the Q-switched laser pulses have been initiated. For the complete mass analysis of a single particle, the quadrupole mass spectrometer will be replaced by a focal plane mass spectrometer with an electro-optical ion detector.[3]

ACKNOWLEDGMENT:

The authors appreciate the continued advice, support, and encouragement of Charles Giffin and David Norris in this project. Financial support for this work was partially provided by the Army Research Office, Research Triangle Park, N.C. and in part by the National Science Foundation.

REFERENCE:

1. M. P. Sinha, C. E. Giffin, D. D. Norris, and S. K. Friedlander, 28th Annual Conf. on Mass Spectrometry and Allied Topics, N.Y., N.Y., May 25-30, 1980, p. 204.
2. M. P. Sinha, C. E. Giffin, D. D. Norris, T. J. Estes, V. L. Vilker, and S. K. Friedlander, J. Colloid Interface Sci. 87, 140 (1982).
3. C. E. Giffin. R. Britten, H. Boettger, J. Conley, and D. Norris, 27th Annual Conf. on Mass Spectrometry and Allied Topics, Seattle, Wa. June 3-8, 1979, p. 214.

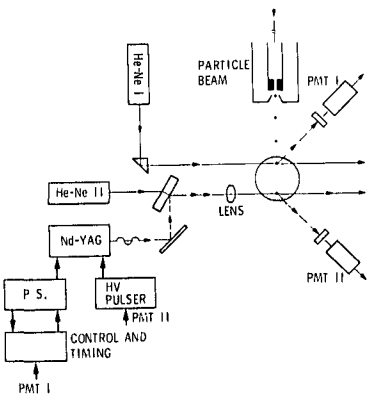


Fig. 1 Schematic of Laser Set-up

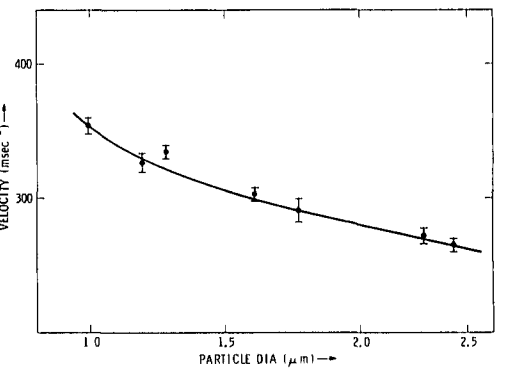


Fig. 2 Velocity versus Particle Diameter

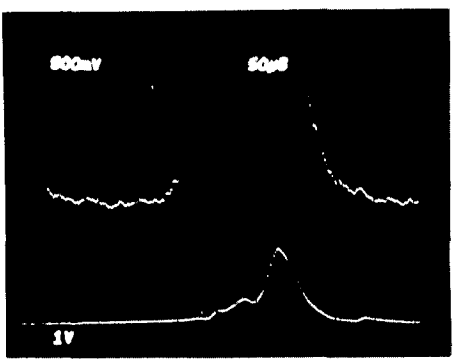


Fig. 3^+ ion Signal from Laser Ionization of Potassium Biphthalate Particle.

CALIBRATION OF A MASS SPECTROMETER FOR DYNAMIC ANALYSIS OF ULTRAMICRO GAS SAMPLES

W. M. Graven and D. E. Gilmartin
The Aerospace Corporation, El Segundo, CA 90245

To analyze for small amounts of residual gases in electronic devices, principally traveling wave tubes, a computerized quadrupole mass spectrometer custom-built by Finnigan Corp. was used. A dynamic method of analysis was developed, since the residual gases had to be transported from the devices that were analyzed to the closed ion-source chamber of the mass spectrometer. With a vacuum system pressure of 10^{-11} Torr, gas transport from device to RGA and quantitative analysis were feasible for amounts of gas as small as 10^{-10} atm-cm^3, corresponding to a pressure of approximately 10^{-9} Torr in the devices. With inert gases, calibration analyses were successfully conducted for much smaller amounts, as illustrated for a 7×10^{-12} atm-cm^3 sample of helium (1). The mass spectrometer was calibrated with seven gases that were found in the devices. Calibrations were made with the same dynamic method that was used for the residual gas analyses. Calibrated gas leaks with leak rates stated to be accurate within ± 10% were the standards to which all measurements of amounts of gas were related. Calibration of the mass spectrometer consisted of accumulating gas from a calibrated leak in a large known volume for a measured time interval, and then introducing a small measured aliquot to the mass spectrometer in the same way that the residual gas sample was introduced for analysis. The instrumental response had a pulse shape similar to that observed if the effluent of a gas chromatograph were introduced for analysis. This is illustrated for a relatively large sample of helium by the digital RGA data and the recorded analog output of the ionization gauge (2). With a spectral scan rate of two scans sec^{-1}, much smaller gas samples could be quantified by the RGA before the gas pulse passed out of the source chamber. Reproducibility of the RGA measurements within a standard deviation of less than 10% of the average value was demonstrated for four gases by analyses of amounts of gas as small as 2×10^{-10} atm-cm^3.

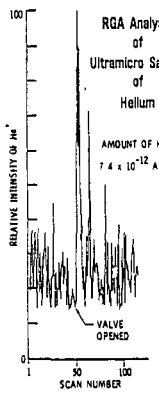
For five gases, the integrated response of the RGA was linear with sample size over a four-decade range. The lower limits of the linearity range were established by the minimum size of the samples that could be accumulated, rather than by the detection limits of the RGA. Multiple calibrated leaks with leak rates that spanned three decades gave consistent results as illustrated for helium (3) and for methane (4). Gases such as carbon monoxide, carbon dioxide and, particularly, oxygen showed evidence of interaction with the walls; the shape of the calibration curve depended on the size of the expansion volume, as illustrated by the results for CO (4). However, linear RGA relations were obtained for amounts of these gases greater than 10^{-8} atm-cm^3, if the smaller expansion volume was used.

The nude ionization gauge located adjacent to the closed ion source also functioned as a sensitive detector of the total amount of gas introduced. Linear relations were found between the amount of gas and the area of the pulse record from the ion gauge, as illustrated for Ar, N_2 and He (5); the slopes of the curves by least squares were 0.98, 1.02 and 0.94, respectively. The linearity extended to the smallest samples that could be detected, namely 5×10^{-10} atm-cm^3.

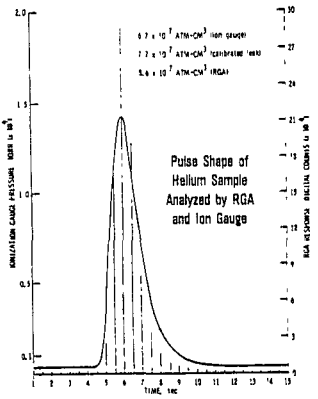
The validity of the dynamic method of analysis was established by demonstrating for each gas that the same response was observed for pulsed and for continuous sample introductions. Responses of both the RGA and the ionization gauge are compared in the table using analyses of accumulated samples and analyses of the effluent of the calibrated leaks for eight gases (6). The least squares slopes of the RGA calibration curves are also tabulated. Except for H_2, CO and O_2, which interact with the heated source filament, the ion gauge results are in approximate agreement with published relative values from measurements at much higher pressures.

Residual gas analyses were conducted for 25 devices. The total amounts of gas found ranged from more than 10^{-5} to less than 10^{-9} atm-cm^3. The devices can be grouped according to the composition of the principal residual gases: 1) argon, 2) methane and/or hydrogen, 3) helium and/or methane. The results of the analysis of a 10-W traveling wave tube have been selected to show the pulse shape produced by transporting the residual gas from the TWT to the RGA (7, 8). Only a slight tailing distinguishes the pulse shapes from those observed in the calibration measurements. From the ratios of the integrated pulses for individual ion intensities to the total ion intensity, the gas composition was determined as 79% CH_4, 3% H_2, 8% Ar and 9% N_2 or CO, or a combination of both. The total gas amounted to 2.7×10^{-6} atm-cm^3.

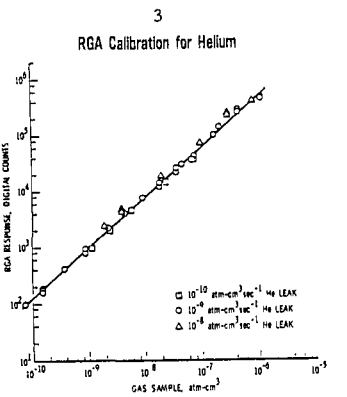
1



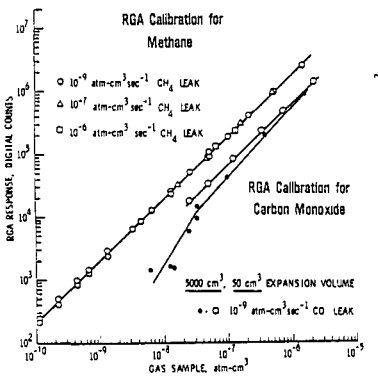
2



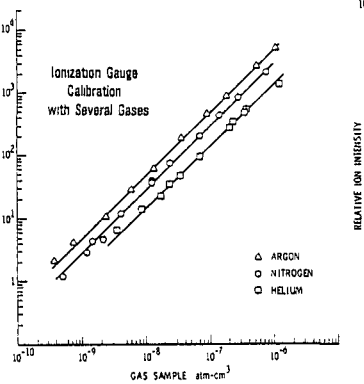
3



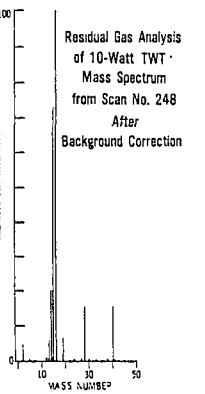
4



5



7

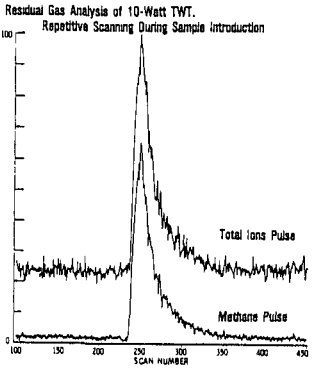


6

RGA AND IONIZATION GAUGE RESPONSES FOR EIGHT GASES USING PULSED AND CONTINUOUS SAMPLE INTRODUCTION

	Accumulated Samples/atm-cm^3			Effluent of Calibrated Leaks/atm-cm^{3}sec^{-1}	
Gas	Empirical Proportionality Exponent	RGA Digital Counts (x 10^{-10})	Ion Gauge Pulse Area, cm^2 (x 3 x 10^{-10})	RGA Digital Counts (x 10^{-10})	Ion Gauge Torr (x 10^2)
Helium	0.904	49	0.46	48	0.45
Argon	0.989	80	1.49	78	1.49
Nitrogen	0.998	111	0.98	113	1.03
Hydrogen	0.984	55	0.14	57	0.13
Methane	0.982	211	1.31	209	1.27
Carbon Monoxide	0.964	68	0.43	60	0.47
Carbon Dioxide	0.982	93	0.86	101	1.10
Oxygen	-	37	0.35	41	0.40

8



ANALYSIS OF AEROSPACE ADHESIVES AND PREPREG COMPOSITE FABRICS

J.G. Moncur,A.B. Campa,P.C. Pinoli, Lockheed Missiles & Space Co., Palo Alto, CA 94304

INTRODUCTION

The development of nonmetal composite materials in the aerospace industry has allowed production of lightweight yet strong multicomponent structures for spacecraft and missiles. In previous work (1), gas chromatography/mass spectrometry has been shown to be useful in trouble shooting manufacturing problems which arise during bonding of multicomponent structures. The examples given in this previous work indicated that bond integrity is often related to the organic adhesives which join dissimilar parts. In addition, the characteristics of functionally bound oxygen on the surface of carbon fiber has been qualitatively and quantitatively assessed by thermal analysis mass spectrometry (2). Functionally bound oxygen on the surface of carbon fibers has been shown to improve polymeric matrix interactions resulting in higher composite interlaminar shear strength.

In the present work, several examples of adhesive analysis will be discussed which demonstrate the use of mass spectrometry in workplace safety studies. Specifically, thermal analysis mass spectrometry (TA/MS) of a divinyl benzene/carbon composite prepreg will be shown to accurately profile volatile content (by plotting molecular ion versus processing temperature) when corroborated with dynamic headspace gas chromatography mass spectrometry (DH/GC/MS). Another example is the DH/GC/MS and pyrolytic (P/GC/MS) analysis of volatiles derived from heating an epoxy resin which is composed of tetraglycidyl methylene dianiline and diamino diphenyl sulfone (TMD/DDS).

EXPERIMENTAL

An instrumentation schematic for DH/GC/MS and P/GC/MS experiments is shown in Figure 1 and has been previously described (1). TA/MS is performed using apparatus similar to that of Chiu, et al (3) for TGA/MS by attaching a high temperature programmable oven which heats a quartz sample tube to a Finnigan Model 4021 GC/MS. All of these techniques rely upon helium to sweep thermally produced volatiles into the GC or MS. In TA/MS the volatiles are swept into the MS via a heated stainless steel transfer line and glass jet separator.

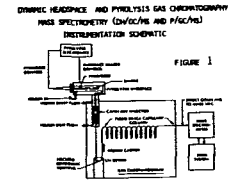
RESULTS AND DISCUSSION

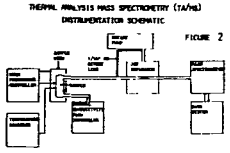
The data presented herein were generated during routine surveys of common aerospace materials for potentially toxic substances. A divinyl benzene/carbon composite prepreg fabric was analyzed for volatiles using the DH/GC/MS technique. This headspace analysis is begun by collecting the volatiles evolved from the fabric in a cryogenically cooled portion of a Carbowax 20M fused silica capillary column during sample heating at 200°C (392°F) for 15 minutes. The high resolution separation of volatiles is shown in Figure 3 as a reconstructed ion chromatogram with molecular ions displayed in the upper portion of the figure. The fabric was found to contain: acetone, methyl ethyl ketone, diethyl benzenes (2 isomers), dimethyl formamide, ethyl vinyl benzenes (2 isomers), acetic acid, divinyl benzenes (2 isomers), cis-1-ethylideneoctahydro-7a-methyl-1H-Indene, naphthalene, and 2,6-ditertbutyl-4-methyl phenol. TA/MS was performed on this material to profile volatile offgassing as a function of processing temperature. Figure 4 plots the intensity of each molecular ion versus processing temperature in °F. It is interesting to note that the nonpolar compounds desorb at low temperatures whereas the polar compounds desorb at higher temperatures. In this case, the affinity of carbon for polar compounds may suggest the presence of polar and/or hydrogen bonding functionalities on the surface of the carbon (2). (Adsorbed water was not studied in this case, only m/z 33-533.)

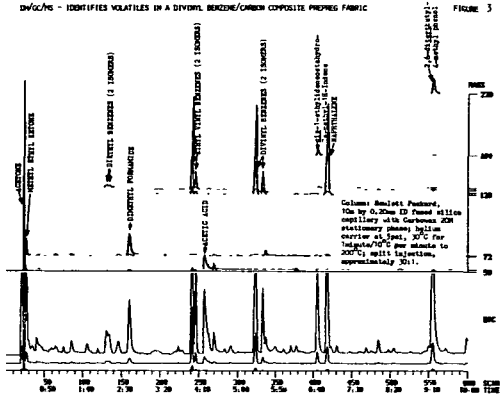
Another workplace safety study surveyed the TMD/DDS epoxy by DH/GC/MS and P/GC/MS. Figure 5 presents the DH/GC/MS chromatogram of TMD/DDS volatiles released upon heating the epoxy at 200°C for 15 minutes. Notably, oxirane (ethylene oxide), acrolein, and epichlorohydrin are seen in this analysis. These compounds are likely liberated during the heat curing of this epoxy which suggests that the vapors generated should be adequately vented. The P/GC/MS analysis of this epoxy suggests caution against its overheating since a very complex mixture of aromatic nitrogen containing compounds is produced upon heating of this epoxy at 480°C for 20 seconds (Figure 6). This analysis used an SE54 fused silica capillary column.

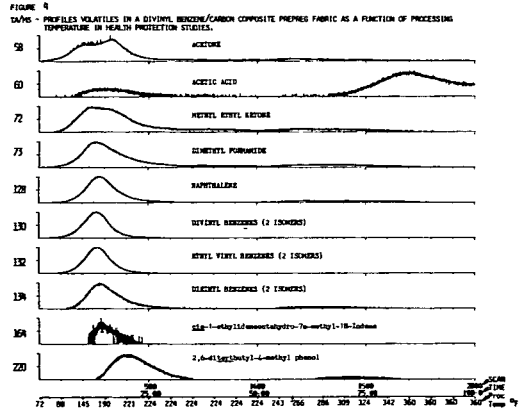
REFERENCES

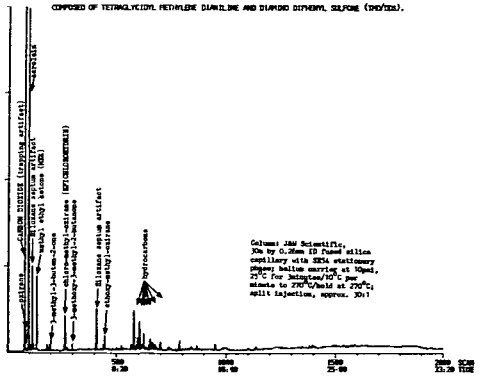
1. J.G. Moncur, T.E. Sharp, E.R. Byrd, HRC&CC, 4 (1981) 603-611.
2. P.C. Pinoli, J.G.Moncur, D.G. McKinstry, "Kinetics of Oxygen Desorption on Pitch Fiber", 15th Biennienl Conference on Carbon, June 1981, Philadelphia, Penn.
3. J. Chiu, A.J. Beattie, Thermochimica Acta, 40 (1980) 251-259.

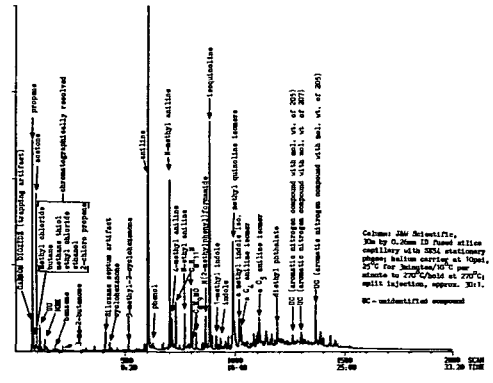

DYNAMIC HEADSPACE AND PYROLYSIS GAS CHROMATOGRAPHY
MASS SPECTROMETRY (Dv/GC/MS AND P/GC/MS)
INSTRUMENTATION SCHEMATIC
FIGURE 1


THERMAL ANALYSIS MASS SPECTROMETRY (TA/MS)
INSTRUMENTATION SCHEMATIC
FIGURE 2


Dv/GC/MS - IDENTIFIES VOLATILES IN A DIVINYL BENZENE/CARBON COMPOSITE PREPREG FABRIC
FIGURE 3
ACETONE
METHYL ETHYL KETONE
DIVINYL BENZENES (2 ISOMERS)
DIMETHYL FORMAMIDE
ACETIC ACID
METHYL VINYL BENZENES (2 ISOMERS)
DIVINYL BENZENES (2 ISOMERS)
sig-1-ethylidenoctahydro-7a-methyl-1H-Indene
NAPHTHALENE
2,6-di-tert-butyl-4-methyl phenol
Column: Restek Fastnet, 10m by 0.2mm ID fused silica capillary with Carbowax 20M stationary phase; helium carrier at 3psi, 30°C for 1minute/10°C per minute to 200°C; split injection, approximately 30:1.
MASS
TIC
72
50
SCAN
TIME


FIGURE 4
TA/MS - PROFILES VOLATILES IN A DIVINYL BENZENE/CARBON COMPOSITE PREPREG FABRIC AS A FUNCTION OF PROCESSING TEMPERATURE IN HEALTH PROTECTION STUDIES.
58
ACETONE
60
ACETIC ACID
72
METHYL ETHYL KETONE
73
DIMETHYL FORMAMIDE
128
NAPHTHALENE
130
DIVINYL BENZENES (2 ISOMERS)
132
METHYL VINYL BENZENES (2 ISOMERS)
134
DIETHYL BENZENES (2 ISOMERS)
168
sig-1-ethylidenoctahydro-7a-methyl-1H-Indene
220
2,6-di-tert-butyl-4-methyl phenol
SCAN
TIME
TOC
Temp °F


FIGURE 5
Dv/GC/MS - SURVEYS AEROSPACE ADHESIVES FOR POTENTIALLY TOXIC COMPOUNDS IN THIS ANALYSIS OF AN EPOXY RESIN COMPOSED OF TETRAGLYCIDYL METHYLENE DIANILINE AND DIAMINO DIPHENYL SULFONE (TMD/IDS).
CARBON DIOXIDE (trapping artifact)
styrene
acetone
chloroform
Methyl chloride
methane thiol
Methanol
ethanol
1-chloro propene
Nitrous oxide artifact
2-methyl-2-butene-3-one
dichloromethyl-nitrane
2-methyl-2-methoxy-1-methene
Nitrous oxide artifact
ethoxy-methyl-nitrane
hydrocarbons
Column: J&W Scientific, 30m by 0.25mm ID fused silica capillary with DB54 stationary phase; helium carrying at 10psi, 70°C for 3minutes/10°C per minute to 270°C/hold at 270°C; split injection, approx. 30:1
SCAN
TIME


FIGURE 6
P/GC/MS - SIMULATES AEROSPACE ADHESIVE THERMAL DECOMPOSITION BY PYROLYSIS OF THE TMD/IDS EPOXY.
CARBON DIOXIDE (trapping artifact)
Methyl chloride
methane thiol
Methanol
ethanol
1-chloro propene
acetone
chromatographically resolved
propene
Nitrous oxide artifact
cyclohexanone
2-methyl-2-propionamine
aniline
4-methyl aniline
2-ethyl aniline
2,6-dimethyl aniline
isoquinoline
methyl isoquinoline isomers
methyl indole
methyl indole isomer
2,6-dimethyl quinoline isomers
2,5 dimethyl aniline isomer
diethyl pyridazole
phenol
DMC (aromatic nitrogen compound with mol. wt. of 205)
DMC (aromatic nitrogen compound with mol. wt. of 205)
DMC (aromatic nitrogen compound with mol. wt. of 205)
Column: J&W Scientific, 30m by 0.25mm ID fused silica capillary with DB54 stationary phase; helium carrying at 10psi, 70°C for 3minutes/10°C per minute to 270°C/hold at 270°C; split injection, approx. 30:1.
DMC - unidentified compound
SCAN
TIME

THE APPLICATION OF METASTABLE MAPPING TO THE ANALYSIS OF NATURAL SUBSTANCES

Warburton G.A., Hazelby D., Taylor K.T., Stradling R.S.
Kratos Analytical Instruments, Barton Dock Road, Urmston,
Manchester M31 2LD, England

Metastable Mapping is a technique which records the intensity of ions formed by unimolecular or collision-induced decompositions in a double-focussing mass spectrometer as a function of the electric and magnetic field strengths, E and B respectively. This work reports results obtained from a suite of computer programs that have been developed to acquire and process these data.

The results were obtained on a Kratos MS25 double-focussing mass spectrometer controlled by a DS55 data system. The apparent mass positions and intensities of peaks bounded by the B and E planes are recorded by repetitively scanning the magnet and changing the voltage applied to the electrostatic sector by a constant value between each magnet scan. The data generated consist of an array of masses and corresponding intensities and a value of E for each scan, stored in conventional DS55 mass data files. A number of simulated metastable scans, such as B/E, B^2/E, constant neutral loss and IKES (ion kinetic energy spectrum) are extracted easily from these data sets. Modern mass spectrometer scan speed and high dynamic range capabilities of modern data systems allow this acquisition to be performed at high speed. The example shown in Figure 1 is a unimolecular metastable map for positive ions in pentadecane. Curves at constant B/E through m/z 212 in the normal mass spectrum and at constant B^2/E through m/z 99 are presented. The constant neutral loss curve for peaks formed by the loss of 56u is also presented.

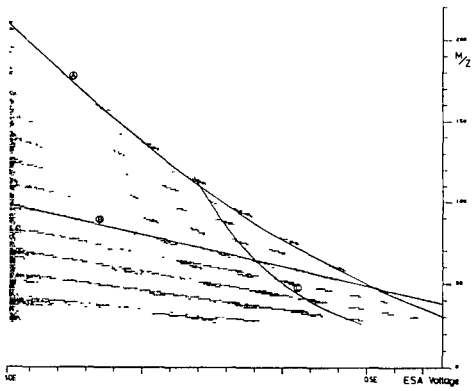


Figure (1) MS25 DS55 METASTABLE MAP FOR POSITIVE IONS IN n-PENTADECANE
Ⓐ is a curve at constant B/E through m/z 212
Ⓑ is a curve at constant B/E through m/z 99
Ⓒ is a curve for constant neutral loss of 56u

Direct mixture analysis of complex mixtures is now becoming an accepted technique although in these cases, electron impact spectra can be extremely complicated. Chemical ionization can greatly simplify these spectra and has a further advantage in that the major ions produced are usually characteristic of the molecular weight of the sample molecules. However, because of the lower internal energy of ions formed in the chemical ionization process little or no unimolecular decomposition occurs. Collision gas is therefore required to induce decomposition allowing the structural information to be obtained.

Figure 2 shows a collision-induced metastable map for positive ions in the CI spectrum of hydroxy-tyranine. The map is much more simple than that produced by electron impact and the fragmentations occurring from the $(M + H)^+$ can be seen clearly.

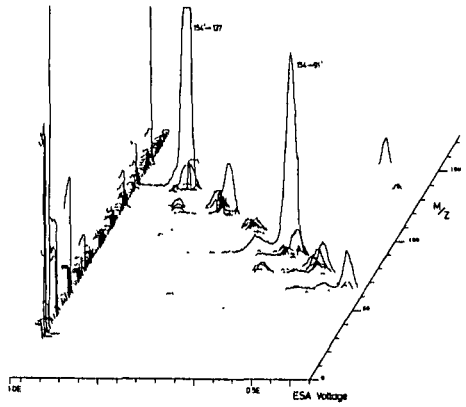


Figure (2) MS25 D555 COLLISION-INDUCED METASTABLE MAP FOR IONS IN THE AMMONIA CI SPECTRUM OF HYDROXY-TYRAMINE (DOPAMINE)

Metastable mapping acquires data from all transistions occurring in the first field free region as a result of this, unexpected processes can be observed in some cases. In the collision-induced map shown in Figure 2, a transition can be seen at approximately 50% of the original E value, yet at a relatively high B value. Further investigation reveals this to be the transistion $(2M + H)^+ - (M + H)^+$, even though the dimeric species is not observed in the normal CI mass spectrum. Figure 3 shows a spectrum obtained at constant B^2/E through $m/z = 154^+$, the $(M + H)^+$ ion in the normal mass spectrum. The existence of both $(M + NH_4)^+$ and $(2M + H)^+$ ions is indicated.

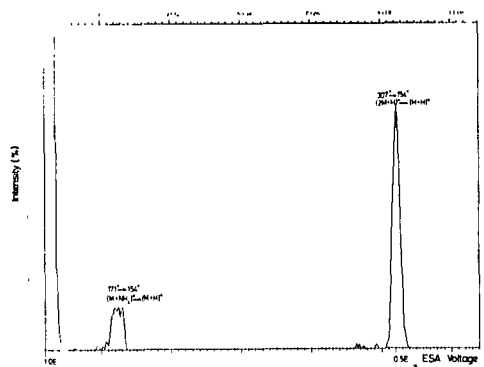


Figure (3) MS25 D555 RECONSTRUCTED SPECTRUM FOR THE COLLISION-INDUCED B^2/E SCAN FROM M/Z=154 IN THE AMMONIA CI SPECTRUM OF HYDROXY-TYRAMINE

CHARACTERIZATION OF HEADSPACE VAPORS OF ABUSED ALKYL NITRITES

C.C. Alley, J.S. Holler, and J.A. Liddle

Clinical Chemistry Division, Center for Environmental Health, Centers for Disease Control, Public Health Service, U.S. Department of Health and Human Services, Atlanta, Georgia 30333

INTRODUCTION. Recent medical investigations have identified significant health problems apparently related to immune system suppression, including Kaposi's sarcoma, Pneumocystis pneumonia, candidiasis, and lymphadenopathy. A predominant number of incidents involve male homosexuals, but there are some indications that such health problems are also increasing in the general adult population.

No agent or factor has been identified as the cause of the observed immunosuppression. Chemotherapeutic agents can cause immunosuppression -- for example, steroids used for preventing graft rejection. Chronic subclinical exposure to certain chemicals may depress immune responsiveness. One common factor in many medical histories of the individuals involved is narcotic abuse, which includes use of volatile nitrites. Our objective is to develop a rapid method for characterizing a number of commercially available volatile nitrites being used for "recreational" purposes.

METHODS AND MATERIALS. One approach for determining the major constituents in volatile mixtures is headspace sampling, followed by analysis by capillary column GC/MS/DS. In headspace sampling, a 100-µl sample of vapor is withdrawn from above the liquid surface by using a 1-ml gastight syringe. Samples are injected via the Grob injection mode onto a 25-m OV-101 fused silica capillary column. The column is maintained at 50°C for 4 min, followed by programming to 100°C at 10°C per min. For these studies, we used a Finnigan 4023 GC/MS/DS system fitted with the PPINICI accessory. Methane reagent gas at a source pressure 1.2×10^{-5} torr was the moderating gas for negative chemical ionization studies. Analytical standards of butyl and isoamyl nitrite were obtained from Chem Services, West Chester, Pa. Samples of commercially available volatile nitrites were obtained from California, New York, and Georgia.

RESULTS AND DISCUSSION. The two alkyl nitrites observed in this study, butyl and isoamyl nitrite, are adequately separated by the chromatographic system. Under electron impact conditions, the retention time for butyl nitrite is 94.7 sec (S.D. = 3.73 for N = 13). The observed retention time for isoamyl nitrite is 119.4 sec (S.D. = 3.58 for N = 12). Slightly longer retention times are observed under negative chemical ionization conditions, possibly because of the higher source pressures acting at the end of the capillary column. Butyl nitrite elutes after 104.2 sec, whereas isoamyl nitrite elutes after 135.1 sec. In each sample analyzed, a trace amount of the corresponding alcohol was observed eluting after the nitrite. Only in a few instances did the alcohol approach 5-10% of the headspace vapor. Individual components are confirmed by electron impact mass spectrum. In the case of the nitrites, the low number of characteristic ions, the overall similarity in the two mass spectra, and spectral distortions due to variable sample concentrations require careful use of the library search routine. A poor FIT is obtained for butyl nitrite in comparison with the reference library spectra. A library search may be improved by using a reference spectrum from authentic standards.

The particular isomer in these mixtures is difficult to identify because of the lack of standards and reference spectra for all isomers. Isoamyl nitrite is the major isomer in the product of commerce; therefore, this is the likely isomer in the C_5 nitrites. The observation of isobutyl alcohol in the samples of C_4 nitrite suggests that the structural isomer is actually isobutyl nitrite.

Negative chemical ionization conditions yield simple mass spectra that indicate the individual nitrite. The predominant ion for each nitrite is loss of (NO) from the molecular ion. Instrument sensitivity is improved in this mode of analysis. The mass spectra for the volatile alcohols appear to be very similar to the corresponding alkyl nitrite with use of this ionization technique. The base peak in each of the alcohols is due to the ion $(M-H)^-$. This ion occurs at the same M/Z as the base peak in the corresponding nitrite. Thus, when this approach is used, good chromatographic separation of these two compounds is necessary for adequately characterizing volatiles.

Of 21 samples submitted for analysis, 10 were found to contain butyl (or isobutyl) nitrite and 10 to contain isoamyl nitrite; 1 sample contained both alkyl nitrites. Laboratory work is under way to complete the confirmation of individual isomers and to identify minor constituents in these mixtures.

CI-MASS FRAGMENTOGRAPHIC ANALYSIS OF METHAMPHETAMINE AND AMPHETAMINE IN HUMAN AUTOPSY TISSUES AFTER ACUTE METHAMPHETAMINE POISONING

T. Kojima, I. Une and M. Yashiki
Department of Legal Medicine, Hiroshima University School of Medicine,
Hiroshima 734, Japan

A 22-year-old male methamphetamine abuser was put under police protection owing to his abnormal state of excitation, but died one hour later.

There were many abrasions and hemorrhages on the face, trunk, upper and lower extremities. Recent needle punctures with hemorrhage were observed on both forearms. Bullae with hemorrhage were at the apices of both lungs, which were moderately congested. The bladder was empty and there were 20 ml of stomach contents without solid material.

The distribution of methamphetamine and amphetamine was determined by CI-mass fragmentography, which has recently been developed for screening and quantifying methamphetamine and its metabolite, amphetamine, in biological materials.

Methamphetamine and amphetamine in tissues were extracted, cleaned and made TFA-derivatives by the method shown in Table 1. CI-mass spectra of TFA-derivatives of amphetamine, methamphetamine and the internal standard, 3-phenylpropylamine, are shown in Fig. 1. CI-mass fragmentograms obtained by using quasi-molecular ions are shown in Fig. 2. The distribution of methamphetamine and amphetamine, and the amphetamine/methamphetamine concentrations in tissues are shown in Table 2. Total amount of methamphetamine-HCl in stomach contents was about 54 mg.

Since the blood level of methamphetamine was found to be at a fatal level of 5.59 μmol/100 g, this indicates that the cause of death was methamphetamine poisoning. The concentration and total amount of the chemical in gastric contents suggest that fatal poisoning occurred by ingestion, but the deceased seemed to be a methamphetamine abuser by intravenous administration, as recent needle punctures were found on both forearms. It is suspected that he swallowed the drug immediately before he was put under police protection to escape punishment for illegal possession of it.

Amphetamine in tissues seems to be a metabolite of methamphetamine, and amphetamine in gastric contents is presumed to result from gastric mucous excretion, since amphetamine concentrations in tissues ranged from 3.2 to 4.3 % of methamphetamine, and was 0.1 % in stomach contents.

Table 1. Procedure

Material(2 g)
↓ add IS(1 ml) and 0.1N-HCl(10 ml)
↓ homogenize(if necessary) and dilute to 20 ml with 0.1N-HCl
Homogenate(2 ml)
↓ add 2N-NaOH(0.5 ml) and ether(10 ml)
↓ shake(10 min) and centrifuge
Ether layer(8 ml) — NaOH layer Discard
↓ add 1N-HCl(2 ml)
↓ shake(10 min) and centrifuge
HCl layer(1.6 ml) — Ether layer Discard
↓ add 10N-NaOH(0.4 ml) and ethyl acetate(1.0 ml)
↓ shake(10 min) and centrifuge
Ethyl acetate layer — NaOH layer Discard
↓ dry with anhydrous sodium sulfate
Ethyl acetate(0.6 ml)
↓ concentrate to 0.1 ml in a nitrogen stream
↓ add trifluoroacetic anhydride(0.1 ml) and incubate(50 °C, 10 min)
↓ evaporate to dryness in a nitrogen stream
↓ add ethyl acetate(40 μl)
GC/MS(CIMF)

IS: 3-phenylpropylamine(5 μg/ml)

Table 2. Results

	MA (μmol/100 g)	A (μmol/100 g)	A/MA (%)
Blood	5.59	0.24	4.3
Liver	9.43	0.41	4.3
Brain	10.02	0.41	4.1
Kidney	9.80	0.37	3.8
Muscle	4.57	0.18	3.9
Subcutaneous fat	0.63	0.02	3.2
Stomach contents	1,464	1.87	0.1

MA: Methamphetamine, A: Amphetamine.

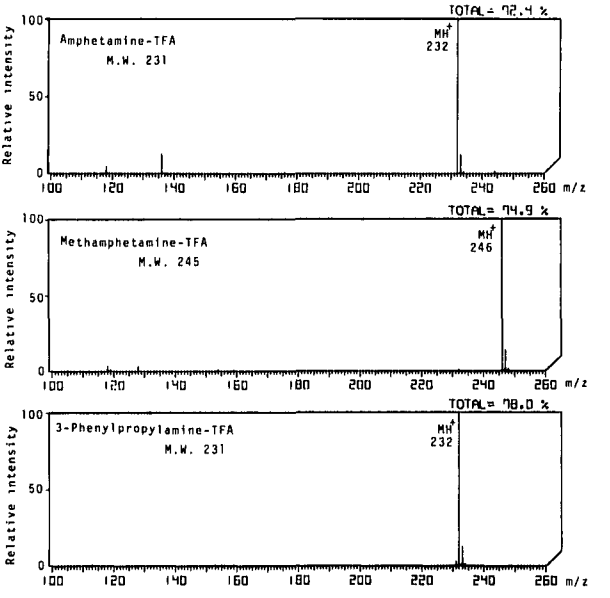


Fig. 1. CI-mass spectra.

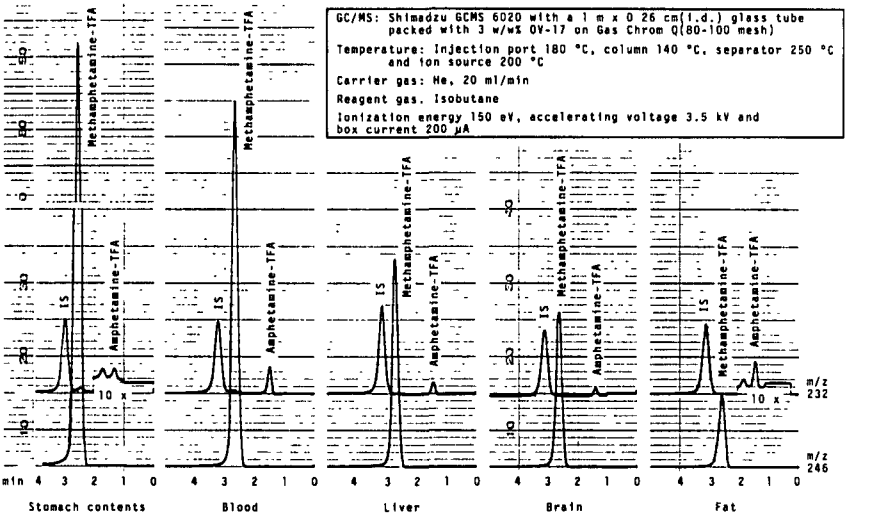


Fig. 2. CI-mass fragmentograms.

TPB 21 GC/MS ANALYSIS OF N-ALKYLATED BARBITURATES; P.S. Callery, M.S.B. Nayar, J. Leslie, M. Stogniew and P.A. Andrews; School of Pharmacy, University of Maryland, Baltimore, MD 21201.

Phenobarbital and other barbiturates were reacted with methyl iodide, trimethylanilinium hydroxide (TMAH) and dimethylformamide dimethyl acetal (DMF-DMA). In each case the major product was identified as the corresponding dialkylbarbiturate. Since earlier reports had indicated that the reaction of barbiturates with DMF-DMA yielded dimethyl acetal derivatives and not N,N'-dimethylbarbiturates, we chose to study this reaction in detail. Reaction of phenobarbital with DMF-DMA was investigated. GC/MS (CI and EI) analysis indicated the molecular weight of the product to be consistent with dimethylphenobarbital which is 18 amu less than the proposed acetal. Methylation of phenobarbital with methyl iodide, TMAH, and DMF-DMA produced compounds with identical GC/MS properties. The structure of the product formed with TMAH was unequivocally established as N,N'-dimethylphenobarbital by spectroscopic and degradation studies. N,N'-Dimethylation with DMF-DMA was accomplished with either free acids or sodium salts of barbiturates. Diethyl and dibutyl acetals of DMF were used to form N,N'-diethyl and N,N'-dibutyl derivatives of phenobarbital. A reaction mechanism for N-alkylation of barbiturates with dimethylformamide dialkyl acetals is proposed.

DETECTION OF WAKE AMINES FROM BODY FLUIDS AND TISSUES BY GC/MS ON MEDICO-LEGAL ASPECTS

Takeaki NAGATA and Mitsuyoshi KAGEURA
Department of Legal Medicine, School of Medicine
Fukuoka University, 814-04 Fukuoka,Japan

GC/MS was used to detect small amounts of wake amines in body fluids and tissues, also under unfavorable conditions leading to decomposition, contamination, etc. The amines examined, methamphetamine, amphetamine and ephedrine,were identified by their retention times and mass spectra. The amines were extracted with ether from liquid or homogenized samples containing 3-phenyl-1-propylamine as internal standard(IS), followed by reverse- and re-extraction steps, and finally derivatized with TFA. Although 1 ml or g of sample was commonly used for analysis, 0.1 ml or 0.1 g would be sufficient if only small samples are available.

Sensitive quantitation was achieved by mass fragmentography. Fig. 1 shows the mass fragmentograms of the amines. The m/z values of the ions used for monitoring the chromatograms were 140 for amphetamine, 154 for methamphetamine and ephedrine, and 162 for the IS. Stable isotopes of these amines were not employed because of legal restrictions in Japan. Each peak was clearly separated without any interference from putrefication products. The peak height of each amine was compared with that of the IS for quantitative analysis. Each calibration curve thus obtained presented a straight line in the range of 10 to 500 ng. The lower limit of detection for routine analysis was 20 pg for methamphetamine as well as amphetamine and 50 pg for ephedrine.

The technique was applied to suspected cases of drug abuse. The table lists the concentrations of methamphetamine detected from autopsy materials. In every case, methamphetamine and small amounts of amphetamine,one of methamphetamine metabolites, were found. The values are expressed in μ mol units to indicate the joint effect of the stimulants. As far as the data indicates,it is likely that there is a close correlation between the degree of intoxication,expressed by mental or physical disorder, and the drug level in the blood listed in order of decreasing concentration. This relationship could help forensic pathologists to estimate not only the cause of death, but also the responsibility at the time of accidents or criminal acts. Among the samples studied, urine had extremely high,but variable concentration levels. It is appropriate for "screening". The viscera and brain showed generally small differences. Their levels were 2 to 3 times as high as for blood and muscle. The results indicate that these tissues, especially, muscle, are possibly substitutes for blood in case of advanced decomposition where blood is unobtainable.

Based on our results as well as on information from the literature, the following criteria of blood levels (μ mol/100 ml or g) were tentatively

established: over 4 for fatal level, over 2 for serious or high level with intense excitement, over 0.5 for intermediate level with various symptoms such as hallucination, excitation, strange acts, over 0.2 for low level with minor or no abnormality and below 0.05 for therapeutic level.

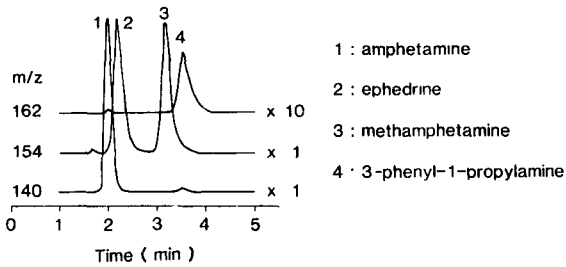


Fig.1. Mass fragmentograms of wake amines.

Table 1. Methamphetamine concentration in body fluids and tissues in autopsy materials

Classification	Age Sex	Concentration*(μ mol/100 g or ml) Bl	Ur	Lv	Br	Sp	Kd	Lg	Ms	Ft	Remarks	Bl. level reported
Fatal	25 M	34		63		42	69	121	22	7.9	Death by poisoning	4.4-30
	34 M	8.3	174	17	14	9.4	16	5.7	6.4	0.6		
Serious(high)	39 M	3.7	131	7.7	11	7.3	11		4.1	0.6	Died in confusional state (near fatal)	5
	25 M	3.2	15	5.1	3.0	2.0	3.5					
	37 M	2.7	58	5.2	6.4	5.3	4.5		2.1	0.8	Fall in confusion	
Intermediate	30 M	2.3	74	2.1	0.9	1.8	3.0		0.9	0.2	Hostility, abuser	
	31 F	1.5	13	4.1	3.0	4.0	2.8	6.0	1.5	0.2	Longtime abuser	
	41 M	1.3	33								Disorientation	
	45 M	0.9	67	1.8	2.6	2.8	2.0	1.7			Impulsive excitation	
	48 M	0.7	26	3.8	1.1	0.9	3.8		0.4	0.06	Hallucination	
	29 M	0.7	6.9								Violent act	
	32 M	0.5	18	1.9	1.7	1.6	1.7		0.6	0.3	Reckless car accident	
	33 M	0.4									Act beyond understanding	
	29 M	0.4	23	1.8	1.0	1.4	1.7			0 1	Threat in excitation	
	44 M			3.3	2.3	0.2	1.1	0.8	1.0	0 14	Longtime abuser	
Slight (low)	41 M	0.2									Abuser,not particular	
	41 M	0.07	1.2	0.06		0.03	0.07	0.3	0.02	0.02	Hallucination before 2 days	tr.-0.6
	39 M	0.03		0.2	0.2	0.17	0.17				Abuser	
Therapeutic												tr.-0.03

Bl:Blood. Ur:Urine. Lv:Liver. Br:Brain. Sp:Spleen. Kd:Kidney. Lg:Lung. Ms:Muscle. Ft:Fat.

* Inclusive of amphetamine 1/10 to 1/20 times as much as methamphetamine

PCP N-OXIDE, A POTENTIAL METABOLITE OF PHENCYCLIDINE

Gösta Hallström and Arthur K. Cho. Department of Pharmacology, UCLA School of Medicine, Los Angeles, CA 90024. (Supported by USPHS grant DA 02411).

Phencyclidine (PCP) is a common drug of abuse, whose diverse psychopharmacological effects could be partly mediated by active metabolites. The drug is rapidly metabolized, and some metabolites remain in the body for several weeks. A few metabolites have been identified, others remain to be positively identified. PCP N-oxide (Fig. 1) has been reported in rat urine on the basis of TLC data (1), but its presence was not unequivocally established. In our laboratory, an enamine that might be a rearrangement product of PCP N-oxide has been identified by GC-MS in in vitro incubates of PCP with rat and rabbit liver preparations. It was therefore of interest to synthesize the N-oxide, investigate its reactions and develop a method to assay the metabolic formation of PCP N-oxide in vitro.

Synthesis: Oxidation of PCP with m-chloroperbenzoic acid in $CHCl_3$ (2) was rapid, but when the reaction mixture was put on a basic alumina column to separate the product from remaining starting material and oxidizing agent, decomposition took place. The eluate contained mainly 1-phenylcyclohexene and N-hydroxypiperidine, the latter characterized as its HCl salt, m.p. 144-7°C (Literature 143-5°C). The decomposition problem was overcome the following way: When ethereal HCl was added after 3 hr to the reaction mixture, subsequent evaporation of the solvent yielded a residue containing m-chlorobenzoic acid and PCP N-oxide hydrochloride. The former was removed by washing with ether, and the N-oxide salt was recrystallized (m.p. 127-9°C from ethanol-ether, analysis $C_{17}H_{26}NOCl$: C,H,N,Cl). Similarly, $^2H_5$-PCP N-oxide HCl, m.p. 125-7°C, was prepared.

Characterization of PCP N-oxide and decomposition products by EIMS: Analysis of fractions from the alumina column initially used in the synthesis, by direct probe MS and GC-MS, revealed that PCP N-oxide had undergone a Cope elimination (3) to form 1-phenylcyclohexene and N-hydroxypiperidine. Although the direct probe spectrum of PCP N-oxide HCl (70 eV; Fig. 1) was similar to that of a hypothetical mixture of the Cope elimination products, the following data indicated that the material was one unique compound that decomposed on electron impact: i) The vaporization of the two elimination products did not coincide in time with that of the N-oxide on identical heating of the probe; ii) The spectrum contained peaks corresponding to losses of O, OH· and H_2O from the molecular ion (which was not detected) occurring at masses greater than those of either of the elimination products; iii) The ratios of m/z 159 to 158 (0.49) and m/z 101 to 100 (1.06) did not match those in the spectra of authentic 1-phenylcyclohexene (0.13) and N-hydroxypiperidine (0.50), respectively.

When PCP N-oxide was subjected to GC analysis (5% QF 1, 6' x 2 mm, 155°C, inj. 210°C), the major GC peak corresponded to 1-phenylcyclohexene, in accordance with a thermal Cope elimination in the injection port. The mass spectrum from the second largest peak suggested that a Meisenheimer rearrangement (4) had also occurred, forming O-piperidino-1-phenylcyclohexanol.

Quantitative analysis of PCP N-oxide: An assay for the N-oxide was developed consisting of reduction of the N-oxide in aqueous solution with $TiCl_3$ after initial extraction with hexane at pH 9.5 to remove any PCP present in the sample. The PCP formed by reduction of PCP N-oxide was quantitated by GC allowing 10 nmol of PCP N-oxide to be measured in the presence of 5000 nmol of PCP.

In vitro metabolism: In experiments using liver microsomes from rabbit, rat and guinea pig and 1 mM concentrations of PCP, no N-oxide could be detected after 10 or 30-min incubation. The analysis would have allowed a formation corresponding to 0.2% of the substrate to be measured. When PCP N-oxide was incubated with rabbit liver microsomes, it disappeared by a NADPH-dependent pathway. Little if any PCP was formed, and the major metabolite was identified as the N-oxide of N-(4-hydroxy-1-phenylcyclohexyl)piperidine based on the MS of the reduced metabolite. However, no significant amount of this secondary metabolite could be detected in 30-min incubations of PCP with rabbit liver microsomes.

Origin of the enamine found in PCP metabolism analysis: GC-MS analysis of extracts from incubations of PCP with rat and rabbit liver preparations identified an enamine, N-(1-phenylcyclohexyl)-1,2,3,4-tetrahydropyridine [20eV: m/z 241(10%), 198(2), 159(10), 91(43), 83(100)]. This compound could have been formed either by a Polonowski rearrangement (5) of PCP N-oxide or by elimination of water from a carbinolamine, α-hydroxy-N-(1-phenylcyclohexyl)piperidine. The direct probe spectrum of PCP N-oxide showed some minor conversion to the enamine (m/z 241), but neither direct GC nor acetic anhydride treatment

(Polonowski conditions) of the N-oxide gave measurable amounts of the enamine. The carbinolamine was proposed as an intermediate in the formation of the amino alcohol metabolite of PCP, via its aqueous equilibrium counterpart, the amino aldehyde [5-(1-phenylcyclohexylamino)valeraldehyde] (6). We have now successfully trapped the amino aldehyde with methoxyamine, and identified the formed O-methyloxime by GC-MS [70eV: m/z 288(3), 257(15), 245(35), 159(35), 91(100)]. In the extracts of methoxyamine-treated incubation mixtures, no enamine was seen, indicating that the carbinolamine is the sole source of this compound, which is probably formed in the GC injection port.

Discussion: Our data from the in vitro metabolism of PCP, where no N-oxide was found, are in contradiction to the findings of Misra et al. (1), who detected a metabolite in rat urine with TLC retention reportedly similar to that of the N-oxide. However, the melting point reported for this reference N-oxide HCl (137-8°C) is different from ours (127-9°C). Since no spectral data were reported by Misra et al., no direct comparison can be made to clarify this discrepancy.

1-Phenylcyclohexene, mentioned above as a product of the Cope elimination, has earlier been identified in metabolism experiments (7,8). In these cases, however, it was a product of a thermal decomposition of PCP itself, which could be avoided by using lower GC injection port temperatures.

The possibility that the enamine found in the GC-MS analysis of PCP metabolism extracts originated from PCP N-oxide was ruled out by showing the involvement of the carbinolamine in the formation of the enamine. Methoxyamine trapping of the aldehyde corresponding to the carbinolamine, followed by identification by MS, is a method that could be applied to studies of the metabolism of other drugs where a carbinolamine has been postulated.

References

1. A.L. Misra, R.B. Pontani, and J.G. Bartolomeo, Life Sci. 27, 2501 (1980).
2. J.C. Craig and K.K. Purushothaman, J. Org. Chem. 35, 1721 (1970).
3. A.C. Cope and H.H. Lee, J. Am. Chem. Soc. 79, 964 (1957).
4. N. Castagnoli, J.C. Craig, A.P. Melikian, and S.K. Roy, Tetrahedron 26, 4319 (1970).
5. R.T. LaLonde, E. Auer, C.F. Wong, and V.P. Muralidharan, J. Am. Chem. Soc. 93, 2501 (1979).
6. A.K. Cho, R.C. Kammerer, and L. Abe, Life Sci. 28, 1075 (1981).
7. D.C.K. Lin, A.F. Fentiman, Jr., R.L. Foltz, R.D. Forney, Jr., and I. Sunshine, Biomed. Mass Spectrom. 2, 206 (1975).
8. L.K. Wong and K. Biemann, Biomed. Mass Spectrom. 2, 204 (1975).

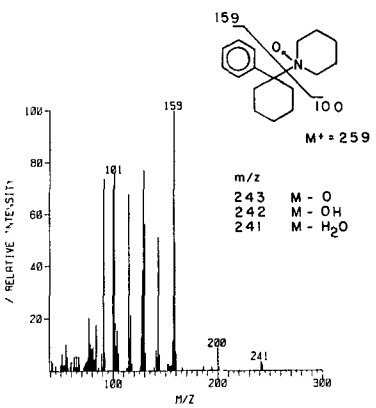


Fig. 1

SELECTED ION MONITORING OF T-BUTYLDIMETHYLSILYL DERIVATIVES OF AMOXAPINE AND ITS 7-OH- AND 8-OH-METABOLITES IN CLINICAL SAMPLES

Harrell E. Hurst[1] and George C. Rodgers[1,2]

(1)Department of Pharmacology and Toxicology
University of Louisville Medical School
and
(2)Kentucky Poison Control Center
Kosair-Children's Hospital

Louisville, KY 40292

The piperazine antidepressant amoxapine, as well as the active (1) metabolites 7-hydroxyamoxapine and 8-hydroxyamoxapine, were quantified by selected ion monitoring (SIM) of the t-butyldimethylsilyl (TBDMS) derivatives. The method was developed and utilized to examine the pharmacokinetics of elimination of amoxapine and metabolites from serum following a suicidal attempt.

Serum samples (0.5 ml) were extracted using 100 mg C-18 Bond Elut columns. Following application of serum and the internal standard perphenazine, the columns were flushed with acetic acid (10 mM) and water. The drugs were eluted with 0.6 ml methanol containing acetic acid (10 mM) and diethylamine (5 mM). The evaporated extracts (N_2, room temperature) were derivatized (80°C, 30 min) with N-methyl-N-t-butyldimethylsilyltrifluoroacetamide (1% t-butyldimethylchlorosilane catalyst) in acetonitrile.

The N-TBDMS-amoxapine and di-(N,O)-TBDMS derivatives of 7-hydroxyamoxapine and 8-hydroxyamoxapine were separated on a 1.8 m x 2 mm glass column packed with 1% SP2100 on 100/120 mesh Supelcoport. The temperature of the column was programmed from 240°C, with initial hold of 2.5 min, to 275°C at a rate of 16°/min. Under these conditions retention times for TBDMS-amoxapine, (N,O)-TBDMS-8-O-amoxapine, (N,O)-TBDMS-7-O-amoxapine, and TBDMS-perphenazine were 5.4 min, 10.3 min, 11.1 min, and 11.2 min, respectively.

Upon EI fragmentation the TBDMS-derivatives of amoxapine and metabolites yielded base peaks of m/z 170, while TBDMS-perphenazine gave a base peak of m/z 246. The centers of mass of these ions were monitored (dwell times, 100 msec) using an HP 5992 quadrupole instrument operating with 0.6 amu peak width at half-height. Confirming ions included $M-57^+$ and/or M^+, which ranged in abundance from 2-12%. Assignments for the monitored ions are:

TBDMS-amoxapine	m/z 170 ($C_9H_{20}NSi^+$)
	m/z 370 ($M-57^+$)
(N,O)-TBDMS-O-amoxapines	m/z 170 ($C_9H_{20}NSi^+$)
	m/z 500 ($M-57^+$)
	m/z 557 (M^+)
TBDMS-perphenazine	m/z 246 ($C_{13}H_9ClNS^+$)
	m/z 517 (M^+)

Internal standardization with perphenazine resulted in linear plots of base peak area ratios versus concentration of amoxapine or metabolites added to drug free plasma. These plots were offset to the right of the origin, and apparent losses of derivatives within the column were responsible in part. After a requisite loading of the column prior to analysis, coefficients of variation at the smallest standard concentration (0.5 µg/ml serum) were approximately 10%.

Quantification of amoxapine, 8-hydroxyamoxapine, and 7-hydroxyamoxapine by this method yielded peak serum concentrations of 1.2, 1.1, and 2.7 μg/ml, respectively, about 12 hr following ingestion. Elimination of amoxapine was biphasic, exhibiting initial and terminal half-lives of 19 and 99 hr, respectively. The initial elimination half-lives of 8-hydroxyamoxapine and 7-hydroxyamoxapine were 26 and 10 hr, terminating in nearly steady-state levels of 0.75 and 0.85 μg/ml, respectively, through the interval 24-56 hr.

The pharmacokinetics of amoxapine and metabolite elimination following this overdose differ from data obtained with subtherapeutic dosage (2). Initial phase half-lives were prolonged (2-3-fold) for amoxapine and 7-hydroxyamoxapine, while the 8-hydroxyamoxapine half-life was not appreciably different than at low dosage. Peak levels of 7-hydroxyamoxapine following this overdose were most substantial, rather than minor. These findings indicate that overdose effects may be more protracted than predicted from the low dose study.

REFERENCES

1. Coupet, J., C.E. Rauk, V.A. Szues-Myers, and L.M. Yunger. 2-Chloro-11-(1-piperazinyl)dibenz[b,f][1,4]oxazepine (amoxapine), an antidepressant with antipsychotic properties - a possible role for 7-hydroxyamoxapine. Biochem. Pharmacol. 28:2514-5 (1979).

2. Cooper, T.B. and R.G. Kelly. GLC analysis of loxapine, amoxapine, and their metabolites in serum and urine. J. Pharm. Sci. 68:216-9 (1979).

ACKNOWLEDGEMENT

The authors gratefully acknowledge the generous gift of amoxapine, 7-hydroxyamoxapine, and 8-hydroxyamoxapine by Harold J. Eisner, Lederle Laboratories, Pearl River, NY.

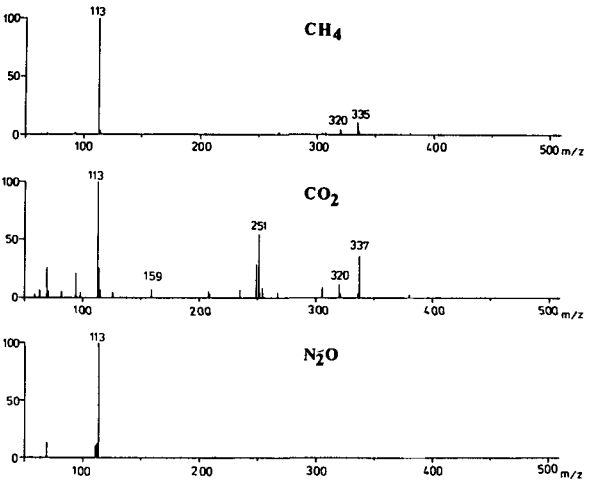
NEGATIVE ION MASS SPECTROMETRY OF PERFLUOROACYLATED OPIATES

Kenji Hara and Hans Brandenberger
Department of Forensic Chemistry, University of Zürich
Zürichbergstr. 8, CH-8028 Zürich, Switzerland.

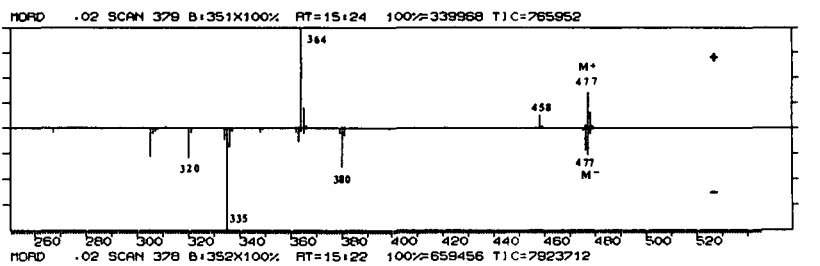
The negative ion mass spectra of trifluoroacetyl(TFA)-, pentafluoropropionyl(PEP)- and heptafluorobutyryl(HFB)-derivatives of morphine (7,8-didehydro-4,5-epoxy-17-methylmorphinan-3,6-diol), codeine (7,8-didehydro-4,5α-epoxy-3-methoxy-17-methylmorphinan-6α-ol), and hydromorphone (4,5α-epoxy-3-hydroxy-17-methylmorphinan-6-one) have been recorded with low pressure chemical ionization using CH_4, CO_2 and N_2O as reagent gases. The ion source pressure was kept in the region of 10^{-2} torr. The corresponding spectra are qualitatively but not quantitatively similar. The spectra of bis-TFA-morphine gave ions at m/z 113 (CF_3COO), m/z 320 (loss of CF_3COOH and CH_2NCH_3), m/z 335 (loss of CF_3CO, CH_2NCH_3 and H_2) and m/z 380 (loss of CF_3CO). Electron attachment with the reagent CH_4 (yielding essentially only secondary electrons as negative particles) gave by far the best sensitivity, 20 times better than a charge exchange mechanism with the reagent N_2O (yielding the anions O^- and $[NO]^-$).

After extraction and perfluoroacylation of opiates in body fluids, GC with selected negative ion detection (electron attachment mode) was used for their trace analysis. The separations were carried out in a packed column with 3% SE-30 at 215°C or a capillary column with OV-1701 at 240°C. The signal intensity (total ion current) increases with the number of fluorine atoms in the derivatives. However, for practical applications, trifluoroacetylation was chosen, since the TFA-derivatives have the shortest retention times and yield characteristic fragment anions suitable for mass specific detection. Trifluoroacetylation was carried out by simultaneous injection of the opiate (in dichloromethane) and N-methyl-bis-trifluoroacetamide as reagent into the GC. Anhydrides were not suitable for this technique.

For detection and dosage of bis-trifluoroacetyl-morphine, m/z 335 and 320 are recommended as tracer anions. Such a chromatographic approach is about 10 times more sensitive than GC with selected cation detection and also more sensitive than GC with electron capture detection of the trifluoroacetylated compound.



Negative CI Mass Spectra of bis-TFA-Morphine with 3 different Reagent Gases
Instrument LKB 2091



bis-TFA-morphine (Mw 477)
CH_4, 5×10^{-3} torr

Quasi-simultaneous recording of positive ion EI- and negative ion CI- mass spectra of bis-TFA-morphine. Upper mass range only. Negative TIC is 10 times higher than positive TIC. Instrument: Nermag R 10/10.

ANALYSIS OF FATTY ACID SYNTHESIS REGULATION BY MASS FRAGMENTOGRAPHY.

Y. Seyama, H. Otsuka, A. Kawaguchi*, S. Okuda* and T. Yamakawa
Department of Biochemistry, Faculty of Medicine and *Institute of Applied Microbiology, University of Tokyo, Bunkyo-ku, Tokyo, Japan

Introduction

Fatty acids are produced from malonyl-CoA, NADPH (and/or NADH) as reducing agent and acetyl-CoA as 'priming' substrate. By adopting a GC/MS technique to follow the incorporation of deuterium atoms from ^2H_2O, we devised a new assay method for fatty acid synthetase by mass fragmentography, which was successfully applied in elucidating the thermal regulation and the termination mechanism of fatty acid synthetase from Brevibacterium ammoniagenes, and the production mechanism of methyl-branched fatty acids with fatty acid synthetase from guinea pig Harderian gland.

Assay Method of Fatty Acid Synthetase

Fatty acid synthetase catalyzes the production of fatty acids with chain length of C_{14} to C_{18}. Fatty acid synthetase from B. ammoniagenes produces oleic acid in addition to palmitic and stearic acids, and the enzyme from guinea pig Harderian gland produces at least 19 kinds of fatty acids in the presence of methylmalonyl-CoA. In studies on the control mechanism of fatty acid synthetase, it became necessary to determine the exact amounts of individual fatty acids produced during incubation.

The fragment ion at m/z 74 [CH_2=C(OH)-OCH_3] of fatty acid methyl esters showed an upward shift to m/z 77 when the enzyme reaction proceeded in ^2H_2O. This enabled us to to differentiate the newly synthesized fatty acids from the endogenous ones by monitoring the intensities of m/z 77 and m/z 74 fragments by mass fragmentography. When a known amount of heptadecanoic acid was added as an internal standard, it was possible to determine the absolute amounts of individual newly synthesized fatty acids (1).

A typical mass fragmentogram is shown in Fig. 1. The reaction was carried out for 10 min at 37°C and terminated by acidification with H_2SO_4. The m/z 74 fragment reflecting the amounts of the internal standard (17:0) and endogenous fatty acids (16:0, 18:1, 18:0), were monitored in channel 1. Newly synthesized fatty acids were monitored by m/z 77 in channel 2. The correlation coefficient between the results of the spectrometric assay and the present method was found to be 0.99. The standard error of the present method was 3.55 % (n=5), and linearity was observed from 0.02 μg up to 4 μg. This procedure is more sensitive and specific than the conventional spectrophotometric method.

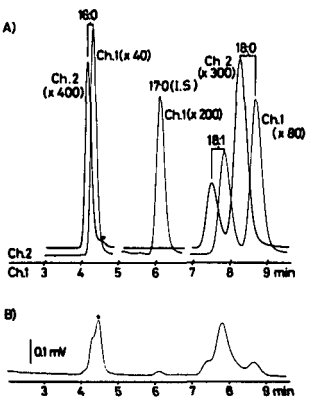


Fig. 1. Mass fragmentogram (A) and total ion monitoring (B) of fatty acids obtained from incubation with fatty acid synthetase from B. ammoniagenes. Channels 1 and 2 were set for m/z 74 and 77, respectively. The amplifications of the channels are shown in the parentheses. The peak area of methyl heptadecanoate corresponded to 0.444 μg. Chart speed was 40 mm/min. *Phthalic acid ester came from n-hexane as a contaminant.

Thermal Regulation of Fatty Acid Synthetase from Brevibacterium ammoniagenes

Living organisms adjust the fatty acid composition of their membrane lipids in response to the environmental temperature. The mechanisms regulating this alteration seem to operate at the levels of both phosphatidic acid synthesis and fatty acid synthesis.

Fatty acid synthetase from B. ammoniagenes is a multienzyme complex. A novel feature of this enzyme complex is its ability to synthesize oleic acid as well as saturated fatty acids. This enzyme synthesizes oleic acid by an anaerobic process involving

ß,γ-dehydration of ß-hydroxyacyl thioester intermediates and subsequent chain elongation of ß,γ-enoate without reduction of the double bond. The enzyme component responsible for this dehydration is tightly associated with the various activities for carbon chain elongation as an integral part of the fatty acid synthetase complex.

The ratio of unsaturated to saturated fatty acids depends on the temperature of the enzyme reaction (Fig. 2A). The amounts of newly synthesized palmitic and stearic acids

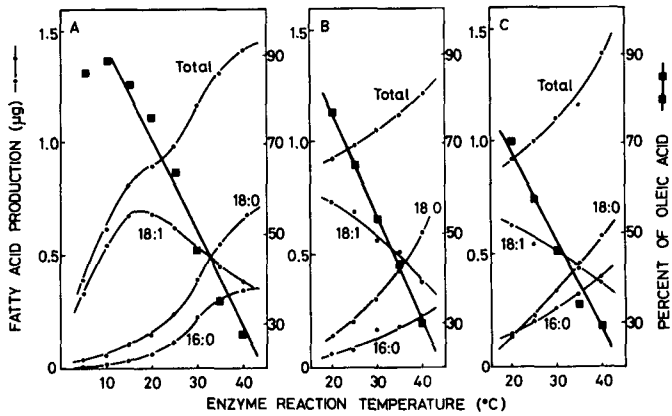


Fig. 2. Temperature-sensitive synthesis of fatty acid species by fatty acid synthetase from B. ammoniagenes. Cells were grown at 30°C (A), 20°C (B), and 37°C (C). Crude enzyme preparation (0.16 mg protein) was used in all experiments and enzyme reactions were carried out for 90 minutes.

increased steadily with increase in the temperature of the enzyme reaction over the range 5°-40°C. On the other hand, the amount of oleic acid was maximal at 20°C and decreased at lower and higher temperatures. The ratio of unsaturated fatty acids decreased with increasing temperature of the enzyme reaction. Enzyme preparations from cells grown at 20°C (Fig. 2B), 30°C (Fig. 2A) and 37°C (Fig. 2C) showed similar profiles of temperature dependent syntheses of palmitic, stearic and oleic acids. The nature of fatty acid synthetase as an enzyme protein appear to be unchanged by the growth temperature. These results suggest that the ratio of products is dependent only on the temperature of the enzyme reaction and is independent of the growth temperature of B. ammoniagenes.

The close correlation between the fatty acids produced in vitro by fatty acid synthetase and those produced in cells supports the idea that the fatty acid composition of B. ammoniagenes may be determined by the temperature dependence of fatty acid synthetase itself (2).

Substrate Control of Termination of Fatty Acid Synthesis

The products of fatty acid synthetase from B. ammoniagenes were palmitic, stearic and oleic acids, and the proportions of these different species are fixed under given conditions of the enzyme reaction. The NADPH and NADH concentrations had substantially no effect on the product distribution of fatty acids. The data in Fig. 3 suggest that the percentage of oleic acid was independent of the ratio of acetyl-CoA to malonyl-CoA, but that the percentage of stearic acid decreased with increase in the acetyl-CoA to malonyl-CoA ratio. In other series of experiments, the ratio of acetyl-CoA to malonyl-CoA was fixed at 2:1 and the patterns of enzymically synthesized fatty acids were determined at various concentrations of malonyl-CoA and acetyl-CoA. The results showed that the chain length of the products was determined primarily by the concentration of malonyl-CoA. Above 100 µM malonyl-CoA, stearic acid accounted for about 90 % of the saturated fatty acids and the pattern of fatty acids synthesized was independent of the malonyl-CoA concentration.

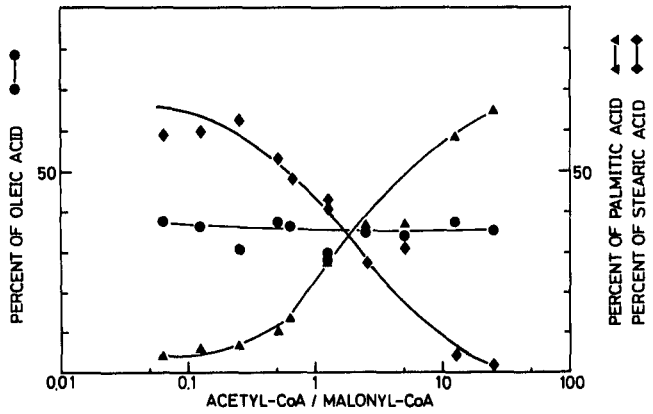


Fig. 3. Effect of the molar ratio of acetyl-CoA to malonyl-CoA on the pattern of fatty acids produced by the B.ammoniagenes synthetase.

Moreover, the percentage of stearic acid was constant (about 60 %) at all ratios of acetyl-CoA to malonyl-CoA tested in the presence of more than 100 μM malonyl-CoA. Below 100 μM malonyl-CoA, the relative proportion of palmitic to stearic acid was dependent on both the absolute concentration of malonyl-CoA and the ratio of malonyl-CoA to acetyl-CoA concentration (3).

Biosynthesis of Methyl-branched Fatty Acids

Fatty acid synthetase from guinea pig Harderian gland exhibited a unique character as compared with the fatty acid synthetase from the liver of the same animal. The former enzyme produced many odd-numbered and methyl-branched fatty acids in the presence of *methylmalonyl-CoA*. *These fatty acids are characteristic components of the lipid secreted* from this gland (4).

Under standard incubation conditions with acetyl-CoA and malonyl-CoA as substrates, a large amount of palmitic acid together with small amounts of myristic and stearic acid was synthesized (Fig. 4a). When methylmalonyl-CoA was added together with malonyl-CoA,

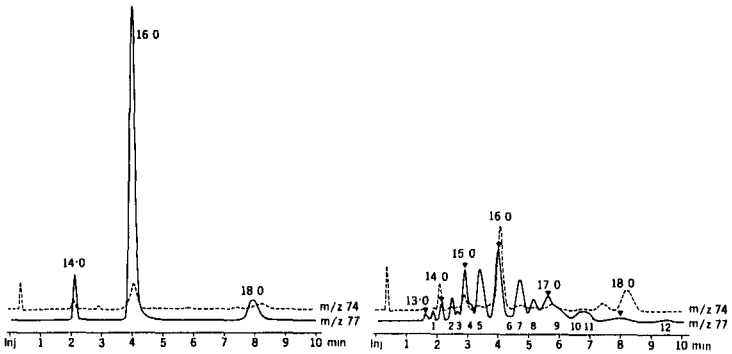


Fig. 4. Fatty acids produced by fatty acid synthetase from guinea *pig Harderian gland. The substrates were as follows:* (a) acetyl-CoA and malonyl-CoA, (b) acetyl-CoA, malonyl-CoA, and methylmalonyl-CoA.

more than 19 kinds of fatty acids were produced (Fig. 4b). Most of the products were methyl-branched fatty acids, but straight chain acids with even and odd numbers of carbon atoms were also produced. The effect of methylmalonyl-CoA concentration on this feature was examined by changing the amount of methylmalonyl-CoA to malonyl-CoA (Fig. 5).

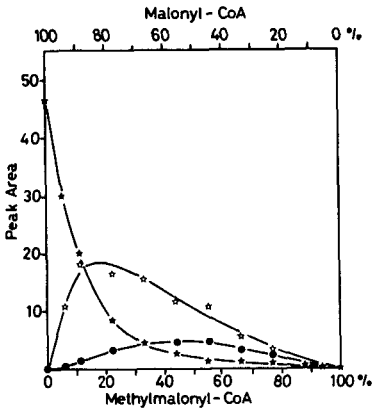


Fig. 5. Effect of methylmalonyl-CoA concentration on fatty acid synthesis. Peak areas (arbitary unit) of even-numbered fatty acids (★), odd-numbered fatty acids (☆), and methyl-branched fatty acids (●) were plotted against the concentrationb ratio of malonyl-CoA and methylmalonyl-CoA.

Production of even-numbered fatty acids was strongly inhibited by methylmalonyl-CoA, but the formation of odd-numbered and methyl-branched fatty acids increased to some extent with increasing amount of methylmalonyl-CoA. The initial velocity, measured by following the reduction of NADPH, decreased with increasing amount of methylmalonyl-CoA (5).

Summary

The overall activity of fatty acid synthetase have been conventionally determined by two methods: (i) spectrophotometric assay measuring the disappearance of NADPH (and/or NADH), and (ii) radioactivity assay of ^{14}C-labelled acetyl-CoA or malonyl-CoA into the fatty acids. Spectrophotometric assay cannot determine the amounts of individual fatty acids. In radioactivity assay, the accuracy is not satisfactory. The present method, mass fragmentography, gives a good separation of individual fatty acids, even between newly synthesized and endogenous fatty acids, and has a great sensitivity.

This assay method was applied to the enzyme system of B. ammoniagenes. (I) The ratio of unsaturated fatty acids synthesized in vitro depends on the temperature of the enzyme reaction but not on the growth temperature of the bacteria. (II) The relative proportion of palmitic to stearic acids depends on the concentration of malonyl-CoA and on the ratio of acetyl-CoA to malonyl-CoA concentrations. It was also applied to the enzyme system from guinea pig Harderian gland. (III) Under an appropriate concentration of substrates, the fatty acid synthetase can produce a set of fatty aicds needed for the synthesis of lipid secreted from this gland.

References

1. Seyama, Y., Kawaguchi, A., Okuda, S. and Yamakawa, T. (1978) J. Biochem., 84, 1309-1314
2. Kawaguchi, a., Seyama, Y., Sasaki, K., Okuda, S. and Yamakawa, T. (1979) J. Biochem., 85, 865-869
3. Kawaguchi, A., Arai, K., Seyama, Y., Yamakawa, T. and Okuda, S. (1980) J. Biochem., 88, 303-306
4. Yamazaki, T., Seyama, Y., Otsuka, H., Ogawa, H. and Yamakawa, T. (1981) J. Biochem. 89, 683-691
5. Seyama, y., Otsuka, H., Kawaguchi, A. and Yamakawa, T. (1981) J. Biochem., 90, 789-797

GC/MS DETERMINATION OF STABLE ISOTOPES OF SELENIUM USED IN HUMAN METABOLIC STUDIES.
C. Veillon, D.C. Reamer, O.A. Levander and C.A. Swanson; Beltsville Human Nutrition Research Center, U.S. Department of Agriculture, Beltsville, Maryland 20705.

Selenium is an essential trace element in human nutrition and its metabolic function is being widely studied. One of the most powerful tools in following the biological pathways of an element is the use of tracers. In animal studies, this is most often accomplished using radiotracers. For in vivo human studies, the use of radiotracers is severely limited, especially in the cases of children, women of childbearing age and during pregnancy. The use of stable isotope tracers avoids many of the problems associated with radioisotopes. No radiation hazards exist, and they can be used for long term studies since decay is not a problem. For several essential trace elements, suitable radioisotopes do not exist, yet stable isotopes do. All of this assumes, however, that suitable means of measuring stable isotope tracers exist.

We wish to describe a method for measuring stable isotopes of selenium and application of the method to tracer studies for the purposes of total selenium analysis, endogenous labeling of foodstuffs and in vivo tracer studies during pregnancy. These techniques permit kinetic studies to be performed and measure such parameters as the size and number of various body pools of selenium.

The measurement employs stable isotope dilution methodology (isotope ratio determinations) and a quadrupole GC/MS system with multiple ion monitoring.

Samples are rapidly digested employing H_3PO_4, HNO_3 and H_2O_2, undigested lipids (free of Se) are extracted with chloroform, and any selenate reduced to selenite. An important advantage of this procedure is that the use of $HClO_4$ is avoided. The selenite is then converted to the nitropiazselenol (Se-NPD) with 4-nitro-o-phenylenediamine, extracted into chloroform and analyzed. By spiking the samples with a known quantity of enriched ^{82}Se, and measuring the $^{80}Se/^{82}Se$ ratio, total selenium can be readily calculated (1).

For tracer studies, another enriched isotope of Se (^{76}Se in this study) can be used as the metabolic tag. Again spiking samples with ^{82}Se and measuring the $^{76}Se/^{82}Se$ and $^{80}Se/^{82}Se$ ratios, one can quantitatively measure both the ^{76}Se tracer and the natural Se along with it. Total Se is then the sum of these. A detailed description of how this is done will be presented.

Hens were depleted for 35 days on a low selenium diet, then repleted by adding enriched ^{76}Se to the diet for 35 days while collecting eggs. The feed was enriched 9.5-fold with respect to ^{76}Se, and this enrichment was reached after 35 days by the egg yolks and livers. Egg whites were enriched about 7-fold and breast meat about 5-fold during this period.

In a controlled metabolic experiment over 21 days, 3 groups of women (non-pregnant, early-pregnant and late-pregnant) were fed a diet containing 150 ug Se/day. On day 8, they were fed a diet containing some of the labeled egg yolks (40 ug of enriched ^{76}Se plus 110 ug natural Se). Urine, feces and blood were collected and analyzed for the remainder of the study. Some examples of the ability of this methodology to monitor the tracer will be presented. From the kinetics involved, it is possible to determine the size of a given metabolic pool and the number of other pools which are in equilibrium with it.

This methodology represents a very powerful analytical tool for the determination of Se in general and for stable isotope tracer techniques in particular. The digestion method employed avoids the problems associated with $HClO_4$ digestions and is rapid since lipids do not have to be destroyed. The combination of chelation, extraction and GC/MS analysis provides a stable isotope method which is extremely specific, sensitive, precise, accurate and rapid.

(1) Reamer, D.C. and Veillon, C. (1981). Determination of selenium in biological materials by stable isotope dilution GC/MS. Anal. Chem. 53, 2166-2169.

STUDY ON METABOLISM OF PHENYLALANINE, TYROSINE AND TRYPTOPHAN AND RELATED COMPOUNDS USING DEUTERATED AMINO ACIDS

H. NARUSE*, T. HAYASHI*, E. SUZUKI*, S. KAMADA*, I. MATSUDA** and R. TAKAHASHI***

* NATIONAL CENTER FOR NERVOUS, MENTAL & MUSCULAR DISORDERS, TOKYO, JAPAN

** DEPT. OF PEDIATRICS, KUMAMOTO UNIV., KUMAMOTO, JAPAN

***DEPT. OF PSYCHIATRY, NAGASAKI UNIV., NAGASAKI, JAPAN

INTRODUCTION

In animal experiments, it was confirmed that in some case, the determination of the turn over rate of certain compounds could reveal the change of function of certain organs, though the determination of pool size of intermediates of certain metabolic pathways did fail to find such a functional change. Therefore, it is assumed that the determination of the turn over rate of certain compounds in vivo could be useful for studying the chemical background of some diseases. We have tried to know the change of turn over rate of amino acids and these derivatives in some psychiatric and neurological diseases based on the usage of stable isotopes.

EXPERIMENTALS

L-[2,3,4,5,6-d]Phenylalanine(Phe-d_5) and L-[2,4,5,6,7-d]Tryptophan(Try-d_5) were synthesized based on a method reported by H. R. Matthews et al,[1] and L-[2,3,5,6-d]Tyrosine(Tyr-d_4) was synthesized based on a method of Y. Tokuhisa et al.[2] These deuterated amino acids were administered orally at 11 a.m., and amounts of the deuterated amino acids was principally kept at 5 mg/kg so that the administration of deuterated amino acids do not cause a pathological increase of the pool size of the related compounds.

Plasma samples were deproteinized by trichloracetic acid, and the acid soluble fraction was treated with Dowex AG 50 W X2 column in order to obtain a fraction containing Phe., Tyr. and Try. The amino acids were derivatized with trifluoroacetic anhydride and diazomethane, and TFA methyl ester of the amino acids were analyzed with GC-MS-SIM method.(Fig. 1)

Finnigan's Q-pole GC-MS(Type-4000) was used, and CI method with isobutane was adopted. Ion monitors were set at m/z 276, 281, 388, 392, 411 and 416 for Phe-d_0, -d_5, Tyr-d_0, -d_4, and Try-d_0, -d_5 respectively. The amino acids between 50 pg to 500 ng were determined exactly. CV % of authentic mixtures of Phe-d_0 and -d_5, and Tyr-d_4 and -d_0 on 30 experiments for six months were 1.18 % for Phe-d_5/d_0, and 1.7 % for Tyr-d_4/d_0.[3] In order to know the change of the metabolic rate of these compounds, a ratio of Phe-d_5 to -d_0, Tyr-d_4 to -d_0 and Try-d_5 to -d_0 were

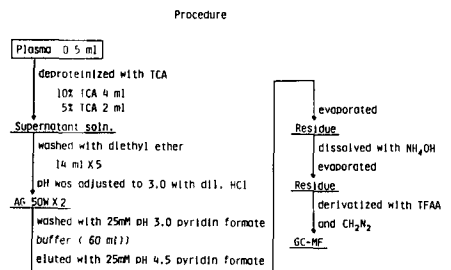


Fig. 1 Preparation and Derivatization of Blood Sample

determined. Amino acid analyzer using OPA was used for the determination of the amounts of endogenous amino acids plus deterated amino acids. An amount of deuterated amino acid was calculated based on the ratio of deuterated and non deuterated amino acids and a total amount of deuterated and non deuterated amino acids.

RESULTS AND DISCUSSION

1) Phenylketonuria [3]

The change of Phe-Tyr metabolism was analyzed in 12 cases of classical PKU and 3 cases of the heterozygote of PKU. In the typical classical PKU, there were no Tyr-d_4 formation during 60 min. after the administration of Phe-d_5 5 mg/kg, and a ratio of Phe-d_5/d_0 was not decrease during the same period. However, there were three cases in whom the ratio of Phe-d_5/d_0 was descreasing significantly. The three cases are called as the B group of the PKU and the others as the A group of PKU. The A group is the typical one and the B group seems to be a mild form. The half life time of Phe was calculated in PKU and the heterozygote of PKU and in the control group. Table 1. shows the half life time in one case of the A group, two cases of the B group and three heterozygotes.

Even in the patients of the B group, no Tyr-d_4 was detected during 60 min. after Phe-d_5 administration and no phenylpyruvate was found in the urine. Therefore, the significant decrease of Phe-d_5/d_0 suggests a possibility of alternative metabolic pathway other than the hydroxylation or transamination. In the heterozygote of PKU, case No. 1 has a same half life time as the control, and case No. 3 has slight prolonged half life times. It was reported that an activity of liver phenylalanine hydroxylase is about 15 to 25% of normal. However, based on present experiments, it could be assumed that the metabolism of Phe in heterozygotes should be rather heterogenous. The ratio of Tyr-d_4 to Phe-d_5 was calculated, and case No. 3 of the heterozygote has shown a very low values in comparison with the control or case No. 1 of the heterogyzotes. The prolonged half life time of Phe seems to result in the decreased formation of Tyr.

Table 1. Half life time of Phe.

Control	No.1	30'
	No.2	35'
	No.3	35'
PKU group A	No.1	>300'
	No.2	>300'
group B	No.1	112'
	No.2	160'
PKU Heterozygote	No.1	40'
	No.2	45'
	No.3	60'

The formed Tyr-d_4 in heterozygotes of PKU degradated as fast as that of the control group. We have tried to calculate the half life time of Tyr, but, since an amount of Tyr came from endogenous or exogenous protein is not determined in our present method, it was impossible to calculate the half life time of Tyr.

2) Depression [4]

The turn over of Phe and Tyr in 15 patients of monopolar depression (major depression in DSM III of America Psychiatric Association) and one of neurotic depression were analyzed. 13 patients of monopolar depression and a neurotic depressive patient have shown the marked

decrease of disappearance curve of Tyr-d_4/d_0 in the blood. These patient are called as the A group of Depression. One patient of monopolar depression has shown a normal pattern of Tyr-d_4/d_0, and is called as the B group. Another one case of monopolar depression has shown a slight decrease of the disappearance curve of Tyr-d_4/d_0. This case might be a very mild one of the A group, but was ommitted from the A group. The change of Phe-d_5/d_0 and Tyr-d_4/d_0 after administration of Phe-d_5 in the A group was shown in Fig. 2.

As described above, the half life time of Tyr could not be calculated, therefore, the change of ratio of Tyr-d_4/d_0 and the change of absolute amounts of Tyr-d_4 in plasma were obtained. These result suggest the significant decrease of the turn over of Tyr in the A group of monopolar depression. The absolute amounts of Tyr-d_4 were almost same in a few cases, and low in other cases, but the rates of disappearance of Tyr-d_4 were significantly decreased in all patients of the A group. These patients have normal liver function, and the decreased turn over rate normalized due to clinical improvements of depressive symptoms.

In order to know whether or not the decreased turn over rate of Tyr relate to the decrease of turn over of cathecolamine, all present aveilable methods are not sensitive enough. Therefore, an ultra-micro technique using the negative ion CI MS is under investigation, and a preliminary results will be reported in the meeting (T. Hayashi, et al.). The disappearance curves of Try-d_5/d_0 of the A group patients have shown that there might be disturbances of cellular up take of Try in some cases of the group. However, the disappearance ratio of Try-d_5/d_0 seems to be in the normal range. The decrease of turn over rate of Tyr in the most cases of depression could be important materials to analyze the metabolic background of depression or of pathological reaction to the stress, though the chemical mechanism of the phenomena is still not clear.

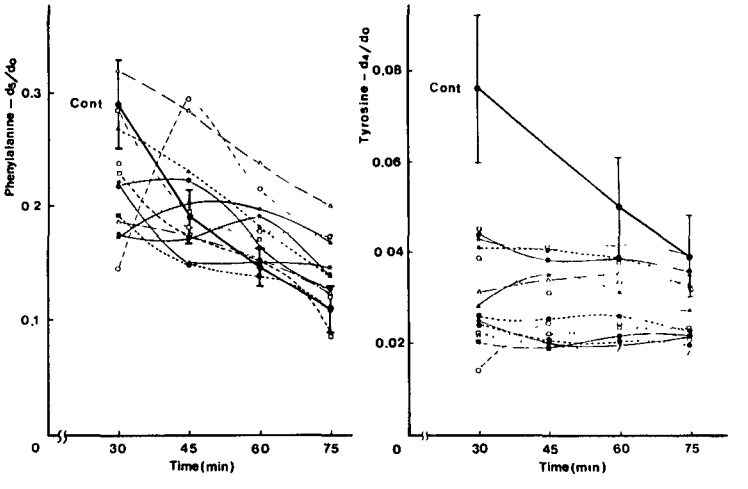


Fig. 2 Change of Phe-d_5/d_0 & Tyr-d_5/d_0 in A group of Depression

3) Infantile Autism

Recently, it is recognized that the infantile autism is a disease caused by a brain damage. Though there were many reports concerning changes of Tyr-cathcolamine metabolism or Try-serotonin metabolism, no detailed study was performed. Therefore, Phe-d_5 and Try-d_5 (5mg/kg) were administered to a typical case of autims with co-operatio of Dr. Takesada in Osaka Children's Hospital. The ratio of Tyr-d_4/d_0 after Phe-d_5 administration, and of Try-d_5/d_0 has suggested the decreased turn over rate of Tyr and Try in this case. In order to study the metabolic change of the Try-serotonin system, a method determining the turn over of free tryptophan in the blood was developed and methods determining turn over rate of serotonin and its metabolite are now under investigation.

SUMMARY

5 mg/kg of Phe-d_5 and Try-d_5 were administered orally to PKU, Heterozygotes of PKU, Depression and Infantile Ausitsm, and change of deuterated amino acids were determined exactly. In PKU and the heterozygotes of PKU, the heterogeneity were recognized based on the use of the deuterated Phe. In the most cases of monopolar depression and a case of neurotic depression, the turn over of Tyr-d_4 derived from Phe-d_5 was markedly decreased. The decrease of the turn over of Tyr-d_4 and Try-d_5 were also found in a case of Infantile Autism. It might be concluded that the use of deuterated -Phe, -Tyr, -Try, or -related compounds should be able to offer important informations of some disease which were suspected to have metabolic disturvances of cathecolamine, serotonin or some other amines.

ACKNOWLEGEMENT

The study was supported by Grant No. 80-06 & No. 81-14 from NCNMMD, of MHW Japan, and Grant from Mother & Child Health Division of MHW. We are very grateful for many technical advises from Prof. Baba, Tokyo Pharma. College.

REFERENCES

1. Matthews, H. R., et al.: Bioch. Biophy Acta 497 1-13, (1977)
2. Tokuhisa, Y., et al.: J. Nutri, Sci, Vitaminol. 26 77-85, (1980)
3. Suzuki, E.: Bulletin of the Japanese Neurochem. Society, 20 48-51, (1981)
4. Naruse, H., et al.: New Vistas in Depression. Academic Press, N.Y. in press.

WOA 4 THE STUDY OF CARBOHYDRATE METABOLISM WITH STABLE ISOTOPES. Kou-Yi Tserng and Satish C. Kalhan. Division of Metabolism, Department of Pediatrics, Case Western Reserve University at Cleveland Metropolitan General Hospital, Cleveland, OH 44109.

The use of radioactive isotope tracer in the kinetic turnover study has played a major role in our understanding of the disorders of carbohydrate metabolism and the homeostatic mechanism. However, radiation hazards associated with these tracers so far has excluded similar studies in pregnant women, children, and women of child bearing ages. There are many conditions, such as prematurity, diabetic pregnancy, and chronic uremia, in which the understanding of their carbohydrate metabolism is an important step in realizing their pathophysiological mechanisms. To those populations, stable isotope labelled compounds provide the answer.

Currently, there are a variety of labelled glucose commercially available, such as [6,6-$^{2}H_{2}$]glucose, [1-^{13}C]glucose, and [ul-^{13}C]glucose. Their enrichment in biological materials can be studied with isotope ratio mass spectrometry after combustion or enzymatic decarboxylation. Alternatively, they can be studied with gas chromatography-mass spectrometry. In the latter, the glucose is converted to penta-acetate, acetonide, butaneboronate, aldononitrile penta-acetate or alditol acetate and then analyzed with electron impact or chemical ionization mass spectrometry. Depending on the derivatives and ionization mode used, a variety of information in carbohydrate metabolism can be obtained.

These techniques have been applied in the quantitation of glucose turnover in premature infants, pregnant women, and chronic uremic patients. Dual tracers are utilized to determine the recycling of glucose in newborn infants. Recycling of glucose is also quantitized in uremic patients using single tracer before and after dialysis. The turnover rates obtained by different tracers are compared and explained by theoretical consideration.

MODELING TECHNIQUES ESTABLISH FEASIBILITY OF MINERAL METABOLISM STUDIES

C.S. Irving, A.L. Yergey, D.L. Hachey and P.D. Klein
USDA/ARS, Children's Nutrition Research Center, Baylor College of Medicine
Houston, TX 77030 and IRP, NICHD, NIH, Bethesda, MD 20205

Mineral nutritional parameters, such as 1) fraction of dietary intake absorbed, 2) urinary and fecal loss, 3) tissue distribution, 4) accretion and resorption of mineral stores, and 5) overall balance, can be evaluated in previously inaccessible infant and maternal populations by the use of stable isotope tracer methods employing mass spectrometric isotope ratiometry (MSIR). The accuracy and precision with which these nutritional parameters can be estimated is determined by the choice of such protocol components as 1) stable isotope tracer, 2) dosage level, 3) route of administration, 4) dose form, 5) sample collection sites and times, and 6) the MSIR method. Since human nutritional studies of mineral absorption and metabolism require major commitments of clinical and analytical resources, it is prudent to evaluate a priori the likelihood that the experimental design and analytical methodology chosen will be able to provide accurate and precise estimates of the nutritional parameters of interest. We describe herein a metabolic modeling technique that can be used to evaluate proposed studies of mineral metabolism.

A hypothetical study of Ca metabolism was evaluated to demonstrate the use of metabolic modeling techniques. The imaginary protocol was designed to test the hypothesis that Ca supplementation of patients in negative calcium balance would lead to positive balance and a decrease in bone Ca resorption. A constant, known Ca intake was to be maintained before and during Ca supplementation. Ca kinetics were to be evaluated in each state by administration of a single I.V. dose of ^{42}Ca and the single oral dose of ^{44}Ca. Blood samples were to be collected at 5, 10, 15, 20, 30, 60, 90, 120, 240, 480 minutes on the first day and once a day for the next 19 days. Total daily urinary collections were to be made for 20 days. Stool samples were to be collected on the first and second days only.

The first step in the metabolic modeling process was the definition of nutritional parameters and a restatement of the hypothesis in terms of the simplified kinetic model

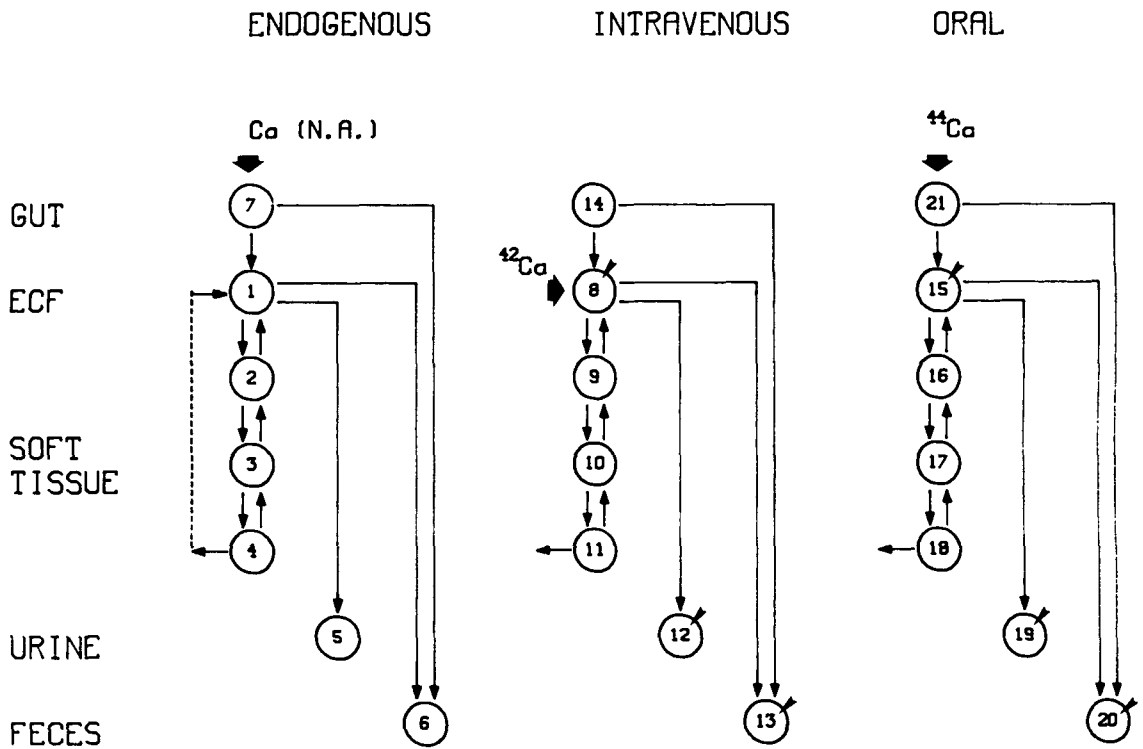


Fig. 1. Multicompartmental model of stable isotope double tracer experiment employing an I.V. dose of ^{42}Ca and an oral dose of ^{44}Ca. ➧ denotes input sites of natural abundance Ca and isotope tracers. Sampling sites are denoted by ➤ .

of calcium metabolism described by Aubert and Milhaud (Biochim. Biophys. Acta 39, 122 1960). Compartmental models of Ca kinetics in the two states were assembled using the parameters given for subject K.M. in the ^{47}Ca radioactive tracer and Ca balance study of Phang et al. (J. Clin. Invest. 48:67, 1969). Maximum dose levels of 1 mmole each of ^{42}Ca and ^{44}Ca were chosen so that the total amount of calcium administered would not exceed 10% of the first miscible Ca pool (30 mmoles) or the daily intake (20 mmoles). The model was then expanded (Fig. 1) and the SAAM-27 program was used to obtain predicted ^{42}Ca and ^{44}Ca atom % excess decay curves of plasma, urine, and stools at the specified times. The next step was the introduction of analysis noise into the simulated curves. A normal Gaussian probability distribution of "observed" values was determined for each sample using the error-free value and the standard deviation of the analytical method. A "noisy" observed value was obtained by randomly choosing a value on the distribution curve. Standard deviations for isotopic analysis by thermal ionization and conventional mass spectrometry were obtained from plots of relative standard deviation against isotope ratio compiled from published data. Multicompartmental analysis using the SAAM-27 program was then used to derive calcium nutritional parameters and their levels of uncertainty from estimates of total urinary Ca excretion, Ca intake, tracer dosage levels, and the "noisy" ^{42}Ca and ^{44}Ca decay curves. The accuracy and precision of estimates of Ca balance (Δ) and bone resorption (V_0^-) for a single evaluation are given in Table 1 for the two methods of MSIR analysis.

Table 1. Comparison of computer simulated determinations of Ca nutritional parameters in the unsupplemented and supplemented state for two methods of MSIR

Parameter	State	Model Value	Thermal Ionization	Conventional Methods
Balance (Δ)	-	-4.12	-4.12 ± 0.03	-8 ± 2
	+	2.80	2.80 ± 0.06	-1 ± 5
Resorption (V_0^-)	-	17.62	17.63 ± 0.03	18 ± 2
	+	10.52	10.50 ± 0.05	12 ± 5

CONCLUSION: The metabolic modeling technique consisting of a single simulation and analysis cycle, indicated for the hypothetical Ca nutritional study evaluated, that statistically significant differences in balance and resorption resulting from Ca supplementation would not be detected using conventional MSIR methods to measure Ca stable isotope enrichment levels; however, highly significant values for the differences would be obtained with thermal ionization measurements. Work supported by the USDA/ARS and NIH.

SIMS CHARACTERIZATION OF INDUSTRIAL ORGANIC COMPOUNDS AND POLYMERIC SYSTEMS

William L. Harrington, Bryan L. Bentz, P. Jane Gale, and Charles W. Magee

RCA Laboratories
Princeton, New Jersey 08540

An HP 5985B GC/MS has been modified to provide SIMS characterization of industrially important organic species, including some polymeric systems. Details of this modification and the performance under various conditions are described in poster paper WPB16 by these same authors. The objectives of this study were to create a sputter-system with which molecular weight and major fragmentation information could be obtained on organics dissolved in a liquid matrix and with which we could assess first-hand the demands on instrument design imposed by static SIMS analysis of solid surfaces. This paper represents a status report. The modifications carried out to date allow for high current density SIMS of liquids. We will report the results of several studies of compounds of interest to the industrial community and will summarize our conclusions about the study of organic molecules on solid surfaces by static SIMS.

Azo dyes, usually prepared as chloride salts, constitute a group of difficult-to-characterize compounds, the cations of which contain all the information on chemical identity. Because of the many by-products possible during synthesis and the fundamental instability of the azo linkage, precise characterization is necessary to assess specific shades and properties of the dyes. The exact molecular weight and principal pathways available from the liquid-matrix SIMS spectra represent major new pieces of information which aid in characterization. Janus Yellow and Janus Green B are two such dyes studied, and their spectra serve to illustrate the deductions which can be made about the stability and purity of the dyes. Figure 1 shows the positive SIMS spectrum of Janus Yellow dissolved in acidified glycerol. Note the single ion at m/e 454, corresponding to the molecular cation, and the major fragments which can be attributed to scissions of the azo linkages. Janus Green B, on the other hand, shows a cluster of ions at m/e 475, 476, 477, and 478, where 475 is the molecular cation of pure Janus Green B, as shown in Figure 2. In cooperation with J. Shabanowitz at the University of Virginia, these ions were examined individually by triple/quad collision-induced-dissociation. M/e 475 was confirmed as the molecular cation of the structure given for Janus Green B, whereas, m/e 476 was deduced to be the molecular cation of a reduced species where reduction has occurred in the phenazenium ring. M/e 477 is then the protonated "pseudomolecular" ion of the reduced species, and m/e 478 is the M+1 isotopic peak of 477.

The anions of sulfonic acids or their sodium salts were found to give structurally significant SIMS spectra. Two compounds serve to illustrate our findings: sodium disulfopropyl disulfide, $NaO_3S(CH_2)_3SS(CH_2)_3SO_3Na$, and hexadecylthiobenzene sulfonic acid, $C_{16}H_{33}S\text{-}\phi\text{-}SO_3H$. The disulfide spectrum in Figure 3 contains a strong signal at m/e 331, $(M\text{-}Na^+)^-$. The ion at m/e 309, $(M\text{-}2Na^+\text{+}H^+)^-$, corresponds to reprotonation of one of the acid groups in the completely dissociated salt. Scission at the disulfide linkage results in ions at m/e 155 and m/e 177, the proton- and sodium-attached species, respectively. CID experiments would be necessary to establish if the monosulfide is present as an impurity or as a result of fragmentation. Confirmation of the molecular weight of the hexadecyl compound was found at m/e 413, $(M\text{-}H^+)^-$, with a major fragment at m/e 188, identifying the alkyl group as hexadecyl, i.e., $(M\text{-}C_{16}H_{33}\text{-}H^+)^-$.

Pure liquids also give structurally significant ions under SIMS conditions. The spectra are of interest in their own right and are also necessary as background information if the liquids are to be used as media in which to dissolve other organic compounds. In addition to glycerol and sulfolane, two polymers, poly(propylene glycol), PPG, and poly(perfluoropropylene oxide), "Fomblin," were studied. Figure 4 shows the positive SIMS spectrum for PPG, dominated by the adduct series MH^+, M_2H^+, M_3H^+, and M_4H^+, where M in this series corresponds to the monomer unit weight. Although the polymer has an average molecular weight of ~754 (n = 13), the character of the spectrum is analogous to that of glycerol. These liquid samples also gave structurally significant negative SIMS spectra, as illustrated in Figure 5 by the spectrum of Fomblin. At low mass the spectrum is dominated by F^- and F_2^- (not shown); ions indicative of the polymer structure are observed above m/e 100. Above m/e 500, the signal-to-noise ratio is too low to provide significant information.

Attempts to study solid polymers directly were predictably futile at the present stage of instrument design. Investigation of solid polymers dissolved and mixed with glycerol was almost equally futile, resulting in only a few instances in which ions characteristic of polymer degradation were observed. During analysis of a liquid latex polymer, however, the

spectrum shown in Figure 6 was obtained. From our previous experience with sulfates and sulfonates, it was suspected that m/e 265 was $(M - Na^+)^-$ for sodium lauryl sulfate. This was confirmed by obtaining a reference spectrum of the pure compound. The peaks at m/e 293 and 321 were interpreted as the tetradecyl ($C_{14}H_{29}$-) and hexadecyl ($C_{16}H_{33}$-) analogues of the impure dodecyl salt.

Our experience with the pure liquids and with polymers leads to several observations and conclusions about the design of instruments for such analyses. Unless efficient extraction geometry is designed specifically for secondary ion collection, high current density of primary particles must be employed. This results in charging of insulating samples if a primary ion beam is used. The high current density also results in the pyrolysis of samples in which no pre-formed ions exist. In addition, line-of-sight geometries allow electrons, photons, neutrals and high-energy scattered ions to reach the detector, producing a high background. Thus, neutral beam bombardment, off-axis extraction and energy-filtering of secondary ions, and off-axis pulse counting detection appear to be of prime importance in static SIMS instrument design. Finally, the unambiguous interpretation of spectra will require the ability to collisionally dissociate sputtered ions.

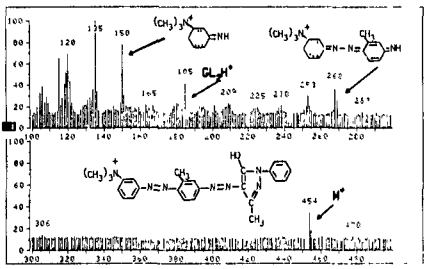


Figure 1

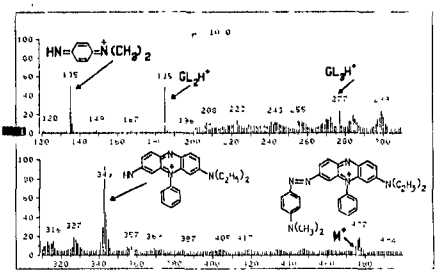


Figure 2

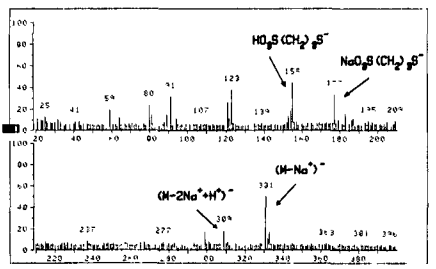


Figure 3

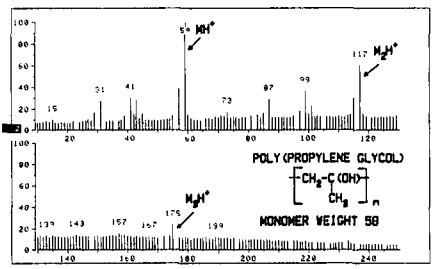


Figure 4

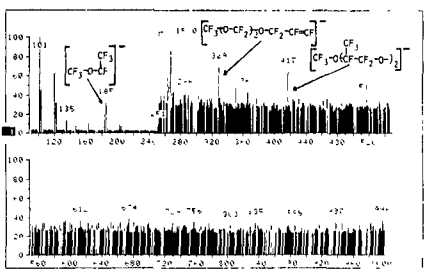


Figure 5

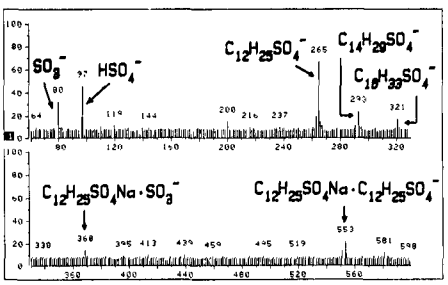


Figure 6

SECONDARY ION MASS SPECTROMETRY: APPLICATIONS TO BIOMOLECULES

K.L. Busch and R.G. Cooks
Department of Chemistry
Purdue University
West Lafayette, Indiana 47907

This paper spotlights the SIMS and LD spectra of a variety of biological compounds as vehicles for a discussion of (i) the analytical characteristics, and (ii) the underlying physical and chemical phenomena in SIMS and related methods of desorption ionization. Table 1 compares analytical characteristics of the DI methods. For molecules with zero net charge, there are two approaches to successful DI analysis. One is "reverse" derivatization to create a species with a net positive or negative charge prior to sputtering (1). The alternative is derivatization in the course of sputtering, for example, by attachment of a cation to the neutral molecule to form the cationized species (C+M). Small peptides and pyridine oximes are two classes of compounds which have been investigated in SIMS by either of these two ionization techniques, and it has been shown that the former is both more sensitive and selective.

SIMS studies on organic and biological compounds have provided significant mechanistic insights into all of DI. This paper reviews these developments with fresh examples. Among the observations are (i) three types of processes (direct desorption, anion or cation attachment, and electron ionization) lead to the parent sputtered ions, (ii) the parent species fragment in the gas phase by metastable processes to give characteristic fragment ions, and (iii) cluster (solvated) ions are generated both by accretion and by fragmentation of higher mass species (2).

The ability to determine the molecular weight of nonvolatile and thermally labile compounds has become a hallmark of DI methodology, and with high performance mass spectrometers, molecules of several thousand daltons have been successfully examined. In organic analysis, the fragmentation pattern generated by a decomposing parent ion provides additional valuable clues as to its structure. SIMS has established a broad base of data on spectral interpretation to which the unimolecular decompositions of desorbed ions can be referenced in all DI spectra.

Figure 1 illustrates the SIMS spectrum of a large organic phosphonium salt (3). Unimolecular fragmentations from the intact cation (observable with a sample loading of just a few nanograms) account for the ions observed at lower mass. The fragmentation patterns of these large cations, and of protonated and cationized species, typically show loss of small neutral fragments and the spectra are dominated by even electron ions. Evidence for the unimolecular nature of these dissociations is provided by comparison of these mass spectra with the MS/MS spectra of the mass selected parent ions (4). Isomeric compounds give distinctive spectra when the chemistry allows, as in the case of ortho interactions between substituents on an aromatic ring (3) and in the case of modified nucleosides which differ in the position of the methyl substituent on the base (5). The enterprising chemist can also devise derivatization reactions which, in addition to providing precharged species primed for desorption, act to distinguish between positional isomers (6), as in Figure 2.

Table 1 indicates that SIMS and some other of the DI methods have been used in conjunction with chromatographic separation. Several groups have developed interfaces to liquid chromatography. Our own work has concentrated on the direct desorption of ionic compounds separated by thin layer and paper chromatography (7). More recently, compounds have been desorbed directly from electrophoretograms, as in Figure 3. The spectra are almost identical with those obtained from ion bombardment of the neat sample, although one difference is the reduced abundance of cluster ions due to a matrix isolation effect. Micrograms of material are needed for this direct chromatographic detection. The joining of electrophoresis with SIMS represents an auspicious combination in that the charged nature of the analyte forms the basis of both its separation and its preferential desorption.

The role of the matrix in the DI analysis of biomolecules is not yet well characterized. Solid matrices such as ammonium chloride have been shown to be useful in obtaining SIMS spectra, and has been shown to reduce the incidence of intermolecular reactions (4) and cluster ion formation (8). Several liquid matrices have been used in SIMS with the same results. (The degree of fragmentation can also be controlled by varying the flux of the primary ion beam, a feature so far unique to SIMS (9)). Desorption from a glycerol matrix in EHD has been shown to result in low energy species; later FAB exploited this same phenomenon in particle induced desorption. The matrix used in DI should satisfy the various criteria of vacuum compatibility and persistence, dispersal and solubility characteristics,

and ideally, a simple reproducible spectrum which does not interfere with the analysis of the encapsulated sample. Fortunately, the nature of the desorption process is such that the matrix can even take the form of a chromatographic medium.

The successes achieved in ionizing larger biomolecules by fast atom bombardment (FAB) should serve to focus attention also upon its direct antecedent secondary ion mass spectrometry. More is known about the underlying processes in SIMS and a far greater variety of experiments have been performed. These and the related PD and LD methods promise to continue to make major contributions to mass spectrometry.

1. K.L. Busch, S.E. Unger, A. Vincze, R.G. Cooks, and T. Keough, J. Am. Chem. Soc., 104, 1507 (1982).
2. R.J. Day, S.E. Unger, and R.G. Cooks, Anal. Chem., 52, 557A (1980).
3. A. Ba-isa, K.L. Busch, R.G. Cooks, A. Vincze, and I. Granoth, submitted.
4. S.E. Unger, R.J. Day, and R.G. Cooks, Int. J. Mass Spec. Ion Phys., 39, 231 (1981).
5. A. Vincze, K.L. Busch, and R. G. Cooks, Anal. Chim. Acta, 136, 143 (1982).
6. S.E. Unger, A.E. Schoen, R.G. Cooks, D.J. Ashworth, J.D. Gomes, and C.-j. Chang, J. Org. Chem., 46, 4765 (1981).
7. S.E. Unger, A. Vincze, R.G. Cooks, R. Chrisman, and L.D. Rothman, Anal. Chem., 53, 976, (1981).
8. L.K. Liu, K.L. Busch, and R.G. Cooks, Anal. Chem., 53, 109 (1981).
9. S.E. Unger, T.M. Ryan, and R.G. Cooks, Anal. Chim. Acta, 118, 169 (1980).

TABLE 1

	SIMS	PD	FAB	LD	FD
SENSITIVITY					
demonstrated limit normal sample size	pg ng-ug	na ug	na ug	ng ng-ug	ng ng-ug
SPECIFICITY					
direct mixture analysis isomer differentiation	yes yes	no yes	no yes	no yes	no yes
SPEED					
acquisition time sample persistence	short long	long long	short long	short variable	short short
FLEXIBILITY					
static chrom. (PC, TLC, Eph) dynamic chrom. (HPLC)	yes yes	yes yes	??? no	no no	no yes
QUANTITATION					
internal standards	yes	no	no	no	yes
DEMONSTRATED MASS RANGE	2100	12000	3500	1500	10000

JUNE 1982

FIGURE 1

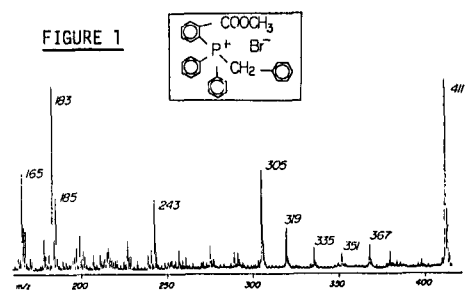


FIGURE 2

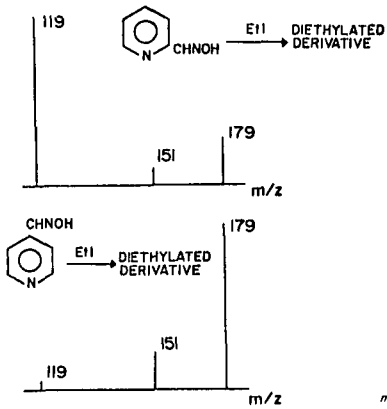
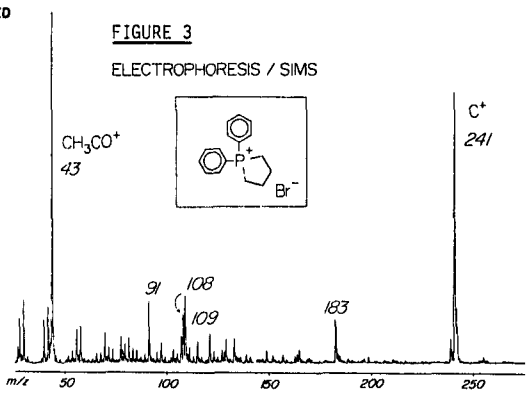


FIGURE 3

ELECTROPHORESIS / SIMS



INTERLABORATORY STUDIES OF FAB-MASS SPECTROMETRY OF SELECTED BIOMOLECULES

R.C. Murphy and K.L. Clay
Department of Pharmacology
University of Colorado Medical School
Denver, Colorado 80262

The variations in ion abundances observed in the fast atom bombardment mass spectrum of a molecule could, in principle, be due to instrumental parameters or sample-related parameters. The types of ions observed in the FAB-experiment include molecular ions (MH^+), alkali attachment ions $(M+Na)^+$, fragment ions as well as typically abundant ions from the glycerol matrix (185,277,369,461 as well as others). In order to assess the influence of instrumental parameters, which include the type of mass spectrometer, atom gun, ion source configuration, target design and accelerating potential, on the relative abundance of ions in the observed FAB spectrum, an intralaboratory investigation was undertaken analyzing the same set of biologically relevant molecules (Table 1).

Table 1
Participating Investigators

Participant	Laboratory	Mass Spectrometer
Catherine Fenselau	Johns Hopkins Medical School	Kratos MS-50
Richard Caprioli	University of Texas	Finn. 3200
William Bone	University of Virginia	Finn. 4000
Kenneth Rinehart	University of Illinois	VG 7070
Vernon Reinhold	Harvard Medical School	MAT 312
Alan Hogg	University of Alberta	Kratos MS-50/MS9
Robert Murphy and Keith Clay	Univ. of Colorado Medical School	VG 7070
K. Biemann and C. Costello	Massachusetts Inst. of Technology	MAT 731

A great deal of experience has been accrued concerning reproducibility of electron impact mass spectra from lab to lab. Caldecourt (1) observed differences in EI-mass spectra from different instruments primarily due to accelerating potential, repeller voltages and magnetic sector design. Beynon (2) reviewed the important effect of ion source temperature on molecular ion abundances. Nevertheless electron impact mass spectra can be regarded as highly reproducible from lab to lab when compared to surface ionization techniques such as field desorption and desorption chemical ionization used in the analysis of non-volatile molecules. The reproducibility in the electron impact mass spectrum of the same methyl stearate sample for this group of investigators in shown in Table 2.

Table 2
Reproducibility of Relative Abundances of Selected ions in the Electron Impact Mass Spectrum of Methyl Stearate by Investigators in Table 1.
70eV, 200° ion source temperature

	Abundance, m/z					
	74	87	143	225	298	299/298
X(n=6)	100	60.8	11.7	4.9	21.4	20.7
SEM	-	3.9	2.9	2.3	10.3	0.29
CV	-	5.3	25	47	48	1.4

In general, each laboratory received identical samples with instructions concerning solvent and amount to be loaded onto the glycerol matrix. Xenon was used for the primary atom beam and ions were recorded above m/z 200 at an arbitrary time period. After subtraction of glycerol-related ions the major ions were normalized to the most abundant ion. As an example, the major ions resultant from dihexdecanoyl phosphatidyl choline were readily discernible and fairly reproducible as seen in Table 3.

Table 3
Dihexadecanoyl phosphatidyl choline
FAB-MS

Laboratory	Relative Abundance (m/z)						MH+/277	Amt (ug)
	478	480	496	551	734	735		
2-3	10	38	24	14	100	38	0.013	2
2-6	11	38	15	9	100	43	1.940	2
2-7	22	63	53	22	100	47	0.029	2
2-8	17	47	32	9	100	44	0.500	2
2-9	45[a]	48[a]	55[a]	24[a]	100	55[a]	8.00[b]	50
2-10	18	48	43	18	100	40	0.058	2
2-11	23	28	47	22	100	41	0.090	25
2-19	25	16	64	0	100	0[c]	0.090	2
X	21	41	42	17	100	44		
SEM	3.9	5.1	5.9	2.4	-	2.1		
CV	18.4	12.4	14.2	14.4	-	4.8		

[a] Signal to noise >2
[b] m/z 277 not above background
[c] Not recorded by computer

With all the test substances there were no major ions other than glycerol adduct ions which were not observed by each laboratory. There was no correlation of glycerol adduct ions and sample-related ions for any compounds in this study. Table 4 lists the compounds under study, the ions selected for comparison, and the coefficient of variation of relative intensities.

Table 4
Reproducibility of Relative Abundances of Selected Ions in the FAB Mass Spectra of Selected Biomolecules

Compound	Major Ions m/z	Normalization ion *m/z*	Coefficient of variation *range*
ATP	530,574,622	552	18-34
Bradykinin	417,638,805,904,1045,1072	1060	10-41
Dihexadecanoyl-PC	478,480,496,551	734	12-18
GSSG	339,484,613	308	12-18
NAD	348,664	428	9,9
Sulfotaurolithocholic acid	359,566,571,587,603	376	26-48
Stachyose	343,487,505,667	325	7-19

The results of this investigation have revealed that the variations in relative abundances of ions in the FAB experiment are similar to that observed for electron impact mass spectrometry of methyl stearate. This suggests that when ions can be obtained by FAB, that the entire mass spectrum primarily reflects the actual sample, including alkali metal and impurity content rather than variation in instrumental parameters.

Acknowledgement

This work was supported in part by the National Institutes of Health (RR01152).

References

1. V. J. Caldecourt. Appl. Spectroscopy 12, 167 (1958).
2. J. Beynon. Mass Spectrometry. Chapt. 10. (Elsevier Amsterdam) 1960.

STRUCTURE DETERMINATION OF A PEPTIDE LIVER TOXIN

The poisoning of cattle and sheep by ingestion of larvae of an Australian species of sawfly (Lophyrotoma interrupta) is a serious problem in several of the grazing areas in Queensland.[1] The toxin isolated was shown to be a peptide containing the following amino acids (molar ratios are given in parenthesis): Asp(1.9), Glu(1.9), Ala(1.0), Val(1.1), Ile(0.8), and Phe(0.9). Electron impact mass spectrometry established the partial sequence of the liver toxin to be: C_6H_5CO.AlaPheValIle...[2]. The amino acid sequence of the liver toxin could be established from the positive and negative ion FAB mass spectra. However, the distinction between the C-terminal residue being Gln or i-Gli could not be made from these spectra. Treatment of the toxin with iodobenzenediacetate resulted in the conversion of the primary amide to a primary amino group.[3] The amino acid content of the rearrangement product was shown to be: Asp(2.0), Glu(1.2), Ala(1.0), Val(1.0), Ile(1.0), Phe(1.0), and 2,4-diaminobutyric acid (0.9). The new amino acid (2,4-diaminobutyric acid) can only be generated from the rearrangement of a Gln residue. Therefore, the amino acid sequence of the liver toxin has been shown to be:

$$C_6H_5CO.AlaPheValIleAspAspGluGln.$$

Analysis of the chirality of the amino acids from the liver toxin using gas chromatography with a chiral capillary column showed that the liver toxin is composed of four D-amino acids (Ala,Phe,Asp,Glu); and four L isomers (Val,Ile,Asp,Glu). Peptide fragments resulting from partial hydrolysis of the liver toxin were separated by reversed-phase HPLC, and their structures were determined by FAB-MS and amino acid analysis. Determination of the chirality of the amino acids from the relevant peptide fragments established that the liver toxin has the following structure:

$$C_6H_5CO.Ala(D)Phe(D)Val(L)Ile(L)Asp(D)Asp(L)Glu(D)Gln(L).$$

Williams, D.H.,[4]
MacLeod, J.K.,[5]
Oelrichs, P.B.,[6]
Santikarn, S.,[4]
Smith, R.J.[4]

1. Roberts, F.H.S., Qd. Agric. J., 37, 41 (1932).
2. Oelrichs, P.B., et al., Lloydia, 40, 209 (1977).
3. Radhakrishna, A.S., et al., J. Org. Chem., 44, 1746 (1979).
4. University of Cambridge Chemical Lab., Lensfield Road, Cambridge, U.K.
5. Research School of Chemistry, A.N.U., Canberra, Australia.
6. Animal Research Institute, Yeerongpilly, Queensland, Australia.

Surface Analysis of Polymers and Other Solid Materials by Fast Atom Bombardment Mass Spectrometry

R. P. Lattimer and J. B. Pausch
The BFGoodrich Research & Development Center
9921 Brecksville Road
Brecksville, OH 44141

and

Gordon E. Hansen
Middle Atlantic Mass Spectrometry Laboratory
The Johns Hopkins University School of Medicine
725 North Wolfe Street, Baltimore, Maryland 21205

Fast Atom Bombardment (FAB) mass spectrometry was developed primarily for structural analysis of polar, nonvolatile chemicals. This report describes the use of FAB-MS for a different type of analysis - surface characterization of polymers and other materials. "Surface FAB" turns out to be very similar to secondary ion mass spectrometry. In principle, there is no reason why a FAB ion source could not be used to do SIMS-type experiments. The main difference is whether the surface is bombarded with ions (SIMS) or fast atoms (FAB). Both techniques produce ions by sputtering, and the ion production mechanisms should be essentially the same with either method. FAB appears to have two principal advantages: (1) surface charging (which may be a problem in SIMS) is greatly reduced or eliminated, and (2) FAB can be carried out with a double-focusing (high voltage) ion source, which allows for extended mass range and higher resolution operation. The ability to do depth profiling may be an advantage for SIMS as compared to FAB, although it was demonstrated in a paper by Surnam at the Pittsburgh Conference.

We conducted a preliminary evaluation of the use of FAB for surface analysis of several solid materials. A Kratos MS-50 mass spectrometer was used with a Kratos DS-55 data system. The following are brief summaries of the FAB mass spectra that were obtained.

Zinc oxide powder. A Sherwin Williams zinc oxide having an organic surface coating was examined. The powder was attached to the flat copper FAB probe with double-sided sticky tape. The principal positive FAB ions were Na^+, K^+, Zn^+, $ZnOH^+$, and numerous alkyl fragment ions (e.g., $C_2H_3^+$, $C_2H_5^+$, $C_3H_5^+$). The principal negative ions were $O^{\cdot-}$, OH^-, F^- and $C_2H_2^{\cdot-}$; $ZnO_2^{\cdot-}$ was also observed at lower intensity.

Copper chloride on alumina. This catalyst powder was attached to the probe with double-sided tape. The principal positive ions were Al^+ and Cu^+, with traces of Na^+, K^+ and $AlOH^+$. The principal negative ions were $O^{\cdot-}$ and Cl^- with some OH^- and F^-.

Poly (vinyl chloride). Two powdered samples were examined. Na^+, K^+, and $C_2H_3^+$ were present in both samples. One sample apparently had trace $CaCl_2$ on the surface, as evidenced by the presence of Ca^+ and $CaCl^+$ ions. The other sample had trace copper on the surface (Cu^+ and $CuOH^+$), probably as CuO and/or Cu_2O. The negative FAB spectra were quite simple; both samples gave abundant Cl^- and $C_2^{\cdot-}$. A sample of chlorinated PVC gave a FAB spectrum not noticeably different than PVC.

Rubber compounds. Two black-loaded rubber stocks were examined. The samples were cut into discs about 5 mm across and 1-2 mm thick. The samples were then attached to the probe with double-sided tape. One sample gave strong positive ion FAB spectra for several minutes. The early spectra showed mostly alkyl fragment ions with some aromatic ions (m/z 77, 91, 106). These ions probably arose from compounding ingredients (e.g., oil), which had bloomed to the surface. In later scans (5-6 minutes into the run), Na^+ and K^+ became dominant.

Another rubber sample contained a surface bloom of ozonized antiozonant (dioctyl-p-phenylenediamine). The positive ion FAB spectrum looked very similar to the other sample, except that aromatic ions from the antiozonant were more intense (m/z 77, 93, 118, 136, 182 et al.).

The following general conclusions can be made regarding the nature of "surface FAB" analysis: (1) the spectra are very similar to static SIMS spectra; (2) the spectra are relatively intense and long-lasting; (3) surface charging does not seem to be a problem; (4) the technique is very sensitive, especially to traces of elements such as Na, K, O and F; and (4) surface FAB is a highly degradative technique. It appears that surface analysis by FAB should be useful in a number of applications, including qualitative characterization of polymers; identification of polymer side-chains; investigation of surface impurities, coatings and blooms; studies of polymer surface reactions or degradation; and investigation of inorganic materials (e.g., catalysts, pigments, and fillers).

RELATIVE YIELDS OF POSITIVE IONS SPUTTERED FROM SILICIDES: Frank G. Satkiewicz, The Johns Hopkins University, Applied Physics Laboratory, Laurel, MD, 20707.

Secondary ion mass spectrometry (SIMS) employing a sputter-ion source is a very useful analytical technique for investigating the composition and distribution of atoms in solids. To obtain quantitative results, a knowledge of ion yields is necessary. The ion yield for atomic species ranges over several orders of magnitude, and for a given element, depends on factors such as type of instrument and instrument conditions, the nature and energy of the primary beam, and the matrix from which the ions are sputtered. Quantitative SIMS analysis thus requires careful attention to experimental parameters and the use of calibration standards. Very often, standards are either not available and/or do not have the same concentration level or matrix as the sample being studied. In an effort to determine the amount of calibration necessary, experiments on sputtering a variety of materials have been underway at APL. These have included metals and glasses (1,2). The current interest in silicides has arisen from the study of thin film polycrystalline silicon being deposited at APL for solar cell application (3). Estimates of the impurity levels in the films were obtained using the relative ion yield factors obtained from the sputtering of glasses of known composition.

The detection limits for many impurities commonly found in Si films using GCA IMS 101B double focusing instrument SIMS is about 5×10^{17} atoms/cm^3 for sputtering with argon and about 2×10^{16} with argon and the sample surface flooded with oxygen. For many elements the solubility limit in silicon is far below either of these figures, so what is being detected is probably an excess precipitated in the silicon matrix as silicides. It was therefore of interest to determine the relative ion yields of X^+ from metallic silicides and to compare them with those previously determined for the glasses. The following silicides were sputtered with a defocused beam of 10 keV Ar^+ ($\sim$ 100 μA/cm^2): $CaSi_2$, $TiSi_2$, V_3Si, VSi_2, $CrSi_2$, FeSi, $FeSi_2$, Ni_2Si, $CoSi_2$, Cu_5Si, $BaSi_2$, and $TaSi_2$.

Characteristic fragmentation patterns were obtained from polyatomic spectra. The intensity fractions of XSi^+, X_2^+, and XSi_2^+ (excluding X^+ and Si^+ from the sum of intensities) showed smooth changes from $Z = 20$ to 27 for XSi_2 silicides suggesting possibility of periodicity in the yields of polyatomic ions analogous to X^+ from the elements.

One of the most difficult problems in determining ion yields is to take into account the influence of both internal and external sources of oxygen. Internal oxygen is important because the silicides used in this investigation were found to differ considerably in their bulk oxygen content. This was evaluated from several approaches including comparison of selected ratios such as XO^+/XSi^+ and $XSiO^+/XSi^+$. The silicides could be ordered in terms of decreasing oxygen content. This was complicated by the possibility that X-O and Si-O bonding extent varies from silicide to silicide.

To investigate the external oxygen influence, the partial pressure of oxygen in the chamber was varied and the effect on the matrix species intensities X^+, Si^+, and O^+ was determined. The energy window was set at 250 $\pm$ 25 eV. The resulting curves were not parallel and the relative ion yields of X^+ to Si^+ ranged from a factor of 10 for VSi_2 to almost no change for $CoSi_2$. The curves for all the silicides flatten at higher pressures making yield comparisons more reproducible. The effect of added oxygen on the mean energy, $\bar{E}$, (calculated from the initial secondary ion energy distribution curves) of X^+ and Si^+ were obtained. In general, oxygen narrows the distribution (smaller $\bar{E}$). There is also a correlation between the lower values of $\bar{E}$ for Si^+ in the "no oxygen" case and the higher population of oxygen-bearing species observed in the polyatomic ion spectra.

The values of $\bar{E}$, and the value of the maximum intensity, I_m, observed in ion energy distribution curves were used in the following expression to obtain relative ion yields ($Y_{Si^+} = 1$):

$$Y_{X^+} = \left(\frac{n_{Si}}{n_X}\right)\left(\frac{(I_m)_{X^+}}{(I_m)_{Si^+}}\right)\left(\frac{F_X}{F_{Si}}\right)\left(\frac{\bar{E}_{X^+}}{\bar{E}_{Si^+}}\right) \qquad (1)$$

where n_{Si} is the number of Si atoms, n_X the number of X atoms in the silicide, and F_X and F_{Si} are isotope correction factors. In place of $\bar{E}$ in Eq. 1, the area under the distribution curve in the energy range of 0-500 eV could also be used. Table I shows the values of Y from the glasses and silicides. The values for the glasses were adjusted to give on the average,

a ratio of [(Y_{X+}) silicide (O_2)] to [(Y_{X+}) glass] of unity. The results from the silicides with O_2 in the background are in somewhat closer agreement with those from the glass. The agreement in yields is considered satisfactory despite the large differences in concentration and matrices.

A tentative conclusion that can be drawn from this work is that it is possible (at least in the case of silicides and Si - based glasses) to use a set of relative ion yields derived from a glass to determine the amount of trace elements in a silicide or vice-versa. Further work is planned on borides and carbides to see whether these fit into the same pattern.

REFERENCES

1. F. G. Satkiewicz, "Initial Energy Distribution of Secondary (+) Ions from the Sputtering of Metals with 10 keV Ar^+," Proceedings of the 27th Annual Conference on Mass Spectrometry and Allied Topics, Seattle, WA, pp 303-304,(1979).

2. F. G. Satkiewicz, "Relative Yields of Positive Ions Sputtered from Several Glasses," Proceedings of the 25th Annual Conference on Mass Spectrometry and Allied Topics, Washington, D. C., pp 312-314,(1977).

3. C. Feldman, F. G. Satkiewicz, and N. A. Blum, "Vacuum-Deposited Polycrystalline Silicon Solar Cells on Foreign Substrates," Thin Solid Films, 90, pp 461-471 (1982).

TABLE I

Comparison of Relative Ion Yields from Silicon Based Glasses and Metallic Silicides

Species	Glasses*	Silicides**	
		O_2 (10^{-5} Torr)	"No O_2"(5×10^{-8} Torr)
O	0.026	-	-
Mg	5.8	-	-
Al	7.1	-	-
Si	1.8	1	1
Ca	11.1	17.1	14.2
Ti	6.4	3.0	13.2
V	-	1.9	8.3 (V_3Si)
V	-	3.0	2.9
Cr	-	2.1	9.4
Mn	2.9	-	-
Fe	1.3	1.3	2.7 (FeSi)
Fe	1.3	2.6	1.4
Ni	-	0.74	0.19 (Ni_2Si)
Co	1.1	1.2	0.73
Cu	0.42	0.28	0.27 (Cu_5Si)
Zn	0.029	-	-
Zr	5.7	-	-
Ba	10.0	10.2	13.3
Ta	0.86	0.56	0.59
Pb	0.16	-	-
Bi	0.12	-	-

*NBS K-glasses (~ 20 at. % Si)

**Silicides not having the stoichiometry of XSi_2 are in ( ).

MASS DISCRIMINATION EFFECTS IN SIMS

J. OKANO and H. NISHIMURA
College of General Education, Osaka University
Toyonaka, Osaka 560, JAPAN

SIMS has been applied to studies of isotope geology, in which a very high accuracy is necessary for the isotope ratio measurement. However, the accuracy of SIMS seems sometimes to be poor compared with that of the results obtained by mass spectrometry with electron bombardment ion sources or with surface ionization ion sources. The purpose of this study is to clarify the causes which lower the accuracy of SIMS and to look for the way of the improvement.

The apparatus used for this work is Hitachi IMA-2A ion microprobe mass analyzer. Samples were metals of magnesium, titanium, nickel, copper and silver, an alloy of nichrome (Ni 80 at %), and a mineral of niccolite (NiAs). A surface of each sample was polished with alumina powder or an emery paper and cleaned ultrasonically in aceton. The surface was bombarded by 12-17 keV O_2^+ ions with normal incidence. The current density and the spot diameter on the sample surface were 1∿10 mA/cm^2 and 100∿250 μm, respectively. Before the isotope ratio measurements, the energy distribution of secondary ions was measured every time and, in usual, the energy window was set at the maximum ion current. The measurements of the isotope ratio have been carried out automatically with a micro computer.

The isotopic ratios of $^{24}Mg^+/^{25}Mg^+$, $^{26}Mg^+/^{25}Mg$, $^{46}Ti^+/^{48}Ti$, $^{52}Cr^+/^{53}Cr^+$ were measured as a function of the bombarding time of the primary ions. They were constant within 5 ‰. Fig.1 shows the energy distribution of $^{48}Ti^+$. Three energy windows with 12 eV widths are shown in the figure. Mass discrimination effect was examined for each energy window. Fig.2 shows the mass discrimination of titanium isotopes. The δ in the ordinate represents the difference in percent between the measured isotopic ratio and the reference ratio in the literature.[1] The results show that low energy component has a slightly high mass discrimination compared with middle and high energy components. Similar result was also obtained for chromium isotopes. The mass discriminations per one percent mass difference were, Mg: 0.89 %, Ti: 0.48 %, and Cr: 0.73 %. The mass discrimination differs from one element to another, so that usually used $\sqrt{m}$ correction can not be applied in SIMS.

In Fig.3 and Fig.4, variations of the measured isotopic ratios with ion bombarding time were shown for nickel. In the beginning of the ion bombardment of a fresh surface, the isotopic ratios, $^{58}Ni^+/^{60}Ni^+$, $^{60}Ni^+/^{62}Ni^+$, $^{61}Ni^+/^{62}Ni^+$, were low, then they increased gradually with time. After several tens minutes, they reached nearly constant values. Contributions of interference peaks, which might give these variations, were throughly examined and they were estimated to be less than 1 ‰. The parallel tendency in these variations of the three sets of the isotopes seems to exclude the interference effect. Similar variations were also observed for the isotopic ratios of $^{63}Cu^+/^{65}Cu^+$ and $^{107}Ag^+/^{109}Ag^+$. The variation of the nickel isotope ratio was small in case of the nichrome sample and there was no variation for the niccolite sample. Nickel, copper and silver have the f.c.c. structure, while the nichrome is the mixture of the f.c.c. and b.c.c. structures and the niccolite is the h.c.p. structure. The variation of the measured isotopic ratio will be due to the mass fractionation which occurs through ion-induced diffusion process in the metals of f.c.c. structure.

REFERENCE

1) J. E. Hogg, Can. J. Chem., 32, 1039 (1954)

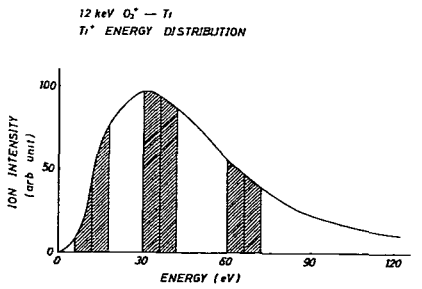


Fig.1 Energy distribution of $^{48}Ti^+$ secondary ions emitted from a titanium metal sample

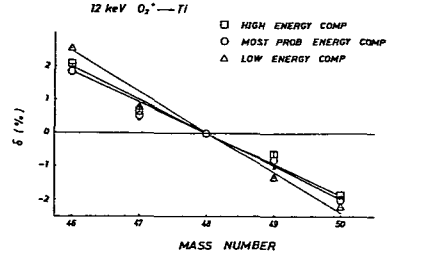


Fig.2 Mass discrimination of titanium isotopes
sample : titanium metal

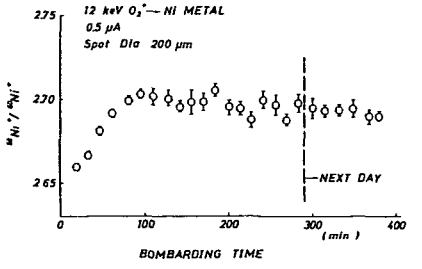


Fig.3 Variation of $^{58}Ni^+/^{60}Ni^+$ ratio as a function of ion bombarding time
sample : nickel metal

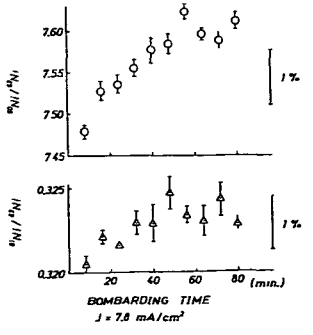


Fig.4 Variation of $^{60}Ni^+/^{62}Ni^+$ and $^{61}Ni^+/^{62}Ni^+$ as a function of ion bombarding time
sample : nickel metal

QUANTITATIVE SIMS ANALYSIS OF TRITIUM PERMEATION BARRIER OXIDE FILMS GROWN ON LASER MODIFIED INCOLOY SURFACES*

W. H. Christie and R. E. Eby
Analytical Chemistry Division
Oak Ridge National Laboratory
Oak Ridge, TN 37830

Secondary ion mass spectrometry (SIMS) was used to quantitatively depth profile oxide films that were grown on steam oxidized Incoloy 800 surfaces. These in-situ formed oxide coatings have been proposed as tritium permeation barriers for candidate heat exchanger materials that would be used in a thermonuclear fusion power reactor. Quantified SIMS data, using indexed sensitivity factors showed that surface pretreatment including milling, polishing, electropolishing, annealing and cold working affected the composition of the oxide film that subsequently forms on the Incoloy surface. As a result of these findings, laser annealing was used as a surface modification technique. Oxide films grown on these surfaces were studied using SIMS analysis. In all cases, the oxide was thinner and more Cr- and Mn-rich in the laser annealed regions relative to the unannealed region. The annealed surface led to favorable corrosion properties for the material.

In this study two types of SIMS profiles were obtained from the Incoloy specimens. When only the oxide film composition was of interest, the sample surface was oriented normal to the sputtering beam. When it was desirable to study sub-surface alteration of the matrix material below the oxide film, the samples were mounted in epoxy so that a transverse cross section was presented for analysis. Samples mounted in this fashion were polished to a smooth metallographic finish prior to analysis. Optical microscopy of a transverse cross section of one of the as-received specimens revealed morphological changes extending 30 to 50 μm below the outer surface. This damage appeared to be a result of the hot extrusion process used in manufacturing Incoloy 800. Subsequent samples were treated to remove this region prior to oxidation and SIMS analysis. Typical oxidation conditions used were 0.94 atm steam at 660°C for times ranging up to 1560 h.

We have prepared suitable indexed sensitivity factor (SF) response curves by recording ion yields from analyzed Incoloy 800 as the O_2 pressure was varied in the sputtering region. We monitored both the CrO^+/Cr^+ and FeO^+/Fe^+ as indexing ratios. Plots were made of the SF's for Al, Si, Ti, Cr, Mn and Ni relative to Fe ≡ 1 versus both indexing ratios. In samples showing low Cr concentrations the FeO^+/Fe^+ ratio was used as the index. Sensitivity factors indexed in this fashion were then used to quantify all subsequent depth profile data obtained from the oxide films studied.

Incoloy 800 is a high strength, heat resistant material well suited for application in heat exchangers. Although this material is considered to be corrosion resistant, we have shown via SIMS analysis that pretreatment of the material strongly influences the type of oxide formed under steam exposure conditions. In this work it was shown that in general cold working and electropolishing led to thick, scaly oxides consisting primarily of Fe, whereas annealed material tended to form thin, adherent oxides rich in Cr and Mn. The different oxidation characteristics of the as-received tabs and the electropolished tabs are probably due to the presence of a thin oxide coating already present on the as-received material prior to the steam oxidation experiments. This Cr-rich film probably inhibited the formation of iron oxides.

Laser annealing was then studied as a surface modification technique that might have a beneficial effect in terms of the type of oxide that would form on the surface during steam oxidation. In this work electropolished samples were irradiated in air with Q-switched ruby laser (λ = 0.694) pulses of energy density 3 J cm^{-2}, and pulse durations of approximately 20 x 10^{-9} sec. On each specimen a region approximately 0.5 cm^2 was irradiated, which then allowed direct comparison of the annealed regions with unannealed regions on the same sample.

*Research sponsored by the U. S. Department of Energy, Division of Basic Energy Sciences, under Contract W-7405-eng-26 with the Union Carbide Corporation.

Oxidation was carried out for 48, 144 and 528 h on three equivalent laser annealed specimens. The observed surface enrichment of all components except Fe and Ni suggest that a thin (<10 nm) oxide film was formed by the in-air laser annealing treatment. For all three steam exposure times employed, the unannealed regions showed thick, Fe rich, scaly oxides. SIMS depth profiling, performed normal to the specimen surface, sputtered only through part of this thick oxide. The oxide in the annealed regions was thin enough so that the sputtered technique provided a complete depth profile of the film.

In all cases the oxide was thinner and more Cr and Mn rich in the annealed regions relative to the unannealed regions. It was noted that the oxide in the annealed region after 24 h exposure was very rich in Cr (66 atom %), while after 144 h the surface of the oxide was Fe rich, and after 528 h the oxide was again rich in Cr. On the basis of earlier work in this laboratory on conventionally annealed material, an initial iron oxide would be expected, which would later spall, leaving a Cr and Mn rich oxide on the surface. The initially high Cr content of the oxide in the laser annealed region may be due to the very thin oxide formed by the in-air laser annealing treatment, which could then initially have a protective effect against iron oxide formation. However, after 144 h exposure the iron oxide did form, and by 528 h this oxide had almost completely spalled leaving behind an oxide rich in Cr and Mn.

The relationship between type of oxide formed and observed tritium permeation inhibition is not well understood at this time. Good correlation exists between oxide composition and barrier effect in some cases. Work is continuing in this laboratory to identify oxide species and their specific relationship to creation of a tritium permeation barrier. A new application of the laser annealing technique was tested for improving the corrosion resistance of Incoloy 800. This technique, which melts the surface of the alloy and quenches it very rapidly, produced a well annealed surface with the bulk of the alloy unchanged. The annealed surface was shown to be more resistant to steam oxidation, which demonstrates its improved corrosion resistance as compared to the unannealed material.

SIMS CHARACTERIZATION OF INORGANIC COMPOUNDS

Gene R. Sparrow, Advanced R&D, Inc., St. Paul, Minnesota

SIMS is still much in its infancy, although its use and application is becoming common and widespread. Professor Benninghoven has pioneered much of SIMS, especially in the areas of static methods and identification of organic compounds on surfaces more recently. Other laboratories, including Navy Research Laboratories, Purdue, and Penn State, have provided substantial additional information concerning SIMS of organic compounds, but presently extensive work has not been done regarding inorganic compounds on surfaces. In general, only elemental identification is accomplished.

SIMS is one of the few techniques which has the potential for determining the molecular structure of materials on surfaces. Our Laboratory has directed extensive efforts at improving both qualitative and quantitative measurements of inorganic compounds on surfaces. The major objectives of these studies are listed below:

1. To enable positive qualitative identification of inorganic compounds on surfaces.
2. To establish Ion Stability Trends & Sputtering Mechanisms.
3. To provide improved Quantitative Methods by SIMS.
4. To determine the effect of Ion Beams on Inorganic Compounds.
5. To provide a reference data base for automatic computer Search/Identify routines.
6. To provide further understanding and information on the SIMS process and Sputtering Mechanisms.

EXPERIMENTAL & INSTRUMENTAL:

Approximately 60 common, pure inorganic compounds have been investigated. Although most of these were powders, the investigations will include analysis of these compounds in the following forms:

Pure Powders	Pressed Pellets
Deposits from Solutions onto Metals	Single Crystals
Deposits from Mixed Solutions	Mixed Powders

Studies are being conducted using both an Extranuclear (ENQ) (1 to 1023 amu) and a UTI (1-300) quadrupole equipped with identical secondary ion prefilters. The UTI SIMSis a 3M/KRATOS Model 535 BX ISS/SIMS system with ion gun and prefilter at 90 . The ENQ has very similar geometry and vacuum. In general, the vacuum system background pressure was in the range of 10^{-8} to 10^{-9} Torr prior to analysis.

Spectra were recorded at four differend sets of instrumental conditions:

$^{4}He^{+}$ at 2 KeV	$^{40}Ar^{+}$ at 2 KeV
$^{4}He^{+}$ at 5 KeV	$^{40}Ar^{+}$ at 5 KeV

All remaining instrument parameters were held constant during analysis. NaCl was used periodically as a reference to calibrate prefilter settings and to establish a consistent gain factor between high mass and low mass for the electron multiplier (CEM).

All spectral data were acquired using a Tracor/Northern Multichannel Analyzer and signal averaging of approximately 32 scans of 10 seconds each. All data were automatically stored on magnetic cartridges.

RESULTS:

Figure 1 shows the raw data from a typical spectrum of KCl. One such spectrum was generated for each different voltage or probe gas, and data were tabulated to 7 orders of magnitude in sensitivity. All spectra were then normalized to 100 as the most intense peak (Figure 2), and plotted as 3-color bar graphs on a linear scale (Figure 3), and on a 6-order Semi-logarithmic Scale (Figure 4). Pertinent physical-chemical information, bond length, bond strength, ionization potentials, etc., were assembled and correlated with corresponding ratios of various cluster ions from selected compounds.

SUMMARY:

Approximately 60 compounds have been subjected to systematic SIMS analysis, and a compilation of representative spectra has been initiated. Several types of compounds such as sulfates, nitrates, and especially carbonates have been observed to decompose rapidly and extensively to oxides when exposed to the ion beam. Rough correlations have been observed between ion cluster ratios such as M_3X_2/M_2X vs. ionization potential and bond energy.

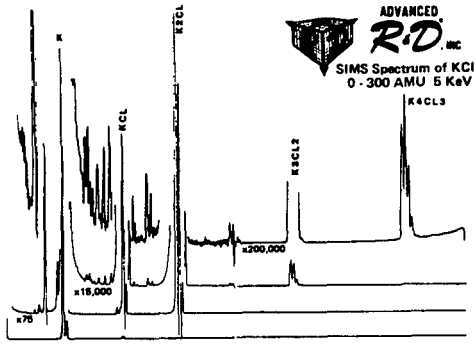
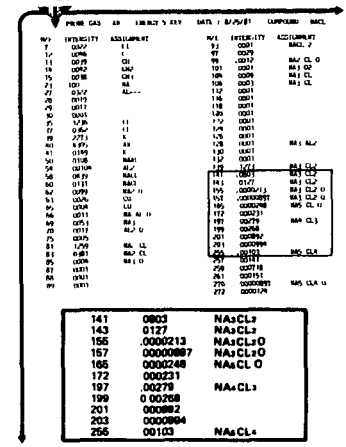


Figure 1 Raw Data KCl Ar^+ 5 Kev



141	0803	$NaCl_2$
143	0127	$NaCl_2$
155	.0000213	$NaCl_2O$
157	00000897	$NaCl_2O$
165	0000248	NaCl O
172	000231	
197	.00279	$NaCl_3$
199	0 00268	
201	000882	
203	0000994	
256	00103	$NaCl_4$

Figure 2 Tabulation NaCl Ar^+ 5 Kev

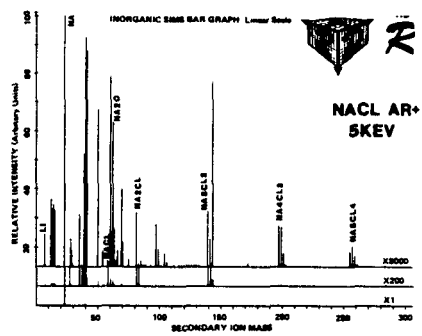


Figure 3 Linear Scale NaCl

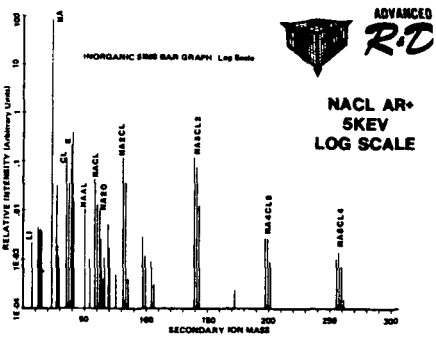


Figure 4 SemiLog Scale NaCl

WOC 1 SIGNALS, NOISE, SENSITIVITY AND RESOLUTION IN ICR SPECTROSCOPY; M. B. Comisarow; Chemistry Department, University of British Columbia, Vancouver, B. C., Canada V6T 1Y6

The fundamental aspects of the title subjects will be discussed in a coherent fashion. The ICR signal is derived from the rotating electric monopole signal model (1) and the temporal dependence of the monopole is conveniently discussed in terms of relaxation mechanisms. The relaxation mechanisms are classified according to their homogeneous or inhomogeneous nature. A quantitative assessment of the relaxation mechanisms is made and related to the ICR resolution. The mechanism which limits the resolution of marginal oscillator-type ICR spectrometers is resistive damping. For FT-ICR spectrometers, ion-ion repulsion and magnetic field inhomogeneities are resolution limiting. The sources of electronic noise in ICR spectrometers are discussed. Knowledge of the noise sources can be used to derive design principles which minimize noise and maximize ICR sensitivity.

(1) M. B. Comisarow, J. Chem. Phys., 69, 4097, (1978)

FOURIER TRANSFORM ICR SPECTROMETER USING HIGH FIELD SUPERCONDUCTING MAGNET

M. Allemann, Hp. Kellerhals
Spectrospin AG, Fallanden, Switzerland

and

K.P. Wanczek
Inorganic Chemistry, University, Bramen, West Germany

A Fourier transform ICR spectrometer is described equipped with a superconducting magnet with 4.7 T field strength.[1] (Bruker BZH-200 WB/A). For optimum field homogeneity a set of super-conducting shim coils is activated, yielding a residual field variation of less than 10^{-5} in the active volume. A cubic cell is used, constructed of nonmagnetic materials. With a turbomolecular pump pressures less than 5×10^{-9} Torr can be reached. The spectrometer can be operated in a small band and a broad band mode. Fourier transform or rapid scan can be used to obtain spectra. Both are carried out with a Bruker ASPECT 2000 computer, which also controls the spectrometer.

Due to the high magnetic field very high resolution and long trapping times are reached. At 10^{-8} Torr the trapping efficiency is 30% for 13.5 h trapping time. At m/e 18 (H_2O^+) a resolution of $m/\Delta m > 10^7$ and for m/e 166 ($C_2Cl_4^+$) of $m/\Delta m > 1.8 \cdot 10^6$ can easily be obtained.

Due to the drift motion of the ions in the cell with frequency ω_d side bands with frequencies $\omega_{eff} \pm n\,\omega_d$ are observed.[2] ($n = 1,2$, ω_{eff}: effective cyclotron frequency of the main peak). The intensity of the side bands is about 5% of the cyclotron peak.

Applying the three-dimensional quadrupolar approximation for the electric field:[3]

$$V(x,y,z) = \tfrac{1}{2}(V_t - V_o) + (V_t - V_o)(-\alpha(\tfrac{x}{a})^2 - \lambda(\tfrac{y}{a})^2 + \beta(\tfrac{z}{a})^2 - \gamma) \qquad (1)$$

the position of the side bands can be described. V_t is the trapping potential, V_o is the potential of the other four cell plates, $\alpha,\beta,\lambda,\gamma$ are constants, defined by the cell geometry. For the trapping frequency one obtains:

$$\omega_t = \left(\frac{2\beta e}{ma^2}(V_t - V_o)\right)^{\frac{1}{2}} \qquad (2)$$

and for the drift frequency:

$$\omega_d = \frac{2(\alpha\lambda)^{\frac{1}{2}}}{a^2 B} (V_t - V_o) \qquad (3)$$

where a is the distance between two parallel cell plates.

For the high frequency side band a frequency ω_R is calculated:

$$\omega_R = (\omega_c^2 - \omega_t^2)^{\frac{1}{2}} + \omega_d \qquad (4)$$

inserting (2) and (3) for ω_t and ω_d respectively and expanding the square root one obtains

$$\omega_R = \omega_c + \omega_{cor} \qquad (5)$$

where ω_R is small compared to ω_c. Therefore ω_R is in very good approximation:

$$\omega_R = \omega_c = \frac{eB}{m} . \qquad (6)$$

In the mass range m/e 18 to 169 the m/e ratio calculated with the aid of the high frequency side band (6) agrees better than 70ppm with the literature values. For this calculation the magnetic field inside the ICR cell was determined including the corrections suggested by Pendleburg.[4] Also the linear dependence of the frequency difference between side bands and main peak $\Delta\omega$ on $V_t - V_o$ can be shown experimentally.

If B and ω_{cor} are chosen as free parameters which can be determined from experimental data the agreement with the literature values is now within 1.5ppm average error in the m/e range 18 to 169.

The deviation of 60ppm between m/e values calculated with (6) and the literature values may be due to small uncertainties in the determination of the magnetic field inside the ICR cell, because for this measurement a stainless steel flange has to be removed to insert the NMR probe utilized. Furthermore the magnetic field of the filament may produce a disturbance large enough to account for the deviation. The frequency shift caused by space charge is only in the order of a few ppm.[5]

If B and ω_{cor} are introduced as free parameters a high-precision mass calibration can be obtained using the side bands. It is stable for several days due to the stability of the superconducting magnet.

References

1. M. Allemann, Hp. Kellerhals and K.P. Wanczek, Chem. Phys. Lett. 75 (1980) 328.

2. M. Allemann, Hp. Kellerhals and K.P. Wanczek, Chem. Phys. Lett. 84 (1981) 547.

3. T.E. Sharp, J.R. Eyler and E. Li, Int. J. Mass Spectrom. Ion Phys. 9 (1972) 421.

4. J.M. Pendleburg, Rev. Sci. Instr. 50 (1979) 535.

5. R.T. McIver, E.B. Ledford and R.L. Hunter, J. Chem. Phys. 72 (1980) 2535.

FOURIER TRANSFORM MASS SPECTROMETRY: A NEW APPROACH TO MS/MS

Sahba Ghaderi, Robert B. Spencer,
Richard E. Hein and John Marra;
Nicolet Instrument Corporation, Madison, WI 53711

Fourier transform mass spectrometry (FT/MS) possesses features that make it a powerful and versatile technique for separation and structure study of organic molecules. Among these are the capabilities of selective ion ejection, long ion trapping time and simultaneous ion detection. Combination of these features provides a means for obtaining collision-induced dissociation (CID) and MS/MS spectra easier and faster than conventional tandom mass spectrometers. This does not require any modifications of the basic instrument and is accomplished by setting up the experimental parameters via some simple computer commands. Ejection of all ions but the ion of interest is followed by excitation of that ion in a collision gas medium and simultaneous mass analysis of the resulting fragment ions. Selectivity, high resolution and efficiency of ion ejection in FT/MS are of key importance to CID - MS/MS experiments.

Due to high ion trapping efficiency of FT/MS instrument, MS/MS experiments can be performed at low pressures in the 10^{-7} to 10^{-6} torr range. It is also possible to obtain CID or MS/MS spectra without the use of a collision gas. Sample neutral molecules can serve as the collision gas if proper reaction time is selected. Figure 1 shows the sequence of events for a MS/MS experiment. All timings, frequencies and rf amplitudes are easily programmed and computer controlled. The first and second rf are used to eject the ions with masses lower and higher than mass ion of interest. The third rf is for exitation and collisionally induced decomposition of the selected ion. The last rf is for excitation of the mass range covering the product ions and is followed by simultaneous ion detection. The first delay is used for chemical ionization and the second delay is the reaction time for CID experiments. Figure 2 shows an example of MS/MS spectra using the FT/MS instrument. The top figure is an EI spectrum of 2:1 mixture of dodecane and acetophenone at a total pressure of 3×10^{-7} torr. Peaks at 105 and 120 are for acetophenone. The middle spectrum is taken after ejection of all ions but molecular ion of acetophenone. The bottom spectrum shows formation of fragment ion m/z 105 after excitation of m/z 120. No collision gas is used in this experiment.

The sequential nature of the FT/MS operation makes it possible to perform higher degrees of separation such as MS/MS/MS experiment, where low pressure of operation results in high resolution MS/MS up to 50,000 on the product ions.

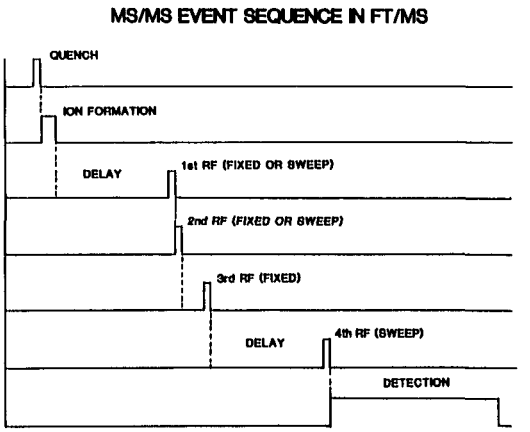


Figure 1.

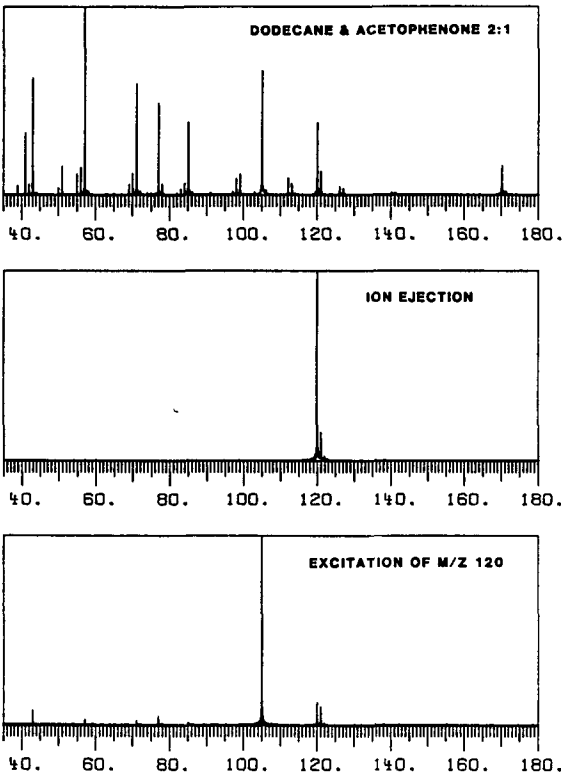

DODECANE & ACETOPHENONE 2:1
40. 60. 80. 100. 120. 140. 160. 180.
ION EJECTION
40. 60. 80. 100. 120. 140. 160. 180.
EXCITATION OF M/Z 120
40. 60. 80. 100. 120. 140. 160. 180.

Figure 2.

WOC 4 DATA TREATMENT OF DISCRETE FOURIER SPECTRA;
C. Giancaspro and M. B. Comisarow; University of British Columbia, Vancouver, B. C., Canada V6T 1Y6

Fourier spectroscopy presents data in the form of discrete spectra which must be further treated to obtain the maximum amount of spectroscopic information. One procedure which can be used to maximize the information content of discrete Fourier spectra is called zero-filling. This procedure has recently been examined in a systematic manner and maximum errors in intensity and frequency have been analytically derived (1). A second procedure for treating discrete Fourier spectra is called interpolation.In this procedure a simple function is fitted to a few points from the discrete spectrum. This procedure has a residual error which results from the mismatch between the simple fitting function and the complex continuous lineshape. The error can be analytically derived for various fitting functions and different forms of discrete Fourier spectra. It is possible in many realizable experimental cases to interpolate exactly by proper choice of the fitting function. The importance of these interpolation procedures in mass spectrometry in general and FT-ICR spectroscopy will be emphasized. Applications to FT-NMR spectroscopy will also be mentioned.

1. M. Comisarow and J. Melka, Anal Chem, 51,2198, (1979)

COMPLEX ORGANIC MIXTURE ANALYSIS USING COMBINED CAPILLARY GC-FTIR-FTMS

Robert L. White, Gary N. Giss, and Charles L. Wilkins
Department of Chemistry
University of California, Riverside
Riverside, California 92521

As a result of continuing improvements in gas chromatography-Fourier transform infrared (GC-FTIR) spectrometers, it is now possible to carry out "on-the-fly" SCOT capillary column GC-FTIR measurements on samples present in quantities of less than 100 nanograms. This increased sensitivity has made even more logical the linkage of GC-FTIR systems with mass spectrometers in order to exploit the complementary information that would thus become available. Early last year, we reported our first successful demonstration of such a system, linking a Kratos MS-50 double focussing mass spectrometer with a Nicolet 7199 GC-FTIR (1). Subsequently, we linked the same infrared system to a Kratos MS-80 mass spectrometer and reported application of the resulting GC-FTIR-MS system to analysis of peppermint oil (2,3). Others, using similar approaches have also linked quadrupole MS systems with other FT-IR spectrometers (4,5). In the present work, we have succeeded in interfacing a Nicolet FT/MS-1000 Fourier transform mass spectrometer with the Nicolet 7199 GC-FTIR system (Figure 1).

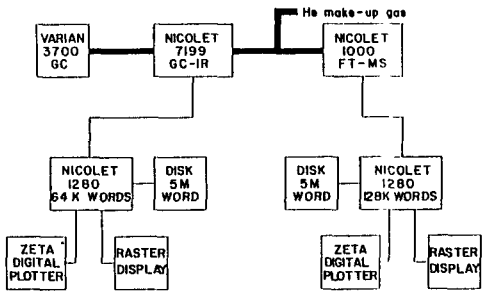


Figure 1

In order to evaluate the suitability of a series-linked GC-FTIR-FTMS system for complex mixture analysis, a commercial lacquer thinner containing over 30 components was analyzed. Because this combination includes a 0.5cc infrared spectrometer lightpipe prior to the mass spectrometer, it was expected that gc resolution would be degraded. As expected, that result was observed (Table 1). However, resolution was still adequate for structure identi-

Table 1 - GC Resolution for Lacquer Thinner[a]

Peaks	FTIR	FTMS
1,3	3.0	2.5
9,10	5.9	5.3
28,29	3.3	1.6

a) $R = \frac{2(t_2 - t_1)}{W_1 + W_2}$

ification purposes. The data analysis approach, as described earlier, was to collect both infrared and mass spectra for each mixture component and to interpret computer library searches by looking for coincidences among the compounds producing the closest matching library spectra in both instances. Following this protocol, 19 of the 30 compounds separated were unambiguously identified. For 7 more, the structural type was clearly indicated, and in 4 cases (minor components) it was difficult to draw structural inferences. In a number of cases, search ambiguities were resolved by methane CI, which is particularily easy to perform under low pressure conditions in the FT/MS-1000.

A detailed account of this work has been submitted to Analytical Chemistry for publication (6).

References

1. C. L. Wilkins, G. N. Giss, G. M. Brissey, and S. Steiner, Anal. Chem., 53, 113-17 (1981).

2. C. L. Wilkins, G. N. Giss, and G. M. Brissey, Presented at 182nd National Meeting, American Chemical Society, New York, N.Y., Sept. 1981, paper ANYL-78.

3. C. L. Wilkins, G. N. Giss, and G. M. Brissey, Presented at 8th Annual FACSS Meeting, Philadelphia, PA., Sept. 1981, paper 46.

4. R. J. Jakobsen and K. H. Shafer, Presented at 8th Annual FACSS Meeting, Philadelphia, PA., Sept. 1981, paper 91.

5. R. W. Crawford, T. B. Hirschfeld, R. H. Sanborn, and C. M. Wong, Anal. Chem., 54, 817-20 (1982).

6. C. L. Wilkins, G. N. Giss, R. L. White, G. M. Brissey, and E. Onyiriuka, Anal. Chem., (submitted, 1982).

THE EXTEND OF PYROLYSIS IN A ICR MASS SPECTROMETER

By Geneviève Boand, Raymond Houriet and Tino Gäumann

Federal Institute of Technology, EPFL-Ecublens, CH-1015 Lausanne, Switzerland

In the reaction of O^- and OH^- with alcohols, nitrites and ethers, the alkoxide anion is a major product ion. According to the structure of the neutral, fragment ions can also be observed, especially the loss of molecular hydrogen from pos.α and β yielding the enolate ion. This ion is partly formed with O^- as direct precursor (Boand, Houriet and Gäumann, Adv. in Mass Spectrometry 8A, 238, 1980), but double resonance experiments showed the existence of a reaction of the following type :

$$C_nH_{2n+1}O^- + M \longrightarrow C_nH_{2n-1}O^- + H_2 + M - 30 \text{ kJ/mol} \qquad (1)$$

This reaction is endothermic and the rate constant depends on the nature of the precursor of the alkoxide ion (in 10^{-11} cm^3/molecule·s) : 20-80 for nitrites, 0.5-1.5 for alcohols and negligible for ethers. The following exothermic reactions can be put forward :

$$\text{alkoxide}^- + \text{RONO} \longrightarrow \text{enolate}^- + \text{HONO} + \text{paraffin} + 23 \text{ kJ/mol} \qquad (2)$$

$$\text{alkoxide}^- + \text{ROH} \longrightarrow \text{enolate}^- + H_2O + \text{paraffin} + 63 \text{ kJ/mol} \qquad (3)$$

$$\text{alkoxide}^- + \text{ROR} \longrightarrow \text{enolate}^- + \text{ROH} + \text{paraffin} + 27 \text{ kJ/mol} \qquad (4)$$

A substitution reaction for the nitrites has been proposed by Noest & Nibbering (Adv. in Mass Spectrometry, 8A, 227, 1980) :

$$RO^- + \text{RONO} \quad \text{ROR} + NO_2^- \qquad (5)$$

However no relationship between the rate constant and the exothermicity for reactions (2) - (4) can be seen.

Caldwell & Bartmess (Int. J. Mass Spectrom. Ion Phys. 40, 269, 1981) presented evidence for pyrolysis of alcohols on the ion gauge, yielding ketones or aldehydes : by switching off the ion gauge, the enolate intensity decreased considerably. We repeated the experiments and found no such effects 3 ms after the ionizing pulse; but by decreasing the effective pumping speed of our vacuum system from 12 l/s to 2 l/s, we observed a fivefold decrease of k_3 and a change in the ratio k_4/k_5 with the ion gauge switched off. We draw the following conclusions :

1. The enolate formed within a few ms with N_2O as reactant gas has mainly O^- as precursor. No pyrolysis products can be detected in normal drift mode conditions.
2. Time dependent spectra and positive ion spectra indicate that the extent of pyrolysis in alcohols amounts to 1 % approximately, corresponding to a "production rate" of about 1 nmol/min at 10^{-6} Torr. The alkoxide reacts with the carbonyl compounds with a rate in the range of 10^{-9} cm^3/molecule.s.
3. The ion gauge acts as a pump. In our case its pumping speed was about 10^{-2} l/s for rare gases and 1 l/s for acetone. The latter value depends on the location and/or the surrounding of the ion gauge.
4. The nitrite pyrolysis is faster. Reaction (5) seems to be the major reaction of RO^- with the neutral nitrite.
5. The determination of the pumping speed of the vacuum system using either the ion gauge or the mass spectrometer showed that the introduction of the substance directly into the ion source is of considerable advantage when pyrolysis is suspected, since the conductance of the ion source is comparable to the pumping speed of the vacuum system.

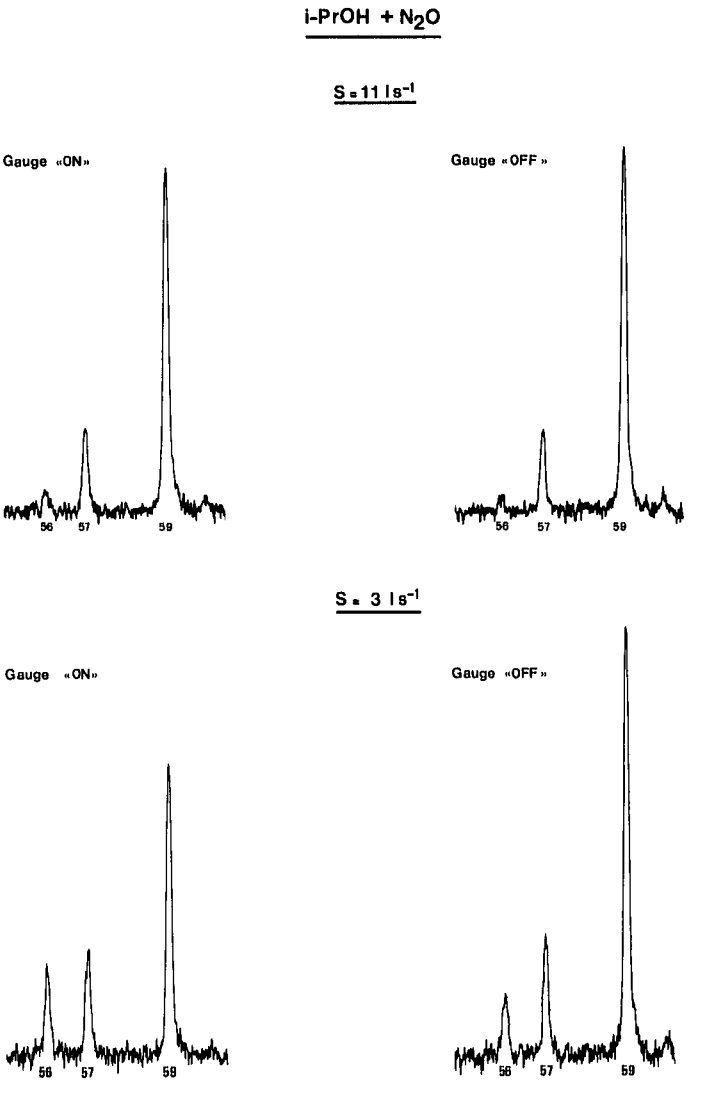


Figure 1: Mixture of N_2O ($8 \cdot 10^{-6}$ Torr) and i-PrOH ($4 \cdot 10^{-6}$ Torr): effect of pumping speed and ion gauge.

Fourier Transform Mass Spectrometry of Mid- to High Mass Molecules

Sahba Ghaderi
Nicolet Analytical Instruments
Madison, Wisconsin 53711

Michael L. Gross
Department of Chemistry
University of Nebraska-Lincoln
Lincoln, Nebraska 68588

Charles L. Wilkins
Department of Chemistry
University of California, Riverside
Riverside, California 92521

The extension of mass spectrometry to investigation of polar and/or non-volatile molecules, especially in the mass range of 1500-20,000 daltons, is of considerable contemporary interest. The well-known and demonstrated capability of Fourier transform mass spectromentry (FTMS) for high mass resolution suggests that this would be a particularily effective tool for obtaining spectra of high mass materials and could possibly yield unit mass resolution for ions ranging in mass from 10,000-20,000 u. Table 1 shows the extrapolated resolution, based upon several measurements made at 1.9 T, that would be predicted for an 8.5T field under otherwise identical measurement conditions.

Table 1 - Extrapolated Resolution for Various m/z values at 8.5 T

m/z	Measured Resolution (1.9T)[a]	Calculated Resolution (8.5T)
28	2.5×10^6	1.1×10^7
156	6.0×10^5	2.7×10^6
1,166	8.3×10^4	3.8×10^5
20,000	-	2.2×10^4

a) m/Δm measuring Δm at 50% peak height

One important aspect of this expected high resolution capability at high mass is the ability to resolve isotopic multiplets in the molecular ion region. This in turn will greatly facilitate determination of elemental compositions for such ions. As is shown in the simulations in Figure 1, for the protected oligonucleotide molecular ion reported by

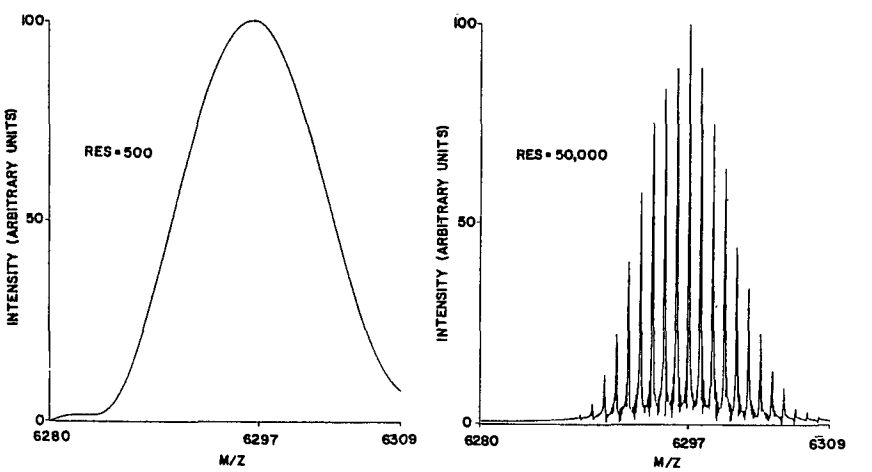


Figure 1

MacFarlane (1) if resolution of 500 is compared with resolution of 50,000, it is clear that the latter yields significantly more information.

Of course, an equally important aspect of the measurement problem is volatilization of the samples in order to make spectral measurements possible. Both laser desorption (2) and fast atom bombardment sources are under investigation for this purpose. The high mass capabilities of FTMS are also being explored by investigation of relatively more volatile highly fluorinated compounds using direct probe methods.

References

1. C. J. McNeal and R. D. MacFarlane, J. Amer. Chem. Soc., 103, 1609-10 (1981).

2. D. A. McCrery, E. B. Ledford, Jr., and M. L. Gross, Anal. Chem. (in press, 1982).

WOC 8 COLLISION-INDUCED DISSOCIATION IN A FOURIER TRANSFORM MASS SPECTROMETER, R. B. Cody, R. C. Burnier, and B. S. Freiser, Purdue University, West Lafayette, IN 47907.

Collision induced dissociation (CID) may be observed in a Fourier transform mass spectrometer by accelerating ions of a given mass at their cyclotron frequency in the presence of a collision gas. Efficient, low energy CID occurs, and the process is comparable to that observed in triple quadrupole instruments. Like the triple quadrupole technique, no slits are employed, and virtually all of the fragment ions formed by the CID process may be detected. Unlike all previous mass spectrometric techniques for studying CID, a tandem instrument is not required, and different experiments are performed by making software modifications rather than hardware modifications. High resolution detection of CID fragments, variation of collision energy, and observation of consecutive CID reactions ("MS/MS/MS") are possible for both primary ions, and products of ion-molecule reactions.

NEGATIVE ION FORMATION BY ATTACHMENT OF ELECTRONS TO RADICALS.

M. INOUE, Univ. of Electro-Communications, Chofu-shi, Tokyo, 182 JAPAN.

The mechanisms of formation of negative ions by low energy electrons in the gas phase have been studied by various techniques. The well-known mechanisms are the dissociative or non-dissociative attachment of electrons to molecules and the pair formation of positive and negative ions. These ions are the primary products from the direct collisions of electrons with molecules. But at higher pressures, in addition to the ions produced by the above mechanisms, ions formed by higher order reactions are also observed. We wish to propose such a mechanism in which negative ions are formed by attachment of electrons to radicals produced in positive ion-molecule reactions[1];

$$HR + e \longrightarrow HR^+ + e + e'$$
$$HR^+ + HR \longrightarrow H_2R^+ + R$$
$$R + e \longrightarrow R^{-*}$$
$$R^{-*} + HR \longrightarrow R^- + HR$$

here HR and R are a molecule and a radical respectively. If R has a positive electron affinity, it can be expected that R^- would be formed by attachment of a secondary electron to R and subsequent stabilizing collisions with HR.

The ICR spectrometry has a unique capability of identifying precursor ions in complex chains of reactions by means of the double resonance technique. If R^- is formed by the proposed mechanism, acceleration of HR^+ in the second reaction by an rf electric field should give rise to a substantial change in the concentration of R and consequently in the R^- intensity. In order to get the HR^+ signal in the double resonance spectrum of R^-, we have developed an ICR cell equipped with venetian blind type trapping electrodes[2] and a trapping voltage modulation technique.

Fig.1 shows a schematic drawing of the cell and motions of positve and negative ions in the cell. X-, Y- and Z-axes are taken as shown . Fig.2 shows cross sections of the cell with equipotential lines, trajectories of positive and negative ions and secondary electrons, and distributions of ions in the Z direction. The trapping electrodes are composed of seven divided small plates and different potentials are applied stepwise from top to bottom plate. Potential difference between top and bottom plates is set to be equal to that of upper and lower drift electrodes. By modulating the bias voltage as shown in the figure to trap positive and negative ions alternatively, it would be possible that for certain negative bias voltages positive ions has enough time in the source region to absorb energy from the accelerating rf field, whereas negative ions are trapped and drift to the analyser region to be detected by the marginal oscillator detector.

Fig.1

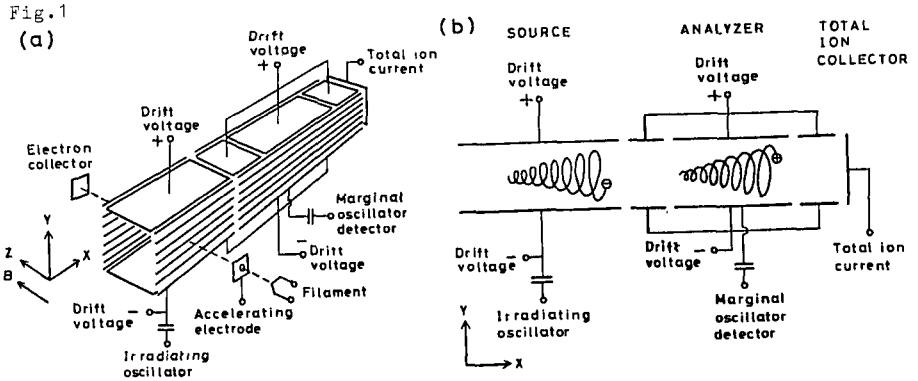


Fig.2

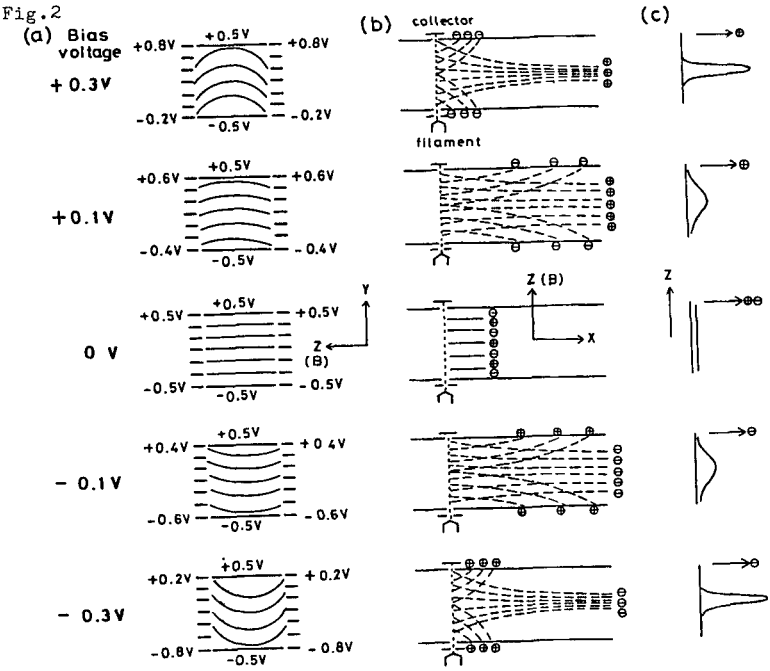
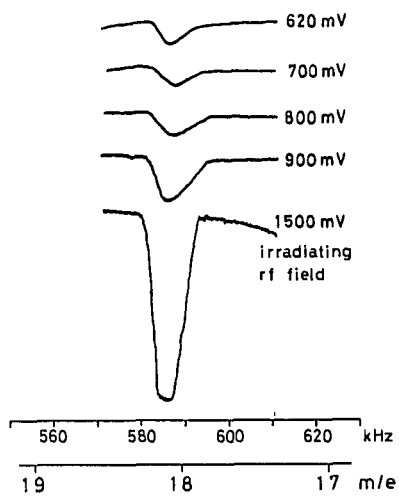


Fig.3



We have studied OH^- ion in water vapor at 3.8×10^{-5} Torr. Fig.3 shows double resonance spectra of OH^-. The ionizing electron energy and current were 50 eV and 0.3 μA respectively. The frequency of the marginal oscillator detector was 624 kHz. The abscissas indicate the frequency of irradiating oscillator and the equivalent mass number. Signals are seen at a frequency corresponding to H_2O^+ ion. The different peaks were obtained by changing the amplitude of the irradiating rf field.[3]

References

1. M. Inoue, J. Chim. Phys., 63, 1061 (1966).
2. J. Urakawa, H. Shibata and M. Inoue, "Ion Cyclotron Resonance Spectrometry", Eds. H. Hartmann and K.-P. Wanczek, Springer-Verlag, Heidelberg, 1978. p.33.
3. M. Inoue, Proceedings of the 2nd International Symposium on ICR Spectrometry, March 23-27, 1981, Mainz, Springer-Verlag (to be published).

Quantitative Analysis of Nutritional Trace Metal Enrichment Using a GC/MS System: Fennessey, P.V., Christie, D., Favier, A., Stage, A., and Hambidge, K.M. University of Colorado Health Sciences Center, School of Medicine, Denver, Colorado 80262.

The use of mass spectrometry and in particular gc/ms for the analysis of trace metal stable isotopes has met with a varying degree of success depending upon the particular metal of interest (1). The causes of the errors in both precision and accuracy has been attributed to co-elution of contaminating peaks, to lack of stability of the chelates, and to exchange of the metals of interest in the mass spectrometer source. Because of these difficulties many researchers have looked to other methods for the analysis of stable isotope enrichment in the study of human nutritional probe. The two prime alternate approaches are neutron activation (2) and direct problems (3). Both of these methods are time consuming and require complex separation schemes and, in addition, neutron activition requires convenient access to a reactor.

It appears to us that the pay off in solving the problems with gc/ms analysis would be well worth the effort, since it would open the door to having the capability of dealing with the multiple analyses required for normal biochemical protocols. In addition, the rapid turn around provided by this method would allow changes in the clinical protocol during the time frame of normal studies.

We divided our research program into two parts. The first dealt with the development of a technique for the quantitative isolation, derivatization and analysis of the trace metals. The second aspect was focused on the measurement of stable isotope enrichment of zinc. Both proved to be difficult.

Based upon literature reports (4,1) we have spent our major effort using diethyldithiocarbamate (DDC) chelates. The isolation procedures involve dry ashing 1 ml of plasma or 1 gm feces and redissolving the metals in 10% HCl. The chelate is formed by simply adding 200 µl of Sat. $NaHCO_3$ and 100 µl of 10% DCC in water and shaking. The chelates are extracted into $CHCl_3$ (2 ml and dryed). The final injection of 1 to 3 µl is made after redissolving the metal chelates in 50µl of $CHCl_3$. Our initial sensitivity was too low when we used either packed columns or capillary columns and standard injection techniques. We attributed this problem to the solvent front where large amounts of unused chelator stripped the column and "activated" it to absorb nanogram levels of trace metals. This problem could be partly overcome by adding small amounts of the chelator vapor to the gas stream. The problem was solved by converting to a falling needle injector (R.H. Allen, Co., Boulder, CO). This device allows one to remove the solvent while retaining all of the sample on the needle prior to injection. As a result there is no solvent front and no overload on our capillary. Using this system we obtained calibration curves that show we can measure down to 2 ng/µl zinc in a plasma sample (normal levels approx. 20 ng/µl). Comparison of our results with data obtained using atomic absorption are shown in Table I.

TABLE I

GC Reproducibility of a single fecal sample (µg/ml)		Correlation of fecal samples by AA	and by GC
1.81	n=7	18.0	14.6
1.90		12.6	11.0
1.82	$\bar{x}$=1.88	1.6	1.0
1.90		2.2	2.2
2.00	σ_n=0.066	8.0	6.5
1.87		7.4	7.5
1.83	CV=3.5%	6.5	6.0
		9.0	8.8

The second phase of this study, likewise, uncovered a number of difficulties. A system was set up on the mass spectrometer consisting of a dropping needle injector and a 10 meter fused silica column (J & W Scentific - DuraBond 5) connected to a Vacuum Generator MM-16 low resolution mass spectrometer. We were surprised by our first gc/ms results which showed the expected peaks for zinc, copper and nickel. However, each peak except Ni showed mass spectra for all these metals. We discovered that our "all glass" inlet consisted of glass lined stainless steel with two 1/16" unions. We replaced this system with a continuous heavy walled glass tube and the aforementioned problem was resolved. In addition, we have replaced the metal source to gc inlet retractable cup with a glass system. In this manner we have an all glass system up to the ion chamber.

Finally, we have obtained a calibration curve using ^{68}Zn as the enriched species. The curve appears to be linear between 1 and 10 atom % enrichment (regression analysis r=0.999) and then deviates between 10 and 20 atom % enrichment. Since we can control our experiment to obtain data in the range of 1-10 atom % enrichment, the curved portions of the curve can be avoided. However, additional work will be needed to understand the cause of this deviation.

We have determined that part, if not all, of the memory problem is associated with the temperature stability of the zinc chelate. We developed a method for the evaluation of this problem using a laboratory gc. The problem was seen by multiple injection of a low level concentration of zinc followed by two or three large concentration sample injections (3X to 5X) and the low level standard. Whenever the conditions were such as to promote dissociation the second set of low level standards showed a higher average concentration of zinc as determined by peak height. This situation was corrected as we adjusted the experimental temperature to the point where decomposition was minimized.

1. Hachey, D.L., Blass, J.C., Klein, P.D.: High Precision Isotope Ratio Analysis of Volatile Metal Chelates. Anal. Chem. 52, 1131 (1980).
2. Janghorbani, M and Young, V.R.: Stable Isotope Methods for Bioavailability assessment of dietary minerals in humans. In Advances in Nutritional Research (H. Draper, ed) Vol 3 (1980).
3. Johnson, P.E.: Use of Stable Isotopes and Mass Spectrometric Analysis ot Measure Absorption of Iron, Zinc and Copper in Human Subjects. XII International Congress of Nutrition, San Diego, Calif. (1981).
4. Tavlaridis, A. and Neeb, R.: Gas Chromatography Multielemental Analysis Using Simple Fluorinated Diethyldithio carbamates. Z. Anal. Chem. 282, 17 (1976).

DETERMINATION OF STABLE METAL ISOTOPES IN MICROLITER VOLUMES OF SOLUTIONS BY INDUCTIVELY COUPLED PLASMA-MASS SPECTROMETRY

Robert S. Houk* and Joseph J. Thompson
Ames Laboratory-USDOE and Dept. of Chemistry
Iowa State University, Ames, IA 50011
(515)294-9462

Solution aerosols from an ultrasonic nebulizer are injected into an inductively coupled argon plasma (ICP) to generate positive ions derived from sample constituents. A fraction of these ions is extracted through a sampling orifice into a differentially pumped vacuum system housing an ion lens and quadrupole mass spectrometer. Sample changing procedures are quick (1-3 minutes) and simple because the sample is directly introduced into the atmospheric pressure ICP. There is no separate ionization source inside the vacuum system (1-4).

A peristaltic pump is used to deliver solution to the nebulizer. A small pipet attached to the sample uptake tube may be used to withdraw and nebulize a discrete volume (50-200 µL). This aerosol "plug" is introduced into the ICP, generating a pulse of sample ions lasting ∿20 s. Positive ions are detected from most of the elements under the same plasma operating conditions. In a selected ion monitoring mode, detection limits are 5-15 mg/L and sensitivity is ∿3 x 10^3 counts/s per mg/L of transition elements, e.g., Fe or Cu. The reproducibility of the sample injection procedure is ± 3 - 10% relative standard deviation; injection precision improves as the injected volume increases.

Alternatively, the mass analyzer may be scanned repetitively during each sample introduction pulse. Individual scans are signal averaged to yield a composite spectrum with improved signal-to-noise ratios. The entire m/z range is scanned for qualitative or survey analysis. Stable metal isotopes are determined by scanning over a smaller m/z range spanning the isotopes of interest. The accuracy and precision for determination of relative isotopic abundances is ± 1 - 3%. Elemental concentrations and isotopic abundances can be determined directly in microliter volumes of biofluids via this pulsed nebulization mode (5).

Table I. Mg Isotope Ratio Determinations

Isotopes	Determined Isotope Ratio*	95% Confidence Limits of Ratio	Accepted Isotope Ratio
24/25	7.581	± 0.052	7.769
24/26	6.885	± 0.056	7.046
25/26	0.908	± 0.089	0.9069

*Values listed are the mean ratios for 13 separate injections of 100 µL of 40 mg Mg/L.

Table II. $^{58}Ni/^{60}Ni$ Isotope Ratio Determinations*

Injection Volume (µL)	Ni Concentration (mg/L)	Number of Injections	Determined $^{58}Ni^+/^{60}Ni^+$	95% Confidence Limits of Ratio
100	2	8	2.570	± 0.077
50	8	10	2.597	± 0.040
100	8	10	2.557	± 0.029
200	8	9	2.571	± 0.043

*Overall mean ratio (37 injections) = 2.574; accepted ratio = 2.588.

1. Houk, R. S.; Fassel, V. A.; Flesch, G. D.; Svec, H. J.; Gray, A. L.; Taylor, C. E. Anal. Chem. 1980, 52, 2283-2289.
2. Houk, R. S.; Fassel, V. A.; Svec, H. J. Dynamic Mass Spectrom. 1981, 6, 234-251.
3. Gray, A. L.; Date, A. R. Dynamic Mass Spectrom. 1981, 6, 252-266.
4. Douglas, D. J.; French, J. B. Anal. Chem. 1981, 53, 37-41.
5. Houk, R. S.; Thompson, J. J. Submitted to Biomed. Mass Spectrom., May 1982.

STUDIES ON THE MECHANISM OF α-OXIDATION OF FATTY ACIDS IN BACTERIA USING $^{18}O_2$

I.Yano[1], E.Yabuuchi[2] and Y.Kishimoto[3]

[1]Niigata University School of Medicine, Niigata 951, Japan,
[2]Kansai Medical School, Osaka, Japan and [3]Johns Hopkins University Maryland, U.S.A.

α-Oxidation is a system oxidizing long chain fatty acids to form 2-hydroxy fatty acids in mammalian or plant tissues. In bacteria, the occurrence of these systems has been extremely rare. Previously, we have reported the existence of α-oxidation system in several gram-positive bacteria[1)2)]. Recently, we have also demonstrated the wide distribution of 2-hydroxy fatty acids among the gram-negative, absolutely aerobic bacteria, such as Pseudomonas, Flavobacterium, Achromobacter and Alkaligenes[3)4)5)]. In order to clarify the mechanism of bacterial α-oxidation systems, we have examined the incorporation of oxygen atoms from $^{18}O_2$ by the short term incubation of cell suspension of various species of absolutely aerobic bacteria.

Achromobacter xylosoxidans and Sphingobacterium multivorum were grown in a medium containing 1 % glucose, 0.5 % peptone and 0.2 % yeast extract, until exponential growth phase. After the cells were harvested by centrifugation the cells were resuspended in a fresh medium and further incubated in $^{18}O_2$ atmosphere for 1 to 4 hours. The reactions were stopped by 6N-HCl and the mixtures were hydrolyzed under reflux. The resultant fatty acids were extracted and methylated, and then analyzed by GC/MS. The incorporation rate of ^{18}O atoms into 2-hydroxy fatty acids was calculated from molecular ions, m/z 90 ion due to C_2-C_3 cleavage, m/z 103 due to C_3-C_4 cleavage and (M-59)ions. Mass fragmentographic analysis was performed by accelerator voltage alternater system of Hitachi M-60 apparatus to obtain precise incorporation rate of ^{18}O.

Among the non-polar, 2-hydroxy and 3-hydroxy fatty acids in both bacteria, Sphingobacterium multivorum and Achromobacter xylosoxidans, a shift of molecular ions by two mass units due to ^{18}O incorporation was shown for the 2-hydroxy fatty acids but not the 3-hydroxy or non-hydroxy fatty acids. Mass fragmentograms of hydroxy fatty acid methyl esters of A.xylosoxidans are indicated in Fig.1, and time course incorporations of ^{18}O atom into various 2 or 3-hydroxy fatty acids are demonstrated in Fig.2. During the incubation of 1 to 7 hours, all the 2-hydroxy fatty acids (C_{12}, 14 and 16) were enriched with ^{18}O, while any significant incorporation was not observed in 3-hydroxy fatty acids ($C_{12, 14 \text{ and } 16}$). Therefore, the bacterial α-oxidation reaction seems very likely to involve 2-hydroxylation reaction using molecular oxygen, like brain microsome systems (Schemel).

Acknowledgments

The authors are indebted to Prof. C.Fenselou for mass fragmentographic analysis of hydroxy fatty acids enriched with $^{18}O_2$ from Sphingobacterium.

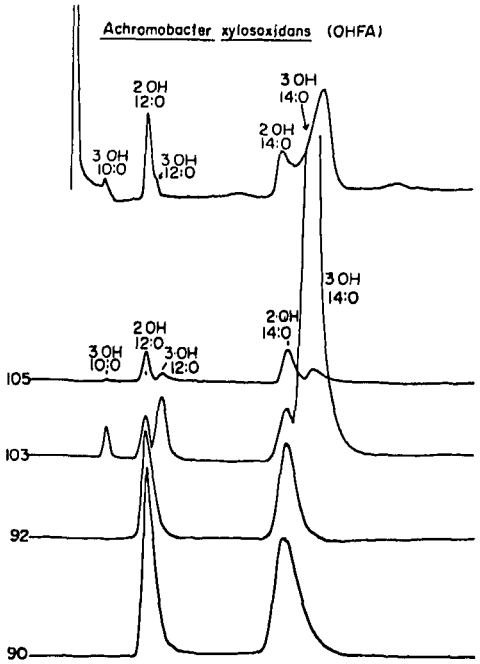


Fig.1 Mass fragmentograms of hydroxy fatty acid methyl esters of A. xylosoxidans after incubation in $^{18}O_2$ for 6 hrs.

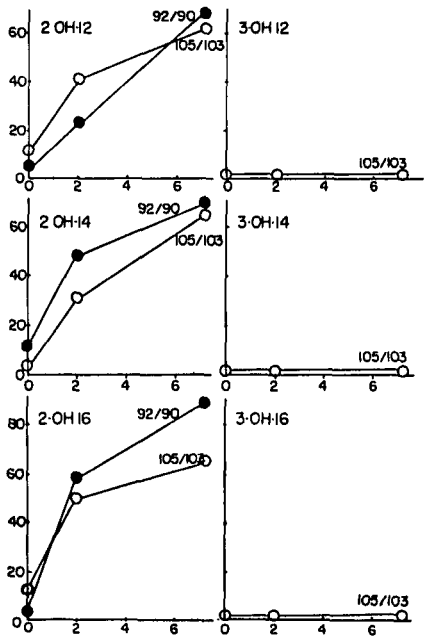
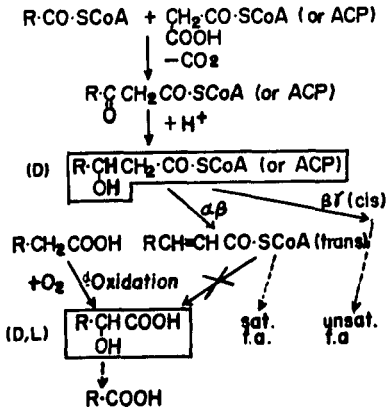


Fig.2 Time course for incorporation of ^{18}O into 2 or 3-hydroxy fatty acids in A.xylosoxidans.

Scheme 1

Proposed Pathway for Biosynthesis of 2 or 3-Hydroxy Fatty Acids in Absolutely Aerobic Bacteria



References

1. I.Yano, Y.Furukawa and M.Kusunose, Biochim.Biophys.Acta., 239 (1971) 513-515.
2. I.Yano, Y.Furukawa and M.Kusunose J.Gen.Appl.Microbiol.,17 (1971) 429-432.
3. A.Yamamoto, I.Yano, M.Masui and E.Yabuuchi, J.Biochem., 83 (1978) 1213-1217.
4. E.Yabuuchi, I.Yano, T.Kaneko and A.Ohyama in the Flavobacterium cytophaga group (H.Reichenbach & O.B.Weeks, Eds.), pp.79-90, (1981) Verlag Chemie, Weinheim.
5. E.Yabuuchi, E.Tanimura, A.Ohyama, I.Yano and A.Yamamoto, J.Gen.Appl. Microbiol., 25 (1979) 95-107.

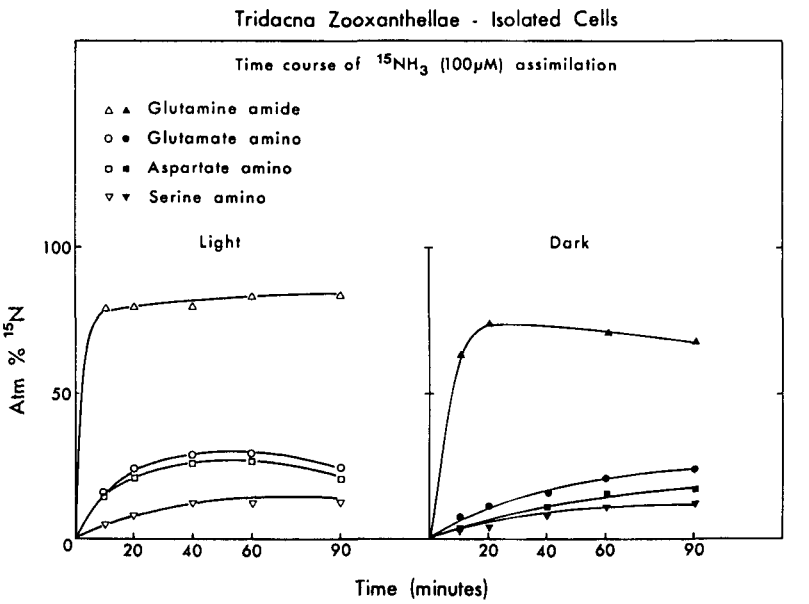
THE STUDY OF NITROGEN METABOLISM IN MARINE ALGAE AND HIGHER PLANTS USING DIRECT ANALYSIS OF ^{15}N INCORPORATION BY GC-MS

R.E. Summons, C.B. Osmond and K.C. Woo

Department of Environmental Biology
Research School of Biological Sciences
Australian National University
P.O. Box 475, Canberra City, A.C.T. 2601, Australia

The stable isotope ^{15}N is being used increasingly as a probe to study nitrogen metabolism in plant tissues as facile techniques are developed for accurately measuring its abundance in critical metabolites. Of fundamental importance is the ability to measure the specific enrichments of the individual nitrogen atoms of glutamine, asparagine, glutamate and aspartate as well as other amino acids. A simple method utilising ion exchange pre-separations followed by GC-MS has been developed to satisfy these requirements.

The method has been used to examine the enzyme pathways and assimilation kinetics of various nitrogenous nutrients likely to be encountered by the symbiotic marine alga Gymnodium microadriaticum (Dinophyceae). These algae, known as zooxanthellae, live in mutualistic associations with many tropical marine invertebrates including the reef building corals and clams of the genus Tridacna. ^{15}N-labeled ammonium chloride, sodium nitrate and urea, when supplied to freshly isolated zooxanthellae were assimilated in light dependent processes and resulted in amino acid labeling patterns indicating activity of glutamine synthetase (GS) and glutamate synthase (GOGAT) rather than the alternative glutamate dehydrogenase (GDH) pathway[1].



A time course feeding experiment using $^{15}NH_4Cl$ at 100 μM resulted in a labeling pattern, shown in the figure, where the glutamine amide nitrogen became heavily labeled in the first few minutes of exposure and remained so for the duration of the experiment. Glutamate, glutamine and other amino acids became amino labeled more slowly, reflecting activity of the transaminating enzyme systems. These results are consistent with primary ammonia assimilation taking place via the GS and GOGAT pathway.

Similar results were observed when leaf discs of a higher plant, Spinacea oleraceae were fed ^{15}N-glycine. The photorespiratory conversion of two moles of glycine to one mole of serine results in the production of one mole each of NH_3 and CO_2. Loss of this ammonia would be a wasteful process. Labeling patterns of glutamine and glutamate, however, showed that this ammonia was reassimilated into the amino acid pool, again via the GS-GOGAT pathway[2].

References

1. R.E. Summons and C.B. Osmond, Phytochemistry, 1982, 20, 575
2. K.C. Woo, J.F. Morot-Gaudry, R.E. Summons and C.B. Osmond, Plant Physiology, 1982, In press

NITROGEN CYCLING IN HIBERNATING BEARS

R.R.Wolfe, R.A.Nelson, M.H.Wolfe, L.Rogers
Shriners Burns Institute, Mass. General Hospital, Boston, MA 02114

Hibernating bears take in virtually no food or water for up to seven months, but maintain a body temperature or 97°, and excrete virtually no nitrogenous wastes. During hibernation there is no loss of lean body mass and urination is not required for several months. It is therefore hypothesized that these bears have a unique ability to re-utilize urea nitrogen. To probe this hypothesis, a tracer amount of di-^{15}N urea was injected into two black bears hibernating in the wilderness area of northern Minnesota, and blood samples were drawn in the first hours and in the following two weeks as snow conditions permitted. The hibernating state of the bears was not disturbed.

Plasma urea enrichment was measured by GC-MS with SIM at M+2 to measure the rate of new urea production. The plasma urea was also measured at M+1 to estimate the re-cycling of nitrogen back into urea. Nitrogen enrichment in plasma albumin and fibrinogen was measured by isotope ratio mass spectrometry after reduction of these proteins to N_2 via ammonia. Free ammonia enrichment was measured by atomic emission. And finally, nitrogen enrichment was measured in 23 plasma amino acids by SIM-GC-MS.

Significant ^{15}N enrichment was detected in several amino acids including ornithine, arginine, glycine, tyrosine, phenylalanine, and threonine. Re-incorporation of amino acids into plasma protein was confirmed by significant levels of 15N in albumin and fibrinogen. Urea production was found to occur continuously since the urea M+2 level declined with time. Free ammonia 15N enrichment was also found to increase. Total body water was measured with a ^3H_2O tracer and lean body mass estimated. Total urea concentration was measured by enzymatic assay. The urea production rate was found to be 1/10th that of a normal bear in summer, awake state.

The combination of GC-MS and IR-MS has led to the elucidation of urea nitrogen re-utilization in a unique mammal, the hibernating black bear. What are normally considered irreversible pathways in the urea cycle appear to be reversible in this hibernating state, and certain keto-acids are transaminated to form what are normally essential amino acids. Artificial stimulation of these pathways would reduce the need for dialysis in anuric patients.

THE USE OF STABLE ISOTOPES TO STUDY ENDOGENOUS NITRATE/NITRITE FORMATION IN HUMANS.

David A. Wagner, John S. Wishnok, and Steven R. Tannenbaum.
M.I.T., Department of Nutrition and Food Science, Cambridge, MA 02139.

A major focus of our research is the possibility that endogenous formation of carcinogenic N-nitroso compounds may contribute to elevated human risk toward cancer in areas where one or more of the precursors of these substances may be present in the diet.

The observation that nitrate is formed in the body, in large amounts relative to those typically ingested (1), prompted a more-detailed investigation of nitrate metabolism in humans as well as in animals especially with regard to the contribution of these processes to total exposure to N-nitroso compounds (2,3), since it is well-known that nitrate is converted to nitrite and thus to nitrosating species - by endogenous bacteria.

For metabolic tracer and isotope dilution studies of $NO_3^{\ominus}$, we used the stable isotope, ^{15}N. To quantitate excreted $^{15}NO_3^{\ominus}$, we adapted the method of Tesch and coworkers (4) for the nitration of benzene in urine. One ml of urine is mixed with 5 ml benzene and 5 ml of concentrated H_2SO_4 is then slowly added. The reactants are mixed in a shaker bath at room temperature for 10 minutes. The benzene layer is removed, passed through a silica Sep-Pak® and then concentrated slowly, under a stream of N_2, to 200 µl.

The ratio of ^{15}N- to ^{14}N-nitrobenzene is determined by gas-chromatography-mass spectrometry on a Hewlett Packard 5992A, with selected ion monitoring at m/z = 122 (M-1), m/z = 123 (M), and m/z = 124 (M+1). Complete mass spectra are obtained periodically to confirm the identity of the compounds being monitored. Since nitroaromatics are susceptible to proton abstraction in the EI mode, it was found that - in addition to corrections for natural isotopic abundances - a correction for this process was required before the ratio ^{15}N-nitrobenzene:^{14}N-nitrobenzene quantitatively reflected the $^{15}NO_3^{\ominus}$:$^{14}NO_3^{\ominus}$ ratio in the urine.

Experiments were conducted in the MIT Clinical Research Center on groups of young adult men. Subjects were fed nutritionally adequate synthetic diets low in nitrate for at least 5 days prior to an experimental period. In studies involving ascorbic acid, 4 x 500 mg of ascorbic acid was given during a 7-day free-choice diet as well as during a 7-day low-nitrate diet. ^{15}N-nitrate (99% atom excess ^{15}N) was then given orally (3500 µmol in 10 ml water followed by 200 ml water). Urine was collected at selected time intervals for 48 hours and analyzed for $^{15}N/^{14}N$ as described above.

In agreement with earlier results, unlabeled nitrate was consistently found in the urine at levels higher than could be accounted for by dietary nitrate (1,3). Urinary excretion of $^{15}NO_3^{\ominus}$ was highest during the first

hour after ingestion but $^{15}NO_3^{\ominus}$ could be detected in the urine at 48 hours post dose.

This was reflected by the behavior of total plasma and salivary nitrate measured independently (3).

The levels of $^{15}NO_3^{\ominus}$ and $^{14}NO_3^{\ominus}$ in the urine of both males and females were unaffected by ascorbic acid.

Most (~60%) of the administered dose of ^{15}N was recovered in the urine as $^{15}NO_3^{\ominus}$, with a much smaller amount (~3%) being recovered in the urine as ammonia and urea. Approximately 35% of the administered $^{15}NO_3^{\ominus}$ remains unaccounted for.

As an initial investigation of possible nitrate precursors, ^{15}N-ammonium ion was administered to rats, and a significant amount of $^{15}NO_3^{\ominus}$ was subsequently detected in their urine. This, along with the detection of ^{15}N-ammonia and ^{15}N-urea following administration of $^{15}NO_3^{\ominus}$ suggests that both reduction of oxidized nitrogen species and oxidation of reduced nitrogen species are involved in mammalian nitrogen metabolism.

Acknowledgement: This work was supported by NCI Grant No. 1-P01-CA26731-03.

References:

1. S.R. Tannenbaum, D. Fett, V.R. Young, P.D. Land, and W.R. Bruce, Science, 200, 1487 (1978).
2. L.C. Green, D.A. Wagner, J. Glogowski, P.L. Skipper, J.S. Wishnok, and S.R. Tannenbaum, Analyt. Biochem., in press.
3. D.A. Wagner, D.S. Schultz, W.M. Deen, V.R. Young, and S.R. Tannenbaum, submitted (Cancer Research).
4. J.W. Tesch, W.R. Rehg, and R.E. Sievers, J. Chromatog., 126, 743 (1976).

BIOSYNTHETIC STUDIES OF MYCOLIC ACIDS IN NOCARDIA USING ^{13}C STABLE ISOTOPES

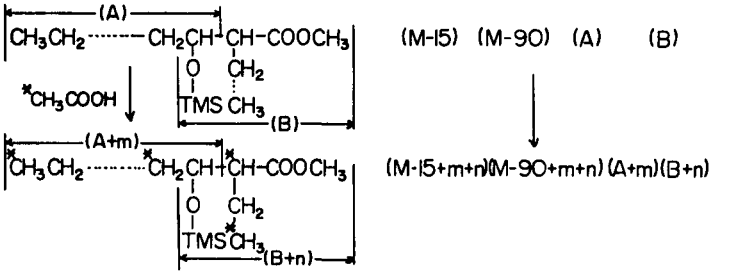
I.Tomiyasu[1], S.Toriyama[2] and I.Yano[2]
[1]Tezukayama Junior College, Nara, Japan and [2]Niigata University School of Medicine, Asahimachi-dori 1, Niigata 951, Japan

Mycolic acid, an α-branched chain β-hydroxy fatty acid, is the most characteristic cell wall lipid component of mycobacteria and nocardia. Recently, the structure of mycolic acids are reported to be concerned profoundly with the physicochemical properties of cell surfaces or the biological activities of cell wall components in immune responses. Since not only for the structural analysis, but also for the biosynthetic studies, the precise analysis of homologues appeared to be essential, we have developed the gas chromatography-mass spectrometry (GC/MS) of molecular species of mycolic acids[1)2)3)4)]. These techniques enabled us to obtaine precise information on the mycolic acid molecule and we have started biosynthetic studies of mycolic acids using stable isotope labelled precursors such as ^{13}C acetate or D_2O.

After incubation of 1- or 2-^{13}C acetate with resting cell suspension of N.rubra for 1 to several hours at 30°C, fatty acids are extracted, methylated and fully separated on TLC and $AgNO_3$ TLC. The trimethylsilyl (TMS) derivatives of mycolic acid methyl esters were analyzed by GC/MS.

As shown in Scheme 1, the ^{13}C incorporation rate of individual mycolic acid is estimated from the shift of molecular ions (or M-15 ions) and the exact numbers and amounts of incorporated stable isotopes are calculated. Our results showed the incorporation, not only into the total molecule, but also into the straight chain alkyl unit and α-branch which can also be estimated from the fragment ions (A) $(CH_3\cdot(CH_2)_n\cdot CHOTMS)$ and (B) $(TMSOCH\cdot CH\cdot(CH_2)_n\cdot CH_3)$-$COOCH_3$, respectively. The shift of (M-15), (A) and (B) ions of C_{48} monoenoic and dienoic acids are demonstrated in Fig.1. From above results, in the case of C_{48} mycolic acids, it was revealed twenty four ^{13}C atoms were incorporated into the total mycolic acid molecule, while eight ^{13}C atoms were incorporated into α-alkyl unit and sixteen ^{13}C-atoms into straight chain alkyl unit, respectively. Results also show that the ^{13}C incorporation rate differred by the molecular species of mycolic acid significantly; the shorter chain homologues such as $C_{38,40,42}$ and more highly unsaturated species such as dienoic acid being synthesized more rapidly than the longer chain homologues such as $C_{44,46,48}$ and less highly unsaturated species such as monounsaturated or saturated acids, respectively.

It is noted that the GC/MS analysis is especially useful for biosynthetic studies of mycolic acid using stable isotope labelled precursors.



Scheme 1 Shift of mass fragment ions of mycolic acid methyl esters enriched with 2-^{13}C-acetate

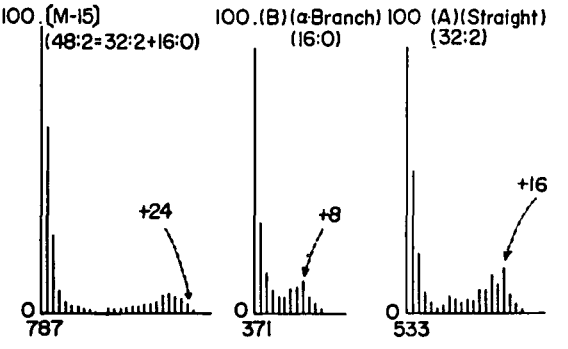


Fig.1 Shift of (M-15), (A) and (B) ions of $C_{48:1}$ mycolic acid after incubation of 2-^{13}C-acetate with the resting cells of N.rubra for 4hs at 30°C

References

1. I.Yano, K.Saito, Y.Furukawa and M.Kusunose, FEBS Lett., 21 (1972) 215-220
2. I.Yano, K.Kageyama, Y.Ohno, M.Masui, E.Kusunose, M.Kusunose and N.Akimori, Biomed.Mass.Spectrom., 5 (1978) 14-24
3. S.Toriyama, I.Yano, M.Masui, E.Kusunose, M.Kusunose and N.Akimori, J.Biochem., 88 (1980) 211-221
4. I.Tomiyasu, S.Toriyama, I.Yano and M.Masui, Chem.Phys.Lipids, 28 (1981) 41-54

WOD 9 ALL YOU'VE ALWAYS WANTED TO KNOW ABOUT COLLISION THEORY BY WERE AFRAID TO ASK;

Michael T. Bowers, Dept. of Chemistry, University of Calif., Santa Barbara, CA. 93106

All of bimolecular gas phase chemistry is initiated by a collision. Collisional properties are determined by the physical, or long range, part of the potential. In some cases reactive properties are strongly dependent on the long range potential while in others the collision merely introduces the reactant partners and the short range, or chemical forces, determine the ultimate outcome of the event. In ion - molecule chemistry collision theory plays an especially important role because the ion - induced dipole or ion - dipole long range forces are strong. Hence, ion - neutral collisions often can energetically access the chemical part of potential surfaces while analogous neutral - neutral collisions are scattered by configurational energy barriers. It should also be noted that unimolecular reactions are just collisions in reverse and collision theory methodology can be usefully applied to them in certain cases.

In this talk a simple introduction will be given to collision theory. Emphasis will be on principles and not mathematical formalism. Numerous examples will be given that indicate the wide range of problems that can be understood and analysed using simple collision theory concepts.

MASS SPECTROMETRIC MEASUREMENTS FOR NUCLEAR SAFEGUARDS*

J. A. Carter, D. H. Smith, and R. L. Walker
Analytical Chemistry Division
Oak Ridge National Laboratory
Oak Ridge, Tennessee 37830

The requirements of nuclear safeguards place great stress on obtaining results of the highest possible precision for uranium and plutonium isotopic abundance measurements from all phases of the nuclear fuel cycle. Because some phases of the cycle necessitate sampling radioactive solutions, it is necessary to analyze small (1-3 ng) samples. The resin bead sampling technique[1,2] provides a convenient means to acquire uranium and plutonium samples while simultaneously separating them from other actinides and fission products. By proper adjustment of acid strength and uranium concentration, only the two elements of interest will adsorb on the beads. For isotope dilution work, Marsh et al.[3] have investigated various plutonium equilibration procedures. The preferred method for fresh dissolver solutions is reduction with Fe(II)-sulfamic acid and oxidation with $NaNO_2$. After 10 minutes agitation of beads and solution on a vortex mixer, each bead will contain 1-3 ng of each element. One bead comprises one sample for mass analysis, where sequential analysis of plutonium and then uranium is performed on a single bead. These quantities are low enough in radioactivity to eliminate the need for heavy and costly shielding during shipment.

To analyze samples of this size, mass spectrometers especially designed for the purpose are required. Instruments built by the various laboratories concerned have been in operation for many years,[4-6] and the newest generation of commercial mass spectrometers approaches the sensitivity requirements.[7] A round robin to evaluate results obtained from resin bead samples has recently been completed,[8] and excellent agreement between laboratories was reported.

Efforts to improve precision beyond what is routinely available through meticulous sample preparation and mass spectrometric analytical procedures are bearing fruit. Two basic approaches are being pursued. The first involves trying to achieve more rigorous control of the evaporation process. The resin bead technique contributes significantly in this area,[9] but overcoating the sample with rhenium seems to be even more helpful.[10] Both electrolytic deposition[11] and addition of rhenium powder in a slurry with a sucrose solution[12] greatly enhance ion emission and reduce evaporation of the sample as oxide species.

The second approach to improving precision is even more promising. This is to use an "internal standard,"[13-16] which is a spike of two isotopes whose ratio is well known (e.g., ^{233}U and ^{236}U). The bias correction necessary to apply for a given filament is calculated on a run-by-run basis and yields far better results than the previous method of applying an average bias correction, determined by analyzing isotopic standards, to all data. Recent work[17,18] has shown that improvements in precision of isotopic ratio measurements of about a factor of five can be attained. The technique is particularly useful in isotope dilution analyses to calculate concentration; its application to improving $^{235}U/^{238}U$ is limited because a truly high purity ^{236}U spike (>99.9% ^{236}U) is not available.

The need of an on-site inspection device to provide isotopic ratio measurements led to the development of a quadrupole mass spectrometer mounted in a van.[19] This mobile laboratory has the ability, through the use of the resin bead technique, to acquire, prepare, and analyze samples of interest to nuclear safeguards. Precision of the measurements is about 1-2%.

*Research sponsored by the U. S. Department of Energy, Office of Safeguards and Security, under Contract W-7405-eng-26 with the Union Carbide Corporation.

By acceptance of this article, the publisher or recipient acknowledges the U S Government's right to retain a nonexclusive, royalty-free license in and to any copyright covering the article

References

1. R. L. Walker, R. E. Eby, C. A. Pritchard, and J. A. Carter, Anal. Lett. 7, 563 (1974).

2. R. L. Walker, J. A. Carter, and D. H. Smith, Anal. Lett. 14, 1603 (1982).

3. S. F. Marsh, R. M. Abernathey, and J. E. Rein, Anal. Lett. 13, 1487 (1980).

4. F. A. White and T. L. Collins, Appl. Spectros. 8, 169 (1954).

5. H. W. Wilson, R. Monro, R. W. Hardy, and N. R. Daly, Nucl. Instrum. Methods 13, 269 (1961).

6. D. H. Smith, W. H. Christie, H. S. McKown, R. L. Walker, and G. R. Hertel, Int. J. Mass Spectrom. Ion Phys. 10, 343 (1972-73).

7. The Finnigan-MAT 260 and the VG-Micromass 54E both have high abundance sensitivity and can analyze samples approaching 10 ng in size.

8. J. D. Fassett and W. R. Kelly in "Analytical Chemistry in Nuclear Technology," W. S. Lyon, ed., Ann Arbor Science, Ann Arbor, MI, 1982, pp. 131-138.

9. D. H. Smith, W. H. Christie, and R. E. Eby, Int. J. Mass Spectrom. Ion Phys. 36, 301 (1980).

10. J. R. Rec, Ph.D. Dissertation at Rensselaer Polytechnic Institute, 1974. Available from University Microfilms, Ann Arbor, MI.

11. R. E. Perrin, D. J. Rokop, J. H. Cappis, and W. R. Shields, Proceedings of 29th Annual Conf. on Mass Spectrometry and Allied Topics, Minneapolis, MN, May, 1981, pp. 422-423.

12. D. H. Smith and J. A. Carter, Int. J. Mass Spectrom. Ion Phys. 40, 211 (1981).

13. L. A. Dietz, C. F. Pachucki, and G. A. Land, Anal. Chem. 34, 709 (1962).

14. L. J. Moore, L. A. Machlan, W. R. Shields, and E. L. Garner, Anal. Chem. 46, 1082 (1974).

15. R. G. Ridley, N. R. Daly, and M. H. Dean, Nucl. Instrum. Methods 34, 163 (1965).

16. M. H. Dodson, Rev. Sci. Instrum. 40, 289 (1963).

17. E. L. Callis in "Analytical Chemistry in Nuclear Technology," W. S. Lyon, ed., Ann Arbor Science, Ann Arbor, MI, 1982, pp. 115-123.

18. D. H. Smith, R. L. Walker, C. A. Pritchard, unpublished results.

19. J. R. Walton, D. H. Smith, H. S. McKown, R. L. Walker, and J. A. Carter, USDOE Report ORNL/TM-8027, Oak Ridge, TN, December, 1981.

THE USE OF MASS SPECTROMETRY FOR SAFEGUARDS AT AN OPERATING REPROCESSING FACILITY;
E.E. Fliby, G. W. Webb, R. A. Rankin, J. E. Delmore, W. A. Emel;
Exxon Nuclear Idaho Company, Inc.; Idaho Falls, Idaho 83401.

Isotope dilution mass spectrometry (IDMS) is a primary tool for uranium accountability analyses at the Idaho Chemical Processing Plant (ICPP). The ICPP reprocesses spent nuclear fuel from reactors in the U. S. and other countries. The fuel is dissolved in batch-type head-end processes[1], and IDMS provides the uranium concentration and isotopic data on the input solutions. The IDMS method is preferred for these measurements because of the high levels of radolactivity associated with the fission products in the input stream[2]. At some times, waste streams are analyzed by IDMS. Finally, IDMS measurements are made on the Plant Product. These accountability results are used along with other data when Safeguards personnel calculate a Material Balance for the Plant. But since the IDMS results are also used for Plant process control, the large number of samples involved must also be analyzed with reasonable speed. The IDMS equipment and methods used at the ICPP reflect the requirements for high sample throughput, rapid turnaround, and high-quality data. Five components of Safeguards mass spectrometry at the ICPP are discussed: (1) the equipment, (2) the operating procedures, (3) operator training and testing, (4) quality control methods, and (5) routine overviews of performance.

The main accountability mass spectrometer has a probe type sample inlet system, a dual-filament thermal ionization source, a 90° magnetic sector mass separator, and a Faraday cage ion collector. Operation of the instrument, data collection, and calculation of the results are controlled by a dedicated minicomputer[3]. The operating procedures used with the instrument are specifically designed to provide the best possible data in a reasonable period of time. A *carefully defined sample loading technique is used and the uranium ion beam is* attained according to a tightly-controlled heating sequence. Finally, data must be taken for the sample only during a particular time "window". Sometimes the operator must intervene in the sequence so that data can be obtained for a sample that is behaving anomalously; the results may not then be used for accountability, though they might serve as a diagnostic tool. The computer printout for each sample will list key parameters, such as beam strength versus time, or time at data taking, for later evaluation by the lab supervisor. Because of this combined need for precision and practicality, operator training is intensive and realistic. Each new operator is first provided a basic familiarization with thermal ionization mass spectrometry through a study of manuals[4] and literature references. Instruction in the operating procedures is then presented in manuals[5], seminars, and personal tutorials. When the trainee has shown a basic level of understanding in written and oral tests, a program of supervised operation is begun to provide hands-on practice with the instruments. Final competence is verified in two operating tests. One is a throughput test to assure that the operator can successfully analyze at least five samples in an 8-hour shift. The other is a "mini" system calibration, in which at least four different uranium Standard Reference Materials are analyzed and the precision on the bias serves as a test of competence. Table I lists the test results for five of the operators trained most recently; for comparison, the results are also shown for re-tests of four of these people after they have had about a year of experience. Only when the trainee has passed both of these test are his results accepted for use in accountability applications.

Table I
Results for Precision Examinatons

Operator	Relative Standard Deviation (%) At Qualification	Relative Standard Deviation (%) After One Year
1	0.16	0.08
2	0.15	0.06
3	0.09	0.05
4	0.15	0.08
5	0.16	--
Std. Dev. on Grand Average:	0.14	0.08

The high level of performance for the mass spectrometric system is maintained in three direct ways: (1) analyses of quality control sample materials, (2) extensive sample tracking, and (3) performance of regular preventative maintenance. Four types of quality control

checks are performed: (1) daily instrument calibrations, (2) "instrument" control runs, (3) analytical control analyses, and (4) pre-defined cross-checks on Plant data. Table II lists the results for precision on uranium concentration obtained for these four levels of quality control. The precisions listed for analytical controls and plant duplicates refer only to those parts of the accountability system from the remote spiking and chemical cleanup of a sample through the mass spectrometric measurement. Instrument controls are the same materials as the analytical controls, but they are weighed on a non-remote analytical balance. Calibrations are performed using solutions of pure uranyl nitrate in dilute nitric acid.

Table II
Precision on Uranium Concentration

Analysis Type	Analyses	Rel. Std. Dev.
Calibrations	70	0.12%
Instrument Controls	36	0.16%
Analytical Controls	52	0.38%
Duplicates, plant	150	0.39%

Three levels of review are routinely performed on the IDMS system: (1) immediate review of all mass spectrometric data, (2) regular evaluation of the quality control data, and (3) weekly critiques by the Uranium Measurements Committee. The immediate data review is performed as soon as a run is completed. The instrument operator checks the timing of the analysis, a peak shape parameter, the precision of the specific sample data set, and so on. If all these parameters are within pre-defined ranges, the operator sets the results aside and goes on to the next sample. The results may be transmitted to plant operations personnel as preliminary data to be used for process monitoring. (When necessary for a crucial process step, it is possible for the analytical sequence to complete a measurement in less than 4 hours.) If the data appear to be questionable, the operator may run another filament from the same sample tube, or a new sample may be requested. Final approval of the results is given by the supervisor of the Mass Spectrometry Laboratory (MSL). The supervisor rechecks the analytical parameters and compares the results to previous data to try to spot any trends that might be developing. If all data entries are correct and the other criteria are met, the results are approved for release from the Lab. The separate Quality Control (QC) group routinely performs a statistical evaluation of the control sample results; the MSL supervisor receives a weekly report on this evaluation. Finally, routine reviews are made of all aspects of the IDMS analytical program (equipment status, analytical methods, operator training, quality control results, etc.) by the Uranium Measurements Committee. This committee has representatives from the chemical laboratory operation, the MSL, the QC group, and the Safeguards Office. They may review plans for development work, recommend new procedures, or perform other actions to improve the performance of the analytical sequence.

The mass spectrometric system described in this paper was devised specifically to address the constraints of turnaround time, throughput, and high data quality. Since the lab can turn a sample around fairly rapidly, has analyzed 350-420 samples per month during peak periods, and obtains the level of precision shown in Table II, it appears that these criteria have been met.

REFERENCES

1. Staff publication, "Idaho Chemical Processing Plant", Exxon Nuclear Idaho Co., Inc. for US-DOE (1981).
2. M.A. Wade, F.W. Spraktes, R.L. Hand, J.M. Baldwin, E.E. Filby, L.C. Lewis, "Performance of an Accountability Measurement System at an Operating Reprocessing Facility", In Nuclear Safeguards Analysis, E.A. Hakkila (Ed.), ACS Symposium Series No. 79, American Chemical Society, Washington, D.C. (1978).
3. J. E. Delmore, "A Computer-Controlled Mass Spectrometer System", Chemical Instrumentation, 3, 251-257 (1972).
4. G.W. Webb, R.A. Rankin, E.E. Filby, "An Introduction to Thermal Ionization Mass Spectrometry at the ICPP", Internal publication, Exxon Nuclear Idaho Co., Inc. (1980).
5. E.E. Filby, G.W. Webb, "Uranium Accountability Measurement Procedures for the Mass Spectrometry Laboratory", ENI-138, Exxon Nuclear Idaho Co., Inc. (1980).

WOE 3 SIMULTANEOUS CONCENTRATION & ISOTOPIC URANIUM ANALYSES OF LOW LEVEL DISCARDS BY ISOTOPE DILUTION MASS SPECTROMETRY

LEWIS F. CASABONA
Teledyne Isotopes, Westwood, N.J. 07675

Tighter restrictions have been imposed on Nuclear Fuels fabrication facilities for purposes of safeguards and environmental considerations, to characterize their low-level waste streams. To date a variety of analytical methods are used, e.g., alpha counting, spectrophotometry, fluorimetry, and X-ray fluorescence. Due to the variety of sample matrices and isotopic composition, these methods have exhibited biases and poor precision and accuracy. Isotope dilution-mass spectrometry offers a relatively interference free analytical approach with a high degree of accuracy and precision. Parallel programs have been conducted and data comparisons will be given in addition to discussing sampling problems.

SAFEGUARDS MEASUREMENTS CAPABILITIES AS OBSERVED BY THE SAFEGUARDS ANALYTICAL LABORATORY EVALUATION PROGRAM,

D. W. Crawford, V. E. Connolly and B. W. Moran, U. S. Department of Energy, New Brunswick Laboratory, Argonne, IL 60439

INTRODUCTION

The New Brunswick Laboratory (NBL) of the U.S. Department of Energy (DOE) administers a variety of interlaboratory measurement programs in support of nuclear material safeguards. The basic goal of these programs is to assess and evaluate nuclear material measurement capabilities of laboratories on an individual as well as a comparative basis. These programs enable laboratories to upgrade their particular measurement capabilities or adopt new methodologies with demonstrated accuracy and precision. These programs also provide information concerning trends or changes in measurement reliabilities over a long period of time. This paper will describe one such program sponsored by DOE/NBL, the Safeguards Analytical Laboratory Evaluation (SALE) Program, which realizes these goals.

There are four (4) types of materials currently being distributed in the SALE Program for measurement evaluation purposes: uranium dioxide pellets, uranyl nitrate solutions, plutonium dioxide powders, and uranium-plutonium dioxide pellets (Table 1). These materials, representative of nuclear fuels measured by analytical laboratories for safeguards purposes, are well characterized for elemental concentration and isotopic abundance using reference measurement techniques verified with appropriate National Bureau of Standards Standard Reference Materials. These materials therefore qualify as reference materials so the measurement data generated by their analyses can be used to evaluate a laboratory's basic ability to handle and measure nuclear materials.

At the present time, forty-seven (47) laboratories from eleven (11) countries participate in the SALE Program (Table 2). These laboratories, analyzing some or all of these four materials on a bimonthly basis, are free to use the assay and isotopic measurement methods with which they are most experienced, as long as these are the methods that are routinely used for safeguards measurements. Thus, the body of data reported by the SALE Program represents a variety of methods, most of which are chosen because they are the most cost- and time-effective for meeting particular nuclear safeguards requirements (Table 3). As a result, the precisions and accuracies of each SALE laboratory's data do not necessarily represent "state-of-the-art" capability. The data, however, do provide good estimates of the "state of the practice" for each method or methods performed on a routine basis. Since the program is designed to evaluate the performance of these laboratories over a period of many years, fluctuations in general performance levels of the nuclear material measurement methodologies used can thus be observed, compared, and monitored.

COMPARISON OF METHODS

All methods used by the SALE Program participants are important in their specific applications. But, an awareness of a given method's limitations and a thorough understanding of its proper application is essential to a SALE laboratory in order to insure a proper utilization of the method. Given that all methods used to perform measurements are inherently subject to sample-to-sample variances (reproducibility) and/or imprecision (repeatability), some methods are better than others. Examples are isotope dilution mass spectrometry (IDMS) and gravimetry for assay determination. Graphs 1 and 2 compare the analyses of uranium dioxide for uranium concentration using these two methods. It is apparent that general precision is better for the gravimetric technique than IDMS. This is due in part to the fact that gravimetric technique is basically a mass measurement on a material whose stoichiometry can be easily reproduced. While impurity element correction must be applied to gravimetric samples, these corrections are seldom greater than 0.05%. However, a large quantity of a highly pure sample is needed for analysis. For very small impure samples, such as waste water and irradiated fuel samples, the IDMS technique generally yields better results, and is a preferred method.

An analogous comparison can be made with two isotopic methods, thermal ionization mass spectrometry (TIMS) and gas source mass spectrometry (GSMS). Although TIMS is more "flexible" in the analysis of a greater number of isotopes of uranium over an entire range of enrichments, as presently practiced, it cannot exceed or compare to GSMS in ^{235}U measurement precision. Table 4 illustrates this and gives a general performance indication as to the precision of TIMS and GSMS data as observed by the SALE Program.

COMPARISON OF LABORATORIES

Variations in the ability of laboratories to measure a material by the same method are frequently observed in participant's data. An example of this is shown in Graph 3, a plot of the 1981 ^{235}U abundance data for uranium dioxide using TIMS. A majority (58%) of the laboratories measuring ^{235}U abundance using TIMS were able to achieve accuracies to within 0.10% of the reference value for the material; other laboratories were unable to achieve the same accuracy and, furthermore, showed significant measurement imprecision.

Several factors contribute to interlaboratory variations for a single method:

(1) Inadequate laboratory resources, especially with regard to the availability and sophistication of technical instrumentation and the level of technical expertise of personnel operating the instrumentation

(2) Lack of uniform quality control limits. This does not imply that participant laboratories do not have quality control programs, but that the established limits determined by their safeguards requirements may not be as stringent for some laboratories as for others.

(3) Improper or lack of chemical pre-treatment of a sample. It is generally accepted that sample composition and impurity levels influence measurement precision and accuracy. This is especially true in the isotopic analyses of plutonium-bearing materials. Decay products, such as americium and uranium, can result in measurement biases and imprecision if not first removed (separated) from plutonium materials prior to using the TIMS method for isotopic analysis.

(4) Lack of or narrow range of operating experience. Various enrichments, chemical forms, impurity levels, and other material characteristics can create analytical problems for a laboratory method if these characteristics are different than those a laboratory normally sees.

(5) Failure to use certified reference materials. This is especially true in mass spectrometry, where mass discrimination corrections are based upon these materials.

PERFORMANCE TRENDS

The SALE Program provides information on performance trends to determine if changes in reliabilities or improvements in safeguards measurements have occurred. In observing the arithmetic means of all data reported during the past five (5) calendar years for the measurement of the uranium concentration and ^{235}U abundance of uranyl nitrate solutions, no notable change in the level of performance and reliabilities of all laboratories can be seen (Graphs 4 and 5). The inclusion of less precise data from "newer" participating laboratories as well as changes in personnel in the "older" more experienced laboratories have produced fluctuations but the overall performance level has remained static. On the other hand, an improvement in the accuracy of ^{241}Pu abundance measurement in the plutonium dioxide using TIMS over the past four (4) years can be seen (Graph 6). A modest improvement is seen in the accuracy of the ^{239}Pu abundance of the same material over the same period of time (Graph 7). The plot showing a change in performance levels for plutonium concentration measurements, Graph 8, shows a decrease in the quality of measurements during 1981. Because of the small number of laboratories performing plutonium measurements, it is difficult to diagnose this negative trend. However, the unavailability of material to some laboratories in 1981 resulted in fewer laboratories able to make measurements and, consequently, less plutonium data being reported.

Generally, the levels of measurement ability of all uranium and plutonium assay and isotopic analyses have followed the same trend as described above.

CONCLUSIONS

The reliability of measurements is closely associated with measurement methods employed by the laboratories. Furthermore, the measurement control within a given laboratory can be responsible for inaccurate or imprecise results irrespective of the method used. These considerations impact on the reliability in safeguards measurements. As it is realized that the most accurate and precise methods are included in the practices of most laboratories

participating in the SALE Program, individual laboratory philosophies and needs prevent their full utilization. What can be determined by the SALE data is the observed "state of the practice" as to how laboratories in the international community are performing safeguards measurements. SALE Program support by participants is necessary in order for meaningful measurement evaluations to be made.

TABLE 1 Reference Materials Used in the SALE Program

Material Type (form)	Measurements	Elemental and Isotopic Composition
Uranium dioxide (UO_2 powder)	Uranium concentration Isotopic ratios	88% Uranium 2.4% ^{235}U
Uranyl nitrate (solution)	Uranium concentration Isotopic ratios	15% Uranium 2 8% ^{235}U
Plutonium dioxide (PuO_2 powder)	Plutonium concentration Isotopic ratios	87% Plutonium 87% ^{239}Pu 12% ^{241}Pu
Plutonium-uranium Mixed oxide, PuO_2-UO_2 (pellet)	Plutonium concentration Plutonium isotopic ratios Uranium concentration Uranium isotopic ratios	22% Plutonium 66% Uranium 0 7% ^{235}U 87% ^{239}Pu 1 4% ^{241}Pu

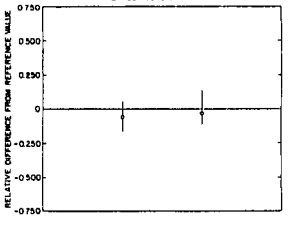
TABLE 2 Countries Currently Participating in the SALE Program

Belgium
Czechoslavakia
Finland
France
Italy
Japan
The Netherlands
Republic of China (Taiwan)
United Kingdom
United States
West Germany

TABLE 3 Methods of Analysis Used by Participants of the SALE Program

Material	Measurement	Method
Uranium dioxide	Uranium concentration	Gravimetry, U_3O_8
		Titrimetry
		Isotope Dilution Mass Spectrometry
	^{235}U abundance	Gamma Spectrometry
	^{235}U uranium isotope ratios	Gas Source Mass Spectrometry
		Thermal Ionization Mass Spectrometry
Uranyl nitrate	Uranium concentration	Gravimetry, U_3O_8
		Titrimetry
		Coulometry
		X Ray Fluorescence
		Isotope Dilution Mass Spectrometry
	^{235}U abundance	Gamma Spectrometry
	^{235}U uranium isotope ratios	Gas Source Mass Spectrometry
		Thermal Ionization Mass Spectrometry
Plutonium dioxide	Plutonium concentration	Titrimetry
		Coulometry
		Isotope Dilution Mass Spectrometry
	^{239}Pu ^{241}Pu plutonium isotope ratios	Thermal Ionization Mass Spectrometry
Uranium plutonium dioxide	Uranium and plutonium concentration	Isotope Dilution Mass Spectrometry
		Titrimetry
		Coulometry
	^{235}U ^{239}Pu ^{241}Pu and uranium and plutonium isotope ratios	Thermal Ionization Mass Spectrometry

GRAPH 1
1981 DATE
MATERIAL-URANIUM DIOXIDE MEASUREMENT-URANIUM CONCENTRATION
METHOD ISO DIL MASS SPEC



GRAPH 2
1981 DATA
MATERIAL-URANIUM DIOXIDE MEASUREMENT URANIUM CONCENTRATION
METHOD-GRAVIMETRY

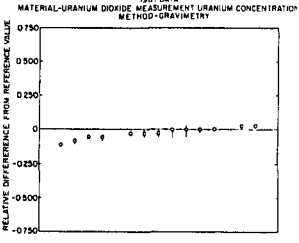


TABLE 4 Gas Source Mass Spectrometry vs. Thermal Ionization Mass Spectrometry in the Measurement of ^{235}U

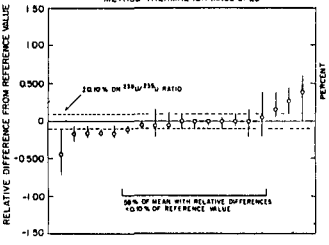
Between Laboratory Standard Deviation (Degrees of Freedom)

	Material Analyzed	Gas Source	Thermal Ionization
1979	Uranium Dioxide	0 032 (3)	0 191 (17)
	Uranyl Nitrate	0 022 (3)	0 141 (25)
1980	Uranium Dioxide	0 010 (3)	0 139 (18)
	Uranyl Nitrate	0 007 (3)	0 144 (17)

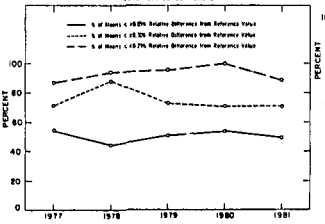
Within Laboratory Standard Deviation (Degrees of Freedom)

	Material Analyzed	Gas Source	Thermal Ionization
1979	Uranium Dioxide	0 043 (28)	0 270 (190)
	Uranyl Nitrate	0 029 (23)	0 193 (157)
1980	Uranium Dioxide	0 047 (22)	0 226 (160)
	Uranyl Nitrate	0.061 (20)	0 216 (163)

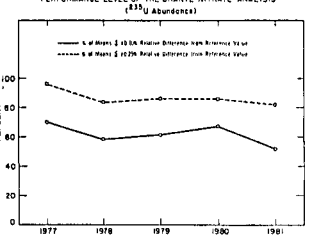
GRAPH 3
1981 DATA
MATERIAL-URANIUM DIOXIDE ANALYSIS, ^{235}U ABUNDANCE
METHOD-THERMAL ION MASS SPEC



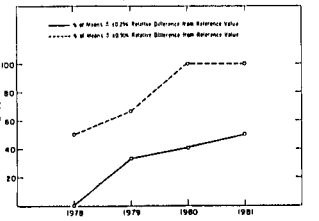
GRAPH 4
PERFORMANCE LEVEL OF THE URANYL NITRATE ANALYSIS
(Uranium concentration)



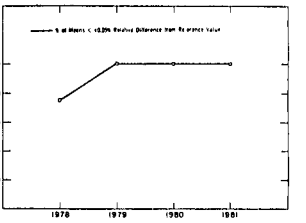
GRAPH 5
PERFORMANCE LEVEL OF THE URANYL NITRATE ANALYSIS
(^{235}U Abundance)



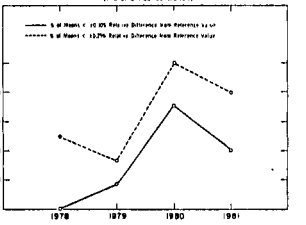
GRAPH 6
PERFORMANCE LEVEL OF THE PLUTONIUM DIOXIDE ANALYSIS
(^{241}Pu Abundance)



GRAPH 7
PERFORMANCE LEVEL OF THE PLUTONIUM DIOXIDE ANALYSIS
(^{239}Pu Abundance)



GRAPH 8
PERFORMANCE LEVEL OF THE PLUTONIUM DIOXIDE ANALYSIS
(Plutonium concentration)



WOE 5 THE CURRENT STATUS AND FUTURE ROLE OF NBS ISOTOPIC STANDARDS FOR NUCLEAR ENERGY.

E. L. Garner, T. E. Gills, and L. J. Moore, Center for Analytical Chemistry and Office of Standard Reference Materials, National Bureau of Standards, Washington, DC 20234.

A summary of currently available special nuclear assay and isotopic Standard Reference Materials (SRMs) and the future role of SRMs for the nuclear energy community will be discussed. Analogous to the steel industry, the maturation of the nuclear industry during the last twenty years has been instrumental in shaping the current NBS policy for SRMs used in the nuclear industry. In essence, this policy limits renewal as well as new SRMs to those which represent a unique measurement or regulatory requirement. Thus, the responsibility for certification and maintenance of key standards for demonstrating traceability to NBS will continue to reside at NBS. Included in the list of key primary standards are SRMs 995 (^{233}U spike), SRM 950b (uranium assay), SRM U500 (equal atomic isotopic standard), 996 (^{244}Pu spike), 949f (Pu metal assay standard), and SRM 957 (a new Pu equal atomic isotopic standard). Other certified reference materials will be provided through lead government agencies and private sector activity. Accordingly, a transfer of standards technology to the public/private sector has begun. The initial steps include the transfer of standards distribution responsibilities for assay and isotopic special nuclear materials to the New Brunswick Laboratory. In addition, a number of obsolete nuclear SRMs are being replaced and others such as the suite of uranium absolute isotopic ratio standards will be upgraded to improve uncertainty statements. From the upgraded suite of 18 uranium isotopic standards, less than half will be selected and recommended for use in systems calibration of mass spectrometers. By providing traceability through a limited number of SRMs and encouraging a strong partnership with other laboratories in the public/private sector, the standardization needs of the nuclear community can be met while improving the NBS ability to respond more effectively to shifting priorities and attendant new demands.

DETERMINATION OF REMOTE ACCOUNTABILITY TANK CONTENT BY ISOTOPE DILUTION MASS SPECTROMETRY

A. E. Perrin, D. J. Rokop, D. J. Frank, and J. Banar, Los Alamos National Laboratory, Los Alamos, New Mexico 87545

IAEA Report SM-201-104 defines the IAEA goals for material balance accuracies for various facilities in the nuclear fuel cycle. For a fuel reprocessing facility the required material balance accuracies for uranium and plutonium are 0.25% and 0.50%, respectively. These accuracies are stated as 1 standard deviation of the overall material balance at the facility.

Independent verification of the material balance at the input measurement end of a reprocessing facility is very difficult due to the high levels of radioactivity. Verification of the calibration of measuring systems located behind radiation shields is particularly difficult.

A verification method was developed by Mathews and coworkers at Bhabha Atomic Research Center which eliminates dependence upon the measurement systems at the processing facility. A known amount of a specific element is added to the accountability tank. After mixing throughly, a sample is withdrawn from the tank. Measurement of the quantity of the added element in the sample provides the needed relationship between the tank content and sample content without reliance on the plant measuring systems. The major uncertainty in the method was the mixing efficiency for the added element.

We have evaluated a modification to the Mathews procedure which utilizes two additionals of separated isotopes of lead. Comparison of the measured 206/208 ratio with the added ratio of 206/208 provides the needed measurement of mixing efficiency.

Because of stringent shipping regulations, it is necessary to accomplish the measurement on quantities of Pb, U, and Pu less than 1 microgram. We have developed precise procedures for these elements at the submicrogram level. The resulting analytical capabilities are listed in Table I.

An error analysis indicates that when these analytical procedures are applied to the double tank tracer method, the over all uncertainty for the input material balance for uranium and plutonium should be 0.2 relative % for each element. The procedure will be tested in cold pilot experiments before application to a hot reprocessing facility.

Table I

Element	Pu	U	Pb
Sample Size	1×10^{-9} g	1×10^{-8} g	1×10^{-7} g
95% CI	0.052%	0.052%	0.052%
Process Blank	5×10^{-13} g	4×10^{-10} g	2×10^{-9} g
Loading Blank	5×10^{-15} g	1×10^{-13} g	1×10^{-15} g
Process Minimum*	2×10^{-7} g	1.6×10^{-5} g	4×10^{-9} g
Transport Minimum*	1×10^{-9} g	8×10^{-9} g	4×10^{-9} g

*Minimum quantity needed to limit blank effect to 0.05% on 0.05 ratio if blank is 100% minor isotope.

AN ON-LINE, AUTOMATED GAS INLET SYSTEM FOR A FIELD MASS SPECTROMETER*

J. C. Newton, R. W. Crawford, R. D. Friesen and C. F. Smith
Lawrence Livermore National Laboratory
Livermore, CA 94550

An inlet system was designed and built for the purpose of analyzing gases obtained from underground nuclear tests in Nevada. These gases are introduced into a mass spectrometer for on-line analysis.[1] The original requirement was that one sample would be analyzed in about three minutes to determine the gross composition. A second sample was to be concentrated by gettering the active gases and then analyzed in approximately three minutes to determine the noble gas content in the diluent air. The analytical system was to be remotely operated by computer control linked by microwave to a control point typically 20-30 miles away. It was required that the system be completely contained due to the radioactivity of the gases. In addition, all components must be able to survive a wide range of temperatures and ground shock. Operation by non-technical personnel in remote locations was necessary.

The inlet system is constructed of stainless steel with double-acting, air actuated valves. The air pressure to operate these valves is controlled by electric solenoids through the DEC LSI-11/2 computer in the analysis trailer. This computer also controls the vacuum pumps, the pressure and temperature transducers and the mass spectrometer. The mass spectrometer is a Balzer's QMG-511 quadrupole chosen for its compatibility with computer control and ability to withstand ground shock. The entire system is installed in a truck-trailer shell for portable operation under field conditions.

The inlet system is shown in Figure 1. This figure is from the CRT display at the control point. Most of the gas from the underground sample hose passes through pump D where the pressure is read by the transducer PT 1 and controlled with the servo valve above pump D at about 120 torr with a Barocel Automatic Pressure Controller. A small amount of flowing gas is sampled by the capillary and then exhausted through an adjustable throttle valve into pump C. An even smaller sample is admitted to the mass spectrometer through the molecular leak for determination of the gross composition. A holdup tank contains the gases exhausted by the vacuum pumps.

In order to measure the noble gases in air, aliquots of the flowing gas from between valves 301 and 302 can be introduced into either Zr-Al getter which operates at 700°C to remove the active gases. This gettering is performed simultaneously during the gross composition determination. Unlike the constant pressure maintained during the gross sample analyses, the pressure of the gettered sample containing noble gases decreases with time.

As stated before, Figure 1 is from the CRT display at the control point. The status of each valve as well as pressure and temperature readings can be monitored during both remote and local operation. A display panel in the instrument trailer with manual switches is used for local operation. A valve number displayed on a dark background indicates the valve is open. PT 1-3 are pressure transducers with digital readouts while tc means thermocouple gauges which indicate low, medium and high pressures. Pumps A-D are Alcatel hermetically-sealed, mechanical pumps. Turbos 1 and 2 are Balzer's TPU-110 turbomolecular pumps.

*Work performed under the auspices of the U.S. Department of Energy by the Lawrence Livermore National Laboratory under contract number W-7405-ENG-48.

1. "A Portable, Remotely Operated, Computer-Controlled, Quadrupole Mass Spectrometer for Field Use," R. D. Friesen, J. C. Newton, C. F. Smith, UCRL-87566 (Preprint) 1982 (FPA7, 1982 ASMS Conference).

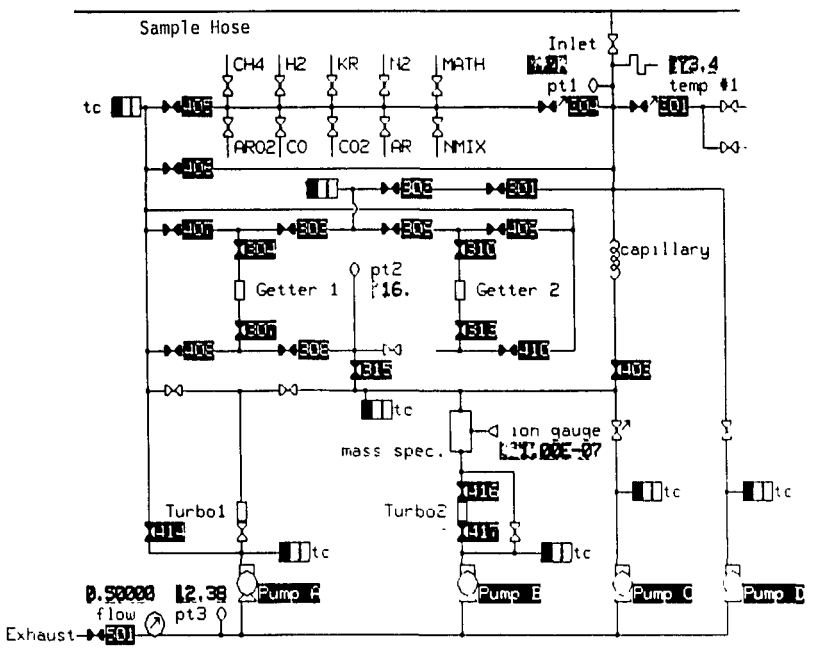
The vacuum manifold shown at the top of Figure 1 contains 10 cylinders of pure gases and gas mixtures used for calibration. Another manifold containing Pump A and Turbo 1 evacuates various volumes during operation cycles.

The software makes it possible for the operator to quickly write a command file to perform a specific function. During operation, it is possible to modify database parameters without stopping the analyses. The basic commands can be individually executed as required, e.g., during troubleshooting. If problems arise which are not remedied by existing hardware interlocks or software protection codes, the operator can quickly place the system in a safe configuration.

Data acquired during a run is displayed on a second CRT display controlled by another LSI-11 computer at the control center. The operator can request a plot of the peak heights vs mass number or have the gas concentrations vs time displayed. The data are also recorded on a disk for further processing in an off-line mode. Peak jumping is employed to improve the S/N. The mass scale is calibrated by using prominent peaks from selected gas standards. A modified multiple regression code is used to calculate gas concentrations on-line.

The system has operated successfully in the field and has met all requirements.

Figure 1. Inlet System Display



Mass Spectrometric Studies of Gaseous Uranium Chlorides

D. L. Hildenbrand and K. H. Lau

Materials Research Laboratory
SRI International, Menlo Park, CA 94025

Very few of the gaseous actinide halide species have been characterized by spectroscopic techniques, and basic thermochemical and molecular property data are scarce. This is particularly true of the lower-valent halide species that will be important in high temperature applications. Among the molecular properties that need to be evaluated are bond dissociation energies, ionization energies, structural parameters, spectroscopic constants, and electronic energy levels. In the studies described here, the gaseous U-Cl system was investigated by high temperature mass spectrometry so as to obtain some of the molecular properties described above. Mass spectrometry offers certain unique capabilities in this regard that cannot presently be matched by other spectroscopic techniques.

The U-Cl species to be studied were generated by the reaction of gaseous Cl_2 or $CaCl_2$ with a UC or UC-Cu sample in a heated graphite effusion beam source. Product species effusing from the molecular beam source entered the slit system of a magnetic sector instrument where they were ionized by electron impact, the resulting ions were then drawn out, mass analyzed, and collected. Gaseous product species were then identified from the masses and, primarily, the threshold appearance potentials (AP) of the ions observed in the mass spectrum of the effusing vapor at various cell temperatures in the range 500 to 2300 K. The lowest threshold AP's of the U-Cl ions and the initial temperatures of observation were: UCl_5^+ (10.2 eV, 525 K); UCl_4^+ (10.0 eV, 525 K); UCl_3^+ (8.5 eV, 1410 K)· UCl_2^+ (6.8 eV, 1970 K); UCl^+ (6.3 eV, 2230 K); and U^+ (6.2 eV, 2230 K). These threshold AP's are in accord with the expected ionization potentials of the corresponding neutrals, based on the increase in orbital energies resulting from successive additions of Cl atoms. These results define the conditions under which the various UCl_x species are present. Significantly higher threshold AP's were observed for UCl_3^+, UCl_2^+, and UCl^+ at lower temperatures, indicating fragmentation from heavier species to be substantial. By working at low ionizing energies, a few eV above the lowest thresholds, it was possible to avoid the complications associated with fragmentation and to monitor the partial pressures of the parent neutrals. This capability of monitoring the composition of complex gas mixtures at high temperatures is one of the unique aspects of mass spectrometry.

After establishment of beam composition, a number of gaseous equilibria involving the UCl_x species were studied over wide temperature ranges using parent ion intensities measured at low ionizing energies as a measure of partial pressure. Fragmentation corrections were also determined so that absolute equilibrium constants could be evaluated. Both enthalpies and entropies of reaction could then be derived solely from the equilibrium constants and their temperature coefficients, as summarized in the table. Since only the properties of UCl, UCl_2, UCl_3, UCl_4, and UCl_5 are unknown, results from the five independent reactions can be used to characterize the unknowns. These lead to the following bond dissociation energies, all in kcal/mole: D(U-Cl) = 108; D(ClU-Cl) = 117; $D(Cl_2U\text{-}Cl)$ = 117; $D(Cl_3U\text{-}Cl)$ = 101; and $D(Cl_4U\text{-}Cl)$ = 49. Absolute entropies evaluated from the equilibrium data show that the electronic contributions are large, ranging from 5 to 7 cal/deg mole at 2000 K. The thermochemical data so obtained are sufficient to predict the equilibrium behavior of the U-Cl system over a wide range of experimental conditions.

SUMMARY OF REACTION THERMOCHEMISTRY

Gaseous Reaction	Range, K	ΔH_T° Kcal/mole	ΔS_T° cal/deg mole
$U + UCl_2 = 2UCl$	2160 - 2440	7.5 ± 1.6	3.4 ± 0.7
$UCl + CaCl = UCl_2 + Ca$	2040 - 2220	-20.5 ± 1.1	-5.9 ± 0.5
$UCl_2 + CaCl = UCl_3 + Ca$	1970 - 2180	-19.0 ± 0.8	-7.8 ± 0.4
$UCl_3 + CuCl = UCl_4 + Cu$	1340 - 1600	- 9.2 ± 0.3	-8.6 ± 0.2
$UCl_4 + 1/2\ Cl_2 = UCl_5$	610 - 920	-20.3 ± 0.3	-14.6 ± 0.3

FORMATION OF METAL ATOM-CLUSTERS AND MEASUREMENT OF IONIZATION POTENTIALS

Yahachi SAITO, Kenzi YAMAUCHI*, Tamotsu NODA and Kazuhiro MIHAMA*

Toyohashi University of Technology, Toyohashi 440, Japan
*Faculty of Engineering, Nagoya University, Nagoya 464, Japan

Interest in small clusters has increased in such areas as the homogenous nucleation and growth of particles in the vapor phase, catalytic reactions and electronic structures. In the present experiment, lead clusters and lead-tin binary clusters are produced by an adiabatic expansion of the metal vapor. Relative abundance and ionization potentials of the clusters are investigated by time-of-flight(TOF) mass spectrometry.

Details of the apparatus design have been given elsewhere.[1] Briefly, the apparatus consists of three vacuum chambers, and each of them is differentially pumped. A boron nitride crucible, which can be heated up to 1700 °C by resistive heating of a tungsten wire, is located in the bottom chamber. The metal vapor expands into a vacuum through a small hole(0.5, 0.7 or 1.0mm in diameter and 6mm in length) of a cap atop the crucible. The clusters are ionized by electron bombardment. After being accelerated, the ionized clusters are chopped by an ion deflector in the middle chamber. The chopped ion beam is focused by an einzel lens to an ion detector at the end of the top chamber. The flight length between the deflector and the detector is 0.95m. The signal from an electron multiplier of the detector system is amplified and observed with an oscilloscope.

Figure 1 shows a TOF mass spectrum of lead clusters generated from the crucible with the hole of 1.0mm in diameter at 1350 °C. Clusters of up to ten atoms are observed, and Pb_7 has the highest intensity. From an estimation of structural stability of atom-clusters under Lennard-Jones interaction, it has been shown that the structure of pentagonal decahedron is the most stable among isomers for the clusters composed of seven atoms.[2] The pentagonal decahedron corresponds to the smallest multiply-twinned particles.[3] This structure has been commonly found in fcc metal particles except for aluminum.

Figure 2 shows relative abundance of Pb_n generated from the hole with three different diameters at 1350 and 1250 °C. The relative abundance is approximately proportional to

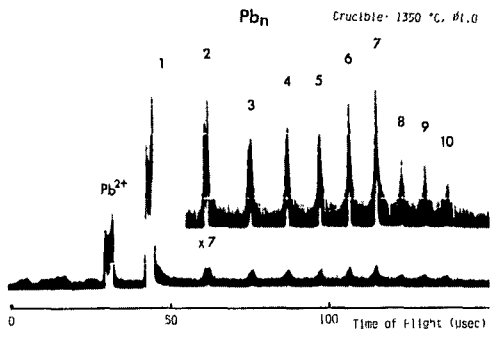


Fig. 1

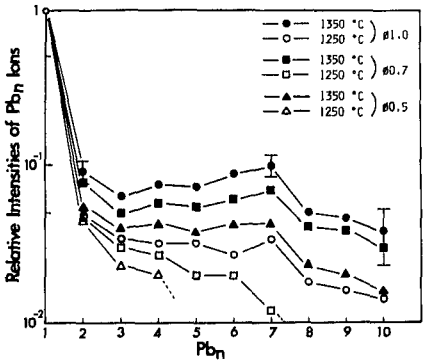


Fig. 2

the hole diameter and to the vapor density in the crucible. Since the region where the clusters are formed may be confined to a small region near the hole due to the divergence of the vapor flow, the abundance is determined by the frequency of collisions among atoms in this region. The size of clusters formed in the present experiment is the same order of magnitide as that of the critical nucleus calculated from the classical homogenous nucleation theory.[1] The lack of clusters of over ten atoms may be due to the small size of the cluster formation region and the high velocity of vapor flow.

Ionization potentials were determined from ionization efficiency curves according to the linear extrapolation method. Pb single atoms were employed as a standard specimen to calibrate the electron energy. The results up to Pb_7 are shown in Fig. 3. The ionization potential of the dimer(6.1eV) is strikingly reduced relative to the monomer(7.415eV), and those of larger clusters have a trend approaching slowly toward the work function of a bulk lead metal(4.02eV). The change in the measured ionization potentials seems likely to agree with the change in the effective work function calculated for classical metal drops[1] which is shown by a solid curve in Fig. 3. Therefore, it can be inferred that these small clusters exhibit metallic properties, since the solid curve in Fig. 3 holds only if the electrons are free.

Figure 4 shows a mass spectrum for lead-tin binary clusters at the crucible temperature of 1250°C and with the hole of 0.7mm in diameter. Pb_n($n \leq 7$), Sn_m($m \leq 4$), Pb_nSn($n \leq 6$) and Pb_nSn_2($n \leq 3$) are observed. Composition of the starting material is about Pb 60-wt%. As consuming the charged material during the experiment, the relative intensities of Pb_n and Pb_nSn_m decrease and those of Sn_m increase because of the high vapor pressure of lead. At the latter part of the evaporation and a high crucible temperature, 1550 °C, clusters observed are Pb_n($n \leq 2$), Sn_m($m \leq 7$) and PbSn.

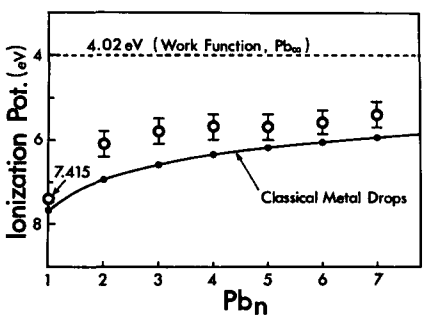


Fig. 3

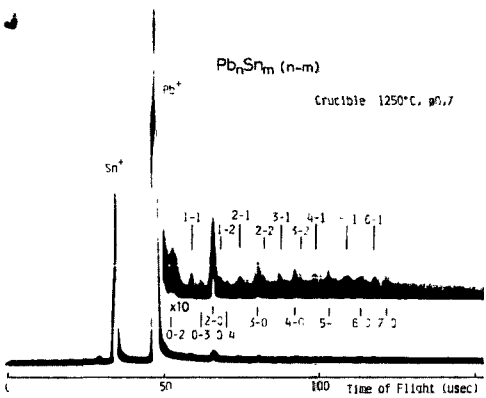


Fig.4

References

1) Y. Saito, K. Yamauchi, K. Mihama and T. Noda: Jpn. J. Appl. Phys. Lett. 21(6) (1982) To be published.
2) M. R. Hoare and P. Pal: Adv. Phys. 24 (1975) 645.
3) R. Uyeda: J. Cryst. Growth 45 (1978) 485.

PLASMA SOURCE MASS SPECTROMETRY OF INORGANIC SAMPLES USING A MICROMASS 12-12S QUADRUPOLE MASS ANALYZER.

Gray, Alan L.,Chemistry Department,University of Surrey,Guildford,Surrey,England.
Date, Alan R., Institute of Geological Sciences, Gray's Inn Road, London,England.
Elliott,R.Martin,and Cantle, John E., V.G. Isotopes Ltd.,Cheshire, England.

The plasma source mass spectrometer system developed at the University of Surrey using an ICP and a Micromass 12-12S quadrupole analyzer has been described in two recent publications (1,2). These however referred almost entirely to operation in a mode where the sample of plasma was taken from within the boundary layer formed over a 70 µm diameter sampling aperture. Recent work at Surrey, using the same basic system, has concentrated on continuum sampling of the plasma with apertures of 0.4 mm. diameter which avoids reaction products from the boundary layer and should provide spectra more typical of the bulk plasma composition.

Solution samples are introduced to a pneumatic nebulizer coupled direct to a standard plasma torch. No desolvator is used. The plasma is normally operated at 1200 watts and the sampling aperture located on the torch axis at 10 mm. from the load coil. The effect of aperture position and plasma power are discussed. A supersonic beam is formed in the expansion stage behind the sampling aperture at a pressure of about 1 torr. The centre of this beam is selected by a 1 mm. diameter skimmer and passed to the ion optics system, and mass analyzer.

Sampling at the full plasma gas temperature of 7,500K provides performance which corresponds more closely than before to that expected from an ICP. The overall ion transmission gives sensitivities within a factor of 3 for elements up to 11ev ionization energy irrespective of mass as shown in Fig. 1. The response for high ionization energy species as shown in Fig. 2 corresponds to an ionization temperature of between 8,500K and 9000K, which also produces doubly charged ions for elements with low second ionization energies. Matrix effects are small and total concentrations of at least 1000 $\mu g.ml^{-1}$ may be run without condensed solid blocking the aperture. The system has a linear response of at least six decades as shown in Fig. 3. System background counts are between 30 and 80 Hz. and detection limits are of the order of 1 $ng.ml^{-1}$. The high temperature of the gas sampled ensures that refractory elements remain dissociated. A spectrum of a thorium solution shown in Fig. 4 demonstrates the small oxide peak associated with the singly charged atomic ion of this highly refractory element.

Although the detection limits obtained so far are considerably poorer than by boundary layer sampling (1), it is thought that the beam forming and skimming process is at present not optimised and that improvement in this will enable the advantages described to be obtained together with lower detection limits.

References.

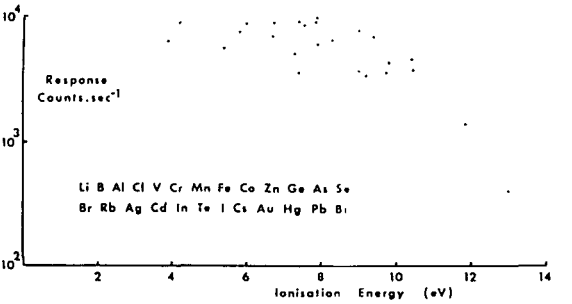
1. Date A.R. and Gray A.L., The Analyst, 106, 1255-1267, Dec. 1981.

2. Date A.R. and Gray A.L., Progress in Plasma Source Mass Spectrometry. Accepted for Proceedings of 1982 Winter Conference on Plasma Spectrochemistry. Spectrochimica Acta B.

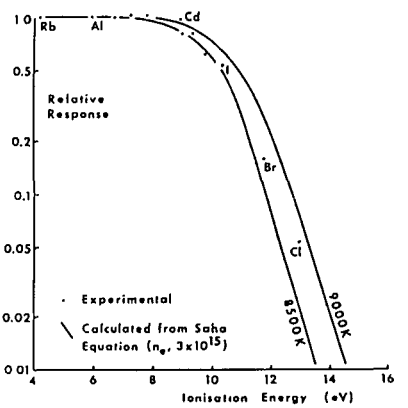
Acknowledgement.

This work is supported by the Institute of Geological Sciences and the European Community's R & D Programme on Uranium Exploration and Extraction. (Contract No. EXU 033-81-UK).

Figure 1

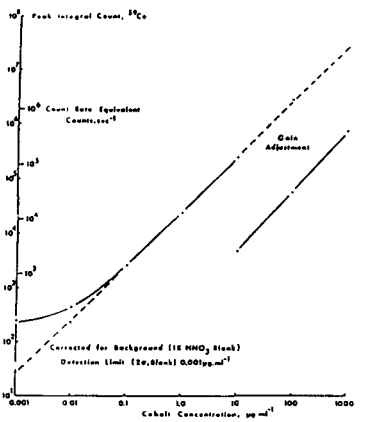


Response to 1μg.ml^{-1} Solution against Ionisation Energy for 25 Elements of Mass Range 7-209 a.m.u



Response against Ionisation Energy

Figure 2.



Linearity of Response

Figure 3.

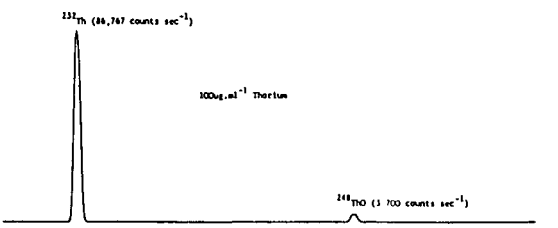


Figure 4. Spectrum of $^{232}Th^{+}$ showing oxide peak.

MASS SPECTROMETRY AS A ROUTE TO VERY ACCURATE THERMOCHEMICAL DATA

E. K. Storms

Los Alamos National Laboratory
Los Alamos, NM 87645

Mass spectrometry can be the most accurate method to obtain thermodynamic information about solids in the difficult high temperature region, i.e. in the region where temperature is measured using optical pyrometry. This paper will describe some techniques which have largely removed the major sources of error when the vaporization behavior of single phase material was used to obtain information about the activity, Gibbs energy, and enthalpy of information.

A vaporization study of single phase material requires that the technique be sensitive and fast to avoid the composition changes which preferential vaporization produces. Therefore, it is necessary to increase the spectrometer sensitivity to the greatest possible extent. We have done this by making the following changes in the ionization region of a single focus, 60° sector, magnetic mass spectrometer:

1. the slits in the ion focus plates were enlarged to sizes shown in Fig. 1,
2. the ionizing current was increased to 2.5 mA using a LaB_6 coated W filament and this was focused into a narrow beam,
3. the Knudsen cell was moved as close as possible to the electron beam, and
4. provision was made for internal bakeout and later cooling of the ionizing region.

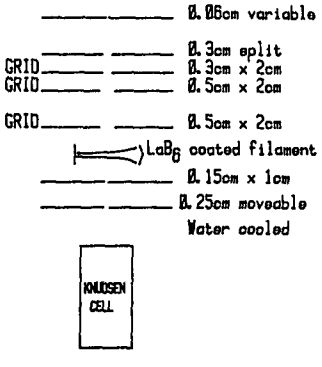


Fig. 1. Diagram of focus electrodes in mass spectrometer.

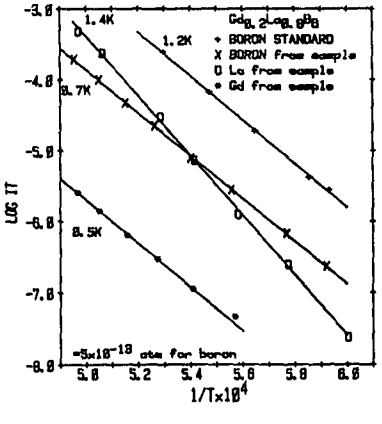


Fig. 2. Example of data obtained using suggested improvements. Temperature variation from line is indicated.

With grids on the indicated electrodes, the ion beam could be focused to a width of 0.06 cm at the primary focus. By coating the filament with LaB_6, the power delivered to the ionizing region was cut in half and this produced a significant reduction in background. The life of the filament was also increased to >700 h even though the emitted current was increased. In addition, the stability of the machine was increased. These changes allowed partial pressures of less than 10^{-13} atm to be measured in the Knudsen cell.

A significant improvement in accuracy can be achieved by using the ion ratio between the component vapor species and the vapor over the pure element. This ratio gives the activity directly thereby eliminating errors introduced by a calibration which uses another element combined with pressure data from the literature. To do this without using a double Knudsen cell requires that the machine sensitivity remain constant between runs. We have reduced this instability to less than ± 5%. This approach results in such a marked improvement in accuracy that the extra care is worth the effort. It is a shame that this is not done more often.

In order to extrapolate the measurements to higher temperatures or to obtain accurate values for the enthalpy of vaporization, the temperature must be accurately known. The temperature error can be largely eliminated by using the newly developed photon counting pyrometer. Although this device is not yet commercially available, it can be constructed from available components by a talented graduate student. The details are given in Ref. 1. This device has the following characteristics:

1. accuracy = ± 1 K at 2000 K,
2. precision = ± 0.1 K at 2000 K,
3. blackbody hole size = 0.05" diameter, and
4. base on a single reference temperature calibration.

Of course, to take full advantage of such an instrument, the temperature at the evaporating surface must be measured independently of any gradients which might exist in the cell.

Figure 2 shows an example of some typical data taken after these improvements were made using a single phase ternary compound. If all of the deviation from the least squares lines were caused by errors in temperature, the indicated average temperature error would result. At the lowest IT value, the boron pressure in the cell would be 5×10^{-13} atm, and the Gd and La pressures would be about 7×10^{-14} atm. These improvements and techniques have the following advantages:

1. systems can be studied at low temperatures where diffusion can compensate for vaporization to reduce composition gradients,
2. systems can be studied over a large temperature range to permit extrapolation to much higher temperatures or to obtain more accurate partial enthalpy values,
3. very accurate Gibbs energy values and chemical activites can be obtained, and
4. systems can be studied within a single phase region as a function of composition.

References

1. E. K. Storms and B. A. Mueller, National Bureau of Standards, Special Publication 561, Proceedings of 10th Materials Research Symposium on Characterization of High Temperature Vapors and Gases, NBS, Gaithersburg, MD., Sept. 18-20, 1978

NEGATIVE IONS FROM CaF_2-Al_2O_3 MIXTURES

E. Kato and T. Shiokawa
Department of Metallurgical Engineering
Waseda University
Tokyo, 160 JAPAN

The vapor species from CaF_2 and the mixtures containing CaF_2 were identified with a mass spectrometer-Knudsen cell combination. The temperatures of the samples were in the range 1127°C to 1565°C. The composition of the samples are shown in Table 1. The mass spectra of positive and negative ions were obtained;the positive ions were produced by electron bombardment, but the ionizing filament was not employed for the measurement of negative ions.

Table 1: Composition of the samples.

1. Pure CaF_2
2. CaF_2-29.9wt%Al_2O_3
3. CaF_2-82.0wt%Al_2O_3
4. CaF_2-10.0wt%SiO_2
5. CaF_2-8.4wt%CaO

Several negative ions were observed in the vapor from CaF_2-Al_2O_3 mixtures as shown in Table 2. The oxyfluoride ions with asterisks have not been reported by other workers. In the vapors from other mixtures than those containing Al_2O_3, negative ions of oxyfluorids were not detected. Large amount of F^- ion was detected in the vapor from any of the samples.

Table 2: Positive and negative ions from CaF_2-82wt%Al_2O_3 mixture.

	Positive ion			Negative ion			
Intensity	S	M	W	V.S	S	M	W
Ion species	AlF^+			F^-	O^-	H^-	C^-
	CaF_2^+	?	?		AlF_4^-	OH^-	CH^-
	AlF_2^+					C_2^-	AlO^-
						C_2H^-	AlO_2^-
						FO^-	$*AlFO^-$
						F_2^-	$*AlFO_2^-$
						AlF_2^-	AlF_3^-
						AlF_2O^-	$*AlFO_3^-$
						$*AlF_3O^-$	$*AlF_2O_2^-$

The positive ions observed in the vapors from CaF_2-Al_2O_3 mixtures are CaF^+, AlF^+ and AlF_2^+. The positive ions of small intensities were not detected, since the peaks of these ions could not be separated from the background peaks owing to the poor resolving power of the mass spectrometer used in this study. The appearance potentials and the ionization efficiency curves of CaF^+, AlF^+ and AlF_2^+ indicate that the precursers of these ions are CaF and CaF_2,

AlF, and AlF and AlF_3, respectively.

The applied voltages to the Knudsen cell, the shuttering slit which is located between the ion source and the Knudsen cell and the ion source are 1.3KV, 0V and -3.6KV, respectively. Therefore, only negative ions existed in the ion source could be detected.

In the ion source, the equilibrium between the molecules and the ions is considered not to have existed. However, thermodynamic consideration can suggest the possible reactions for the production of negative ions. The thermodynamic data and the equilibrium constants for the reactions of F^- with AlF_3, AlF and AlFO are shown in Table 3. These data are computed using the data given in JANAF Thermochemical Tables. The temperature of 500K is close to that of the ion source and the temperature of 1700K is close to that of the Knudsen cell.

Table 3: Thermodynamic data for the formation of negative ions.

Reaction	Temp.(K)	ΔH^o(kcal)	ΔG^o(kcal)	K
$AlF_3+F^-=AlF_4^-$	500	-125	-110	2.3×10^{48}
	1700	-124	-74	4.3×10^{9}
$AlF+F^-=AlF_2^-$	500	-92	-80	1.3×10^{35}
	1700	-93	-50	3.0×10^{6}
$AlFO+F^-=AlF_2O^-$	500	-112	-101	1.7×10^{44}
	1700	-113	-72	1.9×10^{9}

Considerable amount of AlF_3, AlF and F^- existed in the ion source, and the large negative values of the standard free energies of the reactions between these species suggest that AlF_3^- and AlF_2^- ions were produced by the addition of F^- ion to AlF_3 or AlF molecule.

The existance of AlFO molecule in the ion source is not shown in this study. However, Farber and Peterson[1] obtained AlFO vapor by the reaction of AlF_3 vapor with Al_2O_3, and AlFO vapor probably existed in the vapor from the CaF_2-Al_2O_3 mixture. The large negative value of the standard free energy for the reaction of the formation of AlF_2O^- from AlFO and F^- suggests that this reaction is the most probable process of the formation of AlF_2O^-.

The process of the production of other aluminum oxyfluorides is not clear, but these ions were likely produced by the addition of F^- ion to neutral molecules. Accurate determinations of the positive ions will reveal the mechanism of the production of these oxyfluoride ions.

REFERENCE

1. M. Farber and H. L. Petersen, Trans. Farady Soc., 59, 836(1063).

VAPOR PRESSURE MEASUREMENT OF CESIUM IODIDE AND OXIDES BY HIGH TEMPERATURE MASS SPECTROSCOPY

M. YAMAWAKI, M. HIRAI, T. NAGASAKI and M. KANNO

Faculty of Engineering, University of Tokyo, Tokyo, JAPAN

1. Introduction

Cesium iodide and oxides are of highly interest as fission product compounds which are to be accumulated in light water reactor and fast breeder reactor oxide fuels with irradiation. Vaporization behaviors of these compounds were studied with a combination of a Knudsen cell and a mass spectrometer. In advance of the vaporization measurement, an improved pulse counting method was developed to get higher accuracy and sensitivity in vapor pressure measurements.

2. Experimental

A newly developed method to precisely measure the counting efficiency of electron multiplier was used connectedly with the pulse counting vapor pressure measurement. This method is based on the use of a pulse height analyser and a Faraday cup. The conventional DC method was also used to improve the reliability of measurement as well as to expand the measurable temperature range.

3. Results and Discussion

(1) Cesium iodide

A Knudsen cell used was made of molybdenum and had an orifice of 0.7mm diameter. The sample was more than 99.5% pure powder supplied from E. Merck. Identified ions were Cs^+, I^+, CsI^+, Cs_2I^+ and $Cs_2I_2^+$, which gave the heats of sublimation such as tabulated in Table 1. The parent vapor species were determined as monomer(CsI) and dimer(Cs_2I_2) based on the appearance potentials, the heats of sublimation and the shapes of $\log I^+ \cdot T$ vs 1/T curves. By using the total vapor pressure values the absolute partial vapor pressures of both the species were determined as follows:

$$\log P_{CsI} = -9.84 \cdot 10^3/T + 12.4 \quad (592—718K)$$

$$\log P_{Cs_2I_2} = -11.6 \cdot 10^3/T + 13.1 \quad (630—727K)$$

These results are also shown in Fig. 1.

(2) Cesium oxides

A Knudsen cell used was made of platinum and had an orifice of 0.7mm diameter. The samples were prepared from the high purity cesium and oxygen and had compositions of 15, 40 and 64 at.% oxygen. As the ion species Cs^+ and O_2^+ were identified in addition to some hydroxide-originating ion species. Partial pressures of the vapor species of Cs and O_2 were estimated as follows:

Cs-15at.%O: $\log P_{Cs} = -5.42 \cdot 10^3/T + 0.26$ (430—580K)
Cs-40at.%O: $\log P_{Cs} = -6.62 \cdot 10^3/T - 0.92$ (480—620K)
Cs-64at.%O: $\log P_{O_2} = -4.52 \cdot 10^3/T - 2.48$ (550—630K)

These results are also shown in Fig. 2. The congruent vaporization composition of the Cs-O system was estimated to be around 20 at.% oxygen.

References

1) M. Yamawaki et al: Mass Spectroscopy, 28, 317 (1980).
2) M. Yamawaki et al: ibid., 29, 345 (1981).
3) M. Yamawaki, M. Hirai et al: J. Nucl. Sci. Technol., in press.
4) M. Yamawaki et al: High Temperatures-High Pressures, to be published.

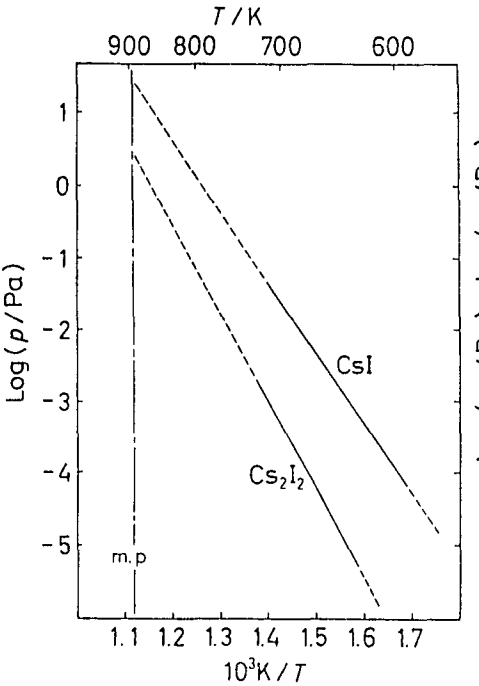


Fig. 1 partial pressues of CsI.

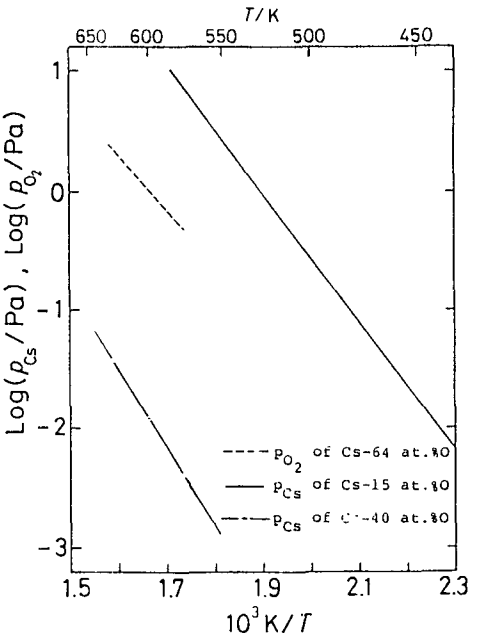


Fig. 2 Partial pressures of Cs-O.

Table 1 Heat of sublimation

Ion	ΔH_s° / kcal·mol^{-1}	$\frac{T}{K}$
I^+	45 9	622-718
Cs^+	45.1	610-716
CsI^+	45.4	592-717
Cs_2^+	52.4	673-727
Cs_2I^+	53 4	630-727
$Cs_2I_2^+$	53.4	688-727

ION-MOLECULE REACTIONS OF PH_3: IMPLICATIONS FOR INTERSTELLAR DETECTION OF PHOSPHORUS CONTAINING MOLECULES.

L. R. Thorne,* V. G. Anicich and W. T. Huntress
Jet Propulsion Laboratory Pasadena, CA 91103

Recent discovery of PH_3 in Jupiter's atmosphere and P^{++} in nearby stellar atmospheres[1] has stimulated interest in the astrochemistry of phosphorus. This coupled with the importance of phosphorus compounds in prebiotic chemical evolution has motivated a search for PH_3 and PN in several interstellar clouds. Neither compound was detected[2]. Consequently, we have investigated a number of ion-molecule reactions which could be important in interstellar phosphorus chemistry and the production of phosphorus containing molecules.

We have used a two step reaction scheme to model interstellar production of phosphorus compounds: (1) production of PMH^+ by a sequence of ion-molecule reactions then (2) dissociative recombination of PMH^+ with an electron to give the neutral products PM and H. M refers to any combination of H, C, N or O.

With this scheme as a guide, we have used Ion Cyclotron Resonance techniques to study a number of reactions of P^+ and PH^+ with neutral molecules thought to be abundant in interstellar clouds. Our results show that neither P^+ nor PH^+ reacts with H_2. Further, there is no simple ion-molecule scheme for production of PH_3 from P. Similarly the reaction, $P^+ + NH_3$ is slow but does produce PNH^+ which can dissociatively recombine with an electron to produce PN. However, the slow reaction rate and the low interstellar abundance of NH_3 suggest PN production may not be significant. On this basis, failure to detect PH_3 is not suprising.

By contrast to PNH^+, our results show that POH^+, POH_2^+, and PCH_2^+ are rapidly produced from $P^+ + H_2O$, $PH^+ + H_2O$, and $P^+ + CH_4$ respectively. Dissociative recombination then gives PO, HPO, and HCP. Of these, HCP is perhaps the most likely candidate for future radio telescope searches because of its simple rotational spectrum.[3]

---

* Present address, Sandia National Laboratory, Livermore, CA 94550.

1. M. Jura and D. G. York, Ap. J. 219, 861(1978).
2. J. M. Hollis, L. E. Snyder, F. J. Lovas and B. L. Ulich, Ap. J. 241, 158 (1980).
3. W. C. Johns, J. Mol. Spectrosc. 38, 437 (1971).

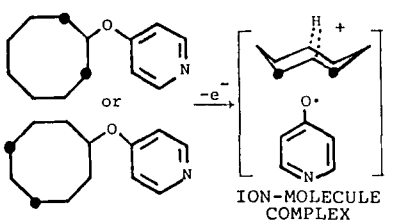
DISTINGUISHING BETWEEN POSITIONAL INTERCHANGE AND RANDOMIZATION OF DEUTERIUM LABEL. A KINETIC ANALYSIS. H.W. Biermann and Thomas Hellman Morton, Department of Chemistry, University of California, Riverside, CA 92521

Specific deuteration is widely used in mass spectrometry. The distribution of labelled products is frequently studied as a function of the isotopic substitution pattern of the neutral precursors. Comparision of two differently labelled neutral reactants sometimes shows that both give the same distribution of deuterated and undeuterated products. This is often used as evidence of an intermediate in which the label is exchanged between sites.

There are two ways that exchange can occur: positional interchange or randomization of label. For instance, if a precursor has a CH_2 and a CD_2 group, positional interchange designates the transposition of the labelled and the unlabelled carbons. Randomization of label, on the other hand, designates that the label itself moves from carbon to carbon; i.e.

$$\overbrace{CH_2\ CD_2} \quad \rightleftarrows \quad \overbrace{CHD\ CHD} \quad \rightleftarrows \quad \overbrace{CD_2\ CH_2}$$

This report describes a kinetic criterion for distinguishing between positional interchange and randomization of label. We shall examine, as an example, the ion-molecule reaction between cyclooctyl cation and the 4-pyridyloxy radical, as shown in reaction 1. We have previously shown that this ion-molecule reaction occurs during photoionization of cycloctyl 4-pyridyl ether. The reactants are produced in an ion-molecule complex from dissociation of the molecular ion, and the reaction obeys first-order kinetics. The ion-molecule reaction involves net transfer of two hydrogens to the pyridyloxy radical to yield protonated 4-hydroxypyridine and a cyclooctenyl radical. As represented in reaction 1, two differently tetradeuterated precursors yield the same distributions of labelled products (labelled carbons are indicated by heavy black dots). In one case, two CD_2 groups are in β-positions. In the other case, the two CD_2 groups are in δ-positions. As depicted, intermediacy of a hydrogen-bridged cyclooctyl cation accounts for the results in terms of positional interchange.

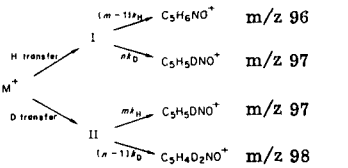


		Relative Abundance
$C_5H_6NO^+$	m/z 96	10
$C_5H_5DNO^+$	m/z 97	2.85
$C_5H_4D_2NO^+$	m/z 98	1.00

(1)

Suppose that, instead, we wish to interpret the result in terms of label randomization prior to any hydrogen transfers. Assume that m H's become completely scrambled with n D's. Scheme I illustrates the kinetics for sequential transfers of two hydrogens after randomization. Let us solve for the product ratios in terms of the kinetic isotope effect on the second step, k_H/k_D = a, and the ratio of steady-state intermediates, [I]/[II] = b. From the statistical weightings of the rate constants in Scheme I, we get the following expressions for product ratios:

Scheme I



$[m/z\ 96]/[m/z\ 98] = ab(\underline{m}-1)/(\underline{n}-1)$ and $[m/z\ 97]/[m/z\ 98] = (\underline{n}a + \underline{m}b)/(\underline{n}-1)$.

If we solve for the kinetic isotope effect, we get a quadratic equation whose solution is $a = (\frac{\underline{n}-1}{2\underline{n}})[\frac{m/z\ 97}{m/z\ 98} + \sqrt{(\frac{m/z\ 97}{m/z\ 98})^2 - \frac{4\underline{n}\underline{m}}{(\underline{n}-1)(\underline{m}-1)}(\frac{m/z\ 96}{m/z\ 98})}\ ]$. If we substitute the experimental values for relative abundances into this expression, we find that there are no positive choices for m and n for which a has a real value. In other words, the discriminant beneath the radical is negative regardless of how many H's and D's are chosen to scramble with one another in a randomization model. This type of analysis can be applied to other cases of double hydrogen transfer.

LEWIS ACID-BASE REACTIONS OF BORATE AND BORONATE ESTERS. John E. Bartmess and Jeff Kiplinger, Department of Chemistry, Indiana University, Bloomington, Indiana 47405, U.S.A.

Boronate esters have been proposed as good derivatization forms for 1,2- and 1,3-diols. Boron is also the best electron withdrawing group known in terms of resonance. We have therefore investigated the positive and negative ion chemistry of the title compounds using ICR spectrometry. The parent cation of borate esters condenses with a neutral borate to give a $(2M\text{-}RO\cdot)^+$ ion as in reaction 1; other fragment ions behave similarly.

$$B(OR)_3^{+\cdot} + B(OR)_3 \rightarrow (RO)_2\overset{+}{B}\text{-}O\text{-}B(OR) + RO\cdot \qquad (1)$$
$$\qquad\qquad\qquad\qquad\qquad\qquad\qquad\qquad\qquad\qquad R$$

Non-nucleophilic cation acids such as CH_5^+ will protonate $B(OMe)_3$; nucleophilic ones such as $EtOH_2^+$, $MeCNH^+$, and amines undergo a Lewis acid-base reaction 2. The Brønsted basicity of

$$MeCNH^+ + B(OMe)_3 \rightarrow MeC\overset{+}{N}\text{-}B(OMe)_2 + MeOH \qquad (2)$$

$B(OMe)_3$ appears to be near that of methanol.

In negative mode, borate esters add nucleophiles readily:

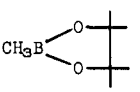
$$NH_2^- + B(OMe)_3 \rightarrow (MeO)_2B\bar{N}H + MeOH$$

$$MeO^- + B(OMe)_3 \rightarrow B(OMe)_4^-$$

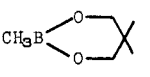
The latter process occurs bimolecularly and appears to involve radiative stabilization of the adduct, consistent with the very strong intensity of the B-O stretch in the IR. The adduct can undergo Ligand switching reactions with either an alcohol or another borate ester.

$$B(OMe)_4^- \xrightarrow[\text{or } B(OEt)_3]{EtOH} (MeO)_nB(OEt)_{4-n}^- \qquad (3)$$

For boronate esters I and II, commonly used as synthons in solution phase chemistry, deprotonation at carbon is a minor channel for all anionic bases. Simple addition at boron,



I



II

addition-fragmentation as in reaction (4), and elimination from the pinacolate methyls in I predominate with NH_2^-, HO^-, and RO^-.

$$CH_3B(OR)_2 + HO^- \rightarrow CH_3\bar{B}(OH)(OR)_2 \xrightarrow{-CH_4} {}^-OB(OR)_2 \qquad (4)$$

Mechanism for the Gas Phase Negative Ion Reaction of Oxygen with 2,3,7,8-Tetrachlorodibenzo-p-dioxin at Atmospheric Pressure

R. K. Mitchum*, W. A. Korfmacher and J. R. Althaus

Department of Health and Human Services
Food and Drug Administration
National Center for Toxicological Research
Jefferson, Arkansas 72079

The reaction of 2,3,7,8-TCDD with oxygen in an electron-rich plasma was first investigated by Hunt et al.[1] and later by Hass et al.[2] using conventional low pressure (1-2 torr) negative ion MS sources. These workers proposed a reaction scheme in which the molecular radical anion of TCDD reacted with O_2 to give the observed 4,5-dichloro-1,2-benzoquinone radical anion (m/z 176) plus the neutral 4,5-dichloro-1,2-benzoquinone.

Mitchum et al.[3,4] have also studied the reaction of O_2 with 2,3,7,8-TCDD at atmospheric pressure. Under these conditions, the same product ion (m/z 176) was observed but the reactant species were thought to be (neutral) 2,3,7,8-TCDD and O_2^-. The scheme was supported experimentally[4] by rigorously excluding O_2 from the system and simultaneously observing that no molecular anion or the corresponding semiquinone was produced. This does not exclude the converse since the transition state for product formation, vide post, is symmetrical for both cases and the accessible electron energies in a low pressure experiment (1-2 torr) could permit electron capture to long-lived negative ion states of the neutral molecule. However, at atmospheric pressure the electron energy population is thermal and the only observed electron attachment channel results in dissociative electron capture to form Cl^-.

In order to further elucidate the mechanism for semiquinone production for this reaction, the $^{18}O/N_2$ experiment described in this report was performed. When the $^{18}O_2/N_2$ was used as the reagent gas, the major product ion (m/z 176) shifted by two mass units (to m/z 178), representing the incorporation of one atom of ^{18}O into the 4,5,-dichloro-1,2-benzoquinone anion. Since the present results are not in agreement with the reaction scheme proposed by Hass[2], we propose a new reaction mechanism which is consistent with the experimental observation. Under APIMS conditions, the reaction mechanism proposed for $^{18}O_2^-$ reacting with 2,3,7,8-TCDD is shown in Figure 1. In this mechanism, $^{18}O_2^-$ reacts with 2,3,7,8-TCDD and proceeds through a Smiles intermediate[5] (Figure 1, #3)[6] which can fragment via two routes (Figure 1, #3a or #3b) to give a neutral and an anionic product each of which contains one atom of ^{18}O. The central part of the proposed mechanism includes a Smiles intermediate anion[5,6] which is very similar to the Smiles intermediate proposed by Nestrick et al.[7] for the condensation of 2,3,6-trichlorophenol in the solid phase producing several TCDD isomers. Further substantiation of the proposed mechanism is illuminated by the findings of Gray et al.[8] and Kende and DeCamp[9] for the condensed phase syntheses of hexachlorodibenzo-p-dioxin, which if a Smiles rearrangement intervenes, would necessarily give rise to an isomer mixture. Employing several different pathways to the desired specific isomer, the same isomer mixture was produced. Kende pointed out that Drozd and coworkers[10] had isolated a related spirocyclic complex which converted to the dibenzo-p-dioxin skeleton (ring system) upon standing in dimethyl sulfoxide. We surmise that the nucleophilicity of the radical anion of O_2 at atmospheric pressure to be similar to that of the phenolates utilized in the condensed phase syntheses.[11] Therefore, we propose that intermediate 3 is generated via intramolecular ipso attack at the adjacent phenyl ether and exists in the high pressure ion source before disassociating to the ion observed (Fig. 1, #4).

The difference between the results under the APIMS conditions and those predicted by Hass et al.[2] could be due to the differences in source conditions (atmospheric pressure and 0.1% O_2 for this work, a few torr total pressure and 10% O_2 for that reported by Hass). However, it is believed that the two reactions should be mechanistically similar.

References

1. Hunt, D. F.; Harvey, T. M.; Russel, J. W. J. Chem. Soc., Chem. Commun. 1975, 151-152.

2. Hass, J. R.; Friesen, M. D.; Hoffman, M. K. Org. Mass Spectrom. 1979, 14, 9-16.

3. Mitchum, R. K.; Moler, G. F.; Korfmacher, W. A. Anal. Chem. 1980, 52, 2278-2282.

4. Mitchum, R. K.; Korfmacher, W. A.; Moler, G. F.; Stalling, D. L. Anal. Chem. 1982, 54, 719-722.

5. Levy, A. A.; Rains, H. C.; Smiles, S. J. Chem. Soc. 1931, 3264.

6. Evans, W. J.; Smiles, S. J. Chem. Soc. 1935, 181.

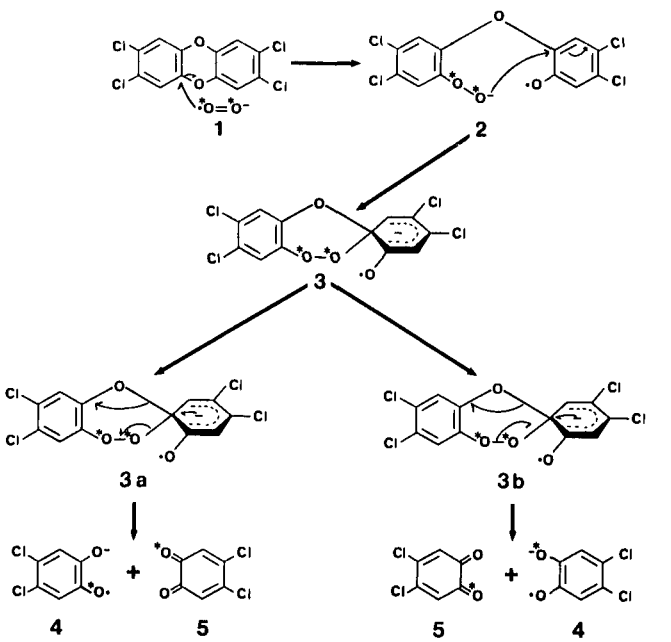
7. Nestrick, T. J.; Lamparski, L. L.; Stehl, R. H. Anal. Chem. 1979, 13, 2273-2281.

8. Gray, A. P.; Cepa, S. P.; Cantrell, J. S. Tetrahedron Lett. 1975, 2873-2876.

9. Kende, A. S.; DeCamp', M. R. Tetrahedron Lett. 1975, 2877-2880.

10. Drozd, V. N.; Knyazev, V. N.; Klimov, A. A. J. Org. Chem., USSR 1974, 10, 828 (English translation).

11. Perrin, C. L.; Skinner, G. A. J. Am. Chem. Soc. 1971, 93, 3389-3394.



WOF 5 NEGATIVE ION CHEMICAL IONIZATION MASS SPECTROMETRY: APPLICATIONS TO PROSTAGLANDIN AND DRUG ANALYSIS; B.J. Sweetman, F. Levin, M. Watson, J. Uetrecht and J.A. Oates; Department of Pharmacology, Vanderbilt University, Nashville, Tennessee 37232.

Electron capture negative ion chemical ionization in our hands has proven to be a useful complementary technique to other ionization modes using the VG 70-70F double focusing mass spectrometer in application to some of the bioanalytical problems presenting themselves in our laboratory. To fully utilize the technique careful consideration must be given to a variety of operational parameters. 6-Keto prostaglandin $F_{1\alpha}$ as the methoxime-trimethylsilyl ether-pentafluorobenzyl ester gives a mass spectrum showing a base peak at m/z 614 corresponding to loss of pentafluorobenzyl, which is a temperature insensitive process. This confirms the work of others using quadrupole mass spectrometers. Using this ion and tetradeuterated analogue as internal standard for selected ion monitoring we have been able to demonstrate sensitivity increases of an order of magnitude compared to existing electron impact-methods. This ion chemistry is also common to other prostaglandins including the major urinary metabolites of PGI_2 and TxB_2. Examples will be presented showing the complementary nature of fragmentation information obtainable comparing negative ion spectra with other ionization modes using procainamide and its metabolites as an example.

WOF 6 ENHANCED SENSITIVITY AND SELECTIVITY FOR DETECTION OF NITROAROMATIC COMPOUNDS USING NEGATIVE CHEMICAL IONIZATION HIGH RESOLUTION GAS CHROMATOGRAPHY/MASS SPECTROMETRY WITH ON-COLUMN INJECTION, Marcia G. Nishioka, Bruce A. Petersen, and Bruce J. Hidy. Battelle Columbus Laboratories, 505 King Avenue, Columbus, Ohio 43201

Methane negative chemical ionization high resolution gas chromatography/mass spectrometry (NCI HRGC/MS) with on-column injection provides enhanced sensitivity and selectivity over conventional EI HRGC/MS methods for the detection of nitro-aromatic compounds (2-5 ring parent PAHS). (1) Nitro-aromatics are thermally labile, thus the use of on-column injection minimizes thermal degradation. Chemical ionization enhances the sensitivity for detection of a molecular ion by decreasing its fragmentation. Minor but readily abundant fragment ions are useful for tentative identification. Data illustrating the enhanced sensitivity and selectivity of the NCI method will be reported. Data will also be presented which demonstrates the influence of reagent gas type, source temperature, and source pressure on the sensitivity for detection of these compounds. Applications of this method for the analysis of nitro-aromatics in environmental samples will be discussed.

(1) M. G. Nishioka, B. A. Petersen, J. Lewtas, Comparison of Direct-Acting Mutagenicity and Nitro-Aromatic Content of Diesel Engine Emission Extracts, 1981. U.S. EPA Diesel Emissions Symposium, October 5-7, 1981, Raleigh, North Carolina

MEDICAL AND BIOCHEMICAL APPLICATION OF NEGATIVE ION CHEMICAL IONIZATION MASS SPECTROMETRY
ULTRA-MICRO ANALYSIS OF BIOLOGICAL COMPOUNDS

T. HAYASHI*, H. NARUSE*, Y. IIDA** and S. DAISHIMA**
* NATIONAL CENTER FOR NERVOUS, MENTAL AND MUSCULAR DISORDERS, TOKYO, JAPAN 187
**DEPARTMENT OF INDUSTRIAL CHEMISTRY, SEIKEI UNIVERSITY, TOKYO, JAPAN 180

INTRODUCTION

Recently, it was reported that negative ion chemical ionization mass spectrometry (NICIMS) could give structural information complementary to that obtained in the positive ion mode of operation, and that electron capture NICIMS could provide sample ion current 100-1000 times greater than that available from positive ion methodology. It was also suggested that the electron affinity inherent to the sample structure would be the most important factor in the sensitivity. But only a few biological compounds show strong electron affinity and there are only a few report dealing with ultra-micro assay of biological compounds with NICIMS. Therefore, studies on derivatization of biological compounds such as phenylalanine, tyrosine, tryptophan and their metabolites.

DERIVATIZATION

The mechanism of the sample ionization is the same under both electron capture detection (ECD) for gas chromatography (GC) and electron capture NICIMS, although the detection mechanism is somewhat different from each other. Therefore, some kinds of fluorinated reagents were used for the derivatization to a molecule with strong electron affinity. One hundred micro-grams of each compound was used for derivatization. One micro-liter of the reaction mixture was injected to measure a methane PPINICI mass spectrum and the ratio of N/P was measured after 1:1000 dilution of the reaction mixture.

METHANE PPINICI MASS SPECTRA

All experiments were performed using a Finnigan 4023 GC/MS/DS equipped with a pulsed positive ion negative ion chemical ionization (PPINICI) system.

Table I and II show the methane PPINICI mass spectra of the derivatives derived from phenylalanine, tyrosine, tryptophan and their metabolites. N/P shown in the Tables is the ratio of the sample ion current of the most abundant negative ion that of the positive one. Therefore, the ratio could be usable as a rough parameter to estimate a detectability enhancement achievable using electron capture NICIMS. For the purpose of application of this method to an experiment using a stable isotope labeled compound, the prominent negative ion produced in the ion-source must contain the labeled moiety of the molecule.

In the case of phenylalanine, tyrosine and their metabolites, the derivatives prepared using fluorinated aromatic reagents provided convenient fragmentation and large N/P value. The introduction of many fluorinated aromatic groups to a molecule mostly provided a low volatile derivative.

On the other hand, in the case of tryptophan and its metabolites, indole compounds, the derivatization using fluorinated aliphatic reagents were as effective as those using fluorinated aromatic ones in the case of phenylalanine, tyrosine and its metabolites.

Table I Methane PPINICI Mass Spectra of the Derivatives of Phenylalanine, Tyrosine and their Metabolites

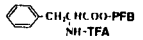
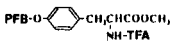
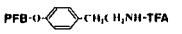
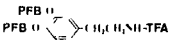
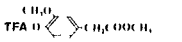
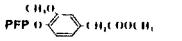
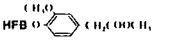
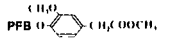
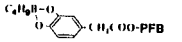
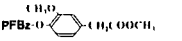
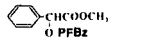
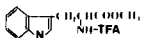
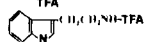
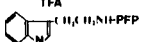
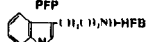
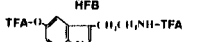
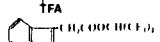
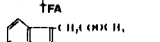
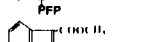
Compound	MW	N/P	m/z of negative ion peak (relative intensity)	m/z of positive base peak
	441	580	260(100) $(M-PFB)^-$	396
	471	100	290(100), 304(60) $(M-PFB)^-$	412
	413	80	232(100), 412(25) $(M-PFB)^-$	414
	609	250	408(100) $(M-PFB-HF)^-$	181
	292	3	113(100), 195(11), 291(11) $(OTFA)^-$	233
	342	50	147(100) $(PFP)^-$	283
	392	20	197(100) $(HFB)^-$	333
	376	760	195(100) $(M-PFB)^-$	317
	390	510	390(100), 306(40), 326(28), $(M)^-$ 391(16), 167(12)	359
	414	230	233(100) $(M-PFB)^-$	181
	360	230	167(100) $(C_6F_5)^-$	149

Table II Methane PPINICI Mass Spectra of the Derivatives of Indole Compounds

Compound	MW	N/P	m/z of negative ion peak (relative intensity)	m/z of positive base peak
	410	200	183(100), 390(70)* $(M-HF)^-$	411
	352	340	332(100)*, 333(18), 351(10) $(M-HF)^-$	353
	452	110	432(100)*, 412(58), 372(35), 451(20) $(M-HF)^-$	453
	552	170	512(100), 532(98)*, 492(64), 472(60) $(M-HF)^-$	553
	464	170	444(100)*, 367(58), 404(20) $(M-HF)^-$	465
	421	60	175(100), 157(48), 401(47)*, 421(42) $(M-HF)^-$	422
	335	20	147(100), 315(53)* $(M-HF)^-$	336
	271	110	174(100)*, 271(45) $(M-TFA)^-$	272

DERIVATIVES FOR ELECTRON CAPTURE NCI: ANALYSIS OF PHENYLACETIC ACID, GAMMA-AMINOBUTYRIC ACID AND THE CATECHOLAMINES AND THEIR O-METHYLATED METABOLITES

Kym F. Faull, Jeffrey Martin and Jack D. Barchas

Pasarow Analytical Neurochemistry Facility, Nancy Pritzker Laboratory of Behavioral Neurochemistry, Department of Psychiatry and Behavioral Sciences, Stanford University School of Medicine, Stanford, California 94305

In order to be applicable to the GC/MS method, a molecule must be sufficiently non-polar, volatile and thermally stable to traverse the chromatographic column. Furthermore, to attain the enhanced sensitivity available in the electron capture NCI mode, the molecule must have a positive electron affinity. Few biological molecules meet these requirements in and of themselves. Accordingly, chemical derivatization is necessary. Derivatizing reactions conferring both volatility and electron capturing ability have found wide application in the area of gas chromatography with electron capture detection. Thus, a great deal of literature is already available regarding the preparation of derivatives which are potentially suitable for NCI GC/MS work. Per-fluoro acylating reagents have perhaps found the most widespread utility as derivatizing reagents for electron capture gas chromatographic applications. These derivatives owe much of their prominence in this area to the volatility and electron capturing properties conferred by the perfluorocarbon group, and the presence of the carbonyl group which synergistically helps to delocalize the captured electron and stabilize the negatively charged ion.

We have attempted to maximize the enhanced sensitivity available in the NCI mode for a number of neurochemicals and their metabolites. This has been done by comparing the sensitivities obtained during SIM with different derivatives. The description of this work is divided into 3 sections, beginning with the most chemically simple example of phenyl-acetic acid, and extending to our work on the multifunctional catecholamines and their metabolites.

The pentafluorobenzyl (PFB) ester of phenylacetic acid has proven a useful derivative for the EI GC/MS assay of this compound in human lumbar CSF (1). The EI mass spectrum of the derivative is characterized by a strong M^+ (m/z 326, 20 percent) and intense fragment ions corresponding to the tropylium ion (m/z 91, 100 percent, C_7H_7) and the structurally analogous fluorinated ion at m/z 181 (40 percent, $C_6F_5CH_2^+$). The EI GC/MS assay can be accomplished by monitoring the ions at m/z 326 or 91 for the d_0-compound, and the ions at m/z 333 or 98 for the d_7-analogue used as the internal standard. We have observed that the NCI (methane) mass spectra of the derivatives of the d_0 and d_7 compounds are characterized by single intense fragment ions at m/z 135 and 142, corresponding to the carboxylate anions $C_6H_5CH_2COO^-$ and $C_6D_5CD_2COO^-$, respectively. These ions arise from the same cleavage which produces the $C_6F_5CH_2^+$ ion under EI conditions.

With this derivative, electron capture NCI yields a remarkable 5000-fold increase in sensitivity over the PEI mode. This sensitivity level allows the quantitation of small samples of cerebrospinal fluid and additionally, allows for split-mode injections when using capillary GC columns. The advantages of split-mode injections include shorter analysis times, while the combination of split injections with NCI detection provides significantly enhanced precision of the quantitative procedure (2). We estimate that with 1 to 3 pg of phenylacetic acid as the PFB ester arriving at the mass spectrometer source, signal to noise ratios in excess of 200/1 are routinely produced.

Gamma-aminobutyric acid (GABA) is an important inhibitory neurotransmitter in the central nervous system, and a number of procedures have been published which use conventional PEI and PCI GC/MS for quantitation in blood, cerebrospinal fluid and brain tissue homogenates. In general, the level of sensitivity demonstrated by these procedures extends to the low nanogram and high picogram concentration ranges. In an attempt to extend the sensitivity of these methods, we have studied the EI and NCI (methane) mass spectra of 6 different fluorinated GABA derivatives.

GABA (NH_2-$(CH_2)_3$-COOH) provides slightly greater chemical complexity than phenyl-acetic acid, with one primary amino and one carboxyl group. The GABA derivatives which we have studied include the PFB esters of the N-acetyl, N-neopentylidine (pivaldehyde) Schiff base and N-pentafluorobenzoyl Schiff base derivatives. These derivatives were prepared in

the hope that the NCI mode would provide a sensitivity increase similar to that found with the PFB ester of phenylacetic acid. We have also studied the N-heptafluorobutyryl (HFB) and N-PFB methyl ester derivatives and the N-pentafluoropropionyl (PFP) pentafluoropropanol (PFPOH) ester. The EI mass spectra of the PFB esters and the N-PFB methyl ester derivative were characterized by an intense ion derived from the reagent at m/z 181 ($C_6F_5CH_2^+$) and less intense diagnostic ions suitable for quantitation. The EI mass spectra of the N-HFB methyl ester and PFPOH ester were characterized by intense, characteristic fragment ions suitable for SIM. The NCI mass spectra of the PFB esters all show intense carboxylate anions which arise from the same cleavage that produces the $C_6F_5CH_2^+$ ion under EI conditions. The NCI spectra of the remaining derivatives show a variety of diagnostic ions, including M^+ and $M-HF^+$ ions, suitable for quantitative SIM analysis. Sensitivity in the EI mode using a suitable diagnostic ion was generally in the low nanogram range for all derivatives. On the other hand, sensitivity in the NCI mode was in the range of 1-300 pg for the same response. The neopentylidine Schiff base PFB ester was particularly sensitive in the NCI mode (1 pg), but unfortunately had a short half-life and decomposed rapidly after formation. The N-PFP PFPOH ester appeared to be the most suitable derivative for routine use, as it was detected at relatively high sensitivity (17 pg) and was stable in solution at room temperature.

Finally, we have studied the EI and NCI characteristics of several different derivatives of the catecholamines and their O-methylated metabolites. The results of this work provide another interesting comparison with the previous two compounds, as the catecholamines represent yet another level of chemical complexity, with catechol, phenolic and aliphatic hydroxyl groups and primary and secondary amino groups. The derivatives which we have show greatest promise for NCI work include the PFP and O-t-butyldimethyl silyl-N-PFB (TBDMS-PFB) derivatives. Their suitability for quantitative work and relative sensitivities have been directly compared for the three catecholamines and their O-methylated metabolites. The PFP derivatives yielded a more sensitive assay in every case, ranging from 1.4 to 8.4-fold sensitivity increases over the TBDMS-PFB derivatives.

The differences in relative sensitivity between the different derivatives observed in this study are likely to be the result of a combination of factors, including a higher yielding derivatization reaction and/or improved mass spectral characteristics with the resulting ions carrying a greater proportion of the ion current. The results demonstrate the increased difficulty experienced when attempting to efficiently convert small amounts of multifunctional compounds to derivatives suitable for NCI GC/MS. The carboxylate anion of phenylacetic acid PFB ester was detected with extraordinary sensitivity in this mode. Although a similar level of sensitivity was obtained for the carboxylate anion derived from the pivaldehyde Shiff base GABA PFB ester, the derivative was too unstable for routine use. Similar levels of sensitivity with other GABA PFB esters were not obtained, although fragmentation patterns similar to that of the phenylacetic acid derivative were produced. In the case of the catecholamines and their O-methylated metabolites, the increased chemical complexity created by multifunctionality further complicates the derivatization process. The requirement of a single derivatization procedure which is suitable to both the primary amino and N-methylated compounds precludes the use of the trimethyl silyl-PFB Schiff base derivative which has excellent senstitivity for dopamine (3). For these compounds, the PFP derivatives provided the best compromise for ease of preparation, sensitivity and rapid elution from the GC column.

Acknowledgements

Supported in part by an NIMH Program-Project Grant MH 23861.

References

1. Fellows, L. E., King, G. S., Pettit, B. R., Goodwin, B. L., Ruthven, C. R. J. and Sandler, M. Biomed. Mass Spec. 5:508-511, 1978.

2. Faull, K. F. and Barchas, J. D. In Methods of Biochemical Analysis, Vol. 29, D. Glick, ed., John Wiley and Sons, New York, in press.

3. Hunt, D. F. and Crow, F. W. Anal. Chem. 197:5, 50, 1711-1784.

MOLECULAR ADDUCT NEGATIVE ION FORMATION BY TRIFLUOROACETYLATED NUCLEOSIDES

R.W. Finney, H. Hughes, J. Nowlin and E.C. Horning. Institute for Lipid Research, Baylor College of Medicine, Houston, Texas 77030

The negative ion mass spectra of the trifluoroacetyl esters of nucleosides were studied, under desorption chemical ionization (DCI) conditions. This mode of sample introduction is particularly suitable for the analysis of involatile polar compounds which are not amenable to vaporization by conventional techniques prior to ionization.

All the presented mass spectral data was obtained from Ribermag R10-10C or Finnigan 1015 mass spectrometers. For introduction to the Ribermag instrument, samples were applied to a 60 μm tungsten wire located at the probe tip. Details of probe modifications and the mode of sample introduction to the Finnigan instrument have previously been reported (1). Methane was used as the primary ionizing source gas and any trifluoroacetic acid present in the mass spectrometer source originated from the derivatization mixture. Derivatives were prepared by the method described by Koenig et al. (2), using trifluoroacetic anhydride as the acylating agent.

Table 1 shows all presented spectra to contain stable molecular adduct ions equivalent to $(M+113)^-$, corresponding to adducts originating from the gas phase binding of trifluoroacetic acid to trifluoroacetyl esters. The relative abundance of molecular adduct ions is generally in excess of 50% and in many instances, the spectral base peak can be attributed to an anion corresponding to a trifluoroacetate molecular adduct.

The formation of trifluoroacetyl adduct ions, directly derived from molecular ions and observed in good intensity, aids in the assigning of molecular masses to compounds which under similar conditions yield low intensity molecular or pseudomolecular ions. This facility, in combination with the enhanced sensitivity of detection and diminished "background" attributable to the analysis of negative ions, should contribute to the study of trace components of biological interest in the presence of contaminants.

References

1. Carroll, D.I., Nowlin, J.G., Stillwell, R.N., and Horning, E.C. (1981). Anal. Chem. 53, 2007.

2. Koenig, W.A., Smith, L.C., Crain, P.F., and McCloskey, J.A. (1971). Biochemistry 10, 3968.

TABLE 1

Desorption Chemical Ionization Mass Spectra
of Trifluoroacetates of Nucleosides

Compound	m/z (Intensity)	
	Adduct ions [a].	Other ions [b].
Adenosine	764(100), 668(44), 572(81)	554(31), 345(25)
N^6-Isopentenyl adenosine	928(79), 832(100), 736(57)	412(21)
1-Methyl adenosine	778(100), 682(25)	761(8), 569(5)
N^6,N^6 Dimethyl adenosine	696(21), 600(79)	582(100), 487(30), 467(14)
Cytidine	740(42), 644(25)	627(43), 399(100)
5-Methyl cytidine	754(100)	641(17), 527(35), 413(24)
Cytosine-1ß-D-arabinofuranosyl	740(68), 644(93), 548(43)	627(30), 531(59), 513(51), 435(15), 417(76), 399(100), 303(35)
Guanosine	684(8)	666(40), 647(100), 570(13), 551(36)
1-Methyl guanosine	698(8)	680(75), 661(50), 584(17), 567(100), 259(58)
Inosine	669(100), 573(14)	556(5), 460(6)
Thymidine	643(12), 547(100)	434(6)
Uridine	645(100), 549(8)	531(13)
5-Bromo-2'-deoxyuridine	613(86), 611(100)	500(43), 498(30)
2,2'-Anhydro-1ß-D-arabinofuranosyl uridine	531(100), 435(35)	645(34), 418(26), 322(5)
2'-Deoxyadenosine	747(75), 652(50)	731(26), 345(100), 326(25)

[a] All adduct ions of relative intensity $\geq$ 5% and derived from the intact molecule are listed.

[b] All spectral ions, other than the above are listed.

NEGATIVE ION MASS SPECTROMETRY BY LOW PRESSURE CHEMICAL IONIZATION AND ITS COMBINATION WITH CONVENTIONAL POSITIVE ION MASS SPECTROMETRY BY ELECTRON IMPACT

H. Brandenberger

Department of Forensic Chemistry, University of Zürich,
Zürichbergstr. 8, CH-8028 Zürich, Switzerland.

Negative CI-MS is more flexible than positive CI-MS. Scheme I lists different possible negative ionization mechanisms. While positive CI requires high source pressure, some of the negative CI modes (1-3) give good yields also in the range of 10^{-3} to 10^{-2} torr.

Negative CI by electron attachment (1), carried out with reagent gases such as CH_4, yielding mainly positive ions and low energy electrons, is an extremely helpful tool for structural characterization and trace detection of compounds with high electron affinity. In combination with chromatographic techniques, it is the electron capture detector (ECD) of the future, more specific and more sensitive than the best conventional ECD. Reagents such as N_2O, which gives - on electron impact - a high negative ion yield (O^- and NO^-), should be chosen to characterize compounds with low electron affinity by charge exchange (2) or proton abstraction (3). CO_2 is the reagent we use to identify unknown components. It yields both the strongly basic anion O^- and a high population of secondary electrons, and is suitable for negative ionization of compounds with low and high electron affinity.

Conventional positive MS by EI is hardly or not at all affected by the presence of reagent gases, as long as the pressure is kept below 10^{-2} torr. This requires a reasonably open ion source. An interesting dual-MS-system is therefore possible in the pressure range of 10^{-3} to 10^{-2} torr. It combines positive ion formation by EI with negative ion production by CI, as illustrated in Figure 1 (pressure dependence of different ionization modes). Such a combination is more informative than two other quasi-simultaneous dual-MS-systems already in use (one consisting of positive and negative CI-MS, the other of EI and positive CI-MS), since it characterizes an unknown

1. by its conventional positive ion spectrum from the hard EI ionization,
2. by an additional negative ion spectrum yielding different and complementary structural information, and
3. by the indication of the molecular mass, usually given by the softer negative CI method.

Examples of applications, taken from toxicological case studies, are given. Figure 2 shows the dual-MS-recording of the metabolite hydroxy-pentobarbital from a urine extract.

Scheme I: Possibilities for negative chemical ionization.

R = reagent gas
M = substrate molecule
e^- = primary electrons, high energy
e^{-*} = secondary electrons, near thermal energy



e^- → R

EI

pos. CI	$R^+ + M \longrightarrow [MR]^+, [MH]^+$		mainly cluster cations
	+		
neg. CI (1)	$e^{-*} + M \longrightarrow M^-$		electron attachment
	or	$[M-H]^-$, $[M-X]^-$	often with dissociation
neg. CI (2)	$R^- + M \longrightarrow M^-$		charge exchange
neg. CI (3)	$R^- + M \longrightarrow [M-H]^-$		proton abstraction
neg. CI (4)	$R^- + M \longrightarrow [M-H+R]^-$		substitution
neg. CI (5)	$R^- + M \longrightarrow [MR]^-$		cluster anions

pos. CI neg. mode 5	only at high pressure
neg. modes 1 to 3	at low and high pressure
neg. mode 4	favored by high pressure

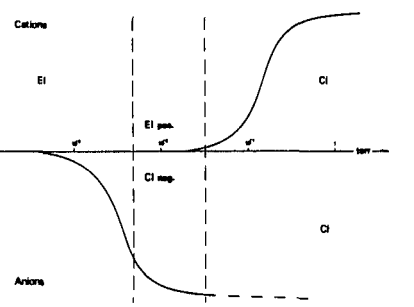
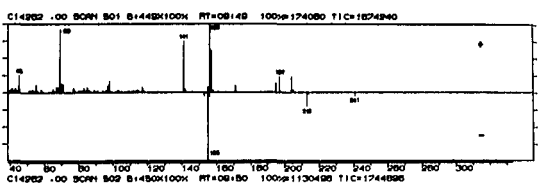
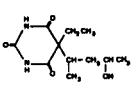


Figure 1





Hydroxypentobarbital

M_r = 242

Figure 2

LASER PHOTOIONIZATION MASS SPECTROSCOPY FOR ISOTOPIC AND ELEMENTAL ANALYSIS

by

N. S. Nogar and C. M. Miller

Los Alamos National Laboratory
Los Alamos, NM 87545

High precision isotope ratio mass spectrometers typically have mass resolutions in the range 10^2-10^3. Consequently, the measurement of the ratios of isotopes of a single element are often complicated by isobaric interferences resulting from incomplete chemical separations. Selective laser photoionization of the element of interest has the potential to reduce or eliminate the isobaric interference while at the same time accurately reflecting the isotopic distribution of the element of interest.

We have applied this technique to the selective ionization of Lu in the presence of Yb. This pair is particularly difficult to separate chemically, or by common physical methods, and so provides an interesting test of the capabilities of selective laser ionization. Samples were prepared by evaporating aqueous chloride solutions of the appropriate rare earth (or mixture) onto the side filaments of a conventional triple filament thermal ionization source. An unfocussed flashlamp-pumped dye laser beam, supplying 1 mJ pulses at 20 Hz, was propagated through the source region parallel to the sample filaments. The laser was tuned to the Lu, 452 nm $^2D_{3/2}(5d6s^2) \rightarrow {}^2D^0_{3/2}(5d6s6p)$ transition via optogalvanic excitation of a commercial Lu hollow cathode lamp (Fig. 1). Excitation to the $^2D^0_{3/2}$ excited state was followed by continuum photoionization using photons of the same wavelength. Laser generated ions were detected and the signals processed with a current integrating multiplier interfaced to a microcomputer.

The resonance-enhanced two-photon ionization process was found to be extremely selective. Figure 1a shows the thermal mass analysis of an equimolar mixture of Lu and Yb. The thermal Yb signal is orders of magnitude larger than that from Lu due to the large difference in volatilities of the two elements. Figure 1b depicts the result of laser photoionization of the same sample under conditions in which thermal ionization is minimized, and shows a dramatic enhancement in the Lu signal.

While rigorous detection limits (S/N $\geq$ 2) have not yet been determined, a preliminary series of experiments has shown that samples $\leq$ 1 ng are detectable. The use of secondary resonances, such as Rydberg or autoionization levels, offers the possibility of further selectivity, through the simultaneous matching of two resonances, and increased sensitivity, through increased cross sections for absorption near or above the ionization threshold. In order to explore this possibility, we have examined the spectroscopy of Lu near the ionization limit.

A XeCl* excimer laser was used to simultaneously pump two dye laser systems for these photoionization experiments. The first, operating with pulse energies of 20 to 100 microjoules, was used to saturate the $5d6s^2\ {}^2D_{3/2} \rightarrow 5d6s6p\ {}^2D^0_{3/2}$ transition of lutetium at 22125 cm^{-1}. The second dye laser, with pulse energies up to 2 millijoules, was tuned through the spectral region corresponding to transitions from the $^2D^0_{3/2}$ state to highly excited Rydberg levels and autoionizing states. Photoionization took place in the source region of

ToF mass spectrometer. Because of the relatively large ionization volume resulting from the use of unfocussed beams, mass resolution was limited to $\sim$ 2 amu.

Figure 2 shows the observed one- (lower) and two- (upper) color, two photon photoionization spectra of lutetium. In the lower trace, a single laser was scanned over the indicated wavelength region; in the upper trace, the second laser at 22125 cm^{-1} (4519 Å) was added. Both traces are shown on the same scale and are uncorrected for the tuning curve of the laser dye. At the laser powers used, optical saturation of several transitions was observed to occur. The spectra suggests that an enhancement of 2-3x in ion yield may be realized from the use autoionizing levels in the photoionization scheme. Further improvement in ion yield, and hence sensitivity, must come from matching sample evaporation and laser photoionization duty cycles.

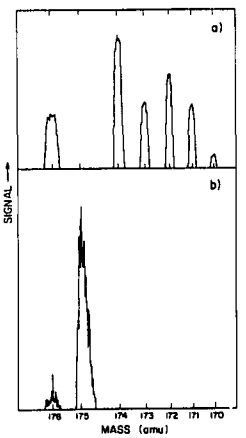


Fig. 1 a) Thermal ionization mass spectrum.

b) Laser ionization of same sample.

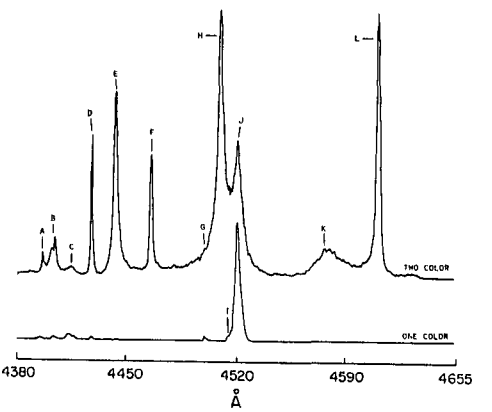


Fig. 2. Photoionization Spectra of Lutetium.

WOG 2 PULSED GLOW DISCHARGE IONIZATION SOURCE FOR ELEMFNTAL ANALYSIS, P. J. SAVICKAS, W. W. HARRISON, Dept. of Chemistry, U. of Va., Charlottesville, VA., 22901

The d.c. glow discharge has previously been applied in our laboratory to the elemental analysis of solid and solution samples. Its stable, high flux of ions for mass spectrometry and atoms for atomic absorption has shown it to be a versatile tool.

We have now designed and constructed a pulsed glow discharge ion source with the intent of maximizing our mass spectral sensitivity. Pulsing the discharge achieves several advantages for such analysis, and has provided some insights into physical glow discharge processes. For example, the source can be run at much higher instantaneous discharge currents than is possible with a d.c. discharge and the time dependent variation at individual elemental and molecular ions in the discharge can give information as to their formation.

Instrumental and discharge parameters, as well as sample and source geometries have been varied to optimize sensitivity for sample ions and to minimize scensitivity for discharge gas ions. A MINC-11 computer has been utilized to allow rapid data handling and to investigate signal processing techniques such as beam modulation and signal averaging.

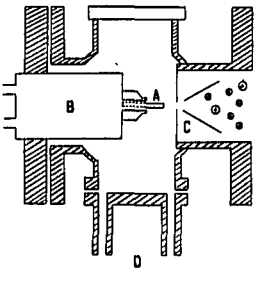
GLOW DISCHARGE MASS SPECTROMETRY OF THE LANTHANIDE ELEMENTS, R. B. Keefe and W. W. Harrison, Department of Chemistry, University of Virginia, Charlottesville, Virginia 22901

Glow discharge mass spectrometry has previously been applied to trace element analysis in a solid conducting sample.[1,2] This methodology has been extended to non-conducting or conducting powdered samples through the use of pressed pins similar to those used in spark source mass spectrometry. A glow discharge source for the sputtering of solution residues from a vitreous carbon cup has also been examined. The lanthanides have been studied because of their major importance as biological probes, and the analytical difficulty they represent for many trace element techniques.

Experimental

In one configuration the source is designed to accomodate a pressed pin held in a shielded vice grip parallel to the quadrupole axis (Figure 1). In the other configuration, up to 50 ul of solution can be applied to a cathode cup held perpendicular to the quadrupole axis (Figure 2). The solution sample is then dried to a residue film and the discharge is initiated.

The rest of the experimental arrangement has been described previously.[1,2]



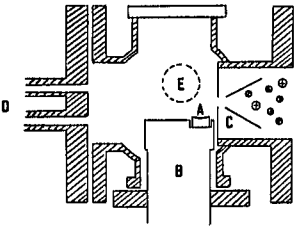


Figure 1. Solids Ion Source (A) Single pressed pin cathode, (B) Water-cooled pin holder, (C) Ion exit orifice leading to high vacuum chamber for quadrupole mass filter, (D) Gas inlet and pumping port.

Figure 2. Solutions Ion Source (A) Vitreous carbon cup cathode, (B) Water-cooled disc holder, (C) Ion exit orifice, (D) Gas inlet and pumping port, (E) Sample injection port.

Results and Discussion

(1) Solids

Figure 3 shows a lanthanide doped graphite pin. The relative sensitivities fall within a factor of 3 of each other. The 2.31% RSD of 50 scans of $^{159}Tb^{+1}$ over 10 minutes shows the homogeneity of the sample.

Not all of the sample is sputtered as singly charged atomic species; LnO^{+} may form as much as 50% of the lanthanide discharge species when the oxide bond is very strong (i.e., Ce). Also, doubly charged atomic species form as much as 16% of an ionized lanthanide, due to its relatively low second ionization potential.

(2) Solutions

Figure 4 shows repetitive scans of $^{151}Eu^+$, $^{153}Eu^+$. Other substances present in the residue matrix can significantly lengthen the time necessary to sputter the sample from the cathode, resulting in a decreased S/N. The scanning rate can be increased and collected on a multichannel analyzer, as in Figure 5. The detection limits range from 4 ppb (0.12 ng) to 41 ppb (1.2 ng).

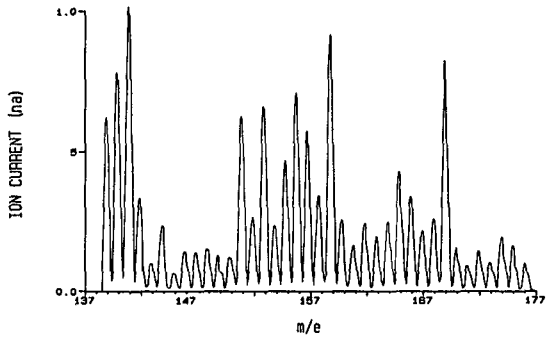


Figure 3. Graphite pin with 1% of 12 lanthanides (no Pm or Lu).

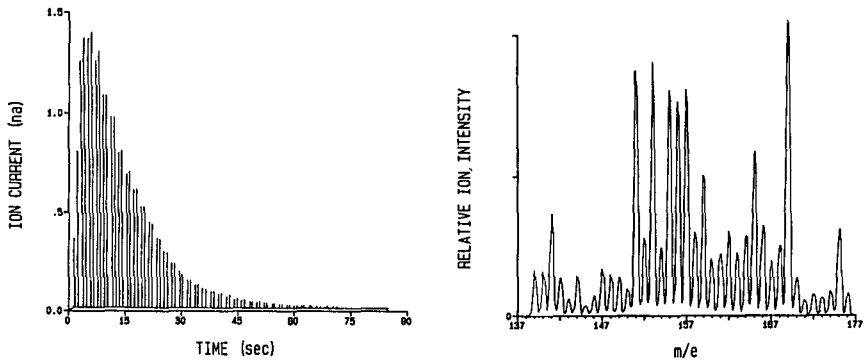


Figure 4. $^{151}Eu^+$, $^{153}Eu^+$. Repetitive scans of a dried solution residue of 30 ul, 1 ppm Eu in 1% HCl.

Figure 5. 25 ul solution of 1 ppm of 12 lanthanides (no Pm or Lu).

References

1. B. L. Bentz, C. G. Bruhn, W. W. Harrison, Int. J. Mass. Spec. Ion Phys., 28, 409 (1978).

2. B. L. Bentz, C. G. Bruhn, W. W. Harrison, Anal. Chem., 51, 673 (1979).

SPARK SOURCE MASS SPECTROMETRIC ANALYSIS OF GALLIUM ARSENIDE FOR TRACE LEVELS OF OXYGEN AND CARBON USING LIQUID HELIUM CRYOPUMPING

D. C. Walters and D. C. Look
Wright State University Research Center, Brehm Laboratory
Wright State University, Dayton, Ohio 45435

Introduction

The relationship between electrical properties of semiconductor materials and their trace elemental composition have been studied for many years and a wide range of effects resulting from both added and unintentional impurities have been documented[1,2,3]. In recent years, oxygen and carbon, which are likely contaminants[4], have received particular attention as they can have pronounced effects on the resistivity characteristics of semi-insulating materials[5]. A thorough characterization of electrically active elemental impurities is essential for an understanding of the electrical behavior of semiconductors and the development of new and better electronic devices. Mass spectrometry is recognized as an effective analytical tool in defining trace element levels in semiconductors and the application of helium cryopumping has been demonstrated to be necessary for optimum reduction of the analytical blank for oxygen and carbon due to the residual gas phase in the source chamber[6].

Instrument Modification

Our laboratory has developed a system using the MS-702 spark source mass spectrometer for trace oxygen and carbon determinations in gallium arsenide while cryopumping the ion source with liquid helium. A diagram of the system is shown in Figure 1. Several significant instrument modifications were incorporated to achieve the helium cryopumping technique.

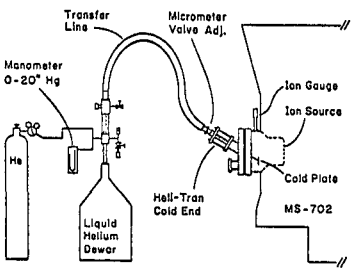
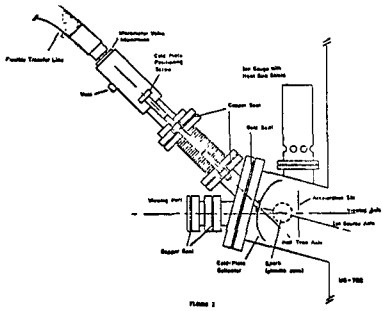


Fig. 1 Spark Source M.S. Cryogenic Pumping Syst.

A stainless steel source flange assembly was fabricated to allow helium transfer from a storage dewar (Cryofab Model CMSH) to a retractable collector which is positioned as desired inside the ion source vacuum housing. The collector, cooled by the regulated flow of liquid helium, is 3" diameter, 10 mil thick copper disc connected to the Cryo-Probe (1/8" copper rod). This probe is coupled through a stainless steel bellows assembly to the source flange and can, therefore, be adjusted by threaded guide rods having knurled knobs without disturbing the vacuum. Transfer of liquid helium to the Cryo-Probe is accomplished by using a Heli-Tran Model LT-3-110 (Air Products and Chemicals, Inc.). This helium transfer system includes a heat-shielded flexible transfer line, which conducts liquid helium through a micrometer needle valve to the top of the cryo-probe, to which is attached the copper cooling disc on which gaseous components are collected.

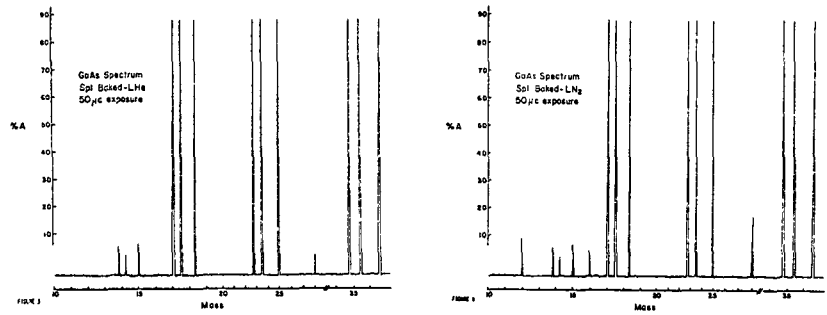
Temperature monitoring is provided by a silicon diode sensor located in the Heli-Tran probe and the temperature is read digitally using an Air Products-APD-G Temperature Indicator/Controller. For more accurate pressure measurement than is possible with the AEI (manufacture) pressure gauges, a CVC ionization gauge was installed directly on the source housing. This dual filament gauge provides vacuum measurements to 10^{-11} torr. The entire cryoflange assembly (shown in Figure 2) has been mounted directly on the ion source housing



with a triple hinge mechanism for convenient sealing (gold "O"-ring) of the flange to the housing chamber.

Results

Operating temperatures of 10°K-12°K are obtained during the analysis and provide source pressures of 2 x 10^{-9} torr following a 12 hour bake-out at 150°C. Recorded spectra for GaAs samples analyzed during the past several months clearly indicate more effective reduction of oxygen and carbon backgrounds using liquid helium than with liquid nitrogen (Figures 3 and 4). Detectabilities of 0.02 ppma for oxygen and 0.05 ppma for carbon have been obtained and



GaAs samples are routinely analyzed by this method with a modest consumption of liquid helium; approximately 2ℓ/hr or 7ℓ/run is used.

We are currently analyzing oxygen-doped and carbon-doped GaAs and other semiconductor materials to establish precision of the SSMS cryogenic method and to study sensitivity coefficients that may be applicable to the observed data.

References

1. D. C. Look, J. Appl. Phys. 48 (12), pp. 5141-5148 (1977).

2. Y. S. Park, B. K. Shin, D. C. Look and D. L. Downing, International Conference on Ion Implantation in Semiconductors, August 26-30, 1974, Osaka, Japan.

3. L. W. Aukerman and R. D. Graft, Phys. Rev. 127, 1576 (1962).

4. G. W. Blackmore, J. B. Clegg, J. S. Hislop and J. B. Mullen, Journal of Electronic Materials, Vol. 5, No. 4, (1976).

5. Phil Won Yu, Solid State Commun., Vol. 32, pp. 1111-1114 (1979).

6. J. B. Clegg, I. G. Gale and E. J. Millett, Analyst, Vol. 98, pp. 69-74, January, 1973.

WOG 5 THE DETERMINATION OF MICROGRAM QUANTITIES OF SULFUR BY THERMAL IONIZATION MASS SPECTROMETRY. P. J. PAULSEN and W. R. KELLY, Center for Analytical Chemistry, National Measurement Laboratory, National Bureau of Standards, Washington, DC 20234.

A new procedure has been developed for the measurement of sulfur isotopic abundances by thermal ionization mass spectrometry using silica gel as an emitter. Sulfur is measured as the AsS^+ ion. Since As is mononuclidic (mass 75), the ion currents at masses 107, 108, 109, and 111 resulting from AsS^+ are directly proportional to the abundances of ^{32}S, ^{33}S, ^{34}S, and ^{36}S, respectively. One microgram of sulfur is sufficient to give a stable ion current of $5x10^{-12}$A $^{75}As^{32}S^+$ for 3/4 hour and yields $^{32}S/^{34}S$ and $^{33}S/^{34}S$ ratios with standard deviations (1σ) of about 0.05% and 0.5%. This procedure utilizes much of the chemistry developed previously for the sulfur isotope dilution spark source mass spectrometric method described by Paulsen, et. al. Sample and ^{34}S enriched spike are equilibrated by dissolution with a mixture of HNO_3 and HCl in a sealed tube which prevents loss of any volatile sulfur compounds. The equilibrated sulfur is reduced to H_2S with a H_3PO_2-HI-HCl mixture and collected in a NH_3-As^{+3} solution. Arsenic sulfide is precipitated by acidification, washed, and redissolved in a NH_3-As^{+3} solution. One microgram of sulfur from this solution is evaporated onto a Re filament along with silica gel and H_3PO_4 for analysis by thermal ionization mass spectrometry. All sample manipulation is performed in a N_2 gas atmosphere to exclude sulfur compounds present in laboratory air. Present blanks range from 0.1 to 0.3 μg and are the limiting factor for analysis at low levels. The main thrust of the NBS effort is to certify a variety of metallic and biological materials for sulfur. There are few techniques capable of measuring sulfur on an absolute basis below 50 μg/g. This technique has been applied to analysis of NBS SRMs ranging from less than 10 ppm in metals to over 4,000 ppm in a citrus leaf sample (SRM 1572).

IMPROVED PRECISION AND ANALYSIS TIMES BY THERMAL IONISATION

P.J. Turner & J.E. Cantle
VG Isotopes Ltd., Winsford, Cheshire, England

Multiple collector arrangements permit simultaneous measurement of two or more ion beams. The benefits to the scientist are:

1. A greater proportion of the total available ion current is collected during a given period of time; hence improved precision is to be expected and analysis times are reduced.
2. The effects of fluctuations of ion beams with respect to time are reduced, removing one of the errors introduced into measurement using the peak jumping technique.
3. Amplifier decay constant effects are eliminated.

Up to the present time the system which has received most experimental attention is double collection for strontium in geochronology. The radiogenic isotope is ^{87}Sr and normalisation is carried out on the assumption that the ratio $^{86}Sr/^{88}Sr$ is constant and equal to 0.1194. Two Faraday collectors separated by unit mass and the $^{86}Sr/^{87}Sr$ ratio and $^{87}Sr/^{88}Sr$ ratio are measured by peak jumping between these two positions. It may be shown that, in this case, the two amplifier gains and any growth or decay of the ion beam during the measurement period no longer affect the value of the $^{87}Sr/^{86}Sr$ ratio.

It is found that the improvement in external (between bead) precision is typically from 0.02 per mil to better than 0.01 per mil, whilst the internal (within bead) reproducibility may well be better than 0.005 per mil.

The precision with which the uranium 235/238 ratio may be measured may be improved by an order of magnitude using simultaneous double collection of the two beams. An internal precision of 0.002% after 50 minutes for an NBS U500 standard is typical. In the case of uranium, however, there is no internal standard for isotopic normalisation.

The individual gain of each amplifier must therefore be calibrated. This is done in one of two ways:

a. by using a rhenium ion beam from the centre ionising filament and switching it to each bucket in turn.
b. by using a constant voltage calibration source to switch a stable signal to each head amplifier in turn.

As the number of collectors increases the second option becomes far more attractive because of the speed of operation.

Multicollector systems having more than two buckets

As the number of collectors increases to provide simultaneous measurement of more than two ion beams, the complexity of setting up the system increases. For this reason - and to provide the maximum versatility to the scientist the VG multicollectors are adjustable, the separation may be varied by the operator from outside of the vacuum system either manually or under computer control via high precision micrometer drives. The reproducibility of bucket precision is $\pm$ 0.01 mm.

A characteristic of the Z focussing ion optics used with extended geometry mass spectrometers is the steeply sloping focal plane represented diagrammatically in Figure 6.

A multicollector configuration aligned along this sloping axis would be prone to secondary ion effects and would make collector adjustability virtually impossible. For these reasons the current VG Thermal Ionisation mass spectrometers have received ion optical modifications to provide a flat focal place at right angles to the ion trajectory. This is illustrated in Figure 7.

This diagram shows a six Faraday collector system. Of the five separations, four are adjustable from outside of the vacuum. The highest mass bucket is fixed to the next highest bucket at a separation defined by the user at the time of manufacture.

This distance is variable only by taking the collector system apart. The axial or central Faraday is displaced with respect to the collectors either side to permit the alternative use of the Daly multiplier detector.

A seven collector system could be readily configured by adding a further fixed bucket on the low mass end. The head amplifiers are all contained in a constant temperature housing maintained at ± 0.01°C. This ensures negligible drift in their gain values.

Figure 8 illustrates some of the isotope systems that may be measured simultaneously with the VG multicollector system. Clearly a collection of fixed buckets would be a severe limitation on the number of isotope systems that would be measurable.

Lead isotope analysis

For highly radiogenic samples it is possible to measure the 204 beam with the Daly detector whilst simultaneously measuring 206, 207 and 208 in Faraday buckets on the high mass side. In this case the highest mass/next highest separation is fixed at 2.602mm.

We have measured the NBS 981 lead standard using our multicollector and obtained the following results.

204/206	0.059009	0.0034%
207/206	0.915077	0.0007%
208/206	2.170111	0.0006%

The precision given is one sigma for a set of 100 sets of 5 second integrations.

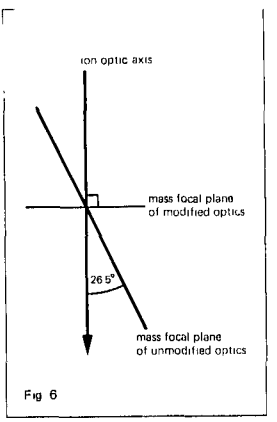


Fig 6

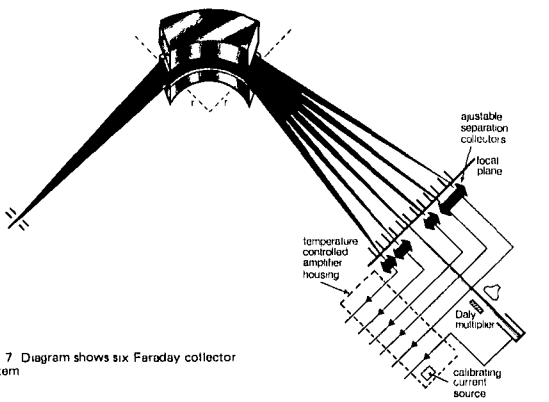
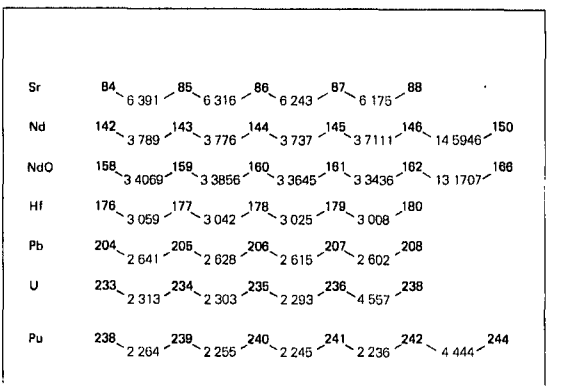


Fig 7 Diagram shows six Faraday collector system

below Fig 8 Peaks which may be measured using adjustable multicollector system



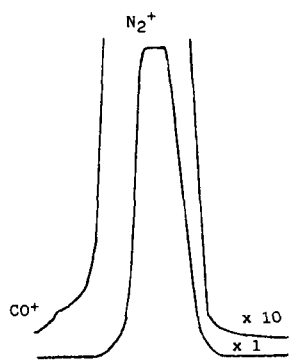
HIGH RESOLUTION, HIGH PRECISION GAS ANALYSIS MASS SPECTROMETRY
DETECTION OF LOW LEVELS OF CO

R.M. Elliott, B. Wright, J.E. Cantle
VG Isotopes Limited, Winsford, Cheshire, U.K.

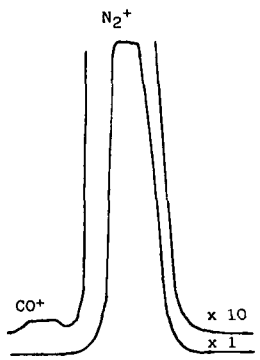
A frequent requirement in precision gas mass spectrometry is the analysis of mixtures containing both CO and N_2 which both have nominal mass 28. Other pairs of peaks of the same nominal mass occur in the analysis of helium/hydrogen isotope mixtures. The relevant species and the resolutions required are shown in the table:

Doublet	Resolution Required	Doublet	Resolution Required
$^4He-D_2$	156		
^3He-HD	512	$^{20}Ne^+-^{40}Ar^{++}$	1780
$HT-D_2$	930	CO-N2	2500
H_2-D	1300		

The group on the left refers to the hydrogen/helium application and these can be covered by an instrument with 1200 to 1500 resolution. The usual design considerations lead to the conclusion that a single focussing instrument with a magnetic dispersion of 30cm, such as the Micromass MM3001, will fulfil the requirements. The question then is how far can the same instrument fulfil the CO-N_2 requirement, in particular when one component is much smaller than the other.



Single Focussing (First stage of GAZAB) 5000ppm of CO in N_2 2500 resolution



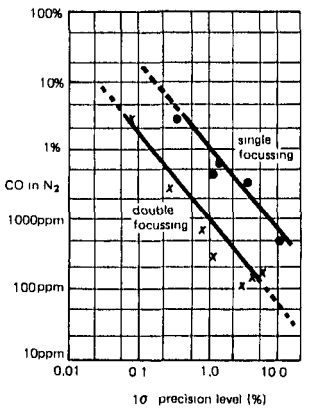
Double Focussing (both stages of GAZAB) 5000ppm of CO in N_2 3000 resolution

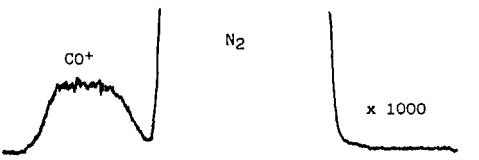
The left-hand trace of the figure shows that in a typical single focussing analyser, operating at 2500 resolution with flat-topped peaks, a low level CO^+ peak (0.5 percent) will appear only as a change in slope in the low level tail of the N_2^+ peak.

A double focussing version of the same mass spectrometer, formed by adding an electrostatic analyser in tandem, has far superior abundance sensitivity and a CO peak at the same level is now well separated.

However, although the single focussing case looks unpromising for precise measurement of the CO^+ intensity, it turns out that by using a modified peak jumping technique, reproducible measurements are possible. The digital field control allows the magnetic field to be switched precisely from the centre of the N_2^+ peak to the nominal position of the CO^+ peak, the number of digital steps being established in a calibration experiment. Also determined in this calibration is the height of the tail at the CO position to be subtracted from the observed intensity.

The measured precision levels achieved at different concentration levels are shown in the graph. However, this plot also shows that the double focussing instrument gives superior precision at a given level and also that CO levels of 100 ppm and below can be measured with an uncertainty of around 10ppm.





This is borne out by a recent example shown in the figure. At 3200 resolution, a 140 ppm CO^+ peak is clearly capable of measurement to 10 ppm or less.

The precision shown for the CO concentration levels in the table below confirm this:

	Daly			Faraday				Daly	
	H_2 ppm	^4He ppm	^{20}Ne ppm	CO ppm	N_2 %	O_2 %	^{40}Ar %	CO_2 ppm	^{84}Kr ppm
	167	13	9	212	78.027	20.899	0.997	373	2.9
	157	13	10	205	78.032	20.895	0.994	393	3.0
	157	13	9	218	78.038	20.887	0.995	399	3.1
	162	13	10	202	78.025	20.900	0.995	405	3.1
	158	13	9	198	78.031	20.896	0.995	401	3.1
	156	13	9	207	78.014	20.911	0.995	411	3.1
Mean	160	13	9.3	207	78.028	20.898	0.995	397	3.1
Std. Dev.	4.2	-	0.5	7.2	0.008	0.008	0.001	13	0.1
R.s.d. (%)	2.6	-	5.6	3.5	0.010	0.038	0.099	3.3	3

GAZAB. Repeat Analyses of Contaminated Air Sample.
3000 Resolution.

ISOTOPIC ANALYSIS WITH THE LASER MICROPROBE MASS ANALYZER

David S. Simons
Center for Analytical Chemistry
National Bureau of Standards
Washington, DC 20234

The Laser Microprobe Mass Analyzer (LAMMA),[1] which combines a laser ablation ionization source with a time-of-flight mass spectrometer, has proven to be a versatile tool for materials analysis of particles and thin sections.[2] Because a mass spectrometer is used as the detector of the emitted ions, the LAMMA is capable of determining isotopic as well as elemental abundance information. However, the author is aware of only one published study to date that has exploited this isotopic capability.[3] It is the purpose of this paper to discuss the performance of the LAMMA in the determination of relative isotopic abundances of an element.

The determination of isotopic abundances in the LAMMA is inherently more precise than the determination of elemental abundances. In the latter case relative ionization efficiencies among elements can be strongly affected by the details of the laser-solid interaction, in analogy with the well-known matrix effects that arise from the ion-solid interaction in secondary ion mass spectrometry (SIMS). Matrix effects are usually not significant for the isotopes of a given element since they all have the same electronic properties.

The best relative precision for a single isotopic ratio determination obtained to date is about 5% (one standard deviation). The isotopic ratios among the major isotopes of lead, which was present as a constituent of a thin glass film, were measured with the LAMMA. The relative standard deviations of the ratios for 10 separate spectra of closely spaced regions in the film ranged from 4% to 6% and were independent of whether the calculation of the ratio was based upon peak amplitudes or integrated peak areas.

One inherent instrumental limitation of precision is the 8-bit resolution of the transient waveform recorder that is used to digitize and store the mass spectrum. The range of uncertainty in the measurement of an intensity that is just below full scale will be approximately ±0.5 of the least significant bit for the peak and the same uncertainty will be present in the background determination. The combined relative error will be about 0.3% for the peak minus background. Since the Pb-206 and Pb-207 peaks were about one-half of full scale in this experiment the digitization error will contribute between 0.6% and 0.8% to the uncertainties in the ratios determined from peak height. For ratios based upon peak area the digitization error has a slightly smaller effect ranging from 0.5% to 0.7%. Clearly, this type of error is not limiting the ratio precision.

The dynamic response of the transient recorder is a second and more important factor that affects the precision of isotope ratio measurements. Although the precision of the analog-to-digital converter may be 8 bits for input signals that vary slowly with time, the effective bit resolution will be severely degraded if the measured waveform has major frequency components that approach the bandwidth of the recorder. Specific sources of error in analog-to-digital conversion that are frequency dependent include integral and differential nonlinearities, missing codes, and aperture uncertainty. Since the channel contents can change by a factor of 2 in adjacent channels when a mass peak is sampled at 10 ns per channel, it is clear that very high frequency components are present in the input signal train from the LAMMA. Therefore it is reasonable to conclude that the precision of the transient recorder for these pulses corresponds to 4 or 5 bits rather than 8.[4] This would completely account for the measured ratio precisions that are observed.

An example of the potential application of the LAMMA to isotopic analysis problems is the determination of the half-life of Re-187 by measuring the ingrowth with time of Os-187 in a sample of rhenium that has been spiked

with a known amount of a reference isotope such as Os-190. For this experiment the total quantity of Os-187 created in one year from 1 kg of rhenium is about 6 ng. With the current state-of-the-art no other mass spectrometric technique can do a routine isotopic analysis of osmium with this amount of material.

As a test of the capability of the LAMMA to perform this type of measurement a blind sample of osmium chloride containing approximately 10 ng of osmium with non-natural isotopic composition was supplied by Dr. Manfred Lindner of Lawrence Livermore Laboratory. A similar sample of natural osmium was used to calibrate the nonlinear response of the electron multiplier detector. The correction factor for this effect was as large as 30% of the measured ratio for the conditions of this experiment.

A spectrum of the non-natural osmium sample is shown in Fig. 1. It is estimated that less than 1 pg of osmium was consumed in acquiring a single spectrum. Isotopic ratios were calculated from peak areas of 10 such spectra, corrected for detector nonlinearity, and averaged. The resulting values are shown in Table I along with the revealed isotopic composition of the sample. It is clear that the LAMMA is capable of determining isotopic ratios from less than 1 ng of osmium with an accuracy better than 3% when the ratio value is greater than 0.2. These preliminary results give confidence that the LAMMA can be used to improve the accuracy with which the half-life of Re-187 is presently known.

This work was supported by the Air Force Technical Applications Center under contract T/0411/NP/NBS.

1. Certain commercial instruments are identified in this paper in order to adequately specify the experimental procedure. Such identification does not imply NBS recommendation or endorsement, nor does it imply that the equipment identified is necessarily the best available for the purpose.

2. F. Hillenkamp and R. Kaufmann, eds., Z. Anal. Chem. 308, 193-320 (1981).

3. P. Engler and U. Herpers, Inorg. Nucl. Chem. Letters 16, 37-43 (1980).

4. N. A. Robin and R. Ramirez, Electronic Design 28, 50-55 (1980).

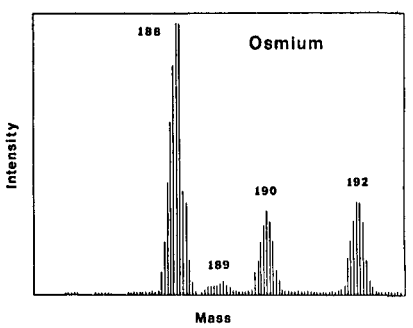


Fig. 1 -- LAMMA spectrum of osmium isotopes. Each vertical line represents contents of a single memory channel. Sampling time is 10 ns/channel.

Table I
Isotopic Ratios of Osmium
Non-Natural Mixture
Average of 10 Spectra

	189/188	190/188	192/188
Ratio determined by LAMMA	0.037 ±0.002*	0.233 ±0.008	0.263 ±0.007
True ratio	0.031	0.232	0.256

*one standard deviation of the mean

TELLURIUM ANOMALIES IN THE METEORITE ABEE?

C.L. Smith*, J.R. De Laeter and K.J.R. Rosman,
School of Physics and Geosciences,
Western Australian Institute of Technology,
Bentley, W.A. 6102. AUSTRALIA.

*Present address: Science Department, Nedlands Campus,
Western Australian College of Advanced Education,
Nedlands. W.A. 6009. AUSTRALIA.

Current theories of formation of the solar system initially require a cold gas-dust cloud, which was until recently thought to be chemically and isotopically homogeneous. However, the discovery of anomalous isotopes in the C3V carbonaceous chondrite Allende, such as ^{16}O (Clayton et al. 1973) and Nd and Ba (McCulloch et al. 1978), tend to indicate that a heterogeneous mix existed in the gas-dust presolar nebula prior to collapse. Some Allende isotopic anomalies could represent the relics of supernova ejecta from an event which may have been the trigger for the collapse of the primordial nebula to form the protosun and condensates of solar system entities.

The element tellurium (Z = 52) is an ideal indicator to test the incomplete mixing hypothesis of the presolar nebula because of:

(a) Its high cosmic elemental abundance of 4.84 normalised to Si = 10^6 atoms (Smith et al. 1977);

(b) High abundance of r-only isotopes ^{128}Te and ^{130}Te (Smith, 1982), and

(c) The unique property of Te in that it possesses three s-only isotopes ^{122}Te, ^{123}Te and ^{124}Te.

As r-process isotopes are synthesised in a supernova event, enrichment in meteoritic ^{128}Te and ^{130}Te could indicate the presence of supernova-derived material. A theoretical study of Heymann and Dziczkaniec (1981) indicated that Te isotopic anomalies are possible at various mass numbers when synthesised during a supernova event.

Manuel and his co-workers have recently claimed anomalous results for several isotopes of Te from Allende (Ballad et al. 1979). Using a neutron activation technique on high refractory mineral spearates from Allende, enrichments have been found in ^{120}Te, ^{122}Te, ^{126}Te and ^{130}Te, and a depletion in ^{124}Te with respect to a terrestrial laboratory standard. The status of these anomalies is uncertain as they have not been verified by mass spectrometry. A number of whole rock meteoritic specimens were isotopically analysed for Te, including Allende (C3V) and Abee (E4) (Smith et al. 1978), but no significant difference between the Te isotopic abundances of meteoritic and terrestrial Te was found.

Oliver et al. (1982) have suggested that the mass spectrometric data of Te in whole rock analyses of the E4 chondrite Abee by Smith et al. (1978) may indicate a depletion in ^{124}Te, although Smith et al. (1978) believed that no isotopic anomalies were present within the limits of experimental error. A depletion in ^{124}Te from Abee would substantiate a similar observed depletion in Allende by Ballad et al. (1979).

To examine the possibility of anomalous Te in Abee, two new analyses of whole-rock samples of this meteorite were carried out on a 30 cm radius, 90° magnetic sector, solid source mass spectrometer equipped with an electron multiplier. The attached figure shows the original data of Smith et al. (1978) together with the two new analyses, plotted as permil variations against the terrestrial laboratory standard. One possible interpretation of the data is that ^{128}Te and ^{130}Te are enriched with respect to ^{124}Te. Since both ^{128}Te and ^{130}Te are r-only isotopes, this implies an enhancement of r-process isotopes in Abee. An alternative explanation is that ^{124}Te is depleted with respect to the other isotopes, which are either r-only isotopes (^{128}Te and ^{130}Te) or a mixture of r and s process material (^{125}Te and ^{126}Te). This latter hypothesis was favoured by Oliver et al. (1982).

To demonstrate a lower limit of sensitivity of ^{124}Te anomaly detection, several synthetic ^{124}Te enriched samples were prepared and analysed. A standard Te solution enriched by 0.17% in ^{124}Te, was analysed to give a 0.16% ^{124}Te anomaly, indicating the level of detection of anomalous Te which is possible with the present instrumentation. An unequivocal answer cannot be given at this time as to the validity of Te anomalies in meteoritic material. Certainly the present data allows the possibility of anomalous Te in Abee, and further high precision analyses of Abee and Allende will be carried out to substantiate the existence of these anomalies.

REFERENCES

Ballad, R.V., Oliver, L.L., Downing, R.G. and Manuel, O.K., Nature, 277, 615-620, (1979).

Clayton, R.N., Grossman, L. and Mayeda, T.K., Science, 182, 485-488, (1973).

Heymann, D. and Dziczkaniec, M., Geochimica et Cosmochimica Acta, 45, 1829-1834, (1981).

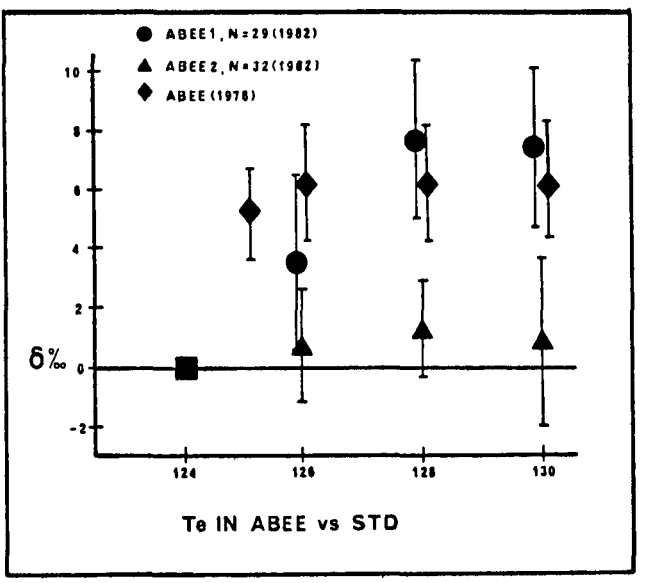
McCulloch, M.T. and Wasserburg, G.J., Astrophysical Journal, 220, L15-L19, (1978).

Oliver, L.L., Ballad, R.V., Richardson, J.F. and Manuel, O.K., *In press*, (1982).

Smith, C.L., Australian Physicist, 19, 2-5, (1982).

Smith, C.L., De Laeter, J.R. and Rosman, K.J.R., Geochimica et Cosmochimica Acta, 41, 676-681, (1977).

Smith, C.L., Rosman, K.J.R. and De Laeter, J.R., International Journal of Mass Spectrometry and Ion Physics, 28, 7-17, (1978).



ISOTOPIC ANALYSIS OF NANOGRAM AMOUNTS OF TELLURIUM AND PALLADIUM IN TERRESTRIAL ROCKS

K.J.R. Rosman, R.D. Loss* and J.R. De Laeter
School of Physics and Geosciences
Western Australian Institute of Technology
Kent Street, Bentley. 6102. W.A. AUSTRALIA.

Prior to 1970 the analysis of microgram amounts of relatively high ionisation potential elements ($\gtrsim$8eV) with conventional solid source mass spectrometers was uncommon. Generally ionisation was achieved with electron impact sources (Tyrrel et al., 1965) which tended to be cumbersome and plagued by hydrocarbon interference originating from residual gases in vacuum systems.

Thermal ionisation was employed very successfully for elements with ionisation potential $\lesssim$7eV, but for elements above this value the analysis of microgram-sized samples was difficult and nanogram amounts impractical. Ion emission from elements with high ionisation potential ($\gtrsim$8eV) was predictably immeasurably small (Langmuir and Kingdom, 1925).

The introduction of the silica gel "activator" (Cameron et al., 1969), in one form or another, into many laboratories in the early 1970's revolutionised solid source mass spectrometry by dramatically increasing the efficiency of the single filament thermal source for a range of elements. The mechanism by which the ionisation occurs is still not understood but the method offers a means of isotopically analysing small samples of many elements. For instance, it is now possible to routinely analyse nanogram samples of Cd, an element having an ionisation potential of 8.99eV. However, the sensitivity of the method is very dependent on the purity of the samples.

In this paper we describe the procedures which have been developed in order to isotopically analyse nanogram amounts of Pd (I.P. 8.3eV) and Te (I.P. 9.01eV) in terrestrial materials. Where high purity samples of Te and Pd are involved, the sample is transferred in conc. HCl (for Pd) or dil. HNO_3 (for Te) to a zone-refined rhenium filament and the liquid is evaporated, then taken briefly to red heat in air. The sample is then transferred to the mass spectrometer and heated to 1000°C for 10 m after which the temperature is increased to achieve ionisation (1150-1200°C for Pd and 1250-1300°C for Te). 100 ng samples yield an ion current of $\sim 10^{-14}$A for several hours. Approximately 2% (95% confidence interval) precision is achieved with 1-5 ng samples of either Pd or Te in our mass spectrometer which is fitted with an electron multiplier.

Where geological samples are analysed they are first digested with aqua-regia, HF and HCl acids, then the Pd and Te are extracted using ion exchange chemistry. The digested sample is loaded on to anion exchange resin (BIORAD,AG1) in conc. HCl. The bulk of the sample is eluted from the resin with between 9M and 3M HCl, then Te with 0.5M HCl and Pd with 0.06M ammonium ion solution. Te is further purified by two cation (BIORAD,AG50) stages. The Te is loaded and eluted at 0.5M HCl concentration. Nanogram-sized samples of Pd and Te require further purification before they can be reliably analysed. An electrodeposition method using a Pt anode, a Re (filament) cathode and NH_4OH/NH_4Cl electrolyte has been developed for this purpose. Efficiencies of 80-90% for Pd and 95% for Te are achieved with potential differences of 5V and 3.5V respectively. After rinsing the filament with water the activator is loaded in the normal way. Analytical blanks for the complete chemistry and loading procedure are typically 0.15 ng for Te and 0.12 ng for Pd.

These procedures have been used for isotope dilution measurements on Geochemical Reference Samples and measurements on samples from the OKLO fossil reactor region (Gabon, Africa). The concentrations found in Reference Samples extend from 0.1ppb in BCR-1 (basalt) to about 3ppb in PCC-1 (peridotite) for Pd and from 0.5ppb in BCR-1 to 474ppb for BX-N (bauxite) for Te. The levels observed at OKLO extend from 172ppm Pd and 162ppm Te in the reactor zones to 0.2ppb Pd and 1.4ppb Te in the country rock surrounding them. It has also been possible to measure the isotopic composition of Pd and Te in country rock samples located hundreds of metres from the reactor zones and detect the presence of fission product Te and Pd in them. These studies enable the mobility of Pd and Te from the OKLO minesite to be evaluated. The results are of value to the storage of radioactive wastes in natural

repositories (Hagemann and Roth, 1978).

REFERENCES

CAMERON, A.E., SMITH, D.H. and WALKER, R.L., (1969),
Mass spectrometry of nanogram-size samples of lead,
Analytical Chemistry, 41, 525-526.

LANGMUIR, I. and KINGDOM, K.H., (1925),
Thermionic effects caused by vapours of alkali metals,
Proc. Roy. Soc. A. 107, 61-79.

HAGEMANN, R. and ROTH, E. (1978),
Relevance of the Studies of the OKLO Natural Nuclear Reactors to the
storage of Radioactive Wastes.
Radiochim. Acta, 25, 241-247.

TYRRELL, A.C., ROBERTS, J.W. and RIDLEY, R.G. (1965),
Electron bombardment ion source for isotopic analysis of solids.
J. Sci. Instrum. 42, 806-807.

* Present address : Education Department of Western Australia, Royal Street,
East Perth. 6000. W.A. AUSTRALIA.

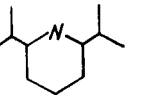
STERIC HINDRANCE OF THE HYDROGEN BOND. QUANTITATIVE EFFECTS ON THE SOLVATION AND CLUSTERING OF PROTONATED BASES, Michael Mautner (Meot-Ner) and L. Wayne Sieck, National Bureau of Standards, Washington, D.C.

1. Experimental
Pulsed high-pressure mass spectrometry.

2. Aqueous vs. Gas-Phase Basicities

Unhindered: 

Substituents in 3,4,5 positions

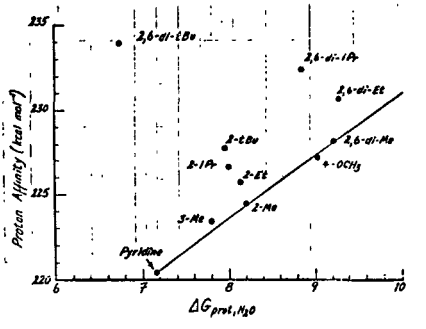
Hindered: 

Bulky substituents in 2,6 positions

Gas-phase basicities of unhindered and hindered pyridines were measured, and compared with aqueous basicities.

Unhindered compounds show linear correlation.

Hindered compounds deviate from correlation: aqueous basicities are decreased due to inefficient solvation of hindered ion.



3. The Gas-Phase Clustering and Hydration of Pyridinium and Ammonium Ions: BH^+B and $BH^+...OH_2$

Observation: Molecular models show that, in some conformations, the substituents keep the neutral B or H_2O molecule away from the H- bonding site. This would cause weakening of the bond--an enthalpy effect. In other conformations, the neutral B or H_2O can approach, but rotational hindrance results--an entropy effect.

Question: Is steric hindrance an enthalpy or entropy effect?

Table I

Entropies and Enthalpies for the Clustering Equilibria $BH^+ + B \rightarrow BH^+ \cdot B$ and for the Equilibria: $BH^+ + H_2O \rightarrow BH^+ \cdot H_2O$

BH^+	$-\Delta H°(BH^+ \cdot B)$[a]	$-\Delta S°(BH^+ \cdot B)$[a]	$-\Delta H°(BH^+ \cdot H_2O)$[a]	$-\Delta S°(BH^+ \cdot H_2O)$[b]
pyridine	24.6	28.2	16.1	27.0
2-Me	23.0	27.8	---	---
4-Me	---	---	14.7	26.6
2,6-di-Me	23.3	33.2	13.2	25.9
2,6-di-Et	22.8	37.4	13.0	28.6
2-iPr	23.0	32.7	14.2	28.8
2-tBu	23.0	39.4	14.2	30.8
2,6-di-iPr	23.6	48.4	12.8	32.1
2,6-di-tBu	23(est)	>60	12.5	41
Me_3NH^+	22.5	32.0	14.5	24.1
Et_3NH^+	23.8	41.0	13.2	27.3
$n\text{-}Pr_3NH^+$	23.5	54.9	12.5	30.2
$n\text{-}Bu_3NH^+$	24.4	56.5	13.6	36.4

[a] kcal mol^{-1}, [b] cal mol^{-1} K^{-1}.

4. Gas-Phase vs. Bulk Solvent Hydration

The steric effects on gas-phase hydration are obtained from the difference between $\Delta S°$ of hydration of hindered vs. unhindered compounds. The steric effects on bulk hydration are obtained from the deviation of hindered compounds from the correlation line of figure 1.

Table II

$XpyrH^+$	$\Delta G°$(steric, gas)[a] = $T\Delta S°$(steric, gas)	$\Delta G°$(steric, bulk water)[a]
2,6-di-Et	0.4	0.7
2-iPr	0.5	0.8
2,6-di-iPr	1.1	1.2
2-tBu	1.3	1.5
2,6-di-tBu	4.1	4.6

[a] kcal mol^{-1}.

5. Kinetic Consequences of Steric Hindrance

The reaction efficiencies (r) of exothermic proton transfer reactions between unhindered and moderately hindered compounds are near unity, and independent of temperature.

However, proton transfer to the highly hindered 2,6-di-tBuPyr is slow ($r < 4$), and substantial negative temperature coefficients (n in $k=CT^n$) are observed.

Table III

Rate Constants and Temperature Coefficients (n in $k=CT^n$) for the Proton Transfer Reactions $AH^+ + B \rightarrow BH^+ + A$

AH^+	B	k(T) (10^{-10} cm^3 s^{-1})	n	-ΔH (Kcal mol^{-1})
2-tBuPyrH$^+$	2,6-di-iPrPyr	8.6 (479) 9.3 (535)		4.6
2,6-di-EtPyrH$^+$	2,6-di-iPrPyr	13.3 (401)		1.8
2-MePyrH$^+$	2,6-di-tBuPyr	10.7 (527)		10.3
2,6-di-MePyrH$^+$	2,6-di-tBuPyr	4.2 (438) 2.9 (533)		5.8
2,6-di-EtPyrH$^+$	2,6-di-tBuPyr	1.9 (357) .16(472)	-7.8	3.4
2-tBuPyrH$^+$	2,6-di-tBuPyr	.65(435) .11(536)	-7.8	6.2
2,6-di-iPrPyrH$^+$	2,6-di-tBuPyr	0.48(357) .0024(483)	-10.1	1.6

6. Conclusions

1. When some conformations allow the ion-molecule complex to approach to optimal distance, the hydrogen bond is not weakened. This is true even when most conformations would block the hydrogen bond. However, steric crowding of the hydrogen bonding site results in unfavorable entropy effects.

2. Steric effects on hydration by one H_2O molecule are similar in magnitude to steric effects on hydration by bulk water.

3. Steric effects are observed in ethyl, i-prop-and t-butyl pyridines, as well as bulky amines. 2,6-di-t-BuPyr exhibits anomalously large effects due to simultaneous freezing of the rotations of the two t-butyl groups.

4. Steric hindrance can slow down the kinetics of proton transfer reactions, and lead to substantial negative temperature coefficients.

WPA 2 CONDENSATION REACTIONS OF HYDROCARBON IONS WITH ACETYLENE AND HYDROGEN CYANIDE. V. G. Anicich, Geoffrey A. Blake, and W. T. Huntress, Jr.; Jet Propulsion Laboratory, California Institute of Technology, 4800 Oak Grove Drive, Pasadena, CA 91109 and Murray J. McEwan, Chemistry Department, University of Canterbury, Christchurch, New Zealand.

The reactions of the ions CH_n^+, $C_2H_n^+$, $C_3H_n^+$, and $C_4H_n^+$, where n = 0 to 4, with both acetylene and hydrogen cyanide were systematically studied. The predominant reaction in all systems is that of condensation, the addition of two carbons with acetylene and CN with hydrogen cyanide. The neutral product is either H_2 or H. In several cases total condensation was observed, presumably being stabilized by a radiative association mechanism. Reaction rate constants and branching ratios were both measured. These types of reactions can be related to soot formation in hydrocarbon flames and formation of large organic molecules in the atmospheres of Titan and dense interstellar dust clouds.

KINETICS AND DEACTIVATION BY NEUTRAL NON-POLAR BATH GASES OF $C_4H_8^+$ AND $(C_4H_8)_2^+$ IONS FORMED IN ISOBUTENE.

K.Nagase and J.A.Herman,
Département de chimie et C.R.A.M., Université Laval, Québec, Canada

Two main channels for disappearance of the iso-$C_4H_8^+$ ions have been proposed: (1) formation of $C_4H_9^+$ by proton or hydrogen atom transfer, and (2) formation of $C_8H_{14}^+$ in a third order process. However, the shape of fractional intensity curves of ions originating from $C_4H_9^+$ and $C_8H_{14}^+$ species suggests the existence of an interrelation between the channels (1) and (2). The purpose of this study is (i) the re-examination of the kinetics of this double-channel mechanism, and (ii) the deactivation of the excited precursor-ion species of the above mentioned ions. As deactivating gases we used non-polar compounds, whose ionization potentials are higher than 10.5 eV.

The following kinetic scheme accounts for the observed fractional intensities:

$$C_4H_8^+ + \text{iso-}C_4H_8 \rightleftharpoons (C_4H_8^+\cdot C_4H_8)^* \xrightarrow{k_2} C_4H_9^+ + C_4H_7^\cdot$$
$$(C_4H_8^+\cdot C_4H_8)^* + \text{iso-}C_4H_8 \xrightarrow{k_3} C_8H_{16}^+ + \text{iso-}C_4H_8$$
$$(C_4H_8^+\cdot C_4H_8)^* + M \xrightarrow{k_4} C_8H_{16}^+ + M^*$$
$$C_8H_{16}^+ + \text{iso-}C_4H_8 \xrightarrow{k_5} C_8H_{14}^+ + \text{iso-}C_4H_{10} \quad .$$

Assuming a steady state concentration of the intermediate $C_8H_{16}^+$ ions, the following kinetic expression can be derived:

$$\frac{I(C_8H_{14})^+}{I(\Sigma C_4H_9^+(C_4H_8)_n)} = \frac{1}{1+R}\left[\frac{k_4}{k_2} + \frac{R\,k_3}{k_2}\right]P_t \quad ,$$

where $R = P(\text{iso-}C_4H_8)/P_M$ is the mixing ratio, P_M is the partial pressure of the gas M and P_t is the total pressure. The ratio k_3/k_2 can be measured in pure isobutene and is equal to 20.6 ± 1.2 (torr^{-1}). A plot of $I(C_8H_{14}^+)/I(\Sigma C_4H_9^+(C_4H_8)_n)$ vs total pressure P_t of the mixture should give a straight line, and from its slope the "relative deactivation efficiency", k_4/k_2 ,can be calculated. Experimentally one finds such linear relation for most of the "inert" gases in the range of 0.1 to ~1 torr. The calculated k_4/k_2 values are presented in Table I.

Reaction (4) represents processes where collision-induced vibrational and collision-induced rotational state changes are taking place. The relative effectiveness of various "inert" gases in bringing some particular transformation in $(C_4H_8^+\cdot C_4H_8) \rightarrow$ products is controlled by a number of molecular parameters. In Figs.1-3 we present some correlations between the ratio k_4/k_2 and some molecular parameters: (i) the intermolecular well depth, ε_{MM} , between pairs of M (ref.1), (ii) the heat of vaporization, ΔH_V , of various "inert" gases, and (iii) the polarizability, α , of "inert" gases. All these representations have in common the consideration of only the attractive part of the intermolecular interaction potential.

Experimental

A high-pressure photoionization (10.03 eV, Krypton resonance line) mass-spectrometer was used in this study. All gases were of the best available purity. The experiments were done at room temperature. The measurements were made under field-free conditions inside the collision chamber.

Reference.

(1). H.M.Lin, M.Seaver, K.Y.Tang, A.E.W.Knight and C.S.Parmenter, J.Chem.Phys., 70, (1979), 5442.

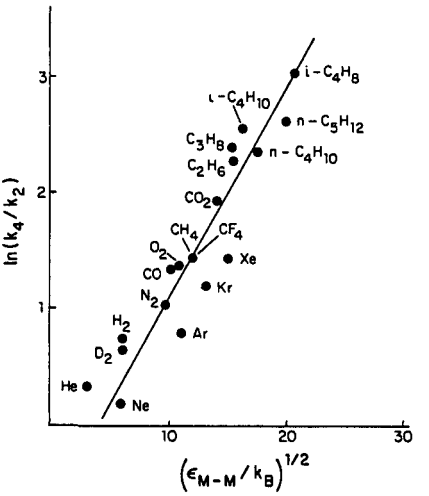


Fig.1 CORRELATION BETWEEN THE DEACTIVATION EFFICIENCY AND THE SQUARE-ROOT OF THE WELL DEPTH.

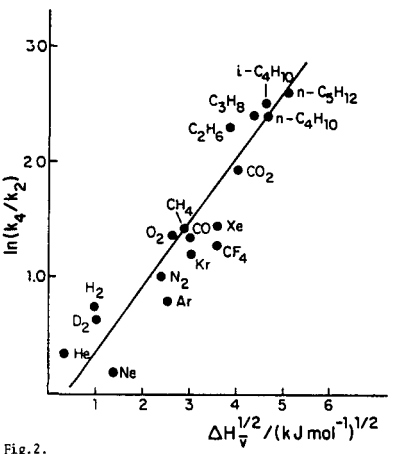


Fig.2. CORRELATION BETWEEN THE DEACTIVATION EFFICIENCY AND THE SQUARE ROOT OF THE HEAT OF VAPORIZATION

TABLE I

DEACTIVATION PARAMETERS, k_4/k_2 (TORR^{-1}).

M	% ISO-C_4H_8	R	PRESSURE RANGE	k_4/k_2
He	9.9	0.11	0.1 - 2.0	1.4 ± 0.3
Ne	10.0	0.11	0.2 - 2.0	1.2 ± 0.8
Ar	10.2	0.11	0.2 - 1.6	2.2 ± 0.9
Kr	9.4	0.10	0.1 - 1.0	3.3 ± 1.1
Xe	9.4	0.10	0.1 - 1.0	4.2 ± 1.5
H_2	18	0.22	0.2 - 1.7	2.1 ± 1.7
D_2	9.5	0.10	0.1 - 1.1	1.9 ± 0.9
N_2	10	0.11	0.1 - 2.0	2.8 ± 1.2
O_2	10.0	0.11	0.2 - 1.2	3.9 ± 1.9
CO	10.9	0.12	0.2 - 2.0	3.8 ± 1.3
CO_2	10.0	0.11	0.2 - 1.0	6.9 ± 2.8
CH_4	21	0.27	0.1 - 1.0	4.1 ± 2.0
C_2H_6	10.0	0.11	0.1 - 1.6	9.8 ± 4.3
C_3H_8	10.2	0.11	0.1 - 1.0	10.9 ± 5.3
n-C_4H_{10}	10.0	0.11	0.2 - 1.0	10.5 ± 4.1
i-C_4H_{10}	10.6	0.12	0.2 - 1.0	12.8 ± 3.4
n-C_5H_{12}	10.0	0.11	0.2 - 1.0	13.6 ± 2.0
CF_4	10.0	0.11	0.2 - 0.8	3.7 ± 0.6

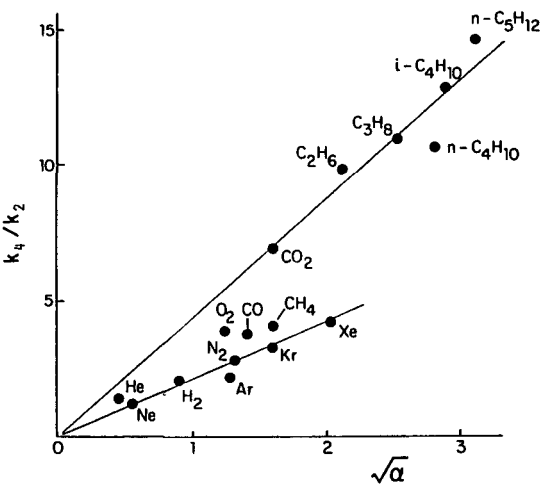


Fig.3 CORRELATION BETWEEN THE DEACTIVATION EFFICIENCY AND THE SQUARE ROOT OF THE POLARIZABILITY.

The Detection of Neutral Products of Ion-Molecule Reactions

Thomas J. Francl, John T. Keech and Robert T. McIver, Jr.
Department of Chemistry
University of California
Irvine, California 92717

Most investigations of ion-molecule reactions in the gas phase can detect just ionic products. Only in the most favorable cases can the neutral products be inferred from thermochemical data. A large number of rearrangement and substitution/elimination reactions can only be understood by knowing the distribution of the neutral products. This problem is a difficult one since the yield of neutral products is typically small compared to the neutral reactants, on the order of one part in a million. In addition, the situation is complicated by any background contamination or interfering radical reactions.

Our approach to the detection of neutral products utilizes a pulsed Ion Cyclotron Resonance (ICR) spectrometer and a Finnigan GC/MS. In the ICR, ions are formed by electron impact in an unusually large gas-tight analyzer cell. The ions are detected by a capacitance bridge detector which monitors the ions formed and how fast they react.[1]

Because ICR is an ultrahigh vacuum technique (base pressures typically in the 10^{-9} Torr range) many problems associated with background contamination are greatly minimized. A 150 ℓ/sec ion pump differentially pumps the filament region to minimize the number of radical products entering the cell. During the course of an experiment, the neutral products produced in the cell via ion-molecule reactions, as well as excess reagents are collected in a liquid nitrogen cooled trap. The collection assembly is interfaced to a Finnigan model 4000 GC/MS for subsequent analysis of the collected species. At operating pressures of 6×10^{-4} Torr of the neutral reagent and 5×10^{-5} Torr of the ionic precursor, approximately 2 ng of product can be collected in a 30 minute experiment.

The first reaction investigated with this technique is the S_N2 reaction shown below:

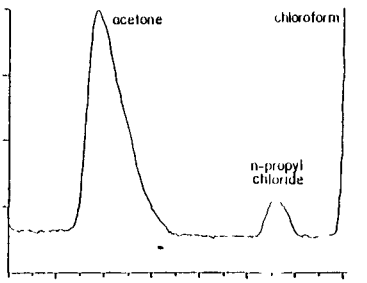
$$C_3H_7Br + Cl^- \longrightarrow C_3H_7Cl + Br^-$$

where Cl^- is formed by electron impact on chloroform. To improve the precision for detection of neutral products, the reaction mixture was doped with a trace amount of acetone. Sequential experiments have shown that the ratio of propyl chloride to acetone remains constant. As shown in Figures 1 and 2, with the electron beam on, the amount of propyl chloride was over 800% greater than with the electron beam off. To verify this increase was due to ion-molecule reactions and not radical reactions on the filament, the filament was left on at 2 amps and the electron energy biased to +5 volts. Under these conditions, no change in the ratio of propyl chloride to acetone was observed when compared to the electron beam off experiment.

These studies have shown that ultrahigh vacuum techniques can be used with ICR to collect and detect the neutral products of an ion-molecule reaction. It has been further demonstrated that the amount of pyrolysis products formed on the hot filament and contri-

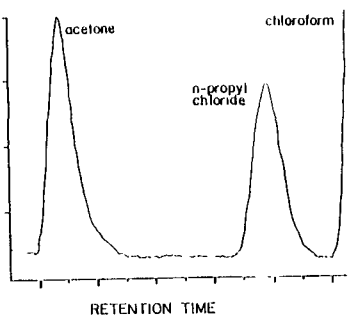
buting to the product number is minimal. System blank studies have shown negligible background contamination. Clearly the ability to detect the neutral products is essential to the understanding of a large number of gas phase ion-molecule reactions.

[1] R. T. McIver, Jr., R. L. Hunter, E. B. Ledford, Jr., M. J. Locke and T. J. Francl, Int. J. Mass Spectrom. Ion Phys., 39, 65 (1981).



Reagents collected at 6×10^{-4} Torr for 30 minutes Electron beam off - no ions formed Propyl chloride is a trace impurity in the propyl bromide The propyl bromide was doped with acetone to provide a relative standard

Figure 1



Reagents at 6×10^{-4} Torr Electron beam on - Br^- observed Collection time - 30 minutes Propyl chloride is over 800% larger than with electron beam off The mass spectra were identical to the reagent blank

Figure 2

A COMBINED DRIFT-TUBE AND BEAM LUMINESCENCE STUDY OF THE CHARGE TRANSFER REACTION OF He^+ WITH Xe IN THE ENERGY RANGE FROM THERMAL (200^oK AND 300^oK) UP TO 2000 eV

F. Howorka, I. Kuen, H. Villinger, W. Lindinger

Institut für Experimentalphysik, Leopold Franzens Universität
A 6020 Innsbruck, Austria

J.H. Futrell

Department of Chemistry, University of Utah
Salt Lake City, Utah 84112, USA

I. Introduction: The title reaction has been studied by a number of investigators using a variety of techniques. These include total charge transfer measurements at collision energies above /1,2/ and below 100 eV /3/, optical excitation cross section measurements above 300 eV /4,5/, in the range 10-500 eV /6/ and. more recently, at and below 100 eV /7,8/. A comprehensive study of the states accessible to the reaction at 100 eV He^+ energy, including cross section values for direct formation and for population cascading of the principal emitting states of Xe^+ were recently reported by Jones et al. /8/. Despite the availability of exoergic states in the Xe^+ atomic ion, Hemsworth et al. /9/ has reported that the thermal-energy rate constant measure in a flowing afterglow has a very low value of 7×10^{-12} cm^3 s^{-1}.

There are two obvious gaps in the investigations of the energy dependence of the reaction cross section (or reaction rate constant) for reaction (1): the energy region between thermal and a few eV for the total rate constant and the energy region from about 100 eV to 300 eV where the optical and VUV excitation cross sections of de Heer et al. /3/ start. We therefore present here a combined study of drift tube investigations of the total charge transfer reaction rate constant and of beam-target interaction causing optical luminescence between 1 and 2000 eV.

II. Experimental: The total charge-exchange rate coefficient for the reaction $He^+ + Xe$ is determined in the energy range of near thermal (0.04 eV) up to 4 eV energy using two different drift tubes. In one drift tube, the ions are produced in a hollow cathode discharge /10/. The second drift tube apparatus has the additional feature of selected ion injection. Additional values of the charge transfer reaction rate coefficient at room temperature (300^oK) and below (200^oK) were measured by D. Smith and N. G. Adams in their selected ion flow tube (SIFT) in Birmingham /11/.

Beam-target studies in the energy range 1-2000 eV are made in an apparatus consisting essentially of a hollow cathode ion source-magnetic sector field mass spectrometer combination to produce a mass-selected beam of He^+. After emerging from the exit slit of the mass spectrometer, the ions (2000 eV) are either slowed down or accelerated in a lens arrangement before entering the collision chamber through a slit of 1 mm width and 1 cm length. Xenon is admitted into the chamber through a leak valve; chamber pressure is measured by an MKS Baratron absolute pressure gauge (accuracy $\pm$ 1%). The wall opposite to the entrance slit of the chamber is insulated to form a Faraday ion collector which accepts narrow-angle and wide-angle scattered ions (180^o), respectively. The photons produced in the reaction volume by luminescence are observed through a fused silica lens imaging part

of the ion path in the chamber on the entrance slit of a Jarrell-Ash 0.5 m Ebert monochromator employing a 1180 lines/mm grating blazed for a 3000 Å. The photons are counted by an EMI 9863/350 QB photomultiplier (-40°C) and an Ortec-Brookdeal photon counting system.

III. Results: The results of the drift tube, flow tube and SIFT measurements are presented together with some beam and spectroscopic results in Figure 1, which presents the rate constant, K, in cm^3 sec^{-1} as a function of center-of-mass kinetic energy in eV. The c.m. kinetic energy in drift tube collisions is calculated from the Wannier formula, using known mobility values of He^+ in He/12/. The triangles represent the drift tube results. The two symbols Φ at an ion kinetic energy of 0.023 and 0.035 eV are values obtained at 200 and 300 K in temperature-controlled flow tubes by Hemsworth et al. /9/ and D. Smith et at. /11/. These values show that the decrease in the rate constant is continued toward lower energies below 0.02 eV, the lowest drift tube energy. The position of the slightly endoergic state of Xe^{+*}, 6s $^4P_{½}$, which is mainly populated in low-energy encounters, is shown by an arrow. At the other end of the scale, the dashed curve shows beam-target results (where the charge exchange cross section is determined from the ion currents in a target chamber) of W. B. Maier II /3/ which are converted to rate constants by multiplication of the cross section by relative velocity. Although the overlapping region of the two methods is rather small, the continuation of the drift results into the beam curve is a striking confirmation of the two kinds of experiments.

Like the 6s $^4P_{½}$ state of Xe^+ already descussed, the three optically emitting states shown (4844 Å: 6p $^4D^o_{7/2}$ → 6s $^4P_{5/2}$, 5419 Å: 6p $^4D^o_{5/12}$ → 6s $^4P_{5/2}$). have endoergicities of 1.64, 1.62 and 1.42 eV, respectively. The cross section curves have experimental onsets which their endothermicities within experimental error; they peak around 60-100 eV, depending on the state. These cross section curves are converted to rate constants by multiplying by relative velocity and shown in Figure 1 to illustrate part of the low energy luminescence which accompanies this charge-transfer reaction.

Figure 2 shows a spectrum obtained by the impact of He^+ on Xe at 1800 eV energy (lab). The lines all orginate from excited Xe^{+*} states. The kinetic energy dependence of the intense lines have been investigated; our results join smoothly to the results of Jaecks et al. /4/ and Jones et at. /8/ and provide a comprehensive picture of the visible luminescence of Xe^{+*}. Quite complex energy dependences are observed, some lines showing one maximum below 300 eV, others a maxiumu around 1 k eV, and others showing both maxima.

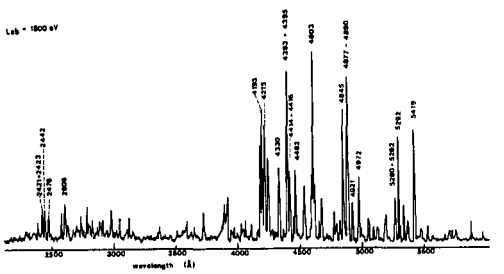
IV. Discussion: The cross section curves observed in the enrgy range 1-2000 eV can interpreted in a Landau-Zener-Stueckelberg model by the consideration of avoided crossings of molecular states. The exact procedure is described elseshere /13/. Three parameters influence the calculated cross section: The radial position of the crossing, the position of the crossing on the incoming potential curve and the Landau-Zener parameter which describes the transition probability. The relative kinetic energy is converted to radial energy, from which the impact parameter region for scattering (charge exchange) is calculated. Integration gives the probability for remaining on the entrance potential curve and the probability for exiting on a different potential curve. From the crossing

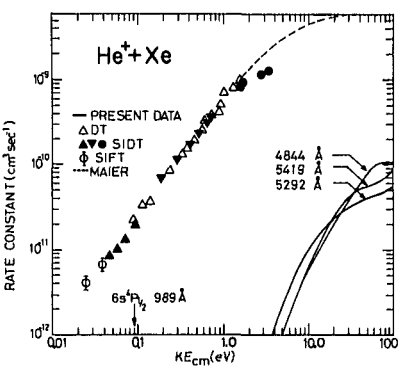
probability and the Landau-Zener parameter the cross section is obtained. In the He Xe^+ system multiple crossings are possible, and it is this feature which appears to be responsible for the structure in the cross section curves.

The atomic exit channels are connected to the incoming channel $He^+ + Xe$ by at least two potential curves of different symmetry (bonding and antibonding) which cross the incoming curve at different energetic and radial positions. Most of the states emitting visible light show two cross section maxima of comparable height. For the state emitting the 2476 Å line the upper crossing seems to have a small probability to populate the state as compared to the lower one. The states emitting VUV lines might show several maxima in the cross section-energy curve but these have not been studied above 100 eV. The general shapes and locations of the maxima observed experimentally are reproduced very well by the calculations.

VII. References:

1. B.H. Stedeford and J.B. Hasted, Proc. Roy. Soc. London A 227, 466 (1955).
2. W. Koopman, Phys, Re. 154, 79 (1967).
3. W.B. Maier, II., Phys, Rev. A5, 1256 (1972).
4. D. Jaecks, F.J. De Heer and A. Salop, Physica (Utrecht) 35, 606 (1967).
5. F.J. De Heer, B.F.J. Luyken, D. Jaecks and L. Wolterbeek-Muller, Physica (Utrecht) 41, 588 (1969).
6. M. Lipeles, R. Novick, and N. Tolk, Phys, Rev. Lett. 15, 815 (1965)
7. E.G. Jones, B.M. Hughes, D. C. Fee and T.O. Tiernan, Phys, Rev. A15, 1446 (1977).
8. E.G. Jones, T.O. Tiernan, D.C. Fee and B.M. Hughes, J. Chem. Phys. 73, 1200 (1980).
9. R.S. Hemsworth, R.C. Bodlen, M.J. Shaw and N.D. Twiddy, Chem. Phys. Lett. 5, 237 (1970).
10. W. Lindinger, F. Howorka, P. Lukac, S. Kuhn, H. Villinger, E. Alge and H. Ramler, Phys. Rev. A 23, 2319 (1981).
11. D. Smith, N.G. Adams, private communication (1981)
12. H.W. Ellis, R.Y. Pai, E.W. McDaniel, E.A. Mason and L.A. Viehland At. Data Necl. Data Tables 17,177 (1976).
13. A. Ding, I. Kuem and F. Howorka, to be published.





ENERGETICS OF NEGATIVE MOLECULAR IONS FORMED IN HIGH TEMPERATURE ENVIRONMENTS

Richard L.C. Wu and T.O. Tiernan
Brehm Laboratory and Departments of Engineering and Chemistry
Wright State University, Dayton, Ohio 45435

Negative ions are present in most plasmas and the formation and reactions of these species are important in various high temperature environments such as discharges, lasers, flames, and certain regions of the earth's and interstellar atmospheres. Accurate knowledge of the thermodynamic properties of various negative molecular ions and their corresponding neutral molecules are therefore of interest for assessment of the reactivity of these species in the various energetic environments. The present study is aimed at measurement of excitation functions and energy thresholds for selected metal oxide negative ions, including, PO^-, PO_2^-, FeO_2^-, BO^-, BO_2^-, MoO^-, and MoO_2^-. From these data, bond dissociation energies and heats of formations of the ions, as well as electron affinities of the neutral species, can be derived.

An in-line tandem mass spectrometer was employed in the present experiments. Various techniques were utilized to generate the projectile ions, including electron impact and microwave discharge of mixtures of N_2O or O_2 with selected organometallic compounds and metal oxides. Translational energy thresholds were determined for collision-induced dissociation (CID) and endothermic charge transfer reactions. Corrections of the measured thresholds were made in order to take account of the incident ion energy distribution and the Doppler motion of the neutral target.[1]

Typical excitation functions obtained for the CID reactions of PO^- and PO_2^- on an Ar target are shown in Fig. 1. The bond dissociation energies deduced from these thresholds were $D^o_s(O^- - P) = 5.6 \pm 0.1$ eV, and $D^o_s(O^- - PO) = 7.4 \pm 0.2$ eV, respectively. The error limits cited here reflect the uncertainties arising from the computer fitting procedure. By inserting these values, along with the previously reported heats of formation of P(3.435 ± 0.002 eV)[3], PO(-0.0633 ± 0.0086 eV)[3] and O^-(1.093 ± 0.02 eV)[3], the heats of formation of PO^- and PO_2^- were determined to be -1.0 ± 0.1 eV and -6.4 ± 0.2 eV, respectively. The latter values, in conjunction with the heat of formation of PO_2(-3.06 eV)[3], can then be used to calculate the electron affinities of the PO and PO_2 molecules, which are found to be 1.0 ± 0.1 and 3.3 ± 0.2 eV, respectively. The electron affinity of PO, determined in the present study is in excellent agreement with the reported value of 1.092 ± 0.01 eV obtained from photodetachment measurements by Zittel and Lineberger.[3] The present electron affinity of PO_2 is also consistent with the value of 3.5 ± 0.5 eV reported by Miller[4] on the basis of flame experiments. Excitation functions for the endothermic charge transfer reactions, $PO_2^-(O_2, PO_2)O_2^-$ and $FeO_2^-(NO_2, FeO_2)NO_2^-$, were also measured. From the measured excitation functions, the translational energy thresholds for the PO_2^-/O_2 and FeO_2^-/NO_2 reactions were determined to be 2.9 ± 0.2 eV and 0.77 ± 0.2 eV respectively. The lower limit to the electron affinity of PO_2 is calculated to be > 3.3 ± 0.2 eV, which is consistent with the CID results. The lower limit to the electron affinity of FeO_2 molecule is found to be > 3.1 ± 0.2 eV. No accurate data on the electron affinity of FeO_2 have been reported previously, although Lineberger et al.[5] estimated this to be > 2.5 eV.

The thermochemical data for metal oxide species derived thus far in the present study are summarized in Table I.

Acknowledgment

This work was supported by U.S. DOE Contract No. DE-AC02-80ER-10668 with Wright State University.

References

1. C. Lifshitz, R.L.C. Wu, T.O. Tiernan and D.T. Terwilliger, J. Chem. Phys. 68, (1978).
2. JANAF Thermochemical Tables, Dow Chemical Co., Midland, MI.
3. P.F. Zittel and W.C. Lineberger, J. Chem. Phys. 65, 1236 (1976).
4. W.J. Miller, "Mass Spectrometric Investigations of the Ion Chemistry of Certain Coal Impurities", in Proceedings of the Conference on High Temperature Sciences Related to Open-cycle, Coal-fired MHD Systems, Argonne National Laboratory Report, ANL-77-21, p. 43 (1977).

5. W.C. Lineberger and P.C. Engelking, "Negative Ion Energetics", in Proceedings of the Conference on High Temperature Sciences Related to Open-cycle, Coal-fired MHD Systems Argonne National Laboratory Report, ANL-77-21, p. 67 (1977).

Table I

Thermochemical Data for Selected Metal Oxide Molecular Negative Ions and For the Corresponding Neutral Species Derived in the Present Studies

	Bond Dissociation Energy (eV)		Heat of Formation (ΔH_f°, eV)		Electron Affinity (eV)	
Ion	This Work	Previous Work	This Work	Previous Work	This Work	Previous Work
PO^-	5.6±0.1(CID)[a]	--	-1.0±0.1(CID)[a]	--	1.0±0.1(CID)[a]	1.092±0.01(PD)[b]
PO_2^-	7.4±0.2(CID)[a]	--	-6.4±0.2(CID)[a]	--	3.3±0.2(CID)[a]	3.5±0.5(Fl)[d]
					3.3±0.2(ECT)[c]	
FeO_2^-	--	--	--	--	3.1±0.2(ECT)[c]	

a. Obtained from threshold for collision-induced dissociation reaction.
b. PD indicates photodetachment data, Ref. 3.
c. Obtained from threshold for endothermic charge transfer reaction.
d. Fl indicates flame study, Ref. 4.

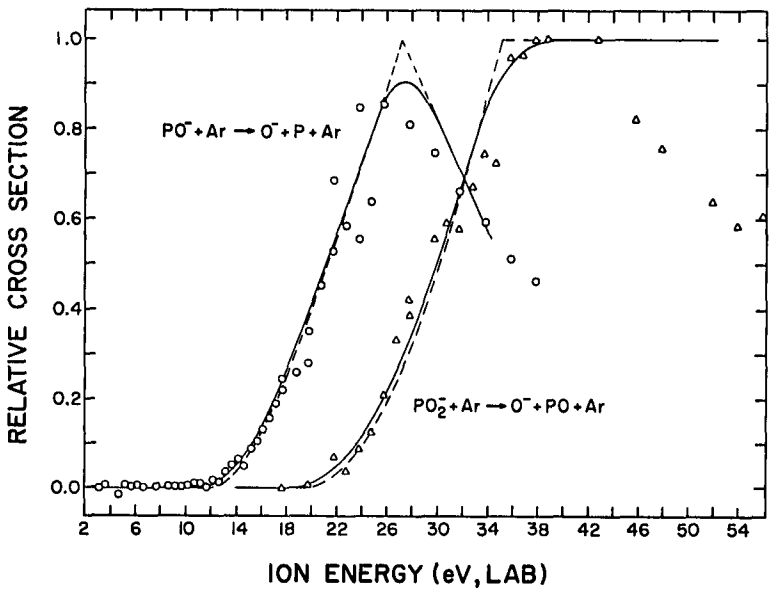


Figure 1. Relative cross section for the collisional dissociation reactions, PO^- + Ar→P + Ar and PO_2^- + Ar→O^- + Ar, as a function of translational energy. Solid lines are the calculated "best fit" excitation functions.

WPA 7 GAS PHASE BASICITIES OF METHYL, PHENYL PHOSPHINES. S. Ikuta and P. Kebarle, Chemistry Department, University of Alberta, Edmonton, Canada T6G 2G2

The phenyl methyl phosphines and particularly Ph_3P are much used bases and ligands in organic synthesis and in transition metal chemistry. The gas phase basicities (proton affinities) of methyl phenyl phosphines were measured by determining proton transfer equilibria like: $Me_3PH^+ + Me_2PhP = Me_3P + Me_2PhPH^+$, with a pulsed electron beam high ion source pressure mass spectrometer. The following proton affinities were obtained: Me_3P = 223.5; Me_2PhP = 226.0; Me_2Ph P = 226.7; $Ph_3P \approx 226.7$ (all values in kcal/mol, based on $Pa(NH_3)$ = 202.3 kcal/mol). The observation that the proton affinities increase when methyl is replaced by phenyl is very interesting. A decrease is observed for the analogous amines i.e. $PA(Me_3N) > PA(Me_2PhN)$. This difference of behavior can be attributed to stabilization in the phenyl phosphonium ions by π conjugation of the aromatic ring with an empty d orbital of the phosphorus. Such a stabilization is not available to the nitrogen compounds.

CHARGE STRIPPING OF HYDROCARBON POSITIVE IONS.

C.G.Herbert, C.J.Proctor, M.Rabrenović, F.M.Harris and J.H.Beynon.

Royal Society Research Unit, University College of Swansea,
Singleton Park, Swansea SA2 8PP, U.K.

Charge stripping of singly-charged ions is an established technique for measuring the differences between single and double ionization energies of atoms and molecules [1]. It has been used in the present work to study a series of singly-charged hydrocarbon ions. When ions having high translational energy collide with neutral gas molecules in a mass spectrometer, a charge stripping process can take place represented by

$$m_1^+ + N \rightarrow m_1^{2+} + N + e^-$$

Charge-stripping experiments have been carried out in the present study using nitrogen collision gas in a cell situated in the second field-free region of a ZAB-2F mass spectrometer. The precursor ions m_1^+ are mass selected, using the magnet of the spectrometer, before they interact with the gas molecules. If E is the voltage which must be applied to the electric sector to transmit m_1^+ ions then the doubly-charged ions generated in the collisions will be transmitted when the electric-sector voltage is approximately E/2. Since some of the translational energy of the m_1^+ ion is needed for its ionization to m_1^{2+} the charge-stripping peak will appear at a sector voltage lower than E/2. The minimum difference in translational energy, Q_{min}, between m_1^+ and m_1^{2+} can be equated to the difference between the double and single ionization energies of m_1 provided both singly- and doubly-charged ions are in their ground states, i.e.

$$Q_{min} = IE\ (m_1^+ \rightarrow m_1^{2+})$$

In order to calibrate the energy scale throughout this work, the process $C_7H_8^{+\cdot} \rightarrow C_7H_8^{2+}$ has been examined repeatedly. The doubly-charged ion peak from the toluene ion is large and well defined and the value of Q_{min} of 15.7 eV is well established from other types of experiments.

In favourable cases, Q_{min} can be measured to within ±0.2 eV. More usually a number of factors can combine to increase the error. These can include:

a) small charge-stripping cross sections for some ions resulting in poor signal-to-noise ratios; and

b) collision induced reactions of the type

$$m_1^+ \rightarrow m_1^+/2 + m_1/2$$

which occur in addition to charge stripping and tend to obscure the charge-stripping peak.

Such factors necessitate the use of long scan times over which it may be difficult to keep instrumental parameters constant. Under such circumstances the errors in Q_{min} may be up to ±0.5 eV.

In excess of thirty different precursor molecules have been examined in order to obtain Q_{min} values for the series of ions represented by $[C_xH_y]^+$ (x=1 to 9; y=0 to 8). The values determined span a wide range from 13.9 eV to 22.8 eV. In all cases these are found to be higher than the corresponding single ionization energies. There does not seem, however, to be a simple relationship between the ionization energy for $m_1 \rightarrow m_1^+$ and that for $m_1^+ \rightarrow m_1^{2+}$.

Trends in the value of Q_{min} with respect to the number of carbon and hydrogen atoms in the ions have been noted. The dependences of Q_{min} values on the number of hydrogen atoms in odd carbon-number ions show the existence of minima at even hydrogen numbers. This suggests that the energy required to remove an unpaired electron from such ions is less than that required to remove a paired electron. A much simpler relationship is observed for ions of even carbon number with increasing number of hydrogen atoms. A minimum in Q_{min} is exhibited for each set of ions when four hydrogen atoms are present.

For a constant number of hydrogen atoms, Q_{min} is found to decrease as the number of carbon atoms increases. The experimental values for the two series C_xH_2 and C_xH_4 are compared with values calculated [2] using the MINDO/3 method. In each case the measured Q_{min} values are higher than the calculated values but the trends with increasing carbon number are the same for both.

References

1. R.G.Cooks, T.Ast and J.H.Beynon, Int.J.Mass Spectrom. and Ion Phys. 11, 490 (1973).

2. T.W.Bentley and C.A.Wellington, Private Communication (1981).

IONIZATION ENERGIES AND ENTROPIES OF CYCLOALKANES. KINETICS OF INTRINSICALLY FAST CHARGE-TRANSFER PROCESS, L. Wayne Sieck and Michael Mautner, National Bureau of Standards, Washington, D.C.

Enthalpies and entropies of ionization (ΔH°_{ion} and ΔS°_{ion}) of alkylcyclohexanes, as well as cycloheptane, cyclooctane, and trans-decalin, have been determined by charge transfer equilibrium measurements. Values of ΔH_{ion}, in units of kcal mol^{-1} (or eV) range from 229.6 (9.96) for cycloheptane to 210.7(9.14) for trans-decalin. A major effect of alkyl substitution is observed following substitution at a site alpha to a tertiary hydrogen atom (as from methylcyclohexane to 1,2-dimethylcyclohexane), or following replacement of a tertiary hydrogen atom (as from methylcyclohexane to 1,1-dimethylcyclohexane). In both cases, ΔH°_{ion} decreases by ca. 5 kcal mol^{-1}. Entropies of ionization are near zero for alkylcyclohexanes, but range up to 5 $cal \cdot deg^{-1} mol^{-1}$ for nonsubstituted cycloalkanes (cyclooctane). The charge transfer reactions involving the cycloalkanes are shown to be fast processes; i.e., the sum of the reaction efficiencies ($r \approx k/k_{collision}$) of the forward and reverse processes is near unity. The efficiencies of these processes appear to be determined uniquely by the overall free energy change (or equilibrium constant K). Specifically, the reaction efficiencies are defined, within a factor of two, by the relation $r = K/(1 + K)$, which can be justified using transition state theory applied to the decomposition of a collision complex over surfaces lacking energy barriers. These reactions are defined as intrinsically fast processes in that they are slowed only by the overall reaction thermochemistry and not by any properties or reactions of the intermediate complex.

* A detailed paper describing this study will appear in the Journal of Physical Chemistry, Sept., 1982.

PHOTOIONIZATION MASS SPECTROMETRY OF NH_2OH: HEATS OF FORMATION OF HNO^+ AND NOH^{+*}

R. E. Kutina, G. L. Goodman and J. Berkowitz
Physics Division, Argonne National Laboratory
Argonne, Illinois 60439

Very little has hitherto been known about the ionization behavior of hydroxylamine (NH_2OH), even by electron impact. We have examined this molecule by photoionization mass spectrometry, with the primary intent of establishing the relative stabilities of potential HNO^+ and NOH^+ fragments. From the absolute heats of formation of these species, we hoped to infer the exo/endo thermicity of the reaction of H_3^+ with NO, postulated to occur in the interstellar clouds.

We prepared samples of NH_2OH and ND_2OD by methods described in the literature. No method has been described for preparing selectively deuterated ND_2OH/NH_2OD, presumably because of rapid internal scrambling. With NH_2OH, the major ion peaks observed and studied were NH_2OH^+ (M33), $H_2NO^+/HNOH^+$ (M32), HNO^+/NOH^+ (M31), NO^+(M30), NH_3^+ (M17) and NH_2^+ (M16). In this brief report, we focus on M31, which was the weakest peak in most of the energy range studied.

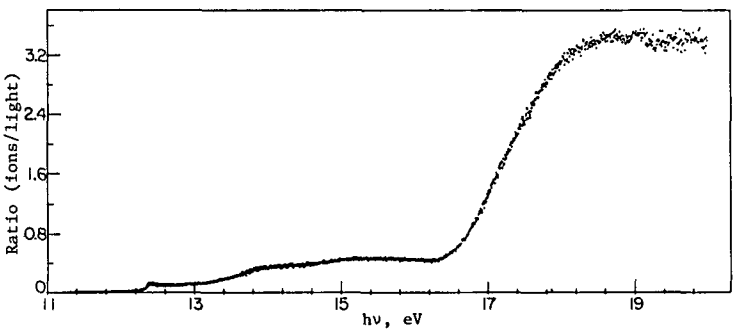


Figure 1. Overview of HNO^+/NOH^+ relative ion from NH_2OH.

Figure 1 is an overview of the ion yield curve for M31, from threshold to ~20 eV. Weak thresholds appear at ~11.6 and 12.3 eV, and a much stronger increase occurs at ~16.2 eV. From available thermochemical data, it is possible to estimate and therefore assign the large increase at ~16.2 eV to the process

$$NH_2OH + h\nu \rightarrow HNO^+/NOH^+ + 2H + e. \qquad (1)$$

The weaker processes at lower energy must therefore involve H_2 (rather than 2H) as fragment. The thresold region is displayed in magnified form in Fig. 2. Thermally corrected thresholds at 11.56 ± 0.06 eV and 12.34 ± 0.03 eV can be seen, followed by a cusp. This cusp coincides with the opening of a new intense channel M32 ($H_2NO^+/HNOH^+$). To interpret this threshold region, we make use of well-established heats of formation of

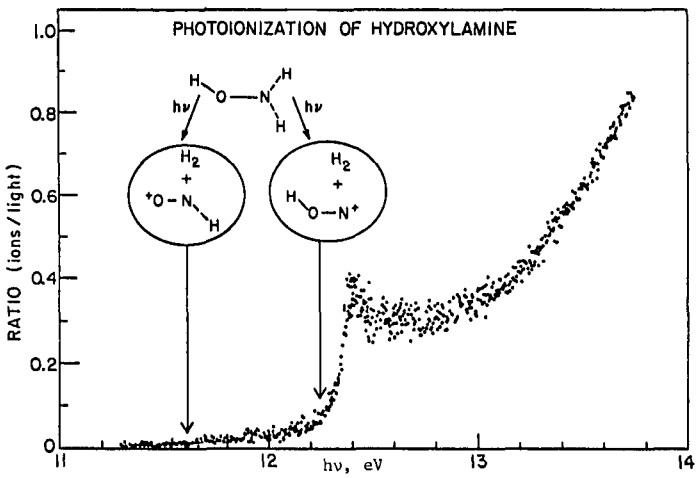


Figure 2. Threshold region for HNO^+/NOH^+.

NH_2OH and HNO and an appearance potential for DNO obtained by electron impact to predict the threshold for the reaction

$$H_2NOH + h\nu \rightarrow HNO^+ + H_2 + e. \qquad (2)$$

The resulting value, ~11.77 eV, is close to but somewhat larger than our lowest threshold. Hence, we identify the lowest threshold with the formation of HNO^+. Franck-Condon considerations restrict the electron impact appearance potential to this entity, rather than NOH^+. The higher energy threshold is assigned to NOH^+. No other reason for an increased ion yield at this energy (such as the onset of a new ionic state) could be found. The heats of formation of HNO^+ ($\Delta H^\circ_{f,0}$ = 256.8 ± 1.4 kcal/mole) and NOH^+ ($\Delta H^\circ_{f,0}$ = 274.8 ± 0.7 kcal/mole) are in excellent agreement with an ab initio calculation[1] involving a double zeta basis set plus extensive configuration interaction (CI), which yields $\Delta H^\circ_{f,0}$ (HNO^+) = 258.8 ± 2 kcal/mole and $\Delta H^\circ_{f,0}$ (NOH^+) = 276.3 ± 2 kcal/mole. It disagrees even in relative stability of HNO^+/NOH^+ with a good calculation[2] that did not include CI. Hence, some of the correlation energy included in CI reverses the relative stability of these species.

From these absolute values, and also that for H_2NO^+, we conclude that the reaction of H_3^+ with NO is exothermic in each of these channels, and hence can deplete NO in interstellar clouds.

References

*Work supported by the United States Department of Energy, Office of Basic Energy Sciences under Contract W-31-109-Eng-38.

1. P. Bruna and C. M. Marian, Chem. Phys. 37, 425 (1979).
2. R. Seeger and J. A. Pople, J. Chem. Phys. 65, 265 (1976).

WPA 11 ENERGY TRANSFER IN THE HIGH ENERGY COLLISIONAL ACTIVATION OF CH_4^+; Frank W. Crow, Kenneth R. Tomer and Michael Gross, Midwest Center for Mass Spectrometry, University of Nebraska, Lincoln, Nebraska 68588 and Jean H. Futrell Department of Chemistry, University of Utah, Salt Lake City, Utah 84112.

The MS-50 Triple Analyzer mass spectrometer at the University of Nebraska, Midwest Center for Mass Spectrometry has been utilized to investigate the collision-induced dissociation of methane molecular ions at kilovolt collision energies with the rare gases He, Ne, Ar, Kr and Xe. The high energy resolution capabilities and high transmission characteristics of the triple analyzer permit a quantitative assessment of energy deposition in the CID process and energy release in the subsequent dissociation of the activated ion.

Methane was chosen because (1) it has been investigated by other techniques at both high and low energy, (2) precise information is available on ion energetics for all possible dissociation paths, and (3) both theoretical and experimental breakdown graphs exist for this ion. Use of the suite of rare gases as collision partners provides a range of center-of-mass collision energies, polarizabilities and ionization potentials to probe mechanistic details of collisional activation.

The data support the interpretation of collision-induced dissociation of organic ions as occurring in a stepwise manner--collisional excitation followed by unimolecular dissociation of the vibronically excited ion. No qualitative differences between low energy (eV range) and high energy (KeV range) activation was noted. Energy release in the dissociation of methane ions is modest but readily measurable with high precision. Comparison of the present results with recent beam data and older collision chamber results suggests that some of the earlier work may have been confounded by multiple collisions and/or poor collection efficiency accompanied by discrimination effects.

ENERGY DEPOSITION IN GAS PHASE IONS: ANGLE RESOLVED MASS SPECTROMETRY AND OTHER TECHNIQUES

S.A. McLuckey and R.G. Cooks
Department of Chemistry
Purdue University
West Lafayette, Indiana 47907

A number of techniques have been employed to control and define internal energies of gas phase ions. Until recently most techniques have centered upon controlling the extent of energy deposition in the ionization process using variable energy photons, electrons, or such chemical reactions as charge exchange. With the advent of MS/MS techniques which rely upon activation subsequent to ionization, interest has focused on controlling and defining energy deposition into mass-selected ions.

The most widely used and experimentally simple method of activating mass-selected ions is via collision with a neutral target gas, termed Collisionally Activated Decomposition (CAD). One can vary the degree of excitation imparted to an ion upon collision by controlling the relative translational energy of the collision or select from the distribution of activation energies a segment of the population by collecting fragment ions at fixed scattering angles. The former approach is most readily accomplished using relatively low precursor ion translational energies (1-150 eV) accessible on hybrid sector/quadrupole, triple quadrupole, and Fourier transform ion cyclotron resonance instruments. Figure 1 shows a comparison of collision energy resolved data for ionized propane as acquired by hybrid MS/MS, FTICR instruments and photoion-photoelectron coincidence. These data indicate a smooth increase in energy deposition with collision energy providing a means for acquiring MS/MS spectra as a function of a parameter (collision energy) related to the degree of excitation.

The alternative technique, termed angle-resolved mass spectrometry (ARMS), can be readily utilized at high collision energy (keV regime). Figure 2 shows a comparison of ARMS data for ionized 2-pentanone with relative fragment ion abundances obtained from statistical calculation. This and other comparisons indicate a smooth increase in internal energy deposition with the angle of scatter. It is important to realize that angular scattering after CAD correlates with energy deposition ($\Delta\varepsilon$) even though two factors may contribute to the measured deflection angle, viz. the scattering angle established during collision and that associated with the subsequent fragmentation of the excited ion (Figure 3). Both these factors give rise to a relationship between $\Delta\varepsilon$ and scattering angle of the form $\Delta\varepsilon \propto \theta^2$.

These two techniques provide to MS/MS means to vary the internal energy of a mass-selected ion over a relatively wide range using ion/neutral collisions as the method of excitation. The internal energies deposited upon collision using these techniques are not as well-defined as with many of the techniques which control energy deposition upon ionization. However, the capability for varying internal energies subsequent to ionization allows for the acquisition of internal energy-resolved data from any ion which can be formed in a mass spectrometer (e.g. protonated species, metal ion adducts, etc.) which have heretofore been inaccessible.

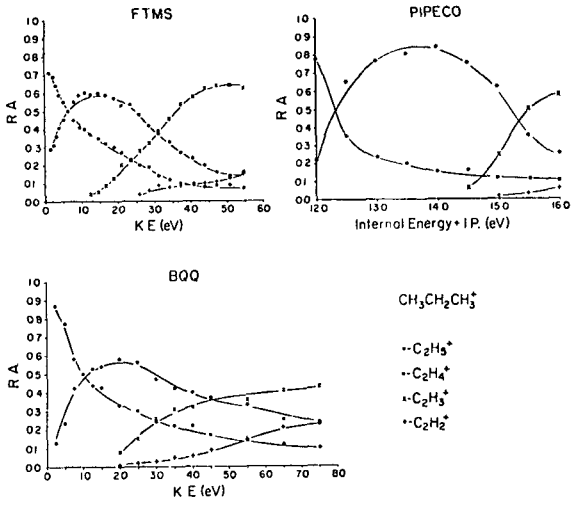


Figure 1

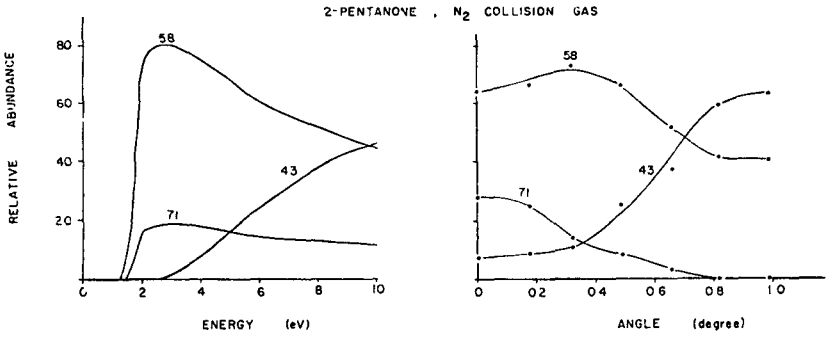


Figure 2

	OBSERVABLE	EXPERIMENTAL VARIABLE	CHIEF DETERMINANT OF θ DISTRIBUTION	FUNDAMENTAL QUANTITY
(a)	R	Θ	T ($T^{\neq}$)	ε ($\varepsilon^{\neq}$)
(b)	R	Θ	b	ε

Figure 3

A STUDY OF THE STRUCTURES OF DECOMPOSING AND NON-DECOMPOSING $[C_6H_5O]^+$ IONS

Hiroshi SAKURAI*, Akira TATEMATSU* and Hisao NAKATA°

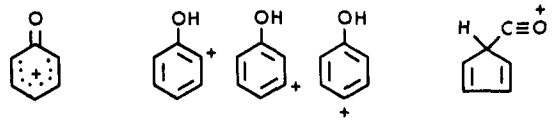
*Faculty of Pharmacy, Meijo University, Tempaku, Nagoya 468, JAPAN

°Department of Chemistry, Aichi Kyoiku University, Kariya 448, JAPAN

Radical cations of the composition $[C_6H_6O]^{+\cdot}$ which are derived from phenol etc. have been investigated by using many different mass spectrometric techniques[1] and photodissociation spectra.[2] On the contrary, ions of $[C_6H_5O]^+$ which are also found in the spectra of a number of phenol derivatives have been paid scant attention. We have studied the structures of decomposing and non-decomposing $[C_6H_5O]^+$ ions by the kinetic energy released ($T_{50\%}$) and by the collision induced dissociation (CID) mass spectra.

Metastable peaks from which kinetic energy released were calculated were recorded on an Hitachi RMU-7 double focusing, reversed geometry mass spectrometer. Spectra of CID products were observed by the method of the B/E linked scan on an Hitachi M-80 double focusing mass spectrometer. CID spectra are averages of three independent measurements obtained under the conditions in which 20% of the main beam is transmitted by introducing helium into a collision chamber in the first field free region.

There are several possible structures for $[C_6H_5O]^+$ ions and some of them (A~E) are shown below. We have produced these probable ions from reasonable precursors, and both the kinetic energy released and CID spectra were examined.



(A) (B_o) (B_m) (B_p) (C)



(D) (E)

Table 1 shows $T_{50\%}$ values which give information about the structures of the decomposing $[C_6H_5O]^+$ ions. These data reveal that anisole and nitrobenzene yield $[C_6H_5O]^+$ ions which have the same structure or a mixture of

structures. On the other hand, compounds which have a hydroxyl group on a benzene ring produce another structure or a mixture of structures. But the $T_{50\%}$ values are not sensitive enough to differentiate the structure (B_m) and (B_p). The existence of the decomposing ions of structures (D) and (E) is not clear, but ions (C), (D), and (E) do not seem to be stable because the peak intensity at m/z 93 is low in the conventional mass spectra of 5-formyl-1,3-cyclopentadiene, dipropargyl ether, and *trans*-2-hexene-4-yn-1-al.

Table 1 Kinetic energy released in the reaction

$$[C_6H_5O]^+ \longrightarrow [C_5H_5]^+ + CO$$

	(meV)		(meV)
Anisole	46	Nitrobenzene	55
Dipropargyl ether	100	*trans*-2-Hexene-4-yn-1-al	94
m-Bromophenol	105	*p*-Bromophenol	104
m-Nitrophenol	107	*p*-Nitrophenol	109
m-Hydroxybenzaldehyde	105	*p*-Hydroxybenzaldehyde	105

The CID spectra (Table 2) mean that non-decomposing ions of $[C_6H_5O]^+$ exist as two distinct structures, probably (A) and a mixture of (B).

Table 2 Partial CID mass spectra of $[C_6H_5O]^+$

Compound m/z	26	29	37	38	39	53	63	64	74	77
Anisole	4	-	7	11	22	-	16	9	-	2
Nitrobenzene	4	-	6	11	23	-	16	10	-	3
m-Bromophenol	2	2	7	9	20	9	12	5	4	-
p-Bromophenol	2	3	7	9	21	8	11	5	4	-
m-Hydroxybenzaldehyde	2	2	6	9	21	8	11	5	4	-
p-Hydroxybenzaldehyde	2	2	7	9	23	8	11	4	3	-

Further studies are under progress.

Acknowledgement: The authors thank Mr. K. Shizukuishi of Naka Works of Hitachi Ltd., for the measurement of CID spectra.

References:

1) H.J. Walther, H. Eyer, U.P. Schlunegger, C.J. Porter, E.A. Larka and H.J. Beynon, Org. Mass Spectrom., 18, 81 (1982) and literatures cited therein.
2) P.N.T. van Velzen, W.J. van der Hart, J. van der Greef, N.M.M. Nibbering and M.L. Gross, J. Amer. Chem. Soc., 104, 1208 (1982).

MASS SPECTROMETRY/MASS SPECTROMETRY STUDIES OF RING-OPENED VS. CYCLIC IONS

D.L MILLER, CHHABIL DASS and M.L. GROSS

Dept. of Chem., Univ. of Nebraska, Lincoln, NE. 68588.

Mass Spectrometry/Mass spectrometry is a technique well suited for the study of gas-phase ions and the determination of their structure. In our laboratory we have applied MS/MS to the question of ring-opening of cyclic hydrocarbons upon ionization. Can MS/MS studies lead to the differentiation of cyclic hydrocarbons and their acyclic counterparts? To answer this question and to examine the mechanisms of ring-opening involved, a variety of experimental methods were used. These methods included ionization at high and low EI ionizing energy or by charge exchange with a variety of gases followed by CID and/or charge stripping of the ion under investigation.

$C_{10}H_{10}$

One of the systems we have studied is that of $C_{10}H_{10}$ isomers. The electrocyclic ring-opening of thermally activated cyclobutene and its derivatives is a well known fact. The question arises as to what happens to these cyclic compounds when ionized in a mass spectrometer. We have investigated this problem by studying 1-phenylcyclobutene and 3-phenylcyclobutene. Other isomers such as, 1,2-dihydronaphthalene and 1-methylindene, are also included in this study. The hydrocarbons under investigation were subjected to various conditions of ionization and then examined by their characteristic CID spectra. Our observation is that the CID spectra of all the isomers are quallitatively similar, but none the less, useful conclusions can be drawn when examined quantitatively. The loss of CH_3 is a major distinguishing feature and the intensity of the resulting ion varies with the ionizing energy. Another characteristic feature is the significant loss of C_2H_4 from 1-phenylcyclobutene. Based on the variation of the intensity ratio of m/z 115/102 (Table I) it can be concluded that all the isomers give distinctive spectra except trans-1-phenyl-1,3-butadiene and 1,2-dihydronaphthalene, which may be interconverting. As a consequence no electrocyclic ring-opening of 1-phenylcyclobutene and 3-phenylcyclobutene has occurred. When high ionizing energy is used the characteristic features of CID spectra of 1-methylindene are still retained. However, 1-phenylcyclobutene, 2-phenyl-1,3-butadiene, trans-1-phenyl-1,3-butadiene and 1,2-dihydronaphthalene tend to isomerize to a common structure, which appears to be a 40:60 mixture of trans-1-phenyl-1,3-butadiene and 1-methylindene.

TABLE I

VARIATION OF M/Z 115/102

IONIZATION						
LOW EV	0.95	2.00	2.25	2.22	3.25	4.06
70 EV	2.06	2.62	2.88	2.66	3.92	4.77
N_2 CE	2.95	2.73	2.89	2.98	3.57	4.04

C_5H_{10}

Another system we have examined is that of cyclic C_5H_{10} isomers and their acyclic counterparts. It has been fairly well established that 3,4, and 5 membered rings open upon ionization to a degree dependent on their internal energy. An often cited example of this is a study in which it is shown that 1-octene and n-pentylcyclopropane have the same CID spectrum. It was proposed that all systems of this type ring-open upon ionization to yield the isomeric 1-alkene. In our investigation of C_5H_{10} isomers we examined a variety of isomers including some alkylcyclopropanes (see Table II).

The CID spectra of the isomers were obtained at both high and low ionization energy. It was observed that the spectra of a particular isomer were identical at both ionizing energies. However, some differences were observed in the CID spectra of the isomers relative to each other. From the CID data it is possible to draw the following conclusions:

1) cyclic C_5H_{10} ions are distinguished from acyclic ions, also,
   A) cyclopentane can be distinguished from other cyclic isomers
   B) 1-pentene can be distinguished from other acyclic isomers.

In an effort to further differentiate the isomers they were subjected to charge stripping and their spectra taken. It was found that each isomer has a unique spectrum (Table III) which allows differentiation of structure when CID spectra are too similar to allow identification. From this we conclude that charge stripping is more sensitive to ion structure than CID for this system.

TABLE II

PARTIAL CID SPECTRA OF SOME C5H10 ISOMERS

SOURCE	M/Z 69	55	42	41
	7	30	6	14
	3	36	8	13
	3	38	10	11
	4	35	10	12
	2	34	17	11
	2	43	20	8
	2	42	12	10
	2	42	11	10
	2	46	13	8
	2	46	14	9

TABLE III

CHARGE STRIPPING SPECTRA OF SOME C5H10 ISOMERS

SOURCE	M/Z 34.5	34.0	33.5	33.0	32.5	32.0
	5	31	17	20	12	14
	10	17	19	20	16	18
	-	34	13	19	16	18
	-	21	21	23	17	18
	8	11	20	26	16	19
	-	18	12	24	21	25
	5	27	14	22	15	17
	-	24	12	19	18	27
	-	27	13	24	16	20
	-	25	24	14	11	26

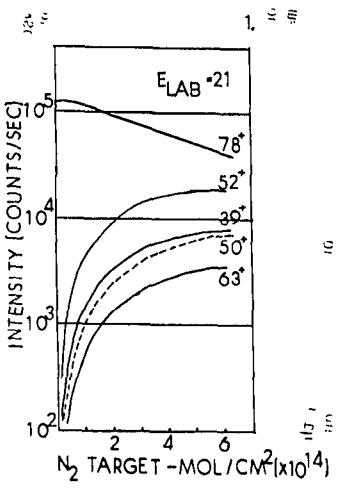
A STUDY OF THE MECHANISM OF THE LOW ENERGY COLLISION INDUCED DISSOCIATION OF $C_6H_6^+$ USING A TRIPLE QUADRUPOLE; P.H. Dawson and W-F Sun, Division of Physics, National Research Council of Canada, Ottawa, Ontario, K1A 0R6

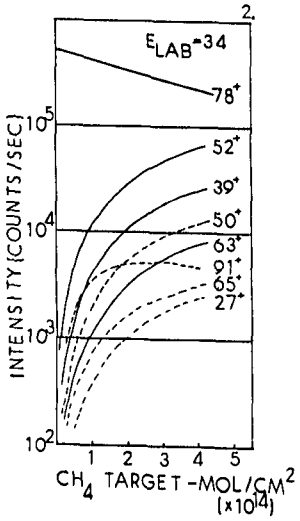
By an appropriate choice of operating conditions, a well-designed triple quadrupole can be used to make quantitative measurements of low energy collision-induced dissociation processes. Considerable care is needed in order to avoid instrumental artefacts. Measurements can be made (a) of the cross-sections for dissociation of ions, (b) of the kinetics of the ionization, which can be analysed in terms of simultaneous and sequential breakdown sequences, (c) of the threshold energies for the formation of each daughter ion, and (d) of the energy distributions of daughter ions and how they vary with collision energy. The latter can indicate the scattering angles that are involved in the dissociation process. This paper reports detailed measurements on $C_6H_6^+$ fragmentation into $C_5H_3^+$, $C_4H_4^+$, $C_3H_3^+$ and $C_2H_2^+$ in collision with target gases such as Ar, N_2 and CH_4. Contrary to some experiments using photoelectron-photoion coincidence techniques, the threshold energies for $C_4H_4^+$ and $C_3H_3^+$ formation are slightly different. The ion-molecule reaction between $C_6H_6^+$ and CH_4 to give $C_7H_7^+$ was also observed to occur quite readily. The yield of $C_7H_7^+$ versus collision energy was measured. The results on $C_6H_6^+$ dissociation complement the studies previously reported for $(H_2O)_nH^+$ and $C_2H_5OH_2^+$ dissociation.

Fig. 1 shows $C_6H_6^+$ dissociation in collision with N_2 at a centre-of-mass energy of 5.6 eV. The parent 78^+ declines exponentially indicating a cross-section of 21 $Å^2$. At low target thicknesses, single collision conditions exist and branching ratios can be determined. Fig. 2 shows results with CH_4 as the target. One major difference is on ion-molecule reaction to form $C_7H_7^+$ which is then itself readily dissociated by further collisions.

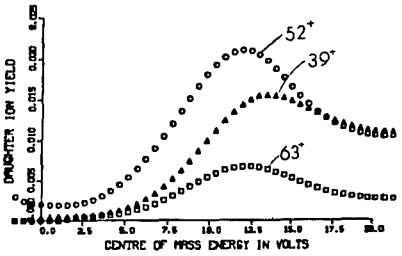
The variation of collision energy is illustrated by Figs. 3 and 4 which show ion yields measured at a low target thickness of argon or krypton. The threshold for $C_2H_2^+$ formation is very high. That for C_4H_4+ is close to the value expected from thermochemical considerations but the C_3H_3+ threshold is 0.9 eV higher. Figure 5 shows the total ion yield as a function of collision energy. With CH_4 as the collision gas, $C_7H_7^+$ formation is observed at centre-of-mass energies above 3 eV and reaches a maximum at 8 eV and then rapidly decreases.

Fragment ion energy distributions are illustrated in Fig. 6. The distributions indicate a narrow range of scattering angles which tend towards zero as the collision energy is increased.

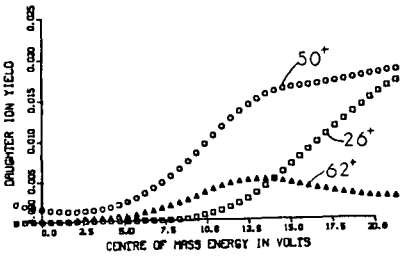




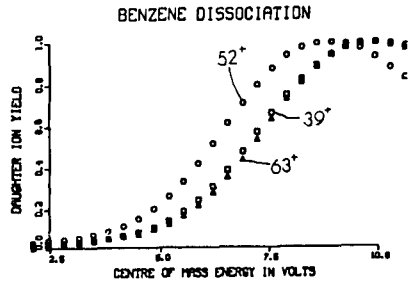
6A


BENZENE DISSOCIATION
DAUGHTER ION YIELD
52+
39+
63+
CENTRE OF MASS ENERGY IN VOLTS

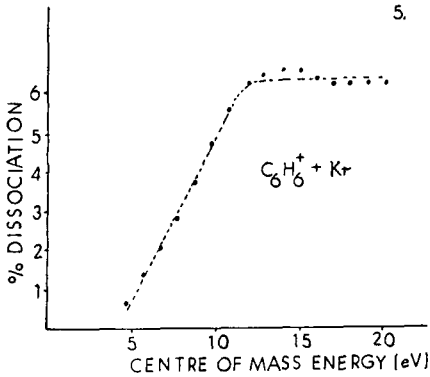
6B

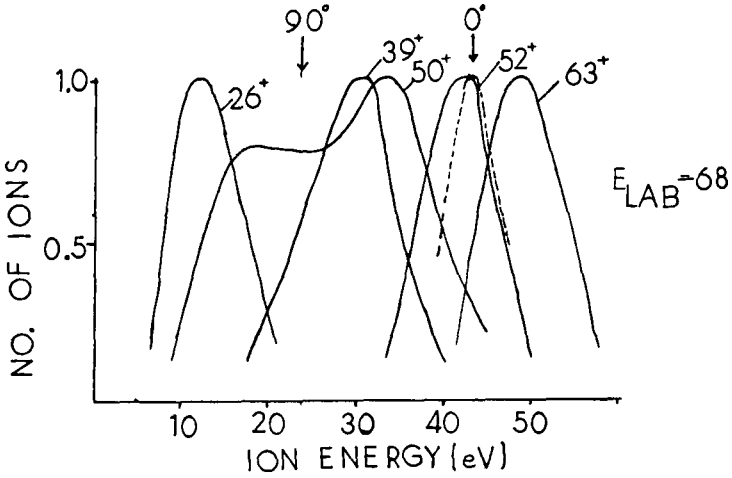

BENZENE DISSOCIATION
DAUGHTER ION YIELD
50+
26+
62+
CENTRE OF MASS ENERGY IN VOLTS

7.


BENZENE DISSOCIATION
DAUGHTER ION YIELD
52+
39+
63+
CENTRE OF MASS ENERGY IN VOLTS

5.


% DISSOCIATION
C6H6+ + Kr
CENTRE OF MASS ENERGY (eV)


90°
0°
39+
50+
52+
63+
26+
NO. OF IONS
ELAB=68
ION ENERGY (eV)

WPA 17 ADVANTAGES OF MS/MS FOR ANALYSIS OF PYRROLIZIDINE ALKALOIDS; William F. Haddon and Russell J. Molyneux, USDA, Albany, CA 94710 and Paul Kershaw, VG Micromass, Ltd., Altrincham, Ches., England.

Several thousand species of plants contain pyrrolizidine alkaloids (PA's), sometimes in concentrations up to 10% dry weight. Many of the PA's are hepatotoxins; their occurrence in Senecio spp. growing on the open ranges of the US and Australia account for significant losses of cattle and sheep. PA's are used by some insects as part of their defense mechanism against predators and as sex pheromones. There is concern that PA's may invade the human food chain, and their natural occurrence in honey and Russian comfrey substantiate this claim.

PA's are biosynthesized from several cyclic amino alcohols and a large suite of necic acids to form both macrocyclic and open chain alkaloids. The strategy we have developed for MS/MS analysis of PA's utilizes a Cl reaction which mimics the reverse of biosynthesis, giving rise to a fragment ion indicative of the amino alcohol. For macrocyclic PA's present in many of the Senecio spp., constant daughter ion scans of the $C_8H_{10}N$ ion yield spectra indicating molecular weights of PA's present in the sample. A comparison with LC, NMR and GC/MS reveals significant advantages for MS/MS in speed of analysis, sensitivity and, most significantly, the ability to measure the PA's together as a chemical class. The work has been carried out using direct probe sample introduction in conjunction with computer-controlled magnetic field-electric sector scanning on an E-B geometry magnetic sector mass spectrometer.

A NEW INSTRUMENT FOR THE ANALYTICAL APPLICATION OF MS-MS

R.H. BATEMAN, B.N. GREEN and D.C. SMITH., VG Analytical Ltd., Tudor Road, Altrincham, Cheshire. England.

INTRODUCTION

Various arrangements of multiple analyser instruments have been developed for MS-MS applications. Those using a magnetic sector or quadrupole as the first analyser, select parent ions with medium resolution only, whilst those using a double focusing configuration are capable of high resolution. Selection of daughter ions by an electrostatic sector usually gives very poor effective mass resolution. A magnetic sector as the daughter ion selector, gives higher resolution, especially if the parent ions are retarded before dissociation in the collision region. The use of a quadrupole collision region plus quadrupole for daughter ion selection offers the advantages of medium resolution combined with high transmission and does not produce artefact peaks which some of the sector arrangements can exhibit.
A new multiple analyser instrument has been designed for the analytical application of MS-MS which combines high parent ion resolution (up to 25,000) with medium daughter ion resolution. It has been developed from the MM7070E double focusing mass spectrometer by the addition of a quadrupole collision region and quadrupole mass analyser after the normal resolving slit to give high overall selectivity and sensitivity. The instrument offers the analyst the powerful combination of high resolution accurate mass measurement and selected ion recording GC/MS with high resolution MS-MS.

INSTRUMENTATION

The instrument consists of a MM7070E double focusing mass spectrometer (EB) after the resolving slit of which has been fitted a quadrupole collision region (Q1) and quadrupole mass analyser (Q2). A schematic diagram of the arrangement is shown in Figure 1. Parent ions are selected by EB and are focused by lenses onto the entrance aperture of Q1. In Q1, the ions undergo collision induced dissociations at energies up to 500 eV. A retarding lens at the entrance to Q1 ensures that the parent ion beam enters Q1 with minimum attenuation. Daughter ions produced in Q1 pass into Q2 where they are mass analysed. Q2 is a high performance quadrupole, with a mass range of 1500. Finally, the daughter ions are detected by a conversion dynode off axis electron multiplier arrangement. A similar detector is situated immediately after the resolving slit of EB to allow the parent ion beam to be selected and, of course, to enable the instrument to be operated as a conventional medium performance mass spectrometer with full performance.
A 3 DAC scan system enables data system control and acquisition of parent ion, daughter ion or neutral loss spectra.

PERFORMANCE

Resolution

Parent ions may be selected by EB at up to 25,000 resolution and daughter ions by Q2 at unit mass resolution up to mass 1500.

Fragmentation Efficiency

The fragmentation efficiency, is defined as the sum of the fragment ion current divided by the total ion current both measured at the final collector.
The measured fragmentation efficiency for N-decane using helium as the collision gas was as high as 80%.

Overall CID efficiency

This is defined as the total fragment current divided by the current of the parent leaving the parent selector (EB).
Preliminary measurements for n-decane and perchlorobutadiene gave a figure of 5% when the daughter ion resolution was unit mass.

Collision Energy Range

The energy of the ions in the collision region can affect the fragmentation pattern. The collision energy in the 70EQ can be varied up to 500 eV and the voltage on Q2 is automatically scanned as a function of parent and daughter ion mass to maintain optimum performance.

Mixture Analysis

Figure 2 shows the necessity of greater than unit mass parent ion resolution to analyse a simple mixture by MS/MS.

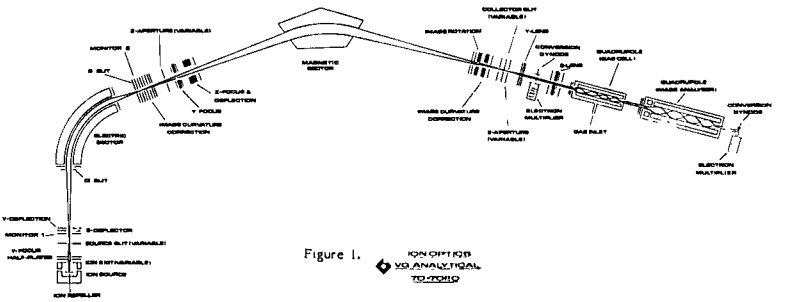


Figure 1. ION OPTICS VG ANALYTICAL TO-ZOMD

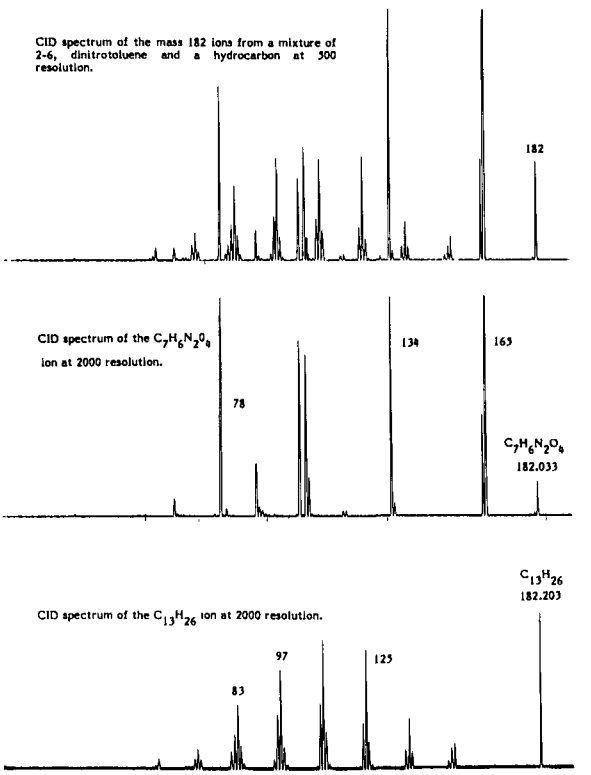


Figure 2. Separation of components in a mixture by medium resolution parent ion selection.

APPLICATION OF AN AUTOMATIC GC-MS-DS SYSTEM TO THE ROUTINE QUALITY CONTROL OF PHARMACEUTICAL PRODUCTS

Ryan P.A., Warburton G.A., Hazelby D., Taylor K.T.
Kratos Analytical Instruments, Barton Dock Road, Urmston
Manchester M31 2LD, England

Modern mass spectrometers are now finding increased application in routine, repetitive analysis, for example in quality control and environmental monitoring. There is also a requirement for the work to be carried out automatically and preferably without an operator in attendance. This paper describes the use of an MS25 fitted with an autosampler and operating under the control of the DS55 data system to provide a routine analysis of a pharmaceutical product.

Software has been developed to automate data acquisition using an autosampler. The software monitors GC temperature to ensure all conditions are correct before proceeding with injection. The sample is selected and identified by rack number, bottle number and injection number, this information being transferred to the data system and incorporated in the runname of that experiment. Wash cycles can also be incorporated in the routine, in which case data acquisition is not initiated.

The solvent vent valve is operated during an initial delay period selected by the user, after which data acquisition starts and the data is written to disk. User-specified processing can be performed on the acquired data before the next injection.

The DS55 Search and Quantitation program is now incorporated in the autosampler procedure. The program requires a calibration file, a retention index file and a known concentration of an internal standard. These are constructed automatically at the user's request.

The following operations are performed:

A Search is executed for the internal standard

The intensity of characteristic ions is calculated

Each library entry is searched for in turn

The concentrations of all entries that have been positively identified are calulated

Reports are produced on all positive identifications.

Each component is detected by its retention index and its identity is confirmed by a reverse library search. The concentration is then calculated by comparison of the maximum intensity of four characteristic ions with that of an ion in the spectrum of the internal standard and a previously acquired calibration.

The example presented in this paper demonstrates the use of an autosampler and the DS55 QSEARCH program in quality control experiments on a pharmaceutical product. This was a proprietary analgesic used for the control of dysmenorrhoea.

Each tablet was crushed and extracted with chloroform/methanol solvent. After addition of an internal standard Anthracene d_{10} - the samples were injected onto a 25M SE52 fused silica capillary column using the autosampler.

Figure 1 shows the chromatograms of three consecutive injections. In order of elution the components were salycilamide, acetaminophen, anthracene d_{10} and caffeine. On this column the acetaminophen yielded a mis-shapen peak, however this had only a relatively small effect on the reproducibility of the results.

The mean concentrations and coefficients of variation obtained for each component are presented below:

	True Concentration	Observed Mean	Coefficient of Variation
Salicylamide	250	250.2	7.4
Acetaminophen	250	246.4	14.5
Caffeine	50	46.7	9.8
Anthracene, d_{10} (Internal Standard)	150	146	9.4

Concentrations are in mg per tablet

The results presented here demonstrate the high reproducibility of the GC-MS-DS package used in this work. The extent of computer control involved makes the combination particularly useful for unattended operations.

Although the application, in this instance, was in quality control, it can be seen that such a system is extremely powerful and has wide applicability.

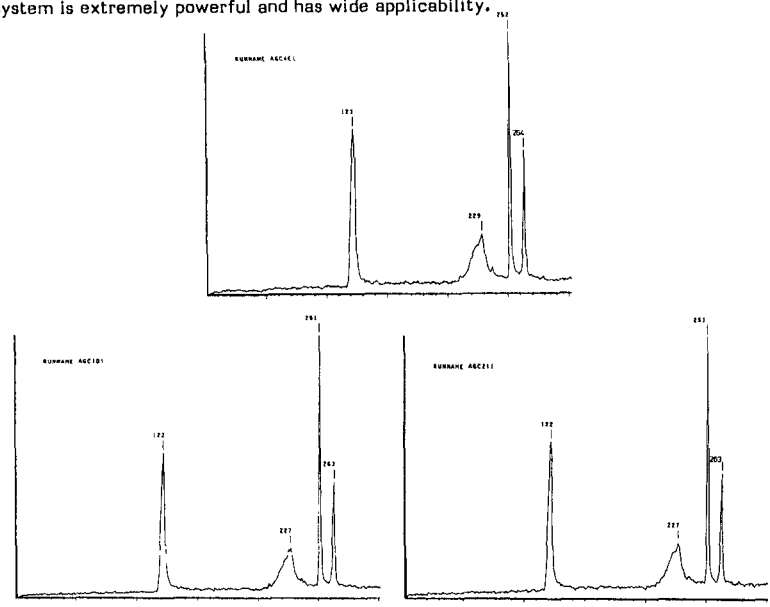


Figure (1) MS25 DS55 TYPICAL CHROMATOGRAMS OF AN ANALGESIC PREPARATION USING AUTOMATED INJECTION & DATA ACQUISITION

Identification of Aflatoxins by Quadrupole MS/MS

R. D. Plattner, G. A. Bennett, and R. D. Stubblefield
Northern Regional Research Center
Agricultural Research Service
U.S. Department of Agriculture
Peoria, Illinois 61604
and
J. R. B. Slayback
Finnigan MAT
Sunnyvale, California 94086

Aflatoxins are compounds that are produced by the fungi Aspergillus flavus and A. parasiticus. They have been found in grains, peanuts, and tree nuts where climatic conditions have been favorable (1). They have been shown to be potent carcinogens in laboratory animals (2). Numerous methods have been devised to identify aflatoxins in complex mixtures based on both biological activity and chemical/physical properties (UV, fluorescence, and chromatography). Confirmation of the identity of aflatoxin in analytical results is essential, especially for regulatory purposes. Aflatoxins are not amenable to gas chromatography, and it is difficult to confirm the identity of these compounds in matrices by mass spectrometry at the low concentrations at which they are found. Recently, Brumley et al. reported a MS procedure consisting of isolation of the aflatoxin by preparatory 2-dimensional TLC, in situ elution of the TLC spot, and analysis by negative ion chemical ionization (NICI) MS (3). Detection was possible at concentrations as low as 10 ng/g. We have applied quadrupole MS/MS (Finnigan MAT triple stage quadrupole mass spectrometer, TSQ™) to the direct analysis of aflatoxins in complex matrices. Aflatoxin B_1 was detected at the 10 ng/g level in corn by monitoring the CAD daughter ions of the major NICI parents at m/z 312, 311, and 297 with no sample cleanup. In this experiment, an aliquot of a contaminated corn $CHCl_3$ extract (10 ng/g aflatoxin B_1) equivalent to 0.1 g corn was analyzed. NICI-MS parent ions at m/z 312, 311, and 297 were focused in Q_1 in successive ~0.5-sec intervals. Several CAD daughter fragments were monitored for each parent experiment as described in Table 1. A 1-ng sample of aflatoxin B_1 and an (0.1-g equivalent) aliquot of clean corn were analyzed by the same procedure as a control. The signals for the daughter spectra were clearly present in the contaminated corn extracts at levels above the background observed in the blank matrix. Stray background signals, the very heavy sample loading (several µl of corn oil), and the relatively few and weak daughter signals observed precluded detection at lower concentration without sample clean-up. However, in corn extracts cleaned up by standard AOAC methods for TLC analysis (4), aflatoxin was detectable at well below 1 ng/g levels. In tissue extracts (loin, liver, bile, and urine) we have successfully confirmed HPLC detection of aflatoxins B_1 and M_1 at levels as low as 0.5 ng/g. This data demonstrates the applicability of MS/MS as a method for confirmation of aflatoxin identity in analytical samples at low levels. Additional work on the quantitative aspects is in progress and will be reported separately.

TABLE 1
MS/MS Daughter Fragments from NI CI-MS/MS of Aflatoxin B_1

Parent	Origin	Rel %	Daughter Fragments (%) Observed[1]
312	$[M]^-$	100	312 (1), 297 (100), 269 (20), 253 (17)
311	$[M-H]^-$	30	311 (100), 296 (62), 283 (12), 267 (18), 253 (12)
297	$[M-15]^-$	50	297 (100), 269 (18), 253 (14)

[1]Underlined fragments chosen for MID experiments.

References

1. Stoloff, L. J. Assoc. Off. Anal. Chem. 63: 1067 (1980).

2. Rodricks, J. V., Hesseltine, C. W., and Mehlman, M. A., Eds., "Mycotoxins in Human and Animal Health," Pathotox: Park Forrest, IL (1977).

3. Brumley, W. C., Nesheim, S., Trucksess, M. W., Trucksess, E. W., Dreifuss, P. A., Roach, J. A. G., Andrzejewski, D., Eppley, R. M., Pohland, A. E., Thorpe, C. W., and Sphon, J. A. Anal. Chem. 53: 2003 (1981).

4. Official Methods of Analysis (1980) 13th Ed., AOAC Arlington, Va., Chapter 26.

ADDUCT ION FORMATION IN THE COLLISION CELL OF A TANDEM QUADRUPOLE MASS SPECTROMETER.
D.I. Carroll, J.G. Nowlin, R.N. Stillwell, and E.C. Horning. Institute for Lipid Research, Baylor College of Medicine, Houston, Texas 77030

OBJECTIVES

During initial studies with a newly designed and fabricated triple quadrupole system, it was noticed that both substituted and unsubstituted aromatic compounds gave ions at masses above the mass of the ion selected for collision induced dissociation. These ions were insignificant at pressures of 1-2 millitorr but became predominant at pressures around 20 millitorr or greater.

One of the major ions observed in the CID spectra of unsubstituted protonated aromatics was that due to the loss of neutral hydrogen:

$$C_6H_7^+ \text{ ---CID---> } C_6H_5^+ + H_2 \qquad (1)$$

The second product ion was then formed from the $C_6H_5^+$ by loss of neutral acetylene:

$$C_6H_5^+ \text{ ---CID---> } C_4H_3^+ + C_2H_2 \qquad (2)$$

The product ions at higher masses than $C_6H_7^+$ corresponded to the formation of a water adduct ion with the $C_6H_5^+$ ion:

$$C_6H_5^+ + H_2O \text{ ---CID---> } C_6H_5OH\cdot H^+ \qquad (3)$$

Careful drying of the collision cell gas eliminated these adduct ions at all but very high collision gas pressures.

The objective of this study was to investigate covalently-bonded adduct ion formation with the $C_6H_5^+$ ion and various other compounds. Adduct ions were found to occur with methane, water, benzene, and ammonia when they were added to the argon collision gas. Simply proton transfer occurred when pyridine or methanol were added.

In this study, the argon collision gas pressure was 20 millitorr, and the ion axial energy was 25 eV.

The collision gas and cell were at room temperature.

CONCLUSIONS

Protonated aromatics in the CID cell at ion axial energies above 15 eV show very characteristic losses, either of the neutral substituent, or if unsubstituted loss of neutral H_2. The resulting ion, typically $C_6H_5^+$ for benzene, easily forms covalently-bonded adduct ions with methane, water, ammonia, and even benzene itself. It may prove possible to use these reactions to further increase the specificity of the CID technique. For example, using argon/methane collision gas and a linked scan with the final analyzer 14 amu above the first analyzer only aromatic compounds would be detected.

Many other characteristic reactions in the collision chamber can probably be found. In this study, using an ammonia/methane collision gas, protonated 4-heptanone gives only NH_4^+, while protonated heptaldehyde loses water and clusters with one and two molecules of ammonia. If this proves to be a general case linked scan CID techniques could be used to distinguish easily aldehydes from ketones.

Characteristic reactions with intentionally added trace gases in the collision gas can often be used to greatly enhance the specificity of the CID technique. The cell can be used both to induce collisional dissociation and/or to serve as a second ary reaction chamber for adduct ion formation with the product ions.

ON THE USE OF TRIPLE-QUADRUPOLE MS/MS FOR PEAK IDENTIFICATION IN COMPLEX INORGANIC SIMS SPECTRA

Charles W. Magee, P. Jane Gale, Bryan L. Bentz
RCA Laboratories, Princeton, New Jersey 08540 and
Jeffrey Shabanowitz, University of Virginia, Charlottesville VA 22901

Inorganic Secondary Ion Mass Spectrometry (SIMS) traditionally supplies information on elemental composition of solids. Ideally the spectra contain peaks which can be assigned unambiguously to atomic species. More often than not the spectra are complicated by the presence of peaks the assignment of which is less straightforward. These peaks are assumed to be polyatomic clusters such as multimers (e.g., Si_2^+), multimetallics (e.g., $SiAl^+$), oxides (e.g., $Ta_2O_3^-$), mixed oxides (e.g., $BaSrO^+$), hydroxides (e.g., $SiOH^+$), and hydrides (e.g., BaH^+). For groups of ions in which a unique isotope pattern can be discerned, the identification of one or more constituents is possible. Many elements, however, are monoisotopic and thus provide no clues as to their presence in a cluster. Quadrupole instruments, on which much of the inorganic SIMS work is carried out, do not provide the high resolution required for exact mass assignment. Collisional dissociation of these clusters provides a novel way of unraveling the composition and structure of sputtered ions [1].

Dissociation experiments at low collision energies were conducted at the University of Virginia on a Finnigan Triple Stage Quadrupole (TSQ). A primary beam for solids bombardment was formed by supplying xenon gas to an Ion Tech particle source operated at 8 kV acceleration potential. A SIMS profile (full scan) of each sample was first obtained without collision gas added to Q2. Each of those ions recorded in the full scan which was thought to be polyatomic was then collisionally dissociated in Q2, using one of the three modes of operation of the TSQ. A Daughter Ion spectrum is obtained by fixing Q1 to pass a particular ion into the collision cell while Q3 is scanned. The fragments produced upon dissociation of the selected parent ion can thus be detected. The acquisition of a Parent Ion spectrum involves the reverse: Q1 is scanned and Q3 is set to pass a particular fragment ion mass. Thus a signal is recorded each time an ion focused by Q1 into the collision cell fragments to yield an ion at the m/e selected in Q3. A Neutral Loss spectrum requires simultaneous scanning of both Q1 and Q3 but with a fixed mass difference between them--that is, at any given time the mass of the ion passed by Q3 is some constant number of amu less than the mass of the ion transmitted to the collision cell by Q1. Note that while the information obtained in each mode is different, all three modes of operation indicate which of the ions transmitted by Q1 fragments in Q2.

A mixed oxide cathode provided a multi-component sample, the analysis of which could be simplified by coupling SIMS with two-stage mass analysis (MS/MS). The full scan survey spectrum is shown in Figure 1. Barium, strontium, and lead are major constituents of this sample, and, as shown in the figure, singly charged atomic ions of these elements are observed. The identification of several other peaks of high intensity as polyatomic species was facilitated by the acquisition of the neutral loss spectrum shown in Figure 2. Q3 was scanned a fixed 17 amu less than Q1. As a consequence, only those ions in the sample which could fragment to lose OH ($XOH \rightarrow X^+ + OH$) reach the detector. The presence of signals at m/e 105, 155, 209, and 259 in the neutral loss spectrum shows that these peaks in the survey spectrum are indeed cluster ions, not atomic species. Subtraction of 17 from each of the parent ion masses can then aid in the identification of X. The assignment of the peak at m/e 138 in Figure 1 to atomic Ba^+ was supported by the Daughter Ion scan using m/e 138 as parent. No fragmentation was observed, as shown in Figure 3, strongly suggesting that the parent ion was atomic.

Figure 4 shows the full scan spectrum of another multi-component sample, a Pb-Ba glass (NBS#89). The strongest signals occur at m/e 23 (Na^+), 28 (Si^+), and 39 (K^+). The signals at m/e 138 and 208 are assumed to be Ba^+ and Pb^+, respectively. These identifications made, there remain a number of peaks which cannot be readily assigned to any atomic species. Since it was thought that some of these peaks were K^+ clusters, a parent ion spectrum using K^+ as daughter was acquired. The spectrum in Figure 5 shows those parent ions which fragmented in Q2 to produce K^+: $KX^+ \rightarrow K^+ + X$. Subtraction of 39 from each of the parent ion masses yields the mass of the neutral fragment X, providing a good clue to its identity. The compositions of clusters deduced by this reasoning are indicated. Daughter ion spectra can also provide information about the polyatomic species. Dissociation of the parent ion NaK^+ (m/e 62) is illustrated in Figure 6. This cluster interacts with the collision gas to yield three products: Na^+, K^+, and $NaKH^+$. The relative intensities of Na^+ and K^+ are determined by the difference in their ionization potentials: 5.14 and 4.34 eV respectively. $NaKH^+$ is presumed to be the result of an ion-molecule reaction with trace water in the collision cell: $NaK^+ + H_2O \rightarrow NaKH^+ + OH$.

The ability to obtain parent, daughter and neutral loss spectra from the collisional

dissociation of selected parent ions produced by sputtering solid targets is a significant addition to the characterization of inorganic solids by SIMS, as illustrated in the foregoing examples. The analysis of complex materials can be considerably simplified if atomic species can be differentiated from polyatomic clusters and if the composition of the polyatomic species can be probed.

Reference

[1] G. L. Glish and P. J. Todd; presented at the 29th Annual Conference on Mass Spectrometry and Allied Topics; Minneapolis, MN, May 24-29, 1981, p. 675.

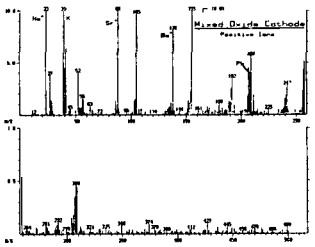


Figure 1

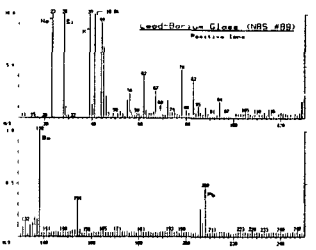


Figure 4

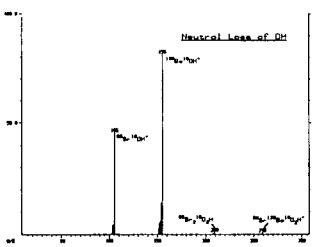


Figure 2

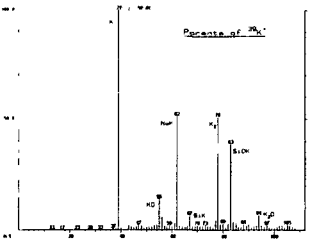


Figure 5

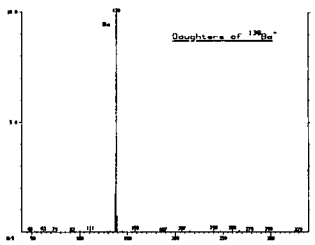


Figure 3

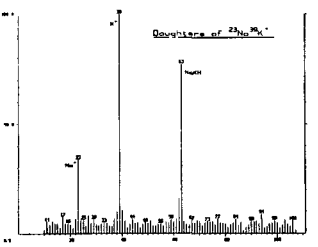


Figure 6

STUDIES IN GC-CI MS

Ta-min Feng, Patrick Rudewicz, and Burnaby Munson
University of Delaware
Newark, Delaware 19711

In our work with NH_3 as a chemical ionization reagent gas, a few interesting and somewhat peculiar (to us) observations were made.

At low pressures (.06 torr) of NH_3 introduced into the CI source of a duPont 492 mass spectrometer, with 0.06 torr of He coming from the gas chromatograph, it was noted that the total ion current increased as the samples were eluted through the mass spectrometer source. This increase is attributed to charge exchange or electron ionization of the samples in addition to reactions with NH_4^+. Some of these fragment ions reacted with ammonia to give new product ions. For example, the $C_6H_5^+$ ion from acetophenone apparently reacts very rapidly with NH_3 to form 94^+, presumably $\emptyset NH_3^+$. These combination CI/EI spectra may be useful for structure determination like the spectra that have been reported previously with mixed reagent gases.

Some of the compounds react by accepting a proton from NH_4^+ and others react by forming the $(M+NH_4)^+$ association ion. We noted that sensitivity for the less basic ions which react by adduct formation decreased with increasing pressure of NH_3, with respect to the strongly basic compounds like pyridine. For example, the ratio of $(M+NH_4)^+$ from cyclohexanol to $(M+H)^+$ from pyridine, I_{118}/I_{80}, decreased from .01 with ~0.06 torr NH_3 to 0.002 with 0.4 torr of NH_3 (for same sample size, He pressure, and temperature). We attribute this to the switching reaction,

$$NH_4^+ + S \rightleftharpoons SNH_4^+$$

$$SNH_4^+ + NH_3 \longrightarrow NH_4(NH_3)^+ + S$$

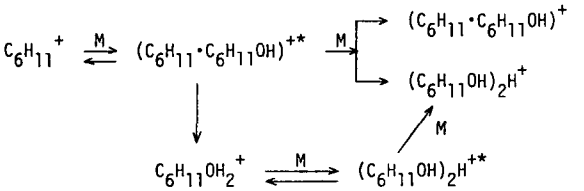
This suggestion is strongly supported by the observation that the $NH_4(NH_3)^+$ ion increases in relative and absolute abundance as the polar, but weakly basic compounds are eluted from the gas chromatograph through the source of the mass spectrometer. Pyridine, on the other hand, (more basic than NH_3) causes a small decrease in the relative and absolute abundances of $NH_4(NH_3)^+$ at m/z = 35.

At pressures of about 0.4 torr of NH_3 and 0.1 torr of He, no significant effects are noted on the absolute or relative abundances of the ammonia ions: NH_4^+, $NH_4(NH_3)^+$, $NH_4(NH_3)_2^+$, $NH_4(NH_3)_3^+$ for polar but weakly basic compounds, unless these compounds have large electron capture cross sections. Bromobenzene, for example, has no effect on the abundances of the ammonia ions, but iodobenzene and nitrobenzene do alter the ratios of ionic abundances: increasing the extent of conversion to the more solvated ions as these strong electron capture agents elute through the gas chromatograph. The small ion current for m/z = 69, $NH_4(NH_3)_3^+$, is roughly tripled as iodobenzene is eluted through the source of the mass spectrometer. The ion current at m/z = 52, $NH_4(NH_3)_2^+$, is almost doubled in the same experiment, a small increase is noted in the $NH_4(NH_3)^+$ ion current, and a 25% decrease is noted in the ion current for NH_4^+. We attribute these changes in ionic distributions to changes in the ionic residence times as these electron capture species elute through the source of the mass spectrometer.

In related experiments a sample is continually in the source (from the probe) and compounds are eluted from the GC. As the electron capture agents elute through the MS source, the ion current for the ions from the probe sample increase significantly, by as much as a factor of two in some cases. Again, we feel that this effect results from an increase in ionic residence time caused by the electron capture reagents.

One interesting complication in CIMS is the occurrence of sample ion/sample molecule reactions. The high mass ions resulting from these reactions with large sample sizes may confuse the interpretation of the spectrum by suggesting that higher mass species are present. A repeating pattern, however, may be helpful in confirming the molecular weight. In GC/CIMS one can deliberately introduce large samples to study the sample ion/sample molecule reactions that result. These studies can provide rapid and reasonable (but not rigorously proven) reaction paths.

A large (0.5 μL) injection of cyclohexanol, for example, gives a very interesting set of ion profiles across the GC peak. The ion current for the major ion ($C_6H_{11}^+$, m/z = 83) shows a minimum at the time corresponding to the maximum of the FID trace which corresponds to the maximum in the trace of the protonated dimer, m/z = 201. Plots of the relative abundances of the major CI productions of cyclohexanol show a distinct minimum for $C_6H_{11}^+$ and little variation across the peak for $C_6H_9^+$ and $C_6H_{10}OH^+$. The molecular weight of the compound is strongly reinforced by the occurrence of ions at 101 and 201, 83 and 183, 99 and 199. The lack of variation for $C_6H_9^+$ and $C_6H_{10}OH^+$ suggests that these ions do not react rapidly by proton transfer with cyclohexanol. The distinct minimum for $C_6H_{11}^+$ and the sharp maxima for the protonated dimer suggests the following reaction sequence: M = $C_6H_{11}OH$, cyclohexanol.



In similar experiments with cyclohexyl propanoate, we note that the major CI ions, $C_2H_5CO_2H_2^+$ and $C_6H_{11}^+$ react rapidly with cyclohexyl propanoate by proton transfer to give the protonated molecule. The protonated molecule reacts rapidly to give the protonated dimer. For cyclohexyl propanoate, the dominant reactions of these and other CI ions are proton transfer, not adduct formation.

A Very High Yield Electron Impact Ion Source for Analytical Mass Spectrometry.

by
S.L.Koontz and M.B.Denton
Chemistry Department, University of Arizona
Tucson, Arizona 85721

Introduction

Previously published results outline the ion optical and operational characteristics of a Very High Yield electron impact ion source(1). In this presentation we report operational characteristics and preformance of two improved versions of the VHY-EI ion source with two r.f. path stability mass filters: 1) A General Electric Monopole 300 and 2) an Extranuclear 4-162-8 0.95 cm quadrupole operated at 2.58 MHz. The VHY-EI ion source is compared directly with the Monopole 300 ion source with respect to both ion yield and the quality of the spectra produced using n-butane at 5 micortorr as the sample gas. The VHY-EI ionizer Extranuclear quadrupole combination is characterized with respect to both residual gas analysis sensitivity and the quality of the spectra produced when organic compounds are used as the sample gas.

Materials and Methods

The ion sources reported here were constructed using components from Kimball Physics eV Parts™ (2). The Monopole 300 version of the VHY-EI ionizer had emissive filaments of 0.025 cm diameter thoriated tungsten wire. Electron Technology Inc. thoriated iridium ribbon (3.175 cm x .005 cm x .068 cm) were used to prepare emissive filament structures in the VHY-EI ionizer Extranuclear quadrupole instrument. Two or three of the ribbon filaments were operated in parallel in the quadrupole instrument. Detailed plans for both ionizers are available on request.

Research grade normal butane (99.995%) was obtained from Phillips Petroleum. Eastman diethylamine was vacuum distilled and refrigerated before use. 2,4-pentanedione, 1-butanol, N,N-dimethylacetamide and 1-pentene were obtained from Matheson,Coleman,and Bell (95% or better) and were used as received. Mehtylcyclohexane was MCB reagent.

Results and Discussion

Normal butane spectra taken with both the VHY-EI ionizer and the monopole ionizer on the Monopole 300 are shown in figure 1. With both ionizers tuned for maximum signal the VHY-EI ionizer is seen to produce a 1000 fold improvement in signal intensity at the same sample pressure and emission current.

In combination with the Extranuclear quadrupole the VHY-EI ionizer produces a residual gas sensitivity of 1.2×10^{-1} A/torr with a resolution of 80 at mass 28. The VHY-EI ionizer quadrupole combination is also able to produce normal electron impact spectra of organic compounds with high ion yield. 70eV spectra of several organic compounds are shown in figures 2 through 5. With sample pressure at 3 microtorr base peak ion currents in excess of 1×10^{-8} A. were obtained for all the compounds shown with resolution 200 at mass 100. In addition low voltage spectra have been obtained. A 15eV spectrum of tributylamine is shown in figure 6. Sample pressure is 1 microtorr and base peak ion current is 5×10^{-11} A. The ion currents reported here were measured with a Faraday cup detector.

Conclusions

A hot cathode Penning ionizer coupled with low spherical aberration focusing optics,the VHY-EI ionizer,can produce higher mass analyzed ion currents than conventional ionizers when the ion beam is mass analysed with r. f. path stability mass filters. Typical electron impact spectra of several organic compounds have been produced at high yield,even at low

electron impact energies. Spectra compare favorably with those shown in the Atlas of Mass Spectral Data(3).

(1) S.L. Koontz abd M.B. Denton, Int. J. Mass Spectrom. Ion Phys.,37(1981) 227-239
(2) Kimball Physics Inc. Wilton, New Hampshire 03086.
(3) E. Stenhagen,S. Abrahamsson,F.W. McLafferty, Atlas of Mass Spectral Data Vol.I(1969) Wiley(interscience) New York.

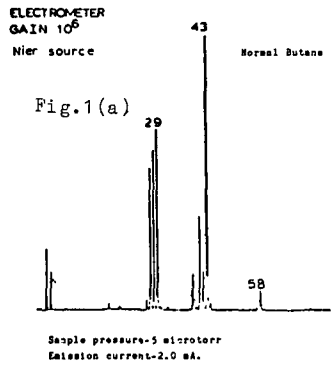


Fig.1(a)

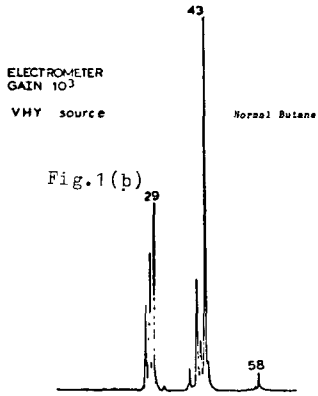


Fig.1(b)

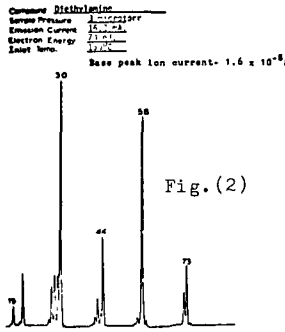


Fig.(2)

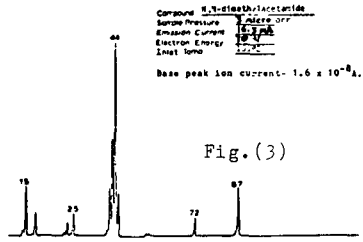


Fig.(3)

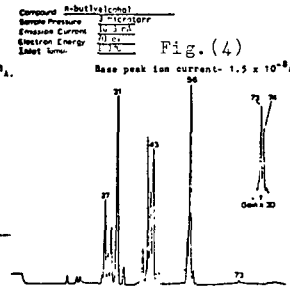


Fig.(4)

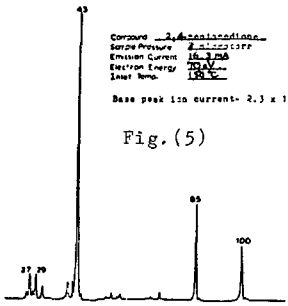


Fig.(5)

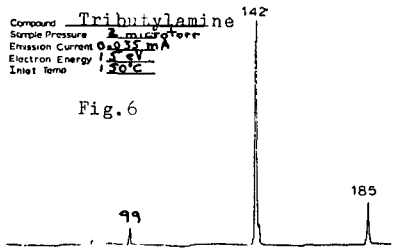


Fig.6

ION OPTICAL PROPERTIES OF ELECTRON-BEAM-GUIDING ION SOURCE AND ITS APPLICATION TO MASS ANALYSER

T.Kishi and T.Takagi

College of Engineering, University of Osaka Prefecture, Sakai, 591, and
Faculty of Engineering, Kyoto University, Kyoto, 606, Japan.

In an ion source using the mechanism of electron beam bombardment vaporization, it is effective to extract the generated ions along the space charge cloud of the electron beam through the center of a cathode. A gun system equipped with such the function was studied from the viewpoint of an ion optics and was applied to the mass analysis of a few solid materials. In order to obtain a small spot size electron beam and to make the ions pass through the center of cathode, a Ta pipe cathode of 1mm, 0.6mm and 8mm as the outside diameter, inside diameter, and length, respectively, was used. The cathode was heated to 2000K by a d.c. current through a few small contact areas of the thin-edged tungsten plates which were arranged to support the emitting end of the cathode symmetrically, as shown in Fig.1. Since the effect of the magnetic fields produced by the heater current on the emitted electrons could be canceled, the electron beam of small size was obtained when the applied bias voltages were suitably adjusted.

T:target
S:sample material
G2:second grid
G1:first grid
W:tungsten plate
K:Ta pipe cathode

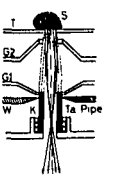


Fig1 Gun column

This electron beam directly bombards the sample material to make it vaporize and ionize simultaneously. The generated ions could be trapped in the space charge cloud of the electron beam. In this case, however, the electric field in front of the target is strong enough, so that the ion trajectories will be influenced also by the gun geometry and the applied bias voltages. The electron beam trajectories were then calculated as functions of the bias voltages taking into account the effect of the space charge. The results of calculations are shown in Figs.2(a) to 2(c) for an acceleration voltage of 2kV and the saturation current of 2mA. In this case it is assumed that these were generated only in front of the target with an energy of 0.1eV and started to move in parallel or in the direction 45° from the optical axis. When the bias voltages are suitably adjusted, not only is the electron beam focused into a small size spot but also the back stream ion beam can pass through the cathode center without sputtering onto the its surface. The electron beam current against the bias voltage Vg1 of the first grid G1 is shown in Fig.3. The rapid increase of the electron beam current near zero bias voltage is due to the contribution of the electrons emitted from the outside face of the cathode. The obtained total ion beam current against the Vg1 and the bias voltage Vg2 of the second grid G2 are also shown in Figs.4(a) and 4(b). The maximum of the ion beam current is obtained at the bias voltages expected from the results of

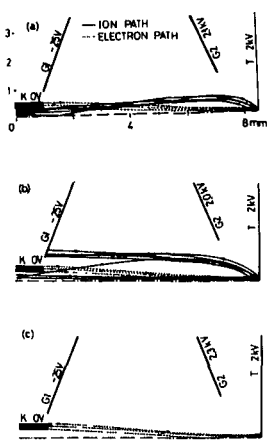


Fig2 Computed electron beam and ion beam trajectories

calculation.

The energy distribution of the obtained ion beam was measured with a conventional cylidrical electrostatic prism. The half width of the ion energy spread is less than 10 to 13eV as shown in Fig.5, but the resolution of the apparatus was of the order of 5 to 6eV. The reasons of this small energy spread can be attributed to the rapid decrease in the vapor pressure distribution of the evaporated atoms along the optical axis or to the lens actions of the gun system and of the extra lens used for focusing the extracted ion beam.

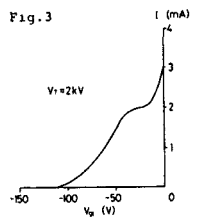
An ore of galena obtained in Hokkaido(Japan) and a piece of boron nitride, which were wrapped in tungsten mesh, were used as the materials for the mass analysis. The extracted ion beam were analyzed by means of a conventional switch magnet. In the case of galena, several characteristic peaks corresponding to Li, Mg, Ca, S, S_2 , Pb, PbS, and Pb_2^{are} detected as shown in Fig.6. In the case of boron nitride the mass peaks corresponding to B_{10} and B_{11} are shown in Fig.7. These material components were also confirmed by chemical analysis. Benzilic acid used as an example of organic compound was analyzed with this gun system. The result is shown in Fig.8, but the mass numbers of the peaks are not given here because the apparatus was not enough to assign the precise mass numbers.

References.

1.T.Kishi, T.Nishida and N.Tanizuka: J. of Vacuum Soc. of Japan, 16,249(1973).

2.T.Kishi, I.Yamada and T.Takagi: Rev. Sci. Instr., 50, 1517(1979).

3.T.Kishi and T.Takagi: will be published in J. Vac. Sci. Technol., 19, May-June(1982).



Electron beam current vs. 1st grid bias voltage

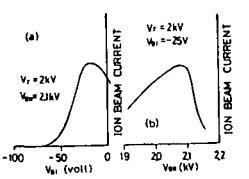


Fig.4 Properties of ion beam current vs V_{B1} and V_{B2}

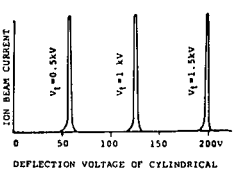


Fig.5 Energy distribution of extracted ion beam

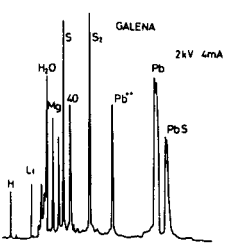


Fig.6 Mass spectrum of galena

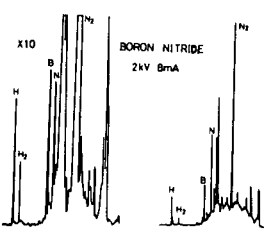


Fig.7 Mass spectrum of boron nitride

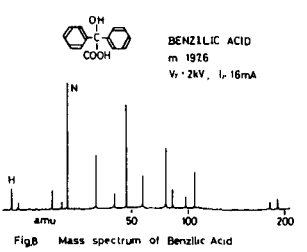


Fig.8 Mass spectrum of Benzilic Acid

AN EHD ION SOURCE WITH A RESERVOIR AND AN EMITTER TIP HEATED BY ELECTRON BOMBARDMENT

T. OKUTANI, K. YAGI and T. NODA
Toyohashi University of Technology, Tempaku, Toyohashi 440, Japan
H. TAMURA, H. OKANO and H. WATANABE
Hitachi Central Research Laboratory, Kokubunji, Tokyo 185, Japan

1. Introduction

Development of the EHD ion source producing a focussed ion beam with a high brightness using liquid metals has attracted a great interest because of its applicability to microfabrication, micro-surface analysis, etc. EHD ion sources reported so far can be classified into two types from their constructions. The first is of the needle type in which an emitter needle is sharpened to a few microns in radius and spot-welded to a heater such as a tungsten hairpin filament(1-3). The other is of the capillary type in which a hollow needle is used with a heating coil(4-6). Although these have been well known as the ion source for fine beam, there still exist some problems. In the needle type, the small amount of liquid metal on the heater rapidly evaporates because its temperature is higher than that of the tip. Hence, the operating life time becomes short. The capillary type equipped with a reservoir for the liquid metal allows long operating life time, but the melting point of the metal must be low to such an extent as galium or cesium is because of the constraint caused by the heating method for the hollow needle and the reservoir. Thus, we have constructed a new type EHD ion source which is equipped with a reservoir and an emitter tip heated by electron bombardment.

2. Construction

First of all, we aimed at constructing an EHD ion source which satisfies the following requirements:

(1) Production of ions from materials even with a high melting point.
(2) Long operating time without refilling.
(3) Ease of replacing the emitter tip and the reservoir, if neccesary, with others at a choice of the material to be ionized.

Figure 1 illustrates the construction of the present ion source(7). Since this heating system allows one to easily raise the tip temperature higher than 3000°C with small electric power, a variety of ion species can stably be produced for a long period of time owing to the reservoir.

In the present study the reservoir is made of quartz pipe of 6 mm ID and cone-shaped bottom with a hole, through which the emitter tip is placed. The tip is made of 0.5 mm tungsten wire, electrolytically polished as sharp as few microns in radius and simply chucked by a tip holder with ease. A tungsten ring filament is placed around the tip as the electron emitter for heating.

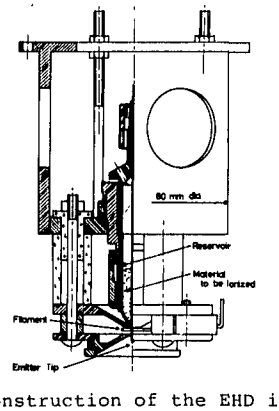


Fig.1 Construction of the EHD ion source

3. Results

We examined characteristics of this ion source using indium and gold. Figure 2 shows probe current vs extraction voltage for indium ions, where the voltage was applied to the tip against an extraction electrode and the probe current emitted within the acceptance half-angle of 20 mrad was monitored by a Faraday cup. It is shown that the ion current steeply rises at a threshold voltage of extraction. The probe current also varies in proportion to squre of the acceptance half-angle which is set at 20, 6.7 and 2.0 mrad, respectively. This shows a current density of ca. 100 uA/sr at the extraction voltage of 10 kV. Figure 3 illustrates the results for gold ions emitted within the acceptance half-angle of 20 mrad. This also shows a steep increase of the probe current as in the case of indium ions. In addition we can see two-stage behavior in the I-V characteristics of gold ions. We have not yet understood the origin, but it may be due to the phenomenon of multiple cusps formation on the emitter needle reported

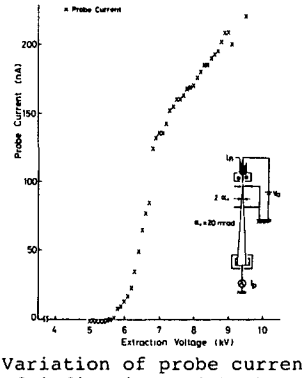


Fig.2 Variation of probe current of indium ions with the extraction voltage.

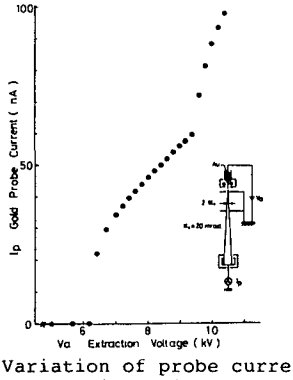


Fig.3 Variation of probe current of gold ions with extraction voltage.

on cesium ions by R. Clampitt et al(8), or to a certain change in the situation of supplying liquid gold to the needle apex. The figure also shows a current density of several tens microampere per unit solid angle for gold ions, which is in the same order as reported so far(2).

A typical example of the probe current fluctuation shows the stability of ca. 5% per hour without using any active stabilization.

4. Summary

We have constructed a new type EHD ion source, which can produce a variety of ion species for a long period of time. Preliminary experiments using indium and gold have shown that the ion source can produce intense and stable ion beam of metals.

References

1. T. Sakurai, R. J. Culbertson and G. H. Robertson, Appl. Phys. Lett. 34(1), 11(1979).
2. M. Komuro and H. Kawakatsu, J. Appl. Phys. 52(4), 2642(1981).
3. K. Gamo, Y. Ochiai, Y. Inomoto and S. Namba, Proc. 28th. Intern. Field Emission Symp. (Oregon, 1981)p83.
4. V. E. Krohn and G. R. Ringo, Appl. Phys. Lett. 27(9), 479(1975).
5. R. L. Seliger, J. W. Ward, V. Wang and R. L. Kubena, Appl. Phys. Lett. 34(5), 310(1979).
6. L. W. Swanson, G. A. Schwind and A. E. Bell, J. Appl. Phys. 51(7), 3453(1980).
7. T. Noda, T. Okutani, K. Yagi, H. Tamura, H. Okano and H. Watanabe, Rev. Sci. Instrum. (submitted, 1982).
8. R. Clampitt and D. K. Jefferies, Low-Energy Ion Beam 1977. Inst. Phys. Conf. Ser. No.38 ch 1.

WPB 4 ATMOSPHERIC PRESSURE PLASMA (ICP or MIP)/MASS SPECTROMETRY FOR ELEMENTAL ANALYSIS.

D.J. Douglas, E.S.K. Quan and R.G. Smith, SCIEX™, 55 Glen Cameron Rd., Thornhill, Ontario, Canada. L3T 1P2.

Progress in the use of a microwave induced plasma (MIP) and an inductively coupled plasma (ICP) as ion sources for quadrupole mass spectrometry will be reported. Solutions are nebulized into these plasmas where the dissolved solids are vapourized and ionized to give a simple mass spectrum characteristic of the solution's elemental composition. As well, isotope ratios may be determined directly for elements in solution with moderate sensitivity (μg) and precision ($\sigma \leq 1\%$) and with very high sample throughput (typically a few minutes per sample). A comparison of the MIP and ICP sources at the current stage of development shows that the ICP can tolerate higher salt content solutions (>1000 ppm) with reduced matrix effects than the MIP but at the expense of reduced sensitivity (detection limits 1-50 ppb). An evaluation of these sources for the analysis of some reference materials and real samples, for isotope ratio determinations of lead and uranium standards, and for isotope dilution measurements will be given. As well a description will be given of the use of an electrothermal atomizer with the MIP to permit the analysis of μL sample sizes and to improve the absolute sensitivity down to picograms or better for some metals, e.g., Pb.

CHARACTERISTICS OF A VOLCANO STYLE FIELD IONIZATION SOURCE AND A HIGH RESOLUTION (MS-9) MASS SPECTROMETER

by

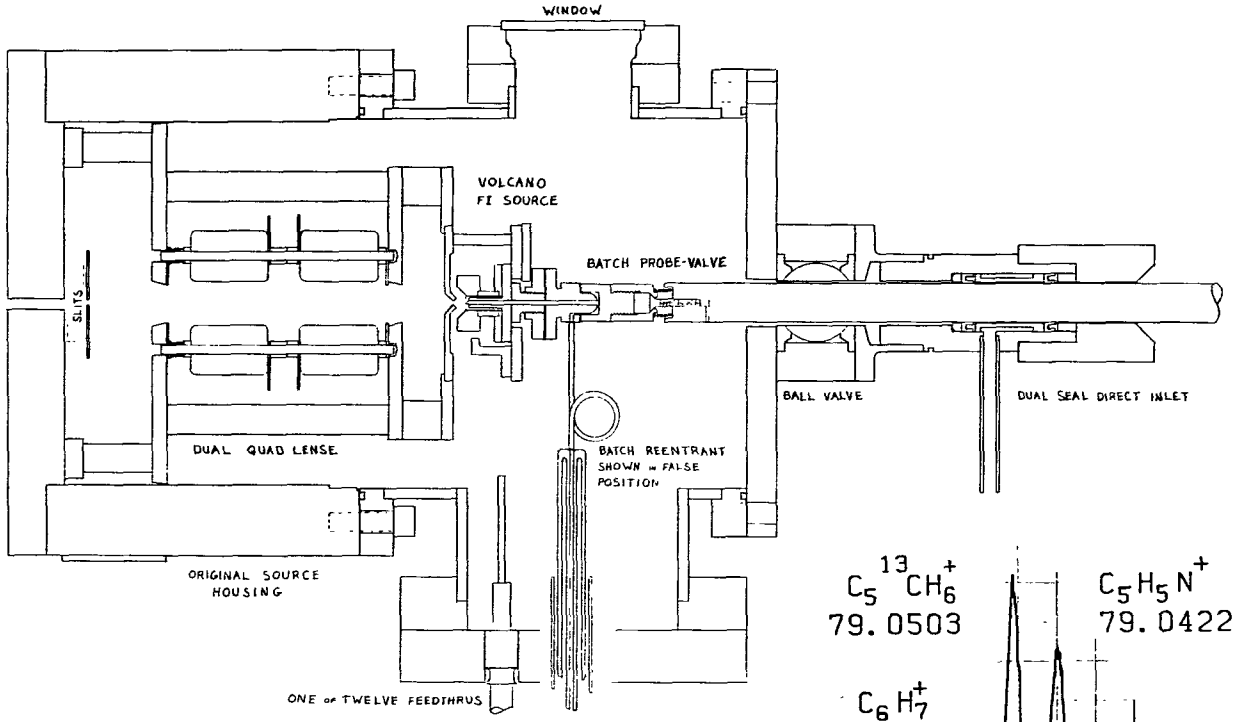
S. E. Young and S. E. Buttrill, Jr.
Mass Spectrometry Development Program
SRI International
Menlo Park, CA 94025

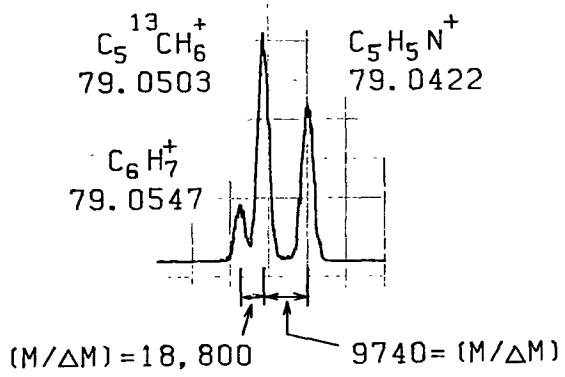
A 1964 vintage Nier-Johnson type (AEI MS-9) double focusing mass spectrometer was purchased and completely overhauled and reconditioned. The entire instrument was completely disassembled, and all parts of the vacuum system and ion optics were thoroughly cleaned. The original discrete dynode multiplier was replaced with a Channeltron continuous dynode multiplier. All of the chopper-stablized DC amplifiers were replaced with solid state amplifiers of our own design using modern integrated circuits. The detector preamplifier was also replaced. The rebuilt instrument in the electron ionization mode achieved a resolution of 33,000 at 8 kV accelerating potential.

The electron ionization source was then removed together with the original direct probe lock, 4-way valve, and batch inlet system reentrant. The source housing was enlarged by adding an extension as shown in the accompanying figure. A new direct probe airlock was also added. The round ion beam from the volcano style field ionization source is shaped and focused by a pair of electrostatic quadrupole lenses.

The batch inlet system was connected to the field ionization source through a new triple wall, vacuum insulated, reentrant. The connection between the ion source and the reentrant is made by a loop of nickel tubing designed to be a firm, springy, fit. A special probe is used to make the final connection between the sample stream from the batch inlet and the volcano. When this probe is pulled back the low pressure side of the batch inlet system leak is pumped by the source housing high vacuum. When the probe is inserted onto the source, the Macor tip sits tightly over the back of the ion source and forms a path connecting the batch inlet sample stream to the volcano. A separate probe used for conventional solid sample introduction connects only with the volcano source. The result of this arrangement is that solid samples can be introduced without contaminating the batch inlet system, and the low pressure side of the batch inlet leak can be pumped by high vacuum when not in use without contaminating the volcano ion source.

The resolution achieved to date with the field ionization source is approximately 20,000. This is illustrated in the second figure. We plan to use the high resolution FIMS system for routine analysis of distillate fuels, for which an operating resolution of about 4,000 is required. Future work will concentrate on modifications and enhancement to the DS-55 Data System for providing automatic analyses of distillate fuels and calculations of fuel compositions from the FIMS spectra. Additional details of the modifications are available from the authors on request.


WINDOW
VOLCANO
FI SOURCE
BATCH PROBE-VALVE
SLITS
BALL VALVE
DUAL SEAL DIRECT INLET
DUAL QUAD LENSE
BATCH REENTRANT
SHOWN IN FALSE
POSITION
ORIGINAL SOURCE
HOUSING
ONE OF TWELVE FEEDTHRUS


$C_5{}^{13}CH_6^+$
79.0503
$C_5H_5N^+$
79.0422
$C_6H_7^+$
79.0547
(M/ΔM) = 18,800
9740 = (M/ΔM)

LIQUID IONIZATION FIELD DESORPTION MASS SPECTROMETRY EFFECT of ELECTRIC FIELD on a SAMPLE PROBE

M.Tsuchiya, T.Nonaka and T.Taira, Faculty of Engineering University of Tokyo, Bunkyo-ku, Tokyo, Japan 113

The effect of electric field applied to a sample probe in the method which we call Liquid ionization[1,2] (a kind of API) mass spectrometry was investigated for the purpose of improving the method and understanding the mechanism of ionization and desorption, especially for nonvolatile compounds. Therefore metastable argon was used as the neutral ionizing species.

A modified quadrupole mass spectrometer (ANELVA TE 600 GC/MS)[1] equipped with a new ion source shown in Fig.1 was used. Argon gas at atmospheric pressure was ionized by corona discharge between a needle electrode-1 and a counter electrode-2. Charged species such as Ar^+ and electrons were eliminated by the electrode-2 and -3, so that only metastable Ar atoms with carrier gas can flow into the ionization chamber and ionize a liquid sample (1-3 ul) deposited on a sample probe which is a silicon emitter (JEOL) made for field desorption (FD) technique. Organic compounds whose ionization energies are lower than 11.72 eV are ionized by collision with metastable argon atoms as follows.

$$Ar^* + M \longrightarrow M^+ + e^- + Ar \quad \text{--- (Penning ioniztion) -- (1)}$$

$$Ar^* + nM \longrightarrow (kM+H)^+ + (mM-H)^- + Ar \quad \text{---- (2)}$$

Major process in this method is thought to be the reaction (2) because of surface ionization. The numbers k and m of observed ions were generally 1 and 2 for involatile compounds such as amino acids and saccharides.

As expected, the ion abundance increased sharply by applying high voltage (900 - 1200 V) to the emitter , more than 100 times of that at low voltage (200 - 300 V). And at a fixed high voltage (e.g. V_E = 1100 V), quite steep increase of ion current was observed at optimum emitter current. This indicates that the electric field accelerates the desorption of ions (not neutral molecules) produced on the emitter.

Less volatile compounds such as -alanine showed mass spectrum similar to that obtained with the previous technique[1] In the case of sucrose, glucose and adenosine, however, the effect of high field (e.g. 1100 V) was significant. The abundnce of MH^+ ion increased and even M_2H^+ ions were observed. Heating is required to observe ions from involatile compounds. The temperature of a sample increases gradually while most of solvent (water) is evaporating from the emitter and then increases quickly to its final temperature. Rapid heating with an optimum emitter current gives a sort of good mass spectrum of sucrose, especially at early period of heating as shown in Fig.2a. This spectrum was obtained by one scan that took about 10 seconds (m/z 80-700). In keep heating, a variety of fragment ions were produced from sucrose as shown in Fig.2b which was the summed mass spectrum of seven scannings. These ions were produced by the loss of water molecules from the M_2H^+, $(M+163)^+$ and MH^+ ions. The $(M+163)^+$ ion is thought to be produced by the elimination of $C_6H_{11}O_5$-OH (mass 180) from the M_2H^+ ion. Selected ion profiles presenting the temperature dependence of major ions of sucrose (Fig.3) indicate that the fragment ions of mass 163 and 181 appeared later at high temperature were produced by thermal decomposition of sucrose molecules.

To find good additives such as glycerin in FAB method is required to obtain better mass spectrum of nonvolatile compounds. For instance, 1,4-butanediol (5×10^{-2} M) was added as an additive (S) to sucrose (1×10^{-2} M) in an aqueous solution. The major ions were MHS^+, $MHS^+ - H_2O$ and the MH^+ and their total abundance was 2-3 times of that obtained with a simple aqueous solution. Acetone showed a little good effect, but glycerin and ethanol showed rather poor effect.

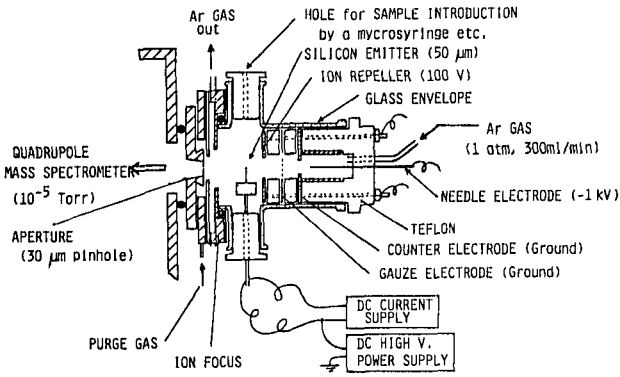
Adenosine in methanol (0.5 μg in 1 μl) was also measured, resulting in only the weak MH^+ ion peak with the abundant fragment ion peak at m/z 136. In contrast, after evaporating methanol on the emitter and adding 1 μl water, the abundant MH^+ ions were obtained as the base peak.

High electric field on the emitter accelerates the desorption of ions of intact molecules, resulting in much abundant MH^+ ions, especially at early stage of heating. The method is useful for nonvolatile compounds.

Additives (reagent) and solvent (matrix) affect mass spectrum and ion abundances, e.g., 1,4-butanediol was better than glycerin for sucrose, probably because of their proton affinities.

Advantages of this method are; a) Soft ionization : MH^+ ions are abundant for most of compounds. b) Ease of sample handling : A microsyringe is enough for sample introduction. Because of 1 atm, too. c) Collision induced dissociation spectrum can be obtained easily. d) Free use of additives and solvent because of 1 atm. e) Very few back ground : No back ground when a clean emitter is used. f) High sensitivity : $10^{-6} - 10^{-9}$ g is enough.

Reference
1) M.Tsuchiya and T.Taira, Int. J. Mass Spectrom. Ion Phys., 34, 351 (1980)
2) M.Tsuchiya, T Nonaka, T Taira, Mass Spectroscopy, 30, 95 (1982)



SCHEMATIC DIAGRAM of an ION SOURCE of LIQUID IONIZATION MASS SPECTROMETER

Fig.1

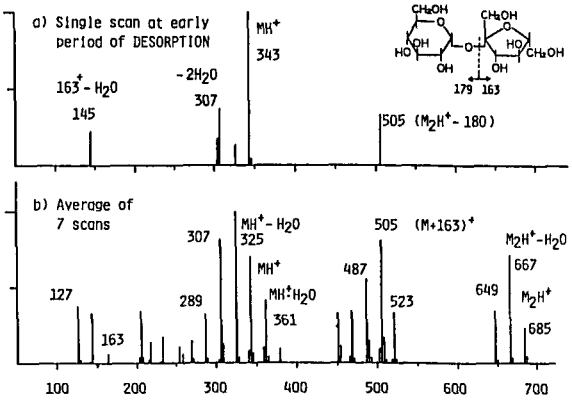
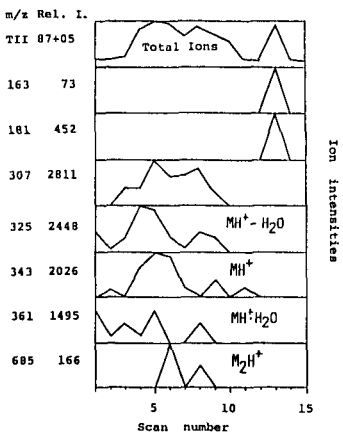


Fig.2 MASS SPECTRA of SUCROSE (10^{-2} M aqueous solution, 1 μl) (V_E : 1100 V)



SELECTED ION PROFILES showing TEMPERATURE DEPENDENCE of IONS from SUCROSE (10^{-2} M aq.)

Fig.3

A Fission Fragment Ionization Study of Chlorophyll a; B.T. Chait and F.H. Field, The Rockefeller University, 1230 York Avenue, New York, N.Y. 10021.

The positive and negative ^{252}Cf fission fragment ionization mass spectra of chlorophyll a are examined. By applying carefully controlled retarding potentials to a set of grids at the end of the flight path of our mass spectrometer, the identities of the various fragmentation reactions occurring in the flight tube can be established[1]. This technique is used to elucidate the majority of the intense flight-tube fragmentations for both positive and negative ions.

Metastable decay rates are measured. It is shown that: (1) Much fragmentation occurs with rate constants in the range 10^4-10^8 s^{-1}. (2) Roughly equal amounts of fragmentation with rate constants greater and less than 10^8 s^{-1} occurs. (3) A wide range of rate constants exists for each fragmentation. (4) Relatively slow fragmentation of the negative molecular ions occurs. These findings are in concurrence with the concepts embodied in the quasi-equilibrium theory of mass spectra and contrary to the explosive (10^{-14}-10^{-12} s) fragmentation hypothesis of Hunt, Macfarlane, Katz and Dougherty[2].

1. Chait, B.T.; Field, F.H. Int. J. Mass Spec. Ion Phys. 1981, 41, 17-20.

2. Hunt, J.E.; Macfarlane, R.D.; Katz, J.J.; Dougherty, R.C. J. Am. Chem. Soc. 1981, 103, 6775-6778.

DISCHARGE IONIZATION SECONDARY ION MASS SPECTROMETRY (DISIMS): GEORGE C. STAFFORD AND Donald C. Bradford; Finnigan MAT Corporation, 355 River Oaks Parkway, San Jose, CA 95134.

The development of the Fast Atom Bombardment (FAB) technique has extended mass spectrometry to many new areas of research. Conventional FAB ionizers require a separate fast atom gun positioned adjacent to the ion source block. A new bombardment source (DISIMS) has been developed utilizing a gaseous discharge system contained within the Finnigan MAT 4500/4600 ionizer.[1] This discharge produces high kinetic energy atoms and ions that strike the sample probe and produce secondary sample ions. The new technique offers good quality FAB type spectra with a simplified and less expensive source of energetic particles.

Figure 1 shows a corss sectional view of the ion source with the DISIMS ionization chamber installed. Xe gas is directed to the discharge region to yield a pressure of 1 torr; operation of the discharge electrode at +5KV will produce a stable gaseous discharge. Positive ions formed in the discharge region are accelerated toward the entrance hole in the DISIMS ionization chamber. Most of these positive ions will undergo charge exchange with neutral Xe atoms to produce fast neutral particles. The resulting beam of fast neutrals and ions strikes the sample/glycerine target producing secondary ions for mass analysis. A side view of the entire ion source system is shown in figure 2. Secondary ions formed at the sample target are extracted by the lens system and mass analyzed by the quadrupole mass filter.

Figure 3 and 4 are examples of spectra which can be obtained utilizing this technique. Figure 3 is a spectrum of vitamin B12 which shows the $(M + H)^+$ ion cluster and the $(M-CN+H)^+$ cluster. Figure 4 shows a spectrum of a penta peptide. This spectrum also shows an ion characteristic of the molecular weight as well as significant fragments which denote partial sequencing information.

This technique has been shown to be useful for a wide variety of compounds which were not applicable to other techniques of ionization.

1. George C. Stafford, Donald C. Bradford, and David R. Stephens, Proc. 29th Annual Conference American Society Mass Spec. and Allied Topics, Minneapolis, May, 1981, p.163.

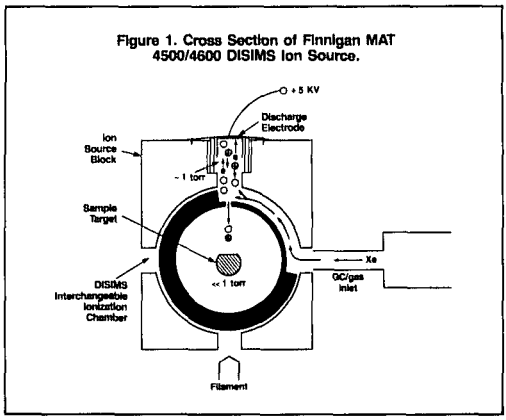


Figure 1. Cross Section of Finnigan MAT 4500/4600 DISIMS Ion Source.

Figure 2. Side View of Finnigan MAT 4500/4600 DISIMS Ion Source.

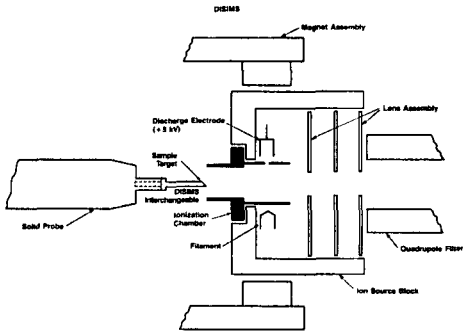


Figure 3. DISIMS Spectrum of Vitamin B_{12}

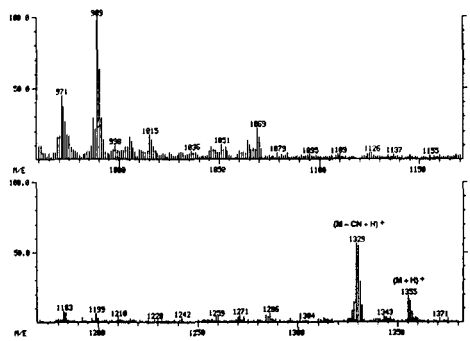
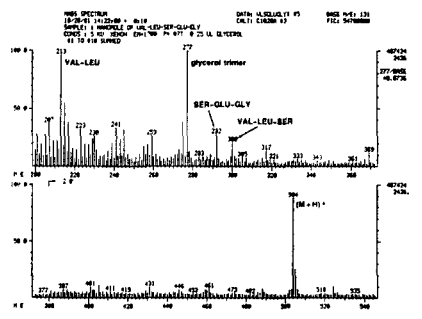


Figure 4. DISIMS of 1 Nanomole of the Pentapeptide VAL-LEU-SER-GLU-GLY



PLASMA DISCHARGE MASS SPECTROMETRY FOR INORGANIC TRACE ANALYSIS

J.E. Cantle, P.J. Turner & D. Kay
VG Isotopes Ltd., Winsford, Cheshire, U.K.

The plasma discharge source enables direct analysis by mass spectrometry of electrically conducting and semi-conducting solid materials. Non-conducting materials may be analysed by compounding the material with an electrically conducting material such as graphite. Liquid samples are analysed following absorption on to a suitable support matrix.

The analysis is essentially a bulk analysis of the material although depth profiling of a very ruidmentary nature is inherent in the technique.

The material to be analysed is placed in the end of a probe and inserted into a source chamber through a vacuum interlock. A gas, such as Argon, is introduced into the source chamber at a pressure of about 0.5 torr and, with the sample as the cathode, a d.c. discharge is struck between the cathode and an anode.

Positive ions formed in the "positive column" of the discharge accelerate towards the cathode. These ions bombard the sample with a few hundreds of eV's of energy and sputter sample material. The sputtered material is mainly neutral atoms and molecules which diffuse towards the "positive column" of the plasma discharge where ionisation occurs by collision with electrons, positive and negative ions. Ions are extracted from the plasma and accelerated towards the source slit of the mass spectrometer for analysis.

The extraction of ions from the plasma takes place through the ion exit slit, the third electrode in this three electrode source. the potential on this electrode may be varied and may be set to be equal to the anode voltage or up to -100 volts with respect to the anode voltage in nine switched steps. Variation of this bias voltage on the ion exit slit in effect changes the point within the plasma from which ions are extracted. This enables the detection of sample ions to be optimised and/or enables the abundance of complex ions formed by interaction of sample ions and discharge supporting gas ions to be minimised.

Detection limits for trace elements in the sample are of the order of 10 ppb. The technique is simultaneous and multielement and can be very favourable compared with spark source mass spectrometry and optical emission spectrometry. It offers the analyst advantages when compared to each of these alternative methods.

1. Versus Spark Source Mass Spectrometry

This technique is characterised by very poor ion beam stability and the complex nature of the mass spectra due to large amounts of multi-charged species viz M^+, M^{++}, M^{+++} etc. Moreover the analysis of one sample satisfactorily may take several hours. The plasma discharge source, however, produces extremely stable ion beams, shows negligible production of multi-charged species and sample turn around is of the order of five minutes.

2. Versus Optical Emission Spectrometry

In this technique the thermally excited atomic emission spectra is generated and analysed optically. Detection limits are limited by the compromise conditions necessary for multielement analysis. Emission spectrum are extremely complicated particularly for complex samples - often beyond the resolving capabilities of commercially available monochromators. The simple mass scale of the plasma discharge mass spectrometer is much more easily interpreted.

Moreover the optical emission technique is found to suffer from the fact that there is a large range of elemental sensitivities where many orders of magnitude separate the most detectable from the least detectable elements. Sensitivity is extremely uniform in the plasma discharge mass spectrometer.

COMPARISON OF DIFFERENT TYPES OF SOLID SOURCE

	Ion Stability	Energy Spread	Ion Optics	Production of Complex & multi charged ions	Sensitivity Range	Matrix Effect	Detection Limit	Sample Size
Spark Source	V. Poor	1000V approx	Double focus + Photoplate	Large Multiply Charged	x 3	Small	10^9	Milligrams
Ion Probe (SIMS)	Good	100V approx	Double focus	Large Complexing	x 10^5	Very Large	10^5-10^8	Micrograms
Plasma Discharge	Good	100V approx	Double focus	Negligible Complex and Double charged	x 3	Small	10^8-10^9	Milligrams
Thermal	Good	1V	Single focus or Double focus	None	x 10^5	Very Large	10^{12}	Nanograms
Inductively Coupled Plasma MS	Good	1-10V	Quadrupole	Relatively Small	x 3	Small/ Large	10^9	Micrograms

DESIGN OF FAST ATOM GUNS AND ION SOURCES FOR FABMS

A.M. Hogg

Department of Chemistry

University of Alberta

Edmonton, Alberta

Canada T6G 2G2

Three AEI/KRATOS mass spectrometers, double focussing MS9 and MS50 and single focussing MS12, have been converted to FAB operation using two basic versions of the saddle field fast atom gun described in Figs. 1 and 2 and Table 1. Samples can be introduced on copper probe tips via insertion locks either at right angles to the ion beam as in EI or axial with the beam as in FI/FD. Suitable probe tip shapes are shown in Fig. 3. The ion source is simply an extraction slit held, together with the sample probe, at the full accelerating voltage and the two beam centering plates held about 500v lower as used in conventional KRATOS sources. Table 2 lists other pertinent details. A full description has been submitted for publication in the International Journal of Mass Spectrometry and Ion Physics.

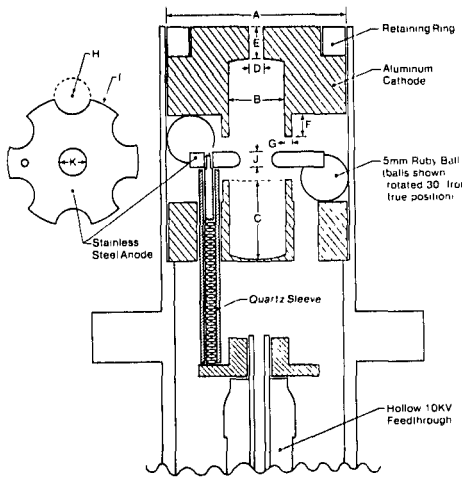


Fig 1

E.A.B. GUN MAJOR DIMENSIONS INCHES (MM)

		ONE INCH GUN	COMPACT GUN
CATHODE DIAMETER	A	.948 (24.08)	.748 (19.00)
CATHODE CAVITY DIAMETER	B	.297 (7.54)	.235 (5.97)
CATHODE CAVITY DEPTH	C	.330 (8.38)	.330 (8.38)
ATOM EXIT DIAMETER	D	.060 (1.52)	.060 (1.52)
ATOM EXIT DEPTH	E	.130 (3.30)	.130 (3.30)
CATHODE SKIRT DEPTH	F	.098 (2.49)	.098 (2.49)
CATHODE SKIRT THICKNESS	G	.060 (1.52)	.030 (0.76)
DIAMETER OF HOLES IN ANODE PERIMETER	H	.160 (4.06)	.160 (4.06)
ANODE DIAMETER	I	.753 (19.13)	.553 (14.05)
ANODE THICKNESS	J	.062 (1.57)	.062 (1.57)
ANODE APERTURE DIAMETER	K	.160 (4.06)	.120 (3.05)

Table 1

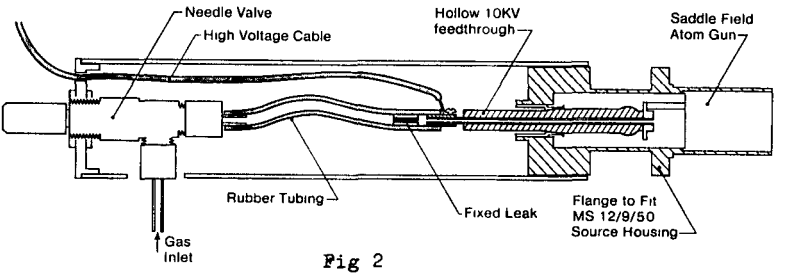
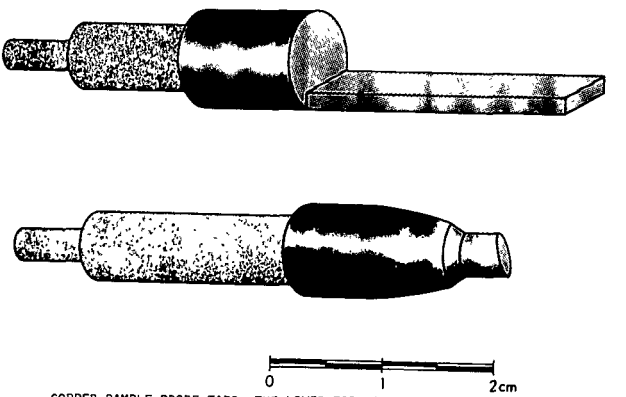


Fig 2



COPPER SAMPLE PROBE TIPS; THE LOWER FOR USE WITH AN AXIAL LOCK
THE UPPER FOR USE WITH A LOCK AT RIGHT ANGLES TO THE ION BEAM.

Fig 3

OTHER DETAILS

HIGH VOLTAGE HOLLOW FEEDTHROUGH: CERAMASEAL 804B4275-6
SUITABLE NEEDLE VALVE: NUPRO SS-2SA OR SS-2SG
FIXED LEAK: APPROX. 6 MM METROSIL ROD #07-561 SEALED IN GLASS OR CEMENTED WITH EPOXY INSIDE 1/8" OD STAINLESS TUBE.
POWER SUPPLY USED: SPELLMAN RHSR15PN60 WITH 3M (30x100K 2 WATT) SERIES RESISTOR.
MORE SUITABLE CURRENT REGULATED SUPPLY: SPELLMAN RHR10P60(CR)
GAS FLOW RATE: APPROX. 0.08 ML/MIN
RESIDUAL POSITIVE ION CURRENT AT 2mA GUN CURRENT: APPROX. 2μA.
OPTIMUM DISTANCE FROM GUN EXIT TO PROBE SURFACE -45 MM.

Table 2

WPB 12 RELEASE OF SECONDARY IONS UNDER VARYING FAB CONDITIONS; Ulrich Giessmann and Douglas F. Barofsky; Oregon Graduate Center, Beaverton, Oregon 97006.

A qualitative understanding of the release of organic ions under fast atom bombardment (FAB) conditions is emerging, and some mechanisms have been postulated[1,2]. The present work has been initiated to generate more specific, empirical data for a better understanding of the basic FAB processes.

Mono- and multivalent ionic compounds were selected as model samples for these experiments because of their relative simplicity and the large body of existing information available on their electric and surface properties. The samples were dispersed on a number of different solid and liquid substrates and bombarded with fast atoms produced either in a cold cathode discharge or a capillaritron atom gun. The primary atom beams were characterized by their atomic identity, average energy, and flux. Variations in emission intensity and speciation of the released secondary ions were observed under different primary beam conditions. Possible mechanisms for the observed results will be discussed.

1 M. Barber, R.S. Bordoli, R.D. Sedgwick, and A.N. Tyler, Nature 1981, 293, 270.

2 D.H. Williams, C. Bradley, G. Bojesen, S. Santikarn, and L.C.E. Taylor, J. Am. Chem. Soc. 1981, 103, 5700.

A UNIQUE FAST ATOM SOURCE FOR MASS SPECTROMETRY APPLICATIONS

J.F.Mahoney, D.M. Goebel, J.Perel and A.T. Forrester
Phrasor Scientific, Inc., Duarte, CA 91010

An alternative source for the generation of fast atom beams developed for fast atom bombardment (FAB) mass spectrometry is described. The principle of operation of the FAB source is based on a Capillaritron source.[2-4] A beam of ions generated from a plasma inside a small capillary nozzle undergoes charge transfer collisions with a flow of un-ionized gas near the nozzle orifice (see Fig. 1). These collisions result in the formation of fast atom beams which are separated by deflecting the residual ion components. A deflection system built into the ion gun unit allows the ratio of ions to fast atoms to be varied. This Fast Atom Capillaritron Source (FACS) can be used to generate fast atom beams from any gas species (typically argon and xenon for FAB) and requires little maintenance. The source can be constructed in miniature configurations, for example, as a small probe used in systems where space is limited.

Power calorimetry was utilized as the diagnostic technique to quantify and evaluate the fast atom beam parameters.[5] Using argon and xenon beams, measurements of ion currents and power density fluxes at FAB targets were made with and without ion beam deflection. It was determined that the power contribution due to fast atoms in an undeflected beam can vary from 40% to 80% of the total power delivered to a target depending upon the gas flow rate and ion beam energy. Fast atom densities up to 50μA/cm^2 have been measured at targets located 2.5cm from the FACS gun. Atom/ion densities up to 90μA/cm^2 have been measured. Power density profiles measured with the power calorimeter show that the fast ion/atom beams are well collimated (see Fig. 2).

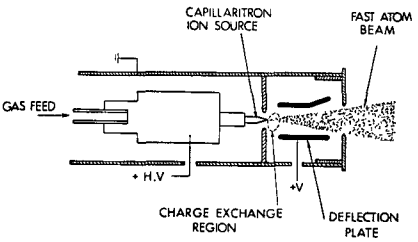


Figure 1.
Fast Atom Capillaritron Source

FACS guns have been successfully operated to produce FAB spectrum on a variety of mass spectrometer systems including quadrupole and magnetic sector instruments. These include the Hewlett Packard 5985B GC/MS System, Finnigan 4000, Kratos MS50, Finnigan MAT 312 and V VG-ZAB-ZF.

The FAB modification using the new FACS gun is excellent for mass analyzing important compounds such as polypeptides, nucleotides, quaternary ammonium alkyls, carbohydrates, porphyrins, glucuronides, proteins, organo-metallics, detergents, dyes, thermally labile and highly polar compounds; substances which thermally decompose prior to reaching a vapor state. A positive ion FAB spectrum of the pentapeptide (Leucine Enkephalene) using xenon as a bombarding gas (7kV, 50μA) is shown in Fig. 3.

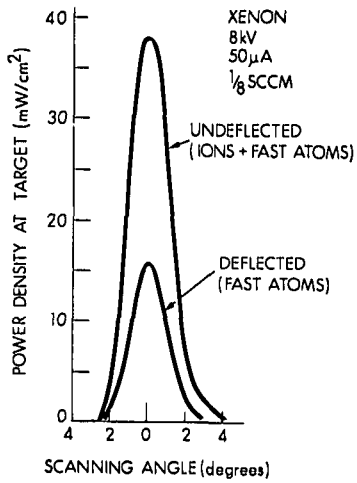


Figure 2.

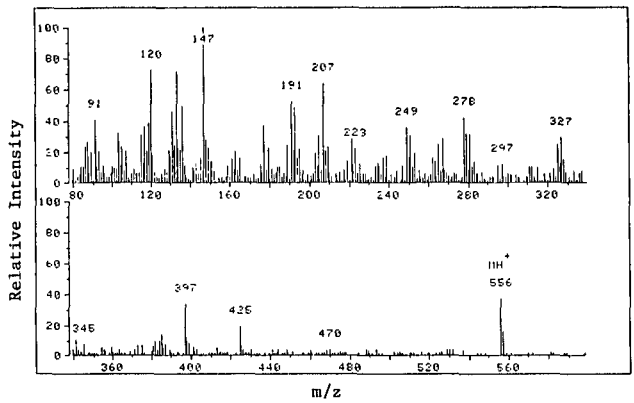


Figure 3.

REFERENCES:

1. R.A.Kerr, "Weight Limit for Mass Spectroscopy Raised", Science, V.216 (9 April 1982).
2. J.F.Mahoney, J.Perel and A.T.Forrester, Appl.Phys.Lett., 38, 320 (1981).
3. J.Perel, J.F.Mahoney, B.E.Kalensher and A.T.Forrester, AIAA-80-0747, 15th Inter. Electric Propul. Conf., Las Vegas, NV (21-23 April 1981).
4. D.M.Goebel, J.Perel, J.F.Mahoney and A.T.Forrester, "Characteristics of the Capillaritron Ion Source", submitted to Journal of Applied Physics.
5. J.F.Mahoney, D.M.Goebel, J.Perel and A.T.Forrester, "A Unique Fast Atom Source for Mass Spectrometry Applications, accepted by Biomedical Mass Spectrometry Journal.

A NEW MINIATURE "ON-SOURCE" FAB GUN

Martin A. Rudat
Central Research and Development Dept.
E. I. du Pont de Nemours & Co.
Wilmington, Delaware 19898

A miniature fast atom or fast ion gun for use in FAB or SIMS, which is mounted on the mass spectrometer ion source within the vacuum housing, has been developed. The source provides an intense, focused atom or ion beam which gives rise to intense, stable FAB or SIMS spectra.

The design is shown in Figure 1, and a schematic of the complete FAB is shown in Figure 2. A capillaritron ion source tip (Phrasor Scientific, Duarte, CA) and a counter electrode, consisting either of a drilled-out Swagelok® fitting (as shown in the Figure) or a stainless steel washer, forms a well-focused ion beam from the gas flowing through the tip (typically argon at 2-4 cc/min). The microdischarge in the 25μm hole at the end of the capillaritron tip also produces an intense fast atom beam by resonant charge exchange with excess gas. If the mass spectrometer ion source is operated at a potential above that of the capillaritron, then the ions produced will be deflected and only an atom beam will enter the source block. If operated below the discharge potential, both ions and atoms will enter the source block. As an alternative, a deflector could be utilized between the discharge and ion source.

Spectra obtained with the miniature source are comparable to published FAB spectra, and exhibit excellent intensity and stability when operating at discharge conditions of only 5-10μA current, a factor of 1000 less than most housing-mounted commercial sources. Figure 3 is the FAB spectrum of hexazinone, in which the glycerol spectrum has been completely suppressed. Spectra have been recorded for a wide variety of compounds, including peptides (such as bradykinin), antibiotics (such as the cyclic antibiotic tyrocidine A), salts, dyes, and polar organic compounds.

A paper describing the new source has been submitted to Analytical Chemistry.

FIGURE 1

FAST ATOM BOMBARDMENT SOURCE

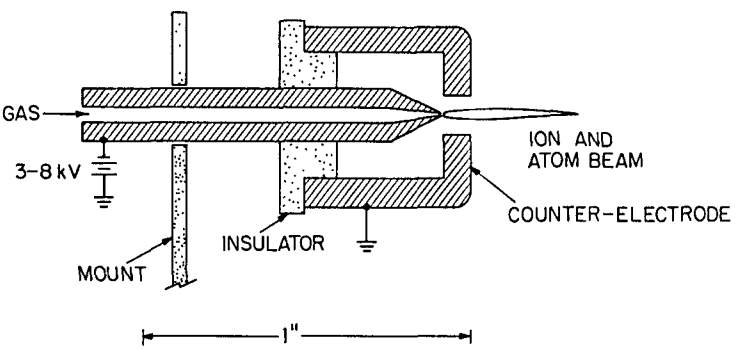


FIGURE 2. VG ZAB-2F FD ION SOURCE MODIFIED FOR FAB

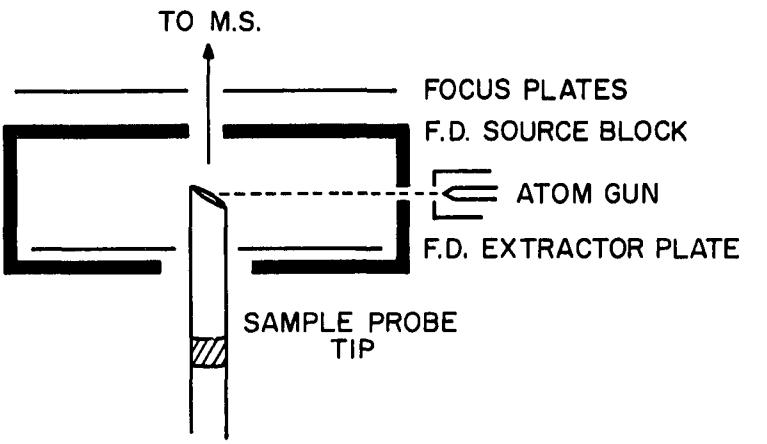
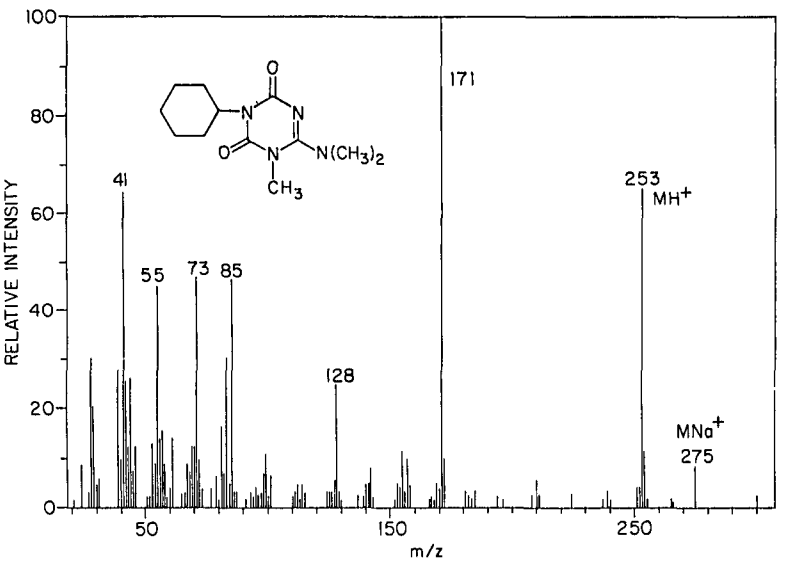


FIGURE 3. ARGON FAB SPECTRUM OF HEXAZINONE IN GLYCEROL



FAB/FD/FI ION SOURCE FOR THE COMPACT GC/MS AND ITS PERFORMANCE

Y. Naito, F. Kunihiro, Y. Kanmei, E. Kubota and M. Naito

JEOL Ltd., Akishima, Tokyo 196 Japan

A unique FAB/FD/FI combination ion source has been developed for the JMS-DX300 double-focusing mass spectrometer. Some important results have been obtained through experiments using this ion source.

A hot filament type ion gun for our Auger microprobe was installed on the ion source housing of the mass spectrometer. This gun has two pairs of deflector plates which can correctly position the ion beam to get an optimum spot. Fast atom energy is variable from 1 to 6 keV. A conventional FD/FI/EI combination ion source was modified to introduce a fast atom beam into the center of the ionization chamber.

Some experiments using this ion source have been conducted especially with the following three different combinations of FAB and FD. These combined methods showed unique features in comparison with FD or FAB alone. They were named as Glycerol-FD, FAB-FD and Emitter-FAB, respectively.

(1) [Glycerol-FD] A sample was deposited on an FD emitter, then coated with glycerol. Its spectrum was taken under high electric field without emitter heating. With this technique, a more distinct spectrum can be obtained than with FD alone, with an intense molecular peak maintained. Also, a ribbon-type silicon emitter was used in order to load as much sample as possible. Fig. 1 shows the differences between various ionization methods. The spectrum by Glycerol-FD using a wire-type emitter shows an intense molecular peak ($[M+H]^+$ or $[M+G+H]^+$) of the sample and no remarkable fragment peaks. On the other hand, the spectrum by Glycerol-FD using a ribbon-type emitter shows an intense fragment peaks as well as a molecular peak, and is rather similar to the FAB spectrum.

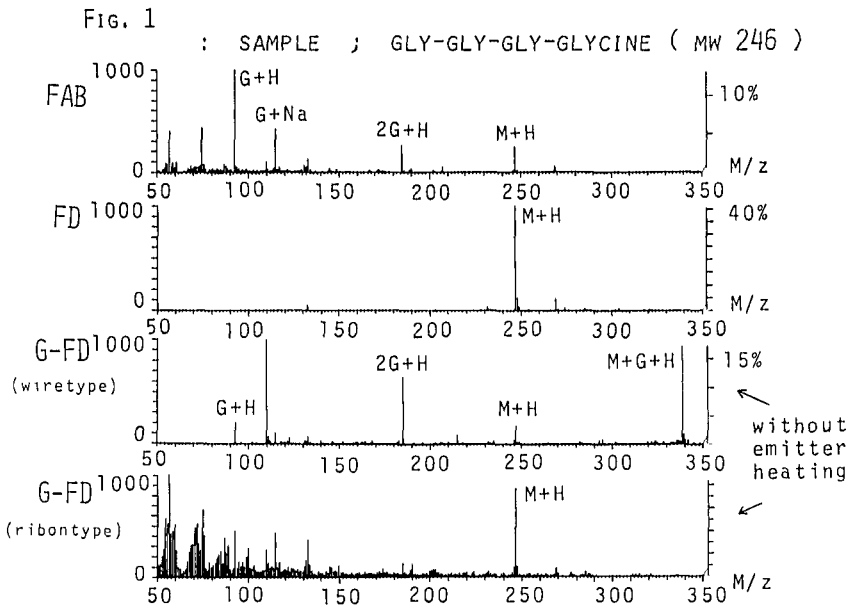
(2) [FAB-FD] A sample (glycerol free) was deposited on an FD emitter, then its spectrum was taken under high electric field and fast atom bombardment. A spectrum of perfluoroalkyl-phosphazine was similar to an added spectrum by FAB and FD.

(3) [Emitter-FAB] A sample was deposited on an FD emitter and coated with glycerol, then heated and subjected to fast atom bombardment. It was noted that the molecular ion intensity became optimum immediately before the glycerol matrix disappeared, and many fragment peaks appeared after the glycerol matrix disappeared. An Emitter-FAB spectrum of adenosine showed a more intense molecular peak than the normal FAB spectrum, and proved that the glycerol-background can be reduced.

Summary

The ionization techniques such as Glycerol-FD and Emitter-FAB have more unique features than FD or FAB, and are expected to expand their application field in the near future.

FIG. 1



MODIFICATION OF AN HP 5985B GC/MS FOR MOLECULAR SIMS

P. Jane Gale, Bryan L. Bentz, William L. Harrington, and Charles W. Magee
RCA Laboratories, Princeton, New Jersey 08540

The sputtering of thermally labile organic molecules from liquids has now become standard procedure in a number of laboratories [1,2], and many molecules, previously out of reach by mass spectroscopists because of their instability during volatilization, have now been characterized. The conversion of mass spectrometers to SIMS devices has in most cases involved simply the addition of an ion gun (with perhaps a charge exchange cell for neutral primary beams). The primary beam is directed toward the target, usually a solids probe modified to accept a copper tip on which the sample can be placed. High current densities can be used because the liquid sample matrix supplies a renewable surface from which sputtering can take place.

The present flurry of activity is an extension of work pioneered by Benninghoven [3] among others [4,5]. These earlier experiments generally involved the sputtering of solid organic species (or adsorbates on solids) using primary current densities low enough to minimize damage to the surface being studied. The constraints imposed by these "static" experiments require much more careful characterization of experimental parameters than is current practice in the liquid surface studies described above.

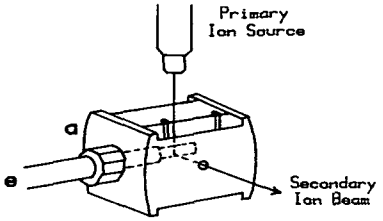
In an effort to understand more fully the design considerations for an instrument capable of both these types of experiments, we incorporated a sputter source and copper probe in the existing hardware of the HP 5985B mass spectrometer in our laboratory, as shown in Figure 1. The current density of the primary beam at the sample surface was estimated by examining the interference fringes obtained by sputtering known thicknesses of Ta_2O_5. Control of beam shape and location was aided by visual observation of beam phosphorescence on ZnS. The effect of neutrals on background noise for line-of-sight geometries was investigated by comparing signals obtained from materials of widely different neutral sputter yields. The effect of lens potentials and minor changes in lens design on collection efficiency for secondaries was also studied, including the interaction between the probe potential and the Einzel lens and between the probe and the quadrupole z-axis potential.

As most other laboratories have reported, we find that this sort of crude modification of existing hardware provides a system with which spectra from pre-formed ions in a liquid matrix can easily be obtained (see Figure 2). As might be expected, however, we find considerable pyrolysis of the sample at high current density, as evidenced by the high intensity of ions below m/e 60. The abundant mass-independent noise visible in the spectra can in part be traced to the neutrals and photons produced in abundance in the sputtering process. Decrease in current density to a level low enough not to damage the surface results in secondary count rates too low to measure with analogue detection. In addition, the use of a primary ion beam instead of a neutral beam causes charging with insulating samples, reducing the escape of secondary ions from the surface. From comparable experiments performed in our laboratory on a SIMS instrument with a mass range limited to 250 amu but which employs good secondary ion optics, an electron beam for charge neutralization, and pulse counting detection, we conclude that the incorporation of these features with an ion gun and sample holder on an organic mass spectrometer would extend the capabilities of analytical SIMS instruments to include direct surface analysis of solid surfaces.

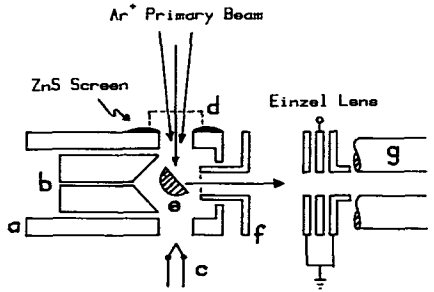
References

[1] M. Barber, R. S. Bordoli, G. J. Elliott, R. D. Sedgwick, and A. N. Tyler, Anal. Chem., 54, 645A (1982).
[2] D. F. Hunt, W. M. Bone, J. Shabanowitz, J. Rhodes, and J. M. Ballard, Anal. Chem., 53, 1704 (1981).
[3] A. Benninghoven, Surf. Sci., 53, 596 (1975).
[4] R. J. Colton, J. Vac. Sci. Technol., 18, 737 (1981).
[5] R. J. Day, S. E. Unger, and R. G. Cooks, Anal. Chem., 52, 557A (1980).

FIGURE 1: VIEWS OF HP 5985B STANDARD EI/CI SOURCE MODIFIED FOR ORGANIC SIMS

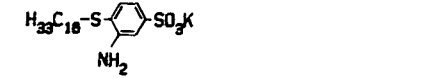


A. SIMPLIFIED PERSPECTIVE VIEW



B. SIDE VIEW

Legend:
- a source block
- b repeller
- c filament
- d electron trap
- e SIMS sample probe
- f draw-out electrode
- g quadrupole rods



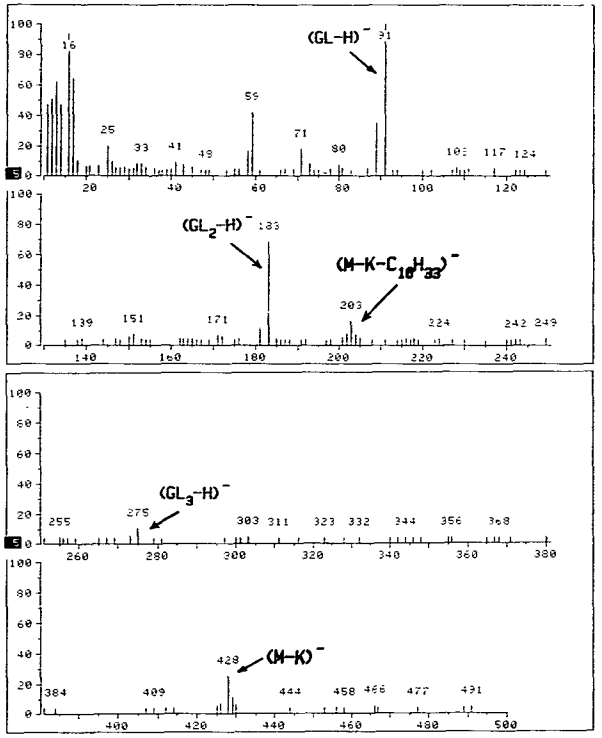


FIGURE 2: NEGATIVE SIMS SPECTRUM OF POTASSIUM HEXADECYLTHIOMETANILATE

A SIMPLE METHOD FOR OBTAINING SIMS (FAB) SPECTRA OF ORGANICS

C. N. McEwen
Central Research and Development Dept.
E. I. du Pont de Nemours and Co.
Wilmington, Delaware 19898

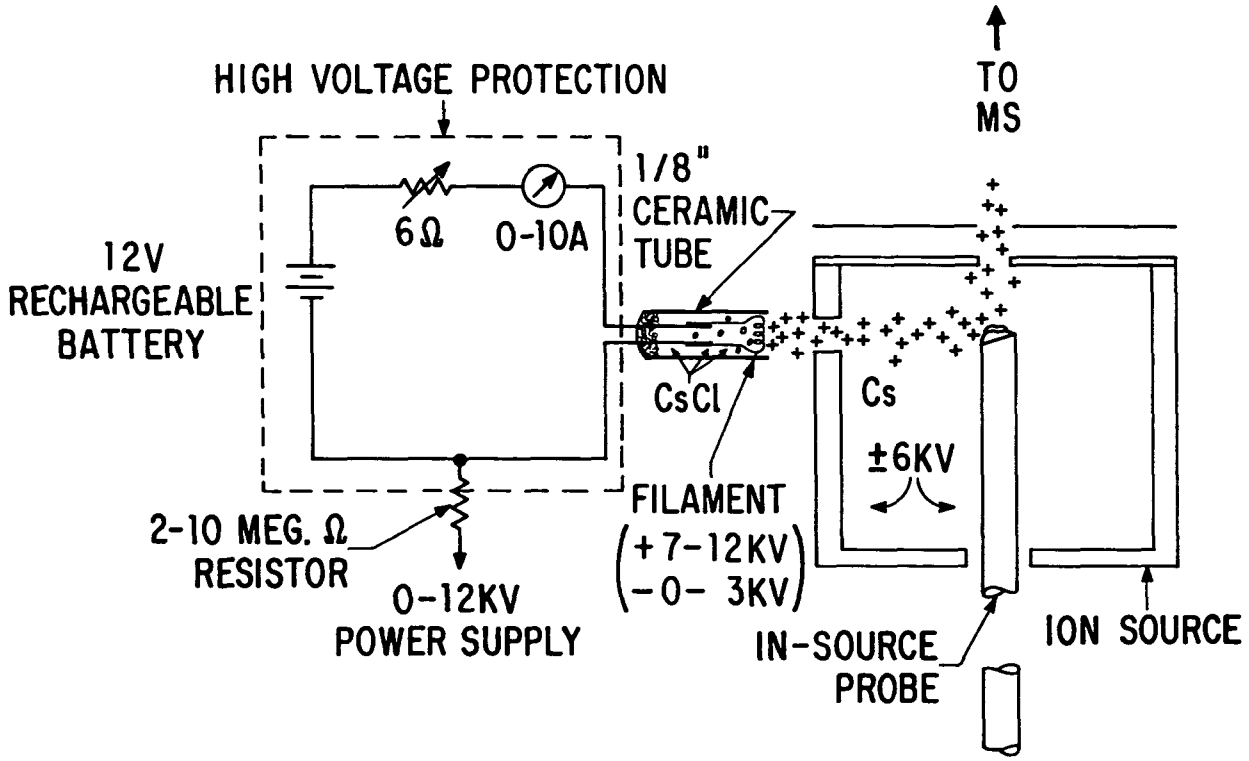
Cesium ion bombardment using a source mounted cesium ion gun has been used to obtain mass spectra virtually identical in intensity and mass spectral pattern to spectra obtained using fast atom bombardment (FAB). For example, the spectrum of the nonapeptide bradykinin obtained by Cs^+ bombardment using a VG-ZAB mass spectrometer was nearly identical to the published FAB spectrum of this compound[1]. Comparison of spectra from several compounds obtained on the same mass spectrometer using Ar° FAB (see paper WPB 14 by M. A. Rudat) and Cs^+ bombardment showed as the only difference in the spectra enhanced high mass intensity using Cs^+. It is expected that Xe° FAB will produce spectra essentially identical to Cs^+ sputtered ion spectra. In all cases, glycerol was used as the matrix and sample charging was not observed.

The cesium ion gun is shown in the figure. It is made from a 1" by 1/8" OD ceramic tube containing a tungsten filament spotwelded at both ends to heavier wire leads. The filament is coiled at one end of the tube and the other end of the tube is sealed (we use Sauereisen #8 electro-temp. cement). The tube is loaded with 100µl of a concentrated CsCl solution (KCl also works well) and dried.

The filament is heated using power from a rechargeable 12V battery. (Note: the battery and accessories float at high voltage and must be encased in an insulating box.) The heat from the filament warms the ceramic tube and lead wires causing the CsCl to evaporate and pass through the red hot filament coils. Cs^+ ions are produced when CsCl comes in contact with the hot filament. Because the filament is biased several KV positive with respect to the source, the Cs^+ ions are accelerated into the source. Positive or negative sputtered ion mass spectra can be obtained from compounds dissolved in a suitable liquid matrix and inserted into the ion beam as shown in the figure.

---

1) M. Barber, R. S. Bardoli, R. D. Sedgwick, A. N. Tyler, and E. T. Whalley, Biomed. Mass Spectrom. 8, 337 (1981).


HIGH VOLTAGE PROTECTION
TO MS
1/8" CERAMIC TUBE
6Ω
0-10A
12V RECHARGEABLE BATTERY
CsCl
Cs
±6KV
FILAMENT (+7-12KV -0- 3KV)
2-10 MEG. Ω RESISTOR
0-12KV POWER SUPPLY
IN-SOURCE PROBE
ION SOURCE

MOLECULAR ION DISTRIBUTIONS OF MIDDLE MOLECULES. J. Yergey, G. Hansen, D. Heller, C. Fenselau and R. Cotter, Deptartment of Pharmacology, Johns Hopkins School of Medicine, Baltimore, Maryland 21205.

For compounds of high molecular weight the molecular ions appear in the mass spectra as a group of many isotopic peaks, which may be displaced several mass units from the nominal mass. The monoisotopic mass may no longer be the most abundant, and when the molecular weight is high enough may no longer be visible. In such cases, the average mass of the entir peak group may take on new importance.

A computer program, designed especially to deal with the larger number of isotopic configurations, has been used to generate theoretical distribution profiles of compounds in the 1,000 10,000 and 100,000 M.W. range, having formulae which provide a variety of mass defects. Nominal, mononisotopic, and average mass are included with an output listing of exact masses, relative abundances, and a plot of these abundances. An expanded listing of every peak includes the individual contributions at each nominal mass, resulting from different isotopic contributions.

In the 1,000 to 3,000 amu range mass defect becomes noticeable for most compounds, but may be somewhat offset when elements with both positive and negative mass defects are contained in the molecule. The monoisotopic mass is usually still visible in this range, and sometimes still the most abundant peak (Figure 1a). The overall shape of the peak envelopr remains non-symmetrcal, but is far wider than experienced below 1,000 amu.

By 10,000 amu mass defect becomes very significant for most compounds, shifting the peak envelope several mass units from the nominal mass (Figure 1b). The monoisotopic mass is usually not the most abundant mass, and quite often not visible. This fact becomes important in accurate mass determinations and calculations of elemental composition. Peak shape becomes relatively symmetrical, and the average and most abundant masses converge. Overall peak envelope width becomes large and relatively independent of the molecule, except for compounds which contain a large number of atoms of a monoisotopic element.

In the 100,000 amu region the monoisotopic mass is invisible for almost all compounds, and therfore becomes somewhat meaningless. Peak shape is extremely symmetrical, and very wide for most compounds (Figure 1c). Individual peaks at unit resolution (R=100,000) are comprised of many isotopic isobars.

Molecular weight assignments at higher masses cannot be accomplished using the monoisotopic mass as is routinely done below 1,000 amu. The situation is complicated by the fact that the most abundant mass is offset from the monoisotopic mass by an unknown number of mass units, and comprised of a number of isotopic isobars which require very high resolution to deconvolute (Table I).

Calculating the average mass, or molecular ion envelope centroid, has been used by other workers to determine molecular weights in situations where unit resolution was not achieved (1). This approach also seems appropriate when unit resolution is attainable, if the monoisotopic mass is no longer clearly distinguishable. It should be noted that there will be many possible and plausible elemental combinations at higher masses which have the same average mass, making the assignment of a unique empirical formula nearly impossible.

As advances in analyzers and ionization allow us to work readily in unit resolution above 3000 amu, new approaches are needed to interpret such spectra. Abundances of monoisotopic ions become vanishingly low, a multiplicity of isotopic isobars contributes to a single mass number, and no individual peak will always be distinctly the most intense in a molecular ion distribution.

We suggest that average masses be calculated with the best accuracy possible, and that theoretical ion distributions for the molecular ion envelopes be exploited to assign and confirm molecular weights.

(1) MacFarlane, R. D. and Torgerson, D. F. Intern. J. Mass Spectrom. Ion Phys. 1976,21,81-92.

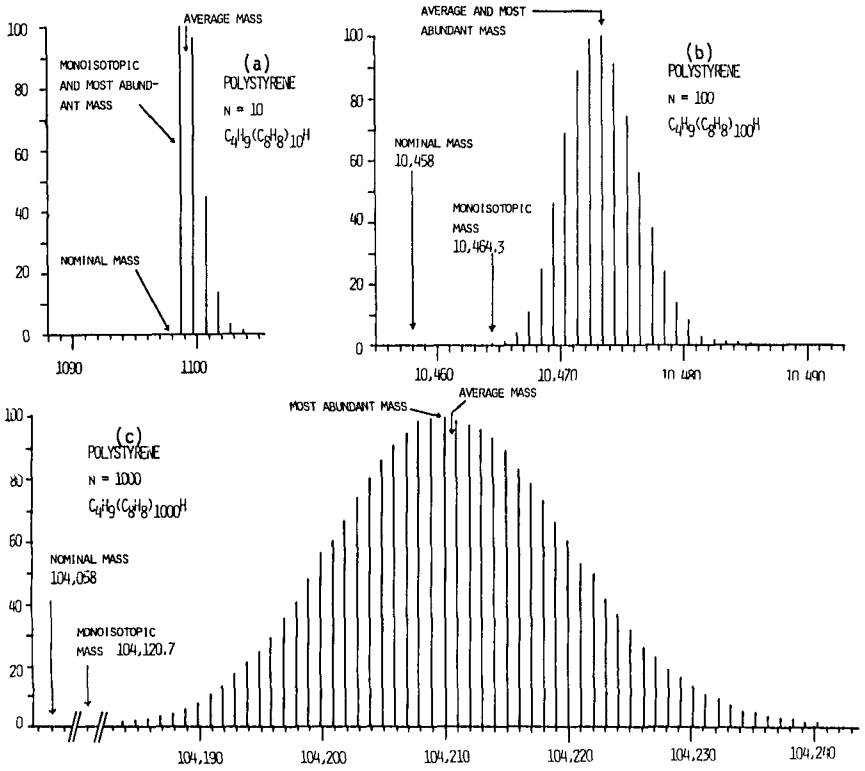


FIGURE 1. Theoretical molecular ion distributions for polystyrene.

TABLE I. Most abundant peak for Glucagon n=3.

FORMULA $C_{459}H_{677}N_{126}O_{150}S_3$	MASS	% COMPOSITION OF TH MOST ABUNDANT PEAK
3 C-13, 1 N-15, 1 S-34	10,450 80	1 95
2 C-13, 1 O-18, 1 S-34	10, 450. 80	0 76
3 C-13, 3 N-15	10, 450. 80	0 51
4 C-13, 1 S-34	10, 450 80	5. 37
4 C-13, 1 N-15, 1 S-33	10, 450 80	0. 45
2 C-13, 2 N-15, 1 O-18	10, 450 81	0. 60
4 C-13, 2 N-15	10, 450 81	4 28
3 C-13, 1 N-15, 1 O-18	10, 450. 81	4. 48
3 C-13, 1 H-2, 1 S-34	10, 450. 81	0. 42
4 C-13, 1 N-15, 1 O-17	10, 450 81	1 05
5 C-13, 1 S-33	10, 450. 81	0 98
5 C-13, 1 N-15	10, 450. 81	19 00
2 C-13, 2 O-18	10, 450 82	0 86
4 C-13, 1 O-18	10, 450. 82	12 35
4 C-13, 1 H-2, 1 N-15	10, 450 82	1 87
3 C-13, 1 O-17, 1 O-18	10, 450 82	0. 54
5 C-13, 1 O-17	10, 450 82	2 31
6 C-13	10, 450 82	34. 74
3 C-13, 1 H-2, 1 O-18	10, 450 82	0. 97
5 C-13, 1 H-2	10, 450. 82	4. 11

MASS CALIBRATION IN FABMS: AN EVALUATION OF CALIBRATION COMPOUNDS SUITABLE FOR ACCURATE MASS MEASUREMENT FOR SPECTRA RECORDED ON PHOTOPLATES

A. Van Langenhove, C.E. Costello, H.-F. Chen, J.E. Biller and K. Biemann

Department of Chemistry
Massachusetts Institute of Technology
Cambridge, MA 02139

Mass spectrometric analysis of samples by fast atom bombardment is routinely carried out by dissolving the sample in glycerol before its introduction in the mass spectrometer. This glycerol matrix produces a strong background spectrum which, in low resolution mass spectrometry, can be used to advantage by serving as a mass reference.

We have found that the glycerol spectrum can also be used successfully for the calibration of high resolution spectra recorded on photoplates. We have created a glycerol reference file consisting of six different groups of cluster ions up to m/z 1013, spaced 92 amu apart (see Table 1; glycerol=G=$C_3H_8O_3$, 92.0473 amu). Accurate mass assignments of the glycerol lines was done in part by peak matching against known reference substances, and in part by photoplate measurements using only the easily recognizable series of the abundant ions $(C_3H_8O_3)_nH^+$ as reference masses.

For photoplate spectra with strong glycerol lines, extrapolation between the glycerol reference lines did not create any problems. For example, in the case of Leu-Enkephalin (H-Tyr-Gly-Gly-Phe-Leu-OH) at a resolution of 10,000, the protonated molecular ion was correctly determined as $C_{28}H_{38}N_5O_7$ (obs. m/z 556.2769; calc. m/z 556.2771; Δmmu=-0.2), and the assignment of the major fragment ions of this molecule confirmed fragmentations (e.g. 1-3) previously reported and based solely on unit resolution FAB spectra. Table 2 lists the sequence determining ions due to cleavage of the CO-NH bond. Also, additional information was obtained by the observation of doublets, e.g. at m/z 177 ($C_9H_9N_2O_2$ and $C_{10}H_{13}N_2O$) and m/z 262 ($C_{13}H_{16}N_3O_3$ and $C_{15}H_{20}NO_3$) and previously unassigned ions, e.g. at m/z 540 ($C_{28}H_{36}N_4O_7$) and m/z 541 ($C_{28}H_{37}N_4O_7$).

Since at a resolution of 10,000 some interference of strong glycerol lines with weak sample lines still can occur (see e.g. at m/z 221, Table 2), exposures with weak glycerol lines would in these cases be preferred. However, where the glycerol lines are weak, extrapolation is difficult because the reference lines are spaced far apart. We therefore evaluated the use of calibration data from a strong glycerol spectrum exposed in the adjacent track of the photoplate. We found that the line positions did not change significantly between consecutive exposures (i.e. neither the magnetic nor the electric fields drifted significantly) even though the sample holder had to be withdrawn and reinserted between exposures. Accurate mass measurements were then obtained by adding the positions of the reference lines in the strong glycerol spectrum to the positions of all the lines in the weaker glycerol and sample spectrum. An example of data obtained in this way is shown in Figure 1.

As an alternative to calibration with glycerol, calibration with overlaid EI Fomblin® was evaluated. This approach had previously been shown useful for calibration of FD spectra (4). Accurate mass measurements were achieved by this technique (see Figure 2). However, the hot filament causes the ion source temperature to rise somewhat during the recording of the EI spectrum and this approach is, therefore, less convenient than the FAB reference approach.

The same procedure (reference lines in one track, compound lines in the adjacent one) should be extendable to higher masses using mixtures of phosphazenes as the reference lines.

REFERENCES

1. Barber, M., Bordoli, R.S., Garner, G.V., Gordon, D.B., Sedgwick, R.D., Tetler, D.W. and Tyler, A.N., Biochem. J. 197, 401-404 (1981).
2. Barber, M., Bordoli, R.S., Sedgwick, R.D. and Tyler, A.N., Nature 293, 270-275 (1981).
3. Williams, D.H., Bradley, C.V., Santikarn, S. and Bojesen, C., Biochem. J. 201, 105-117 (1982).
4. Costello, C.E., Carr, S.A., Mancuso, N.R. and Biemann, K. "Use of Complete Field Desorption Mass Spectra for Structural Studies in Biological Chemistry", 1979 ASMS meeting, Paper No. MAM088.

TABLE 1. REFERENCE FILE OF GLYCEROL (G) CLUSTER IONS

	El. Comp.	m/z		El. Comp.	m/z		
1.	$C_3H_9O_3$	93.0552	(+G)	$C_6H_{17}O_6$	185.1025	(+G)	.....
2.	$C_4H_9O_3$	105.0552	(+G)	$C_7H_{17}O_6$	197.1025		
3.	$C_4H_{11}O_4$	123.0658	(+G)	$C_7H_{19}O_7$	215.1132		
4.	$C_6H_{11}O_3$	131.0709	(+G)	$C_9H_{19}O_6$	223.1182		
5.	$C_6H_{13}O_4$	149.0814	(+G)	$C_9H_{21}O_7$	241.1288		
6.	$C_6H_{15}O_5$	167.0920	(+G)	$C_9H_{23}O_8$	259.1394		

TABLE 2. Leu-Enkephalin· ACCURATE MASS ASSIGNMENTS OF THE SERIES OF SEQUENCE IONS PRODUCED BY CO-NH CLEAVAGE.

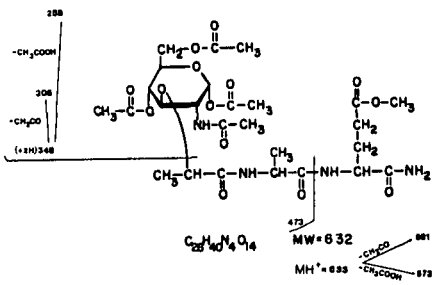
A. CHARGE RETENTION ON THE C-TERMINAL FRAGMENT

Obs. m/z	Calc. m/z	Δ,mmu	El.Comp.
393.2150	293.2138	+ 1.2	$C_{19}H_{29}N_4O_5$
336.1925	336.1923	+ 0.2	$C_{17}H_{26}N_3O_4$
279.1679	279.1709	- 3.0	$C_{15}H_{23}N_2O_3$

B. CHARGE RETENTION ON THE N-TERMINAL FRAGMENT

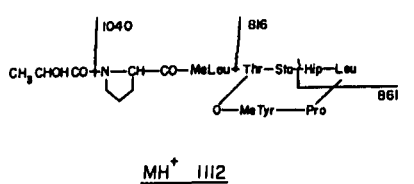
Obs. m/z	Calc. m/z	Δ,mmu	El.Comp.
425.1832	425.1825	+ 0.7	$C_{22}H_{25}N_4O_5$
278.1141	278.1141	0.0	$C_{13}H_{16}N_3O_4$
221.0971*	221.0926	+ 4.5	$C_{11}H_{13}N_2O_3$

*Glycerol line at m/z 221.1025 interfering (at Res.=10,000).



OBSERVED m/z	CALCULATED m/z	EL. COMP.	Δ, mmu
288.1079	288.1084	$C_{12}H_{18}NO_7$	-0.5
306.1200	306.1190	$C_{12}H_{20}NO_8$	+1.0
348.1283	348.1295	$C_{14}H_{22}NO_9$	-1.2
473.1801	473.1772	$C_{20}H_{29}N_2O_{11}$	+2.9
573.2432	573.2408	$C_{24}H_{37}N_4O_{12}$	+2.4
591.2552	591.2514	$C_{24}H_{39}N_4O_{13}$	+3.8
633.2596	633.2620	$C_{26}H_{41}N_4O_{14}$	-2.4

Fig. 1. An example of accurate mass measurements obtained by FAB(+)MS calibration using an adjacent glycerol exposure for reference lines.



OBSERVED m/z	CALCULATED m/z	EL. COMP.	Δ, mmu
1112.6437	1112.6495	$C_{57}H_{90}N_7O_{15}$	-5.8
1040.6255	1040.6283	$C_{54}H_{86}N_7O_{13}$	-2.8
861.4932	861.4973	$C_{43}H_{69}N_6O_{12}$	-4.1
816.4748	816.4759	$C_{42}H_{66}N_5O_{11}$	-1.1

Fig. 2. An example of accurate mass measurements obtained by FAB(+)MS calibration with overlaid EI Fomblin.

HIGH RESOLUTION AND ACCURATE MASS MEASUREMENTS USING FAST ATOM BOMBARDMENT;

D. HELLER, G. HANSEN, J. YERGEY, R. J. COTTER AND C. FENSELAU; **Middle Atlantic Mass Spectrometry Facility; Johns Hopkins U.; Baltimore, MD**

OBJECTIVE

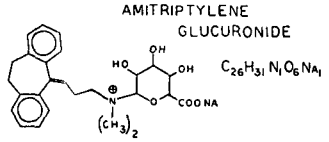
TO EXPLORE ACCURATE MASS MEASUREMENT BY FAST ATOM BOMBARDMENT; high ion current with low energy spread

NARROW RANGE VOLTAGE SCANNING:

SCANS SUMMED BY SOFTWARE MULTICHANNEL ANALYZER

3000

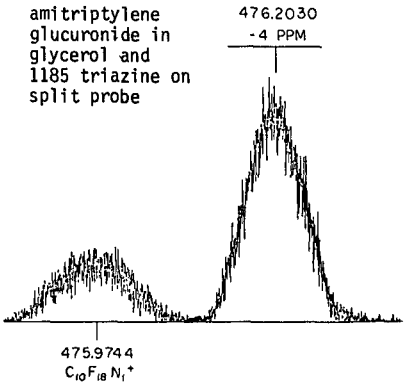
AMITRIPTYLENE GLUCURONIDE

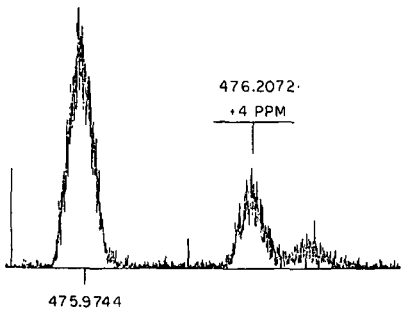


$C_{26}H_{31}N_1O_6Na_1$

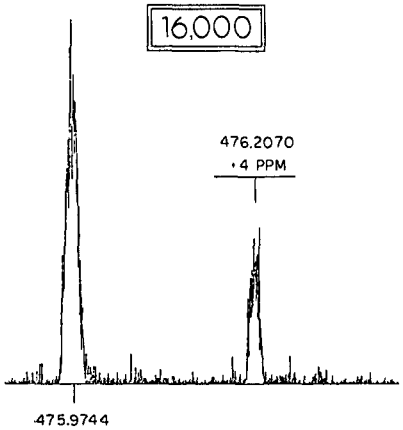
8000

amitriptylene glucuronide in glycerol and 1185 triazine on split probe

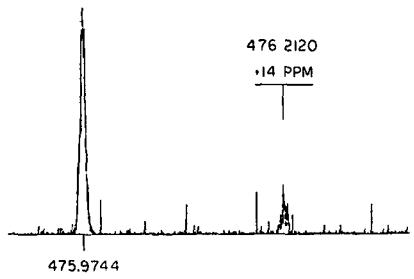




16,000



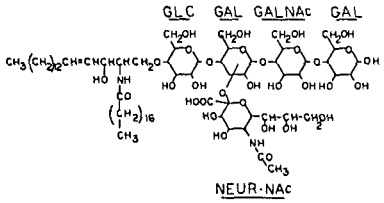
30,000



VOLTAGE JUMPING (PEAK MATCHING)

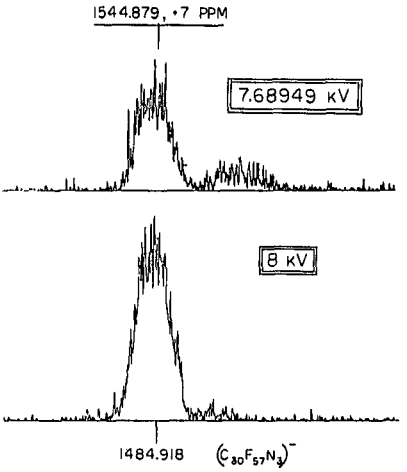
COMPUTER ACQUIRED RAW DATA

Ganglioside GD1 in triethanolamine and 1485 triazine on split probe; negative ion mode



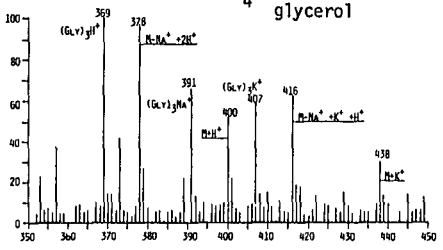
GANGLIOSIDE GD1

$C_{73}H_{131}N_3O_{31}$

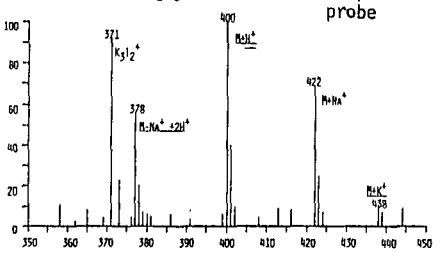


WHY WE USE A SPLIT PROBE

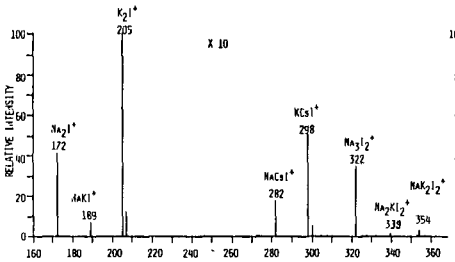
7-Me Guanosine Mono-PO_4 and KI mixed in glycerol



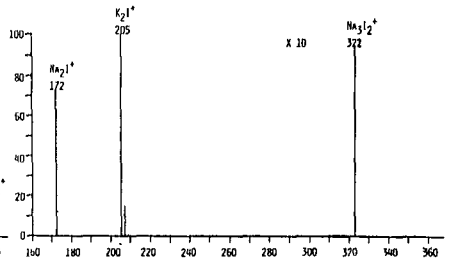
7-Me GMP in glycerol and KI on split probe



NaI, Ki and CsI mixed on single probe



NaI, KI and CsI on three ribbon probe



CONCLUSIONS

HIGH RESOLUTION MEASUREMENTS CAN BE MADE IN FAST ATOM BOMBARDMENT.

ACCURATE MASS MEASUREMENTS CAN BE MADE IN FAST ATOM BOMBARDMENT.

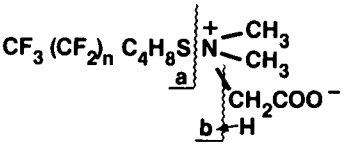
APPROACHES TO ACCURATE MASS DETERMINATION IN FABMS

J. L. Occolowitz and P. W. Landis, Lilly Research Laboratories
Indianapolis, IN, U.S.A. 46285

Mass measurements at a resolution of 15,000 using a modified Finnigan-MAT 731 mass spectrometer showed that FABMS was capable of attaining an accuracy at least as good as that using EIMS (~ 1 ppm). For peaks of moderate intensity this accuracy could be obtained if the standard and sample were in the same glycerol matrix. However, having sample and standard in the same matrix often created the following problems:

1. The standard suppressed the sample spectrum or vice versa,
2. In ternary or quarternary mixtures, i.e., those containing a proton source such as oxalic acid, a precipitate formed, and
3. Mass standards such as fomblins and phosphazenes, which are suitable for EIMS and FDMS, were not suitable for use in glycerol. They did, however, yield good FAB spectra if used neat.

Design of a routine method of accurate mass measurement required finding an internal standard which did not create the problems enumerated above, or development of a split target geometry which would separate standard and sample. The search for a suitable internal standard has been successful over a limited mass range. The amphoteric surfactant Zonyl FSB®

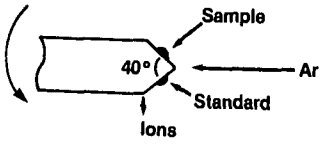


n = 3,5,7,9

as a 0.2 percent solution in glycerol was useful over a mass range of m/z 277 to 780 for peak matching with a 10 percent maximum mass separation between standard and sample. The [M + H] peaks plus the peaks resulting from the fragmentations "a" and "b" provided the requisite mass standards. It is likely that analogs of Zonyl FSB could be used for other mass ranges.

Split targets, where sample and standard were placed on adjacent areas and observed simultaneously, proved unsatisfactory. Although the separation of sample and standard did not exceed several tenths of a mm, different focusing conditions were observed for each. Additionally, when a compromise focus was achieved, peak matching gave unacceptable errors.

Following a suggestion of Dr. C. Brunee, Finnigan-MAT, Bremen, we examined a rotatable target for mass measurement. The principle of the target is illustrated below.



At a resolution of 25,000 with glycerol on both target faces, no peak shift was observed when ions were generated from either face. With Ultramark on both faces, the mass of the ions at m/z 1521 derived from one face was determined within 2.1 mMU using ions at m/z 1470 derived from the other face. The rotatable probe has been used routinely and has measured the mass peptides up to m/z 1350 with accuracies generally between 1-2 ppm.

Currently the probe is rotated manually. A stepping motor drive is being constructed to rotate the probe in phase with the peak matching unit.

The probe is potentially useful for accurate mass determination using photoplates. Successive exposures from both faces without moving the plate would supply superimposed spectra suitable for mass measurement.

® Registered Dupont

FAST ATOM BOMBARDMENT AS AN IONIZATION TECHNIQUE: SENSITIVITY AND APPLICABILITY STUDIES

Mark E. Hemling, J. Carter Cook, Jr., Kenneth L. Rinehart, Jr., and Keith L. Olson; School of Chemical Sciences, University of Illinois, Urbana, IL 61801

Fast atom bombardment (FAB) has quickly evolved as a useful ionization technique for non-volatile, thermally labile compounds (1-6). Field desorption (FD) had previously been the method of choice for many of these compounds despite the difficulty of the technique and the transient nature of the signal produced. Claims of high pseudo-molecular ion sensitivity and the applicability of FAB to any molecule suitable for FD (1) have spurred interest in the analysis of such molecules in many laboratories. We address the question of sensitivity in a quantitative manner and also present some data about the applicability of FAB *vis-a-vis* FD.

FD sensitivity was previously reported (7) as coulombs/nanogram for the molecular or pseudo-molecular ion, M^+ or $(M+H)^+$, and previously unreported data were also available expressed as coulombs/mole (8). In the present work we determined static ion currents after three minutes of fast atom bombardment for the pseudo-molecular ion, since $(M+H)^+$ is typically the base peak in the glycerol-corrected spectrum. Moreover, it was found that the ion current was essentially constant during the first three minutes and coulombs could, therefore, be calculated.

Progesterone and pimaricin were used as model compounds for the determination of the amount of sample consumed, since they exhibit UV absorption. Sample utilization curves follow an exponential decay and it can be determined that approximately 15% of the sample is consumed in the first three minutes. This contrasts with an earlier report (9) that sample use is negligible, allowing prolonged analysis under non-destructive conditions.

Sensitivity, in coulombs/mole, was calculated from the measured ion current and the sample consumed based on the results above, as shown below.

AMINO ACIDS AND DIPEPTIDES

COMPOUND[1]	M	I_{norm}[2,3] amps$\times 10^{-11}$	coul/mole $\times 10^{-2}$,FAB	coul/mole $\times 10^{-2}$,FD	coul/mole $\times 10^{-2}$,FAB (TIC)
GLYCINE (a)	75	2 7	14	2.1	24
PROLINE (a)	115	4 5	37	1.5	53
ASPARAGINE (a)	132	2.0	19	1.7	28
PHENYLALANINE (c)	165	7.5	88	0.020	144
GLY-LEU (c)	188	9.8	130	0.36	250
HYP-GLY (c)	188	1.4	18	1.2	23

NUCLEOSIDES

COMPOUND[1]	M	I_{norm}[2,3] amps$\times 10^{-11}$	coul/mole $\times 10^{-2}$,FAB	coul/mole $\times 10^{-2}$,FD	coul/mole $\times 10^{-2}$,FAB (TIC)
THYMIDINE (a)	242	0.33	5.8	3.6	24
CYTIDINE (a)	243	0.39	6.8		23
CYTIDINE (c)	243	0.51	8.8		30
URIDINE (c)	244	0.15	2.6	2.1	9.4

STEROIDS

COMPOUND[1]	M	I_{norm}[2,3] amps$\times 10^{-11}$	coul/mole $\times 10^{-2}$,FAB	coul/mole $\times 10^{-2}$,FD	coul/mole $\times 10^{-2}$,FAB (TIC)
β-ESTRADIOL (c)	272	0.080	1.60	2.2	5.0
TESTOSTERONE (c)	288	5 0	103	3.2	104
PROGESTERONE (c)	314	0.85	19	11	50
CORTICOSTERONE (c)	346	3.3	82	1.5	168
CHOLIC ACID (c)	408	0.032	0.94	0.098	156

ANTIBIOTICS

COMPOUND[1]	M	I_{norm}[2,3] amps$\times 10^{-11}$	coul/mole $\times 10^{-2}$,FAB	coul/mole $\times 10^{-2}$,FD	coul/mole $\times 10^{-2}$,FAB (TIC)
NEAMINE (b)	322	0 10	2.3	9 3	5.0
NEAMINE (c)	322	0 26	6.0	9.3	13
SPECTINOMYCIN (b)	332	0.083	2.0	0.021	20
CHALCOMYCIN (b)	700	0.014	0.71	0.11	35
LANKAMYCIN (b)	832	0.0050	0.30	0.021	20
TYLOSIN (b)	915	0.011	0.72	0 039	28

[1] (a) 7070, 4-8-82, (b) 311A, 4-19-82, (c) 311A, 5-23-82

[2] IN 2μL GLYCEROL

[3] NORMALIZED TO M/Z 93 PEAK OF GLYCEROL ON 5-23-82 VALUE OF $2\,6\times 10^{-10}$ A

FAB sensitivities are generally better than those for FD but seldom more than an order of magnitude. It has previously been noted (10) that the sensitivities for the two techniques appear to be the same but that spectral intensity may be increased in FAB by using larger sample loadings. Sample loadings in FD are limited to the nanogram range. Working curves determined for progesterone and two quaternary salts show that ion current may be increased by increasing the sample loading up to about 30 micrograms in several microliters of glycerol.

The FAB (TIC) sensitivities were determined by totaling all of the non-glycerol peaks in oscillographically recorded spectra. TIC sensitivities are greater than pseudo-molecular ion sensitivities by up to two orders of magnitude. The low $(M+H)^+$ sensitivity for cholic acid results from its propensity to dehydrate, losing as many as three molecules of water. The difference between $(M+H)^+$ and TIC sensitivity for the nucleosides and antibiotics results at least in part from the labile glycosidic bonds.

Over 350 samples, organic and inorganic, have been analyzed in our laboratory in the past year on three spectrometers with four ion sources. Ninety per cent of the samples were amenable to FAB analysis. Of those that did not give spectra by FAB, approximately seventy per cent yielded results by FD, indicating that FAB will probably not replace FD but will complement it. Over 90 accurate mass measurements, facilitated by the high ion intensity, have also been made employing FAB on 47 different compounds. These include both positive and negative molecular and fragment ions and are routinely performed with a multichannel signal averager(11).

(1) Barber, M., Bordoli, R. S., Sedgwick, R. D.; Tyler, A. N. J C S Chem Commun 1981, 325-327.

(2) Barber, M., Bordoli, R. S., Sedgwick, R. D., Tyler, A. N. Nature 1981, 293, 270-275

(3) Rinehart, K. L., Jr., Cook, J. C., Jr., Pandey, R. C., Lee, M. D., Schaffner, C. P., Barber, M., Bordoli, R. S., Sedgwick, R. D., Tyler, A. N., Green, B. N. Abstracts, 29th Annual Conference on Mass Spectrometry and Allied Topics, Minneapolis, MN, May 24-29, 1981, 369-370

(4) Williams, D. H., Bradley, C., Bojesen, G.; Santikarn, S., Taylor, L. C. E. J Am Chem. Soc 1981, 103, 5700-5704

(5) Rinehart, K. L., Jr., Gaudioso, L. A.; Moore, M. L., Pandey, R. C., Cook, J. C., Jr. J Am Chem Soc 1981, 103, 6517-6520.

(6) Samain, D., Cook, J. C., Jr., Rinehart, K. L., Jr. J Am Chem Soc 1982, 104, in press

(7) Olson, K. L.; Cook, J. C., Jr., Rinehart, K. L., Jr. Biomed. Mass Spectrom 1981, 1, 358-362

(8) Olson, K. L., Ph D Thesis, University of Illinois, Urbana, 1976

(9) Barber, M., Bordoli, R. S., Sedgwick, R. D., Tyler, A. N.; Whalley, E. T. Biomed Mass Spectrom 1981, 8, 337-342

(10) Morris, H. R., Dell, A., Etienne, A. T., Judkins, M., McDowell, R. A., Panico, M., Taylor, G. W. Pure Appl Chem 1982, 54, 267-279

(11) Snelling, C. R., Jr., Cook, J. C., Jr., Milberg, R. M., Rinehart, K. L., Jr. Abstracts, 29th Annual Conference on Mass Spectrometry and Allied Topics, Minneapolis, MN, May 24-29, 1981, 602-603

CHEMICAL FACTORS INFLUENCING FAB MASS SPECTROMETRY

W.M. Bone, D.F. Hunt, and J.M. Marasco, Department of Chemistry, University of Virginia, Charlottesville, Virginia 22901

The chemical factors which influence FAB mass spectra can be explained in terms of solution phase chemistry. The intensity of the protonated or deprotonated molecular ion is dependent on the acidity or basicity of the sample relative to glycerol. Compounds with very acidic functional groups yield intense anions under FAB conditions. Samples containing very basic functional groups become protonated in the glycerol and produce intense cations.

Solubility is another important factor to consider when obtaining FAB mass spectra. Sample molecules need to be soluble in the liquid matrix to ensure the production of intense sample ion peaks. Sulfolane and/or DMSO are two solvents often used to help dissolve difficult samples in the glycerol matrix.

Surfactants often yield excellent FAB mass spectra. This is perhaps due to a variety of things. Most surfactants contain either very basic or very acidic functional groups and are quite soluble in glycerol. However being surfactants they may reside primarily on the surface of the matrix where they are exposed to the primary beam and can be readily sputtered. In these cases both the functional groups present and the formation of surface films may work together in allowing these classes of compounds to be analyzed by FAB-MS.

Dodecyl, hexadecyl and octadecyl compounds contains various functional groups were analyzed by FAB-MS in both the positive ion and negative ion modes. Mixtures of the compounds were also subjected to FAB-MS and the relative ratios of PI and NI molecular ion intensities were compared. In nearly all cases the more basic compounds yielded more intense PI spectra and the more acidic compounds produced enhanced NI spectra. Indeed the molecular ion intensity can be related to the acidity or basicity of a compound in glycerol. Compounds which didn't follow this pattern often were somewhat insoluble in glycerol or were slightly volatile.

The C_{12}, C_{16} and C_{18} amines were analyzed as their primary, secondary, tertiary and quaternary derivatives (methyl substituted). In each case the quaternary ammonium compounds showed the most intense positive ions followed by the secondary amines. The primary and tertiary amines were similar in intensity with the primary amines yielding slighter greater molecular ion intensities than the tertiary amines. This is in keeping with the idea that solution phase acidity or basicity is the important concept to remember when using FAB-MS rather than gas phase acidity or basicity.

In conclusion it appears that ionization of sample molecules under FAB conditions appears to occurs in the glycerol matrix with relative abundance of positive and negative ions being related to a sample acidity or basicity compared to glycerol. Solubility of a sample in the glycerol is necessary with molecules capable of forming soluble monolayers producing very intense FAB mass spectra.

OPTIMIZATION OF EXPERIMENTAL PROCEDURES FOR FAST ATOM BOMBARDMENT MASS SPECTROMETRY

S.A. Martin, C.E. Costello and K. Biemann

Department of Chemistry
Massachusetts Institute of Technology
Cambridge, MA 02139

A systematic investigation of the experimental variables in Fast Atom Bombardment Mass Spectrometry has been undertaken in order to optimize the experimental technique especially for exact mass measurements at high resolution. Among the parameters studied have been the shape and material of the target, the nature of the ionizing gas, sample preparation, concentration and matrix. Measurements have been made in both positive and negative ion modes and both low (1000) and high (10,000) resolution. Interferences and artifacts have been identified and methods have been developed to minimize their effects. A series of recommendations for Fast Atom Bombardment mass spectral experiments is presented as the result of these studies.

A double focusing (Varian MAT 731) mass spectrometer of Mattauch-Herzog geometry with a mass range of 1-2000 amu at 8 kV accelerating potential was used for this work. The EI/FI/FD ion source was used without modifications. The MAT 731 ion source housing is equipped with ports directly opposite each other and perpendicular to the ion optical system. The Ion Tech atom gun was attached to the ion source housing via one of these ports through an adapter connecting a 69 mm OD Conflat flange which fits the atom gun to a 75 mm OD gold seal flange which fits the port on the ion source housing (Figure 1).

The sample is introduced into the EI/FI/FD combination ion source on the tip of a probe which is positioned on the end of the FD push rod. The standard probe tip is made of 303 stainless steel, SS, with $\Theta = 60°$ (Figure 2), and has a sample surface area of 5.7 mm. Table I lists a few standard sets of operating conditions for FABMS with varying neutral beams.

The standard procedure for FAB analysis was as follows. The stainless steel tip is coated with 50% v/v nitric acid for a few seconds, then rinsed with distilled water, followed by nanograde methanol and allowed to dry. The sample, usually at a concentration of 1 μg/μl, is applied with a 10 μl syringe or 5 μl graduated capillary to the sloped surface of the probe. The volumem 0.3 μl, is spread so that a thin, uniform film is visible to the unaided eye. The probe was then placed in the path of the neutral beam and the mass spectrum was recorded.

The conversion of an existing ion source, with an available vacuum port, to accommodate a FAB gun is shown to be straightforward and effective.

The material we found of the best overall performance was 303 SS, which produced the least interference and was inert to most substances. The angle of incidence of the beam with the SS tips which yielded the highest ion abundance was found to be $\Theta = 60°$ (Figure 3), at least in our instrument. Furthermore, the ion yield for the sample is related to the probe size. A plateau in sensitivity was noted with the 2.5 mm diamter tips. The ion beam spread caused by the neutral beam/sample/tip surface interaction is a factor in the absolute ion sensitivity.

The wide range of gases studied support the assumption that, of the commonly used gases, xenon was the most efficient neutral beam for the ionization of the sample on the probe tip (Figure 4).

The most important aspect of the FABMS technique is sample preparation because a number of contaminants have the property of suppressing ionization of the sample, sometimes completely (Table II). This is especially critical for those samples that have been derivatized, exposed to buffers or treated with enzymes. The sample cleanup procedure which we have found most effective consists of repeated dilution followed by lyophilzation, the use of Sep-Pak® or separation by HPLC, depending on the nature of the impurity. The most efficient method for the preparation of homogenous solutions consists of first dissolving the sample in a solvent and then adding the matrix. Furthermore, the addition of acids or bases to the sample matrix is often required to produce an observable sample spectrum above the glycerol background (Table II).

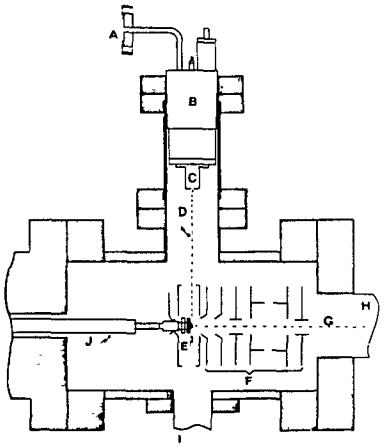


Figure 1 Schematic diagram of the MAT 731 combination EI/FI/FD ion source in the FAB configuration; (A) gas inlet; (B) FAB gun, Ion Tech Ltd ; (C) flight tube; (D) neutral beam; (E) sample probe tip; (F) ion focusing lenses; (G) ion beam; (H) analyzer; (I) direct insertion probe; (J) FD push rod

TABLE II. MATRIX-ASSOCIATED IONS OBSERVED IN FAB SPECTRA

Matrix component	Masses observed, comments
Glycerol	$(93 + (92)_x)^+$ $(91 + (92)_x)^-$
	$(Sample\ MW + 75)^+$
	$(Sample\ MW + 93 + (92)_x)^+$
Sodium	$(Sample\ MW + 23)^+$
	$(Sample\ MW + 23 + (22)_x)^+$
	$(23 + (92)_x)^+$
Potassium	(Same as sodium, 16 amu higher)
Chloride	$(Sample\ MW + 35,37)^-$
Ammonium	$(18 + (92)_x)^+$
Formic Acid	$(93 + (92)_x + (28)_{1\ or\ 2})^+$
Guanidine hydrochloride	$(93 + (92)_x + 58)^+$
Phosphate	$[93 + (92)_x + (98,99,100)^*]^+ = [93 + (92)_{x+1} + (6,7,8)^*]^+$
	*pH dependent
Diaminobutane	$(Sample\ MW + 73)^+$
Oxalic Acid	$(92)_x + 73$
Comments	
Oxalic Acid	Protonates well, oxidizes sulfur amino acids slowly on standing.
Acetic Acid, HCl(dil)	Both protonate well, do not interfere
Heptafluorobutyric Acid	Very complex pattern of interference
Ammonium Trifluoroacetate	Dilute/Lyophilize 2-3 times

TABLE I. OPERATING PARAMETERS FOR FAB/IS

$P_s^a = 8 \times 10^{-6}$ Torr, $T_s^b = 32^0$C, SEM^c Gain = 1×10^6

Gas	HT^d (KV)	LC^e (mA)	IC^f (μA)
Xenon	4 8	0.2	10 0
	5 7	0 5	20 0
	6.6	0 8	30 0
	7.3	1 1	40.0
Argon	4 8	0 2	10 0
	5 2	0 6	20 0
	5.8	1 0	30 0
	6 2	1.2	40 0

a pressure in ion source housing
b temperature in ion source housing
c secondary electron multiplier
d high voltage of 850 power supply
e limiting current of 850 power supply
f equivalent ion current of neutral beam

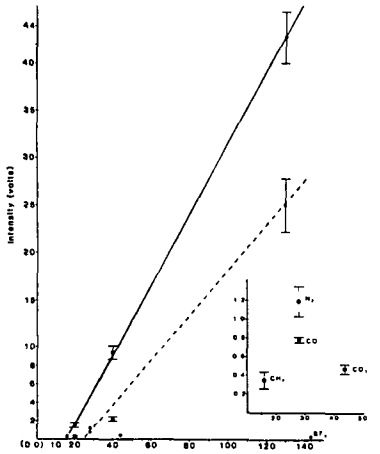


Figure 4. The ion abundance of MH^+ versus the atomic/molecular weight of the neutral beam at constant FAB gun ion current; (●) Xenon; (■) Argon; (▲) Neon; (——) Leucine enkephalin, m.w. 555; (---) Angiotensin II (Asp^1 Ala^5), m.w. 925

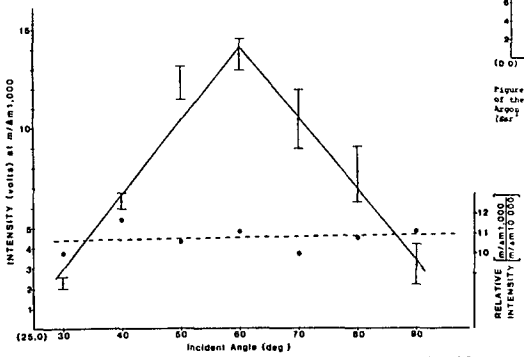
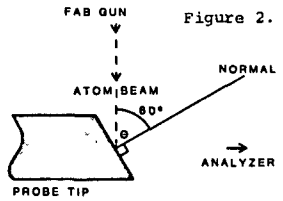


Figure 3. Relationship of sample ion abundance and incident angle of the neutral beam for a 2.5 mm diameter tip at constant ion source housing pressure and temperature and constant neutral beam flux (solid line and error bars) Dotted line: relationship of the ratio of ion intensity at low resolution (1:1,000) versus high resolution (1:10,000) and angle of incidence.

Figure 2.



KINETICS OF ION FORMATION FROM INORGANIC AND ORGANIC SALTS BY PULSED LASER IRRADIATION

B. Schueler, P. Feigl
Institut für Biophysik -Physik für Mediziner-, Th.-Stern-Kai 7, D-6000 Frankfurt/M. 70

F. R. Krueger
Max-Planck-Institut für Kernphysik, D-6900 Heidelberg, West Germany

Nonvolatile and polar compounds can be ionized by pulsed laser irradiation and the instantaneously produced ions analyzed by time-of-flight mass spectrometry. Also inorganic salts, especially alkali halides, organic salts and other compounds have been analyzed by the well known LAMMA 500® technique. In order to obtain more reproducible data suitable for thermodynamic analysis a new irradiation arrangement, LAMMA 1000® was set up by two of us.(P.F,B.S) A schematic picture of the LAMMA 1000® setup, capable of bulk surface analysis is shown in fig.1. The laser beam is focused (λ=266, 355, 532 nm, τ=10 nsec) onto the sample. The produced ions are extracted from the same side of the target and accelerated into the time-of-flight system. The spatial resolution of the analysis is about 1 µm. High resolution sample observation (num. ap. = .6 Ø=.5 µm) and selection of the target spot to be analyzed is realized by a light/dark field microscopic objective.

Typical ion types occuring from salts are the parent monomer kation and anion, but also dimers and polymers (e.g. $Cs_{n+1}J_n^+$, n=0,1,2,..) and fragments of organics. The ion yields represent the acidity and basicity of the related types in the condensed phase, as already shown by one of us (F.R.K) in the last year Minneapolis meeting. Ions resulting from gas phase reactions (electron impact, radical ions) are scarce. Gas phase born polymer ion yields should decrease, at least relatively, with increasing laser irradiance, contrary to our experimental results. Those gas phase reactions can essentially be ruled out for irradiances below 10^9 W/cm^2. For alkali halides the thermodynamic parameters are well known and are thus used to discuss the ion formation process representatively in more detail below.

One specific feature of ion generation from alkali halides is the formation of cluster ions of the type $(alk_{n+1}hal_n)^+$ and $(alk_nhal_{n+1})^-$. When assuming a quasireversible isothermal ion formation process the relative ion yields can be described in terms of ion formation free enthalpies: $Y_n = Y_o/n \exp(-\Delta H_n/RT)$, where Y_n is the yield of a cluster of order n, 1/n an entropy factor, ΔH_n the enthalpy of formation of cluster ion n, and T the temperature. Such an Arrhenius-type behaviour is indeed experimentally obtained (see fig.2). The evaporation "temperature" due to this isothermal model process can be fitted with the above linear dependence. Those "cluster temperatures" T_{cl} are typically $5\text{-}8\cdot10^3$ K. It seems noteworthy that T_{cl} remains constant for a special substance if the laser irradiance varies in the region $2\cdot E_{th}$ to $10\cdot E_{th}$. (E_{th}=: irradiance at ion detection threshold). This behaviour is analoguous to that observed in heavy ion induced desorption (HIID), where the relative yields (and line widths!) of the mass spectra ions are independent from the primary ion energy loss as observed by Dück et al. [1]

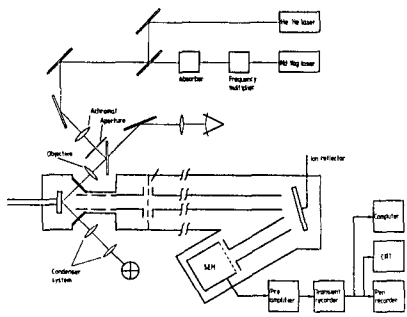


Fig.1: Schematic view of the LAMMA 1000® system

However, there are still some other consequences of this quasiisothermal model of solid evaporation: With the above "temperatures" T_{cl}~6000 K the model yields a ratio of neutral to charged particles to be produced of $Y_{no}/Y_{n+}^{cl} = \exp((\Delta H_{n+} - \Delta H_{no})/RT) \approx 10^5$, where ΔH_{no} is the enthalpy of formation for the neutral particles $(alk_nhal_n)^{no}$. The experimentally obtained ratio is $Y_o \ll 10^3 \cdot Y_+$ this corresponding to a "temperature" $T \gg 10^4$ K, which is in disagreement with a quasiisothermal ion- and neutral-formation model. On the other hand, the ions produced in the solid-gas transition have to be stable for at least some 10^{-8} sec (acceleration time) to be detected in the straight-line TOF system, but some 10^{-5} sec in the TOF reflection system, respectively. It follows from quasiequilibrium theory and experimental stability analysis

that in any case the ion excitation temperatures are lower than 10^3 K ! However, the absolute ion formation rates, not being lower than the total ion yield per laser shot duration, point again to much higher "temperatures". All these facts show that any temperature determined from a quasi-adiabatic model can only be called a pseudo-temperature. Consequently, a new, very non-adiabatic, view was adopted:

The effect of laser irradiation (and related methods of fast dissipation) can be described as probing the in-situ solid state dielectric charge (and momentum) distribution) by an electric sudden perturbation process allowing charge bearing species to leave the surface with little additional excitation.

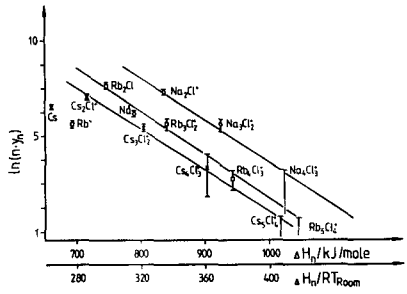


Fig.2: Alkali chloride positive ion cluster distribution. Irradiance $3 \cdot E_{th}$

Thus also a new interpretation of the cluster distribution is necessary. The slope of the line $\ln(n \cdot Y_n) = f(-\Delta H_n / RT_r)$ (T_r = specimen (e.g. room-) temperature before irradiation) provides the average number of correlated degrees of freedom (proportional to atoms n_c) around every central atom "frozen" during the very short but strong perturbation resulting from the irradiation. Typical n_c are in the order of 10 for alkali halides.

Furthermore, a dependence of the relative and absolute ion yields from the sample temperatures T_s (above T_r) before the laser irradiation is predicted. Altering the sample temperature is equivalent to an alteration of the microscopic correlation statistics. Static heating of the sample T_s=300 - 800 K before laser irradiation increases the atomic kation yield and decreases the yields of cluster ions (see fig.3) in good agreement with the model. More quantitatively one is able to say, that the correlation number defined above related to $(T_c - T_s)$ (T_c =: critical temperature near the melting point) obeys a potency function with a critical exponent as known from phase transition theory.

For complex molecules the model predicts, that for components of higher condensed phase acidity of the neutrals anions are preferred against cations and reverse for the basicity. Also clustering should be enhanced and low molecular fragment ionization hindered with lower sample temperatures. However, only minor effects should arise from the irradiance (if not higher than 10^{10} W/cm^2), wavelength and pulse duration in this limit of a high amplitude high-frequency (fast) electric perturbation. (Longer wave lengths may increase the mean n_c thus increasing clustering slightly; lower durations in the picosecond range may enhance the number of phase-correlated substructures enhancing the number of lines in the mass spectra; both is consistant with preliminary measurements.)

All these model features seem to be relevant for 252-Cf-f.f.i.d., SIMS, and FAB-MS, too. Namely, relative yields, distribution of momenta of the secondary ions should be less sensitive to the primary ion/atom property, but very sensitive to sample parameters in the condensed phase like temperature, acidity, basicity, and microscopic structure.

1) P. Dück et al., Nucl.Instr.&Meth. 168 (1980), 601

® Registered trade mark for: Leybold-Heraeus, D-5000 Köln, West Germany

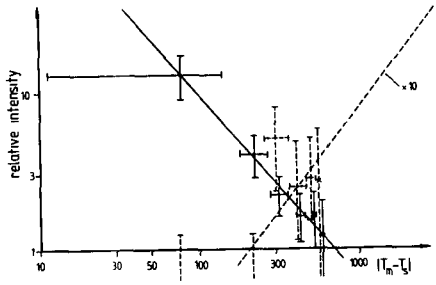


Fig.3: Atomic kation —— and cluster ion ----- yield dependence on sample temperature. $Y_{atom} = c \cdot (T_c - T)$ $Y_{cluster} = c' \cdot (T_c - T)^{-\gamma}$ $(T_c = T_m)$

WPB 26 LC-MS SYSTEM EMPLOYING THERMOSPRAY SAMPLE WITH BELT TRANSPORT AND LASER DESORPTION:

E.D. HARDIN and M.L. VESTAL; Dept. of Chem.,Univ. of Houston, Houston, TX 77004

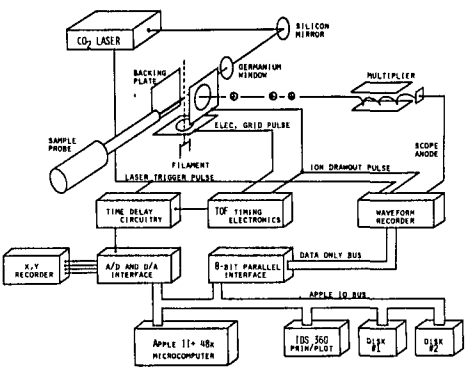
A new LC-MS system has been developed which employs a moving belt onto which the nonvolatile samples are deposited using the thermospray technique. This approach effectively vaporizes the solvent and causes nonvolatile samples to be efficiently sprayed onto the belt with no visible accumulation of liquid. Samples on the belt are transported to the ion source of a laser desorption quadrupole mass spectrometer where they are efficiently desorbed and ionizaed by the focused beam from a 30 watt Q-switched YAG laser operating at repetition rates in the kilohertz range. Differentially pumped chambers between the vaporizer and the ionizer allow operation with both aqueous and nonaqueous mobile phases at flow rates up to at least 2 ml/min. A gated boxcar integrator is used to process the pulsed ion signal, and with the use of the high pulse rates possible with the new laser, mass scan rates of several hundred amu/sec can easily be achieved using the standard quadrupole electronics and conventional data system. Data on the performance of this system are presented and the results are compared with other recently developed techniques for LC/MS interfacing.

LASER DESORPTION MASS SPECTROMETRY

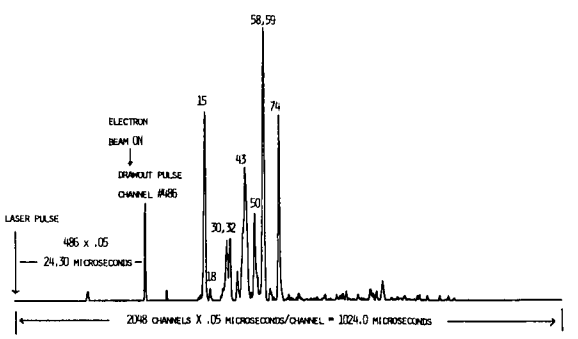
Robert J. Cotter, Richard VanBreemen, and Mark Snow
Department of Pharmacology, The Johns Hopkins University
Baltimore, Maryland 21205 USA

INTRODUCTION: A laser desorption mass spectrometer has been developed to study the details of the desorption process, in particular:
(1) to examine the competition between the desorption of ions, neutrals, clusters and pyrolysis prducts
(2) to evaluate the thermal model for the laser desorption of preformed ions.

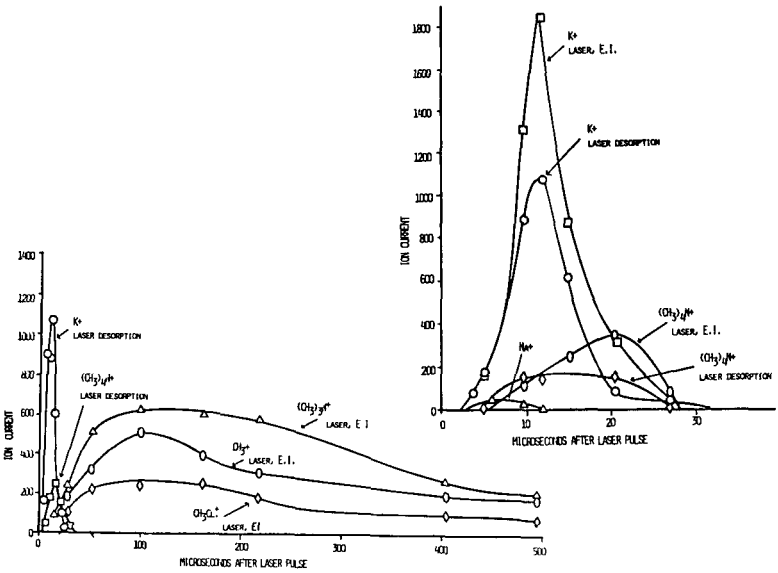
METHOD: LASER DESORPTION (LD) to examine the ions desorbed
LASER DESORPTION/ELECTRON IMPACT (LEI) to also observe the neutrals
TIME RESOLVED LASER DESORPTION (TLD) to observe competing processes which take place with different reaction rates, by variation of the time delay between the LASER PULSE, the ELECTRON BEAM PULSE, and the ION DRAWOUT PULSE.



INSTRUMENTAL: A block diagram of the laser/time-of-flight system is shown in FIGURE 1. Either the ion drawout pulse or the laser trigger pulse may be used to trigger the waveform recording of the mass spectrum. If the latter is used, the record will also indicate the time delay (FIGURE 2).



RESULTS: Tetramethyl ammonium chloride is generally considered a thermally labile compound which, upon heating, decomposes to the tertiary amine, $(CH_3)_3N$. However, other studies have shown that neutral clusters $(CH_3)_4N^+Cl^-)_n$ are also vaporized, and that quaternary ammonium compounds are also an excellent source of "preformed" ions. The competition between these processes was studied using time resolved LD and LEI mass spectrometry (FIGURES 3 and 4).



CONCLUSIONS:

(1) Kistemaker et.al.(1) have described a thermal model in which the substrate absorbs the laser power, reaches maximum temperature very quickly, but cools down more slowly as it transfers heat to the sample and to the surroundings. This can be seen by the order in which alkali and preformed ions are desorbed:

(2) The competing processes observed in other thermal techniques can be resolved:

REFERENCES.

(1) G.J.Q. van der Peyl, J. Haverkamp and P.G. Kistemaker, Int. J. Mass Spectrom Ion Phys , 42, (1982) 125

(2) R. Stoll and F.W. Rollgen, J. Chem Soc , Chem Commun. 789 (1980)

(3) R J Cotter and A.L. Yergey, J Am. Chem. Soc , 103 (1981) 1596

(4) G.D Daves, Jr., et. al. Anal. Chem , 53 (1981) 304

WPB 28 MIXTURE ANALYSIS BY MULTIPHOTON IONIZATION MASS SPECTROMETRY. D. M. Rider, J. Durant, S. Anderson, and R. N. Zare; Department of Chemistry, Stanford Univ., Stanford, CA 94305

Multiphoton ionization rates depend strongly on the optical absorption spectrum of a compound. Thus, mass spectra of individual components of a mixture can be recorded by selectively ionizing compounds at their characteristic absorption features. The analysis is carried out using a Nd:YAG pumped dye laser in conjunction with a time-of-flight mass spectrometer. The samples are introduced into the ion source with a pulsed nozzle. The supersonic expansion from the nozzle cools the molecules to below 50°K, thus greatly simplifying their absorption spectrum. This simplification increases the selectivity of MPI and aids in the identification of a compound. Results will be presented for phosphonates and aromatic hydrocarbons.

Support of the Army Research Office (DAAG-29-80-K-0097) is gratefully acknowledged.

Mass Spectrometry of Aromatic Molecules with Resonance Enhanced MPI

David M. Lubman and Mel N. Kronick
Quanta-Ray, Inc.
Mountain View, CA 94043

In this presentation we report the use of resonance enhanced laser multiphoton ionization as an ionization source for mass spectrometry. The technique of multiphoton ionization (MPI) has many attributes which make it potentially useful in performing chemical analysis. The MPI technique is a very efficient means of ionization, allowing in the best case 100% of the molecules to be ionized. Further, MPI enables one to obtain soft ionization of molecules with high efficiency. Soft ionization implies ionizing a molecule and obtaining only the molecular ion. With electron beam ionization soft ionization can be achieved only with a significant decrease in ionization efficiency. In the case of MPI, the fragmentation can be adjusted to provide the parent ion or ion fragments by simply adjusting the laser power. Extensive fragmentation can occur as the power density is increased.

The truly unique and most important property of MPI as compared to other means of ionization is the wavelength selectivity of the technique. When MPI occurs through a real resonant intermediate state the process is resonantly enhanced. Thus, the ionization spectrum will reflect the spectrum of this state. Since the MPI process creates ions, the compounds can be mass identified in a mass spectrometer. Thus, the laser can be used as a real-time means of achieving spectral selection of a compound prior to mass analysis. Thus, we can obtain a 3-parameter identification of a molecule where the three parameters are mass, intensity and wavelength. In the first class of experiments performed we demonstrate the effect of wavelength and power on the MPI of molecules in thermal beams. Valuable analytical features of such ionization processes are discussed for a variety of compounds which can be ionized by the absorption of 2 photons. In particular we demonstrate the efficient soft ionization of a large number of polyaromatic hydrocarbons.

Most large polyaromatic molecules have broad, unresolvable spectra at room temperature. We therefore have used a supersonic expansion of a sample molecule in an inert carrier gas, i.e. He, in order to simplify the spectra by "freezing-out" many of the vibrational and rotational modes. Thus, molecules may be identified on the basis their unique spectra, just as molecules are identified by IR fingerprinting. This procedure, when used in conjunction with a TOF mass spectrometer, is analogous

to GC-MS. The tunable laser becomes the means of separation. A three-dimensional analysis of 4 molecules in a TOF mass spectrometer is shown in Figure 1. In addition, we have been able to discriminate the isomers azulene and naphthalene in a cooled beam using their unique MPI spectra in the near UV.

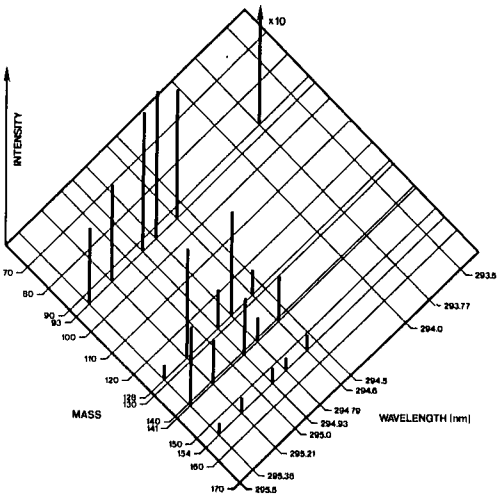


fig. 1

Three dimensional plot of a mixture of aniline, naphthalene, methylnaphthalene, and dimethylnaphthalene using the LMS technique.

ROA 1 THE (^{252}CF-PDMS, SIMS, LD, FAB) OF THIN FILMS OF BIOMOLECULES-CONDENSED STATE CHEMISTRY IN THE HIGH ENERGY-SHORT TIME DOMAIN; R. D. Macfarlane, Texas A&M University, College Station, TX 77843

It is now recognized that the new surface ionization techniques applied to organic molecules (^{252}Cf-PDMS, organic SIMS, LD, and FAB) produce essentially the same kind of mass spectra for involatile biomolecules. This implies that in the mechanism for ion formation there must be some similarities even though the primary energy depostition processes are quite different. In this review, an attempt is made to draw together the salient features of the processes involved from experimental data: how electronic and nuclear excitation can lead to the same set of molecular desorption states for thermally-labile species but not for stable molecules. A model for the molecular states of surface molecules will be proposed based on the Lundqvist-Nørskov theory that takes account of adsorbate-substrate interactions to give adsorbed species a "partial ionic character" distribution. Drawing from recent experimental data, the dynamics of the surface ionization process that ultimately determines which ions enter into the gas phase from the surface will be discussed. This research was sponsored by the National Science Foundation (CHE-79-04863), the National Institutes of Health (GM26096) and the Robert A. Welch Foundation (A-258).

Sputtering of Organic Molecules

Charles W. Magee
RCA Laboratories
Princeton, NJ 08540

I. Introduction

Kiloelectron-volt ion bombardment has been used for many years to produce secondary ions from inorganic solid surfaces [1]. Several years ago, it was realized that this same method of producing ions from involatile samples could be used for organic solids as well [2] and has since been put to use on a wide range of problems [3]. Recently, this same technique has been used with great success to produce ions from involatile organic liquids and from solids dissolved in liquids [4]. The mechanism of particle emission from a sample surface common to all of these techniques involves momentum transfer from the primary ion to sample atoms. In the case of organic samples, the emission of large, intact molecules will be dependent on (a) the nature of the momentum transfer process, and (b) the amount of radiation damage incurred by the uppermost monolayer of the sample from which the molecules are emitted. This paper will address these two areas of critical importance.

II. Particle-Solid Interactions

Production of secondary ions from an involatile sample surface due to primary particle bombardment is a direct result of the interaction of the energetic projectile with sample atoms [5]. Upon impact with the solid surface, the primary particle will transfer its momentum to the sample atoms through screened coulombic interactions between the respective nuclei. Clearly, the chemical bonding of the sample atoms is unimportant when considering energy-loss processes of this type. Likewise, it is unimportant to distinguish between ions and atoms as primary particles because upon impact, these two types of particles become indistinguishable. This process will produce a "collision cascade" within the solid, displacing or "recoiling" many sample atoms along the penetration track of the primary particle.

Since ejection of sputtered material is a result of sample atoms being displaced by the impact of the primary particle, a qualitative picture of the process can be obtained by examining the paths taken by these recoiled atoms as simulated by three-dimensional Monte Carlo calculations [6]. Figure 1 is a pictorial representation of such a calculation for 10 keV Ar^+ normally* incident on Cu [7]. It shows the trajectories of Cu atoms recoiled as a result of a direct collision with the Ar ion or as a result of secondary and higher-order collision cascades. While this calculation is not for an organic sample, the qualitative results are still applicable. The large number of atomic displacements induced by the primary ion are apparent at the surface within a radius of 10 Å around the point of impact. This large scale atomic displacement with resultant bond breaking (often referred to as "radiation damage") extends to a depth roughly equivalent to the range of the ion in the sample. However, only that portion of the collision cascade which intersects the surface can result in a sputtering event.

Ejection of material from the surface will then occur by two principal mechanisms [5], direct-knockon sputtering and linear cascade sputtering. Both of these regimes are depicted in Figure 2. In the direct-knockon regime, the bombarding particle transfers energy to a target atom which, after undergoing a small number of further collisions, is ejected from the surface if energetic enough to overcome binding forces. In the linear cascade regime, recoiled sample atoms are energetic enough to generate secondary and higher-generation recoils, some of which may intersect the target surface with enough energy to overcome the surface barrier. For organic samples in particular, these two ejection mechanisms will produce secondary particles which vary considerably in number of constituent atoms, angle of emission, and kinetic energy [8]. The relative probabilities of these two types of sputtering events will thus determine, in large part, the character of the mass spectrum observed.

If one now examines the atomic motion induced within the uppermost region of the sample surface from which sputtered particles originate, it becomes clear how ejection of large, intact organic molecules is possible. Figure 3 is also a Monte Carlo calculation for Ar → Cu, in which only those trajectories of sample atoms are plotted which result in a particle being ejected from the surface. It is apparent that most sputtered particles emanate from a small volume within several Angstroms of the point of ion impact -- a volume severely damaged by the collision cascade with most interatomic bonds broken. In this region, the direct knockon mechanism of sputtering will dominate, and particles will be ejected as single atoms or small clusters. Moreover, they will be highly energetic (10-100 eV) [10], and will have an angle of emission which is preferentially oriented away from the angle of incidence of the primary ion beam [11].

Figure 3 also shows that some particles can be ejected into the vacuum from as far away as 30 to 40 Å from the original point of impact of the primary particle. These sputtering events must arise from the linear cascade mechanism of energy transfer, and the particles ejected can have characteristics quite different from those of particles ejected by direct knockon. Linear cascade sputtering produces secondary particles which are emitted with a cosine distribution about the surface normal and with low kinetic energy. Because of the low energy of the cascade particles at these considerable distances from the impact point, the material sputtered suffers minimal radiation damage, thus making possible the ejection of large, intact organic molecules [12].

*The angle of incidence of a particle beam upon a surface is defined with respect to the surface normal [9] and is denoted by the symbol θ. Thus, "normally" incident implies θ = 0°.

III. Discussion

In the linear cascade regime of energy transfer, as described previously, the energy of the bombarding particles is distributed over a large volume due to the sequential and multiplicative nature of the collision cascades involved. When a cascade extends to a distance of 40 Å from the track of the primary particles, the energy of the recoiled atoms is small and the directions in which the atoms move are totally random due to the large number of interatomic collisions that must take place in order to transfer energy over such distances. As a consequence of such low-energy atomic motion near the surface, one can easily visualize how a large organic molecule on the sample surface could receive a concerted "push" from the moving atoms underneath [13], giving the molecule just enough energy to overcome the surface binding forces, but not enough to cause it to fragment [12]. Such large sputtered molecules have low kinetic energies (<1 eV) and due to the random motions of the recoiled atoms which "push" it off the surface, the sputtered molecules will be ejected in a cosine distribution centered about the surface normal.

The concept of sputtering large, intact, organic molecules from surfaces presupposes, of course, that such entities exist on the surface prior to the initiation of the sputtering event. Clearly, after prolonged ion bombardment of a solid, this would not be the case due to the radiation damage produced by the bombarding particles [14]. Sputtering of such intact molecular species is possible only if there is a high probability that the molecule will be ejected from a previously unbombarded area on the sample surface [2]. For solids, this will be the case until approximately 10% of the surface area has been damaged (equivalent to 10^{13} part./cm^2 assuming each particle damages an area of 100 Å^2). This limitation can pose serious problems concerning the use of sputtering in organic mass spectrometry. If one assumes the critical dose of 10^{13} bombarding particles/cm^2 mentioned above, and limits the experiment to this dose, then one can perform the experiment in several ways. To first approximation, a sample can be bombarded with a current density of 10^{-9} A/cm^2 for 1000 sec before the critical dose is reached. This allows more than enough time to take several scans of the mass spectrum. Such a low primary particle density, however, will produce, under optimum conditions, only ~10^5 structurally significant ions/sec. For fast-scanning, standard MS data systems using analogue detection circuits, this signal level is simply too low to provide usable mass spectra. More signal can be obtained if one simply uses a higher flux of bombarding particles--but at commensurate sacrifice in experiment duration. Signal levels can be raised three orders of magnitude by bombarding with 10^{-6} A/cm^2 but at that fluence rate, the critical dose of 10^{13}/cm^2 would be reached in one second! The experiment would result in only a short, intense flash of polyatomic and molecular ions; also an unacceptable situation. Clearly, one is being severely limited by the restriction of 10^{13} bombarding particles/cm^2 of sampled area. One solution to this restriction is to sample a larger area. This can be done through the use of sophisticated secondary ion extraction techniques, such as dynamic emittance matching [15] or by simply translating a large sample area under the bombarding particle beam.

Large areas of undamaged sample can also be presented to the bombarding particle beam if the molecules of interest are dissolved in a liquid [16]. Liquids have diffusion coefficients of the order of 10^{-5} cm^2/sec [17]. This results in molecular velocities of approximately 30 μm/sec, sufficient to completely renew the radiation-damaged upper 100 Å of the liquid film every 3 x 10^{-4} sec. Thus, the critical dose for detectable sample damage can be delivered to the sample in that period of time, which is equivalent to a bombarding current density of 10^{-2} A/cm^2. This very high flux density would generate quite intense signals indeed, and one could expect to sputter intact molecular ions from the surface until the liquid matrix is pumped away into the vacuum system. Such large secondary ion currents for a duration of minutes are ideally suited to many mass spectrometer/data systems in use for organic analysis, and as such, have resulted in a very popular sample preparation technique [4].

IV. Observations and Conclusions

From this brief review of particle-solid interactions and how they affect the sputtering of organic molecules from surfaces, one can make the following observations:

a) The charge on the primary bombarding particle in no way affects the sputtering process because it results from elastic interactions between the partially screened nuclei of the bombarding and target atoms. This point is relevant in light of the sputtering method which uses keV-energy atom beams for sample bombardment. fast atom bombardment (FAB). It should be noted that atom bombardment [18-20] of insulating samples will result in less sample charging than will ion bombardment. This is especially important for quadrupole-type mass spectrometers due to their low accelerating potentials. (Any surface charge represents a much larger fraction of the total ion energy than would be the case with magnetic sector-type instruments). There are, however, several methods available for neutralizing surface charge build-up on insulating samples under ion bombardment. They are summarized in reference 21. They include negative primary ion bombardment [22], use of conducting grids over the sample [23], use of an auxiliary conducting electrode near the sample surface [21], flooding the sample with electrons from a heated filament [24] or from a low-energy (5 eV) [25] or high energy (2 keV) [26] electron gun.

b) On the time scale of a collision cascade, particle bombardment of a liquid is identical to that of a solid. The time which elapses from initial impact of the bombarding particle until all atomic motion has ceased is about 10^{-13} to 10^{-12} seconds [13]. During this period, the molecules of a typical liquid (with a diffusion coefficient of 10^{-5} cm^2/sec) are essentially stationary On this time scale thermal vibrations may also be ignored.

c) Liquid sputtering matrices are useful for rapid exchanging the sample surface exposed to the radiation damage caused by the sputtering beam. This allows one to bombard with particle fluxes high enough to generate large numbers of sputtered organic molecules, but without exceeding the critical dose for detectable sample damage. In addition, liquids generally have lower surface binding energies than do similar solids and thus produce higher yields of sputtered particles than do solids.

d) Contrary to the theory now in vogue, energetic particle bombardment is not a "soft ionization" technique. Rather, it is a "graded ionization" technique, capable of producing organic ions of varying structural complexity, from atomic carbon ions to intact molecular ions of Vitamin B12 [27]. One must remember that these ions are created from different areas on the sample surface which span a wide range of energy available for particle ejection--energies of several hundred eV only a few Angstroms away from the point of projectile impact, to energies of several eV tens of Angstroms away. In addition, the more structurally complex the sputtered ion, the lower will be its initial kinetic energy [8]. This can be seen in the energy distributions of sputtered atomic and cluster ions in Figure 4. The differences between these distributions can be used to vary the amount of fragmentation observed in a mass spectrum. Using secondary ion optics with an energy bandpass of ~1 eV, one can "tune in" or "tune out" portions of the energy spectrum of sputtered ions as desired. In addition, *the degree of fragmentation observed in a mass spectrum is influenced by the balance between direct-knockon sputtering* (which produces small, high-energy clusters), and linear cascade sputtering (which can produce large, low-energy clusters). Several factors influence this balance. Low bombarding particle energy will favor direct-knockon sputtering events due to a lack of energy necessary to initiate large, extended collision cascades [8]. Low mass bombarding particles (e.g., N) will likewise favor direct-knockon sputtering of organic compounds due to the more favorable energy transfer incurred between atoms of similar mass [5]. This creates recoiled atoms with much more energy as opposed to those created with heavy projectile (e.g. Xe) bombardment. In fact, the single knockon regime of sputtering organic compounds as depicted in Figure 2(a) is not possible when bombarding with massive projectiles due to the kinematics of elastic collisions. (One cannot bounce a bowling ball off a golf ball.)

Finally, one can affect the degree of fragmentation observed in a mass spectrum by changing the angle of incidence, θ, that the bombarding beam makes with the surface normal. Figure 1 depicts normal incidence ($\theta = 0°$) in which case only the short, still highly energetic collision cascades, close to the point of impact reach the surface to produce sputtering. The direct radiation damage in this area of the sample surface is severe, resulting in a high degree of molecular fragmentation. On *the other hand, if the angle of incidence is increased to 70°, more of the lower energy, extended* cascades will reach the surface to produce a sputtering event, as illustrated in Figure 5. This situation results in a higher overall yield of sputtered particles with a lower degree of fragmentation than is observed at $\theta = 0°$ [29].

The author gratefully acknowledges the helpful conversations with R. E. Honig, W. L. Harrington, P. J. Gale and B. L. Bentz of this laboratory, and with P. Sigmund of Odense University. R. Shimizu of Osaka University and W. R. Wampler of Sandia Laboratories are also acknowledged for their Monte Carlo calculations.

References

(1) R. E. Honig, J. Appl. Phys. 29, 549 (1958).
(2) A. Benninghoven, Org. Mass. Spectrom. 12, 595 (1977).
(3) R. J. Day, S. E. Unger and R. G. Cooks, Anal. Chem. 52, 557A (1980).
(4) M. Barber, R. S. Bordoli, G. J. Elliott, R. D. Sedgwick and A. N. Tyler, Anal. Chem. 54, 645A (1982).
(5) For a complete review of particle-solid interactions, see P. Sigmund in "Sputtering by Ion Bombardment-I", R. Behrisch, Ed., Springer-Verlag Topics in Applied Physics, Berlin, 1981, Chap. 2.
(6) J. P. Biersack and L. G. Haggmark, Nucl. Instrum. Meth. 174, 257 (1980).
(7) T. Ishitani and R. Shimizu., Phys. Lett. 46A, 487 (1974).
(8) For a complete review of emission characteristics of sputtered particles, see W. Hofer in "Sputtering By Ion Bombardment-III, R. Behrisch, Ed., Springer-Verlag Topics in Applied Physics, (in preparation).
(9) J. Thewlis, in "Concise Dictionary of Physics and Related Subjects", Pergamon Press, 1973).
(10) K. Wittmaack, Phys. Lett. 69A, 322 (1979).
(11) T. Okutani, M. Shikata, S. Tchimura, R. Shimizu, J. Appl. Phys. 51, 2884 (1980).
(12) A. Benninghoven in, "Secondary Ion Mass Spectrometry-SIMS III", A. Benninghoven, J. Giber, J. Laszlo, M. Riedel and H. W. Werner, Eds., Springer-Verlag Series in Chemical Physics, Vol. 19, Berlin, (1982), p. 438.
(13) B. J. Garrison, J. Am. Chem. Soc. 102, 6553 (1980).
(14) A. Benninghoven and W. K. Sichtermann, Anal. Chem. 50, 1180 (1978).
(15) J. E. Campana, J. J. DeCorpo and J. R. Wyatt, Rev. Sci. Instrum. 52, 1518 (1981).
(16) D. F. Hunt, W. M. Bone, J. Shabanowitz, J. Rhodes and J. M. Ballard, Anal. Chem. 53, 1704 (1981).
(17) Handbook of Chemistry and Physics, 44th Edition, Chemical Rubber Publ. Co., Cleveland OH, 1963 p. 2274.
(18) N. H. Tolk, I. S.T. Tsong and C. W. White, Anal. Chem. 49, 16A (1977).
(19) A. Iino and A. Mizuike, Bull. Chem. Soc. Jpn. 54, 1975 (1981).
(20) M. Barber, R. S. Bordoli, R. D. Sedgwick and A. N. Tyler, J. Chem. Soc., Chem. Commun. 325 (1981).
(21) H. W. Werner and A. E. Morgan, J. Appl. Phys. 47, 1232 (1976).
(22) C. A. Andersen, H. J. Roden and C. F. Robinson, J. Appl. Phys. 40, 3419 (1969).
(23) G. Slodzian, Ann. Phys. (Paris) 9, 591 (1964).
(24) R.F.K. Herzog, W. P. Poschenrieder, F. G. Rüdenauer and F. G. Satkiewicz, Proceedings of the 15th Annual Conference on Mass Spectrometry and Allied Topics, Denver, May, 1967 p.301.
(25) G. Muller, Appl. Phys. 10, 317 (1976).
(26) C. W. Magee and W. L. Harrington, Appl. Phys. Lett. 33, 193 (1978).
(27) M. Barber, R. S. Bardoli, R. D. Sedgwick and A. N. Tyler, Proceedings of the 29th Annual Conference on Mass Spectrometry and Allied Topics, Minneapolis, May, 1981, p. 351.
(28) B. J. Garrison, N. Winograd and D. E. Harrison, Jr., J. Chem. Phys. 69, 1440 (1978).
(29) C. J. McNeal, Anal. Chem. 54, 43A (1982).

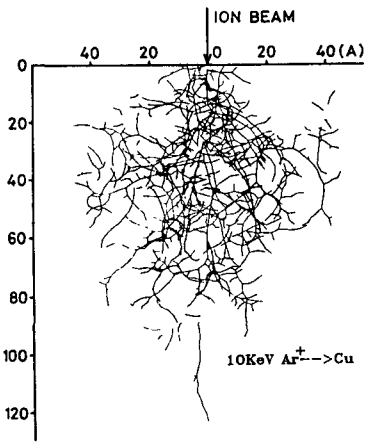


Figure 1. Monte Carlo simulation of the trajectories of recoiled sample atoms due to 10keV Ar bombardment of Cu. (from ref. 10).

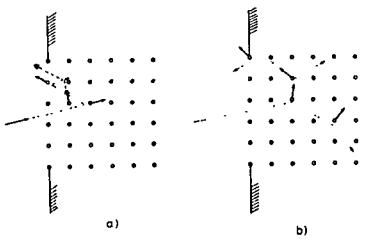


Figure 2. Two regimes of sputtering by elastic collisions: a) The direct-knockon regime. Recoil atoms from projectile-target collisions get ejected directly. b) Linear cascade regime. Recoil atoms from projectile-target collisions generate higher-order cascades of recoil atoms which are then ejected. (from ref. 5).

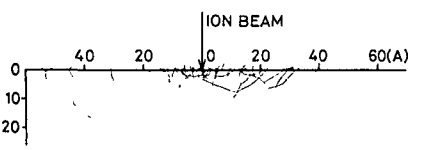


Figure 3. Monte Carlo simulation of the trajectories of recoil sample atoms which result in a sputtering event. (from ref. 7, Ar → Cu).

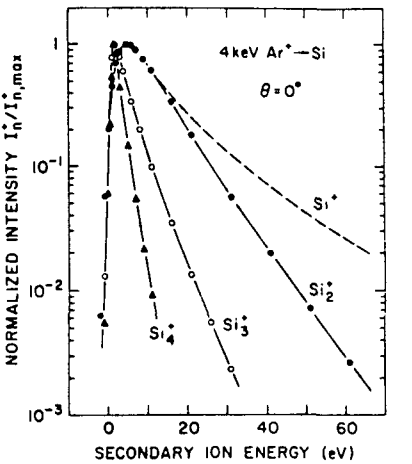


Figure 4. Energy distributions of sputtered atomic and cluster ions. Unlike large, intact organic sputtered ions (13), however, small polyatomic clusters may be formed by recombination above the sample surface (28). (from ref. 10).

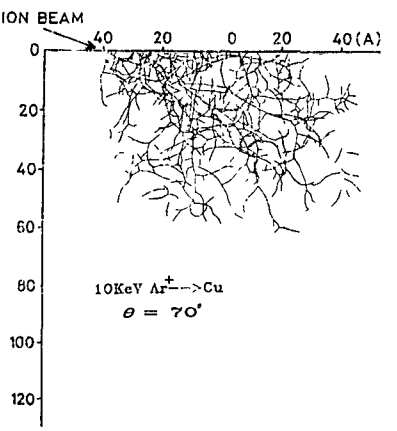


Figure 5. Monte Carlo simulation of the trajectories of recoiled atoms from Figure 1, except tilted to simulate bombardment at θ=70°. Note how many more of the low-energy collision cascades intersect the sample surface in this case as contrasted with those of Figure 1.

SECONDARY ION MASS SPECTROMETRY OF ORGANIC COMPOUNDS

A. BENNINGHOVEN

PHYSIKALISCHES INSTITUT DER UNIVERSITÄT MÜNSTER,
D-4400 MÜNSTER, FED. REP. OF GERMANY

PARENT-LIKE SECONDARY IONS OF THE GENERAL COMPOSITION $(M+H)^+$ AND $(M-H)^-$, WHERE M STANDS FOR AN ORGANIC MOLECULE, ARE EMITTED WITH VERY HIGH ABSOLUTE YIELDS FROM CORRESPONDING MOLECULAR LAYERS ON SOLID SURFACES DURING ION BOMBARDMENT. THAT WAS THE SURPRISING RESULT OF TWO SYSTEMATIC SIMS INVESTIGATIONS ON 40 MOSTLY THERMALLY LABILE ORGANIC COMPOUNDS AS AMINO ACIDS, PEPTIDES, VITAMINS, DRUGS, PHARMACEUTICALS ETC., PUBLISHED IN 1976 /1/ AND 1977 /2/.

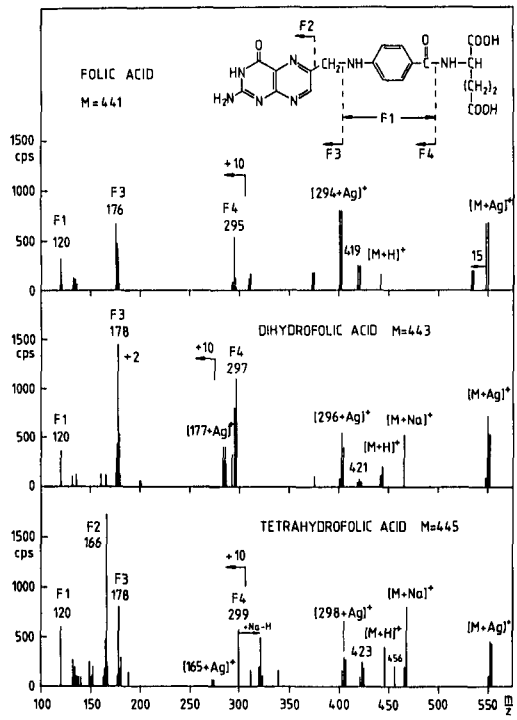


FIG. 1:
POSITIVE SIMS-SPECTRUM OF FOLIC ACID (DERIVATES). 1 NG HAS BEEN DEPOSITED ON 0.1 CM^2 OF A SILVER SUBSTRATE, BY DRYING 1 µL OF A 10^{-4} MOL/L AQUEOUS SOLUTION.
BOMBARDMENT CONDITIONS: AR^+, 3 KEV; $3 \cdot 10^{-10}$ A ON 0.1 CM^2

THIS EMISSION OF UNDESTROYED LARGE ORGANIC MOLECULES WAS A COMPLETELY UNEXPECTED EFFECT. SPUTTERING HAS BEEN REGARDED TO BE HIGHLY DESTRUCTIVE AND ONLY FRAGMENTS WERE EXPECTED TO BE EMITTED FROM BOMBARDED LARGE ORGANIC MOLECULES. IN CONTRAST TO THIS, VERY OFTEN PARENT-LIKE SECONDARY IONS REPRESENT THE BASE PEAK IN AN ORGANIC SIMS SPECTRUM /1-3/. FOLLOWING OUR FIRST CONFERENCE

REPORTS AND PUBLICATIONS, AN INCREASING NUMBER OF OTHER GROUPS ENTERED THIS NEW FIELD /5-8 E.G./. TODAY A LARGE BODY OF EXPERIMENTAL MATERIAL IS AVAILABLE. GENERAL RESULTS ARE:

- FROM VIRTUALLY ALL ORGANIC COMPOUNDS, THAT HAVE BEEN INVESTIGATED SO FAR, PROTONATED AND DEPROTONATED MOLECULES $(M+H)^+$ AND $(M-H)^-$ (WHERE M STANDS FOR THE SAMPLE MOLECULE) ARE EMITTED. DEPENDING ON THE STRUCTURE OF M AND ITS CHEMICAL ENVIRONMENT ON THE SAMPLE SURFACE, OTHER PARENT-LIKE SECONDARY IONS AS $(M+CATION)^+$ /5/, $(M+ANION)^-$, $(M+2CATION-H)^+$, $(2M+H)^+$, $(2M-H)^-$ ETC. OCCUR.

- THE ABSOLUTE AS WELL AS THE RELATIVE YIELDS OF ALL THESE PARENT-LIKE SECONDARY IONS COMPLETELY DEPEND ON THE CHEMICAL ENVIRONMENT OF THE SAMPLE MOLECULES ON THE TARGET SURFACE. THIS ENVIRONMENT IS DETERMINED BY THE SUBSTRATE MATERIAL (AT LEAST IN THE CASE OF MONOLAYER DEPOSITION), BY THE COMPOSITION OF THE SOLVENT (FOR "WET" TARGET PREPARATION), AND THE CONCENTRATION OF ADDITIONAL ATOMIC OR MOLECULAR SPECIES IN THIS SOLVENT, OR BY THE CHEMICAL NATURE OF A LIQUID MATRIX (GLYCEROL E.G.).

- BY AN APPROPRIATE SAMPLE PREPARATION (SURFACE CHEMISTRY) EXTREMELY HIGH YIELDS (UP TO SOME 10 %) FOR AT LEAST ONE OF THESE PARENT-LIKE IONS CAN BE ACHIEVED /4/.

- IN ADDITION TO THE PARENT-LIKE SECONDARY IONS, CHARACTERISTIC FRAGMENT IONS, POSITIVE AS WELL AS NEGATIVE, ARE EMITTED (FIG. 1), SOME OF THEM OF THE GENERAL COMPOSITION $(M-A)^{\pm}$, WHERE A IS A SMALL STABLE COMPLEX SUCH AS CO_2, H_2O, ETC.

- DISAPPEARANCE CROSS SECTIONS σ (SEE FIG. 2), FOR ION AS WELL AS FOR ELECTRON BOMBARDMENT, AND DISAPPEARANCE TEMPERATURES MAY BE VERY DIFFERENT FOR DIFFERENT PARENT-LIKE SECONDARY IONS FROM THE SAME SAMPLE MOLECULE M AS $(M+H)^+$ AND $(M-H)^-$ /4/.

- ISOTOPE EXPERIMENTS FOR AMINO ACIDS PROVE, THAT THE PROTON TRANSFER, RESULTING IN THE FORMATION OF $(M+H)^+$- AND $(M-H)^-$-IONS, OCCURS IN THE SAME WAY AS IN A SOLUTION, I.E. ONLY THE HYDROGEN ATOMS IN THE CNH_2-COOH GROUP CONTRIBUTE TO THIS TRANSFER /4/.

- THE CHARGE STATE OF THE BOMBARDING PARTICLE HAS VIRTUALLY NO, AND ITS COMPOSITION, MASS, ENERGY AND ANGLE OF INCIDENCE ONLY A VERY LIMITED INFLUENCE ON THE SECONDARY ION EMISSION.

CONSIDERING THESE AND OTHER GENERAL FEATURES OF ORGANIC SECONDARY ION EMISSION, A PRECURSOR MODEL FOR THE ION FORMATION PROCESS MAY BE ESTABLISHED /9/:

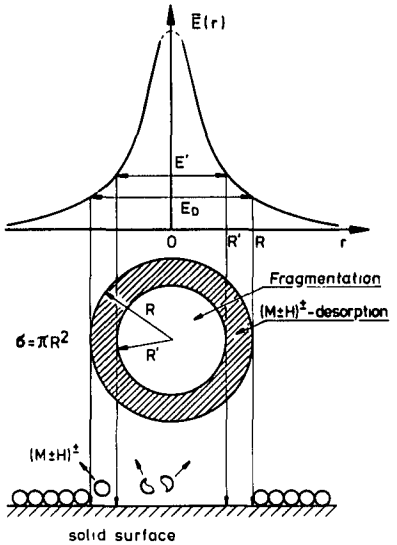


FIG. 2:
MOLECULAR ION FORMATION DURING SPUTTERING OF LARGE ORGANIC MOLECULES M FROM A SOLID SURFACE. THE ENERGY DISTRIBUTION E(ν) REPRESENTS THE AVERAGE ENERGY WHICH IS TRANSFERRED BY AN IMPACT CASCADE TO A SUBSTRATE SURFACE ATOM AT A DISTANCE R FROM THE POINT OF PRIMARY ION IMPACT (R = 0). THE FAST ($< 10^{-12}$ S) ENERGY TRANSFER TO THE MOLECULES M RESULTS IN A DISAPPEARANCE OF M FOR $\nu \leq R$. ONLY FOR $R' \leq \nu \leq R$ DOES THIS DISAPPEARANCE RESULT IN THE EMISSION OF PARENT-LIKE IONS. NOTE THAT THIS SCHEME DOES NOT DESCRIBE ONE SINGLE IMPACT PROCESS, BUT AVERAGES A LARGE NUMBER OF SUCH EVENTS !

1. PRECURSOR FORMATION: PRIOR TO ANY PARTICLE BOMBARDMENT, A PRECURSOR OF THE FINALLY EMITTED SECONDARY ION EXISTS AT THE TARGET SURFACE. THIS CONCERNS THE ATOMIC COMPOSITION AS WELL AS THE AVERAGE CHARGE STATE OF THE FINALLY EMITTED SECONDARY ION.

2. FAST EVAPORATION: THE LOW ENERGY TAIL OF THE IMPACT CASCADE, THAT IS GENERATED NEAR THE SURFACE AS A RESULT OF THE BOMBARDMENT, IS RESPONSIBLE FOR THE FAST EVAPORATION ($< 10^{-12}$ S) OF THE UNFRAGMENTED PRECURSORS.

3. CHARGE SIGN CONSERVATION: A TENDENCY EXISTS TO MAINTAIN THE AVERAGE CHARGE SIGN OF THE PRECURSOR DURING ITS TRANSFORMATION IN THE CORRESPONDING SECONDARY ION.

4. FRAGMENTATION: THE HIGH ENERGY REGION OF THE SURFACE CASCADE PRODUCES FRAGMENTS OF THE SURFACE PRECURSOR, INCLUDING ATOMIC SPECIES (FIG. 2). ADDITIONAL FRAGMENT FORMATION MAY OCCUR DURING THE DECOMPOSITION OF EXCITED MOLECULAR SECONDARY SPECIES AFTER THEIR SEPARATION FROM THE SURFACE.

ORGANIC SIMS HAS AN EXTRAORDINARY ANALYTICAL POWER. IT ENABLES THE INVESTIGATION AND IDENTIFICATION OF EVEN NON-VOLATILE ORGANIC COMPOUNDS UP TO SOME 1000 AMU IN THE SUBNANOGRAM RANGE, ALREADY WITH THE EXISTING INSTRUMENTS. ORGANIC SIMS IS INCREASINGLY APPLIED IN DOUBLE FOCUSSING MAGNETIC INSTRUMENTS, WHERE FOR TECHNICAL REASONS NEUTRAL ATOMS ARE USED AS BOMBARDING PRIMARY PARTICLES (FAB) /10/, AND A CONTINUOUS SURFACE REGENERATION OF THE

BOMBARDED SAMPLE SURFACE IS ACHIEVED BY DEPOSITING THE SAMPLE MOLECULES IN A GLYCEROL MATRIX. IMPROVEMENTS IN SAMPLE PREPARATION (CHEMICAL ENVIRONMENT) AND INSTRUMENT TRANSMISSION (TOF E.G.) WILL INCREASE THE SENSITIVITY BY ORDERS OF MAGNITUDE. EVEN THE PRESENT SENSITIVITY IN THE SUBNANOGRAM RANGE MAKES ORGANIC SIMS AN EXTREMELY USEFUL DETECTOR IN LIQUID (11) AND THIN LAYER (12) CHROMATOGRAPHY, AND A POWERFUL TOOL FOR DRUG DETECTION (13), FOR THE TRACE DETECTION AND IDENTIFICATION OF ORGANIC COMPOUNDS IN BODY FLUIDS (14), ETC.

LITERATURE

1 A.BENNINGHOVEN, D.JASPERS AND W.SICHTERMANN, APPL.PHYS. 11 (1976) 35

2 A.BENNINGHOVEN AND W.SICHTERMANN, ORG.MASS SPECTROM. 12 (1977) 595

3 A.BENNINGHOVEN AND W.SICHTERMANN, ANAL.CHEM. 50 (1978) 1180

4 A.BENNINGHOVEN, D.HOLTKAMP, D.JIRIKOWSKY, W.LANGE, TO BE PUBLISHED IN SURF.SCI.

5 H.GRADE, N.WINOGRAD AND R.G.COOKS, J.AM.CHEM.SOC. 99 (1977) 7725

6 R.J.COLTON, J.S.MURDAY, J.R.WYATT AND J.J. DE CORPO, SURF.SCI. 84 (1979) 235

7 R.J.DAY, S.E.UNGER AND R.G.COOKS, ANAL.CHEM. 52 (1980) 557

8 H.KAMBARA AND S.HISHIDA, ORG.MASS.SPECTROM. 16 (1981) 167

9 SIMS III, PROCEEDINGS OF THE THIRD INTERNATIONAL CONFERENCE ON SECONDARY ION MASS SPECTROMETRY, A.BENNINGHOVEN ET AL., EDS., SPRINGER HEIDELBERG, 1982, P. 438

10 M.BARBER, R.S.BORDOLI, R.D.SEDGWICK AND A.N. TYLER, J.C.S.CHEM. COMM. 1981, 325

11 A.BENNINGHOVEN ET AL., ORG.MASS SPECTROM. 15 (1980) 459

12 S.E.UNGER, A.VINCE, R.G.COOKS, R.CHRISTMAN, AND E.D.ROTHMAN, ANAL.CHEM. 53 (1981) 976

13 A.BENNINGHOVEN AND W.SICHTERMANN, INT.J. MASS SPECTROM.ION PHYS. 33 (1981) 351

14 W.SICHTERMANN, M.JUNACK, A.EICKE, AND A.BENNINGHOVEN, FRESENIUS Z.ANAL.CHEM. 301 (1980) 115, AND 311 (1982) 410 AND 411

LASER DESORPTION, SECONDARY ION MASS SPECTROMETRY, AND OTHER FORMS OF DESORPTION IONIZATION. PHENOMENA AND UTILITY

R.G. Cooks and K.L. Busch
Department of Chemistry
Purdue University
West Lafayette, Indiana 47907

Desorption ionization (DI) that is, methods in which ions are generated from molecular solids by the rapid input of energy into a sample, has developed to the point where it has begun to rival CI and EI. This presentation traces this development with emphasis on new capabilities available for the analysis of nonvolatile compounds.

Laser desorption (0.1 J/pulse, 10 nsec pulse width, 10 Hz repetition rate) and secondary ion mass spectrometry (Ar^+, 5 keV, ca 10^{-10} A/cm^2) are the main subjects of discussion.

Spectral Comparison

When the same analyzer is used, remarkably similar LD and SIMS spectra are recorded. A typical comparison is illustrated in Figure 1 for an organic salt. The spectra shown here are also quite similar to the spectrum obtained with PD. Neutral compounds are readily ionized in SIMS by cationization, preferably using an isotopically distinctive transition metal ion. This cationization process is also observed for laser desorption.

Ionization and Fragmentation Mechanisms

Three types of reactions account for the parent anions and cations observed in DI (1). They are, in decreasing order of importance, (i) direct emission of precharged ions, (ii) ion transfer processes, especially the formation of adducts between neutral molecules and cations, viz. cationization and anionization, and (iii) electron transfer processes yielding radical ions. Fragment ions are generated by unimolecular processes which parallel those observed in EI and CI, and can be interpreted to deduce the presence of certain structural features. These concepts were developed under the aegis of molecular SIMS, but serve to explain spectra in all forms of DI. Figure 2 compares the unimolecular fragmentations of a collisionally activated cation generated by LD and examined by MS/MS, with the SIMS spectrum of the corresponding salt. This type of result indicates that it is unimolecular reactions of internally excited parent ions which lead to the fragments observed in SIMS, and in other forms of DI.

A Model for Desorption Ionization

Several years ago (MÜnster Conference, 1980) we developed a simple model (2) which accounts for many of the phenomena reported for the new direct ionization procedures. The subsequent development of fast atom bombardment (FAB) has provided further experimental support for these ideas. The elements of this model are given in Figure 3.

"Reverse" Derivatization and Surface Reactions

Efficient analytical utilization of DI suggests that the sample be converted into a precharged state. This derivatization is the reverse of that normally employed in preparing compounds for GC/MS, where non-polar derivatives are desired (3). Derivatization can be conducted *in situ* or prior to sample introduction. Figure 4 illustrates the dramatic effects of converting zwitterions to the cationic form prior to obtaining an LD mass spectrum.

An emerging field of study is the reactions of organic compounds at interfaces. DI methods, particularly LD and SIMS, should have much to offer. For example, it has already been found that thiophene undergoes dehydrosulfurization and C-C scission at a silver surface. This process, discovered in SIMS, was subsequently verified in a catalytic reactor (4).

Internal Energies in DI

One of the most significant characteristics of an ionization method must be the internal energy transferred to the parent ion. This is also one characteristic in which the various methods of DI differ most strongly. For example, electrohydrodynamic ionization produces ions from a glycerol solution with energies such that no fragmentation is observed.

A measure of internal energy can be had by examining a series of compounds in which dissociation is increasingly likely. This is conveniently done by taking a series of doubly-charged salts and varying the intercharge distance and hence the coulombic energy. Results for such experiments using SIMS have been published (5) while EHMS (K. Cook, personal communication) data show much lower internal energies.

The matrix from which ionization occurs profoundly affects internal energies. Ejection from the surface of solvated ions may be followed by desolvation which serves to produce an energetically relaxed form of the ion. Ammonium chloride has been found to be a superior matrix for SIMS (9). Figure 5 illustrates this, showing the decreased fragment ion abundance relative to the parent cation. In addition, there is a small increase in total signal and a dramatic improvement in S/N when the sample is run from a large excess (10-100 x) of ammonium chloride.

Mass Spectrometry/Mass Spectrometry and Desorption Ionization

One of the first combination of these procedures employed pulsed laser desorption and collision-induced dissociation (7). The techniques are complementary since DI sometimes (FD, EHMS) produces fragments of insufficient abundance to provide structural information, or else (FAB) there is a high background and interference from solvent peaks.

It is possible to obtain good MS/MS spectra on peaks for which chemical noise makes the MS itself analytically useless. This important feature of MS/MS is illustrated, for laser desorption, in Figure 6.

Analytical applications to direct mixture analysis can be made by DI alone, as in the identification of quaternary alkaloids from intact plant materials. However, MS/MS facilitates such determinations, as in the detection of candicine (1) chloride in a cactus species (Figure 7). It should be noted that the two major fragment ions arise by simple unimolecular dissociations of the intact cation (Scheme 1).

Analytical Applications and Chromatography

DI techniques are capable of directly ionizing involatile, ionic compounds separated by chromatography. Interfacing of SIMS to reversed phase LC has been reported. In addition to such dynamic modes of chromatography, there are advantages in using DI methods with procedures such as thin layer, paper chromatography and electrophoresis. These have now been accomplished using SIMS (8). The latter, used to separate compounds on the basis of charge, seems particularly well suited for DI analysis, which shows an enhanced selectivity for these charged compounds.

An overall comparison of the state-of-the-art of desorption ionization methods for analysis is provided in Table 1.

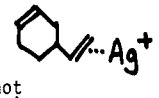
New Trends

Many of the above topics themselves represent new developments. It is nevertheless possible to foresee several quite new growth points for desorption ionization. Those in which we have commenced experiments are:

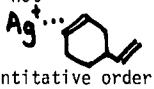
(i) Reactions at surfaces. These involve chemical manipulation of surfaces using ion beams, especially to form new chemical entities. An example is the formation of the organometallic complex by the sequence shown (Figure 8); note the role of DI in characterizing the product.

(ii) Metal-organic bonding. The strengths and site of metal bonding to organic

molecules is accessible using DI combined with MS/MS (9). For example, laser desorption is used to bind silver ions to the diolefin; the product is complexed with a test olefin and then mass analyzed and dissociated. From a series of MS/MS spectra such as that shown in Figure 9 it is possible to determine that the bonding is predominantly



and not



Quantitative ordering of metal affinities is also possible by this method.

(1) R.J. Day, S.E. Unger and R.G. Cooks, Anal. Chem., 52, 557A (1980).
(2) K.L. Busch, S.E. Unger and R.G. Cooks, Proceedings of the Conference on Ion Formation from Organic Solids, University of Münster, October 1980, Springer-Verlag, New York, 1982.
(3) K.L. Busch, S.E. Unger, A. Vincze, R.G. Cooks and T. Keough, J. Am. Chem. Soc., 104, 1507 (1982).
(4) S.E. Unger, R.G. Cooks, B.J. Steinmetz and W.N. Delgass, Surf. Sci., 116, L211 (1982).
(5) T.M. Ryan, R.J. Day and R.G. Cooks, Anal. Chem., 52, 2054 (1980).
(6) L.K. Liu, K.L. Busch, and R.G. Cooks, Anal. Chem., 53, 109 (1981).
(7) D. Zakett, A.E. Schoen, R.G. Cooks and P.H. Hemberger, J. Am. Chem. Soc., 103, 1295 (1981).
(8) S.E. Unger, A. Vincze, R.G. Cooks, R. Chrisman and L. Rothman, Anal. Chem., 53, 976 (1981).
(9) S.A. McLuckey, A.E. Schoen and R.G. Cooks, J. Am. Chem. Soc., 104, 848 (1982).

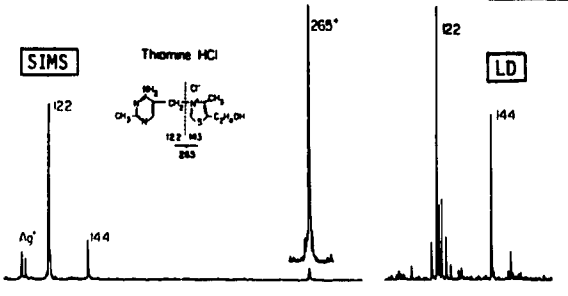


FIGURE 1

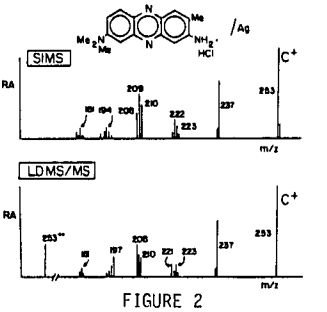


FIGURE 2

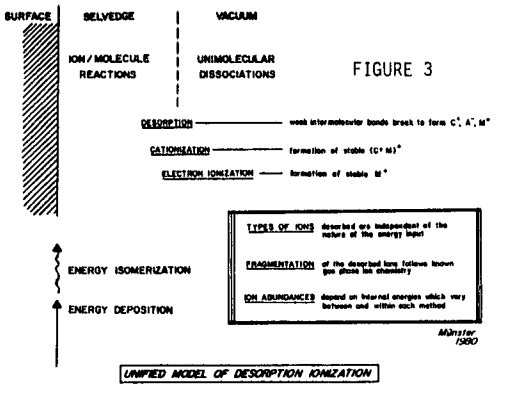


FIGURE 3

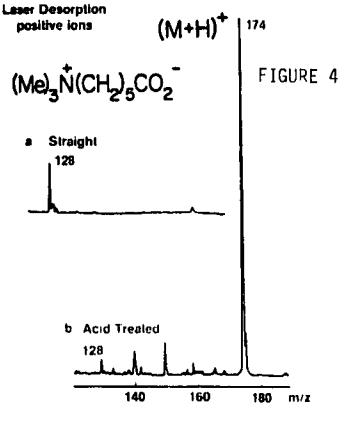


FIGURE 4

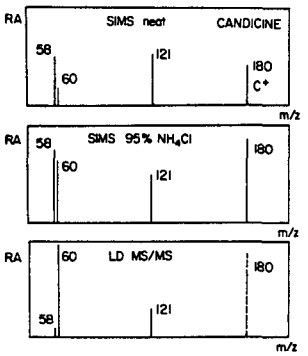


FIGURE 5

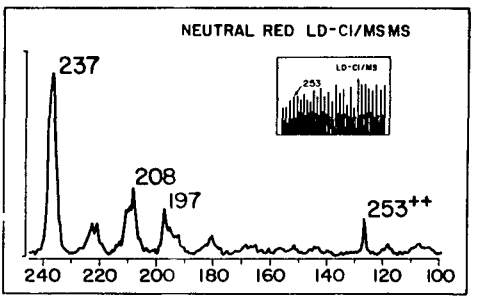


FIGURE 6

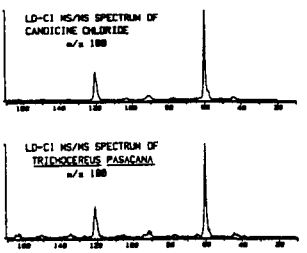
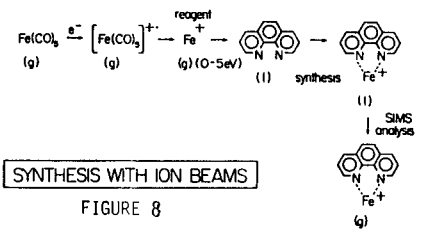


FIGURE 7



SYNTHESIS WITH ION BEAMS

FIGURE 8

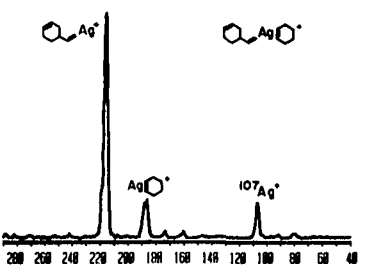


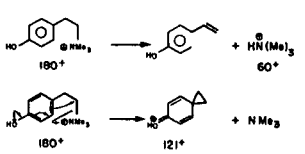
FIGURE 9

TABLE 1

	SIMS	PD	FAB	LD	FD
SENSITIVITY					
demonstrated limit normal sample size	pg ng-ug	ng ug	ng ug	ng ng-ug	ng ng-ug
SPECIFICITY					
direct mixture analysis isomer differentiation	yes yes	no yes	no yes	no yes	no yes
SPEED					
acquisition time sample persistence	short long	long long	short long	short variable	short short
FLEXIBILITY					
static chrom (PC, TLC, Eph) dynamic chrom (HPLC)	yes yes	yes yes	??? no	no no	no yes
QUANTITATION					
internal standards	yes	no	no	no	yes
DEMONSTRATED MASS RANGE	2100	12000	3500	1500	10000

JUNE 1982

SCHEME 1



Isotope analysis of noble gases and some applications in Earth sciences

Erhard H. Hebeda
Z.W.O. Laboratorium voor Isotopen-Geologie, De Boelelaan 1085, 1081 HV Amsterdam, The Netherlands

The measurement of the elemental distribution and isotopic composition of noble gases has been recognized as a powerful technique for the understanding of nuclear processes. Investigation of noble gases has played a key role in the understanding of the formation and history of extraterrestrial matter, the meteorites and lunar samples (1, 2). In the Earth sciences, the analysis of argon isotopes is widely used for the potassium-argon dating method (3), but the study of other radiogenic noble gas isotopes from geological samples is as yet not very common (4, 5, 6). In recent years, however, the study of noble gases in terrestrial materials has found a wide range of applications for gaining a better understanding of geochemical processes in the evolution and degassing history of the crust and mantle and in the evolution of the atmosphere (7, 8, 9).

The low natural abundances of particularly the heavy noble gases require mass spectrometry of high sensitivity and precision. In order to obtain this sensitivity the isotope measurements are performed under static conditions, with the spectrometer system isolated from the vacuum pumps. Memory, mass discrimination and blank are the limiting factors for the precision and accuracy in the determination of small samples of noble gases and their isotopic composition. Memory is the contamination of the gas sample by the release of gas molecules from previous samples, both adsorbed molecules and those implanted as ions with energies of several thousands volts into the surfaces, especially in the ion source of the mass spectrometer. The implanted gases will not be released completely during a bake-out but only by bombardment with an ion beam. In conventional ion sources, with transmissions in the order of few percent, the majority of the ions will be implanted and never reach the detector. Pressure dependent mass discrimination and sensitivity are inherent to Nier-type ion sources with source magnets. A new type of ion source designed by Baur (10) uses no magnets and has an unique axial design with Z-focussing and a ring-shaped filament which produces a conical electron beam. This source combines high sensitivity and stability with negligible pressure dependent non-linearities and has been incorporated into noble gas mass spectrometer systems in which the mass discrimination was minimized by the use of pulse-counting technique (11, 12).

With carefully designed furnaces and purification systems for the extraction of noble gases from the samples very low "hot blanks" are obtainable: 10^{-8} - 10^{-9} ccSTP of ^{40}Ar at 1600°C for advanced systems, $< 4 \times 10^{-11}$ cc STP of ^{40}Ar for more sophisticated systems (11, 13). In geochronology a very high sensitivity for argon is in most cases not necessary. But high precision and accuracy are

required, especially for dating very young samples or determining initial isotope ratios for the detection of excess radiogenic argon. The precision and accuracy still will be limited by the memory, even when mass discrimination and blank are controlled. By the simultaneous detection of the different ion species the time necessary for a complete isotopic analysis is greatly reduced (14). In this way the uncertainties in the computation of the isotopic ratios back to the time of gas-inlet and the errors of the intensity interpolations due to beam fluctuations are minimized. The combination of a multi-collector noble gas mass spectrometer equipped with a Baur-source could very well represent an ideal system for the analysis of noble gases in geological samples.

References:

1 Reynolds J.H. (1967) Isotopic Abundance Anomalies in the Solar System. Ann. Rev. Nucl. Sci. 17, 253.

2 Sabu D.D. and Manuel O.K. (1980) Noble Gas Anomalies and Synthesis of the Chemical Elements. Meteoritics 15, 117.

3 Dalrymple G.B. and Lanphere M.A. (1969) Potassium-Argon Dating, W.H. Freeman, San Francisco.

4 Shukoljukov J., Kirsten T. and Jessberger E.K. (1974) The Xe-Xe Spectrum Technique, A New Dating Method. Earth. Planet. Sci. Let. 24, 271.

5 Teitsma A. and Clarke W.B. (1978) Fission Xenon Isotope Dating. J. Geophys. Res. 83, 5443.

6 Hebeda E.H. and Freundel M. (in prep.) Uranium, Lead, Xenon and Krypton Systematics of Zircons from the Botnavatn Igneous Complex, SW Norway.

7 Alexander, Jr. E.C. and Ozima M. (1978) Terrestrial Rare Cases. Adv. in Earth and Planetary Sci. 3, Japan Sci. Soc. Press.

8 Alexander, Jr. E.C. (1978) Noble Gases; in: Handbook of Geochemistry, Wedepohl K.H., Editor, Springer, Berlin, Heidelberg, New York.

9 Manuel O.K. and Sabu D.D. (1981) The Noble Gas Record of the Terrestrial Planets. Geochem. J. 15, 245.

10 Baur H. (1980) Numerische Simulation und Praktische Erprobung einer Rotationssymmetrischen Ionenquelle fuer Gasmassenspektrometer. Thesis ETHZ Zürich.

11 Hohenberg C.M. (1980) High Sensitivity Pulse-Counting Mass Spectrometer System for Noble Gas Analysis. Rev. Sci. Instrum. 51, 1075.

12 Reynolds J.H., Lumpkin G.R. and Jeffery P.M. (1980) Search for ^{129}Xe in Mineral Grains from Allende Inclusions: An Exercise in Miniaturized Rare Gas Analysis. Z. Naturforsch. 35a, 257.

13 Huneke J.C. (1978) ^{40}Ar-^{39}Ar Microanalysis of Single 74220 Glass Balls and 72435 Breccia Clasts. Proc. Lunar Sci. Conf. 9th, 2345.

14 Stacey J.S., Sherrill N.D., Dalrymple G.B., Lanphere M.A. and Carpenter N.V. (1981) A Five-Collector System for the Simultaneous Measurement of Argon Isotope Ratios in a Static Mass Spectrometer. Int. J. Mass Spectrometry Ion Phys. 39, 167.

ROB 2 URANIUM-LEAD MINERAL GEOCHRONOLOGY; Halfdan Baadsgaard; Department of Geology, The University of Alberta, Edmonton, Canada T6G 2E3

Radiometric dating of minerals using the U-Pb system is now a widely used geochronological method. Many natural uranium-bearing minerals are amenable to this method, but zircon, apatite and sphene are the most common and widespread in their occurrence. The use of U-Pb on several minerals enables internal testing of results by concordance and between minerals. Minerals vary in the way in which they give discordant dates, and this variable behaviour yields additional geological inferences. Modern mass spectrometric techniques enable U-Pb dating to be applied with high reliability to minerals containing microgram amounts of U and Pb. U-Pb dating of zircons from the major igneous rock types of the Archean in West Greenland gives times of emplacement for all but the oldest examples. Addition of sphene and apatite data to that of the West Greenland zircons shows the presence and effects of secondary metamorphism on the oldest primary intrusive rocks. The paragenetic sequence of secondary uranium mineralization in ores from northern Saskatchewan, Canada, may be followed and outlined by U-Pb dating of pitchblendes. Igneous zircons in the Cretaceous Bayonne batholith of British Columbia, Canada, are demonstrably contaminated by older material. U-Pb determinations on pyroclastic zircon from Montana furnish a geological time-scale calibration point at 63.9 million years ago for the Cretaceous-Tertiary boundary.

ROB 3 PRECISE URANIUM-LEAD AGES USING ZIRCONS;
T. E. Krogh; Mineralogy and Geology Department, Royal Ontario Museum, Toronto, Ontario, Canada M5S 2C6

Zircon is ideal for isotopic dating because it is geologically inert, crystallizes in many rocks at high temperatures, excludes background Pb, and incorporates trace amounts of U which provides two parent-daughter systems. Whereas crystals can withstand melting of their host and not lose their age, eventually at low temperatures, radiation damage accumulates and hydration and open isotopic systems can occur. Precise dating requires specialized analytical abilities, as well as techniques to eliminate such open domains.

Analytical procedures and their associated lead contamination (blank) are as follows: dissolution by HF at 220°C in a confined teflon vessel (Krogh, 1973), blank 10-30 pg, lead extraction by anion exchange, blank 10-15 pg, isotopic measurements on a solid sample mass spectrometer by thermal ionization, loading blank 1-2 pg. Total Pb is 5 to 200 ng, total Pb blank 50-100 pg. Concentrations by isotope dilution using a ^{205}Pb-^{235}U mixed tracer (Krogh and Davis, 1975) give Pb/U ratios to $\pm$ .5%, 2 sigma. Ratios of ^{207}Pb to ^{206}Pb change with time by about 0.1% every 2 Ma and are reproducible to this level after minor common Pb corrections indicated by ^{204}Pb abundances. Historically, errors due to corrections for isotopic disturbances (geological factors) far exceeded analytical errors. Now, errors of 1 to 3 Ma are achieved for rocks 200 to 3600 Ma old by creating and concentrating closed system domains (Krogh, 1980a, b). Abrasion removes outer surfaces as well as U-rich regions softened by radiation damage, and high gradient paramagnetic methods again remove U-rich grains, probably through coupled RE substitution (a low gradient device was previously employed). Abrasion also reduces background Pb and allows detection of ancient inherited cores. Duplicate samples and numerous tests against known geological sequences indicate that our new small errors are meaningful and that closely-spaced ancient geological events can now be resolved.

U-PB AGES WITHIN SINGLE ZIRCONS USING A SENSITIVE HIGH MASS-RESOLUTION ION MICROPROBE

W. Compston, I.S. Williams and S.W. Clement

Research School of Earth Sciences,
Australian National University.

A sensitive high mass-resolution ion microprobe, SHRIMP, has been constructed at the Australian National University for geological and meteoritical applications. The positive or negative primary ion beam, produced from a duoplasmatron source, can be focussed to ≈20 μm and strikes the target at 45°. Secondary ions are extracted normally and transferred to the entrance slit of the secondary mass analyzer (SMA) by a series of ion lenses and steering plates (Fig. 1). The SMA is based upon one of the designs of Matsuda (1974) for minimal second order abberation coefficients in energy and directional refocussing. It involves a cylindrical 85° electrostatic field, an electrostatic quadrupole lens and a homogeneous 72.5° magnetic field with non-normal entry (Fig. 2). The magnet has a large turning radius (1 m) to allow use of a wide source slit at resolution ≈10^4 for high sensitivity.

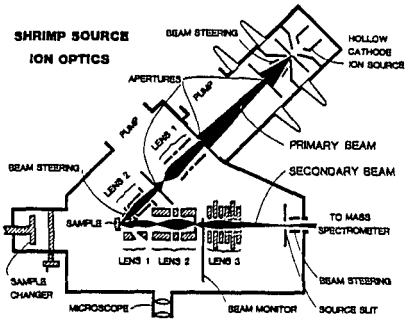


Figure 1

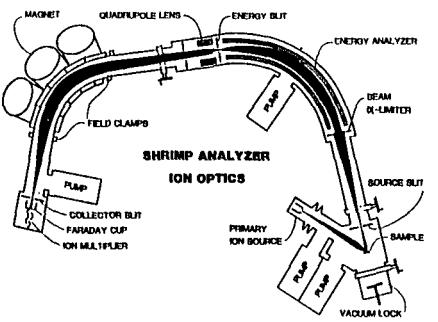


Figure 2

Zircon ($ZrSiO_4$) has several desirable characteristics which have resulted in its becoming widely used for U-Pb geochronology. Zircon crystallizes with very high initial U/Pb ratios and retains radioactive decay products particularly well. Further, it occurs as a trace mineral in most rocks and has such physical and chemical stability that it may survive several cycles of geological processes, including high temperature metamorphism and magma genesis.

For the isotopic analysis of Pb in zircon, the primary beam, O^- at energy 10 KV and a current of 10 - 15 nA,is focussed to a 35 μm waist on the sample. Positive secondary ions at 11 KV energy are extracted. Of these, 15% are intercepted by the source monitor (Fig. 1), 45% of the remainder are transmitted through the source slit set at 45 μm, and more than 90% of these are transmitted through the SMA to the collector slit set at 65 μm. The SMA forms a demagnified image about 20 μm in width so that flat-topped peaks are obtained (Fig. 3). The resolution under these conditions is 6500 (defined at the 1% valley), and the sensitivity is ≈100 ions/sec per ppm of each Pb isotope in the zircon. This resolution is the minimum necessary to separate the Pb isotopes from isobaric spectral interferences arising from dioxides of hafnium and heavy

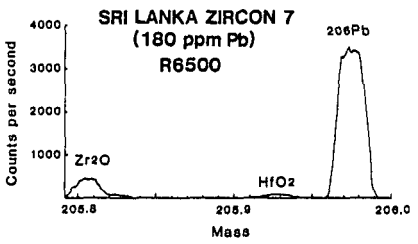


Figure 3

rare-earth elements. PbH^+ remains as a possible interference but the abundance of such ions relative to Pb^+ is < 0.1%. Isotopic ratios are measured by cyclic stepping of the magnetic field under computer control through the nominal mass sequence $^{196}(Zr_2O)$, ^{204}Pb, ion counter zero (0.040 AMU above ^{204}Pb), ^{206}Pb, ^{207}Pb, ^{208}Pb, $^{228}(Zr_2O_3)$, ^{238}U, $^{232}Th^{16}O$ and $^{238}U^{16}O$. The Pb isotopes and zero are counted for 10 seconds and the others for 1 second. During stepping, the signal from the Hall-plate field controller that the set field has been reached is followed by a delay of 1.2 seconds. This allows for small field changes elsewhere in the pole-gap due to slowly decreasing eddy currents in the magnetic circuit. The magnet yoke has been laminated and the soft-iron pole-pieces segmented to minimize such currents. The smallest digital field increment is 5 milligauss, equivalent to 0.001 AMU at mass 200. The stepped magnetic field stations are empirically trimmed at high resolution by determining the position of each collected beam with one movable edge of the collector slit, which is remotely adjustable and digitally displayed. The trimmed values correspond closely to the nuclidic masses of the beams, but not exactly. The precision observed for the Pb isotopic ratios is almost completely attributable to counting statistics.

The use of standard zircons has provided targets of accurately-known $^{206}Pb/^{238}U$ and $^{207}Pb/^{206}Pb$ and approximately-known (on a 30 μm scale) Pb concentrations. Relative to Zr_2O^+, all other species measured in the cycle decrease in intensity over the first 15 minutes of sputtering of a fresh spot and the observed $^{206}Pb^+/UO^+$ usually also decreases. This may represent the establishing of steady-state concentrations of the various elements in the target, after disturbance by the sputtering process. In addition, the observed $^{206}Pb^+/UO^+$ differs from place to place on the same uniform zircon. However, the correction factor required (d) is well correlated with changes in the observed UO^+/U^+ (Fig. 4), so that the latter can be used to relate the observed $^{206}Pb^+/UO^+$ to the true $^{206}Pb/^{238}U$ in the target. Replicate data show that the precision for the target $^{206}Pb/^{238}U$ thus measured is ≃ 3% for the mean of 5 measurement cycles, which is satisfactory for the construction of Concordia co-ordinates ($^{206}Pb/^{238}U$ *vs* $^{207}Pb/^{235}U$) used for the geological analysis of U-Pb data. Measurements are taken in cycles of 5 to allow for changes in the target composition. U concentrations in the target can be estimated by the empirical correlation between the observed UO^+/Zr_2O^+ and UO^+/U^+. Fixed analysis conditions must be employed (e.g. energy and ion density of primary beam, secondary extraction optics) to maintain fixed correlations with UO^+/U^+.

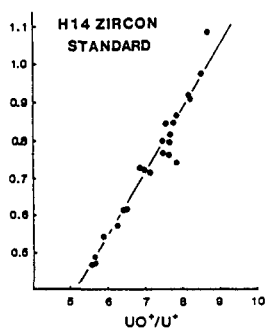


Figure 4

SHRIMP has been applied to the analysis of zircon from a variety of geological environments. An emphasis has been placed on the study of zircon populations already analyzed by conventional techniques. There are advantages in being able to compare ion probe analyses directly with those made by conventional methods. First, in the proving stages of the ion probe's operation, it provides a test of the accuracy of the probe data. Secondly, conventional analyses give average compositions of heterogeneous zircon mixtures and complement the necessarily extremely selective analyses of the probe, indicating in each case the extent to which the set of probe analyses represents all components in the sample.

Our most important conclusion so far concerns zircons' retention of radiogenic Pb. In conventional zircon studies it is usual to do several analyses of different zircon subpopulations from any one sample and thereby to define the zircons' pattern of U-Pb discordance. Common experience is that the variation in U/Pb generating the discordance pattern is consistent with variable loss of radiogenic Pb relative to U during a recent or ancient geological episode. Ion probe studies of zircon from several igneous and metamorphic rocks have shown that in most cases the conventionally-defined discordance pattern is in fact an array of compositions generated by the mixing of two or more discrete zircon components. Significantly, it is common for these components to be concordant, that is, apparently to be closed U-Pb systems. Other components may be extremely discordant, apparently having lost the majority of their radiogenic Pb, in some cases in an ancient episode, in some cases in the recent past. Several components commonly are present within single zircon grains, the crystals being comprised of layers of zircon

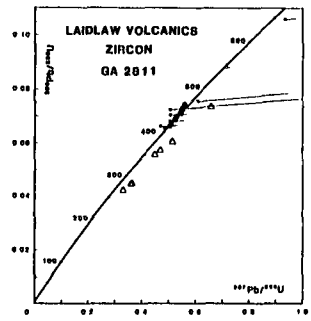


Figure 5

of different ages.

The Laidlaw Volcanics, NSW, Australia, have been dated by mineral and total-rock Rb-Sr methods at 421 ± 2 Ma. Conventional zircon analyses by Gulson and Rankin (1977) (Fig. 5, triangles) show the effects both of an inherited older component, and of a recent loss of radiogenic Pb. Ion probe analyses of the same zircon sample (circles) show most of the zircon to contain concordant U-Pb systems 421 ± 8 Ma old. We consider this zircon to be the magmatic component. The cores of a few crystals are much older, with Pb-Pb ages up to 750 Ma. Ion probe analysis has not yet identified the highly-discordant Pb-U component which the conventional analyses show must also be present.

The Dalgety Granodiorite, NSW, Australia, was formed by the melting of much older sedimentary rocks and conventional monazite U-Pb dating gives its age as 430 Ma. Conventional zircon analyses show that the granite contains zircon at least 880 Ma old which either is mixed with younger zircon or has lost radiogenic Pb in an episode less than 530 Ma ago. More recent Pb loss also is indicated. The ion probe has identified several zircon components. The predominant component, comprised of both whole grains and the rims of grains, has a Pb-Pb age that agrees with the monazite to within the analytical uncertainties which we interpret as the magmatic component. A second component, represented by the core of one grain, is at least 95% deficient in radiogenic Pb and contains high common Pb, suggesting major post-crystallization exchange between Pb in the crystal and Pb in the rest of the rock. A third component consists of grains containing discordant U-Pb systems which have a range of Pb-Pb ages up to 2800 Ma. We interpret such zircons as having survived from the granite's sedimentary source rock. One zircon crystal has been found which is comprised of layers of zircon of three distinct ages: a core at least 2800 Ma old, an intermediate layer with a Pb-Pb age ≈2300 Ma and a thin rim ≈400 Ma old (Fig. 6).

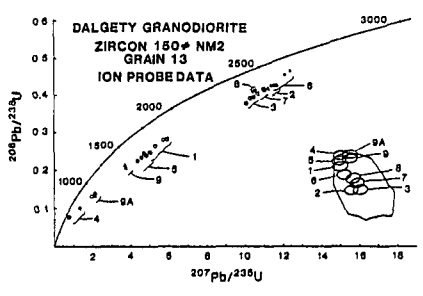


Figure 6

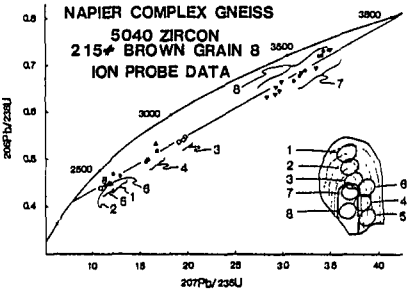


Figure 7

The original igneous rocks of the Napier Complex, Enderby Land, Antarctica, have been subject to several episodes of high grade metamorphism and deformation. Conventional analyses give zircon Pb-Pb ages between 2500 and 2700 Ma. Ion probe work has shown most of the zircon to be 2500 Ma old and only slightly discordant. Several of the grains studied have discordant older cores with Pb-Pb ages up to 3500 Ma and 2500 Ma rims. In one grain (Fig. 7), comprised mostly of ≈2500 Ma zircon, was found a tiny (100 μm) core with a slightly discordant U-Pb age of at least 3700 Ma.

Gulson, B.L. & Rankin, P.C. Geochemical comparison of Woodlawn and Mount Painter acid volcanics, southeastern Australia. *J. Geol. Soc. Aust.*, 24, (1977) 427-438.

Matsuda, H. Double focussing mass spectrometers of second order. *Int. J. Mass Spectrom. Ion Phys.*, 14 (1974) 219-233.

ROB 5 ARCHEAN GEOCHRONOLOGY OF INDIA:

Asish R. Basu, Dept. of Geological Sciences, University of Rochester, Rochester, New York 14627.

The stratigraphic, tectonic and metamorphic-plutonic history of the Indian shield, in conjunction with some reliable radiometric age data, reveal at least four regions with Archean crust. These regions are: Bihar and Orissa in the east, the Eastern Ghat Belt (coastal), southern Indian region and the Rajasthan-Bundelkhand area in the northwest. Recently, Rb-Sr and Sm-Nd data have been reported from two of these above areas. Rb-Sr whole rock data for Archean gneisses from the Gorur-Hassan area in the Southern Indian crator reveal an age of 3358±66 Ma with low initial 87Sr/86Sr ratio of 0.7000±0.0004. This low initial ratio of Sr implies a Rb-depleted source for the gneisses in the mantle. A separate study includes a Sm-Nd whole-rock isochron age of 3775±89 Ma for nine granitic and tonalite gneisses occurring as remnants within a vast granitic batholithic complex in the Bihar Orissa region. The initial Nd-isotopic ratio for this latter isochron implies a non-chondritic mantle source for these tonalites.

Because of the good control of stratigraphic and field correlations, and aided by the Sm-Nd data, the following geochronology has been established for the Archean nucleus in the eastern region: 3800 Ma - Deformation and metamorphism of the supracrustal with synkinematic intrusion of tonalite; 3000 Ma - Folding and metamorphism of the Iron Ore Group accompanied by the intrusions of a granodiorite batholith. The 3800 Ma Basement Complex of this eastern region has probable equivalents in south India and in the Eastern Ghats Belt.

QUANTITATIVE TRACE ANALYSIS BY REVERSED-PHASE LC/MS EMPLOYING CONTINUOUS SAMPLE PRECONCENTRATION

R. G. Christensen, H. S. Hertz, S. Meiselman, and E. White V
Center for Analytical Chemistry
National Bureau of Standards
Washington, DC 20234

Several methods of combining HPLC with mass spectrometry have been reported, each with its particular advantages. In the LC/MS system which we developed, the entire effluent (one to three mL/minute) from a liquid chromatograph is concentrated by allowing it to flow down the outside of an electrically heated wire. The effluent, concentrated by a factor of five to twenty, is drawn by the vacuum of the mass spectrometer through a nickel tube constructed with a miniature needle valve at the vacuum end, and is sprayed directly into the ion source of a differentially pumped quadrupole mass spectrometer. A complete description of the above LC/MS system and some examples of its application to quantitation by normal-phase liquid chromatography have been published [1].

Difficulties, which are apparently caused by the high surface tension and heat of vaporization of water, occur when attempting to spray aqueous solutions with only one atmosphere as the driving pressure. In order to extend the usefulness of the LC/MS system to reversed-phase chromatography, a "sonic sprayer" has been developed. This device utilizes the magnetostrictive behavior of the nickel capillary to induce longitudinal vibrations at 16,000-50,000 Hz. Related devices have been reported [2,3], but in each case the spray device has been separated from the ion source of the mass spectrometer by one or more skimmer nozzles or pinholes and most of the sample therefore discarded. The device constructed in our laboratory disperses the high surface tension solutions typically used in reversed-phase LC directly into the ion source as drops about 20 μm in diameter and gives uniform source pressures with water and alcohol solutions.

We have successfully applied the system, using solvent systems of methanol/water/acetic acid, to the quantitation of the anticonvulsant, valproic acid, in human serum with the results shown in Table I and the measurement of aliphatic acids in a shale oil process water as shown in Table II. In both cases, the determination was by direct injection of sample into the liquid chromatograph without any pretreatment or clean-up.

Table I

Concentration of Valproic Acid (μg/g) in SRM 1599 (Human Serum)

Level	LC/MS[a]	Certified Values[b]
Low	13.5 ± 1.4	14.5 ± 0.3
Medium	65.4 ± 10	69 ± 1.0
High	139 ± 12	143 ± 1

[a]Mean ± standard deviation of a single measurement.

[b]Mean ± standard error of the mean.

Table II

Concentration of Aliphatic Acids (μg/g) in a Shale Oil Process Water
(Mean ± Standard Deviation of a Single Measurement)

Acid	LC/MS	GC/MS[a]
Butanoic acids	91 ± 10[b]	49.6 ± 7.6
Pentanoic acid	84 ± 10	71.9 ± 8.9
Hexanoic acid	87 ± 13	87.8 ± 4.4
Heptanoic acid	136	149.5 ± 9.2

[a]Specific for n-acids.

[b]Includes n-butanoic and 2-methylpropanoic acids.

[1] Christensen, R. G., Hertz, H. S., Meiselman, S., White V, E., Anal. Chem., 1981, 53, 171-174; and U.S. Patent 4,281,246, July 28, 1981.

[2] Udseth, H. R., Orth, R. G., Futrell, J. H., 26th Annual Conference on Mass Spectrometry and Allied Topics, Paper No. RP-4.

[3] Jpn. Kokai Tokkyo Koho 81 61,643, 27 May 1981 (CA 95:125567h); Jpn. Kokai Tokkyo Koho, JP 82 00,836, 05 Jan. 1982 (CA 96:173649d).

ION EVAPORATION/MASS SPECTROMETRY OF LABILE COMPOUNDS - ANALYSIS BY MS/MS AND LC/MS

Bruce A. Thomson, SCIEX™, 55 Glen Cameron Rd., Unit 202, Thornhill, Ontario, Canada, L3T 1P2; J.V. Iribarne and P.J. Dziedzic, McLennan Laboratories, University of Toronto, Toronto, Ontario, Canada.

Last year we reported on the current status of the new technique of Ion Evaporation/ Mass Spectrometry, and presented some examples of the mass spectra of labile and polar molecules showing almost exclusively quasi-molecular ions. The technique involves the direct nebulization of solutions containing the pre-ionized species of interest, and has proven suitable for compounds which are intractable using conventional thermal vaporization techniques. These include amino acids, peptides, alkaloids, nucleosides and nucleotides.

Experimental

The technique of ion evaporation has been described in other publications (1,2). Preionized species in aqueous solution are sprayed into an atmospheric pressure gas (air or nitrogen) in the form of highly charged droplets. Ions are emitted from the droplets as they evaporate, and are drawn into the mass spectrometer system for analysis. No heat is employed, and in general, the unfragmented parent ions (MH^+ or $[M-H]^-$) which are present in the solution are detected by the mass spectrometer.

In these experiments, a Waters 6000A pump with a 440 UV detector was connected to the nebulizer with .009" ID stainless steel tubing. A μ-Bondpak C-18 column was used to separate the compounds, with water and MeOH/water solvents at a flowrate of 1 ml/min. Acetic acid at 1% was added to the solvent carrier to ensure ionization of the basic species.

The mass spectrometer system is a TAGA® 6000 triple quadrupole system equipped with an atmospheric pressure interface assembly for sampling ions directly from atmospheric pressure. Data was collected in both the MS mode (one quadrupole resolving) to identify the parent ions and the MS/MS mode to detect specific daughter ions, using both full scan and selected-ion-monitoring during the LC runs.

Results

Dopamine (MW 153), epinephrine (MW 183) and norepinephrine (MW 169) (catecholamines) are labile biogenic amines of biological interest. Their ion evaporation mass spectra (2) reveal abundant MH^+ along with minor peaks at MH^+-18. Figure 1 shows the response to an injection on column of a mixture containing 300 ng of each, monitored at the parent ion masses of m/z 170, 184 and 170, with H_2O/1% acetic acid as a solvent. Current detectibilities for these compounds are in the range of tens of nanograms.

Figure 2 shows the LC/MS analysis of a mixture of four amino acids: creatine (MW 131), valine (MW 117), leucine (MW 131) and isoleucine (MW 131). Data was collected by full scan MS, and the mass spectrum of each compound showed MH^+ as the base peak with almost no indication of fragments. The extracted ion current profiles of m/z 118 and m/z 132 are shown. Leucine and isoleucine are not resolved when the parent ions are plotted, but multiple-reaction-monitoring of specific daughter ions does reveal the presence of the two components (Figure 3). The 132 ---> 69 reaction is specific to isoleucine, while the 132 ---> 86 occurs for both leucine and isoleucine. Less than 100 ng could be detected in either the MS or MS/MS mode. Arginine, another labile amino acid, could be detected at the 20 ng level.

The tripeptide isomers Ala-Leu-Gly and Gly-Leu-Ala were separated with H_2O/1% acetic acid on the C18 column. Both showed m/z 260 $(MH^+)^*$ as the base peak, but the daughter ion spectra showed differences. Ala-Leu-Gly gave daughter ions of m/z 185 and m/z 86, while Gly-Leu-Ala gave daughter ions of m/z 142 and m/z 86. The isomers could therefore be resolved by both retention time and by specific daughter ions.

Several alkaloids have been tested and shown to give strong signals by ion evaporation. Procaine-HCl was injected in a 20/80 MeOH/H_2O solvent with 1% acetic acid, and was readily detected at the level of 2 ng on-column in either MS (at m/z 237) or MS/MS (237 ---> 100) mode.

(1) B.A. Thomson and J.V. Iribarne, J. Chem. Phys., 1979, 71, 4451-4463.
(2) B.A. Thomson, J.V. Iribarne and P.J. Dziedzic, submitted for publication to Anal. Chem.

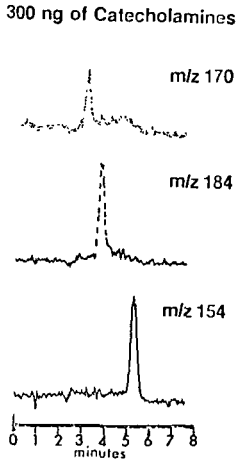


Figure 1. LC/MS of 300 ng of norepinephrine (MW=169), epinephrine (MW=183) and dopamine (MW=153).

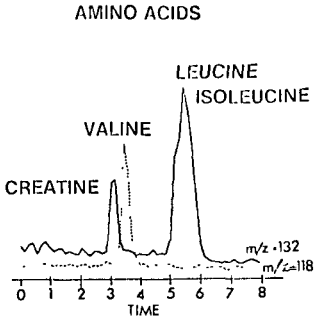


Figure 2. Extracted ion current profiles from LC/MS full scan of creatine, valine, leucine and isoleucine.

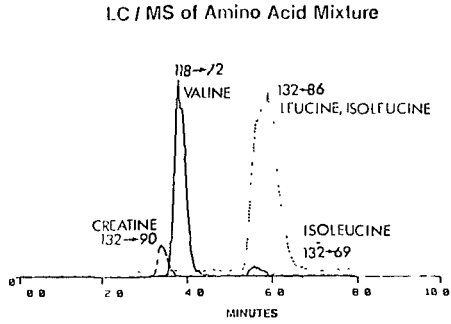


Figure 3. LC/MS/MS (multiple reaction monitoring) of specific daughter ions of amino acids.

APPLICATION OF DIRECTLY COUPLED LIQUID CHROMATOGRAPHY-MASS SPECTROMETER USING A NEW VACUUM NEBULIZING INTERFACE INCORPORATED WITH A COOLING JACKET TO THE ANALYSIS OF NONVOLATILE AND/OR THERMALLY UNSTABLE COMPOUNDS

S. TSUGE, K. MATSUMOTO, H. YOSHIDA, K. OHTA and Y. HIRATA
Department of Synthetic Chemistry, Faculty of Engineering, Nagoya University, Nagoya 464, JAPAN

A vacuum nebulizing interface for a directly coupled LC-MS was improved by incorporating a small water cooling jacket to protect the feeded LC-effluent from the overheating which otherwise caused either boiling-up or thermal decomposition of thermally untable polar compounds in the effluent at the top of the heated nebulizer. In addition, a bubble saturator was inserted in the line of the nebulizing gas supplier to adjust the nature of the nebulizing gas by saturation with a desired solution vapor which in turn acted as the reagent gas for chemical ionization(CI). Fig,1 shows a schematic diagram of the LC-MS system with the improved vacuum nebulizing interface, where a quadrapole mass spectrometer, JMS-Q10A from JEOLCO and a micr-LC, FAMILIC-100 or -300 from JASCO were used.

By these improvements, the applicability of the micro-LC-MS system was remarkably extended to various nonvolatile and/or thermally unstable natural compounds such as amino acids, small peptides, free fatty acids, saccharides and nucleosides. Fig.2(a) and (b) show typical CI mass spectra of various fatty acids observed using benzene and methanol as developing(reagent) solvents, respectively. In each mass spectrum, fairly strong quasimolecular peaks of $(M+H)^+$ can be seen. Fig.3 and 4 demonstrate the results of free fatty acid analysis in bean oil and palm oil, respectively, which were taken by 4-channel selective ion monitoring system, where a ODS separation column (0.15 mm, i.d. x 14.5 cm long) was used by a developing solvent(methanol/water =9/1) at 16 µl/min, and the nebulizing temperature wasmaintained at 200°C.

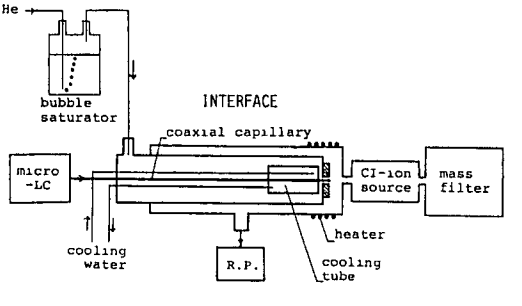
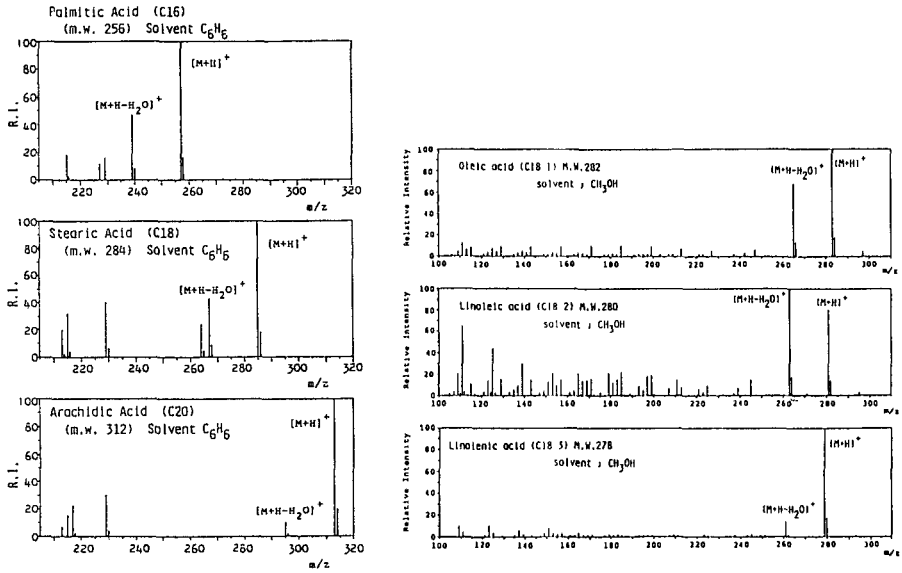


Fig.1 Flow diagram of directly coupled LC-MS system using vacuum nebulizing interface



(a) (b)

Fig.2 CI mass spectra of variou free fatty acids

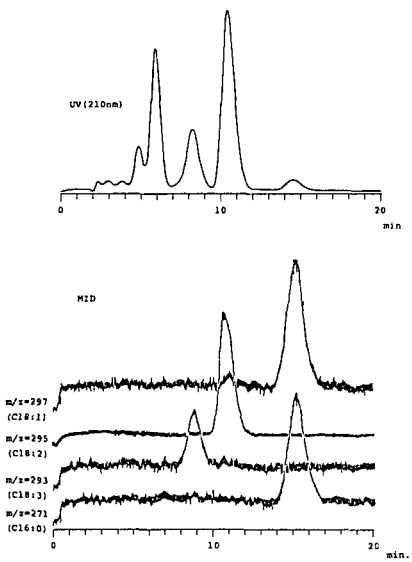


Fig.3 Mass fragmentograms of fatty acids from bean oil

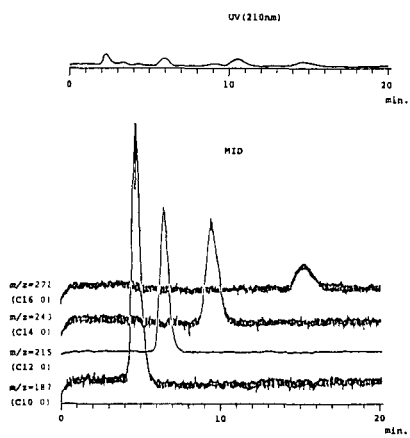


Fig.4 Mass fragmentograms of fatty acids from palm oil

THE INJECTION OF LIQUID SOLUTIONS INTO A CI SOURCE UNDER LC/MS CONDITIONS. APPLICATION TO QUATERNARY AMMONIUM SALTS IN AN ACETONITRILE SOLUTION.

P.J. Arpino(1),J.P. Bounine(2), M. Dedieu (3),G. Guiochon (1).

(1) Ecole Polytechnique, Laboratoire CAP, 91128 Palaiseau,France
(2) Rhône-Poulenc Recherches, 94400 Vitry, France
(3) Nermag Corp. 92500 Rueil-Malmaison, France.

Early LC/MS system were based on the assumption that ionization in the mass spectrometer must follow vaporization of the intact neutral solute. This meant in practice:(1) introduction of the effluent from the HPLC column into the mass spectrometer;(2) selective removal of the chromatographic carrier by a separator or by a vacuum; (3) vaporization of the neutral solute; and (4) ionization and mass analysis. However, a series of results obtained under the conditions of LC/MS, or that of other ionization techniques for mass spectrometry strongly suggest that solute ions could arise directly from a liquid solution[1]. Consequently, we now attempt to introduce liquid droplets directly into the CI source block of a quadrupole mass spectrometer.

A special device for concentrating the droplets and accelerating their speeds to sonic velocities prior to introduction into the CI source is described in paper MPA7. Interesting application work have been conducted on several non volatile molecules, including vitamin B12. An other droplet tranfer line has been tested concurrently. It is also placed between a conventional DLI nebulizer and the CI source block. The major difference (fig.1) is that the desolvation chamber is a convergent cone held at various electrical potentials. The chamber is thermally and electrically insulated from both the DLI probe and the CI source. The droplets produced by the DLI nebulizer are naturally charged as a result of the nebulization process. By applying a voltage to the desolvation chamber, it was expected that the droplets could be focussed along the chamber axis and would be repelled from the hot chamber walls. Voltages were varied in the range $\pm$ 200 V. A strong positive enhancement for the MS signals is obtained for voltages ca 80 V (the value depends on the nature and the flow-rate of the nebulized liquid. 30 µl/min of acetonitrile were injected in the experiments). For values ca 180 V, a stable Townsend discharge is obtained. The energy of the ionizing electrons from a heated rhenium ribbon can be changed from 100 eV to 3 eV, producing no visible change in the recorded mass spectrum.

Methylphenanthridinium iodide and trideuteromethylphenanthridinium iodide were successfully analyzed,using this device. As expected, when both the CI source and the desolvation chamber are at temperatures ca 200C, the salt looses methyl iodide thermally, thus the spectrum only shows a peak corresponding to the protonated molecule of phenanthridine. However, the quaternary ammonium ion is the base peak when the temperatures of both zones are set at 90°C (i.e. 100°C below the temperature of the melting point of the salt). The molecular ion is sometime accompanied by a satellite peak at 2 amu higher. Both peaks are shifted by 3 amu in the spectrum of the deuteriated analog.(figure 2).

1 Arpino, P.J.;Guiochon,G. J.Chromatogr.1982,251,153.

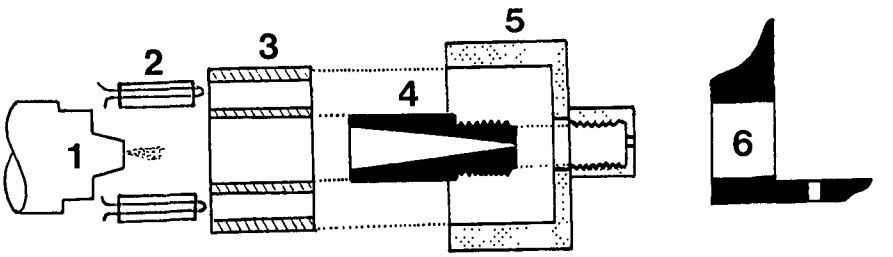
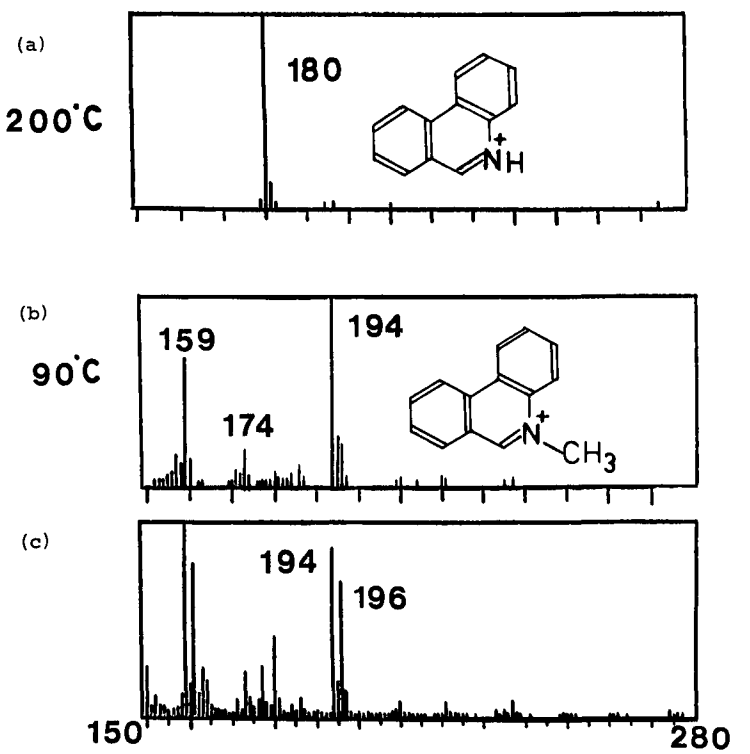


figure 1: Schematic diagram of the desolvation chamber . (1) vespel end of the DLI probe; (2) electrical heater; (3) copper heater housing; (4) copper convergent desolvation chamber held at variable voltages; (5) Macor insulator; (6) CI source block.

figure 2: Mass spectra of methylphenanthridinium iodide in an acetonitrile solution. (a) parts 4 and 6 are at 200°C; (b) and (c) parts 4 and 6 are at 90°C. The spectra (b) and (c) were recorded during the same run, at two different times, during the elution of the sample. Other spectra sometimes show m/z 196 as the base peak.

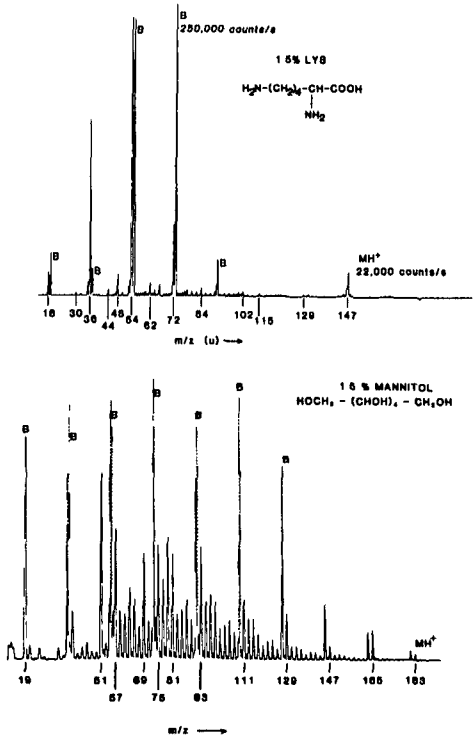


MASS SPECTRA OF POLAR ORGANIC COMPOUNDS IN AQUEOUS SOLUTIONS INTRODUCED INTO AN INDUCTIVELY COUPLED PLASMA

Robert S. Houk* and Jose A. Olivares
Ames Laboratory-USDOE and Dept. of Chemistry
Iowa State University, Ames, IA 50011
(515)294-9462

Aqueous aerosols of amino acids, saccharides, and other relatively nonvolatile compounds are introduced into an atmospheric pressure ICP that serves as the ion source for a quadrupole mass spectrometer (1). The ICP is "cooled" to limit the dissociation of sample molecules. The major peaks observed during nebulization of deionized H_2O are $H^+(H_2O)_n$ (n=1-7). These peaks are marked by the letter B in the spectra shown below. Protonated molecular ions (MH^+) of the above compounds are observed at count rates ranging from 10^2 to 10^4 counts/s. The detection limits for MH^+ ions of glycine and tartaric acid are 100 and 160 µg/mL, respectively. Numerous fragment and cluster ions are observed. The most prominent fragment ions correspond to either a) loss of small, stable molecules (H_2O, CO, CO_2) from MH^+, or b) formation of small, stable ions, e.g., NH_4^+ from amino acids. These observations agree qualitatively with those expected if fragment ions are formed via thermal degradation in the ICP (2). The ease of aqueous sample introduction into ICPs make them potentially valuable ion sources for organic mass spectrometry provided the powers of detection can be improved and the ionization, fragmentation, and ion sampling processes become better understood.

1. Houk, R. S.; Fassel, V. A.; Flesch, G. D.; Svec, H. J.; Gray, A. L.; Taylor, C. E. Anal. Chem. 1980, 52, 2283-2289.
2. Houk, R. S.; Fassel, V. A.; Svec, H. J. Org. Mass Spectrom. 1982, 17, 240-244.



MH^+ = 1200 counts/s

NUCLEOSIDE ANALYSIS BY COMBINED LIQUID CHROMATOGRAPHY-MASS SPECTROMETRY: TRANSFER RNA HYDROLYSATES; C. G. Edmonds, H. Pang and J. A. McCloskey, Departments of Medicinal Chemistry and Biochemistry, University of Utah, Salt Lake City, Utah 84112; C. R. Blakely and M. L. Vestal, Department of Chemistry, University of Houston, Houston, Texas 77004.

Transfer RNAs, functional intermediaries in protein biosynthesis, contain a high proportion of modified nucleosides. A specific modified residue, of the 60 so far identified, may occur once per isoaccepting tRNA molecule and that molecule typically contains 5-15 such residues. Two dimensional paper chromatography or methods based on ^{32}P post labeling of enzymatic hydrolysates are conventionally used to detect these modified compounds in tRNA. These procedures ultimately rely on chromatographic mobility for identification and are sometimes ambiguous. Mass spectrometry and combined gas chromatography-mass spectrometry are occasionally restricted by the insufficient volatility of many highly modified nucleosides and chemical instability to procedures for the preparation of volatile derivatives. Particularly where sample is limited, combined liquid chromatography-mass spectrometry employing particle beam interface offers unique advantages in the direct analysis of these mixtures.

The basic instrument and its operation have been previously described.[1] In brief, eluted components in a conventional reverse-phase LC eluate are concentrated into an aerosol created by the passage through a narrow heated capillary. Vapor is removed in a peripheral vacuum and the rapidly moving particle beam directed into an axially pumped ion source. Final impact-vaporization, chemical ionization of the resulting vapor cloud and quadrupole mass analysis afford useful data on a wide range of modified nucleosides. The details of this ion source configuration are shown on the left in Figure 1.

It was found that when the source of ionizing electrons was removed in the above system under appropriate conditions, ions continue to be produced.[2,3] This so-called "thermospray" ionization provides analytically useful mass spectra on a variety of involatile and thermally labile materials showing strong affinities for data obtained by other desorption ionization methods. The ion source configuration which optimizes this performance is shown on the right in Figure 1. The vaporizer is connected directly to the ion source and "thermospray" ion collection optimized by a conical sampling aperture extending to near the axis of the source volume.

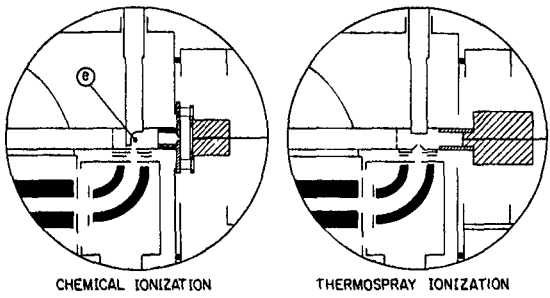


Figure 1: Alternative ion source configurations for the particle beam LC/MS instrument: CI operation (left) with an external source of ionizing electrons entering at /e/, "thermospray" operation (right) with direct vaporizer connection and conical ion exit.

These source configuration are now maintained as interchangeable options for the analysis of nucleic acid constituents. Table 1 compares system sensitivities for adenosine at the BH_2^+ fragment ions, m/z 136 and the protonated molecular ion, MH^+, m/z 268.

Table 1: Typical LC/MS System Sensitivities*
(Coulombs/microgram Adenosine)

	Ionization Mode			
Configuration	Chemical Ionization		Thermospray Ionization	
	m/z 136	m/z 268	m/z 136	m/z 268
Flat ion exit + probe	3.6×10^{-10}	3.3×10^{-13}	6.2×10^{-12}	1.7×10^{-12}
Conical ion exit + direct vaporizer inlet	1.1×10^{-13}	1.1×10^{-13}	1.4×10^{-11}**	2.5×10^{-11}**

* LC conditions: 0.01M NH_4COOH, pH 5.4, 20% MeOH.
** LC conditions: 0.1M NH_4OAc, pH 5.6, 20% MeOH.

The flat ion exit with probe operated in CI mode affords higher absolute sensitivity at m/z 136 and has proven somewhat more stable and reproducible. Markedly lower noise and a predominance of ionization in molecular species make "thermospray" operation with conical ion exit and direct vaporizer inlet the most attractive mode for qualitative investigations.

Chromatographic analysis of modified nucleosides relying on UV absorbance for detection or visualization are complicated by the occurrence of poor UV absorbing species such as for such as dihydrouridine. The advantage afforded by LC/MS analysis in positive ion CI are illustrated below by the MID experiment on three uridine derivatives separated under the conditions indicated.

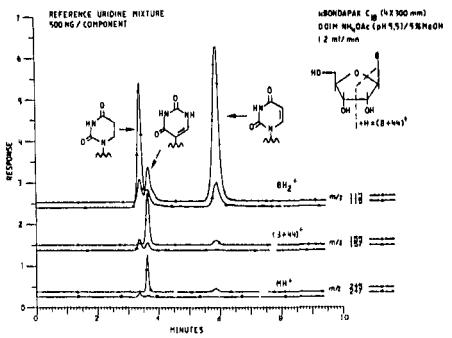


Figure 2: Chemical ionization LC/MS experiment on reference uridine mixture.

Dihydrouridine is separated from pseudouridine and is detected with uridine in positive ion CI by monitoring the protonated molecular ion (m/z 245 and 257), the protonated base (m/z 113 and 115) and ions arising from a cleavage of the ribosyl moiety as indicated at m/z 155 and 167.

MS and GC/MS analyses of thiolated nucleosides as 4-thiouridine and 5-methylaminomethyl-2-thiouridine are difficult or impossible because of instability of the free compounds and their sensitivity to procedures for derivative preparation. "Thermospray" ionization LC/MS has proven particularly useful in their detection in tRNA hydrolysates down to the level of a few nanograms.

REFERENCES

1. C. R. Blakely, J. J. Carmody and M. L. Vestal, Anal. Chem., 52, 1636 (1980).
2. C. R. Blakely, J. J. Carmody and M. L. Vestal, J. Am. Chem. Soc., 102, 5933 (1980).
3. J. J. Carmody, C. R. Blakely and M. L. Vestal. 29th Ann. Conf. Mass Spectrom. and Allied Topics, 1981, paper MPC7.

LC-MS OF NUCLEOSIDES USING A COMMERCIALLY AVAILABLE DIRECT-LIQUID INTRODUCTION PROBE.

E.L.ESMANS,Y.LUYTEN,F.C.ALDERWEIRELDT
University of Antwerp (RUCA)
Laboratory for Organic Chemistry
Groenenborgerlaan 171
B2020 Antwerp BELGIUM

P.KRIEN,G.DEVANT
Nermag S.A.
Paris FRANCE

HPLC as an analytical tool for the separation and identification of nucleosides has received growing interest in the past years. The analysis of such polar compounds is mostly performed by anion exchange-;cation exchange- and reverse phase chromatography,using non-volatile buffers ,such as phosphates,as mobile phase[1,2]. Identification of unknowns can either be accomplished by co-injection of a known standard or by enzymic peak shift procedures. In view of the already existing mass spectrometric techniques of identifying nucleosides,such as GC-MS[3],F.D.[4],F.I.[5],D/C.I.[6] etc.,the coupling of a liquid chromatograph to a mass spectrometer could broaden the analytical possibilities of structure identification of this type of compounds.

Since the early results of continuous monitoring LC-MS several interface systems have been elaborated[7].Amongst these interface systems,the direct liquid introduction (DLI)probe ,can be situated as a system capable of handling relative large amounts of water.The use of buffers is not prohibited provided that volatile salts such as ammonium acetate,ammonium formate etc. are used.

In order to establish suitable mass spectral conditions,our first experiments consisted in introducing pure nucleosides. The experimental set-up was as follows: A Spectra -Physics SP 8700 HPLC system,was connected to a Ribermag 10-10 quadrupole mass spectrometer equipped with a Sidar data-system. The connection was achieved with a DLI-probe manufactured by the same firm(Nermag S.A.).The amount of solvent (CH_3OH) ,passing through a 1-2 µm pinhole was regulated in such a way that the pressure in the ion source housing was about 2.10^{-4} Torr at 230°C. Introduction of uridine,adenosine cytidine etc.,was done separately on a LiChrosorb 10 RP 8 column (25cm,I.D.=4.6 mm) using methanol/water(80/20) and acetonitrile/water(90/10)mixtures as the effluent. All compounds show strong

$(M+H)^+$-peaks.From thymidine and inosine,the negative chemical ionization spectra were recorded,introducing the compounds in pure methanol. In this case a more recent desingn of DLI-Probe was used.[8] Typical ions were observed at m/z= B^- and m/z= $(M-H)^-$.

Further experiments were directed towards the analysis of mixtures: a) a separation of adenosine,inosine,thymidine and uridine on a μ-Bondapack C-18 column using gradient elution.(100% 0.2M NH_4OOCH^+ 100%CH_3OH in 20 min.) b)a separation of uracil,hypoxanthine,uridine,inosine,adenine etc. on a CP^{tm} Microspher C-18 column.(Fig.1)

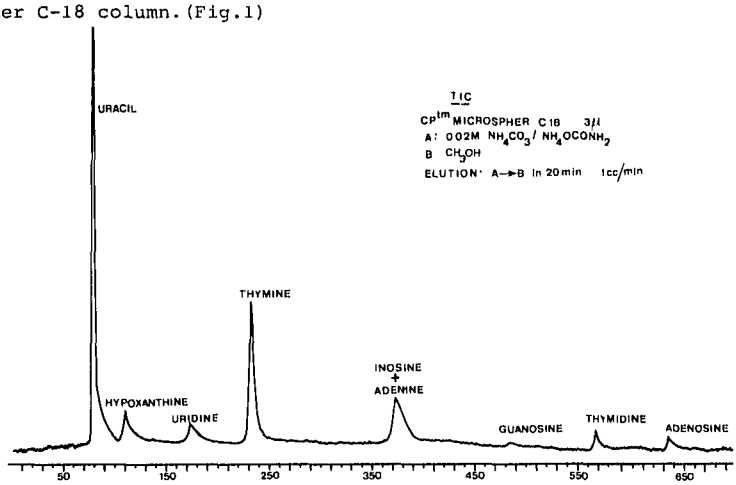


Fig.1.: TIC chromatogram of the separation of a mixture of nucleosides and nucleobases using a DLI-probe in a gradient elution experiment

ACKNOWLEDGEMENTS.

We thank the NFWO for financial support.

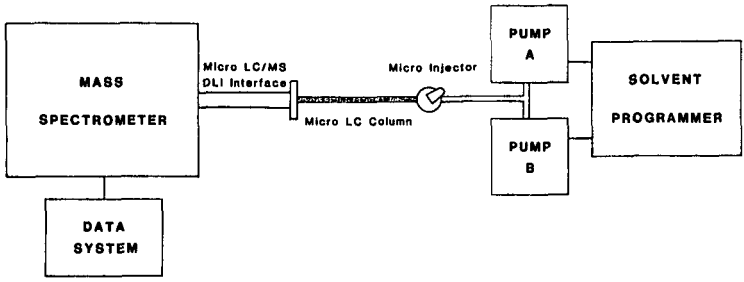
REFERENCES.

1. K.H.SCHRAM,J.A.Mc Closkey in GLC and HPLC determination of Therapeutic agents,part3,K.Tsuji Editor, Marcel Dekker Inc.,1979,P.1149
2. P.R.Brown,R.A.Hartwick,A.M.Krstulovic in Biological/Biomedical Applications of Liquid Chromatography.G.L.Hawk,Editor.Marcel Dekker Inc. 1979,p.295
3. K.H.Schram,Y.Taniguchi,J.A.Mc Closkey,Journ.Chrom.155,355(1978).
4. H.-R.Schulten,H.D.Beckey,Org.Mass Spectrom.,155,355(1978).
5. P.R.Brown,G.R.Petit,R.K.Robins,Org.Mass Spectrom.,2,521(1969).
6. E.L.Esmans,E.J.Freyne,J.H.Vanbroeckhoven,F.C.Alderweireldt,Biom.Mass Spectrom.,7,377(1980)
7. W.H.Mc Fadden,Journ.Chrom.Science ,18,97(1980)
8. M.Dedieu,C.Juin,P.J.Arpino,J.P.Bounine,G.Guiochon,Journ.Chrom.,251,203(1982)

oooooooooooooooo

APPLICATIONS OF MICRO LC/MS TO THE DETERMINATION OF DRUG RESIDUES FOUND IN EQUINE PLASMA AND URINE J.D. Henion, C. Eckers and G.A. Maylin, Diagnostic laboratory, NYS College of Veterinary Medicine, Cornell University, Ithaca, NY 14853 and J.C. Greenfield, The Upjohn Co., Kalamazoo, MI 49001

Figure 1 shows a schematic drawing of the overall micro LC/MS system used in this work. The micro LC system is set up with commercially available hardware. It consists of two piston pumps driven by a modified solvent programmer, a micro loop injector connected to the pumps by narrow bore tubing, a packed microbore LC column, the micro LC/MS interface described herein, and a quadrupole mass spectrometer with its associated data system.

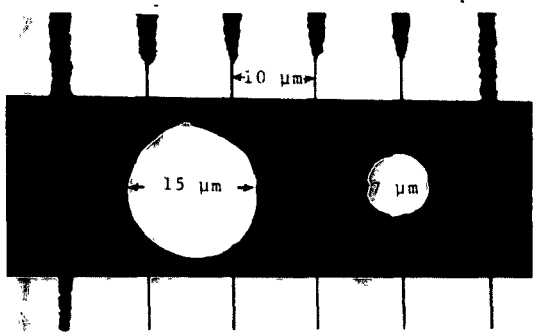


Modified DLI Micro LC/MS Probe

The micro LC/MS probe utilized in this work includes a modification of that reported earlier. In the revised micro LC/MS probe the central two concentric small bore tubes have been replaced by one tube whose dimensions are 0.004 in. i.d. x 0.062 in. o.d. x 13.5 in. This central one-piece throughput microbore tube eliminates the considerable construction details associated with the earlier device. It also eliminates the occasional plugging of the original microbore tubing.

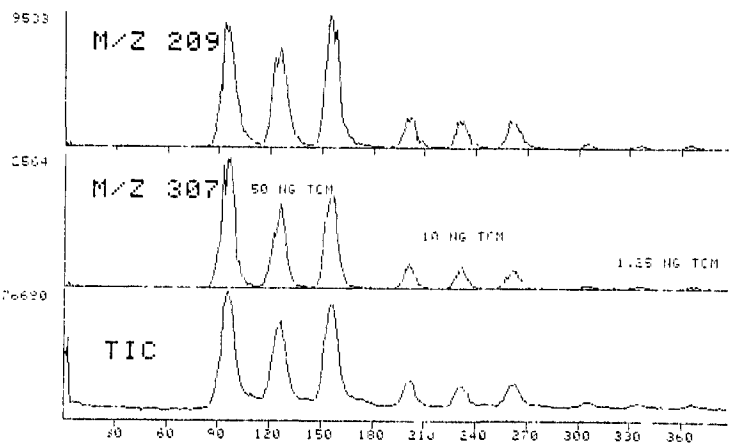
Experimental

Recently we have observed considerable variation in the performance of our DLI LC/MS technique. This variation has been traced to over-sized pinholes in the diaphragm through which the micro LC effluent passes. Figure 2 shows an 1800x photograph of two different pinholes which have actually been used for micro LC/MS. The vender reported each diameter



as 5 microns with a tolerance of plus or minus one micron. The practical detection limit for the 15 μm orifice shown on the left side of Figure 2 was 500 ng and that for the 7 μm orifice shown to its right was about 1 ng. Thus the size of the orifice in the diaphragm is critical for high sensitivity and in fact should not be greater than 5 microns in diameter.

The mass spectral ion current profiles shown in Figure 3 were obtained from triplicate injections of the diuretic trichlormethiazide (TCM). Successive on-column injections were made at 50 ng, 10 ng and 1.25 ng levels onto a Chrompack C_{18} 50 cm microbore column. This experiment reveals the typical ion current stability and reproducibility of a thirty minute micro LC/MS DLI run, and the practical detection limit of the technique for such a thermally labile molecule.



These data were obtained by operating the MS in the negative ion chemical ionization (NCI) mode with 80% CH_3CN/H_2O at a micro LC flow rate of 40 μL/min. Due to the construction of the micro LC/MS probe the entire micro LC/MS effluent is transferred to the MS. It is this feature of the interface which provides low nanogram full scan micro LC/MS detection limits from conventional MS hardware.

Micro LC/MS can be useful for the determination of antibiotics produced in fermentation broths. We have analyzed authentic standards of nodusmicin, nargenicin A, and 18-deoxynargenicin A, kindly donated by the Upjohn Company, by micro LC/MS with 73/27 CH_3OH/H_2O at a flow rate of 40 μL/min on a Whatman ODS-3 25 cm glass-lined column. These antibiotics are readily amenable to either PCI or NCI micro LC/MS displaying molecular weight and useful fragment information in each ionization mode.

A methylene chloride extract of a crude fermentation broth was analyzed by micro LC/MS with the above micro LC conditions. Although the total ion current indicated the presence of many components, the three antibiotics could be detected and verified by their NCI and PCI mass spectra. One antibiotic component was present in trace quantities but readily verified by SIM micro LC/MS experiments. These antibiotics ranged from 422 to 515 in molecular weight and are not amenable to GC/MS analysis. Since HPLC is the method of choice for their separation in the complex matrix of a fermentation broth, micro LC/MS may be the preferred method for their verification.

THE DETERMINATION OF STEROIDS AND RELATED COMPOUNDS BY MICRO LC/MS, Christine Eckers, D. Skrabalak and J.D. Henion, Diagnostic Laboratory, NYS College of Veterinary Medicine, Cornell University, Ithaca, NY 14853

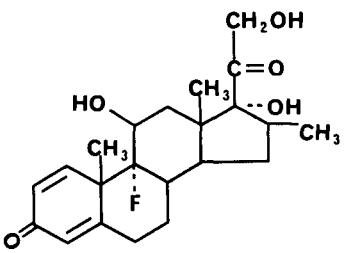
The combination of a micro LC interfaced to a mass spectrometer (micro LC/MS) by a direct liquid introduction LC/MS interface, has been shown to be a sensitive, routine method for the determination of drugs in biological and organic matrices. The equipment previously described for micro LC/MS has been used for the determination of corticosteroids in equine urine.

EXPERIMENTAL

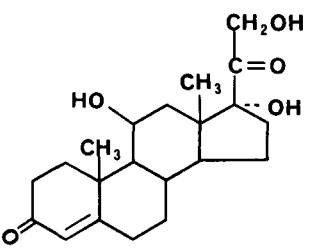
An unchanged Hewlett-Packard Model 5985B GC/MS instrument equipped for LC/MS operation was used for this work. The liquid nitrogen cooled cryopump was used in all CI LC/MS experiments as recommended by the manufacturer. Although LC/MS experiments may be conducted without cooling the cryopump, micro LC flow rates up to 50μL/min may be utilized when the cryopump is cooled by liquid nitrogen.

RESULTS AND DISCUSSION

Betamethasone (I) is a potent anti-inflammatory agent. Since very low doses produce therapeutic efficacy and the drug is rapidly metabolized, its detection in biological fluids is difficult.



I



II

The conditions for separation of betamethasone from the endogenous steroid cortisol (II) and a major metabolite, were optimized by micro LC/MS. These conditions have been used to examine urine extracts from horses administered betamethasone. Figure 1 shows the total ion current trace and mass chromatograms of major fragment ions obtained by micro LC/MS analysis of an equine urine extract. It was possible to identify the presence of betamethasone (peak C) and its major metabolite (peak A) in the extract. From examination of the chromatograms and mass spectra it was possible to detect another compound (peak B) which is not present in an extract of pre-betamethasone administration urine from the same horse. This compound had not been previously detected by TLC or micro LC with UV detection, and since it shows similar mass spectral characteristics to betamethasone and its metabolite, it appears to be another metabolite.

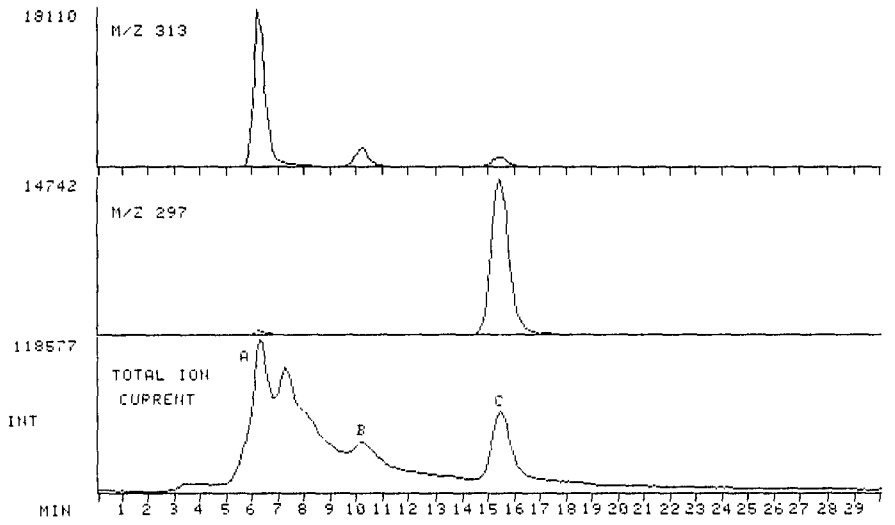


FIGURE 1. MICRO LC/MS OF URINE EXTRACT AFTER ADINISTRATION OF BETAMETHASONE. COLUMN: 50CM X 1MM ZORBAX ODS. MOBILE PHASE: 65/35 METHANOL/WATER. FLOW RATE: 40 UL/MIN.

This application illustrates the advantage of interfacing the mass spectrometer and micro LC, allowing detection of previously undetermined compounds.

HIGH-PRESSURE MASS SPECTROMETRY OF SOME LC-MS LIQUID REAGENTS

Jehuda Yinon and Aviad Cohen

Department of Isotope Research, Weizmann Institute of Science, Rehovot, Israel

When using the direct liquid introduction LC-MS interface, a part of the solvent/sample effluent enters the CI source. In such case the LC - solvent acts as the CI reagent. In an effort to optimize the CI conditions in the ion source of the mass spectrometer, we have investigated the high-pressure mass spectra of several reversed-phase LC solvents including methanol, acetonitrile and mixtures of methanol: water and acetonitrile: water. Mass spectra were recorded with a Varian MAT CH7 CI mass spectrometer. Samples were introduced through a short, heated liquid inlet system connected to the source through a needle valve.

We have recorded the mass spectra of these solvents as function of repeller voltage, temperature and pressure. As has already been reported previously (1,2) methanol at CI pressures forms a series of protonated ions of the type $[(CH_3OH)_nH]^+$, the abundances of which are pressure dependant. Similarily, in acetonitrile a series of protonated ions of the type $[(CH_3CN)_nH]^+$ are formed.

In both acetonitrile and methanol, with increasing temperature there is a decrease in the relative abundances of the cluster ions and an increase in the relative abundance of the MH^+ ion. The increase of repeller voltage brings a decrease in the relative abundances of the MH^+ and the cluster ions.

Figure 1 shows the relative abundance of the MH^+ ion as function of source pressure in pure acetonitrile and in two mixtures of acetonitrile with water. A slight shift of the maximum is observed towards higher pressures with the increase of the amount of water in the mixture. This could indicate that the ion - molecule reaction in acetonitrile leading to formation of the MH^+ ion is more dominant than the proton transfer reaction from the H_3O^+ ion to the acetonitrile. This can also be seen in the mass spectra of acetonitrile: H_2O (25:75) and acetonitrile:D_2O (25:75) as shown in Figure 2. In the mass spectrum of the acetonitrile: D_2O mixture we can differentiate between that part of the MH^+ ion formed by ion - molecule reaction (m/z 42) and the part of MH^+ formed by proton transfer from the D_3O^+ ion (m/z 43).

In methanol: water mixtures no differences in pressure dependance of the MH^+ ions were observed for different amounts of water.

The CI mass spectra of some amino acids were recorded with methanol:water and acetonitrile:water as reagents at various pressures. At 0.05 Torr a small MH^+ ion and fragment ions are observed. At 0.1 Torr the MH^+ forms the base peak with the addition of small fragment ions and some adduct ions. At 1 Torr the adduct ions carry the majority of the ion current.

The decision what pressure to use should depend on the particular application. As the flow rate of the solvent is determined mainly by chromatographic considerations, one should be able to determine independantly the pressure in the ion source.

References

1. M.A. Baldwin and F.W. McLafferty, Org. Mass Spectrom. 7, 111 (1973)
2. P. Arpino, M.A. Baldwin and F.W. McLafferty, Biom. Mass Spectrom. 1, 80 (1974)

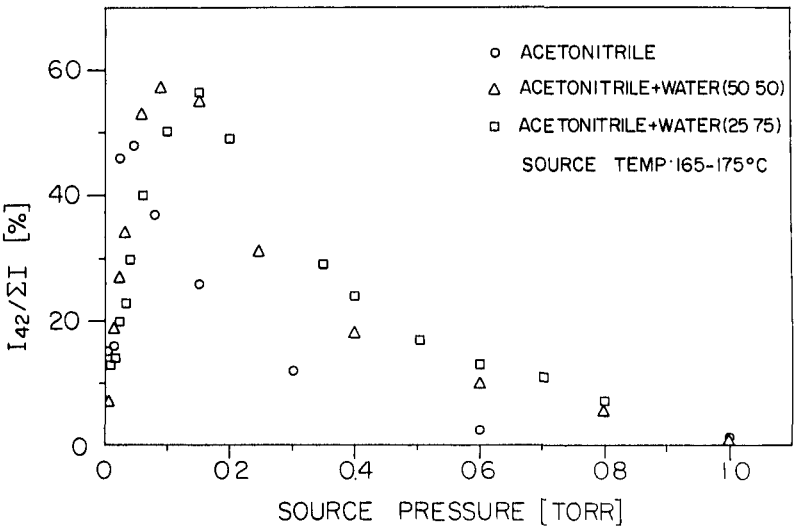


Figure 1

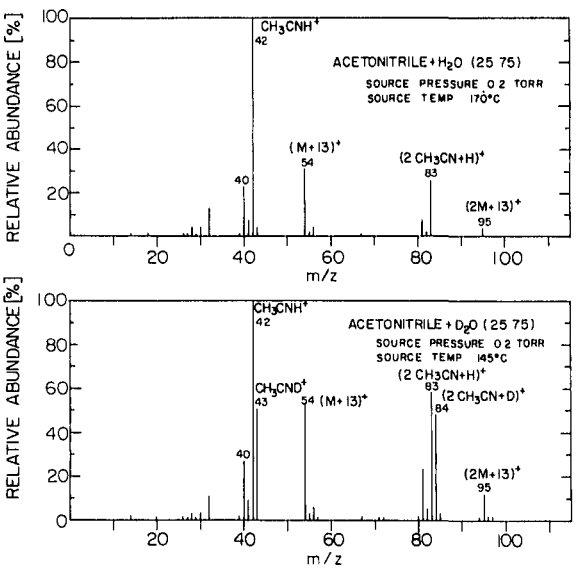


Figure 2

APPROACHES TO ON-LINE ION-PAIR EXTRACTION AND DERIVATIZATION FOR HIGH-PERFORMANCE LIQUID CHROMATOGRAPHY-MASS SPECTROMETRY

PAUL VOUROS*, E.P. LANKMAYR, M.J. HAYES and B.L. KARGER

Institute of Chemical Analysis and Department of Chemistry,
Northeastern University, Boston, MA 02115 (U.S.A.)

and

JOHN M. McGUIRE

U.S. Environmental Protection Agency, Athens Environmental Research Laboratory
Athens, GA 30605 (U.S.A.)

The use of ion-pairing reagents to increase the compatibility of high-performance liquid chromatography (LC) coupled with mass spectrometry (MS) is demonstrated. Counter-ions were selected for examination on the basis of the structural requirements for mass spectrometric fragmentation and the on-line extractability of their ion pairs with different solutes into organic solvents. The use of aromatic (e.g. naphthalenesulfonate, picrate) instead of aliphatic (e.g., n-decylsulfate) counter-ions shows a significant simplification of the resulting electron impact mass spectra of the solutes. Thus, structural information on the solutes can be easily obtained, especially when relevant peaks occur at lower m/z values. A second example of on-line chemical transformation for LC-MS is shown in the use of trimethylanilinium hydroxide for selective methylation. These results along with previous work, demonstrate practical approaches to enhance the on-line LC-MS method using the moving-belt interface. The incorporation of on-line chemical procedures between the HPLC and the mass spectrometer may provide practical approaches to the solution of a variety of analytical problems. Moreover, such approaches permit the optimization of HPLC separation procedures relatively independent of the specific mass spectrometer and/or interface.

Journal of Chromatography, 251, 175 (1982)

PHOTOIONIZATION MASS SPECTROMETRY OF CH_3SH, CD_3SH AND CH_3SD: HEATS OF FORMATION OF $CH_3S^+(CH_2SH^+)$, CH_2S^+, CH_2S AND HCS^+ *

R. E. Kutina, A. K. Edwards,** G. L. Goodman and J. Berkowitz
Physics Division, Argonne National Laboratory
Argonne, Illinois 60439

The first (lowest energy) intense fragment observed in the decomposition of thiomethanol ion involves loss of an H atom, as in methanol. The structure of this fragment from methanol has been clearly established to be CH_2OH^+, whereas electron impact studies show that CD_3S^+ has a lower appearance potential from CD_3SH than does CD_2SH^+, implying that CH_3S^+ is more stable than CH_2SH^+. We have examined this process by photoionization mass spectrometry on both CD_3SH and CH_3SD (see Figs. 1 and 2).

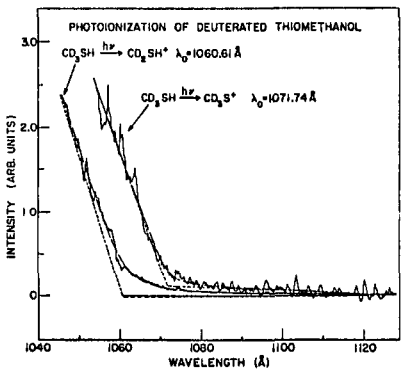


Figure 1

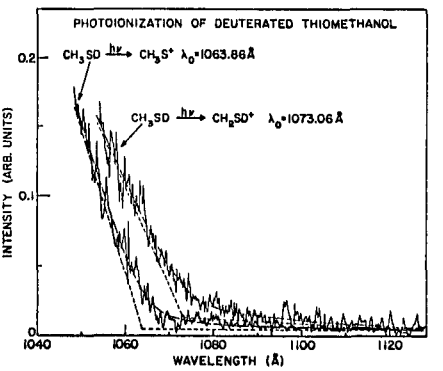


Figure 2

Our results for CD_3SH are in qualitative agreement with the electron impact data; CD_3S^+ has a lower threshold than CD_2SH^+, by ~0.11 eV. However, the corresponding experiment on CH_3SD yields a lower threshold for CH_2SD^+ than CH_3S^+, by ~0.10 eV. Detailed examination of several isotopic combinations using known frequencies and calculated frequencies based on a normal coordinate analysis shows that these thresholds are compatible with a single structure, the alternate thresholds resulting from zero point energy differences. If two structures are involved, they differ in heats of formation by <0.03 eV. An examination of the evidence from this and other studies does not clearly establish which (if either) structure is the more stable one.

At higher energy, this fragment decomposes further to $HCS^+ + H_2$ (or deuterated analog). From the threshold for HCS^+, we deduce $\Delta H^\circ_{f,0}$ (HCS^+) $\leq$ 259.2 ± 0.9 kcal/mole, which is in excellent agreement with a bracketed proton affinity[1] for CS, that can be converted to $\Delta H^\circ_{f,0}$ (HCS^+) = 256 ± 4.5 kcal/mole. These values differ by at least 30 kcal/mole from an ab initio CI level calculation. The experimental results can be used to

predict that HCS^+ should be formed in interstellar clouds by an exothermic reaction and, in fact, it has recently been observed.

When the various ion yield curves from CH_3SH are differentiated and normalized, their sum is in good agreement with the photoelectron spectrum of CH_3SH. However, the higher energy peaks in the derivative curve, whose origin is the HCS^+ ion yield curve, are about 1/3 as intense as in the corresponding photoelectron spectrum. A plausible interpretation is that HCS^+ is produced primarily with excess kinetic energy of ~1 eV, but also weakly at threshold without excess kinetic energy. These results support Harrison's[2] observation of metastable ions with ~0.9 eV kinetic energy in the decomposition of CD_3S^+ and CD_2SH^+. The detailed nature of this decomposition remains an enigma, partly because of uncertainty regarding the structure of the first daughter (CH_3S^+ or CH_2SH^+). Various alternatives will be discussed.

References

*Work supported by the United States Department of Energy, Office of Basic Energy Sciences under Contract W-31-109-Eng-38.

**A. K. Edwards - Permanent address: University of Georgia, Athens, GA 30602

1. T. McAllister, Astrophys. J. 225, 857 (1978).

2. A. G. Harrison, J. Am. Chem. Soc. 100, 4911 (1978).

^{252}Cf-PDMS OF PHOTOACTIVATED AL_2O_3 FILMS; D. Jacobs and R. D. Macfarlane; Texas A&M University, College Station, Texas 77843

The ^{252}Cf-PDMS spectra of thin Al_2O_3 films is dominated by a set of cluster ions in the positive and negative ion spectra of the type $AlO^+ \cdot xAl_2O_3$ and $AlO_2^- \cdot xAl_2O_3$ extending beyond m/z 3000. In addition, there are minor sets of cluster ions (e.g. $H^+ \cdot xAl_2O_3$, $OH^- \cdot xAl_2O_3$) that appear to originate from sites in the film that are reactive. Illumination of these films by 185 nm light results in the attachment of up to 3 hydrogen molecules to these cluster ions but not to the others. This phenomenon is believed to be the result of photoactivation of particular surface states. Previous studies on photo-induced processes in Al_2O_3 have also demonstrated H_2 adsorption using other spectroscopic methods. This work shows that the recently developed surface MS methods may be useful in obtaining more detailed information on photo-induced surface interactions. This research was sponsored by the National Science Foundation (CHE-79-04863) and the Robert A. Welch Foundation (A-258).

THE EFFECT OF SOURCE TEMPERATURE ON THE PHOTODISSOCIATION OF POSITIVE MOLECULAR IONS.

F.M.Harris, I.W.Griffiths, E.S.Mukhtar and J.H.Beynon.

Royal Society Research Unit, University College of Swansea, Singleton Park, Swansea SA2 8PP, U.K.

Over the past three years, commercial double-focusing mass spectrometers have been successfully modified in this Laboratory [1,2] for studies of photodissociation of ions. With the ZAB-2F spectrometer, ions of a pre-selected species enter the second field-free region where they are irradiated with light from an argon-ion laser. This region is highly evacuated and the photoexcited ions are unlikely to experience collisions with neutral molecules. Further, the number density of ions is such that photoexcited or photofragment ions are unlikely to experience ion-ion interactions. The photoexcited ions, if they dissociate, thus do so in a collision-free environment which is an important aspect of this experimental technique. It follows that competing dissociation reactions of isolated photoexcited ions can be studied and in the case of some ions the relative rates have been shown to be highly dependent on the photoexcitation energy [2,3]. Changes as small as 0.1 eV in the total internal energy of the photoexcited ions can produce significant changes in the ratios of the fragment ions formed via competing dissociation pathways. Another aspect which has been studied in detail is the release of translational energy in a particular dissociation reaction; for several ions this also has been shown to depend sensitively on the photoexcitation energy [4].

Because the results from both types of experiments are sensitively dependent on the total internal energy of the photoexcited ions, it was decided to investigate if changes in the average internal energy of the ions prior to photoexcitation could be detected. In these experiments the photoexcitation energy was held constant by working with one laser-light wavelength; changes in the internal energy of the parent ions were effected by changing the temperature of the EI source in which the ions were formed over the range 70°C to 240°C.

The effect of source temperature on competing photodissociation reactions of *n-butylbenzene and n-pentylbenzene molecular ions photoexcited with 2.41 eV photons* was studied. Earlier results had shown that competing dissociation reactions for each species give rise to photofragment ions 91^+ and 92^+ and that at a fixed source temperature the ratio $91^+/92^+$ increased rapidly as the photoexcitation energy increased. The present work showed that at a fixed photoexcitation energy the ratio $91^+/92^+$ increased significantly as the source temperature changed in the range 70-240°C. By comparing results from these two experimental procedures it is estimated that a 100°C change in source temperature changes the average internal energy of the photoexcited ions by about 0.27 eV.

In a separate and different type of experiment, the effect of source temperature on the average translational energy, $\overline{T}_t$, released when ions photo-excited through a fixed energy dissociate has been studied. Increases in $\overline{T}_t$ were observed on increasing the source temperature and again the magnitude of the change in internal energy necessary to cause the effect can be estimated by comparing the results with those obtained at one source temperature and various photoexcitation energies. Such a comparison indicates that for the ions studied (t-butylbenzene, nitrobenzene and n-propylbenzene molecular ions) the average change in the internal energy of the photoexcited ions is about 0.21 eV when the source temperature changes from 400 to 500K.

The present experiments show that the average internal energies of the ions reaching the second field-free region of the ZAB are increased by between 0.2 and 0.3 eV when the source temperature is increased by 100°C. Thermal excitation of the ions after they are generated in the source is unlikely because (a) the ions are extracted by a weak electric field and don't make contact with the walls of the ionization chamber; and (b) the sample pressure in an EI source is not high enough to give rise to significant ion-molecule collisions. The effects observed must thus be due to thermal excitation of the sample molecules which is reflected in the average internal energy of the ions. Using available thermochemical data [5] for some of the samples investigated, it is calculated that changes in the average internal energy of the molecules of between 0.2 and 0.3 eV occur as the source temperature changes from 400 to 500K. These changes are approximately the same as those observed in the ions over the same temperature range.

References

1. F.M.Harris, E.S.Mukhtar, I.W.Griffiths and J.H.Beynon, Proc.Roy.Soc. A.374 461 (1981).
2. E.S.Mukhtar, I.W.Griffiths, F.M.Harris and J.H.Beynon, Int.J.Mass Spectrom. and Ion Phys. 37, 159 (1981).
3. E.S.Mukhtar, I.W.Griffiths, F.M.Harris and J.H.Beynon, Org.Mass Spectrom. 15, 51 (1980).
4. E.S.Mukhtar, I.W.Griffiths, R.E.March, F.M.Harris and J.H.Beynon, Int.J.Mass Spectrom. and Ion Phys. 41, 61 (1981).
5. F.D.Rossini, K.S.Pitzer, F.L.Arnett, R.M.Braun and G.C.Pimentel, Selected Values of Physical and Thermodynamic Properties of Hydrocarbon and Related Compounds, Carnegie Press, Pittsburgh (1953).

ROD 4 PHOTOFRAGMENT SPECTROSCOPY STUDIES: ENERGY PARTITIONING AND ION STRUCTURE, R.E. Krailler, A.E. McLaurin and D.H. Russell, Dept. of Chem., Texas A&M Univ., College Station, TX. 77843.

Photodissociation spectroscopy (PDS) has provided important information on structure and rearrangement reactions of gas phase ions. The bulk of these studies were performed on an ion cyclotron resonance (ICR) mass spectrometer. Using ICR-PDS the fate of the energy dilvered to the ion in photon absorption cannot be investigated; however, photodissociation of ions in the ion beam of double focussing mass spectrometer, in combination with metastable ion scanning methods, can be utilized to probe the conversion of internal energy of the fragmenting (photoactivated) ion into translational degrees of freedom. The latter technique has been coined photofragment spectroscopy (PFS). In our laboratory we are presently using PFS for investigations on energy partitioning and for studies on rearrangement reactions of unsaturated hydrocarbon systems. These studies will be discussed with particular emphasis on results from energy partitioning data.

ROD 5 ION FRAGMENTATION KINETICS AS A PROBE OF MULTIPHOTON IONIZATION. D. M. Rider, J. Durant, S. Anderson and R. N. Zare; Department of Chemistry, Stanford Univ., Stanford, CA 94305

The production of metastable ions is a common occurence in VUV photoionization. It is then surprising that only a few metastables have been observed in molecules ionized by multiphoton absorption. We have found that metastables can be produced by multiphoton ionization of substituted benzenes. The fragmentations of the metastables produce daughter ions that appear as broad assymetric peaks in the time-of-flight mass spectrum. Fragmentation rates of the metastables can be derived from the peak shape. The fragmentation rate is found to vary with the excitation wavelength. This rate is very sensitive to the internal energy of the parent ion and is used as a probe of the multiphoton ionization process.

Supported by the Air Force Office of Scientific Research (AFOSR 81-0053-A).

MULTIPHOTON IONIZATION--POTENTIAL AND LIMITATIONS

J. W. Hudgens, M. T. Duignan, T. G. DiGiuseppe, and J. R. Wyatt
Naval Research Laboratory, Washington, D.C. 20375

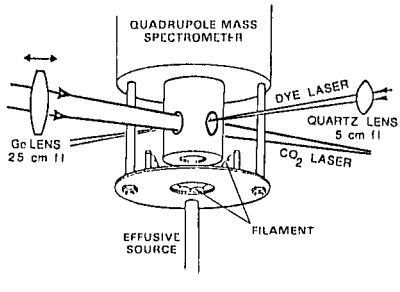
Mass Spectrometry has the ability to detect ions of a given mass with unit efficiency. Hence, the principal improvement in mass spectrometry can only occur in the method of ionization. New methods of ionization cannot only improve the sensitivity of ionization but the selectively as well. In fact, for many analytical problems the ultimate detection limit is determined by the selectivity more than the sensitivity.

In spite of the rapid advance of many areas of technology, electron impact remains the technique of choice for the ionization of molecules in the gas phase. Electron impact is not a selective form of ionization as all molecules having an ionization potential less than the electron energy are ionized.

An alternative to electron-impact ionization is photon impact. The principal photon source for laboratory experiments has been the resonance lamp. The advent of lasers, in particular the recent advent of the excimer laser, provides a new source of ionizing radiation for the mass spectrometrist. Since laser radiation is monochromatic, can be focussed to a small volume, and does not have a space charge limit, it can overcome these drawbacks.

Unfortunately the single photon energy of lasers (6.42 eV ArF, for example) is insufficient to produce ionization. However, the high powers make possible ionization *via* multi-photon absorption. In fact, this process can occur although the molecule being ionized has no resonant absorption for a single-photon process. If the molecule being ionized has a single or multi-photon resonant state, both the selectivity and sensitivity of the ionization can be dramatically increased. The technique of resonance enhanced multiphoton ionization has been given the acronym REMPI.

The experimental apparatus is depicted in the Figure. Particular care was taken to assure that none of the photons struck any of the ionizer surfaces. Previous work at this laboratory using a high-powered CO_2 laser had shown that ions can readily be produced when the ionizer surfaces are irradiated. Samples were introduced directly as gases from an effusive source. To study radicals this source was modified so that radicals could be produced by pyrolysis.



For our initial experiments investigating multiphoton ionization we used an ArF excimer laser.[1] Mass spectra were obtained using the laser and 10eV and 70eV electrons.

Most of the fragmentation patterns using the laser were similar to the low-energy electron-impact patterns. Since ions produced by electron impact and multiphoton ionization are produced in somewhat different regions of the ionizer, their kinetic energy and acceptance by the mass filter would vary. Therefore, it is best to compare the intensities of ions which vary slightly in mass. For example the m/z ratio 91/92 for ions from toluene by multiphoton ionization and 10eV electron impact is approximately 0.5 whereas by 70eV electron impact it is 1.3. Similar results were observed for the m/z ratios of 30/29 and 29/28 of ethane. A simpler molecule such as ammonia also shows the same trend in the m/z 17/16 ratio. Not all compounds behave in this manner. For example the benzaldehyde spectrum produced by multiphoton impact shows little intensity at m/z 106 and 105, which are major peaks in the electron-impact spectra.

For the majority of the molecules studied, the multiphoton-ionization mass spectra and low-energy electron impact mass spectra are virtually identical. From this result, we infer that the ionization process is due to the sequential absorption of two photons. The process must involve non-resonant absorption of the first photon since molecules such as the alkanes have no excitation by 6.42 eV photons. Even in molecules such as benzene, in which excited states are accessible, there must be little dissociation of these states during the time (20 ns) of the irradiation. The fact that certain molecules, most notably benzaldehyde, show multiphoton-ionization mass spectra significantly different from low-energy electron-impact implies different mechanisms than direct ionization are operative. The most reasonable mechanism would be that benzaldehyde rapidly dissociates upon absorption of one photon such that only its dissociation products are available for ionization.

More recently, we investigated the use of tunable lasers to ionize selectivity by REMPI. We have used REMPI to distinguish between cis and trans isomers.[2] For example, the ion current for both cis and trans dichloroethene has strong absorption peaks between 440 to 460 nm. Since these features do not overlap it is possible to ionize selectively one of the isomers in a tenfold excess. The major ion produced is C_2H_2 for which two HCl molecules have been eliminated from the parent molecule prior to ionization.

REMPI also can be used to detect radicals in the presence of neutral species which produce strong interferences at the masses used for radical detection. We have used REMPI to detect methyl radicals produced by the the thermal decomposition of azomethane.[3] The intensity of the methyl ion shows a strong resonance at 451 nm which corresponds to a resonant three-photon absorption. The absorption data correlates well with VUV spectroscopy of the methyl radical. Absorptions observed by REMPI at 328-334 nm for CH_3 have led us to postulate new previously unobserved states for the methyl radical.[4]

REMPI also has been used in this laboratory to compare CF_2 radicals produced by thermal decomposition and infrared multiphoton photolysis (IRMPD) of CF_2 containing compounds.[5] CF_2 shows a rich three-photon absorption spectra in the 410-490 nm region. Only CF_2 produced from CF_2I IRMPD showed any wavelength dependence. We have postulated that this effect is due to vibrationally-hot CF_2 produced by IRMPD such that the structure in the REMPI absorption spectrum washes out.

References

1. M. E. Seaver, J. W. Hudgens, and J. J. DeCorpo, Int. J. Mass Spectrom. Ion. Phys., 34, 175(1980).

2. J. W. Hudgens, M. E. Seaver, and J. J. DeCorpo, J. Phys. Chem., 85, 761(1981).

3. T. G. DiGiuseppe, J. W. Hudgens, and M. C. Lin, J. Phys. Chem., 86, 36(1982).

4. T. G. DiGiuseppe, J. W. Hudgens, and M. C. Lin, J. Chem. Phys, 76, 3338(1982).

5. T. M. Duignan, J. W. Hudgens, and J. R. Wyatt, submitted for publication.

ANALYTICAL MULTIPHOTON IONIZATION STUDIES OF IRON-CONTAINING COMPOUNDS

W. W. Harrison,* D. M. Rider, and R. N. Zare
Department of Chemistry
Stanford University
Stanford, CA 94305

Multiphoton ionization (MPI) techniques have been directed to the study of numerous organometallic compounds,[1-5] usually with the intent of examining dissociation/ionization mechanisms. The efficiency with which such multiple photon absorption can produce ionization of the metal atom is evident from the mass spectra obtained, which show the singly charged metal ion to be the overwhelmingly dominant species. Our interest in these studies is to explore potential analytical aspects of MPI methodology for trace element analysis. In principle, MPI could lead to enhanced sensitivity and selectivity in comparison to current analytical mass spectrometric approaches.

Experimental

A Nd:YAG laser (Quanta Ray DCR-1A) is used to pump a tunable frequency doubled dye laser (Quanta-Ray PDL-1), the output of which is coupled to a time-of-flight mass spectrometer, designed and built in this laboratory.[6] Mass spectra and wavelength ionization spectra were obtained for iron pentacarbonyl and 1,1'-dimethyl ferrocene, which were introduced through a heated leak valve from glass vials containing the pure compound. A small auxiliary vacuum manifold is used to prepare organometallic/argon dilutions in one-liter flasks for analytical studies. The collimated laser beam had a diameter of 3-5 mm and delivered approximately 4 mj/pulse at peak dye response.

Results and Discussion

A mass spectrum taken at 280 nm of iron pentacarbonyl (5×10^{-8} torr) is dominated by the iron isotopes plus minor contributions from such species as $Fe(CO)^+$ and $Fe(CO)_2^+$. Using the dye R590, 275-285 nm wavelength scans were then obtained for $^{56}Fe^+$ and $Fe(CO)_2^+$. The latter is continuous and unstructured. The spectrum for $^{56}Fe^+$ was highly structured, as shown in Figure 1. The lines can be identified as arising from iron atomic transitions

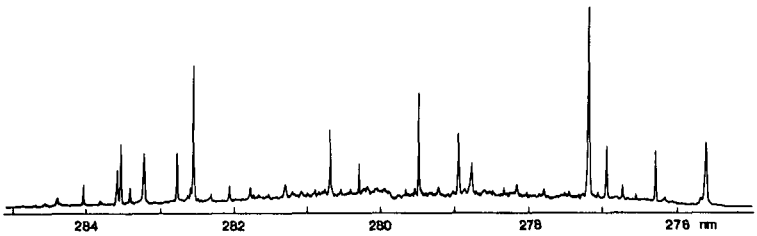


Figure 1. Wavelength ionization spectrum of $Fe(CO)_5$ for $^{56}Fe^+$.

wherein the tunable laser radiation is absorbed by resonant states, thus leading to sharp increases in the $^{56}Fe^+$ signal. At wavelength regions between these transitions, a small nonresonant ion signal is observed. When the laser beam is focused (the power density increasing ~100×), nonresonant ionization becomes much more significant and the spectrum begins to lose its line-like characteristics. The most sensitive analytical line is seen at 277.2 nm. Another wavelength range explored was 247-254 nm, obtained by anti-Stokes Raman shifting with H_2 of the frequency doubled R590 output. While the nominally best iron analytical line is to be found at 248.3 nm,[7] because of the reduced power levels resulting from the Raman shifting, the 277.2 nm unshifted line actually gave better sensitivity. Coumarin 500 dye was used to scan the 264-274 nm region. Sharp line spectra similar to Figure 1 resulted, but no line was found to be more intense than the 277.2 nm

*On leave from the Department of Chemistry, University of Virginia

line. Since iron has nearly 5,000 spectral lines covering the UV and visible regions, it would require many dyes and much time to thoroughly evaluate its rich spectrum. However, 277.2 nm serves as a quite sensitive transition in a convenient working region. Using this line, Figure 2 shows the effect of laser power on $^{56}Fe^{+}$ ion intensity. The response

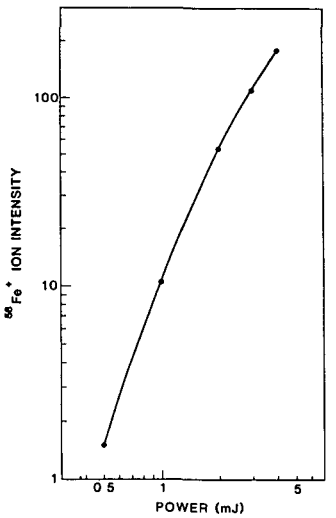


Figure 2. Effect of laser power on $^{56}Fe^{+}$ signal intensity at 277.2 nm.

tends to break off from linearity at the higher power levels, an effect which is aggravated when using focused laser radiation to produce higher power densities. Mass spectra and wavelength ionization spectra have also been obtained for 1,1'-dimethyl ferrocene. The mass spectrum shows primarily the iron isotopes with a parent molecular ion at about 3% the intensity of $^{56}Fe^{+}$. The Fe^{+} wavelength spectra yield the same response as shown in Figure 1; no spectral structure was observed for the parent ion. For sensitivity studies, iron pentacarbonyl samples at 1 torr and 0.1 torr, respectively, were diluted to atmospheric pressure with argon. From signal/background response, calculated sensitivities in the low ppm range have been obtained.

References

1. P. C. Engelking, Chem. Phys. Lett. 74, 207 (1980).
2. M. A. Duncan, T. G. Dietz, and R. E. Smalley, Chem. Phys. 44, 415 (1979).
3. Z. Karny, R. Naaman, and R. N. Zare, Chem. Phys. Lett. 59, 33 (1978).
4. D. W. Trainor and S. A. Mani, J. Chem. Phys. 68, 5481 (1978).
5. D. P. Gerrity, L. J. Rothberg, and V. Vaida, Chem. Phys. Lett. 74, 1 (1980).
6. D. Proch, D. M. Rider, and R. N. Zare, Chem. Phys. Lett. 81, 430 (1981).
7. G. F. Kirkbright and M. Sargent, "Atomic Absorption and Fluorescence Spectroscopy," Academic Press, London, 1974.

Support of the Department of Energy (DE-AS058010635) and the Army Research Office (DAAG-29-80-K-0097) is gratefully acknowledged.

LASER DESORPTION TLC/CI MASS SPECTROMETRY

L. Ramaley and Margaret-Anne Vaughan, Dept. of Chemistry, Dalhousie University, Halifax, N.S., W.D. Jamieson, National Research Council of Canada, Halifax, N.S., and N.H. Burnett, National Research Council of Canada, Ottawa, Ont., Canada.

A TLC scanning apparatus which interfaces directly to a Finnigan 4000 quadrupole mass spectrometer through the direct sample probe inlet has been previously described (1). A 1 X 10 cm TLC plate passes under a source of desorption energy and CI gas, flowing over the plate, carries the desorbed sample from the plate chamber through an isolation valve and heated, glass-lined transfer line to the ion source. This arrangement offers the advantages of requiring no modifications to the ion source, of rapid changeover to another sample introduction technique, of direct analysis of chromatograms with no intermediate chemical steps, and of only using a portion of the sample without altering the plate material.

The original source of desorption energy (1) was a 150 W incandescent lamp focused through a silica window onto the plate by an ellipsoidal mirror. This was found to perform well with thermally stable compounds such as polyaromatic hydrocarbons. However, less stable materials degraded significantly or were not observed at all. In an attempt to improve performance a small CO_2 laser (20 mJ/pulse, 1.5 to 6 pulses/second) was substituted for the lamp (2). With laser desorption, materials such as methyl stearate and cholesterol were observed on occasion with little or no degredation, but these measurements were not reproducible. To improve reproducibility the laser and its power supply have been modified to operate at higher pulse rates (15 mJ/pulse up to 50 pulses/second). On testing the modified system it became obvious that sensitivity was highly dependent on desorption chamber temperature (the laser produces no heat in the chamber whereas the lamp causes a significant temperature increase). Cartridge heaters were installed in the chamber which provided temperatures up to approximately 80°C near the desorption area.

Under these conditions compounds such as phenanthrene are quite obvious in the RIC at the 1.0 µg level, can be seen in the RIC at the 0.1 µg level, and can be detected in a mass chromatogram at the 10 ng level (3 second sweep scan, m/z 120-250). Sensitivity would obviously be higher using an MID scan. Plates can be rescanned with about 50% loss in sensitivity. Peak shape depends on volatility and inlet system temperature. At low temperatures, for example, benzoquinone provides a high, narrow, symmetric peak while anthraquinone is difficult to detect at all with a broad, tailing peak. Increasing the temperature broadens the peak for benzoquinone while narrowing that for anthraquinone and greatly improving its sensitivity.

Overall reproducibility is about 20%, mainly due to variations in TLC sampling and in laser energy. Best results are obtained with relatively non-polar aromatic compounds. Amines, nitro compounds, ketones,quinones, and ethers are readily observed. Aromatic alcohols and acids are usually not observed at all. Increasing the length of aliphatic side chains decreases sensitivity significantly. For example, dimethyl phthalate shows moderate sensitivity (10% of phenanthrene), diethyl phthalate loses sensitivity by a factor of two and dibutyl phthalate is not detected at all. Aliphatic compounds are at least 10 to 100 times less sensitive than aromatics and tend to fragment much more readily.

Studies are just beginning on the effect of the TLC surface itself on compound desorption. Silica gel without indicator has been the only medium studied so far. However, HPTLC plates (0.1 mm layer) show higher sensitivities than standard plates (0.25 mm layer), especially with compounds of lower volatility.

Finally, significant background effects are observed. These are caused by materials adsorbed from the atmosphere by the plates, and residues of elution solvent. In addition to increasing the RIC at the beginning of a scan and thus making peaks more difficult to observe, this background affects the CI reagent gas chemistry of some materials, usually increasing the ionization of those materials. Thus sensitivity, affected by background, may decrease with position on the plate. Prescanning the plate with the laser off significantly reduces this effect, but at the risk of removing some of the more volatile samples.

REFERENCES

1. L. Ramaley, W.D. Jamieson and R.G. Ackman, 28th Annual Conference on Mass Spectrometry and Allied Topics, New York, NY, May 25-30, 1980, paper TPMP3.

2. L. Ramaley, M.E. Nearing, W.D. Jamieson and R.G. Ackman, 29th Annual Conference on Mass Spectrometry and Allied Topics, Minneapolis, MN, May 24-29, 1981 paper MPB8.

LASER DESORPTION FOURIER TRANSFORM MASS SPECTROMETRY

David A. McCrery, Edward. B. Ledford, Jr., and Michael L. Gross
Department of Chemistry, University of Nebraska
Lincoln, Nebraska 68588

An operational laser desorption Fourier transform mass spectrometer (LD/FTMS) system has been demonstrated and shown to be suitable for the analysis of nonvolatile and thermally labile organic molecules and organic salts. Features which make FTMS well suited for laser desorption studies are fast mass scan rates, high mass resolution, and the capability of mass analyzing heavy ions.

The vacuum and detection electronics used in this study have been described in detail elsewhere (1,2). The laser used was a grating-tuned, pulsed TEA CO_2 laser based on a Tachisto Model 215 laser head. Approximately 0.9 Joule of energy is delivered in 50 ns at 10.6 μm wavelength. The pulse repetition rate was 0.5 Hz. The laser beam was brought in transverse to the magnetic field of the FTMS, entered a cubic analyzer cell diagonally, and struck the sample probe inserted along the opposing diagonal (Figure 1). The beam was focused with a germanium lens to a diameter of 2 mm at the target. Beam intensity was adjusted by placing polyethylene sheets in the path of the unfocused beam. The sample surface was subjected to power densities in the range of 10^6 W/cm^2. Because the laser pulse was not synchronized with the FTMS pulse sequence, the analyzer cell was operated with the quench pulse turned off and functioned as a static ion accumulator. About 12 FTMS decay transients were digitized and signal averaged per laser pulse. The spectra in Figure 2 result from one or two laser bursts.

The negative ion spectrum of citric acid (Figure 2a) consists of a single major ion, the $[M-H]^-$ citrate ion at m/e 191. Succinic and adipic acids also produce strong $[M-H]^-$ peaks but, as in the case of citric acid, exhibit no significant fragment ions.

As with the carboxylic acids, the only distinguishing feature in the negative ion spectra of the underivatized dipeptides glycyltyrosine (Figure 2b), glycylserine, leucylglycine, and glycylphenylalanine is the characteristic $[M-H]^-$ peak.

Reversing the polarity of the trapping plates allowed the detection of the positive tetrabutylammonium cation (Figure 2c) desorbed from a layer of tetrabutylammonium perchlorate. As in the previous cases, there is a lack of structurally significant fragment ions.

The high resolution capabilities of LD/FTMS were investigated using succinic acid. Displayed in Figure 2d is a mass range of a fraction of an amu centered at the succinate ion, m/e 117. At a pressure of 1×10^7 we obtained a resolution of 10,000 (fwhh). This is the highest resolution reported in any laser desorption experiment and demonstrates the inherent high resolution capabilities of FTMS.

In general, negative ion spectra were far more intense than positive ion spectra. Stable, long lasting ICR transients with amplitudes of 2 mV peak-to-peak on the cell receiver plates (no amplification) could be achieved routinely. It has not been possible to generate ICR signals of such quality using an electron beam. Considering that the sample is positioned just outside the analyzer cell, the ions cannot be formed in a collision free environment. If they were, they could not be trapped in the cell. Consequently, we postulate that a "plume" of ions and neutrals, or perhaps a neutral plasma, allows the ions to travel the several millimeters transverse to the magnetic field before neutral and ionic components of opposite polarity to that of the trap plates are rapidly removed, leaving sample ions of desired polarity trapped for mass analysis.

These results will be published in the July, 1982, issue of Analytical Chemistry.

1. Ledford, E.B., Jr.; Ghaderi, S.; White, R.L.; Spencer, R.B.; Kulkarni, P.S.; Wilkins, C.L.; Gross, M.L. Anal. Chem. **1980**, 52, 463-468.
2. Ledford, E.B., Jr; White, R.L.; Ghaderi, S.; Wilkins, C.L.; Gross, M.L. Anal. Chem. **1980**, 52, 2450-2451.

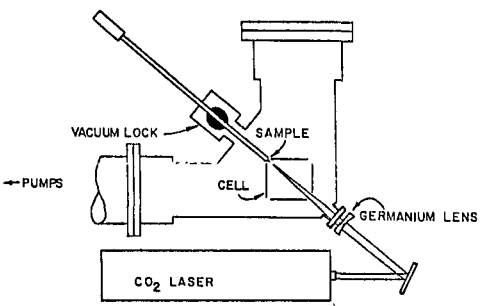


Figure 1.

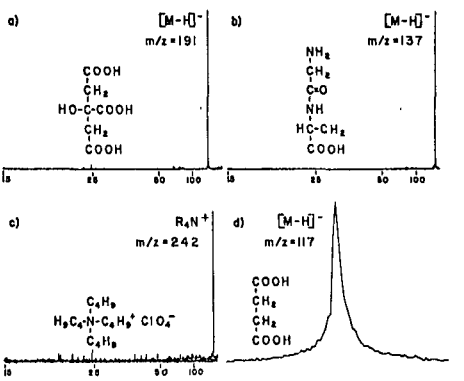


Figure 2.

ROD 11 MASS SPECTROMETRIC ELUCIDATION OF CHEMICAL BEHAVIOR ON COPPER-COPPER OXIDE CATALYSTS;

George M. Wood, Billy T. Upchurch,* Ronald F. Hoyt, Patricia A. Paulin, Ruth Anna Holmes,* and Edwin L. Wildner,** NASA, Langley Research Center, Hampton, VA 23665.

NASA's interest in applying laser technology in satellite measurement systems requires gas lasers with long-term continuous operation capabilities. These requirements have fostered research efforts in the study and evaluation of several catalytic and reactive substrate systems for the regeneration or removal of product species formed during the lasing process which ultimately lead to laser malfunction.

A method for observing reaction products to determine oxidation of carbon-containing compounds over heated copper (II) oxide was discussed at a prior (1981) ASMS meeting. Data are obtained by passing the gaseous reactants through a heated quartz tube containing the metal-metal oxide catalyst, and then through a heated capillary inlet into the source region of a modified Dempster 180° spectrometer. The technique, along with the isotopic labeling of the substrate or reactant, provides a direct measure of reaction mechanisms.

In this paper, we discuss measurements and results involving oxygen, carbon monoxide, carbon dioxide, elemental copper, cupric oxide, and stainless steel. Monitoring of gaseous species as a function of temperature and mass transport when in contact with the reactive substrate has enabled us to gain insight into the reaction mechanisms. With the aid of isotopic labeling, the mechanism for the reaction between oxygen gas and carbon in stainless steel has been postulated. The data obtained for carbon monoxide and oxygen, and their reaction with the cupric oxide/copper substrate are indicative of a regenerative catalytic mechanism. These data are presented and their use in the elucidation of reaction mechanisms and in support of laser technology development will be discussed.

*Dept. of Chem., Old Dominion University, Norfolk, VA 23508.
**Consultant, 4 Merry Terrace, Newport News, VA 23606.

Direct Analysis of Industrial Polymers by Mass Spectrometry - An Introduction

Robert P. Lattimer
The BFGoodrich Research & Development Center
9921 Brecksville Road
Brecksville, OH 44141

Despite its numerous analytical advantages, mass spectrometry has been underutilized in the past for studying polymeric systems. The prinicpal problem, of course, is the nonvolatility (or thermal lability) of polymers. In order to analyze any material by mass spectrometry, the sample first has to be vaporized and ionized into the instrument's vacuum system. Because of this rather severe limitation, most mass spectral methods of polymer analysis involve degradation of the material prior to analysis of the volatile fragments. Degradative methods, principally pyrolysis (thermal degradation), constitute the vast majority of work in mass spectral analysis of industrial polymers.

In the ideal situation, however, the polymer chemist would like to use the mass spectrometer for direct analysis of polymer systems. Much can be learned about the composition of the polymer if the mass spectrometer can produce a spectrum of molecular (or quasimolecular) ions for the various oligomers that are present. For the analysis of an oligomeric mixture, it is preferable that fragmentation and decomposition processes be absent, or at least minimal, in the mass spectrometer. The direct analysis of high polymers (MW ~10^4-10^7 amu) by mass spectrometry has not yet been effectively achieved, but some exciting developments in this quest have recently been reported. The "middle molecule" region (MW ~10^3-10^4 amu) is now accessible by a number of techniques. The applications to date have mainly been in the area of large biomolecules, but several reports have recently issued describing the characterization of industrial polymer systems as well.

In the analysis of higher molecular weight materials, all components of the mass spectrometer system need to be considered: the inlet (vaporization) system, the ionization method, the mass analyzer, and the ion detector. All common types of analyzers have been adapted for higher mass transmission; these include high field or large radius magnets, low frequency quadrupoles, time-of-flight analyzers, and the plasma chromatograph (ion mobility analyzer). Normally for higher mass operation these analyzers are operated at rather low resolution. Resolution is normally not of prime concern in oligomer analysis, however, since the objective is only to separate oligomers with relatively large mass differences (~40-100 amu). Detection of higher mass ions can present special problems. Standard electron multipliers, for example, become progressively less efficient as the mass of the molecule increases (or, conversely, as the ion velocity decreases). Current methods of improving higher mass detection include the use of post-acceleration (e.g., Daly) detectors or else devices that fragment larger ions into smaller ones (after mass separation).

The vaporization/ionization of higher molecular weight molecules is currently the most restrictive area relative to the mass spectral analysis of polymers. Several vaporization/ionization approaches have been used with varying degrees of success, and the numerous techniques are listed in Figure 1 with a tentative assessment of their past use and future potential. At this point no one technique has emerged as a dominant or preferred method. Field desorption has thus far received the most attention for direct oligomer analysis, but it is certainly not the ultimate technique.

Some people might question the necessity or advisability of pursuing techniques for analysis of higher molecular weight polymers, since a number of "classical" methods (e.g., gel permeation chromatography, vapor pressure osmometry, laser light scattering, infrared spectroscopy, magnetic resonance) are available. It turns out there are important reasons to pursue these developments other than the scientist's curiosity and desire to constantly

improve the methodology. Classical techniques, for example, are always averaging methods; i.e., they never measure exact masses of individual oligomers. Furthermore, classical techniques do not investigate the different types of oligomers that may be present, nor do they distinguish impurities in polymer samples. Copolymers and blends will often not be distinguished as to polymer type. Finally, classical methods do not provide absolute direct molecular weight distributions for polymers; instead they rely on calibrations made with accepted standards. Mass spectrometry clearly has great potential for direct analysis of polymers, but the full realization of that potential must await the development of new and improved techniques that can overcome the formidable obstacles that currently exist. Various aspects of the instrumentation used for polymer analysis and the results obtained are discussed in the Symposium on "Analysis of Industrial polymers," which could be titled a progress report in "macromass" spectrometry.

FIGURE 1

VAPORIZATION/IONIZATION

Technique	Direct Analysis of Industrial Polymers	
	Past use	Potential
Direct probe EI/CI	Yes	No
Rapid heating EI/CI	Yes	Some
Desorption CI	No?	Some
Laser Desorption	No?	Some
^{252}Cf Plasma Desorption	No?	Some
Secondary Ion MS	Yes	No
Fast Atom Bombardment	Yes	Yes
Field Desorption	Yes	Yes
Electrospray	Yes	Yes?
Electrohydrodynamic Ionization	Yes	Yes

SOME SUBSTRATE TEMPERATURE EFFECTS ON MOLECULAR IONS SPUTTERED FROM POLYMERIC LIQUID SURFACES, Woodfin V. Ligon, Jr. and Steven B. Dorn, General Electric Company, Corporate Research and Development, P. O. Box 8, Schenectady, NY 12301.

It is now widely recognized that in secondary ion mass spectrometry (SIMS) of organic compounds, there are significant advantages to be gained for some compounds by generating secondary ions from solution in certain liquids rather than from the solid state. Sample lifetimes in particular are frequently greatly extended by this approach. Extended sample lifetimes have been attributed to continuous renewal of the surface by migration of sample from the bulk liquid (1), although other explanations are certainly possible. We have attempted to verify this mechanism by looking for a temperature (T) dependence in the surface renewal. Such a temperature dependence might be considered to arise in the following manner. A much simplified expression for the observed ion intensity is the following

$$I = I_0 E C$$

where I is the observed intensity (ions/sec), I_0 is the primary beam intensity (particles/sec), E is a term related to the efficiency of conversion, and C is the surface concentration of the sample (molecules/cm^2). If C and E are constant clearly I should be constant. Also, it is possible that C might be so great that the observed signal, I, is limited by I_0E, and I would not change with C.

Assuming that renewal processes actually exist, a rough expression for the surface concentration at a given time would be:

$$C = C_0 - At + Bt$$

where C_0 is the original concentration, A is the sum of the rates of all processes removing sample (molecules/cm^2 sec), B is the sum of the rates of all processes renewing the surface (molecules/cm^2 sec) and t is time. The major component of A is, of course, the sputtering process itself removing both ions and neutrals, and A is dependent largely therefore on I_0. The major components of B might include diffusion, convection, and any surface milling which exposes fresh surface.

It is well established that diffusion and convection are functions of temperature. Accordingly, at increased temperature, one could reasonably assume that more rapid surface renewal would occur. One way, therefore, to probe for the importance of these processes would be to search for changes in intensity with time which are temperature dependent.

Since, clearly, such changes in I with time (dI/dt) could reflect changes in either C or E, it is necessary to consider what other processes might be temperature dependent. The most likely cause of a change in E would be a buildup of decomposition products on the surface ("beam damage"). One might argue that if these products are to some extent removed by diffusion into the liquid matrix then changes in E might also be temperature dependent to some degree. It is probable, however, that the materials which truly interfere are in fact insoluble and not subject to these effects. We consider, therefore, that this process is unimportant. Along the same lines, a buildup of surface decomposition products might also reduce the effectiveness of renewal processes, such as diffusion. Rapid removal of these products might diminish this effect, but again it is likely that the insoluble products would be most important and therefore equally probable that no temperature effect would apply. Finally, since incident particle energies are so very high, it is not reasonable to expect that small changes in substrate temperature would significantly affect ion production efficiency (E) and it should be safe to assume that over a 40°C temperature range, changes in E should be insignificant.

From these considerations we conclude that the most important temperature dependent processes affecting I should be diffusion or convection and that changes in dI/dt should arise from changes in C, not E. If we find $dI/dt \neq 0$ and invariant with temperature then we do not know if E or C is changing since both are potentially sensitive to I_0. It is also important to note that any experiment must be carried out in a concentration range where I is dependent on C. If C is so large that I is limited by I_0E, then dI/dt is independent of C and would reflect only changes in E. If I is much less than the I_0E maximum value, however, then we can safely assume that the surface does not have any arbitrarily limiting surface concentration such as a monolayer (1). An experiment carried out under these conditions in which dI/dt shows no change with T strongly suggests that diffusion and convection are unimportant or are very fast and not rate limiting.

Such an experiment is relatively easy to design. It is important to avoid liquid carriers which evaporate since this introduces yet another mechanism for concentration of sample on the surface. On this basis the most common matrix, glycerol, is unsuitable for the experiment. We have chosen to use polyethylene glycol (PEG) of average molecular weight 1000 as the matrix liquid. At room temperature this material is a solid but at 40°C it is a liquid with a viscosity considerably less than that of glycerol (glycerol = 756 centistokes (25°C), PEG-1000 = 100 centistokes (40°C)). Between 80°C and 40°C the viscosity of PEG-1000 changes by a factor of about 4. PEG-1000 has no significant volatility at 80°C. As sample molecules we have chosen two ammonium salts which give very strong signals in positive ion mode. These are: tetrabutylammonium bromide and benzethonium chloride. In both cases we have chosen to use a concentration of 1000 ppm -- well below the level where I is no longer dependent on C. At this level, molecular ions from the matrix are partially suppressed by both samples but fragment ions from the matrix are quite abundant. Both of the samples are completely soluble in the matrix at this level. In addition, we have studied the m/z 942 molecular ion from the PEG matrix itself.

Significant values of dI/dt were obtained by using thin films which were relatively rapidly depleted. Isothermal measurements of dI/dt were taken for the five minute period between 10 and 15 minutes after primary beam irradiation was begun (presumably due to mechanical movement of the liquid sample and possibly due to charging effects, dI/dt was erratic before the 10 minute point). Seventy points were taken to establish each slope and the average of 3-5 independent experiments taken. Measurements were taken using the primary beam from an Ion Tech B11-NWF neutral beam gun mounted on a Varian-MAT 731 mass spectrometer as described previously (2). For m/z 942 from the pure PEG-1000 matrix, $dI/dt = 0$ between 80°C and 40°C in the time frame of the experiment. The primary intensity (I_0) was that intensity corresponding to a power supply current of 1ma as measured by the B-50 power supply. The absolute intensity of m/z 942 is also insensitive to temperature between 80° and 40°C but disappears below 40°C as the material crystalizes. Since m/z 942 is a matrix ion, $dI/dt = 0$ is not unexpected. The bulk concentration is 100% and I should be limited by I_0E. This result does suggest, however, that beam damage induced changes in E are also not detectable over this time frame.

For tetrabutyl ammonium bromide ($dI/dt)_{80°C} = 0$ at $I_0 = 0.1$ma but is negative for $I_0 = 1.0$ma as shown in Figure 1. We find, however, that dI/dt is, invariant between 80°C and 40°C at $I_0 = 1$ma. (See Figure 2) We must suspect in this case that diffusion is either not important or is very fast. If it is not important then surface renewal must be by ion milling. This mechanism would require a long time period where dI/dt was near zero (assuming E constant) and then a sudden drop as the matrix was used up. Our results show a long fairly constant drop in dI/dt suggesting that continuous renewal is depleting the bulk concentration. Diffusion may, therefore, be important and very fast. Such a mechanism would require that sample ions be sputtered in preference to matrix ions in order to generate a concentration gradient. We have no direct evidence for such differential sputtering. We also have no direct evidence that our observed change in dI/dt arises from changes in C not E although the constancy of dI/dt for the m/z 942 matrix ion and the much extended lifetime of larger sample volumes may offer support here.

Our only certain conclusion can be that diffusion is not directly limiting the observed intensity. We can not show whether diffusion in fact occurs or not. For benzethonium chloride $(dI/dt)_{80°}$ is negative for $I_0 = 1$ma and less negative at lower temperatures. This is the opposite effect to that which would be expected for active transport. We have been able to attribute the effect to sample instability in the chemical sense at elevated temperature. The increased (more negative) slope at 80°C is due, therefore, to simple thermal decomposition.

We do not feel that suppression of matrix ions is positive evidence of monolayer formation and, therefore, of diffusion (1). As a case in point, 1000 ppm benzethonium chloride in glycerol completely suppresses matrix ions in positive ion mode. In negative ion mode at exactly the same level, sample ions are small while matrix ions are quite abundant. Clearly, if a monolayer exists in positive ion mode it must also exist in negative ion mode. The conclusion must be that if a monolayer exists it does not prevent simultaneous sputtering of underlying matrix ions and is, therefore, an inadequate explanation of suppression of positive matrix ions.

Our experience suggests that suppression of matrix ions is simply a function of the presence or absence of sufficient low ionization potential sample ions to satisfy the thermodynamic requirement for positive charge carriers at a given incident particle energy. According to this explanation a higher incident particle energy should require a higher sample concentration to suppress matrix ions. This has been observed by us for benzethonium chloride in glycerol at 1000 ppm.

We feel strongly that the crucial question is not whether one sputters from a liquid but rather whether or not the bombarded surface polymerizes. Consider that 0.1% tetrabutylammonium bromide in PEG-1000 gives very long lived signal whereas under the same conditions a PEG-6800 matrix heated to give an identical viscosity gives signals which last only seconds because of rapid formation of a polymer skin. Furthermore, urea a solid gives very long lived signals because it does not polymerize. It is clear, therefore, that some liquids give very short lifetimes and some solids give very long lifetimes. The secret is, does the matrix (either solid or liquid) develop polymeric decomposition products on the surface.

Proper sample preparation for organic SIMS, therefore, involves finding a matrix which does not readily polymerize under particle bombardment, has a higher ionization potential than your sample and which makes a nicely homogeneous solution. Slow matrix evaporation might possibly be exploited to enhance surface concentration and may be important in the glycerol case

1. M. Barber, R. S. Bordoli, G. J. Elliot, R. D. Sedgwick, A. N. Tyler, Anal. Chem., 54, 645A (1982).

2. W. V. Ligon, Int. J. Mass Spec. Ion Phys., 41, 204 (1982).

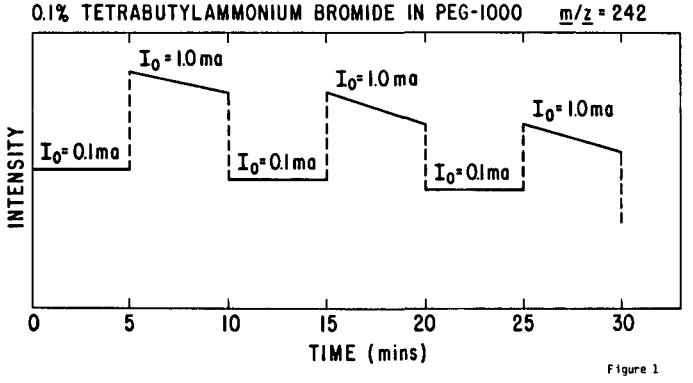
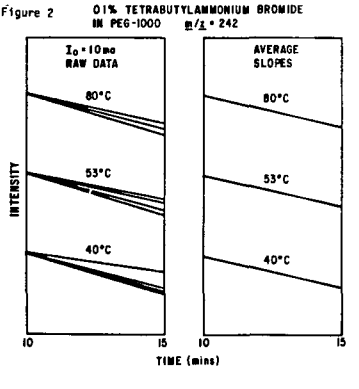


Figure 1



FIELD DESORPTION OF POLYMERS

A. Grey Craig, Christine E. McCrae
and Peter J. Derrick

School of Chemistry, University of New South Wales
P.O. Box 1 Kensington, NSW 2033
Australia

It is shown that the degree of fragmentation induced in field desorption of polyethylene glycol increases as the cathode potential, and hence the electric field, is raised. The relative ionization probabilities of different polymers (i.e. different chain lengths) appears to be insensitive to cathode potential. The degree of fragmentation is not strongly dependent upon emitter heating current, whereas the relative intensities of psuedomolecular ions of different masses are strongly affected by emitter heating current. It is concluded that the fragmentation observed in field desorption of polyethylene glycol is induced by the electric field i.e. field dissociation.

A model[1] is advanced in which field desorption is seen as involving two steps: ionization and field evaporation (or sublimation) of ions. The height of the potential energy barrier, over which evaporation is regarded as occurring, is determined by the local field. It is proposed that the model is relevant not only to the field desorption of polymers but also to other classes of compounds such as peptides. It is suggested that the formation of gaseous ions by sputtering techniques such as fast atom bombardment may be described in terms of a similar model. In these cases, the fields necessary for ionic evaporation might arise at the surfaces of colloidal liquid droplets (aerosol).

The technique of mass spectrometry - mass spectrometry has been applied to psuedomolecular ions of polymers. The molecules of different masses within a polymer sample can be separated, and the dependence of properties upon chain length investigated. Collisional activation spectra are presented for $(M+H)^+$ ions of different masses formed from a number of polymers.

1. *To be published in Organic Mass Spectrometry*

THE APPLICATION OF FIELD DESORPTION MASS SPECTROSCOPY TO QUANTITATION AND STRUCTURAL ELUCIDATION OF PHENOLIC RESIN OLIGOMERS

G. Herman, P. Skotnicki and A. F. Weston
Occidental Chemical Corporation, Research and Development
Long Road, Grand Island, New York 14072

The use of field desorption and field ionization for the characterization and quantitation of Industrial Polymers has been a continuing interest to this laboratory.

The resins which we have investigated are made up of a series of oligomers of increasing molecular weight. We have compared electron impact and chemical ionization mass spectra of the oligomers with field desorption and have found that FD is the technique of choice for our application. Oligomers of molecular weight greater than 2000 have been successfully separated and characterized using the technique.

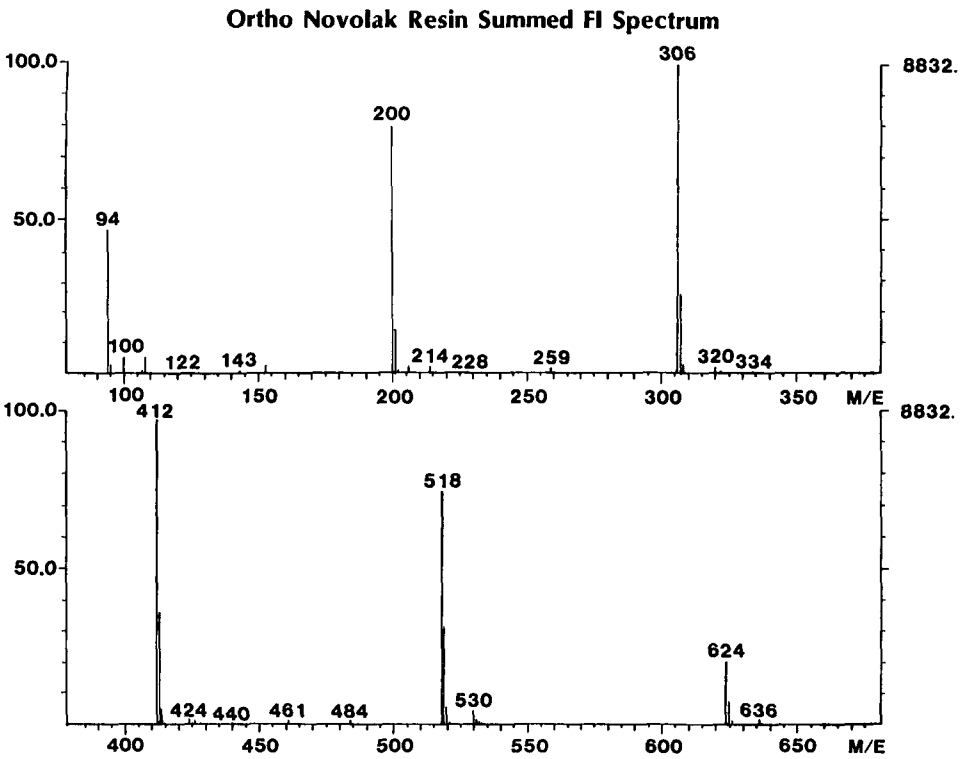
Instrument calibration has been a continuing problem in the application of field desorption. Changes in source stability reduce mass accuracy if an electron impact calibration is used for field desorption mass spectra. Fomblin has been used successfully by several laboratories but we have noted that fluorocarbons cause faster deterioration of emitter wires. Fomblin does not have a high ionization efficiency compared to the phenolic resins and, therefore, when it is used as a spectral calibrant for high resolution applications it gives a very weak spectrum unless significant quantities are used. To avoid the use of Fomblin we have investigated the use of the phenolic oligomers themselves as calibrants and have developed several oligomer mixtures which can be used for different mass ranges. The critical criterion is that the oligomers should have similar volatilities so that they produce optimum ion current at about the same time. Figure 1 shows an ion chromatogram of a typical oligomer mixture which can be used to calibrate the mass range in field desorption or ionization mode. An unknown sample can be spiked with the mixture, then scans including the mixture can be used to obtain high resolution data for the unknown oligomer. When the

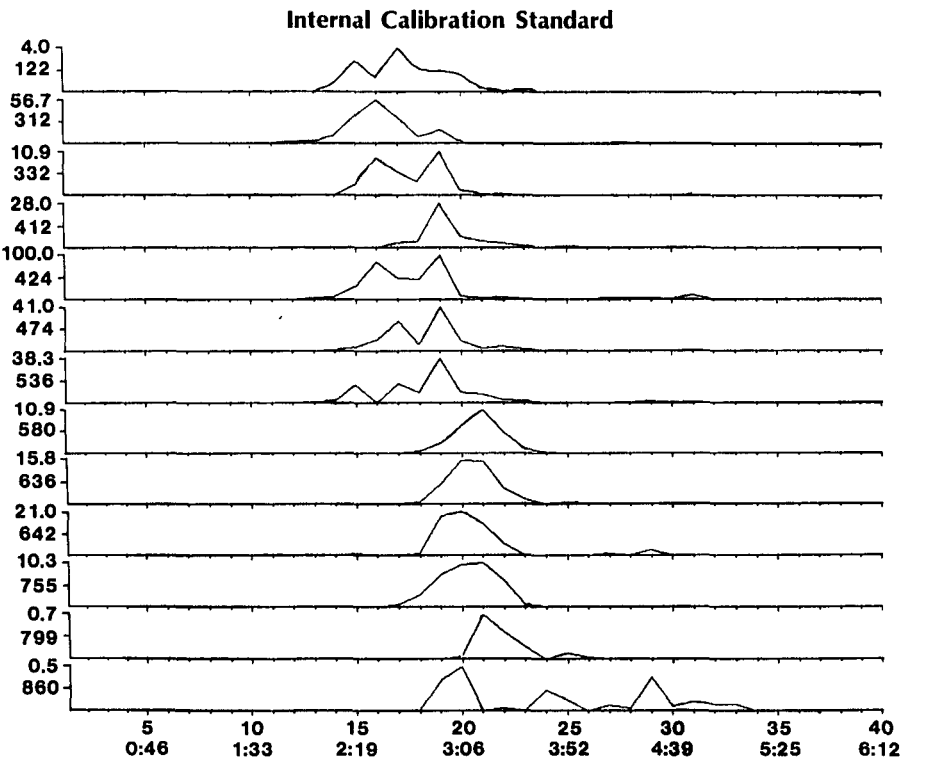
oligomers do not have sufficient overlap in their volatility range, it is possible to create a spectrum for calibration by editing several mass spectra together. The resulting calibration can then be used to assign masses to other spectra of the resins.

Quantitation of oligomers in resins is important because different oligomer distributions create resins with different properties. Traditionally, this has been accomplished using ^{13}C NMR. Changes in signal size of different functional groups are used to determine differences in average molecular weight. This technique is not oligomer specific and, therefore, field desorption and field ionization are used to determine changes in the oligomer composition.

The mass spectrum of a typical ortho-Novolac resin is shown in Figure 2. The mass spectrum shown was produced by summation of fifty scans so that all the oligomers appear on one trace and their peak heights are in about the correct proportion. This data takes into account small differences in volatility, but does not reflect any possible difference in ionization efficiency. Several samples which had been spiked with increasing amounts of a pure ortho-Novolac dimer were analyzed and the ratio of dimer to timer plotted.

The spiking resulted in a linear increase in dimer response relative to trimer. By using known weights of the compounds the relative amount of dimer in the original resin can be calculated from the intercept and the amount of dimer in a resin of unknown compositions can also be determined. The results of these experiments were confirmed by comparison with ^{13}C NMR data.


Ortho Novolak Resin Summed FI Spectrum
100.0
50.0
8832.
306
200
94
100
122
143
214
228
259
320
334
100
150
200
250
300
350
M/E
100.0
50.0
8832.
412
518
624
424
440
461
484
530
636
400
450
500
550
600
650
M/E


Internal Calibration Standard
4.0
122
56.7
312
10.9
332
28.0
412
100.0
424
41.0
474
38.3
536
10.9
580
15.8
636
21.0
642
10.3
755
0.7
799
0.5
860
5
0:46
10
1:33
15
2:19
20
3:06
25
3:52
30
4:39
35
5:25
40
6:12

HIGH-RESOLUTION HIGH-SENSITIVITY MASS SPECTROMETERS FOR HIGH MASS ANALYSIS

Hisashi Matsuda

Institute of Physics, College of General Education
Osaka University, Toyonaka, Japan

1. Introduction

The improvement of the mass spectrometer is indispensable for obtaining good results in high mass analysis. The requirements for the instrument are as follows: (1) high resolution, (2) high sensitivity, (3) high mass range and (4) precise mass calibration. Ion optical considerations to satisfy these requirements are described and several examples of improved mass spectrometers are shown.

2. Resolving power and sensitivity

The resolving power of a mass spectrometer is given by the equation

$$R = \frac{A_\gamma}{A_x s + \Delta + d}$$

where s and d are the widths of source and collector slits, respectively, and A_γ, A_x and Δ are mass dispersion, image magnification and total amount of image aberrations, respectively. The width of the collector slit is chosen to be $(A_x s + \Delta)$ in order to achieve most efficient detection. A large numerator and a small denominator are necessary to get large resolving power. For this purpose it is most important to reduce the aberrations. A high resolution is obtained by making s small. However, a small source slit decreases the ion intensity from the ion source. Therefore, a large value of A_γ/A_x is desirable for obtaining high resolution and high sensitivity simultaneously. A stigmatic and wide angle focusing is also useful to increase the sensitivity.

3. Second order double focusing mass spectrometer

The main cause of image aberrations in a double-focusing mass spectrometer is the second-order aberration. According to the trajectory calculation, the final position of an ion at the collector slit is given by

$$\begin{aligned} x_f = {} & A_x x + A_\alpha \alpha + A_\gamma \gamma + A_\delta \delta \\ & + A_{\alpha\alpha}\alpha^2 + A_{\alpha\delta}\alpha\delta + A_{\delta\delta}\delta^2 + A_{yy}y^2 + A_{y\beta}y\beta + A_{\beta\beta}\beta^2 \\ & + A_{\alpha\alpha\alpha}\alpha^3 + A_{\alpha\alpha\delta}\alpha^2\delta + A_{\alpha\delta\delta}\alpha\delta^2 + A_{\delta\delta\delta}\delta^3 + A_{\alpha yy}\alpha y^2 + A_{\alpha y\beta}\alpha y\beta \\ & + A_{\alpha\beta\beta}\alpha\beta^2 + A_{\delta yy}\delta y^2 + A_{\delta y\beta}\delta y\beta + A_{\delta\beta\beta}\delta\beta^2 \end{aligned}$$

in the third order approximation, where α and β denote the radial and axial inclination of the incident beam, x and y the coordinates within the object slit, δ and γ the relative energy and mass deviation, respectively. The first

order double focusing condition requires that $A_\alpha = A_\delta = 0$. The coefficients A_{ij} are the second order and A_{ijk} the third order aberration coefficients. Here those terms which include x are neglected because x is expected to be very small. The computer program "TRIO" (Third Order Ion Optics) has been developed to calculate aberration coefficients[1]. The influence of the fringing field is taken into consideration.

The possibilities of correcting for second order aberration coefficients have been investigated by using TRIO, and found many examples of second-order double-focusing mass spectrometers[2]. The apparatus shown in Fig. 1 was constructed at Osaka University. The aberration coefficients are given in Table 1. The FD mass spectrum of polystyrene up to M = 11000 was obtained by this apparatus[3].

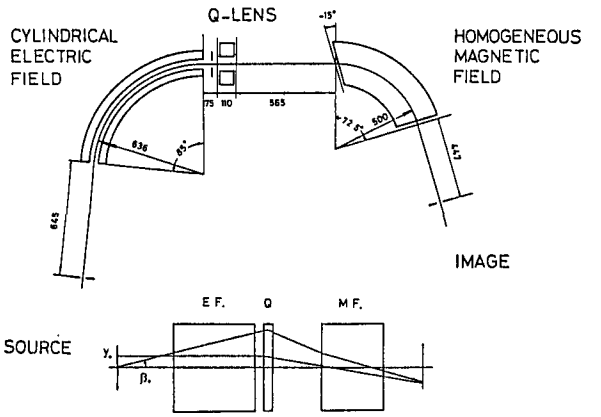


Fig.1. Schematic diagram of the second-order double-focusing mass spectrometer. Vertical trajectory is shown in the lower part.

Table 1. Aberration Coefficients

	Calculated	Measured
$A_{\alpha\alpha}$	0.03	-0.03
$A_{\alpha\delta}$	-0.02	-0.01
$A_{\delta\delta}$	0.01	0.01
A_{yy}	-0.20	-0.1
$A_{y\beta}$	0.13	0.2
$A_{\beta\beta}$	-0.04	0.1
$A_{\alpha\alpha\alpha}$	15	17
$A_{\alpha\alpha\delta}$	-11	-5
$A_{\alpha\delta\delta}$	16	9
$A_{\delta\delta\delta}$	-6	-3

4. Virtual image type mass spectrometer

The focul length of a Toroidal electric sector field depends on the field index c, which is defined as the ratio of two radii of curvature of electric potential surface perpendicular to each other. If c > 2, the toroidal electric field has a diverging focusing action which corresponds to a concave lens in light optics as shown in Fig. 2. A concave lens makes a small virtual

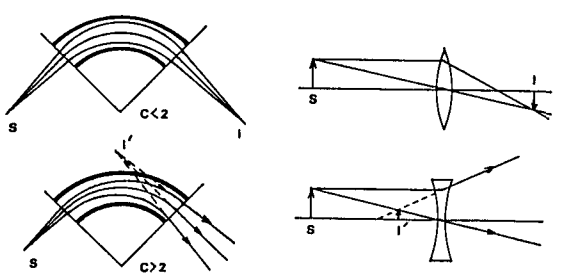


Fig. 2. Focusing action of Toroidal electric sector field

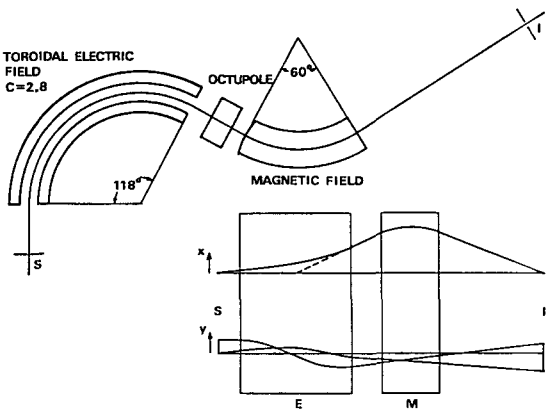


Fig. 3. Virtual image type mass spectrometer. Horizontal and vertical ion trajectories are also shown.

image. Therefore, a large value of A_γ/A_x is expected. A double focusing mass spectrometer of virtual image type is shown in Fig. 3. The ratio A_γ/A_x of this apparatus is about 4. The second order image aberration is corrected by geometry and the third order by a octupole. A resolving power of 30000 (10% valley) was obtained by the apparatus with $r_e = r_m = 15$ cm. A mass spectrometer with larger value of A_γ/A_x is proposed in ref. 4.

5. A new type of improved mass spectrometer

The high mass analysis requires a strong magnetic field. A narrow magnet gap is desirable to obtain strong magnetic field. However, if the narrow gap restricts the transmission of ion beam, then the sensitivity decreases. Therefore, the desirable beam cross-section in the magnetic field is narrow in the vertical direction and wide in the horizontal direction. A wide horizontal cross-section makes the image magnification small. A quadrupole lens system shown in Fig. 4(c) is useful for this purpose. A new type of mass spectrometer with an arrangement QQHQC (Q - lens, Q - lens, Homogeneous magnetic field, Q - lens, Cylindrical electric field) is shown in Fig. 5. The ion optical characters are shown in Table 2. Since the value of A_γ/A_x is about 8, a resolving power of 5000 can be obtained by using 0.2 mm source slit in a mass spectrometer with $r_m = 25$ cm.

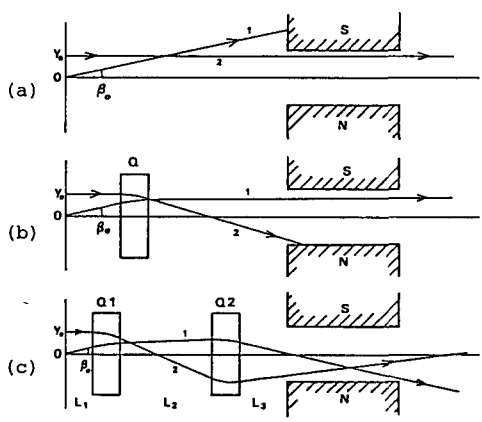
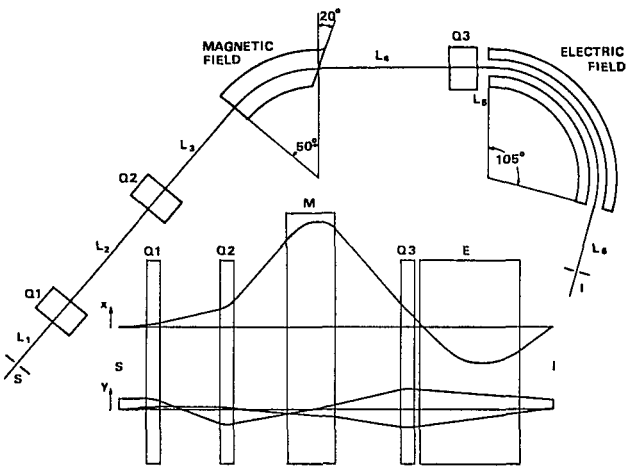


Fig. 4. Effect of quadrupole lens system on ion trajectory.

References

1) T. Matsuo, H. Matsuda, Y. Fujita and H. Wollnik, Mass Spectroscopy (Japan), 24 (1976) 19.
2) H. Matsuda, Int. J. Mass Spectrom. Ion Phys. 14 (1974) 219.
3) T. Matsuo, H. Matsuda and I. Katakuse, Anal. Chem. 51 (1979) 1329.
4) H. Matsuda, Nucl. Instr. Meth. 187 (1981) 127.



ϕ_m	50
ϕ_e	105
$r_e=r_m$	1.0
RM_1	-0.410
ε_2	-20
RE_2	-2.66
QL	0.25
QK_1	-2.85
QK_2	-2.85
QK_3	-1.85
L_1	0.5
L_2	1.1
L_3	0.97
L_4	1.195
L_5	0.1
L_6	0.617

Fig. 5. New mass spectrometer system QQHQC. Horizontal and Vertical ion trajectories are also shown.

Table 2. Aberration Coefficients, Values of A_γ/A_x and Maximum Beam Height

	CQH	QQHT	QQHQC	N-J	R.N-J
A_x	0.440	0.217	0.147	0.679	1.553
A_γ	0.776	-1.742	-1.169	0.840	-1.237
$A_{\alpha\alpha}$	0.02	-0.03	-0.02	0.13	-0.09
$A_{\alpha\delta}$	-0.02	0.15	-0.04	-0.06	0.60
$A_{\delta\delta}$	0.01	0.54	-0.06	0.32	-1.06
A_{yy}	-0.17	0.80	0.13	-0.87	1.26
$A_{y\beta}$	0.21	0.37	0.12	-9.94	4.42
$A_{\beta\beta}$	-0.02	0.34	0.13	-28.7	4.11
A_y	-1.63	0.35	0.73	1.10	1.30
A_β	-1.31	0.04	0.12	8.04	8.68
A_γ/A_x	1.76	8.03	7.95	1.24	0.80
g (mm)	5.3	4.4	5.7	20.5	11.2
h (mm)	11.4	1.9	4.0	25.6	28.8

g and h are the maximum vertical beam size in the magnet and that at the final collector, respectively, when the incident beam is assumed to be $y_0 = \pm 2.5$ mm, $\beta_0 = \pm 0.005$ and $r_m = 25$ cm.
CQH : mass spectrometer of Fig. 1
QQHT : instrument with T (toroidal electric field) instead of QC
N-J : Nier-Johnson type
R.N-J : reverse Nier-Johnson type

HIGH MOLECULAR WEIGHT MASS SPECTROMETRY. R. J. Beuhler and L. Friedman, Chemistry Department, Brookhaven National Laboratory, Upton, New York 11973

One of the first mass spectral analyses of high molecular weight industrial polymers was the technique pioneered by M. Dole and co-workers, utilizing an electrospray source coupled to an electric retardation field to determine a coarse value of M/e for the "seeded" ion beam. This experiment has been studied in this laboratory; the problems encountered have led to the development of techniques for mass analysis of ions with M/e ratios up to 180,000. Critical developments have been T.O.F. and low frequency quadrupole mass spectrometry coupled to high voltage post-acceleration detectors utilizing the secondary electron emission process. A significant reduction of threshold velocity for ejection of secondary electrons has been found for negative macroions striking oxide surfaces. Source technology for high molecular weight ions has been extended through studies of clustering reactions of solvent molecules to ions at high pressures, allowing mass scale calibration up through M/e 20,000. For smaller polymers and sugars, results have been obtained with rapid sample heating techniques, utilizing different chemical ionization gases, sample heating rates, and sample matrix isolation techniques to yield structural information.

This research was performed under grants from the Basic Energy Science Division of the Department of Energy.

PROBING ION-POLYMER INTERACTIONS BY ELECTROHYDRODYNAMIC IONIZATION MASS SPECTROMETRY.
K.W. CHAN and KELSEY D. COOK*, School of Chemical Sciences and Materials Research Laboratory, University of Illinois, Urbana, IL 61801

The nature of the electrohydrodynamic ionization (EH) process makes it particularly well suited as a probe of soluble, thermally labile samples. The EHMS experiment relies on low energy solution phase chemistry (dissociation or ion attachment) for ionization of salts and polar substrates, and therefore is accompanied by apparently negligible internal energy deposition. Furthermore, the need for conventional vaporization in the EH ionization process is obviated by the "field evaporation" process of ion emission directly from solution at the EH emitter tip. Thus, even systems predisposed to fragmentation (e.g., diquaternary ammonium salts, which are destabilized by intramolecular coulombic repulsions) show little or no evidence of degradation in their EH mass spectra. This "softness" provides one major advantage of EH ionization and sampling for polymer M.S. Another also stems from the mechanism of solution phase ionization; EH mass spectra are perhaps uniquely reflective of the solution chemistry of ion-polymer interactions.

In earlier EH studies of poly(ethylene glycols)[1] (PEG's), detection of exclusively quasimolecular oligomer ions (produced in glycerol solution by sodium attachment) allowed determination of molecular weight distributions with averages in excellent agreement with values determined using ASTM titrations. In that study, a trend toward multiple ion attachment by larger oligomers was noted, and tentatively ascribed to spiraling of the PEG chain around sodium ions, in a manner analogous to complexation by crown ethers. For example, chains containing more than about 12 oligomers (twice as many ether oxygen atoms as present in 18 crown 6) could attach two sodium ions. This observation led to a prediction that (within the limits of solubility in glycerol), heavier oligomers might be brought within the mass range of the spectrometer by virtue of multiple charge. This expectation has been at least partially realized; Figure 1 shows portions of an EH mass spectrum of PEG 4000 (average molecular weight specified by manufacturer: 3,000-3,700). Although this sample exceeds the nominal range of the MS9 mass spectrometer (~ 1800 at 4 kV) by about a factor of 2, analyte ions are nevertheless evident in the spectrum. These are detected because their mass to charge ratio has been appreciably lowered by incorporation of up to four sodium ions per molecule. Despite the low signal to noise ratio of the spectrum (which results in part from the low solubility of the polymer), a reasonable estimate of average molecular weight ($\bar{M}_n$ ~ 3200) can be made by using oligomer peak heights to estimate concentrations.

If increased polymer charge can facilitate analysis, use of a doubly charged cationization agent might be expected to extend applicability even further. To test this hypothesis, salts of barium were employed as supporting electrolyte. $BaSO_4$ was found to have glycerol solubility too low to be useful. Table I summarizes analyte ions in the EH mass spectrum obtained from a glycerol solution of PEG 400 ($\bar{M}_n$ = 406 [1]) with barium acetate. Similar data was obtained with $BaCl_2$. Although some doubly charged ions resulting from association of PEG with Ba^{2+} were present, most barium evidently retained acetate (or chloride) ion, resulting in singly charged adducts. Lowering the electrostatic sector voltage to examine ions undergoing metastable decomposition (solvent evaporation [2]) in the first field-free region revealed that much of the barium in solution was heavily solvated, possibly impeding interaction with PEG.

If stronger interactions lead to more extensive cationization, an alternative approach to increasing polymer charge could be to employ cations which interact with analyte more strongly than does sodium. If the analogy to crown ether complexation drawn above is accurate, PEG of size comparable to 18 crown 6 (or larger) would be expected to interact more strongly with potassium than with sodium in polar solvents.[3] Figure 2 summarizes analyte ion intensities from an EH mass spectrum of a glycerol solution of PEG 400 containing equimolar KI and NaI. As expected, each oligomer binds preferentially to potassium. Nevertheless, multiple ion attachment did not appear to be promoted by the stronger interactions. In fact, although analogy to crown ethers would suggest that barium complexation should be stronger than either sodium or potassium, the EH spectrum of PEG 400 with a mixture of Ba^{2+} and Na^{+} in glycerol (Figure 3) was dominated by sodium adducts. This may be due to the low availability of barium because of extensive solvation, as mentioned above. Alternatively, PEG selectivity in glycerol may intrinsically differ from that of crown ethers in methanol. Experiments are under way to test these possibilities.

Maximum mass range extension by introduction of multiple charge might be predicted for sampling of polyelectrolytes, which can achieve multiple charge in solution by ionic dissociation, rather than association. However, preliminary studies with poly(styrene sulfonate) (PSS) failed to generate any ions of analytical interest. Again, extensive solvation may be responsible, although studies are under way to assess the alternative explanation that the sodium salt of PSS may not dissociate appreciably in glycerol solution with

NaI supporting electrolyte.

Clearly, EHMS promises to be a useful tool for characterization of polymers and their solution chemistry. Before the full potential of mass range extension by incorporation of multiple charge can be realized, fundamental understanding of the role of charge and solvation in EH sampling will have to be improved. Furthermore, for optimum utility, limitations imposed by the requirement for solvents of low vapor pressure (primarily glycerol) must be relieved. Studies presently under way are aimed at answering these and related questions.

ACKNOWLEDGEMENT:

This work is partially funded jointly by the National Science Foundation and the Army Research Office, under grant number NSF-DMR-80-24632. The Materials Research Lab is supported in part by NSF grant DMR-80-20250.

REFERENCES

1. S.-T. F. Lai, K. W. Chan, and K. D. Cook, Macromolecules 13, 953 (1980).
2. B. P. Stimpson, D. S. Simons, and C. A. Evans, Jr., J. Phys. Chem. 82, 660 (1978).
3. J. D. Lamb, R. M. Izatt, C. S. Swain, and J. J. Christensen, J. Am. Chem. Soc. 102, 475 (1980).

Table 1

Relative Intensities of Analyte Ions in the 8kV EH Mass Spectrum of PEG 400(1.0 mole %) with $Ba(OAc)_2$ (4.5 mole %) in Glycerol

Structure	Degree of Polymerization											
	5	6	7	8	9	10	11	12	13	14	15	16
$[PEG + BaOAc]^+$	1	7	71	100	90	62	36	24	14	8	4	3
$[PEG + Ba]^{2+}$				1	3	3	2	2	2	1		

Fig. 1 Portions of the 4.5 kV EH Mass Spectrum of PEG 4000 (0.1 mole %) with NaI (6.0 mole %) in Glycerol

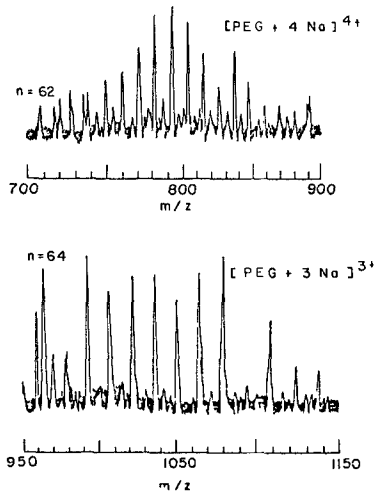


Fig. 2 Relative Adduct Ion Intensities in the 8 kV EH Mass Spectrum of PEG 400 (1.0 mole %) with NaI (3.0 mole %) and KI (3.0 mole %) in Glycerol

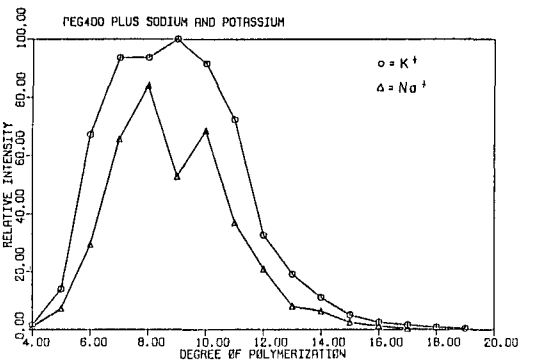
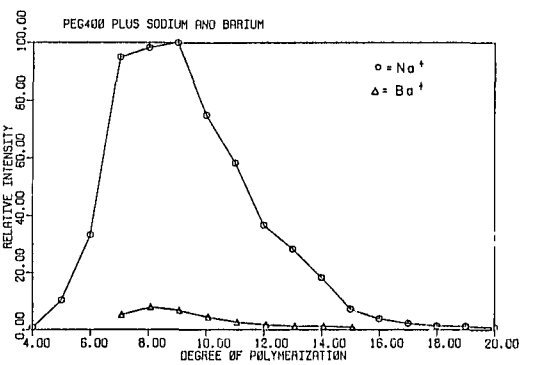


Fig. 3 Relative Adduct Ion Intensities in the 8 kV EH Mass Spectrum of PEG 400 (1.0 mole %) with NaI (3.0 mole %) and $Ba(OAc)_2$ (3.0 mole %) in Glycerol



Using the Mass Spectrometer as a Chlorine-Selective Detector

J. LaBrosse and R. J. Anderegg, Department of Chemistry, University of Maine at Orono, Orono, Maine 04469

Element selective detectors have long been used in gas chromatography. The electron capture detector (ECD), for example, responds to compounds, often halogenated, which have a high affinity for electrons. The extreme sensitivity of the ECD has led to its routine use in pesticide analysis. The ECD suffers from two limitations. Because the response is to electrophilic species, there is a lack of specificity of the detector. Nitro compounds, aromatics such as phthalate esters, and halogenated species all produce a response. Secondly, little or no structural information is generated by the detector.

Mass spectrometry, on the other hand, produces a wealth of structural information, but responds to any compounds which are ionized and detected. Certain elements will produce, by virtue of their natural isotopic distributions, very characteristic patterns of ions in the mass spectrometer. These patterns are easily recognized in spectral examination and can be used to indicate the presence of certain elements in the compound under study. We have been involved in writing computer programs to search a GCMS data set for these characteristic isotope clusters with the intention of using the computer as an "element-selective detector" for chlorine or bromine.

Last year, we described a technique called isotope cluster chromatography (1) to search a GCMS data set for the presence of a particular isotope pattern. We have made two significant improvements in that program. The introduction of several presearches serves to screen potential clusters and eliminate unnecessary calculations, increasing the efficiency of the search. In addition, when a cluster is located, it is checked against the predicted clusters containing one more or one less chlorine atom. This greatly reduces the number of "false finds" due to chlorine clusters other than the one under study. The result of these two modifications in the generation of more accurate isotope cluster chromatograms with a time savings of about 65% over the previous version.

By repetitively searching the GCMS data set for one-chlorine clusters, two-chlorine clusters, three- etc. up to a pre-set maximum, one generates a "chlorine selective chromatogram". Compounds whose mass spectra display any of the distinctive chlorine isotope clusters are shown as peaks in this computer-constructed chromatogram. The scores, which measure the likelihood of a cluster's presence, are weighted for the number of chlorines implied. That is, a 1 μg injection of monochlorobenzene will produce a peak with a score of about the same size as a 0.5 μg injection of dichlorobenzene.

The detector has selectivity with respect to species containing only carbon, hydrogen, nitrogen or oxygen, because such compounds do not display the distinctive chlorine isotope patterns. For example, phthalate esters, nitro-compounds and aromatics are undetected. Bromine, because of its own isotope pattern, causes a substantial interference.

Both the isotope cluster search and the chlorine-selective detector programs are used routinely in our laboratories for the analysis of metabolites of the chlorinated anti-cancer drug, Lysodren, (1-(o-chlorophenyl)-1-(p'-chlorophenyl)-2,2-dichloroethane). The figure below shows a typical urine extract experiment. The lower trace shows the total ion profile for the GCMS experiment, the upper trace is the computer generated chlorine-selective chromatogram. Of the many compounds appearing as peaks in the total ion profile, only a few contain chlorine, and these are readily located by the chlorine-selective chromatogram.

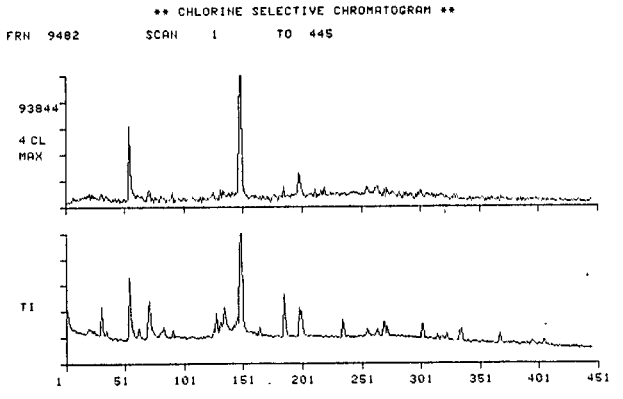


Figure 1.

1. R. J. Anderegg, Anal. Chem. 53, 2169-2171 (1981).

CAPILLARY GC/MS AND CAPILLARY GC/FID PROTOCOL USED FOR THE IDENTIFICATION AND CHARACTERIZATION OF CHROMATOGRAPHABLE COMPONENTS OF INDUSTRIAL EFFLUENTS TO THE CHESAPEAKE BAY BASIN.

B. Mason Hughes, S. Mitrosky, and J. J. Brooks, Monsanto Research Corporation, Dayton Laboratory
1515 Nicholas Road, Dayton, OH 45418

Monsanto Research Corporation's 27-month, 3-phase program entitled "Toxic Point Source Assessment of Industrial Discharges to the Chesapeake Bay Basin" (EPA contract No. 68-02-3161) was designed: (1) to determine the industrial contribution to increasing levels of toxic compounds being found in the Chesapeake Bay Basin, and (2) to develop a comprehensive, cost-effective toxicity identification protocol for long-term use by state agencies within the region. This presentation contains, principally, the results of the 7-month, Phase III study, designed to verify the final protocol recommended at the end of Phase II. It contains only the capillary GC/FID and capillary GC/MS protocol used in this multidisciplinary study.

In phase III, final effluent grab samples were collected at 28 plants and sediment samples were collected from the bay at 22 of these plants. The effluent samples were submitted for aquatic, acute toxicity testing and a series of chemical analyses. Sediment samples were solvent extracted in a different manner than were effluent samples, but they were analyzed by techniques similar to those used for the effluents. Effluent data were evaluated in terms of a "decision analysis" which was first presented in the Phase II report. This decision analysis determined, on an individual effluent basis, the complexity of the chemical analyses necessary to identify the cause of the aquatic toxicity. Employing this decision analysis resulted in the successful identification of the probable causes of the acute toxicity in 22 of 28 effluent samples.

Capillary GC/FID Protocol

TCO/TCG Method - An automated capillary GC/FID analysis was used to provide four types of information on the Phase III samples: total chromatographable organics (TCOs), total chromatographable gravimetrics (TCGs), relative retention indices, and recoveries of deuterated surrogate spiking compounds.

The TCO analysis is a gas chromatographic procedure for quantitating materials boiling in the 100°C to 300°C range. The area of all peaks eluting between compounds having boiling points of 98°C and 302°C is integrated, and by comparison with standards, is reported as the TCO value in mg/L of original effluent water [1], or mg/g of sediment.

The end-points of the boiling range are defined by the retention times of n-heptane (C_7), b.p. 98°C) and n-heptadecane (C_{17}, b.p. 302°C). Quantitation is based on standard solutions of known amounts of normal C_8, C_{12}, and C_{16} hydrocarbons, with corrections made for solvent blanks and spiked deuterated compounds.

The TCG analysis was included in the Phase III protocol to determine what fraction of the GRAV organics can actually be chromatographed by capillary GC. For TCG, the areas of all peaks eluting between the retention times of n-heptadecane and the end of the FID chromatogram (51.00 min) are integrated. The boiling point range is from 300°C to about 500°C. Quantitation is based on standards composed of n-C_{20} and n-C_{24} alkanes, with corrections made for solvent blanks and spiked deuterated compounds. The results are reported in mg/L of original effluent water, or mg/g of sediment.

The samples were analyzed using a Hewlett-Packard 5880 capillary column gas chromatograph interfaced to an HP 3356 Laboratory Automation System. A 30 m fused silica column with SE-54 stationary phase, identical to that used in the capillary GC/MS analyses, was used.

[1] U.S. Environmental Protection Agency, IERL-RTP Procedures Manual: Level I Environmental Assessment, 2nd ed. EPA-600/7-78-201. 1978, October

Relative Retention Indices

Relative retention indices (RRI) for peaks eluting within the GC/FID and GC/MS chromatograms were determined in order to compare the data obtained during the TCO/TCG analyses with mass spectrometric data and other chromatographic information. This allows a preliminary identification of aromatic components present in the sample based upon their RRI values. A standard mixture of PNAs was prepared and analyzed several times over the course of each sample set. RRIs for all sample peaks falling in the range of the PNA marker compounds ($RRI_{biphenyl}$=100, $RRI_{phenanthrene}$=200, RRI_{pyrene}=300, $RRI_{chrysene}$=400, $RRI_{perylene}$=500, and $RRI_{benzo(ghi)perylene}$=600) were automatically calculated by the 3356 Laboratory Automation System. Linear interpolation was used to calculate RRIs relative to the retention times of the marker compounds. When long series of runs were scheduled, as was the case with the 56 effluent extracts, PNA marker standards were analyzed at frequent intervals to monitor any retention time shifts. When slight fluctuations did occur, the relative retention time data were corrected for these shifts.

Capillary GC/MS Protocol

All GC/MS analyses were performed by automated capillary column chromatography using a Hewlett-Packard 5985-A GC/MS with a 5934 data system, which used Revision C Software and included a 7920 multi-drive disc unit. Since the peaks obtained in capillary column GC/MS analysis are only a few seconds wide, it is necessary to scan the mass spectrometer at its maximum rate to generate reliable mass spectra -- approximately 4500 spectra for a 40-minute run, depending on the initial MS scan delay, as compared to perhaps 700 for a 40-minute, packed-column run. A low detection threshold must also be used to capture the information contained in small peaks, which combines with the large number of spectra to consume enormous amounts of computer disc space in a given analysis. In some cases several GC/MS analyses could fill a data disc cartridge. Thus, to perform a series of 10 to 20 analyses, using the automatic injection system, requires the use of several discs for data acquisition. This is only possible in an automated mode on the Hewlett-Packard system by using the multi-disc drive in which the equivalent of up to 19 auxillary discs could be accessed simultaneously.

Method

The relevant GC/MS parameters used for the Phase III analyses are summarized below:

- 30 m fused silica SE-54 WCOT column
- Column head pressure, 7+ [psi
- MS operating pressure, 1 x 10^{-5} to 4 x 10^{-6} torr
- Backflush on at 0.5 min
- Initial temperature, 50°C
- Initial temperature held for 4 minutes
- Heating rate, 8°C/min
- Final temperature, 280°C
- Total analysis time, 40 min
- Injector, splitless mode, temperature, 250°C
- Transfer line temperature, 250°C (fused silica column through this zone, directly to the MS source)
- Electron energy, 70eV
- Source temperature, 200°C
- A/D rate, 1 measurement/0.125 amu; scan rate, approximately 0.6 s/scan
- Mass spectrometer scan delay, 3.0 min

The routine procedure used for GC/MS analysis was to transfer 150 µL of the sample extract into 1.5 mL sample vials along with 150 µL of a 100 µg/ml anthracene-d_{10} in methylene chloride internal standard. The vial was capped and placed in the autosampler, which injected approximately 1 µL into the GC, operating in the splitless mode.

Interpretation of Mass Spectra

The following protocol was followed in interpreting the mass spectral data obtained from the Phase III extracts:

(1) Spectra of compounds detected as peaks in the Hewlett-Packard BATCH program with a 1% to 5% threshold (depending upon the complexity of the sample) were automatically compared with standard spectra in the computerized EPA/NIH mass spectral data base using the Probability Based Search (PBS) software supplied by Hewlett-Packard. A goodness of fit parameter was generated (1.0 being a perfect match) for the ten matches closest to 1.0.

(2) The results from these searches were reviewed by an experienced mass spectroscopist using the Hewlett-Packard supplied spectral comparison software, SPDIF, to compare the sample spectra with the standard spectra identified by the SEARCH program.

(3) In cases where the spectral agreement was judged to be adequate, compound identities were assigned. When compound isomers produced similar spectra, no specific isomer could be identified based solely upon mass spectral data.

(4) In cases where the agreement was not adequate, identifications were made on the basis of manual interpretation (when obvious), or compounds were listed as unknown with their major masses given in parentheses. If a high even mass was present with odd fragment masses, the even mass was underlined to indicate a possible molecular ion.

QA/QC for Extractable Organics

In Phase II, MRC developed a routine procedure for assessing the condition of the mass spectrometer and the column in the gas chromatograph. The mass spectrometer was tuned approximately once a week using perfluorotributylamine (PFTBA) which is the basis for the Hewlett-Packard AUTOTUNE program.

Samples were run in the automated BATCH AQUIRE mode overnight, and with each batch of samples a system performance standard was analyzed. This included the compound decaflurotriphenylphosphine (DFTPP) which was analyzed by the Hewlett-Packard program: DFTPP EPA Criterion Verifier.

Typically, the m/e 51 and 127 on our instrument fell somewhat below the normal range specified by the EPA criterion. This fact was taken into account in interpreting mass spectra. If other peaks fell outside the ranges, the tuning of the mass spectrometer was re-examined.

The substances present in the system performance standard were: (1) 2,6-dimethylphenol, (2) 2,6-dimethylaniline, (3) decanol, (4) pentachlorophenol, (5) anthracene-d_{10} added prior to analysis, (6) octadecene, (7) octadecane, (8) DFTPP, (9) eicosane, (10) heneicosane, (11) pyrene, (12) methyl stearate, and (13) chrysene. By examaning the resoltuion of components 5-7 and 10-12, and by looking at the tailing of certain peaks such as decanol and pentachlorophenol, the condition of the column was visually evaluated. When the resolution and tailing were substantially worse than in a new column, the injection port insert was replaced, the front end of the column was broken off, or the column was replaced.

Analysis of Standards

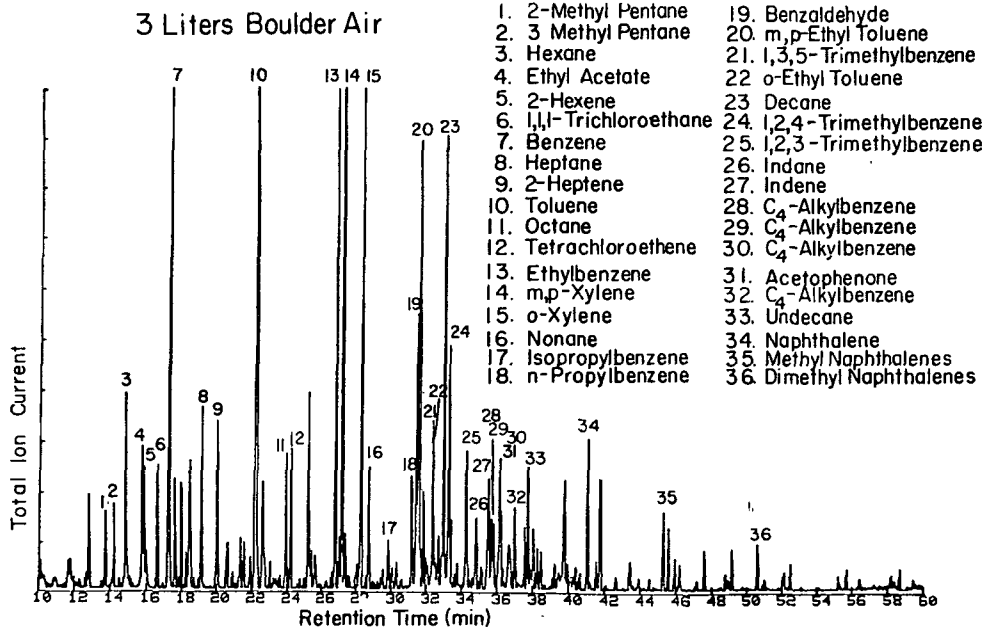
Four standard solutions were routinely analyzed along with effluent or sediment extracts in order to verify that good quality capillary chromatography and mass spectrometric analyses were being performed on sample extracts. In addition, capillary chromatographic/flame ionization detector system performance was also verified using the same set of standards analysis. One standard included all acid priority pollutants; a second standard included over 80% of the pesticide priority pollutants (excluding the Aroclor and toxaphene multicomponent priority pollutants); the third standard contained over 80% of the base/neutral extractable priority pollutants and the fourth was the system performance standard, discussed above. Excellent agreement was observed between the total ion chromatograms obtained from capillary GC/MS analyses and chromatograms obtained from capillary GC/FID analyses of these standards. Therefore, the correlation of data obtained from these two analytical techniques should exclude any differences between chromatography from these two analytical systems.

COMBINED FUSED SILICA CAPILLARY COLUMN GAS CHROMATOGRAPHY/MASS SPECTROMETRY IN ENVIRONMENTAL CHEMISTRY

R. E. Sievers, R. M. Barkley, R. S. Hutte,
E. J. Williams, M. K. Conditt, and S. B. Hawthorne
Department of Chemistry and CIRES
University of Colorado
Campus Box 449
Boulder, CO 80309

A variety of environmentally important samples has been studied using combined fused silica capillary gas chromatography/mass spectrometry. For these analyses the capillary column was coupled directly to the ion source of the mass spectrometer. This analytical system exhibits more inertness, better apparent chromatographic resolution and higher sensitivity than other GC/MS configurations that we have used. Results will be described for studies of volatile and moderately volatile organic compounds in potable and wastewaters, including a home-scale water treatment system in which domestic wastewater is recycled for potable re-use. Potable water from this system contained less than one microgram per liter total trihalomethanes, while Boulder municipal water contains thirty to eighty micrograms per liter total trihalomethanes. Studies of the organic constituents present in oil shale wastewater indicate the advantages of using an inert fused silica GC/MS system. It is not otherwise possible to separate and obtain distinguishable mass spectra of the constituents of these complex samples, which contain hundreds of compounds, many of which are phenols, acids, amines and N-heterocycles. Thick-film(1μm) cross-linked silicone polymer-coated fused silica columns have been used in our studies of volatile organic compounds in air and exhaust gasses. The use of these fused-silica capillary columns has allowed 10-mL samples of water-saturated air from headspace over aqueous solutions to be injected into the column for cryogenic trapping and subsequent analysis of the vapor-phase organic compounds. This can be done without any pre-concentration with porous polymeric sorbents. This type of analysis has revealed the presence of alkanes, alkenes, alkyl thiophenes, alkyl benzenes, and alkylated nitrogen-containing heterocycles in the headspace above shale oil wastewaters. The emission of these compounds during storage and disposal of shale oil wastewaters may be a significant and difficult to control cause of air quality degradation in the shale oil region.

The figure below shows an air sample collected during a temperature inversion which occasionally traps atmospheric pollutants in the Boulder Valley. Benzene and toluene were present at 8.3 and 8.9 parts per billion by volume during this pollution episode. In contrast, air samples collected in rural western Colorado contained only 0.7 and 0.2 ppbv of benzene and toluene.


3 Liters Boulder Air
1. 2-Methyl Pentane
2. 3 Methyl Pentane
3. Hexane
4. Ethyl Acetate
5. 2-Hexene
6. 1,1,1-Trichloroethane
7. Benzene
8. Heptane
9. 2-Heptene
10. Toluene
11. Octane
12. Tetrachloroethene
13. Ethylbenzene
14. m,p-Xylene
15. o-Xylene
16. Nonane
17. Isopropylbenzene
18. n-Propylbenzene
19. Benzaldehyde
20. m,p-Ethyl Toluene
21. 1,3,5-Trimethylbenzene
22 o-Ethyl Toluene
23 Decane
24. 1,2,4-Trimethylbenzene
25. 1,2,3-Trimethylbenzene
26. Indane
27. Indene
28. C4-Alkylbenzene
29. C4-Alkylbenzene
30. C4-Alkylbenzene
31. Acetophenone
32. C4-Alkylbenzene
33. Undecane
34. Naphthalene
35. Methyl Naphthalenes
36. Dimethyl Naphthalenes
Total Ion Current
Retention Time (min)

PRECISION AND ACCURACY OF MEASUREMENTS AT HIGH RESOLUTION WITH A FAST SCANNING MAGNET AND A CAPILLARY GAS CHROMATOGRAPHIC INLET SYSTEM; William L. Budde, James W. Eichelberger, and John P. Donnelly; U. S. Environmental Protection Agency, Cincinnati, Ohio 45268.

The development of fused silica capillary columns, fast scanning magnets, and very fast data acquisition systems has renewed interest in exact mass measurements of many ions in spectra as components of a complex mixture emerge from a high resolution capillary column. This work was performed to determine the precision and accuracy of the mass measurements and the precision of the ancillary measurements of retention time, relative retention time, peak area, and relative peak area. All experiments were carried out using Grob splitless injection and on-column injection into the capillary column.

A mixture of compounds was prepared which gave ions with masses representative of a variety of mass defects. The mixture included three internal standards for computation of relative retention times and relative peak areas (response factors). Seven replicate injections were made with each injector over a period of several working days. The gas chromatographic column was a 30 meter 0.32 mm i.d. fused silica capillary column coated with SE54. The mass spectrometer was operated at 3000 and 10,000 resolution in the repetitive scanning electron impact mode from 45 to 450 amu at a one second cycle time. The experiments were repeated with both injectors at each spectrometer resolution. Both perfluorokerosene and tetraiodoethylene were evaluated as sources of ions for reference in exact mass measurements.

Results are presented in terms of mean mass measurement errors, standard deviations, and relative standard deviations. The precision of the ancillary measurements are given in terms of their mean values with standard deviations and relative standard deviations.

TRACE WATER ANALYSIS IN GASES USING THE IPC-200

L. C. Frees, D. H. Holkeboer and J. Farden
INFICON Leybold-Heraeus, Inc., 6500 Fly Road, E. Syracuse, NY 13057

The measurement of trace water vapor in gases is often difficult and time consuming. Experiments utilizing the IPC-200 mass spectrometer, equipped with the capillary continuous sampling inlet, have shown that it is possible to measure water vapor concentrations from 50 to 5,000 ppm in certain gases. The analysis time, under appropriate conditions, is less than 5 minutes.

The purpose of the capillary inlet is to reduce the sample pressure from atmospheric to high vacuum without distorting the sample gas composition, with minimum response time. Pressure reduction is accomplished in two stages, through the capillary and across a molecular leak. In the capillary, conditions of viscous flow prevail. The gas flows through the capillary, past one side of the molecular leak, through a restriction, and into a mechanical pump. Some of the gas flows through the molecular leak into the mass spectrometer high vacuum chamber, and finally into a turbomolecular pump. In order to establish a definite pressure ratio across the leak for all gases, the pumping speed is restricted by system components to about 35 l/sec, thus isolating the chamber from pumping speed variations in the turbomolecular pump.

The capillary was equipped with a heating jacket which was controlled with a variable transformer. The mass spectrometer vacuum chamber was installed in a thermostated oven, permitting bake-out at 300°C. A thermostated heating tape was wrapped around the turbo pump inlet port.

The calibration gases used in this experiment were UHP (ultra-high purity grade) N_2 and He, and a certified standard mixture of 45 ppm H_2O in N_2. Samples with varying H_2O content were prepared by passing the UHP gases through a thermostated hydration chamber. All gas cylinders were equipped with high purity regulators. A multi-port valve was attached to the inlet of the capillary to facilitate switching between samples. Connections to the valve were made with copper tubing and brass fittings that had been carefully cleaned and dried.

In all cases, the net water vapor content of the sample gas was determined from the difference between the mass 18 signal for the wet gas and the dry UHP standard. This allowed for changes in the water background signal between runs without affecting the results.

Initial experiments involved measurements made on the 45 ppm H_2O calibration standard. The capillary and oven temperatures were varied systematically (with the turbo pump at ambient), and the effects on the background and net H_2O signals and response times (the time required for the mass 18 signal to reach equilibrium) were recorded. The capillary temperature, over the range from 25 to 200°C, had no significant effect. The mass spectrometer oven temperature had a great effect on both the response time and the net H_2O content, with the time varying from 32 to 7 minutes and the net H_2O signal varying from ~40 to 70 ppm for oven temperatures of 50 and 200°C, respectively. Heating the turbo decreased the response times by a factor of three, with no other noticeable effect.

An additional restriction, having a conductance of 3 liters/sec, was inserted between the vacuum chamber and the turbo pump to ensure that pumping speed variations were not responsible for the observed results. This considerably reduced the relative water background, and led to the observation of a new phenomenon. The cracking pattern for H_2O appeared to change over the course of several minutes when N_2 was admitted into the chamber. The mass 18 peak decreased to a fraction of its earlier value, while the 16 and 17 amu peaks increased in intensity until they were larger than the mass 18 peak had been initially. No such phenomenon was observed when UHP He was substituted for the N_2. It appears that the H_2O was reacting with the N_2 to form NH_3, although not by a simple gas phase reaction. When wet N_2 was used, the amount of NH_3 formed increased with increasing H_2O content.

The depletion of H_2O in the presence of N_2, although very noticeable for the 45 ppm mix, was insignificant for H_2O concentrations above 500 ppm. Measurements of H_2O concentration for samples containing 600 to 3500 ppm of H_2O yielded values within the experimental error in preparing the samples (due mostly to the temperature stability of the hydration chamber). The data are presented in Table 1. With the capillary at 100°C, the oven at 200°C, and the turbo pump at 67°C, the time required for each measurement was less than 5 minutes.

Table 1. The net water concentration as measured by the mass spectrometer vs. the sample composition as calculated from the dew point.

Sample H_2O ppm	Net H_2O ppm
600	530±56
1100	1225±7
1450	1465±35
2250	2090±85
3500	3700±396

The IPC-200 has proved itself very useful for the reasonably rapid and reproducible determination of water vapor concentration in certain gases. For H_2O concentrations from 500 to 5,000 ppm in N_2, the calibration and measurement procedures are straightforward. For concentrations between 50 and 500 ppm, the depletion of the H_2O by reaction with the N_2 results in decreased sensitivity and marked nonlinearity. For accurate results, careful calibration is necessary. The lower limit of detectability is set by the background water signal. For reproducible results, the temperature of the mass spectrometer vacuum chamber must be carefully controlled.

DETERMINATION OF TRACE AMOUNTS OF AMINES IN WATER WITH 2,4-DINITROPHENYLAMINE DERIVATIVES BY GAS CHROMATOGRAPHY/CHEMICAL IONIZATION MASS SPECTROMETRY.

Minoru Koga, Takashi Akiyama, and Ryota Shinohara; Department of Environmental Health Engineering, School of Medicine, University of Occupational and Environmental Health, 1-1 Iseigaoka, Yahata-nishi-ku, Kitakyushu 807, Japan.

The sensitive analytical method for trace amounts of aliphatic amines in water has been developed by GC/CI-MS after preparing 2,4-dinitrophenylamine derivatives (DNPA) with 1-fluoro-2,4-dinitrobenzene (FDNB). Aliphatic primary amine (methylamine, ethylamine, n-propylamine, isopropylamine, n-butylamine, isobutylamine, sec-butylamine, and tert-butylamine) and secondary amines (dimethylamine, diethylamine, di-n-propylamine, diisopropylamine, di-n-butylamine, diisobutylamine, pyrrolidine, piperidine, and morpholine) were examined.

Analytical procedure is shown in Fig. 1. The tested amines, except tert-butylamine and diisopropylamine, were reacted with FDNB and their derivatives were extracted with benzene quantitatively. The reactivities of tert-butylamine or diisopropylamine with FDNB are considered to be insufficient. Though pyrrolidine also reacted with FDNB, the DNPA derivative of pyrrolidine could not be analyzed by gas chromatography, because it is thermally unstable. Ammonia in water reacted with FDNB to form 2,4-dinitroaniline, and its recovery efficiency under this condition was about 50 %. Residual FDNB, 2,4-dinitroaniline produced by reaction of FDNB and ammonia, and bis(2,4-dinitrophenyl)ether produced by hydrolysis of FDNB could be removed from benzene extract by alumina-column chromatography.

The chemical ionization mass spectrum of each DNPA in which isobutane was used as reactant gas, showed a $(M+H)^+$ cluster ion as the most abundant ion. Quantitative analysis by GC/CI-MS equipped with MID were carried out by using these cluster ion. MID gas chromatogram of synthesized DNPA is shown in Fig. 2. The amount of each DNPA is 1.0 ng. Use of several different GC column were attempted to separate DNPA derivatives, and the mixture of 2% OV-17 and 3% PZ-179 liquid phase was the most suitable for their analyses. Minimum detection limit of each DNPA was in the range of 50-100 pg with MID. The calibration curves of amines were made from peak area ratio of DNPA against the derivative of deutrium labeled methylamine. In the range of 1.0-50 ppb, the linearity was satisfactory enough for quantitative analyses. The recoveries of amines spiked to sewage water at the μg/L level were examined, and the quantitative recoveries were obtained.

Table 1 listed the amines detected in the river water and the sewage. By using this method, we can sensitively and specifically determine aliphatic amines present in water at the ppb level.

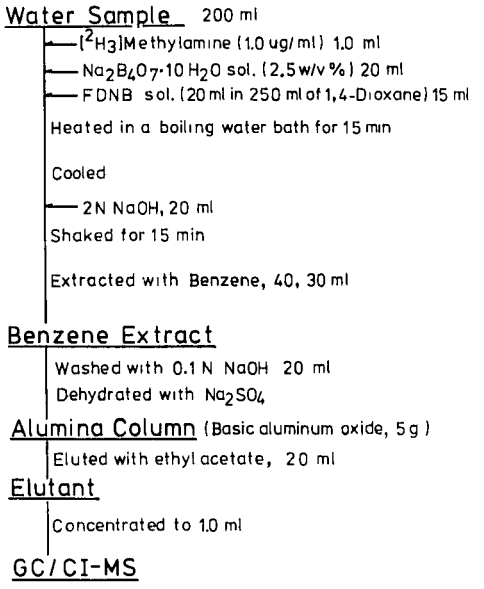


Fig. 1. Analytical procedure for amines in water.

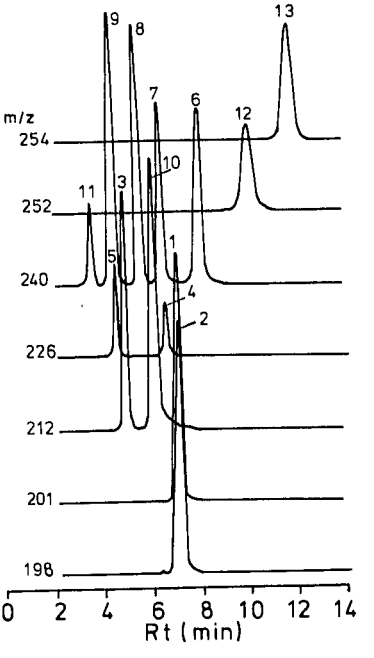


Fig. 2. Gas chromatogram of 2,4-dinitrophenylamines
1:[$^2H_3$]Methylamine (I.S.) 2:Methylamine 3:Ethylamine 4:Propylamine 5:Isopropylamine 6:Butylamine 7:Isobutylamine 8:s-Butylamine 9:t-Butylamine 10:Dimethylamine 11:Diethylamine 12:Piperidine 13:Morpholine, Amount of each DNPA was 1.0 ng. Column: 2% OV-17+ 3% PZ-179, 2m, Temp.:290°C, Reactant gas :Isobutane.

Table 1. Concentration of amines in water (ppb)

Sampling site	River water 1	2	3	Sewage Secondary effuluent
Methylamine	7.6	7.3	4.2	15.5
Ethylamine	1.8	2.3	2.7	ND
Propylamine	1.8	ND	ND	ND
Isopropylamine	6.3	5.8	4.5	10.5
Butylamine	1.3	1.3	1.0	ND
Isobutylamine	1.6	2.0	1.8	ND
sec-Butylamine	2.3	2.9	2.3	ND
tert-Butylamine	ND	ND	ND	ND
Dimethylamine	3.0	5.2	3.3	3.3
Diethylamine	4.5	9.2	6.2	1.3
Dipropylamine	ND	ND	ND	ND
Dibutylamine	ND	ND	ND	ND
Diisobutylamine	ND	ND	ND	ND
Piperidine	ND	ND	ND	2.1
Morpholine	ND	ND	ND	3.1

ND: Not detected; detection limit: 1.0 ppb.

PARTS PER TRILLION ANALYSIS OF SEMIVOLATILE PRIORITY POLLUTANTS BY CLOSED LOOP STRIPPING - GC/MS

**Albert R. Trussell, Robert R. Clark,
Dean L. Hartley, Raphe J. Pavlick**

**JMM Environmental Research Laboratory
Pasadena, California 91101**

INTRODUCTION

The Closed Loop Stripping (CLS) procedure for the analysis of trace organic components in drinking water was developed by Grob in 1972 and first reported in 1973 (1). The technique offerred detection limits in the low nanogram/liter range for compounds amenable to dynamic headspace stripping. Several years later the procedure was used in the United States by Reinhard for the analysis of treated wastewaters (2). More recently the CLS procedure has become popular in the U.S. for the analysis of synthetic contaminants in drinking water (3,4) and for the quantification of taste and odor compounds (5). The authors' current work focuses on the precision and accuracy of the CLS procedure as applied to the analysis of certain priority pollutants and naturally occurring taste and odor compounds.

EXPERIMENTAL

Stripping

The CLS technique used by the authors was adapted from the work conducted by Grob (1). The only major modification from the original apparatus was the incorporation of all glass and teflon parts. Twenty grams of sodium sulfate were added to a 500 ml water sample which was maintained at 60°C. The sample was then stripped by a recirculating air flow for 60 minutes at a flow rate of approximately 100 ml/min. Activated carbon filters were extracted sequentially with two 10 microliter portions of carbon disulfide to yield a total of 16 µl of extract.

GC/MS

The CLS extracts were analyzed on a Finnigan 4021 GC/MS (Finnigan Corporation, Sunnyvale, California). Two µl of sample were injected splitless onto a 30 meter SE-54 fused silica capillary column (J&W Scientific, Rancho Cordovo, California) at room temperature. The column was then held isothermally at 50°C for two minutes, programmed to 95°C at 4°C per minute, then to 280°C at 6°C per minute where the temperature was held for the duration of the run. The mass spectrometer was run in the electron impact, direct mode, with an emission current of 0.5 ma, an electron energy of 70 eV, the electron multiplier at 1600 volts and the ion source at 250°C. The data system was programmed to scan from m/e 34 to 450 in 0.95 seconds with a 0.05 second hold at the bottom.

RESULTS

Table I shows the results of seven replicate runs for a 100 ng/l spike in blank water. The accuracy shown includes adjustment for recovery. Table II shows the results of a 50 ng/l spike into a wastewater matrix. Although not all compounds tested are shown in the tables attached, the authors can summarize as follows: (1) with internal standard and recovery correction average relative error was 20% for 35 compounds spiked in wastewater at 50 nanograms/liter; (2) average precision for 44 compounds tested in 7 replicate runs was 22%; (3) actual recoveries range from 1-90% and are dependent on the polarity, ionic character, and boiling points of specific organic compounds tested.

Table I
RECOVERY AND PRECISION @ 100 ng/liter

Compound	Recovered(ng/l)	% Std. Dev.
Chlorobenzene	89	5.4
Ethylbenzene	79	7.6
Bromoform	82	17
2-Chloronaphthalene	82	16
Geosmin	78	12
Fluorene	106	30
Hexachlorobenzene	90	21
o-Dichlorobenzene	89	5.4

Based on 7 runs

Table II
WASTEWATER SPIKE RECOVERY

Compound	Original Sample (ng/l)	After 50 ng/l Spike	% Recovery
Chlorobenzene	2.4	53	102
Ethylbenzene	52	100	96
Bromoform	1.0	43	84
2-Chloronaphthalene	ND	59	118
Geosmin	4.6	50	100
Fluorene	ND	58	116
Hexachlorobenzene	ND	33	66
o-Dichlorobenzene	2.4	56	112

REFERENCES

1. Grob, K., "Organic Substances in Potable Water and in its Precursor, Part I. Methods for Their Determination by Gas-Liquid Chromatography." J. Chromatogr., 84:255 (1973).

2. McCarty, P.L., Reinhard, M., and Argo, D.G., "Organics Removal by Advanced Wastewater Treatment." Proc. 97th AWWA Annual Conf., Anaheim, CA (May 1977).

3. Melton, R.G., et al., "Comparison of Grob Closed-Loop Stripping Analysis with Other Trace Organic Methods," Advances in the Identification and Analysis of Organic Pollutants in Water Vol. 2., pp. 597-673, Ann Arbor Science (1981).

4. Trussell, A.R., Moncur, J.G., "Extended Use of the Purge and Trap Technique on Low Volatility Organics in Water" Proceedings 29th Annual ASMS Conference (May 1981).

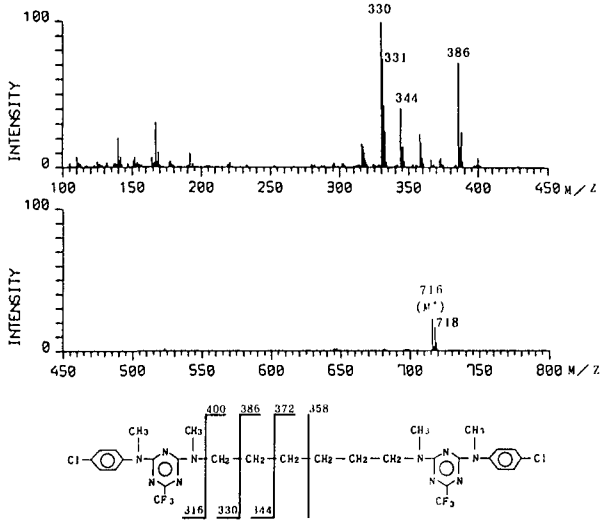
5. Krasner, S.W., Hwang, C.J., and McGuire, M.J., "Development of a Closed-Loop Stripping Technique for the Analysis of Taste and Odor Causing Substances in Drinking Water," Advances in the Identification and Analysis of Organic Pollutants in Water Vol. 2., pp. 689-710, An Arbor Science (1981).

ANALYSIS OF CHLORHEXIDINE IN WASTE WATER USING AN EXTRELUT COLUMN, ON-COLUMN METHYLATION AND MASS FRAGMENTOGRAPHY

Hajime Matsushima and Nobuo Sakurai; Department of Hygiene, Hamamatsu University School of Medicine, 3600 Handa-cho, Hamamatsu 431-31, Japan

We have developed a new method to determine chlorhexidine {1,6-di(4'-chlorophenyldiguanido)hexane, CH}, a disinfectant, in waste water from medical center by mass fragmentography. The followings are the procedures: To 100 ml of the waste water, 1.0-3.0 ml of 1N NaOH solution was added to adjust the pH to 12.5-13.0. Twenty-ml of the solution was transferred to an Extrelut column and then eluted with 40 ml of ethyl acetate. To the eluate concentrated to about 0.1 ml under reduced pressure, 0.2 ml of trifluoroacetic anhydride was added and mixed vigorously for 2 min at room temperature. The solution containing a CH triazine derivative was evaporated to dryness under N_2 gas, dissolved in 0.2M trimethylanilinium hydroxide in methanol, and subjected to on-column methylation in a gas chromatographic column by mass fragmentography. CH amounts were determined by monitoring at m/z 330, 331 and 386.

The mass spectrum of the CH triazine N-methyl derivative from standard working solution is shown in the Figure.



MASS SPECTRUM OF A CH TRIAZINE N-METHYL DERIVATIVE AND SUSPECTED FRAGMENTATION MECHANISMS

As the CH derivative has two chlorines, there were fragment ions at m/z 718 and 720 and a molecular ion m/z 716, with an intensity ratio of 9:6:1. The base peak was at m/z 330 with additional ions at m/z 331, 344 and 386. The suspected fragmentation mechanisms are depicted also in the Figure.

The analyses were performed on a JEOL D-300 gas chromatograph/mass spectrometer equipped with a JEOL 2000E computer-controlled data analysis system. The gas chromatographic separation was made on a 1.0m × 2mm glass column packed with 1% Silicone OV-1 on Chromosorb W 60-80 mesh. Two to four µl of the derivatized sample was injected onto a column. The gas chromatographic conditions were: injection temperature 320°C, column temperature 290°C and helium flow rate 30 ml/min. The mass spectrometer conditions were: electron energy 70 eV, separator temperature 320°C, ionizing chamber temperature 250°C, ion accelerating voltage 3.0 kV and ionizing current 300 µA.

The CH derivative was identified on the basis of retention time and mass spectrum by direct comparison with that of the standard compound. The CH derivative was determined by absolute calibration curve of the peak area of the mass fragmentograms.

About 90% of CH added to waste waters was recovered in amounts from 1 to 10 µg. The Table shows the concentrations of CH in waste water from Hamamatsu University School of Medicine using the present method. CH in medical waste water and sewage was found to have concentrations of 85-1940 and 15-107 µg/l, respectively.

This method is simple, rapid, sensitive, and quite specific for CH.

CH IN WASTE WATER FROM HAMAMATSU UNIVERSITY SCHOOL OF MEDICINE

(µg/l)

Date	Medical Waste Water	Sewage
22 Jul., 1981	213	77
19 Aug., 1981	85	92
16 Sep., 1981	228	107
21 Oct., 1981	216	88
18 Nov., 1981	1940	92
16 Dec., 1981	509	15
20 Jan., 1982	1310	38
17 Feb., 1982	237	51
17 Mar., 1982	134	33

ROF 9 QUALITY CONTROL PROTOCOL FOR THE FUSED SILICA CAPILLARY COLUMN GAS CHROMATOGRAPHY/MASS SPECTROMETRY DETERMINATION OF SEMIVOLATILE PRIORITY POLLUATANTS; Viorica Lopez-Avila. Acurex Corporation, 485 Clyde Avenue, Mountain View, California 94042; Andrew D. Sauter Environmental Protection Agency, Las Vegas, Nevada 89114

A quality control protocol for the determination of priority pollutants (acids, base/neutral, pesticides) using a fused silica capillary column GC/MS procedure has been developed. The protocol gives column specifications, installation and operating details, requirements for system calibration and retention time reproducibility. The QC procedures recommended in this protocol will be discussed. An interlaboratory study using this protocol demonstrated excellent precision and accuracy for the priority pollutants. Furthermore, the protocol has been tested using various environmental samples; other results obtained in the development and testing of this protocol will be discussed.

ROF 10 ANALYSIS OF ORGANIC POLLUTANTS IN ENVIRONMENTAL SAMPLES BY GC/MS INCLUDING POSITIVE/NEGATIVE EI/CI TECHNIQUES by R. C. Lao, R. S. Thomas and J. Lockwood. Laboratory Services Division, Air Pollution Control Directorate,Environment Canada,Ottawa,Canada,K1A 1C8

There has developed a global concern, in the last two decades, over the worldwide exposure of the environment to a broad range of industrial pollutants with unknown or ill-defined characteristics which may represent significant hazards. One of the fundamental approaches to hazard assessment is the detailed chemical identification and quantification of all organic compounds present in multi-media emissions and effluents. In 1979, EPA published a set of guidelines for the formulation of analytical procedures for the organic priority pollutants. GC/MS is the technique to be used to characterize the individual components present in the sample. A variety of modifications to the original EPA protocol have been proposed including the MAS(master analytical scheme - 1981) for organics in water. Running in parallel to many other efforts, we have endeavoured to develop and apply GC/MS techniques to the analysis of organic substances at ppt/ppb levels in highly complex multi-media matrices. Negative/positive CI techniques and Townsend Discharge Ionization are used to determine polychlorinated hydrocarbons present in the samples. Quality control programs including recovery studies are enhanced to include a broad cross-section of compounds to be determined by the analytical GC/MS procedures. Results from various samples will be presented and discussed.

NEGATIVE (CCl_4) AND POSITIVE (NH_3) CHEMICAL IONIZATION OF THE EXPLOSIVE HEXANITROSTILBENE; R O. YELTON; Monsanto Research Corporation, Mound Facility,* Miamisburg, OH 45342

The use of mass spectrometry in the analysis and characterization of explosives and explosive residues has steadily been increasing over the last decade; as a result, positive and negative ion electron impact and chemical ionization mass spectra of many commonly encountered explosives have been reported by several workers in the open literature.

The nitro-aromatic explosive hexanitrostilbene (HNS) is finding increasing application because of its low sensitivity to shock, friction, and impact, combined with its excellent stability at elevated temperatures (M.P. >315°C); however, mass spectrometric data on this relatively low vapor pressure, high temperature explosive have not been thus far reported. This investigation has been directed toward obtaining a suitable mass spectrum for HNS by examining positive and negative electron impact (EI) and chemical ionization (CI) techniques

Experimental - Mass spectra have been recorded on a Kratos MS-25/DS-55 double focusing, magnetic sector mass spectrometer/data system equipped with a combined EI-CI source. Reagent gases were admitted via the multiple reagent gas inlet system. The samples were introduced into the ion source by direct insertion probe and were typically 100-200 μg in size. The mass spectrometer operating parameters were adjusted as follows:

Electron Impact Mode (Pos + Neg)

Source Temperature	250°C	Scan Speed	10 s/decade
Electron Energy	70 eV	Accelerating Voltage	2 kV
Trap Current	100 μA	Bandwidth	100 Hz

Chemical Ionization Mode (Pos + Neg)

Source Temperature	150-250°C	Scan Speed	10 s/decade
Source Pressure	0.5-1.0 torr	Accelerating Voltage	2 kV
Emission Current	1.5 mA	Bandwidth	100 Hz
Electron Energy	100 eV	Reagent Gas	CCl_4, NH_3

Magnetic scanning and data collection were allowed to proceed under computer control.

Results and Discussion- The positive EI mass spectrum of HNS (M.W. 450) was recorded at an ion source temperature of 250°C and a probe temperature of 270°C. The base peak in the spectrum appears at M/Z 30[NO]$^+$, with large ions present at M/Z 44[N_2O]$^+$, M/Z 119[C_6HNO_2]$^+$ and M/Z 167[$C_6H_3N_2O_4$]$^+$. The molecule has undergone extensive fragmentation with the most massive peak appearing at M/Z 240[$C_6H_6N_3O_6$]$^+$. No molecular ion was detected.

The negative ion EI mass spectrum of HNS was recorded at an ion source temperature of 250°C and a probe temperature of 260°C. The base peak appears at M/Z 212[$C_6H_2N_3O_6$]$^-$ and yields a large (~50% B.P.) molecular anion at M/Z 450[M]$^-$ with structurally informative ions at M/Z 404[M-NO_2]$^-$; M/Z 387[M-HNO_3]$^-$; M/Z 375[M-$CHNO_3$]$^-$; M/Z 358[M-$2NO_2$]$^-$; M/Z 46[NO_2]$^-$, etc , indicating subsequeht losses of C, N, and O The negative EI mass spectrum of HNS has been found to yield more structural information and ion current than positive EI mass spectra.

The ammonia positive chemical ionization (PCI) mass spectrum of HNS is shown in Figure 1. The spectrum is similar to that obtained in positive EI and could only be obtained when the ion source temperature was increased to 250°C. As the probe temperature was increased to 280°C, extremely weak ions at M/Z 468[M+NH_4]$^+$, formed by ammonia attachment, M/Z 451[MH]$^+$ and M/Z 438[M+NH_4-NO]$^+$ were detected. The sensitivity of this technique was quite poor and experiments with other common PCI reagent gases failed to produce a suitable PCI mass spectrum.

*Mound Facility is operated by Monsanto Research Corporation for the U. S. Department of Energy under Contract No. DE-AC04-76-DPO0053

The carbon tetrachloride negative chemical ionization (NCI) mass spectrum obtained for hexanitrostilbene is given in Figure 2. The spectrum was recorded at an ion source temperature of 150°C and a probe temperature of 240°C. These experiments resulted in the production of an extremely simple mass spectrum for HNS with a base peak at M/Z 450[M]$^-$, the molecular anion resulting from resonance electron capture, which accounts for >80% of the ion current, and a large (20% B.P) ion at M/Z 46[NO_2]$^-$. The spectrum is completely devoid of structural information, but, by increasing the source temperature to 200°C, diminished [M]$^-$ ion intensity and increased fragmentation have been observed. The sensitivity of the technique is comparable to that obtained in negative ion EI experiments.

Severe ion source contamination presented many problems throughout this investigation owing to the fact that optimum temperatures for chemical ionization are 100-150°C below the temperature required to obtain sufficient vapor pressure of HNS. At a source temperature of 250°C, condensation of HNS in the ion source was still encountered.

Negative electron impact and negative ion chemical ionization have been found to be the most sensitive and informative techniques for generating mass spectra containing structural as well as molecular weight information on HNS. Ammonia PCI has been found to be a useful confirmatory technique in the analysis of HNS only when high sensitivity is not required.

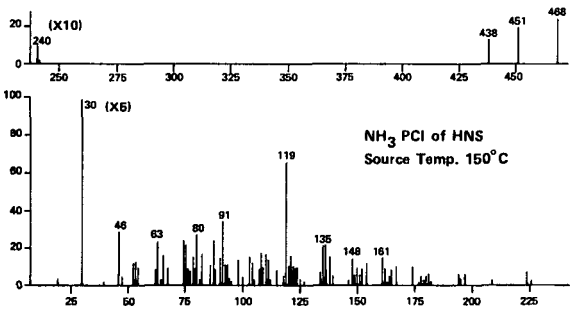


FIGURE 1 - Ammonia PCI spectrum of HNS

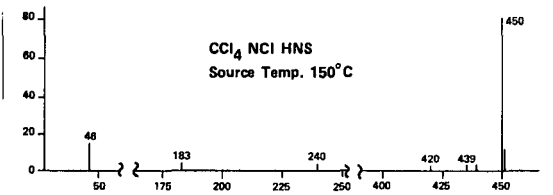


FIGURE 2 - Carbon tetrachloride NCI spectrum of HNS

AMMONIA CHEMICAL IONIZATION OF THE EXPLOSIVES PENTAERYTHRITOLTETRANITRATE AND DIPENTAERYTHRITOL HEXANITRATE; R. O. YELTON; Monsanto Research Corporation, Mound Facility*, Miamisburg, Ohio 45342

The electron mass spectrum of the secondary explosive pentaerythritoltetranitrate[1] (PETN) is dominated by three major ions: M/Z 46$[NO_2]^+$, the base peak, M/Z 30$[NO]^+$, and M/Z 76$[CH_2O\ NO_2]^+$. Thus, its distinction from the spectra of other functionally similar explosives is difficult by this ionization method alone. Positive chemical ionization mass spectra of PETN (M.W. 316) have previously been acquired by several workers utilizing various reagent gases, such as methane,[2] isobutane,[3] hydrogen,[4] and water.[5] The present investigation evaluates the potential analytical application of ammonia as a complementary chemical ionization reagent for the analysis of PETN and its homolog dipentaerythritol hexanitrate (DIPEHN) (M.W. 524).

Experimental - Ammonia positive chemical ionization (PCI) mass spectra have been recorded on a Kratos MS-25/DS-55, double focusing, magnetic sector mass spectrometer operated in the chemical ionization mode. Anhydrous ammonia was admitted into the ionization chamber via the multiple reagent gas inlet system. The samples were introduced into the mass spectrometer source by direct insertion probe and were typically 100-200 μg in size. The mass spectrometer operating parameters were adjusted as follows:

Source Temperature	- 50-150°C	PCI Reagent Gas	- NH_3
Source Pressure	- 0.5-1 torr	Scan Speed	- 10^3s/decade
Emission Current	- 1.5 mA	Accelerating Voltage	- 2 kV
Electron Energy	- 150 eV	Bandwidth	- 100 Hz

Magnetic scanning and data collection were allowed to proceed under computer control.

Results and Discussion - The ammonia PCI mass spectrum of PETN is presented in Figure 1. This spectrum was obtained at an ion source temperature of 150°C and a probe temperature of 120°C. The most massive ion was observed at M/Z 351$[M+NH_4 \cdot NH_3]^+$ but was of very weak intensity. A large adduct ion (~50% B.P.) was present at M/Z 334$[M+NH_4]^+$. The base peak appeared at M/Z 289 and is believed to have been formed in a ternary reaction involving the attachment of ammonia at M/Z 334, the loss of a single nitro group, and subsequent site protonation $[M+NH_4-NO_2+H]^+$. Other large ions appeared at M/Z 244$[289-NO_2+H]^+$, M/Z 199$[244-NO_2+H]^+$, M/Z 104, and M/Z 30$[NO]^+$. The formation of an extremely weak $[MH]^+$ ion was occasionally observed. The source pressure, while still maintaining the ammonia PCI reagent ion intensity at M/Z 18$[NH_4]^+$ and M/Z 35$[NH_4 \cdot NH_3]^+$, had a negligible effect on the spectrum obtained. When the source temperature was decreased to room temperature, the intensities of the higher mass ions were decreased, the base peak appeared at M/Z 52, and a higher probe temperature was required to obtain sufficient sample vapor pressure. Source temperatures greater than 150°C resulted in poor formation of PCI reagent ions and produced spectra similar to those produced by electron bombardment.

The ammonia PCI mass spectrum obtained for DIPHEN is shown in Figure 2. The spectrum was obtained at an ion source temperature of 150°C and a probe temperature of 200°C. The most massive ion detected appeared at M/Z 542$[M+NH_4]^+$; the formation of fragment ions appeared to

*Mound Facility is operated by Monsanto Research Corporation for the U.S. Department of Energy under Contract No. DE-AC04-76-DP00053.

be quite similar to that of PETN with significant ions at M/Z 497$[M+NH_4-NO_2+H]^+$, and at MZ 452, 420, 375, 357, and 312. The base peak in the spectrum appeared at M/Z 30$[NO]^+$ and a large M/Z 46$[NO_2]$ ion was also observed. Only in extremely rare cases has a weak $[MH]^+$ ion at MZ 525 been observed. Some decomposition was also found to occur at elevated probe temperatures. The effects of varying the source pressure and source temperature generally yielded the same results as in the experiments with PETN.

Ammonia chemical ionization has, therefore, been found to be a useful confirmatory tool in the analysis of PETN and DIPEHN when used in conjuction with previously described techniques.

[1]R. Boschan and S. R. Smith (1957), "Mass Spectra of Nitrate Esters, Nitrite Esters, Nitro Compounds and Several Other Nitrogen Compounds," NAVORD Report 5412, U.S. Naval Ordnance Test Station, China Lake, California.

[2]S. Zitrin and J. Yinon (1976), Advances in Mass Spectrom. in Biochem. and Medicine, 1, 369.

[3]R. Saferstein, J. M. Chao and J. J. Manura (1975), J. Assoc. Offic. Anal. Chem., 58, 734.

[4]R. G. Gillis, M. J. Lacey and J. S. Shannon (1974), Org. Mass Spectrom, 9, 359.

[5]J. Yinon (1974), Biomed. Mass Spectrom, 1, 393.

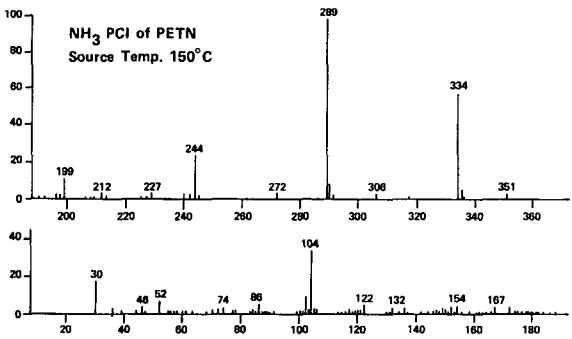


FIGURE 1 - Ammonia PCI spectrum of PETN with a source temperature of 150°C.

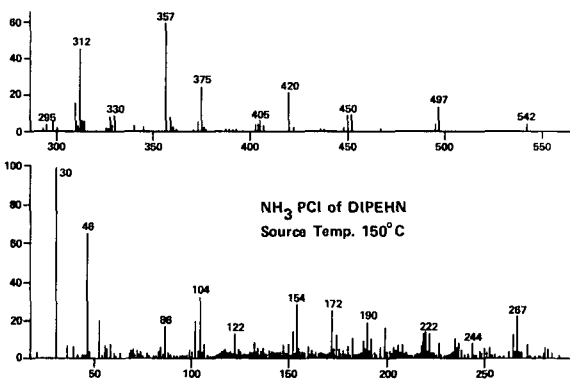


FIGURE 2 - Ammonia PCI spectrum of DIPEHN with a source temperature of 150°C.

ASPECTS OF SINGLET OXYGEN CHEMISTRY IN CHEMICAL IONIZATION MASS SPECTROMETRY; D. C. Lane*and J. M. McGuire, U.S. EPA, Environmental Research Laboratory, Athens, Georgia 30613. *NRC-EPA-ORD Research Associate.

Singlet oxygen ($^1O_2$), which is known to react readily with molecules of environmental interest, including polycyclic aromatic hydrocarbons (PAH), heterocyclics, phenols, polymers, and olefins,[1] may be useful as an analytical reagent as well as a probe for mechanistic studies via mass spectrometry. Considerable interest in $^1O_2$ chemistry stems, for example, from its presence in photochemical smog through the decomposition of peroxyacetylnitrate and subsequent reaction with biological systems and atmospheric components.[2] Experiments have shown that using oxygen as the reagent gas in the presence of a Townsend discharge in CI-MS analyses of PAHs leads to the formation of $(M+32-nH)^-$ ions, where nH represents loss of hydrogen.[3] Identification of the role played by $^1O_2$ in the formation of oxygenated products in the CI ion source is an objective of the present study.

Singlet oxygen can be generated chemically by means of thermolysis of 9,10-diphenylanthracene endoperoxide (DPAE).[4] The reactivity of 1,3-diphenylisobenzofuran (DPBF) with $^1O_2$ to produce o-dibenzoylbenzene (DBB) is well known.[1,4] Preliminary experiments have involved looking for reactivity between DPBF and $^1O_2$ from DPAE on the direct inlet probe of the mass spectrometer under CI conditions. The paper describes the synthesis and purification of DPAE and discusses the observed mass spectra of DPAE, DPBF, and DPAE/DPBF mixtures.

The synthesis of DPAE involves a two-phase system in which $^1O_2$ generated by the slow addition of bromine to alkaline hydrogen peroxide in the lower aqueous phase reacts with 9,10-diphenylanthracene (DPA) in chlorobenzene making up the organic layer.[5] Side reactions include the bromination of DPA. The organic phase is reduced in volume and subjected to column and thin layer chromatography. Electron impact mass spectra of samples taken from TLC plates show that brominated compounds are eluted from the alumina column with unreacted DPA in the petroleum ether/toluene fractions as well as with DPAE in the toluene fraction. Structures and possible decomposition pathways to explain observed ions are suggested for the brominated species.

Isobutane CI-MS of DPAE, introduced via the direct inlet probe, yields ions at m/Z 363, 347, 331, and 387, corresponding to $(M+1)^+$, $(M-16+1)^+$, $(M-32+1)^+$, and $(M-32+57)^+$, respectively. Ions at m/Z 331 and 387 can be explained by the loss of molecular oxygen from DPAE to yield DPA, i.e., thermal decomposition of DPAE on the probe, or by the contamination of DPAE by DPA. The latter contribution is minimized by taking the DPAE sample from a TLC plate. The presence of ions at m/Z 347 and 73 indicates the loss of atomic oxygen and the interaction of atomic oxygen with $C_4H_9^+$ reagent gas ions, respectively.

Isobutane CI-MS of DPBF gives rise to ions at m/Z 271 and 327 corresponding to $(M+1)^+$ and $(M+57)^+$. Low intensity ions at m/Z 287 also appear, probably due to contamination from DBB as a result of the ease with which DPBF undergoes autoxidation in air.

To obtain evidence for singlet oxygen reactivity, mixtures of DPAE and DBPF were heated rapidly on the solids probe to induce thermal decomposition of DPAE and subsequent $^1O_2$ reaction with DBPF. The isobutane CI mass spectra contained ions typical of DPAE and DBPF with ions at m/Z 287 corresponding to $(DBPF+16+1)^+$ or $(DBB+1)^+$, at intensities greater than those observed for DBPF mass spectra. Ions at m/Z 303, which could be correlated with a DBPF-$^1O_2$ Diels-Alder adduct, were not observed.

Mass spectra of DPAE, DPBF, and DPAE/DPBF mixtures using helium under CI conditions also show evidence of reactivity: ions at $(M-16)^+$ and $(M-32)^+$ from DPAE decomposition as well as the increased intensity for

ions at m/Z 286 associated with DBB formation from DPBF. Similar experiments with mixtures of DPAE and $^1O_2$ reactive substrates, difluorophenylfuran and indene, give inconclusive results.

Experiments thus far completed indicate evidence for the release of oxygen via thermolysis of DPAE on the solids probe and subsequent interaction of the oxygen species with DPBF. Further work will involve introducing the $^1O_2$-reactive substrates, i.e. dimethylfuran, indene, and cyclohexadiene, as CI reagent gases, not only to increase the potential for $^1O_2$ reactivity in the CI-MS source, but also to identify variations in DPAE CI mass spectra with source conditions.

REFERENCES

1 H. H. Wasserman and R. W. Murray, Singlet Oxygen, Academic Press, New York (1979).

2 K. L. Demerjian, J. A. Kerr, and J. E. Calvert, Ad. Environ. Sci. Technol., 4, 1 (1974).

3 D. F. Hunt, G. C. Stafford, Jr., F. W. Crow, and J. W. Russell, Anal. Chem., 48, 2098 (1976); D. F. Hunt, et al., in Mass Spectrometry, Part B, C. Merritt, Jr. and C. N. McEwen, eds., Marcel Dekker, Inc., New York (1980).

4 H. H. Wasserman, J. R. Scheffer, and J. L. Cooper, J. Am. Chem. Soc. 94, 4991 (1972).

5 E. McKeown and W. A. Waters, J. Chem. Soc. (B), 1040-1046 (1966).

NOTE: This is an abstract of a proposed presentation and does not necessarily reflect EPA policy.

CONFORMATIONAL AND CONFIGURATIONAL EFFECTS IN THE AMMONIA CHEMICAL IONIZATION MASS SPECTRA OF CYCLIC MONOALCOHOLS.

F.O. Gülaçar*, F.J. Winkler**, F. Mermoud* and A. Buchs*

*Mass Spectrometry Center, University of Geneva, 16 Bd. d'Yvoy, 1211 Geneva 4, Switz.
**Institut fÜr Chemie Weihenstephan, Technische Univ. MÜnchen, Freising, West Germany.

Chemical ionization mass spectrometry has been shown to be a useful technique for the investigation of the stereochemistry of epimeric compounds, and more particularly epimeric diols[1]. Recently, our preliminary work on isobutane and ammonia chemical ionization of a restricted set of epimeric cyclic monoalcohols has demonstrated that CI could also be an adequate technique for stereochemical assignments of these compounds[2]. In the present work, we discuss the ammonia CI mass spectra of a large number of cyclic monoalcohols in order to demonstrate the reliability of the energetic correlation approach for studying the stereospecificity of the fragmentation of even-electron ions.

Ammonia CI mass spectra of cyclic monoalcohols exhibit the MNH_4^+ adduct ions, the $(MNH_4\text{-}H_2)^+$ and $(MNH_4\text{-}H_2O)^+$ ions, as well as some other ions formed through further fragmentations. The competing dehydrogenation and dehydration reactions of the adduct ions are a priori good candidates for studying the influence of stereochemistry. In the case of the deydrogenation reaction, where the epimeric adduct ions fragment to the same product ions, the differences in the yields of the $(MNH_4\text{-}H_2)^+$ ions in the spectra of the two epimers of any given pair correlate with the difference in the steric compression energies in the precursor ions.

The results presented in Table 1 clearly show that for the flexible hexa- and penta-cyclic monoalcohols, the $(MNH_4\text{-}H_2)^+/MNH_4^+$ abundance ratios are definitely higher for the epimers having mainly an 'axial' OH conformation. For epimeric pairs with a bulky vicinal alkyl substituent, the differences are considerably reduced, or even reversed. The strong vicinal gauche alkyl-hydroxyl interactions, which is the same for both epimers of a pair, probably surpasses the C(1)-OH and C(1) H diaxial interactions with the ring hydrogen atoms. A correlation between the $(MNH_4\text{-}H_2O)^+$ ion abundance and the conformation of OH does also exist, but it is much less pronounced, because of the low abundance of the former ions.

Table 1 - Dehydrogenation and dehydration of the MNH_4^+ ions in the NH_3/CI mass spectra of flexible cyclic monoalcohols.

	MNH_4^+ (% Σ_{60})		$(MNH_4\text{-}H_2)^+/MNH_4^+$		$(MNH_4\text{-}H_2O)^+/MNH_4^+$	
Conformation of OH:	ax	eq	ax	eq	ax	eq
Me-1-Cyclohexanol	25	-	0.09	-	0.87	-
Me-2-Cyclohexanol	4.5	13	9.2	2.1	0.46	0.22
Et-2-Cyclohexanol	13	23	1.7	0.68	0.17	0.12
n-Bu-2-Cyclohexanol	10	12	2.9	2.6	0.21	0.25
t-Bu-Cyclohexanol	7.4	9.4	2.9	2.8	0.34	0.25
Menthol	9.0	12	3.2	1.9	0.17	0.17
Me-3-Cyclohexanol	5.1	11	6.0	2.1	0.27	0.15
Me-4-Cyclohexanol	7.5	12	4.5	1.8	0.13	0.10
t-Bu-4-Cyclohexanol	5.6	9.1	6.9	3.2	0.11	0.07
Me-2-Cyclopentanol	1.5	3.4	29	9.8	0.93	0.59

Table 2 - Dehydrogenation and dehydration of the MNH_4^+ ions in the ammonia chemical ionization mass spectra of rigid cyclic monoalcohols.

	MNH_4^+ ($\%\Sigma_{60}$)	$(MNH_4-H_2)^+/MNH_4^+$	$(MNH_4-H_2O)^+/MNH_4^+$
Trans-1-decalol	6.5	5.3	0.22
Trans-2-decalol (OH axial)	6.9	4.2	0.12
Trans-2-decalol (OH equat)	10.1	2.1	0.07
Borneol (exo)	1.8	14.9	8.0
Isoborneol (endo)	1.6	20.1	1.09
Norborneol (exo)	0.54	12.2	47.4
Norborneol (endo)	2.9	7.0	0.49
Fenchol (endo)	3.5	6.4	0.59
Adamantanol-2	6.4	5.5	0.59
Adamantanol-1	36.1	0.04	0.88

Table 2 shows the results obtained with some rigid cyclic monoalcohols. The two epimers of trans-2-decalol can be distinguished in the same way as the epimers of the cyclohexanol series. In the borneol series, the main difference between the endo and the exo epimers is the loss of the elements of water from the MNH_4^+ adduct ions. The exo epimers, with the more hindered OH substituent, exhibit high yields for the formation of $(MNH_4-H_2O)^+$, while the same ions are of negligible abundance in the mass spectra of the endo epimers. On the above basis, the mass spectrum of the unknown fenchol isomer may be attributed to the endo epimer, thus showing the utility of the NH_3/CI technique.

Adamantanol-2 and adamantanol-1 exhibit the characteristics which permit to distinguish secondary from tertiary alcohols in the cyclohexanol series. The dehydrogenation reaction of adamantanol-2 occurs with a facility similar to that of the 'axial' epimers of the cyclohexanol series, while adamantanol-1 behaves exactly like methyl-1-cyclohexanol.

The results which are presented here were obtained with a Finnigan GCMS 4000 instrument, at a ion source temperature of 60° C. The stereospecificity of the two reactions which serve as a probe for stereochemical assignments is not affected when the temperature of the ion source is increased stepwise up to 250 ° C., in spite of the fact that the mass spectra are temperature dependent. A more complete account of this research will be published elsewhere.

Literature

1- See for example: a) F.J. Winkler and F.W. McLafferty, Tetrahedron 30, 2971 (1974); b) B. Munson, B.L.Jelus, F. Hutch, T.K. Morgan Jr. and R.K. Murray Jr., Org. Mass Spectrom. 15, 161 (1980); c) F.J. Winkler and D. Stahl, J. Am. Chem. Soc. 101, 3685, (1979); d) R. Wolfschütz, H. Schwarz, W. Baum and W.J. Richter, Org. Mass Spectrom. 16, 37 (1981).

2- F.J. Winkler, O.F. Gülaçar and A. Buchs, Proc. of the 8th International Symposium on Recent Developments in Mass Spectrometry in Biochemistry, Medicine and Environmental Research, Venice (Italy), 18-19 June 1980.

QUANTITATIVE ANALYSIS OF VITAMINS BY MASS SPECTROMETRY

D.J. FRAISSE[+], F.F. MAQUIN[+], C.E. BOURGEOIS[++] and S. ALAMERCERY[+]

\+ Mass Spectrometry Center - SCA - CNRS - BP 22 - 69390 VERNAISON - FRANCE
++ Hoffmann-La Roche - 59 rue Pasteur - 94120 FONTENAY-sous-BOIS - FRANCE

The analysis of vitamins in foodstuffs, has been increasingly used to obtain compositional and nutritional data and to follow changes in food composition during processing and storage. Vitamins are labile compounds and are difficult to analyse due to their sensitivity to the action of light, heat or enzymes. Existing techniques such as titrimetry, colorimetry UV spectrometry, microbiological assay, fluorimetry and gas-liquid chromatography lack the necessary specificity and reliability (1). Even liquid chromatography is unsatisfactory because each vitamin requires specific operating conditions and is subject to interferences. Quantitative analysis of derivatized vitamin D (2) and vitamin E (3) in plasma by combined GC-MS-MID (Multiple Ion Detection) have been reported ; however this method is limited to the types of vitamins which can be derivatized which may head to the introduction of contamination, require intensive cleanup and additional time. The work described in this demonstrates the importance of the technique of mass spectrometry for the analysis of vitamins. Fat soluble vitamins have been analysed in EI, PCI and NCI techniques (table I).

TABLE I - EI and CI MASS SPECTRA OF VITAMINS

	EI - 70 eV		PCI - NH_4^+		NCI - OH^- (CH_4+N_2O)	
	m/z	I	m/z	I	m/z	I
Vitamin E α tocopherol $C_{29}H_{50}O_2$ MW = 430	430 205 165	100 % 9,1 % 90 %	431 165	100 % 18 %	429 164	90 % 100 %
Vitamin E-acetate α tocopheryl acetate $C_{31}H_{52}O_3$ MW = 472	472 430 207 165	15 % 100 % 12 % 38 %	490 473 472 430	100 % 60 % 19 % 43 %	472 471 429 164	78 % 100 % 74 % 55 %
Vitamin D_2 ergocalciferol $C_{28}H_{44}O$ MW = 396	396 136 118 117 55	71 % 85 % 100 % 29 % 95 %	397 398	100 % 29 %	396 395 377	43 % 100 % 17 %
Vitamin D_3 cholecalciferol $C_{27}H_{44}O$ MW = 384	384 136 118 117	27 % 100 % 73 % 51 %	386 385	29 % 100 %	384 383 365	67 % 100 % 15 %
Vitamin A Renitol $C_{20}H_{30}O$ MW = 286	286 268	13 % 100 %	287 269	11 % 100 %	285 267 268	100 % 73 % 66 %
Vitamin A acetate Renityl acetate $C_{22}H_{32}O_2$ MW = 328	328 269 268 69	90 % 31 % 59 % 100 %	329 269	2 % 100 %	327 59	1 % 100 %

Electron impact mass spectra show intense peaks due to the molecular ions, but often unfortunately are accompanied by many fragment ion peaks which is a limiting factor of this ionisation technique making it unsuitable for simultaneous quantitative analysis of several vitamins.

Negative chemical ionisation with OH^- as reagent gas give very intense molecular proton abstracted ion $(M-H)^-$.
Positive chemical ionisation spectra show very few fragment ions and very intense molecular protoned ions. This technique has been selected in our work keeping in mind that negative chemical ionisation $(OH)^-$ might be an alternative in some cases.
Three fat-soluble vitamins, extracted from polyvitamins mixtures used in foods, i.e,retinol acetate (vitamin E acetate), cholecalciferol (vitamin D_3) and tocopheryl acetate (vitamin E acetate) have been measured.
The perdeuterated vitamins are often difficult to obtain. Initialy cholesterol was used as internal standard but since this compound is also present in foodstuffs and could lead to possible interference it has been replaced by lupeol which gives a very simple mass spectrum by (NH_3) positive chemical ionisation.
Direct probe introduction technique and repetitive scanning under NH_3) CI^+ conditions of selested ions, i.e, m/z 269 $(MH-60)^+$ of retinyl acetate, m/z 385 $(MH)^+$ of cholecalciferol m/z 490 $(M+NH_4)$ of tocopheryl acetate was used. The select ions of the internal standard were m/z 369 of cholesterol $(MH-H_2O-NH_3)^+$or m/z 409 of lupeol $(MH-H_2O)^+$.
Calibration curves were plotted by running standard solutions in hexane of pure vitamins each containing 50 µg/ µl of internal standard. Table 2 shows the three different curves which were obtained which may be seen to be linear over the range 200 µg/ µl to 1 mg/ µl of vitamin. The measurements obtained for the unknow extract match with those obtained by other conventionnal methods.

Extract	Vitamin E acetate tocophenyl acetate	Vitamin A acetate renityl acetate	Vitamin D_3 cholecalciferol
Expected value	3-10 mg/ml	344-1032 µg/ml	50-125 µg/ml
Result by direct probe introduction	8,5 mg/ml	680 µg/ml	138 µg/ml

It appears that mass spectrometry can be an alternative method for quantitative analysis of vitamins. Howerver quantitative measurements on three or more vitamins simultaneously has not yet been completed.

(1) A.A. CHRISTIE, R.A. WIGGINS, Dev. Food Anal. Tech. 1,1 (1978)

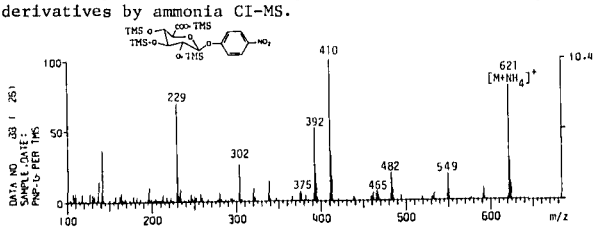
(2) D.A. SEAMARK, D.J-H. TRAFFORD, H.L.J. MAKIN, Clinica Chimica Acta 106, 51 (1980)

(3) M. NAKANISHI, K. TSUCHIYA, K. SAKAGUCHI and T. FUJITA, YAKUGAKU ZASSHI 99, 10, 1037 (1979)

RPA 6 CHARACTERIZATION OF GLUCURONIDES BY AMMONIA CHEMICAL IONIZATION MASS SPECTROMETRY(CI-MS) USING LINKED SCANNING MODE

Y.HASHIMOTO,M.ISHIBASHI and H.MIYAZAKI,Pharmaceutical Divi. Nippon Kayaku Co.,Tokyo,JAPAN
K.NOZIMA,E.YAMAUCHI and T.AOYAMA,Application Lab.Mass Spectrometer Department,JEOL Ltd.,Tokyo,JAPAN

We have found that ammonia CI-MS of per-TMS derivatives of glucuronides provides us useful information for their structural elucidation. The figure shows an ammonia CI mass spectrum of the per-TMS derivatives of p-nitrophenyl-ß-glucuronide (PNP-G) as a representative sample. The ion at m/z 410 yielded from the glucuronic acid moiety was observed as a base peak and the ion at m/z 621 corresponding to $[M+NH_4]^+$and m/z 229 from the aglycon moiety appeared as prominent peaks. A shift technique using $[^2H_3]$-ammonia as a reagent gas was applied to estimate the structure of these ions, indicating that the ions at m/z 621,410 and 229 were the ion species attached NH_4^+, and the ions at m/z 482 and 329 were those attached nuetral NH_3. However, the ion structure of m/z 302 could not be clarified by this technique, because this ion was shifted to m/z 304 by the use of $[^2H_3]$-ammonia. High resolution ammonia CI-MS gave the formula of $C_{12}H_{22}NO_4D_2Si_2$ as the most favorite composition of $TMSO^2H$ from the ion of m/z 395. Thus a linked scanning technique and TMS-dimethylethylsilyl exchange reaction were applied to confirm the fragmentation pathway. These facts indicated that there were two different pathways in the fragmentation of the PNP-G-per-TMS derivatives by ammonia CI-MS.



CHEMICAL IONIZATION MASS SPECTROMETRY OF BIFUNCTIONAL COMPOUNDS

H. Nakata and H. Konishi
Department of Chemistry, Aichi Kyoiku University
Kariya, Aichi, 448, Japan

N. Takeda, M. Suzuki, and A. Tatematsu
Faculty of Pharmacy, Meijo University, Nagoya, 468, Japan

The purpose of this work is to re-examine empirical rules for fragmentations in chemical ionization mass spectrometry of bifunctional compounds X-P-Y, where X and Y = NH_2, OCH_3, OH, and P = rigid or flexible carbon skeleton.

1) Site of Protonation

If the carbon skeleton P is rigid, the effective proton exchange would not occur between $\overset{+}{H}X$-P-Y and X-P-$\overset{+}{Y}H$. Therefore, both types of protonated molecule are formed regardless of the proton affinity of X and Y.

2) Local Bond Weakening on Protonation

Bond cleavages often seem to be triggered by the formal positive charge arising from the protonation of the substrate molecule (1). We calculated the bond index differences between protonated and neutral molecules of a model compound by INDO MO method. It is clear that when the protonation occurs at one functional group, bond weakening, indicated by positive values in the following figure, also takes place around that functional group, and this may cause a cleavage of that part of the molecule. In fact, the model compound shows both $[MH-NH_3]^+$ and $[MH-CH_3OH]^+$ peaks in the CH_4 mediated mass spectrum (Table 1).

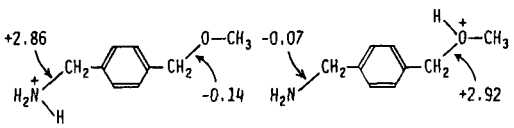


Table 1

	m/z	Σ_{100} Methane	Isobutane	
$[MH]^+$	152	13 %	45 %	NH_2-CH_2-⟨benzene⟩-CH_2-O-CH_3
$[MH-NH_3]^+$	135	32	7	
$[MH-CH_3OH]^+$	120	31	20	
$[\ ?\ ]^+$	106	6	6	
$[MH]^+$	180	36 %		$(CH_3)_2N$-CH_2-⟨benzene⟩-CH_2-O-CH_3
$[MH-(CH_3)_2NH]^+$	135	5		
$[MH-CH_3OH]^+$	148	40		

3) Internal Energy of Protonated Molecule

The protonated molecule initially acquires a part of energies of the protonation exothermicity (heats of protonation). About 2×10^2 collisions occurring in the ion source would then result the dissipation of the excess energies, and average internal energies of the protonated molecule tend to shift to the lower side.

4) Fragmentation Selectivity

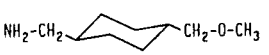
Although the quantity of fragment ions depends on P(E) and k(E) curves, fragmentations may usually take place more favorably from the protonated molecule that has protons at less basic site, because the product states HX + $[PY]^+$ and HY + $[PX]^+$ would be in similar energies, if X or Y does not have any strong interactions to the charged site. A useful corollary is that the less basic functional group can be cleaved more easily.

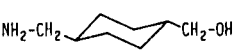
5) Product Stability Criterion

As far as the simple bond cleavage is concerned, the activation energy of the fragmentation is approximated by the heats of reaction as in EI fragmentations. This is the basis of product stability criterion for fragmentation: the more stable products are formed more preferentially. As a result, if the product state becomes less stable, fragmentations will occur less favorably. For example, when the aromatic nucleus above is replaced by a cyclohexane ring, fragmentations are suppressed substantially (Table 2).

Table 2

	m/z	Methane		m/z	Methane
$[MH]^+$	158	56 % Σ_{100}	$[MH]^+$	144	48 % Σ_{80}
$[MH-NH_3]^+$	141	--	$[MH-NH_3]^+$	127	--
$[MH-CH_3OH]^+$	126	10	$[MH-H_2O]^+$	126	20
$[MH-CH_3OH-NH_3]^+$	109	6	$[MH-H_2O-NH_3]^+$	109	13





6) Structure Reactivity Correlation

In a pair of compounds of the type X-P-Y and X-P-Z, the similar argument can be applied. Thus the less basic functional group Z (e.g., OH) can be cleaved more easily than more basic Y (e.g., OCH_3) at a constant X (e.g., NH_2)(Table 2).

Reference:

(1) H.Nakata, M.Suzuki, K.Harada, N.Takeda, and A.Tatematsu, Org. Mass Spectrom., 16, 188 (1981).

RPA 8 POSITIVE AND NEGATIVE ION HYDROGEN CHEMICAL IONIZATION OF PORPHYRINS AND METALLOPROPHYRINS BY QUADRUPOLE MS/MS. P. Sundaraman[1], E.J. Gallegos[2], J.R.B. Slayback[3], M. Johnston[3] and E.W. Baker[4]
[1]Chevron Oil Field Research Company, Richmond, CA 94805; [2]Chevron Research Company, Richmond, CA 94805; [3]Finnigan MAT, Sunnyvale, CA 94086; and [4]Florida Atlantic University, Boca Raton, FL 33432

The EIMS of porphyrins and metalloporphyrins provide very limited structural information. Recently the hydrogen chemical ionization MS of porphyrins was shown to be useful in determining the structure of individual porphyrins. The positive and negative ion hydrogen chemical ionization MS and MS/MS of both porphyrins and metalloporphyrins were obtained. In these experiments, a Finnigan MAT triple stage quadrupole was used to collect CIMS and collision-activated decomposition spectra (CAD) under various instrumental conditions.

The results show that the nickelporphyrin undergoes hydrogenation in the ion source followed by demetallation using CAD processes to give the free base porphyrin which undergoes further fragmentation. On the other hand the vanadyl porphyrin undergoes hydrogenation followed by loss of water, ethyl and methyl groups. No loss of the metal was observed.

Under CAD conditions, daughter spectra of the free base porphyrins showed formation of the mono, di and tri-pyrroles.

In the negative ion experiments, the free base porphyrins did not ionize significantly whereas the metalloporphyrins produced intense molecular anions with little fragmentation. Implications of these experiments will be discussed.

RPA 9 THE DETECTION OF SULFUR AND NITROGEN OXIDES IN THE ATMOSPHERE BY API/MS; F.M. Benoit, Health and Welfare Canada, Environmental Health Directorate, Ottawa, Canada, K1A 0L2.

The presence of sulfur and nitrogen oxides in the atmosphere can result in environmental damage either by direct attack, if present in high concentrations, or by indirect attack such as acid rain, if present in low concentrations. A novel technique for the detection of vapours in air is atmospheric pressure ionization mass spectrometry (API/MS) whereby ionization may be effected by proton transfer, proton abstraction or charge transfer depending upon the mode of ionization and the reagent ion selected. The usual reagent species in the positive mode is a collection of protonated water clusters generated by electron impact of the water molecules usually present in the atmosphere.

An API/MS, the TAGA 3000, mounted in a mobile laboratory has recently been used in field trials to detect vapours in the atmosphere. A number of sulfur and nitrogen oxides were detected. The identification and reactive sequences of the oxides detected will be discussed. The use of additional reagent ions will be commented on.

HIGH PRESSURE LIQUID CARBON DIOXIDE EXTRACTION OF TETRACHLORODIBENZO-P-DIOXINS (TCDDs).

Fred L. DeRoos, Dan G. Aichele, Joe E. Tabor, and Mike Larson, Battelle's Columbus Laboratories, 505 King Avenue, Columbus, Ohio 43201.

INTRODUCTION - The technique of high pressure soxhlet extraction using liquid carbon dioxide as the solvent was investigated for the extraction of TCDDs from environmentally significant samples. This technique was found to be faster than conventional soxhlet extraction and able to efficiently extract TCDDs from most sample matrices. A comparison of the High Pressure Soxhlet Extraction Technique with Conventional Low Pressure Soxhlet Extraction is shown in Figure 1.

FIGURE 1. COMPARISON OF HIGH PRESSURE AND CONVENTIONAL LOW PRESSURE SOXHLET EXTRACTIONS

Conventional Low Pressure Soxhlet Extraction	High Pressure Liquid CO_2 Extraction
Analyte extracted into relatively large volume of solvent	Analyte extracted into dry flask
Analyte may be lost during solvent concentration step	Solvent removed through sublimation at -78°C
Solvent impurities are concentrated along with the analyte	Solvent is distilled before entering the extraction flask
May have poor extraction of samples containing moisture (dependent upon solvent)	Liquid carbon dioxide is miscible with water

EXTRACTION PROCEDURE - The sample (typically 5 grams) spiked with native 2,3,7,8-TCDD is loaded into the extraction thimble of the soxhlet apparatus. The soxhlet apparatus is placed inside the pressure vessel and approximately 125 grams of dry ice are added around the extraction flask. The needle valve on the vessel cover is fully opened and the cover is attached to the vessel using high strength machine screws. After the carbon dioxide has displaced the air from the pressure vessel, the valve is closed and the lower portion of the vessel is placed in a water bath maintained at 40°C. The cold finger condenser is kept at 0°C using ice water.

After the extraction, the pressure vessel is cooled with dry ice and the needle valve is opened. The vessel is then removed from the dry ice and allowed to reach ambient temperature. The cover is removed and the soxhlet apparatus taken out. The internal standard (2,3,7,8-TCDD-$^{13}C_{12}$) is added to the flask and the extract is transferred to the liquid chromatography columns using three 5 ml rinses of hexane.

Each extract was cleaned up by passing it through a multilayered silica column containing sulfuric acid and sodium hydroxide layers followed by activated alumina and activated florisil columns. The levels of 2,3,7,8-TCDD were quantified using combined high resolution gas chromatography/high resolution mass spectrometry (HRGC/HRMS).

RESULTS

Sample Matrix - Paper

2,3,7,8-TCDD SPIKE LEVEL	2,3,7,8-TCDD LEVEL DETERMINED	
1000 ppt	1005 ppt	
1000 ppt	985 ppt	$\bar{X}$ = 1044 ppt
1000 ppt	1143 ppt	
400 ppt	320 ppt	
400 ppt	374 ppt	$\bar{X}$ = 356 ppt
400 ppt	375 ppt	
100 ppt	111 ppt	
100 ppt	122 ppt	$\bar{X}$ = 123 ppt
100 ppt	136 ppt	

Sample Matrix - Electrostatic Fly Ash

2,3,7,8-TCDD SPIKE LEVEL	2,3,7,8-TCDD LEVEL DETERMINED	
200 ppt	201 ppt	$\bar{X}$ = 176 ppt
200 ppt	150 ppt	
80 ppt	80 ppt	$\bar{X}$ = 78 ppt
80 ppt	75 ppt	
20 ppt	31 ppt	$\bar{X}$ = 28 ppt
20 ppt	26 ppt	
Sample Matrix - Soil		
200 ppt	180 ppt	$\bar{X}$ = 199 ppt
200 ppt	218 ppt	
80 ppt	77 ppt	$\bar{X}$ = 76 ppt
80 ppt	75 ppt	
20 ppt	13 ppt	$\bar{X}$ = 18 ppt
20 ppt	23 ppt	
Sample Matrix - Fish		
200 ppt	209 ppt	$\bar{X}$ = 216 ppt
200 ppt	224 ppt	
100 ppt	116 ppt	$\bar{X}$ = 118 ppt
100 ppt	120 ppt	
20 ppt	16 ppt	$\bar{X}$ = 20 ppt
20 ppt	24 ppt	

CONCLUSIONS - The high pressure liquid carbon dioxide soxhlet extraction technique is a viable alternative to conventional low pressure soxhlet extractions. It is often faster and eliminates evaporative losses which may occur during solvent removal. Further studies should be designed and carried out to directly compare the extraction efficiencies of the two techniques using split samples.

RPA 11 MASS SPECTRAL CHARACTERIZATION OF DIESEL ENGINE PARTICULATE EMISSION EXTRACTS, Marcia G. Nishioka, Fred L. DeRoos, and Bruce A. Petersen, Battelle Columbus Laboratories, 505 King Avenue, Columbus, Ohio 43201

Negative chemical ionization high resolution gas chromatography/mass spectrometry (NCI HRGC/MS) is an especially sensitive technique for the identification of polar PAH derivatives including quinone, semi-quinone, nitro and carboxaldehyde types.(1) A high sensitivity results from the electronegativity of the substituent group which readily accepts a negative charge. Their mass spectra are typically dominated by the molecular ion (M^-) with very little fragmentation. The use of NCI HRGC/MS in conjunction with conventional electron impact HRGC/MS and high resolution mass spectrometry (HRMS) techniques has proved to be very effective in determining formulas, structures, and compound classes of species which are present in extracts of diesel engine exhaust particulates. Data will be presented from the characterization of standards and polar PAH derivatives in extracts of diesel engine exhaust particulate.

(1) M. G. Nishioka, B. A. Petersen, J. Lewtas, Comparison of Direct-Acting Mutagenicity and Nitro-Aromatic Content of Diesel Engine Emission Extracts, 1981. U.S. EPA Diesel Emissions Symposium, October 5-7, 1981. Raleigh, North Carolina.

RPA-13: **GC/MS analysis of the biodegradation products of 4-chlorobiphenyl by gram-negative microorganisms. Robert Massé, François Messier and Marie-France Lévesque, Institut National de la Recherche Scientifique - Santé, Montréal H1N-3M5, Québec, Canada and Michel Sylvestre, Institut Armand-Frappier, Ville Laval, Québec, Canada.**

Polychlorinated biphenyls (PCB's) are a class of relatively inert compounds which industrial use dates back to the 1930th. As a result of the extensive use and the resistance to biodegration, PCB's are now found present in the constituants of the food chains and are recognized as one of the most ubiquitous and persistant environmental pollutants. We have undertaken studies on the microbial biodegradation of PCB's in order to develop bacterial strains with the capability to degrade PCB's into non toxic metabolites for man and animal and to assess the environmental impact of PCB's biodegradation. This abstract describes the GC/MS analysis of the biotransformation products of 4-chlorobiphenyl (4-CB) with gram-negative strain B-206 (1).

EXPERIMENTAL

In a typical experiment, strain B-206 was grown in the presence of 4-CB for 96 hours. The culture was centrifuged and the supernatant extracted at pH 7.0, 3.0 and 1.2 with ethylacetate. The organic extracts were evaporated and the residues derivatized. Chromatographic separation was carried out on a SE-30 30 meters capillary column, directly connected to the EI source of the mass spectrometer (Kratos, MS-25). GC/MS parameters: injection mode: splitless, injector temperature: 250°C, column temperature: 140°C for 5 minutes then programmed to 280°C at 5°/minute, source temperature 250°C, ionizing voltage 70 eV, scanning speed: 1 second/decade.

RESULTS AND DISCUSSION

A typical total ion chromatogram (TIC) obtained by GC/MS analysis of a trimethylsilylated extract (pH 3.0) of the culture medium is shown in Figure 1. Two classes of metabolites resulting from the biotransformation of 4-CB by strain B-206 were detected: a) 4-chlorobiphenylols (peaks 2,3,4,5 and 6) and b) acid metabolites resulting from the oxydative cleavage of 4-CB non chlorinated aromatic ring (peaks 1 and 7). The mass spectra of peaks 1 and 7 (Figure II and III) are identical to that of p-chloro cinnamic acid TMS ester and 2-hydroxy -6-oxo-p-chlorophenylhexanoic acid TMS derivative respectively. Compound 7 is the saturated analog of 2-hydroxy-6-oxo-chlorophenylhexa-2,4-dienoic acid already reported in biodegradation studies of PCB's (2,3). Peaks 2 and 3 (Figure IV and V) were identified as the isomeric 2 and 4-hydroxy-4'-chlorobiphenyl TMS ether derivatives. The latters may derived from 4'-CB 2,3 and 3,4-oxide intermediates. Peaks 4 and 5 were identified as 2,3-dihydro-2,3-dihydroxy and 3,4-dihydro- 3,4-dihydroxy-4'-chlorobiphenyl. The mass spectra of their corresponding TMS derivatives are illustrated in Figure VI and VII. Finally, peak 6 was found homogeneous and its mass spectrum (TMS derivative, Figure VIII) correspond to that of 2,3- and/or 3,4-dihydroxy-4'-chlorobiphenyl. The structure assignments proposed for the dihydroxy metabolites 4,5 and 6 were corroborated by the mass spectra of their n-butyl boronate cyclic ether derivatives. Deuterated TMS (d_9) derivatives were also prepared and analyzed by GC/MS in order to ascertain the structure of the bacterial metabolites.

Interesting observations were made in this study on the microbial metabolism of 4-chlorobiphenyl, in that a) 4-CB was metabolized to monohydroxylated compounds 2 and 3 as it is in mammals, b) 2,3 and 3,4-dihydrodiol metabolites were isolated and c) saturated meta-cleaved metabolite 6 instead of the expected 2-hydroxy-6-oxo-(4-chlorophenyl)-hexa-2,4-dienoic acid was isolated and identified. These data indicate that strain B-206 possesses aryl hydroxylase activity (monooxygenase) similar to that displayed by mammalian hepatic microsomal mixed function oxydase which metabolized PCB's to monohydroxylated compounds via arene oxyde intermediates (4).

REFERENCES

1. Michel Sylvestre, Applied and Environmental Microbiology 39:1223 (1980).
2. B.D. Preston and J.R. Allen, Drug Metabolism and Disposition 8:197 (1980).
3. O. Yagi and R. Sudo, Water Pol. Cont. Fed. 1035 (1980).
4. K. Furukawa, N. Tomizoka and A. Kamibayashi, Applied and Environmental Microbiology 38: 301 (1979).

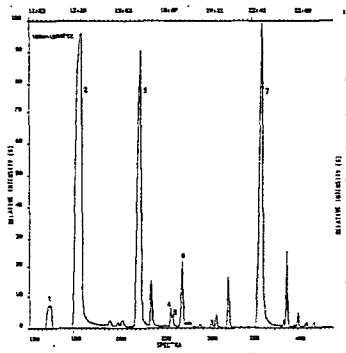


Figure 1. Total-ion chromatogram (TIC) of .3n dichloromethylene extract (gn.1.0) obtained from the growth medium incubated for 96 hours

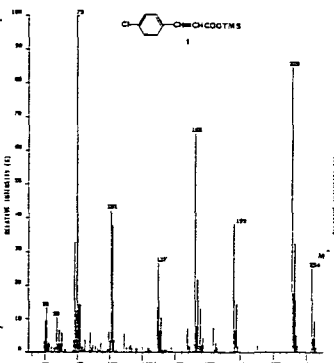


Figure 2 Mass spectrum of compound 1

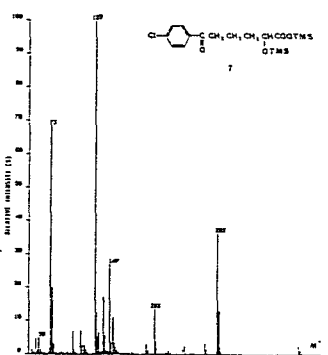


Figure 3. Mass spectrum of compound 7

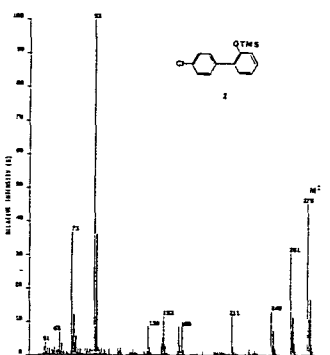


Figure 4. Mass spectrum of compound 2

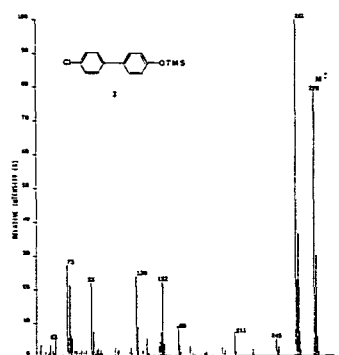


Figure 5. Mass spectrum of compound 3

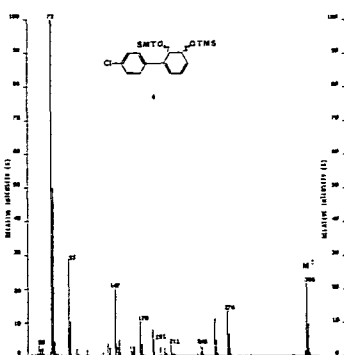


Figure 6 Mass spectrum of compound 4

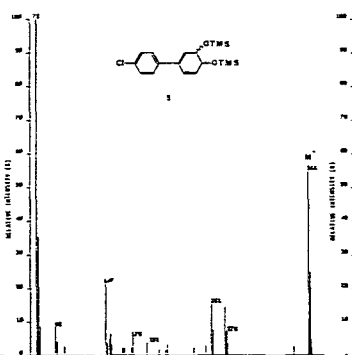


Figure 7 Mass spectrum of compound 5

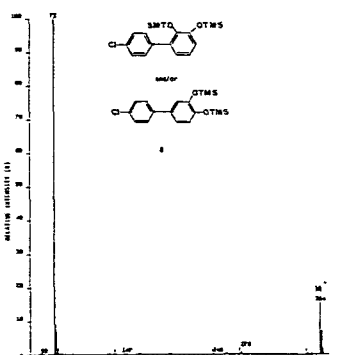


Figure 8 Mass spectrum of compound 6

PENTACYCLIC TERPANES IN A 420-MILLION-YEAR-OLD (SILURIAN) BITUMEN

by Anders, D. E. and King, J. D., USGS, Denver, CO., 80225
Marschner, R. F., Standard Oil (Indiana), Naperville, IL., 60540

Introduction: Niagaran (Silurian) carbonate rocks (300-1,200 m thick) extend from subsurface depths of 3,050 m in the central part of the Michigan basin, to surface exposures along the periphery of the basin (Fig. 1). Niagaran carbonates contain abundant reef-type structures. In the subsurface, along two reef belts, the pinnacle reefs contain commercial oil accumulations. Some reefs outcrops contain tarry bituminous residues. One such example is the Thornton Reef complex (south Chicago IL.) where solid bitumen residues and tarry oozes have become exposed.

Several theories have been proposed for the origin of the Thornton bitumens: 1) the Thornton bitumens are residual products of oil that migrated from Silurian reservoirs of southern Michigan; 2) they are from local organic-rich facies; and 3) they are derived from underlying Ordovician source rocks such as the Utica shale. Using gas chromatographic-mass spectrometric (GC-MS) biomarker correlation techniques, this report considers only the first and third theories.

Experimental: Thornton Reef bitumen occurs as small, black, solid to tarry particles dispersed in the carbonate rock. This bitumen and the bitumen from a Utica shale sample were isolated and analyzed by GC/MS. Also analyzed were three Silurian Michigan basin crudes. A heavy sour crude (API, 18°) from the Salina A-2 carbonate member, Dorr Field, Allegan Co., S.W. Michigan, and two sweet crudes (API, 39°), one from the Niagaran Dolomite, Marine City Field and the other from the Salina A-1 member, Hessen Field, both in S.E. Michigan. The GC separations were achieved using a SE-54 bonded phase WCOT column, 30 m x 0.36 mm I.D.. The mass spectra and ion chromatograms were produced using an AEI MS-30 mass spectrometer coupled to a DS-50 data system.

GC analysis of the alkanes from Thornton bitumen show this material to be devoid of n-alkanes and chain isoprenoids, but rich in heavy cyclic alkanes (Fig. II). This unusual distribution of alkanes is attributed to microbiological degradation. The most abundant cyclic alkanes are the pentacyclic triterpanes of the hopane series (C_{27}-C_{40}). Also present are minor amounts of 5α-steranes (C_{28} and C_{29}) and a number of 3- and 4-ring structures whose mass spectral fragmentation patterns resemble those for pentacyclic triterpanes (principle fragment ion m/z 191). The hydrocarbons of major significance are all numbered on the chromatogram in Fig. II and identified in Table I.

Gas chromatograms and ion chromatograms (m/z 191 and 217) of alkanes isolated from the Thornton bitumen are compared with the chromatograms of hydrocarbons from the Silurian crudes and the Utica shale (Figure II, the Hessen and Marine City are genetically similar, therefore only the Hessen chromatograms are shown).

Results: Compounds 1-3 and 5-7 form a homologous series of condensed-3-ring-extended diterpanes that appear to differ only in the length of the alkyl chain attached to ring C Table II). The principal fragment ion in the spectra of each compound is m/z 191. Also observed was a prominent (M-15) fragment ion, indicating a labile methyl substituent. The geometric configurations of naturally occuring cyclic diterpanes and triterpanes, giving m/z 191 as their principal fragment ion, has been documented widely in the literature (Budzikiewicz, et al, 1963; and others).

Components 8 and 9 fall in the four ring series, but are not steranes as evidenced by the absence of a prominent m/z 217 fragment ion. These components also give m/z 191 as the dominant fragment ion. Component 8 has a prominent M-15 ($-CH_3$) fragment, but little else that is definitive of the alkyl substituents; however, the spectrum of component 9 shows an additional fragment ion at M-29 that is indicative of ethyl loss.

The suggested structures for components 1-3 and 5-9 (Table I) are based on fragmentation patterns of natural occurring hydrocarbons.

The pentacyclic alkane identifications (peaks 11-13, 18 and 20-46, Table I, Figure II) are based on a comparison of GC elution times (SE-54) and MS fragmentation patterns with published data.

Summary and Conclusions: Pentacyclic triterpanes in alkane fractions provide an excellent means of comparing oils with potential source rocks; this is particularly applicable to biodegraded samples wherein pentacyclic triterpanes, resistent to bacterial attack are concentrated. For example, the pentacyclic triterpane distribution (PTD) of the Thornton Reef is identical to the PTD of the Dorr Field crude oil, but significantly different from the PTD of the Marine City and Hessen Field crudes and the Utica shale. The data suggests that oils similar to the Dorr crude may be the source of the Thornton Reef bitumens or

that both bitumens and oils are derived from similar carbonate source rock facies. Further studies of nonstained carbonate source rocks in the vicinity of these samples are required to refine the interpretations.

Extended and degraded hopanes in sediments were once thought to be evidence of higher plant material. However, our identification of hopanes (C_{27}-C_{40}) in Silurian hydrocarbon deposits now place them in sediments that may predate the origin of higher plants. A probable explanation for their abundance in these Silurian deposits is that they were derived from algae or bacteria.

In this report, α, β extended hopane C_{22} diastereomers (S and R) are identified through C_{40}. To our knowledge, previous investigators have identified hopanes only through C_{35}.

References: Budzikiewicz, H., Wilson, J. M., and Djerassi, C., 1963. Mass spectrometry in structural and stereochemical problems. XXXII. Pentacyclic triterpanes: Journal of American Chemical Society, v. 85, p. 3688-3699.

Table 1
Structural Assignment of Biomarkers in Thornton Reef

GC Peak No.	Molecular ION	Empirical Formula	Identification[a]
1	278+	$C_{20}H_{36}$	
2	290+	$C_{21}H_{38}$	
3	304+	$C_{22}H_{40}$	
4	328+	--	
5	318+	$C_{23}H_{42}$	
6	332+	$C_{24}H_{44}$	
7	346+	$C_{25}H_{46}$	
8	330+	$C_{24}H_{42}$	
9	358+	$C_{26}H_{46}$	
10	--		
11	370+	$C_{27}H_{46}$	18αH 21βH - Trisnorhopane
12	370+	$C_{27}H_{46}$	17βH, 21βH - Trisnorhopane
13	384+	$C_{28}H_{48}$	17βH 21βH - Bisnorhopane
14	386+	$C_{28}H_{50}$	C_{28} - Sterane
15	400+	$C_{29}H_{52}$	C_{29} - Sterane
16	400+	$C_{29}H_{52}$	C_{29} - Sterane
17	400+	$C_{29}H_{52}$	C_{29} - Sterane
18	386+	$C_{29}H_{50}$	17βH 21βH - Norhopane
19	400+	$C_{29}H_{52}$	C_{29} Sterane (Silicotane)
20	398+	$C_{29}H_{50}$	17αH 21βH - Normoretane
21	412+	$C_{30}H_{52}$	17αH 21βH - Hopane
22	412+	$C_{30}H_{52}$	17βH 21βH - Moretane
23	426+	$C_{31}H_{54}$	17αH 21βH - Homohopane (22S)
24	426+	$C_{31}H_{54}$	17αH, 21βH - Homohopane (22R)
25	412+	$C_{30}H_{52}$	Gammacerane
26	440+	$C_{32}H_{56}$	17αH 21βH - Bishomohopane (22S)
27	440+	$C_{32}H_{56}$	17αH, 21βH - Bishomohopane (22R)
28	440+	$C_{32}H_{56}$	17αH, 21βH - Bishomohopane
29	454+	$C_{33}H_{58}$	17αH 21βH - Trishomohopane (22S)
30	454+	$C_{33}H_{58}$	17αH 21βH - Trishomohopane (22R)
31	454+	$C_{33}H_{58}$	17αH, 21βH - Trishomoretane
32	468+	$C_{34}H_{60}$	17αH, 21βH - Tetrakishomohopane(22S)
33	468+	$C_{34}H_{60}$	17αH, 21βH - Tetrakishomohopane(22R)
34	468+	$C_{34}H_{60}$	17αH 21βH - Tetrakishomoretane (S or R)
35	482+	$C_{35}H_{62}$	17αH 21βH - Pentakishomohopane(22S)
36	482+	$C_{35}H_{62}$	17αH, 21βH - Pentakishomohopane(22R)
37	496+	$C_{36}H_{64}$	17αH 21βH - Hexakishomohopane(22S)
38	496+	$C_{36}H_{64}$	17αH 21βH - Hexakishomohopane(22R)
39	510	$C_{37}H_{66}$	17αH 21βH - Heptakishomohopane(22S)
40	510	$C_{37}H_{66}$	17αH 21βH - Heptakishomohopane(22R)
41	524	$C_{38}H_{68}$	17αH 21βH - Octakishomohopane(22S)
42	524	$C_{38}H_{68}$	17αH 21βH - Octakishomohopane(22R)
43	538	$C_{39}H_{70}$	17αH 21βH - Nonakishomohopane(22S)
44	538	$C_{39}H_{70}$	17αH 21βH - Nonakishomohopane(22R)
45	552	$C_{40}H_{72}$	17αH 21βH - Decakishomohopane(22S)
46	552	$C_{40}H_{72}$	17αH, 21βH - Decakishomohopane(22R)

a Assignments based on mass spectral interpretation, GC retention times, and comparison with authentic standards

Figure I

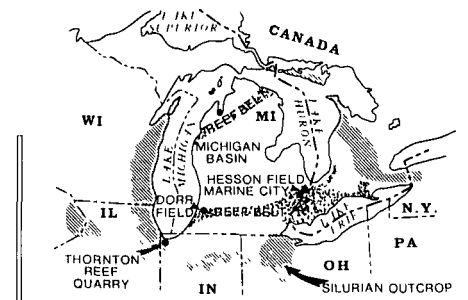
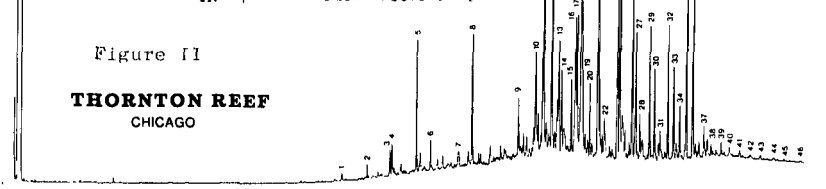


Figure II



THORNTON REEF
CHICAGO

RPA 15 .A NEW TECHNIQUE FOR DETERMINING PETROLEUM STERANE DISTRIBUTIONS USING SELECTIVE METASTABLE ION MONITORING; John E. Zumberge, Cities Service Research, Box 3908, Tulsa, OK 74102; Geoff A. Warburton and R. S. Stradling, Kratos Limited, Barton Dock Road, Urmston, Manchester M312LD, UK.

Steroidal hydrocarbons are common constituents of crude oils and ancient sedimentary rocks. The distributions of these compounds are indicators of source rock depositional environments and are useful in petroleum exploration as correlation and thermal maturity parameters. Routine capillary GC/MS analysis of steranes monitors the electron impact m/z 217 fragment ion; the resulting mass fragmentogram often reveals a complex and incompletely resolved structural and stereoisomeric mixture of C_{27}, C_{28}, and C_{29} steranes. Chromatographic co-elution of sterane homologs places constraints on the accurate measurement of various sterane ratios which are geochemically significant. Increased specificity and sensitivity can be achieved by monitoring the spontaneous (unimolecular) fragmentation of sterane parent ions occurring in the first field free region of a double focusing mass spectrometer in which the electrostatic sector precedes the magnetic sector. The sterane metastable parent ion transitions, $372^+ \rightarrow 217^+$, $386^+ \rightarrow 217^+$, and $400^+ \rightarrow 217^+$, can be separately observed during a single GC/MS run by using a programmable power supply to vary the accelerating voltage while holding the magnetic and electrostatic fields at appropriate constant values. Thus, the complete resolution of sterane homologs allows for a more accurate determination of the relative abundances of geochemically important steranes. Metastable ion monitoring is presently more sensitive to sterane detection than high resolution single ion monitoring of the normal m/z 217 ion. Furthermore, it is calculated that metastable sensitivity for steranes could still be increased a factor of five by using a collision gas.

ELUCIDATION OF CHEMICAL CHARACTERISTICS OF COAL FROM PYROLYSIS MASS SPECTRAL PATTERNS; Alice M. Harper, David L. Pope, G. Steven Metcalf, Henk L. C. Meuzelaar; Biomaterials Profiling Center, University of Utah, Salt Lake City, Utah 84108.

Among the often quoted limitation of pyrolysis mass spectrometry is that of interpretation of pyrolysis patterns. Elucidation of chemical information from the Py-MS patterns of coals is a good example of the degree of complexity that can arise from application of Py-MS techniques to those problems for which it is ideally suited. Our laboratory has been developing over the past two years an in-house multivariate statistical protocol for the processing of coal pyrolysis patterns.

Eighty-one Rocky Mountain coal samples from the Pennsylvania State Coal Collection were analyzed in quadruplicate by Curie-point pyrolysis over a four day period. Statistical methods developed by Eshuis *et al.* [1] were used to monitor reproducibility within the coal replicates and to eliminate inconsistent data. Each spectrum was normalized using the NORMA [2] procedure, a method which detects and deletes irreproducing masses and uses the resulting reproducible portion of the spectra for normalization to total ion intensity. The quadruplicate analyses for each coal sample were averaged and this average spectrum was used in subsequent data analysis. Twenty five conventional coal measurements reflecting metamorphic, maceral, depositional and elemental composition on the same set of coal samples were obtained from the Penn State/DOE Data Base.

The data processing portion of this study which used the ARTHUR [3] program took place in four stages: 1) factor analysis of the Py-MS data base, 2) factor analysis of the conventional measurement data, 3) target rotation [4] of the Py-MS factor space to the conventional factor space, and 4) development of prediction models for coal rank using classification analysis and calorific value using least squares fitting. The Karhunen-Loéve (K-L) projection of the first two Py-MS factors is shown in Figure 1. Figure 2 is the K-L plot derived from factor analysis of the conventional data base. The loadings on the measurements for these first two factors of both sets indicated a tendency for the factors to mix rank and depositional information. A striking similarity exists between the K-L plots from the two data bases. In fact, the correlation coefficient between the first axis of both plots was 0.82.

The factor loading spectrum from rotation of the Py-MS data to the first conventional factor (fit correlation - 0.89) is shown in Figure 3. Not only does the target rotation between the two sets of data reveal a great deal of overlap in information contained in the results of the two vastly different analysis techniques, but also the rotation produces simple pictures of the mass peaks which give rise to the chemical nature of the behavior seen in the conventional data factors. Figure 4 shows a loading spectrum obtained from least squares modeling for the prediction of calorific value from Py-MS patterns. Five randomly selected prediction sets produced an average error of ± 173 BTU, a result consistent with the expected error between interlaboratory values.

Despite the overall complexity of Py-MS patterns on coal samples, simple trends in the chemical nature of the coal matrix are readily extracted with the aid of factor analysis and pattern recognition techniques. Moreover, the information provided in a single Py-MS spectrum is comparable to that of more time consuming conventional organic measurement techniques for complex matrices such as coal and shale.

1. Eshuis, W., Kistemaker, P.G., Meuzelaar, H.L.C., in *"Analytical Pyrolysis"*, eds. C.E.R. Jones and C.A. Cramers, Elsevier, Amsterdam, 1977, pp. 151-166.
2. Meuzelaar, H.L.C., Futrell, J.H., Hill, G.R., Pope, D.L., Iwamoto, D.J. and Tomlinson, J.H., First semiannual progress report to DOE (Grant # DE-FG22-80PC30242), 1980.
3. Harper, A.M., Deuwer, D.L., Kowalski, B.R., Fasching, J.L., in *"Chemometrics: Theory and Application"*, ed. B.R. Kowalski, American Chemical Society, Washington D.C., 1977, pp. 14-52.
4. Howery, D.G., in *"Chemometrics: Theory and Application"*, ed. B.R. Kowalski, American Chemical Society, Washington D.C., 1977, pp. 73-79.

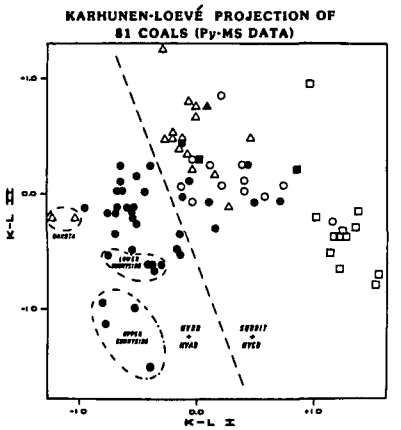


Figure 1. Karhunen Loéve projection of 81 coals (Py-MS data).

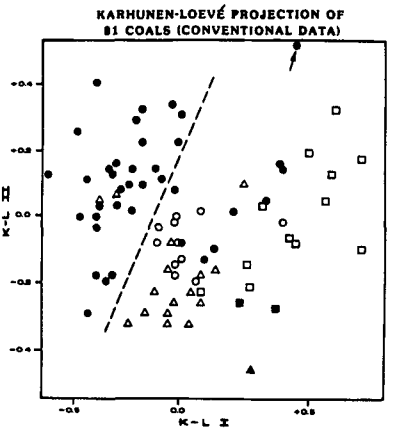


Figure 2. Karhunen Loéve projection of 81 coals (conventional data).

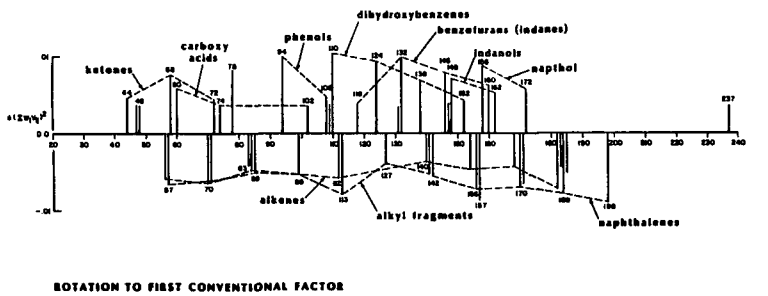


Figure 3. Loadings for the rotation of the pyrolysis mass spectra to the first conventional factor.

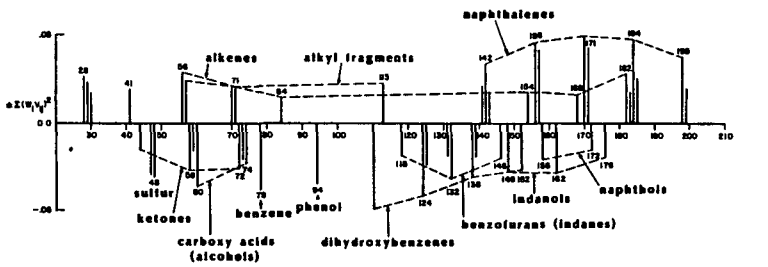


Figure 4. Loadings for the rotation of the pyrolysis mass spectra to calorific value.

CLASS ASSIGNMENT OF UNKNOWN COAL LIQUID CONSTITUENTS BY COMPUTERIZED PATTERN RECOGNITION TECHNIQUES. G. Steven Metcalf, William H. McClennen, Alice M. Harper, David L. Pope, Henk L. C. Meuzelaar; Biomaterials Profiling Center; George R. Hill; Department of Chemical Engineering, University of Utah, Salt Lake City, Utah 84108.

The renewed emphasis on the development of liquid synthetic fuels from coal has necessitated an increase in the variety of analytical methods used to characterize the compound classes present in these liquids. Analytical problems, however are formidable due to the multitude and variety of compounds present. Even with the use of modern "on-line" separation techniques, such as LC/MS, GC/MS, MS/MS, etc., one is often limited to a best-guess approach in identification. Indeed, the growth in magnitude of new compounds to be characterized from these and other processes has outpaced the rate at which standard compounds and/or reference spectra have become available for use in positive, unambiguous identification.

In our laboratory, distillates from the Exxon Donor Solvent (EDS) and H-Coal processes were investigated for oxygen containing compounds by a combination of analytical techniques, including LC, GC/MS, Py/MS and MS/MS [1], resulting in the tentative identification of alkylphenols and a series of alkylindanols consisting of 4-indanol, 5-indanol and their higher homologs. The latter series was noteworthy because of unexpectedly high abundances and the apparent consumption of 5-indanol (and corresponding homologs) during EDS hydrotreatment.

Since unambiguous identification of mass spectra usually requires matching of unknown spectra with spectra obtained from standard compounds and/or reference libraries, and only a limited number of suitable standards were available, we were prompted to investigate the use of computer-assisted pattern recognition, as available in the ARTHUR program package [2], to assign mass spectra of "unknown" products to correct compound classes.

Selected spectra from GC/MS analyses were extracted to form two sets of data files. The first set (labeled PH/IN) contained only spectra of suspected alkylphenols and alkylindanols from the distillates and spectra of two standard compounds: 5-indanol and 5-hydroxytetralin. This set was used to examine the degree of separation achieved between the two classes and the relationship of the 5-hydroxytetralin spectrum to these classes. The second set (labeled MULTI) contained spectra of a variety of hydrocarbons in addition to spectra of suspected alkylphenols and alkylindanols. This set was formed to examine the separation possible between hydroxy- and nonhydroxy-compound classes. In addition, each set was divided into data files of two types: a normal type (fragment ion spectra) and a corresponding reverse type (neutral-loss spectra). The former was used to obtain molecular core information and the latter to investigate fragmentation tendencies.

After submission to ARTHUR, the data of each file were "auto-scaled" [3] (mean normalization followed by variance division), to form new features from the original measurements with the same initial potential of class separation. Loadings were calculated for each feature according to a Fisher ratio criterion [4] (interclass variance over intraclass variance) and the features of lowest Fisher weight discarded so that only the most reliable features (low intraclass variance) that effectively separate classes (high interclass variance) were used. These loadings were either retained to effect better class separation (MULTI) or removed to observe natural clustering tendencies (PH/IN) in subsequent analyses. All files were subjected to factor analysis via the Karhunen-Loéve transform [5] (an eigenvector/eigenvalue extraction from correlation matrices followed by an orthogonal rotation of factors). Plots of the major axes of variance (eigenvectors with highest eigenvalues) for each file are shown in Figures 1-4. These results tend to confirm our tentative identification. Further supportive evidence was indicated by 100% correct compound classification obtained from discriminant analyses via the KNN (K-nearest neighbor) and SIMCA [6] (Statistical Isolinear Multicategory Analysis) routines. The former, based on distance matrices, utilizes "committee voting" of each spectrum's nearest neighbors to obtain classification, while the latter is a sophisticated "intra-category" factor analysis approach, using principal components to derive models for each class.

1. G. R. Hill, *et al.*, "Characterization of Coal Liquefaction Fractions", 2nd Annual Report to DOE # DE-AT2279ET-14808 (1981).
2. A. M. Harper, *et al.*, "ARTHUR and Experimental Data Analysis: The Heuristic Use of a Polyalgorithm", in *Chemometrics: Theory and Application*, B. R. Kowalski, ed., ACS Series 52, Washington D.C., 1977.
3. B. R. Kowalski and C. F. Bender, *J. Amer. Chem. Soc.*, 94:16 (1972) 5632.
4. R. A. Fisher, *Annals of Eugenics*, 7 (1936) 179.
5. J. Mendel and K. Fu, *Adaptive, Learning and Pattern Recognition Systems*, Academic Press, NY (1970).
6. S. Wöld and M. Sjöstrom, "SIMCA: A Method for Analyzing Chemical Data in Terms of Similarity and Analogy", in *Chemometrics: Theory and Application*, B. R. Kowalski, ed. ACS Series 52, Washington D.C., 1977.

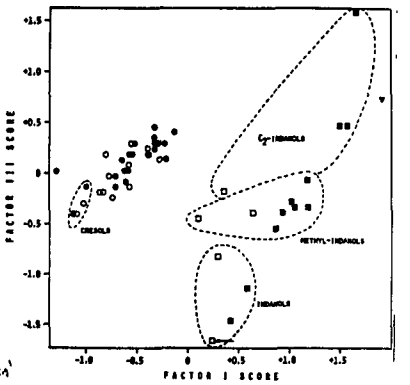


Figure 1. K-L projection of the 1st and 3rd factors extracted from the PH/IN-normal data file. Factor I effectively separates the two classes while Factor II exhibits a wide degree of variance for the alkylindanols but yields a compact cluster for the alkylphenols.

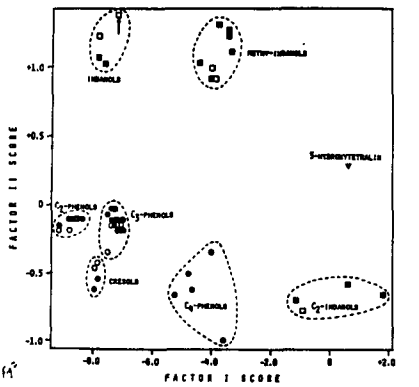


Figure 2. K-L projection of the 1st two factors extracted from the PH/IN-reverse data file. In contrast to Fig. 1, the tendency here is for sub-clustering based upon degree and type of substitution in addition to overall class separation. The 5-hydroxytetralin spectrum occupies a position that is in the overall hydroaromatic region, but that is inconsistent with its molecular weight.

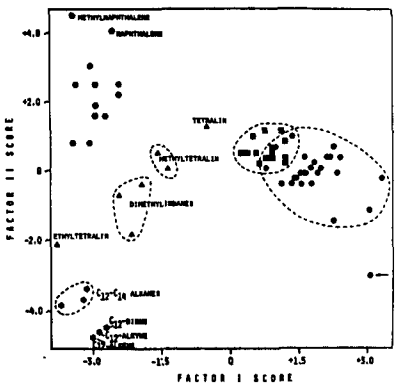


Figure 3. K-L projection of the 1st two factors extracted from the MULTI-normal data file. Factor I separates the hydroxyspectra from all others while Factor II ranks low for aliphatics, high for aromatics and intermediate for hydroaromatics.

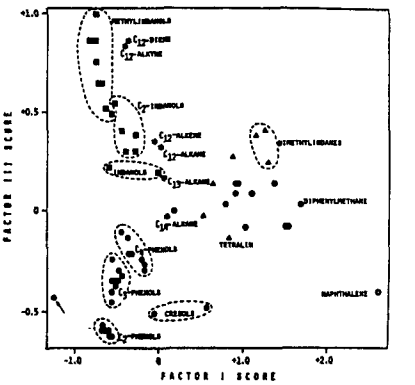


Figure 4. K-L projection of the 1st and 3rd factors extracted from the MULTI-reverse data file. Again, sub-clustering dominates in this plot when compared to Fig. 3.

● PHENOLS ■ INDANOLS ✱ ALIPHATICS ⬡ NAPHTHALENES

▲ TETRALINS, INDANES ⬢ BIPHENYLS, ACENAPHTHENES

PYROLYSIS GC/MS OF SPECIFICALLY TREATED COALS*

G. L. Glish, E. H. McBay, and W. T. Rainey
Oak Ridge National Laboratory
Oak Ridge, TN 37830
R. Liotta, Exxon Research and Engineering
Linden, NJ 07036

Coal that has been modified by replacement of hydroxy H's with ^{13}C methyl and perdeuteromethyl groups has been pyrolyzed, with the products being analyzed by GC/MS in an effort to gain some insight into the coal structure. The coal is prepared by the following reactions.[1]

$$(Coal)\text{-}OH + (C_4H_9)_4OH \xrightarrow{THF} (Coal)\text{-}O(C_4H_9)_4 + H_2O$$

$$(Coal)\text{-}O(C_4H_9)_4 + CH_3I \xrightarrow{THF} (Coal)\text{-}OCH_3 + (C_4H_9)_4I.$$

The reaction is very mild and causes little or no other change in the coal structure. Elemental analysis shows that the composition of Illinois 6 coal changes from $C_{100}H_{84}O_{11}S_{1.8}N_{1.4}$ to $C_{105}H_{94}O_{11}S_{1.8}N_{1.4}$ and that Rawhide coal changes from $C_{100}H_{85}O_{21}NS_{0.3}$ to $C_{108}H_{101}O_{21}NS_{0.3}$.

The pyrolysis experiments were performed using the following instrumentation: a Chemical Data Systems pyroprobe 100 pyrolysis unit; a Perkin-Elmer Sigma III gas chromatograph with a Hewlett-Packard 25 meter fused silica capillary column; a Kratos MS25/DS55 mass spectrometer/data system. GC/MS runs were done on untreated, perdeuteromethylated and ^{13}C methylated samples for both coals at 600, 800 and 1000°C pyrolysis temperatures. A typical mass chromatogram is shown along with a table identifying the peaks. The modified coals showed very similar chromatograms with the addition of several peaks due to anisole and its methylated homologs (resulting from the O-methylation of phenol and methyl phenols).

The mass spectra for each chromatographic peak were averaged into one spectrum. This spectrum was then corrected for contributions from naturally occurring ^{13}C, ^{33}S, ^{34}S and then subsequently corrected for fragmentations (i.e., loss of H, D). This gave a molecular ion distribution showing the amount of ^{2}H or ^{13}C incorporated into the compound.

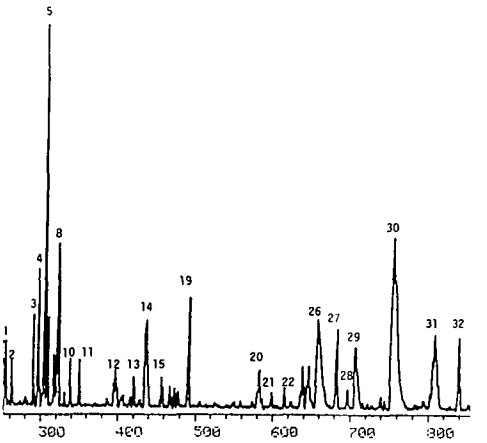
Several tentative conclusions can be drawn from the results. Pyrolysis temperature, over the range studied, has little or no effect upon deuterium or ^{13}C incorporation into the products. The xylenes, ethylbenzene, m-cresol and dimethylphenol are formed to a large extent by methyl group transfer during pyrolysis, while p-cresol and dimethylthiophenes show little methyl group transfer. Compounds without alkyl groups have various degrees of label incorporation. Naphthalene shows a surprisingly high amount of ^{13}C incorporation while indene shows some and phenol has essentially no ^{13}C incorporation. From the deuterium results it seems that most compounds have two radical sites on the ring structure and that each methyl group adds one radical site to the compound.

---

*Research sponsored by the U. S. Department of Energy, Division of Basic Energy Sciences, under Contract W-7405-eng-26 with the Union Carbide Corporation.

Reference

1. R. Liotta, Fuel 58, 724 (1979).



A PORTION OF THE MASS CHROMATOGRAM OF UNTREATED ILLINOIS 6 COAL PYROLYZED AT 800°C.

PEAK	COMPOUND	PEAK	COMPOUND
1	C_8H_{16}	17	$C_{10}H_{22}$
2	C_8H_{13}	18	C_9H_{10}
3	ETHYLBENZENE	19	INDENE
4	ETHYLTHIOPHENE	20	METHYLBENZOFURAN
5	XYLENE	21	$C_{11}H_{22}$
6	DIMETHYLTHIOPHENE	22	$C_{11}H_{24}$
7	DIMETHYLTHIOPHENE	23	METHYLINDENE
8	XYLENE & STYRENE	24	METHYLINDENE
9	DIMETHYLTHIOPHENE	25	METHYLINDENE
10	C_9H_{18}	26	PHENOL
11	C_9H_{20}	27	NAPHTHALENE
12	C_3-BENZENE	28	BENZOTHIOPHENE
13	TRIMETHYLTHIOPHENE	29	CRESOL
14	BENZOFURAN & C_5-BENZENE	30	CRESOL
15	$C_{10}H_{20}$	31	DIMETHYLPHENOL
16	C_3-BENZENE	32	METHYLNAPHTHALENE

ON THE INTERPRETATION OF THE MASS SPECTRA OF MIXTURES

J.L. Stauffer
Arthur D. Little, Inc.
Cambridge, MA 02140

A mass spectrum is a set of ordered pairs $[(m_1,i_1), (m_2,i_2), (m_3,i_3),\ldots,(m_n,i_n)]$ where m_k and i_k are the mass and intensity values, respectively, of the ion k. When spectral sets A and B are combined, the result is a new spectral set C which contains all of the members of A and B, such that $(m_{ci}, i_{ci}) = (m_{ai},i_{ai})$ and $(m_{cj},i_{cj}) = (m_{bj}, i_{bj})$, except if $m_{ak} = m_{bk}$, then $m_{ck} = m_{ak} = m_{bk}$ and $i_{ck} = i_{ak} + i_{bk}$.

A specific spectrum, S_x, is included in or is a subset of another spectrum S_y if and only if for every $(m_x,i_x)\in S_x$, $(m_x,i_x)\in S_y$ where $(m_x,i_x)\in S_y$ if $m_{xj}=$some m_{yj} and for that $m_{yj},i_{yj}\geq i_{xj}>0$.

If a mixture is made up of components C_1, C_2, $C_3,\ldots,$ C_n, then the spectrum of the mixture, M, is the union of the spectral sets S_1, S_2, $S_3,\ldots,S_n$ of the individual components,

$$\bigcup_{K=1}^{n} S_k = M$$

and the individual component spectra are identifiable subsets of M:

$$S_1,S_2,S_3,\ldots,S_n \subseteq M$$

Axiom 1

The collection of all spectra that are subsets of M represent all possible assignments to M.

Axiom 2

Any collection of subset spectra that partitions M is an interpretation of M.

Partition Procedure

An effective procedure for partitioning the mixture spectrum M_{70} into individual subsets can be developed if, in addition to the primary spectrum, a mixture spectrum subset M_{15} is obtained under the same sample conditions, but with reduced ionization energy. If M_{70} is the mixture spectrum obtained at 70 eV, and M_{15} is the mixture spectrum obtained at 15 eV, then $M_{15}\subseteq M_{70}$, and, as a first approximation,

M_{70} = the reference matchable set,

M_{15} = the molecular ion set,

$M_{70}-M_{15}$ = the fragment ion set.

Those elements of M_{15} that

1. are in approximately the upper half of the spectrum set,
2. are not isotopic satellites of another peak, and
3. have satellite isotope peaks,

are tentatively assumed to represent molecular ions. These m values from M_{15} are used to select, from an indexed collection of reference spectra, specific molecular weight collections to be matched against M_{70}. Only spectra that are subsets of M_{70} are retained for further consideration. From the resulting collection of M_{70} subset spectra, a partition of M_{70} is formed.

Identification Procedure

The interpretation that is indicated by a partition of a mixture spectrum can be tested for consistency and uniqueness if the sample is introduced into the MS by a means that offers some preliminary separation, such as is obtained by thermal fractionation from the solids probe.

If a reference spectrum subset of M_{70} is also the spectrum of a component of the mixture being analyzed, then that spectrum S_a will be a subset of every thermally adjacent spectrum in which the major ion (m_j,i_{100}) S_a appears, providing that S_a is the sole or principal contributor to the i component at m_j. In general, where M_t is the mixture spectrum at temperature T, and where M_{tx} is any of the thermally contiguous series of spectra, and S_a is an authentic subset spectrum of the mixture,

$$[(m_j,i_{100})\in S_a \wedge S_a \subseteq M_t] \rightarrow [(m_j,i_k)\in M_{tx} \rightarrow S_a \subseteq M_{tx}]$$

If this test fails at mj and $S_a \not\subseteq M_{tx}$ in which $(m_j,i_k)\in M_{tx}$, then $(m_j,i_k)\in(S_a \cap S_x)$ where $S_x \subseteq \overline{S_a}$. Successive iterations using different major intensity ions of S_a can establish which, if any, belong exclusively to S_a.

A spectrum that has at least one interference free $(m_e,i_x)\in S_a$ can be tested throughout for interference by comparing the ion intensity vs. probe temperature profile for all of the remaining $(m_l,i_m)\in S_a$ with that of the exclusive member. The ion intensity curves of all interference free $(m_l,i_m)\in S_a$, scaled i_x/i_m , will be identical with that of (m_e,i_x) over the domain D_e that $(m_e,i_x)\in M_{tx}$. Any ion of S_a that has an interference from a spectrum other than S_a will exhibit an ion intensity value higher then expected, over the domain D_f of the interference.

SECONDARY ION MASS SPECTROMETRY OF FROZEN SOLUTIONS OF INORGANIC SALTS.

Dusan Stulik, Robert G. Orth and Josef Michl, Department of Chemistry, University of Utah, Salt Lake City, Utah 84112

Matrix-isolation secondary ion mass spectrometry[1] (SIMS) permits the measurement of mass spectra of species imbedded in excess material at temperatures as low as 15-20 K. While the low-temperature matrix materials used so far were primarily the rare gases, water can also be used. Using a low-temperature SIMS instrument, we have observed the positive SIMS spectra of frozen aqueous solutions of the chlorides of alkali and alkaline earth metals.

A UHF chamber of the SIMS instrument[2] was equipped with an Extranuclear Laboratories quadrupole mass spectrometer (2-1000 m/e), with a Bessel box energy prefilter, Riber differentially pumped ion gun (0-4 keV) and a flood gun for surface charge neutralization. The system was pumped by a Varian 500 l/s ion pump. The base pressure was in 10^{-10} Torr range.

Samples were introduced into the main chamber from a preparation chamber equipped with a Balzers 100 l/s turbopump and with a differentially pumped sealing system for cryostat movement. The chlorides of Li, Na, K, Rb, Cs, Mg, Ca, Sr and Ba were dissolved in ultrapure water with molarities 10^{-1} - 10^{-7}. The solutions were deposited with a capillary pipet on a cleaned OHC copper plate attached to a precooled cryostat. The samples were introduced into the main chamber when sample temperature reached 15-20 K and the pressure in the preparation chamber reached 10^{-9} Torr.

Like other matrix materials, solid water produces a SIMS spectrum of its own. The spectrum is dominated by the ions H^+, O^+, OH^+, OH_2^+ and by the cluster ion series $H^+(H_2O)_n$. The positive SIMS spectrum of a frozen 10^- M solution of Li, Na, K, Rb, and Cs chlorides shows simple peaks of Li^+, Na^+, K^+, Rb^+ and Cs^+ and a series of hydrated metal ions $M^+(H_2O)_{n-3}$. Similar hydrated metal clusters are known from high pressure mass spectrometry.[3] The spectrum of a binary solution LiCl and CsCl measured in the mass range 1-500 m/e shows the presence of hydrated metal clusters as large as $Cs^+(H_2O)_{13}$, $Li^+(H_2O)_6$ in addition to water clusters up to $H^+(H_2O)_{27}$.

Alkali metal cations are easily detectable even in the highly diluted 10^{-7}M solutions where the series of water clusters is dominant. The detection limit for alkaline earth metals is a little higher.

The results of this study show that SIMS provides new possibilities for the study of complexation and aggregation in solutions of inorganic salts. The sensitivity of detection depends considerably on the nature of the ions and for alkali metals it appears that concentration 10^{-9}M can be detected. These observations may also have application in chemical analysis.

Acknowledgement. This work was supported by the National Science Foundation (CHE78-27094).

References

1. Jonkman, H.T.; Michl, J. J. Chem. Soc. Chem. Commun. **1978**, 751.

2. Jonkman, H.T.; Michl, J. J. Am. Chem. Soc. **1981**, 103, 733.

3. Märk, T.D.; Peterson, K.I.; Castleman, A.W. Jr. Nature, **1980**, 285, 392.

MASS SPECTROMETRY OF VIC-DIOXIMATE COMPLEXES OF NICKEL, PALLADIUM AND PLATINUM

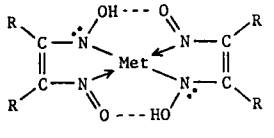
JOHN B. WESTMORE AND DANIEL K. C. FUNG

Department of Chemistry,
University of Manitoba,
Winnipeg, Manitoba R3T 2N2
Canada

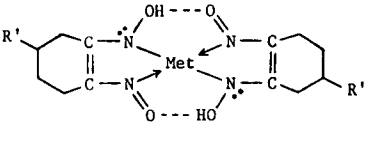
The mass spectra of metal-containing compounds have often been discussed in terms of the valence-change concept (1,2) for rationalizing the major fragmentation pathways. It was proposed that the odd- or even-electron character of a metal-containing ion is determined by the capacity of the metal to accept one or more electrons from the ligands (valence decrease) or to donate one or more electrons to the ligands (valence increase). Thus, ion abundances in mass spectra will be influenced by the ion structures and relative stabilities of oxidation states of metals in gaseous metal-containing ions. In the absence of substantial information on these points it has been necessary to discuss spectra in terms of the general chemistry of the particular metal. While recognizing the perhaps unwarrented assumptions inherent in this procedure, considerable success has been achieved in rationalizing ion decompositions of "classical complexes" (3) in this way (5). The concept has been applied in reviews of the spectra (6) and energetics (7) of ion decompositions of coordination compounds of many transition and non-transition metals. However, there are many complexes for which the oxidation state of the metal is vague or ambiguous, particularly when the metal-ligand bond is highly covalent and/or multiple, e.g. π-acceptor or π-bonded ligands are involved. In these cases the mass spectra differ in important qualitative ways from those of classical complexes and the valence-change concept becomes less useful.

The nickel(II), palladium(II) and platinum(II) complexes shown below, of five dialkyl and di-aryl vicinal dioximes, have been studied by positive ion electron-impact mass spectrometry. These complexes have complicated mass spectra which are of fundamental importance because while the initial compounds may be regarded as classical complexes it is found that many of the fragment ions have ligand residues which fall into the π-acceptor or π-bonded classifications. The spectra can be used as a sensitive probe to investigate the variations in mass spectral behavior between the metals of this group.

Some important generalizations are illustrated by the accompanying data. The molecular ions of every complex are very stable and correspond to the base peak in 12 of 15 spectra. For most ligands the stability of the molecular ion is in the sequence Pt > Ni > Pd. Ion types and structures correlate well with the known chemistry of the metals. Significant differences between the behaviors of the three metals are observed. Among prominent fragment ions there appears to be a trend towards increasing prominence for even-electron oxidation states in the sequence Ni → Pd → Pt. A more conspicuous trend involves the formation of fragment ions with metal-carbon σ bonds and metal-acetylene bonds. Such ions increase in prominence in the spectra of the metal complexes in the sequence Ni → Pd → Pt. Both trends are consistent with the known chemistry of the metals.



1. $Met(DMG)_2$; R = CH_3
2. $Met(DPG)_2$; R = C_6H_5
3. $Met(AFD)_2$; R = 2-C_4H_3O



4. $Met(Niox)_2$; R' = H; [R_2 = $-(CH_2)_4-$]
5. $Met(MNiox)_2$; R' = CH_3; [R_2 = $-(CH_2CHCH_3CH_2CH_2)-$]

% RELATIVE ABUNDANCES OF SELECTED IONS IN THE POSITIVE ION ELECTRON-IMPACT MASS SPECTRA:

$[MetL_2]^+$

L	Ni	Pd	Pt
DMG	100	100	100
	28	23	29
DPG	100	96	100
	20	20	40
AFD	100	91	100
	31	27	37
Niox	100	93	100
	32	15	48
MNiox	100	100	100
	51	34	51

Lower data give M^+ as % of total current of metal-containing ions.

$[MetLH]^+$

L	Ni	Pd	Pt
DMG	44	97	5
DPG	78	100	-
AFD	28	100	3
Niox	9	83	1
MNiox	6	17	2

Note low % RA for Pt complexes.

$[MetL]^+$

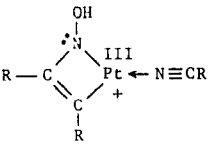
L	Ni	Pd	Pt
DMG	9	22	6
DPG	28	15	-
AFD	10	-	-
Niox	5	32	4
MNiox	3	27	3

Note low % RA for Pt complexes.

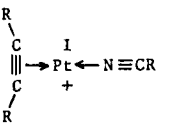
$[Met(C_2R_2)]^+$

L	Ni	Pd	Pt
DMG	9	8	27
DPG	29	26	30
AFD	25	14	34
Niox	-	-	-
MNiox	-	-	-

The enhanced abundances for the DPG and AFD complexes are consistent with the known greater stability of aryl acetylene than alkyl acetylene complexes. Complexes involving cyclic alkynes are known to be less stable.



$[Pt(L - NO)(NCR)]^+$



$[Pt(C_2R_2)(NCR)]^+$

Fragment ions involving metal-carbon or metal-acetylene bonds become more prominent in the sequence Ni → Pd → Pt, with the result that ions such as those above are unique to platinum. Such bonding is a characteristic feature of the chemistry of platinum.

REFERENCES AND FOOTNOTES.

1. J. S. Shannon and M. J. Swan, Chem. Commun. 33 (1965)
2. M. J. Lacey and J. S. Shannon, Org. Mass Spectrom. 6, 931 (1972)
3. Classical complexes can, for the most part, be described in terms of (a) a set of ligands with a discrete electron population, and (b) a metal atom with a well-defined oxidation number, ref. 4, p. 62.
4. F. A. Cotton and G. Wilkinson, "Advanced Inorganic Chemistry", 4th Edn., Interscience, New York (1980)
5. J. Charalambous (Ed.), "Mass Spectrometry of Metal Compounds", Butterworths, London (1975), p. 50 et seq.
6. J. B. Westmore, in ref. 5, chapter 9, pp. 147-253.
7. J. B. Westmore, Chem. Rev. 76, 695 (1975)

A MOLECULAR BEAM/MASS SPECTROMETER SYSTEM FOR DYNAMIC PYROLYSIS STUDIES

Thomas A. Milne and Michael N. Soltys

Thermochemical and Electrochemical Research Branch
Solar Fuels and Chemicals Division
Solar Energy Research Institute
1617 Cole Boulevard, Golden, CO 80401

A system has been developed to permit the direct mass spectrometric observation of primary and secondary pyrolysis processes, when small specimens of biomass or related materials are heated rapidly in hot gases at atmospheric pressure.[1] The approach chosen combines the burnt-gas region of a stoichiometric H_2-O_2-Ar flame as a pyrolysis reactor with a free-jet expansion, molecular-beam mass spectrometer sampling system. This system, shown in Fig. 1, has the following advantages when the goal is the molecular study of pyrolysis under conditions simulating those of technological interest:

- Direct sampling of both highly condensible and non-condensible species.
- Rapid quenching of hot-gas composition from one atmosphere or higher pressure pyrolysis environments, without condensation.
- Real-time measurement of the sequence of both primary and secondary pyrolysis events.
- Direct coupling of sampled gas with a "universal" detector such as the mass spectrometer.
- "Wall-less" pyrolysis and sampling.
- Achieving internal-state cooling of sampled species without condensation.

The last advantage is achieved through the fact that the initial adiabatic expansion of sampled gases to molecular flow results in remarkable cooling of the sampled species including significant vibrational and rotational relaxation. We are thus able to escape the usual sampling dilemma of (1) either allowing the gases to cool, thus risking condensation and secondary reactions, or (2) directly introducing the hot gases into the mass spectrometer ion source (as in most high-temperature Knudson cell studies) and having to interpret the fragmentation patterns of hot molecules. Alterations in parent-to-fragment ion ratios can be particularly dramatic for organic molecules at temperatures above 300°C. Under our conditions, room temperature fragmentation patterns are obtained from methanol, propane, and n-butane sampled from a 900°C flame.[2]

Figures 2, 3, and 4 show typical positive ion mass spectra of the primary pyrolysis products from cellulose (filter paper), lignin (steam-exploded aspen-ethanol extracted) and wood. The spectra represent the integrated pyrolysis of about 10 mg of sample, with the quadrupole mass spectrometer tuned to favor high masses. (Resolution is further degraded by the rapid scan and time constant of the phase-sensitive amplifer used to record the modulated molecular beam signal only.) More complex materials, such as coal, may also be examined as shown in Fig. 5.

This system has been used to study the secondary pyrolysis of primary products, by allowing the latter to spend a longer time in the hot flame gases before sampling. Such studies show the formation of acetylene and olefins when the primary tars and oils are cracked at 900°C for tens of milliseconds. Effects of pyrolyzing sample size and impurities have also been charted.[3]

The technique described here is complimentary to those used in analytical pyrolysis (e.g., Curie point probes with more or less direct evaporation of micrograms of material in or very near the ion source ionizing region). In our case, much larger samples are used but a more faithful simulation of conditions applicable to applied pyrolysis reactors is achieved.

References

1. Soltys, M. N.; Milne, T. A. 1982. The SERI High-Pressure, Molecular Beam, Mass Spectrometric, Sampling System. SERI/TR-622-1172. Golden, CO: Solr Energy Research Institute.

2. Milne, T. A.; Soltys, M. N. 1981. Pyrolysis Mechanisms -- Quarterly Report: April-June, 1981. SERI/PR-622-1347. Golden, CO: Solar Energy Research Institute.

3. Milne, T.A.; Soltys, M.N. 1982. Fundamental Pyrolysis Studies -- Quarterly Report: October-December, 1981. SERI/PR-234-1537. Golden, CO: Solar Energy Research Institute. (Forthcoming)

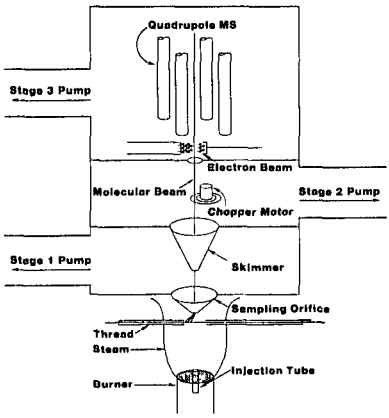


Figure 1. Molecular-Beam Apparatus for Fast Biomass Pyrolysis

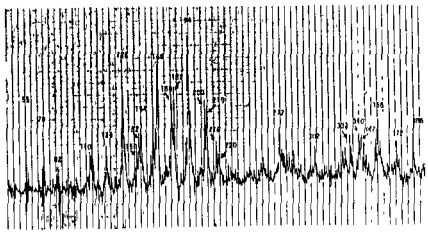


Figure 4. Mass Spectrum of Primary Pyrolysis Products from a Toothpick (16.5 eV Electron Energy).

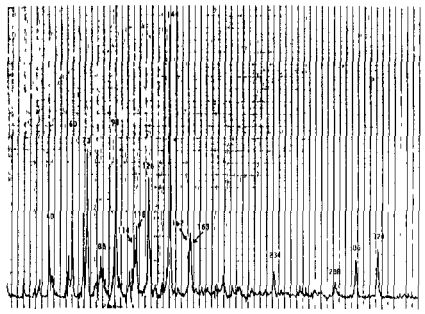


Figure 2. Mass Spectrum of Primary Pyrolysis Products from Cellulose (16.5 eV Electron Energy).

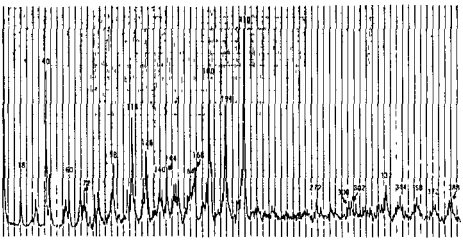


Figure 3. Mass Spectrum of Primary Pyrolysis Products from Steam-Exploded Hardwood Lignin (16.5 eV Electron Energy).

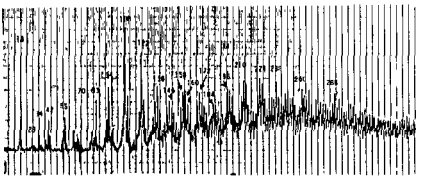


Figure 5. Mass Spectrum of Primary Pyrolysis Products from Crushed Kentucky #9 Coal (16.5 eV Electron Energy).

PHOTOELECTRON SPECTRA OF GAS PHASE LANTHANIDE TRIHALIDES*

B. Ruščič, G. L. Goodman and J. Berkowitz
Physics Division, Argonne National Laboratory
Argonne, Illinois 60439

Gas phase ultraviolet photoelectron spectroscopy (UVPES) provides a method for revealing the molecular orbital composition of the valence shells of molecules. It has been applied most extensively to permanent gases, but some of the more interesting problems involve normally involatile species. These must be studied by high temperature beam techniques, combined with UVPES.

One such problem which we had previously studied[1] was the involvement of transition metal 3d orbitals in molecular bonding in transition metal dihalides. We found that early members of the series (Mn, Fe) had metal 3d orbitals as the uppermost occupied (least bound); the 3d orbitals were drawn in, relative to the halogen ligand orbitals, and became core-like at the end of the transition series (Zn).

The present investigation posed a similar problem regarding the lanthanide 4f electrons in lanthanide trihalides. While this work was in progress, Potts and Lee[2] reported preliminary data on some lanthanide trichlorides. We focus here on the tribromides and triiodides, which provide a greater splitting in the valence shell, and thereby more detail. The vapors were generated at temperatures of 1000 - 1200 K. For each species, spectra were obtained at two wavelengths - 584Å (21.2 eV) and 304Å (40.8 eV). It is known that ionization from orbitals having high angular momentum ($\ell > 2$) is retarded near threshold, due to an angular momentum barrier for escape of the photoelectrons. Therefore, the experiments at 21.2 eV can be expected to yield data emphasing the ligand p orbitals, whereas the 40.8 eV experiments should reveal the influence of f and/or d orbitals.

In this brief report, we show 21.2 eV and 40.8 eV spectra of $CeBr_3$ (representing an early member of the lanthanide series) in Fig. 1a,b and LuI_3 (the terminus of the lanthanides) in Fig. 2a,b. The iodides can be compared to the chlorides, and are seen to

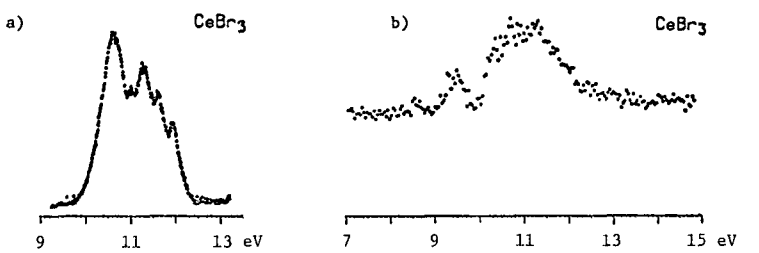


Fig. 1. a) He I (21.2 eV) and b) He II (40.8 eV) photoelectron spectra of $CeBr_3$ vapor.

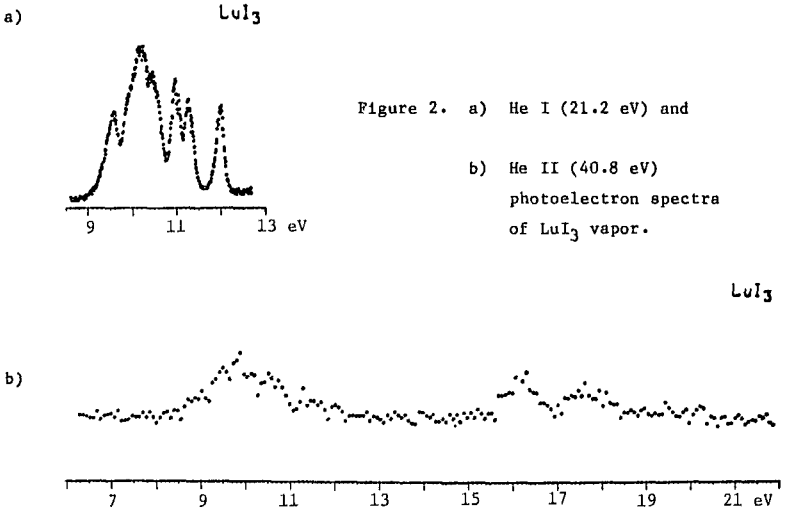


Figure 2. a) He I (21.2 eV) and b) He II (40.8 eV) photoelectron spectra of LuI_3 vapor.

provide much greater detail. In CeI_3, an additional low ionization energy peak is observed in the 40.8 eV spectrum, whereas in LaI_3 the additional peaks at 40.8 eV occur at higher energy than the ligand orbitals. Hence, a picture similar to that of the transition metal halides is beginning to emerge.

Quantum mechanical calculations for such heavy systems are almost non-existent. These molecules are too big for Hartree-Fock, and parametrizations for semi-empirical calculations such as extended Hückel or CNDO are too uncertain. A published[3] extended Hückel calculation on the lanthanide trihalides did not even include the Ln 4f orbitals. We have utilized relativistic self-consistent charge Xα calculations and have had reasonable success in reproducing the experimental results. It was found necessary to perform transition state calculations on each orbital, and to adjust the basis set for that particular orbital, in order to obtain the best results. A complete table of experimental and calculated ionization energies, together with atomic orbital compositions of the molecular orbitals, will be presented at the conference.

References

*Work supported by the United States Department of Energy, Office of Basic Energy Sciences under Contract W-31-109-Eng-38.

1. J. Berkowitz, D. G. Streets and A. Garritz, J. Chem. Phys. 70 1305 (1979).
2. A. W. Potts and E. P. F. Lee, Chem. Phys. Lett. 82, 526 (1981).
3. C. E. Myers, L. J. Norman II and L. M. Leow, Inorg. Chem. 17, 1581 (1978).

ANALYSIS OF CORRECTION FACTORS USED FOR MOLECULAR BEAM MASS SPECTROMETRY

D. A. Stevenson and D. W. Kisker, Stanford University/ Department of Materials Science
Stanford, CA 94305

Introduction

Molecular beam sampling techniques for mass spectromery have been developed for the analysis of atmospheric pressure-high temperature gaseous systems. The present work concerns the correction factors for this sampling procedure, with special emphasis on the detection of species in low concentration levels (ppm range). Correction factors may be divided into two groups: those arising from the transfer of the sample to the mass analyzer chamber; and those concerned with the detection process. Our principal emphasis is on the first group.

Molecular Beam Sampling

In molecular beam sampling of atmospheric pressure systems, the gas sample is expanded into a multi-stage differentially pumped system which directs a portion of the sample, in the form of a molecular beam, to the final mass analyzer stage. The regions of interest in the sampling process are: the initial jet expansion region; the selection of a portion of the beam by a skimmer orifice; and the transport of the molecular beam to the final detection chamber. Major considerations for composition changes upon sampling are: pressure diffusion (1); cluster formation (2); background penetration (3); skimmer interference (4); and free molecular diffusion (5). Both theory and experiment establish the first and last as the most important for the experimental conditions encountered in the present study.

Pressure Diffusion

The pressure diffusion effect was analyzed by Sherman (1). The enhancement of heavy species along the beam axis due to this effect is:

$$\alpha_p = X_h/X_{h,o} = 1 + \frac{11.7(1-X_{h,o})}{Re_o Sc_o}\left(\frac{\gamma}{\gamma-1}\right)\left(\frac{m_h - m_\ell}{X_{h,o}m_h+(1-X_{h,o})m_\ell}\right) \quad , \qquad (1)$$

where X_h and $X_{h,o}$ are the observed and actual concentrations of the heavy species, m_h and m_ℓ are molecular weights of the heavy and light species, γ is the heat capacity ratio and Re_o and Sc_o are the stagnation Reynolds and Schmidt numbers. If $X_{h,o} << 1$ and $m_h >> m_\ell$, Eq. (1) simplifies to:

$$\alpha_p \simeq 1 + \frac{11.7}{Re_o Sc_o}\left(\frac{m_h}{m_\ell}\right)\left(\frac{\gamma}{\gamma-1}\right) \qquad (2)$$

Figure 1 shows a plot of calculated α_p versus concentration for Xe, Kr, Ar, and N_2 in H_2 taking $Sc_o = 1$ and $Re_o = 500$. It is seen that for concentrations below about 0.1%, Eq. (2) is a good approximation and α_p can be a significant enhancement term in this low concentration limit.

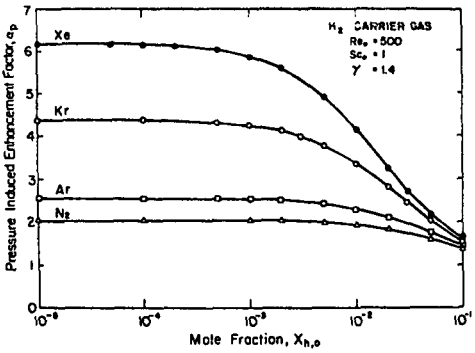


Fig. 1. Pressure induced enhancement factor versus mole fraction of heavy species in hydrogen.

Molecular Diffusion:

Once the expansion proceeds and the beam is sampled by the skimmer orifice, another phenomenon occurs as a result of the residual thermal energy of the molecules. Although the axial velocity components of all species are essentially the same, the residual

thermal velocities correspond to different radial velocities, with the lighter molecules diffusing more rapidly from the center of the beam. The resulting molecular diffusion enhancement factor, α_d, is given by (1):

$$\alpha_d = X_d/X_s = m_h/m_\ell \quad , \tag{3}$$

where X_d and X_s are the mole fractions of the heavy species at the detector and skimmer entrances, respectively. Although other factors, such as skimmer interference, cluster formation, and background penetration can cause changes in composition, these effects are not important under properly controlled operating conditions. The total enhancement factor, α_T, for the case of the low concentration limit is the product of α_p and α_d;

$$\alpha_T = \frac{m_h}{m_\ell} + \frac{11.7}{Re_o Sc_o} \left(\frac{\gamma}{\gamma-1}\right) \left(\frac{m_h}{m_\ell}\right)^2 \tag{4}$$

For low concentrations of high molecular weight species ($m \gtrsim 40$):

$$\alpha_T \approx K_\alpha m_h^2 \tag{5}$$

Analyzer Correction Factors and Overall Behavior of the Response Coefficient

Once the molecular beam enters the mass analyzer chamber, there are several processes whose efficiency is species dependent. For quadrupole mass analyzers these processes are: ionization, transmission, and ion detection. For the UTI 100C quadrupole analyzer used in the present study, the relative efficiencies of these processes showed the following mass dependence; $K_I m$; $\exp(-m/K_T)$; $K_G m^{-1/2}$, where K_I, K_T, and K_G are appropriate constants for the ionization, transmission and gain, respectively. When fragmentation effects are suitably considered, one may show that the mass dependence of the sampling and the detection process, defined as the response coefficient, C_i, is:

$$C_i \propto K_\alpha m^{5/2} \exp(-m/K_T) \tag{6}$$

To verify the above prediction, carefully calibrated gas mixtures of several gaseous species in a hydrogen gas were prepared, with concentrations in the 1-20 ppm concentration range. The linear response behavior was established by plotting the ion intensity of the species versus its concentration. The validity of Fig. 6 was then tested by plotting $C_i \exp(m_i/67.1)$ versus m_i. The results, shown in Fig. 2, provide good confirmation for this relation, for the relatively simple molecular species used in this study.

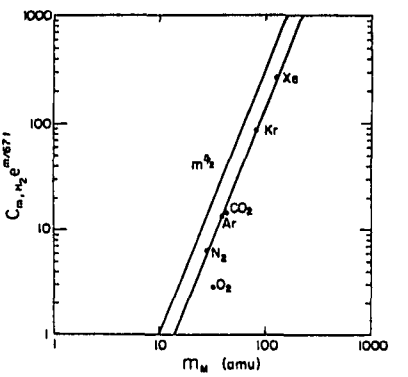


Fig. 2. Mass dependence of the response coefficient

1. F.S. Sherman, Phys. Fluids 8(1965) 773.
2. O.F. Hagena, in "Molecular Beam Low Density Gasdynamics", ed. P. Wegener (Dekker, N.Y., 1974), ch. 2.
3. R. Camparague, J. Chem. Phys. 52 (1970) 1975.
4. V.H. Reis and J.B. Fenn, J. Chem. Phys. 19(1963) 3240.
5. P.C. Waterman and S.A. Stern, J. Chem. Phys. 31 (1959). 405.

STRUCTURAL DETERMINATION OF GAS PHASE METAL ION COMPLEXES USING FOURIER TRANSFORM MASS SPECTROMETRY-COLLISION INDUCED DISSOCIATION

D.B. Jacobson, G.D. Byrd, T.J. Carlin, and B.S. Freiser

Department of Chemistry
Purdue University
West Lafayette, Indiana 47907

The combination of a laser ionization source used in conjunction with a Fourier transform mass spectrometer (FTMS) provides a powerful method for generating and studying the chemistry of atomic metal ions (1,2). The FTMS yields the complete mass spectrum from one laser pulse. In addition the FTMS also has the advantages of high mass range, high resolution, and low energy collision-induced dissociation (CID) capabilities (3-5). Several of the examples presented are discussed below.

In the reaction of Fe^+ with butanone, high resolution studies demonstrate that both of the isobaric ions $FeCO^+$ and $FeC_2H_4^+$ are produced. Deuterium exchange reactions yield ion structural information (6). Five H/D exchanges are observed in the sequential reactions of $RhC_3H_6^+$ (produced by the reaction of Rh^+ with propane) with D_2 suggesting an allyl-hydride structure, while six H/D exchanges are observed for $CoC_5H_6^+$ (produced by the reaction of Co^+ with norbornadiene) suggesting a cyclopentadienyl-hydride structure. Finally, in this paper we apply FTMS to study the structures of $NiC_nH_{2n}^+$ complexes generated from reactions of Ni^+ with a variety of hydrocarbons and demonstrate that different isomeric structures can readily be distinguished both by collision-induced dissociation and by specific ion-molecule reactions (5). Evidence is provided for four unique structures of $NiC_4H_8^+$ generated from reactions of Ni^+ with butane, hexane, 2,2-dimethylpropane, and cyclopentanone. Dehydrogenation reactions of Ni^+ with n-alkanes yield bisolefin complexes which are distinguishable from their isomeric mono-alkene complexes. Ni^+ is found to be highly selective for cleaving internal bonds and highly selective against insertion into terminal C-C bonds. Dehydrogenation becomes more competitive with alkane elimination when β-hydride transfers from secondary carbons are involved instead of primary β-hydride transfers. Selected ion Fourier transform mass spectrometry (SIFTMS) is an aid in yielding this information.

References

1. D.B. Jacobson, G.D. Byrd, and B.S. Freiser, J. Am. Chem. Soc., 104, 2320 (1982).
2. R.C. Burnier, G.D. Byrd, and B.S. Freiser, J. Am. Chem. Soc., 103, 4360 (1981).
3. R.B. Cody and B.S. Freiser, Int. J. Mass Spectrom. Ion Phys., 41, 199 (1982).
4. R.B. Cody, R.C. Burnier, and B.S. Freiser, Anal. Chem., 54, 96 (1982).
5. D.B. Jacobson and B.S. Freiser, J. Am. Chem. Soc., submitted.
6. J.L. Beauchamp, A.E. Stevens, R.R. Corderman, Pure and Appl., 51, 967 (1979).

HOW TO MAKE THE DS-50/55 SYSTEM ACTUALLY WORK

D. THOMAS TERWILLIGER

Department of Chemistry, University of Pennsylvania, Philadelphia, Pa. and
Terwilliger Software, 29 Chetwynd Road, Paoli, Pa.

The DS-50/55 system is designed to be a comprehensive mass spectrometer data system capable of handling all phases of data collection, storage, and processing. However, like most commercial systems, it has been designed to do what the manufacturer thinks you want, which may or may not be what is required. It has been designed primarily for high-speed GC/MS, and so most of its focus is on collecting data rapidly. This concern for speed, while absolutely essential for capillary GC/MS, is irrelevant for processing probe samples. As an example, the peak profile data is generally ignored; only the peak area and time centroid are saved. When running probe samples, more real-time processing could be performed, and more elaborate time-to-mass and multiplet separation algorithms could be used.

The system is also partial to Kratos mass spectrometers, being particularly intolerant of data from a noisy instrument with a crooked scan law such as the Hitachi RMH-2. Portions of the high resolution software are so inaccurate on data from this instrument that it was difficult to obtain correct mass values at the extremes of the mass range. Reference peaks are very widely separated at low mass, and magnet saturation causes severe non-linearities at high mass. As an example, the systematic mass measurement error at m/e 58 using the Kratos interpolation routine is in excess of 30 PPM. The modified routine, specifically optimized for the RMH-2, reduces this error to less than 1 PPM. The mass spectrometer interface was also rewired substantially to aid in interfacing the V.G. 7070-H. The rewired interface only necessitated using one relay in the RMH-2, rather than the seven often malfunctioning ones preciously in use, thus increasing reliability substantially.

Another difficulty is that the user is expected to purchase all equipment upgrades from the data system supplier. This approach is not feasible for university laboratories in general, and totally unnecessary if the laboratory is able to assume "system responsibility" itself. In order to interface any additional devices, a number of patches and fixes to the operating system are usually required, as Kratos will not distribute the system generation programs, except to those who have purchased the latest revision. Even if one is willing to purchase equipment from the data system supplier, key portions of the system are often "obsoleted" or "orphaned" on a regular basis. This requires the user to upgrade to the latest revision in order to expand the system in any way, thus adding more unnecessary costs. The DS-50/55 system is also not designed to communicate with any other systems, be they duplicate DS-50/55 systems, other laboratory data systems, or main-frames such as the EPA-NIH computer.

Aside from the major deficiencies cited above, the ability to modify a commercial data system provides other advantages. Numerous unused system capabilities can be tapped, thus greatly simplifying operation. Our sample log book has been integrated into the data system, so all information is automatically recorded as the sample is run. This provides ready access to the log book, the user directory, and monthly billing statements, all automatically prepared by the data system. Many other "purely Fortran" utility programs greatly aid operation (such as a word processing program used to prepare abstracts, memos, and manuals). In addition, many system programs are very inefficient, such as the "Atomic Composition" program, which in its original form took 93 minutes to process one scan of data with multiple selenium isotopes. The modified version generates the same report in less than three minutes.

Despite all these inevitable drawbacks, it is still not usually advisable to write your entire data system from scratch. Here, there was a need for immediate results, so the time was not available. As a result, the data system modifications described were undertaken one at a time as the need arose and time was available. This provided the advantage of a system that did work (more or less) initially, but gave us the capacity to improve it steadily over the years as the capability and scope of the laboratory has increased.

The most cost-effective modifications were those undertaken to provide support for non-standard peripherals. Our data system has grown from a single user system with only a

single 2.5 M-byte disk to a dual processor system with two mass specs, 30 M-bytes of storage, and complete facilities for interchange of data between processors. Shortly, we will be adding a third mass spec, C.P.U., and disk; providing another 10 M-bytes of storage, and allowing three users simultaneous access to all data collected on any of the systems. The total cost of all these additions will come to less than one-fourth the estimated cost of obtaining a comparable package from the manufacturer. Much of this savings is a result of the thriving market that exists for used Data General (and D.E.C.) equipment, thanks in part to the rush of many organizations to discard their supposedly "obsolete" 16-bit equipment for the new 32-bit processors.

None of these additions would have been of any value without a satisfactory (and inexpensive) method for transfering data between processors. No such capability was available from Kratos, and buying the equipment from D.G. would have been expensive, and would have required some sort of system generation capability. Our net expenditure came to under $700 for an intercomputer communication system which works better than the D.G. equipment. It operates in the foreground of an unmapped system, and has been integrated into the data system so that a single command will transfer data from an entire run (consisting of many separate files).

Other modifications have substantially extended the system capability by:

1. Permitting direct data transfer to either the EPA/NIH or the PBM/STIRS library search systems.
2. Storing peak profile data as well as mass data (probe samples only) so any real-time processing errors can be corrected later on.
3. Performing a statistical analysis of high resolution mass accuracy, and using the statistically significant limits as tolerances for the "Atomic Composition" matching program.

In addition, much time has been saved by fixing the numerous bugs that complicated systems always seem to have. This is usually far simpler than trying to hassle the manufacturer about them.

The DS-50/55 system is divided into five basic sections as follows:

1. Operating System Software (written by Data General).
2. Real-time Data Acquisition Software.
3. Data Access Library.
4. Post-processing Software (Primarily in Fortran).
5. Parameter Control Module for #2 and #4.

Source programs and documentation are distributed only for the post-processing software. However, even it is designed to be modified only to the extent that no changes are required to the parameter control module, which means in practice, that not very much can be accomplished. Since the problems requiring modification occur throughout the system, much needed documentation was missing. This necessitated development of numerous utilities to produce this missing information and to work around various resultant problems. Some of these utilities were supplied with the system, but most were developed by Terwilliger Software specifically for this purpose. They provide the capability to modify and/or expand any portion of the data system, regardless of what language it is written in, and whether or not source programs and/or listings are available. Only limited use can be made of the supplied assemblers, compilers, and linkers, as the source codes are unavailable. These utilities can also be extremely useful in debugging user programs, and in recovering from hardware failures, as they can diagnose and patch-up almost anything.

The principal results of the modifications performed have been:

1. A vast extension of system capability.
2. Greater ease of use, especially by technicians and students.
3. Substantial dollar savings on upgrades.
4. Greatly reduced down time.
5. Greater flexibility in performing special tasks.

There has been a tremendous advantage in having the capability to meet any specialized need that might arise through an appropriate modification to the data system. The basic goal has been to produce a data system which is tailored to the operation of the laboratory, and not the reverse.

PRIORITY POLLUTANT PROGRAMS FOR THE VG-2050 DATA SYSTEM

Stephen R. Shrader
Shrader Laboratories Detroit, Michigan

INTRODUCTION

An increasing number of laboratories are being asked to analyze water and waste streams by GC/MS for industrial chemicals, often referred to as "Priority Pollutants". Many of these analyses have been, and are, performed by laboratories with quadrupole instruments and data systems which automatically calibrate and process the sample data. The VG Data Systems have no such set of programs.

This paper describes a set of programs, written in Fortran, which serve to perform all necessary data processing functions for a "Priority Pollutant" analysis using a VG-2050 data system. The programs may also be used to detect and quantitate any other defined series of compounds giving characteristic mass spectra.

REFERENCE FILE SET-UP

The first step is the establishment of one or more data files containing the following information about the compounds of interest:

COMPOUND NAME
MAJOR INTEGRATING ION
SECONDARY IONS

The COMPOUND NAME may consist of up to 30 alphanumeric characters.

The MAJOR INTEGRATING ION should be one of the more intense ions in the spectrum, but should also be characteristic of the compound.

Up to four (4) SECONDARY IONS may be used for confirmation of the presence of a compound.

The first compound in a data file is the internal standard.

DATA FILE SAMPLE

"ACID Priority Pollutants"

Compound Name	Major Ion	Secondary Ions
D10-Anthracene Internal Standard	188	---
2-Chlorophenol	128	130, 54, 92
2,4-Dichlorophenol	162	164, 166, 126, 63
2,4-Dimethylphenol	122	107, 121, 77
4,6-Dinitro-o-cresol	198	77
2,4-Dinitrophenol	184	77
2-Nitrophenol	139	109, 94, 65
4-Nitrophenol	139	109, 65, 53
p-Chloro-m-cresol	142	144, 107, 77
Pentachlorophenol	266	264, 268, 165, 167
Phenol	94	66, 65
2,4,6-Trichlorophenol	196	198, 200, 132, 134

CALIBRATION

A solution containing known concentrations of each of the compounds to be measured, as well as the internal standard, is analyzed under the conditions to be used with the actual samples.

The CALIBRATION program evaluates the spectra obtained, looking in turn for each of the MAJOR INTEGRATING IONS. The operator has the choice of allowing the computer to search an adjustable scan window for the ion, or of entering the exact scan in which the ion maximized. The program then

integrates the ion intensity over a scan window of 5-13 scans, correcting for the background level of the ion.

Following entry of the known concentration, the program computes a response factor and relative retention time, both related to the internal standard. This new calibration data is stored in the REFERENCE FILE.

BLANKS

An injection of a solvent blank is processed with the BLANK program in order to determine instrument background levels for each of the compounds. These levels are stored in the REFERENCE FILE, and subtracted during processing of samples.

A concentrate obtained by extraction of a sample blank may alternatively be processed at this stage to store method background levels.

SAMPLE PROCESSING

Samples are automatically processed by the SAMPLE program. Each compound is quantitated by integrating through an adjustable scan window which centers at the scan expected by the relative retention time.

The program allows entry of the RUN DATE, SAMPLE ORIGIN, and defined DETECTION LIMIT.

If a compound is detected at a concentration greater than one-third the DETECTION LIMIT, the program then searches for the SECONDARY IONS. The result of this search and a summary of the integration are displayed for the operator, who then confirms whether the compound is present.

If the integrating ion is overloaded, the program asks the operator to enter an alternative integrating ion and an intensity factor. An isotope ion is commonly used. This facility expands the effective dynamic range of the analytical system to more than 10^5.

FEATURES

*Each compound is integrated in 40-60 seconds.

*System accommodates a wide range of concentrations, from PPB to PPM.

*Programs are interactive, allowing the operator flexibility in determining scan windows, detection limits, and final confirmation of the presence of a compound.

*Programs are easily adaptable to any series of compounds.

*Programs may be modified to accommodate multiple internal standards, including isotopically labelled standards.

*Hard copy records of the integration and the final results are generated.

GEOCHEMICAL DATA PROCESSING WITH THE DS-50 DATA SYSTEM. J. David King, U.S. Geological Survey, Box 25046, MS977, Denver, Colorado 80225

INTRODUCTION

Geochemical analysis of the organic chemical constituents of sedimentary rocks and crude oil samples provides results that can be of assistance in determining the biological origin of the organic matter and the compositional effects of natural geological processes such as thermal alteration and migration. In addition, crude oil-source rock and oil-oil correlations can be established. Samples of rock such as shales and carbonates are generally examined along with samples of petroleum in an attempt to understand the history of petroleum formation. Mass spectral (MS) and gas chromatographic - mass spectral (GC/MS) results are often supplemented by other geochemical data. Analytical techniques utilized (besides MS and GC/MS) are listed in Table 1. The results of these analyses are used to select a suite of samples for further study by MS and GC/MS. Post data acquisition computer programs have been written which reduce these data to a form readily useable by geochemists. These programs are written in FORTRAN utilizing the DS-50 programmer's package provided by Kratos, Inc. for the DS-50 mass spectrometer data system.

SAMPLE TREATMENT

For the saturated hydrocarbon fraction, mass spectral analyses most commonly used are shown in table 2. Out of a sample suite, usually one or two representative samples are analyzed by GC/MS, scanning complete spectra to insure positive identification of compounds that can be separated by gas chromatography. Compound identifications are performed by a computer program utilizing the scheme of Wardroper and others (1977) for classifying spectra of steranes and pentacyclic triterpanes on the basis of characteristic mass spectral fragmentations for these classes of biological markers. Another program performs group-type analyses on each scan of the GC/MS run, producing chromatograms representative of the number of fused cyclic rings present. This is an extension of the technique developed by Brown (1951). Examples of the reports produced by these programs for the classification and group-type analyses are shown in figures 1 and 2, respectively.

After this preliminary examination, the entire suite of samples is subjected to bulk group-type analysis then, for the purpose of oil to source rock and oil to oil correlations, each sample is analyzed by GC/MS/MID (multiple ion detection) for selected ions (m/z 217.1956 and m/z 191.1800, Figure 3) representative of the steranes and pentacyclic triterpanes. A third program allows comparison of mass chromatograms from different GC/MS/MID analyses utilizing two reference peaks in each run to properly scale the display for direct visual examination (Figure 5). The fourth program in this package calculates relative abundances of the major biological markers and certain ratios of geologic importance. The output of this program is shown in figure 4.

INTERPRETATION OF RESULTS

Figure 5 is a comparison of an Eocene oil-source rock pair from the Ouchai Basin, People's Republic of China. These chromatograms show excellent correlation. The effects of migration on the ratios of some of the steranes and triterpanes is also evident. These samples were two from a suite representing rock-oil pairs from continental basins in Asia. Figure 6 is a graphical representation of the relative amounts of 5(alpha)H + 5(beta)H C_{27},C_{28} and C_{29} steranes from this same suite. Wen-Yen Huang and W.G. Meinschein (1979) proposed that the precursor sterols present in the primordial sediment are a good indicator of the paleobiological environment because C_{27} sterols are more prevalent in simpler organisms and C_{29} sterols are found predominantly in higher plant forms. This generally holds true for the reduced sterols (steranes) (Figure 6); most of the oils and rocks points lie within the lacustrine (inland lake) environment. An univestigated phenomenon is responsible for alteration of the steranes for the oils that lie toward the open marine area of the plot.

An example of thermal maturation is shown in figure 7. A suite of coal and shale samples of Pennsylvanian age was collected from the Cherokee group throughout Iowa, Missouri, Kansas and Oklahoma. This set of coal and shale samples illustrates that the ratio of 22S/22R isomers of the extended (>C30) hopanes is related to vitrinite reflectance. Vitrinite reflectance is generally accepted as an indicator of maturation of source rocks or rank of coals. However, not all source rocks of petroleum contain sufficient higher plant macerals to obtain good values of vitrinite reflectance. In this event, the 22S/22R ratios of the Hopanes may provide evidence of the degree of thermal

maturity of rocks. The shales and coals labeled similarly (A,B,C,D,E) in Figure 7 lie stratigraphically near each other and thus have experienced a similar geothermal history. Petroleum generation from the shale begins when the coal vitrinite reflectance reaches a value of approximately 0.5, corresponding to a 22S/22R hopane value of 1.5 in the shale.

SUMMARY

It is to be emphasized that data collected by MS and GC/MS cannot be productively utilized without also critically examining all available geologic, geophysical and geochemical data. With few exceptions, a suite of samples should be analyzed rather than a single sample, and documentation of the sample collection must be reliable. Automation of data reduction by computer programs can substantially increase sample throughput for a statistically valid treatment of the results aside from allowing the geochemist more time for intepretation.

REFERENCES

Brown, R.A., 1951, Compound types in gasoline by mass spectrometer analysis: Analytical Chemistry, v.23, p.430

Huang, Wen-Yen and Meinschein, W.G. ,1979, Sterols as ecological indicators: Geochimica et Cosmochimica Acta, v. 43, p.739

Wardroper, A.M.K., Brooks, P.W., Humberston, M.J., and Maxwell, J.R., 1977, Analysis of steranes and triterpanes in geolipid extracts by automatic classification of mass spectra: Geochimica et Cosmochimica Acta, v.41, p.499

fig 1.4

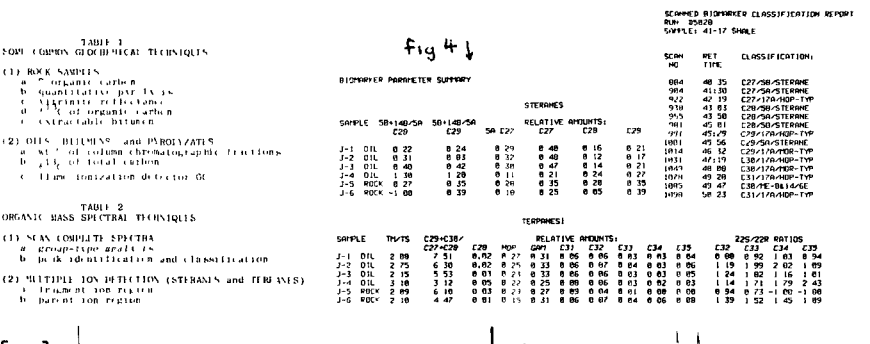


TABLE 1
SOME COMMON GEOCHEMICAL TECHNIQUES

(1) ROCK SAMPLES
- a. % organic carbon
- b. quantitative pyrolysis
- c. vitrinite reflectance
- d. ^{13}C of organic carbon
- e. extractable bitumen

(2) OILS, BITUMENS and PYROLYZATES
- a. wt % of column chromatographic fractions
- b. ^{13}C of total carbon
- c. flame ionization detector GC

TABLE 2
ORGANIC MASS SPECTRAL TECHNIQUES

(1) SCAN (COMPLETE SPECTRA)
- a. group-type analysis
- b. peak identification and classification

(2) MULTIPLE ION DETECTION (STERANES and TERPANES)
- a. fragment ion region
- b. parent ion region

fig 4

BIOMARKER PARAMETER SUMMARY

SAMPLE	5B+14B/5A C29	5B+14B/5A C29	5A C27	STERANES RELATIVE AMOUNTS: C27	C28	C29
J-1 OIL	0.22	0.24	0.29	0.48	0.16	0.21
J-2 OIL	0.31	0.83	0.32	0.48	0.12	0.17
J-3 OIL	0.40	0.42	0.38	0.47	0.14	0.21
J-4 OIL	1.38	1.20	0.11	0.21	0.24	0.27
J-5 ROCK	0.27	0.35	0.24	0.35	0.28	0.35
J-6 ROCK	1.08	0.39	0.10	0.25	0.05	0.39

TERPANES:

SAMPLE	TM/TS	C29+C30/ C27+C29	C29	HOP	GAM	C31	C32	C33	C34	C35	22S/22R RATIOS C32	C33	C34	C35
J-1 OIL	2.89	7.51	0.02	0.27	0.31	0.06	0.06	0.03	0.03	0.04	0.00	0.92	1.03	0.94
J-2 OIL	2.75	6.30	0.02	0.25	0.33	0.06	0.07	0.04	0.03	0.06	1.19	1.99	2.02	1.89
J-3 OIL	2.15	5.53	0.01	0.21	0.33	0.06	0.06	0.03	0.03	0.05	1.24	1.82	1.16	1.01
J-4 OIL	3.18	3.12	0.05	0.22	0.25	0.09	0.06	0.03	0.02	0.03	1.14	1.71	1.79	2.43
J-5 ROCK	2.89	6.18	0.03	0.21	0.27	0.03	0.04	0.01	0.00	0.00	0.94	0.73	<1.00	<1.00
J-6 ROCK	2.10	4.47	0.01	0.15	0.31	0.06	0.07	0.04	0.06	0.08	1.39	1.52	1.45	1.89

fig 1.4

SCANNED BIOMARKER CLASSIFICATION REPORT
RUN: 8582B
SAMPLES: 41-17 SHALE

SCAN NO	RET TIME	CLASSIFICATION:
884	40 35	C27/5B/STERANE
904	41:30	C27/5A/STERANE
922	42 19	C27/17A-HOP-TYP
939	43 03	C28/5B/STERANE
955	43 50	C28/5A/STERANE
981	45 01	C28/5D/STERANE
977	45:49	C29/17A-HOP-TYP
1001	45 56	C29/5A/STERANE
1014	46 12	C29/17A/MOR-TYP
1031	47:19	C30/17A/HOP-TYP
1049	48 08	C30/17A/MOR-TYP
1074	49 20	C31/17A-HOP-TYP
1095	49 47	C30/ME-B&14&5E
1098	50 23	C31/17A/HOP-TYP

fig. 2

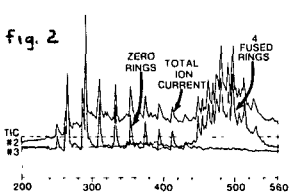
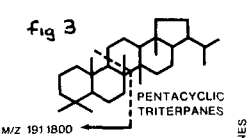


fig 3



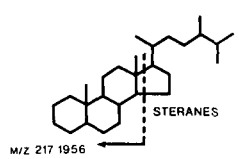


fig 5

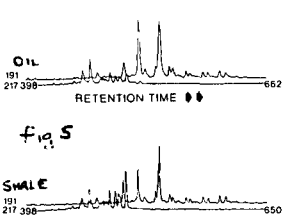


fig 6

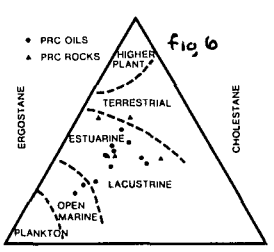
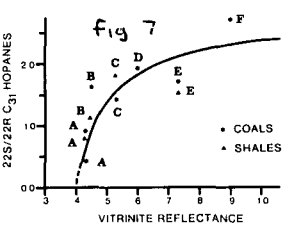


fig 7



PLT10 - A New Interpretive Program for Hewlett Packard GC/MS Data Systems

D. M. Schoengold

Battelle Pacific Northwest Laboratory, Richland, WA 99352

PLT10 is a new interpretive program for Hewlett Packard GC/MS data systems which replaces both manufacturer supplied programs - SPEED and ANSWER. It was designed to provide faster and easier interpretation of complex capillary chromatograms which require extensive use of background subtraction and reconstructed single ion chromatograms to verify the masses in a spectrum. PLT10 is faster than either SPEED or ANSWER for most applications. It is also more versatile and has a friendlier operator-program interaction than either program. PLT10 is written in BASIC for easy user modification and for inter-system compatibility.

Advantages of PLT10 over SPEED are:

1. Plots up to 10 single ion reconstructs/page instead of just 3.
2. Goes directly to scan number or time range of interest without having to scroll the X-axis.
3. Runs up to 3 times faster.
4. All output is indexed by both scan number and retention time making comparison with stand-along GC output easier.
5. Output includes useful data such as total ionization, base peak intensity and largest single ion intensity that is absent in SPEED.
6. Peaks are normalized to the largest value within the range plotted instead of the largest value for the entire run.

Advantages of PLT10 over ANSWER are:

1. PLT10 has a much more convenient background correction routine.
2. Interpretive throughput is usually faster.
3. Output includes useful data not printed on ANSWER output.
4. Both scan numbers and retention times are always printed.
5. Mass spectral output is much "prettier".

PLT10 will run on all Hewlett Packard data systems which use either 21MX or HP1000 computers. It will support a Tektronix 4012 or a HP 2648 graphics terminal.

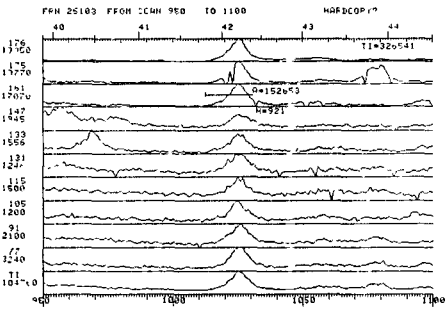
Basic Program Options

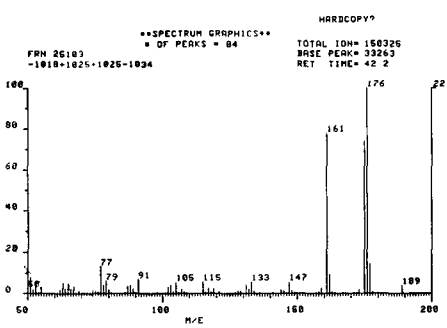
1. Normal Reconstructed Single Ion Chromatograms.
   This is equivalent to single ion reconstructs in SPEED or ANSWER.

2. Homologous Series.
   This option automatically generates homologous series plots which are single ion reconstructs separated by 14 AMU. The only data entry needed are the number of masses to be plotted and the first mass in the series.

3. Store Mass Groups.
   If several sets of mass groups are used repetitively, this option simplifies keyboard entry. Up to 9 groups of 10 masses may be entered and stored. To call a mass group, the user has to merely enter the group number(1-9). This reduces keyboard entry time and also reduces errors.

4. Unattended Data Plotting.
   This option permits up to 90 sets of up to 10 ions per set to be stored for later, unattended plotting. This permits the operator to set up a group of plots and then do other work while the computer is generating data. The data system can be used in the same manner to produce data during the night for off-line interpretation during the day. Since generation of 90 plots of 10 ions each would take about 30 hours of operator time using SPEED, 5 to 10 hours of operator time with ANSWER and about 5 hours of unattended time with PLT10, this gives the interpretive throughput effect of 2nd and even 3d shift operation without having someone work those shifts.





RUN TIME COMPARISONS(MINUTES) FOR PLT10, ANSWER AND SPEED

	HP1000 Computer			21MX Computer	
	SPEED	ANSWER	PLT10-8206	SPEED	PLT10-8092
1. Generate a 10 ion chromatogram	19 2*	2.8	1 7	16.0*	1.9(1.3)#
2 After plotting a spectrum, replot a 10 ion chromatogram using the same mass set	0 3**	0 3	0.9	0.3**	1 0(0.7)#
3. After plotting a spectrum, replot a 10 ion chromatogram using a new mass set	4.5**	2.5	1 8	3.7**	2 1(1 4)#
4. Plot a 10 ion chromatogram, do a background correction, replot the same set of ions and then do a new background correction	5.9**	5.6	3.9	5.8**	5.8(4.7)#
5. Plot a 10 ion chromatogram, do a background correction, check the peaks in the subtracted spectrum by plotting a new 10 ion chromatogram and then do a new background correction	8.7**	7.9	4.7	8.8**	6.8(5.3)#
6. Plot a 10 ion chromatogram, do a background correction, then do a second background correction by entering scan numbers directly(PLT10 "B" option)	****	5.0***	2.9	****	4 7(4 1)#

* It is not possible to generate 10 ion chromatograms with SPEED. The times are obtained by multiplying the 3 ion plot times by five.

** It is not possible to plot 10 ion chromatograms in SPEED The times shown are for the equivalent 3 ion chromatogram operation.

*** The "B" option does not exist in ANSWER The time shown is for the closest equivalent operation

**** This operation is not possible in SPEED.

\# The first time is for a 10 ion chromatogram, the second is for a 3 ion chromatogram. The second time provides an exact comparison with the 21MX SPEED run times

EXTENSIONS TO AN INCOS DATA SYSTEM*

W. D. Jamieson and E. Lewis
Atlantic Research Laboratory
National Research Council
1411 Oxford Street
HALIFAX, N.S., Canada B3H 3Z1

Several extensions and modifications have been made to our Finnigan MAT INCOS data system. All are compatible with Level 3.1 Revision B or Revision C versions and are in regular use with our dual terminal, dual acquisition system. The system is interfaced to Finnigan MAT 4000 (equipped for positive/negative ion chemical ionization) and CEC 21-110B mass spectrometers, and to a Varian 620/L-100 minicomputer on which is based a system developed for automated acquisition of photoplate high resolution mass spectral data (1).

Over 20 MSDS programs have been modified or extended. Some extensions involve new overlay program modules, called automatically (user - "transparent") where relevant. Input/output activity with the Varian 620/L-100 is supported by some new software, and runs as a background job.

User convenience was improved by a disk identification system and related revision of the STATus program; provision for day/month/year file dating and sorting; expansion of the file description information displayed by the PARAmeters program and its extension to be a fully capable editor for data-file headers.

Processing and interpretation of high resolution or accurate mass data was improved by major revision and extension of the elemental COMPosition set of programs to provide more kinds of hardcopy products more efficiently; to optionally restrict masses considered to those within specified mass defect limits, or those ions of less than a specified recorded intensity; to compute masses and double bond equivalent values for specified elemental compositions and, optionally, find alternative elemental compositions within specified mass error limits (candidate "interferences"); to allow masses considered to be ordered by decreasing recorded intensity; to allow candidate elemental compositions for a mass to be output ordered by error; to allow identification and error-reporting in the output for masses assigned to ions on which the mass assignment calibration was based (.CT entries).

Major revision and extension of the PROFile set of programs improved user information and interaction, aided consideration of multiplet occurrences and provided for hardcopy output of multiplet diagnostic displays.

Mass assignment operations in difficult cases have been aided by revision of the CALI, HCAL calibration programs, and the EDRT, EDCT programs to increase user information and convenience, enable more interaction and allow more detailed documentation.

*NRCC No. 19913

The STABility set of programs was revised to display more information including, optionally, graphical display of statistical calculations and wider user choice of display modes. These revisions have helped users assessing the quality of high accuracy mass data and with such GC/MS low mass resolution operations as detecting sample-derived ions of the same nominal mass as ions derived from column-bleed or other "background" contaminants.

Fine-tuning of mass spectrometer adjustments, the design and documentation of GC/MS and other experiments were aided by revisions to the GAIN, SYSTem, MID and ACQU program sets. Major changes to MID and ACQU improved calibration practice, increased information to the user and improved documentation of experiments, requesting and filing data appropriate to GC, LC, direct-probe or TLC sample introduction modes. These changes have helped the operators of our mass spectrometers to do better experiments, consistently. Experienced operators appreciate the convenience, the less experienced learn more quickly and make fewer mistakes.

Software changes for more effective processing of photoplate-derived data have been described previously (1). A Varian 620/L-100 minicomputer is used to control operation of a microcomparator-densitometer and acquire the data, then reformat it as an INCOS 'profile' data file. This INCOS-compatible data is transferred to INCOS using a system described in another paper presented at this Conference (2). The INCOS MSDS CALI/HCAL, COMP, COPY, ENHA, PARA, PROF, SAVE, STAB and SYST program sets were extended to better handle this photoplate data. The ENHAnce extension provided for creation in INCOS of index (.TX) files needed for data from multiple comparator scans. The other changes ensured preservation of a file-header flag (in ITCON) that the file contained photoplate data, altered displayed information to show photoplate documentation or ensured appropriate processing action (e.g., CALI/HCAL, SYST, EDCT).

Minor revisions provided for selection of smaller graphics hard-copy dimensions, removed a few bugs and allowed user "B1" to hear music.

Our revised software is usable on systems equipped with 10, 32 or 96 megabyte disc drives.

Program listings and other information are available. Colleagues who have already obtained some of this software have not reported problems with it. We can record it on either 5 megabyte (Wangco, Perkin Elmer, etc.) or 16 megabyte (CMD) discs.

We acknowledge gratefully the assistance of E. W. Dyer.

REFERENCE

1. W. D. Jamieson, F. G. Mason and D. E. Webber. Automated Acquisition and Processing of Photoplate High Resolution Mass Spectral Data by an 'INCOS'-'VARIAN' System. Presented at the 29th Annual Conference on Mass Spectrometry and Allied Topics, Minneapolis, May, 1981. Proc., pp. 457-8.

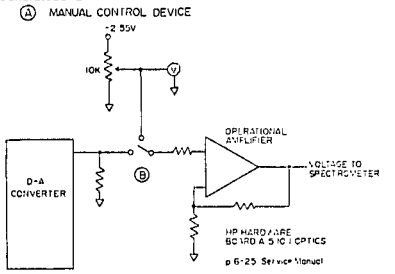
2. W. D. Jamieson, E. W. Dyer and F. G. Mason. Linking an INCOS Data System to Another Minicomputer. Presented at the 30th Annual Conference on Mass Spectrometry and Allied Topics, Honolulu, June, 1982. Paper RPB7.

PERFORMANCE OPTIMIZATION OF HP-5985A MASS SPECTROMETER VIA OPERATOR INTERACTION; B.D. Musselman, M.J. Davenport, J.F. Holland, and G. Dolnikowski, NIH/MSU Mass Spectrometry Facility, Michigan State University, East Lansing, Michigan 48824.

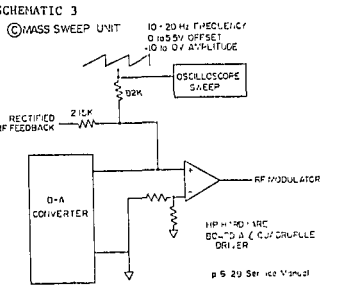
In recent years, the manufacturers of data systems for GC-MS have made progress toward automating the mass axis calibration and instrument tune-up procedures. Specifically, the HP-5985A has all of the major ion source functions under complete computer control. Situations can arise in which the computer cannot reach satisfactory status as defined in the computer algorithm. To overcome this problem, a manual control device was designed observing three basic concepts. First, to display the detector output in real time and thus allow for interaction between the operator and instrument. Second, to allow for manual control of each parameter individually or collectively. Third, to incorporate minimal changes in the HP electronics system. With these principles in mind, the following controller was designed and implemented.

Manual control of the ion focussing parameters was implemented by interrupting the DAC output from the computer to the corresponding operational amplifiers on the Ion Optics board A-5. This modification is outlined in schematic 1. The 10KΩ potentiometer provides a voltage of 0 to -2.55V thus emulating the normal computer operational range. Schematic 2 outlines the circuits used for each individual control device including the HP part numbers for easy reference. All of the new circuits are identical except for the Entrance Lens control section. The entrance lens potential is ramped as a function of mass being filtered in the analyzer. The ramping action of the manual control is accomplished by substituting the fixed 2.15KΩ resistor on the output of the DAC for an equivalent 2.15KΩ parallel resistor combination consisting of a 10KΩ potentiometer and a 2.7KΩ resistor.

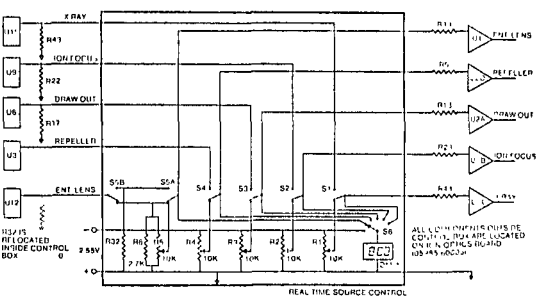
SCHEMATIC 1



SCHEMATIC 3



SCHEMATIC 2



The switches incorporated in the modification allow us to fulfill our second requirement. The instrument can be run in either computer or manual mode with a switch distinguishing between the two modes. Manual adjustments can be completed on individual lens elements, after which their voltages are recorded using a DVM. Subsequently, these optimum voltages can be entered into the OVERRIDE* program for permanent storage and use. The measured voltages on the DVM are multiplied by the appropriate gains in order to determine the proper voltage entry for OVERRIDE.

Selection of the mass values for transmission through the quadrupole filter is completed by utilizing the HP SIM* program. Sets of ions are entered via standard format, with longer delay times (i.e. 1-5 sec) being used to allow for visual inspection of the output generated at each ion. Scanning over a desired peak is completed by superimposing a sawtooth DC voltage on the RF modulator as detailed in schematic 3. This allows observation of a small mass range and permits the evaluation of the ion focus as a function of peak shape and intensity.

The output from the detector is split between the oscilloscope and the ion current amplifier in the HP system. The sweep generator used to apply the sawtooth voltage to the RF modulator also controls the horizontal plates of the oscilloscope, this links the scope horizontal position with the mass being examined. By adjustment of the sweep generator offset an ion peak can be centered on the scope face for real time display of the ion throughput.

The modifications outlined in this control device are not major. The requirements for this system are listed below for your reference.

To date, there have been several beneficial uses of this system. The main use has been in the area of optimization of ion focus. Significant reduction in the time required for this task have been noted. The optimization of peak shape and intensity can be completed in less than one minute of operation, where AUTOTUNE* typically required 5-10 minutes and OVERRIDE* took as long as 3 minutes to examine one source element alone. Reducing this time factor was a primary concern since introduction of calibration compound into the source is a major factor reducing source sensitivity.

In summary, this system has been designed to aid the operator in keeping the instrument in top condition. It serves as a diagnostic tool for the user and can be added to an existing instrument with minimal hardware change, thereby providing a more versatile system.

Parts

5 - 10KΩ 10-turn potentiometer (R1-R5)
1 - 2.7KΩ , 1/4 watt resistor (R6)
4 - SPDT miniature switch (S1-S4)
1 - DPDT miniature switch (S-5)
1 - 6 Pos Rotary switch, Centralab PA-1001 (S-6)
1 - DVM with display to -3.00V

Misc. 22 gauge wire for switch wiring, knobs for potentiometer and rotary switch, shielded cable to and from HP-5985A mass spec., box to house controls, 2 banna jacks for power supply

Equipment

1 - Oscilloscope with external sweep
1 - Coax Tee Connector (UG247/U)
1 - Sweep Generator with offset
1 - Regulated power supply (for -2.55V in control unit)

LINKING AN INCOS DATA SYSTEM TO ANOTHER MINICOMPUTER*

W. D. Jamieson, E. W. Dyer and F. G. Mason
Atlantic Research Laboratory
National Research Council
1411 Oxford Street
HALIFAX, N.S., Canada B3H 3Z1

We reported earlier (1) on how we had provided for hardwired data transfers at 9600 baud (serial 8-bit binary) between an INCOS data system (dual acquisition, dual terminal configuration) and a separate system which used a Varian 620/L-100 minicomputer. Cable distance between the two systems is about 60 metres. The software we had used for this required alteration of the IDOS operating system of the INCOS data system. Updating our software to compatibility with successive INCOS revisions probably would have required changes each time, since our original software which had been developed with Level 3.1 Revision B would not run with Revision C. We now report on a software approach which does not require IDOS alteration. We have used this successfully for over a year, through two INCOS revisions.

Further hardware modifications were not made. Neither were changes to Varian 620/L-100 resident software, although there was some further development of this, to increase operator convenience when transferring Varian-acquired photoplate-derived mass spectral data to the INCOS data system for processing and interpretation (2,3). To aid in modification of Varian-resident software written in assembler, Varian assembler and editor utilities were modified so the INCOS disc storage, source-file editor (GE) and listing or hard-copy facilities could be used for development of programs to be coded in Varian assembler. The Varian-resident input/output handling software and the modified Varian utilities use INCOS assets as a background job as allowed by other INCOS system activity.

Our new INCOS-resident input/output handling software is a set of subroutines accessed and controlled through a main program, "LINE", written in FORTRAN IV to be compatible with MSDS. LINE provides some functions similar to those available through the INCOS "PHONE" program and others such as those checking for input/output errors, allowing remote (Varian 620/L-100) operation or operation by MSDS method files, as well as user aids such as usually appropriate default values for description of files to be input/output and some protection against operator errors. LINE also deals with points of software incompatibility between INCOS and Varian system conventions (e.g. use of "control-C").

The Varian minicomputer can be "boot-strapped" from INCOS, and can thus be dealt with as a remote INCOS peripheral.

With the Varian-based hardware we use (16 K core, no disk drives, data storage on cassette tape) data transfer time for large amounts of data are determined mainly by the time used by the Varian system to read from or write to cassette tape storage. This has not been a serious difficulty. For example, after multiply-scanned photoplate high

*NRCC No. 19912

resolution mass spectral data has been acquired by Varian operation of the microcomparator -densitomer (2), then formatted as INCOS "profile" files and stored on cassette tape, it usually requires less than 5 minutes use of an INCOS terminal to set up and complete input of the data to INCOS.

Program listings and other information are available.

We acknowledge gratefully the assistance of D. J. Embree and the late D. E. Webber of this laboratory and M. Weiss, Finnigan MAT, San Jose, California.

References

1. W. D. Jamieson, E. W. Dyer, F. G. Mason and M. Weiss. Data Transfer Between an INCOS Data System and a VARIAN 620/L-100 Minicomputer. Presented at 27th Annual conference on Mass Spectrometry and Allied Topics, Seattle, June, 1979, Proc. pp. 258-9.

2. W. D. Jamieson, F. G. Mason and D. E. Webber. Automated Acquisition and Processing of Photoplate High Resolution Mass Spectral Data by an 'INCOS'-'VARIAN' System. Presented at the 29th Annual Conference on Mass Spectrometry and Allied Topics, Minneapolis, May, 1981. Proc., pp. 457-8.

3. W. D. Jamieson and E. Lewis. Extensions to an INCOS Data System. Presented at the 30th Annual Conference on Mass Spectrometry and Allied Topics, Honolulu, June, 1982. Paper RPB5.

EXPANSION OF THE INCOS LIBRARY SEARCH

L.E. Slivon, D.G. Aichele
Battelle Columbus Laboratories
Columbus, OH 43221

Introduction

Selected enhancements were made to the Incos data system in an effort to accomodate and support the growth of the EPA/NIH/MSDC mass spectral data base. The enhancements include the modification of existing MSDS programs and the creation of new MSDS compatible utilities.

Library Search

The 1982 release of the EPA/NIH/MSDC mass spectral data base containing approximately 38,800 mass spectra was transformed into an Incos compatible library. This library represents a growth of approximately 7,000 new spectra beyond that previously available on an Incos system. 89 percent of the new spectra were determined to be in the 100-400 molecular weight range providing added capability for unknowns identification in GC/MS analyses.

Since the Incos forward search program is limited to 32,767 spectra in a single library, modification of the program was required in order to fully utilize the new library. No modifications were made to the library storage format or the conventional search options in order to retain compatibility with previous issues of the library and user procedures. The revised program is able to accomodate up to approximately 65,000 reference spectra in a single library. In addition to providing access to large libraries, the graphic display feature of the program was expanded to to include the unknown and the five best matches.

Library Listing

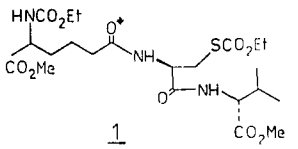
Due to the size of the new library, it was necessary to replace the Incos procedure conventionally used to list the entire library. A single MSDS compatible program was developed for this purpose. New features of the listing include CAS registry numbers and up to 70 characters of compound name.

Submission of Spectra

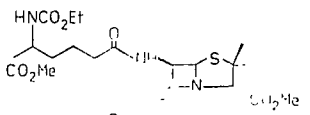
In order to promote the continued growth of the EPA/NIH/MSDC data base, a program was developed to serve as a mechanism for submission of reference quality spectra. This program eliminates the time consuming and error prone transcription of mass-intensity pairs. The process of spectrum documentation is also simplified. The program transforms background corrected mass spectra into the National Standard Reference Data System (NSRDS) format on standard magnetic tape. The format of the data produced by this program is identical to that used for national distribution of the data base allowing the data to be readily assimilated by those responsible for review and maintenance of this collection. The mass spectral data used by the program is that which remains in the Incos system following a conventional "List" or "Spec" display. This approach minimizes the effort required. Successive spectra are maintained in a disk file which may be later copied to magnetic tape. The majority of the NSRDS fields are available to the analyst. Instrument parameters necessary for proper documentation of the data may be saved and used for successive spectra eliminating the need to repetitively enter equivalent information. After the program is called, entry of compound identification information is generally all that is required to process the spectral data.

ACE; DCI; IN BEAM EI; AND LINKED SCAN B/E, STUDIES ON δ-(L-α-AMINOADIPYL)-PEPTIDES PRECURSORS OF THE PENICILLIN AND CEPHELOSPORIN ANTIBIOTICS. R.M. ADLINGTON, R.T. APLIN, DYSON PERRINS LABORATORY, OXFORD UNIVERSITY, OXFORD, U.K.

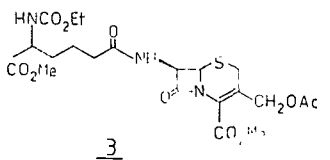
The detailed fragmentation pathways of N,S-ethoxycarbonyl-carboxymethyl deviations of the δ-(L-α-aminoadipyl)-peptide ACV(1), iso-Penicillin N(2) and cephalosporin-C(3) have been determined.



1



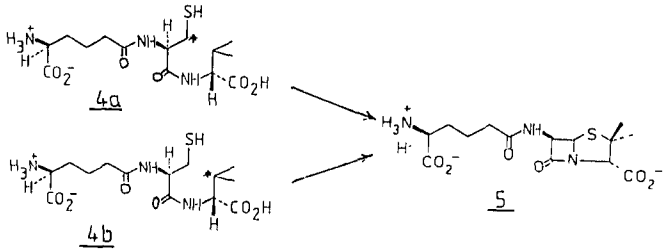
2



3

Site specific [17/18] oxygen labelling at O* has shown that NO loss of label occurs in the conversion of ACV into iso-Penicillin N. This eliminates all mechanisms which involve intramolecular dehydration/hydration steps[2,3,4] and all mechanisms involving intermolecular esters, thioesters, amides, amidenes etc.

The conversion of a 1:1 mixture $^{2}H:^{1}H^{*}$ labelled ACV(4a,b) in a cell free system



shows no build up of ^{2}H labelled ACV as the biosynthesis proceeds. This indicates, since hydrogen is lost from these positions in the formation of iso-Penicillin-N(5), that these reactions are not rate determining in the biosynthesis.

1. P.B. Loder and E.P. Abraham, Biochem J., 1971, 123, 471.
2. A.I. Scott, S.E. Yoo, S.K. Chung, and J.A. Lacadie, Tetrahedron Letters, 1976, 1137.
3. R.D.G. Cooper, J. Am. Chem. Soc., 1972, 94, 1018.
4. S. Nakatsuka, H. Tanino, and Y. Kishi, J. Am. Chem. Soc., 1975, 97, 5008, 5010.

CHARACTERIZATION OF LIPOXYGENASE METABOLITES OF ARACHIDONIC AND LINOLEIC ACID BY GC/MS

Magda Claeys, Marie-Claire Coene and Cor Van Hove
Division of Pharmacology, Department of Pharmaceutical Sciences, University of Antwerp, Universiteitsplein 1, B-2610 Wilrijk, Belgium.

Recent studies on the biotransformation of arachidonic acid (AA) have indicated that metabolism by various lipoxygenases is an important event in certain cell types, particularly in cells of the reticuloendothelial system such as platelets, leucocytes and macrophages. As interest grows in the physiological function of lipoxygenase metabolites, methods are needed to study their formation in and their release from cells or tissues. In an attempt to determine lipoxygenase and to some extent also cyclo-oxygenase and thromboxane synthase activity, we have devised a profiling method for monohydroxylated metabolites of polyunsaturated fatty acids, i.e. AA and linoleic acid (LA). The measured metabolites are listed in Table I.

Experimental

The procedures for generation of lipoxygenase, cyclo-oxygenase and thromboxane synthase metabolites and for isolation of monohydroxylated metabolites have been described previously (1). After methylation using ethereal diazomethane, catalytic hydrogenation with PtO_2 as catalyst and trimethylsilylation with BSTFA, the derivatives were analyzed by GC/MS using a Finnigan 4000/Incos datasystem combination. Separations were performed on a 2m x 2mm 1% OV-1 column, which was programmed from 180 to 230°C at a rate of 5°C/min. Selected ion monitoring was carried out at the two specific and abundant ions, listed in Table I.

Results and Discussion

Electron impact analysis of the derivatized monohydroxylated metabolites of AA and LA results in two abundant and specific ions, formed through the fragmentation directing effect of the trimethylsilylated hydroxyl group. The catalytically hydrogenated derivatives allow as such to distinguish between positional isomeric monohydroxylated metabolites. Fig. I shows the profile for monohydroxylated metabolites formed from endogenously released polyunsaturated fatty acids by rabbit peritoneal tissue, a tissue rich in mesothelial cells of the same embryonic origin as the endothelial cells of the blood vessel wall. The products of the AA cascade are HHT, formed through the combined action of cyclo-oxygenase and thromboxane synthase, 11-HETE, due to incomplete cyclo-oxygenase action, and 12- and 15-HETE, which are lipoxygenase metabolites. With regard to LA metabolites, three products are detected, i.e. 9- and 13-HODD, and a minor metabolite containing a hydroxyl group at the 12-position, of which the enzymic origin is not elucidated yet. The profiling method has also been employed to investigate the biotransformation of endogenously released polyunsaturated fatty acids in macrophages and to detect metabolic shifts induced by indomethacin, a known inhibitor of the cyclo-oxygenase pathway.

For quantitation purposes, two homologs each containing 3 double bonds and 19 or 22 carbon atoms, biosynthesized from the corresponding polyunsaturated fatty acids using soyabean lipoxygenase, have been evaluated as internal standards (Table I). The C_{19}-homolog could not be employed because of an interference on the m/z 173 ion trace, due to hydrogenated dioctyl phtalate. As it is practically impossible to make biological extracts free from phtalate plasticizers, the higher C_{22}-homolog had to be utilized. So far, only semi-quantitative data have been obtained. For the estimations, the assumption is made that all the derivatives have the same ionization efficiency. Furthermore, a correction is carried out for the differences in the intensities of the ions used to quantitate the various metabolites and the internal standard. The determination of the precision and the accuracy will be a subject for future research in our laboratory.

Acknowledgment

This work was supported by the Belgian National Fund for Scientific Research (Grant nr. 3.9001.79).

Reference

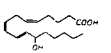
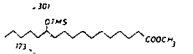
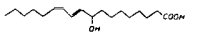
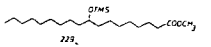
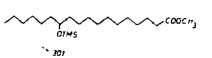
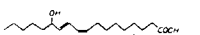
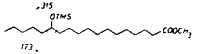
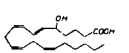
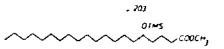
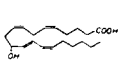
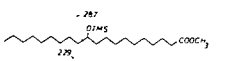
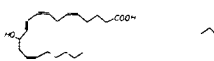
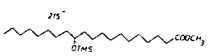
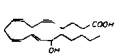
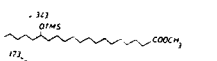
(1) M. Claeys, M.-C. Coene, A.G. Herman, M. Van der Planken, G.H. Jouvenaz and D. H. Nugteren. Arch. int. Pharmacodyn. 250, 305 (1981).

Abbreviations

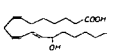
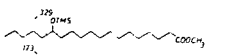
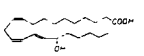
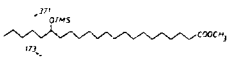
HETE, hydroxy eicosatetraenoic acid; HHT, hydroxy heptadecatrienoic acid; HODD, hydroxy octadecadienoic acid.

TABLE I :

MEASURED METABOLITES

	n° C. atoms	structure	derivative
HHT	17		
9-HODD	18		
12-HODD	18		
13-HODD	18		
5-HETE	20		
11-HETE	20		
12-HETE	20		
15-HETE	20		

INTERNAL STANDARDS

19		
22		

MONOHYDROXYLATED METABOLITES OF ARACHIDONIC AND LINOLEIC ACID FORMED BY RABBIT PERITONEAL TISSUE

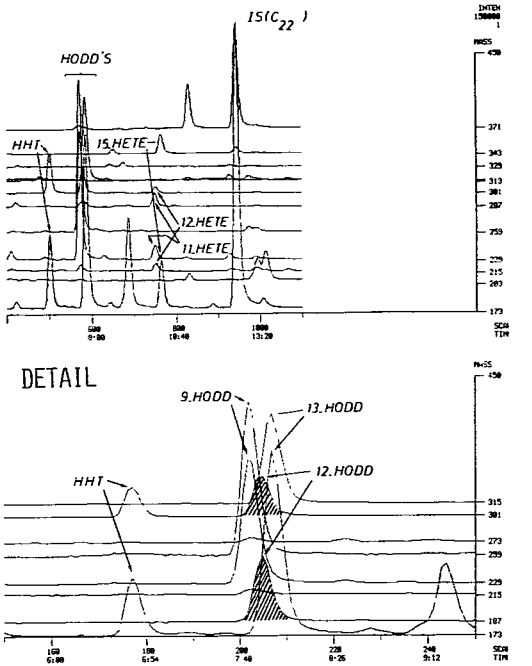


FIG. I

Peptide Sequencing and Amino Acid Mixture Analysis by GCMS. Ketoacid Ester Formation in One Procedural Step from Amino Acids and Peptides.

C. J. Metral, K. Jayasimhulu, A. Kornel, and R. A. Day
Department of Chemistry and Department of Environmental Health, University of Cincinnati
Cincinnnati, OH 45221

The α-amino group of amino acids and peptides may be replaced by an α-keto (2-oxo-) group under relatively mild conditions utilizing reagents that effect transamination. Transamination can be carried out with various reagents in organic or aqueous solutions that may be neutral to acidic. The reactions proceed at acceptable rates from room temperature to 120°. Esterification may be done prior to, simultaneously with, or after the transamination.

Reagents and typical conditions examined:

1) 2-Pyridinecarboxaldehyde (2PC)/3N HCl/MeOH at room T, reflux, and at 105° sealed tube, and gl HOAc 120° sealed tube.[1]

2) 4-Pyridinecarboxaldehyde (4PC) under the same sets of conditions as used with 2PC.

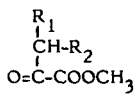
3) N-Methyl-4-pyridinecarboxaldehyde (MPC) salts, aqueous, pH 4-7,[2] room T to 105° sealed tube; or in 3N HCl/MeOH at 105°.

4) Glyoxalic acid/pyridine/water pH 7/$NiAc_2$ room T.[3]

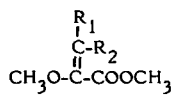
The wide range of conditions and solvents available for the reaction include the very mild through moderately severe conditions. The solvents used in transamination are good peptide solvents. The reactions offer a degree of specificity not always seen with other amino acid modifying processes. The yields range up to quantitative for favorable cases, e.g., amino acids and their amides.

The transamination by-products may complicate the GC pattern. However, the 2PC by-products[1] are readily extracted into aqueous acid or could be removed by cation exchange resins. The MPC gives very few volatile by-products. The GC-volatile glyoxalate by-products are very numerous and in high yield.

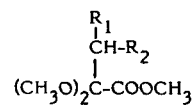
When the reactions were carried out in 3N methanolic HCl, esterification occurred simultaneously. The transaminations effected in an aqueous solution required a separate esterification. Esterification after transamination of amino acids gave variable yields of the 2-oxoester (I), the vinyl ether ester (II), and the 2,2-dimethoxyester (III) with some amino acids (aromatic > aliphatic)



I



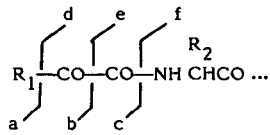
II



III

Peptides showed no detectable amounts of type II or III products. An alternative esterification previously demonstrated to work with peptide derivatives is pyrolytic permethylation accomplished by injecting alkaline quaternary alkyl amine salts into a GC with a suitable injection port temperature.[4] In spite of their polarity, up to tetrapeptide derivatives have been successfully separated.

The fragmentation patterns around the 2-oxoacyl functions give clear identifica on of the N-terminal residue (III):

IV: 

For the expected cleavages (a-f), the order of decreasing ion current for each generally is a, b, f > e, M. For examples, see Table I.

Table I

2-oxo Derivative of	Relative Ion Intensities						
	a	b	c	d	e	f	M^+
Valine	100	82	-	-	15	-	9
Alanine	-	100	-	-	37	-	100
Leucine	100	83	-	-	20	-	7
Isoleucine							
Methionine	78	-	-	4	35	-	78
Phenyl alanine	100	20	-	-	10	-	20
Alanyl-alanine	-	20	-	2	10	87	4
Leucyl-valine	91	96	-	2	62	100	45
Isoleucyl-valine	94	86	-	-	34	100	10
Leucyl-glycyl-glycine	94	98		100	-	-	-

Molecular ion intensities by EI vary from base peak to zero intensity and in general the 2-oxoacyl function should be classified among the more electronegative, higher ionization potential substituents[5] in its effect on fragmentation, i.e., weak or undetectable M^+.

Among the other advantages attending the use of the 2-oxo derivatives is the unambiguous differentiation of leucine from isoleucine.[6] Asparagine and glutamine are modified without loss of the ω-amide. However, some N-terminal amino acid residues are not readily converted to their 2-oxo derivatives. Tryptophan,[7] histidine[7] and proline[4] give characteristic heterocyclic products. Simple fragmentation patterns suggest the development of computer identification and sequencing. Software for this is being developed.

References

1. K. Jayasimhulu and R. A. Day, Biomed. Mass. Spectrom. 7, 7 (1980); R. A. Day, K. Jayasimhulu, J. V. Evans, G. Bhat, L. C. Lin, and M. J. Wieser, J. Heterocyclic Chem. 17, 1651 (1980).

2. J. R. Maley and T. C. Bruice, J. Am. Chem. Soc. 90, 2843 (1968).

3. H. B. F. Dixon and R. Fields, Methods in Enzymol. XXV, 409 (1972).

4. R. E. Hamilton, G. V. Patil, K. Jayasimhulu and R. A. Day, Org. Mass. Spectrom. 9, 211 (1974).

5. A. Prox and K. K. Sun, Z. Naturforsch. B. 21, 1028 (1966); R. A. Day, H. Falter, J. P. Lehman, and R. E. Hamilton J. Org. Chem. 38, 782 (1979).

6. R. A. Day, C. J. Metral, and K. Jayasimhulu, These Proceedings. Also see K. Jayasimhulu and R. A. Day, Biomed. Mass. Spectrom. 7, 321 (1980).

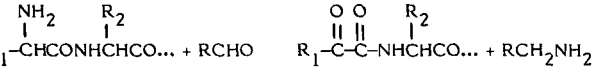
7. K. Jayasimhulu and R. A. Day, Biomed. Mass Spectrom. 7, 321 (1980).

Differentiation Between Leucine and Isoleucine in Peptides by α-C=X Derivatives: 2-Oxoacids, 2-Oxoacyl Derivatives and Oxazinones.

R. A. Day, C. J. Metral, K. Jayasimhulu and J. Baatz
Department of Chemistry and Environmental Health
University of Cincinnati
Cincinnati, OH 452212

Differentiation between leucine and isoleucine residues in peptides by mass spectrometry has generally been done by utilizing quantitative differences in appropriate fragment ion intensities. Recently, we showed that 2-oxoacyl derivatives could be readily characterized by conversion to their naphtho[1,4]-oxazin-2-one derivatives.[1,2] These derivatives proved to yield unambiguous information in the form of McLafferty rearrangement products that differentiated isoleucine from leucine.

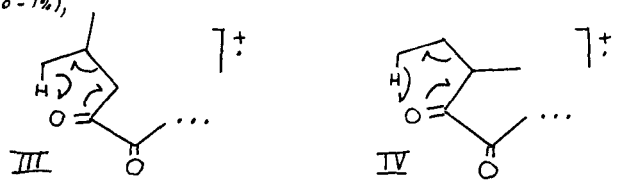
Conversion of peptides to 2-oxoacyl derivatives[2,3] involves transamination of the α-amino group of the N-terminal residue of a peptide(I) by a suitable amino group acceptor(II):



Methods: Suitable acceptors were 2- and 4-pyridinecarboxaldehyde (2PC and 4PC) and N-methyl-4-pyridinecarboxaldehyde salts (MPC) under a variety of conditions.[3] Conditions for transamination varied from room T, a few hours, aqueous pH 4-7 with MPC to 105°, 10-30m, 3 N-methanolic HCl with 2PC and 4PC. The amount of acceptor was varied from stoichiometric to a two- or three-fold excess although much higher excesses have been used.[4]

Oxazinone formation proceeded rapidly at room T. The stock 1-amino-2-naphthol·HCl (0.1M) was made up in 2-chloroethanol or 2,2,2-trifluorethanol, clarified by centrifugation and stored for up to one week at room T in the dark. In the preparation of the oxazinone the 2-oxoacid or the 2-oxoacyl derivative were combined in 3:1 absolute (EtOH/HOAc. Oxalic acid reacted as a 2-oxoacid as well. The reaction is conveniently monitored by the appearance of the oxazinone fluorophore (λ_{ex} 370, λ_{em} 440). The reaction times varied from a few minutes to over an hour.

When the N-terminal residue is LEU or ILE, the resulting oxo-LEU(III) or oxo-ILE(IV) residue fragments upon EI in characteristic ways. The distinguishing fragment ion arises from a McLafferty rearrangement; III in all derivatives examined exhibited ion current in the M-42 ion. IV showed an M-28, usually weak (0 - 1%),



but not an M-42 (Table I). In addition the characteristic fragmentation pattern (V) of 2-oxoacyl derivatives was noted.

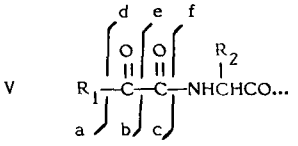


Table I. Fragment Ions Arising from oxoLEU and oxoILE Derivatives (III,IV,V).

DERIVATIVE	FRAGMENT INTENSITY								
	a	b	c	d	e	F	M-28	M-42	M
ISOLEUCINE	100	100	-	-	20	-	-‡	-	10
LEUCINE	100	100	-	-	20	-	-	4	10
LEUCYL-VALINE	100	100	3	18	25*	100	-	4**	20
ISOLEUCYL-VALINE	100	40	-	-	12	72	-‡	-	4

* d - 2
** M-43
‡ < 1%

In addition, the ratios of m/Z 43 to m/Z 29 were characteristic; oxoLEU derivatives typically showed 2:1 and oxoILE derivative 0.7:1.

The characteristic and distinguishing McLafferty rearrangement only occurs if the LEU or ILE are at the N-terminus. Where ambiguities may arise (an) other set(s) of peptides should be generated so that the residues in question are at the N-terminus in one or more peptide.

References

1. K. Jayasimhulu and R.A. Day, Biomed. Mass Spectrom. 7, 7 (1980).

2. R.A. Day, K. Jayasimhulu, J.V. Evans, G. Bhat, L.G. Lin, and M.J. Wieser, J. Heterocyclic. Chem. 17, 1651 (1980).

3. C.J. Metral, K. Jayasimhulu, A. Kornel, and R.A. Day, These Proceedings (1982).

4. J.R. Maley and T.C. Bruice, J. Am. Chem. Soc. 90, 2843 (1968).

FAST ATOM BOMBARDMENT AND DIRECT CHEMICAL IONIZATION MASS SPECTROMETRIC ANALYSIS OF GLYCOSPHINGOLIPIDS. Steven A. Carr and Vernon N. Reinhold, Dept. of Biol. Chem., Harvard Medical School, Boston, Ma 02115.

The glycosphingolipids (GSL's) are a class of cell membrane components which have been implicated in many fundamental cellular processes. Mass spectrometry has had an essential role in the structural analysis of these compounds. Electron impact MS of samples prepared as permethylated GSL's and also as permethylated-reduced and silylated GSL's can, in many cases, allow the determination of oligosaccharide sequence, presence of branch points, and composition of the ceramide portion. Large amounts of sample (100-200 μg) are needed for each analysis and, unfortunately, molecular ions are often of very low abundance or absent.

In the present study we have explored the utility of ammonia-direct chemical ionization (NH_3-DCI) and fast atom bombardment (FAB) MS in the structural analysis of underivatized and permethylated GSL's. For underivatized GSL's containing up to two sugar units NH_3-DCI produces intense protonated and ammonia cationized molecular ions and abundant fragment ions indicative of sugar sequence and ceramide structure using only 0.1 to 0.3 μg of material[1]. The composition and sequence of the sugar portion is provided by fragments representing sequential loss of oxonium-pyran sugar units from the terminal end, with the charge retained on the ceramide portion of the molecule. For underivatized GSL's containing 3 or more sugar residues the abundance of M.W. related ions decreases markedly, although ions related to sugar sequence and ceramide structure are still observed.

We have found that permethylation in conjunction with NH_3-DCI can be used to obtain both M.W. and structural information on large and complex glycolipids with sub-microgram amounts of material. The utility of this approach can be appreciated by considering the NH_3-DCI mass spectrum of the permethylated ganglioside GM3 (Fig. 1). The mass spectra of these permethylated derivatives exhibit intense $(M+NH_4)^+$ adduct ions, and abundant ions corresponding to ammonia-cationized hexose sequence fragments originating from the terminal end of the oligosaccharide; many of these cleavages have their corollary in the oligosaccharide DCI-MS data[2].

The FAB mass spectra of low M.W. glycolipids are highly informative. In addition to abundant cationized molecular species, structurally diagnostic ions due to sequential loss of terminal anhydro-sugar units (with charge retained on the newly generated glycolipid) and loss of the fatty acyl moiety are commonly present. The ratio of fragment to molecular ions is greater than that observed by NH_3-DCI. For example, the base peak in the FAB mass spectrum of N-palmitoyl dihydrolactocerebroside arises from the loss of both sugar residues with the charge remaining on the protonated ceramide portion. Ions due to the loss of water from the fragments are also prominent. This fragmentation behavior is also observed for underivatized GM3 and for globoside (GalNAc-Gal-Gal-Glc-ceramide) for which the base peaks correspond to $((HO\text{-ceramide}+H)-H_2O)^+$. As the number of sugar residues increases, the contribution of M.W. related ions to the spectra becomes even smaller, although they are still readily apparent. Permethylation can improve the intensity of high mass ions in the FAB mass spectra of GSL's, but the overall quality of the spectra and the sensitivity of analysis are much lower than for NH_3-DCI.

Phosphorylated and sulfated glycoconjugates, an important class of biopolymers, can also be analyzed by FAB MS. Phosphoglycolipids fail to yield useful structural information by NH_3-DCI, and permethylation is usually not successful. However, ions related to sugar sequence, fatty acid composition, base structure and molecular weight are readily apparent in the FAB spectra of mannose-inositol-phosphate-ceramide (Fig. 2). Clusters of molecular- and ceramide-related ions confirm that the ceramide portion of this molecule is heterogeneous, consisting predominantly of C_{26}-OH and C_{28}-OH fatty acids attached to phytosphingosine. The P-O bonds are not observed to cleave; rather, the intense ceramide ion series (C) arise by fission of the base-oxygen ether bonds. In general, the spectra of these highly charged GSL's are much more intense and informative than those of neutral GSL's.

The sensitivity for the FAB analysis of GSL's is strongly influenced by the solubility of these compounds in glycerol. We have observed that the addition of dipolar aprotic solvents of low volatility such as DMSO and tetramethylene sulfone (solvolane) to the glycerol matrix impedes micelle formation and improves the sensitivity and reproducibility of the FAB mass spectral data. In general, 2-10 μg of material are required to obtain good results using these methods.

[1]Reinhold, V.N. and Carr, S.A. (1982) Anal. Chem. 54, 499-503.

[2]Reinhold, V.N. and Carr, S.A. (1982) 30th Annual Conf. on Mass Spec. and Allied Topics, Honolulu, Hawaii; paper RPB-14.

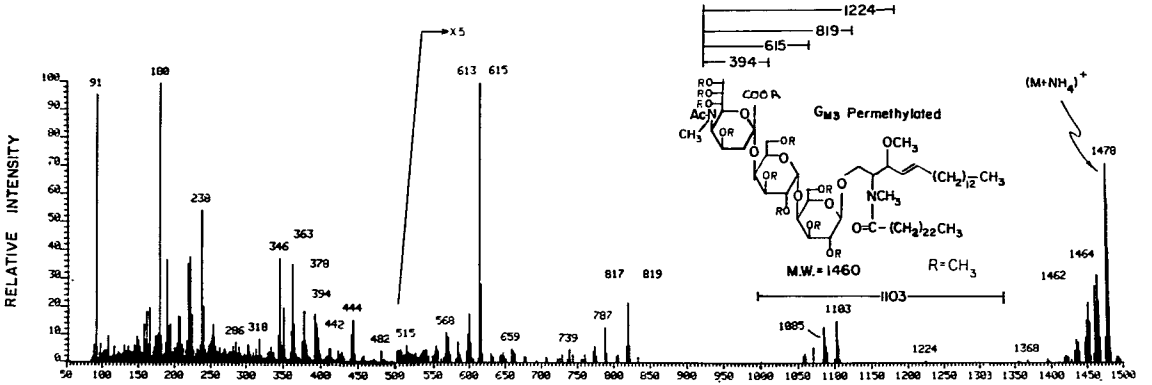


Fig. 1. NH_3-DCI mass spectrum of permethylated NANA-Gal-Glc-Ceramide (GM3); 2.0 µg on polyimide coated wire.

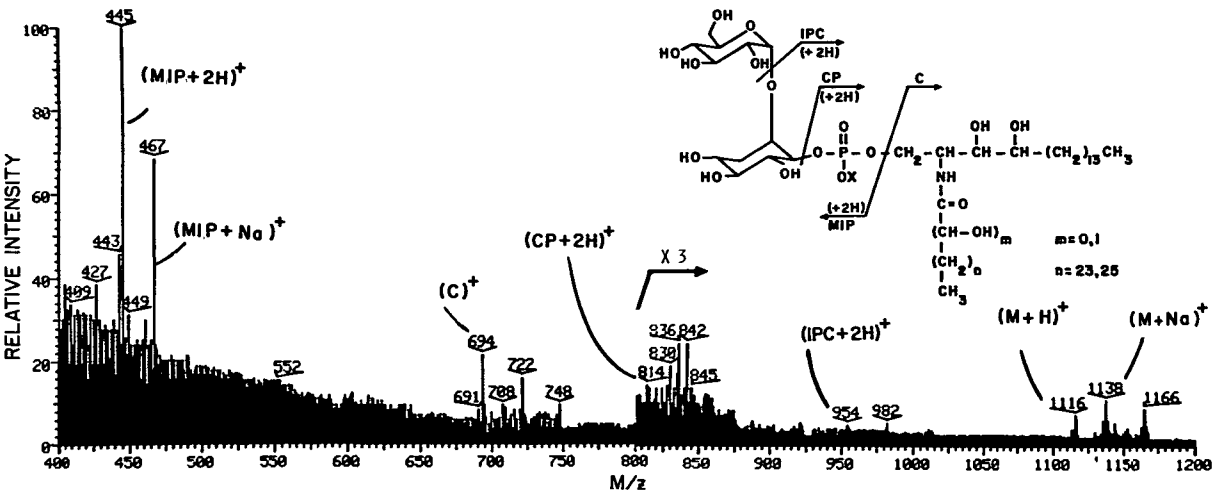


Fig. 2. FAB mass spectrum of Mannose-Inositol-Phosphate-Ceramide; 5 µg in glycerol and tetramethylene sulfone. Labeled ions correspond to n=23, m=1 in fatty acid.

STRUCTURAL STUDIES OF CARBOHYDRATE OLIGOMERS BY FAST ATOM BOMBARDMENT AND DIRECT CHEMICAL IONIZATION MASS SPECTROMETRY

Vernon N. Reinhold and Steven A. Carr

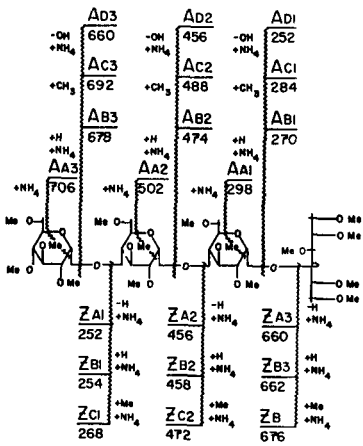
Department of Biological Chemistry, Harvard University Medical School, Boston, MA 02115.

The study of carbohydrate material (oligosaccharides, glycoproteins, and glycolipids) is currently undergoing a renaissance sparked by the recognition that these ubiquitous components of biological tissue have manifold and vital physiological functions. Mass spectrometry has played an increasingly important role in the structural analysis of the glycoconjugates because considerable structural detail can be gleaned on the vanishingly small amounts of material frequently available. Various soft ionization methods have been used to analyze free and derivatized carbohydrate materials. One of the most promising approaches is direct chemical ionization (DCI) using ammonia as a reagent gas. We have previously shown that analysis of reduced and permethylated oligosaccharides by NH_3-DCI using polyimide coated wires produces both abundant molecular weight and sequence related ions (1). Molecular ion adducts of these permethylated oligosaccharides show remarkable stability extending well beyond the 2000 mass range, and equally as important, their spectra are annointed with fragment and sequence ions of considerable structural significance. This approach has been used to determine the structure of oligosaccharides isolated from the membrane of E. coli. One of those fractions, purified by HPLC, was found to be a nonasaccharide of very complex branching when analyzed by this NH_3-DCI method (Fig. 1a). This work has now been expanded into a detailed study of fragmentation, using as probes, a combination of stable isotopes both in the reagent gas and the sample. With a series of standard oligosaccharides we have been able to propose a fragmentation scheme that accounts for the major sequence ions when analyzed by this method (Scheme 1).

The new ionization method of fast atom bombardment (FAB) has also been evaluated on oligosaccharides using glycerol as the dispersive matrix. These studies have shown that FAB provides molecular weight information for large oligosaccharides but sequence related ions are absent or of very low abundance. This is an interesting contrast to the lower saccharides which show sample sequence fragments with bond ruptures very analogous to that observed when ionized by intense electrical fields (FD) or charged ion particles (SIMS). Neutral oligosaccharides, when ionized by FAB and focusing positive ions appears to be less sensitive when compared to the DCI technique. An intermediate molecular weight cyclic oligosaccharide is shown in Figure 2.

References: (1) Reinhold, V.N. and Carr, S.A. Anal. Chem., (1982), 54, 499-503.

Scheme 1.)



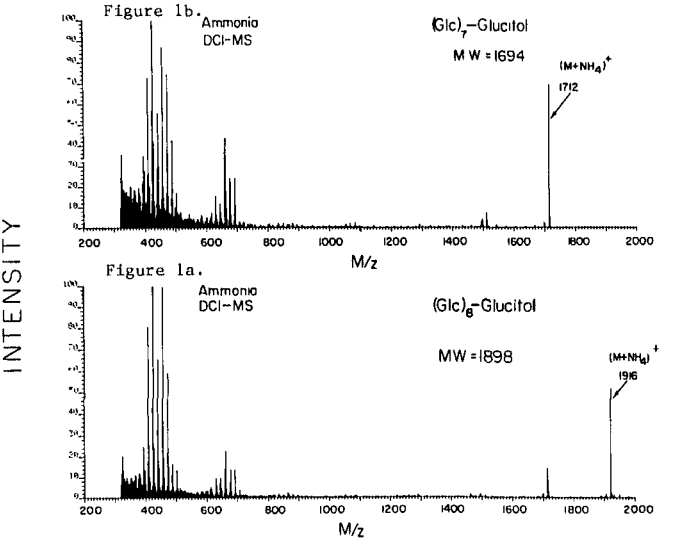


Figure 1.) Two major oligosaccharides isolated from E. coli membrane after HPLC purification, reduction, permethylation and NH_3-DCI/MS.

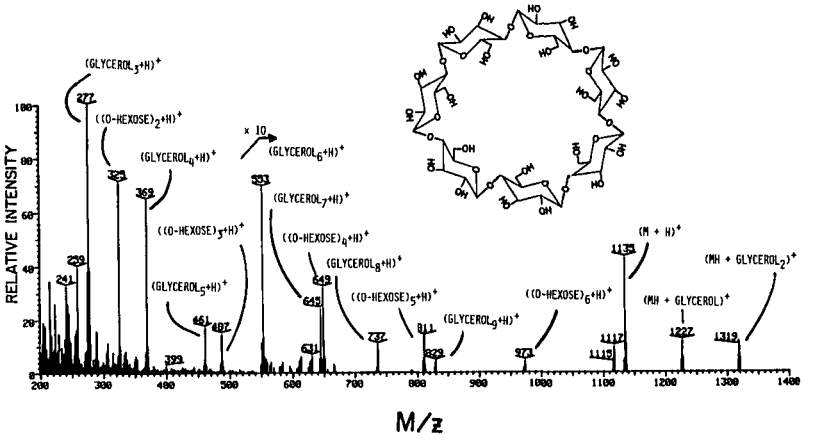


Figure 2.) Cyclodextran, a bacteria product, analyzed by FAB using a glycerol matrix.and xenon as gas for primary beam.

FD/MS ANALYSIS OF HIGHLY UNSATURATED MYCOLIC ACIDS AND THEIR TREHALOSE ESTERS

S.Shizukuishi[1], N.Akimori[1], I.Tomiyasu[2] and I.Yano[3]

[1]Hitachi Naka Works, Katsuda, Ibaragi-Japan, [2]Tezukayama Junior College, Nara, Japan and [3]Niigata University School of Medicine, Niigata 951, Japan

The most characteristic component in the cell wall lipids in acid-fast bacteria, such as Mycobacteria, Nocardia and Corynebacteria is mycolic acids and related compounds. They are high molecular weight β-hydroxy fatty acids possessing a long chain alkyl branch at 2-position and associated with trehalose or cell wall polysaccharide molecule. The structure of mycolic acids are related profoundly to the taxonomical situation, biological activities and cell wall properties. However, owing to instability at high temperature, the analysis of intact molecule of such types of fatty acids was extremely difficult. Recently, we have developed a powerful analytical technique using gas chromatography-mass spectrometry (GC/MS) and revealed the detailed structure of individual mycolic acid molecule can be determined as intact molecule[1)2)3)4)]. Field desorption mass spectrometry (FD/MS) is now used widely to determine the molecular weight of polar and thermolabile molecule. This method also gives information on only limitted numbers of fragment ions. Therefore, we tried to introduce to estimate the molecular species composition of complex mixture of highly unsaturated mycolic acids and mycolic acid containing lipids such as trehalose esters.

The bacterial cells were grown in a medium containing 1 % glucose, 0.5 % peptone and 0.2 % yeast extract with a pH adjusted 7.0. Cells were harvested by centrifugation and mycolic acids were extracted after alkyline hydrolysis[2)3)]. Mycolic acid methyl esters were prepared by thin-layer chromatography on Silica gel and further separated on $AgNO_3$ silica. FD/MS analysis was performed with Hitachi M-80 apparatus as intact methyl esters and GC/MS analysis was carried out as TMS derivatives of methyl mycolate.

The results showed the molecular weight of mycolic acids ranging from C_{30} to C_{80} from Mycobacteria, Nocardia, Gordona and Rhodococcus group, possessing one to seven double bonds, were clearly determined from (M+H)ions and the species composition was also estimated (Fig.1). The composition of trehalose mono- and diesters of mycolic acids were also determined from (M+H)ions, clearly (Fig.2).

References

1. I.Yano, K.Saito, Y.Furukawa and M.Kusunose, FEBS Lett., 21 (1972) 215-220
2. I.Yano, K.Kageyama, Y.Ohno, M.Masui, E.Kusunose, M.Kusunose and N.Akimori, Biomed.Mass Spectrom., 5 (1978) 14-24
3. S.Toriyama, I.Yano, M.Masui, E.Kusunose, M.Kusunose and N.Akimori, J.Biochem., 88 (1980) 211-221
4. I.Tomiyasu, S.Toriyama, I.Yano and M.Masui, Chem.Phys.Lipids, 28 (1981) 41-54

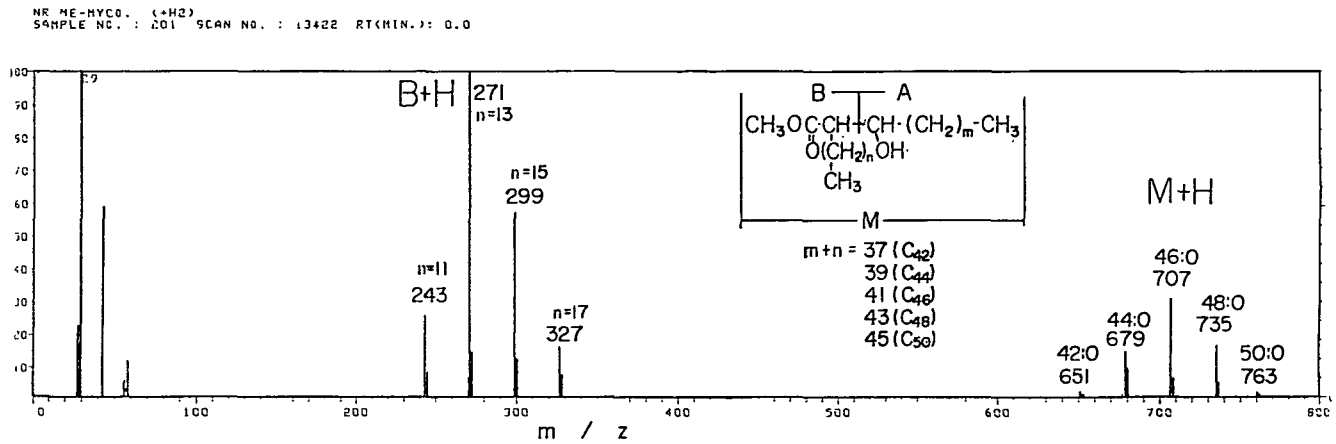


Fig.1 FD mass spectrum of fully hydrogenated methyl mycolate from Nocardia rubra

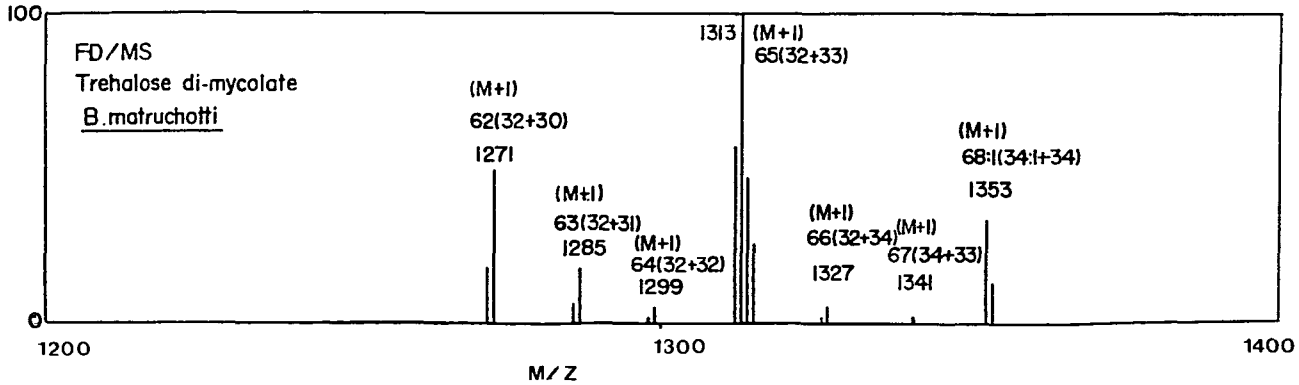


Fig.2 FD mass spectrum of trehalose mono-mycolate from Bacterionema matruchotti

ANALYSIS OF N-ACETYLNEURAMINIC ACID AND ITS DERIVATIVES BY GAS CHROMATOGRAPHY-MASS SPECTROMETRY. III.

Satoshi Mineo, Masaaki Numata and Koichi Metori

The Kohno Clinical Medicine Research Institute
3-3-24 Kitashinagawa, Shinagawa-ku, Tokyo 140, Japan

In general, acylneuraminic acids (sialic acid) occupies the non-reducing end of the heterooligosaccharide chains in glycoproteins and in gangliosides. Schauer[1] reported in his review on "Chemistry and Biology of the Acylneuraminic Acids" that the recent knowledge on biological importance of acylneuraminic acids were as follow; 1) increase in the viscosity of glycoproteins in aqueous solution 2) binding and transport of molecules and viruses 3) effects on surface charge, aggregation, and shape of cells 4) further functions in reproduction 5) protection of macromolecules against proteolytic attack 6) regulation of the "Normal" behavior and of the lifetime of cells 7) masking of cellular antigen. An assay of sialic acid has been usually based on the colorimetric determination using thiobarbituric acid by Warren[2] and Aminoff[3]. Recently Sugahara et al.[4] reported enzymatic assay of serum sialic acid which included neuraminidase hydrolysis and cleavage of sialic acid to pyruvate by N-acetylneuraminic acid-aldolase. The increasing interest in the structure and biological functions of sialic acid requires for a more accurate and convenient analytical method.

Previously we reported[5] the quantification of trimethylsilyl (TMS), trifluoroacetyl (TFA) and acetyl (Ac) derivatives of N-acetylneuraminic acid (NANA) and its derivatives. Here we report the quantification of TMS derivatives of NANA which were obtained from NANA-lactose or human sera. Trimethylsilylation of NANA β-methylglycoside methylester (β-di-Me) was carried out with pyridine-trimethylsilylimidazole (Py-TSIM) instead of pyridine-bis(trimethylsilyl)trifluoroacetamide (Py-BSTFA) or pyridine-hexamethyldisilazane-trimethylchlorosilane (Py-HMDS-TMCS). Py-TSIM is better trimethylsilylating reagent than Py-BSTFA or Py-HMDS-TMCS for trimethylsilylation of acylneuraminic acids. When NANA-lactose was treated with 0.1N or 0.05N MeOH-HCl,

two peaks of β-di-Me and neuraminic acid β-methylglycoside methylester (β-de-Ac were observed using GC/MS. Only one peak of β-di-Me was obtained from acetylation of the standard sample of β-de-Ac with Py-Ac_2O following the trimethylsilylation with Py-TSIM (Fig.). Neutralization of the acid hydrolysis solution did not afford the good results for the quantitative analysis of sialic acid by the use of MeOH-HCl hydrolysis. The study involved the analysis of women's peripheral sera during and after pregnancy, umbilical cord sera and human mothers' milk. It was observed that serum NANA increased just before delivery and alkaline phosphatase activity became very high at the same time. Other interesting results were discussed.

ACKNOWLEDGEMENT The authors are indebted to Professor H. Ogura and Ph. Dr. K. Furuhata for a gift of NANA and its derivatives.

1) R. Schauer, Angew. Chem. internat. Edit., 12, 127 (1975)
2) L. Warren, J. Biol. Chem., 224, 1971 (1959)
3) D. Aminoff, Biochem. J., 81, 384 (1961)
4) K. Sugahara, K. Sugimoto, O. Nomura and T. Usui, Clin. Chim. Acta, 108, 493 (1980)
5) S. Mineo, M. Numata, K. Metori and S. Ito, Pro. Jap. Soc. Med. Mass Spectrom., 6, 133 (1981)

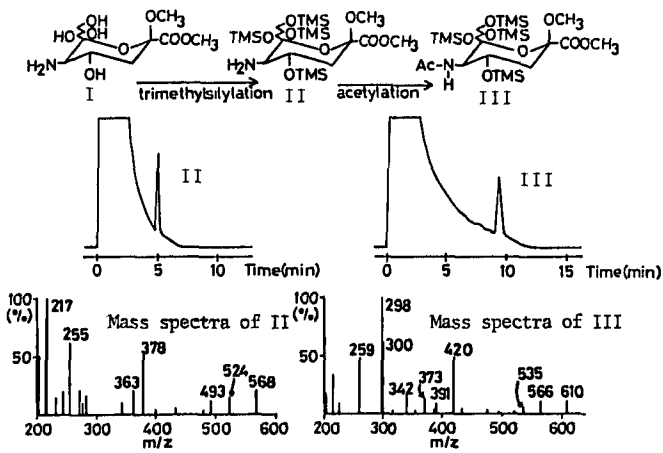


Fig. Gas chromatogram and mass spectra of the TMS derivatives of β-de-Ac (II) and β-di-Me (III)

DI/MS OF THE MOLECULAR SPECIES OF DEUTERATED GLYCEROPHOSPHOLIPIDS

Kunihiko Saito, Kiyoshi Satouchi and Masami Gamo, Department of Medical Chemistry, Kansai Medical School, Osaka, JAPAN 570

There has been many evidences to confirm the hypothesis that membrane functions, such as permeability and membrane-associated enzyme activities are affected or controlled by the properties of lipid molecules existing in biomembrane. Based on these facts, it would be quite feasible that many increasing demands to establish the complete analytical method for determination of molecular species of membrane phospholipids have been arising.

So long as we know, there are three analytical procedures to determine the molecular species. The first one is the combination method of Ag-TLC and GLC (1) and the second is application of HPLC (2). The last one is GC(DI)-EI-MC method, which was introduced in the previous meeting at Seatle and Minneapolis by us (3) and (4).

There is a tendency that molecular species containing polyunsaturated fatty acid were more labile against GC-EI than less unsaturated species. The intensities of molecular weight determining ions were severely influenced with the changes of chain length and degree of unsaturation of fatty acids esterified in glycerophospholipid molecules. The above disadvantage was considerably improved by the applications of direct inlet system and t-BDMS derivative, however, for the complete analysis, it still remained to be resolved. In order to overcome these problems, two possible methods have arisen. The one is application of calibration factor using the known synthetic phospholipids and internal standard. The alternative procedure is direct saturation of molecular species containing unsaturated fatty acids using deuterium. With the expectation that there are almost same sensitivities for producing molecular weight determining ions among saturated and deuterated species, we chosed the latter procedure as the first step.

In the present experiment, PC 34=2 (C 16=0/C 18=2), PC 36=4 (C 16=0/C 20=4), PC 36=2 (C 18=0/C 18=2) and PC 38=4 (C 18=0/C 20=4) have been used as the model species. They were subjected to hydrolysis with phospholipase C and the resulting diglycerides were immediately converted to t-BDMS derivatives. Then, they were subjected to catalytic deuteration using tristriphenylphosphine rhodium chloride as catalyst (5).

At the level of fatty acid analysis, comparing with Adams' catalyst, the random distribution of deuterium in molecular ion region could be prevented using Wilkinson's (Fig.1). At the level of diglyceride, deuterium ion was incorporated, thereby four peaks, PC 34=2, PC 36=4, PC 36=2 and PC 38=4 were resulted to reduce into three peaks (PC 34=2, d=4, PC 36=4, d=8, PC 36=2, d=4 and PC 38=4, d=8). Mass spectra of each molecular species also confirmed the adequate incorporation of deuterium ion, for example, molecular weight determining ion of PC 36=2 at m/z 677 was shifted to m/z 685, PC 36=4 at m/z 673 to 689, respectively. Using the above characterized specimens, the mass distribution of each molecular species was determined by the procedure of DI-EI-MC and assessed the effect on quantification due to deuteration.

At present, the deuteration method have not given so improved effect on determination of molecular species as we anticipated, however, it could be amply applicable if the calibration factor for deuterated species was available. It would be also worth noting that the increase in intensity of the ion at RCO + 74 of polyunsaturated fatty acid was observed as the one of benefits of deuteration.

(1) B.J. Holub and A. Kuksis, Adv. Lipid Res. 16, 1-125 (1978).

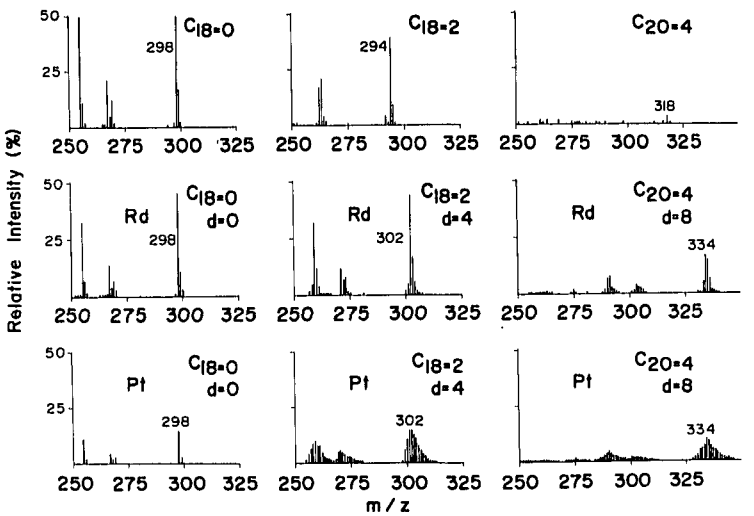
(2) G.M. Patton, J.M. Fasulo and S. Robins, J. Lipid Res. 23, 190-196 (1982).

(3) K. Saito, H. Ogino and K. Satouchi, in "MEMBRANE FLUIDITY: Biophysical Techniques and Cellular Regulation", ed. by M. Kates & A. Kuksis: The Humana Press Inc., Clifton, New Jersey; p 33-41 (1980).

(4) J. Sugatani, M. Kino, K. Saito, T. Matsuo, H. Matsuda and I. Katakuse, Biomed. Mass Spectrom. 9, in press (1982).
(5) J.A. Osborn, F.H. Jardine, J.F. Young and G. Wilkinson, J. Chem. Soc. A, 1711-1732 (1966).

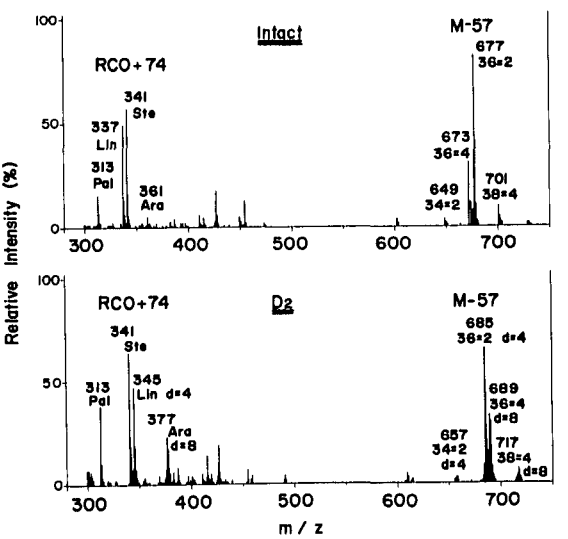
GC-MS of FAME

Fig. 1



DI-MS of DG-tBDMS

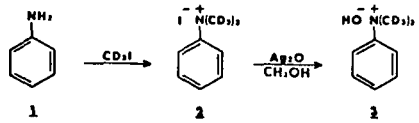
Fig. 2



DEUTERATED TRIMETHYLANILINIUM HYDROXIDE; PREPARATION AND UTILITY FOR ON COLUMN PERMETHYLATION OF MODIFIED NUCLEOSIDES, Schram, K.H., Teece, R.G. and Slowikowski, D., Univ. of Arizona, College of Pharmacy, Tucson, AZ 85721.

The conversion of nucleosides to their permethyl derivatives has been described using various anion solutions with CH_3I or CD_3I.[1,2,3] More recently the utility of "on column" methods using trimethylanilinium hydroxide (TMAH) for the preparation of permethylated nucleosides and nucleotides has been described.[1,4,5] The main advantage of using the TMAH method for permethylation is to simplify sample preparation. The use of CD_3I with DMSO anion effects incorporation of a CD_3 group at all free exchangeable positions. Similarly, labeled TMAH (TMAH-d_9) is shown to perform the same function although this compound is not commercially available and the synthesis has not been described in the literature.

Trimethylanilinium hydroxide-d_9 is prepared as described. To 10 ml of CD_3I was added 1.2 ml of aniline (1). The mixture was stirred for 1 h at rt and then 20 ml of EtOAc was added and stirring continued for an additional 12 h. The precipitate formed was collected by filtration, recrystallized twice from a minimum amount of warm EtOH and dried in vacuo at 117° C to give 2. A sample of 2 (27.2 mg) was dissolved in MeOH (5.0 ml) and Ag_2O (13.2 mg) was added with stirring over a 15 min. period to give 3. The reaction mixture was filtered and 50 ug of sample was dissolved in 50 ul of the filtrate. A 1 ul sample was introduced into the injection port (300°C) of the GC to effect the "on column" permethylation.



1 2 3

Gas chromatography/mass spectrometry experiments were performed on adenosine and 2'-O-methyladenosine using TMAH and TMAH-d_9. Using TMAH on either nucleoside results in the same product (Figure 1a). However, the analysis of spectrums generated from TMAH-d_9 derivatives showed two distinct compounds (Figure 1b and 1c). The location and number of "native" methyl groups present in the base (B+2H ion) or the sugar (S-1 ion) as seen with 2'-O-methyladenosine can easily be determined. Thus, the utility of this reagent can be seen for studying the structure of naturally occurring methylated nucleosides.

References

1. R.G. Teece and K.H. Schram, "Preparation and Gas Phase Analysis of Permethylated Nucleosides" in Nucleic Acid Chemistry, ed. by L.B. Townsend and R.S. Tipson, Wiley-Interscience, New York, in press.
2. A.P. DeLeenher and C.F. Gewlijkens, Anal. Chem., 48, 2203 (1976).
3. D.L. vonMinden and J.A. McClosky, J. Amer. Chem. Soc., 95, 7480 (1973).
4. K.M. Baker in Advances in Mass Spectrometry in Biochemistry and Medicine, Vol. 1, ed. by A. Frigerio and N. Castagnoli, p. 231. Spectrum Publications, New York (1976).
5. G.R. Pettit, J.J. Einck and P. Brown, Biomed. Mass Spectrum, 5, 153 (1978).

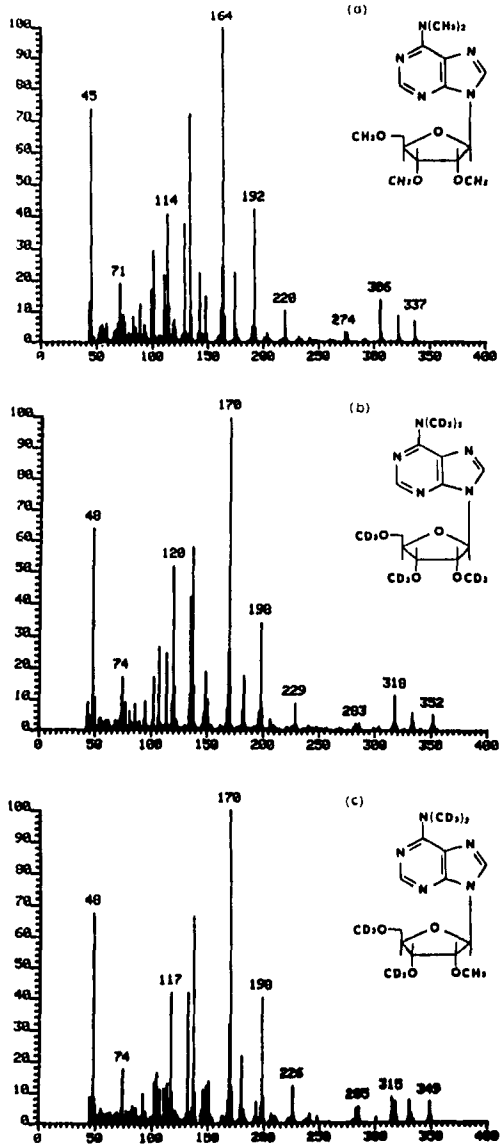


Figure 1. Low resolution mass spectra of (a) permethyl adenosine, (b) permethyl adenosine-d_{15} and (c) permethyl 2'-O-methyladenosine-d_{12}.

DETERMINATION OF ^{18}O LABELING IN NUCLEOSIDE ALPHA-PHOSPHATES

T. P. KRICK[1], T. F. WALSETH[2], S. J. EIDE[2] AND N. D. GOLDBERG[2]
DEPTS. OF BIOCHEMISTRY[1] AND PHARMACOLOGY[2]
UNIVERSITY OF MINNESOTA, ST. PAUL, MN 55108

OBJECTIVE:

Since certain specific metabolic processes can be monitored by determining the amount of ^{18}O incorporated into the α-phosphoryls of nucleotides after incubation of cells with ^{18}O water, a method was developed to measure the amount and distribution of ^{18}O labeling in these molecules from tissue and cell sample representing less than 10 mg of protein.

RATIONALE:

Initially the ^{18}O incorporation was measured by analyzing the inorganic phosphate released from the purified nucleoside monophosphates by 5' nucleotidase. However, this analysis was limited by interference from ubiquitous inorganic phosphate. Also, the direct analysis of nucleoside monophosphates was found to be unreliable in our hands due to GLC and derivatization difficulties. It was determined that the analysis of glycerol-3-phosphate (G3P), obtained from Smith degradation of nucleoside monophosphate (Fig. 2), provided reliable results. The mass spectrum of labeled and unlabeled G3P is shown in Figure 1.

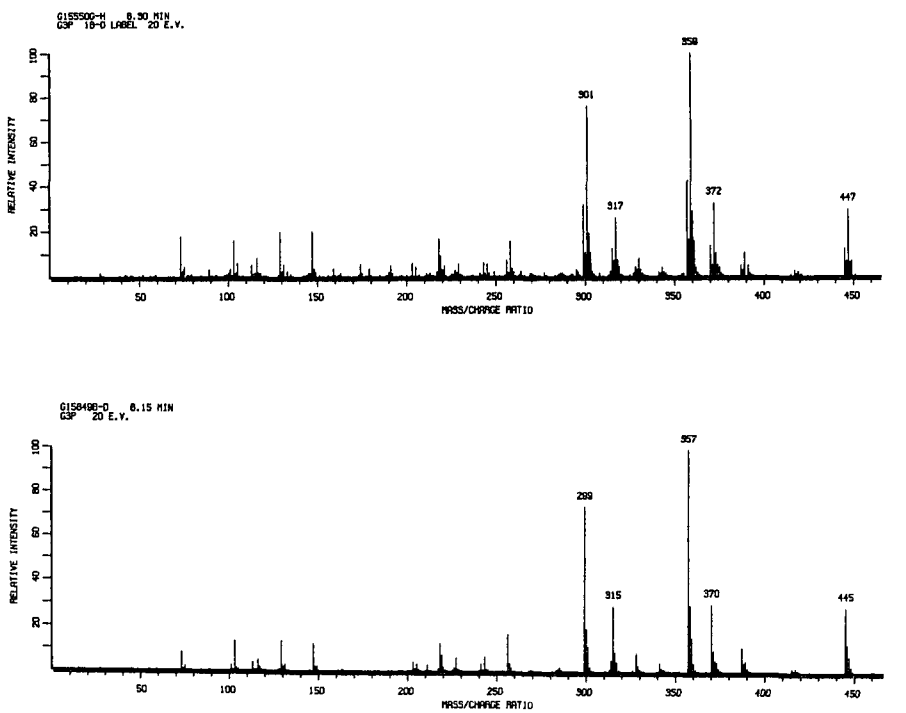


Figure 1. Mass spectra of labeled and unlabeled TMS-G3P.

METHOD:

The procedure involves preparing acid extracts of cells equilibrated with ^{18}O water. The extracts are then chromatographed on a phenylboronate resin which seperates nucleotides from inorganic phosphate. The isolated nucleotides are then chromatographed on DEAE-cellulose to fractionate nucleoside mono-, di-, and tri-phosphates. Next, the nucleoside di- and tri-phosphates are degraded enzymatically to their respective monophosphates. The endogenous nucleoside monophosphates and the nucleoside monophosphates deriving from the nucleoside di- and tri-phosphate fractions are purified by ion-pair reverse phase HPLC employing a volatile solvent. Because of a contaminant in the AMP samples at this stage of isolation, it was found necessary to convert the AMP to IMP with adenylate deaminase. The resulting IMP is purified by rechromatography on the same HPLC system. The AMP (IMP) and GMP recovered from each of the three fractions are then subjected to a Smith degradation to generate glycerol-3-phosphate (G3P), which is purified free from reactants and side products by anion-exchange chromatography. The G3P, which contains the α-phosphoryl of the nucleotide is analyzed for atom percent excess of ^{18}O by gas chromatography-mass spectrometry after conversion to its trimethylsilyl (TMS) derivative. The TMS-G3P is analyzed by selective ion monitoring of the three major phosphate containing fragments (m/z 299 to 307, m/z 357 to 365, and m/z 445 to 453). Three to five injections are made for each sample.

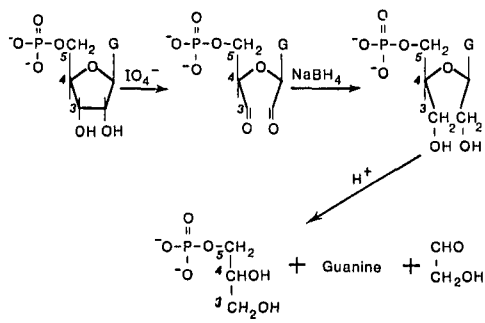


Figure 2. Smith degradation of nucleoside monophosphate.

An alternative approach is used when the labeling of the β and γ-phosphoryls of ATP and the β-phosphoryl of ADP are also determined. The ADP and ATP are isolated by anion-exchange chromatography of the nucleotide fraction from the phenylboronate step. The γ-phosphoryl of ATP is analyzed as G3P after its transfer of glycerol in a reaction catalyzed by glycerol kinase. The β-phosphoryl of ADP and ATP (after its conversion to ADP with glycerol kinase) are also analyzed as G3P by employing ADP as the substrate in an adenylate kinase catalyzed reaction to continuously generate ATP in the presence of glycerokinase. The γ-phosphoryl of the ATP derived from β-ADP in the exchange is transferred to glycerol with glycerokinase. The AMP generated in this coupled reaction represents the α-phosphoryl of ADP to ATP. Both are analyzed for ^{18}O content as described above. The inorganic phosphate isolated from phenylboronate chromatography is also analyzed for ^{18}O labeling as its TMS derivative.

CONCLUSIONS:

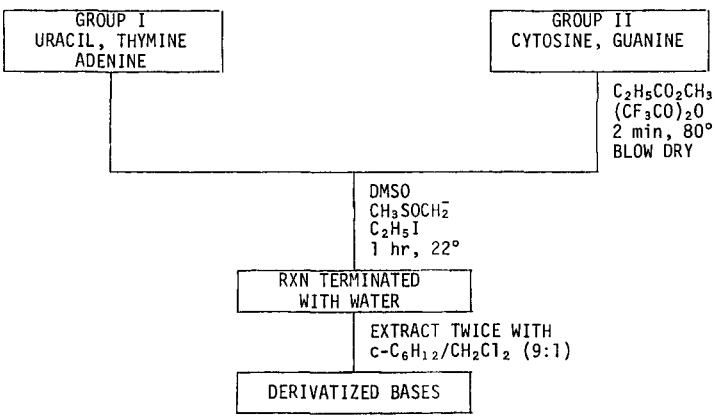
Analyzing for the ^{18}O content of G3P was found to be superior to either direct analysis of nucleoside monophosphates or to the analysis of the phosphoric acid derived from the nucleotide. In general, the standard errors are within a range that are less than 5% of the mean. The lower limit of mass spectral sensitivity is approximately 100 pmol of TMS-G3P.

CHARACTERIZATION OF PURINE AND PYRIMIDINE BASES AS THEIR N,O-PERALKYL AND TRIFLUOROACETYL/N,O-PERALKYL DERIVATIVES

C. F. Gelijkens, David L. Smith and J. A. McCloskey
Departments of Medicinal Chemistry and Biochemistry
University of Utah
Salt Lake City, Utah 84112

The detection and quantification of chemically or biologically modified bases is important in several areas, including studies of carcinogenesis and the structure and function of transfer RNA. Capillary gas chromatography, when coupled with mass spectrometry, is both highly selective and sensitive and may be used to analyze small quantities of nucleic acid hydrolysates for the presence of modified bases. This method of analysis is particularly useful when such bases are very minor constituents. Because of their low volatility and high chemical reactivity, bases must be derivatized prior to gas chromatographic analyses. We report here a general procedure for making N,O-peralkyl or trifluoroacetyl/N,O-peralkyl derivatives of many of the purine and pyrimidine bases. The methylsulfinyl carbanion solution was prepared using a previously reported procedure.[1]

DERIVATIZATION PROCEDURE



These derivatives have excellent chromatographic properties when analyzed either on non-polar (SE-30) or polar (Superox-FA) capillary columns. Relative retention times expressed in methylene units as well as the number of alkyl and trifluoroacetyl groups added are summarized in the table below:

Relative Retention Times of N,O-Perethyl and N-Trifluoroacetyl/Perethyl Derivatives of Bases

Parent Base	Mol Wt	C_2H_5 Groups	CF_3CO Groups	SE-30	Superox-FA
GROUP I					
Uracil (1)	168	2	-	14.34	23.53
5-Fluorouracil (2)	186	2	-	14.40	24.00
Thymine (3)	182	2	-	14.75	23.22
2-Thiouracil (4)	184	2	-	14.80	22.92
5-Hydroxymethyluracil (5)	226	3	-	17.01	24.99
N^6,N^6-Dimethyladenine (6)	191	1	-	17.25	26.94
Orotic acid (7)	240	3	-	17.46	25.34
N^6-Methyladenine (8)	205	2	-	17.78	26.92
Adenine (9)	219	3	-	18.24	26.82
N^2,N^2-Dimethylguanine (10)	235	2	-	19.88	30.73
1-Methyladenine (11)	205	2	-	20.08	34.74
N^2-Methylguanine (12)	249	3	-	20.31	30.71
GROUP II					
5-Fluorocytosine (13)	281	2	1	16.97	27.33
Cytosine (14)	263	2	1	17.13	27.17
5-Methylcytosine (15)	277	2	1	17.94	28.29
5-Hydroxymethylcytosine (16)	321	3	1	18.96	28.81
Guanine (17)	331	3	1	22.33	35.72
7-Methylguanine (18)	317	2	1	22.30	37.75

The principal fragmentation reaction of many of the derivatized purine and pyrimidine bases have been examined using metastable ion and exact mass measurements. Further understanding of the fragmentation mechanisms of these compounds is derived from mass shifts observed for isotopically labeled bases as well as for when deuterated alkyl substituents have been used. These results are briefly summarized below:

Uracil (ET)

$$M^{\cdot+}\ (60) \xrightarrow{-C_2H_4} (61) \xrightarrow{-C_2H_4} (38)$$

Cytosine (TFA, ET)

$$M^{\cdot+}\ (1) \xrightarrow{-CF_3} (100) \xrightarrow{-C_2H_4} (57)$$

Adenine (ET)

$$M^{\cdot+}\ (60) \xrightarrow{-C_2H_5} (100)$$
$$\xrightarrow{-CH_3} (77)$$
$$\xrightarrow{-C_2H_5N} (73)$$

Guanine (TFA, ET)

$$M^{+}\ (6) \xrightarrow{-CF_3} (100) \xrightarrow{-C_2H_4} (29)$$

(1) E. J. Corey and M. Chaykovsky, J. Am. Chem. Soc., 84, 866 (1962).

IDENTIFICATION OF N^4-DIMETHYL-5-METHYL-2′-DEOXYCYTIDINE FOLLOWING THE REACTION OF DIMETHYLCARBAMYL CHLORIDE WITH THYMIDINE; Jerome J. Solomon, Alvin Segal, Urszula Maté and Benjamin L. Van Duuren. Lab. Org. Chem. and Carcinogenesis, Inst. of Env. Med., New York Univ. Med. Center, New York, N.Y. 10016.

The direct-acting carcinogen and mutagen dimethylcarbamyl chloride (DMCC) was reacted with thymidine (dThd) under physiological conditions (37°C, pH 7-7.5, 4h) to characterize carcinogen modified nucleosides prior to in vitro reaction of DMCC with calf thymus DNA. A new adduct was isolated, N^4-dimethyl-5-methyl-2′-deoxycytidine, and characterized by UV, NMR and EI and CI mass spectrometry. This apparent base change is believed to result from an O^4-dimethylcarbamyl-dThd intermediate which undergoes a novel nucleophilic aromatic substitution of the dimethylcarbamyloxy group by dimethylamine formed during hydrolysis of DMCC. This type of nucleophilic substitution was previously(1) observed to occur with O^6-acylated derivatives of deoxyguanosine and DMCC, and the O^6 intermediate could be isolated and identified by source insertion CI. The O^4-acyl thymidine intermediate could not be detected indicating a more rapid displacement. Considering the presence of dimethylamine in biological fluids of humans and rodents this substitution reaction may play an important part in the genotoxic damage of DMCC and other acylating agents. Supported by USPHS Grants CA 24124, CA 13343 and ES 00260.

1. A. Segal, J.J. Solomon, U. Maté and B.L. Van Duuren. Chem. Biological Interactions, in press, 1982.

RPB 23 A STUDY OF THE UNUSUAL CHEMICAL REACTIVITY OF 7,8,9,10-TETRAHYDROBENZO(a)PYRENE DERIVATIVES AT CARBON 10 BY MASS SPECTROMETRY. Peter P. Roller, National Cancer Institute, NIH, Bethesda, MD 20205; Shen K. Yang, Uniformed Services Univ. of Health Sci., Bethesda, MD 20814.

The 7,8-trans-dihydroxy-9,10-epoxy derivatives of 7,8,9,10-tetrahydrobenzo(a)pyrene (4H-BaP) are metabolically activated carcinogenic forms of benzo(a)pyrene, binding to DNA at the C-10 position. Our chemical studies demonstrate the unusual chemical reactivity at C-10 of several 4H-BaP derivatives using ^{18}O labeling and mass spectral analysis. Thus, the hydroxyl group at C-10 of certain isomers of 7,8,9,10-tetrahydroxy-4H-BaP is susceptible to solvolytic exchange in acid. Also, the 9,10-trans diol analog exchanges with ^{18}O labeled solvent isomerizing to the 9,10-cis compound. Such is not the case for the 7,8 analog. Derivatization to the acetonides makes these compounds amenable to mass spectral analysis. Very dissimilar reactivity was found toward acetonide formation for the 7,8 and 9,10 diols of 4H-BaP. Experiments show, that the 7,8-cis diol forms an acetonide derivative with ^{18}O-acetone : $CuSO_4$, with complete loss of the ^{18}O label, as expected, according to the established mechanism, and that the 7,8-trans diol does not form a derivative. Surprisingly, the 9,10-trans diol also forms an acetonide with complete retention of ^{18}O label from ^{18}O-acetone with apparent inversion of configuration at C-10. In a parallel experiment the 9,10-cis diol forms an acetonide with 33% retention of ^{18}O from the acetone reagent through a probable carbonium ion at C-10 of the molecule. The mass spectra of the isomeric 7,8 and 9,10 acetonide derivatives exhibit distinct spectral characteristics.

MASS SPECTROMETRIC STUDIES IN STRUCTURAL AND STEREOCHEMICAL PROBLEMS OF 1-OXACEPHEMS

Yuzo NAKAGAWA and Yuji IKENISHI
Shionogi Research Laboratories
Fukushima-ku, Osaka 553, JAPAN

INTRODUCTION The mass spectrometric behavior of 1-oxacephems has been investigated using in-beam EI mass spectra. Structural and stereochemical studies of the fragmentation and the hydrogen rearrangement mechanism are discussed.

1-Oxacephems including a new semisynthetic β-lactam antibiotic, latamoxef, have two asymmetric centers at C-6 and C-7 and thus there are two possible stereoisomers. We examined the in-beam EI mass spectra of the 1-oxacephems (1) shown in Table 1, and observed the ions as they are important ions for determining the stereochemistry at C-6 and C-7. The present paper describes the effective use of EIMS for determining the stereochemistry at C-6 and C-7 in 1-oxacephems.

RESULTS AND DISCUSSION Mass spectra of cis isomer 1a (α-hydrogen at C-6, and at C-7) and trans isomer 1b (α-hydrogen at C-6, β-hydrogen at C-7) are shown in Fig. 1 and the relative abundances of the fragment ion peaks in the spectra of 1-oxacephems are also shown in Table 2 (see also Fig. 2). The accurate mass spectra are measured to determine the element compositions of ions. Comparisons of the ion abundances *a*, *a'*, *b*, and *b'* show that in the spectra of the cis isomer (1a~7a), *a'* and *b'* are more abundant than *a* and *b*, respectively, but vice versa for the trans isomer (1b~4b). Ions *b'* and *c* of the cis isomer are more abundant than those of the trans.

Thus, we could distinguish between cis and trans isomer of the 1-oxacephems by comparing the abundances of the fragment ions *b*, *b'* and *c* in their mass spectra. If the abundance of the *b* ion is of 5% or more relative abundance and is larger than that of *b* ion in the mass spectra of 1-oxacephems, the stereochemical arrangement at C-6 and C-7 is cis. On the other hand, if the abundance of the *b'* ion is less than 1% and smaller than that of the *b* ion, the stereochemical arrangement at C-6 and C-7 is trans. Hence, if both stereoisomers of 1-oxacephems exist, they can be classified as cis or trans by comparison of the abundance of the ions, *a*, *a'*, *b*, *b'*, and *c*. The in-beam EI mass spectrum of latamoxef dimethyl ester indicated that the relative abundance of ion *b'* at *m/z* 270 is greater (40.4%) than that of ion *b* at *m/z* 269 (8.0%). Thus, latamoxef dimethyl ester should be of the cis arrangement at C-6 and C-7. This conclusion is consistent with the results of X-ray analysis. (2).

The generation mechanism of ion *b'*, which has different abundance in cis and trans isomers, was investigated. The collision induced dissociation spectrum of the molecular ion of 7a indicated the ion *b'* (*m/z* 346) was directly produced from the molecular ion, which suggested it was produced by cleavage across the β-lactam ring after hydrogen transfer to the dihydrooxazine ring and not by protonation of the ion *b* (*m/z* 345) which could be generated from the molecular ion. Since substitution of H to the methoxyl group at C-7 did not affect the abundance of the *b'* ion (see compounds 1a, 1b, 3a, and 3b), the hydrogen rearranged was not the hydrogen at C-7 nor the hydrogen of the methoxyl group at C-7 but the hydrogen of amide group at C-7 (and/or the hydrogen of amino group of compounds 2a and 2b). This was confirmed by observing the spectra of 7-amide deuterium compounds. The peaks corresponding to ions *a*, *a'*, *b'*, and *c* shifted one mass unit higher, but those for ions *a''* and *b* did not shift. This spectrometric behavior supported our assumption that the hydrogen transferred to the dihydrooxazine ring originated from the C-7 amide hydrogen.

The hydrogen can be received by two sites in the dihydrooxazine ring — the nitrogen and the oxygen atom each of which has a lone pair of electrons. The fact that ion *b'* is more abundant in cis than in trans isomer indicates that the rearrangement of the amide hydrogen to the nitrogen or the oxygen atom proceeds more easily in cis isomer. According to a stereomodel examination, the amide hydrogen in the cis isomer is located close to the oxygen atom (2.38Å) and at a distance from the nitrogen atom (3.30Å) but in the trans isomer, is located near the nitrogen atom (3.31Å) and at a distance from the oxygen atom (4.03Å) (Fig. 3). Consequently, the amide hydrogen in cis isomer favors to transfer to the oxygen rather than nitrogen. In addition, since one of the two lone paired electron orbitals of the oxygen atom extend upward out of the dihydrooxazine ring plane, it is suited to receiving the amide hydrogen in the cis isomer. Information on the electron densities and the total energies given by M.O. calculations indicated the easy formation of the hydrogen rearranged intermediate [⁻ÖH] for the cis isomer and the easy fission of the bond between C-6 and C-7 of it. While for the trans iso-

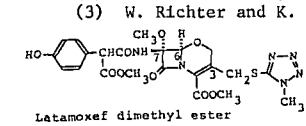
mer, it is rather difficult to form the intermediate ion ($\geq\dot{O}H$) and the other possible ion [$\geq\overset{+}{N}H$] has a large bond order of the bond between C-6 and C-7. Thus the ion *b'* is more abundant in the cis isomer than that of the trans isomer. Our results led to the conclusion that the C-7 amide hydrogen is transferred to the oxygen atom in the dihydrooxazine ring and further fragmentation gives ion *b'*. Ion *b'* was assumed to be the dihydrooxazine ion protonated on the oxygen atom as shown in Fig. 2, and was not compatible with the structure of the dihydrothiazine ion protonated at the nitrogen atom (ion b_2 in Fig. 2) from cephalosporins reported by Biemann et al. (3).

The compounds labeled with deuterium did not give any shift for ion *a''*, which indicated the ion had no amide deuterium — this ion was generated after loss of the labeled deuterium atom — and the structure of ion *a''* was assumed to be that shown in Fig. 2.

Finally, we inferred the structure of the main fragment ions and the fragmentation of 1-oxacephems to be as shown in Fig. 2.

ACKNOWLEDGEMENT The M.O. calculations carried out by Dr. M. Yamamoto and Miss T. Takeuchi are greatly appreciated.

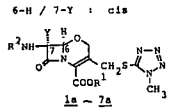
REFERENCES (1) M. Narisada et al., J. Med. Chem., 22, 757 (1979), and others.
(2) M. Shiro et al., to be published in Cryst. Struct. Comm., (1982).
(3) W. Richter and K. Biemann, Monatsch. Chem., 96, 484 (1965).



Latamoxef dimethyl ester

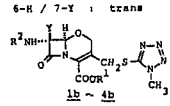
Table 1. 1-Oxacephems

6-H / 7-Y : cis



1a ~ 7a

6-H / 7-Y : trans



1b ~ 4b

	R^1	R^2	Y
1a , 1b	$CH(C_6H_5)_2$	$C_6H_5CH_2CO$	H
2a , 2b	$CH(C_6H_5)_2$	H	OCH_3
3a , 3b	$CH(C_6H_5)_2$	$C_6H_5CH_2CO$	OCH_3
4a , 4b	$CH(C_6H_5)_2$	C_6H_5CO	OCH_3
5a	CH_3	$C_6H_5CH_2CO$	OCH_3
6a	$CH_2C_6H_5$	$C_6H_5CH_2CO$	OCH_3
7a	$CH_2C_6H_5$	$C_6H_5CH_2CO$	H

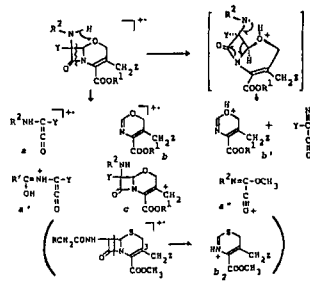


Fig. 2. Fragmentation of 1-oxacephems

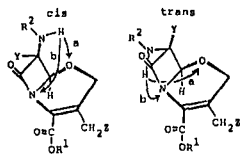


Fig. 3. Possible paths of H-transfer

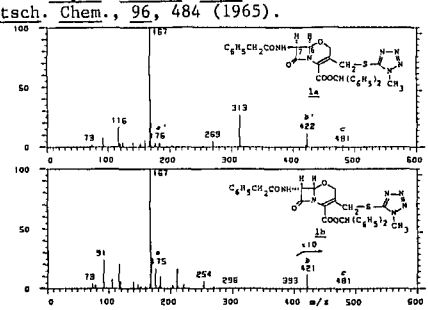
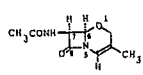


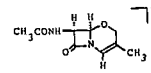
Fig. 1. Mass spectra of the compounds 1a and 1b

Table 2. Relative abundances of the main fragment ions of 1-oxacephems

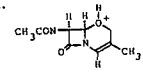
	a''	a	a'	b	b'	c	$M^{+\cdot}$	Base peak m/z
1a		2.8	3.5		9.2	1.5		167
1b		20.6	4.5	2.5		0.2		167
2a	2.1	1.0	2.8	0.9	1.5	0.3		167
2b	0.1	1.2	1.0	0.7	0.6			167
3a	2.1	3.0	1.3		9.3	1.2		167
3b	7.5	3.8	0.7	1.3	0.4	0.1		167
4a	38.7	5.2	0.9	0.4	5.3	0.1		167
4b	14.3	1.8	0.1	0.7	0.4			167
5a	12.6	3.1	2 6	12 9	32.5	23.3	2.1	155
6a	22.2	8.2	18.4	6.2	62.2	9.6	1.8	91
7a		2.9	18.4	5.8	100 0	39.1	20.3	346



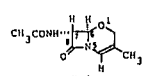
A-1
-151.7009 a.u.



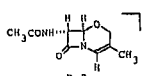
A-2
-151.3457 a u.



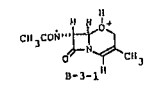
A-3
-151.3435 a.u.



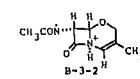
B-1
-151.6814 a.u.



B-2
-151.3334 a.u.



B-3-1
-151.3290 a.u.



B-3-2
-151.3690 a.u.

Total energy of cis and trans isomers

CALCULATED ANGULAR DISTRIBUTION OF FRAGMENT IONS FROM POLYATOMIC ION COLLISIONS

P. J. Todd, R. J. Warmack, E. H. McBay
Oak Ridge National Laboratory
Oak Ridge, Tennessee

Mass resolution observed in MIKES spectra from the collision induced fragmentations of high (~keV) energy polyatomic ions suffers due to the energy released in fragmentation, T [1]. Associated with T is a recoil velocity vector, $\bar{v}_1$ the precursor ion center of mass reference frame. $\bar{v}_1$ is the velocity with which the fragment ion departs the precursor ion center of mass. Projection of $\bar{v}_1$ onto the mean ion velocity, $\bar{v}_0$, either parallel or antiparallel, causes a substantial uncertainty in fragment ion kinetic energy, ΔE, in the laboratory reference frame [2]. This reduces mass resolution. The magnitude of $\bar{v}_1$ is given by equation (1):

$$|v_1| = \left[\frac{2(M-M)}{Mm}\right]^{\frac{1}{2}} T^{\frac{1}{2}} \qquad (1)$$

where M = precursor mass
m = daughter ion mass.

If v_1 has some orientation other than parallel or antiparallel to the mean ion axis, the fragment ion formed will be deflected by an angle from the mean ion axis, given by:

$$\tan \Phi \approx \Phi = \frac{v_1}{v_0}\frac{\sin \alpha}{} = \left(\frac{M-m}{m}\right)^{\frac{1}{2}}\left(\frac{T}{E_0}\right)^{\frac{1}{2}} \sin \alpha \qquad (2)$$

where Φ = laboratory observed scattering angle
α = angle between $\bar{v}_1$ and $\bar{v}_0$
E_0 = precursor ion kinetic energy.

Collisions were induced between various precursor ions in the region between the ion source and electrostatic sector (ESA) of an MS-50 mass spectrometer. Values for T were measured from peak widths at half height, using HV scans [2]. These values were, in turn, used to calculate an angular distribution of fragment ions using Eq. 2. It was thus possible to calculate and plot the relative abundance of fragment ions as a function of laboratory angle, ϕ, i.e., construct a so-called ARMS plot. An example is shown in Figure 1 for the fragments of nitromethane molecular ion: $CH_2NO_2^+$ (T = 134 meV), NO_2^+ T = 36.2 meV) and NO^+ (T = 34.9 meV). Also plotted are the angular results observed by R. G. Cooks and his students at Purdue [3]. Despite the simplifying assumptions incumbent with the calculations, the degree of fit is surprising. Equally good fits are found for other systems [4]. In general, smaller mass ions are almost invariably found to increase in relative abundance with increasing angle ϕ. This can be understood from the mass term in Eq. 2. While other factors such as precursor ion scatter may be contributory, these data indicate that relative fragment ion mass and energy released play a dominant role in the angular distribution observed in collision induced dissociation of polyatomic ions.

*Research sponsored by the U. S. Department of Energy, Division of Basic Energy Sciences, under Contract W-7405-eng-26 with the Union Carbide Corporation.

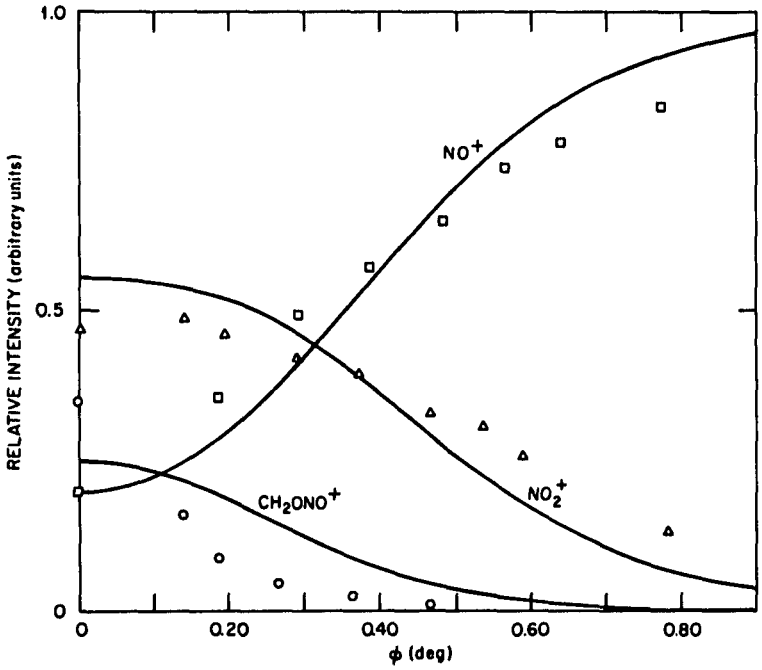


Figure 1. Calculated and reported [3] relative intensities of collision induced fragment ions from 7.5 keV CH_3ONO^+ precursor ions, as a function of laboratory angle, φ.

References

1. Tuithof, H. H., Int. J. Mass Spectrom. Ion Phys. 23, 147-151 (1977).

2. Cooks, R. G., Beynon, J. H. Caprioli, R. M., Lester, G. R., "Metastable Ions," Elsevier, Amsterdam (1973).

3. Hubik, A. R., Hemberger, P. H., Laramee, J. A., Cooks, R. G., J. Amer. Chem. Soc. 102, 3997-4000 (1980).

4. Laramee, J. A., Hemberger, P. H., Cooks, R. G., Int. J. Mass Spectrom. Ion Phys. 33, 231-241 (1980).

Ionic Decomposition Maps; R. S. Mason, M. J. Farncombe and K. R. Jennings;
Department of Chemistry and Molecular Sciences, University of Warwick,
Coventry CV4 7AL, England.

Linked scans in which both the magnetic sector field strength B and the electric sector field strength E are varied simultaneously have recently been used increasingly in the study of ion structures and in mixture analysis. The three most commonly-used scans are those in which (i) B/E remains constant giving all daughter ions of a chosen parent ion, (ii) B^2/E remains constant giving all parent ions of a given daughter ion and (iii) $B^2(1-E'/E'^2$ remains constant giving daughter ions formed by the loss of a constant neutral mass from parent ions ($E' = E/E_o$ where E_o is the electric sector field strength required to transmit the main beam). If scans of these types were carried out for the majority of ions observed in the mass spectrum of a given compound, it would be very time-consuming and would require the use of a considerable amount of sample.

Since each scan is essentially a method of investigating the intensity distribution within the B,E plane, a method has been developed which rapidly acquires, processes and stores this data on disc and which allows subsequent off-line simulation of the three linked scans for any chosen ion in the spectrum. A MINC-11 mini-computer was used to generate reference voltages for E and the accelerating voltage V of an MS50 mass spectrometer and DS55 data system (Kratos Analytical Instruments Ltd.). Rapid consecutive scanning of the magnetic field strength B is controlled by the DS55 data system, which also performs time to mass conversion, and the MINC-11 decrements the reference voltage for E between each scan. The size of the decrement is preset and may be relatively small so as to produce a detailed picture of part of the surface or may be made sufficiently large for the whole plane to be investigated. The complete set of stored spectra constitute the scan of the B,E plane and several methods have been developed for the display of the spectra. Although the B,E plane is the simplest to visualize in terms of instrumental parameters, a plot of intensity within a B^2,E plane has the advantage that $M \propto B^2$, but the plot is still not easy to interpret. A more readily-interpreted plot is one in which the parent ion mass M_1^+ is plotted against the daughter ion mass M_2 in which the normal mass spectrum appears along the diagonal line for which $M_1 = M_2$, as described by Yost and Enke for triple-quad collision-induced decomposition spectra.[1] Simulated B/E, B^2/E and constant neutral loss scans can then be obtained by following paths parallel to the M_2 axis, the M_1 axis and diagonal respectively.

In this way, ion intensity distributions within the B,E plane are converted to ion decomposition maps (metastable transition or collision-induced decompositions). The signals given by simulated linked scans are found to be in good agreement with those given by normal linked scans and the identification of artefact peaks is considerably facilitated by reference to the intensity distribution within the B,E plane. Weak signals which arise from decompositions occurring during acceleration or within the electric sector are clearly shown as continua and scans which cross these continua necessarily contain artefact peaks.

A detailed study of maps given by methanol and n-decanol has been made and an example of the use of the method in identifying the constituents in an analgesic tablet has been described.[2] A preliminary report of the use of the technique in the study of angle-resolved fragmentation products of collision-induced decomposition has also been accepted for publication.[3]

References

1. R. A. Yost and C. G. Enke, Anal. Chem., 51, (1979), 1251.

2. M. J. Farncombe, R. S. Mason, K. R. Jennings and J. Scrivens, Int. J. Mass Spectrom. Ion Phys. (in press).

3. R. S. Mason, M. J. Farncombe, K. R. Jennings and R. G. Cooks, Int. J. Mass Spectrom. Ion Phys. (in press).

A STUDY OF THE FRAGMENTATION BEHAVIOR OF ANISOL BY THRESHOLD PHOTOELECTRON COINCIDENT PHOTOION (TPEPICO) MASS SPECTROMETRY

Jerome P. Gilman, Pradip R. Das, Toshihiro Fujii*, and G.G. Meisels, Department of Chemistry, University of Nebraska, Lincoln, Nebraska 68588-0304

The Quasiequilibrium Theory (QET) of mass spectra is accepted widely because it describes the fragmentation of large gaseous ions highly successfully. Calculations based on this theory normally assume that any initial electron excitation is converted rapidly to vibrational excitation of the ground electronic state by radiationless transitions. Evidence that some molecules may fragment from non-interconverting electronic states has been reported recently (1), but the existence of these states is difficult to establish unambiguously.

Non-interconverting states may be more probable for molecular ions which contain a heteroatom. Several molecular ions containing oxygen, such as CH_3ONO, C_3H_6O, CH_2O, and CH_3NO_2, may exhibit non-statistical behavior (1). In our attempt to gain further insight and understanding of the role the heteroatom may play in the competition between statistical and state-specific processes, we are investigating anisol and report here that this molecular ion may possibly exist in non-interconverting states.

It has been reported previously that the loss of formaldehyde (H_2CO) from the anisol molecular ion shows a composite metastable peak (2). The authors suggested that H_2CO elimination occurred via two reaction channels involving four and five centered transition states, respectively, and led to two different product ion structures from the same reactant ion. However, ion-molecule reactions of the product $C_6H_6^+$ ions and of $C_6H_6^+$ formed from benzene are identical (3), suggesting that the composite peak may also arise from fragmentation of non-interconverting states of anisol molecular ion to identical product ions.

We have examined the fragmentation behavior of anisol using TPEPICO mass spectrometry. Fragmentation at photon energies less than 14 eV is characterized by 4 major fragment ions at m/z 93, 79, 78 and 65, representing loss of CH_3, CHO, H_2CO and C_2H_3O, respectively. The time-of-flight (TOF) mass spectra of anisol (Fig. 1) do not resolve m/z 78 from 79 and m/z 107 from 108. Separation of these ions is accomplished by quadrupole mass analysis.

A breakdown graph (BDG) (Fig. 2) which represents the relative abundance of parent and fragment ions, normalized to 100%, as a function of internal energy, was constructed and corrected for the contribution of non-threshold electrons transmitted through the threshold photoelectron detector (4). The abundance of the molecular ion begins to decrease at 11.5 eV, is zero at least from 12.5 to 13.2 eV, but rises again at that energy with a maximum abundance of ca. 13% at 13.53 eV.

The TOF peak shape of the resolved m/z 78 ion indicates that at 13.53 eV asymmetric broadening may occur but that the peak may be symmetrically broadened at 12.99 and 13.98 eV. TOF peaks between these energies (except at 13.53 eV) were not obtained since the photon intensity of the light source is very low in this region, making collection time prohibitively long.

Mass selected TOF spectra were obtained for m/z 78 under single field conditions at two energies (Fig. 3-dots). Under these conditions, collection times averaged about 100 hours. Calculated TOF curves (Fig. 3-solid lines), based on a single unimolecular rate constant that is varied until a best fit between calculated and observed TOF curves is obtained, yielded rate constants of 1.0×10^6 sec^{-1} and 2.0×10^5 sec^{-1} at 12.99 and 13.53 eV, respectively.

We believe that the increase in parent ion abundance at 13.5 eV may arise from the population of an electronic state other than the ground electronic state. Comparison of the PES with the breakdown graph of anisol (Fig. 4, m/z 79 and 65 not shown), shows that the increase in the parent ion abundance occurs at the onset of the 6th PES band (approximately 13.5 eV photon energy). Although direct correspondence with a PES band is not observed, it is possible that interconversion from lower vibrational levels of the state corresponding to the 6th PES band does not occur efficiently but that the probability of internal conversion to the ground state of the ion increases with increasing quantum number. Fragmentation of states with low quantum numbers may proceed via a surface crossing. Alternate explanations include fluorescence from the lower vibrational states of the 6th band, and an undetected autoionizing state at ca. 13.5 eV; these will be the subject of future investigations.

Acknowledgments: We wish to thank Dr. Toshihide Nishimura for many helpful discussions, and the Department of Energy for support under contract number AT(11-1)-2567.

References: *National Institute for Environmental Studies, P.O. Yatabe, Tsukbaraki, Ibaraki 300-21 Japan. (1) (a) G.G. Meisels, T. Hsieh and J.P. Gilman, J. Chem. Phys. **73**, 4126 (1980). (b) J.P. Gilman, T. Hsieh and G.G. Meisels, 29th Ann. Conf. on Mass Spectrom. and Allied Top., Minneapolis, MN (1981); (c) C. Lifshitz and E. Tzidony, ibid.; (d) R. Bombach, J. Dannacher, J.P. Stadelmann and J. Vogt, ibid.; (e) Y. Niwa, S. Tajima and T. Tsuchiya, Int. J. Mass Spectrom. Ion Phys., **40**, 287 (1981). (2) R.G. Cooks, M. Bertrand, J.H. Beynon, M.F. Rennekemp, and D.W. Setser, J. Am. Chem. Soc., **95**, 1732 (1973). (3) M.L. Gross, D.H. Russel, R.J. Aerni, and S.A. Bronczyk, J. Am. Chem. Soc., **99**, 3603 (1977). (4) J.P. Gilman, T. Hsieh, and G.G. Meisels, to be sumbitted.

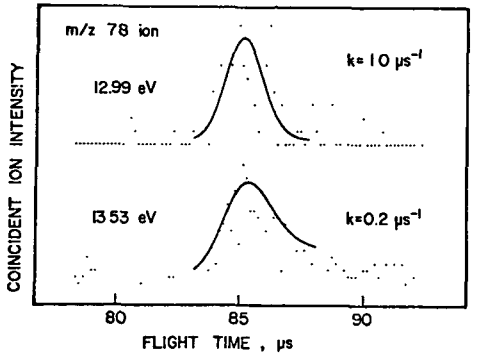


Fig. 3: Rate constant fits to m/z 78 TOF curve

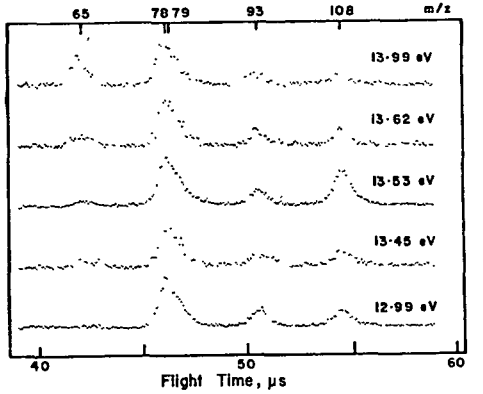


Fig. 1: TOF mass spectra at selected energies.

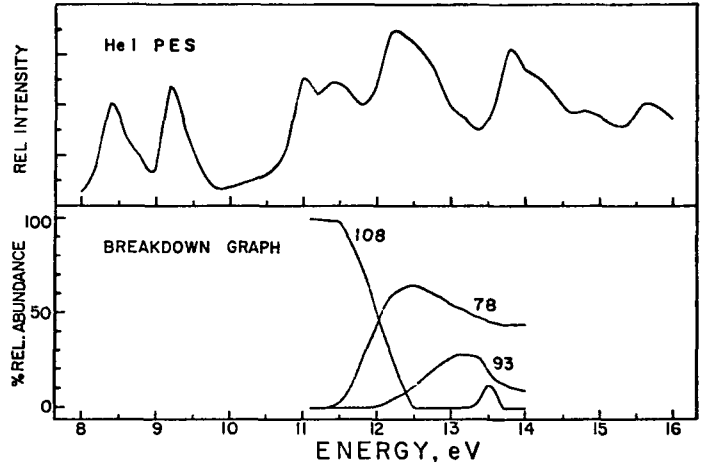


Fig. 4: P.E.S. and partial BDG.

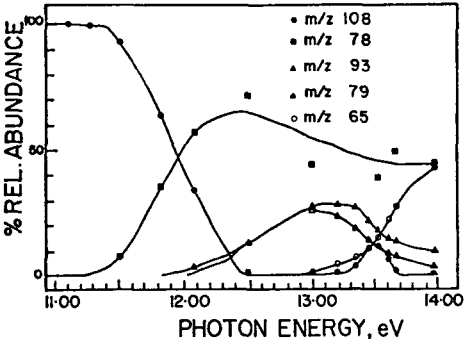


Fig. 2: Breakdown graph of anisol.

STRUCTURES AND FRAGMENTATION MECHANISMS OF THE IONS OF ETHANOL BY TRIPLE QUADRUPOLE MASS SPECTROMETRY

R. Kazmer Latven, Margaret B. McFarland, Christie G. Enke
Department of Chemistry
Michigan State University
East Lansing, Michigan 48824

The purpose of this study was to probe the usefulness of triple quadrupole mass spectrometry in providing detailed structural and mechanistic information. Ethanol was chosen as the compound of interest because its relatively simple structure can yield unambiguous information in many cases. In addition, this compound has been studied in high energy CID experiments, hence results from both high and low energy collision experiments can be compared.

Figure 1 shows an EI mass spectrum obtained by the TQMS in single MS mode (RF/RF/DC). Ethanol ions of interest are those at m/z 46, 45, 43, 42, and 31. The structures of these ions and the mechanisms of their formation and decomposition are the object of this study. Stable isotopes CH_3CH_2OD and CD_3CH_2OH were used to provide additional spectra whose interpretation must be consistent with the structures and mechanisms postulated for the ions of the unlabeled isotope.

Electron impact ions of ethanol were formed in the ion source at a sample pressure of 5 mtorr, with the source block at 225° C. Ions selected by the first quadrupole were accelerated to a translational energy of 25 eV in the second quadrupole where they undergo collisionally activated decomposition (CAD) upon impact with argon target at 4×10^{-4} torr. Fragmentation products were then analyzed by the third quadrupole and detected.

The molecular ion of ethanol (m/z 46) yields daughter ions at m/z 45 and 31. The mechanism ascribed to both decompositions is simple alpha cleavage of the hydrogen at the one position, and the cleavage of the C-C bond respectively. The ethanol-OD isotope similarly loses H and CH_3 to yield ions at m/z 46 and 32, while the D_3 analog loses H and CD_3 providing daughter ions at m/z 48 and 31.

Since the ion at m/z 45 was formed by loss of H at the one position, the fragmentation reactions of this ion must assume $[CH_3CHOH]^+$ as the parent ion structure, with the charge on the number one carbon. $[CH_3CHOH]^+$ loses H_2 by the four centered reaction seen in Figure 2a, loses methyl radical by electron unpairing to form two odd-electron products (2b), loses methane by the combination of terminal methyl and hydroxyl proton (2c), and water by combination of hydroxyl and the proton at the number one position. Figure 3 shows CAD spectra of CH_3CHOH (3a), CH_3CHOD (3b), and CD_3CHOH (3c). The daughter spectra of the deuterated analogs are consistent with the mechanisms described in Figure 2.

The ion at m/z 43 has the structure $[CH_2 = COH]^+$ with the charge on the number one carbon (2a). Evidence suggests that this 'enol' form has a concurrent 'keto' tautomer. The most abundant daughter peaks arise from the keto form of the parent, and the unlabeled, -OD labelled, and D_3-labelled analogs provide daughter ions at m/z 15, 16, and 17, which correspond to CH_3^+, CH_2D^+, and CHD_2^+. Less abundant peaks are observed at m/z 14, 14 and 15, and 15 and 16 respectively which could arise from the enol form of the parent after scrambling.

The parent at mass 42 is of the form $[CH_2C = O]^+$ and has one daughter peak at m/z 14. The -OD and D_3-analogs again provide consistent data with ions at mass 14 and 16 respectively.

Figure 4 summarizes the structures postulated for these ions of ethanol. Quadrupole MS/MS has been shown to provide detailed information on ionic structure and fragmentation pathways, particularly when used in conjunction with labeled isotopes.

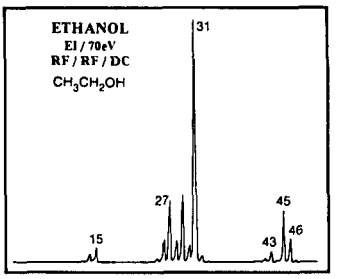


Figure 1

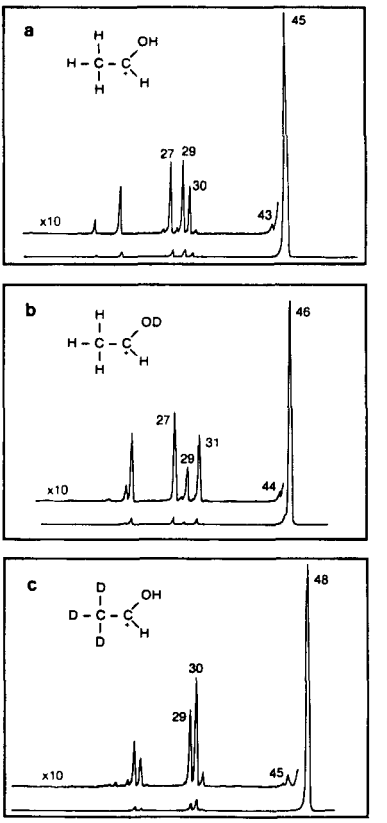


Figure 3

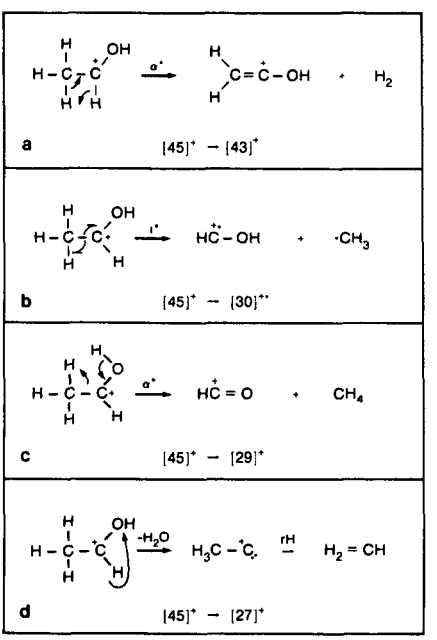


Figure 2

MAJOR IONS OF ETHANOL

$[46]^{+\cdot}$	$H_3C-CH_2-\ddot{O}H$
$[45]^+$	$H_3C-\dot{C}H-OH$
$[43]^+$	$H_2C=\dot{C}-OH \rightleftharpoons H_3C-\dot{C}=O$
$[42]^{+\cdot}$	$H_2\dot{C}-\dot{C}=O$
$[31]^+$	$H_2\dot{C}-OH$

Figure 4

THE DIECKMANN CONDENSATION AND RELATED REACTIONS IN THE MASS SPECTROMETER

DAVID J. BURINSKY and R. GRAHAM COOKS
Department of Chemistry
Purdue University
West Lafayette, IN 47907

This paper concerns structure elucidation and reaction mechanisms in the gas phase and their relationship to well known solution reactions. In some cases a great deal of similarity is observed between reaction mechanisms in the two phases, while in others striking differences occur.

Species which are transient in solution, e.g. enolate anions and carbonium ions, are generated as stable gas-phase entities by chemical ionization. Reaction products are isolated by electrostatic extraction and mass selection and then characterized by their ms/ms spectrum following collision-induced dissociation.

Two types of questions have been posed using this methodology:

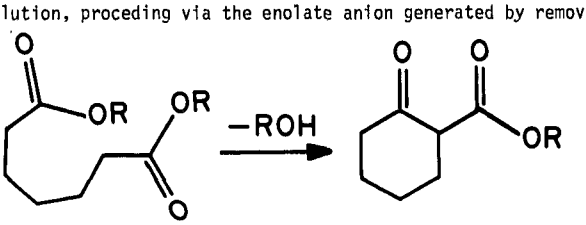
(i) What is the site of reaction in bimolecular processes such as electrophilic aromatic substitution?
(ii) Are particular elimination reactions accompanied by cyclization?

The first type of question is typified by the methylation of phenol and aniline. The ms/ms methodology was used to distinguish between substituent (O or N) methylation and ring methylation. Results were obtained using two different ms/ms instruments operating at low (ca 20 eV) and high (7 keV) collision energies. It was observed (Table 1) that ring methylation predominated for phenol, while substituent methylation was the dominant process for aniline. In solution, the substituent is far more nucleophilic than the ring toward alkylation.

Table 1.

SITE OF ALKYLATION	MIKES	TSQ[R]
Aniline		
N-Methylation	80-90%	95%
Ring Methylation	10-20%	5%
Phenol		
O-Methylation	20%	35%
Ring Methylation	80%	65%

The second question is epitomized by the Dieckmann condensation of aliphatic diesters to yield cyclic ketoesters after elimination of an alcohol molecule. The reaction is base-catalyzed in solution, proceding via the enolate anion generated by removal of an α-proton.



THE DIECKMANN CONDENSATION

Figure 1 compares the ms/ms spectrum of the product of the alcohol elimination of the enolate from α-methyl diethyl pimelate with two isomeric ketoesters which might be generated in this reaction. Evidently, one route is followed with the other product not being observed. This conclusion, based on charge-inversion ms/ms spectra was further supported by conventional (negatively charged parent ion → → negatively charged fragment ions) ms/ms spectra, by results for analogous esters, and by isotopic labeling.

The chemical ionization ms/ms methodology used here was first described in 1976[1]. It has been used to investigate the following reactions: Claisen-Schmidt[2], Cannizarro[3], Aldol[4], Wagner-Meerwein[5], Fischer indole synthesis[6], barbituric acid synthesis[7], as well as protonation, alkylation, and other electrophilic reactions of aromatic systems[1].

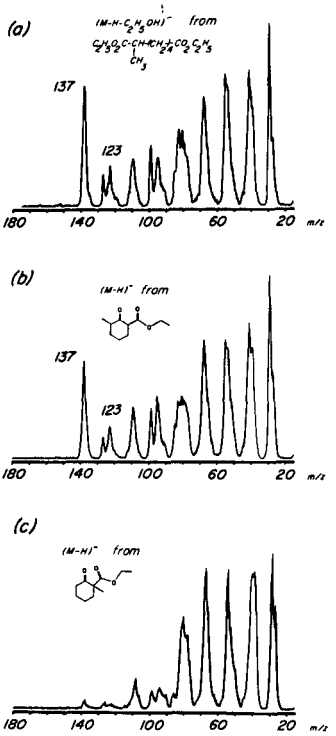


Figure 1. - (a) Charge-inversion spectrum of 183^-, ethanol elimination product of deprotonated α-methyl diethyl pimelate (gas-phase reaction product). (b) Product analysis of the conjugate base of authentic 6-methyl-2-carbethoxycyclohexanone (charge-inversion spectrum of 183^-). (c) Positive fragment ion (charge-inversion) spectrum of 183^- from deprotonated 2-methyl-2-carbethoxycyclohexanone.

Analogous methods, using laser desorption and ms/ms are currently being used to examine the structures of organometallic ions generated in the gas phase[8].

REFERENCES

1 Kruger, T.L.; Flammang, R.; Litton, J.F.; Cooks, R.G. Tetrahedron Lett. 1976, 50, 4555.
2 Burinsky, D.J.; Cooks, R.G., to be published.
3 Burinsky, D.J.; Cooks, R.G., to be published.
4 Wesdemiotis, C.; McLafferty, F.W. Org. Mass Spectrom. 1981, 16, 381.
5 Wolfschutz, R.; Schwarz, H.; Blum, W.; Richter, W.J. Org. Mass Spectrom. 1979, 14, 462.
6 Glish, G.L.; Cooks, R.G. J. Am. Chem. Soc. 1978, 100, 6720.
7 Burinsky, D.J.; Cooks, R.G., to be published.
8 McLuckey, S.A.; Cooks, R.G., to be published.

MS/MS OF OXIDATIVE INSERTION REACTIONS

C. N. McEwen
Central Research and Development Dept.
E. I. du Pont de Nemours & Co.
Wilmington, Delaware 19898

Beauchamp, et. al.[1] have shown that $CpNi^+$ ions produced from Cp_2Ni in an ICR spectrometer, react with acetaldehyde molecules to give $[CpNiC_2H_4O]^+$ ions which unimolecularly decompose to $[CpNiCO]^+$ and CH_4. Likewise, $CpNi^+$ ions were shown to react in the ICR spectrometer with benzaldehyde to give $[CpNiC_7H_6O]^+$ ions which in turn fragment to give $[CpNiC_6H_6]^+$ and CO. $[CpNiC_2H_4O]^+$ and $CpNiC_7H_6O]^+$ ions can be produced in a similar way under chemical ionization conditions. Unimolecular decomposition of these ions gives results analogous to those obtained by ICR spectrometry. Analysis of the results suggests that the metastable ions are isomerizing and decomposing by the lowest energy pathway available.

On the other hand, collision induced decomposition (CID) of the "stable" intermediate ions from these reactions produces considerably different results. The large amount of internal energy deposited in the ion during the collision process and the limited time available (ca. 10^{-7}s) for decomposition favors direct bond breaking over the lower energy, but more ordered (lower entropy) process of isomerization. Thus, the structures of the stable intermediate ions are accessible from the CID spectra.

Collision induced dissociation of the $[CpNiC_2H_4O]^+$ ions shows predominant loss of CH_3CHO indicating that the dominant intermediate structure for these ions is $[CpNi...O{=}CHCH_3]^+$. CID of the $[CpNiC_7H_6O]^+$ ions shows loss of C_6H_5CHO and CO in about equal amounts indicating that these ions have the structures $[CpNi...O{=}CHC_6H_5]^+$ and $[CpNi(CO)(C_6H_6)]^+$.

The reactions of Fe^+ with acetaldehyde[2] and benzaldehyde were also studied using MS/MS as were the reactions of $FeCO^+$ with methane and benzene. CID shows that the $[FeC_2H_4O]^+$ ions from the reaction of Fe^+ with acetaldehyde have primarily the $[Fe...O{=}CHCH_3]^+$ structure, whereas the $[FeC_2H_4O]^+$ ion from the reaction of $FeCO^+$ with methane have primarily the $[Fe(CO)(CH_4)]^+$ structure. In the reaction of Fe^+ with benzaldehyde, the intermediate ions were found to have the structures $[Fe...O{=}CHC_6H_5]^+$ and $[Fe(CO)(C_6H_6)]^+$. These same structures, although in different intensity ratios were found for the intermediate ions from the reaction of $FeCO^+$ with benzene. Unimolecular decomposition of the $[FeC_7H_6O]^+$ ions from either of these reactions showed nearly exclusive loss of CO.

These studies indicate that CID MS/MS can be used to determine the intermediate structures of oxidative insertion reactions occurring in a chemical ionization source, and that the lowest energy path available for decomposition can be identified from the metastable spectra. Thus, MS/MS along with ICR mass spectrometry becomes an important tool for studying these catalytically important gas phase reactions.

---

[1] J. L. Beauchamp, A. E. Stevens, and R. R. Conderman, Pure and Appl. Chem., 51, 967 (1979).

[2] R. C. Burnier, G. D. Byrd, and B. S. Freiser, J. Am. Chem. Soc., 103, 4360 (1981).

DIFFERENTIATION OF POSITIONAL ISOMERS WITH COLLISION ACTIVATED REACTIONS IN A TRIPLE QUADRUPOLE MASS SPECTROMETER

J.A. Chakel and C.G. Enke

Department of Chemistry
Michigan State University
East Lansing, MI 48824

Chemically specific ion-molecule reactions may be used with a triple quadrupole mass spectrometer (TQMS) for the analysis of positional isomers. In TQMS, ions generated in the source are mass-selected by the first quadrupole. The selected ion can undergo low energy collision activated dissociation/reaction (CAD/CAR) in the center rf-only quadrupole collision cell. The ionic collision/reaction products are focused into and mass-analyzed by the third quadrupole.

Opportunities for chemically specific reactions exist in both the source and the collision cell. Benefits similar to those from chemical ionization in the source can be realized by employing ion-molecule reactions in the collision cell. The isomers selected for this study were the three dichlorobenzenes, the three monohydroxybiphenyls, the three monobromobiphenyls and 2,2'-dibromobiphenyl and 4,4'-dibromobyphenyl. The collision gases used in second quad and the collision activated reaction for each are presented in the following table:

Collision Gas	Collision Activated Reaction
N_2	$M^+ + N_2 \rightarrow M^{+*} \rightarrow$ Fragments
NH_3	$MX^+ + NH_3 \rightarrow (M - X + NH_3)^+$
D_2O	$(M - H)^- + D_2O \rightarrow (M - H - Hy + Dy)^-$
SF_6	$(M - H)^- + SF_6 \rightarrow (M - H)^{+*} \rightarrow$ Fragments

In all cases maximum CAR product formation occurs at low collision energy with the exception of the charge inversion process which occurs at high (180 V Lab) collision energy. Collision with nitrogen is useful for differentiating between the two dibromobiphenyl isomers. The 2,2'-dibromobiphenyl favors the loss of one bromine from M+ by a factor of 60 over the 4,4'-dibromobiphenyl which in turn favors the loss of both bromines by a factor of 14. When NH_3 is utilized as the collision gas for these same two isomers the ammonia substitution product corresponding to $(M - Br + NH_3)^+$ is slightly larger for the 2,2'-dibromobyphenyl and the peak corresponding to $(M - Br_2 + NH_3)^+$ is five times larger for 4,4'-dibromobiphenyl. Occurring individually, these isomers could be readily distinguished.

D_2O as a collision gas provides unique results for both the dichlorobenzenes and the dibromobiphenyls. Both ortho and para dichlorobenzene readily undergo deuterium incorporation in $(M-H)^-$ to give primarily three deuterium and 1 deuterium incorporation, respectively. The meta isomer preferentially picks up two deuteriums at 70% R.A. Single deuterium incorporation is preferred for 2,2'-dibromobiphenyl and a surprising seven deuterium incorporation is preferred for 4,4'-dibromobiphenyl. All collision gas pressures were approximately 3×10^{-4} Torr.

SF_6 provided charge inversion spectra for the hydroxybiphenyls although no striking differences were observed for the three different isomers. Further optimization of the process will be made and may prove quite useful for isomeric studies.

In summary, many reactions are possible within the quad collision chamber and examples of the utility they provide for dramatically enhancing spectral differences between positional isomers has been demonstrated.

This work was supported in part by the MSU Agriculture Experiment Station.

SURVEY OF THE ENERGY DEPENDENCE OF THE COLLISIONALLY ACTIVATED DECOMPOSITION (CAD) SPECTRA OF ORGANIC SALTS PRODUCED BY FAB/MS/MS

D. Zakett and J. C. Tou
Dow Chemical Company
Midland, Michigan 48640

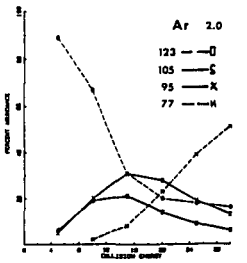
The dependence of the low energy MS/MS spectra for two compounds, didodecyldimethylammonium chloride and p-ethylphenol has been investigated as a function of collision energy and collision cell pressure using three different collision gases (Ar, Xe, SF_6). Results indicate that substantial changes in the relative abundances of fragment ions can occur, including the appearance and disappearance of certain fragment ions, as the collision energy and/or the collision gas pressure is varied over the range of 3-30 eV and 0.1-5.0 mtorr, respectively. The different collision gases were found to cause more or less energetic fragmentation of the parent ion for a given set of collision energy and pressure conditions. Xenon caused the most energetic fragmentation followed by argon and then SF_6. This ordering was determined by plotting the relative abundances of fragment ions from protonated 4-ethylphenol as a function of collision energy for each of the gases and observing the energy at which the abundance of 77^+ exceeded that of 95^+ and 105^+ as illustrated in figure 1. Additional confirmation of this ranking scheme is provided by the fact that 51^+ and 65^+ fragments which were observed at higher energies and pressures (>25 eV, ~5 mtorr) for both Ar and Xe were not detected using SF_6 as collision gas under the same conditions. It is noteworthy that SF_6 transferred the least energy in the collision activated decomposition process. In this instance energy transfer for Xe and Ar increases with atomic mass, for SF_6, however, energy transfer appears more consistent with the atomic weight of fluorine or sulfur than with the molecular weight of SF_6. These experiments were performed using a Finnigan TSQ (triple quadrupole) mass spectrometer with a model 4500 ion source.

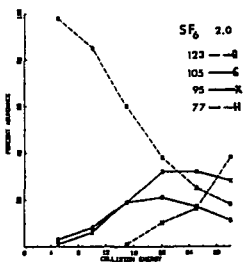
Didodecyldimethylammonium chloride was ionized by fast atom bombardment using an Iontech atom gun which had been adapted to fit on the flange normally used for the liquid chromatographic interface. The quaternary ammonium chloride was supported in glycerol and introduced via solid probe using a specially constructed probe tip. The atom gun was normally operated at 6KV with an indicated ion current of 20μA. Xenon was used for the atom beam.

The MS/MS spectrum of m/z 382, the C_{26} quaternary ammonium cation, was rather simple, containing an alkyl ion series at m/z 43, 57, 71 and 85, and a single peak corresponding to loss of a neutral C_{12} olefin from the parent ion. The fragmentation behavior of this and other long chain quaternary ammonium compounds exhibited less variability with collision pressure and energy than did protonated ethylphenol which was ionized by methane chemical ionization.

The MS/MS data was acquired in the same manner regardless of whether FAB or chemical ionization was used. The collision cell pressure was held constant during the course of data acquisition and the axial ion energy (nominal collision energy) stepped repetitively thru the set of 3, 5, 10, 15, 20, 25, 30 volts. A daughter spectrum (at a given collision energy) was obtained approximately once per second. The experiment was terminated after approximately 20 cycles of the collision energy set had been completed. Points plotted in figures 1 and 2 represent the ion abundances obtained after averaging from 5-10 individual MS/MS spectra obtained at that particular energy. Ions are plotted as percent of all ions detected (including parent ion m/z 123 but excluding SF_5^+ m/z 127). The collision pressure was measured using an MKS Baratron and is accurate to ±0.05 mtorr.

Figure 2 shows the energy and pressure dependence of three fragment ions from protonated p-ethylphenol (m/z 123) using xenon as collision gas.





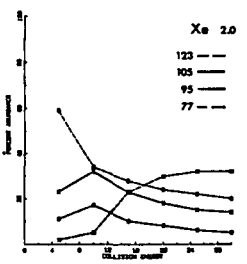


Figure 1. Comparison of energy dependence of m/z 77, 95 and 105 fragment ions from protonated p-ethylphenol at 2.00 mtorr for argon, sulfurhexafluoride and xenon collision gases.

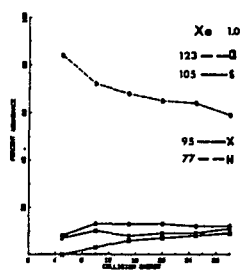


Figure 2. Energy and pressure dependence of m/z 77, 95 and 105 fragment ions from p-ethylphenol using xenon collision gas at pressures of 1.00, 2.00 and 4.30 mtorr.

METASTABLE PEAK SHAPES AND THE PARTITION OF INTERNAL ENERGY IN REACTIONS $(C_2H_5O)^+ \rightarrow (CHO)^+ + CH_4$

Kevin F. Donchi, Bruce A. Rumpf and Peter J. Derrick

School of Chemistry, The University of New South Wales,
P.O. Box 1 Kensington, NSW 2033
Australia

The two ions $(CH_3CHOH)^+$ and $(CH_3OCH_2)^+$ both react unimolecularly to eliminate methane. The metastable peak for the reaction $(CH_3OCH_2)^+ \rightarrow (CHO)^+$ is "gausian" in shape, whereas that for $(CH_3CHOH)^+ \rightarrow (CHO)^+$ is "dished".

The metastable peak for the reaction of the perdeuterated ion $(CD_3OCD_2)^+ \rightarrow (CDO)^+$ is also "gausian", but is broader than that for $(CH_3OCH_2)^+$. That is to say, substitution of D for H increases the amount of internal energy released as translation.

The metastable peaks for the reactions $(CH_3CHOD)^+ \rightarrow (CHO)^+$, $(CD_3CDOH)^+ \rightarrow (CDO)^+$ and $(CD_3CDOD)^+ \rightarrow (CDO)^+$ are all "dished". The peaks decrease in breadth on going from $(CH_3CHOH)^+$ to $(CH_3CHOD)^+$ to $(CD_3CDOH)^+$ to $(CD_3CDOD)^+$. That is to say, progressively greater degrees of substitution of D for H reduce the amount of internal energy released as translation.

These observations are in accord with predictions of the dynamical theory of energy partition[1], based on dynamic transition states obtained through calculation using the semi-empirical molecular orbital method MINDO/3 (ref. 2). By "dynamic transition state" is meant a transition state configuration in which not only the geometry but also the relative motions of all the individual atoms are defined.

The dynamic transition state for the reaction $(CH_3CHOH)^+ \rightarrow (CHO)^+$ involves motion of the H atom from the oxygen atom towards the methyl group in what might be termed a "front-side" attack. The dynamic transition state for the reaction $(CH_3OCH_2)^+ \rightarrow (CHO)^+$ involves what might be termed a "back-side" attack. An H atom from the methylene group moves to interact with the oxygen atom and from there to the methyl group.

1. *P.J. Derrick and K.F. Donchi, in "Comprehensive Chemical Kinetics", eds. C.H. Bamford and C.F.H. Tipper, Suppl. Vol. 1, Elsevier Scientific Publ. Co., 1982, pp. 54-247.*

2. *K.F. Donchi, B.A. Rumpf and P.J. Derrick, to be published.*

MASS SPECTROMETRIC ANALYSIS OF SELECTED
DISTILLATE FRACTIONS FROM SHALE OIL

R. A. Heppner, F.D. Guffey, and J.H. Weber;
Laramie Energy Technology Center; Department of Energy; Laramie, WY 82071

Mass spectrometry is used extensively at our laboratory for characterizing fuel products derived from shale oil. Two areas in which mass spectrometry has been applied will be discussed: I. GC/MS of hydrocarbon fractions, and II. High Resolution Mass Spectrometry (HRMS) of nitrogen concentrates.

I. GC/MS of Hydrocarbon Fractions

Because hydrocarbons are the most prominent compound types in fuel products derived from shale oil, fuels can be characterized by a careful analysis of the hydrocarbon compounds. The characterization provides a measure for the fuel quality and a basis for comparison of fuels and fuel sources.

Obtaining hydrocarbon fractions requires using a column chromatographic separation scheme. With this separation saturate, olefinic, and aromatic hydrocarbon fractions can be obtained and subsequently individually analyzed using GC/MS. The GC/MS analysis is very complete in that the resolvable components can all be assigned a relative contribution to the sample from their area percentages. However, when a large number of different components are present it is easier to group the components into their Z series classes, summing individual compound intensities within each Z series. This "type analysis" form of reporting is shown in figure 1 for the naphtha and light distillate saturate hydrocarbon fractions from shale oil. Normal and branched saturates correspond to Z=+2, olefinic compounds to Z=0. Similar information is shown for the aromatic fraction in figure 2. By presenting the data in this way it is easy to quickly see gross differences between the fuels, and, if necessary, the GC/MS data is always available for determination of finer differences among fuels at the individual component level. The data shown in figures 1 and 2 has been compared with the results from the application of type analysis methods to these same samples and good agreement was obtained. This work was done for the ASTM E-14 committee.

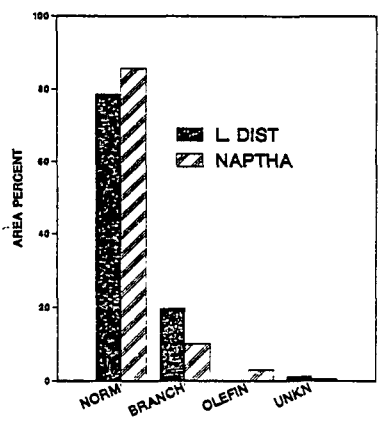


Figure 1. GC/MS Analysis of Saturates

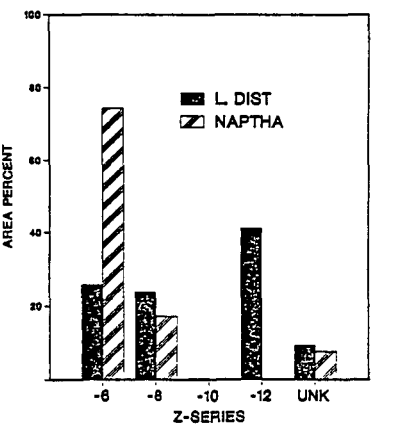


Figure 2. GC/MS Analysis of Aromatics

GC/MS has also been used to examine jet fuel samples. Because these fuels are blended from various refinery streams (reformate, alkylate, hydrocracker,etc.), they can vary widely in composition and yet still meet the standards required for classification as jet fuels. Tables 1 and 2 summarize the results obtained from analyzing two jet fuel samples. The first fuel is rich in aromatic species, while the second fuel is completely opposite, being rich in saturate species. Each of these fuels contained the order of 100 resolvable GC peaks, but the differences can be readily summarized in the Z series form as shown in the two tables. Separation of these fuels into saturate and aromatic fractions is time consuming. However, the reduced complexity of each fraction enables better GC/MS measurements to be made. It is a case of trading off analysis time for analysis accuracy. Future work will involve more jet fuel analyses both by GC/MS and using type analysis methods. Separation methods may also be employed. The aim will be to obtain better agreement among the analysis methods.

TABLE 1

Component Type Analysis of the Sample VN-80-48

Saturates		Area%
Z = +2	n-alkanes	9.48
	branched alkanes	2.70
Z = 0	cycloaklanes	2.02
Total Saturates		14.20
Aromatics		
Z = −6	alkyle benzenes	15.13
Z = −8	indans/tetralins	2.43
Z = −12	naphthalenes	68.22
Total Aromatics		85.78

TABLE 2

Component Type Analysis of the Sample VN-80-41

Saturates		Area %
Z = +2	n-alkanes	30.42
	branched alkanes	23.66
Z = 0	cyclohexane	14.24
Z = −2	decalins	0.62
Total Saturates		68.94
Aromatics		
Z = −6	alkyl benzenes	26.40
Z = −8	indans/tetralins	0.46
Z = −2	naphthalenes	4.29
Total Aromatics		31.15

II. HRMS Analysis of Nitrogen Concentrates from Hydroprocessed Shale Oil

It is important to characterize nitrogen containing species in both crude and hydroprocessed shale oil for several reasons: nitrogen containing species oxidize and can form gums and gels that are detrimental to fuel storage stability, they can form environmentally hazardous compounds, NO_x, upon burning, and optimization of catalytic hydrotreating processes requires knowledge of the types of nitrogen compounds present. To obtain a comprehensive characterization of nitrogen species several analytical techniques are employed. These are: column chromatography to provide simpler fractions from a complex oil, IR spectroscopy to identify major functionalities present in each fraction, differential titration (DT) to determine acid/base strengths of major species within each fraction, and HRMS for identifying compound types, their carbon number range, and their relative contribution to each fraction.

The column chromatographic separation scheme used for analysis of nitrogen concentrates splits the oil into 5 nitrogen containing fractions: pyridine 1, pyridine 2, pyrrole, pyrrole/arylamine, and amide/pyridine 3.[1] These names are chosen because they represent the major functionalities present in each fraction. The 3 different pyridine types have different structures attached to the basic pyridine ring. An example of the type of data available from DT is shown in table 3. This table summarizes the results of the analysis of the pyridine 2 fraction from a hydroprocessed diesel fuel marine

TABLE 3

Base Types for P2 Fraction from Diesel Fuel Marine

Base Type	pKa	wt. %
Strong Base	9 to 11	
Weak Base I	7 to 9	91
Weak Base II	2 to 7	
Very Weak Base	-2 to 2	6
Non-Basic		3

distillate cut. The weight percent contribution of nitrogen containing species to 5 different base types is measured. This data provides an indication of the chemical nature of the species in the pyridine 2 fraction and can be related to the ease with which they can be hydrotreated.

Table 4 gives a partial listing of the results of the HRMS analysis of the same pyridine 2 fraction. Data was obtained using two different ionizing voltages: 12 V and 70 V. For the 12 V data primarily only parent species are seen. The ratio of the individual series intensity to the summed intensity of all series is the "series intensity" value at 12 V. For the 70 V data the method of Peters and Bendoraitis[2] was used to analyze the data. Here P^+ and $(P-1)^+$ are summed and the sum is treated in the same manner as the P^+ series in the 12 V data. Table 4 shows that there is good agreement between the two methods, and since each has certain analytical advantages, both methods have been used in the analysis of nitrogen concentrates. Use of column chromatographic retention information and the functional information provided by IR enables compound types to be suggested for each series in the pyridine 2 fraction, as shown in table 4.

TABLE 4

HRMS Analysis of P2 Fraction from Hydrotreated Diesel Fuel Marine

Formula Type	Series Intensity 12V.	70V.	Suggested Compounds
$C_nH_{2n-5}N$	.29	.28	Pyridines + other
$C_nH_{2n-7}N$	.19	.22	Naptheno Pyridines
$C_nH_{2n-9}N$	.40	.33	Di-Naptheno Pyridines
$C_nH_{2n-11}N$	.09	.11	Quinolines
$C_nH_{2n-13}N$	.02	.03	Naptheno Quinolines

(cont.)

The compound types suggested for each series have reasonably well defined pKa values and thus can be classified as strong base, weak base I, etc. By summing the series intensities that fall into each of the base classifications, the HRMS data can be compared with the DT measurements made on each fraction. This comparison is shown in Table 5. For the five nitrogen fractions listed across the top of the table, the DT and the HRMS results are given. The HRMS measurements are listed above the dividing line, the DT results are below the line. In nearly all cases the agreement is within 10% absolute. This is surprisingly good considering that there are several factors which could cause differences between the DT and HRMS results. These factors are: 1) The pyrrole (PYR)

TABLE 5

DT (wt. %) and HRMS (M+M−1) Analysis of Hydrotreated Diesel Fuel Marine (70V)

Base	P1	P2	AM/P3	PYR	PYR/AR
Strong			12/3		
Weak I	100/92	99/91	61/62		
Weak II			6/12	3/0	72/84
Very Weak	0/8	0/6	16/24	81/60	19/16
Non-Basic		1/3	9/0	19/40	9/0

and pyrrole/arylamine (PYR/AR) fractions are difficult to analyze completely because of volatility problems (Polymerization, oxidation, and gel formation occur quite rapidly in these fractions. Their character can change dramatically even though they originally were distillable in the diesel fuel marine cut.). 2) Using low ionizing voltage HRMS, bi-modal distributions of parent intensities are seen for several of the series. This indicates that perhaps there is more than one compound type and thus base type contributing to the series. 3) There is some uncertainty in the application of the Peters and Bendoraitis method to these nitrogen concentrates. There are no independent methods of analysis for these materials with which the results from applying this method can be compared. It is interesting that the method works so well even without any sensitivity corrections for the various series.

One can conclude from the comparison presented in table 5 that HRMS can provide a reasonably quantitative weight percent measure of the compound types and base classes present in nitrogen concentrates from hydroprocessed shale oils. Using this technique both distillate fractions and whole oils have been characterized. Several species believed to be reaction intermediates in catalytic hydroprocessing have also been identified. These include alkyl amines/alkyl piperidines and alkyl anilines. These species are not found in the raw shale oil and must be produced during the hydrotreating process. Careful consideration of the effect of hydroprocessing conditions on the various types of compounds should enable refineries to both remove noxious compounds and deliver a better fuel product.

References

[1]S.A. Holmes and L.F. Thompson, "Nitrogen-Type Distribution in Hydrotreated Shale Oils: Correlation with Upgrading Process Conditions", 14th Oil Shale Symposium Proceedings, Colorado School of Mines Press, pp 235-248.

[2]A.W. Peters and J.G. Bendoraitis, "High Resolution Mass Spectrographic Method for the Analysis of Nitrogen-and Oxygen-Containing Material Derived from Petroleum", Anal. Chem. 48, pp 968-973 (1976).

GC/MS/C ANALYSIS OF PARAHO SHALE OIL <400°F

By E. J. Gallegos
Chevron Research Company, Richmond, California 94802

A B S T R A C T

Paraho shale oil <400°F was analyzed by GC/MS/C with the intent of establishing a preliminary set of guidelines and conditions under the auspices of ASTM for the GC/MS analysis of shale oil.

A 60-meter DURABOND-1, DB-1, fused silica capillary column coupled directly to our fast scanning 7070H double-focusing mass spectrometer was chosen. GC/MS/C operating parameters were selected so that the total ion monitor, TIM, GC trace would match that of an FID GC trace obtained previously under optimized conditions for a DB-1 column.

Preliminary results show the presence of homologs of n-alkanes, isoalkanes, alkenes and/or cyclic alkanes, alkyl benzenes, naphthalenes, indanes, tetralins, thiophenes, pyridines, analines, indoles, phenols, etc.

The data were reduced using an automatic quantitation INCOS computer procedure designed by J. Karnofsky specifically for this laboratory.

Instrumentation

The analysis of Paraho shale oil <400°F was performed using a 60-meter DB-1 fused silica capillary column from J and V Scientific in a 5700A Hewlett-Packard gas chromatograph. The column was coupled directly to the source of a VG 7070H double-focusing mass spectrometer tuned to a resolution of ~1000.

The column was programmed from 30°C to 200°C at 1°C/minute. Data were collected using a magnet scan cycle of 1.5 seconds from mass 12 to 300 using an INCOS instrument control and data collection computer system.

A 0.005 µl sample was injected using a 1 µl No. 7001 Hamilton syringe. The injection port is designed so that the needle is received by a 0.03-inch sleeve which couples to either 0.010-inch OD fused silica column or 0.03-inch OD stainless steel columns.

Sample

The Paraho shale oil sample was obtained from the Laramie Energy Research Center specifically for method development and use by ASTM Subcommittee E-14.

Results and Discussion

Qualitative Aspects

Figure 1 shows the gas chromatogram, FID, detection trace of the Paraho shale oil <400°F using a 60 M DB-1 fused silica capillary column. This is compared to that obtained using a second 60 M DB-1 column on the GC/MS/C system. Note comparable resolution of the traces.

Figure 2 is the even mass intensity retention time MAP of the C_nH_{2n+2} and C_nH_{2n-12} components in Paraho shale oil. The mass chromatographic peaks include n-C_6 to n-C_{17} normal alkanes and C_{13} to C_{16} isoalkanes. The latter are very likely the α-methyl alkanes. The blue colored mass chromatographic peaks include naphthalene, the two methyl naphthalenes, and the (2C, 3C, 4C) naphthalenes. This is only one of seven possible maps on the sample.

Quantitation

The automatic quantitation procedure first determines the total area from the reconstructed ion chromatogram, then the data are enhanced, i.e., by background subtraction,

deconvolution, smoothing, etc., then individual GC peaks are quantitated by area and compared to a library entry. Those peaks which do not match a library entry within a 50-100% fit limit are put into an "unknown" list along with their areas. Those GC peaks which do not match a library entry are put into a "known" list along with the area. The "known" list entries are then grouped along with the area. The "known" list entries are then grouped along with their subtotaled aras into their respective z category, where z = 2 to z = -16. z comes from the formula C_nH_{2n+z}. A final summary lists the z categories found in the sample, the number of components, and the concentration of all components within a z category. The automatic quantitation procedure, designated GCK, produced the summary in Table I.

An example of the automatic quantitation procedure output are shown in Table II.

Table I

	Number	Total, %
Unknowns	100	13.4
z = +2	52	33.84
z = 0	61	15.47
z = -1	2	0.58
z = -2	1	1.03
z = -4	7	0.42
z = -5	6	0.83
z = -6	50	9.03
z = -7	3	0.41
z = -8	26	4.11
z = -9	2	0.11
z = -10	8	0.8
z = -11	1	0.1
z = -12	14	4.1
z = -14	1	0.10
z = -16	1	0.03

In some cases, the same identification will be given to two or more different GC peaks. This means that their mass spectra are very similar and the same library entry gave the best fit. The category in which they are entered, however, is probably correct. In some cases, a component is identified but the concentration is below 0.01% of the entry. Found is given. The total concentration of identified components and unknowns will be under 100%. The difference is background noise, column bleed, and baseline computation differences between total GC area and individual peak area.

At a resolution of ~6000, mass chromatograms were obtained from CH_2N+, CHS+, $C_2H_{50}+$, etc., shown in Figures 3 and 4.

This converts the MS into an elemental specific detector showing the location of S, N, and O compounds in a GC/MS run.

Conclusions

Optimum conditions for the GC/MS/C analysis of a sample containing heteropolar and nonpolar hydrocarbons such as Paraho shale oil, thus far, includes the use of a DB-1 fused silica column and a mass spectrometer which can scan at a cycle rate of at least 1.5 sec. from mass 10 to ~350.

Shale oils contain a fair amount of nitrogen- and oxygen-containing species. Paraho shale oil, for example, showed the presence of pyridines, indoles, phenols, ketones, alkane and cyclic alcohols, and some indication of NO compounds.

The automatic quantitation procedure, GCK, is only a first approximation, 50% or better, fit of identified to actual components in a GC/MS run.

TABLE II

QUANTITATION OF PARAHO SHALE OIL <400°F
ARRANGED BY Z CATEGORY

		Scan	Ret Time	Conc
Z = -3	C_nH_{2n-1}			
1	7-AZABICYCLO[4.1.0]HEPTANE, 1-METHYL-	2699	67:17	0.12
2	PYRIDINE 2,3,4,5-TETRAMETHYL-	3161	79:01	0.27
Z = -2	C_nH_{2n-3}, C_nH_{2n-10}			
2	CYCLOPENTENE,1,3-DIMETHYL-	512	12:48	0.09
3	BICYCLO[3.2.1]HEPTANE	553	13:49	0.08
4	CYCLOPENTANE,1-METHYL-2-(2-PROPENYL)-, TRANS-	629	29:12	0.03
5	CYCLOPENTANE,2-ETHYL-1,1-DIMETHYL-	924	23:04	0.25
6	CYCLOPENTANE,1-ETHYL-2-METHYL-,1,2-DIMETHYL-	926	23:12	0.25
7	CYCLOPENTANE,1 1'-ETHYLIDENEBIS-	1073	26:49	0.07
8	4-NONYNE	1263	31:34	0.01
9	FURAN,2 3-DIHYDRO-3-METHYL-	1309	32:43	0.03
10	CYCLOHEXENE, 1,2-DIETHYL-	1393	34:49	0.04
11	CYCLOHEXENE, 1-BUTYL-	FOUND		
12	PROPANE, 2-(1-METHYLETHYL)CYCLOPROPYLIDENE)-	1652	41:18	0.22
13	CYCLOHEXANE, METHYLENE-	1973	49:16	0.01
14	PROPANE, 2-(2-ISOPROPYL-1-BENE-3 METHYLCYCLOPROPYL)-,	FOUND		
15	17-HEPTADECYN-1-OL	2490	62:15	0.02
16	1,11-DODECADIENE	2645	71:04	0.23
17	CYCLOHEXANE, 1,1'-(1-BUTYL)-2,1-ETHANEDIYL)BIS-,4-METHY	3078	76:45	0.27
18	2-OCTENAL, 3-BUTYL-	FOUND		
19	2,5-DODECADIENE,3,8-METHYL-	3321	83:01	0.05
20	6-OCTEN-1-OL, 3,7-DIMETHYL-, PROPANOATE	3383	84:34	0.47
21	4-OCTANONE,2,2-EPOXY-2-METHYL-	3573	89:19	0.42
22	BICYCLO[4.1.0]HEPTANE,2-METHYL-7-(METHYL-	FOUND		
23	BUTANE, 1,4-BIS(CYCLOPENTYL-	3880	95:00	0.03
24	CYCLOHEXENE, 2,3,5-TRIMETHYL-	4048	133:42	0.02
Z = -4	C_nH_{2n-4}, C_nH_{2n-12}, C_nH_{2n-16}			
2	2-CYCLOPENTENE-1-THIONE, 3-METHYL-	238	11:38	0.01
3	THIOPHENE,2,3,5-TRIMETHYL-	245	12:15	0.01
4	CYCLOHEXANOL, 1-ETHYNYL-	342	17:06	0.02
5	THIOPHENE,2,3,4-TRIMETHYL-	434	21:42	0.06
6	THIOPHENE,2,3,4-TRIMETHYL-	FOUND		
7	1-CYCLOHEXENE-1-CARBOXALDEHYDE,2,6,6-TRIMETHYL-	684	34:32	0.04
8	3R,7-METHANO-3AH-CYCLOPENTACYCLOOCTENE, DECAHYDRO-3	1767	88:21	0.26
Z = -5	C_nH_{2n-18}			
2	PYRIDINE,4-ETHYL-	382	15:06	0.02
3	PYRIDINE,2,3,5-TRIMETHYL-	546	27:18	0.06
4	PYRIDINE,2,3,5-TRIMETHYL-	568	28:24	0.06
5	PYRIDINE,2,3,5,5-TRIMETHYL-	FOUND		
6	BENZENAMINE,2,3,4,5,6-PENTAMETHYL-	1888	49:00	0.20
7	PYRIDINE,2,3,5-TRIMETHYL-	1983	93:09	0.05

TOTAL + CHROMATOGRAM MAP
12/01/81 15:13:00
SAMPLE: PARAHO SHALE <400F

DATA: YC225.01
SCANS 1 TO 2568
SCANS 86 TO 298

Figure 1

TIM AND FID TRACES OF
PARAHO SHALE OIL <400°F

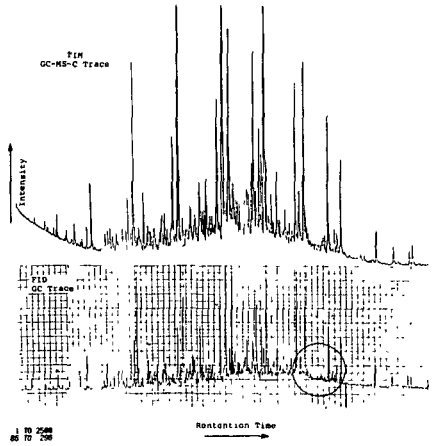


Figure 2

MAP OF THE C_nH_{2n+1} ...12 COMPONENTS
ALKANES, ORANGE, AND NAPHTHALENES BLUE

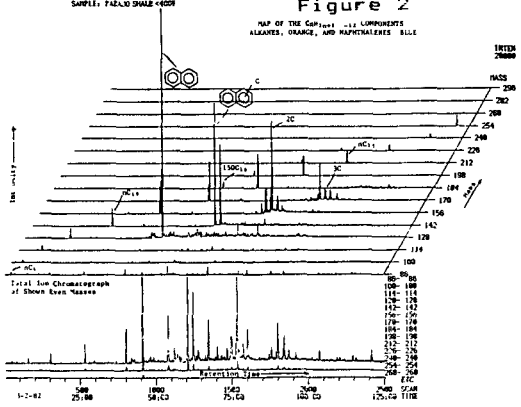


Figure 3

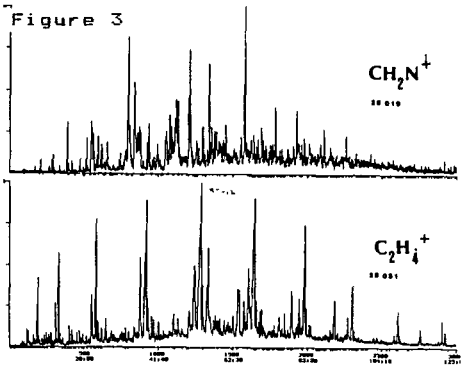
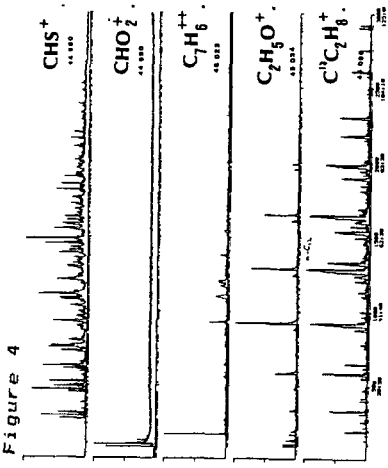


Figure 4



GC/MS Comparison of Selected Ketones and Nitriles in Green River and Australian Shale Oils

R. J. Pancirov, T. R. Ashe, W. K. Robbins
Exxon Research and Engineering Co., Linden, NJ

A series of aliphatic ketones and nitriles have been identified in Green River and Australian shale oils. The shale oils were subjected to an extensive separation scheme to isolate the ketones and nitriles.

The procedure involves separation on silica gel that has been 10% water deactivated with an elution program of n-pentane (saturates), 6% CH_2Cl_2/94% n-pentane (aromatics), 50% CH_2Cl_2/50% n-pentane (neutral nitrogens), 10% C_2H_5OH/90% CH_2Cl_2 (basic nitrogens) and C_2H_5OH (polars). The neutral fraction was subdivided into three fractions using an isopropyl alcohol elution from sephadex LH-20. The first fraction off the sephadex contained nitriles and ketones, the second fraction also contained ketones, and the third fraction is a N-PNA concentrate.

The nitrogen in the neutral nitrogen fraction from the silica gel separation amounts to c. 18% for the Australian oil and 26% for the Green River oil. The Green River neutral nitrogen fraction covered C_{11} to C_{33}. The bulk of the nitrogen containing material was of the indole - carbazole type. There was very little material of the nitrile type present in the Green River shale oil.

The ketone content of the Green River oil fraction accounted for a considerable portion of the sample. The ketones were located by using a selected ion chromatogram of the m/z 58 rearrangement ion. This ion is characteristic for just about all aliphatic ketones but is very specific for methyl ketones. The methyl ketones covered the range from C_{11} to C_{33}.

A detailed examination of the spectra which exhibited a m/z 58 rearrangement ion showed that they are the methyl, ethyl, propyl, butyl, etc., ketones. There are therefore a series of ketones present at each carbon number. We also found in Green River oil the C_{18} isoprenodial ketone derived from pristane probably through bacterial action. In addition to this biomarker ketone we also found a pentacyclic ketone of the hopane type.

The Australian shale exhibited a cleaner RIC than did the Green River neutral nitrogen fraction. This is mainly due to the fact that the primary nitrogen containing materials in this shale oil are of the straight chain alipahtic nitriles. Additionally, in the Australian shale oil, the same ketone distribution was observed as in the Green River material.

There was an anomaly in the nitrile distribution of the Australian shale oil. This was a material which was present in high concentration and exhibited a parent ion at m/z 405.

FOB 4 APPLICATION OF MASS SPECTROMETRY TO PETROLEUM EXPLORATION; W. K. Seifert, J. M. Moldowan, and E. J. Gallegos; Chevron Oil Field Research Company, Richmond, California 94802.

Compounds significant to the petroleum chemist concerned with petroleum exploration are those hydrocarbons possessing biological marker characteristics, i.e., possessing intact steroid, terpenoid, and isoprenoid skeletons. These hydrocarbons are so closely related to the compounds occurring in the living organism from which petroleum was formed that they are capable of yielding very specific information regarding source, maturation, migration, and biodegradation of petroleum. Examples how source shales can be related to petroleum reservoirs using computerized GCMS are shown. The terpane GCMS MAP approach can be used to differentiate source shales of different degree of maturity and, thus, to determine source rock quality. Heavily biodegraded oils can be characterized and correlated by GCMS fragmentograms of steranes and terpanes. Ratios of specific biomarkers obtained by quantitation from GCMS data are used to differentiate oils of different degree of migration. Examples from the exploration arena worldwide are given to illustrate these applications.

FOB 5 COMBINED GAS CHROMATOGRAPHY-MASS SPECTROMETRIC ANALYSIS OF SELECTED SULFUR COMPOUNDS IN OIL SHALE RETORT GASES; F. D. Guffey and W. E. Blanton; Laramie Energy Technology Center, Department of Energy, Laramie, WY 82071

Analysis of low-molecular-weight, sulfur-containing species generated during the retorting of oil shale is important for both environmental and engineering considerations. Combined gas chromatography/mass spectrometry (GC/MS) was chosen as a potential nonroutine method of analysis of these compounds as they are sampled in the gas collection system of an oil shale retort. An on-line sampling and collecting system was designed to collect the samples and introduce them into the instrument for real-time analysis. Selected sulfur-containing species found in the parts-per-million range have been quantified using this method and verified with an external standard. Hydrogen sulfide was confirmed to be the most abundant sulfur-containing species present in the production gas. Other species determined to be present in the gas at significant concentrations include methylmercaptan, carbonyl sulfide and carbon disulfide. The advantages of using the GC/MS method for the analysis and the suggested applications of this method to engineering and environmental sciences will be discussed.

MASS SPECTRAL CHARACTERIZATION OF THE ACID AND BASE FRACTIONS FROM AN EASTERN AND WESTERN SHALE OIL

Gil J. Greenwood, Phillips Petroleum Company, Research and Development, Bartlesville, Oklahoma 74004

Oils from an eastern and a western shale oil sample were separated into acidic, basic and neutral fractions by anion- and cation-exchange chromatography and analyzed by low resolution field ionization and high resolution 70 eV mass spectrometry. Methylene chloride replaced benzene in a modified separation scheme.[1] Table I lists the weight per cent and volatility data for the acids, bases and neutrals from both oils. The western shale oil contained approximately 3 times the concentration of acids and 2.5 times the percentage of bases in the eastern shale oil. The volatility of the eastern shale oil acids and bases was considerably higher than the corresponding western fractions.

The singly oxygenated compound types identified in the eastern shale oil acid fraction are summarized in Table II. The mass spectra were dominated by ions at m/z 122, 136, 150 and 164 consistent with the presence of benzoic acids. The remaining single oxygen components were identified as phenolic with an average of six carbons exocyclic to the parent compounds. The type of side chain (i.e., branched vs. linear) can not be determined from the mass spectral data. However, infrared data show an absorption at 720 cm^{-1} which indicates unbroken methylene units. This suggests that the carbon structure exocyclic to the basic phenolic nucleus is a singly or doubly substituted unbranched side chain. Several doubly oxygenated species summarized in Table III were also detected in the eastern shale oil acid fraction. For the doubly oxygenated materials the number of carbons exocyclic to the nucleus generally averaged four. The exceptions were the $-14(O_2)$ series and the $-16(O_2)$ series which ran 13 and 8 carbons long, respectively. The parent formulas are also consistent with either acids and/or furanols. Because of the limited analytical data available on eastern shale acids, an exact statement of composition for the doubly oxygenated compounds can not be made at this time.

Greater than 70% of the western shale acids was made up by three compound types summarized in Table IV. The major component in this fraction was benzoic acid. Another significant feature of this fraction was the presence of a series of aliphatic acids ranging from $C_7H_{14}O_2$ to $C_{32}H_{64}O_2$. Previous analysis of western shale oil acids from the Green River formation has shown these compounds to be a characteristic feature of western shale oils.[2,3] The large suite of phenol types observed in the eastern shale oil acids was not detected in the western sample.

The mass spectral data for the single nitrogen containing compounds in the eastern and western shale oil bases are summarized in Table V. Azaaromatic compound types consistent with each z series are drawn. However, isomers with the nitrogen exocyclic to the aromatic nucleus are also possible.[5-7] A number of differences between the different base fractions can be seen in Table V. The number of carbons exocyclic to a given z series nucleus is much higher in the western bases than the eastern bases, an average of 22 and 15, respectively. As with the acids, mass spectrometry can not detail the exact nature of the carbons substituted on a given nucleus. However, infrared data support the presence of unbranched alkyl substituents in the eastern shale bases. The base fraction isolated from western shale oil appears to have either greater substitution by shorter alkyl side chains or more branching in the alkyl substituents than the eastern sample. The mode for both the eastern and western compound distributions occurs, on the average, four carbons exocyclic to the base compounds. Lastly, only compounds up to the z=-27(N) series were detected in the western shale bases whereas the eastern base fraction showed compound types up to the z=-33(N) series.

Compounds containing both nitrogen and oxygen were detected in the eastern and western shale oil base fractions from z=-5(NO) to z=-19(NO). No attempt has been made to assign a tentative structure because of the functional combinations possible with N and O and because of the limited knowledge concerning the basicities (pK_b) of NO compounds isolated from shale oils. Infrared data suggest some amide type absorptions. Therefore, it is possible that some of the N, O structure is in the form of amides.

References

1. Jewell, D. M.; Weber, J. H.; Bunger, J. W.; Plancher, H.; Latham, D. R., Anal. Chem., 44, 1391 (1972).
2. Lawler, D. L. and Robinson, W. E., Am. Chem. Soc., Div. Petrol. Chem., Prepr., 10(1), 5 (1965).
3. Burlingame, A. L. and Simoneit, B. R., Am. Chem. Soc., Div. Petrol. Chem., Prepr., 13 (2) F132 (1968).

References (Cont'd.)

4. Dinneen, G. U.; Cook, G. L.; Jensen, H. B., Anal. Chem., 30 (12), 2026 (1958).
5. Simoneit, B. R.; Schnoes, H. K.; Haug, P.; Burlingame, A. L., Chem. Geol., 7, 123 (1971).
6. Poulson, R. E., Am. Chem. Soc., Div. Fuel Chem., Prepr., 20 (2), 183 (1975).
7. Ford, C. D.; Holmes, S. A.; Thompson, L. F.; Latham, D. R., Anal. Chem., 53, 831 (1981).

TABLE I

SEPARATION AND VOLATILITY DATA FOR AN EASTERN AND WESTERN SHALE OIL

	Weight Per Cent in Eastern Shale Oil[b]	Weight Per Cent in Western Shale Oil[c]	Per Cent volatiles in 21-1100[a] Eastern Shale Oil	Per Cent volatiles in 21-1100[a] Western Shale Oil
Acids	2 6	10 0	62.1	51.5
Bases	15 0	38.2	70 5	43.0
Neutrals	80 3	49.9	78 7	83 0
Total Recovery	96.3	96.0		

[a]Samples were volatilized at 300°C and 10^{-5} torr

[b]Represents 73 4% of the total liquid

[c]Represents 62 7% of the total liquid

TABLE II

SINGLY OXYGENATED COMPOUNDS DETECTED IN EASTERN ACID OILS

Z#	Compound Type	Parent Formula	Exocyclic C's
-6(O)		C_7H_6O	4
-8(O)		$C_{10}H_{12}O$	6
-12(O)		$C_{10}H_8O$	7
-14(O)		$C_{12}H_{10}O$	6
-16(O)		$C_{13}H_{10}O$	7
-18(O)		$C_{14}H_{10}O$	6
-20(O)		$C_{15}H_{10}O$	7
-22(O)		$C_{16}H_{10}O$	6
-26(O)		$C_{18}H_{10}O$	4

TABLE III

DOUBLY OXYGENATED COMPOUNDS DETECTED IN EASTERN ACID OILS

Z#	Compound Type	Parent Formula	Exocyclic C's
-8(O$_2$)		$C_7H_6O_2$	3
-14(O$_2$)		$C_{14}H_{14}O_2$	13
-16(O$_2$)		$C_{13}H_{10}O_2$	8
-18(O$_2$)		$C_{16}H_{14}O_2$	4
-20(O$_2$)		$C_{18}H_{16}O_2$	4
-24(O$_2$)		$C_{19}H_{14}O_2$	4

TABLE IV

MAJOR COMPONENTS OF WESTERN SHALE ACID OIL FRACTION

Z#	Compound Type	Parent Formula	Exocyclic C's
-0(O$_2$)		$C_{17}H_{34}O_2$	25
-6(O)		C_6H_6O	8
-8(O$_2$)		$C_7H_6O_2$	4

TABLE V

NITROGEN COMPOUND TYPES PRESENT IN EASTERN AND WESTERN SHALE OIL BASE FRACTIONS

Compound Type	Starting Member	Eastern Exocyclic C#	Eastern Mode C#	Western Exocyclic C#	Western Mode C#
	$C_9H_{11}N$	14	4	25	4
	$C_9H_{11}N$	11	3	25	4
	C_9H_9N	16	5	21	4
	$C_{10}H_9N$	15	3	20	4
	$C_{12}H_{11}N$	16	4	22	4
	$C_{12}H_9N$	12	3	23	4
	$C_{13}H_9N$	16	4	22	4
	$C_{15}H_{13}N$	17	4	17	4
	$C_{16}H_{11}N$	17	4	16	4
	$C_{17}H_{11}N$	17	4	14	4
	$C_{20}H_{15}N$	17	-	11	3
	$C_{19}H_{11}N$	13	4	-	-
	$C_{20}H_{13}N$	11	-	-	-
	$C_{21}H_{13}N$	11	-	-	-
	$C_{21}H_9N$	15	3	-	-

FOB 7 PYROLYSIS-MASS SPECTROMETRY STUDIES OF OIL SHALE AND OIL SHALE KEROGENS: Henk L.C. Meuzelaar, Alice M. Harper; Biomaterials Profiling Center; Jean H. Futrell; Biomaterials Profiling Center and Department of Chemistry, University of Utah, Salt Lake City, UT 84112; and Steve Larter; Union Oil, Brea, CA.

Pyrolysis mass spectrometry has been established as a valuable technique for characterizing chemical compounds, mixtures and materials of high molecular weight and/or limited volatility. New instrumental methods - fast scanning mass analyzers, molecular beam sampling, automated sampling, tandem mass spectrometry - for Py-MS developed by this laboratory have been described at the 1980 and 1981 Annual Conferences of the ASMS. The present paper will describe the applications of these methods to the analysis of oil shales and separated kerogens.

A focus of our recent research has been the development of multivariate statistical methods for processing the enormous amount of data generated by Py-MS. These programs monitor the self-consistency and reproducibility of the data, providing objective criteria for rejecting inappropriate data. Pattern recognition and factor analysis identify chemical characteristics within the pyrolysis patterns. The most distinguishing features - individual mass peaks or linear combinations - may then be investigated further by time-resolved or tandem Py-MS to characterize the samples in more detail.

Although our work has emphasized kerogen from Green River shale from the Piceance Basin of Utah/Colorado, data will also be presented on kerogens from other shales as well as from alginite rich coals and coal macerals. It will be shown that this rapid, highly-automated technique provides chemical information strongly complementary to the data obtained by more conventional methods in use for oil shale characterization.

FIELD IONIZATION MASS SPECTROMETRIC ANALYSIS OF SATURATES IN SHALE OIL

S. E. Scheppele and Q. G. Grindstaff

Bartlesville Energy Technology Center, U.S. Department of Energy, Bartlesville, OK 74005

Unlike ASTM 2786(1), field-ionization mass spectrometry should be capable of providing carbon-number distributions for saturated hydrocarbons. The sensitivities for saturates are dependent upon hydrocarbon structure (2) and are altered by the addition of acetone (3). Consequently, sensitivities were determined for FI of 37 saturated hydrocarbons in the 2(H;H), 0(H;H), -2(H;H), and -4(H;H) Z series in the presence of acetone. The FI sensitivities used in quantitative analysis were determined at acetone concentrations resulting in relative sensitivities independent of the partial pressure of acetone.

Let p and r represent the first homolog in a specific-Z series and the reference compound, respectively, and $(\Delta/C_i)_p$ be the variation of the relative FI mole sensitivity on carbon-number in a specific-Z series (2). The variation in the relative gram sensitivity in a given Z series has a slope, M, equal to

$$M = MW_p \left[1 - \frac{(\Delta/C_i)_p (MW)_p}{14} \right].$$

If the relative mole sensitivity is carbon-number independent, i.e., $\Delta/C_i = 0$, then $M = MW_p$. If $\Delta/C_i > 0$ or $\Delta/C_i < 0$, then M will be less than or greater than MW_p, respectively.

A plot of the gram sensitivities for FI of alkanes relative to the gram sensitivity for FI of decalin versus MW^{-1} is shown in the Figure. The least-squares fit of $s(g)_i$ to MW^{-1} is excellent. Since the FI sensitivities must be greater than zero the functional form of $s(g)_i$ on MW^{-1} must change at a carbon number less than 28. Preliminary results suggest that this phenomenon occurs at a carbon number of *ca.* 26 as indicated in the Figure. Acetone enhances the sensitivity for carbon numbers less than this value but appears to have a much smaller effect on the sensitivity for alkanes possessing in excess of *ca.* 28 carbons. For present purposes, (Δ/C_i) for the 2(H;H) series was assumed to be zero above C_{28}.

Table 1 summarizes the results obtained for other compounds. Acetone induces a significantly greater falloff in relative gram sensitivity in the 0(H;H) and -2(H;H) series than would be predicted for the normal assumption that $\Delta/C_i = 0$. In contrast, the decrease in the relative gram sensitivity in the -4(H;H) series is less than predicted by a slope of 192. The x-axis intercept for 0(H;H) and -2(H;H) compounds occurs at carbon numbers of 30 and 32, respectively. For predictive purposes Δ/C_i was taken as 0 at carbon numbers equal to or greater than 26 and 30 in these series, respectively.

Tables 2 and 3 present compositional results obtained from FI/MS, 70-eV EI/MS, and GC analysis of the saturates obtained from a hydrotreated shale oil. Direct comparison of the FI and ASTM 2786 results requires that the densities are not varying significantly. Thus, the agreement in the two MS analyses for the 200-325 °C saturates shown in Table 2 is satisfactory although the 70-eV EI/MS analysis did not reveal compounds in the -8 and -10 Z (H;H) series. Likewise, the carbon-number distributions for and the total weight percents of 2(H;H) compounds by FI and by GC, shown in Table 3, are in good agreement. The value 34.4 by GC is a lower limit to the percentage 2(H;H) compounds because the analysis does not explicitly consider branched alkanes.

In contrast, the results in Table 2 reveal that FI and ASTM 2786 yield significantly different results from the 325-425 °C and > 425 °C distillates. The disagreement appears to be inconsistent with density effects. Although the GC results in Table 3 show the presence of significant amounts of n-alkanes in both distillates, the carbon-number distributions are not in good agreement with those obtained

by FI. Realization of agreement between the two analyses would require the presence of significant amounts of branched alkanes having the higher carbon numbers.

In summary, sensitivities for FI of saturates are influenced in a complex manner, which is presently not understood, by addition of acetone. Three different analytical methods yielded reproducible results for 3 saturate fractions having different boiling ranges. The agreement between the methods is quite good for the lowest boiling fraction but very poor for the two higher boiling samples.

1) Annual Book of ASTM Standards, Petroleum Products and Lubricants, II, 24(1977)700.
2) S. E. Scheppele, C. S. Hsu, T. D. Marriott, P. A. Benson, K. N. Detwiler, and N. B. Perreira, *Int. J. Mass Spectrom.*, 28(1978)335.
3) Unpublished results of Q. G. Grindstaff and S. E. Scheppele.

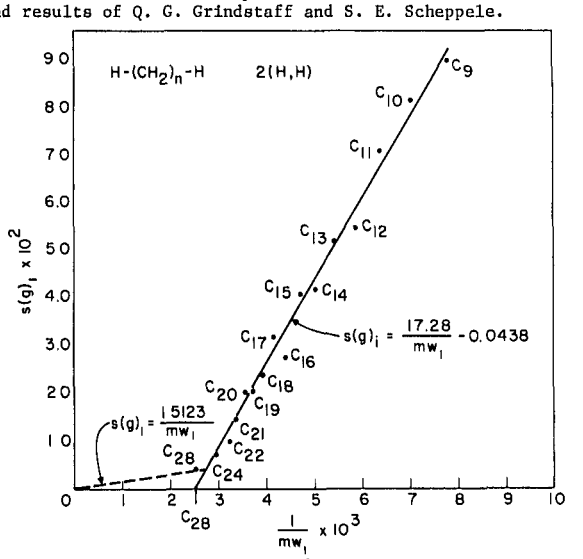


TABLE 1 Carbon-Number Dependence of Relative Mole Sensitivity for FI of Saturates on Reciprocal of Molecular Weight in Presence of Acetone

Compounds	Z(H,H)	$\langle \Delta/C_i \rangle_p$	$M(L\ S)_p^a$	$M(MW)_p^b$	$\frac{M(L\ S)_p}{M(MW)_p}$
Alkanes	2	-0 058[c]	213[c]	142[c]	1 5
Cyclohexanes	0	-0 018	111	84	1 3
Decalins	-2	-0.050	195	138	1 4
Perhydrophenanthrenes	-4	0 021	126	192	0.7

[a] Least-squares slope of relative gram sensitivity versus MW^{-1}.
[b] Slope of relative gram sensitivity versus MW^{-1} for $\Delta/C_i = 0$
[c] Calculated relative to decane rather than methane.

TABLE 2 Compositional Data for Saturate Fractions from Hydrotreated Shale Oil Distillates

Z(H,H)	200-325 °C Distillate Wt % FI	200-325 °C Distillate Vol % ASTM 2786	325-425 °C Distillate Wt % FI	325-425 °C Distillate Vol % ASTM 2786	>425 °C Distillate Wt % FI	>425 °C Distillate Vol % ASTM 2786
2	37 0	42.0	70 2	38 9	59 5	35.9
0	33 0	24 3	15 8	24 1	20 2	23 2
-2	19 5	21 0	6 1	15 2	7 2	11 4
-4	5 9	7.9	3.0	8.8	2 2	18 0
-6	3 1	3.1	2 8	6.9	3 6	6 5
-8	1 3	--	1 4	5 4	6 6	2.6
-10	0 2	--	0 7	--	0 7	2 1

TABLE 3 Carbon-Number Distributions for Z(H,H) Compounds in Saturate Fractions from Hydrotreated Shale-Oil Distillates

	Distillate 200-325 °C			Distillate 325-425 °C			>425 °C		
Carbon No	Wt % FI	Wt % GC	Carbon No	Wt % FI	Wt % GC	Carbon No	Wt % FI	Wt % GC
11	0 9	--	19	2 5	8 7	27	4 6	5 6
12	7 9	9.6	20	3 6	8 5	28	8 1	15 0
13	7.1	7 0	21	3 8	6.6	29	6 8	15.1
14	5.0	5.0	22	4.2	6.3	30	5 9	8 0
15	4.5	4 0	23	5 8	5.6	31	6 6	6.6
16	3.7	3 3	24	7 1	5 4	32	5 5	2 6
17	1 2	3 1	25	9 7	5 5	33	4 7	1 6
18	3.0	2 4	26	12.1	4 6	34	4.8	0 7
19	0.9	--	27	8 2	2 6	35	4.5	0 3
20	0 8	--	28	6 8	0 2	36	5 2	0 1
			29	4.0	--	37	2 8	--
			30	2 5	--			
Total	37 0	34 4		70 3	54.0		59 5	55 6

AN EVALUATION OF TRIPLE QUADRUPOLE MS/MS FOR ON-LINE GAS ANALYSIS OF TRACE SULFUR CONTAINING SPECIES FROM OIL SHALE PROCESSING*

Carla M. Wong and Richard W. Crawford
Lawrence Livermore National Laboratory
Livermore CA, 94550

Richard A. Yost
Univ. of Florida
Gainesville, Florida 32611

Many processes are being evaluated for efficiently releasing oil from oil shale. It is important for both environmental protection and process control to monitor trace levels of sulfur containing species released as part of the gaseous products.

At LLNL we have used computer interactive time-of-flight mass spectrometry to do on-line monitoring of underground coal gasification product gas and have determined that this technique does not have enough sensitivity/selectivity for analysis of sulfur gas species. Other techniques such as GC, Laser Raman and FTIR, have been evaluated in the past at LLNL and other places, and all exhibit problems of either speed, sensitivity and/or selectivity. Therefore, we have used our "home made" triple quadrupole MS/MS to evaluate the applicability of this technique to the sulfur gas analysis problem.

We will describe both the sensitivity and selectivity measured for key mercaptans and thiophenes. A series of pure compounds, known mixes and unknown samples are employed in the evaluation. If funding permits, a commercial MS/MS will be evaluated also.

*Work performed under the auspices of the U.S. Department of Energy at the Lawrence Livermore National Laboratory under contract number W-7405-ENG-48.

FOC 1 STRUCTURAL AND STEREOCHEMICAL INFORMATION FROM TANDEM MASS SPECTROMETRY; M. T. Cheng, M. P. Barbalas, R. F. Pegues, C. J. Proctor, F. Turecek, and F. W. McLafferty, Department of Chemistry, Cornell University, Ithaca, NY 14853

Secondary mass spectra formed by collisionally activated decomposition (CAD) of fragment ions in the mass spectra of unknown molecules can provide specific information on substructures present. Types of fragment ions whose CAD spectra have the greatest structural utility are those which are odd-electron, of the highest abundance, and which have the most hydrogen atoms. Fragment ions produced by chemical ionization often arise from parts of the molecule complementary to those of fragment ions in EI mass spectra. Complementary pairs of fragment ions whose masses and/or elemental compositions total that of the molecule are sought; for each of these pieces further complementary pairs are sought, and this process is continued until the individual ions are small enough to determine their structures with confidence by matching against reference CAD spectra or by interpretation. Repeating the process starting with a different complementary pair from the molecular ion can provide further details as well as confirmation of the structure. Elemental compositions from exact mass measurements in MS-II as well as MS-I are helpful for this pairing. This general approach will be illustrated by applications to steroids, polypeptides, and fentanyl compounds.

Acknowledgement: We are grateful for generous financial support from the National Institutes of Health (grant GM16609).

Dimethyl Ether: A Versatile Reagent Gas for Organic-Functional-Group Recognition by Chemical Ionization Mass Spectrometry, T. Keough, The Procter & Gamble Co., Miami Valley Laboratories, P.O. Box 39175, Cincinnati, OH 45247.

Dimethyl ether (DME) CI is particularly useful for the recognition of organic functional groups. This technique readily differentiates cycloalkanes from alkenes, conjugated and nonconjugated dienes, and some polycyclic aromatic hydrocarbons. It can also differentiate aldehydes from ketones, acids from esters, and alcohols from ethers. Dimethyl ether appears to be more versatile than nitric oxide and it has the added advantage of not requiring a special (Townsend discharge) ionization source. In contrast to methane CI, DME CI exhibits a wide range of sensitivities depending upon the class of compound being ionized.

The intensities of the major ions generated by electron ionization of DME, as a function of source pressure, are given in Fig. 1. The major reactant ions at 0.2 torr are $CH_2{=}OCH_3^+$ and $C_2H_7O^+$. Increased source pressure results in excessive clustering of these ions with neutral DME.

A variety of ionization mechanisms are observed depending upon the functional group(s) present in the organic analyte. The $C_2H_5O^+$ ion abstracts a proton from alkanes and cycloalkanes, yielding $(M-H)^+$ ions, but adds to alkenes, yielding $(M+C_2H_5O)^+$ and $(M+C_2H_5O-CH_3OH)^+$ ions. The double bonds in nonconjugated dienes react independently, while significantly enhanced ratios of $(M+C_2H_5O)^+/(M+C_2H_5O-CH_3OH)^+$ are observed for conjugated diene isomers. This latter result suggests that a cycloaddition process competes with CH_3OH loss from the $(M+C_2H_5O)^+$ ions generated from conjugated dienes. As shown in Fig. 2, the cycloaddition process can also be used to differentiate some polycyclic aromatic hydrocarbons. Anthracene (upper), which is known to undergo Diels-Alder cycloaddition in solution, exhibits an intense $(M+C_2H_5O)^+$ ion in DME CI. Isomeric phenanthrene (lower), which does not undergo cycloaddition in solution, does not yield an abundant $(M+C_2H_5O)^+$ ion in DME CI. As shown in Fig. 3, aliphatic aldehydes and ketones are readily differentiated by DME CI. The ketones yield intense $(M+H)^+$ ions, while aldehydes also yield $(M-H)^+$. Acids and esters are readily differentiated since acids yield intense $(M-OH)^+$ ions while esters yield $(M+H)^+$ and $(M+C_2H_5O)^+$ ions. Finally, alcohols and ethers are readily differentiated by DME CI, Fig. 4. Pentanol (upper) yields $(M-OH)^+$ and $(M+C_2H_7O)^+$ while methyl butyl ether yields $(M-H)^+$ and $(M+H)^+$ ions.

Relative response factors, obtained for a number of molecules differing greatly in gas-phase basicity, are compared in Table 1 with results obtained using CH_4 CI. In contrast to CH_4 CI, DME exhibits a wide range of sensitivities depending upon the functional group present in the organic analyte. This suggests selective ionization applications.

Finally, the reactivity of two other simple oxonium ions, $CH_2{=}OH^+$ and $CH_3CH{=}OC_2H_5^+$, was compared with that of $C_2H_5O^+$ to more fully assess the utility of oxonium ions for analytical CI applications. As shown in Table 2, CH_2OH^+ is $\sim$14 kcal/mole more acidic than DME. Therefore, the ion chemistry of $CH_2{=}OH^+$ is dominated by the non-structure-specific proton transfer reaction. Diethyl ether is $\sim$8 kcal/mole less acidic than DME. Therefore, proton transfer reactions are minimized. However, the $C_4H_9O^+$ ion is $\sim$26 kcal/mole more stable (less reactive) than $C_2H_5O^+$. In fact, the $C_4H_9O^+$ ion is not sufficiently reactive to be useful for general CI applications. Only DME strikes the appropriate compromise between acidity and reactivity required to be useful for organic-functional-group recognition.

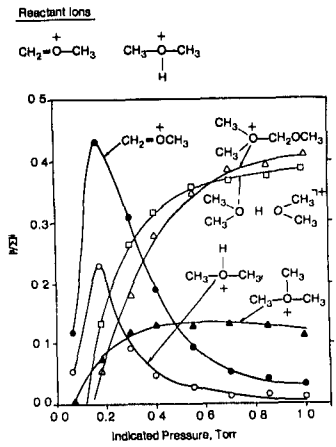


Figure 1: Normalized intensity of reagent ions vs. pressure.

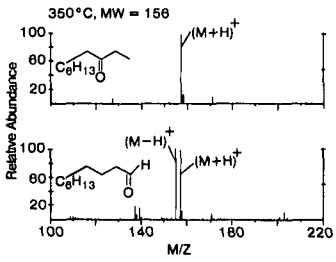


Figure 3: DME CI spectra of 3-decanone (upper) and decanal (lower).

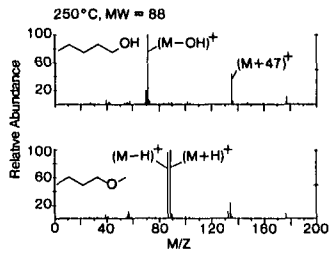


Figure 4: DME CI spectra of pentanol (upper) and methyl butyl ether (lower).

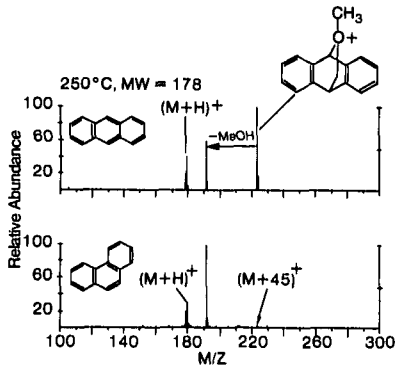


Figure 2: DME CI spectra of anthracene (upper) and phenanthrene (lower)

Relative Response Factors with Methane and Dimethyl Ether Reagent Gases

	Relative Response Factor	
Compound	CH_4	DME
Octane	0.63	0.00
Octene	1.28	0.24
Octyl Bromide	1.17	0.04
Octanol	1.21	0.27
Biphenyl	—	0.16
3-Decanone	1.00	1.00
Dodecanal	0.73	0.04
m-Anisidine	0.55	0.45

Table 1

Summary of Thermochemical Data for Some Simple Oxonium Ions.[a]

Reactant Ion (R^+)	Source (M)	$\Delta H_f(R^+)$	PA(M)
$CH_2{=}O{-}H^+$	$CH_2{=}O$	172	175
$CH_2{=}O{-}CH_3^+$	CH_3OCH_3	157	189
$CH_3CH{=}OC_2H_5^+$	$C_2H_5OC_2H_5$	121	197

a. $\Delta H_f(R^+)$ and PA(M) are expressed in kcal/mole

Table 2

DERIVATIVES FOR THE STRUCTURAL DETERMINATION OF BRANCHED, UNSATURATED AND CYCLOPROPYL LONG-CHAIN ACIDS, ALCOHOLS AND 1,2-DIOLS BY MASS SPECTROMETRY

D.J. HARVEY

University Department of Pharmacology,
South Parks Road,
Oxford, OX1 3QT, U.K.

Wax esters containing a range of normal, branched and unsaturated fatty acids and alcohols are major constituents of several avian and mammalian glandular secretions. Although mass spectrometric methods are available for the structural determination of the constituent acids[1] and to a lesser extent, the alcohols, these are not ideal for a variety of reasons. For example, double bond position can be determined from the spectra of TMS derivatives of glycols prepared by the action of osmium tetroxide on the double bond but the spectra become complicated for the derivatives of polyunsaturated acids. Sample preparation time is lengthy, the reagents are toxic, and the resulting derivatives have high molecular weights. Pyrrolidides partially overcome these problems; their spectra contain a series of ions produced by radical-induced cleavage following hydrogen abstraction from any position of the hydrocarbon chain but the abundance of these ions is very low. There is, therefore, a need for more satisfactory derivatives for structural determination of these long-chain compounds.

Vetter and Meister[2] have recently introduced nicotinyl derivatives for the structural determination of long-chain alcohols. The spectra of these derivatives resembled those of the pyrrolidide derivatives of the acids but the relative abundance of the series of diagnostic ions was much higher. We have adapted this method to the structural determination of fatty acids and have introduced picolinyl derivatives[3], prepared from the action of 3-pyridylcarbinol on the derived acid chloride.

The acid (20 µg) was reacted with an excess (about 100 µl) of thionyl chloride at room temperature for 30 sec. The thionyl chloride was removed with a nitrogen stream and 10 µl of a 10% solution of 3-pyridylcarbinol in acetonitrile was added. This was mixed and allowed to stand at room temperature for 30 sec - 1 min Samples of the resulting esters could be examined directly by GLC or GC/MS, but more usually, and always in the case of biological mixtures, 20 µl of a mixture of BSTFA, TMCS and acetonitrile (2:1:2) was added to silylate any hydroxy compound and the excess of 3-pyridylcarbinol. Samples were examined directly by GC-MS using a V.G. Micromass 12B mass spectrometer interfaced via a glass jet separator to a Varian 2440 gas chromatograph which was fitted with a 2 m x 2 mm (ID) glass column packed with 3% SE-30 on 100-120 Mesh Gas Chrom Q. The mass spectrometer operating conditions were: accelerating voltage, 2.4 kV; electron energy, 25 eV; trap current, 100 µA; separator and ion source temperatures, 300 and 260°C. The gas chromatographic column was temperature programmed from 150 to 300° at 2°C/min for biological samples and held isothermally at a temperature which gave a retention time of about 5 min for the derivatives of individual acids.

Derivatization appeared to be quantitative as judged by GLC and the spectra of the derivatives contained a moderately abundant series of ions produced, as in the case of the pyrrolidides by radical-induced cleavage following hydrogen abstraction by the pyridine ring. The position of chain branching could be determined (Fig. 1) by the fact that a single carbon fragment could not be lost by cleavage of the chain at the branch point and thus the ion which would have represented a one-carbon loss was absent or very weak. This is clearly seen in Fig. 1. Double bond positions were apparent from the spacing of the characteristic series of ions. Normally 14 mass units separated these but where double bonds were present the ion formally representing cleavage through the double bond was weak and adjacent ions were separated by 26 rather than 28 mass units. This pattern was also present in the spectra of polyunsaturated acids. Cyclopropane acids gave similar spectra with the major difference being a very abundant ion representing cleavage through the cyclopropane ring; thus differentiation from the isomeric monounsaturated acids could be achieved and also the position of the ring could be determined.

A series of derivatives of long branched-chain alcohols and diols was examined. Acetates enabled the position of chain branching to be determined by vertue of the high

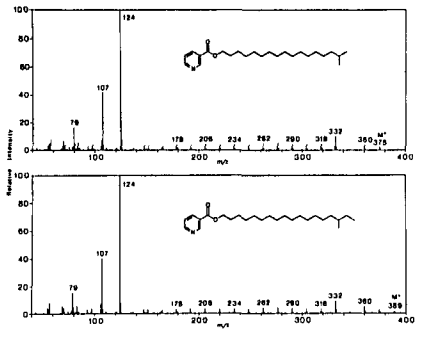


Fig. 1. 25 eV mass spectra of the picolinyl derivatives of iso-octadecanoic acid (top) and anteiso-nonadecanoic acid (bottom).

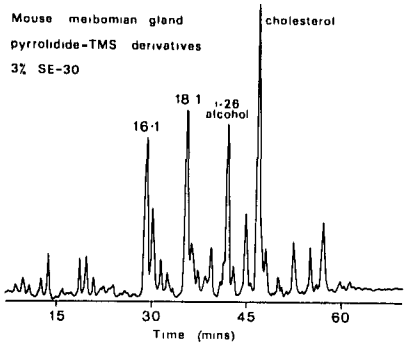


Fig. 2. Total ion current chromatogram of the constituent acids, alcohols and sterols from the meibomian glands of the mouse.

abundance of ions at m/z 56 and m/z 70 in the spectra of iso- and anteiso- methyl branched alcohols respectively. (Methyl group on the ω-1 and ω-2 carbon atoms respectively). The best results, however, were achieved with nicotinates which were applied for the first time to alcohols of the iso- and anteiso- series and to branched-chain diols.

Extracts from mouse meibomian glands were examined using these derivatives. The glands were dissected from the eyelids, washed with ethyl acetate and slit several times with a scalpel blade. The exposed lipids were extracted with ethyl acetate. These were either hydrolysed with NaOH and converted into picolinyl-TMS derivatives as described above or were reacted directly with pyrrolidine and acetic acid to form the amides from the esterified fatty acids[4]. Alcohols were trimethylsilylated in the usual way. Only moderate yields of the picolinyl derivatives were obtained because of the tendency for the acid chlorides to recombine with the meibomian alcohols. The spectra, however, were strong enough to yield the required information on chain structure. Quantitative formation of the pyrrolidide-TMS derivatives was obtained (Fig. 2). The results showed that palmitoleic (16:1,ω7) and oleic (18:1,ω9) acids were the major constituent acids, accompanied by a homologous series of acids belonging to the ω9 series. The major alcohols were cholesterol and iso-hexacosanol. Semiquantitative measurements of the constituent acids and alcohols could be achieved in this mixture using selected ion monitoring of the pyrrolidide-TMS derivatives. Acids were monitored using m/z 113, the base peak, and alcohols were monitored using m/z 103.

Acknowledgements

I thank the Medical Research Council for support under a Programme Research Grant and the Wellcome Trust for additional financial support.

References

1. D.E. Minniken, Chem. Phys. Lipids, 21, 313 (1978).
2. W. Vetter and W. Meister, Org. Mass Spectrom., 16, 118 (1981).
3. D.J. Harvey, Biomed. Mass Spectrom., 9, 33 (1982).
4. B.Å. Andersson and R.T. Holman, Lipids, 9, 185 (1974).

FRAGMENTATION OF 3-DEAZAURIDINE AND SELECTED DERIVATIVES

Karl H. Schram, Department of Pharmaceutical Sciences,
College of Pharmacy, University of Arizona, Tucson, AZ 85721

During an investigation of the fragmentation of modified nucleosides of interest to the NCI as potential antitumor agents, a striking resemblance of the mass spectrum of 3-deazauridine (1) (Figure 1a) to the spectra of cytidine type compounds, most especially ara-C (2) (Figure 1b), was noted. Not only are the m/z values of 1 and 2 coincident as a result of the isobaric base moieties, but the relative intensities of all major fragment ions, except for slight variations, render the spectra almost identical. These results are contrary to a priori expectations where the spectrum of 1 was expected to resemble that of uridine (3) (Figure 1c). The most notable differences in the spectra of 1 and 2 vs 3 are 1) the presence of a strong b+41 ion in 1 and 2 and 2) the virtual absence of a sugar ion ($S^{+\cdot}$) in 1 and 2 and the presence of a very stong S-H ion in the spectrum of 3[1]. These differences are attributed to the facile formation of a b+41 ion in the spectra of 1 and cytidine type compounds but not in 3. Thus, 1 is an exception to the proposal[2] that the presence of a strong b+41 ion is diagnostic of cytidine base.

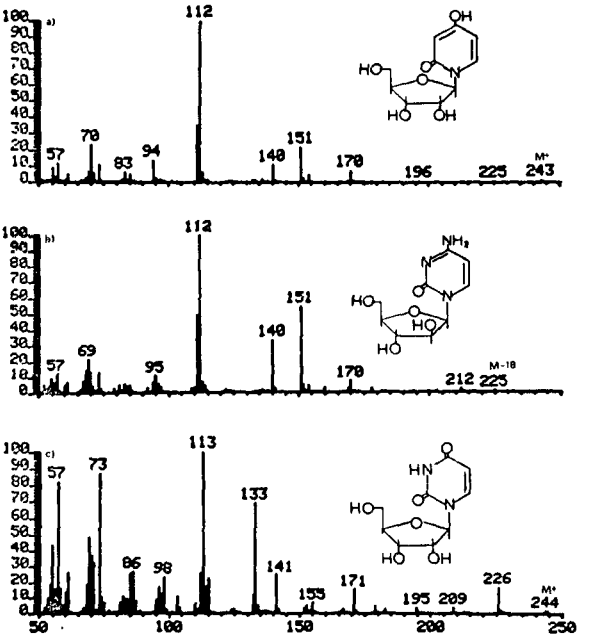


Figure 1.

The spectrum of 3-deazauridine (4) -TMS_4 (Figure 2a) shows fragmentations common to nucleoside TMS derivatives in general[1], but the overall appearance of the spectrum is seen to resemble ara-C-TMS_4 (5) (Figure 2b) to a much greater degree than uridine-TMS_4 (6) (Figure 2c). The similarity of the spectra of 4 and 5 is less striking than with the free nucleosides but the presence of a strong b+41 ion at m/z 223 in 4 and 5 again reflects the similarity of 4 to cytidine type compounds. However, the gas chromatographic properties of 4 are significantly different from 5 so these compounds can be individaully identified.

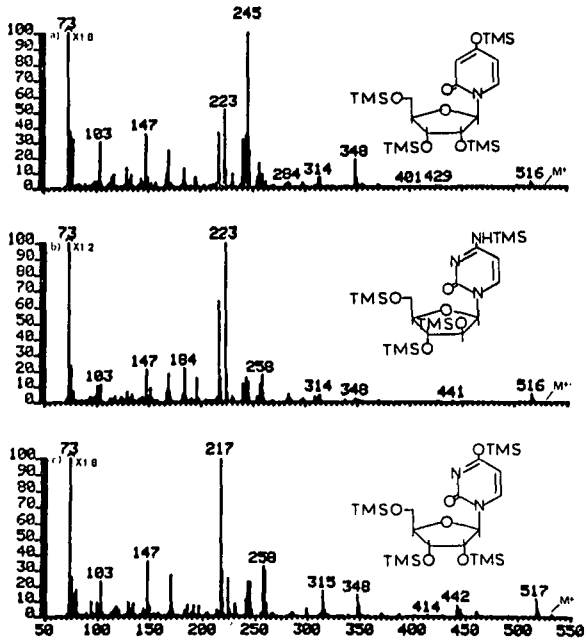


Figure 2.

The fundamental conclusion of this work is that caution should be used in assigning a cytosine base to the structure of an unknown nucleoside based solely on the presence of a strong b+41 ion in the mass spectrum of the compound.

Acknowledgement. This investigation was supported by Grant Number CA24690 awarded by the National Cancer Institute, DHHS.

References

1. J.A. McCloskey, "Mass Spectrometry" in Basic Principles in Nucleic Acid Chemistry, Vol. 1., P.O.P. Tso, Ed., Academic Press, New York, 1974.

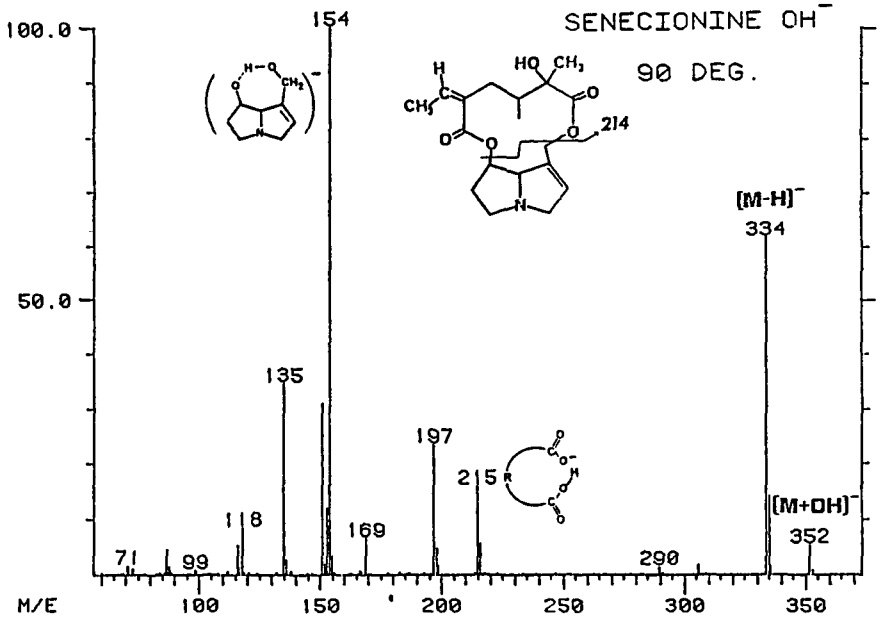
2. J.G. Liehr, D.L. von Minden, S.E. Hattox and J.A. McCloskey, Biomed. Mass Spectrom., 1, 281 (1974).

NEGATIVE ION CHEMICAL IONIZATION MASS SPECTROMETRY OF PYRROLIZIDINE ALKALOIDS

Peter A. Dreifuss, Edward A. Caress(1), William C. Brumley, and James A. Sphon
U.S. Food and Drug Administration, Washington, DC 20204

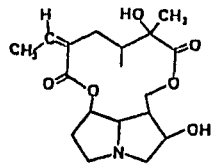
A number of pyrrolizidine alkaloids (PAs) were examined by resonance electron capture (REC) and hydroxide reactant ion (OH-) negative ion chemical ionization mass spectrometry. The purpose of the study was to determine the structural information which could be obtained from these multifunctional esters using these two techniques. The study was aided by the use of high resolution exact mass measurements, mass-analyzed ion kinetic energy (MIKE) spectrometry, and linked B**2/E scans. A major emphasis was placed on the use of OH-.

The 11- or 12- membered macrocyclic ring PAs exhibited abundant (M-H)- ions, (M+17)- ions, and extensive fragmentation when analyzed using OH-. Senecionine, a 12- membered macrocyclic ring PA with an unsaturated necine (the bicyclic pyrrolizidine ring system), is a good example. Its spectrum is shown below. A collisionally induced MIKE spectrum was obtained on the (M-H)- ion at m/z 334 to examine the decompositions occurring from this ion. The most abundant daughter ions were observed at m/z 306, 290, 234, 222, 215, 197, 169, 154, and 135. The (M+17)- ion at m/z 352 was studied by high resolution and collisionally induced MIKE spectrometry. The exact mass was consistent with the elemental composition of an (M+OH)- adduct. The most abundant daughter ions in the MIKE spectrum of m/z 352 were observed at m/z 215, 197, 169, 154, and 153. The fact that daughter ions were obtained (which include no loss of water) from the adduct ion suggests that this interaction of OH- with the PA is a bond to carbon, rather than an attachment to hydrogen or a hydration of the (M-H)- ion. The (M+OH)- adduct has not been reported for other compounds where the OH- was produced with nitrous oxide and methane. The observation of the (M+OH)- adduct ion with these compounds may be due to the ability of the macrocyclic ring to open with attack of the nucleophile. No (M+OH)- adduct ions would then be expected for the non-macrocyclic PAs and none are observed.



High resolution mass measurements were consistent with the assignment of m/z 215 as the even electron ion corresponding to the intact side chain, as depicted in the spectrum of senecionine. The ion structures in the spectrum are intended to demonstrate the structural significance of those ions and are not intended as the actual ion structures. A collisionally induced MIKE spectrum was obtained on m/z 215 to determine which of the ions in the spectrum are fragments of the side chain. The most abundant ions were observed at m/z 197, 171, 169, 153, 125, 116, and 87. The side chain dehydration fragment (at m/z 197 in senecionine) is also an important fragment in that it appears in the OH- spectra of all the macrocyclic PAs. m/z 197 in the OH- spectrum of senecionine can arise from a direct loss of water from the m/z 215 ion side chain. However, pathways directly from the (M+OH)- or (M-H)- ions also exist.

A very small m/z 215 ion can also be observed in the REC spectrum of senecionine, but m/z 154 is unique to OH- ionization. The assignment of m/z 154 as a necine anion, as depicted in the spectrum, was arrived at by the high resolution elemental composition. It was further substantiated by the OH- spectra of compounds such as rosmarinine(1), where the corresponding ion is shifted to m/z 172 because of the saturation of the double bond and an additional hydroxyl group on the bicyclic pyrrolizidine base.



(1)

Some variations in the fragmentation exhibited by senecionine and similar PAs have been observed for other types of PAs. The 11- membered macrocyclic ring PAs give a much smaller response for the necine structural component. PAs with saturated necines often give a weak response for the even electron side chain ion, but the side chain dehydration ions - which also indicate the mass of the side chain - are still present. The fact that the side chain dehydration ion is consistently observed may be due to the multiple pathways that exist for its formation; it can arise from (M+OH)-, (M-H)-, or the side chain ion. The spectra of the noncyclic monoester alkaloids provide a good indication of the mass of both structural components but produce a weak (M-H)- ion and no (M+OH)- ion.

An understanding of the fragmentation which occurs in these known compounds can surely aid in the structural elucidation of unknowns. Furthermore, it should be possible to compare the MS/MS spectra of carboxylate side chain ions or necine ions produced from the OH- ionization of different PAs. This would certainly aid the identification of structure and eliminate the need for extensive sample purification.

(1) Department of Chemistry, The George Washington University, Washington, DC 20052

STRUCTURAL DETERMINATION OF ECDYSTEROIDS AND BRASSINOSTEROIDS BY MASS SPECTROMETRY

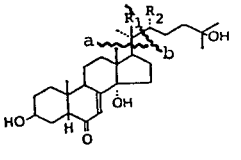
N.IKEKAWA, S.TAKATSUTO, AND T.IKEDA
Department of Chemistry, Tokyo Institute of Technology,
Meguro-ku, Tokyo, 152, Japan

Mass spectrometry is an essential technique for structural determination of natural ecdysteroids, insect moulting hormone, and brassinosteroids, plant growth hormone.

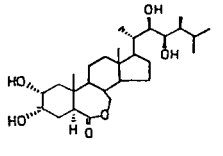
Most characteristic fragment ions of the steroidal skeleton of 20-hydroxyecdysone are m/z 363 and 327. The peaks of m/z 347 and 311 of 2-deoxy-ecdysteroid correspond to those peaks. The most important peak of the 6-oxo-7-ene-2,3,14-triol structure is m/z 250. The peak m/z 234 for 2-deoxy compound corresponds to m/z 250 of the 2,3-diol compound.

For determination of the side chain structure of the ecdysteroids, the fragment ions are also very useful. In the case of 20,22-dihydroxy compound, the cleavage at C_{17}-C_{20}(cleavage a) give an odd numbers peaks. In the case of 20-hydroxy and 22-hydroxy compounds, we found a different fragmentation. The prominent peaks of a-cleavage of 22-hydroxy compound are caused by single cleavage, showing odd number peaks. But the b-cleavage gives an even number peak for the part of steroidal skeleton. A hydrogen transfer is observed. So the number of odd or even of the steroid ring fragment is useful for determination of the position of the hydroxy group in 20 or 22-position.

We have isolated new ecdysteroids from the ovaries of the silkworm, Bombyx mori, and determined their structures as 2-deoxyecdysone(R_1=H, R_2=OH), 2-deoxy-20-hydroxyecdysone(R_1=R_2=OH), and 2,22-dideoxy-20-hydroxy-ecdysone(R_1=OH, R_2=H).[1,2,3] These ecdysteroids can be considered to be biogenetic precursors of 20-hydroxyecdysone.



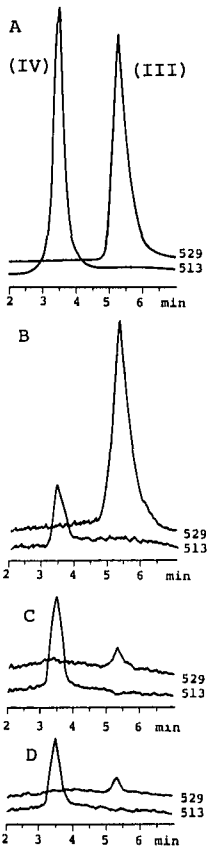
(I)



(II)

Recently, a novel plant growth-promoting substance named brassinolide (II) has been isolated from rape pollen. The presence of brassinolide-like substances have been suggested in other pollen and also many other plants. Although the biological functions in plant are remained to be clarified, establishment of microanalytical technique of brassinolide and its analogs becomes an important problem in order to investigate its biological significance and its distribution in plant kingdom.

We have developed a microanalysis of brassinolide as bismethaneboronate by gas chromatography[4]. Thus, by the computerized mass fragmentography using GC-CIMS system, picogram amount of brassinosteroids could be detected. Since brassinolide has two vicinal diols, methaneboronate is most suitable derivative for gas phase analysis. The derivative exhibits moderate volatility, strong molecular ion in CI-MS as a base peak, and methaneboronic acid is a specific reagent for vicinal diol function, causing easy separation from other contaminants in the plant. The molecular ions m/z 529 of brassinolide derivative(III) and m/z 513 of (24S)-24-methylbrassinone derivative(IV) can be effectively used for selected ion monitoring as shown in Fig. 1.



This microanalysis was applied to the identification and screening of brassinolide and its analogs in the extracts obtained from three different kinds of plants, the immature seeds and sheaths of Chinese cabbage, Brassica campestris var. pekinensis, the leaves of green tea, Thea sinensis, and the insect galls of the chesnut tree, Castanea spp, demonstrating the possibility of the ubiquitous presence of brassinolide and (23S)-24-methylbrassinone in the plant kingdom.

References

1. E.Ohnishi, T.Mizuno, N.Ikekawa, N.Awata, and S.Sakurai, J. Insect Physiol.,23, 317(1977).
2. E.Ohnishi, T.Mizuno, F.Chatani, N.Ikekawa, and S.Sakurai, Science, 197, 66(1977).
3. N.Ikekawa, T.Ikeda, T.Mizuno, E.Ohnishi, and S.Sakurai, J.Chem.Soc.,Chem. Comm.,1980, 448.
4. S.Takatsuto, B.Ying, M.Morisaki, and N. Ikekawa, J. Chromatog., 239, 233(1982).

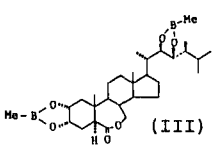


Fig. 1. Identification of brassinolide and (24S)-24-methylbrassinone in plants. (A) Standard mixture, (B) in chinese cabbage, (C) in green tea, (D) in chestnut gall. [A Shimadzu GC-MS 6020 with CI sources and a CSAP-1123 was used. A column packed with 2% OV-17, 0.5 m X 2 mm i.d. was used at 290°. The reagent gas was isobutane.]

COMPUTER-AIDED INTERPRETATION OF MASS SPECTRA; L. Baczynskyj and D. J. Duchamp, Physical and Analytical Chemistry Research, The Upjohn Company, Kalamazoo, MI 49001

Attempts to use computers in the interpretation of mass spectra of organic compounds of unknown structure have been described in the past and were summarized.[1] However, the vast majority of mass spectra recorded in our and in other laboratories pertain to compounds of known or suggested structures. Recently we have implemented a structure entry program which allows the operator to enter and store a structure with each mass spectrum stored in our library. Each structure can be displayed with the corresponding mass spectrum on a Tektronix 4014 CRT terminal. A series of interactive programs have been written which allow the operator to break any of the bonds of the displayed structure and to display the elemental compositions, the nominal and exact masses of both fragments alongside the mass spectrum and structure under investigation. Several bonds can be consecutively broken, yielding ions that correspond to consecutive reactions occurring in the mass spectrometer. In addition, the operator can add or subtract hydrogens and other ionic or neutral species to or from any ion in the mass spectrum. This is particularly important in chemical ionization (C.I.) and fast atom bombardment (F.A.B.) mass spectrometry. Ions that correspond to intense or important peaks in the mass spectrum are kept in a separate table. They can be plotted alongside the structure and the mass spectrum under investigation. The mass spectrum can also be displayed at any time with deletion of the ions that have already been interpreted. Also, the original mass spectrum and the spectrum with the deleted ions can be displayed to see if further interpretation is warranted.

Using the electron impact mass spectrum of cholesterol as an example, the structure of cholesterol was entered into the computer using the Tektronix 4014 CRT terminal, the associated tablet and the pen. This structure is permanently stored in our structure library under the same ID as the displayed mass spectrum. The interpretation begins when the mass spectrum is shown on the top half of the screen and the structure of cholesterol on the bottom half. By pointing the cross-hair of the cursor to a given bond, e.g., the C_{17}-C_{20} bond and by hitting the "B" (break) key, the elemental compositions along with the nominal and exact masses for both fragments thus generated appear on the bottom left hand of the screen. This area of the screen is used as a scratch area. A wavy line across the C_{17}-C_{20} bond also appears on the structure. The operator then inspects the mass spectrum. Since there is a relatively intense ion at m/z 273, he points the cursor to the lower fragment (ring system) of cholesterol and hits the "K" (keep) key. This puts the "structure" of this ion in the assigned ion table, appearing at the bottom right hand corner of the screen. Similarly, by breaking the C_{13}-C_{17} and C_{14}-C_{15} bonds and then subtracting a hydrogen radical from the resulting formula, a fragment having an elemental compositon of $C_{16}H_{23}O_1$ and a mass of 231 is displayed. Since this is an intense ion in the mass spectrum of cholesterol, this ion is also kept in the assigned ion table. This table can accommodate up to 20 entries. Any structure from this table can be displayed by pointing to it with the cursor and hitting the "Q" (querry) key or it can be deleted from the table by pressing "X" (expunge) key. In the final interpretation step all the structures of the ions kept in the assigned ions list can be displayed around the original structure of the compound investigated.

This interpretation system is in daily use in our laboratory and hundreds of mass spectra and structures have been correlated and interpreted in this manner. Further refinement and new options will be developed in the future.

1. P. V. Fennessey, "Computer Assisted Interpretation of Mass Spectra" in "Mass Spectrometry - Techniques and Applications." G. W. A. Milne, Ed., Wiley-Interscience, New York, 1971.

PREPARATION OF PEPTIDES LABELED WITH DEUTERIUM ON THE PHENYLALANINE AND TYROSINE AROMATIC RINGS

Kym F. Faull and Jack D. Barchas

Pasarow Analytical Neurochemistry Facility, Nancy Pritzker Laboratory of Behavioral Neurochemistry, Department of Psychiatry and Behavioral Sciences, Stanford University School of Medicine, Stanford, California 94305.

Stephen Murray and Berthold Halpern*
Department of Chemistry, University of Wollongong, N.S.W. Australia.
*Paper prepared posthumously.

Recent developments in mass spectrometry have led to a heightened level of interest in the use of this technique for quantitative analysis of peptides. These developments include negative chemical ionization of suitably derivatized peptides (1) and field desorption (2) and fast atom bombardment (FAB) (3) mass spectrometry of underivatized peptides. However, the successful application of these developments to peptide quantification will depend upon the availability of suitable internal standards.

The metal catalyzed exchange of aromatic ring protons in deuterium oxide has long been a subject of study by physical chemists who continue to strongly debate the mechanism of the exchange process (4, and references cited therein). It would seem, however, that this exchange process has merit for the preparation of deuterated analogues of a wide variety of biologically interesting molecules for studies involving mass spectrometry and NMR. We have successfully used this route for the preparation of a number of deuterated aromatic biogenic amine metabolites (5), and now report the application of this technique to the preparation of deuterated analogues of leucine-enkephalin and related peptides.

The deuterated compounds were prepared using a previously described technique (5) in which the peptides or N-acetyltyrosine were incubated with catalyst and deuterium oxide in an evacuated sealed glass ampoule. Carefully washed catalyst was prepared immediately prior to use by reduction of platinum IV oxide with sodium borohydride. Approximate weight ratios of 1 to 10 mg of peptide or N-acetyltyrosine (acetate salt or free acid), platinum derived by reduction of 33 mg of Pt_2O and 1.1 ml of D_2O were used. Reactions were carried out for 4 weeks at room temperature with continuous agitation of the contents of the ampoule.

A comparison of the proton NMR spectra (100 MHz in D_2O) of the dipeptides Phe-Leu and Gly-Phe, and the tripeptide Tyr-Gly-Gly which had undergone hydrogen-deuterium exchange, with the spectra of the same compounds which had not undergone exchange labeling, demonstrated a virtual complete loss of the aromatic protons in the exchange-labeled samples. The integrated signals obtained from the NMR spectra of the two dipeptides also indicated a partial loss of the benzylic protons adjacent to the aromatic Phe and Tyr rings. Furthermore, the integrated areas of the NMR peaks provided no suggestion that exchange-labeling resulted in loss of any other protons on the dipeptides.

A comparison between the EI mass spectra of the N,O-HFB methyl esters of the deuterated and undeuterated dipetides Phe-Leu, Gly-Phe and Tyr-Gly showed the presence of predominantly 5,6 and 7 deuterium atoms on the labeled samples. The location of the label on the aromatic residues was indicated by the shift in mass of the tropylium ion (C_7H_7), present in the spectra of Phe containing dipeptides, from m/z 91 to m/z 96, 97 and 98, and the shift in mass of the corresponding $C_3F_7COO\text{-}C_6H_4\text{-}CH_2^{\ddagger}$ ion, present in the spectra of the Tyr containing dipeptides, from m/z 303 to m/z 308 and 309. The absence of deuterium incorporation at positions other than the side-chain of the aromatic residues was evident in the spectrum of the Gly-Phe derivative, which demonstrated that exchange labeling did not result in a shift in mass of the intense fragment ion at m/z 226 which is attributed to the Gly portion of the molecule ($C_3F_7CO\text{-}NH\text{-}CH_2^{\ddagger}$).

These results were confirmed by FAB mass spectra (obtained in glycerol/HCl matrix, with zenon as the bombarding species at 7 Kv and 40 microamps) of the underivatized peptides. The results demonstrated the presence of predominantly 5, 6 and 7 deuterium atoms in exchange-labeled samples of Gly-Phe, Tyr-Gly, Tyr-Gly-Gly and leucine-enkephalin (Figure 1). The incorporation of label into the aromatic residues was evident from the shift in

mass of the ions at m/z 120 (attributed to $NH_2^+=CHCH_2C_6H_5$) and 136 (attributed to $NH_2^+=CHCH_2C_6H_4OH$) derived from Phe and Tyr residues respectively.

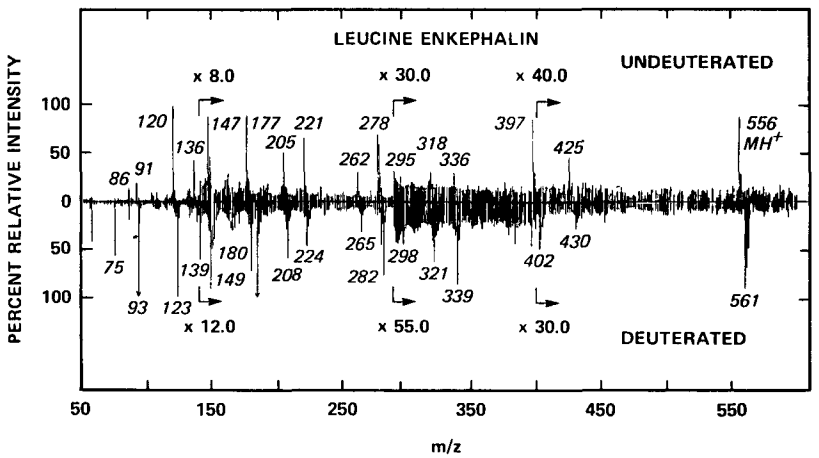


Figure 1.
Positive Ion FAB Mass Spectrum of Deuterated and Undeuterated Leucine-Enkephalin

Studies on the time course of label incorporation were carried out with N-acetyltyrosine (a water soluble form of this amino acid) and Tyr-Gly. N-Acetyltyrosine was converted within 1 week of reaction to primarily a ring-labeled tetradeuterated species. Extending the reaction period up to 4 weeks did not result in significant incorporation of additional deuterium atoms. On the other hand, Tyr-Gly was converted to a ring-labeled tetradeuterated species within 1 week of reaction, but extending the reaction period up to 4 weeks resulted in incorporation of two additional deuterium atoms in the benzylic position adjacent to the aromatic ring. One month after the reaction was started the hexadeuterated species was most abundent and accounted for 76 percent of the Tyr-Gly.

These results suggest this route has merit for the preparation of deuterated analogues of peptides which contain aromatic residues.

Acknowlegements

We are pleased to acknowledge the cooperation of the Middle Atlantic Mass Spectrometry Laboratory, Johns Hopkins University, and the Space Sciences Laboratory, University of California, Berkeley, where the first FAB spectra of the deuterated peptides were recorded. Supported in part by NIMH program-project grant, MH 23861.

References

1. Morris, H. R., Dell, A., Judkins, M., McDowell, R. A., Panico, M. and Taylor, G. W. In "Proceedings of the 7th American Peptide Symposium", D. H. Rich and E. Gross, eds., Pierce Chemical Co., Rockford, IL, 1981, pp. 745-755.

2. Desiderio, D. M., Yamada, S., Sabbatini, J. Z. and Tanzer, F. Biomed. Mass Spectrom. 8:10, 1981.

3. Barber, M., Bordoli, R. S., Sedgwick, R. D. and Tyler, A. N. Nature 293:270, 1981.

4. Fraser, R. R. and Renaud, R. N. J. Am. Chem. Soc. 88:19, 1966.

5. Faull, K. F., Anderson, P. J. and Barchas, J. D. J. Labelled Compounds 18:1075, 1981.

FOD 1 MATRIX EFFECTS IN DIRECT MIXTURE ANALYSIS BY MS/MS. W.R. Davidson, B.A. Thomson, B.I. Shushan and J.E. Fulford; SCIEX™, 55 Glen Cameron Rd., Unit 202, Thornhill, Ontario, Canada, L3T 1P2.

One of the more desirable features of tandem mass spectrometry (MS/MS) is the ability to directly analyze complex mixtures for trace components without resorting to extended sample workup and chromatographic separations. However, some sample matrices are so complex that components in the matrix quantitatively and/or qualitatively affect the analysis for the trace compounds. This paper describes several applications of a triple quadrupole MS/MS system, the TAGA™ 6000, to the direct analysis of crude sample extracts including diesel exhaust, fish, fried bacon, oil residue, grain and human serum for the detection and quantitation of trace constituents. Several techniques are presented which circumvent or diminish matrix effects. These methods include software algorithms which determine whether or not an isobaric interfering compound is producing daughter ions of the same mass as the compound of interest and which can in many cases automatically remove the false readings. Rapid pre-analysis or in-situ separation steps may also be necessary. Internal standards should always be used in quantitative direct mixture analysis. Standard addition techniques (spiking) also provide quantitative results and can be used in cases where no internal standards are available. If matrix effects are too severe to use the techniques described above, a more rigourous sample workup may be necessary.

TLC/MS/MS OF DRUGS IN BIOLOGICAL SAMPLES

Jack D. Henion, Dale S. Skrabalak, Diagnostic Laboratory, New York State College of Veterinary Medicine, Cornell University, Ithaca, NY 14853 and Bruce A. Thomson, SCIEX™, 55 Glen Cameron Rd., Unit 202, Thornhill, Ontario, Canada, L3T 1P2.

Tandem mass spectrometry has been shown to be a highly specific and sensitive technique in targeted compound analysis. The ability to analyze relatively complex samples for trace species offers a real savings in both manpower and time over more conventional techniques of GC and GC/MS. Examples have been published showing that direct probe analysis with an MS/MS instrument could allow many samples to be rapidly screened for the presence of specific compounds or compound classes, with confirmation of the few positive samples by GC/MS or GC/MS/MS. There are other situations, however, in which it would be more efficient to screen the samples with an inexpensive technique and use the high specificity of MS/MS to provide confirmation. In a previous paper we reported on the use of LC/MS/MS for the detection of administered drugs in crude equine plasma and urine extracts (1). We are currently exploring the use of MS/MS for the confirmation of drugs and metabolites in plasma and urine samples which have been screened by Thin Layer Chromatography (TLC). In this paper, we report on the analysis of urine samples by Direct Probe/MS/MS with an Atmospheric Pressure Ionization Source. Results are presented comparing analysis of crude urine extracts, with analysis of the same samples which are first screened by Thin Layer Chromatography (TLC). The developed TLC spots were analyzed both by eluting the silica scrape and depositing the extract on the probe, and by placing the silica directly in the probe and thermally desorbing the material. The latter technique was successful for only one of the three drugs studied.

Experimental

A TAGA® 6000 Triple Quadrupole Mass Spectrometer System equipped with an atmospheric pressure ionization source was used for the analysis. Samples were introduced on glass surfaces in a direct insertion probe.

Three drugs were chosen for the study: caffeine in human urine (from a coffee drinker and smoker), and butorphanol and betamethasone in equine urine (both administered drugs). Each of the three samples was analyzed in three ways: in a crude extract, in an eluted TLC scrape and by thermal desorption directly from the silica.

Caffeine was extracted from urine directly into chloroform at pH 7.1. The same urine sample was also placed on a TLC plate and developed, with the spot which appeared beside the caffeine standard being scraped off. One half of the scrape was eluted with methanol, and the other half was reserved.

The equine urine samples were treated similarly. Butorphanol was extracted from urine into petroleum ether at a pH of 10. The TLC scrape was eluted with ethyl acetate. Betamethasone was extracted into 2:1:1 ether:dichloromethane:isopropanol at a pH of 4.5 and the TLC scrape was eluted with methanol.

Results

The API mass spectrum of a caffeine standard shows only the MH^+ at m/z 195. The CID spectrum with an argon collision gas and a lab collision energy of 44 volts showed daughter ions at m/z 138, 110, 83, 69, 56 and 42. The mass spectrum of a 2 μl aliquot of the crude urine extract showed abundant peaks at m/z 163, 177, 195, 237, 255, 353, 371 and 389 (Figure 1). The CID spectrum of m/z 195 matches that of a caffeine standard (Figure 2) while that of m/z 163 matches the reference CID spectrum of a nicotine standard. The m/z 177 was probably due to cotinine, a nicotine metabolite, although a reference spectrum was not available for comparison. The eluted TLC spot showed only the m/z 195 caffeine peak, again identified by the CID spectrum. Direct thermal desorption of the silica scrape in the probe also showed a strong m/z 195 identified by CID as caffeine.

The API mass spectrum of butorphanol shows only the MH^+ at m/z 328. The crude extracts of equine urine containing butorphanol and butamethasone did not show the presence of either of the drugs, due probably to the matrix effects of other components in the crude extracts. However, the eluted TLC scrape of butorphanol showed a strong m/z 328 peak (MH^+). A CID spectrum of this peak matched that of the butorphanol standard.

The betamethosone API mass spectrum indicates some decomposition of this compound on the probe. The base peak is m/z 333, with the parent MH^+ at m/z 393 at 5 to 10% intensity. Bethamasone could not be detected in the crude extract, but was readily detected in the eluted TLC scrape, the CID spectrum of m/z 333 matching that of the standard. Neither betamethasone nor butorphanol could be detected by direct thermal desorption from the silica scrapes.

Conclusions

While crude urine extracts could be readily desorbed into the API source without reducing the system performance, only caffeine and nicotine could be directly identified in the extract. Even in complex mass spectra, CID spectra of the mass peaks of interest show good specificity in the fragmentation patterns and closely match those of the pure standard, with no interference from other components or solvents. Analysis by TLC provides a pre-screening of the samples (only positives need be further analyzed), and result in sufficient sample cleanup to obtain good mass spectra and CID spectra of the peaks of interest. Only caffeine could be detected by direct thermal desorption from silica. The combination of TLC screening followed by MS/MS confirmation appears to offer an attractive combination of speed, efficiency and specificity in a situation where many samples must be analyzed daily.

(1) J.D. Henion, B.A. Thomson and P.H. Dawson, Anal. Chem., 1982, 54, 451-456.

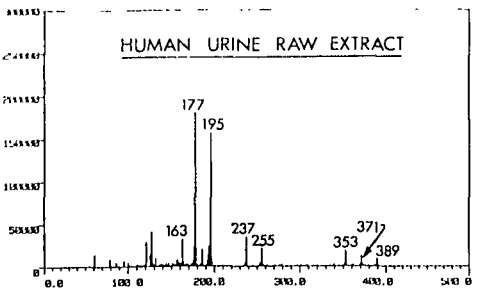


Figure 1. Full scan MS of raw extract of human urine.

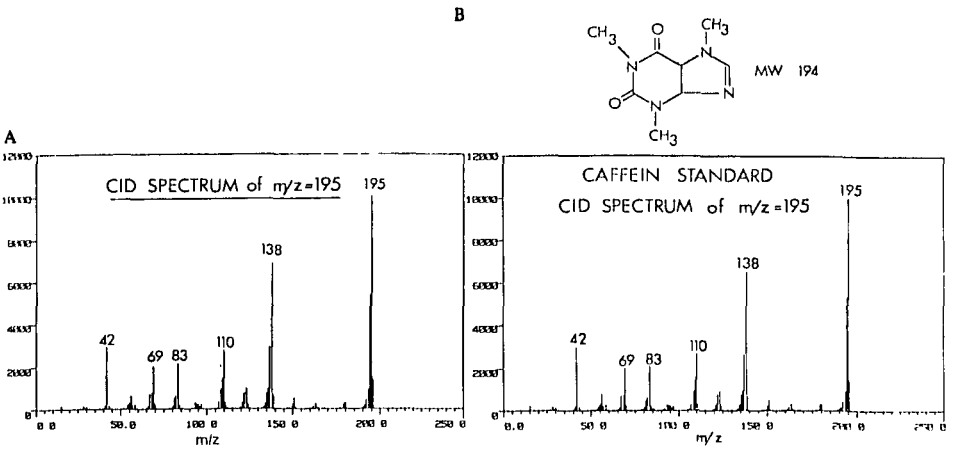


Figure 2. a) CID spectrum of m/z 195 from raw urine extract. b) CID of m/z 195 from caffeine standard.

MASS SPECTROMETRY/MASS SPECTROMETRY OF ENZYME CLEAVAGE PRODUCTS

R. G. KALEY and H. I. WEINGARTEN
Corporate Research and Development
Monsanto Company
St. Louis, MO 63167

One important application area for mass spectrometry/mass spectrometry (MS/MS) is the identification and structure verification of target compounds in complex matrices. The unique capability of a tandem mass spectrometer to generate protonated molecular weight ions in a chemical ionization (CI) ion source, select those ions in the first mass spectrometer, fragment the ions by collisionally activated dissociation (CAD) in a collision chamber, and obtain the spectra in the second mass spectrometer is the basis of the technique. This report describes the results for one such application: the verification of enzyme cleavage products of a heptapeptide. The problem is well-suited for MS/MS, since the expected cleavage products are known and the molecular weights of the cleavage products are well within the mass range of the triple quadrupole mass spectrometer. Previous mass spectral analysis required separation, isolation, and derivatization of each compound. It was hoped that direct analysis of the reaction mixture by MS/MS would provide the necessary mass spectral information without requiring the extensive sample workup.

Preliminary experiments demonstrated that the protonated methyl esters of the tri- and tetrapeptide cleavage products (Figure I) could be volatilized from a direct insertion probe (DIP), ionized, fragmented by CAD, and identified with respect to molecular weight and amino acid sequence. (Figures II and III) A simple sample workup procedure was developed for the analysis of the reaction mixture, involving lyophilization of the reaction mixture, methylation by thionyl chloride in methanol, and re-lyophilization, yielding a solid sample containing methylated cleavage products, residual buffer and small amounts of enzyme and substrate. An actual reaction mixture, initially containing 5 µmole/ml of substrate, which had been treated as described, was run by CI mass spectrometry. The CI mass spectrum is shown in Figure IV. The mass spectrum contains ions at 243, 342, and 429 daltons as expected. The ion at 243 daltons is the 2M + H ion from the buffer and the ions at 342 and 429 are the M + H ions for the tri- and tetrapeptide respectively. The ions at 463 daltons and 550 daltons were not anticipated. Based on CAD work, these almost certainly result from addition of protonated buffer ions (122 daltons) to the tri- and tetrapeptides. This "buffer CI" is a result of the large excess of buffer in the ion source. However, since the ions are clearly identifiable by CAD MS/MS, their presence in the CI spectrum is of no concern. Comparison of the CAD daughter spectra of the ions at 342 and 429 daltons with the spectra of the authentic materials showed they were identical, verifying the identity and structure of the cleavage products in the reaction mixture. MS/MS daughter spectra are an unequivocal verification of the expected action of the enzyme on the substrate.

CLEAVAGE PRODUCTS (METHYLATED)

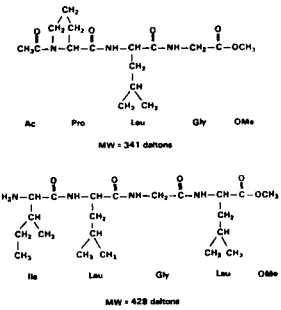


Figure 1

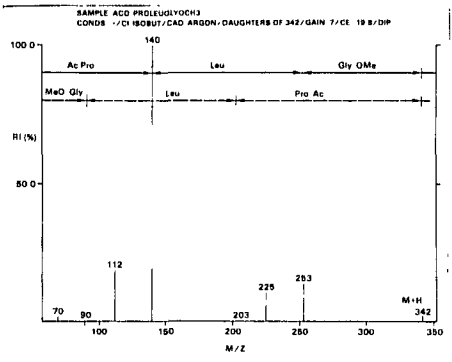


Figure 2

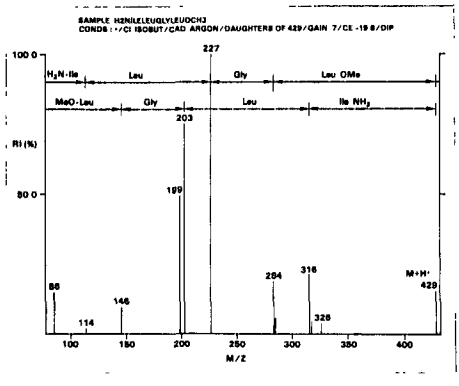


Figure 3

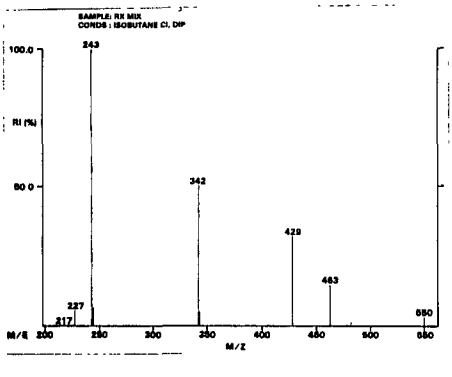
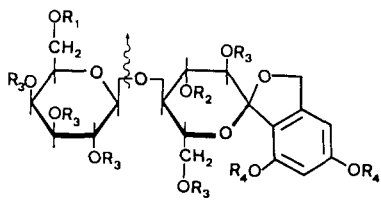


Figure 4

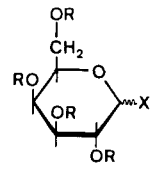
'SOFT COLLISION' GC/MS/MS AS A PROBE INTO THE STEREOCHEMISTRY OF SUGAR SUBUNITS IN COMPLEX NATURAL MOLECULES.

W. J. Richter and W. Blum, Ciba-Geigy AG, Central Function Research, CH-4002 Basel, Switzerland.

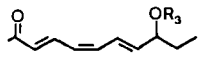
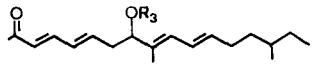
In previous work, structure 1 had been assigned to papulacandin B, the chief representative of a new class of antibiotics, mainly on grounds of NMR and MS measurements in combination with extensive chemical degradation (1,2). E.g., the non-spirocyclic sugar moiety embodying a D-galactose unit was identified after i) removal of the two long-chain unsaturated fatty acids (R_1 and R_2 substituents) by selective hydrolysis, ii) selective methylation, and iii) methanolysis. A spirocyclic diglycoside 2, its dimethyl derivative 3, and methyl α-D-galactoside 4 (together with the product retaining the larger portion of the molecule) are formed in due course. Identification of 4 required its isolation as a pure compound from the reaction mixture with subsequent preparation of the tetraacetate 4a for spectral comparison with an authentic sample. In the present work, this same task is shown to be amenable to GC/MS/MS using a triple stage quadrupole (QQQ) mass spectrometer, with less effort and on a much smaller scale.



1 - 3



4

1 R_1 =  R_2 =  R_3, R_4 = H; 2 R_1, R_2, R_3, R_4 = H; 2a R_1, R_2, R_3, R_4 = CH_3CO; 2b R_1, R_2, R_3, R_4 = $(CH_3)_3Si$; 3 R_1, R_2, R_3 = H, R_4 = CH_3; 4 R = H, X = α-OCH_3; 4a R = CH_3CO, X = α-OCH_3; 4a' R = CH_3CO, X = +; 4b R = $(CH_3)_3Si$, X = α-OCH_3; 4b' R = $(CH_3)_3Si$, X = +;

For the intended stereochemical characterization by MS/MS, the ion 4a' at m/z 331 appeared suitable since the 6-ring structure of the non-spirocyclic sugar moiety should be preserved intact as a low internal energy population can be generated and collected. Glycosidic heterolysis induced by CI(CH_4)

was found to furnish this ion from the nonaacetate precursor 2a (MH^+ at m/z 841) in high yield when analyzed in the DCI mode. In a typical low kinetic energy MS/MS experiment with a QQQ instrument (Finnigan TSQ), m/z 331 of 2a was mass-selected by Q_1, fragmented (after acceleration to about 15 eV) by collision-induced dissociation (CAD) in (RF only) Q_2 with argon as the target gas, and its CAD daughter ion spectrum recorded by operating Q_3 in the full scan or selected ion monitoring mode.

For identification, the CAD 'fingerprint' of ion 4a' is to be matched with relevant CAD reference spectra, i.e. those of the more common diastereoisomers of the structure in question (cf. Fig.). These reference spectra were obtained by preparing, in single batches, the methyl glycoside tetraacetates of authentic D-galactose, D-mannose and D-glucose, and introducing the crude reaction products (chiefly α- and β-anomers) via capillary GC. In the required successive runs the MS/MS conditions (parent ion kinetic energy, collision gas pressure) were carefully maintained. As can be seen, 2a-derived ion 4a' differs from its glucose-derived stereoisomer considerably while matching closely the patterns of both the galactose- and mannose-derived counterparts. With glucose thus ruled out, the necessary distinction of the two latter was readily achieved in an analogous GC/MS/MS experiment using trimethylsilyl derivatives instead of the acetates. While, then, 2b-derived ion 4b' (m/z 451) matches closely the galactose/glucose pair, mannose can be promptly discounted.

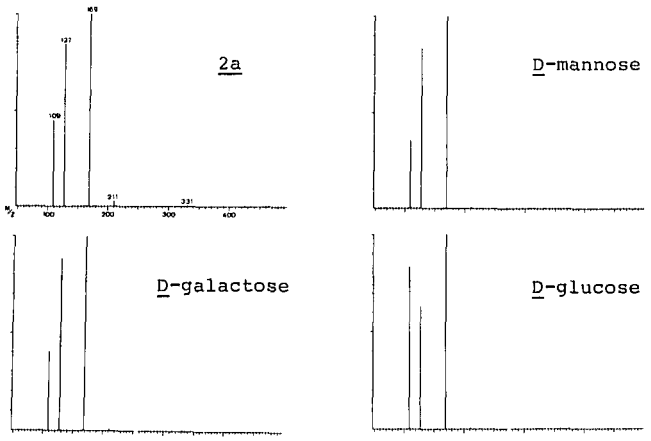


Fig.: m/z 331 CAD spectra of 'unknown' and reference derivatives

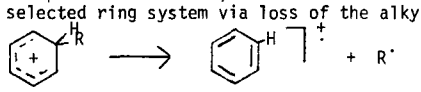
(1) P. Traxler, H. Fritz and W. J. Richter, Helv. Chim. Acta 60, 578 (1977).
(2) P. Traxler, H. Fritz, H. Fuhrer and W. J. Richter, J. Antibiot. 33, 967 (1980).

CHARACTERIZATION OF ORGANICS IN COAL LIQUIDS AND DIESEL PARTICULATES BY MS/MS

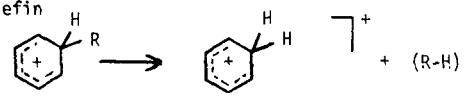
Zhong-min Li, J.D. Ciupek, K.V. Wood, R.G. Cooks
Department of Chemistry
Purdue University
West Lafayette, Indiana 47907

Fuel-related materials are complex mixtures of compounds containing many different functional groups as well as a wide distribution of molecular weights. Direct analysis of these materials can be achieved using mass spectrometry/mass spectrometry (MS/MS). Parent spectra, obtained by scanning the first mass analyzer so as to characterize the set of parent ions which yield a specified daughter ion, and neutral loss spectra, obtained by simultaneously scanning both mass analyzers with a mass difference characteristic of a particular functional group, are of particular value in the analysis of these types of complex mixtures. Daughter spectra, obtained by scanning the second mass analyzer so as to characterize a selected parent ion, provide confirmatory information as to the exact nature of a given molecular weight component. Supplementary ionization techniques like negative ion chemical ionization and laser desorption as well as internal energy variation through controlled collision-induced dissociation are rapidly becoming more useful.

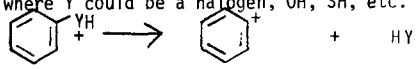
Three principal types of parent spectra have been found to be particularly valuable in the analysis of complex mixtures: 1) even electron to odd electron, identifying alkyl substituents on a selected ring system via loss of the alkyl substituent



2) Even electron to even electron identifying alkyl substituents on a selected ring via loss of the olefin



3) Even electron to even electron identifying heteroatom substituents on a selected ring via loss of HY where Y could be a halogen, OH, SH, etc.



These reactions can be illustrated in a coal-derived mixture taking the parent spectrum of m/z 127-129 for naphthalene ring substituents. The primary ions detected in the m/z 128 spectrum result from protonated naphthalene, m/z 129 and the C_1-C_4 alkyl substituted homologs, m/z 143, 157, 171, 185... The same series (loss of olefin) are observed for the m/z 129 spectrum except that instead of detecting protonated methylnaphthalene, protonated methylquinoline m/z 144 is observed. Evidence for protonated hydroxyquinoline m/z 146 is also seen. Some of the ions seen in the m/z 127 spectrum are m/z 129, loss of H_2 from protonated naphthalene, m/z 143, loss of CH_4 from protonated methylnaphthalene and of particular interest m/z 145, loss of H_2O from protonated hydroxynaphthalene. Another ion of interest detected is m/z 155, loss of C_2H_4 from protonated acenaphthene.

Daughter spectra of the ions of interest can be used to confirm the presence of suspected constituents. In the above example, it is particularly important to confirm, with an authentic that protonated dimethylnaphthalene does in fact lose, ethylene, and that m/z 144 is protonated methyl quinoline and not the ^{13}C isotope of protonated methylnaphthalene.

Neutral loss spectra are particularly well-suited for characterization of complex mixtures, but can present a problem with false positives. For example, the neutral loss 33 spectrum (loss of HS· from sulfur aryls) from a coal-derived liquid is very complex, indicating many sulfur containing species. Daughter spectra of suspected components recorded for confirmation, show that many of the suspected components are probably not sulfur containing. One reason is the occurrence of successive dissociations in the collision cell, like 18 amu (H_2O) and 15 amu (methyl), which sum to 33 amu. There

are many cases where neutral loss spectra can provide valuable data, however, like the neutral loss spectra of 18 amu (H_2O), which is indicative of the hydroxy containing constituents in a complex mixture.

Besides parent and neutral loss scans,supplementary techniques like collision energy variation and novel ionization techniques are particularly suited for MS/MS analysis of complex mixtures. Collision energy in the MS/MS technique, can be varied in the low energy regime to provide additional information for the analysis of complex mixtures. This variation enables certain dissociation pathways of interest to be enhanced. Decreasing the collision energy in certain instances reduces fragment ions that are not of interest relative to diagnostic fragment ions. Conversely increasing the collision energy can in certain cases enhance a particularly weak dissociation pathway that is characteristic of a certain molecular species.

Laser desorption is an alternative ionization technique for nonvolatile compounds that is just developing for MS/MS. This enables components that normally would not be ionized to be analyzed by MS/MS for identification in a complex mixture. Examples include the higher molecular weight amino compounds which occur in coal liquids.

To exemplify the advantages of the newer scan techniques Figures 1 and 2 show neutral loss and parent spectra for a coal liquid. Figure 1 is a neutral loss 18 spectrum indicating the presence of phenols in a coal-derived liquid. Figure 2 is a parent scan of m/z 154 indicating those substituents which dissociate from even-electron to odd-electron ions(ionized acenaphthene/biphenyl in this case).

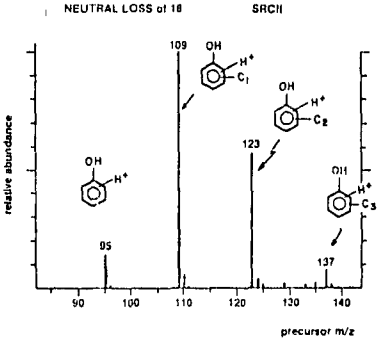


Figure 1

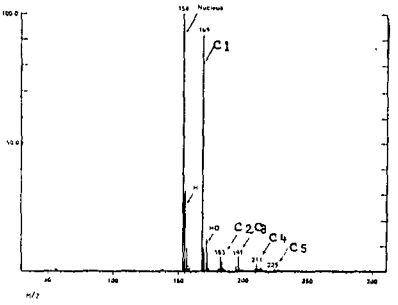


Figure 2

A COMPREHENSIVE ANALYTICAL SCHEME FOR THE ANALYSIS OF ORGANICS IN ENVIRONMENTAL MATRICES BY MS/MS

Hunt, D.F.; Shabanowtiz, J.; Harvey, T.M.; and Coates, M; Department of Chemistry, University of Virginia, Charlottesville, Virginia 22901

Analysis of environmental samples for the 114 toxic organic chemicals on the EPA priority pollutant list presently involves separation of the organics from the matrix using a combination of wet chemical extraction steps, sample concentration and clean-up by various types of chromatography, and final analysis by a gas chromatograph/mass spectrometer/data system. Diasadvantages of the above approach include: (a) the inability to detect highly polar compounds too involatile or thermally labile to pass through the gas chromatograph, (b) the high labor costs dictated by the need for extensive sample clean-up prior to sample analysis and (c) the large amount of time required to perform a single analysis on a gas chromatograph/mass spectrometer/data system.

To overcome these problems, we have initiated research to develop a cost effective, comprehensive analytical scheme based on tandem mass spectrometry for the direct, rapid, qualitative-semiquantitative analysis of both known and unknown organics in gaseous, liquid, and solid environmental matrices. Elimination of all or most wet chemical and chromatographic separation steps, detection limits in the 10-1000 ppb range, and a total analysis time per sample of under 20 minutes are achievable.

Our approach is to analyze the organics in complex mixtures by functional group. The matrix components are volatilized directly into the ion source and converted to positive or negative ions charactersitic of sample molecular weight using chemical ionization methods. The tandem mass spectrometer system is then operated under collision activated dissociation conditions with the two mass analyzers scanning under computer control in either the parent ion or neutral loss mode.

Parent ion spectra are obtained by scanning the first analyzer over the desired mass range while the second analyzer is set at a particular m/z value. In this configuration the only ions that reach the detector are those that are selected by the first mass analyzer and suffer dissociation in the collision cell to give a fragment ion having a m/z value corresponding to that being monitored by the second analyzer. The resulting spectra contain only the parent ions that form the particular fragment being transmitted by the fixed 1 amu window of the second analyzer. If the fragment ion being monitored is both highly characteristic of a particular functional group and exhibited by all members of the class of compounds containing that functionality, then the parent ion scan mode can be employed to determine both the molecular weight and approximate concentration of all the organic compounds in the mixture with that particular functional group.

Similar results are obtained by operating the tandem instrument in the neutral loss mode. Here the two mass analyzers are scanned under computer control over the desired mass range at a fixed mass separation. Under these conditions the only ions to reach the detector are those that undergo collision activated dissociation with loss of a specific moiety having a mass equal to the fixed mass separation of the two analyzers. As long as the neutral elimination is highly characteristic of a particular functional group, the neutral loss scan can be employed to determine the molecular weight and relative concentrations of all the compounds in the mixture containing that specific functional group.

Success of the above approach depends on the assumption that ions characteristic of the molecular weight of each class of organic compounds will suffer collision activated dissociation with high efficiency and either lose a highly characteristic neutral or form a highly characteristic charged fragment. Unfortunately this is not the case for several types of organic compounds under the low energy conditions employed in the collision cell of the triple quadrupole instrument. Those compounds that fail to meet the above criteria must therefore be derivatized in order to promote the desired behavior in the collision activated dissociation process. Ideally the derivatization reaction should (a) employ volatile reagents that can be easily removed from the matrix, (b) proceed in high yield under mild conditions, and (c) introduce a functional group which is sufficiently acidic or basic to localize proton addition or abstraction at the site of the newly introduced substituent. Dissociation of the resulting ion characteristic of sample molecular weight on collision with molecular nitrogen in quadrupole 2 should also proceed with high ef-

ficiency, and preferably lead to a small number of abundant fragment ions highly characteristic of the functional group in the derivative.

Analysis of the derivatized matrix is accomplished by thermally desorbing the organics directly into the ion source of a Finnigan triple quadrupole mass spectrometer, which is operated under computer control and cycled repetitively through a number of different parent ion and neutral loss scans. The following is a summary of our current methodology for different classes of organic compounds.

CLASS	DERIVATIVE	PARENT SCAN (positive or negative ion CI)	NEUTRAL LOSS (positive or negative ion CI)
Phthalates	—	(+) 149	—
Aldehydes/Ketones	o-benzyloximine	(+) 91	—
Amines	urea	—	(+ or -) 57
Phenols	carbamate	—	(+) 57
PAHs	nitro	—	(+) 17/46
Chlorocarbons	—	—	(+) 35/36
Acids	—	—	(-) 44/62
Sulfur[a] sulfides	sulfone	(+) 30	—
Sulfur[a] heterocyclics	—	—	(+) 33

[a]See Anal. Chem., 54, 574-578 (1982) for details.

Collision activated dissociation (CAD) of $(M+H)^+$ ions from all phthalates except dimethyl phthalate results in the loss of one molecule of alcohol and one molecule of olefin to give protonated phthalic anhydride at m/z 149. Accordingly, members of this class of compounds are monitored selectively by a parent scan of the m/z 149 fragment. Aldehydes and ketones are also detected in a parent ion scan mode. In this case, the carbonyl compounds are converted to oximes with o-benzylhydroxylamine and the abundant m/z 91 ion formed by CAD is monitored.

Amines and phenols are readily converted to their respective urea and carbamate derivatives upon treatment with methylisocyanate in ethyl acetate. CAD of the methyl carbamate $(M+H)^+$ ions results in the loss of methyl isocyanate (57 amu). CAD of the methyl urea $(M-H)^-$ ions also results in a neutral loss of 57 amu. Thus the phenols are monitored in a positive ion neutral loss scan while the amines are differentiated by monitoring a negative ion neutral loss scan.

Due to the low efficiency of the CAD analysis, polynuclear aromatic hydrocarbons (PAHs) are converted to their nitro derivatives using N_2O_4. The nitro group is highly basic and easily protonated under CI conditions. The resulting $(M+H)^+$ ions suffer facile dissociation in the CAD process and afford abundant fragment ions resulting from elimination of $OH\cdot$(17amu) and $NO_2\cdot$(46amu). A neutral loss scan of 17 amu and 46 amu can be employed to monitor the PAHs.

Chlorocarbons can be analyzed directly by using 35 amu and 36 amu neutral loss scans from $(M+H)^+$ ions.

Under negative ion CI conditions, carboxylic acids are converted to carboxylate anions which suffer loss of CO_2 (44 amu) upon CAD. Hydroxy-acids will also exhibit a loss of 62 amu (CO_2 and H_2O). Thus, a neutral loss scan of 44 amu and 62 amu (if desired) can be utilized to monitor most carboxylic acids.

The procedures outlined here are sufficient to monitor most of the known toxic compounds, which are on the EPA priority pollutant list. However, without any additional work, information is also obtained on unknown but related compounds which potentially may be considered hazardous and of interest.

Preliminary results obtained from samples run by both MS/MS and an independent high accuracy GC/MS laboratory correlate very well and verify the promising future of MS/MS for rapid analysis of organic compounds and complex matrices.

A MICRO COMPUTER CONTROLLED TANDEM QUADRUPOLE MASS SPECTROMETER USING A DIRECT LIQUID INTRODUCTION PROBE FOR SCREENING ANALYSIS: R.D. Voyksner 1,2; J.R. Hass 1; M.M. Bursey 2; 1. NIEHS, P.O. Box 12233, Research Triangle Park, NC 27709; 2. Dept. of Chem., University of NC at Chapel Hill 27514

INTRODUCTION

The increasing number of environmental and clinical samples indicate the desirability that some screening procedures be used to reduce the burden on GC/MS. Mass spectrometry/mass spectrometry (MS/MS) has been proposed to perform such screening analysis. Observation of a characteristic neutral loss or single and multiple reaction monitoring (SRM) (MRM) are screening techniques used in MS/MS. The direct probe sample introduction procedure is used instead of the GC inlet because of the capability of high sample through-put. Yet this method of sample introduction has a number of drawbacks and can be the slowest step in the analysis. Loss of volatiles in the vacuum lock, temperature programming the probe to vaporize the involatiles, and constant insertion and removal of the probe are a few limitations of the method. An alternative way of sample introduction we now present involves the use of the direct liquid introduction (DLI) probe. 2,4,5-trichlorophenol (TCP), the analyte investigated by the DLI method, is representative of many polychlorinated contaminates and screening for TCP in spiked urine samples should demonstrate the validity of the DLI-MS/MS technique.

EXPERIMENTAL

Screening was carried out on an Extranuclear Laboratories Tandem Quadrupole MS/MS using the Hewlett-Packard DLI interface or a homebuilt micro DLI probe. The samples were carried into the source by an 80/20 CH_3CN/H_2O mixture, which served as the chemical ionization reagent gas. A 5cm ODS guard column served to filter out the particulates that could plug the probe. The screening analysis was performed by monitoring the loss of HCOCl (m/z 132) from the molecular ion of TCP (m/z 196). This loss was observed at a collision energy of 35V with N_2 collision gas.

An Apple II computer and ISAAC (Cyborg Co., MA) interface controlled both quadrupoles, collected data, and performed the data reduction. The SRM program set both quadrupoles to monitor the 196 → 132 reaction and acquired data at a rate of 2 Hz (the rate can be varied from 1000 - .05 Hz). The data is displayed in real time then stored on the disk for later data reduction. The other screening programs allow both quadrupoles to be stepped with a constant offset between them, neutral loss scan, as well as perform MRM from a given parent.

RESULTS AND DISCUSSION

The DLI probe provided adequate results for the first experiments. The probe was capable of introducing a new sample every 30 sec. and once the probe was optimized it did not have to be moved. The calibration (fig. 1) was linear and the concentration of the TCP in the unextracted urine sample determined from the plot was within 10% of the spiked value. The major drawback of the technique was a detection limit of 700ng due to the 1/100 split in the probe. The use of column extraction techniques and a micro DLI probe were two methods investigated to improve the detection limits.

The column extraction involved concentrating the TCP on the stationary phase of the guard column, then flushing the band of TCP off the phase and into the MS. The analysis procedure is as follows:

(A) H_2O ——→ TCP ——→ CH_3CN/H_2O ——→ Detect ——→ goto (A)

300 s. 15-180 s. 90 s. 60 s.

The results for concentrating a 7.7 ng/ul solution of TCP at a 1.5 ml/min flow rate are shown on fig. 2. The longer concentration times resulted in less efficient extraction of the TCP in addition to larger sample volumes. The detection limits could be reduced to the 100pg/ul range with a 2 min. extraction with an increase in analysis time to 10 min., no faster than GC/MS.

The micro DLI probe showed the best compromise in speed, small sample volumes, and sensitivity. The SRM chromatogram fig. 3 shows adequate sensitivity for TCP, with an analysis time of 1 min. The calibration proved linear over the 9.3 - 90ng range (fig. 4). Again the urine sample concentrations from the calibration plot were within 10% agreement of the known spike value.

CONCLUSIONS

The DLI screening procedure proves to be fast, easy, and capable of being automated. The column extraction techniques or the micro probe provides the capability of performing screening in the low ng range. The screening analysis is not to be confused with confirmation or analysis for the analyte. Its purpose is to separate samples that give a positive response, which require further analysis, from those that give no signal above the threshold. The Apple II computer and interface are capable of controlling the tandem quadrupole and proves to be an adequate and inexpensive data system for screening analysis.

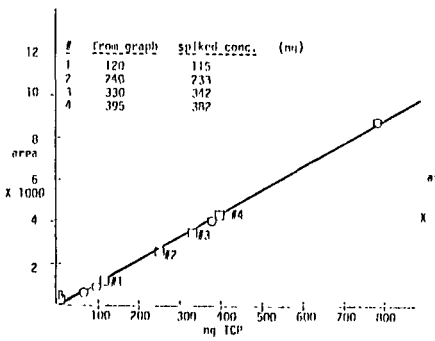


Fig. 1 Calibration for TCP using DLI probe.

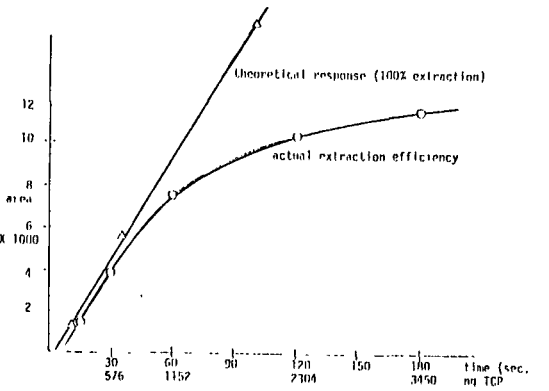


Fig. 2 Extraction of 7.7 ng/ul TCP solution on the 5 cm ODS guard column.

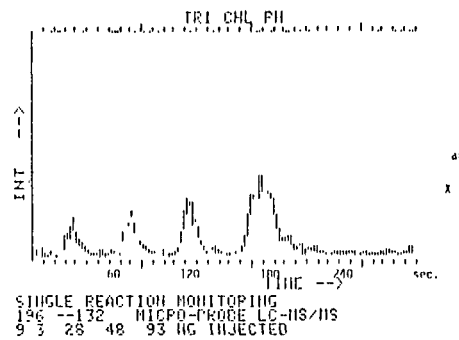


Fig. 3 SRM chromatogram for TCP using the micro DLI probe.

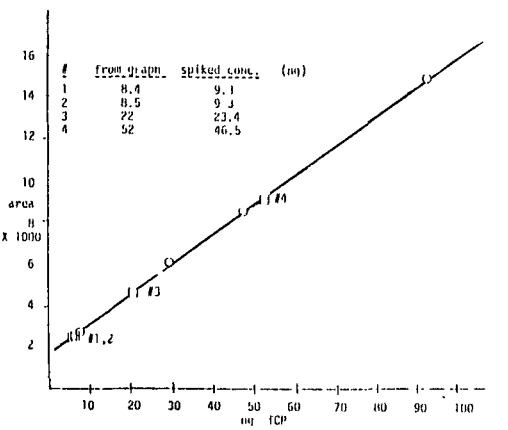


Fig. 4 Calibration for TCP using the micro DLI probe.

FOD 9 TANDEM MASS SPECTROMETRY WITH IMPROVED MASS RANGE; C. J. Proctor, I. J. Amster, M. A. Baldwin, M. P. Barbalas, F. W. McLafferty, and R. S. Yalow*; Department of Chemistry, Cornell University, Ithaca, NY 14853 and Veteran's Administration Medical Center*, Bronx, NY 10468.

The exploitation of exciting new mass spectrometric methods for the ionization of non-volatile molecules has been limited by the resolution and/or mass range of available instrumentation. The MS-I magnet of the Cornell tandem double-focusing mass spectrometer has been replaced with a 60 cm, 23 Kgauss magnet which has an upper mass limit for 8 KV ions of m/z 12,000; the upper mass limit of its MS-II magnet is m/z 4,700 for such ions. The new MS-I magnet also minimizes the second order aberration of the original Hitachi RMH-2 instrument used. This extended mass range should be especially important for biologically important molecules such as polypeptides, polynucleotides, and polysaccharides. MS/MS instrumentation is valuable for such studies, as MS-I offers a unique way not only to detect impurities, but to separate them for structural analysis in MS-II. Further, fragment ions of molecular species separated in MS-I can be structurally characterized from the secondary spectrum resulting from collisionally activated decomposition measured in MS-II. A key assumption in such applications is that the CAD spectrum (omitting peaks arising from low energy processes) is quantitatively characteristic of the structure of the precursor ion, independent of its internal energy. In support of this, changing the average internal energy of $C_7H_7^+$ ions by 1.5 eV changes their absolute CAD cross-sections by $\leq$5%, consistent with theoretical predictions. Applications to biologically-important molecules will include a number that have been examined extensively with sophisticated techniques such as radioimmunoassay. These include a number of variants of the important polypeptides cholecystokinin and insulin.

Acknowledgment: Financial support has been provided by the National Institutes of Health (grant GM-16609).

HIGH PRESSURE COLLISIONAL ACTIVATION MASS SPECTROMETRY

K. Blom and B. Munson
University of Delaware
Newark, Delaware 19711

Chemical Ionization (CI) can produce simplified spectra which contain abundant ions characteristic of the sample's molecular weight. These ions can be collisionally activated by increasing the field strength within the CI source to produce fragment ions which can be correlated to the structural features of the sample. High pressure collisional activation (HPCA) may be a complementary method to CI for characterization of a sample.

The HPCA processes are different from high energy CA in the modes of excitation, time scales of the reactions, and subsequent fate of decomposition products. Reported here are some of the major types of processes observed in HPCA and the basic methodology used for studying them.

Figure I shows the modified drift-tube source used to study HPCA processes. The block consists of a stack of Au-plated Al drift rings separated by Teflon insulators. The reaction chamber is divided into three regions by fine mesh (200 lines/inch), high transparency (≥78%) wire grids. The field strength within each region can be controlled independently to allow activating and reactive collisional processes to be separated and identified.

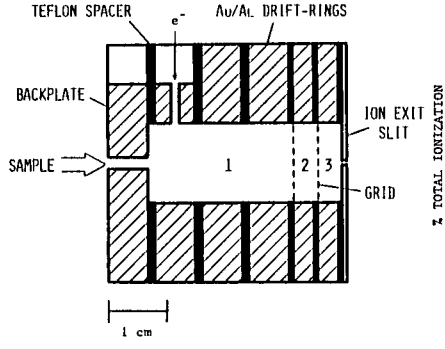


FIGURE I

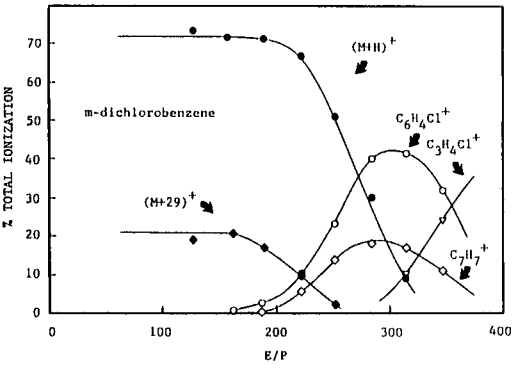


FIGURE II

In one mode of operation of this source, sample ions are produced by CI reactions under low field conditions (5-15V/cm) in regions 1 and 2. These ions are collisionally activated in region 3 by field strengths as high as 200V/cm. The breakdown curves obtained in this way for $(M+H)^+$ and $(M+29)^+$ from m-dichlorobenzene under CH_4 CI conditions are shown in Figure II. The plot represents the distribution of parent and fragment ions as a function of ion energy (E/P = field strength/pressure and is approximately proportional to ion energy). At low energies there is little fragmentation and the CI spectrum is observed. As field strength is increased the CI ions disappear and the major new ion is $C_6H_4Cl^+$ resulting from the fragmentation processes

$$C_6H_4Cl_2H^+ \xrightarrow[*]{CH_4} C_6H_4Cl^+ + HCl \qquad (1)$$

$$C_6H_4Cl_2C_2H_5^+ \xrightarrow[*]{CH_4} C_6H_4Cl^+ + (C_2H_4 + HCl) \qquad (2)$$

The less abundant new ion, $C_7H_7^+$, does not result from a simple fragmentation process, but rather involves the subsequent reaction of $C_6H_4Cl^+$ with the CH_4 reagent gas.

$$C_6H_4Cl^+ + CH_4 \longrightarrow C_7H_7^+ + HCl \qquad (3)$$

The extent of subsequent reaction can be increased by reconfiguring the source so that the fragmentation is initiated by a high field in region 2. The fragment ions then flow into region 3 where they are allowed to react under low field conditions. The ionic distributions obtained with both modes of the source under similar conditions (E/P = 300V/cm torr in CA region) are shown in Figure III. In the "3 region" configuration the $C_6H_4Cl^+$ has essentially disappeared while the $C_7H_7^+$ is the only ion which has increased significantly.

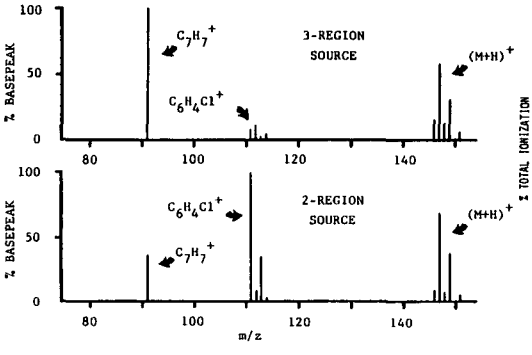


FIGURE III

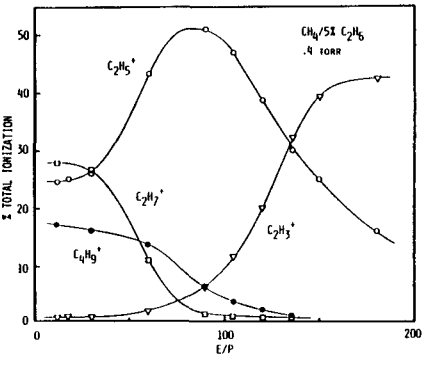


FIGURE IV

In Figure IV are the breakdown curves for the ions in a $CH_4/5\%\ C_2H_6$ mixture, showing the step-wise fragmentation sequence,

$$C_2H_7^+ \xrightarrow[*]{CH_4} C_2H_5^+ + H_2$$

$$C_2H_5^+ \xrightarrow[*]{CH_4} C_2H_3^+ + H_2$$

Step-wise fragmentation appears to be quite common under HPCA conditions and is possible because of the large number of activating collisions an ion undergoes in the CA region.

Since the field strength within the CA region can be changed very rapidly it is possible to obtain CI and CA spectra on consecutive scans of the mass spectrometer. This type of experiment is directly analogous to simultaneous EI/CI in information acquired, but is much simpler from an instrumental standpoint. When combined with a GC it is possible to characterize complex unknown mixtures in a single analysis. Figure V shows the CI and CA spectra for diethylbenzene obtained on consecutive scans at the top of a GC peak.

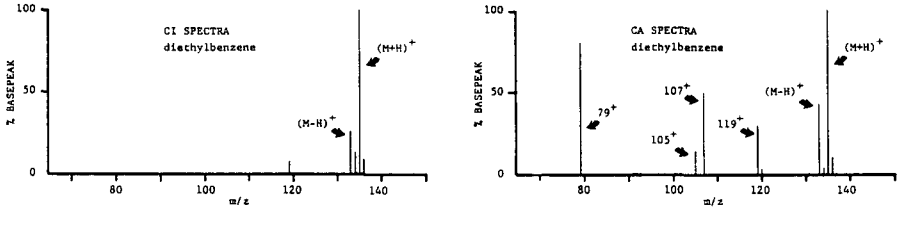


FIGURE V

FOE 1 AN IMPROVED METHOD FOR CALCULATING COMPOUND TYPES IN HYDROCARBON MIXTURES; F.M. Bockhoff and B. Asamoto; Sohio Research Center, Cleveland, Ohio 44128.

The standard method for determining hydrocarbon types by mass spectrometry in C_6-C12 range petroleum mixtures is ASTM Method D 2789. This method reports volume percentages of paraffins, cycloparaffins (naphthenes), and aromatics along with saturate and aromatic carbon numbers. The inverted matrix used to perform calculations is calibrated from hydrocarbon mixtures representative of a virgin naphtha. However, it has been found here that significant errors can occur in the results when some mixtures that vary substantially from a naphtha feed are analyzed by this method.

These errors are caused primarily because of variations in isomer ratios between samples. Especially prone to error are paraffin distributions which are calculated from molecular ion intensities that can vary widely between isomers. For example the relative abundance of molecular ion m/z 86 from n-hexane is 30% versus 0.1% from 2,2-dimethylbutane.

Computer software modifications are presented which reduce errors by taking into account isomer variations between sample types and by allowing isomer bias corrections to be made. This results in increased accuracy in analysis over a wide range of hydrocarbon sample types.

FOE 2 IDENTIFICATION OF SULPHUR COMPOUNDS IN A GASOLINE BY GAS CHROMATOGRAPHY/ QUADRUPOLE MASS SPECTROMETER

GUIEZE (1), DEVANT (2), LOYAUX (2)

1 - FLOPETROL-SCHLUMBERGER, 228, rue Einstein 77530 VAUX LE PENIL FRANCE

2 - NERMAG S.A., 49, quai du Halage 92500 RUEIL-MALMAISON FRANCE

Sulphur compounds are present in gas-oil fractions at very low concentration which makes qualitative and quantitative determinations a rather difficult task.

However, with the help of negative ions detection with CI mode using ammonia as reactant gas, the hydrocarbons are almost completely eliminated which causes the sulphur compounds to appear as intense peaks.

A direct application is to be presented : gasoline, condensed from natural gas pit containing hydrocarbons in the range of C1 to C26 in which concentration of sulphur compounds do not exceed 2 % in weight.

FIELD DESORPTION-HIGH MASS SPECTRAL ANALYSIS OF COAL LIQUEFACTION BOTTOMS AND PETROLEUM RESIDS

Thomas Aczel and James A. Laramee
Exxon Research and Development Division
Exxon Research and Engineering Company
Baytown, Texas

and

Gordon J. Hansen
Johns Hopkins University, Pharmacy Department
Baltimore, Maryland

Introduction

Analysis of heavy ends of both petroleum and coal liquefaction products is of paramount importance in view of the increasing need for the practical utilization of these materials as source for fuels and chemicals. This presentation summarizes preliminary work in this field, using field desorption mass spectrometry (FDMS), coupled with a high field magnet mass spectrometer and high resolution, low voltage mass spectrometry (HRLV MS). FDMS is particularly suited for heavy ends analysis, as the low volatility and low solubility of these materials hinders detailed characterization by conventional MS, GC/MS, NMR and IR techniques.

Experimental

Ground particles from a coal liquefaction bottoms and a highly refined petroleum resid were analyzed by the FDMS method using the Kratos model MS50, equipped with a high field magnet at the Mid-Atlantic MS Center at Johns Hopkins University. The petroleum resid was soluble in THF; the bottoms was only dispersed but nevertheless gave good spectra. FDMS data were obtained at about 3000 resolution. Emitter temperature was increased stepwise from 0 to about 30 mA filament current.

HRLV spectra were obtained at Exxon Research and Engineering Company, Baytown R&D Division using a Kratos MS50. Resolving power was 50,000, and samples were volatilized from a reservoir type inlet at 300 C and 10^{-2} tor. Most of the petroleum resid but only about 10 percent of the bottoms were volatilized. HRMS data were handled with proprietary computer programs.

Results

Field desorption increased the mass range that could be analyzed by a large factor with respect to a conventional probe; from 300-1000 daltons to 300-4000 daltons in the case of the petroleum resid and from 200-600 daltons to 200-1200 daltons in the case of the bottoms. For the mostly naphthenic resid the maximum MW observed corresponds to a C_{270} type saturated molecule, a very noteworthy achievement. Detailed examination of the time resolved FD spectra showed in both cases that increased emitter temperatures lead to regularly increasing MW ranges. The concentrations of the lower MW components decreased regularly with increasing temperatures; no pyrolysis products could be detected. The MW distribution of the petroleum resid showed a distinct, gaussian maximum extending to 3800 daltons. The MW distribution of the bottoms was essentially triangular, with maxima at about 800 to 1000 daltons.

Separations and detailed high and low resolution MS analyses of the petroleum resid showed that it contained 68 percent saturates, mostly naphthenes, and 30 percent aromatics, mostly one and two ring types. Measurable carbon number range was 27 to 57 with maxima in the middle forties.

High resolution, low voltage data of the volatile portion of the bottoms showed it to be a very complex mixture, containing approximately 1000-1200 carbon number homologs. It consisted of 59 percent hydrocarbons, 16 percent mono-oxygen compounds, 3 percent dioxygen and poly-oxygen compounds, 17 percent nitrogen compounds and 5 percent miscellaneous multi-element compounds. The latter included nitrogen-oxygen and sulfur-oxygen types. Aromatics condensation ranged from two to seven plus rings per molecule with an average condensation of about 5.

It can be concluded from these data that FDMS can indeed be used for the MW characterization of both petroleum resids and coal liquefaction bottoms. Susppensious of insolubles in strong solvents yield acceptable spectra. The data seem reasonably reproducible and there was no evidence for pyrolysis. On the other hand, unit resolution is not sufficient for detailed characterization given the enormous complexity of the materials analyzed.

Future research will therefore emphasize high resolution FDMS using relatively low scan speeds; fast sample depletion will be compensated for by slower heating rates, scanning of small segments of spectra, computerized integration of intensities. Other areas of interest will be quantitation and extension to other materials. Calibration of GBC with FDMS data will also be investigated.

Acknowledgements

We thank Professor Catherine Fenselau of Johns Hopkins for gracious encouragement of this effort and helpful discussions; Bob Cuttler of the same organization; Dr. Ann Dell of Imperial College, London, for running some of the samples and helpful discussions; and Exxon Research and Engineering Company.

HIGH PERFORMANCE MS IN THE OPTIMIZATION OF COAL LIQUEFACTION PROCESSES

Bary W. Wilson and Edward K. Chess. Physical Sciences Department, Battelle, Pacific Northwest Laboratory, Richland, WA 99352 and Michael L. Gross. Midwest Center for Mass Spectrometry, University of Nebraska, Lincoln, NE 68588

Determination of higher molecular weight substituted polyaromatics in complex mixtures continues to be a major problem in the analytical chemistry of coal liquids. Heteroatomic polyaromatics having molecular weights in excess of about 250 amu are of particular interest to us, primarily because most of the mutagenicity and much of the carcinogenicity for many coal-derived liquids are found in fractions with components in this molecular weight range.(1)

We have recently conducted a preliminary evaluation of fast atom bombardment (FAB) mass spectrometry for analysis of polar fractions from SRC-II heavy coal liquids. FAB offers several theoretical advantages over other ionization modes as well as over "soft" ionization techniques such as field ionization (FI), field desorption (FD), or chemical ionization (CI) for the analysis of polar, high molecular weight species. EI, CI and FI require the sample to be sufficiently volatile to leave the solids probe inlet during analysis. FD also requires sample heating, and spectra from complex samples may change drastically during analysis. FAB on the other hand, ionizes materials directly from the condensed phase and hence should not discriminate against nonvolatile components. Because FAB ionization has been known to yield spectra comprised essentially of molecular ions species, we also investigated the possibility of applying MS/MS techniques to identify individual components within complex coal liquid fractions.

All collisional activation and fast-atom bombardment data were acquired using a Kratos MS-50 triple analyzer mass spectrometer.(2) The instrument was equipped with a standard Kratos FAB source and was operated with an accelerating potential of 8000 eV. The ion source temperature was maintained at approximately 80°C for the FAB experiments.

FAB mass spectra of several amino polycyclic aromatic hydrocarbons (APAH), a 3° polyaromatic nitrogen heterocycle (PANH) cyano compound, phenazine and benzoquinolines, as well as hydroxylated 2° and 3°PANH were characterized by intense molecular ion clusters in which the base peak corresponded to the protonated molecular ion. Dibenzcarbazole was the single exception and was characterized by a protonated molecular ion (m/z 268) that was only 80% as intense as the base peak molecular ion at m/z 267. Little or no fragmentation was evident in any of the spectra. Main beam ion densities for standards ionized by FAB were sufficient for analysis by collisional activation (CA) mass-analyzed ion kinetic energy spectrometry (MIKES). FAB CA spectra of the protonated molecular ions for several standards showed major differences in relative fragment ion abundances when compared to EI CA spectra for the molecular ion of the same materials.

The FAB CA spectrum of biquinoline, for example, showed an intesense product ion corresponding to the quinoline monomer (Figure 1a). CA MIKES analysis of m/z 257 ion from the 3° PANH fraction of SRC-II 850°F$^+$ coal liquid (Figure 1b) yielded a similar pattern, which was unique among molecular ions from this sample for which CA spectra were obtained. We believe that the striking similarity between the spectra is good evidence for the presence of biquinolines which had not been previously detected in these coal liquids.

Biologically active APAH, 2°PANH and 3°PANH nitrogen subfractions from the 750° to 800° and 850°F$^+$ coal liquid distillates from SRC II all yielded excellent spectra. Molecular ion intensities comprised an essentially Gaussian distribution about the base peak, as would be expected for narrowly cut distillate material.

An interesting difference was noted between samples run using neutral and acidic glycerin as a sample medium: the spectra obtained from the acid matrix were some 50 amu higher in their average molecular weight as estimated by the m/z value of the base peak, and the distribution of molecular ion intensities. Thus, the base peak for the spectrum obtained with neutral glycerin had a base peak of m/z 268 (corresponding to the m/z 267 base peak observed in the EI spectra of this particular fraction). The FAB spectrum of the same fraction obtained with acidified glycerin exhibited a base peak at m/z 314 (see Figure 2). EIHRMS analysis of the nitrogen fractions yielded required elemental compositions for the m/z 267, m/z 281, m/z 299 and m/z 313 ions to assign the first two molecular ions as alkylated benzopyrenes or isomers, and the latter two as alkylated azabenzanthracenes (see Table 1). Elemental compositions with similar fits were found for alkyl homologs of azabenzanthracenes as high as C_8.

This shift in average m/z value was reproducible for each of the APAH, 2°PANH and 3°PANH fractions analyzed. Our working hypothesis regarding this effect is that the more highly alkylated nitrogen compounds do not compete well with the less alkylated species for the available protons in the mixture and hence are less likely to become cationized: the

TABLE 1

m/z	Elemental Composition	Exact Mass	
		Calculated	Found
267	$C_{20}H_{13}N$	267.1048	267.1044
281	$C_{21}H_{15}N$	281.1204	281.1194
299	$C_{22}H_{21}N$	299.1674	299.1660
313	$C_{23}H_{23}N$	313.1830	313.1813

increased availability of protons resulting from the addition of acid to the glycerin allows cationization of the more highly alkylated species.

In these preliminary evaluations, FAB appears to be a useful technique in analysis of polar fossil fuel materials and thus may provide a good complement to other ionization modes which are more suitable to neutral aromatic and aliphatic fractions. With only slight modifications of reference files, calibration may be carried out routinely with customary standards such as perfluorotributylamine. Analysis is straightforward and rapid compared to FD, for example. Since the sample probe need not be heated to effect ionization; spectra do not change noticeably during analysis as is the case in conventional ionization modes when sample probe heating is required.

Average molecular weight estimations for complex mixtures made on the basis of FAB spectra appear to be more accurate and reliable than those made on the basis of FI or CI analyses, particularly when dealing with higher molecular weight materials. Of greatest importance however, with respect to heavy-end coal liquid analysis, is the fact that MIKES spectra may be readily obtained for single ions in complex mixtures, and although these spectra vary substantially in some cases from those obtained by EI, they nonetheless appear to be as unique as EI MIKES spectra and show many of the same structural features. FAB potential in analysis of highly alkylated heteroatomic PAH, which has been demonstrated in these studies, may also prove to be useful in the analysis of fossil fuels in general.

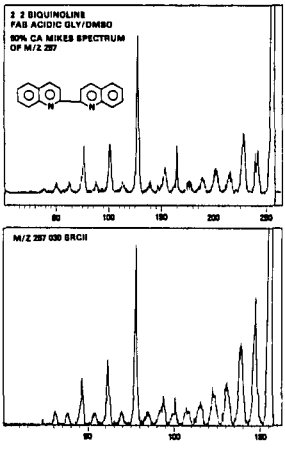


FIGURE 1

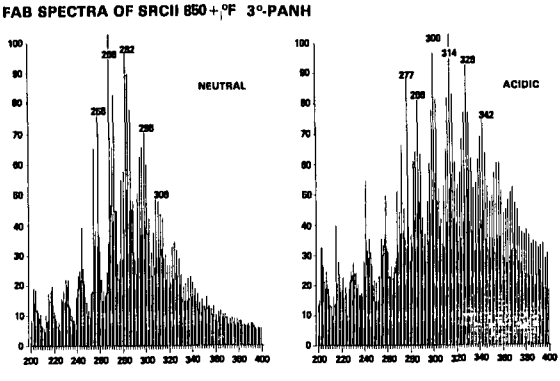


FIGURE 2

1. Wilson, Bary W., Richard A. Pelroy and Dennis D. Mahlum. 1982. Chemical Characterization and Genotoxic Potential Related to Boiling Point for Fractionally Distilled SRC-I Coal Liquids. PNL-4277, Pacific Northwest Laboratory, Richland, Washington.

2. Gross, M. L., E. K. Chess, F. W. Crow, P. A. Lyon, S. Evans, and H. Tudge. 1982. "Triple Analyzer Mass Spectrometry for High Resolution MS/MS Studies." Int. J. Mass Spectrom. Ion Phys. (in press).

Research sponsored by the U.S. Department of Energy under Contract DE-AC06-76RLO 1830.

SCREENING AVIATION FUELS FOR THIOPHENES USING TRIPLE QUADRUPOLE MASS SPECTROMETRY

C.A. Myerholtz and C.G. Enke

Department of Chemistry
Michigan State University
East Lansing, Michigan 48824

The application of triple quadrupole mass spectrometry (TQMS) to the screening of jet aircraft fuels for thiophenes has been examined in our laboratory. Jet fuels present a complex hydrocarbon matrix which makes identification of low-level components difficult. The chance of finding unique molecular ion peaks in the raw fuel mass spectrum for each compound or class of compounds is almost negligible. Tandem mass spectrometry (MS/MS) offers several modes of component specificity besides the molecular ion mass. For particular components, characteristic combinations of parent and daughter masses can provide a high degree of selectivity. In addition, particular daughter ion or neutral loss masses may be highly indicative of certain compound classes. However, in such a complex mixture as raw jet fuel, even these techniques may not provide unique identification for the components of interest.

For the particular case of the thiophenes several characteristics were used to screen for the thiophenes and confirm their presence. Table 1 shows in a condensed form the results of a search for identifiable characteristics of thiophenes. Pure reference compounds, known to be present in aviation fuel were used. Notice that the parent mass (such as 84) alone is inadequate to identify the presence of a thiophene. The cycloalkanes and olefins are isobaric with the thiophene family. However, the neutral loss of 45 (representing CHS) qualified by the parent mass, provides a unique identification for the thiophenes.

This approach is sufficiently selective to readily detect thiophenes containing between zero and four carbon sidechains in samples of commercial aviation fuel (JET-A) with no prior workup. Figure 1 shows a conventional EI mass spectrum obtained from a sample of JET-A. Figure 2 is the result of performing a neutral loss scan for a loss of 45 in the collision cell on the same sample. The peaks due to the thiophenes at 84, 98, 112, 126 and 140 are prominent.

To confirm the presence of the thiophenes a number of secondary experiments were performed. One was scanning for a neutral loss of 32 (representing the loss of sulfur). This scan also produced a set of peaks occurring at 84, 98, 122, 126, and 140 indicating the presence of thiophenes. However, the intensity of these peaks was about a factor of five lower than the peaks resulting from the loss of 45, which makes the loss of 32 a less desirable screening characteristic. Another experiment involved scanning for all the parents of a 97^+ daughter ion. As can be seen fropm Table 1, the 97^+ daughter ion is apparently characteristic of the substituted thiophenes. This experiment generated intense peaks at 98, 112, 126 and 140, identifying the substituted thiophenes. The limitation of this check is that it cannot confirm the presence of thiophene itself.

This work illustrates a method for the development of screening and confirmation procedures for a particular compound class in a given sample type. The great selectivity of TQMS is seen to be expanded still further through the use of secondary confirming characteristics. The ability to analyze for minor components in such a complex matrix without workup confirms the effectiveness of this approach.

This research was supported in part by a grant from NASA.

	PARENT MASS						NEUTRAL LOSS			DAUGHTER
	84	98	112	86	98	114	45	32	33	97
THIOPHENE	X						X	X	X	
METHYL-THIOPHENE		X					X	X	X	X
ETHYL-THIOPHENE			X				X	X	X	X
DIMETHLY-THIOPHENE			X				X	X	X	X
1-HEXENE	X									
CYCLO-HEXANE	X									
2-HEPTANE		X								
METHYL CYCLOHEXANE		X								
2-OCTENE			X							
N-HEXANE				X			X			
N-HEPTANE					X		X			
N-OCTANE						X	X			

Table 1

JET-A

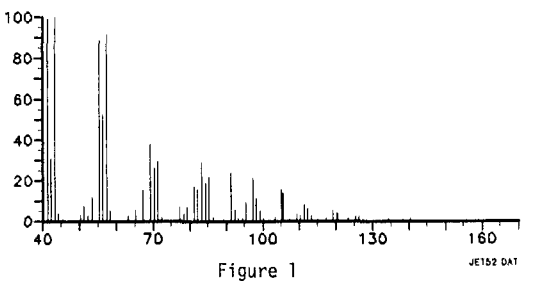


Figure 1

45 LOSS FROM JET-A

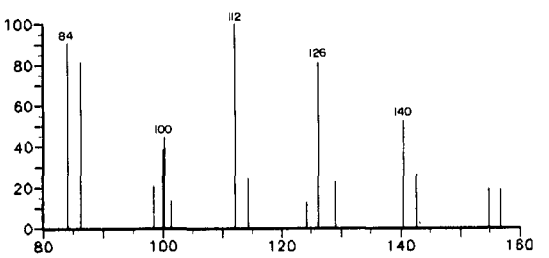


Figure 2

GC/MS AND MS/MS STUDIES OF DIESEL EMISSIONS FROM CHEMICALLY DEFINED FUELS

T. R. Henderson, J. D. Sun, A. P. Li, R. L. Hanson, W. D. Bechtold and J. S. Dutcher
Inhalation Toxicology Research Institute
Lovelace Biomedical and Environmental Research Institute
P. O. Box 5890
Albuquerque, NM 87185

and

T. M. Harvey, J. Shabanowitz and D. F. Hunt
Department of Chemistry
University of Virginia
Charlottesville, VA

Use of diesel engines in light duty vehicles is expected because of increased fuel economy and the ability to utilize a variety of fuels. Mutagenic activity in soot extracts has raised concern over potential adverse health effects. The mutagenicity of soot extracts varies with fuel aromaticity.[1] Fuels from alternate energy sources have increased aromatic content, thus the need for studies of aromatic hydrocarbons in fuels on emissions.

METHODS

A single cylinder, direct-injection Swan engine[2] was operated at 2000 RPM (75% of maximum) and 900 watts load (75% of maximum) on the electric generator to which the engine was coupled. The soot emissions from 300 ml of fuel were collected on Pallflex T60A20 filters after a 1:10 dilution; the filters were extracted with CH_2Cl_2,[2] and evaporated. For GC/MS, 10 to 50 mg of dried extract were spiked with 0.2 mg each of d_{10}-pyrene and d_{12}-benzo(a)pyrene as internal standards. The aromatic fraction was isolated by DMSO fractionation[2] and a 1 µl aliquot was injected into a Finnigan 4023 GC/MS/DS equipped with a 20 m J & W DB-5 fused silica column. The temperature program was 50 to 250°C at 10°/min with a 2 min hold at 50°. Quantitation used the m/z 178, 202, 212, 252 and 264 peak areas. Relative response factors, recoveries of standards, linearity of responses and reproducibilities averaged less than 10% error. MS/MS analyses were carried out on a Finnigan 4500 TSQ at the University of Virginia. Neutral loss (M - 17) scans from m/z 100 to 400 were carried out for 1 sec.[2] MID scans of 0.1 sec were carried out sequentially for nitropyrenes, d_9-nitropyrene and dinitropyrene parent-daughters at m/z 248 to 231; 257 to 240 and 293 to 276, respectively. The low sensitivity for dinitropyrenes resulted not detecting these compounds in the extracts used here. Mutagenicity assays were conducted with Salmonella typhimurium TA98 as described previously.[1,2,4]

RESULTS

Operation of the Swan engine on a pure aliphatic fuel, hexadecane, showed that the PAH emissions were much lower than with a reference diesel fuel[4] of 19.2% aromatic content (Table 1). The specific activity of direct mutagens was similar in both cases, but there were 33% extractable organics associated with soot from reference fuel combustion vs. only 13% from hexadecane, resulting in much lower total mutagen emissions from aliphatic fuels as previously reported by Yergey et al.[5]

Adding PAHs to hexadecane fuel resulted in two types of emissions effects. PAHs which were relatively refractory to combustion in diesel engine were more concentrated in soot extracts than in the fuel and did not alter the emissions of other PAHs. Table 1 shows that 1% pyrene in hexadecane increases the pyrene emissions but had only minor effects on other PAH emissions. Soot-promoting PAHs, such as methylnaphthalenes, acenaphthenes or benzo(a)pyrene increased particulate emissions by 2 to 4 fold and increased emissions of a variety of other PAHs. Table 1 shows the changes in emissions from addition of 1% benzo(a)-pyrene to hexadecane fuel.

Table 2 shows that there was no quantitative correlation between MS/MS estimates of nitropyrene concentrations in aromatic soot fractions and direct mutagenicity. DMSO fractionation removes dinitropyrenes, which partition into polar fractions, thus removing their contribution to mutagenicity.[2] MS/MS comparisons of soot extracts from 0.01%, 0.10% and 1.0% pyrene supplemented fuels showed that the only difference from this non-soot promoting PAH was increased peak intensities at m/z 231, the daughter ion from nitropyrenes/nitrofluoranthenes.

MS/MS spectra of emissions from the addition of 1% benzo(a)pyrene to hexadecane showed overall changes in nitro-PAHs emissions as expected from the altered PAH emissions. The major nitro-PAH ion was m/z 202, which corresponds to dinitronaphthalenes. Single ring

nitro-PAHs were also noted which are not known to be active mutagens. Dinitronaphthalenes are also low in mutagenic activity.[6]

A new mechanism for soot production during combustion has recently been proposed.[7] This model proposes that reactive aromatic intermediates such as PAH radicals are the immediate precursors for soot formation. These reactive intermediates are proposed to be interconvertible with PAHs. This mechanism provides an explanation of why soot-forming PAHs increase the emissions of many other PAHs as well as soot. This mechanism also explains why relatively refractory PAHs such as pyrene may not affect either soot or other PAH emissions.

TABLE 1
EFFECTS OF FUEL ALTERATIONS ON DIESEL SOOT EXTRACT* COMPOSITION

Fuel	Revertants/µg TA98 Mutagenicity	mg PAH emissions/l fuel		
		Phenanthrene	Pyrene	Benzo(a)pyrene
Reference[4]	20	22	41	2.6
Hexadecane	18	1.4	6.2	2.5
Hexadecane + 1% Pyrene	20	1.8	75	0.4
Hexadecane + 1% Benzo(a)pyrene	2.5	73	97	93

*Unfractionated extracts of soot.

TABLE 2
MS/MS NITRO-PYRENE LEVELS VS MUTAGENICITY OF AROMATIC* SOOT FRACTIONS

Fuel	PPM Nitropyrenes	Revertants/µg TA98 Mutagenicity
Reference	342	53
Hexadecane	590	55
Hexadecane + 1% Pyrene	1000	41
Hexadecane + 1% Benzo(a)pyrene	15	2

*Extracts fractionated with DMSO[2,4]

REFERENCES

1. Clark, C. R., Henderson, T. R. Royer, R. E., Brooks, A. L., McClellan, R. O., Marshall, F. and Naman, T. M., Fund. Appl. Toxicol. (in press, 1982).
2. Henderson, T. R., et al., Paper presented at 1981 EPA Diesel Emissions Symposium, Raleigh, N.C. Oct 5-8, 1981.
3. Henderson, T. R., Royer, R. E. and Clark, C. R., Proceedings 29th Annual Conference ASMS (1981). p. 642-643.
4. Henderson, T. R., Royer, R. E., Clark, C. R., Harvey, T. M. and Hunt, D. F., J. Appl. Toxicol. (in press, 1982).
5. Yergey, J. A., Risby, T. H. and Lestz, S. S., Paper delivered at 1981 EPA Diesel Emissions Symposium, Ibid.
6. Tokiwa, H., Nakagawa, R., and Ohnishi, Y., Mutation Res. 91:321-325 (1981).
7. Pasternak, M., Zinn, B. T. and Browner, R. F., in Eighteenth Annual Symposium on Combustion, the Combustion Institute, Philadelphia, Pa., 1981.

ACKNOWLEDGEMENTS

Research performed under U.S. Department of Energy Contract DE-AC04-76EV01013.

CAPILLARY COLUMN GC-LOW RESOLUTION MS TECHNIQUES FOR MONITORING TOXIC ORGANIC COMPOUNDS IN COMBUSTION EFFLUENTS*

T.O. Tiernan, J.H. Garrett, J.G. Solch, G.F. VanNess, and M.L. Taylor
Brehm Laboratory and Depts. of Chemistry and Pharmacology/Toxicology
Wright State University, Dayton, Ohio 45435

Recent reports indicating the presence of highly toxic chlorinated dibenzo-p-dioxins (CDDs) and chlorinated dibenzofurans (CDFs) in the effluents from combustion of municipal waste[1,2] have prompted the development of elaborate analytical schemes for determining the quantities of entire series of these and other related compounds in combustion products. The present paper describes analytical procedures in which such samples are extracted, fractionated, and analyzed for CDDs, CDFs, chlorinated phenols (CPs), chlorinated benzenes (CBzs), and polychlorinated biphenyls (PCBs) using coupled gas chromatography-mass spectrometry.

Stack effluents from a waste-fueled boiler were sampled by using an EPA Method V Sampling Train, which is comprised of a quartz-lined probe, a filter for trapping particulates, three cooled glass impingers (the first containing water, the second being empty, and the third containing silica gel), and a glass trap containing XAD-2 resin. Following sampling, the train was disassembled and the particulate filter, the resin trap and the impinger contents were removed for analyses. In addition, the front portion of the train was rinsed with methanol and toluene, successively, and the back portion of the train was rinsed with toluene, and the rinses were also retained and analyzed. Each train thus yielded six samples for analysis.

Both liquid and solid samples from the train were spiked prior to analyses with a set of internal standards, which included $^{37}Cl_4$-2,3,7,8-tetrachlorodibenzo-p-dioxin; $^{37}Cl_4$-1,2,3,4,6,7,8-heptachlorodibenzo-p-dioxin; $^{37}Cl_8$-octachlorodibenzo-p-dioxin; D_6-3,3',4,4'-tetrachlorobenzene; $^{13}C_6$-pentachlorophenol and $^{13}C_6$-hexachlorobenzene. Liquid samples were extracted with hexane, except for the methanol rinses, which were extracted with benzene in a Soxhlet apparatus. All of the organic extracts were cleaned-up and fractionated by using a sequence of acid, base, and H_2O washes, followed by sequential liquid chromatographic separation using base modified silica and alumina columns. One fraction was isolated containing the PCBs and CBzs, while a second fraction, containing the CDDs and CDFs was obtained. A third fraction, containing the CPs, was derivatized to yield the acetylated chlorophenols.

Portions of extracts of each of the fractions prepared as described above, were analyzed using a Perkin-Elmer Sigma III Gas Chromatograph coupled to a Kratos MS-25 Mass Spectrometer equipped with a DS-55SM Data System. The gas chromatographic column utilized was a 50 meter WCOT OV-101 fused silica capillary column, operated with hydrogen carrier gas, and was temperature programmed during the analyses. The mass spectrometer was operated in the Selected-ion Monitoring Mode. Computer controlled operating sequences were developed and utilized, in which the ion masses monitored, the sweep widths, dwell times and other parameters were automatically adjusted to permit detection of the entire series of all of the compounds monitored (tetra- through octa- CDDs and CDFs, di- through hexa- CBzs, tri- through penta- CPs, and tetra- thru deca- PCBs). In general, at least two ion masses characteristic of each chlorinated class of each of these compounds were monitored at the appropriate GC elution period. The instrumental operating sequence, showing the GC and MS parameters utilized in the analyses of the CDDs and CDFs are shown in Table 1. Similar sequences were developed and applied for the other classes of compounds monitored.

Typical data obtained using the analytical procedures described are shown in Table 2. In some cases, information on specific isomeric composition of the various chlorinated classes was also obtained, although this was limited by the availability of pure standards. The groups of compounds of interest here comprise a total of some 450 discrete isomers.

*Supported in part by the U.S. Environmental Protection Agency.

1. J.W.A. Lustenhouwer, K. Olie and O. Hutzinger, Chemosphere 9, 501 (1980).
2. T.O. Tiernan, M.L. Taylor, J.G. Solch, G.F. VanNess and J.H. Garrett, Resources and Conservation, in press (1982).

TABLE 1

SEQUENCE OF OPERATIONS IN GC-MS-25-DS ANALYSES OF SAMPLE EXTRACTS FOR CHLORODIBENZO-p-DIOXINS AND CHLORODIBENZOFURANS

Elapsed Time (min)	Event	GC Column Temperature	Temperature Program Rate (°C/Min)	Ions Monitored By Mass Spectrometer (m/z)	Compounds Monitored
0.00	Injection, splitless	190°C	--		
1.50	Turn on split valve	190°C	--		
2.00	Begin temp program to 220°C	190°C	5°C/min		
5.00	Open column flow to Mass Spect.	205°C	5°C/min		
16.00	Start MID PROGRAM #4	220°C	--	303.902	Cl_4 furans
	Sweep - 100 ppm			305.899	Cl_4 furans
	Time on Cl_4 mass = 0.15 sec			319.897	Cl_4 dioxins
	Time on ^{37}Cl-TCDD = 0.05 sec			321.894	Cl_4 dioxins
				327.885	$^{37}Cl_4$ labelled TCDD
23.75	Stop MID PROGRAM #4	220°C	--		
24.25	Start PROGRAM #5	220°C	--		
	Sweep = 750 ppm			337.863	Cl_5 furans
	Time on penta mass = 0.2 sec			339.860	Cl_5 furans
				353.858	Cl_5 dioxins
				355.855	Cl_5 dioxins
25.00	Begin Temp program to 230°C	220°C	5°C/min		
34.50	Stop MID PROGRAM #5	238°C			
35.00	Start MID PROGRAM #6	230°C		373.821	Cl_6 furans
	Sweep - 150 ppm			375.821	Cl_6 furans
	Time on each mass = .25 sec			389.816	Cl_6 dioxins
				391.813	Cl_6 dioxins
50.00	Begin temp program to 235°C		5°C/min		
53.50	Stop MID PROGRAM #6	235°C	--		
54.00	Start MID PROGRAM #7				
	Sweep = 750 ppm				
	Time on each mass = 0.35 sec	235°C	--	407.782	Cl_7 furans
				409.779	Cl_7 furans
				423.777	Cl_7 dioxins
				425.774	Cl_7 dioxins
				431.765	$^{37}Cl_4$ labelled TCDD
70.00	Stop MID PROGRAM #7				
85.00	Start MID PROGRAM #8	235°C	--	441.743	Cl_8 furans
	Sweep = 750 ppm			443.740	Cl_8 furans
	Time on each mass = 0.50 sec			457.738	Cl_8 dioxins
95.00	Stop MID PROGRAM #8	235°C		459.735	Cl_8 dioxins
130.00	Return to initial temp			471.717	$^{37}Cl_8$ labelled TCDD

TABLE 2

QUANTITIES OF CDDs, CDFs, CPs, AND CBzs IN EFFLUENTS FROM A REFUSE INCINERATOR

No. of Chlorine Atoms in Molecule	Quantity (nanograms per sample) CDDs	CDFs	(% of Total Compounds Detected) CPs	CBzs
3	-	-	299000 (54)	4820 (0.86)
4	3160 (0.56)	14700 (2.6)	128000 (23)	6130 (0.11)
5	4150 (0.74)	5220 (0.94)	38800 (6.9)	22500 (4.0)
6	6970 (1.2)	6320 (1.1)	-	8320 (1.5)
7	3450 (0.62)	2660 (0.48)	-	-
8	910 (0.16)	144 (0.03)	-	-

GCMS ANALYSIS OF POLAR COMPONENTS IN THE OIL PRODUCTS AND WASTEWATER EFFLUENT FROM THE GFETC SLAGGING FIXED-BED GASIFIER

Edwin S. Olson, John W. Diehl, and David J. Miller
Grand Forks Energy Technology Center
Box 8213, University Station
Grand Forks, ND 58202

Characterization of the polar constituents of the oil product and effluent water condensate from the GFETC slagging fixed-bed gasifier has been carried out to identify toxic substances present, to better understand the effects of different process conditions, and to help in designing effluent or product treatment processes. Of special interest are phenolics, amines or azarenes, and polar carbonyl compounds, many of which are not extractable with organic solvents.

Phenolics were separated from the oil product and effluent water by solvent extraction schemes. Identification of the phenols was done with gcms (EI) and retention index matching, using a silicone bonded-phase fused silica capillary column. Good resolution of alkylphenols was obtained by using low starting temperatures and slow heating rates; however, overlap of alkylphenol with guaiacol peaks was evident from the mass spectra. A normal phase hplc separation using 10% chloroform in hexane on a cyano column was effective in resolving the phenolics into classes of guaiacols and 2,6-dialkylphenols, ortho-phenols, meta- and para-phenols, and naphthols. Only five guaiacols were present; however, almost every C_1, C_2, and C_3 alkylphenol isomer was found. Numerous alkyl substituted indanols, naphthols, and phenylphenols were also present.

A significant amount of organic material was not extracted from the condensate water at acidic or basic pH by methylene chloride or other solvents. Most of this material was removed by adsorption on charcoal. Extraction of the charcoal with methylene chloride, ethanol, or DMF yielded fractions which were analyzed using a Superox-FA fused silica column. The major constituents were five different 5,5-dialkylhydantoins, 5,5-dimethylhydantoin, 5-ethyl-5-methylhydantoin, 5,5-diethylhydantoin, 5-methyl-5-propylhydantoin, and 5-methyl-5-isopropylhydantoin. These were presumably derived from the reaction of various ketones with cyanide and ammonia in the condensate. Methylation of the hydantoins was carried out and the N,N-dimethyl-derivatives analyzed by gcms on a silicone column. These derivatives gave more intense molecular ions than the underivatized hydantoins.

DIAGNOSIS OF ORGANIC ACIDEMIAS BY GAS CHROMATOGRAPHY MASS SPECTROMETRY

Yong Y. Lin, J.A. Heininger: N.Y.S. Institute for Basic Research in Developmental Disabilities, 1050 Forest Hill Road, Staten Island, N.Y. 10314
and
T. Shinka, I. Matsumoto: Kurume University, School of Medicine, Kurume, Japan
and
T. Aoyama, T. Higuchi, K. Nojima: JEOL, Ltd., Tokyo, Japan
and
I. Arad, Hadassah University Hospital, Jerusalem.

GC-MS has become an important tool for the diagnosis and studies of metabolic disorders. The application to the diagnosis of organic acidemia, in particular, has been well established in many clinical laboratories. We, the Institute for Basic Research in Developmental Disabilities at New York and the GC-MS Institute of Kurume University at Japan, use the GC-MS analysis as the routine diagnostic studies for organic acidemias involving many inborn error metabolic diseases or neurological disorders.

The standard method of analysis involves solvent extraction of urine (plasma, CSF, or amniotic fluids, etc.) by ether-ethyl acetate, trimethylsilylation by bis (trimethylsilyl)-trifluoroacetamide (BSTFA), and GC-MS analysis. Most of nonvolatile organic acids in the biological fluids can be detected, identified and diagnosis of organic acidemia can be made; amino acids analysis are made in parallel for detecting metabolic disorders involving amino acids.

While many organic acidemia can be diagnosed successfully by this standard method, demands of improvement in sample separation techniques and mass spectrometric characterizations emerge from time to time in order to achieve more efficient diagnosis and studies of intricate profiles of metabolic disorders. We report here two examples of our approaches.

I) Aromatic Amino Acids Metabolic Disorders by GC-CIMS Using NH_3 as the Reagent Gas:

Aromatic amino acids, Phe, Tyr and Trp are biochemical precursors of important neurotransmitters or biogenic amines. Metabolic disorders involves with aromatic amino acids may closely relate to mental retardation and other psychoneurosis. We established an accurate and rapid analysis of aromatic amino acids metabolites by utilizing selective absorption of the metabolites into Amberite XAD resin and characterization of the metabolites by GC-CIMS using NH_3 as the reagent gas.

One ml of urine from patient with phenylketonuria (PKU) or tyrosinemia was adjusted to pH 2.0 with formic acid and absorbed to a short column of XAD-4. The column was washed thoroughly with water. The aromatic amino acids metabolites absorbed was eluted from the column with methanol. TMS derivatives were made with BSTFA in acetonitrile. GC-CIMS analysis was carried out with an 3% OV-17 column and ammonia as the reagent gas. The RIC chromatograms of urines from PKU and typrosinemia patients are shown in Fig 1 and 2. Accumulation of metabolites, PLA, PHE, PPA, and N-Acetylphenylalanine in PKU and 4-HPLA, Tyr, 4-HPPA in tyrosinemia patients, are quickly characterized.

The mild ionization of NH_3 CI gave quasi-molecular ions, M+1 or M+18, as the base peaks in all of the CI spectra of metabolites. These ions were utilized for the ion monitoring of the metabolites; thus, sensitive and reproducible quantitation of the metabolites were achieved.

II) GCMS Analysis of Glutaric Aciduria:

The urine, plasma and CSF of a child who developed severe metabolic acidosis, hypoxemia and hypoglycemia shortly after birth was studied by GC-MS analysis. The urinary organic acid pattern (Fig. 3) shows remarkable elevation of glutaric acid, lactic acid and 4-hydroxyphenyllactic acid; similar organic acid profiles were also obtained from the GC-MS of plasma and CSF. Characterization of most metabolites were made by identification of the fragmentations from their EI spectra; however, additional information such as molecular weights, obtained from GC-CIMS (isobutane) facilitate the characterization. The EI spectra of peak 4 in Fig. 3 caused considerable concerns initially with three peaks, m/z 173, 145 and 75. However the mw of 188 was clearly shown by the isobutane CI; m/z 189, 173 and 99. An easy loss of a methyl group from the parent molecule rather than from a TMS group in the CI spectra was further indicated from the isobutane CI spectra of the tetradeuteriomethyl derivative, which gave m/e 198, 182 and 99. The compound was identified to be a mono-TMS derivative of the lactol form of 4-oxopentanoic acid (levulinic acid).

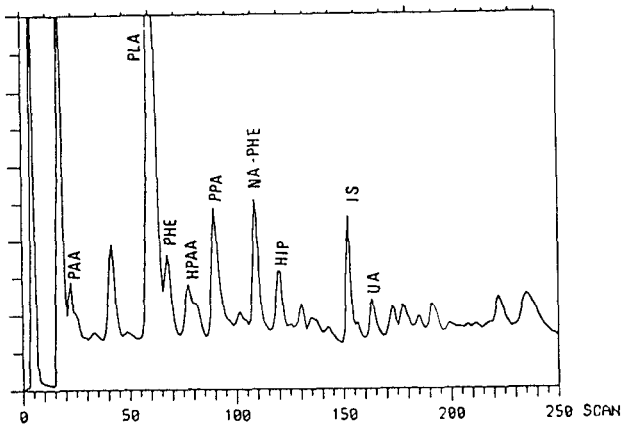


Fig. 1 - Urinary metabolites of 3 year old PKU patient.
PAA = phenylacetic acid; PLA = phenyllactic acid; PHE = phenylalanine;
HPA = 4-hydroxyphenylacetic acid; PPA = phenylpyruvic acid;
NA-PHE = N-acetylphenylalanine; HIP = hippuric acid;
IS (int. standard) = hexadecanoic acid; UA = uric acid.

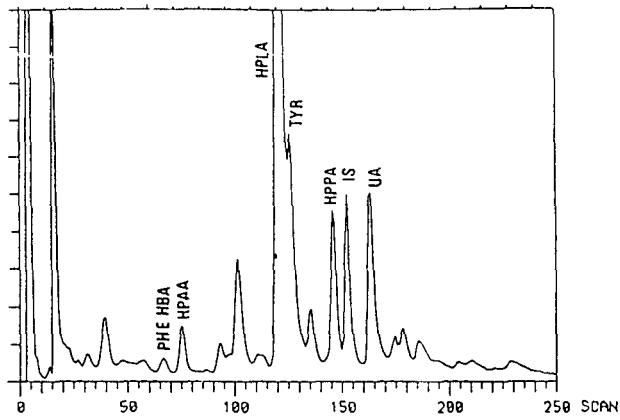


Fig. 2 - Urinary metabolites of 1 year old tyrosinemia patient.
HPLA = 4-hydroxyphenyllactic acid; TYR = tyrosine;
HPPA = 4-hydroxyphenylpyruvic acid.

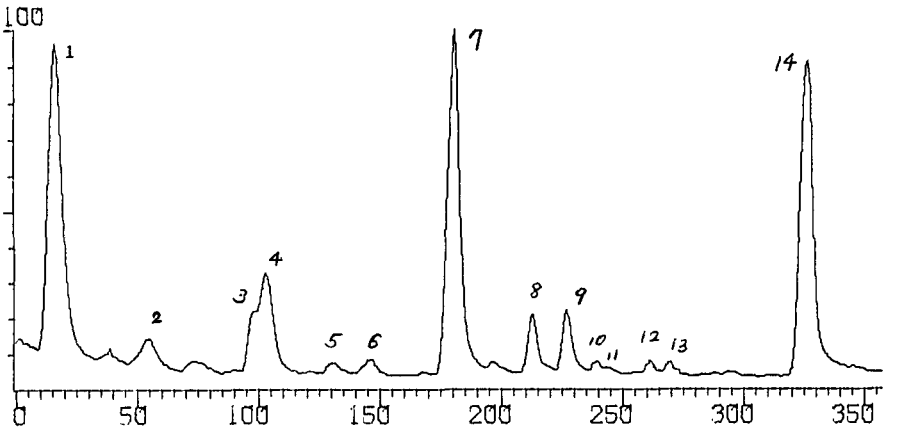


Fig. 3 - Urinary metabolites of Glutaric Aciduria

1) lactic acid
2) 3-hydroxybutyric acid
3) 3-hydroxyvaleric acid
4) 4-oxopentanoic acid
5) phosphoric acid
6) succinic acid
7) glutaric acid
8) adipic acid
9) 2-hydroxyglutaric acid
10) isovalerylglycine
11) 2-hydroxyfurane-5-carboxylic acid
12) 4-hydroxyphenylacetic acid
13) suberic acid
14) 4-hydroxyphenyllactic acid

AMMONIA METABOLISM OF A PATIENT WITH ORNITHINE TRANSCARBAMYLASE DEFICIENCY DETECTED BY ^{15}N TRACER

H. Yabuuchi, H. Kodama, K. Samukawa, O. Nose, S. Okada

Department of Pediatrics, Osaka University Medical School
Fukushima-ku, Osaka, Japan

Ammonia metabolism was studied in an 8 year-old girl with ornithine transcarbamylase deficiency using ^{15}N tracer. The patient was asymptomatic until 2 years of age, when she began to have intermittent episode of vomit, lethargy, anorexia and inappropriate behavior. Her plasma ammonia level was 250-500 μg/dl (normal level: less than 50 μg/dl) and her blood urea nitrogen was 6-8 mg/dl. Her serum and urine glutamine levels were increased (serum: 1,450 μmole/l, urine: 1.48 μmole/mg of creatinine), but other amino acids in the serum and urine were within normal ranges. Orotic acid excretion in her urine was 97.4 μg/mg of creatinine (control: 4.4-7.3 μg/mg of creatinine). Her liver ornithine transcabamylase activity was a few percent of that of normal control.

The patient was given 500 mg of 99.6 atom % excess of ^{15}N-ammonium chloride (25 mg/kg) orally after overnight starvation. Blood samples were taken before and 0.5, 1, 2, 3 and 6 hours after administration. Urine were collected at 2 hours intervals during the first 6 hours and then urine collection was continued for 2 days. ^{15}N-excess ratios of urinary ammonia and urea were measured separately by Conway's diffusion method and analyzed by mass spectrometry. Amino acids in the serum and urine were separated by ion exchange resin. The N-TFA-O-butyl ester derivatives of these amino acids were analyzed by GC-MS. The fragment ion m/e at 140 was used for determining the ^{15}N-excess ratio of alanine, because it had the highest relative intensity and included nitrogen. The ratio of the relative intensity value of m/e 141 to that of 140 was calculated and the ^{15}N-excess ratio was obtained using Vanden Heuvel's equation. The fragment ion that had the highest relative intensity and included nitrogen was selected from the mass spectrum of each amino acid for examination of the ^{15}N-excess ratio of each amino acid.

The serum level of ammonia in the patient increased to a maximum 30 min. after loading of ammonium chloride and serum glutamine also increased. However, the levels of other amino acids did not change significantly. In the patient, 4.6 % of administered ^{15}N was recovered as ammonia-^{15}N in the urine and most of them were excreted within 6 hours. The patient excreted 20.4 % of administered ^{15}N as urea in two days. On the contrary, the control excreted very small amount of ammonium and excreted 63.6 % of administered ^{15}N as urea in 2 days (Fig. 1). After administration of ^{15}N-ammonium chloride much of ^{15}N was incorporated into α-amino N of glutamine and of glutamate in

both control and patient. The incorporation was greater in the patient(Fig. 2). The incorporation of ^{15}N into asparagine was low in the control but was high in the patient(Fig. 2). Large amount of ^{15}N was rapidly incorporated into alanine and serine in the patient compared with that of the control. On the other hand, labeling of serum ornithine in the control reached a maximum of 1.46 atom % excess after 1 hour, but it was 0.66 atom % excess after 3 hours in the patient(Fig. 2). The incorporation of ^{15}N into other amino acids, i.e. valine, glycine, isoleucine, leucine, threonine and lysine were very small and were not significantly different between patient and control.

These results show that much ^{15}N was incorporated into glutamine, alanine, asparagine and serine and this suggest that the formation of these amino acids can serve to remove excessive ammonia in the patient. The ^{15}N-excess ratio of amino acid could be measured with a small amount of sample by GC-MS. This technique is useful for examining the amino acid and ammonia metabolism in humans.

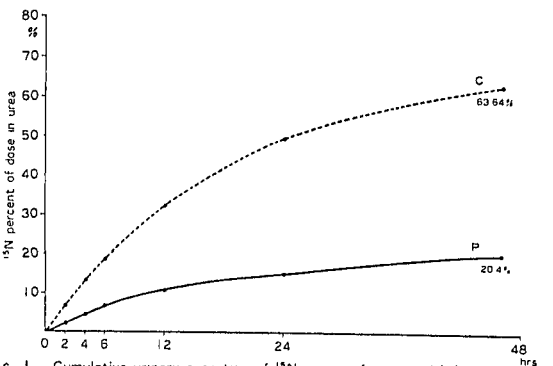


Fig. 1 Cumulative urinary excretion of ^{15}N in urea, for control (C) and patient (P) expressed as percentages of dose given.

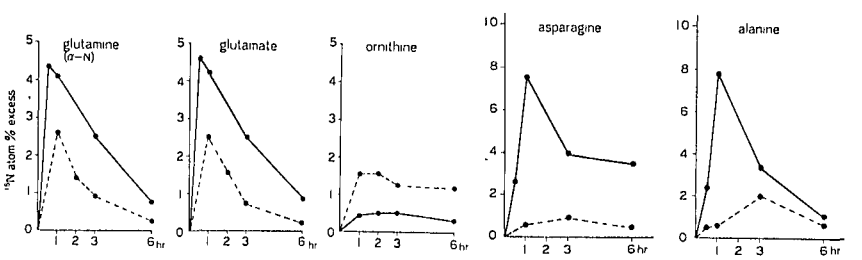


Fig. 2 ^{15}N specific activity curves following oral administration of $^{15}NH_4Cl$ ●—● patient with OTC deficiency. ●---● control

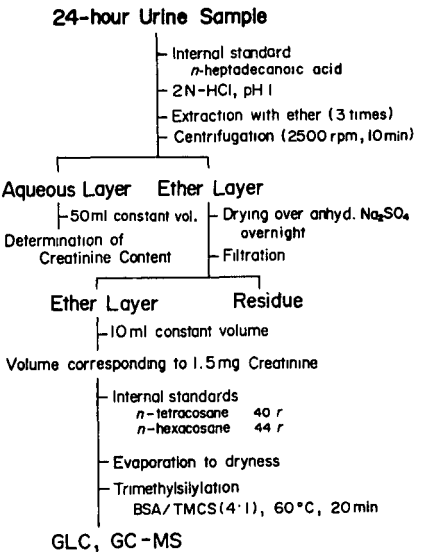
STUDIES OF HYPERTENSIVE RAT URINARY ORGANIC ACIDS USING CAPILLARY GC/MS

Akira Hayashi and Masanori Morita*

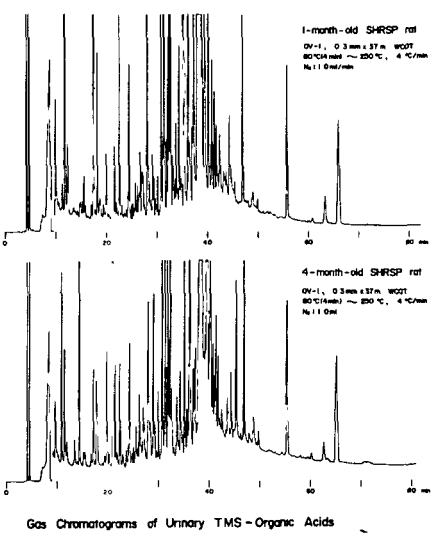
Department of Chemistry, Faculty of Science and Technology, and Research Laboratory of GC/MS*, Kinki University, Higashi-Osaka 577, Japan

The relationship between urinary organic acid profiles and the onset of hypertension was investigated using capillary column GC/MS to improve diagnosis of spontaneous hypertension.

Two kinds of rats were used: spontaneously hypertensive rat-stroke prone (SHRSP)[1] and Wistar Kyoto (WKY) rats of ages 1 and 4 months. SHRSP rats were normal at 1 month of age, but already hypertensive at 4 months. The 24-hour urine was collected from four 1-month-old rats for 7 days and six 4-month-old rats for 5 days and stored at -20°C. Organic acids were extracted as shown in Scheme 1, and ether layer aliquots corresponding to 1.5 mg creatinine were trimethylsilylated with BSA/TMCS (4:1) at 60°C for 20 min., then analyzed by gas chromatography using an open tubular glass capillary column wall-coated with OV-1 (0.3 mm x 37 m), programmed from 80° to 250°C at 4°C/min. Preliminary experiments showed that these reaction condi-



Scheme 1



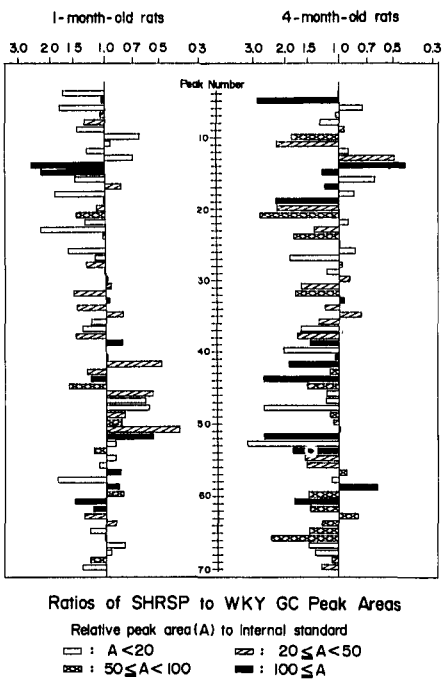
Gas Chromatograms of Urinary TMS-Organic Acids

Fig.1

tions were adequate for trimethylsilylation of urinary organic acids.

About 70 well-defined peaks (of a total of 130 peaks) were obtained with good reproducibility as shown in Fig. 1. Most of these were identified by retention time[2], GC-EI-MS[3,4] and GC-CI(isobutane)-MS. The peak area ratio of SHRSP to the corresponding peak area of WKY was calculated for both 1- and 4-month-old rats, and is shown in Fig. 2. As the peaks showing significantly high peak ratio (2.3-2.6) in 1-month-old rats, we found methylmalonic acid (peak no. 14) and benzoic acid (15), while 3-hydroxy-3-methylglutaric acid (42), dodecanoic acid (46) and 3-hydroxyphenyllactic acid (52) were very low-ratio (0.5-0.6) compounds. These peaks could be utilized as signs of the onset of hypertension.

When the SHRSP/WKY ratio of each peak of 1-month-old rats is compared with that of 4-month-old rats for the values shown in Fig. 2, many peaks show marked variation between 1- and 4-month-old rats. Some of these compounds may have some relation with the outbreak mechanism of hypertension. Methylmalonic acid (peak no. 14) showed the most significant variation.



Ratios of SHRSP to WKY GC Peak Areas

Relative peak area(A) to internal standard

□ : A<20 ▨ : 20≦A<50

▨ : 50≦A<100 ■ : 100≦A

Fig.2

1) Yamori, Y., Nagaoka, A. and Okamoto, K., Jap. Circ. J., 38, 1095 (1974)

2) Tanaka, K., Hills, D.G., West-Dull, A. and Lynn, T.B., Clin. Chem., 26, 1839 (1980)

3) Goodman, S.I. and Markey, S.P.,-"Diagnosis of Organic Acidemias by Gas Chromatography-Mass Spectrometry", A.R. Liss, Inc., New York (1981)

4) Niwa, T. et al., Clin. Chim. Acta, 108, 113 (1980); 110, 51 (1981)

METABOLIC PROFILING OF DIABETIC KETOACIDOSIS USING GC-MS

T. Niwa, K. Maeda, H. Asada, N. Yamamoto, M. Shibata, T. Ohki* and K. Yamada

Department of Internal Medicine, Nagoya University Branch Hospital
1-4, Daiko-cho 1-chome, Higashi-ku, Nagoya 461, JAPAN

*The Bio-Dynamics Research Institute
3-2, Tamamizu-cho 1-chome, Mizuho-ku, Nagoya 467, JAPAN

SUMMARY

The organic acids in the urine and serum of diabetic patients with ketoacidosis were analyzed by gas chromatography-mass spectrometry. In the urine some 50 compounds were identified. 3-Hydroxyvaleric acid, 5-hydroxyhexanoic acid and 2-hydroxy-2-methyllevulinic acid were newly identified in the urine from the diabetic patients with ketoacidosis. The acids became undetectable in their urine after insulin therapy when the patients became nonketotic. The acids were not detected in the urine and serum of healthy subjects or diabetic patients without ketosis. The diabetic patients with ketoacidosis showed the elevated urinary excretion of lactic acid, 2-hydroxybutyric acid, 3-hydroxyisovaleric acid, adipic acid and 2,3-dideoxypentonic acid.

INTRODUCTION

Gas chromatography-mass spectrometry (GC-MS) has been used to study the altered metabolism in diabetic ketoacidosis by profiling the organic acids in the urine and serum of diabetic ketoacidotic patients. The increased urinary excretion of adipic acid, suberic acid, 3-hydroxyisovaleric acid, 3-hydroxyisobutyric acid, 2-methyl-3-hydroxybutyric acid, 2-hydroxyisovaleric acid, and 2-hydroxybutyric acid has been reported. We investigated the organic acid profile of diabetic patients with ketoacidosis and identified 3-hydroxyvaleric acid, 5-hydroxyhexanoic acid and 2-hydroxy-2-methyllevulinic acid for the first time. (1, 2)

MATERIALS AND METHODS

Samples: Urine samples were obtained from four diabetic patients with ketoacidosis, three diabetic patients without ketosis and five healthy adults. Serum samples were obtained from four diabetic patients with ketoacidosis, six diabetic patients without ketosis and six healthy adults.

Sample preparation: Serum was ultrafiltrated by a filter (Amicon CF 25). One ml of urine or serum ultrafiltrate was acidified to pH 1 with HCl, and saturated with NaCl. As an internal standard 50 µg or 10 µg of p-(n-amyl)-benzoic acid was added to the urine or serum ultrafiltrate respectively. The organic acids were extracted three times with 3 ml of ethyl acetate. The organic phase was dehydrated over anhydrous sodium sulfate, and evaporated with N_2 stream. One mg of methoxylamine hydrochloride in 50 µl of ethyl acetate was added to the extract and the keto groups were methoximed at 60°C for 30 min. After evaporation 100 µl or 20 µl of N,O-bis(trimethylsilyl)trifluoroacetamide was added to the extract from urine or serum respectively, and the hydroxy groups and carboxyl groups were trimethylsilylated at 90°C for 1 hour.

GC/MS: A Hewlett-Packard 5710 A gas chromatograph was directly coupled to the source of JMS D-300 double focussing mass spectrometer (JEOL, Tokyo, Japan). The gas chromatograph was equipped with a 30 m x 0.25 mm i.d. OV 101 open tubular glass capillary column and a splitless injector. The column temperature was programmed from 70°C to 250°C at 3°C/min.

RESULTS AND DISCUSSION

In the diabetic patients with ketoacidosis the urinary excretion of lactic acid, acetoacetic acid, 2-hydroxybutyric acid, 3-hydroxybutyric acid,

2-hydroxyisovaleric acid, 3-hydroxyisovaleric acid, 2-hydroxyvaleric acid, 5-hydroxyhexanoic acid, 2-hydroxy-2-methyllevulinic acid, adipic acid and 2,3-dideoxypentonic acid was increased as compared with the healthy subjects.

In the diabetic patients with ketoacidosis the serum levels of lactic acid, acetoacetic acid, 2-hydroxybutyric acid, 3-hydroxybutyric acid and 2,3-dideoxypentonic acid were higher than in the healthy subjects.

3-Hydroxyvaleric acid was detected in the urine of 3 out of 4 diabetic patients with ketoacidosis, but was not detected in the patients' sera. 3-Hydroxyvaleric acid was not detected in the urine and serum of the diabetic patients without ketosis or healthy subjects.

5-Hydroxyhexanoic acid was detected in the urine of four diabetic patients with ketoacidosis, but was not detected in the patients' sera. 5-Hydroxyhexanoic acid was not detected in the urine and serum of the diabetic patients without ketosis or healthy subjects.

2-Hydroxy-2-methyllevulinic acid was detected in the urine of four diabetic patients with ketoacidosis and in the serum of two out of the four patients. The identification of 2-hydroxy-2-methyllevulinic acid was confirmed by comparing the mass spectrum with that of the trimethylsilylated authentic 2-hydroxy-2-methyllevulinic acid, which was synthesized from pyruvic acid and acetone. 2-Hydroxy-2-methyllevulinic acid was not detected in the urine and serum of the diabetic patients without ketosis or healthy subjects.

3-Hydroxyvaleric acid, 5-hydroxyhexanoic acid and 2-hydroxy-2-methyllevulinic acid disappeared from the patients' urine when the patients became non-ketotic with the insulin therapy.

Although 3-hydroxyvaleric acid has never been reported as a normal component of human physiological fluids, the compound was reported to be detected in the blood of a child with propionic acidemia and methylmalonic acidemia. Propionyl Co A is a metabolite of isoleucine, methionine, threonine, phytanic acid, old chain fatty acids, the side chain of cholesterol, and the propionic acid produced by the intestinal microflora. In diabetic ketoacidosis the catabolism of protein followed by the catabolism of amino acids such as isoleucine etc. is enhanced to cause the accumulation of propionyl Co A. The condensation of propionyl Co A and acetyl Co A may occur to form 3-ketovaleric acid. Then, 3-hydroxyvaleric acid may be formed by the reduction of 3-ketovaleric acid.

5-Hydroxyhexanoic acid has also never been reported as a normal component of human physiological fluids. The compound was reported to be detected in the urine of a child with Reye's like syndrome such as hypoglycemia and coma and in the urine of a child with episodic hypoglycemia. The source of 5-hydroxyhexanoic acid in the diabetic ketoacidosis may be the ω-1 oxidation of the long-chain fatty acids in the cytosol of liver followed by the β-oxidation of the ω-1 hydroxylated fatty acids.

2-Hydroxy-2-methyllevulinic acid has never been detected in human physiological fulids. Since the compound was detected in the urine of diabetic patients with ketoacidosis and a child with pyruvic acidemia and ketosis, it is considered to be specific to the ketotic state. The metabolic pathway for its formation is not yet known.

REFERENCES

1. T. Niwa, K. Maeda, T. Ohki, A. Saito and I. Tsuchida (1981) Gas chromatographic-mass spectrometric profile of organic acids in urine and serum of diabetic ketotic patients. J. Chromatogr. 225, 1-8.

2. T. Niwa, K. Maeda, T. Ohki and J. Sakakibara (1982) Identification of 2-hydroxy-2-methyllevulinic acid in urine and serum of diabetic patients with ketoacidosis. J. Chromatogr. 228, 59-65.

3-HYDROXY-3-ETHYLGLUTARIC ACID AND ITS METABOLISM IN PATIENTS WITH PROPIONIC ACIDEMIA

T. Kuhara, I. Matsumoto, T. Shinka and M. Matsuo°
Research Institute of Medical Mass Spectrometry,
Kurume University School of Medicine, Kurume, Fukuoka 830 and
°Kobe Children's Hospital, Kobe, Hyogo 654, Japan

Propionic acidemia is caused by a defect of propionyl CoA carboxylase activity. The metabolism of propionyl CoA in propionic acidemia patients seems to proceed via normal acetyl CoA metabolism except for glycine conjugation and β-oxidation of propionyl CoA. In a previous paper(1) we have reported that the concentrations of several precursors of acetyl CoA found in the urine of a propionic acidemia patient increased during clinical episodes. It was suggested that the mitochondrial acetyl CoA level is higer than that speculated from the urinary concentrations of 3-hydroxybutyric acid plus acetoacetic acid. In this communication we report the identification of 3-hydroxy-3-ethylglutaric acid in the urine of propionic acidemia patients.

Two patients with propionyl CoA carboxylase deficiency excreted an unknown compound(X) as well as a large number of propionyl CoA metabolites characteristic to this disorder. Healthy controls or other patients without propionic acidemia did not excrete X. In the mass spectrum of X as trimethylsilyl derivative, the highest mass peak was detected at m/z 377, indicating a molecular mass of 392. When X was silylated with N,O-bis(nonadeuterotrimethylsilyl)acetamide, the $[M-CD_3]$ ion was found at m/z 401, indicating a molecular mass of 419. As the mass difference of these two derivatives was 27 mass units, the presence of three functional group in the molecule is evident. The presence of an ethyl radical in the molecule was indicated by ions at m/Z 363 and 273, and at m/z 390 and m/z 291 in the perdeuterotrimethylsilyl derivative. They correspond to $[M - C_2H_5]$ and $[M - C_2H_5 - TMSOH]$ respectively. The presence of these two prominent peaks indicated that the ethyl group and a hydroxy group are attached to the same carbon with respect to α-cleavage of TMS ether bond. The presence of one hydroxy group at C3 position was demonstrated by an intense ion at m/z 261 $[M - CH_2COOTMS]$. The ion at m/z 245 is produced through the rearrangement of TMS group(2). The fragmentation pattern of 3-hydroxy-3-methylglutaric acid is quite similar to that of X. From these observations X was identified as 3-hydroxy-3-ethylglutaric acid. The mass spectrum of trimethylsilyl derivative of authentic 3-hydroxy-3-ethylglutaric acid was identical with that of X, as was the methylene uint value on gas chromatography.

A recent publication reported only the detection of traces of 3-hydroxy-3-ethylglutaric acid in human urine as methyl ester derivative(3). We detected the metabolite only in the urine of propionic acidemia patients. The amount of 3-hydroxy-3-ethylglutaric acid detected was far less than the amount of 3-hydroxyvaleric plus 3-oxovaleric acid detected at the same time in all cases. We think that 3-hydroxy-3-ethylglutaric acid is formed as a result of side reaction, deacylation of 3-hydroxy-3-ethylglutaryl CoA. Baker and Schooley(4) have identified 3-hydroxy-3-ethylglutaric acid as diethyl ester from [1-^{14}C] propionyl CoA plus acetyl CoA, incubated with cell-free preparations of Manduca sexta corpora cardiaca allata complexes. Their mode of radiolabelling was in agreement with their hypothetical role as intermediates of juvenile hormon biosynthesis. They also demonstrated that 3-hydroxy-3-ethylglutaryl CoA is produced by a cytosole fraction obtained from rat liver. Enzymes responsible for ketone body formation are associated mainly with the mitochondria. Although an experiments using a mitochondrial fraction has not been carried out, the substrate specificity of mitochondrial 3-hydroxy-3-methylglutaryl CoA synthetase may be the same as cytosolic one.

We suggest that patients with propionic acidemia excrete in catabolic state 3-oxovaleric acid and 3-hydroxyvaleric acid in order to remove propionyl CoA as well as acetyl CoA and that most of 3-oxovaleric acid and 3-hydroxy-valeric acid are formed as follows:

1. One molecule of propionyl CoA and one molecule of acetyl CoA condenses to give 3-oxovaleryl CoA catalyzed by a thiolase (EC 2.3.1.9.).
2. 3-Oxovaleryl CoA condenses with another acetyl CoA to give 3-hydroxy-3-ethylglutaryl CoA catalyzed by 3-hydroxy-3-methylglutaryl CoA synthetase (EC 4.1.3.5.).
3. 3-Hydroxy-3-ethylglutaryl CoA is cleaved to 3-oxovaleric acid and acetyl CoA catalyzed by 3-hydroxy-3-methylglutaryl CoA lyase (EC 4.1.3.4.).
4. 3-Hydroxyvaleric acid is formed from 3-oxovaleric acid by 3-hydroxy-butyrate dehydrogenase (EC 1.1.1.30.).

ACKNOWLEDGEMENT

The authors thank Dr. David A. Schooley, Zoecon Corporation Research Laboratory, Palo Alto, California for the kind gift of authentic 3-hydroxy-3-ethylglutaric acid.

References

1. T. Kuhara, T. Shinka, M. Matsuo and I. Matsumoto, Clin. Chim. Acta, (1982) in press
2. G. Petersson, Tetrahedron, 26, 3413 (1970)
3. M. Spiteller and G. Spiteller, J. Chromatogr., 164, 253 (1979)
4. F. C. Baker and D. A. Schooley, J. Chem. Soc. Chem. Commun., 292 (1978)

FOF 6 QUANTITATIVE URINARY STEROIDS OF HYPER-ANDROGENIC WOMEN BY FINNIGAN OWA 1020 GAS CHROMATOGRAPHY-SPECTROMETRY, Shen-Nan Lin, Jane Ao, R. M. Caprioli, L. J. Rodriquez, K. D. Smith and E. Steinberger. Analytical Chemistry Center and Department of Reproductive Medicine and Biology, University of Texas Medical School at Houston, Houston, Texas 77025

Routine measurements of urinary steroids of hyperandrogenic women were carried out by a Finnigan, OWA 1020 Gas Chromatograph-Mass Spectrometer. Separation of stereoisomers of steroids was achieved by a 30 m x 0.32 mm fused silica capillary column coated with an SE-30 stationary phase. It was found that this column maintained good separation efficiency for four months with an average of six analyses per day. Based on measurements of five 25 ml portions of a typical 24 hr urine sample, the reproducibilities of quantitative measurements of 20 urinary steroids by GC/MS were in the range from 12.5 to 29.7% C.V. For clinical purposes, the first urine sample in the morning of the patients was used for measurement. The objective of this investigation was to evaluate the possible usage of urinary steroid profile for acute adrenal suppression test which is particularly useful in identification of women who will not respond to chronic glucocorticoid suppression therapy. Preliminary data of 11 hyperandrogenic women's urines before and after oral ingestion of dexamethasone showed changes in urinary steroid profile which correlated well with the suppression of plasma levels of testosterone and cortisol in these patients. It appeared that urinary steroid profile may be used to replace or at least, to supplement the more difficult plasma steroid determinations for acute dexamethasone suppression test.

QUANTITATION AND IDENTIFICATION OF URINARY STEROID HORMONES IN PRECOCIUS PUBERTY: A.W. Pike, P.V. Fennessey and Celia Moynihan; Departments of Pediatrics and Pharmacology, University of Colorado School of Medicine, Denver, Colorado 80262.

Introduction

Precocious puberty is the premature onset of secondary sexual characteristics before the age of ten years. In the majority of cases, it is usually as a result of tumors of the pituitary, adrenals, testis or of C.N.S. lesions. Individuals with true precocious puberty have been shown to have a functional hypothalamic, pituitary, gonadal axis. This form is usually more common in females than in males. Routine urinary steroid analysis by GC and GC-MS can usually facilitate in the diagnosis of the more common forms of this disorder and determine the type of sexual precocity present.

Virilizing associated with a number of steroid biosynthetic enzyme defects can be determined using this technique. Urinary steroid profiling will usually reflect the position of the enzyme defect. In some instances this will be indicated by an increase in androgen production and a decrease in cortisol metabolites. Abberations in the pituitary-adrenal feedback mechanism due to adrenal tumors or ACTH like producing tumors can also be distinguished. ACTH producing tumors will stimulate adrenal steroidogenesis which will result in a marked increase in most steroids of adrenal origin. While some adrenal tumors could result in the excessive production of just a select few. This will therefore depend on the location of the tumor. Using the technique of GC and GC-MS we have been investigating a comparatively rare form of true precocious puberty in a family with a history of the condition. The trait in this family is dependent upon a sex limited autosomal dominant gene. Only the proband C.D., is of prepubertal age.

Twenty-four hour urine samples were collected from most of the affected males, and processed in the following manner.

To 5 cm^3 aliquots of urine was added 5-25 µg of 5β-epitestosterone as internal standard. The concentration of internal standard being determined by the age of the individual. The urine was then passed through a SEP-PAK (Waters Assoc.) and after washing with water, the steroid rich fraction was eluted with methanol. This was dried down under nitrogen and subjected to enzyme hydrolysis using *Helix pomatia* for 48 hours. Steroid were then extraced with methylene chloride. After washing with base and distilled water, cholesterol butyrate was added as a second internal standard. Keton groups were protected using methoxyamine hydrochloride in pyridine. Hydroxyl groups were converted to their corresponding trimethylsilyl ethers.

The extracts were then analyzed by GC and confirmed by GC-MS. GC profiles of normal prepubertal individuals are predominatly composed of cortisol metabolites. As expected C19 steroids are very low during this period of life. GC profiles from normal adult males exhibit marked elevation of C19 steroids. Androsterone and etiocholanolone being the major androgen metabolites followed by their 11-oxo and 11-hydroxy isomers.

Comparison of these profiles to the prepuberscent individual expressing the trait indicated a profile similar to that of an adult male. Indeed quantitation of these components give values which were within the normal range for adult males. Also cortisol metabolites were significantly elevated for his age. Extensive clinical evaluation of this individual revealed an intact pituitary, adrenal, testicular axis, wit no evidence of tumor. This then would indicate a case of true precocious puberty of unknown etiology.

Examination of the profiles from the other males expressing the trait indicated normal adult male androgen values, but again significantly elevated cortisol metabolites. It is interesting to note that only those C21 adrenal steroids which were 11β-hydroxylated were significantly elevated above normal in these affected individuals.

In conclusion these profiles did not exhibit patterns similar to any of the classical steroid biosynthetic enzyme defects. We believe that this condition is not due to a common enzyme block. The trait in this family fits sex-limited autosomal dominant gene inheritance with 93% penetrance. It is transmitted by affected males and carrier females to about half their offspring, but is only expressed in the male.

In the male one deleterious gene is sufficient for precocious puberty, whereas in the female two genes may be required for expression of the trait. However, since marriage between carrier males and females have not been found, we cannot determine what the clinical status of the homozygous dominant female would be. This type of marriage would most likely come from a consanguinous relationship since the trait is so rare in the population.

We have not eliminated the possibility that although the carrier females do not express the gene, they may exhibit an endocrine dysfunction.

ψ-KETO AND ψ-HYDROXY ACID EXCRETION IN AN ERROR OF FATTY ACID CATABOLISM; O.A. Mamer, J.A. Montgomery, J. Miller and E. Colle. The Montreal Children's Hospital - McGill University Research Institute, and the McGill University - Medical Research Council of Canada Biomedical Mass Spectrometry Unit, 1130 Pine Ave W, Montreal, CANADA. H3A 1A3.

Three unrelated children (2 female, 1 male) have been found to present with various symptoms resembling Reye's syndrome (among them, acute recurrent hypoglycemia, enlarged liver, moderate urinary ketones, low insulin, and low non-protein-bound serum free fatty acids). GCMS profiling of the TMS derivatives of their acute serum and urinary organic acids revealed large concentrations of octanoic (Oct), 5-hydroxyhexanoic (5-HH), 7-hydroxyoctanoic (7-HO), and 9-hydroxydecanoic (9-HD) acids {1}, collectively termed ψ-hydroxy fatty acids (by analogy with α, β, and ω-hydroxy fatty acids). Present in smaller amounts were the corresponding ψ-keto fatty acids, best shown as the hydroxylamine derivatives {2}.

Patient 1 on first admission had the following urinary ψ-hydroxy acid concentrations: (acid, conc. in mg/g creatinine) Oct, 7; 5-HH,70; 7-HO, 30; 9-HD, 3. On second admission 8 months later, these were: Oct, 90; 5-HH, 140; 7-HO, 190; 9-HD, 13. Following brief supportive treatment with intravenous glucose, patient 1 regained apparent good health but continues to excrete these acids: Oct, 29; 5-HH, 26; 7-HO, 39; 9-HD, estimated 1-2. Present also at all times were comparably large concentrations of urinary adipic, suberic and sebacic acids. The second admission acute serum contained the following (acid, μMolar): Oct, 14; 5-HH, 1.5; 7-HO, 1.3; adipic, 2.7; suberic, 0.9, sebacic, 0.6. Serum β-hydroxybutyric and acetoacetic acids were approximately 3 times normal.

Oral loadings with medium chain triglycerides rapidly precipitated gross ψ-hydroxyaciduria and dicarboxylic aciduria while long chain loadings produced a much less pronounced effect. The loadings did not reproduce the hypoglycemia or any other symptom.

Proposed is a defect in mitochondrial medium chain β-oxidation that results in the extrusion of accumulated C_6-C_{10} acids into the extra-mitochondrial volume where they undergo ψ- and ω-oxidation {3}. Restriction of acetyl-CoA production from fatty acid metabolism may inhibit ATP synthesis in the Krebs cycle and curtail gluconeogenesis. Significantly, urinary succinic acid is usually low or absent in the acute state. In vitro determination of the rate of medium chain β-oxidation is greatly reduced in fibroblasts of patient 1 relative to controls. Long chain oxidation is unaffected.

1 O.A. Mamer, J.A. Montgomery, and E. Colle. Biomed. Mass Spectrom. 7, 53-57 (1980).
2 G. Lancaster, P.Lamm, C.R. Scriver, S.S. Tjoa, and O.A. Mamer. Clin. Chim. Acta 48, 279 (1973).
3 M. Hamberg and I. Bjorkhem. J. Biol. Chem. 246, 7411 (1971).

THE NIH/EPA MASS SPECTRAL DATABASE SEARCH SYSTEM

D. P. Martinsen, Fein-Marquart Associates, Inc., 7215 York Rd., Baltimore, MD 21212
S. R. Heller, US Environmental Protection Agency, 401 M St., SW, Washington, DC 20460
W. L. Budde, US Environmental Protection Agency, 26 W. St. Clair St, Cincinnati, OH 45628
G.W.A. Milne, National Cancer Institute, 8300 Colesville Rd., Silver Spring, MD 20910
R. G. Oldham, Radian Corporation, Austin, TX 78766

The NIH/EPA Mass Spectral Search System (MSSS) is one of the components of the NIH/EPA Chemcial Information System (CIS). The CIS is a collection of various types of chemical data which may be searched and retrieved using the commands of the system. In addition to mass spectral data, both EI and CI, the CIS contains C-13 NMR, IR, and crystallographic data. There are also a number of data bases in the CIS which contain toxicity values, spill response information, Federal Register citations, and chemical structure and nomenclature. The CIS, including MSSS, is available on a commercial computer which may be accessed via local telephone calls from most major cities in the United States and Western Europe.

MSSS consists of a set of programs to search data bases of EI spectra, CI spectra, and proton affinity/gas-phase basicity values. The EI data base contains spectra of nearly 39,000 compounds taken from an archival file of over 70,000 spectra. The spectra for the public file are chosen on the basis of their quality index(1). Spectra are received from laboratories around the world and are used to update the data base approximately once a year. The EPA, through its Cincinnati office and with the assistance of Radian Corporation, is attempting to add to the data base spectra for 2,500 compounds from the Toxic Substances Control Act (TSCA) Inventory List and from the list of chemicals for priority testing for which mass spectral data are not available. The current data base contains almost 700 spectra from that project which have been measured under very carefully controlled conditions. Each day, prior to measuring the spectra of any reference compounds, the instrument must be calibrated using the compound bis(pentafluorophenyl)phenylphosphine (CAS RN 5074-71-5). The spectrum of the calibration compound must meet the published criteria(2). A recent study has shown that the quality indices of these spectra are considerably higher than the average quality index of the rest of the data base(3).

In addition to being accessible through MSSS, the EI data base is also available on magnetic tape from the National Bureau of Standards(4), and in printed form from the U.S. Government Printing Office(5).

The CI data base contains approximately 1,500 spectra, most of which were obtained using methane as a reagent gas. An effort is currently underway to develop a quality index algorithm for CI spectra. The CI algorithm is based on the EI algorithm(1), but a number of changes are being made to account for the differences between the methods. For CI spectra, electron voltages greater than 70 eV are allowed, specific ions greater than the molecular ion are possible and are dependent on the reagent gas, and illogical losses are based on $(M+1)^+$ as well as on M^+. In addition, the number of peaks in a CI spectrum should, in general, be less than for an EI spectrum.

The NBS file of proton affinity and gas-phase basicity values contains approximately 650 measurements for 420 compounds. Citations to the literature describing the measurements are also included.

The MSSS programs allow one to search the data base in a number of ways to retrieve information. Compounds may be retrieved on the basis of molecular weight, molecular formula, and partial formula. Because of the capabilities of other components in the CIS, compounds may also be retrieved on the basis of chemical names, trade names, CAS Registry Number and structure. The mass spectrum may be used as the basis for an interactive peak search, in which compounds containing specific peaks with specific ranges are retrieved. The KB and PBM searches retrieve spectra similar to an unknown spectrum based on algorithms comparing abbreviated forms of the spectra.

Although the data base of EI spectra contains many compounds, it is by no means complete. Therefore, a number of pattern recognition programs have been developed to provide certain information about a compound even when the library searches fail to provide any good matches. The MOLION program, written by Dromey and co-workers at Stanford University, determines likely molecular weights for a compound based on the spectrum. The MSTREE option, developed by Technology Service Corporation, uses a decision tree approach to determine the presence or absence of specific structural groups and assigns a probability to each determination(7). An examination of the entire data base yields spectral features which are useful for distinguishing compounds containing a given structural group from those which do not. When an unknown spectrum is tested for these spectral features in an established sequence (following the paths of the decision tree), the compound is classified as either containing or not containing the structural group. While the generation of the decision tree is a time-consuming process, the actual analysis of an unknown spectrum is very fast. The program currently checks for chlorine, bromine, nitrogen and phenyl.

1. D.D. Speck, R. Venkataraghavan, and F.W. McLafferty, Org. Mass Spectrom. 13, 209 (1978).

2. J.W. Eichelberger, L.E. Harris, and W.L. Budde, Anal. Chem. 47, 995 (1975).

3. G.W.A. Milne, W.L. Budde, S.R. Heller, D.P. Martinsen, and R.G. Oldham, Org. Mass Spectrom., accepted for publication.

4. U.S. National Bureau of Standards, Office of Standard Reference Data, Building 221, Room A318, Washington, DC 20234.

5. U.S. Government Printing Office, Washington, DC 20402 (Order numbers NSRDS-NBS #63, 003-003-01987-9 and NSRDS-NBS #63, Supplement 1, 003-003-02268-3).

6. R.G. Dromey, B.G. Buchanan, D.H. Smith, J. Lederberg and C. Djerassi, J. Org. Chem. 40, 770 (1975).

7. W.S. Meisel, M. Jolley, S.R. Heller, and G.W.A. Milne, Anal. Chim. Acta 112, 407 (1979).

PERSONAL MASS SPECTRAL DATABASE IN FLOPPY DISK SYSTEM

Yasuji KOYAMA, Toyohiko TAZAWA* and Kogoro MAEDA
Electrotechnical Laboratory, 1-1-4 Umezono, Sakura-mura, Niihari-gun, Ibaraki, JAPAN
* Nippon Data General, 2165, Mochida, Gyoda, Saitama, JAPAN

Performance of small systems using microcomputers with relatively large scale storage peripherals has gradually come up to the levels of large scale computer systems in the age of 1960 to 1970, and central processing of the present style using large computer systems will be replaced by a group of the small computer systems. Manipulation of huge storage of data will also be distributed into local and/or personal database systems in small but appropriate scales in near future. It would be main trend in the future, therefore, that in parallel to the usage of large databases, the small databases will usually be handled personally in the small systems. It is because that information is inherently of personal matter, and information that is really useful and effective is to be made, compiled and used by the person who really needs the information.

With this basic ideas, mass spectral databases of hydrocarbons C_nH_m and one-oxygen containing coumpounds $C_nH_mO_1$ were constructed so far for personal use in two floppy disks of a small computer system. The original data were taken from NIH/EPA Mass Spectral Data Base. The extracted data are represented in six terms, compound name, molecular weight, chemical form, ionization method and mass numbers of molecular ion, if present, and its fragment ions and further the CAS number. The mass numbers are taken for only maximum 10 or 13 peaks higher than 10% to the height of the base peak in the order of their peak heights. No exact peak height information was included. With this format, the information of about 2500 compounds can be stored in one floppy disk of the standard size.

Construction and retrieval programs are all described with extended BASIC language. Long period experience has proved that the usage of BASIC language is convenient and the total system used is effective for construction, addition and amendment of the database. Numbers of the compounds stored in each floppy disk are so far 1813 for C_nH_m and 2281 for $C_nH_mO_1$. Using the floppy disks, the retrieves of the stored data could be made effectively without the peak height values. For example, the most abundant base peak for hydrocarbons was m/z 43, and the number of the molecules having the m/z 43 peaks as the base peak was 151. Even with this large number, only several compound names could be extracted as the candidates for the unknown sample having the m/z 43 base peaks from the 1813 C_nH_m data by keying further 5 to 10 m/z values as the search peaks. The search can be made by keying the largest 5 peaks regardress the order of the peak heights, corresponding to the well-known non-reproducibility of the peak heights in the mass spectra, and it was found that even for the hydrocarbons

the candidates less than several can be extracted for every molecule, except for the compounds whose base peaks are m/z 43, 57 and 55.

Statistical treatments were also made, and some clear correlations were obtained between the base peak values and the molecular structures. The sort number of the base peaks was found 196 for 1813 C_nH_m data in the present database, and the largest 15 base peaks are shown in the table. These base peaks can be classified by sorting with the m-values in C_nH_{2n-m}(m=-2 to 8) as can be seen in the table. The table indicates that, for example, the structures of molecules giving $C_6H_7^+$ peaks (m/z 79) as the base peak always correspond to C_nH_{2n-4}, and the number of the corresponding hydrocarbons is 28. No other structure was given from the present analysis. The table also indicates that there is no corresponding C_nH_{2n+2} structure for the molecules giving m/z 41, 55, 69 or 83 as the base peaks. With the results obtained, we are able to confirm the mass spectral information found by experienced organic chemists and also able to find some inconsistency in the database, as indicated by parentheses in the table. Base peak distribution for 2281 $C_nH_mO_1$ compounds were also revealed that the most abundant base peaks are m/z 43, 41, 57, 55, 69, 45, 81, 71, 91, 59 etc. in this order, and among them, the two m/z values 45 and 59 are not given as the base peaks for hydrocarbons C_nH_m.

BASE PEAK		CnH2n-m (m)					
M/z		-2	0	2	4	6	8
43	$C_3H_7^+$	108	24	7	1	5	1
57	$C_4H_9^+$	106	6	5	1	4	
41	$C_3H_5^+$		50	20	14	8	5
55	$C_4H_7^+$		72	25	8	2	5
69	$C_5H_9^+$		26	3		2	2
83	$C_6H_{11}^+$		24	23	5		
56	$C_4H_8^+$	(2)	42				
67	$C_5H_7^+$			67	2	2	
81	$C_6H_9^+$			44	1	6	2
95	$C_7H_{11}^+$			27	1	3	
79	$C_6H_7^+$				28		
93	$C_7H_9^+$				28	5	
91	$C_7H_7^+$					62	7
105	$C_8H_9^+$					38	3
119	$C_9H_{11}^+$				(1)	30	2

All peak distributions in the present data base for 4094 C_nH_m and $C_nH_mO_1$ compounds are further obtained, and almost the same distribution scheme were found for both C_nH_m and $C_nH_mO_1$, except several peak values like m/z 45 and 59, which are characteristic peaks for alcohols and ethers.

Present database can give structural information on the compounds C_nH_m and $C_nH_mO_1$ that the rates of ring-structured compounds to total compounds for a given C_n number are almost constant above about 15 of C_n values. Further, as for a series of base peak values m/z 31, 45, 59, 73 and 87, no or quite small numbers of the compounds having the peaks was found for C_nH_m, whereas for $C_nH_mO_1$ compounds, these peaks are found to be the base peaks for alcohols and ethers. The database gives us, as well as the structural information, the fact that the total number of these compounds was 122, and so on. Some other interesting information have been obtained by utilizing the present constructed database.

Pascal language, which is widely used in the microcomputer systems, was also used for improving the processing time. Simultaneous usage of both languages was quite advantageous. It was found that the retrieves of candidates by compound names could be made effectively.

FPA 3 REAL-TIME PBM MATCHING OF UNKNOWN MASS SPECTRA ON A GC/MS/COM SYSTEM; J. K. Mun, D. B. Stauffer, W. Staedeli, C.-J. Guo, F. W. McLafferty, D. W. Peterson*, and J. W. Serum*, Department of Chemistry, Cornell University, Ithaca, NY 14853 and Scientific Instrument Division*, Hewlett Packard, Palo Alto, CA 94304.

Both the Probability Based Matching (PBM) and Self-Training Interpretive and Retrieval System (STIRS) have been implemented on a gas chromatograph/mass spectrometer/computer (GC/MS/COM) system, the H-P 5985 with H-P 1000 computer. The searching speed of PBM has been improved by nearly two orders of magnitude through two levels of file ordering, so that on-line PBM matching against a data base of 41,000 reference spectra, simultaneously with the GC/MS data acquisition and reduction, requires 5-20 seconds. Thus for GC/MS analyses of complex mixtures the PBM identifications of GC peak-top spectra of most mixture components can be displayed during the GC/MS run. STIRS has also been implemented on the computer of the H-P 5985 system, so that computer interpretation of unknown spectra not in the reference file can be done off-line. STIRS predicts molecular weight and substructural information; for 600 common substructures the prediction reliability is also given.

A major expansion of the Cornell data base has just been completed using spectra donated by a large number of leading mass spectrometry laboratories and spectra transcribed from the literature. The magnetic tape containing 70,000 different mass spectra of 55,000 different compounds will be distributed by John Wiley & Sons as the expanded "Registry of Mass Spectral Data".

Acknowledgment: Generous financial support was provided by the National Science Foundation (grant CHE-7910400) through their Industry-University Cooperative research grant program.

FPA 4 A RAPID AND RELIABLE PROGRAM FOR THE DETERMINATION OF TARGET COMPOUNDS IN GC/MS DATA FILES; P.W. Ryan and B.N. Colby, S-CUBED, La Jolla, CA, 92038.

Processing of GC/MS data files for qualitative and quantitative determination of large numbers of target compounds requires the use of rapid, reliable computer programs and algorithms in order to maintain a data reduction pace equivalent to that of data acquisition. For example, if 100 target compounds are to be determined using a 45-min fused silica capillary column run, approximately 2700 spectra will be acquired. These must be processed for target compounds in about 30 min or at a rate of one target compound per 18 seconds. Because user interactive software is at least a factor of 10 to 20 too slow to achieve this rate, a variety of strategies which lend themselves to noninteractive data reduction have been investigated. Using the information generated from these studies, a highly flexible program has been developed which reliably processes target compound data at a rate of approximately one compound per 3 seconds. The purpose of this presentation is to report the results of these studies and to describe the program which has resulted from them.

COMPUTERIZED LABORATORY MANAGEMENT SYSTEM FOR ENHANCED QUALITY CONTROL AND SAMPLE TRACKING IN VOLUME ORIENTED GC/MS ANALYSES

John W. Russell and Kent H. Fulton
Mead CompuChem®,
Research Triangle Park, N.C. 27709

The ability of a laboratory to perform quality GC/MS analyses on large numbers of samples requires the creation of a sophisticated laboratory management system. In order to achieve this capability, a Computerized Laboratory Management System (CLMS) which provides for receipt, scheduling, and tracking of large volumes of routine and non-routine samples through the GC/MS laboratory is essential. Once implemented, a CLMS also provides additional information retrieval benefits not available to laboratories which use manual systems.

Generally, the first input into the CLMS is the entry of an order for analytical services by marketing, which is typically placed before the sample arrives. This information is tracked by Production Planning and Control to ensure that the laboratory is prepared to perform the requested analyses without delay upon sample receipt and that the laboratory does not commit to perform work in excess of capacity. Production Planning and Control has responsibility for creating and maintaining analysis codes, issuing work assignments, and tracking the progress of samples through the laboratory.

Upon sample receipt, sample custodians inspect the sample while the CLMS assigns a unique CompuChem® number and confirms the requested analysis. This action initiates the scheduling of all requisite tasks including sample preparation, instrumental analysis method, technical and quality control reviews, and preparation of the final report. Because the CLMS is able to provide each specific group in the laboratory with daily work queues which list what samples require a particular task, the system becomes a valuable human and instrument resource allocation and scheduling tool.

Further, when a sample is entered into the CLMS, it will have a designated group of standards associated with the analysis. The standards laboratory maintains an inventory of all required standards for work in progress and makes them available when and where needed.

The sample preparation laboratory is designed to process large volumes of different types of samples. These include environmental (air, water, and soil/sediment) and biomedical (blood/plasma and urine) samples. The completion of the sample preparation phase is entered into the CLMS which then releases the prepared sample to the analytical laboratories.

The gc/ms laboratory is equipped with twenty-four (24) instruments which are optimally configured based on the existing and anticipated workload. These instruments are capable of performing volatile and semi-volatile analyses by either packed or capillary column chromatography. Automated software is used for the identification and quantitation of target compounds.

The gc laboratory is equipped with eight (8) dual column, dual detector gas chromatographs interfaced to a laboratory data system. In addition to performing herbicide and pesticide analyses, the laboratory performs screening analyses of hazardous waste, process streams, and solvent wastes to determine the correct sample preparation procedure prior to gc/ms analysis.

The accumulation and review of quality control data is accelerated and enhanced by the CLMS. The CLMS has responsibility for the automated introduction into the laboratory of Quality Control (QC) samples such as blanks, spikes, and duplicates. This assures that requisite QC samples are not omitted, while at the same time preventing redundant QC samples which create an unnecessary expense. The Quality Control group monitors surrogate recovery data and the results of spike and duplicate analyses and maintains data bases of response factors and the results of standards analyses. The computerization of this QC data is the only credible approach when large volumes of data are involved.

Finally, the computerization of all scheduled events allow for immediate status reports on all samples as they proceed through the laboratory. The ability to provide analytical progress reports and to forecast completion dates is not only a valuable service to the individual needing the analysis data, but is a requirement for successful laboratory operation.

A DATA BASE MANAGEMENT SYSTEM FOR MS/MS AND OTHER MULTI-DIMENSIONAL INSTRUMENTS

Richard W. Crawford, Hal R. Brand and Carla M. Wong*
Lawrence Livermore National Laboratory
Livermore, CA 94550

Hugh R. Gregg, Phil A. Hoffman and Chris G. Enke†
Michigan State University
East Lansing, MI 48824

Multi-dimensional instruments, such as MS/MS, are capable of producing large volumes of information detailing the sample studied. A prerequisite for the analysis of any data is a method for its collection, storage, retrieval and display. We have developed a data base management system to efficiently meet the latter three goals for multi-dimensional instruments.

In tandem mass spectrometry there are a large number of variables or instrument parameters besides the mass selected by the two analyzers. These variables include all ion path potentials, chemical ionization and collision chamber pressures, source and direct inlet probe temperatures and all gas chromatographic conditions. The alteration of n of these variables in an experiment produces an n+1 matrix of data which is stored in the experimental data base.

The retrieval system is capable of extracting any plane of information contained in the data base, even if that specific type of scan were not performed. For example, if several daughter scans of a selected parent ion are collected at various collision energies, an energy versus intensity scan for any of the daughter ions can be extracted and displayed. Also, in a temperature ramp experiment collecting data from one or more parents, the intensity of any daughter ion from a selected parent can be displayed versus time, scan or temperature. The organization of files is shown on the next page.

The data base system is designed to be flexible, efficient and easy to use. The data extraction routines use English style commands; for example SCAN VS INTENSITY, MASS=41, PARENT=102 produces an intensity profile with respect to scan number (time) of the mass 41 daughter ion from the mass 102 parent. An extraction of this type from a file of 1000 scans takes less than 10 seconds.

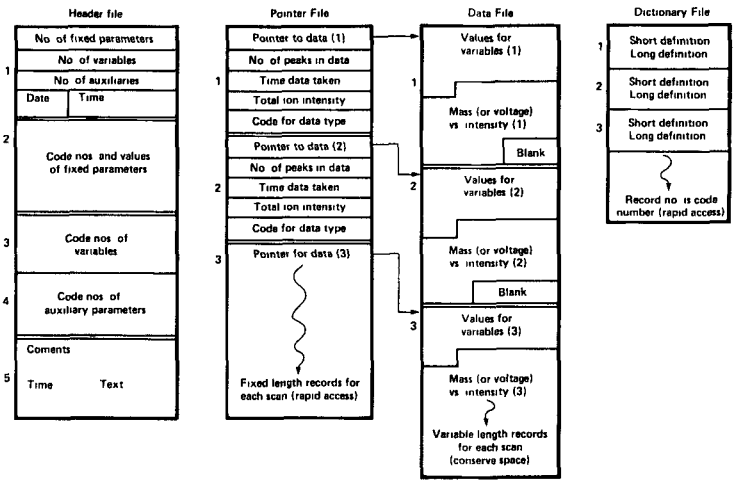
The programs and subroutines that comprise this system are written primarily in FORTRAN for a DEC PDP-11 mini-computer. The modularity of these programs makes modifications and incorporation of new features easily accomplished.

A variety of graphics capabilities are included in this system, which range from very fast, simple plots, to publication quality output. Graphical output can be directed to a variety of graphics terminals and hard copy units, both color and black and white.

*Work performed under the auspices of the U.S. Department of Energy at the Lawrence Livermore National Laboratory under Contract W-7405-ENG-48.

†Work performed under the auspices of the National Institute of Health at Michigan State University.

BLOCK DIAGRAM OF DATA MANAGEMENT SYSTEM



FILES ARE DESIGNED FOR FLEXIBILITY, SPEED

1. HEADER FILE—computerized notebook

   Contains code numbers and starting values for all instrument parameters, code numbers for all variable parameters, code numbers for auxiliary parameters, and comments.

2. POINTER FILE—index to the data

   Contains pointer to the start of the data for each scan, the number of data points in the scan, elapsed time since the experiment began, the sum of all intensities in the scan, and a code number for each scan.

3. DATA FILE—the raw data

   Contains the values for the variable parameters, the intensities and the masses (voltages).

4. DICTIONARY FILE—define codes

   Contains a short and long definition of all code numbers of instrument and auxiliary parameters.

A PORTABLE, REMOTELY OPERATED, COMPUTER-CONTROLLED, QUADRUPOLE MASS SPECTROMETER FOR FIELD USE

R. D. Friesen, J. C. Newton, C. F. Smith
Lawrence Livermore National Laboratory
Livermore, California 94550

EXTENDED ABSTRACT

A portable, remote-controlled mass spectrometer was required at the Nevada Test Site to analyze prompt post-event gas from the nuclear cavity in support of the underground testing program. A Balzers QMG-511 quadrupole was chosen for its ability to be interfaced to a DEC LSI-11 computer and to withstand the ground movement caused by this field environment. The inlet system valves, the pumps, the pressure and temperature transducers, and the quadrupole mass spectrometer are controlled by a read-only-memory-based DEC LSI-11/2 with a high-speed microwave link to the control point which is typically 30 miles away. The computer at the control point is a DEC LSI-11/23 running the RSX-11 operating system. The instrument was automated as much as possible because the system is run by inexperienced operators at times. The mass spectrometer has been used on an initial field event with excellent performance. This paper describes the gas analysis system, including automation by a novel computer control method which reduces operator errors and allows dynamic access to the system parameters.

INTRODUCTION

The Nuclear Chemistry Division at Lawrence Livermore National Laboratory routinely collects gas samples from the vicinity of underground nuclear explosives tests conducted at the Nevada Test Site and analyzes them to evaluate device performance. In an effort to improve the quality of the sampling and to obtain composition data in real time, a mass spectrometer was added to the existing gas sampling program. The information obtained by the spectrometer is used in determining when, and at what intervals, samples are to be taken for extensive further analysis. This instrument had to be operated remotely from a test control point 30 miles away.

The mass spectrometer we needed had to be portable to allow it to be moved from one test location to another. The instrument had to operate in a desert environment with high winds, dust, high and low temperatures, and extensive ground movement. The instrument had to be easy to install and convenient and fool-proof in operation because people available for installation and operation at each site have limited laboratory experience and no mass spectrometer background. The system also had to be completely contained since the gas to be analyzed is radioactive.

To meet these requirements we selected a rugged quadrupole mass spectrometer with built-in computer interface. Control was accomplished using two computers: one at the spectrometer location to provide local control, and one at the remote control point for operator interfacing and data processing. In addition to being simple to operate, we also wanted the system to be flexible enough to run a variety of samples and to allow an experiment to be reprogrammed on-line. (Since we also assumed that, although the setup and operation would be done by inexperienced personnel, there would be a scientist present during the actual test.) Environmental protection and mobility were obtained by installing of the instrument in a truck-trailer shell.

HARDWARE DESCRIPTION

The quadrupole selected was the Balzers QMG-511. This instrument has an interface for the DEC LSI-11 Q-bus and is available with FORTRAN-compatible software. Also Balzers had experience with their quadrupole in mobile environments. The two computers are Digital Equipment Corporation's LSI-11s. The processor in the forward area is an LSI-11/2 with read-only memory (PROM). A PROM-based computer allows computer-controlled interlocking in the local area, and since system software is not volatile, helps ensure reliable communication to the control point over a microwave link. THe processor at the control point is an LSI-11/23 running the RSX-11/M operating system. This is a time-shared system and allows control, graphics, data reduction, and operator interaction to take place simultaneously and independently. The LSI-11/23 processor has 128 Kwords of memory, a floppy disk, and a 5 Mbyte hard disk. There are two Tektronics 4025 graphics terminals. One displays the status of the inlet system and the other displays the processed data. Hard copy output for the system is produced by a Tektronics 4631.

The spectrometer's gas inlet system was designed at LLNL (1). It is all stainless steel with double-acting air-actuated valves. The air pressure to operate these valves is controlled by electric solenoids through the local LSI-11/2. All exhaust gases from the system are contained by a large steel tank that is evacuated prior to the experiment.

SOFTWARE DESCRIPTION

The software is divided into separate tasks. Some tasks are begun automatically when the system is started and others are started under operator control. The communication control link, the interactive communication with the operator, and the status display tasks are started automatically.

The operator has access only to the master database, a set of command files, and to a powerful set of control procedures. The inexperienced operator is instructed to use only the command files, which are predetermined sequences of control procedures. The database is a list of all the control settings, limits, and display parameters for the system. These may be changed dynamically during operation, but they are automatically copied into a working database at controlled intervals to prevent change at a time when it would interfere with system operation.

The data coming from the forward area is recorded in a disk file and then read by the data reduction and display control tasks. Display options include both numeric data tables and graphs of peak height versus mass, peak height versus time, and gas concentrations versus time. These displays are automatically hard copied after each update. The status information is routed directly to the display task and the graphics screen is updated immediately. Instructions for system operation are kept in a text file on the disk. The operator can read them at any time by dismissing the data display and requesting information. When these instructions are called, they are automatically passed to the hardcopy unit for the operator.

Following completion of analysis, an extensive set of graphical and tabular display options are available (e.g., ratios of components versus time or air-corrected concentrations). The control procedures are written in a language developed in-house that allows the scientist to program the system with plain language statements such as OPEN VALVE 104, WAIT 10 sec, etc. At any time the operator can abort a run and restore the system to a "safe" condition if problems do arise.

RESULTS

This system of hardware and software allows the scientist almost complete control over any test. He can sit at the console and run each step by hand or set up as much automation as he desires using the command files. He can change any database parameter before or during a run and can plot any peak (or peaks) or gas concentrations as a function of time. Alternately, he can set up any experiment in advance and turn it over to an inexperienced operator to run.

The operator has a system that is relatively easy to operate. He has a complete list of step-by-step instructions available from the computer at any time. He does not have to know a great deal about mass spectrometry to run the instrument. If something does go wrong he can easily regain control and restore the system to a "safe" condition.

The system programmer is not required to participate in the experimental "loop" for each individual experiment. The software is set up to perform specific discrete operations whenever called by the operator. Sequencing these operations to perform a desired analysis does not require the programmer. Since the various tasks are modular, they can be worked on independently. Also the interaction with the operator does not interfere with the system operation.

This system has been in the field since October 1981 and has met or exceeded all requirements. The Balzers QMG-511 has proven itself to be as rugged and reliable as the manufacturer claimed, and the few minor problems that seem to be in all new instruments were dealt with quickly by Balzers. After the initial software debugging, the computer system has given no problems and the ease of system operation has proved the value of the programming technique.

REFERENCES

1. An On-Line, Automated Gas Inlet System for a Field Mass Spectrometer, J.C. Newton, R. W. Crawford, R. D. Friesen, and C. F. Smith, UCRL ABS, 1982. (In preparation.)

This work was performed under the auspices of the U.S. Department of Energy by Lawrence Livermore Laboratory under contract No. W-7405-Eng-48.

DISCLAIMER

This document was prepared as an account of work sponsored by an agency of the United States Government. Neither the United States Government nor the University of California nor any of their employees, makes any warranty, express or implied, or assumes any legal liability or responsibility for the accuracy, completeness, or usefulness of any information, apparatus, product, or process disclosed, or represents that its use would not infringe privately owned rights. Reference herein to any specific commercial products, process, or service by trade name, trademark, manufacturer, or otherwise, does not necessarily constitute or imply its endorsement, recommendation, or favoring by the United States Government or the University of California. The views and opinions of authors expressed herein do not necessarily state or reflect those of the United States Government thereof, and shall not be used for advertising or product endorsement purposes.

A VERSATILE SOFTWARE CONTROL SYSTEM FOR A TRIPLE QUADRUPOLE MASS SPECTROMETER

C.A. Myerholtz and C.G. Enke

Department of Chemistry
Michigan State University
East Lansing, Michigan 48824

The flow of experiment execution of the TQMS in our laboratory is diagrammed in Figure 1. The user definition of his or her experiment includes how the data will be displayed, what mode of data acquisition will be used, and the conditions under which the experiment will be performed. Nearly all aspects of operation of our TQMS instrument have been placed under computer control which allows the control system computer to automatically configure the instrument for its many different operating modes.

A convenient command structure was needed to allow the operators to take easy advantage of the extensive flexibility provided by the high level of computer control of the instrument. Software for the control system was written in the programming language FORTH, which proves to be an excellent programming environment for laboratory control applications. FORTH is an extensible language where existing commands are strung together to form new commands that can be used to generate more new commands, and so on. As a result, a high level language can be generated for the specific control application. Examples of the results of this implementation in our laboratory are shown below.

	Operation	Command
1.	Scan Quadrupole three:	3 SCAN
2.	Daughter Scan of mass 100:	100 MS1 DSCAN
3.	Daughter scan of parents 58, 72, and 100:	58 MS1 DSCAN 72 MS1 DSCAN 100 MS1 DSCAN or 58 72 100 DAUGHTERS

In the command for operation 2 above, 100 MS1 selects the desired parent ion and DSCAN configures the instrument for a daughter ion scan and performs the scans. An alternative approach to listing the sequence of commands for operation 3, above (especially if it is frequently used to define a new command called EXPT1. This is done as follows:

```
: EXPT1 58 MS1 DSCAN 72 MS1 DSCAN 100 MS1;
```

The colon marks the beginning of the new command; the semi-colon terminates the definition of the new command. Now typing EXPT1 will produce the three daughter scans. Another option would be to define a new command called DAUGHTERS as follows:

```
: Daughters BEGIN MS1 DSCAN DUP = END;
```

where MS1 and DSCAN are new mass spec functions that have been added to FORTH, and the words BEGIN, END form a looping construct. This new command word can now be used as illustrated in the second command for operation 3 above.

The capabilities of the TQMS control system include: scanning any system parameter and generating either a linear or logarithmic display of the result, automatic sequencing of experimental modes, generation of three dimensional plots of any two instrument parameters verses ion current, and computer linked scanning of any combination of parameters. Figures 2 and 3 show the EI spectrum of 3 hexane displayed in both a linear and logarithmic format respectively. Figure 4 is a three dimensional plot generated by the control system. In this experiment, ion current was measured as a function of source block voltage (IV) for successive values of the source repeller voltage (RP) and then plotted automatically. Even this relatively complex experiment and display is readily produced by the simple command RP IV CONTOUR-DATA 3D-PLOT.

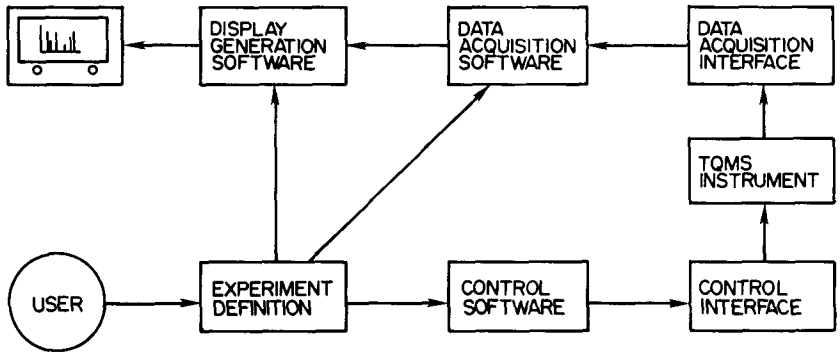


Figure 1

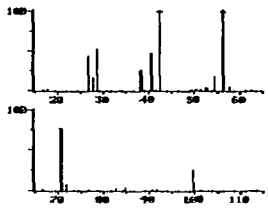


Figure 2

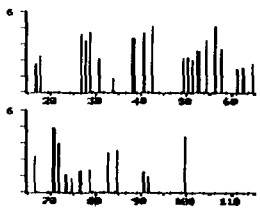


Figure 3

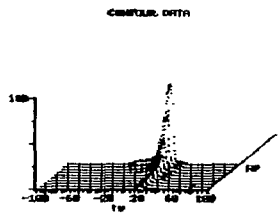


Figure 4

FPA 9 MICROCOMPUTER-BASED DATA ACQUISITION SYSTEM FOR ION CYCLOTRON RESONANCE MASS SPECTROMETRY: T. J. Buckley and J. R. Eyler, Department of Chemistry, University of Florida, Gainesville, FL 32611

We have added a general purpose laboratory interface to our microcomputer-based Fourier transform detection system so that it can now be used with a marginal oscillator, capacitance bridge, or Fourier transform ion detection system. The system is based on an Apple II microcomputer operated either by itself or in a master-slave configuration with a KIM I microcomputer and an S-100 bus. Because of its use in Fourier transform experiments, the system can also control a Rockland frequency synthesizer and a Biomation waveform recorder. Using data acquisition routines written in-house and commercially available curve fitting and plotting software the system makes possible facile signal averaging in ion-molecule reaction kinetics and laser-irradiation experiments. Block diagrams and examples of applications in these areas will be presented.

INVESTIGATING THE USES OF A COMMODORE PET MICROCOMPUTER IN CONVENTIONAL ION * CYCLOTRON RESONANCE SPECTROMETRY; McElvany, S.; Hardebeck, P. and Allison, J., Michigan State University, Chemistry Department, East Lansing, MI 48824

The application of an inexpensive microcomputer system (less than $4000) for recording mass spectra from an ICR spectrometer, rapidly reporting spectra in tabular and bar graph forms, and manipulating data was investigated. One goal was to minimize the hardware development required in the interface. This was achieved using the following system: (see figure 1)

1) Commodore PET 2001 Microcomputer (6502 Based, 16K RAM)
2) High Resolution Graphics Board (MTU 1008-6) 8K RAM
3) 32K Expansion RAM (MTU K-1032)
4) CBM 2040 Dual Disk Drive (340 kBytes)
5) CBM 2022 Dot Matrix Printer
6) Connecticut Microcomputer 8-bit, 16 channel A/D Converter (100 μsec conversion)

A simple interface of the magnet controller to the A/D converter was described which allowed mass determination.

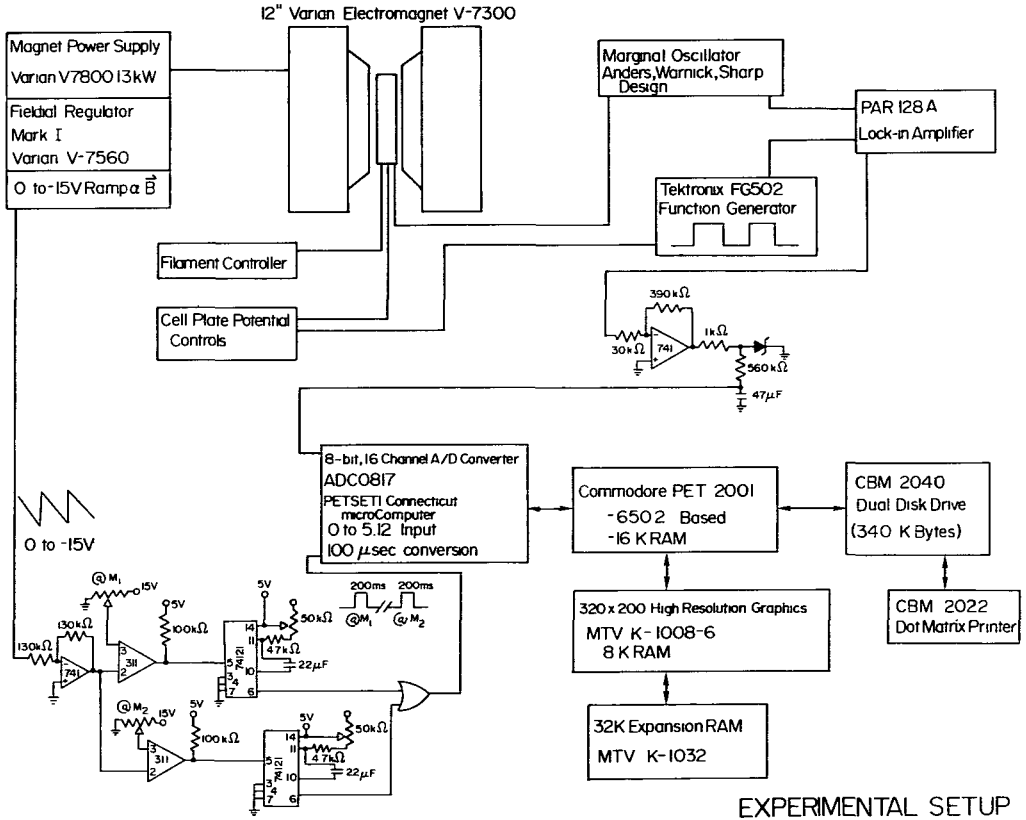
At this time the software development includes the following:

1) A main BASIC program which allows access to various subroutines.
2) A subroutine for monitoring instrumental parameters such as plate voltages in the ICR cell.
3) Machine Code subroutine for data acquisition and simultaneous display of the spectrum on the CRT. The present system records 16,000 data points in a five minute scan of the magnetic field. The maximum data acquisition rate is 10,000 points per second.
4) Machine Code peak finding subroutine and subsequent display of the Mass/Intensity catalog and bar graph of the spectrum.

Future software development will include:

1) Spectral arithmetic - addition and subtraction of spectra.
2) Pressure plots from sets of spectra.
3) Calculation of rate constants from double resonance experiments.

Those interested in obtaining the software as it develops should contact the authors.



EXPERIMENTAL SETUP

FIGURE 1

ANALYSIS OF MALEIC ANHYDRIDE IN DIETS OF RODENTS BY GAS CHROMATOGRAPHY-MASS SPECTROMETRY.
E. L. White, H. d'A. Heck and J. M. Cheplen, Chemical Industry Institute of Toxicology, Research Triangle Park, NC 27709.

Maleic anhydride (MA) is used primarily in the manufacture of polyester resins, and in the production of agricultural chemicals. Vapors and dust of (MA) are acute irritants of eyes, skin and upper respiratory tract. Maleic acid (MAC), the hydrolytic product of MA is used in the manufacture of polymers, dyeing and finishing of cotton, wool, and silk, and is also an irritant. MA is readily hydrolyzed to MAC in the presence of water. Previous attempts to determine MA in test diets have been unsuccessful due to instability and hydrolysis of the anhydride to the acid and/or irreversible binding of MA/MAC to chemical components of the feed. A method was developed to determine the concentration of MA by hydrolysing it to MAC, followed by gas chromatographic-mass spectrometric analysis. Test diets were prepared at concentrations (0.2% range) that would allow oral administration of 100 mg/kg/day in a 2 yr chronic study. To determine if specified dose requirements were obtained, randomly selected samples of rat chow were analyzed. Feed samples were mixed with dilute HCl containing internal standard ($^{2}H_{2}$-MA), extracted with diethyl ether, and then derivatized with diazomethane. Effluent of a 25m SE54 fused silica capillary column is selectively monitored at the major fragment ions (M/Z 113 and M/Z 115) for the dimethyl esters of MAC and $^{2}H_{2}$-MAC, respectively. Results of these analyses showed that actual concentrations (on the average) were 64% and 65% of the expected for male and female diets, respectively. Analysis of freshly prepared MA in feed yield 95-106% of expected, while samples prepared in our laboratory approximately 2.25 yr earlier gave essentially identical results (65-69%) as test diets. Diet samples ranged from 2 to 4 yr old. This results show, contrary to previous reports, that MA/MAC concentrations can be determined in diets stored for extended periods of time.

FPA 12 THE RAPID SCREENING OF FOOD PRODUCTS FOR MYCOTOXINS BY MS/MS. W.R. Davidson, S.D. Tanner and A. Ngo; SCIEX™, 55 Glen Cameron Rd., Unit 202, Thornhill, Ontario, Canada, L3T 1P2; and R. Greenhalgh, Agriculture Canada, Neatby Building, Ottawa, Ontario, K1A 0C6.

Mycotoxins are toxic secondary metabolites of microfungi which infest mainly cereals and nuts both during growth and storage. In order to detect low levels of the more potent varieties of mycotoxins, a highly sensitive and selective analytical technique must be used. Tandem mass spectrometry (MS/MS) provides both these criteria with minimal sample workup and direct sample introduction (i.e., without chromatographic separation) in the rapid screening of foods for mycotoxins. This paper deals mainly with vomitoxin (deoxynivalenol) and T-2 toxin, both members of the trichothecene class of mycotoxins associated with moldy grain, as well as aflatoxin B_1, a secondary metabolite of Aspergillus fungi. The collision induced dissociation spectra, obtained on the TAGA™ 6000 MS/MS system, for the above mycotoxins and other related compounds will be presented. Calibration curves for pure standards of vomitoxin, T-2 toxin and aflatoxin B_1 were obtained in a multiple reaction monitoring mode of operation. Detection limits obtained using a series of specific daughter ions for each toxin are observed to be approximately 50 picograms. Actual grain extract samples were analyzed at various stages of clean-up to determine whether or not the MS/MS technique could simplify the analysis for these substances. A comparison was made between various methods used to analyze grain, flour and bread for vomitoxin. These methods include the MS/MS technique as well as GC/MS and HPLC. Results of these comparative analysis will be presented.

CONFIRMATION OF VOLATILE NITROSAMINES IN MEAT FOOD PRODUCTS BY GAS CHROMATOGRAPHY/MEDIUM RESOLUTION MASS SPECTROMETRY; Tung Sun; USDA-FSIS, P. O. Box 6085, Athens, GA 30604

It has been known that many nitrosamines are potent carcinogenic compounds and have been found in a wide variety of meat food products. Thus, they are monitored by U. S. Department of Agriculture, Food Safety and Inspection Service. Since nitrosamines will usually be present at sub-ppb or less in very complex mixture, a very sensitive and nitrosyl radical selective detector, thermal energy analyzer (TEA), is used to screen the extracts. As a regulatory agency, we also need to use the most reliable and available instrument, GC/MS, to confirm the nitrosamine violative samples. In order to reach the required sensitivity and specificity, GC/medium resolution MS with multiple peaks monitoring is necessary to confirm nitrosamines unequivocally from quite complex sample extracts. The nitrosamines are confirmed if all the following criteria are reached: (a) GC retention times are correct, (b) molecular ion, characteristic nitrosyl ion NO^+ and two other fragment ions are detected, and (c) no interferences of the suspect nitrosamines are in the reagent blank.

Experimental

(A) Sample Handling and Clean-up (1,2): Place 25 g ground meat sample and 200 ml 3N KOH into a round-bottom flask. Vacuum is applied, and the contents of the flask are slowly heated to 110°C. The aqueous distillate is trapped in vapor traps immersed in liquid nitrogen. The aqueous distillate is then acidified and extracted with dichloromethane (DCM) to remove amines and other basic compounds. The DCM extract is then washed with 50 ml 1N KOH solution to remove acidic contaminants and drys over anhydrous sodium sulfate and is concentrated to 1 ml for GC/TEA detection and quantitation. When the nitrosamines are found above 5 ppb, either selica gel column followed by acid celite column or alumina column only are used to further clean up the sample extracts before carrying out the GC/MS confirmation.

(B) Gas Chromatograph: A Pye Unicam Model 104 equipped with a 9 ft x 4 mm i.d. glass column and packed with 5% FFAP on 60/80 chromosorb WHP is used. Ultra pure helium is used as carrier gas at a flow rate of 25 ml/min. Column temperature is usually at isothermal 140°C. Typical retention times (in min:sec) are: Dimethylnitrosamine (DMNA), 2:45; Diethylnitrosamine (DENA), 3:21; N-Di-n-propylnitrosamine (DPNA), 5:05; N-nitrosoazetidine (NAZE), 8:10; N-Di-n-butylnitrosamine (DBNA), 9:25; N-nitrosopiperidine (NPIP), 10:47; N-nitrosopyrrolidine (NPYR), 12:23; and N-nitrosomorpholine (NMOR), 14:36.

(C) Thermal Energy Analyzer (3): It is a Model 502 TEA from Thermo Electron Corp., Waltham, MA. Nitrosamines are separated by GC column and enter a catalytic pyrolysis chamber which is heated to 450°C to liberate •NO and other pyrolysis products. These pyrolysis products are removed from gas stream through a cold trap (-150°C). The •NO then passes into a reaction chamber where it is allowed to react with ozone, formed by high voltage electric discharge (7.5 KV across a 1 mm glass dielectric) in oxygen, to produce electronically excited nitrogen dioxide. The $•NO_2^*$ decays to its ground state with the emission of light in the near infrared region. This emission is detected by a photomultiplier tube, amplified and recorded.

(D) Mass Spectrometer (4,5): A Kratos AEI MS 30 double beam mass spectrometer with multiple peak monitoring is used almost exclusively in electron impact mode, because all volatile nitrosamines show sufficiently intense molecular ion and quite simple EI mass spectra. The static resolution at 10% valley definition is usually higher than 3000 to separate the significant nitrogen containing fragment ions or molecular ions from commonly interfered hydrocarbon ions. Maximum sensitivity at beam 1 is often necessary in order to detect the trace amount of nitrosamines. A reference mass is monitored at beam 2 to view and correct the drift should it happen.

(E) Data System: Data acquisition is accomplished with DS-50S software with a Data General NOVA 2 computer.

Results and Conclusions

(A) Because samples are prepared involving low temperature vacuum distillation, there are more interference peaks around low GC retention time area. Thus, DMNA and DENA need to be confirmed very carefully either by using higher resolution mass spectrometry or monitoring more characteristic ions.

(B) The m/z 30 at low resolution contains at least two significant ions of NO^+ and CH_4N^+ for all volatile nitrosamines. Other common fragment ions are CH_xN^+, $C_2H_yN^+$, and $(M-H_zNO)^+$ where x = 2,3; y = 2,3,4,5,6; and z = 0,1,2,3. Only DENA and DMNA have significant NH_4^+ ion. DPNA and DBNA have quite intense $(M-OH)^+$ ion.

(C) The most commonly occurring nitrosamine in cured meat products are NPYR and trace DMNA. We haven't found any violative sample containing DPNA and NAZE in meat food products. Thus, they are usually used as internal standards for TEA quantification.

References

(1) N. P. Sen, S. Seaman and W. F. Miles, J. Agr. Food Chem., 27, 1355 (1979).
(2) J. H. Hotchkiss, J. Assoc. Off. Anal. Chem., 64, 1037 (1981).
(3) D. H. Fine, F. Rufeh, D. Lieb and D. P. Rounbehler, Anal. Chem., 47, 1188 (1975).
(4) T. A. Gough, Analyst, 103, 785 (1978).
(5) J. H. Beynon, R. A. Saunders and A. E. Williams, The Mass Spectra of Organic Molecules, Chapter 5, pp 258-346, Elsevier Pub. Co., New York (1968).

MS ANALYSIS OF THE LINKAGE OF PESTICIDE RESIDUES AND HUMUS CONSTITUENTS

Robert D. Minard, J. M. Bollag and S. Y. Liu, Dep'ts. of Chemistry and Soil Microbiology, Penn State University, University Park, PA 16802.

INTRODUCTION: Bollag and coworkers have done extensive research on the environmental fate of pesticide degradation intermediates. Mass spectrometry has played a key role in the success of this work. Chromatographic fractions (some selected by radio label detection) containing µg quantities of material, can be rapidly examined by mass spectrometry and these results then guide further effort and research. In this presentation, I will present several examples of how mass spectral results not only answered structural questions but led us in new directions.

ENZYME CATALYZED OXIDATIVE COUPLING OF 1-NAPHTHOL AND OTHER PHENOLS: In 1975, we were able to isolate an extracellular phenol oxidase (laccase) from a culture of the soil fungus, Rhizoctonia Praticola and found that this enzyme polymerizes phenolic products from various pesticides [2,4-dichbrophenol from 2,4-D, Naphthol from Sevin for example]. This oxidative coupling activity was detected by mass spectrometric analysis of the more volatile oligomers. Some phenol-enzyme product mixtures contain only dimer or trimer molecular ions in their spectra, but others yield a distribution of oligomers (ref. 1-3).

Often sufficient quantities of dimers or trimers could be chromatographically isolated to allow nmr analysis and this helped to define the exact location and type (carbon-carbon or carbon-oxygen) of coupling. We also examined cross-coupling between two different phenols (for example 2,4-dichlorophenol and 2-chloro-4-bromo phenol) and mass spectrometric analysis made product identification quite simple.

SYRINGIC AND VANILLIC ACID OLIGOMERS: At the same time that we studied the oxidative coupling of xenobiotoc phenols, we examined the oligomeric reaction products from naturally occurring, lignin-derived phenols such as syringic acid and vanillic acid. Mass spectrometry provided us with the best insight into the structural nature of these humic acid model compounds to date (ref. 4, 5).

CROSS COUPLING OF HUMUS CONSTITUENTS AND 2,4-DICHLOROPHENOL: The data from the oxidative coupling experiments of xenobiotic and naturally occurring phenols immediately suggest the direct linkage of pesticide derived phenols to soil phenols such as syringic acid or vanillic acid. Indeed when these soil phenols are incubated with the laccase enzyme in the presence of 2,4-dichlorophenol, mass spectrometric analysis of the products showed dimers to pentamers containing both dichlorophenol and syringic or vanillic acid units (ref. 6). Although the exact location and type (C-C or C-O) of coupling shown in the structures below is purely postulative, the chlorine isotope patterns and molecular weights as determined by Mass Spectrometry are compatible with these suggested oligomeric structures. Thus, MS analysis provides data that implies the potential incorporation of xenobiotic phenols into soil humus, an implication that may have environmental consequences.

CONCLUSIONS: Mass spectrometry is absolutely essential to our study of the environmental fate of pesticides:

1). It allows analysis of the small amounts of products available. 2) It provides a rapid screening method of crude extracts or partially separated product mixtures in order to see the extent of substrate transformation. 3) Within a series of related products, molecular weight and isotope pattern analysis allows "reasonable" structure assignments even if too little material exists for other spectral analyses (nmr, ir). 4) It often produces results that effect the direction of further work.

REFERENCES:

1. R. Sjoblad, R. Minard and J.-M. Bollag, Pesticide Biochemistry and Physiology, 6, (1976).
2. R. Minard, S. Liu, J.-M. Bollag, J. Ag. Food. Chem., 29, 250 (1981).
3. J.-M. Bollag, S. Liu and R. Minard, App. and Env. Microbiology, 38, 1564 (1981).
4. S. Liu, R. Minard, J.-M. Bollag, Soil Sci. Soc. American Journ. 45, 1100 (1981).
5. J.-M. Bollag, S. Liu, R. Minard, Soil Biol. Biochem. 14, 157 (1982).
6. J.-M. Bollag, S. Liu, R. Minard, Soil Sci. Soc. of America J. 44, 52, 1980.

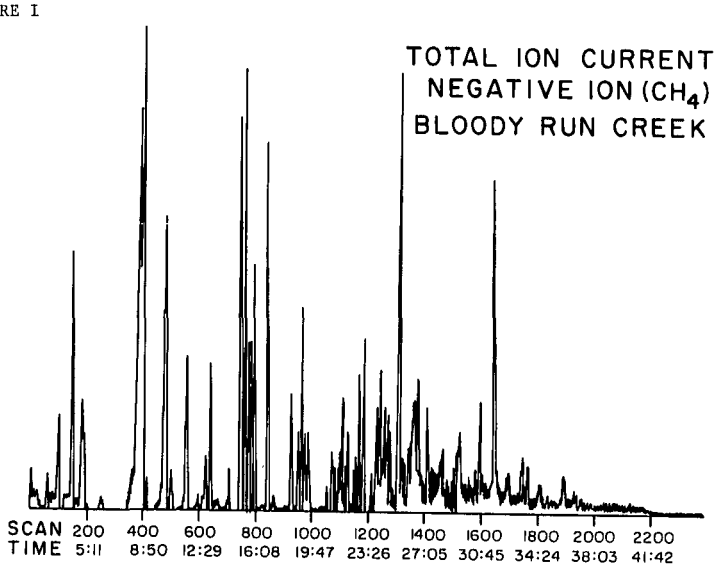
IDENTIFICATION OF TRIFLUOROMETHYLBENZENE DERIVATIVES BY NEGATIVE ION CHEMICAL IONIZATION MASS SPECTROMETRY, Bertha L. Proctor, University of Texas at Dallas, Richardson, TX 75080

Trifluoromethylbenzenes are important feed stock chemicals in the production of a variety of biologically active compounds including pharmaceuticals, herbicides and germicides (1). Bloody Run Creek in Niagara Falls, New York receives runoff from the Hyde Park disposal area which contains over 8,000 tons of trifluoromethylbenzene derivatives (2).

After researching the industrial synthesis of Trifluoromethylbenzenes(Table I A,B,&C) and the types of compounds dumped in Hyde Park (over 80,000 tons), I postulated probable by-products. Several of these compounds were synthesized in the laboratory, fingerprinted by gas chromatograph retention time, and negative ion chemical ionization mass spectrometry.

Bloody Run Creek sediments were extracted and analyzed for these trifluoromethylbenzene derivatives by selected ion monitoring methane negative chemical ionization mass spectrometry. Figure 1 is the Total Ion Current for methane negative ion chemical ionization mass spectrometry of soxhlet extract of Bloody Run Creek. Table 1 is a partial listing the the trifluoromethylbenzenes identified. Figure 2 is the negative ion chemical ionization mass spectra of one of the compounds thought to be a result of reactions taking place in the disposal site.

FIGURE I



REFERENCES

1. Kirk, R.E.; Othmer, D. F.; Grayson, M.; Eckroth, P. "Kirk-Othmer Encyclopedia of Chemical Tecknology" 3rd Edition; Wiley & Sons, NY 1980

2. "Draft Report on Hazardous Waste Disposal in Erie and Niagara Counties, New York" Interagency Task Force on Hazardous Waste, March 1979

TABLE I

TRIFLUOROMETHYLBENZENE DERIVATIVES

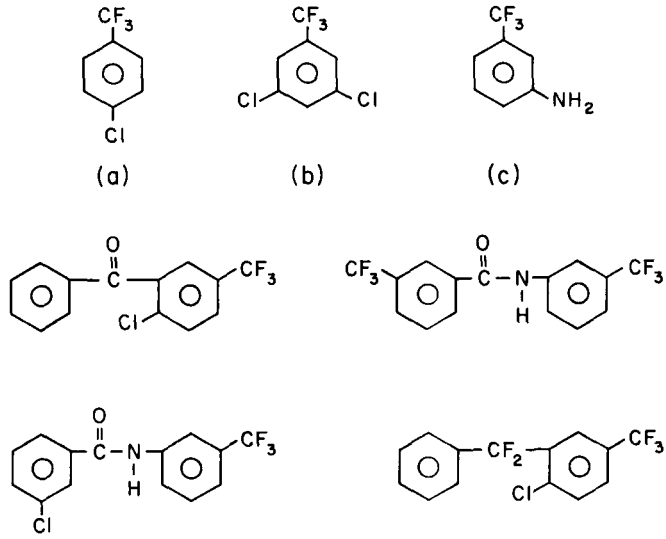
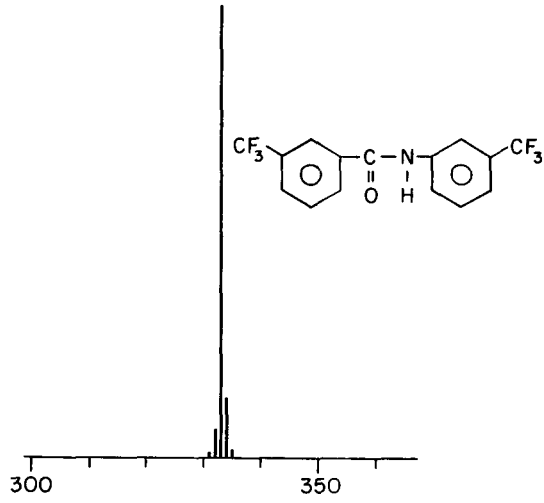


FIGURE 2

NEGATIVE ION CH_4 IONIZATION
BLOODY RUN CREEK



FPA 16 NEGATIVE ION CHEMICAL IONIZATION MASS SPECTROMETRY OF PHENOLIC PRIORITY POLLUTANT COMPOUNDS; Charlene W. Bayer and Luis E. Lowe, U.S. Geological Survey, National Water Quality Laboratory - Atlanta, Doraville, Georgia 30340

Negative ion chemical ionization mass spectrometry was evaluated as a method for the qualitative and quantitative determination of trace quantities of phenolic priority pollutant compounds in complex environmental mixtures. The phenolic compounds in the organic extracts were derivatized with pentafluorobenzylbromide, using hexaoxacyclooctadecane as the catalyst. Each mixture was analyzed by capillary gas chromatography/mass spectrometry using positive ion electron impact ionization, positive ion chemical ionization, and negative ion chemical ionization modes. The negative ion chemical ionization technique allows for greater sensitivity of the derivatized priority pollutant compounds in the environmental matrices due to the reduction of undesirable background moieties.

LONG TERM RESPONSE AND RETENTION TIME PRECISION OF COMBINED ACID AND BASE/NEUTRAL FRACTION PRIORITY POLLUTANT ANALYSES USING FUSED SILICA CAPILLARY COLUMN GC/MS;
B.N. COLBY, P.W. Ryan and J.E. Wilkinson; S-CUBED, La Jolla, CA 92038

The use of fused silica capillary columns has recently been reported as a means of increasing priority pollutant analysis efficiency by analyzing combined acid and base/neutral fractions. Because this results in repeated coinjection of compounds possessing highly divergent physical properties, there has been some uncertainty about the long term stability of the system under routine operating conditions. In order to evaluate long term stability, 28 acidic, basic and neutral priority pollutants were investigated over a one month period during which extracts from synthetic fuel production waste waters were being routinely analyzed. Stability of quantitative response was evaluated using absolute area as well as relative area referred to both conventional and isotopically labeled analogue internal standards. Retention time stability was evaluated from absolute retention times and from relative retention times using the same conventional and labeled analogue internal standards. The results of this study will be presented.

STUDIES OF AQUEOUS SOLUTION OF GLUTARALDEHYDE BY CAPILLARY GAS CHROMATOGRAPHY-MASS SPECTROMETRY

Y.MASADA, K.HASHIMOTO, Y.SUMIDA and S.TERADA, Kyoto college of Pharmacy, Misasagi, Yamashina, Kyoto, Japan
T.TASHIMA and N.SATOH, Maruishi Paharmaceutical Co. Ltd., 2-2-41, Imazu-naka, Tsurumi-ku, Osaka, Japan

Introduction

Glutaraldehyde has become an important compound in a number of different areas. Since the introduction for electron microscopy by Sabatini et al., glutaraldehyde has become commonly used as a fixative reagent for tissues being analyzed by electron microscopy. Biochemically, its bifunctional nature has also been utilized successfully to immobilize various enzymes and to cross-link various proteins, and technologically, it has been used in the tanning of leather.

More recently, due to its excellent bactericidal and sporicidal properties, it has been used in the chemosterilization of hospital instruments.

In spite of its widespread, it is generally agreed that the chemistry of aqueous glutaraldehyde is very complex. Many workers indicated that commercial glutaraldehyde is a mixture of the monomeric dialdehyde and amounts of ipurities, mainly polymerization products.

Despite the large number of papers on this subject, however, the impurities in aqueous glutaraldehyde have yet to be determined, as an assay of purity the relative values of U.V. absorbance at 235 and 280nm has been generally used.

In order to ascertain the species present in aqueous glutaraldehyde, we subjected a few of commercial samples, which were assayed for electron microscopy, experimental and industrial use, to gas chromatography and gas chromatography-mass spectrometry.

Gas chromatography

The typical gas chromatogram of aqueous glutaraldehyde marketed as general grade is shown in Figure 1, by using fused silica capillary column coated with SE-54 (0.2mm X 25m).

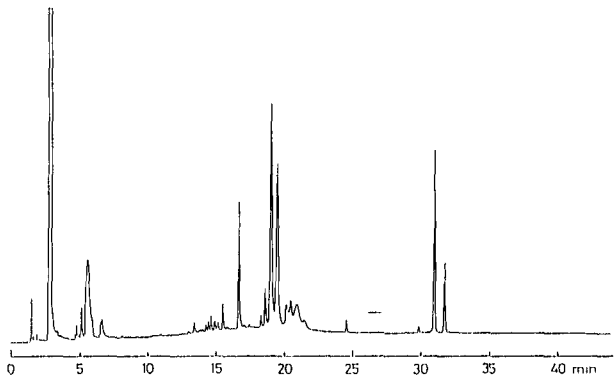


Figure 1.

In order to find the appropriate gas chromatographic system, we tested various column systems, by changing column types(glass packed and capillary column) and liquid phases(PEG-20M, OV-101, OV-1, SE-54, etc.).

The good gas chromatogram was obtained by using SE-54 coated on fused silica capillary column in comparison with other column systems. Many peaks were found in the chromatogram of commercial glutaraldehyde for general use, as shown in Figure 1, however, they were not produced by thermal decomposition of glutaraldehyde in an injection port, because of the following experimental result.

It is generally thought that glutaraldehyde decomposes in thermal condition, but various chromatogram were got from each of different samples, which had been marketed as electron microscopy and industry grade, etc. Particularly no peak was found in the case of specially purified solution without a large peak of glutaraldehyde and a few of peaks.

The relative values of U.V. absorbance at 235 and 280nm has been generally used as an index of purity:glutaraldehyde has an absorbance peak at 280nm and indeterminate impurities have an absorbance peak at 235nm. However, many peaks(on the gas chromatogram) were found in a someone of commercial samples, which had a lower absorbance peak at 235nm than at 280nm.

As the above fact, we proporse that the analysis of aqueous glutaraldehyde by gas chromatography shall be used as an assay of purity.

Gas chromatography-mass spectrometry

In an effort to ascertain the species present and detected in our gas chromatographic system, we subjected several aqueous solutions to gas chromatography-mass spectrometry(GC-MS).

The capillary GC-MS analyses were performed with SE-54 coated on fused silica capillary column(0.3mm X 50m) and the electron impact(EI) mode, the chemical ionization(CI) mode using iso-butane, ammonia, iso-butane-pyridine and ammonia-pyridine as the reagent gases.

It was difficult to detect molecular ions by the EI mode. Even if molecular ions were observed, they showed very weak intensities.

Wheares, the CI mass spectra provided the informations of molecular weight for the several main peaks in the gas chromatogram.

It was assumed that a few of species, which were produced by aldol condensation and hydration-polymerization, existed in aqueous solution of glutaraldehyde.

Conclusion

The good gas chromatogram of aqueous glutaraldehyde was obtained by using fused silica capillary column coated with SE-54.

As an assay of purity the analysis by gas chromatography is more precise and available than by U.V. absorption spectrometry.

We recognize the existence of dimers and trimers by GC-MS, especially using CI mode.

They were assumed to be the species which arose from glutaraldehyde in aqueous solution by aldol condensation and hydration-polymerization.

The CI mass spectra of species produced by aldol condensation showed prominent ions as MH^+, $(M + \text{pyridine-H})^+$, however, the species of hydration-polymerization showed as M^+ and $(M - H_2O + \text{pyridine-H})^+$.

* Sabatini D., K. Bensch and R. Barnett, J. Cell. Biol.,17(1963) 19.

MASS SPECTROMETRIC DETERMINATION OF TRACE ORGANIC COMPOUNDS IN AQUEOUS WASTES ASSOCIATED WITH ENERGY PRODUCTION

L. R. Hilpert, K. L. Richie, and H. S. Hertz, Center for Analytical Chemistry, National Bureau of Standards, Washington, DC 20234.

Over the past few years, increasing concern has been expressed over the potentially hazardous wastes associated with energy production. The Resource Conservation and Recovery Act of 1976 requires the identification of hazardous wastes based, in part, on chemical characterization of the waste and, in part, on the mobility or leachability of certain toxic chemical components of wastes. The National Bureau of Standards has been involved in developing measurement methods for the analysis of potentially toxic organic compounds in energy process by-product waters and aqueous leachates of hazardous wastes. GC/MS with selected ion monitoring has been used to quantitate organic acids in a shale oil process water at the µg/mL level and various aromatic compounds (PAH) in aqueous leachates of an SRC II coal liquid vacuum still bottom material at the ng/mL level.

- Analysis of Shale Oil Process Water -

The water analyzed in these studies was obtained from a simulated in situ retort, operated by the Laramie Energy Technology Center, Laramie, WY. One hundred mL of the process water were acidified to pH 2 or less with H_2SO_4 and then extracted with 2 x 50 mL methylene chloride. The organic extract was dried by filtering through a cone of anhydrous sodium sulfate and concentrated under a stream of dry nitrogen. The concentrated extracts were analyzed by GC/MS. Gas chromatographic separations were carried out on a 30 m x 0.26 mm i.d. Carbowax 20M fused silica capillary column. The column was interfaced directly to the ion source of a quadrupole mass spectrometer. Figure 1 shows a chromatogram of the organic acids extract from the shale oil process water. The normal aliphatic acids and phenol are identified on the chromatogram.

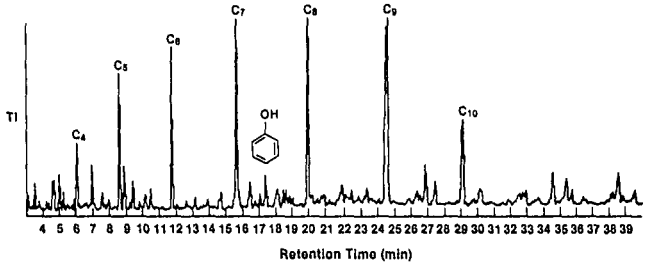


Figure 1. Shale Oil Process Water Acids

Quantitative determinations were made by GC/MS with selected ion monitoring (SIM) using a standard addition technique. Three standard additions were made over a range of 0 to twice the approximate concentration in the process water (based on preliminary quantitation using external standards). In the SIM experiments, ions at m/z 60 for the aliphatic acids and m/z 94 for phenol were monitored in 0.1 amu increments to insure that the voltage was sampled at the top of the mass peak; a dwell time of 100 ms was used to give at least 20 data points across the chromatographic peak. The results of these determinations are shown in Table I.

Table I

Shale Oil Process Water Analysis

Compound	Concentration (ppm)
n-butanoic acid	49.6 ± 7.6
n-pentanoic acid	71.9 ± 8.9
n-hexanoic acid	87.8 ± 4.4
n-heptanoic acid	149.5 ± 9.2
n-octanoic acid	140.5 ± 7.8
n-nonanoic acid	82.5 ± 5.0
n-decanoic acid	38.5 ± 2.1
phenol	16.1 ± 4.2

- Analysis of Aqueous Leachates of SRC II Vacuum Still Bottom Material -

Aqueous leachates of a ground SRC II vacuum still bottom material (particle size approximately 250 μm) were prepared using the EP leach procedure described in "Test Methods for Evaluating Solid Wastes: Chemical/Physical Properties," Federal Register, Vol. 45, No. 98, May 19, 1980, and the ASTM leaching method described in "Proposed Methods for Leaching of Waste Materials," 1979 Annual Book of ASTM Standards, Part 31. The aqueous leachates were carried through a solvent extraction scheme to isolate the acids and base-neutrals. The organic extracts were analyzed by GC/MS in the SIM mode for quantitation, and the full scanning mode for confirmation of identifications. The results of quantitative determinations are shown in Table II.

Table II

Concentrations of Compounds in Bulk Leachates of SRC II Vacuum Still Bottom Material

Analyte	Concentration (μg/L)[a] ASTM-A Leachate	EP Leachate
2-picoline	0.24	---
phenol	6.68	1.09
o-cresol	1.63	0.18
naphthalene	0.38	0.20
quinoline	0.39	---
1,4-naphthoquinone	0.15	0.08
dibenzothiophene	0.02	---
phenanthrene	0.06	0.05
carbazole	0.76	0.46
fluoranthene	0.02	0.02

[a]Values are the average of two determinations.

The ground SRC II vacuum still bottom material itself was also extracted with methylene chloride. An aliquot of this extract was analyzed by GC/MS on a 30 m SE-52 fused silica capillary column. The total ion chromatogram is shown in Figure 2. Most of the peaks identified were a series of polynuclear aromatic hydrocarbons (PAH). Concentrations of the PAH identified in the aqueous leachates (see Table II) were in the low part per billion range, due in part to their inherently low aqueous solubility, and to losses encountered during the sample extraction and work-up steps.

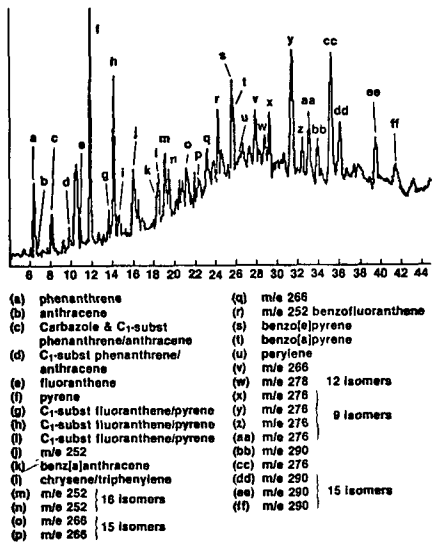


Figure 2. Total Ion Chromatogram of CH_2Cl_2 Extract of SRC II Vacuum Still Bottom Material

GAS CHROMATOGRAPHY - FIELD IONIZATION MASS SPECTROMETRY (GC-FIMS)

R. H. Fleming, S. E. Buttrill, Jr., J. H. Smith, and J. C. Harper

SRI International, 333 Ravenswood, Menlo Park, CA 94025

Field ionization (FI) produces only molecular ions from the vast majority of compounds. Thus FIMS is often used for analysis of easily fragmented substances. Because there is only one type of ion for each component, FIMS analysis of complicated mixtures is also useful. Interpretation of the FIMS spectra is straightforward except that more than one component of the mixture could have the same molecular weight. To gain analytical specificity for such components, capillary column gas chromatography capability has been added to a FIMS system, thus providing a second dimension of information. The goals of these experiments are to demonstrate GC-FIMS at high capillary column resolution and high mass spectrometer sensitivity.

GC/FIMS Instrumentation

Chromatographic separation of compounds prior to delivery to the FIMS was accomplished with a Hewlett Packard 5840A gas chromatograph equipped with a 30m SE-30 fused silica capillary column. Helium was used as the carrier gas with the column flow adjusted to 50 cm sec^{-1}. To reduce the amount of injected solvent passing into the mass spectrometer. the GC was operated in the split mode with a split ratio of 200:1. A sample volume of 1 µl was injected in each case.

The interface consists of a heated (170°C) dimethyl silicone membrane (0.025 mm x 46 mm^2) placed between the field ionization source and the GC column. The membrane is 15 to 500 times more permeable to organic substances than to air or helium. It thus serves to concentrate organic molecules at the same time it provides a barrier between the high vacuum of the mass spectrometer and the carrier gas exiting from the GC column.

The organic substances pass from the membrane separator to the ion source. The SRI volcano type field ionization source has been described in detail by Aberth and Spindt.* Its unique high sensitivity results from its extremely efficient sample handling. Sample molecules may escape only by passing through the high field region at the throat of the volcano. Field ionization occurs by virtue of the large potential difference (typically 1200 V) maintained between the volcano and a nickel mesh counterelectrode.

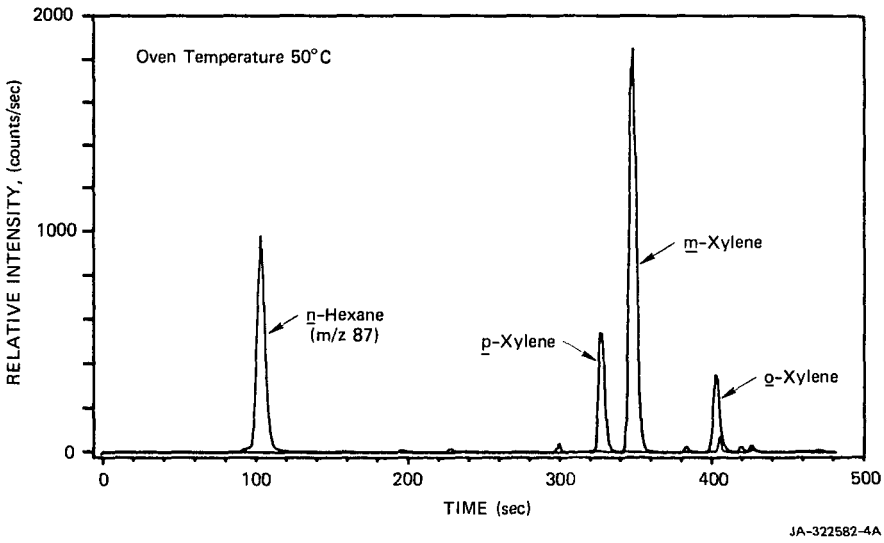
---

*W. Aberth and C. A. Spindt, Int. J. Mass Spectrom. Ion Phys., 25, 183 (1977).

A conventional quadrupole mass analyzer and ion counting detector system are used. A Digital Equipment Corp. LSI-11 computer collects data and controls the mass analyzer. Most compounds are ionized, mass analyzed, and detected with an efficiency of about 2 x 10^{-6} ions/molecule. This sensitivity is about 50 times greater than that obtained with the best commercial FIMS instrument.

RESULTS

Selected ion chromatograms were acquired for several fuels and hydrocarbon mixtures. The GC column resolution is equivalent to that obtained with a flame ionization detector and demonstrates that the membrane interface does not increase the GC peak width. In the figure the M + 1 ions of n-hexane solvent at m/z 87 ($^{13}C^{12}C_5H_{14}$) were monitored at the same time as the molecular ions of a mixture of xylene isomers at m/z 106. The smallest peak represents 125 pg of o-xylene injected onto the column and detected with a signal-to-noise ratio of 40:1.



SELECTED ION CHROMATOGRAMS (m/z 106) XYLENES (1 ng total) IN *n*-HEXANE

Dry Injector Regains Sensitivity and Maintains Separation for Capillary GC-MS Analysis: Allen, R.H., Pike, A., and Fennessey, P.V. R.H. Allen, Co., Boulder, Colo. and University of Colorado Health Sciences Center, Denver, Colo. 80262.

There are several types of injection systems currently in use today. Of these split, splitless and "on column" appear to have gained most popularity. Their technical aspects have been well documented.

The choice of inlet system in usually dependent on the material to be analyzed. In the majority of the above mentioned techniques, samples are introduced into the inlet system using solvent as a vehicle. There they undergo flash evaporation in the heated zone of the inlet before being swept onto the column by the carrier gas.

These techniques have shown considerable application in the analysis of volatile compounds. However, there are a number of fundamental practical details that must be followed if one is to obtain the desired chromatographic resolution and efficiency. Of these initial column temperature, solvent boiling point, the amount of solvent injected and injection rate appear to be of major importance in obtaining the desired solvent effect. The all-glass solid sampling device developed by Van der Berg (1) and modified by us allows the quantitative analysis of compounds with boiling points at least 70°C higher than the solvent.

In principle, the material to be analyzed is deposited on the tip of the glass needle with a standard microlitre syringe. The choice of solvent is of little consequence. However, it is probably faster in terms of analytical time to use solvents of high volatility.

The carrier gas enters the system at a point well below the tip of the needle. The gas stream is split downwards onto the column, and upwards carrying the evaporating solvent out into the atmosphere. After a few minutes the solvent has completely evaporated and the needle is rapidly introduced into the heated zone of the inlet system. There volatilization of the sample occurs which is simultaneously swept onto the capillary column by the carrier gas. After several seconds the glass needle is returned to its original position. It is then ready to receive the next sample.

This system offers two major advantages for the analysis of trace quantities of material. The first is that one can connect the capillary column directly into the mass spectrometery without the usual divert valve needed to keep the large solvent loads off the source. As a result one can maintain the sensitivity and stability of the M.S. for longer periods of time. The second advantage is that the basic sensitivity of the capillary analysis is increased. This is because one does not need to split the sample in the injector or handle the rather large solvent loads. When we compare our basic sensitivity to injectors that split the sample we see a 10 to 100 fold increase in sensitivity using the falling needle. And when we compare this injector to on-column types we see a 4-5 fold increase in sensitivity with excellent resolution.

Reference

1. van den Berg, P.M.J. and Cox, Th.P.H.: "An all glass sampling device for open tubular columns in gas chromatography". Chromatographia 5, 301 (1972).

A CHEMICAL REACTION INTERFACE FOR CAPILLARY GC/MS. Fred P. Abramson and Sanford P. Markey. Clinical Pharmacology Branch, National Cancer Institute and Laboratory of Clinical Science, National Institute of Mental Health, NIH, Bethesda, MD 20205, and Department of Pharmacology, George Washington University Medical Center, Washington, DC 20037

Gas chromatography with detection of radioactivity has long utilized nuclear decay to permit very specific compound localization in complex chromatograms (1). The design of combustion chambers and radiochemical detectors significantly degrades the chromatographic resolution attainable with capillary columns (2,3). The amount of ^{14}C normally employed in metabolism experiments suggests that mass spectrometric detection of ^{14}C should compete with radiochemical detection--i.e., 1000 dpm equals approximately 100 pg of ^{14}C. The limitation of mass detection is interference from ^{13}C, ^{2}H, ^{18}O, etc. which contribute to a significant and variable M+2 background for most organic molecules. Quantitative degradation of organic molecules to di- or triatomic products simplifies heavy nuclide detection by eliminating interfering background. We have exploited a low pressure microwave induced plasma interface to convert all carbon containing compounds in a capillary gc effluent to CO and CO_2 which can be measured in a conventional mass spectrometer without loss of chromatographic resolution and with a detection limit of 300-500 dpm.

EXPERIMENTAL

A Varian 1400 gas chromatograph equipped with a capillary splitter inlet set at 400:1 (Supelco) was used with a Hewlett-Packard 50 m x 0.3 mm ID SE 54 coated fused silica capillary column. The end of the column was extended into a 1/4" Swagelok "T" where its 1 ml/min helium flow was mixed with 0.1 ml/min of oxygen (UHP Matheson) and then passed through a 1/4" OD, 4 mm ID, 10 cm long quartz tube into a microwave discharge cavity. Connections to the quartz tube were made with Vespel SP22 (40% graphite) ferrules and Swagelok fittings. The polyimide coating on that part of the capillary column which extended into the make-up "T" was burned off prior to assembly to minimize background. The microwave cavity was of a novel design* to perform under a relatively high pressure oxygen-rich environment, and was powered by a 2450 MHz Raytheon Microtherm microwave power supply. The quartz tube was coupled to a 1 m section of 0.030" ID stainless steel capillary tubing which ran concentrically through the direct introduction probe into the mass spectrometer ion source. The interface was heated to approximately 230°C up to the discharge cavity, and operated at ambient temperature from that point on.

A mixture of 514 ppm butane in helium was obtained from Matheson. The 1-^{14}C-palmitic acid (50 mCi/mmole, New England Nuclear) was methylated with diazomethane in ether and compared for purity with unlabeled methyl palmitate and palmitic acid using conventional GC/MS techniques. A Finnigan Model 1015 quadrupole mass spectrometer with Extranuclear SpectraEl electronics and differential pumping was used to obtain mass spectral data recorded with a Ribar SADR data system or Finnigan PROMIM.

RESULTS AND DISCUSSION

Because of the low operating pressures in the discharge tube, ca, 1 Torr, no make-up gas was needed to ensure high chromatographic resolution. Only 0.1 ml/min of O_2 was needed to completely combust any analyte introduced. Approximately 1 ml/min of the butane/He mixture was introduced via the make-up gas line and its spectrum analyzed both without and with the discharge. No ions representing intact butane were observed after the discharge was turned on; the summed intensities of major product ions approximately equals the intensities of butane.

The chromatographic resolution obtainable with the interface was demonstrated by injecting a sample of isomeric hexanes which separated at room temperature. The peak width at half-height was approximately 1.8 seconds at a retention time of 2 minutes.

---

*The chamber was designed and built by Dr. Robert L. Bowman. Details are avilable upon request.

The potential of this technique as a radioactivity monitor was assessed with a sample of 1-^{14}C-methyl palmitate which was chromatographed isothermally at 215°C. $^{14}CO_2$ was detected at m/z 46 along with the natural $^{12}CO_2$ at m/z 44. The time from the injection was 4.2 minutes and the half-width was 4 seconds. After accounting for purity, derivatization yield, and split, the methyl palmitate peak was calculated to contain 150 pCi which is 330 dpm.

The reaction GC/MS interface is not limited to oxygen as the reactant gas nor to carbon as the analyzable element. We have seen complete reaction of carbon with either nitrogen to form HCN and $(CN)_2$, or with H_2 to form CH_4. Other preliminary studies have shown detection of nitrogen, sulfur, chlorine and bromine in the oxygen-scavenged discharge.

The use of a destructive interace has the advantage of generality; no information is needed about the position or the chemistry of the element or nuclide under investigation. In this way, it may be useful in metabolic studies where all the products of a labeled precursor are sought, or in survey analyses where an element- or nuclide-specific chromatographic detector is desired. Its construction permits retention of the high resolution of open tubular gas chromatgraphic columns.

REFERENCES

1. Campbell, I.M. Anal, Chem. 1979, 51, 1012A-1021A.

2. Weber, H., Höller, M., Breuer, H. J. Chromatogr, 1982 235, 523-526.

3. Ernst, L.A., Emmons, G.T., Naworal, J.D., Campbell, I.M. Anal. Chem, 1981, 53, 1959-1961.

THE INTEGRATED GC PROBE: A NEW ANALYTICAL TOOL FOR HIGH BOILING COMPOUNDS AND MS/MS

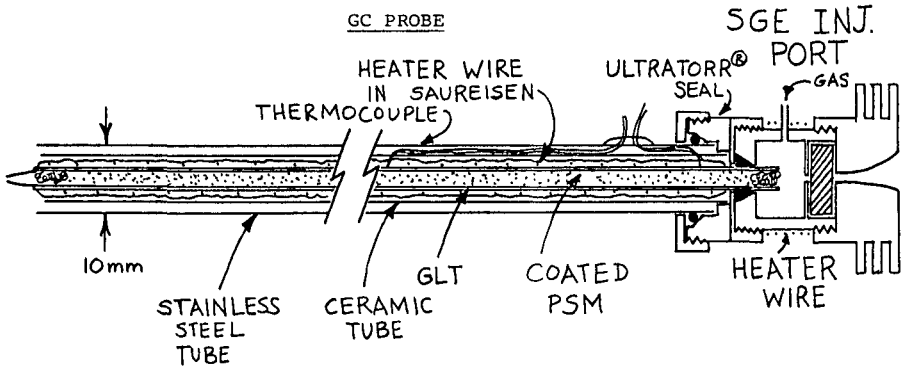
Martin A. Rudat
Central Research and Development Dept.
E. I. du Pont de Nemours & Co.
Wilmington, Delaware 19898

A complete, integrated GC system (inlet, column, heaters, and GC/MS interface) that is no larger than a standard direct inlet solids probe has been developed. The new device provides an inexpensive means of obtaining the GC/MS combination, while providing capabilities beyond those typically available with standard GC/MS systems.

The figure shows a schematic diagram of the "GC probe", the column of which is a glass-lined stainless tube packed with 0.5% coated (SP-2100 or SP-1000) porous silica microspheres. Up to 2000 plates may be obtained in the 30cm x 1.5mm column, although significantly fewer effective plates have thus far been typically obtained due to intentional sample overloading. Helium gas flow rates are compatible with most modern mass spectrometers, optimizing at 3-5 cc/min. This is advantageous, since the transfer line and gas separation normally required for packed columns is eliminated, yet the capacity of the column is greater than that of a capillary column operated similarly. Due to the vacuum at the outlet, the entire column operates at sub-atmospheric pressure.

The combination of short length, light liquid loading, and reduced pressure operation provide the GC probe with improved capabilities for high boiling point and thermolabile compounds, since the injection port temperature and column temperature required for elution (in 0.5-3 minutes, typically) are comparatively very low. For example, squalene elutes in 20 seconds from a column at only 160°C. Similarly, injected solids elute very rapidly at reasonable temperatures. An additional feature of the GC probe is the dramatic variation in retention time introduced by changing the column temperature. The approximate doubling of retention in 10°C provides the probe with a retention dynamic range of about 250000:1 over the normal range (room temperature to 250°C).

The combination of these unique characteristics should make the GC probe useful for the rapid analysis of high boiling point compounds and thermolabile compounds, and for the "prefiltering" of mixtures for MS/MS analysis.



GC/MS and GC/FT-IR; A Comparison

K.L. Gallaher and D.B. Lukco,
Sohio Research Center, Cleveland, Ohio 44128

Although both mass spectra and infrared spectra have substantial information content, GC/MS has been far ahead of GC/FT-IR as a practical technique. GC/FT-IR has been hindered by a data rate several times larger than that of GC/MS, by data processing requirements too large to perform in real time and by data storage requirements which limited most systems to a few hundred scans. However, 1982 technology has solved these problems. Several commercial GC/FT-IR systems now have array processors or dedicated fast Fourier processors which allow real time computation. New megabyte disk drives allow over 10,000 scans.

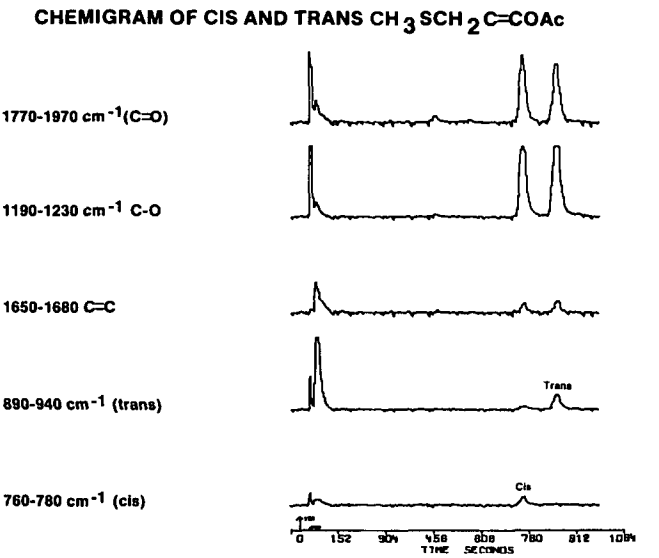
Quoted full scan MS and IR detection sensitivities are similar. Identification sensitivity for specific compounds can vary substantially. Quadrupole MS sensitivity decreases with mass which can obscure the parent ion and other important high masses. Some molecules produce primarily negative ions undetected by a normal positive ion scan. FT-IR sensitivity is a function of the polarity of the compound observed. Sensitivity varies across the infrared spectrum as a function of source intensity and detector response reaching a maximum in the middle of the spectrum and decreasing to zero at 400 to 800 cm^{-1} depending on the particular system. Poor low wavenumber sensitivity can decrease the ability to determine aromatic or olefinic substitution.

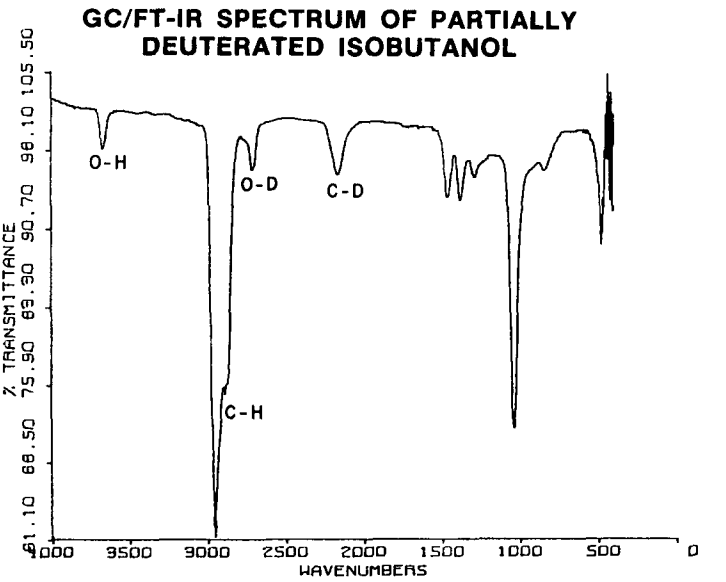
Mass spectroscopy is the method of choice for molecular weight determination and in the identification of a wide variety of homologous series. Spectral search methods for known compounds are easy because of mass spectroscopy's intrinsically digital nature.

Infrared spectroscopy is better at distinguishing isomers and at screening for specific functionalities, especially polar functionality. For example, this GC/FT-IR "Chemigram" (figure 1) easily distinguishes cis and trans isomers of $CH_3SCH_2CH{=}CHOAc$ which gave identical mass spectra.

In another unusual example GC/FT-IR quickly determined that deuterium is indeed in the backbone of isobutanol even though it is in methanol-d_1 (CH_3OD) solution. GC/MS would have required derivatization.

As improvements in GC/IR data storage capability, computation speed, data analysis software and spectral libraries are implemented, GC/IR is increasingly becoming a technique which can indeed be considered as an alternative or an addition to GC/MS for the information content it can offer.


CHEMIGRAM OF CIS AND TRANS CH3SCH2C=COAc
1770-1970 cm-1(C=O)
1190-1230 cm-1 C-O
1650-1680 C=C
890-940 cm-1 (trans)
760-780 cm-1 (cis)
Trans
Cis
0
152
304
456
608
760
912
1064
TIME SECONDS


GC/FT-IR SPECTRUM OF PARTIALLY DEUTERATED ISOBUTANOL
% TRANSMITTANCE
105.50
98.10
90.70
83.30
75.90
68.50
61.10
O-H
O-D
C-D
C-H
4000
3500
3000
2500
2000
1500
1000
500
0
WAVENUMBERS

MODIFICATIONS OF AUTOMATED REVERSE LIBRARY SEARCHING ALGORITHMS (MSSMET) BASED ON EXPERIMENTAL OBSERVATIONS; J.D. Pinkston, J. Vrbanac, J.F. Holland, L. Westover and C.C. Sweeley, NIH/MSU Mass Spectrometry Facility, Michigan State University, East Lansing, Michigan 48824

The automated qualitative and quantitative program MSSMET has been applied to the analysis of urinary acids, urinary steroids, and plasma acids (1,2,3). This program incorporates a reverse library search that uses chromatographic retention time as the independent parameter delineating the constraints in the library prior to searching. Library entries are characterized by their retention index, a designate ion (most definitive of that compound in the sample milieu), and a confirming ion set (4). Both capillary and packed column chromatography have been utilized as the separation mode.

Experiences encountered in these applications have led to modifications of the algorithms utilized and the nature of the computer-operator interactions. Of particular importance has been the continuing need for operator surveillance of the data files. This situation is caused by the wide variations in the type and amount of components found in these complex biological mixtures. New problems are continuously appearing with compounds not interferred with in samples of prior experience. The fidelity of the library entries must be continuously evaluated as new combinations and concentrations of sample constituency are encountered. With this established pattern of operator interaction, observations have been made on the efficacy of several of the original logical assumptions upon which the analysis algorithms are based.

In general, it has been found that complex mathematical schemes work very well in simple situations, however, they fail unpredictably in complex cases. Simpler logic has been employed with the same results, i.e., success in simple cases, difficulty in complex cases. It has been found that, in most cases, the simple algorithms offer a much greater execution speed with no loss in accuracy. Since operator input has been required, a method of choice has slowly evolved which embodies simpler logical construction with computer selection of defined options, computer output of the options used, and the flagging of situations in which the analysis was not definitive. Examples of the more significant logical alterations are presented below.

In post-run analysis, the collected data are searched for all ions of interest, i.e., the designate and confirming ions of library entries located within a retention time window. The ion profiles are then screened for peaks occurring within the defined window and height and area calculations are made for each peak. For simplicity, the qualitative and quantitative calculations will be separated in this description with qualitative factors presented first.

Confirmation of component identity has been based upon a Grotch-type confidence factor calculation. The original applications included the designate ion. This inclusion became a source of error under certain circumstances and the designate ion has been removed from the calculations and given a weight of one or zero. A simple assumption that the designate ion must be present for the compound to be present has resulted in a substantial decrease in false positives. The remaining calculation as shown in Figure 1 has been expanded to include a bias against peaks of lesser intensity. This change has prevented low level ion peaks, where noise has an increased significance, to overly influence the factor calculation.

An additional factor based upon the proximity of each peak to the expected retention index has been incorporated to resolve situations of multiple positive findings within the retention time window. This factor, shown in Figure 2, weighs the intensity confidence factor against the retention time deviation using an empirical formula based upon past observations.

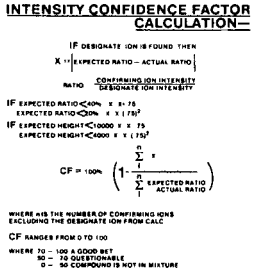


Figure 1

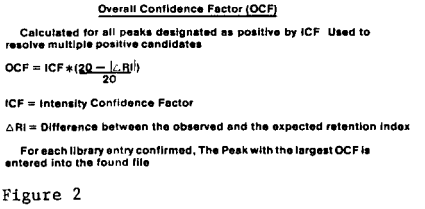


Figure 2

The base line subtraction routine has been changed from a polynominal fit to a simple lowest side value. This simplification has not significantly effected the overall accuracy and has reduced the incidence of errors produced when peaks are located near the extremes of the window region. The area calculations have been simplified and two major unresolved situations have been defined as shown in Figures 3 and 4. If the ratio of peak heights is less than 3, a simple perpendicular drop is used for area calculations. If the peak ratio exceeds 3, the smaller peak is skimmed from the larger peak as shown in Figure 4. For all area calculations, the computer outputs the option employed. When the situation is very complex, even the simple algorithms run into trouble. The computer will highlite these cases for rapid visual attention.

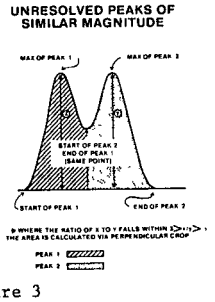


Figure 3

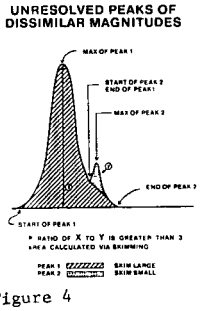


Figure 4

The results of these logical simplifications have greatly improved execution speed and reduced the number of gross errors. All internal checks to date indicate that this has been done with an apparent increase in precision and accuracy. The computer output of options used and flagging of trouble regions undoubtedly have assisted in this improvement.

1. S.C. Gates, C.C. Sweeley, S. Krivit, D. Dewitt, and B.E. Blaisdell, Clin. Chem., 24 (1978) 1680.
2. J.J. Vrbanac, W.E. Braselton, Jr., J.F. Holland, and C.C. Sweeley, J. of Chromatog., 239 (1982) 265-276.
3. D. Issachar and C.C. Sweeley, Analytical Biochemistry 113 (1981) 43-50.
4. S.C. Gates, M.J. Smisko, C.L. Ashendel, N.D. Young, J.F. Holland, and C.C. Sweeley, Anal. Chem., 50 (1978) 433.

CHARACTERIZATION OF POLYAROMATIC NITROGEN COMPOUNDS IN CRUDE OILS

J.M. SCHMITTER, M. DORBON, G. DERYCKE, I. IGNATIADIS and P.J. ARPINO

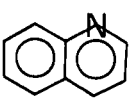
Ecole Polytechnique, Laboratoire de Chimie Analytique Physique
F- 91120 PALAISEAU, FRANCE

Basic and non-basic nitrogen containing compounds from various crude oils were analysed by a combination of chromatographic techniques (liquid and gas) and low resolution mass spectrometry (EI and CI).

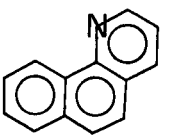
Nitrogen bases were selectively isolated by trapping on HCl modified silica. These compounds are mainly mono-azaarenes ($C_nH_{2n+Z}N$) with 2 to 7 fused aromatic rings. Distributions according to the Z number were obtained by probe microdistillation /CIMS analysis. The major series of compounds are quinolines (Z= -11, the maximum of the distribution found at $C_{15}H_{19}N$, i.e. C_6-alkylquinolines) benzoquinolines (Z= -17, maximum at $C_{15}H_{13}N$) and dibenzoquinolines (Z= -23, maximum at $C_{19}H_{15}N$).

Some differences are found in the relative distribution of azaarenes, but the same individual compounds are present in all crude oil samples. Total identifications were the result of a combination of glass capillary column GC/MS and spectroscopic methods (UV, LC/UV, fluorescence). A few authentic molecules were synthesized in the di-and tri-aromatic series. In particular, alkylated benzo[h] quinolines, all substituted by a methyl group in the alpha position to the nitrogen atom, represent the major triaromatic structures.

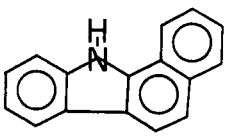
Fractions highly enriched in non-basic nitrogen compounds of the carbazole type were obtained by using a combination of liquid chromatographic techniques on acid/base modified silica and alumina adsorbents. Individual benzocarbazoles and dibenzocarbazoles were identified by means of capillary column GC/MS and coinjections with reference compounds.



quinoline



benzo[h]quinoline



benzo[a]carbazole

AUTHOR INDEX

AUTHOR	PAGE
ABBOTT, F S	98
ABERTH, W	47
ABRAMSON, F P	866
ACHEAMPONG, A A	98
ACZEL, T	808
ADAMS, D	53
ADAMS, J M	282
ADAMS, T	248
ADLINGTON, R M	720
AICHELE, D G	679
AICHELE, D G	719
AKIMORI, N	732
AKIYAMA, T	658
ALDERWEIRELDT, F C	149
ALDERWEIRELDT, F C	608
ALKALAY, D	172
ALKALAY, D	43
ALLEN, R H	865
ALLEY, C C	360
ALLISON, J	5
ALLISON, J	64
ALLISON, J	848
ALPIN, R T	720
ALTHAUS, J R	458
AMIR, J	183
AMSTER, I J	804
ANDEREGG, R J	648
ANDERS, D E	684
ANDERSON, D J	248
ANDERSON, S	622
ANDERSON, S	573
ANDREWS, P A	364
ANICICH, V G	455
ANICICH, V G	490
ANICICH, V G	67
AO, J	830
AOYAMA, T	675
AOYAMA, T	819
ARIKAWA, T	90
ARPINO, P J	603
ARPINO, P J	125
ARPINO, P J	873
ASAMOTO, B	807
ASHE, T R	769
AUE, D H	248
BAADSGAARD, H	591
BACZYNSKYJ, L	788
BACZYNSKYJ, L	247
BAIRD, M A	36
BAKER, A L	178
BAKER, E W	678
BALDWIN, M A	804
BALLATORE, A M	234
BARBALAS, M P	777
BARBALAS, M P	804
BARCHAS, J D	789
BARCHAS, J D	464
BARKLEY, R M	653
BARLAK, T M	251
BAROFSKY, D F	545
BARRON, R P	155
BARTMESS, J E	70
BARTMESS, J E	457
BARTNER, P	147
BASS, L M	71
BASU, A R	596
BATEMAN, R H	516
BAYER, C W	857
BAYLIS, F P	167
BEAVIS, R	229
BEAVIS, R	316
BECCHI, M	151
BECKNER, C F	234
BECKNER, C F	231
BENCSATH, F A	177
BENNETT, G A	520
BENNINGHOVEN, A	581
BENOIT, F M	678
BENSON, W R	155
BENTZ, B L	523
BENTZ, B L	386
BERKOWITZ, J	617
BERKOWITZ, J	700
BERKOWITZ, J	504
BERLEC, D	869
BEUHLER, R J	644
BEYNON, J H	14
BEYNON, J H	501
BEYNON, J H	620
BIEMANN, K	243
BIEMANN, K	567
BIEMANN, K	558
BIEMANN, K	232
BIERBAUM, V M	22
BIERBAUM, V M	78
BIERMAN, H W	456
BIERMANN, H W	249
BILL, J C	286
BILL, J C	246
BILLER, J E	558
BLAKE, G A	490
BLAKLEY, C R	117
BLAKLEY, C R	118
BLAKLEY, C R	606
BLANTON, W E	770
BLOM, K F	805
BLUM, W	796
BOAND, G	412
BOCKHOFF, F M	807
BOHRINGER, H	74
BOLLAG, J M	854
BONE, W M	49
BONE, W M	566
BORMAN, C H	172
BOSE, A K	147
BOUNINE, J P	125
BOUNINE, J P	603
BOURGEOIS, C E	673
BOWERS, M T	248
BOWERS, M T	431
BOWERS, M T	71
BRADFORD, D C	539
BRADLEY, C V	392
BRADLOW, H L	177

AUTHOR INDEX

AUTHOR	PAGE
BRAND, H R	841
BRANDENBERGER, H	371
BRANDENBERGER, H	468
BRENT, D A	226
BRILL, F W	77
BRITTEN, R A	337
BROOKS, J J	650
BROOKS, P W	286
BROOKS, P W	310
BROTHERTON, H O	224
BROWN, J E	167
BROWNSEY, B G	310
BRUMLEY, W C	784
BRUNNEE, C	348
BUCHS, A	671
BUCKLEY, T J	847
BUDDE, W L	655
BUDDE, W L	833
BURINSKY, D J	755
BURLINGAME, A L	47
BURNETT, N H	627
BURNIER, R C	704
BURSEY, M M	802
BURTON, R R	98
BUSCH, K L	585
BUSCH, K L	388
BUTRILL, S E	863
BUTTARS, L W	328
BUTTRILL, S E	43
BUTTRILL, S E	534
BYRD, G D	704
CADIZ, M	112
CALDECOURT, V	86
CALDWELL, G	70
CALLERY, P S	364
CAMPA, A B	356
CAMPANA, J E	251
CANADA, D C	124
CANTLE, J E	478
CANTLE, J E	541
CANTLE, J E	480
CAPRIOLI, R M	830
CAPRIOLI, R M	231
CAPRIOLI, R M	234
CARDACIOTTO, S J	300
CARESS, E A	784
CARLIN, J R	159
CARR, S A	728
CARR, S A	270
CARR, S A	730
CARROLL, D I	522
CARROLL, D I	288
CARTER, J A	432
CASABONA, L	436
CASTLEMAN, A W	205
CASTLEMAN, A W	209
CASTRO, M	248
CHAIT, B T	538
CHAKEL, J A	758
CHAN, K W	57
CHAN, K W	645
CHANDRASURIN, P	226
CHANG, C J	198
CHANG, T T	318
CHANG, T	300
CHATFIELD, D A	60
CHEN, H F	558
CHENG, M T	777
CHEPLEN, J M	850
CHESS, E K	810
CHIBA, K	161
CHIBA, K	274
CHO, A K	367
CHRISTENSEN, R G	597
CHRISTIE, D	419
CHRISTIE, W H	399
CHUNG, K M	92
CIUPEK, J C	798
CLAEYS, M	722
CLARK, C R	814
CLARK, J S	7
CLARK, J S	220
CLARK, J S	335
CLARK, J S	218
CLARK, R R	660
CLAY, K L	390
CLEMENT, S W	593
CLINE, R E	187
COATES, M	800
CODY, R B	704
CODY, R B	416
COENE, M C	722
COHEN, A	614
COLBY, B N	838
COLBY, B N	858
COLLE, E	832
COLTON, R J	325
COLTON, R J	251
COLVIN, D M	110
COMISAROW, M B	403
COMISAROW, M B	409
COMPSON, K R	240
COMPSTON, W	593
CONDITT, M K	653
CONNOLLY, V E	437
COOK, J C	564
COOK, K D	57
COOK, K D	645
COOKS, R G	585
COOKS, R G	388
COOKS, R G	798
COOKS, R G	755
COOKS, R G	255
COOKS, R G	507
COSTELLO, C E	243
COSTELLO, C E	270
COSTELLO, C E	567
COSTELLO, C E	558
COTTER, R J	560
COTTER, R J	571
COTTER, R	556
CRAIG, A G	635
CRAIN, P F	34
CRAWFORD, D W	437

AUTHOR INDEX

AUTHOR	PAGE
CRAWFORD, R W	776
CRAWFORD, R W	841
CRAWFORD, R W	442
CRIDDLE, M J	7
CRIDDLE, M J	218
CRIDDLE, M J	220
CRIDDLE, M J	335
CROW, F W	323
CROW, F W	506
DAISHIMA, S	462
DAN, P	173
DAN, P	135
DAS, P R	751
DASS, C	511
DATE, A R	447
DAVENPORT, M J	715
DAVIDSON, W R	791
DAVIDSON, W R	851
DAVIES, R O	159
DAWSON, P H	290
DAWSON, P H	513
DAY, R A	726
DAY, R A	724
DE LAETER, J R	484
DE LEENHEER, A P	38
DECORPO, J J	251
DEDIEU, M	125
DEDIEU, M	603
DEKANAL, J	197
DELMORE, J E	328
DELMORE, J E	434
DELONGCHAMP, R R	165
DENNE, D R	282
DENTON, M B	527
DEPUY, C H	78
DEROOS, F L	679
DEROOS, F L	681
DERRICK, P J	761
DERRICK, P J	13
DERRICK, P J	635
DERRICK, P J	263
DERYCKE, G	873
DESIDERIO, D M	264
DEVANT, G	807
DEVANT, G	125
DEVANT, G	603
DIEHL, J W	818
DIGIUSEPPE, T G	623
DJERASSI, C	143
DOBBERSTEIN, P	320
DONCHI, K F	761
DONNELLY, J P	655
DORBON, M	873
DORN, S B	633
DOUGHERTY, R C	197
DOUGLAS, D J	533
DREIFUSS, P A	784
DUBAY, G R	112
DUCHAMP, D J	788
DUGGER, D L	341
DUGGER, D L	343
DUHOLKE, W K	153
DUIGNAN, M	623
DUNLAP, B I	251
DURANT, J	622
DURANT, J	573
DURFEE, S L	268
DYER, E W	717
DZIEDZIC, P J	599
EATON, D	185
EBY, R E	399
ECKERS, C	612
ECKERS, C	610
EDMONDS, C G	606
EDWARDS, A K	617
EICHELBERGER, J W	655
EIDE, S J	740
EINOLF, W N	131
EISEMAN, J L	226
ELLIOTT, R M	480
EMEL, W A	434
ENDELE, R	45
ENKE, C G	758
ENKE, C G	5
ENKE, C G	753
ENKE, C G	841
ENKE, C G	812
ENKE, C G	845
ENS, W	229
ENS, W	316
ESMANS, E L	608
ESMANS, E L	149
EVANS, F E	242
EYLER, J R	77
EYLER, J R	847
FAHEY, D	74
FARDEN, J	656
FARNCOMBE, M J	750
FARR, F L	220
FARR, F L	335
FARR, F L	7
FAULL, K F	789
FAULL, K F	464
FAVIER, A	419
FEHSENFELD, F	74
FENG, T M	525
FENNESEY, P V	831
FENNESEY, P V	865
FENNESEY, P V	419
FENSELAU, C	556
FENSELAU, C	560
FENSELAU, C C	139
FENSELAU, C C	228
FENSELAU, C	175
FERGUSON, E E	74
FERGUSON, E E	200
FERGUSON, M D	74
FERGUSON, R K	159
FIELD, F H	538
FIELD, F H	177
FILBY, E E	434
FINNEY, R W	466
FJELDSTED, J	84
FLEMING, R H	863

AUTHOR	PAGE
FLEMING, R H	55
FORRESTER, A T	546
FOSTER, N G	129
FRAISSE, D	151
FRAISSE, D J	673
FRANCL, T J	493
FRANK, D J	441
FREEMAN, J P	242
FREES, L C	656
FREISER, B S	416
FREISER, B S	704
FRIEDLANDER, S K	352
FRIEDMAN, L	644
FRIESEN, R D	843
FRIESEN, R D	442
FUJII, T	9
FUJII, T	751
FUKUDA, E K	68
FUKUI, M	102
FUKUSHIMA, S	198
FULFORD, J E	791
FULTON, K H	839
FUNG, D	696
FUTRELL, J H	205
FUTRELL, J H	495
FUTRELL, J H	506
FUTRELL, J H	773
GALE, P J	386
GALE, P J	552
GALE, P J	523
GALLAHER, K L	869
GALLEGOS, E J	766
GALLEGOS, E J	770
GALLEGOS, E J	678
GAMO, M	736
GANGULY, A K	147
GARNER, E L	440
GARRETT, J H	816
GASKELL, S J	310
GAUMANN, T	412
GELFAND, M J	173
GELIJKENS, C F	742
GELLENE, G I	72
GEOFFROY, G L	321
GHADERI, S	407
GHADERI, S	414
GHADERI, S	280
GIANCASPRO, C	409
GIANG, B Y	294
GIBSON, B W	232
GIESSMANN, U	545
GILLS, T E	440
GILMAN, J P	751
GILMARTIN, D E	354
GIRIJAVALLABHAN, V	147
GISS, G N	410
GLISH, G L	691
GOEBEL, D M	546
GOLDBERG, N D	740
GOLDENBERG, M	96
GOODBLATT, R S	172
GOODLEY, P C	82
GOODLEY, P C	145
GOODMAN, G L	617
GOODMAN, G L	700
GOODMAN, G L	504
GOTO, J	236
GRABOWSKI, J J	78
GRAVEN, W M	354
GRAY, A L	447
GRAYSON, M A	1
GREAVES, J	227
GREEN, B N	286
GREEN, B N	516
GREEN, B N	310
GREENE, F T	347
GREENHALGH, R	851
GREENWOOD, G	771
GREGG, H R	841
GREGOR, I K	141
GRIFFITH, R S	282
GRIFFITHS, I W	620
GRINDSTAFF, G G	774
GRIZZLE, P L	774
GROENEWOLD, G S	258
GROSS, M L	323
GROSS, M L	414
GROSS, M L	628
GROSS, M L	258
GROSS, M L	511
GROSS, M L	810
GROSS, M	506
GUFFEY, F D	770
GUFFEY, F D	762
GUIEZE,	807
GUILHAUS, M	141
GULACAR, F O	671
GUO, C J	837
HABFAST, K	334
HABFAST, K	345
HACHEY, D L	383
HADDON, W F	515
HALL, E	541
HALLSTROM, G	367
HAMBIDGE, K M	419
HAMBURGEN, W R	82
HANNA, A	280
HANSEN, G	556
HANSEN, G	560
HANSEN, G E	393
HARA, K	371
HARADA, K I	302
HARADA, K I	314
HARAGUCHI, K	30
HARDIN, E D	570
HARDY, M	125
HARPER, A M	687
HARPER, A M	773
HARPER, A M	689
HARPER, J C	863
HARPER, T	127
HARRINGTON, W L	386
HARRINGTON, W L	552
HARRIS, F M	14

AUTHOR	PAGE
HARRIS, F M	620
HARRIS, F M	501
HARRIS, T H	220
HARRIS, T R	218
HARRISON, A G	260
HARRISON, W W	625
HARRISON, W W	472
HARRISON, W W	473
HARTMAN, H	92
HARVEY, D J	780
HARVEY, D J	28
HARVEY, T M	800
HASHIMOTO, K	859
HASHIMOTO, Y	171
HASHIMOTO, Y	675
HASS, J R	802
HATCH, F	157
HAWTHORNE, S B	653
HAYASHI, A	824
HAYASHI, A	41
HAYASHI, T	378
HAYASHI, T	462
HAYES, M J	616
HEBEDA, E H	589
HECK, H A	32
HECK, H A	850
HEIN, R E	407
HEIN, R	280
HELLER, D	556
HELLER, D	560
HELLER, S R	833
HEMLING, M E	564
HENDERSON, T R	814
HENION, J D	792
HENION, J D	610
HENION, J D	612
HEPPNER, R A	762
HEPPNER, R A	3
HERBERT, C G	501
HERMAN, G	636
HERMAN, J A	491
HERTZ, H S	597
HERTZ, H S	861
HEUBI, J E	173
HIDY, B J	461
HIGA, S	41
HIGUCHI, T	236
HIGUCHI, T	819
HILDENBRAND, D L	444
HILL, G R	689
HILPERT, L R	861
HINTON, M L	226
HIRAI, M	453
HIRANO, Y	143
HIRATA, Y	601
HITES, R A	188
HO, B	106
HOD, M	183
HOFFMAN, P A	841
HOGG, A M	543
HOHN, M	320
HOLKEBOER, D H	656
HOLLAND, J F	871
HOLLAND, J F	5
HOLLAND, J F	227
HOLLAND, J F	715
HOLLER, J S	187
HOLLER, J S	360
HOLLER, J S	36
HOLMES, R A	630
HOPSON, W	9
HORNING, E C	466
HORNING, E C	288
HORNING, E C	522
HOUK, R S	605
HOUK, R S	421
HOURIET, R	412
HOWORKA, F	495
HOYT, R F	630
HSU, S T	198
HUANG, S K	64
HUDGENS, J W	623
HUDSON, C E	137
HUGHES, H	466
HUGHES, S M	650
HUNT, D F	800
HUNT, D F	49
HUNT, D F	566
HUNTER, R L	93
HUNTRESS, W T	67
HUNTRESS, W T	455
HUNTRESS, W T	490
HURST, H E	369
HUTTE, R S	653
ICHIKAWA, H	260
ICHIMURA, K	161
ICHIMURA, K	274
IGARASHI, K	102
IGNIATIADIS, I	873
IIDA, Y	462
IKEDA, T	786
IKEKAWA, N	786
IKENISHI, Y	746
IKUTA, S	204
IKUTA, S	500
INMAN, R C	104
INQUE, M	417
IRIBARNE, J V	599
IRIE, T	171
IRVING, C S	383
ISHIBASHI, M	171
ISHIBASHI, M	675
ISHII, D	120
ITAGAKI, Y	236
ITAKURA, Y	298
JACOBS, D	619
JACOBSON, D B	704
JAMIESON, W D	627
JAMIESON, W D	713
JAMIESON, W D	717
JARDINE, I	238
JARROLD, M F	71
JAYASIMHULU, K	724
JAYASIMHULU, K	726

AUTHOR	PAGE
JENNINGS, K R	750
JOHN, G A	55
JOHNSON, L P	40
JOHNSTON, M	678
JONCKHEERE, J A	38
JONKMAN, H T	212
JOST, B	569
JUDSON, C M	332
KADLUBAR, F F	242
KAGEURA, M	365
KALEY, R G	794
KALHAN, S C	382
KALMAN, D	185
KAMBARA, H	314
KAMINSKY, R	188
KANAZAWA, K	90
KANMEI, Y	550
KANNO, M	453
KARGER, B L	616
KASHIMOTO, T	198
KASUYA, F	102
KATO, E	451
KATO, K	274
KATO, K	161
KATO, T	18
KAUFMANN, H	348
KAWAGUCHI, A	373
KAY, R	541
KEBARLE, P	204
KEBARLE, P	500
KEBARLE, P	76
KEECH, J R	493
KEEFE, R B	473
KEESEE, R G	209
KELLER, W C	104
KELLERHALS, H	404
KELLEY, W R	477
KEMP, T R	246
KEMPER, P R	71
KENNISH, J M	100
KENYON, C N	145
KEOUGH, T	778
KERSHAW, P	515
KING, J D	709
KING, J D	684
KINSINGER, J	280
KIPLINGER, J	457
KIRBY, H	292
KIRLEW, P	197
KISHI, T	529
KISHIMOTO, Y	175
KISHIMOTO, Y	422
KISKER, D W	702
KLEIN, P D	383
KODAMA, H	822
KOGA, M	658
KOJIMA, H	108
KOJIMA, T	362
KOMORI, T	298
KONDO, T	41
KONISHI, H	676
KOONTZ, S L	527
KOPRIO, J	350
KORALEWSKI, C	222
KORFMACHER, W A	458
KORFMACHER, W A	165
KORNEL, A	724
KOTAKE, A N	178
KOYAMA, Y	835
KOYANO, I	18
KRAILLER, R E	622
KRICK, T P	740
KROGH, T E	592
KRONICK, M N	574
KRUEGER, F R	569
KUBODERA, T	284
KUBOTA, E	550
KUEN, I	495
KUHARA, T	828
KUHARA, T	306
KUHARA, T	308
KUMAR, R	238
KUNIHIRO, F	550
KUNITA, N	198
KUROKI, H	30
KUTINA, R E	617
KUTINA, R E	504
LABROSSE, J	648
LAETER, J R	486
LAMBERT, G H	178
LAMBERT, W E	38
LANE, D C	669
LANKMAYR, E P	616
LAO, R C	664
LAPIDOT, A	183
LARAMEE, J A	808
LARSEN, D J	693
LARSEN, J W	691
LARSON, J W	257
LARSON, M	679
LARTER, S	773
LASER, B	345
LATTIMER, R P	631
LATTIMER, R P	393
LATVEN, R K	753
LAU, K H	444
LAU, P Y	196
LAU, Y K	204
LAUBER, R	135
LAY, J O	258
LEDFORD, E B	628
LEDFORD, E B	326
LEHMAN, J P	110
LESLIE, J	364
LETHAM, D S	40
LEUSCHNER, J T	28
LEVANDER, O A	377
LEVIN, F	460
LEVINS, P L	693
LEWIS, E	713
LEWIS, I A	246
LI, Z M	798
LIEHR, J G	234
LIFSHITZ, C	96

AUTHOR	PAGE
LIGON, W V	633
LIN, S N	830
LIN, Y Y	819
LINDINGER, W	495
LIOTTA, R	691
LITTLE, J A	360
LIU, S Y	854
LO, H H	115
LOCKWOOD, J	664
LOMBARSKI, M	64
LOOK, D C	475
LOPEZ-AVILA, V	664
LOSS, R D	486
LOWE, L E	857
LOWENTHAL, A	149
LOYAUX,	807
LUBMAN, D M	330
LUBMAN, D M	574
LUYTEN, Y	608
MACFARLANE, R D	576
MACFARLANE, R D	619
MACLEOD, J K	40
MAEDA, K	826
MAEDA, K	304
MAEDA, K	835
MAETANI, I	298
MAGEE, C W	577
MAGEE, C W	386
MAGEE, C W	523
MAGEE, C W	552
MAGGIO, J	392
MAGIN, D F	131
MAGNERA, F	204
MAGNERA, T F	76
MAHONEY, J F	51
MAHONEY, J F	546
MAKLAE, G	341
MALBICA, J O	169
MALINOVICH, Y	96
MAMER, O A	832
MAOLYNEUX, R J	515
MAQUIN, F	673
MARASCO, J	49
MARASCO, J	566
MARESCAU, B	149
MARK, T D	205
MARKEY, S P	866
MARRA, J	280
MARRA, J	407
MARTIN, J	464
MARTIN, S A	567
MARTIN, S A	243
MARTINSEN, D P	833
MASADA, Y	859
MASON, F G	717
MASON, R S	750
MASSEL, R	682
MASUDA, Y	30
MATE, U	744
MATSUDA, H	640
MATSUDA, I	378
MATSUMOTO, I	819
MATSUMOTO, I	828
MATSUMOTO, I	306
MATSUMOTO, I	308
MATSUMOTO, K	601
MATSUO, M	828
MATSUOKA, K	120
MATSUOKA, S	80
MATSUSHIMA, H	662
MATTOX, V R	238
MAUTNER, M	503
MAYLIN, G A	610
MCADOO, D J	137
MCBAY, E H	691
MCCLENNEN, W H	689
MCCLOSKEY, J A	34
MCCLOSKEY, J A	606
MCCLOSKEY, J A	742
MCCRAE, C E	635
MCCRERY, D A	628
MCELVANY, S	848
MCELVANY, S	64
MCEWAN, M J	490
MCEWEN, C N	757
MCEWEN, C N	554
MCFARLAND, M B	753
MCGUIRE, J M	669
MCGUIRE, J M	616
MCIVER, R T	68
MCIVER, R T	93
MCIVER, R T	493
MCLAFFERTY, F W	777
MCLAFFERTY, F W	804
MCLAFFERTY, F W	837
MCLAURIN, A E	622
MCLOUGHLIN, R G	24
MCLUCKEY, S A	255
MCLUCKEY, S A	507
MCMAHON, T B	257
MEISELMAN, S	597
MEISELS, G G	751
MEISELS, G G	9
MEOT-NER, M	488
MESSIERI, F	682
METCALF, G S	687
METCALF, G S	689
METORI, K	734
METRAL, C J	724
METRAL, C J	726
MEUZELAAR, H L	773
MEUZELAAR, H L	687
MEUZELAAR, H L	689
MICHELSEN, H	348
MICHL, J	212
MICHL, J	695
MIHAMA, K	445
MILLEN, W G	300
MILLER, C M	470
MILLER, D J	818
MILLER, D L	511
MILLER, J	832
MILNE, T A	698
MILNE, W A	833

AUTHOR INDEX

AUTHOR	PAGE
MINARD, R D	854
MINARD, R D	321
MINEO, S	734
MINSKER, D H	167
MINTZ, D M	296
MITCHUM, R K	242
MITCHUM, R K	458
MITCHUM, R K	165
MITROSKY, S	650
MIYATA, H	198
MIYAZAKI, H	171
MIYAZAKI, H	675
MIZUTANI, T	181
MOCHIKI, A	859
MOLDOWAN, J M	770
MOLER, G F	165
MONCUR, J G	122
MONCUR, J G	356
MONSON, K R	169
MONTGOMERY, J A	832
MOORE, L E	282
MOORE, L E	240
MOORE, L E	358
MOORE, L E	518
MOORE, L J	440
MOORE, S E	268
MORAN, B W	437
MORITA, M	824
MORRISON, J D	24
MORTON, T H	249
MORTON, T H	456
MOSER, A B	175
MOSER, H W	175
MOYNIHAN, C	831
MUKHTAR, E S	620
MUN, I K	837
MUNSON, B	805
MUNSON, B	525
MURPHY, R C	127
MURPHY, R C	390
MUSSELMAN, B D	715
MYERHOLTZ, C A	812
MYERHOLTZ, C A	845
NAGASAKI, M	453
NAGASE, K	491
NAGATA, T	365
NAITO, M	550
NAITO, Y	550
NAITO, Y	236
NAKAGAWA, Y	746
NAKAJIMA, Y	260
NAKAMURA, H	80
NAKAMURA, K	222
NAKATA, H	676
NAKATA, H	509
NAMBARA, T	236
NARABAYASHI, H	41
NARUSE, H	378
NARUSE, H	462
NAYAR, M S	364
NEILSON, K L	169
NELSON, R A	426
NEMER, M J	316
NEUMANN, G M	263
NEWSOME, W H	196
NEWTON, J C	442
NEWTON, J C	843
NGO, A	851
NIELSEN, J W	247
NISHI, I	216
NISHIMOTO, K	133
NISHIMURA, H	397
NISHIOKA, M G	681
NISHIOKA, M G	461
NIWA, T	826
NIWA, T	304
NODA, T	445
NODA, T	531
NOGAR, N S	470
NOJIMA, K	819
NONAKA, T	536
NORMAN, E J	174
NORMAN, E J	173
NORWOOD, K C	693
NOSE, O	822
NOWLIN, J G	522
NOWLIN, J G	288
NOWLIN, J	466
NOZAKI, Y	274
NOZAKI, Y	161
NOZIMA, K	675
NUMATA, M	734
O'DONNELL, J E	347
OATES, J A	460
OCCOLOWITZ, J L	562
OHASHI, M	155
OHASHI, M	266
OHI, G	198
OHKI, T	304
OHKI, T	826
OHTA, K	601
OHTA, K	304
OKADA, S	822
OKANO, H	531
OKANO, J	397
OKUDA, S	373
OKUTANI, T	531
OLDHAM, R G	833
OLIVARES, J A	605
OLSON, E S	818
OLSON, K L	564
ORTH, R G	695
ORTH, R G	212
OSMOND, C B	424
OTSUKA, H	373
OVADIA, Y	183
PALLANTE, S L	175
PANCIROV, R J	769
PANG, H	606
PARKER, C W	40
PARR, A C	25
PATON, W D	28
PATTERSON, D G	36
PAULIN, P A	630

AUTHOR	PAGE
PAULSEN, P J	477
PAUSCH, J B	393
PEDLEY, M	248
PEGUES, R F	777
PERCHALSKI, R J	224
PEREL, J	51
PEREL, J	546
PERES, M	96
PERRIN, R E	441
PESCH, R	320
PESCH, R	348
PETERSON, B A	681
PETERSON, B A	461
PETERSON, D W	837
PIKE, A W	831
PIKE, A	865
PINKSTON, J D	871
PINKSTON, J D	5
PINOLI, P C	356
PLATTNER, R D	520
POMPLIANO, D L	473
POPE, D L	687
PORTER, R F	72
POWELL, M L	163
PRAKASH, O	147
PRAMANIK, B N	147
PROCTOR, B L	855
PROCTOR, B L	190
PROCTOR, C J	804
PROCTOR, C J	501
PROCTOR, C J	777
PRZYBYLSKI, M	262
QUAN, E S	533
RABRENOVIC, M	501
RACHE, H	334
RADECKI, B	64
RAINEY, W T	691
RAMALEY, L	627
RAMANA, D V	62
RANKIN, P C	339
RANKIN, R A	434
RANKIN, R A	328
RAPP, U	320
RAPP, U	348
RAYNAUD, J	151
REAMER, D C	377
REINHOLD, V N	728
REINHOLD, V N	730
REINHOLD, V N	270
REINHOLD, V N	276
REISNER, S R	183
REMPEL, D	326
RHODES, W H	343
RICHIE, K L	861
RICHTER, W J	796
RIDER, D M	622
RIDER, D M	573
RIDER, D M	625
RIDGE, D P	253
RINEHART, K L	564
ROACH, D	242
ROBBINS, R C	129
ROBERTSON, R T	167
ROBOZ, J	227
RODGERS, G C	369
RODRIGUEZ, L J	830
ROGERS, J D	159
ROGERS, L	426
ROITMAN, E	312
ROKOP, D J	441
ROLLER, P P	745
ROSELIUS, H	350
ROSENSTOCK, H M	25
ROSMAN, K J	486
ROSS, M M	325
RUDAT, M A	868
RUDAT, M A	548
RUDEWICZ, P	525
RUMPF, B A	761
RUOCCO, J J	268
RUSCIC, B M	700
RUSSELL, D H	622
RUSSELL, D H	248
RUSSELL, J W	839
RYAN, P A	358
RYAN, P A	518
RYAN, P W	838
RYAN, P W	858
SAITO, A	304
SAITO, K	736
SAITO, K	161
SAITO, K	274
SAITO, Y	445
SAKAMOTO, K	298
SAKODA, S	41
SAKURAI, H	509
SAKURAI, N	662
SAMUKAWA, K	822
SANDERS, R A	278
SANTIKARN, S	392
SATHO, N	859
SATKIEWICZ, F G	395
SATOUCHI, K	736
SAUTER, A D	664
SAVICKAS, P J	472
SCANLAN, G F	238
SCHEPPELE, S E	774
SCHLUNEGGER, U P	135
SCHMITTER, J M	873
SCHMITZ, M C	32
SCHOELLER, D A	178
SCHOELLER, D A	222
SCHOENGOLD, D M	711
SCHRAM, K H	782
SCHRAM, K H	738
SCHRAM, K H	272
SCHROEDER, D H	226
SCHUCH, D	92
SCHUELER, B	569
SECOR, H	131
SEGAL, A	744
SEIFERT, W K	770
SENN, M	45
SENSHARMA, D K	76

AUTHOR	PAGE
SERUM, J W	837
SEYAMA, Y	373
SHABANOWTIZ, J	800
SHABONOWITZ, J	523
SHACKLETON, C H	312
SHADOFF, L A	95
SHARP, T E	122
SHIBATA, M	826
SHIMADZE, K	284
SHIMIZU, K	180
SHINKA, T	819
SHINKA, T	306
SHINKA, T	828
SHINOHARA, R	658
SHIOKAWA, T	451
SHIRATSUCHI, K	284
SHIZUKUISHI, K	859
SHIZUKUISHI, S	732
SHRADER, S	707
SHUSHAN, B I	791
SIECK, L W	488
SIECK, L W	503
SIEGEL, M W	88
SIEGEL, M W	115
SIEVERS, R E	653
SILIDES, D	227
SIMONS, D S	482
SINHA, M P	352
SKOTNICKI, P	636
SKRABALAK, D	612
SLAYBACK, J	292
SLAYBACK, J R	678
SLAYBACK, J R	520
SLIVON, L E	719
SLOWIKOWSKI, D	738
SMITH, C F	442
SMITH, C F	843
SMITH, C L	484
SMITH, C	447
SMITH, D C	516
SMITH, D H	392
SMITH, D H	432
SMITH, D L	24
SMITH, D L	742
SMITH, J H	863
SMITH, K D	830
SMITH, L A	231
SMITH, R D	11
SMITH, R D	84
SMITH, R G	533
SOKOLOW, S	292
SOLCH, J G	816
SOLOMON, J J	744
SOLSTEN, R T	272
SOLTYS, M N	698
SPARROW, G R	401
SPENCER, R B	407
SPERLING, M A	173
SPHON, J A	784
STAEDELI, W	837
STAFFORD, G C	539
STAGE, A	419
STANDING, K G	229
STANDING, K G	316
STAUFFER, D B	837
STAUFFER, J L	693
STEINAUER, R	135
STEINBERGER, E	830
STEINER, U	292
STEPHAN, K	205
STEVENSON, D A	702
STILLWELL, R N	288
STILLWELL, R N	522
STOFFELS, J J	329
STOGNIEW, M	364
STORMS, E	449
STORY, M	345
STOUT, S J	192
STRADLING, R S	686
STRADLING, R S	240
STRADLING, R S	282
STRAUB, K	47
STRAUB, K	312
STUBBLEFIELD, R D	520
STULIK, D	695
STULIK, D	212
STULTS, J T	5
SUMIDA, Y	859
SUMMONS, R E	424
SUN, J D	814
SUN, T	852
SUN, W F	513
SUNDARAMAN, P	678
SUZUKI, E	378
SUZUKI, M	314
SUZUKI, M	302
SUZUKI, M	676
SUZUKI, R	227
SUZUKI, T	41
SWANSON, C A	377
SWEELEY, C C	871
SWEETMAN, B J	460
SYLVESTRE, M	682
TABET, J C	151
TABOR, J E	679
TAGUCHI, S	298
TAIRA, T	536
TAJIMA, K	181
TAKAGI, T	529
TAKAHASHI, R	378
TAKATSUTO, S	786
TAKEDA, N	302
TAKEDA, N	676
TAKEDA, T	284
TAKEUCHI, T	120
TAKEUCHI, T	133
TAMURA, H	531
TAMURA, T	80
TANAKA, K	18
TANG, S Y	197
TANG, S Y	198
TANNENBAUM, S R	427
TANNER, S D	851
TASHIMA, T	859

AUTHOR	PAGE
TATEMATSU, A	676
TATEMATSU, A	302
TATEMATSU, A	314
TATEMATSU, A	509
TATSUTA, L	216
TAYLOR, K T	358
TAYLOR, K T	518
TAYLOR, L C	240
TAYLOR, M L	816
TAZAWA, T	835
TECON, P	143
TEECE, R G	738
TERWILLIGER, D T	705
THOMAS, R S	664
THOMPSON, J A	106
THOMPSON, J J	421
THOMPSON, T A	172
THOMSON, B A	792
THOMSON, B A	599
THOMSON, B A	791
THOMSON, M L	300
THORNE, L R	455
TIERNAN, T O	816
TIERNAN, T O	475
TIERNAN, T O	498
TODD, P J	748
TOMER, K B	323
TOMER, K R	506
TOMIYASU, I	429
TOMIYASU, I	732
TOMIZAWA, G	216
TORIYAMA, S	429
TOU, J C	759
TOU, J	86
TRUSSEL, A R	660
TSANG, R C	173
TSAO, R	268
TSARBOPOLOUS, A	64
TSERNG, K Y	382
TSUCHIYA, M	536
TSUGE, S	601
TSUGITA, A	262
TSUJIMOTO, K	266
TUNG, T C	198
TURECEK, F	777
TURNER, P J	447
TURNER, P J	478
TURNER, P J	541
TWAY, P C	194
UDSETH, H	11
UETRECHT, J	460
UNE, I	362
UPCHURCH, B T	630
VAN BREEMEN, R B	228
VAN DEN BROEK, R	262
VAN DUUREN, B L	744
VAN HOVE, C	722
VAN KOPPEN, P	71
VAN LANGENHOVE, A	243
VAN LANGENHOVE, A	558
VANBREEMEN, R B	571
VANDENHEUVEL, W J	159
VANDENHEUVEL, W J	167
VANNESS, G F	816
VAUGHAN, M A	627
VEILLON, C	377
VESTAL, M L	59
VESTAL, M L	118
VESTAL, M L	570
VESTAL, M L	117
VESTAL, M L	606
VILLENGER, H	495
VOLK, J	172
VOORHEES, K J	268
VOUROS, P	616
VOYKSNER, R D	802
VRBANAC, J	871
WAGNER, D A	427
WAKEFIELD, C J	240
WAKEFIELD, C J	282
WALKER, R L	432
WALKER, R W	167
WALLACE, W D	7
WALLS, F	47
WALSETH, T F	740
WALTERS, D C	475
WANCZEK, K P	404
WARBURTON, G A	358
WARBURTON, G A	518
WARMACK, R J	748
WATANABE, H	531
WATSON, J T	5
WATSON, M	460
WEBB, G W	434
WEBB, H M	248
WEBER, J H	762
WEBER, M	334
WEDDLE, G	253
WEE, E L	174
WEIL, M	227
WEINGARTEN, H I	794
WEISBERGER, M	163
WESTMORE, J B	696
WESTMORE, J B	229
WESTMORE, J B	316
WESTON, A F	636
WESTOVER, L	871
WHITE, E L	850
WHITE, E L	32
WHITE, E	597
WHITE, R L	410
WILDNER, E L	630
WILKINS, C L	410
WILKINS, C L	414
WILKINSON, J E	858
WILLIAMS, D H	392
WILLIAMS, E J	653
WILLIAMS, I S	593
WILLIAMS, P	53
WILSON, B W	810
WINKLER, F J	671
WISHNOK, J S	427
WOLF, C J	1
WOLFE, M H	426

AUTHOR	PAGE
WOLFE, R R	426
WONG, C M	776
WONG, C M	841
WOO, K C	424
WOOD, G M	630
WOOD, G W	62
WOOD, K V	798
WRIGHT, B	480
WRONKA, J	253
WU, R L	498
WYATT, J R	623
WYATT, J R	251
YABUUCHI, E	422
YABUUCHI, H	822
YAGI, K	531
YALOW, R S	804
YAMAKAWA, T	373
YAMAMOTO, K	181
YAMAMOTO, M	133
YAMAMOTO, S	198
YAMANAKA, N	304
YAMASHITA, K	171
YAMAUCHI, E	675
YAMAUCHI, K	445
YAMAWAKI, M	453
YANG, S K	745
YANO, I	422
YANO, I	429
YANO, I	732
YASHIKI, M	362
YELLE, L	139
YELTON, R D	665
YELTON, R D	667
YERGEY, A L	118
YERGEY, A L	383
YERGEY, J	556
YERGEY, J	560
YERT, L W	187
YINON, J	614
YOSHIDA, H	601
YOSHIDA, T	108
YOST, R A	224
YOST, R A	776
YOUNG, S E	534
YOUNG, S E	43
YU, K D	104
ZAKETT, D	759
ZAKETT, D	95
ZAKETT, D	86
ZARE, R N	330
ZARE, R N	622
ZARE, R N	573
ZARE, R N	625
ZARETSKII, Z V	135
ZIMMERMAN, E F	174
ZINGG, D S	124
ZOUTENDAM, P H	153
ZUMBERGE, J E	686

Business Meeting of the
American Society for Mass Spectrometry

Wednesday, June 9, 1982, 5:30 P.M.

President Munson introduced Henry Fales as the Parliamentarian for the business meeting to the approximately 90 assembled members of the Society. He then asked for corrections to the Minutes of the previous year which were then approved as published in the "Abstracts of the 29th Annual Conference on Mass Spectrometry and Allied Topics."

The Secretary then introduced the recipients of the travel fellowships. He then exhibited the election results and introduced the successful candidates.

Vice President for Programs	R. Graham Cooks	316
	Mike Gross	233
Treasurer	Jim DeCorpo	262
	Floie Vane	242
Member-At-Large	Fred Abramson	229
	Marvin Vestal	307

Brief mention was made of the deaths of three members and the Secretary requested those assembled to inform him if they were aware of any other losses.

President Munson then expressed the Society's appreciation of the efforts of the departing Board Members. Vice President for Programs Fenselau presented President Munson and Past President McCloskey with tokens of the Society's appreciation of their efforts.

Treasurer Frisch then gave the financial picture of the Society. The balance on hand as of May 28, 1982 was $116,408.20. In light of the lower registration and projected Conference deficits, the Treasurer advised that the registration fees would probably be increased for the 1983 Conference.

Vice President for Programs Fenselau presented a review of the Honolulu program, noting that over 530 abstracts had been submitted. She then presented the demographic distribution of authors, noting that the Conference truly had increased Japanese, Australian and New Zealand contributions.

Munson then thanked several Corporate Members for making extraordinary one-time financial contributions for the success of the Conference. The Corporate Members acknowledged were:

Colorado Group (In Memory of Glenn Kerfoot)
Extranuclear Laboratories
Hewlett-Packard
Kratos Scientific Instruments
Nicolet Instruments
Phrasor Scientific
Scientific Glass Engineering
Sciex

Vice President for Arrangements Compson then discussed future meeting sites. The schedule is as follows: Boston, MA, May 8-13, 1983; San Antonio, TX, 1984; San Diego, CA, 1985; East Coast, 1986. Compson announced that negotiations are underway with both Cincinatti and Pittsburgh for 1986. Compson asked for a straw

vote of the attendees concerning a mid-week social affair in Boston. Nothing had been planned for Honolulu due to variety of activities available. The clear concensus of those attending was that a formal social event was desirable. Compson solicited suggestions from the membership for possible 1987 meeting sites.

Member-At-Large Fred Lampe then discussed the Conference Abstracts which will again be produced with the aid of Judith Watson (ASMS Staff) and ASTM's publishing facilities. Lampe urged that all authors citing work in the Conference Abstracts conform to the citation notice printed in the Conference Abstracts.

Munson praised the technical success of the FAB Workshop held in Baltimore and discussed the new workshop "Theory and Applications of Multiple Analyzer Mass Spectrometers" proposed for Fall, 1982. He then acknowledged the efforts of the Nomenclature Committee and urged authors to conform to their recommendations.

Munson then introduced Judith Watson (PAM) to the attendees. One of the Society Office's functions is to act as a clearing house for employment. Prospective employees can obtain a list of available openings by contacting the Society Office, resumes will not be circulated.

The meeting was adjourned at 6:31 P.M.

T. R. Ashe

ASTM E-14 1982 BUSINESS MEETING MINUTES SUMMARY

The Business Meeting of ASTM Committee E-14 on Mass Spectrometry was held on June 8, 1982 in Honolulu, Hawaii, It was attended by 18 individuals representing industrial, government and academic interests. The meeting was opened by Chairman, Thomas Aczel, who introduced the current officers.

Chairman:	Thomas Aczel, Exxon Res. and Eng. Co., Box 4255, Baytown, TX 77520
Vice Chairman:	P.C. Price, Union Carbide Corp., Bldg. 770-120, Box 8361, S. Charleston, WV 25303
Secretary-Treasurer:	B.N. Colby, S-CUBED, Box 1620, La Jolla, CA 92038

Minutes of the previous meeting were presented by B.N. Colby and approved.

A letter prepared by Louise Neall, the ASTM Staff Manager who was unable to attend, was read. It described the current status of standards and ballot results:

Revision of E 304-68 (1975)	Approved September, 1981
Revision of E 137-68 (1975)	Ballot in progress
82-1 Concurrent E14/E14.14	Issued April, 1982

Current membership totals 56 including 3 affiliates and reflecting 7 resignations and 8 new members since May, 1981. E-14 Financial Report indicates a balance as of January 1, 1982 of $3,903.19.

A discussion of an Affiliate Member status took place. It was decided to limit this membership status to the current and elect ASMS Presidents and to invite the past ASMS Presidents to join ASTM E-14 as regular voting members.

Subcommittee Reports were then heard.

M.C. Hamming, Chairman of Subcommittee E14.04 on Data and Information Problems, suggested the possibility of tabulating ASMS papers by analytical subject.

D. Cameron, Chairman of Subcommittee E14.10 on Definitions and Terms, provided a list of definitions to be discussed jointly with the corresponding ASMS Committee. ASTM, ASMS and IUPAC have been working together in this area. The effort is behind the anticipated schedule, but is progressing.

T.J. DeStefano (for P.C. Price), Chairman of Subcommittee E14.14 on General Practices, reviewed the status of balloting. Included were results indicating that E137-68(1975) had been approved.

D. Cameron, Chairman of Subcommittee E14.15 on New Instrumentation and Techniques, described his efforts in working with ASMS to establish standards for acquiring MS-MS spectra. This effort includes participation in an ASMS workshop later in the week.

T. Aczel, Chairman of Subcommittee E14.91, Liaison, gave a brief update on the activity of Committee D-2 where oil shale methods are being worked on. He also described the symposium on the "Characterization of Shale Oils" being jointly sponsored by ASTM and ASMS to be held later this week.

B.N. Colby, Chairman of Subcommittee E14.93, on Long Range Planning, indicated that he planned to go through the survey results provided by M.C. Hamming, in an attempt to establish a better prospective of E-14 members and their activities. M.C. Hamming described the survey which he was responsible for carrying out.

J.F. Litton, Chairman of Subcommittee E14.13 on GC/MS was unable to attend the meeting but had indicated that review of the GC/MS practice in preparation continues.

No new business was discussed and the meeting was adjourned.

An informal Executive Committee Meeting was held by the Officers of the Business Meeting. They discussed the above and other related topics.

Respectfully Submitted,

Bruce N. Colby

Bruce N. Colby
Secretary-Treasurer

PROCEEDINGS OF ASTM COMMITTEE D-2,

RESEARCH DIVISION IV, SECTION M

The annual meeting of ASTM D-2, Research Division IV, Section M on mass spectrometry was held at 5 p.m. June 7, 1982 in Honolulu, Hawaii. Thomas Aczel presided. Twenty-one people attended the meeting (Table I).

The meeting was opened by T. Aczel, who presented the following agenda:

1. Revision of Existing D-2 Methods on MS (T. Aczel, T. R. Ashe).
2. Report of Shale Oil Task Group (G. Greenwood)
3. Report of Saturates Analysis Task Force (G. Greenwood)
4. New Business

Notes were taken by T. R. Ashe, who acted as temporary secretary.

1. Revision of Existing Methods (T. Ashe, T. Aczel)

A list of currently used methods is given in Table II. T. Ashe pointed out that most of these were written in the late 1950's, early 1960's aaand contain references to obsolescent instruments or instrument parts. A poll of the audience revealed that essentially no one used methods ASTM D-1658, 2424, 2498, 2567, 2601 (see Table II) any more. It was voted unanimously that these methods be submitted to the general membership for balloting for cancellation. On the other hand, it was recognized that methods presently in use required some updating. It was decided to proceed in 1982-83 with methods ASTM D-2786 and D-2789. Mike Story of Finnigan will chair an "ad hoc" group to revise D-2786 with bold emphasis on suitability for other than CEC instruments, and involving all manufacturers of potentially suitable instrumentation. Frank Bockhoff of SOHIO will be in charge of revising D-2789. T. Aczel will arrange for the ballotting.

T. Aczel proposed that calibration matrixes that were obtained on CEC instruments be modified, if required, to be usable on new type instruments by regression analysis on widely variable petroleum streams.

2. Shale Oil Task Group (G. Greenwood)

Fifty-five gallons of Paraho shale oil were set apart by Gil Greenwood of Phillips for cooperative proposes. Simdis, C, H, N, O, S determinations are wanted yet on the total oil, and its IBP to 400 F to 1000 F cuts. Gil will carry out these tests, that will also cross-checked by volunteers (T. Aczel) T. Ashe, F. Bockhoff).

E. Gallegos of Chevron reported on the GC/MS analysis of the IBP to 400 F fraction (50 to 600 F in reality). Only 50% of the sample eluted; polymer formation was observed; components detected included numerous pyridines, phenols, sulfur compounds.

Gil Greenwood reported on Amoco's HRMS, LV analysis of the 400 F+ fraction, at 40,000 rp. Main types determined included 1 to 4 ring aromatics, mostly -16 to -22 types and aromatic thiophenes, mostly -10S and -16S. Total

aromatics and thiophenes amounted to 95.3 percent of the aromatics plus polars (saturates were not seen at low voltages); oxygen, disulfur and nitrogen compounds were present in only very minor amounts. The low nitrogen concentration, 0.2 percent, is particularly puzzling for a shale oil, and the possibility of a sample mix-up can not be excluded. A new sample will be thus sent both to Amoco and Exxon Research (T. Aczel) for reanalysis.

T. Aczel reported on the purity of acidic and basic fractions separated from eastern and western Colorado Shale Oils by Gil Greenwood. Up to 1000-1200 components were found in each of these by HRMS at LV, 50,000 rp., including oxygen, di-oxygen, nitrogen, di-nitrogen, nitrogen-oxygen, nitrogen-dioxygen, dinitrogen-oxygen compounds. A satisfactory separation was achieved between acidic and basic types. The acid fraction contained essentially all phenolics and only minor amounts of neutral nitrogen and nitrogen-oxygen compounds. The basic fraction contained most nitrogen and nitrogen-oxygen compounds, as well as the dinitrogen types; most of these appeared basic according to the carbon number distribution; only very minor amounts of oxygen compounds were found in this fraction. Neither fraction contained but trace aromatics hydrocarbons; condensation ranged from 1 to 8 rings; and up to 20 carbon atoms were in side chains with maxima at 3 to 4. Rick Heppner of LETC will titrate these fractions for basic N types. Detailed data can be obtained from T. Aczel or G. Greenwood.

A working group, including E. Gallegos and G. Greenwood, was established to work out a reliable separation method that is clearly essential before fractions can be analyzed by MS methods.

3. Saturates Analysis (G. Greenwood)

A generally good agreement was obtained from several laboratories. Mono-aromatics content, however, was too high; T. Ashe will check purity of fraction by UV; T. Aczel will reseparate, if required.

4. New Business

Stu Scheppele of DOE, Bartesville, raised the issue of reproducibility vs. accuracy in ASTM methods in general. Only the former can be established reliably; but all present agreed that accuracy is of paramount importance. Stu proposed an exchange of lists of available pure compounds for calibration; T. Aczel, T. Ashe, Ron Fleming and R. Heppner volunteered.

The meeting was adjourned by the chairman at 7 p.m.

TABLE I

D-2 ATTENDANCE, 6/7/82

Name	Affiliation/Address
Arthur Moore	Marathon Oil Company, Box 269, Littleton, CO 80160
Frank Guffey	LETC-DOE, P. O. Box 3395, Laramie, WY 82071
Stephen Shrader	Shrader Labs, 3450 Lovett, Detroit, MI 48210
Emilio Gallegos	Chevron Research Company, Richmond, CA
Paul C. Samson	UOP Inc., Des Plaines, IL 60016
Larry Rapp	ARCO, 400 E. Sibley Blvd., Harvey, IL 60426
Ron Fleming	SRI International, 333 Ravenswood (PS029), Menlo Park, CA 94025
B. M. Hughes	Monsanto Research Corporation, 1515 Nicholos Road, Dayton, OH 45459
Bob Sievers	Department of Chemistry, University of Colorado, Campus Box 215, Boulder, CO 80309
Frank M. Bockhoff	SOHIO Research Center, 4440 Warrensville Center Raod, Cleveland, OH 44128
Mike Story	Finnigan Corporation, 845 West Maude Avenue, Sunnyvale, CA 94086
Jurg Koprio	Balzers, Balzers Company, Liechtenstein
Quirinas Grindstaff	BETC, Bartlesville, OK 74003
Terry D. Marriott	Rice University of Chemistry, P. O. Box 1892, Houston, TX 77251
Richard Heppner	Laramie Energy Technology Center DOE, Box 3395 Union Station, Laramie, WY 82071
Curt Brunnee	Finnigan MAT, Barkhausenstr. 2, 2800 Bremen, Germany
Stuart Scheppele	Bartlesville Energy Technology Center, P. O. Box 1398, Bartlesville, OK 74003
T. R. Ashe	Exxon Research and Engineering Company, P. O. Box 121, Linden, NJ 07036
S. E. "Bud" Buttrill	SRI International, 333 Ravenswood, Menlo Park, CA 94025
Gil Greenwood	Phillips Petroleum, 150 Place, Bartlesville, OK 74003
Thomas Aczel	Exxon Research and Engineering Company, P. O. Box 4255, Baytown, TX 77520

LIST OF D-2 PROCEDURES RELATED TO

MASS SPECTROMETRY

Number			
D 1658	(23)	1980	• Carbon no. distribution of aromatics in naphthas; C_6 to C_9, HV, benzenes.
D 2424	(24)	1977	• Hydrocarbon types in propylene polymer; C_9 to C_{15}, -2, -4, -6, -8, HV.
D 2425	(24)	1978	• Hydrocarbon types in middle distillates; 400 to 650°F, 11 types, +2 through -18, HV.
D 2498	(24)	1978	• Isomer distribution of Detergent Alkylate Systems (based on 2567); C_{15}-C_{24} phenyl-n-alkanes, HV.
D 2567	(24)	1978	• Carbon no. distribution of Mono-alkylbenzenes in Detergent Alkylates; C_{13} to C_{42} aromatics, 99% plus aromatics: HV.
D 2601	(24)	1978	• Hydrocarbon types in propylene polymer by low ionizing voltage MS; C_9 to C_{18}, 0 to -6, LV.
D 2650	(24)	1978	• Chemical composition of gas mixtures; H_2, CO, CO_2, N_2, O_2, Ar, H_2S, C_1-C_2 mercaptans, C_1-C_6 hydrocarbons, HV.
D 2786	(24)	1976	• Hydrocarbon types in gas-oil saturates; +2 through -10, plus monoaromatics, C_{16}-C_{32}, HV.
D 2789	(24)	1976	• Hydrocarbon types in low olefinic gasoline; +2, 0, -2, -6, -8, -12 in naphthas up to 411°F, and less than 3% olefins, HV.
D 3239	(81)	1981	• Aromatic types in gas-oil aromatics 18 aromatics, 3 thiophenes, HV.

ASMS COMMITTEE REPORT - QUALITATIVE ORGANIC TECHNIQUES

WORKSHOP ON SPECIAL PROBLEMS IN CALIBRATION AND SAMPLE HANDLING FOR THE MASS RANGE 1500 TO 5000u.

The Workshop was held on Wednesday, June 9, from 3:00 to 4:45 PM.

Panel members for the discussion were J. Carter Cook (Univ. of Illinois), B. N. Green (V. G. Analytical, Ltd.), C. J. McNeal (Texas A. and M. Univ.), H. Matsuda (Osaka Univ.), H. R. Morris (Imperial College) and C. E. Costello, who served as the discussion leader.

The topics addressed by the panelists included the selection of reference compounds and the assignment of mass scale for the 1500 to 5000u region, the possibility of reduced detector response as higher mass ions are recorded, and sample handling techniques such as purification, derivatization and solubilization of large molecules. The question of accurate mass measurement at high mass evoked comments also from the audience, and there was, in fact, no consensus reached as to the necessity of even unit mass assignment in this mass region nor of the instrumental limitations on such measurements.

Reference compounds which had been found useful for nominal mass assignments included potassium iodide and/or cesium iodide and their clusters (FAB) and polystyrene (FD). Peak matching against known compounds has been used for both FAB and FD spectra, usually with the aid of a multichannel analyzer. Both Fomblin® oil and phosphazenes have been used to generate EI spectra which can be used to provide calibration for FAB or FD spectra using either a multichannel analyzer or photoplates, but, as yet, most of this work has been done below m/z 2000.

Although secondary electron multipliers have been used for detection of ions as high as m/z 25,000, it was difficult to assess relative molar responses for high mass compounds, because of uncertainties about ionization efficiencies and lifetimes, according to most panel members. Dr. McNeal did report results obtained in the laboratory of Bo Sundquist in Sweden which indicated that high accelerating fields had to be applied at the detector for recording high mass ions (e.g. 20 KV for m/z 6000). Prof. Morris illustrated the observation that, even for species of similar mass, sensitivity may be quite variable, by showing results in the range around m/z 5000 for the two chains of monellin, peptides of nearly equal weight but differing in amino acid composition and showing a factor of five or more difference in signal intensity for equimolar quantities.

Sample preparation was important for all the ionization techniques employed. Desalting biological samples was frequently a necessity. HPLC was most commonly preferred as a purification method. A variety of solvents were suggested to help dissolve specific compound classes, and the importance of proper solvent selection was generally made apparent. Conversion of samples to simple derivatives helped both to improve solubility and to determine the numbers of certain types of functional groups, such as free acids or amines.

About two hundred people attended the workshop. A few of these attended the brief business meeting which followed. Possible future activities of the committee were discussed at the meeting, but no decisions were made at that time.

Respectfully submitted,

Catherine E. Costello

Catherine E. Costello

Mass Spectrometry Facility
Department of Chemistry
M. I. T.

COMMITTEE REPORT

BIOMEDICAL APPLICATIONS

The Biomedical Applications Committee meeting was held at 5:00 p.m. on June 10, 1982, and was attended by the chairman, J. Clark, M. Criddle, C. Costello, W. Elliott, H. Fales, V. Reinhold, B. Sweetman, and B. Thomson.

A discussion was held on the subject of how groups with special interests in biomedical applications could obtain help with specific analytical problems. The example brought up by J. Clark and M. Criddle was a special requirement in respiratory gas analysis. It was agreed that, in this case as in others in which this committee has played a role in recent years, the functions could as well have been carried out by other committees and that the Biomedical Applications Committee has perhaps out-lived its usefulness.

It is suggested that the committee not be continued next year and that the Board of Directors observe whether the demise is regretted by the membership. It is hoped that any member with a contrary opinion will communicate his or her wishes to the Board.

Respectfully submitted,

WILLIAM R. SHERMAN
Chairman

ASMS Committee on Fundamentals

Technical Activities:

In 1982 Committee II sponsored one symposium and one workshop. The symposium "Ions and Light," was composed of 5 talks of 1/2 hour duration. There was one speaker each from Japan, Australia and Great Britain with the remaining two from the USA. Attendance was good, between 50-150, with the lower number attained during direct competition with an Introductory Lecture. The workshop "Internal Energy Effects in Collision Induced Dissociation Studies" was organized by K.R. Jennings. It was well attended and much lively debate ensued. A more detailed report is given elsewhere in these proceedings. It was the consensus opinion of those attending ($\sim$70) that the subject should be looked at again next year.

Business Meeting:

The business meeting was only sparsley attended (10-15). The principle cause of the poor attendance was the meeting location (Hawaii) and scheduled time of the meeting (5:00pm Thursday). In spite of the low attendance the committee had a very lively hour of discussion and formulated several recommendations to be considered by the board. These include: Recommendations for several plenary lectures; Recommendations for several symposia; A recommendation to institute an annual lecture, the Franklin lectures; Recommendations regarding Introductory lectures; Recommendations regarding workshops; Recommendations regarding the chairmanship of Committee II; And, finally, recommendations regarding a restructuring of ASMS along topical lines. Details of these recommendations will be sent to the appropriate association officers under separate cover.

Respectfully submitted,

Mike Bowers

Michael T. Bowers, Chairman
Committee II, Fundamentals

ASMS EDUCATION COMMITTEE REPORT

Workshop on "Short Courses in Mass Spectrometry:
What Needs Should They Serve?"

A workshop on short courses in mass spectrometry was held Tuesday, June 8, 1982 at 2:00 p.m. Approximately 40 people attended the workshop, the major aim of which was an evaluation of the short course needs and priorities for the Society. Introductory comments were made by panel participants who represented providers and users of short courses. These panel participants were Dr. Martin Rudat - E.I. DuPont, Dr. Lubomir Baczynskyj - The Upjohn Co., Dr. Don DeJongh - Finnigan Institute, Dr. Fred McLafferty - Cornell University, and Dr. Throck Watson - Michigan State University.

Dr. Rudat recently completed a survey of DuPont employees who have taken short courses in mass spectrometry. Three populations of employees were included in these short courses: organic chemists who used mass spectrometry but were basically unfamiliar with the technique, mass spectrometer operators who were familiar with instrumentation but not always with spectrum interpretation, and technicians. The technicians were not interested in detailed reaction mechanisms but wanted a "phenomenological" approach to the interpretation of spectra. The mass spectrometrists' main interest was in education on quantitative mass spectrometry and on the interpretation of "imperfect" spectra. The organic chemists were interested in a more basic, detailed education. These differences point to the difficulties in presenting courses which will answer the needs of all possible students.

Dr. Baczynskyj's comments, again from the point of view of a user of short courses, echoed those of Dr. Rudat. Dr. Baczynskyj also mentioned the desire of a number of people for an audio-cassette course on the interpretation of mass spectra.

Dr. DeJongh categorized the needs of students in mass spectrometry short courses into three distinct groups: 1) training, which is a basic introduction on how to run specific instruments, 2) development, which is instruction for someone who will not necessarily operate an instrument but wants technical knowledge related to mass spectrometry, and 3) education, which is intended for a scientist who is possibly outside the field but wants general education in mass spectrometry.

Dr. McLafferty stated that it was his opinion that the training aspects were not in his sphere of major influence as an educator and that he attempted to make his presentations relate most closely to the education end of the scale presented by Dr. DeJongh.

Dr. Watson commented that in his experience a very important aspect of the short course has been the presentation of information on distinguishing "good" data from "bad" data. Also, students in the courses he has taught have been extremely interested in how to evaluate an instrument and how to make the appropriate choice in purchasing an instrument to meet a particular need.

In the discussion which followed the audience expressed the opinion that the "Interpretation of Mass Spectra" short course should be closest to the training/development approach expressed by Dr. DeJongh. The "Quantitative Mass Spectrometry" short course should be addressed to the chemist who is beginning to perform quantitative analyses by mass spectrometry.

There was also considerable interest in advanced topics short courses such as the capillary GC course presented by Professor Grob at the Honolulu meeting. Two possible courses for consideration in Boston were discussed; one course on high performance liquid chromatography and the other course on the basics of ion optics. Both courses will be explored in more detail and then final decisions will be made about short course offerings for the 1983 ASMS meeting.

Respectfully submitted,

Harry S. Hertz
Education Chairman

ASMS Committee on Quantitative Organic Analysis

A committee meeting was held on Tuesday, June 8, 1982 at 5:00 p.m. Approximately 10 people attended the meeting. The following statement of goals and purposes was approved for recommendation to the Society:

"The committee on Quantitative Organic Analysis shall be responsible for activities supporting the use of mass spectrometry in the quantitative determination of organic substances. As primary goals, the committee should foster the exchange of ideas and techniques to improve accuracy, reproducibility and sensitivity of existing techniques and applications, should actively seek to extend the use of mass spectrometry for quantitative analysis and should promote the development of better instruments for this purpose. Workshops should be held at periodic intervals at national meetings, guidelines should be developed when appropriate, and advice should be made available on occasion when needed by officers of the society."

Various possible formats for the presentation of quantitative methodology at the next ASMS meeting were discussed. Dr. Stuart Scheppele, representing the ASTM Committee D-2, said that his committee would like to participate more closely with ASMS in this area. He proposed the possibility of a symposium that would include invited speakers from the petroleum industry to discuss such topics as performance characteristics of GC, batch inlet for bulk samples, computerized probe distillation for quantitative profiling analysis, and capillary GC injection techniques. Other approaches that were discussed to sponsor information transfer about quantitative methods included workshops of the type held several times in the past, and a short course.

The next item of business concerned terms that would be appropriate for definition by the Nomenclature Committee. Response factors, sensitivity, detection limit, isotope dilution, reverse isotope dilution, reconstructed ion chromatogram, mass chromatogram and noise were discussed in this connection.

A workshop, entitled "Quantitative Mixture Analysis. Performance Characteristics of GC-MS, MS-MS and Direct Probes," was held prior to the committee meeting; it was joint with the Environmental Applications Committee chaired by Ralph Daugherty. The format was similar to that which was used by Graham Cooks in 1981 for a discussion of MS/MS. Panel members were Toshihiro Fugui, William Budde, Andre de Leenheer, Isamu Matsumoto, Graham Cooks and Michael Gross. Questions previously submitted to Ralph Daugherty or Charles Sweeley were fielded by one or more of the panel members and audience participation was invited. The questions dealt with reference versus definitive methods in clinical chemistry; stable isotope dilution for quantitative analyses; accuracy and precision of GC-MS, MS-MS and probe analyses; limits of detection routinely attainable by GC-MS, MS-MS and probe analysis; matrix effects on precision and accuracy, especially in FAB analyses; and standards for evaluation of performance of the various techniques. The problem of matrix effects was of great interest, and much discussion was devoted to the evaluation of precision and other aspects of performance. The workshop was well attended by about 150 persons.

C. C. Sweeley 7/1/82

Charles C. Sweeley
Michigan State University

COMMITTEE REPORT

HIGH TEMPERATURE MASS SPECTROMETRY

The Committee met briefly following the sponsored workshop on quadrupole mass spectrometry. Several topics for future workshops were discussed, along with other activities for the future meetings in Boston and San Antonio. These topics will be developed through correspondence and discussions in the coming months. The general area of pyrolysis mass spectrometry was discussed again, and it was agreed that aspects dealing with reaction mechanisms and kinetics could well be included in Committee activities. T. A. Milne, Solar Energy Research Institute, agreed to coordinate activities in this area.

D. L. Hildenbrand
Chairman

ASMS Committee IV. Isotope Ratio Measurements

The activities of the Committee on Isotope Ratio Measurements at the 1982 ASMS Meeting included two symposia entitled "Mass Spectrometry for Nuclear Safeguards" and "Isotopes in Geochemistry and Geochronology;" and a workshop, "Laser Mass Spectrometry for the Production and Measurement of Inorganic Ions." The sessions were well attended, and the special opportunity for interchange of information with Australian, New Zealand, and Japanese scientists was very beneficial. I would like to express my appreciation to Dick Perrin, Sam Goldich, and Larry Moore for an excellent job of organizing this year's activities, and to the ASMS board for enabling us to conduct such a diverse program.

The laser workshop, which is described elsewhere in this volume, attracted a number of scientists from outside of the isotope ratio core group, and the suggestion has been made to provide a follow-up session for the 1983 meeting in Boston. Other suggestions for 1983 include a short course on mass spectrometry theory and design, which would address such topics as ion optics, vacuum technology, and measurement circuit electronics, as well as sessions on statistical methods of reporting data and a general session on elemental analysis by mass spectrometry. We are in need of people who are willing to assume leadership positions within the Committee and organize activities such as symposia, workshops, and any other activities which would benefit the isotope ratio community.

I have been asked by Catherine Fenselau, the incoming ASMS President, to continue as Chairman of the Committee for 1983-84. I would like to thank all of you for your suggestions and cooperation over the past two years, and hope that, with your continued support, we can maintain a diversified program which will attract a wider range of scientists with interests in isotope ratio measurements.

Respectfully submitted,

L. J. Powell
Chairman, Committee IV

ASMS NOMENCLATURE COMMITTEE WORKSHOP -

Honolulu, 1982

One Workshop was held on Tuesday, June 8, 1982, which was co-sponsored by the ASTM E14.10 subcommittee on nomenclature. Due to various committments, those who volunteered last year to supply terms and definitions for the 1982 meeting were either unable to do so or could not do so until a few months prior to the meeting. This prevented the list of terms from being circulated until the day of the Workshop. For this reason, it was decided that the attached list be published in the bound volume of this year's meeting, and that comments on these terms be solicited from the ASMS membership. It was also decided that a separate cover letter be sent to the membership alerting them to the list and the request for their comments.

A letter was read by Prof. Burnaby Munson regarding the view of the ASMS Board of Directors on the list of definitions produced at last year's Workshops. This letter is reproduced in part below.

> "The Board of Directors of ASMS approves the list of terms as presented in the Bound Volume of Abstracts for the 1981 meeting subject to periodic review and extension by the Nomenclature Committee and the Board, such that this shall be a living document. The Board recommends that authors' usage conform to this nomenclature."

All comments on this year's list of definitions should be sent to:

Doug Cameron
Science and Technology Div.
Union Oil Company
P. O. Box 76
Brea, CA 92621

All comments received prior to December 31, 1982, will be considered for inclusion into the list, and a revised version of the definitions will be sent to all interested persons prior to next year's meeting.

Doug Cameron

Doug Cameron
Chairman

ANALYZERS

Electrostatic Analyzer. A velocity focusing device composed of means for producing an electrostatic field perpendicular to the direction of ion travel. Effect is to bring to a common focus all ions of constant velocity. Usually used in combination with a magnetic analyzer for mass analysis.

Magnetic Analyzer. A direction focusing device composed of means for producing a magnetic field perpendicular to the direction of ion travel. Effect is to bring to a common focus all ions of constant momentum.

Quadrupole Analyzer. A true mass filter consisting of means of creating a quadrupole field of a constant component and a varying component in such a manner as to allow transmission of only a selected mass to charge ratio.

Time of Flight. An ion travel time device consisting of a means to measure the flight time of ions with an equivalent kinetic energy over a fixed distance.

Wien Analyzer. A velocity filter composed of means for creating a crossed homogeneous electric and magnetic field such that only ions of a fixed velocity are transmitted.

Mass Resonant Spectrometer. A mass analyzer composed of means for mass dependent resonant energy transfer and measurement of the resonance frequency, power or ion current of the resonant ions.

(The following are standard instrumental configurations utilizing one or more of the above techniques.)

Double Focusing Mass Spectrometer . The combination of a magnetic analyzer and electrostatic analyzer in either sequence to effect direction and velocity focusing.

Ion Cyclotron Resonance Spectrometer. A device to determine the mass of an ion by measuring its resonant frequency.

Ion Trap Mass Spectrometer. A mass resonance spectrometer composed of means for creating a three dimensional rotationally symmetric quadrupole field capable of storing ions at selected masses.

Mass Spectrometer Configurations. Multianalyzer instruments should be named for the mass analyzers in the sequence in which they are traversed by the ion beam. Using B for a magnetic analyzer, E for an electrostatic analyzer, Q for a quadrupole analyzer we have a BE mass spectrometer ("reversed" geometry double focusing instrument), BQ mass spectrometer (hybrid sector and quadrupole instrument), EBQ (high resolution followed by a quadrupole). Note that a triple quadrupole which has two mass analyzers is a QQ mass spectrometer.

Problem: Time of flight, simultaneously or sequentially with other mass analyzers.

IONIZATION

Desorption Ionization (DI). General term to encompass the various procedures (secondary ion mass spectrometry, fast atom bombardment, californium fission fragment desorption, thermal desorption) in which ions are generated directly from a solid sample by energy input.

Note: Intent is to establish a broad term analogous to chemical ionization which also encompasses a group of related ionization processes.

SAMPLE INTRODUCTION

Sample Introduction System. This is a system used to introduce sample to a mass spectrometer ion source before and/or during analysis. (Sample Introduction System, Introduction System, Sample Inlet System, Inlet System, and Inlet are synonymous terms.)

Reservoir Inlet. This is an Inlet System having an enclosed volume (the reservoir), with provision to evacuate the reservoir, to admit sample to the reservoir, and to allow gas or vapor from the reservoir to flow through a leak to the mass spectrometer ion source. A complete description of a Reservoir Inlet should include a description of the method by which the sample is introduced into the reservoir (e.g. with gas-metering, septum, fritted-disc, or teflon-cup introduction), an indication as to whether the leak provides viscous or molecular flow, and an indication whether the reservoir is heated.

Batch Inlet. This is the historic term for a Reservoir Inlet. Reservoir Inlet is preferred because a Direct Inlet Probe is also a form of Batch Inlet. Batch Gas Inlet or Batch Vapor Inlet is, however, a completely descriptive term.

Dual Viscous-Flow Reservoir Inlet. This is an inlet having two reservoirs, used alternately, each having a leak that provides viscous flow. This inlet is used for making precise comparisons of isotope ratios in two samples.

Continuous Inlet. This is an inlet in which gas or vapor passes continously into a mass spectrometer ion source, as distinguished from a Reservoir Inlet or a Direct Inlet Probe.

Non-Fractionating Continuous Inlet. This is a Continuous Inlet in which gas flows from a gas stream being analyzed to the mass spectrometer ion source without any change in the conditions of flow through the inlet or by the conditions of flow through the ion source.

Direct-Inlet Probe. This is a rod having a sample holder at one end, which is inserted into the vacuum system of a mass spectrometer through a vacuum lock, placing the sample near to, at the entrance of, or within the ion source, so that the sample can be vaporized after introduction to the vacuum system by heat from the ion source or by heat applied to the probe from an external source. (Direct Inlet Probe, Direct-Introduction Probe or Direct-Insertion Probe are synonymous terms. The use of DIP as an abbreviation for these terms is not recommended.)

Vacuum-Lock Inlet. This is an inlet in which a sample is placed in a chamber, the chamber is pumped out, and a valve is opened so that the sample can then be introduced to the mass spectrometer ion source. A Vacuum-Lock Inlet commonly uses a Direct-Inlet Probe which passes through one or more sliding seals, but other kinds of Vacuum-Lock Inlets are possible.

Extended Direct-Inlet Probe. This probe provides for insertion of a sample on an exposed surface (such as a flat surface or a wire) into (rather than up to the entrance of) the ion source of a mass spectrometer. (This term is synonymous with Direct-Exposure Probe.)

Crucible Direct-Inlet Probe. With this probe, the sample is held in a cup-shaped device (the crucible) rather than on an exposed surface. A Direct-Inlet Probe is assumed to be a crucible type unless otherwise specified.

GC/MS Interferface. This is an interface between as gas chromatograph and a mass spectrometer which serves to provide continuous introduction to a mass spectrometer ion source of effluent gas from a gas chromatograph during the period for which the effluent gas is to be analyzed.

Direct GC/MS. This is an interface in which the entire effluent from the gas chromatograph passes to the mass spectrometer ion source during an analysis, without any splitting of this effluent.

Splitter GC/MS Interface. This is an interface in which the effluent from the gas chromatograph is divided before admisssion to the mass spectrometer, without enrichment of sample with respect to carrier gas.

Separator GC/MS Interface. This is an interface in which the effluent from the gas chromatograph is enriched in the ratio of sample to carrier gas. (Separator, Molecular Separator, and Enricher are synonymous terms.) A separator should generally

be defined as an Effusion Separator, a Jet Separator, or a Membrane Separator.

Effusion Separator (or Effusion Enricher). This is an interface in which carrier gas is preferentially removed from the gas entering the mass spectrometer by effusive flow (e.g. through a porous tube or through a slit).

Jet Separator. This is an interface in which carrier gas is preferentially removed by diffusion out of a gas jet flowing from a nozzle. (Jet Separator, Jet-Orifice Separator, Jet Enricher and Jet-Orifice Enricher are synonymous terms.)

Membrane Separator. With this separator, the gas or vapor passes to the mass spectrometer through a semi-permeable membrane (e.g. a silicone membrane) which selectively transmits organic compounds in preference to carrier gas. (Membrane Separator, Membrane Enricher, Semi-Permeable Membrane Separator, and Semi-Permeable Membrane Enricher are synonymous terms.)

Solvent-Divert System. This system is used in conjunction with an interface which permits temporary interruption of the flow from a gas chromatograph to a mass spectrometer by opening a valve to a pumping line, so that an effluent present at a high concentration (usually solvent) does not enter the mass spectrometer ion source at a high concentration.

Liquid Chromatograph/Mass Spectrometer (LC/MS) Interface. This interface is between a liquid chromatograph and a mass spectrometer which serves to provide continuous introduction to a mass spectrometer ion source of the effluent from a liquid chromatograph during the period for which the effluent is to be analyzed.

Moving Belt (Ribbon or Wire) Interface. With this interface, all or a part of the effluent from a liquid chromatograph is continously applied to a belt (ribbon or wire), which passes through two or more orifices, with differential pumping, into the mass spectrometer vacuum system; after which heat is applied, to remove the solvent, and then to evaporate the solute into the ion source.

Direct Chemical Ionization Interface. With this interface, all or a part of a liquid chromatograph effluent passes continuously to the mass spectrometer, in which the solvent is used as a chemical ionization agent for ionization of the solute.

ION/MOLECULE REACTIONS

Collision-Induced Dissociation (CID). The fragmentation of a polyatomic ion due to the collision of the ion with a target, usually a neutral gas molecule. (Collision Activated Dissociation (CAD) and Collisional Activation (CA) are synonomous terms, but Collisional Activation is not recommended.)

Collisional Activation (CA). This refers to the increase in internal energy of an ion as the result of a collision between the ion and a target.

APPENDIX

SECONDARY ION MASS SPECTROMETRY (SIMS)

(The terms in this section have been provided entirely by ASTM Subcommittee E42.06 and are part of a list which is presently under consideration by this subcommittee. Their contribution is gratefully acknowledged.)

Analysis Area. The area of the specimen from which the secondary ion signal is accepted.

Angle of Incidence. The nominal angle between the incident Primary Ion Beam, and the normal to the original sample surface.

Angular Distribution. The variation of Secondary Ion Yield as a function of emission angle from the specimen.

Background Signal. Signal from both the continuum background on either side of the

mass of interest and from species not completely resolved from the mass of interest.

Channeling. The process by which particles preferentially penetrate along crystallographic directions because of the long range atomic order in a crystalline specimen.

Charge Neutralization. A technique in which a surface under ion bombardment is maintained at a constant potential by compensating for any accumulated charge.

Collection Angle. The angle between the normal to the original sample surface and the secondary ion collection optics.

Collision Cascade. A sequential energy transfer between excited atoms moving through a solid as a result of bombardment by an energetic primary ion.

Crater Wall Effect. A potential interference by secondary ions which originate from depths shallower than the maximum depth of the crater formed by ion bombardment.

Depth Profile. A plot of secondary ion signal as a function of sputtering time as a representative measure of the relative distribution of that species as a function of depth.

Depth Resolution. The depth range over which the secondary ion signal for one species increases from 10 to 90% at an ideally sharp interface between two dissimilar media.

Detection Limit. The lowest concentration of a substance which may be detected, i.e. the concentration which yields a signal twice the standard deviation of the background signal at the mass of the detected species. Contributions from both a continuum background and species of interfering mass must be included in the background measurement. The background ideally should be determined from an identical specimen except that it contains none of the constituent being determined.

Dynamic SIMS. SIMS analysis at sufficiently large primary ion currents such that more than one mono-layer of material is removed during the analysis.

Energy Distribution. A plot of the number of secondary ions of a particular species leaving the sample surface as a function of the energy of those ions.

Equilibrium Composition. The steady state surface composition produced by sputter-etching a homogeneous sample under fixed conditions for the vacuum ambient and the primary ion beam.

Fractional Sputter Yield. The Sputter Yield of a particular component with respect to the total ion yield in a multicomponent matrix.

Interface Width. The measured distance over which a 10 to 90% change in composition is measured at the junction of two dissimilar matrices.

Ion Beam. A directed flux of charged atoms or molecules.

Ion Beam Current. The measured total ion current incident upon the specimen.

Ion Beam Current Density. The current incident on the specimen per unit area.

Ion Beam Energy. The energy of the ions incident on the specimen surface, expressed in kilo electron volts, KeV.

Ion Implantation. The introduction and retention of an energetic ion within a target material.

Ion Neutralization. A process in which a charged species is converted into a neutral species.

Knock-In. The movement of a constituent of the target deeper into the target matrix as a result of recoil collisions with the primary ion beam.

Matrix Effect. The change in Sputtering Yield, Fractional Sputter Yield, ion yield

or other experimental quantities which are caused by the difference in composition or structure between various samples.

Molecular Ion (in SIMS). A charged multi-atom species detected in the secondary ion emission.

Negative Ion Yield. The number of negative ions sputtered from a target per incident ion of given mass, energy, charge, and angle of incidence.

Positive Ion Yield. The number of positive ions sputtered from a target per incident ion of given mass, energy, charge, and angle of incidence.

Preferential Sputtering. The phenomena which occurs when the Fractional Sputter Yield for a species is different from the fractional composition of that species in the specimen.

Primary Ion Beam. A beam of charged particles incident on the sample which causes removal of the surface by sputtering.

Primary Ion Beam Profile. The spatial distribution of the primary ion current in a plane perpendicular to the primary beam axis.

Raster. The periodic deflection of an ion beam.

Sample Charging. The accumulation of electrical charge on the sample caused by bombardment by a charged species.

Secondary Ions. Ions ejected from a sample surface as a result of sputtering by the primary ion beam.

Secondary Ion Signal Gating. The process of accepting secondary ion signal from only a portion of the sputtered area of the sample to avoid crater wall effects.

Secondary Ion Yield. The number of positive or negative ions sputtered from a target per incident, ion of given mass, energy, charge and angle of incidence.

Selected Area Aperture. The mechanical equivalent of signal gating commonly used in stigmatic mass spectrometers.

Selective Sputtering. The same as Preferential Sputtering.

Sensitivity Factor. The factor used to convert the net counts per unit time, for a particular species, matrix and experimental conditions, to concentration.

Signal to Background. The ratio of signal above background to that of the background.

Signal to Noise Ratio. The ratio of signal above background to either the standard deviation of the signal including background, or one fifth the maximum variation in the signal including background.

SIMS Ion Image. The x-y distribution of a particular species sputtered from the sample surface representing the concentration distribution of that substance over the sample surface.

Sputter Rate. The amount of material removed per unit time as a result of ion bombardment.

Sputter Yield. The average number of particles ejected from a sample surface per primary ion.

Static SIMS. SIMS analysis at sufficiently small primary ion current density such that less than one mono-layer of material is removed during the analysis.

Target Current. The current striking the sample during primary ion bombardment.

Useful Ion Yield. The ratio of ions detected to atoms sputtered from the analysis

area.

Zone of Mixing. The layer of the target surface within which the primary beam causes atomic motion.

Integer Ion m/z Values. Two definitions are proposed.

1. The set of positive integers, produced by appropriate changes in the magnitude of at least one of the independent variables in the laws-of-motion applicable to a given geometry instrument.

2. The set of positive integers generated by assigning integer values to the members of the sets of singly-charged homologous ions in the mass spectrum of a reference substance. This *m/z* scale establishes the integer *m/z* values for the ions in the mass spectra of other substances by the mathematical process of rounding these latter values to the nearest integer.

Integer Ion Mass. The integer ion *m/z* value multiplied by the number of charges on the ion.

Nominal Ion Mass. Let $a(j)$ and $MN(j)$ represent the atomic coefficients and the mass numbers, respectively, of the $X(j)$ nuclides comprising a given formula. The nominal ion mass is thus defined by the expression

$$NM\ X(1)_{a(1)}\cdots X(j)_{a(j)}\cdots X(m)_{a(m)} = \sum_{j=1}^{m} a(j)\cdot MN(j)$$

Calculated Ion Mass and Associated Error. Let $a(j)$ and $M(j)$ represent the atomic coefficients and the masses, respectively, of the $X(j)$ nuclides comprising a given formula. Let $\sigma^2_{M(j)}$ be the variance in $M(j)$ and M_e represent the rest mass of the electron. The following expressions then define the calculated ion mass and its associated standard error, respectively.

$$CM\ X(1)_{a(1)}\cdots X(j)_{a(j)}\cdots X(m)_{a(m)} = \sum_{j=1}^{m} a(j)\cdot M(j) - M_e$$

$$\sigma_{CM} = \pm \left(\sum_{j=1}^{m} a(j)^2 \cdot \sigma^2_{M(j)} + \sigma^2_{M_e} \right)^{\frac{1}{2}}$$

Calculated Ion m/z Value and Associated Error. The calculated ion mass divided by the number of charges on the ion. The standard error is $\pm(\sigma_{CM}/z)$.

Experimental Ion m/z Value and Associated Error. The experimental ion *m/z* value is the mass to charge ratio determined at a resolution R using a given mass spectrometer. Let the resolution be $R = m/z/\Delta(m/z)$ where $\Delta(m/z)$ is the width of the peak due to an ion having a mass-to-charge ratio of *m/z* at 5% of its height. If the peak shape is Gaussian, then $\Delta(m/z) = 4.9\ \sigma$ where σ is the standard deviation in the mass-to-charge ratio of the ions defining a given peak. The contribution of the ion statistics to the ppm standard deviation in *m/z* is thus

$$\sigma_{m/z} = \frac{10^6}{(4.9)(R)(N_i \cdot N_s)^{\frac{1}{2}}}$$

where N_i is the number of ions in the peak and N_s is the number of scans averaged.

Experimental Ion Mass. The experimental ion m/z value multiplied by the number of charges on the ion.

Error in the Experimental Ion Mass. Let $EM(i,j)$ be the experimental determination of the known mass of the jth ion, $CM(j)$, in the ith scan of the spectrum of a known substance acquired at a resolution R. For N_s scans of the spectrum, the average ppm error in determining $CM(j)$, $E(j)$, and its associated standard deviation, $\sigma_{E(j)}$, are given by the following equations, respectively.

$$E(j) = \frac{10^6}{CM(j)} \cdot \left[\frac{CM(j) - \sum_{i=1}^{N_s} EM(i,j)}{N_s} \right]$$

$$\sigma_{E(j)} = \frac{10^6}{CM(j)} \left[\frac{\sum_{i=1}^{N_s} (E(j) - EM(i,j))^2}{N_s - 1} \right]^{\frac{1}{2}}$$

The root-mean-square (rms) error, σ_E, in the experimental errors for all j ions, which is a measure of the overallaccuracy in mass measurement at the resolution R, is

$$\sigma_E = \left[\frac{\sum_{j=1}^{N_j} E(j)^2}{N_j - 1} \right]^{\frac{1}{2}}$$

The quantity σ_E can also be calculated using the values of $\sigma_{m/z}$ calculated from N_i, N_s, and R in the equation defining $E(j)$.

Random and Systematic Contributions to the Error. Let r be the random contribution to the rms error in mass measurement for a single scan and s be the systematic contribution to the error. Let σ_E' and σ_E be the rms errors for a single scan of the spectrum and for the average spectrum obtained from N_s scans of the spectrum. The following equations express σ_E' and σ_E as functions of r, s, and N_s.

$$\sigma_E' = r + s$$

$$\sigma_E = (r/N_s^{\frac{1}{2}}) + s$$

Error Tolerance for Formula Acceptability. Let <EM> be the average experimental mass and CM be the calculated mass for the formula under consideration. The error tolerance for formula acceptability, (ET), is defined by the following equation where N is a positive integer.

$$ET = |CM - \langle EM \rangle| \leq \sigma_{CM} + 10^{-6} \cdot N \cdot \sigma_E \cdot \langle EM \rangle$$

MINUTES OF THE "ORPHANED INSTRUMENTS" WORKSHOP
June 8, 1982 - Waikiki, Hawaii

The meeting opened with a discussion of independent service, by Bill Frasure who outlined typical charging arrangements. The broad experience in mass spectrometers possessed by many independents often compensates for in-depth instrumental familiarity of the affiliated service engineers. Prices of the independent appear to be in general lower (about $70/hr on the average). It was suggested that persons requiring service a given area get together to share the independent's travel expenses. Frasure stressed the need for use of common terms by all servicemen and suggested ions/millisec for sensitivity and volts/msec/ion for response. Frasure has compiled the following list of servicemen and welcomes other names.

Don Raimey, Reading, MA	tel:	617-644-6594	
John Kelley, Columbus Ohio		614-267-8098	
Mike Claus, Barnegat, NJ		609-698-1720	
Joel Johnson, Wilmington, DE		302-655-9291	
Rafael Cistoza, Springfield, VA		703-451-2826	
Al Cox, Catharpin, VA		703-591-4632	
David Minks, Ithaca, NY		607-273-6819	
Ray Allen, Boulder, CO		303-442-2141	(glassware)
George E. Davis,		408-496-0323	
Davco Co., San Jose, CA		(Finnegan boards & computers)	
Bob Dutky, Colesville, MD		301-384-5305	
Jim Wilder, Pleasant Hill, CA		415-229-0325	(multipliers
Bill Frasure, St. Louis, MO		314-962-8648	and sources)

The session's audience of about sixty represented 11 from LKB, 2 MAT, 3 Finnegan, 2 CVC, 8 AEI, 3 Hitachi, 16 Dupont, 2 Bendix, 1 Teknivent owners who consider themselves "orphaned".

Some discussion about turbopumps ensued and several failures had been noted. The Chairman recalled that Macfarlane (Texas A&M) recommends attaching a storage battery plus invertor to maintain power to the oil pump for the bearings when the mains power is lost.

The group then broke up into 3 smaller groups, LKB, AEI, Dupont and miscellaneous to discuss specialized topics and the appended list of orphans was collected.

ORPHANED INSTRUMENTS

NAME	INSTRUMENT	ADDRESS
Walt Chamberlin	CEC-21-620 CEC 21-110 Dupont 21-104	Los Alamos National Lab Box 1663 M/S G780 Los Alamos, NM 87545 505-667-2054 FTS 843-2054
George R. Dubay	LKB-9000 Dupont DP1	Bristol Myers Pharm. Res. & Dev. P.O. Box 657, Bldg. 23A-305 Syracuse, NY 13201 315-432-2265
Bill Elliott	LKB 9000 2091	St. Louis University School of Medicine
Hank Fales	LKB 9000 2091	NIH, Bethesda, MD 20205 301-496-2135
Larry Gilbert	Manuf TOF-MS	CNC Products, Inc. 525 Lee Road Rochester, NY 14603
G. Greenwood	CEC 21-103 21-110	Phillips Petroleum Co. 150 PL Bartlesville, OK 74003
Ron Grigsby	CEC 21-110B	Masspec, Inc. 275 Turkey Creek Road Bartlesville, OK 74003
L. F. Herzog	most upgrades	Nuclide 642 E. College Ave State College, PA
B. J. Hidy	1015 & AEI MS9	Battelle Columbus Labs 505 King Avenue Columbus, Ohio 43201
W. D. (Dave) Jamieson	Dupont 21-491 Dupont/CEC 21-110B 21-620A	National Research Council 1411 Oxford Street Halifax, N.S Canada B3H3Z1 902-426-8279
Margith Jansson	LKB 9000 2091	Karolinska Institute Masspectrometri lab, FACK S-1040 Stockholm, Sweden
Alfred Kornel, Jr.	Bendix Modifier TOF #12-101	Univ. of Cincinnati Dept. of Chemistry Cincinnati, Ohio 45221
Climaco J. Metral	RMU-7	"
Tom Krick	LKB 9000	Univ. of Minnesota Biochemistry Dept. St. Paul, MN
John C. Newton	CEC P1-103C	Lawrence Livermore National Lab Livermore, CA 94550

Kenneth Ng		CIBA Geigy Corp 444 Saw Mill River Rd. Ardsley, NY 914-478-3131 ext 2914
Vincent O'Connell	Data systems for magnetic MS, older HP & Finnigan MS	Teknivent Corp 10774 Trenton St. Louis, MO
Larry Rapp	CGC 102, 103, 104 106	Arco 400 E. Sibley Harvey, IL 60426
Louis Romaley	Dupont 21-104	Dalhousie University Dept. of Chemistry Halifax, N.S. Canada
Paul C. Samson	CEC 21-103 (2) Bendix TOF Model 12	UOP Inc Ten UOP Plaza Des Plaines, IL 60016
David Smith	LKB 9000S	Univ. of Utah 311 Skaggs Hall Salt Lake City, UT 84112
Jim Stauffer	Dupont/CEC 2110B Finnigan 6100	Arthur D. Little, Inc. Acorn Park Cambridge, MA 02140 617-864-5770 x2559
Brian J. Sweetman	LKB 9000	Vanderbilt University Dept. of Pharmacology Nashville, TN 37232
Tom Terwilliger	Hitachi RNH-2 also provide independent data system service upgrades	University of Pennsylvania Department of Chemistry Philadelphia, PA 19104
George Wood	CEC 21-14 21-621	NASA - Langley Res. Center Hampton, VA 23665
Steve Young	MS-9 (1964) Dupont 21-490	SRI International 333 Ravenswood Avenue Menlo Park, CA 94025 415-859-4806

Henry M. Fales

COMMITTEE REPORT

ENVIRONMENTAL COMMITTEE

WORKSHOP: QUANTITATIVE MIXTURE ANALYSIS

(Jointly Sponsored with Quantitative Organic Committee)

This workshop was attended by more than 150 people. The subjects discussed spanned the range of quantitative mixture analysis from direct analysis of complex mixtures by direct probe introduction to specific analysis of individual compounds or metabolites using isotopically altered internal standards. The most widely used and discussed technique was capillary gc mass spectrometry using electron ionization. C. Sweeley and other practitioners of biochemical profiling pointed out the fact that the normal range of biological variability is sufficiently large that quantitation with precisions of better than 1% is not needed so that internal standards that are not structurally related to the components under analysis are acceptable for the purposes of quantitation. It was generally agreed that isotope dilution mass spectrometry provides the highest sensitivity precision and accuracy in quantitative analysis. Isotope dilution is the method of choice where high precision and accuracy are required. R.G. Cooks pointed out the virtures of multiple analyzer mass spectrometry for mixture analyses. When using MS/MS techniques the ion beam is attenuated by as much as two orders of magnitude; however, the increase in the certainty in chemical analyses that results from the presentation of the daughter ion spectrum and the decrease in chemical noise can result in no effective change in detection limits. The workshop concluded with a lively discussion of the EPA capillary gas chromatography mass spectrometry quality control protocol which was lead primarily by W.L. Budde.

COMMITTEE MEETING

The meeting of the Environmental Committee was held immediately after the workshop it was attended by a representative group of the active scientists in this field. There was a consensus that the society should organize a symposium on the subject of "Quality Assurance in Quantitative Analysis: Screening to High Precision Analyses". There were strong feelings that the society should invite two individuals who are not members of the society to discuss the respective themes of development of a quality assurance program and statistical evaluation of chemical data.

Considerable interests was expressed in two subjects for workshops for the 1983 meeting. These topics are "Hazardous Sample Analysis: Sample Collection, Storage, Analysis and Disposal" and "The Implementation of the EPA Capillary Gas Chromatography Mass Spectrometry Quality Control Protocol".

This committee feels that it would be worthwhile for the society to schedule an introductory lecture in 1983 on the subject of high performance capillary gas chromatography.

Ralph Dougherty
Florida State University

ASMS COMMITTEE REPORT-SURFACE ANALYSIS AND SOLIDS

Workshop on Ion Optics for Extraction of Secondary Ions from Surfaces

An informal workshop co-chaired by Peter Williams (Arizona State University) and Charles Magee (RCA) was held in which some of the expertise in the area of ion extraction optics gained by inorganic SIMS investigators over the years could be shared with those organic mass spectrometrists just getting into the field of sputtered ion mass spectrometry. The co-chairmen gave brief presentations in their areas of interest (Williams-Magnetic sector instrum., Magee-quadrupole instrum.) then together fielded questions from the 100 + attendees, or called upon other knowledgeable persons in the audience for answers. The following points were made:

1) Characteristics of sputtered organic ions:
   - A. 1-2 eV energy spread,
   - B. Average kinetic energy of ≈2 eV
   - C. Emitted in a cosine distribution centered about the surface normal.
   - D. One has the advantage of knowing exactly where in space the ions are generated.
2) Secondary ion optics for quadrupole-type sputtered ion mass spectrometers.
   - A. High extraction fields cannot be used.
   - B. Use of an immersion lens in close proximity to the sample surface is quite effective at focusing the secondary ions emitted with a cosine distribution.
   - C. Energy analysis of the emitted secondary ions, while not mandatory, is advisable.
   - D. In order to obtain low noise levels at the detector, the photons and high energy neutrals emitted from the bombarded surface must be blocked from direct entry into the quadrupole.
3) Secondary ion optics for magnetic-sector-type sputtered ion mass spectrometers.
   - A. The instruments currently being employed by practitioners of FAB reflect little effort toward optimization of transmission of ions emitted from a planar surface.
   - B. High performance inorganic instruments (e.g. CAMECA ims-3f) have transmissions approaching 10%.
   - C. Use of a high extraction field directly above the sample surface forms a strong lens which can be used to focus into the MS nearly 100% of the ions emitted with initial kinetic energies $\leq$2 eV.
   - D. The emittance of the sample and extraction lens must be carefully matched with "transfer optics" to the acceptance characteristics of the mass spectrometer.

After these discussions, a brief presentation was made by J. Campana (Naval Research Laboratory) on the optics needed for efficient extraction of ions from a large sample area, which is necessary for low-primary-particle-dose or "static" SIMS as practiced by Benninghoven, Cooks and others. After a discussion period on the principles involved (called "dynamic emittance matching"), the workshop was adjourned.

A brief business meeting was then held in which it was decided that a re-ordering of the two parts of the Committee title would more accurately reflect the emphasis of the active members. It was deemed important, however, to retain the word "solids" in the title to provide a forum for the spark source mass spectroscopists who originally formed the Committee.

Charles W. Magee
RCA Laboratories
Chairman

HARDWARE AND SOFTWARE FOR INTERCOMPUTER COMMUNICATIONS

Thursday, June 10, 1982, 3:30 P.M.

Participants:

Brian Musselman	Michigan State University
Tom Krick	University of Minnesota
Mike Grayson	McDonnell Douglas (St. Louis)
Tom Terwilliger	University of Pennsylvania

The purpose of this workshop was to focus on the problems involved in transferring information between computer systems. Many laboratories have more than one computer of some sort, and systems differ drastically in their ability to communicate with one another. If one has duplicate data systems from the same manufacturer with compatible mass storage devices on both, then it is easy (although sometimes slow) to hand carry a disk cartridge (or tape) from one to the other. This workshop addressed the problems that often occur when the above condition is not met.

Approximately 75 people attended, at least at the start. Of these, roughly 60% have more than one data system in their laboratory. Nearly all of these are currently transferring data between systems in one way or another. Most of them wrote the necessary programs themselves, with only two admitting to having gotten the required material from the manufacturers. (N.B. This seems a little surprising.)

Brian Musselman started by describing his hardware foreground-background dual processor system. He has two PDP-8's connected together such that one is a "foreground" data acquisition processor, and the other is used for "background" data processing and output. This enables simultaneous acquisition and processing at a much greater speed than would be possible if a single processor were used. He also has the PDP-8 connected to another PDP-11 system, as well as an H.P. GC/MS data system interfaced to a time-shared PDP-11/44. Both of these interconnections are primarily for data transfer; the latter permitting access to the much larger PDP-11/44 system. The PDP-8/PDP-11 interface was custom designed, but no modifications were required to the RSX-11 software operating on the PDP-11.

Tom Krick then described the work he has done connecting two of his laboratory data systems (LKB-9000 and HP-5985) to the University of Minnesota mainframe computer, and thus indirectly to each other. All communication with the mainframe is done via the telephone modem at 1200 Baud and date transmission is in ASCII. Handshaking problems are overcome by sending one line at a time using a specially designed "transmission protocol", and by insuring that internal buffers are large enough to prevent overflow. The principal accomplishment has been to gain access to the greater facilities of the mainframe such as better graphic capability and increased storage, and to be able to transfer data from one laboratory system to the other.

Mike Grayson then described the transfer of data between his MINC laboratory data system used on a time-of-flight mass spectrometer, and a CYBER 750/730. He is able to transfer small files over the telephone in much the same way as described previously, but finds this impractical for the large volumes of data generated by his MS-30 GC/MS system. Here he writes the raw data directly to magnetic tape and hand carries the tape to the computer center. Since the tape drives were directly compatible, this only necessitated writing the proper re-formatting programs on the CYBER. He had no particular problems with either the hardware or software; his primary difficulties were in the personnel category.

Tom Terwilliger concluded the presentations by describing the University of Pennsylvania system. Here there are two DS-50-S systems with incompatible disk drives and shared peripherals. A direct CPU-CPU hookup was made using specially modified RS-232-C interfaces. Baud rates were raised to 33,000 and hardware handshaking on a character by character basis was implemented. This simplified the software considerably, and allowed the transfer-control program to operate in the foreground so it could run simultaneously with other tasks including data acquisition. Operating System modifications were required: (1) to increase speed, (2) because no "system generation" capability was available to add an extra "device" into the operating system, and (3) because the modified interface boards were no longer compatible with the original operating system.

In the discussion that followed, the use of a common mass storage device (tape or disk) that is "dual ported" or simultaneously connected to two C.P.U.'s was mentioned. This is very efficient if the hardware allows this option and the data systems are both from the same manufacturer. Several people mentioned a need to communicate between G.C. data systems and/or from a GC system to a GC/MS system. Mason Hughes (Monsanto Research - Dayton) described an easy method for transferring data from an H.P.-5985 GC/MS system to an H.P.-3356 lab data system. He has a direct CPU interconnection using RS-232-C lines which allows the 3356 system to function as an "output device" for the 5985 system. ASCII data can be transferred simply by directing the 5985 to "print" on the transfer line, thus permitting access to the much larger storage facilities of the 3356 system.

There seemed to be a general feeling that given the cost of mass spectrometer data systems, they should be better able to communicate with other systems. This would necessitate adoption of some sort of standardized data format and transmission protocol for it to work successfully. It also seemed apparent that there is a much greater interest in this topic than existed when it was last discussed (roughly four years ago); and that many people have created useful systems on their own. There seem to be almost as many ways to communicate between systems as there are laboratories needing this capability.

The workshop concluded at roughly 4:45 PM, although attendance had dwindled somewhat at this point.

Respectively submitted,

Tom Terwilliger

D. Thomas Terwilliger

Good Laboratory Practices Workshop

The Good Laboratory Practices (GLP) workshop was held on Thursday, June 10 at 2:00 p.m. Approximately 35 people attended. The meeting began with a review of the objectives of the GLP committee. These are:

1. To keep mass spectroscopists aware of the government regulations which might affect their work.

2. To provide a conduit for discussion and response to current and proposed regulations.

3. To serve as a link between ASTM Committee E-14 and ASMS. This should serve to broaden the consensus for ASTM documents.

4. To provide a continuing forum for the discussion of quality assurance as it applies not just to government regulations but to the entire range of mass spectrometry.

5. To provide a nonadversarial setting for discussions between government regulators and those being regulated.

Two articles regarding computer-generated data were brought to the attention of the attendees: Computer Evidence in Federal Courts, Commercial Law Journal, 266, Aug/Sept 1979 and Proposed Changes to the Federal Rules of Evidence as Applied to Computer Generated Evidence, Journal of Computers, Technology and Law, Vol. 7, 157, 1979. A general discussion regarding long-term data storage followed. Dr. William Budde, U.S.E.P.A., said that he had begun using a magnetic tape called Inmac Plus from Inmac Corp., 2465 Augustin Dr., Santa Clara, CA 95051. This is a thicker, more durable tape than most. Similar types of tapes are probably available from most magnetic tape manufacturers.

Dr. James Sphon, F.D.A., showed a slide presentation outlining the reasons behind, and the major sections of, the GLP regulations. This was followed by a discussion about what FDA inspectors look for in our audit. The final part of the meeting was devoted to a more general discussion regarding quality assurance in mass spectrometry laboratories with Drs. Sphon, Budde and Alkalay (Ciba-Geigy) answering questions from the floor.

Respectfully Submitted,

Anthony DeStefano

st/AJDglp
6/18/82

Report on Workshop: Resolution in MS/MS

Introduction: Desorption methods of ionization and mass spectrometry/mass spectrometry are two major advances in recent years. These two techniques, although developed in parallel, may operate in series in the future to provide a powerful method for the analysis of biological materials. The disadvantages of fast atom bombardment or SIMS include simple spectra showing little fragmentation and poor signal-to-noise ratios. Furthermore, real samples will often be impure leading to difficulties in assigning observed mass peaks to the various components. These problems can be addressed using MS/MS instrumentation. Decomposition reactions can be induced by collision to give structural information and to connect fragmentation peaks. Chemical noise can be removed by using the two stages of mass analysis.

Theme of Workshop: In the framework of the above ideas, it becomes important to assess the state-of-the-art in terms of mass resolving powers and upper mass limits of the various mass analyzers used as MS-I and MS-II in MS/MS. A panel consisting of R.G. Cooks (Purdue University), P.H. Dawson (NRC-Canada), R.T. McIver (U. of California-Irvine), F.W. McLafferty (Cornell University) and R.S. Stradling (Kratos) was assembled to review the current status of MS/MS in terms of resolution and upper mass limit.

It is recognized at the outset that the overall capability of MS/MS is greater than the sum of its individual analyzers. Therefore, the capabilities of each analyzer may not serve as an adequate "figure-of-merit" for the combined system. Nevertheless, this is the only approach to evaluation that can be taken at this time, particularly for evaluation of MS/MS for use with desorption ionization methods.

Discussion: It was suggested (Cooks) that perhaps only one stage of high resolution in MS/MS is needed. It was also suggested (Stradling) that a normal geometry (Nier-Johnson) instrument is all that is needed for MS/MS applications. The difficulties with such instruments are that they give low resolution primary beam selection in the linked scan mode, and the scans are subject to artifact peaks. A discussion of the mass resolution of MS-I followed. It was pointed

MS-I Instrument	Mass Resolution	Upper Mass Limit
E in EB	500	3000[1]
B in BE	5000	3000
B in BQ	5000	3000
EB in EBE	100,000[2]	3000
Fourier Transform MS	500	Unknown[3]
Q in QQQ	Unit(?)	1000-2000

(1) Magnet system on commercially available high performance instrument.
(2) Demonstrated at the Univ. of Nebraska.
(3) Unlimited upper mass in theory; ca. 1500 demonstrated at 1.9 Tesla.

out that with careful design of the collision cell, CID spetra can be acquired with modest signal averaging at the resolving power of MS-I (Gross). A paper covering the design and evaluation of an EBE instrument will appear soon in Int'l. J. M. S. I. P.

The demonstrated capabilities of MS-II are also varied, and they are summarized as follows: The resolution of the ESA as in BE or EBE

MS-II	Mass Resolution	Upper Mass Limit
B as in EB	1000	Det'd by B
E as in BE & EBE	200	Det'd by E
B as in BEB[1]	300	Det'd by B
Q as in BQ or QQQ	1000	1000-2000
FT-MS	10,000 at m/z 43	Unknown

(1) New instrument under construction at VG. Quoted R for MS-II operated after deceleration of ion beam, CID, and reacceleration is 3000. Demonstrated R to date is 300.

instrument is adequate for many applications at low molecular weight, but it will be found inadequate for studies of higher molecular weight substances. The resolving power of the quadrupole is adequate for many current applications, but its mass range and transmission at high mass are not sufficient for studies above m/z 1000-1500. Some improvements can be made, however, such as lengthening the rods and lowering the frequency (Dawson).

The resolution of FT-MS for MS/MS studies can be improved by admitting the collision gas using a pulsed valve and removing it for mass analysis (McIver). Pulsed gas studies are underway at the Univ. of California-Irvine, Purdue, and Nebraska. Higher magnetic fields currently used will permit greater excitation of the ion to be studied as well as better resolution for daughter ion analysis.

The proposed BT instrument (Enke) may be useful for studies of biological materials. The present expectations are to obtain a mass resolution of ca. 1000.

It was suggested that the best resolution of tandem sector instruments will be achieved by deceleration of the beam prior to collision followed by reacceleration (Cooks, Gross). However, the location of collision cells beyond the object focus of Nier-Johnson instruments is not optimum, and results taken with these innstruments should not be viewed as measures of the optimum resolving power achievable using linked scanning EB analyzers as MS-II.

One objective of the workshop was to examine whether an ideal instrument exists for MS/MS studies of higher mass materials. Although some conclusions are possible in terms of what analyzers should not be excluded, the form of the MS/MS instrument of the future is not yet established.

Submitted by:

Michael L. Gross
Professor of Chemistry
University of Nebraska-Lincoln
Lincoln, NE 68588

WORKSHOP — Standard Operating Conditions for Triple Quadrupoles While Acquiring Library MS/MS Spectra

Organizer — P.H. Dawson, National Research Council of Canada

Panel Members — J.D. Morrison, LaTrobe University
C. Enke, Michigan State University
W.R. Davidson, Sciex Inc.
U. Steiner, Finnigan /MAT

The chairman presented a brief introduction, pointing out that low energy collision-induced dissociation spectra are a very strong function of the chosen operating conditions - especially collision energy and target thickness (or pressure × length of the collision cell) and also depend upon the mode of operation of both the second and the third quadrupoles. There has already been some move towards establishing spectral libraries and if these are to be useful in a general way, that is, with transferability of data from one laboratory to another and one machine to another, it is essential that, at the minimum, the conditions under which they are acquired be well defined and preferable that the spectra be acquired under a standard set or sets of conditions.

The first question put to the panel was if the development of the instrumentation and our knowledge of the CID mechanism had reached the stage where such conditions could be adequately defined. Chris Enke said that he would be pleased if the outcome of the workshop discussion was a consensus on how conditions could be defined and compared in different laboratories - for example, by comparisons of results on a specified parent ion. Bill Davidson agreed that this was a necessary first step but, as an analytical chemist involved in applications, he felt that it was urgent to move to agreement on some standardised conditions for library spectra before each user began collecting his own personal libraries under a wide variety of conditions. Jim Morrison supported the idea that it should be possible to establish comparisons of conditions of operation. He drew the parallel with early discussion concerning EI spectra and their reproducibility. Urs Steiner strongly took the view that comparisons of spectral intensities are not and would not be useful and that libraries, if used at all in a general way, would have to be restricted to the presence or absence of particular daughters with no information on relative magnitudes. This point-of-view was discussed at some length from the floor. In response to questions, both manufacturer's representatives expressed confidence that their instruments leaving the factory gave highly reproducible data, and the general opinion seemed to be that it therefore should be possible to make some meaningful quantitative comparisons using a few selected ions or, at least, that an attempt should be made. The possibility of a round-robin test among different laboratories of a variety of different ions under a single defined set of conditions had been raised. However, in the light of the discussion, it was agreed that it would be better to concentrate on one or two ions under a variety of different experimental conditions. Since several different triple quadrupoles were to be available at the MS/MS workshop at Purdue, it was suggested that this could be the starting point for a comparison. In the absence of any participants from Purdue, this suggestion was well received.

The discussion passed on to consider some specific parameters. It seemed likely that more than one collision energy should be chosen as a standard so that the necessary degree of fragmentation for unambiguous identification could always be achieved. It was suggested also that it might be possible, with a given collision gas, to empirically calibrate the energy scale using a known cross-over point in ion yields from a chosen compound. Target thickness (pressure × length of collision cell, or density × length of collision cell) could be standardised at that necessary to reduce the parent intensity to $1/e$ or $1/e^2$ of its initial value. There was a brief discussion of quadrupole operation but insufficient time to fully pursue these questions.

One point which clearly needed clarification for some members of the audience is that the intent is not to try to impose a standard set of operating conditions in a "black-box" type of situation. Indeed, variation of collision energy is seen as an added dimension to low energy CID which will bring some distinct advantages. For particular analytical problems, the optimum set of conditions will always be sought. However, standard, defined conditions would provide a starting point for the exchange of information and libraries would be useful when dealing with unknowns (as opposed to targetted analysis). These libraries might be organised to search for neutral loss spectra or parent spectra as well as daughter spectra.

As a result of the workshop, it is proposed to initiate a comparison of the spectra from two or three chosen ions taken at various specified conditions (collision energy, target thickness) in different laboratories. As is usual in a round-robin of this sort, the submitted data will be treated in a statistical fashion with no attribution of individual results. This will allow a better assessment of the degree of variability that exists and allow a more concrete discussion at future meetings of what the next step should be. Anyone willing to take part in this simple test should contact as soon as possible

P.H. Dawson
Division of Physics
National Research Council of Canada
Ottawa, Canada K1A 0R6

Workshop Report

"Collision-Induced Decompositions - Internal Energy Effects"

In his introductory remarks, the Chairman outlined the generally accepted procedure for the use of collision-induced decomposition of ions in the study of ion structure but emphasized the need for a carefully-argued logical discussion of observations, which was not always evident in some publications. This was particularly important in establishing the credibility of the technique with chemists who did not work in the field of mass spectrometry. Professor McLafferty suggested that the strengths and weaknesses of the technique were similar to those of electron ionization but asserted that as the size of the ion increases (reducing the possibility of the existence of isolated states) the chances of interference from internal energy effects decrease. The relative abundances of fragment ions given by the collision-induced dissociation of ions of the same structure may vary by ±5% and it is possible that for some ions, part of this irreproducibility may be due to small differences arising from internal energy effects. On the other hand, Professor Bowers described several systems, exemplified by protonated dimethyl ether and protonated ethanol, in which interconversion between the two structures was not possible and for which the relative peak intensities in the collision-induced decomposition spectra varied by considerably more than ±5% as the pressure was varied in the chemical ionization source ion in which the ions were generated. This was interpreted as being due to the decrease in average internal energy due to collisional deactivation as the source pressure was raised.

A lively discussion ensued and it was clear that opinions were divided on the likelihood that internal energy effects were a general complication in the interpretation of the collision-induced spectra of ions. Professor Cooks pointed out that identical internal energy distributions would give identical breakdown curves and insofar as the technique produces identical internal energy distributions, it works reasonably well in the investigation of ion structures. Nevertheless, one could not rule out the existence of internal energy effects in some systems. After contributions from Professor Freiser on the use of FTICR to study collision-induced decomposition of ions, Professor Gross on the need to improve reproducibility if small differences were to be judged of significance, together with other contributions from the floor, it was necessary to stop at 4:55 p.m. A continuation of the discussion at the 1983 meeting would certainly be appropriate.

The attendance at the workshop was estimated to be approximately 65-75.

K. R. Jennings

WORKSHOP REPORT ON

FAB: WHERE ARE WE NOW?

A work shop was held to discuss current applications in several laboratories, focus on outstanding problems and evaluate relevant reports presented earlier in the week of this 30th ASMS meeting.

Panel members included:

Dr. Richard M. Caprioli, University of Texas Medical School, U.S.A.
Dr. Catherine E. Costello, Massachusetts Institute of Technology, U.S.A.
Dr. Yasuhiro Itagaki, Joel Ltd., Japan.
Dr. Dudley H. Williams, University of Cambridge, U.K.

The combined expertise of the panel members included a broad cross-section of FAB experience including quadrupole and sector instruments, low and high resolution as well as low and high mass analysis.

The meeting was opened with a short review of current applications in each of the panel members' respective laboratories followed by discussions and questions from the audience. This was followed by a series of short comments by selected attendees of the symposium.

Although the panel members presented and discussed many new applications utilizing FAB MS, from their own and other laboratories, the experimental approaches described indicated surprising continuity when considering the short period of time that the technique has been with us and the breadth of analyzed samples. The similarity of ion fragments obtained from SIMS and FAB MS was mentioned and this point was described in greater detail in Paper WOB 2, presented by K.L. Busch and R.G. Cooks. Moreover, an interlaboratory study coordinated by R.C. Murphy and K.L. Clay, Paper WOB 3, was summarized. This discussion indicated that for analysis of a broad range of compound classes, utilizing a number of different instruments, that FAB MS analyses were as reproducible as EIMS.

Comments were brought forth about the little success in finding alternative material to serve as a sample matrix which would replace glycerol. However, conclusions gleaned from these discussions suggest, that in some cases, FAB sensitivities can be enhanced when additives or dopants are added to the glycerol which appears to increase the sample solubility.

Comments from the floor were presented on instrumental operation, inexpensive electrostatic vs oscillograph recording (W. Ligon) and data system modifications to accept FAB data (S. Carr).

The session had 122 attendees.

Organizer
Vernon N. Reinhold, Ph.D.
Harvard University Medical School

Workshop Report

QUANTITATIVE QUADRUPOLE MASS SPECTROMETRY

The objective of the workshop was to explore several of the instrumental factors affecting the use of quadrupoles in accurate relative abundance measurements. The workshop was sponsored by the ASMS Committee on High Temperature Mass Spectrometry. About 28 persons were in attendance.

Discussion centered primarily on two topics, (1) mass discrimination effects in quadrupole mass filters, and (2) the mass dependence of particle multiplier detection efficiency. M. A. Frisch, IBM Research Lab; A. Yergey, NIH; D. L. Hildenbrand, SRI International; and R. J. Colton, Naval Research Lab presented relative abundance data obtained with quadruoples over variable mass ranges. These results showed that, although mass discrimination effects could be very serious and even misleading under certain conditions, it was possible to minimize discrimination effects with careful attention to variable ion energy programming. A great deal of lively discussion ensued regarding the extraction and transmission of ion beams in quadrupoles, and comparisons with magnetic sector instruments, but it was generally agreed that useful spectra can be obtained with proper cognizance of the inherent instrumental effects.

R. J. Buehler, Brookhaven National Lab, then discussed the results of some measurements of secondary electron multiplier efficiencies for ions of different mass and energy. The results, summarized in Int. J. Mass Spectrom. Ion Phys. 23, 81 (1977), showed again that mass effects could be serious, and defined the energies required to efficiently detect ions of increasing mass. It was pointed out that these effects would be more serious for quadrupoles with their lower ion energies than for magnetic instruments, where the higher source voltages supplement the multiplier operating voltage. It was strongly recommended that serious consideration be given to high-voltage "post acceleration" of ion beams when mass sensitivity effects of particle multipliers are to be brought under control. Following this, F. T. Greene, Midwest Research Institute, discussed some unusual mass discrimination effects in sampling of high pressure sources with both quadrupole and magnetic instruments.

All in all, the nature of the discrimination problem was brought into sharper focus, and there was much useful information exchanged among the workshop participants.

D. L. Hildenbrand

Workshop Report

Laser Mass Spectrometry for the Production and Measurement of Inorganic Ions

Within the last few years, dramatic developments have occurred in the physics and chemistry communities that command the attention of all who are interested in the efficient and selective formation and measurement of ions. The laser-mass spectrometry interface that results from these developments encompasses a large variety of optical mechanisms and measurement capabilities ranging from "single atom" atomic detection to the complex multi-photon ionization and laser desorption of higher molecular weight organic molecules. Since it was not feasible to condense the complete scope of this interface into a single workshop that is constrained to inorganic isotope considerations, the theme of this workshop was the formation and measurement of inorganic ions, principally atomic, by laser mass spectrometry.

More specifically, the objectives of this workshop were to highlight selected emerging areas of research related to the use of lasers for ion formation and measurement in mass spectrometry, and to provide an opportunity for dialogue among current and candidate researchers. The scientific and technical backgrounds of various optical mechanisms for ion formation were combined with perspectives on applications and an overview of current and projected laser technology. Audience participation was encouraged through discussion and questions during the workshop. Specifically addressed were questions of current interest, including laser duty cycle, range of applicability, ionization efficiency and selectivity, and the measurement potential for selected isotopes.

Principles leading to the formation of ions using resonance ionization were summarized by T. Whitaker, Atom Sciences, Inc., Oak Ridge, Tennessee. Previous research was described for the ionization and detection of alkali and rare gas atoms using pulsed laser systems. A new mass spectrometer was described whose ion source will utilize a pulsed ion bombardment beam synchronized with a repetitively pulsed laser. This arrangement would maximize the duty cycle or "on-time" and permit selective and efficient resonance ionization of the ablated neutral species produced during ion bombardment. Questions were posed regarding the optimal position of the laser beam relative to the ablated plume and the apparent limitation of accessing a single element with a given laser configuration. Suggestions were given by the speaker that dye changes and attendant wavelength accessibility are easily achieved to permit sequential elemental measurements, and that preliminary calculations indicated an optimal laser beam position about one mm above the sample surface. The attributes of ionization efficiency ($\geq$ 90%) and selectivity were discussed as the predominant features of the new mass spectrometry measurement capability, and the potentially broad elemental coverage of the periodic table available with existing laser technology was mentioned.

Some of the calculations and considerations involving the use of continuous wave (cw) lasers for the production of inorganic ions were summarized by N. Nogar of Los Alamos National Laboratory. Although most research directed toward the formation of inorganic ions has used pulsed laser technology, there are substantial measurement advantages to be realized in many experimental problems from the use of a continuous source of ions instead of pulsed ion packets. The possibilities of ion formation were compared generally for pulsed vs. cw technology, leading to a conclusion that by cleverly applying cw lasers, a large number of elemental ionization and isotopic measurement capabilities could be realized. A mass spectrometer using an isotopically selective cw detection system was described that may lead to isotopic abundance sensitivities approaching 10^{11} for single magnetic sector instruments.

Basic instrumentation and performance characteristics of the Laser Microprobe Mass Analyzer (LAMMA-500) manufactured by Leybold-Heraeus, were summarized by D. Simons of the National Bureau of Standards. Ion formation by laser ablation was characterized briefly, and the tendency of the ionization process to form singly charged ions was described. The relatively high abundance of Mo^{++} from a metallic molybdenum target was noted. Dynamic range and measurement limitations of the 100 MHz transient digitizer were described, and the inability to produce 8 bit measurement resolution in the analyses of real samples was cited. Although it was possible to demonstrate the measurement of osmium isotopic ratios from nanogram samples to within 5% RSD, it was felt that the detector system currently

used may be a limitation in the measurement accuracy. The development of a sample stage and associated laser and ion optics for reflection ionization was briefly described by B. Schueler of the University of Frankfurt for the new LAMMA-1000.

To familiarize mass spectroscopists with the kind and level of laser technology required for typical laser mass spectrometry configurations, R. Mortensen of Quanta-Ray presented a laser overview. A range of laser systems was described and categorized according to continuous wave and pulsed sources. The wavelength capabilities of the various lasers were discussed and the requirements described for covering the wavelength range from the infrared to the near-UV. A system comprised of a tunable dye laser pumped by a Nd·YAG pulsed laser, together with appropriate frequency multiplication, was described as a way to access a broad spectral range of tunable radiation. The investment for these systems was described, which ranged from a few thousand dollars for the simplest to well over a hundred thousand dollars for a broadly tunable and versatile system. Finally, the range of capabilities was roughly categorized by level of required maintenance. Optimism was also expressed for a future of steady progress in breadth of wavelength capability, solid state tunability, ease of use and applicability to a broad spectrum of measurements.

L. J. Moore
National Bureau of Standards
Workshop Chairman

OFFICERS

ASTM COMMITTEE E-14 AND THE AMERICAN SOCIETY FOR MASS SPECTROMETRY

Year	President	Vice President (Programs)	Vice President (Arrangements)	Vice President (Data & Stds.)
		ASTM E-14		
1961-2	V.H. Dibeler	R.E. Fox	R.A. Brown	-
1963-4	R.E. Fox	N.D. Coggeshall	A.G. Sharkey	-
1965-6	N.D. Coggeshall	H.M. Rosenstock	M.K. Testerman	-
1967-8	H.M. Rosenstock	J.L. Franklin	D.B. Harrington	-
1968-9	J.L. Franklin	R.E. Honig	C.E. Johannsen	-
		ASMS		
1970	J.L. Franklin	R.E. Honig	C.E. Johannsen	H.R. Harless
1971-2	R.E. Honig	F.H. Field	G.L. Kearns	H.R. Harless
1972-4	F.H. Field	H.J. Svec	A.H. Struck	E. Lumpkin
1974-6	H.J. Svec	J.H. Futrell	W.H. Brubaker	*
1976-8	J.H. Futrell	J.A. McCloskey	E.J. Bonelli	-
1978-9	J.A. McCloskey	B. Munson	E.J. Bonelli	-
1979-80	J.A. McCloskey	B. Munson	W.A. Wolstenholme	-
1980-1	B. Munson	C.C. Fenselau	W.A. Wolstenholme	-
1981-2	B. Munson	C.C. Fenselau	K.R. Compson	-

*ASTM E-14 Chairman was dropped as a Vice President and made Member-at-Large in 1974.

Year	Secretary	Treasurer	Members-at-Large	
		ASTM E-14		
1961	C.F. Crable	-	J.H. Beynon	C.F. Robinson
1963-4	H.E. Lumpkin	-	S. Meyerson	A.L. Wahrhaftig
1965-6	G.L. Cook	-	H.I. Schiff	W.M. Hickam
1967-8	A.B. King	-	E.E. Muschlitz	R.M. Teeter
1969	J.M. McCrea	-	R.F. Porter	J.T. Herron
		ASMS		
1970	J.M. McCrea	H.D. Cook	R.F. Porter	J.T. Herron
1971-2	F.E. Saalfeld	H.D. Cook	A.G. Sharkey	A.L. Wahrhaftig
1972-4	F.E. Saalfeld	M.T. Laug	J. Berkowitz	E.B. Owens
1974-6	J.A. McCloskey	M.T. Laug	P. Kebarle +E.M. Emery	J.L. Margrave
1976-7	K.E. McCulloh	M.T. Laug	H.M. Fales	A.G. Harrison
1977-8	H.M. Fales	M.A. Frisch	H.M. Fales +E.G. Carlson	A.G. Harrison
1978-9	H.M. Fales	M.A. Frisch	C.C. Fenselau +M.C. Hamming	A.G. Harrison
1979-80	H.M. Fales	M.A. Frisch	C.C. Fenselau +M.C. Hamming	W.L. Fite
1980-1	H.M. Fales	M.A. Frisch	J.T. Watson +M.C. Hamming	W.L. Fite
1981-2	T.R. Ashe	M.A. Frisch	J.T. Watson +T. Aczel	F.W. Lampe

+ASTM E-14 Chairman

MEMBER NAME	ADDR1	ADDR2	ADDR3	CITY	STATE	ZIP CODE
ABBOTT F S	UNIV BRIT COLUMBIA	PHARMACEUTICAL SCI		VANCOUVER, BC		V6T 1W5
ARSENAULT GUY P	RR 2	MIDDLE ROAD		KINGSTON,ONTARIO		K7L 5H6
BAADSGAARD HALFDAN	5220-114 B STREET			EDMONTON,ALB		T6H 3N5
BENUIT F M	HEALTH-WELFARE DEPT	ENVIRONMENTAL HEALTH	TUNNEYS PASTURE	OTTAWA, ONTARIO		K1A 0L2
BERTRAND M J	UNIV OF MONTREAL	CHEMISTRY DEPT	C.P. 6210 SUK.A	MONTREAL, QUEBEC		H3C 3V1
BOURDONNAIS CLAUDE R	14 MICHAEL ST			KIRKLAND,QUEBEC		
BUCKLEY J A	SCIEX INC	55 GLENCAMERON RD	SUITE 202	THURNHILL, ONTARIO		L3T 1P2
CUMISAROW M B	UNIV BRIT COLUMBIA	CHEMISTRY DEPT	2036 MAIN MALL	VANCOUVER, BC		V6T 1Y6
COULOMBE P L	ANALYTECH	742 MOONEY'S BAY PL		OTTAWA, ONTARIO		
DAVIDSON W R	SCIEX INC	55 GLENCAMERON RD	SUITE 202	THORNHILL, ONTARIO		L3T 1P2
DAWSON P H	NAT RESEARCH COUNCIL	PHYSICS DEPT		OTTAWA, ONTARIO		K1A 0R6
DOUGLAS D J	SCIEX INC	55 GLENCAMERON RD	SUITE 202	THORNHILL, ONTARIO		L3T 1P2
DURDEN DAVID A	PSYCHIATRIC RES DIV	508A UNIV HOSP		SASKATOON,SASK		S7N 0X0
FULFORD J E	SCIEX INC	55 GLENCAMERON RD	SUITE 202	THORNHILL, ONTARIO		L3T 1P2
HERMAN J A	UNIVERSITE LAVAL	CHEMISTRY DEPT		QUEBEC, QUEBEC		G1K 7P4
HOGG A M	UNIV OF ALBERTA	CHEMISTRY DEPT		EDMONTON, ALBERTA		T6G 2G2
HOGGE LAWRENCE R	NAT'L RES COUNCIL	110 GYMNASIUM RD		SASKATOON,SASK		S7N 0W9
JAMIESON W D	NRC	1411 OXFORD ST		HALIFAX, NOVA SCOTIA		B3H 3Z1
KALLOO M	MERCK SHARP & DOHME	PO BOX 899		POINTE CLAIRE QUEBEC		H9R 4P7
KEBARLE P	UNIV OF ALBERTA	CHEMISTRY DEPT		EDMONTON, ALBERTA		T6G 2G2
LAO R C	ENVIRONMENT CANADA	CHEMISTRY DIV	APCD	OTTAWA, ONTARIO		K1A 1C8
LAU BENJAMIN P	HEALTH & WELFARE CAN	FOOD RESEARCH	TUNNEY'S PASTURE	OTTAWA,ONTARIO		K1A 0L2
LOVETT A M	SCIEX INC	55 GLENCAMERON RD	SUITE 202	THORNHILL, ONTARIO		L3T 1P2
MAGNERA T	UNIV OF ALBERTA	CHEMISTRY DEPT		EDMONTON, ALBERTA		T6G 2G2
MAMER OKVAL	MCGILL UNIV	1130 PINE AVE WEST		MONTREAL, QUEBEC		H3A 1A3
MARTIN TREVOR I	XEROX RESEARCH CTR	2480 DUNWIN DR		MISSISSAUGA ONT		L5L 1J9
MASSE ROBERT	INRS-SANTE	7401 HOCHELAGA		MONTREAL,QUEBEC		H1N 3M5
MCMAHON T B	UNIV NEW BRUNSWICK	CHEMISTRY DEPT		FREDERILTON, NB		E3B 5A3
MILES W F	PLANT PRODUCTS	LAB SERVICES DIV	BLDG #22, C.E.F.	OTTAWA, ONTARIO		K1A 0C6
NACSON S	SCIEX INC	55 GLENCAMERON RD	SUITE 202	THORNHILL, ONTARIO		L3T 1P2
RAMALEY L	DALHOUSIE UNIVERSITY	CHEMISTRY DEPT		HALIFAX, NOVA SCOTIA		B3H 4J3
REID N M	SCIEX INC	55 GLENCAMERON RD	SUITE 202	THORNHILL, ONTARIO		L3T 1P2
REYNOLDS JAMES	SCIEX	55 GLENCAMERON RD		THORNHILL,ONT		L3T 1P2
ROSENBLATT GORDON	SCIEX	55 GLENCAMERON RD		THORNHILL,ONT		L3T 1P2
SAULIER R W	10 WOODMAN SR	NO. 402		HAMILTON, ONTARIO		L8K 4E1
STANDING K	UNIV OF MANITOBA	PHYSICS DEPT		WINNIPEG, MANITOBA		R3T 2N2
TANNER SCOTT D	SCIEX INC	55 GLENCAMERON RD		THORNHILL, ONTARIO		L3T 1P2
TASSONE ROSINA	SCIEX	55 GLENCAMERON RD		THORNHILL,ONT		L3T 1P2
THOMSON B	SCIEX INC	55 GLENCAMERON RD	SUITE 202	THORNHILL, ONTARIO		L3T 1P2
WESTMORE J B	UNIV OF MANITOBA	CHEMISTRY DEPT		WINNIPEG, MANITOBA		R3T 2N2
WOOD G W	UNIV OF WINDSOR	CHEMISTRY DEPT		WINDSOR, ONTARIO		N9B 3P4
YAMDAGNI R	UNIV OF CALGARY	CHEMISTRY DEPT		CALGARY, ALBERTA		T2N 1N4

MEMBER NAME	ADDR1	ADDR2	ADDR3	CITY	COUNTRY
NIWA TOSHIMITSU	3584-4,KOHRI	KONAN		AICHI	JAPAN
NOMURA HIROSHI	1-5-3 CHIGUSA	OBAMA		FUKUI 917	JAPAN
OHASHI M	DEPT MATERIALS SCI	UNIV OF ELEC-COMMUN	CHOFU	TOKYO 182	JAPAN
PANNELL LEWIS K	P O BOX 13447			CHRISTCHURCH 1	NEW ZEALAND
PESCH REINHOLD	FINNIGAN CORP	355 RIVER OAKS PKWY		SAN JOSE	
PRZYBYLSKI M P	UNIV MAINZ	INST ORG CHEMIE		D-6500 MAINZ	WEST GERMANY
RACE JOHN A	VG ANALYTICAL LTD	3 TUDOR RD		ALTRINCHAM WA145RZ	ENGLAND
RICHTER WILLIAM J	CIBA GEIGY	K 127.508		CH-4002 BASEL	SWITZERLAND
ROSMAN K J	WA INST OF TECH	PHYSICS DEPT		SO BENTLEY, WA 6102	AUSTRALIA
RYAN P A	KRATOS SCIEN APP LTD	BARTON DOCK ROAD	URMSTON	MANCHESTER, M31 2LD	ENGLAND
SAITO K	KANSAI MEDICAL SCH	DEPT MEDICAL CHEM	MORIGUCHI	OSAKA 570	JAPAN
SAKAI IKUO	TORAY RESEARCH CTR	1111 TEBIRO		KAMAKURA	JAPAN
SANTIKARN SITTHIVET	28 STRETTEN AVE			CAMBRIDGE CB4 3EP	ENGLAND
SCHUCH D	LEGIENSTRASSE 33A			D-6230 FRANKFURT 80	WEST GERMANY
SCHUELER BRUNO	MESSELER STR 24			DARMSTADT D-6100	W GERMANY
SENN M	BUEHRINGER MANNHEIM			D-6800 MANNHEIM	WEST GERMANY
SHINKA T S	KURUME UNIVERSITY	RES INST OF MED MS		FUKUOKA, 830	JAPAN
SMITH CLIFTON	14 GARLAND RD	ROLEYSTONE		PERTH 6111	AUSTRALIA
STRADLING ROD	KRATOS LTD	BARTON DOCK RD	URMSTON	MANCHESTER M31 2LD	ENGLAND
SUMMONS ROGER E	AUSTRALIAN UNIV	BIOLOGICAL SCIENCES		CANBERRA A.C.T.	AUSTRALIA
SUZUKI M	MEIJO UNIVERSITY	PHARMACY FACULTY	TEMPAKU	NAGOYA, 468	JAPAN
TATEMATSU A	MEIJO UNIVERSITY	PHARMACY FACULTY	TEMPAKU	NAGOYA, 468	JAPAN
TAYLOR KEITH	KRATOS LTD	BARTON DOCK RD	URMSTON	MANCHESTER M31 2LD	ENGLAND
TSUCHIYA M	4 37 27 KUGAYAMA	SUGINIMI KU		TOKYO, 168	JAPAN
VINCZE ADAM	ISRAEL INST BIOL RESPO	BOX 19		NESS ZIONA 70450	ISRAEL
WANCZEK K P	PARKALLEE 197			D-2800 BREMEN	WEST GERMANY
WILLIAMS DUDLEY H	UNIV OF CAMBRIDGE	CHEMICAL LAB	LENSFIELD RD	CAMBRIDGE LB2 1EW	ENGLAND
WOODWARD HAROLD	135 PENINSULAR RD			GRAYS POINT NSW 2232	AUSTRALIA
WOODWARD HILDA	135 PENINSULAR RD			GRAYS POINT NSW 2232	AUSTRALIA
YAMAGUCHI SANAE	506 HOMAN BIL,8-27	3 CHOME, SHIMIZU	MINAMI-KU	FUKUOKA 815	JAPAN
YINON J	WEIZMANN INS SCIENCE			REHOVOT	ISRAEL
YOUNG HARRY	DSIR	MT ALBERT RES CTR	PRIVATE BAG	AUCKLAND	NEW ZEALAND
ZARETSKII Z	ISOTOPE DEPT	WEIZMANN INST		76 100 REHOVOT	ISRAEL
ARIKAWA TATSUA	TOKYO UNIV OF AG & TA	PPLIED PHYSICS	NAKA-MACHI 2-24-16	TOKYO 181	JAPAN
FUJII TOSHIHIKO	NAT'L INST FOR	ENVIRONMENTAL STUDIE	TSUKUBA	IBARAKI 305	JAPAN
FUKUI MIYOSHI	1229-32 KITANO	NOGUCHI-CHO	KAGOGAWA	HYOGO 675	JAPAN
HARA KENJI	FUKUOKA UNIV	34 NANAKUMA	NISHI-KU	FUKUOKA 814-01	JAPAN
HASHIMOTO YUTAKA	3-31-12 SHIMO	KITA-KU		TOKYO	JAPAN
HAYASHI AKIRA	2-45,SAKUKAGAOKA	YAO		OSAKA 577	JAPAN
HAYASHI AKIRA	9-5 3-CHOME	TSUKUMODAI	SUITA	OSAKA 565	JAPAN
HAYASHI TOKISHI	2620 OGAWAHIGASHI-MA	KODAIRA		TOKYO 187	JAPAN
HIRAI KUISUMI	1-18-14 HARAMACHI	MEGUROKU		TOKYO	JAPAN
HIROSE HIROSHI	4898-4 NAKANE	KATUTA		IBARAK	JAPAN
ICHIMURA KAZUYOSI	302 SIRUBA-COPO	9-20,DAIKYO-TYO	SHINJUKU-KU	TOKYO 160	JAPAN
IGAKASHI KAZUO	1218-30-9-2 MAIKODAI	TARUMI		KOBE,HYOGO 655	JAPAN
IKUTA SHIGERU	TOKYO METRO UNIV	FUKASAWA	SETAGAYA	TOKYO 158	JAPAN
INOUE MASAO	13-2-404 SHIROKANEDA	3-CHOME	MINATO-KU	TOKYO 108	JAPAN
KAMMEI Y	1418 NAKAGAMI	AKISHIMA		TOKYO 196	JAPAN
KATO EIICHI	3-34-9 DAITA	SETAGAYAKU		TOKYO 155	JAPAN
KATO RYUICHI	35 SHINANOMACHI	SHINJUKU-KU		TOKYO 160	JAPAN
KINOSHITA HARUKI	3-41-8 TAKAO	TOSHIMA-KU		TOKYO	JAPAN
KISHIMOTO TAKAO	4-3-32 TAISUMI-HIGAS	IKUNOKU		OSAKA 544	JAPAN
KUGA MINORU	1-4-205 ISEIGAOKA	YAHATANISHI-KU		KITAKYUSHU 807	JAPAN
KOJIMA HARUMI	26-2 TOOGOK	8-CHOME	102 SETAGAYA-KU	TOKYO	JAPAN
KOJIMA TOHRU	AJINADAI 1-20-19	HATSUKAICHI-CHO	SAEKI-GUN	HIROSHIMA 738	JAPAN

MEMBER NAME	ADDR1	ADDR2	ADDR3	CITY	COUNTRY
ALDERWEIRELDT FRANK	UNIV OF ANTWERP	GROENENBORGERLAN 171		2020 ANTWERP	BELGIUM
APLIN R T	DYSON PERRINS LAB	SOUTH PKS RD		OXFORD	ENGLAND
ARPINO P J	ECOLE POLYTECHNIQUE	LAB CHIM ANAL PHYS		91128 PALAISEAU	FRANCE
BENNINGHOVEN ALFRED A	DOMAGKSTRASSE 75			4400 MUNSTER	W GERMANY
BILL JOHN C	VG ANALYTICAL LTD	4 TAXMERE CLOSE	SANDBACH	CHESHIRE	ENGLAND
BLUM WOLFGANG	HEINRICH HAAS STR.26			D 7858 WEIL-5	W GERMANY
BRANDENBERGER HANS	GERICHKEMISCHE	ABTEIHING	UNIV OF ZURICH	8028 ZURICH	SWITZERLAND
BRUNNEE C	FINNIGAN MAT	BARKHAUSENSTR 2	POSTFACH 14 4062	D-2800 BREMEN 10	WEST GERMANY
BUCHS A P	UNIV DE GENEVE	MASS SPECTROMETRY	16 BD D'YVOY, SCI 1	CH-1211 GENEVE 4	SWITZERLAND
BUCHS MINA	9 CHEMIV DES VVATTES			GENEVA	SWITZERLAND
CANTLE JOHN	VG ISOTOPES	ION PATH ROAD 3		WINSFORD CHESHIRE	ENGLAND
CLAEYS M M	UNIV INSTELL ANTWERP	PHARMACY DEPT	UNIVERSITEITSPLEIN 1	B-2610 WILRIJK	BELGIUM
DE LEENHEER ANDRE P	FARMACEUTISCH INST	MELKERIJSTRAAT 96		B-9000 GENT	BELGIUM
DERRICK PETER J	UNIV OF NEW S WALES	CHEMISTRY DEPT	PO BOX 1	KENSINGTON NSW 2033	AUSTRALIA
DIXON DAVID	HEWLETT PACKARD GMBH			WALDBRONN D-7517	W GERMANY
ELLIOTT MARTIN	VG ISOTOPES	ION PATH	ROAD THREE	WINSFORD, CHESHIRE	ENGLAND
ESMANS E	UNIV ANTWERPEN	ORGANISCHE SCHEIKUND	GROENENBORGLN 171	B-2020 ANTWERPEN	BELGIUM
FRAISSE DANIEL J	SPEC DE MASSE	SCA-CNRS	BP 22	69390-VERNAISON	FRANCE
GASKELL S J	TENOVUS INSTITUTE	WELSCH NAT'L SCH OF		CARDIFF CF4 4XX	WALES
GAUMANN T	EPFL-ECUBLENS	INST DE CHIMIE PHYS		CH-1015 LAUSANNE	SWITZERLAND
GREEN B N	VG ORGANIC LTD	TUDOR RD		ALTRINCHAM, CHESHIRE	ENGLAND
GREGOR IAN K	PO BOX 1			KENSINGTON, NSW2033	
HABFAST K E	VARIAN MAT GMBH	BARKHAUSENSTR 2	POSTFACH 14 4062	D-2800 BREMEN 10	WEST GERMANY
HAKAGUCHI KOICHI	307 NISSHIN CORP	1-22-24,SHIMIZU	MINAMI-KU	FUKUOKA 815	JAPAN
HARRIS FRANK	ROYAL SOC	RESEARCH UNIT	UNIV COLL OF SWANSEA	SWANSEA SA2 8PP	ENGLAND
HARRISON ALAN	VG MICROMASS	TRIBUNE AVENUE	ALTRINCHAM	CHESHIRE WA14 5TP	ENGLAND
HARVEY D J	OXFORD UNIVERSITY	PHARMACOLOGY DEPT	SOUTH PARKS RD	OXFORD, OX1 3QT	ENGLAND
HEBEDA ERNARD H	DEBOELELAAN 1085			1081 HV AMSTERDAM	NETHERLANDS
ICHIKAWA H	HOSHI COLL PHARMACY	2-4 EBARA	SHINAGAWA-KU	TOKYO, 142	JAPAN
ISSACHAR D	WEIZMANN INST SCIENC			REHOVOT 76100	ISRAEL
ITAGAKI Y I	JEOL LTD	AKISHIMA	NAKAGAMI CHO 1418	TOKYO, 196	JAPAN
JANSSON MARGITH	KAROLINSKA INSTITUTE	MASS SPECTROMETRY LA		S-10401 STOCKHOLM	SWEDEN
JENNINGS K R	UNIV OF WARWICK	CHEMISTRY &MOLECULAR	SCIENCES DEPT	COVENTRY, CV4 7AL	ENGLAND
JONCKHEERE J A	BRANDSTRAAT 61			B-9131 BEERVELDE	BELGIUM
KANDEL CHARLES K	52 BALACLAVA RD			MELBOURNE VIC 3183	AUSTRALIA
KISHI T	UNIV OSAKA PREF	MUZU UMEMACHI SAKAI	COLL ENGINEERING	SAKAI, 591	JAPAN
KOPRIO JURG	BALZERS	DEPT ECA		9496 BALZERS	LIECHTENSTEI
KRUEGER FRANZ	MESSELER STR. 24			D-61 DARMSTADT 12	WEST GERMANY
KUROKI HIROAKI	403, 2-5-12 NANOKAWA	CHUO-KU		FUKUOKA 810	JAPAN
LAPIDOT AVIVA	WEIZMANN INSTITUTE			REHOVOT 76100	ISRAEL
LAVOLD TORLEIF	P O BOX 26			JARFALLA S-17521	SWEDEN
LIFSHITZ CHAVA	HEBREW UNIV	PHYSICAL CHEM DEPT	MAIL CODE 91904	JERUSALEM	ISRAEL
LOSS ROBERT R	38 GLADSTONE AVE			SOUTH PERTH	W AUSTRALIA
LYNAUGH NORMAN	VG ANALYTICAL LTD	ALTRINCHAM		MANCHESTER	ENGLAND
MACLEOD J K	AUSTRALIA NAT UNIV	RES SCHOOL OF CHEM	PO BOX 4	CANBERRA, ACT 2600	AUSTRALIA
MAEDA KOGORO	ELECTROTECHNICAL LAB	SAKURAMURA		IBARAGI-KEN	JAPAN
MARKLUND STELLAN	UNIV OF UMEA	ORGANIC CHEMISTRY		S-901 87 UMEA	SWEDEN
MATSUDA H	OSAKA UNIV	1-1 MACHIKANEYAMA-CHO	TOYONAKA	OSAKA, 560	JAPAN
MATSUMOTO I M	KURUME UNIVERSITY	RESEARCH INST GC-MS	SCHOOL OF MEDICINE	FUKUOKA, 830	JAPAN
MCEWAN M J	UNIV OF CANTERBURY	CHEMISTRY DEPT		CHRISTCHURCH	NEW ZEALAND
MIZUTANI TAMIO	45-8 NAKABAYASHI-CHO	SHUGAKUIN		KYOTO 606	JAPAN
MORRIS H R	IMPERIAL COLLEGE	BIOCHEMISTRY DEPT		LONDON	ENGLAND
MORRISON J D	LA TROBE UNIVERSITY	PHYSICAL CHEMISTRY		BUNDOORA, VIC 3083	AUSTRALIA
NAKAGAWA Y	SHIONUGI RESEARCH LB	FUKUSHIMA-KU		OSAKA, 553	JAPAN
NIWA T	NAGOYA UNIV HOSPITAL	INTERNAL MEDICINE	1-1-4, DAIKO-CHO	HIGASHI-KU, NAGOYA	JAPAN

MEMBER NAME	ADDR1	ADDR2	ADDR3	CITY	COUNTRY
KOMORI TAKUJI	GOKEN-CHO,1-1-1-105	MITO-SHI		IBARAKI-KEN 310	JAPAN
KOMORI TETSUYA	CHIYO 1-31-5	HAKATA-KU		FUKUOKA 812	JAPAN
KUBUTA E	1418 NALCAGAMI	AKISHIMA		TOKYO 196	JAPAN
KUHARA TOMIKO	991 KOIKE	KOMORINO-MACHI	KURUME	FUKUOKA 830	JAPAN
LUMI TATSUTA	5102-1 TOZUKA	HAWAGUCHI		SAITAMA 333	JAPAN
MASANORI MURITA	3-4-1 KOWAKAE	HIGASHIOSAKA		OSAKA 577	JAPAN
MASUDA YOSHITO	548 KASHIIGAOKA	MATSUZAKI	HIGASHI-KU	FUKUOKA 813	JAPAN
MATSUOKA SHINGO	91 SHIRAKATA	TOKAIMURA	NAKAGUN	IBARAGI 319-11	JAPAN
MATSUSHIMA HAJIME	3776 HANDA-CHO	HAMAMATSU		SHIZUOKO 431-31	JAPAN
METORI KOICHI	1-20-3,NISHIKOUJIA	OOTA-KU		TOKYO 144	JAPAN
MINEO SATUSHI	7-4-16 TAMAGAWAGAKUE	MACHIDA-SHI		TOKYO 194	JAPAN
MIYATA HIDEAKI	82-1,UMEZUNOCHO	MORIGUCHI		OSAKA 570	JAPAN
MORI K	3-3-1 NEW TOKYO BIL	MARUNOUCHI	CHIYAKU	TOKYU	JAPAN
NAGANAWA HIROSHI	3-17,DEN-ENCHOFU	HONCHO	OTA-KU	TOKYO 145	JAPAN
NAGATA TAKEAKI	1327-260,KASHIWARA	MINAMI-KU		FUKUOKA 815	JAPAN
NAKAMURA KANICHI	776 OSUNE-CHO	KOHOKU-KU		YOKOHAMA 222	JAPAN
NAKATA HISAO	147-24,ARIMATSU-URA	NARUMI-CHO	MIDORI-KU	NAGOYA 458	JAPAN
NARUSE HIROSHI	2620 OGAWAHIGASHI-MA	KODAIRA		TOKYO 187	JAPAN
NISHI ISAO	4-21 YAYOICHO	KASHIWASHI		CHIBA 277	JAPAN
NODA TAMOTSU	HIGASHIURA 2-1	5-203,KITAYAMACHO		TOYOHASHI 440	JAPAN
NOGUCHI HIDEYO	FUJISAWA PHARMACEUTI	2-1-6,KASHIMA	TODOGAWA-KU	OSAKA	JAPAN
OKUTANI TSUYOSHI	WAKAMATSU 137	SHATO-AKEBONO 101	AKEBONOCHO	TOYOHASHI 440	JAPAN
SADAYUKI NIIKUNI	DAICHI TAKAHASHISOU	6-9 MINATO	ICHIKAWA	CHIBA	JAPAN
SAITO YAMACHI	KASATORI-CHO 2-57-2	NISHI-KU		NAGOYA 451	JAPAN
SERIZAWA SHIGEO	5-7-15 MAZARIKANE			SHIZUOKA 422	JAPAN
SEYAMA YOUSUKE	16-12 NISHIKATA	2-CHOME	BUNKYO-KU	TOKYO 113	JAPAN
SHIMIZU KYUTARO	TOTTORI UNIV MED SCH			683 YONAGO	JAPAN
SHINKA TOSHIHIRU	55,NOKYU APARTMENT	358-9 NAGATOISHI-MA	CKURUME	FUKUOKA 830	JAPAN
SUZUKI TOMOKAZU	9-30-307,4-CHOME	OKAMOTO	HIGASHINADA-KU	KOBE 658	JAPAN
TAKEDA NAOHITU	1-6-21,SHINSAKAE	NAKA-KU	NAGOYA	AICHI 460	JAPAN
TAKEDA TAKEHIKO	KAKUSAI	SHINBAYASHI	KITA-KODAN 9-701	KYOTO 610-11	JAPAN
TAKEUCHI TAKAE	2,HANDATSUKINUKE-CHO			NAHA 630	JAPAN
TAKEUCHI TOYOHIDE	NAGOYA UNIV	APPLIED CHEMISTRY	CHIKUSA-KU	NAGOYA-SHI	JAPAN
TANAKA KENICHIRO	38 MYODAIJI	OKAZAKI		AICHI 444	JAPAN
TASHIMA TOSHIO	1-7-13-1206 SHINMORI	ASAHIKU		OSAKA 535	JAPAN
TOMIYASU IKUKO	6-4-16 MINAMITSUMORI	NISHINARI-KU		OSAKA 557	JAPAN
TOMIZAWA GIICHI	5-31-13 YATU	NARASHIMI-SHI		CHIBA	JAPAN
TOYOKAZU OHKI	1-3-2 TAMAMIZU-CHO	MIZUHO-KU	NAGOYA	AICHI 467	JAPAN
TSUGE SHIN	NAGOYA UNIV	SYNTHETIC CHEMISTRY		NAGOYA 464	JAPAN
WATANABE KAZUE	MIYAMA 5-1-10	FUNABASHI		CHIBA 274	JAPAN
WATANABE YOSHIO	3-3-1 MARUNOUCHI	CHIYODAKU		TOKYO	JAPAN
YABUUCHI HYAKUJI	OMIYA 4-19-18	ASAHI-KU		OSAKA 535	JAPAN
YAMAMOTO MASAO	1-6-31,KAMIUICHI	NISHINOMIYA		HYOGO 663	JAPAN
YAMAMOTO KENJI	1-12-7 MITSUKUCHI SH	IMACHI		KANAZAWA 920	JAPAN
YAMAMURA YUICHI	1-9-22,TAKADAI	NIKAWA	TAKAKAZUKA	HYOGO 665	JAPAN
YAMAWAKI MICHIO	6-19 BENTEN	URAYASUSHI		CHIBA 272-01	JAPAN
YAMAZOE YASUSHI	931-1 DAIZUTOMACHI	KITAKU	YUKOHAMASHI	KANAGAWA 222	JAPAN
YAMAZOE YASUSHI	35 SHINANOMACHI	SHINJUKU-KU		TOKYO 160	JAPAN
YANO IKUYA	106 KOGANE CHYO			NIIGATA 951	JAPAN
YUTAKA NOZAKI	1110 SHIMOKATO	TAMAHO-MURA	NAKAKUMAGUN	YAMANASHI-KEN 409-38	JAPAN

MEMBER NAME	ADDR1	ADDR2	ADDR3	CITY	STATE	ZIP CODE
ABERTH WILLIAM H	3146 MANCHESTER			PALO ALTO	CA	94303
ABRAMSON F P	GEORGE WASHINGTON UNPHARMACOLOGY DEPT			WASHINGTON	DC	20037
ALZEL T	EXXON R/E	PO BOX 4255		BAYTOWN	TX	77520
ADAMS R A	3480 TANBARK CT NE			ATLANTA	GA	30319
AGNEW MARC N	75 NEW ROAD			KENDALL PARK	NJ	08824
ALKALAY D	CIBA-GEIGY CORP	444 SAWMILL RIVER RD		ARDSLEY	NY	10502
ALKHATIB H	2929 N STREET, NW			WASHINGTON	DC	20007
ALLEN R H	R H ALLEN CO	PO BOX 27		BOULDER	CO	80302
ALLISON J	MICHIGAN STATE UNIV	CHEMISTRY DEPT		EAST LANSING	MI	48824
ANDEREGG R J	UNIV OF MAINE	473 AUBERT HALL		ORONO	ME	04469
ANDERS DON	11473 BRIARWOOD DR			LAKEWOOD	CO	80226
ANICICH V G	8036 GRAYSTONE			SUNLAND	CA	91040
ASHE T R	EXXON R/E	PO BOX 121	"	LINDEN	NJ	07036
AUE D H	UNIV OF CALIFORNIA	CHEMISTRY DEPT		SANTA BARBARA	CA	93106
BACZYNSKYJ L	THE UPJOHN CO	301 HENRIETTA		KALAMAZOO	MI	49001
BAFUS D A	4114 CLOVERNOOK LANE			SEABROOK	TX	77586
BAILEY J	5 JOSH COURT			CLIFTON	NJ	07011
BAN VLADIMIR	1061 GREAT ROAD			PRINCETON	NJ	08540
BARDFSKY D F	OREGON GRAD CTR	19600 NW WALKER RD		BEAVERTON	OR	97006
BARRON K P	FDA	HFD-420	200 C ST SW	WASHINGTON	DC	20204
BARTMESS J E	INDIANA UNIV	CHEMISTRY DEPT		BLOOMINGTON	IN	47405
BAYER CHARLENE W	USGEOLOGICAL SURVEY	6481H PEACHTREE	INDUS BLVD	DORAVILLE	GA	30340
BAYER FORREST	COCA-COLA CO	PO DRWAER 1734		ATLANTA	GA	30301
BECK MARY D	FOREMOST MCKESSON	DUBLIN RES & DEV	6363 CLARK AVE	DUBLIN	CA	94566
BENTZ B L	1017 SALISBURY CT			LANCASTER	PA	17601
BERGER P S	TEKNIVENT CORP	10774 TRENTON CORP		ST LOUIS	MO	63132
BERGKNUT LARS	1214 HELE STREET			KAILUA	HI	96734
BERKOWITZ JOSEPH	ARGONNE NAT'L LAB	PHYSICS DIV	9700 S CASS AVE	ARGONNE	IL	60439
BEUMLER ROBERT J	BROOKHAVEN NAT'L LAB	CHEMISTRY DEPT		UPTON	NY	11973
BIEMANN K	MIT	CHEMISTRY, 56-010		CAMBRIDGE	MA	02139
BIERBAUM V M	UNIV OF COLORADO	CHEMISTRY DEPT	CAMPUS BOX 215	BOULDER	CO	80309
BLOM KARL	6 WENARK DR	APT 1		NEWARK	DE	19713
BOCKHOFF FRANK M	STANDARD OIL CO	4440 WARRENSVILLE CT		CLEVELAND	OH	44128
BONE WILLIAM M	UNIV OF VIRGINIA	CHEMISTRY DEPT	MC CORMICK RD	CHARLOTTESVILLE	VA	22903
BOSHOFF PHILIP	UNIV OF CALIF	CHEMISTRY DEPT		SANTA BARBARA	CA	93106
BOWERS M T	UNIV OF CALIFORNIA	CHEMISTRY DEPT		SANTA BARBARA	CA	93106
BRADFORD DON C	FINNIGAN MAT	845 W MAUDE AVE		SUNNYVALE	CA	94086
BRENT D A	BURROUGHS WELLCOME	3030 CORNWALLS		RESEARCH TRIANGLE PKNC		27709
BRIGGS PHILIP R	HARVARD UNIVERSITY	CHEMISTRY DEPT	12 OXFORD ST	CAMBRIDGE	MA	02138
BRITTEN R A	84 WEST MARIPOSA ST			ALTADENA	CA	91001
BRODASKY THOMAS F	6215 WESTLINS AVE			KALAMAZOO	MI	49009
BROWN C L	CALIFORNIA STATE UN	CHEMISTRY DEPT		LOS ANGELES	CA	90032
BRUBAKER W M	1954 HIGHLAND OAKS			ARCADIA	CA	91006
BRUNFELDT ROBERT J	2721 EVERGREEN DR			BARTLESVILLE	OK	74003
BUDDE W L	EPA	26 W ST CLAIR ST		CINCINNATI	OH	45268
BURINSKY D J	PURDUE UNIVERSITY	CHEMISTRY DEPT	BOX 321	WEST LAFAYETTE	IN	47907
BURLINGAME A L	UNIV OF CALIFORNIA	PHARMCEUTICAL CHEM		SAN FRANCISCO	CA	94143
BURROWS D G	NORTHWEST & ALASKA	FISHERIES CENTER	2725 MONTLAKE BLVD E	SEATTLE	WA	98112
BUSCH KENNETH L	3000 N 300 W	NO 6		W LAFAYETTE	IN	47906
BUTTRILL S E	SRI INTERNATIONAL	333 RAVENSWOOD AVE	RM 204A	MENLO PARK	CA	94025
CALDECOURT VICTOR J	DOW CHEMICAL CO	1603 BLDG,ANAL LAB		MIDLAND	MI	48640
CALLERY P S	UNIV OF MARYLAND	636 W LOMBARD ST		BALTIMORE	MD	21201
CAMERON DOUGLAS	UNION OIL CO OF CA	SCI & TECH DIV		BREA	CA	92621
CAMPANA JOSEPH E	NAVAL RES LAB	CHEMISTRY DIV	CODE 6110	WASHINGTON	DC	20375
CANADA DAVID C	UNION CARBIDE	PO BOX P	K1004B	OAK RIDGE	TN	37830

MEMBER NAME	ADDR1	ADDR2	ADDR3	CITY	STATE	ZIP CODE
CAPRIOLI R M	UNIV OF TEXAS HSC	PO BOX 20708		HOUSTON	TX	77030
CARDACIOTTO STANLEY	AMER CYANAMID CO	PO BOX 400		PRINCETON	NJ	08540
CARLIN J R	MERCK SHARP & DOHME	RESEARCH LABORATORY	PO BOX 2000	RAHWAY	NJ	07065
CARR STEVEN A	LMRRB RM B-08	45 SHATTUCK ST		BOSTON	MA	02115
CARROLL DAVID I	BAYLOR COLL MEDICINE	INST LIPID RESEARCH	TEXAS MEDICAL CENTER	HOUSTON	TX	77030
CARTER JOEL A	RT 7	BOX 487-C		CLINTON	TN	37716
CASABONA L P	TELEDYNE-ISOTOPES	50 VAN BUREN AVE		WESTWOOD	NJ	07675
CHAIT B T	ROCKEFELLER UNIV	1230 YORK AVE		NEW YORK	NY	10021
CHAKEL J A	MICHIGAN STATE UNIV	CHEMISTRY DEPT		EAST LANSING	MI	48824
CHAMBERLIN W S	2183 B 36TH ST			LOS ALAMOS	NM	87544
CHAN C L	E LOS ANGELES COLLEGE	CHEMISTRY DEPT	1301 E BROOKLYN AVE	MONTEREY PARK	CA	91754
CHANDRASURIN PISAL	BURROUGHS WELLSOME	3030 CORWALLIS ROAD		RES TRI PARK	NC	27709
CHANG C	WRIGHT STATE UNIV	BREHM LAB		DAYTON	OH	45431
CHANG S Y	MCNEIL PHARMACEUTICAL	WELSH & MCKEAN RD		SPRING HOUSE	PA	19477
CHANG T L	AMERICAN CYANAMID	1937 W MAIN ST		STAMFORD	CT	06904
CHATFIELD D A	SAN DIEGO STATE UNIV	CHEMISTRY DEPT		SAN DIEGO	CA	92182
CHENG MICHAEL T	CORNELL UNIV	BOX 396	BAKER LAB	ITHACA	NY	14850
CHENG CHIN S	2806 S CONNOR ST			SALT LAKE CITY	UT	84109
CHESS EDWARD K	BATTELLE NWST LABS	PO BOX 999		RICHLAND	WA	99352
CHING STEPHANIE	HAWAIIAN SUGAR PLANT	PO BOX 1057		AIEU	HI	96701
CHINN D M	UNIV OF UTAH	CTR HUMAN TOXICOLOGY	SKAGGS HALL 38	SALT LAKE CITY	UT	84112
CHO D K	SYNTEX RESEARCH	3401 HILLVIEW AVE		PALO ALTO	CA	94304
CHRISTIE W H	ORNL, UNION CARBIDE	PO BOX Y, BLDG 9735		OAK RIDGE	TN	37830
CLARK JUSTIN S	PRIMARY CHDN'S HOSP	BIOPHYSICS DEPT	320 12TH AVE	SALT LAKE CITY	UT	84103
CLAUS MIKE	PO BOX 751			BARNEGAT	NJ	08005
CLAY R L	UNIV OF COLORADO	MEDICAL CENTER	4200 E 9TH AVE	DENVER	CO	80262
CODY R B	PURDUE UNIVERSITY	CHEMISTRY DEPT	PO BOX 355	WEST LAFAYETTE	IN	47907
COLBY BRUCE N	S-CUBED	BOX 1620		LAJOLLA	CA	92038
COLLINS G J	STAUFFER CHEM CO			DOBBS FERRY	NY	10522
COLTON R J	NRL	CODE 6110		WASHINGTON	DC	20375
COMPSON K R	26A FRANKLIN AVE			MONTVALE	NJ	07645
CONNELL JOHN D	KRATOS SCIENTIFIC	603 ROSE CT		LISLE	IL	60532
CONRAD EDWARD C	355 COMMERCE DR			AMHERST	NY	14226
CONTRATTO FRANK	5225-1 VERONA RD			MADISON	WI	53711
COOK J C	UNIV OF ILLINOIS	CHEMICAL SCIENCES		URBANA	IL	61801
COOK KELSEY D	UNIV OF ILLINOIS	44 ROGER ADAMS LAB,	61209 W CALIFORNIA	URBANA	IL	61801
COOKS R G	PURDUE UNIVERSITY	CHEMISTRY DEPT		WEST LAFAYETTE	IN	47907
COOMBS K A	106 COLEMAN AVE			CHATHAM	NJ	07928
COSTELLO C E	MIT	CHEMISTRY, 56-029	77 MASS AVE	CAMBRIDGE	MA	02139
COTTER R J	JOHNS HOPKINS UNIV	MID ATLANTIC MS LAB	725 N WOLFE ST	BALTIMORE	MD	21205
CRAIN PAMELA F	UNIV OF UTAH	310 SKAGGS HALL		SALT LAKE CITY	UT	84112
CRAWFORD D W	US DEPT OF ENERGY	9800 S CASS AVE		ARGONNE	IL	60439
CRAWFORD RICHARD W	LLNL	PO BOX 808	L 310	LIVERMORE	CA	94550
CRIDDLE MICHAEL J	PRIMARY CHDN'S HOSP	BIOPHYSICS DEPT	320 12TH AVE	SALT LAKE CITY	UT	84103
CROW F W	UNIV OF NEBRASKA	CHEMISTRY DEPT	MCMS	LINCOLN	NE	68588
CROWLEY JAN R	UNIV OF FLORIDA	RADIOLOGY DEPT	BOX J374	GAINESVILLE	FL	32601
CURRY Z F	51 OAKHURST CIRCLE			PITTSBURGH	PA	15238
CURTIS TOMMIE G	MONSANTO CO U-C	800 N LINDBERGH		ST LOUIS	MO	63166
DAN PNINA	UNIV OF CINCINNATI	COLL OF MEDICINE	231 BETHESDA AVE	CINCINNATI	OH	45221
DASS CHHABIL	UNIV OF NEBRASKA	CHEMISTRY DEPT	30 HAMILTON HALL	LINCOLN	NE	68588
DAVIDSON WALTER	HALCON	PHILLIPS PKWY		MONTVALE	NJ	07645
DAVIS WILLIAM S	TOSCO CORP	18200 W HIGHWAY 72		GOLDEN	CO	80401
DAY R A	UNIV OF CINCINNATI	CHEMISTRY DEPT		CINCINNATI	OH	45221
DEAL D E	34 WAKONA ST			SAN FRANCISCO	CA	94127
DECORPO JAMES J	NAVAL SEA SYSTEM	COMMAND	CODE 05R14	WASHINGTON	DC	20362

MEMBER NAME	ADDR1	ADDR2	ADDR3	CITY	STATE	ZIP CODE
DEINZER MAX L	OREGON STATE UNIV	AGRICUL CHEM DEPT		CORVALLIS	OR	97331
DEJONGH DON C	FINNIGAN INST	11 TRIANGLE PARK DR		CINCINNATI	OH	45246
DELMORE JAMES E	EXXON NUC IDAHO CO	BOX 2800		IDAHO FALLS	ID	83401
DEROOS F L	BATTELLE LABS	505 KING AVE		COLUMBUS	OH	43201
DESIDERIO D M	UNIV OF TENNESSEE	STOUT, NEUROSCIENCE	800 MADISON AVE	MEMPHIS	TN	38163
DE STEFANO ANTHONY J	PROCTOR & GAMBLE	MIAMI VALLEY LAB	PO BOX 39175	CINCINNATI	OH	45247
DOUGHERTY R C	FLORIDA STATE UNIV	CHEMISTRY DEPT		TALLAHASSEE	FL	32306
DUBAY GEORGE K	BRISTOL LABORATORIES	BLDG 23A-336	PO BOX 657	SYRACUSE	NY	13201
DUGGER D L	114 LEDLEIS DR			MARLBORO	MA	01752
DUHOLKE W K	THE UPJOHN CO	7171 PORTAGE RD		KALAMAZOO	MI	49001
DURAN DAVID	4839 HIGH ST			LINCOLN	NE	68506
DURFEE STEVEN L	3608 MARIPOSA ST			DENVER	CO	80211
DURYEA ANTHONY	BOX 324A	RD 1		CHESWICK	PA	15024
DUTKY R C	14112 NEW HAMP AVE			COLESVILLE	MD	20904
DZIDIC ISMET	1220 BARTLETT	NO 2		HOUSTON	TX	77006
ECKERS CHRISTINE	NY COLL OF VET MED	DIAGNOSTIC LAB	CORNELL UNIV	ITHACA	NY	14853
EDMONDS C G	UNIV OF UTAH	COLLEGE OF PHARMACY	MEDICINAL CHEM DEPT	SALT LAKE CITY	UT	84112
ELLIOTT W H	ST LOUIS UNIV	BIOCHEMISTRY DEPT	1402 S GRAND	ST LOUIS	MO	63104
ELLIS ROBERT H	HEWLETT PACKARD	SCIEN INSTR DIV	1601 CALIFORNIA AVE	PALO ALTO	CA	94304
ENKE C G	MICHIGAN STATE UNIV	CHEMISTRY DEPT		EAST LANSING	MI	48824
EVANS JAMES E	E KENNEDY SHRIVER CT	200 TRAPELO RD		WALTHAM	MA	02254
EYLER J R	UNIV OF FLORIDA	CHEMISTRY DEPT		GAINESVILLE	FL	32611
FALES H M	6502 STONEHAM RD			BETHESDA	MD	20034
FAULL K F	STANFORD UNIVERSITY	PSYCHIATRY DEPT	MEDICAL SCHOOL	STANFORD	CA	94305
FEIL V J	1438 3RD ST N			FARGO	ND	58102
FENNESSEY P V	UNIV OF COLORADO	MEDICAL CENTER, C234	4200 E 9TH AVE	DENVER	CO	80262
FENSELAU C C	JOHNS HOPKINS UNIV	PHARMACOLOGY DEPT	725 N WOLFE ST	BALTIMORE	MD	21205
FERGUSON ELDON	AERONOMY LAB	NOAA		BOULDER	CO	80303
FERGUSON MARIE	205 BROOKSIDE CT			BOULDER	CO	80302
FIELD F H	ROCKEFELLER UNIV	1230 YORK AVE		NEW YORK	NY	10021
FIES W J	155 CHEROKEE WAY			PORTOLA VALLEY	CA	94025
FILBY EVAN E	1431 WOODRUFF AVE			IDAHO FALLS	ID	83401
FINNIGAN R E	FINNIGAN CORP	845 W MAUDE AVE		SUNNYVALE	CA	94086
FINNEY RAYMOND J	MONSANTO RES CORP	MOUND FACILITY, R-2		MIAMISBURG	OH	45342
FITE WADE L	EXTRANUCLEAR LAB	100 BETA DR	PO BOX 11512	PITTSBURGH	PA	15238
FLEMING R H	SRI INTERNATIONAL	333 RAVENSWOOD		MENLO PARK	CA	94025
FOLK T L	227 WASHINGTON AVE			CUYAHOGA FALLS	OH	44305
FOLTZ R L	UNIV OF UTAH	CTR HUMAN TOXICOLOGY		SALT LAKE CITY	UT	84112
FOREMAN JOHN B	A H ROBINS INC	1211 SHERWOOD AVE		RICHMOND	VA	23220
FOSTER N G	2719 ROBINWOOD LANE			DENTON	TX	76201
FRALEY DAVID F	903 SARBROOK DR			CINCINNATI	OH	45231
FRANCL MICHELLE	UNIV OF CALIFORNIA	CHEMISTRY DEPT		IRVINE	CA	92717
FRANCL T J	UNIV OF CALIFORNIA	CHEMISTRY DEPT		IRVINE	CA	92717
FRANKLIN J C	141 CUMBERLAND VIEW			OAK RIDGE	TN	37830
FRASURE W	326 MARION AVE			ST LOUIS	MO	63119
FREEMAN JOHN A	BALZERS	8 SAGAMORE PARK RD		HUDSON	NH	03051
FREES LOUIS C	INFICON LEYBOLD	6500 FLY ROAD		E SYRACUSE	NY	13057
FREISER B S	PURDUE UNIVERSITY	CHEMISTRY DEPT		WEST LAFAYETTE	IN	47907
FRENCH SCOTT B	4110 KINGSTON DR			ANCHORAGE	AK	99504
FREY CARL	459 GRANITE SPRINGS			YORKTOWN HEIGHTS	NY	10598
FRIESEN R D	LLL	PO BOX 808, L-230		LIVERMORE	CA	94550
FRISCH M A	IBM RESEARCH CENTER	PO BOX 218		YORKTOWN HEIGHTS	NY	10598
FU EMIL W	SANDOZ, INC	59 ROUTE 10	BLDG 404, RM 376	E. HANOVER	NJ	07936
FUHRHOP RALPH W	MONSANTO CO	800 N LINDBERGH BLVD		ST LOUIS	MO	63166
FUJIWARA H	MONSANTO CO	800 N LINDBERGH BLVD		ST LOUIS	MO	63166

MEMBER NAME	ADDR1	ADDR2	ADDR3	CITY	STATE	ZIP CODE
FUKUDA E K	UNIV OF CALIFORNIA	CHEMISTRY DEPT		IRVINE	CA	92717
FUNKE P T	E R SQUIBB	PO BOX 4000		PRINCETON	NJ	08540
FUTRELL J H	UNIV OF UTAH	CHEMISTRY DEPT		SALT LAKE CITY	UT	84112
GALE P J	RCA	DAVID SARNOFF RES CT		PRINCETON	NJ	08540
GALLAHER KENNETH L	SOHIO	4440 WARRENSVILLE RD		CLEVELAND	OH	44128
GALLEGOS E J	CHEVRON	PO BOX 1627		RICHMOND	CA	94804
GARRETT JOHN H	WRIGHT STATE UNIV	3640 COLONEL GLENN H		DAYTON	OH	45435
GELLENE GREGORY I	CORNELL UNIV	BAKER LAB, BOX 168		ITHACA	NY	14853
GERBER J N	HEWLETT PACKARD	1021 EIGHTH AVE		KING OF PRUSSIA	PA	19406
GHADERI SAMBA	NICOLET INST CORP	ANAL BLDG	5225 VERONA RD	MADISON	WI	53771
GIANG B Y	STAUFFER RESEARCH	1200 SO 47TH ST		RICHMOND	CA	94804
GIBLIN D E	4526 PRESCOTT			LINCOLN	NE	68506
GIBSON BRADFORD W	MIT	CHEMISTRY DEPT	BLDG 56-028	CAMBRIDGE	MA	02139
GIESSMANN ULRICH P	OREGON GRAD CTR	19600 NW WALKER RD		BEAVERTON	OR	97006
GIFFIN C E	JET PROPULSION LAB	11-116	4800 OAK GROVE DR	PASADENA	CA	91103
GILBERT L	CVC PRODUCTS	525 LEE RD		ROCHESTER	NY	14603
GILLECE-CASTRO BETH	TRAVENOL LABS INC	6301 N LINCOLN AVE		MORTON GROVE	IL	60053
GILMAN J P	UNIV OF NEBRASKA	CHEMISTRY DEPT		LINCOLN	NE	68588
GLISH G L	OAK RIDGE NATIONAL LA	PO BOX Y	BLDG 9735	OAK RIDGE	TN	37830
GOETZ ANN G	BEST FOODS CPC INT'L	1120 COMMERCE AVE		UNION	NJ	07040
GOHLKE ROLAND S	1231 IMPERIAL DR			WEBSTER	NY	14580
GOO REGINALD	1255 NUUANU AVE	APT. E 401		HONOLULU	HI	96817
GOODLEY PAUL C	HEWLETT PACKARD	SCI INST DIV	1601 CALIFORNIA AVE	PALO ALTO	CA	94304
GORETSAS GWEN D	STATE LAB OF HYGIENE	465 HENRY MALL		MADISON	WI	53706
GORMAN LEO A	VG INSTRUMENTS	134 JUNEDALE DR		CINCINNATI	OH	45218
GRAVEN WENDELL M	1157 TENTH ST			MANHATTAN BCH	CA	90266
GRAYSON M A	427 GLENMEADOW DR			BALLWIN	MO	63011
GREENE F T	MIDWEST RESRCH INST	425 VOLKER BLVD		KANSAS CITY	MO	64110
GREENHOUSE S H	21 OAK TERRACE	APT 1A		SOMERVILLE	NJ	08876
GREENWOOD GIL J	PHILLIPS PETROLEUM	150 PL		BARTLESVILLE	OK	74003
GREGG H R	MICHIGAN STATE UNIV	CHEMISTRY DEPT		EAST LANSING	MI	48824
GRIGSBY RONALD D	DEPT OF ENERGY	PO BOX 1398		BARTLESVILLE	OK	74003
GRINDSTAFF W G	BARTLESVILLE ENERGY	TECHNOLOGY CENTER	BOX 1398, DOE	BARTLESVILLE	OK	74003
GRITTER ROY J	40 W BROKAW RD			SAN JOSE	CA	95116
GROENEWOLD G S	UNIV OF NEBRASKA	720 HAMILTON HALL		LINCOLN	NE	68588
GROSS M L	UNIV OF NEBRASKA	CHEMISTRY DEPT		LINCOLN	NE	68588
GROSTIC M F	THE UPJOHN CO	DEPT 7820		KALAMAZOO	MI	49001
GUFFEY F D	US DEPT OF ENERGY	PO BOX 3395		LARAMIE	WY	82071
HACHEY DAVID L	BAYLOR COLL OF MED	PEDIATRICS DEPT	1200 MOUR SAND	HOUSTON	TX	77030
HAGEMAN LYNN R	MON ST DEPT OF AG	MCCALL HALL	MONTANA STATE UNIV	BOZEMAN	MT	59717
HALLIDAY FRED	VALLECITOS NUCLEAR C	PO BOX 460		PLEASANTON	CA	94566
HALLSTROM GOSTA	UNIV OF CALIFORNIA	PHARMACOLOGY DEPT		LOS ANGELES	CA	90024
HAMMING MYNARD C	CONOCO INC			PONCA CITY	OK	74601
HARDIN E D	DEPT OF CHEMISTRY	UNIV OF HOUSTON		HOUSTON	TX	77004
HARE JERRY	NICOLET INST	5225-1 VERONA RD		MADISON	WI	53711
HARPER ALICE M	BIOMATERIALS PROFIL	391 CHIPETA WAY	RESEARCH PARK	SALT LAKE CITY	UT	84108
HARPER TIMOTHY	UNIV OF COLORADO	BOX C236	4200 EAST NINTH AVE	DENVER	CO	80220
HARRINGTON W L	RCA LABORATORIES			PRINCETON	NJ	08540
HARRISON W W	UNIV OF VIRGINIA	CHEMISTRY DEPT		CHARLOTTESVILLE	VA	22901
HARTWIG MARK A	HEWLETT PACKARD	5201 TOLLVIEW DR		ROLLING MEADOWS	IL	60008
HATCH F W	BOEHRINGER INGELHEIM	90 EAST RIDGE	PO BOX 368	RIDGEFIELD	CT	06877
HAWKS R L	2032 BELMONT RD	APT 507		WASHINGTON	DC	20009
HEARN JOHN	FINNIGAN CORP	845 W MAUDE AVE		SUNNYVALE	CA	94086
HEIN R E	NICOLET INSTRUMENTS	5225 VERONA RD		MADISON	WI	53711
HELLER D N	JOHN HOPKINS UNIV	6-6 BIOHPYSICS DEPT	725 N WOLFE ST	BALTIMORE	MD	21205

MEMBER NAME	ADDR1	ADDR2	ADDR3	CITY	STATE	ZIP CODE
HELLER S R	2413 LILLIAN DRIVE			SILVER SPRING	MD	20902
HELLMANN ROBERT	NLO, INC	PO BOX 39158		CINCINNATI	OH	45239
HEMLING MARK E	UNIV OF ILLINOIS	456 RAL, BOX 76-5	1209 W CALIFORNIA	URBANA	IL	61801
HENDERSON T R	5609 DON FELIPE CT S			ALBUQUERQUE	NM	87105
HENION J D	CORNELL UNIVERSITY	NYS COL VET MEDICINE	132 DIAGNOSTIC LAB	ITHACA	NY	14853
HENKEL PAUL R	GALILEO ELECTRO OPT	GALILEO PARK		STURBRIDGE	MA	01518
HEPPNER RICHARD A	ENERGY TECH CTR	BOX 3395	UNIV STATTION	LARAMIE	WY	82071
HERON ELAINE J	HP SCIENTIFIC INSTR	BLDG 29A	3172 PORTER DRIVE	PALO ALTO	CA	94304
HERTZ H S	NBS	A113 CHEMISTRY		WASHINGTON	DC	20234
HERZOG L F	NUCLIDE CORP	642 E COLLEGE AVE		STATE COLLEGE	PA	16801
HEURING DENNIS L	TMS ANAL SERV	PO BOX 13		EVANSVILLE	IN	47701
HIDY B J	BATTELLE LABS	505 KING AVE		COLUMBUS	OH	43201
HIGNITE C E	VETERANS ADMIN HOSP	4801 LINWOOD BLVD		KANSAS CITY	MO	64128
HILDENBRAND D L	SRI INTERNATIONAL			MENLO PARK	CA	94025
HINDENLANG D M	ALLIED CHEMICAL CORP	PO BOX 1021R		MORRISTOWN	NJ	07960
HINES H B	3901 MEADOWBROOK CIR			PITTSBURG	CA	94565
HITES RONALD A	INDIANA UNIV	400 E 7TH ST,RM 433		BLOOMINGTON	IN	47405
HOLKEBOER D H	231 WINDCREST DR			CAMILLUS	NY	13031
HOLLAND J F	MICHIGAN STATE UNIV	BIOCHEMISTRY DEPT		EAST LANSING	MI	48824
HOLLER J S	CENTER DISEASE CNTRL	TOXICOLOGY BRANCH		ATLANTA	GA	30333
HOPPE J J	VACUMETRICS INC	2261-#1 PALMA DR		VENTURA	CA	93003
HORNING E C	11610 STARWOOD DR			HOUSTON	TX	77024
HORNING M G	BAYLOR COLL MEDICINE	INST LIPID RESEARCH	TEXAS MEDICAL CENTER	HOUSTON	TX	77030
HOUK ROBERT S	IOWA STATE UNIV	CHEMISTRY DEPT		AMES	IA	50011
HRIBAR J D	G D SEARLE & CO	PO BOX 5110		CHICAGO	IL	60680
HSIEH CHRISTINA	UNIV OF HOUSTON	CHEMISTRY DEPT	4143 MARLOWE	HOUSTON	TX	77005
HSIEH TACHENG	VELSICAL CHEM CORP	ANAL RESEARCH	341 E OHIO ST	CHICAGO	IL	60611
HUDSON L E	MARINE BIOMEDICAL	200 UNIVERSITY BLVD		GALVESTON	TX	77550
HUGHES B M	1563 LINDENHURST			DAYTON	OH	45459
HUGHES HELEN	INST FOR LIPID RES	BAYLOR COLL OF MED	1200 MOURSUND	HOUSTON	TX	77030
HUNTER R L	UNIV OF CALIFORNIA	CHEMISTRY DEPT		IRVINE	CA	92717
HUNTRESS W T	JET PROPULSION LAB	SSD		PASADENA	CA	91103
HURST H E	UNIV OF LOUISVILLE	PHARMACOLOGY DEPT		LOUISVILLE	KY	40292
IDEN CHARLES R	SUNY-STONY BROOK	PHARMACOLOGY DEPT		STONY BROOK	NY	11794
IRVING CHARLES S	920 W BELLFORT	NO 88		HOUSTON	TX	77031
ISABELLE LORNE M	OREGON GRAD CTR	19600 NW WALKER RD		BEAVERTON	OR	97006
ITEN R T	E I DUPONT	EXPERIMENTAL STATION	BLDG 336	WILMINGTON	DE	19898
JACOBS M L	COMMERICAL TESTING	AND ENGINEERING	490 ORCHARD ST	GOLDEN	CO	80401
JAMES RUBY H	SOUTHERN RES INST	2000 9TH AVE SOUTH		BIRMINGHAM	AL	35255
JAMIESON GENE C	ZOECON CORP	975 CALIFORNIA ST	PO BOX 10975	PALO ALTO	CA	94304
JARDINE I	MAYO CLINIC	PHARMACOLOGY DEPT		ROCHESTER	MN	55901
JAYASIMHULU KOKA	810 MORGEN HALL			CINCINNATI	OH	45219
JENSON ALFRED H	602 ARBOR VALLEY			CAMPBELL HALL	NY	10916
JOHNSON STEVEN L	JEOL	235 BIRCHWOOD AVE		CRANFORD	NJ	07016
JONES GILBERT G	AMOCO RES CTR	PO BOX 400		NAPERVILLE	IL	60566
JUDSON CHARLES M	UNIV OF KANSAS	CHEMISTRY DEPT		LAWRENCE	KS	66044
KALEY PAMALA L	MONSANTO CO	800 N LINDBERGH BLVD		ST LOUIS	MO	63167
KALEY ROBERT G	MONSANTO	800 N LINDBERGH		ST LOUIS	MO	63167
KALMAN DAVID A	ENVIRONMENTAL HEALTH	UNIV OF WASHINGTON	SC-34	SEATTLE	WA	98195
KAN NANCY M	FINNIGAN CORP	845 W MAUDE AVE		SUNNYVALE	CA	94086
KANSAKO SIDNEY	98-1063 KAONOHI ST			AIEA	HI	96701
KEARNS G L	56 BUCKINGHAM DR			STAMFORD	CT	06902
KEEFE RONALD B	UNIV OF VIRGINIA	CHEMISTRY DEPT	MCCORMICK RD	CHARLOTTESVILLE	VA	22901
KEESEE ROBERT G	1422 HARRIS ST			STATE COLLEGE	PA	16801
KELLEY PAUL E	FINNIGAN CORP	845 W MAUDE AVE		SUNNYVALE	CA	94086

MEMBER NAME	ADDR1	ADDR2	ADDR3	CITY	STATE	ZIP CODE
KELLY W R	NAT'L BUR OF STAN	BLDG 222, A355		WASHINGTON	DC	20234
KENNISH J M	UNIV OF ALASKA	CHEMISTRY DEPT	3221 PROVIDENCE DR	ANCHORAGE	AK	99504
KENYON C N	HP SCIENTIFIC INSTR	1601 CALIFORNIA AVE		PALO ALTO	CA	94304
KEOUGH F W	8557 CAVALIER DR			CINCINNATI	OH	45231
KILLMER LEWIS B	325 N EDGEMONT ST			MEDIA	PA	19063
KING J D	DFC	MS977	PO BOX 25046	DENVER	CO	80225
KING J W	3850 GAVOTA AVE			SAN JOSE	CA	95124
KINNEL ROBIN B	3037 GULSTON ST			HONOLULU	HI	96816
KINSER R D	PHILIP MORRIS USA	RESEARCH CENTER	PO BOX 26583	RICHMOND	VA	23261
KINSINGER JAMES A	NICOLET ANAL	5225 VERONA ROAD		MADISON	WI	53711
KIRBY HELEN M	FINNIGAN INST	355 RIVER OAKS PRKWY		SAN JOSE	CA	95134
KISER R W	781 GLENDOVER ROAD			LEXINGTON	KY	40502
KITSON F G	3 HARTFORD PLACE			NEWARK	DE	19711
KLEIMAN JOSEPH P	18915 BEDFORD			BIRMINGHAM	MI	48009
KLOEK JAMES A	800 N LINDBERGH BLVD			ST LOUIS	MO	63167
KNIGHT J B	FINNIGAN CORP	845 W MAUDE AVE		SUNNYVALE	CA	94086
KOLOR M G	GENERAL FOODS CORP	555 SO BROADWAY		TARRYTOWN	NY	10591
KOONTZ S L	UNIV OF ARIZONA	CHEMISTRY DEPT		TUCSON	AZ	85721
KORNEL ALFRED	UNIV OF CINCINNATI	CHEMISTRY DEPT		CINCINNATI	OH	45221
KRASNER S W	METRO WATER DIST	WATER QUALITY BRANCH	700 NORTH MORENO AVE	LA VERNE	CA	91750
KREEK MARY J	ROCKEFELLER UNIV	1230 YORK AVE		NEW YORK	NY	10021
KRICK T	UNIV OF MINNESOTA	BIOCHEMISTRY DEPT		ST PAUL	MN	55108
KRUSE JAY R	UCLA	68-124 NPI-MRRC	760 WESTWOOD PLZ	LOS ANGELES	CA	90024
KUHNLE JUDITH	HAWAIIAN SUGAR PLANT	99-193 AIEA HGHTS DR		AIEA	HI	91701
KURZWEG LUTZ	EXTRANUCLEAR LAB	100 BETA DR	PO BOX 11512	PITTSBURGH	PA	15238
KYLE GLENNA M	12220 GUD OAK PL			WOODLAND	TX	77380
LAGERGREN C R	2110 HOWELL AVE			RICHLAND	WA	99352
LANE DOROTHY C	115-4 ACROPOLIS DR			ATHENS	GA	30605
LANKELMA JAN	STANFORD UNIV	CHEMISTRY DEPT	MASS SPEC LAB	STANFORD	CA	94305
LARKA BARBARA A	4954 ABBOTT AVE SO			MINNEAPOLIS	MN	55410
LARKA EDMUND A	4954 ABBOTT AVE S	N/A	N/A	MINNEAPOLIS	MN	55410
LATTIMER R P	B F GOODRICH R & D	9921 BRECKSVILLE RD		BRECKSVILLE	OH	44141
LATVEN R K	HEWLETT PACKARD	3003 SCOTT BLVD		SANTA CLARA	CA	95050
LAY J O	1431 D STREET	APT 9		LINCOLN	NE	68502
LEDFORD E B	4511 SOUTH ST			LINCOLN	NE	92506
LEE TERRY D	CETUS CORP	600 BANCROFT WAY		BERKELEY	CA	94710
LEHMAN J P	3645 ELMLEY AVE			BALTIMORE	MD	21213
LEIKER THOMAS	BUR OF RECLAMATION	DENVER FEDERAL CTR	PO BOX 25007	DENVER	CO	80225
LEMIEUX ROBERT E	1211 SHERWOOD AVE			RICHMOND	VA	23220
LEVENBERG M I	ABBOTT LABS	DEPT 417		NORTH CHICAGO	IL	60064
LEWIS S G	UNIV OF CALIFORNIA	SPACE SCIENCES LAB		BERKELEY	CA	94720
LIEHR J G	UNIV OF TEXAS MSC	ANALYTICAL CHEMISTRY	PO BOX 20708	HOUSTON	TX	77030
LIGON W V	GENERAL ELECTRIC CORD	R&D CENTER	BLDG K1, PO BOX 8	SCHENECTADY	NY	12301
LIN DENNIS	ENVIR TEST & CERT CO	284 RARATAN CTR PKY		EDISON	NJ	08837
LIN S N	UNIV OF TEXAS MSC	ANALYTICAL CHEMISTRY	PO BOX 20708	HOUSTON	TX	77030
LIN YUNG Y	INST BASIC RESEARCH	1050 FOREST HILL RD		STATEN ISLAND	NY	10314
LINCOLN K A	2016 STOCKBRIDGE AVE			REDWOOD CITY	CA	94061
LIPPSTREU D L	UNIV OF NEBRASKA	CHEMISTRY DEPT		LINCOLN	NE	68588
LITTLE DAVID	12251 ANGEL WING LT			RESTON	VA	22091
LITTON J F	UOP RESEARCH	PO BOX 19601		IRVINE	CA	92713
LIU NORMAN W	SEARLE RES LAB	PO BOX 5110		CHICAGO	IL	60680
LLOYD M A	NIH	BLDG 10, RM 7N312		BETHESDA	MD	20205
LO MSI M	EXTRANUCLEAR LABS	PO BOX 11512		PITTSBURGH	PA	15238
LOPEZ-AVILA V	MIDWEST RESRCH INST	425 VOLKER BLVD		KANSAS CITY	MO	64110
LUBMAN DAVID M	QUANTA-RAY	1250 CHARLESTON RD		MOUNTAIN VIEW	CA	94043

MEMBER NAME	ADDR1	ADDR2	ADDR3	CITY	STATE	ZIP CODE
LUCAS S V	BATTELLE LABS	505 KING AVE		COLUMBUS	OH	43201
LUEG VOLKER R	FINNIGAN CORP	355 RIVER OAKS PKWY		SAN JOSE	CA	95134
MACDONALD J L	RALSTON PURINA CO	3KS CHECKERBOARD SQ		ST LOUIS	MO	63188
MACFARLANE R D	TEXAS A&M UNIVERSITY	CHEMISTRY DEPT		COLLEGE STATION	TX	77843
MAGEE C W	RCA LABORATORIES			PRINCETON	NJ	08540
MAGIN DONALD F	PHILIP MORRIS RED	BOX 26583		RICHMOND	VA	23261
MAHLER KENNETH O	SCI GLASS ENGIN	2007 KRAMER LANE	SUITE 100	AUSTIN	TX	78758
MAHONEY JOHN	PHRASOR SCIENTIFIC	1536 HIGHLAND AVE		DUARTE	CA	91010
MALIK JOSEPH M	MONSANTO	U2E	800 N LINDBERGH	ST LOUIS	MO	63141
MARCUS MARK	STAUFFER CHEMICAL	400 FARMINGTON AVE		FARMINGTON	CT	06032
MARKWART UWE	FINNIGAN CORP	355 RIVER OAKS PKWY		SAN JOSE	CA	95134
MARKIOTT T D	RICE UNIVERSITY	CHEMISTRY DEPT		HOUSTON	TX	77005
MARTIN S A	MIT	BLDG 56-035	77 MASSACHUSETTS AVE	CAMBRIDGE	MA	02139
MARTINSEN DAVID	302 SOPHIA COURT			BALTIMORE	MD	21208
MATTSON DAVE R	6389 DEMARCO TR			VERONA	WI	53593
MAUTNER M	NBS			WASHINGTON	DC	20234
MAYLIN GEORGE A	676 CODDINGTON RD			ITHACA	NY	14850
MCLAMAN M W	CITY OF HOPE MED CTR			DUARTE	CA	91010
MCCLOSKEY J A	UNIV OF UTAH	COLLEGE OF PHARMACY	MEDICINAL CHEM DEPT	SALT LAKE CITY	UT	84112
MCCLURE C R	FINNIGAN CORP	845 W MAUDE AVE		SUNNYVALE	CA	94086
MCCLUSKY GARY A	WARNER LAMBERT CO	PO BOX 1047		ANN ARBOR	MI	48106
MCCRERY D A	1201 S 24TH ST			LINCOLN	NE	68502
MCELVANY STEPHAN W	MICH STATE UNIV	CHEMISTRY DEPT		EAST LANSING	MI	48824
MCEWEN C N	24 COACHLIGHT CT			NEW CASTLE	DE	19720
MCFADDEN W H	FINNIGAN CORP	845 W MAUDE AVE		SUNNYVALE	CA	94086
MCHUGH J A	GENERAL ELECTRIC CO	KNOLLS ATOM POW LAB	PO BOX 1072	SCHENECTADY	NY	12301
MCIVER R T	UNIV OF CALIFORNIA	CHEMISTRY DEPT		IRVINE	CA	92717
MCLAFFERTY F W	CORNELL UNIVERSITY	CHEMISTRY DEPT	BAKER LABORATORY	ITHACA	NY	14853
MCLUCKEY S A	PURDUE UNIVERSITY	CHEMISTRY DEPT	PO BOX 600	WEST LAFAYETTE	IN	47907
MCNEAL C J	TEXAS A&M UNIVERSITY	CHEMISTRY DEPT		COLLEGE STATION	TX	77843
MEHNERT R M	US GEOLOGICAL SURVEY	ISOTOPE GEOLOGY		DENVER	CO	80225
MEISELS G G	UNIV OF NEBRASKA	CHEMISTRY DEPT	HAMILTON HALL	LINCOLN	NE	68588
MERRITT CHARLES	SCI & ADV TECH LAB	US ARMY NATICK LABS		NATICK	MA	01760
METCALF STEVEN	BIOMATERIALS PROFIL	391 S CHIPETA WAY	SUITE F	SALT LAKE CITY	UT	84108
METRAL CLIMACO	3482 HAZELWOOD AVE	APT 7		CINCINNATI	OH	45211
MICHL JOSEF	UNIV OF UTAH	CHEMISTRY DEPT		SALT LAKE CITY	UT	84112
MILKELSON D L	THE UPJOHN CO	LOC 1140-91-1		KALAMAZOO	MI	49001
MICKELSON MARY M	1601 GREENVIEW			PORTAGE	MI	49801
MIDGETT C H	US TOBACCO CO	905 HARRISON ST		NASHVILLE	TN	37203
MILLEN W G	CYANAMID	PO BOX 400		PRINCETON	NJ	08540
MILLER D L	UNIV OF NEBRASKA	DEPT OF CHEMISTRY		LINCOLN	NE	68588
MILLS GLENN W	ELI LILLY RES LABS	DEPT MC 525		INDIANAPOLIS	IN	46258
MILNE T A	SERI	1536 COLE BLVD		GOLDEN	CO	80401
MINARD R D	PENN STATE UNIV	152 DAVEY LAB		UNIVERSITY PARK	PA	16802
MINTZ DONALD M	1610 BELLEVILLE WAY			SUNNYVALE	CA	94087
MITCHUM RONALD K	NAT'L CTR TOXICOLOGI			JEFFERSON	AR	72079
MOKHALLAWHATI M	PENN STATE UNIV	CHEMISTRY DEPT	152 DAVEY LAB	UNIVERSITY PK	PA	16802
MOL GORDON J	1662 PUERTO VALLARTO			SAN JOSE	CA	95120
MONCUR JAMES	LOCKHEED	3251 HANOVER ST		PALO ALTO	CA	94304
MONSON R R	ICI AMERICAS INC	BIOMEDICAL RES LAB		WILMINGTON	DE	19897
MONTGOMERY FREDERICK E	NERMAG, INC	PO BOX 31483		HOUSTON	TX	77035
MOORE ARTHUR	MARATHON OIL CO	BOX 269		LITTLETON	CO	80160
MOORE LARRY J	NBS	A-21 PHYSICS		WASHINGTON	DC	20234
MORTENSEN ROBERT L	3105 BANDERA DR			PALO ALTO	CA	94304
MORTON T H	UNIV OF CALIFORNIA	CHEMISTRY DEPT		RIVERSIDE	CA	92521

MEMBER NAME	ADDR1	ADDR2	ADDR3	CITY	STATE	ZIP CODE
MUNSON B	UNIV OF DELAWARE	CHEMISTRY DEPT		NEWARK	DE	19711
MURPHY R C	UNIV OF COLORADO	MEDICAL CENTER	PHARMCOLOGY DEPT	DENVER	CO	80262
MUSSELMAN BRIAN D	MICH STATE UNIV	BIOCHEMISTRY DEPT	MASS SPEC FACIL	EAST LANSING	MI	48824
MYERHOLTZ CARL A	MICHIGAN STATE UNIV	CHEMISTRY DEPT		EAST LANSING	MI	48824
NEWTON JOHN C	LAW LIV NAT'L LAB	L-310	PO BOX 808	LIVERMORE	CA	94550
NG K T	CIBA-GEIGY CORP			ARDSLEY	NY	10502
NISHIOKA MARCIA G	BATTELLE COL LABS	RM 7238	505 KING AVE	COLUMBUS	OH	43201
NOGAR NICHOLAS S	446 CONNIE ST			LOS ALAMOS	NM	87545
NORMAN E J	1044 SUNWOOD CT			CINCINNATI	OH	45231
NOWLIN J G	6535 FANNIN	FONDREN F524		HOUSTON	TX	77030
OCCOLOWITZ J L	ELI LILLY RES LABS			INDIANAPOLIS	IN	46285
O'CONNELL V P	TEKNIVENT CORP	10774 TRENTON AVE		ST LOUIS	MO	63132
ODOM R W	4331 PEMBROKE DR			CONCORD	CA	94521
OLDHAM R G	RADIAN CORP	PO BOX 9948		AUSTIN	TX	78766
OLSON EDWIN S	GRAND FORKS ENERGY	TECHNOLOGY CTR	PO BOX 8213 UN STN	GRAND FORKS	ND	58202
ONAK THOMAS P	CHEMISTRY DEPT	5151 STATE UNIV DR		LOS ANGELES	CA	90032
ORTH ROBERT G	301 SOUTH 15TH AVE	NO 2		BOZEMAN	MT	59715
PALLANTE S L	JOHNS HOPKINS UNIV	PHARMACOLOGY DEPT	725 N WOLFE ST	BALTIMORE	MD	21205
PARR A C	NBS	BLDG 221, RM A251		WASHINGTON	DC	20234
PARTRIDGE LESLIE G	SYNTEX RESEARCH	3401 HILLVIEW		PALO ALTO	CA	94304
PATEL S M	1339 VENTURA DRIVE			LAKEWOOD	NJ	08701
PATTERSON PAUL L	DETECTOR ENG & TECH	2212 BRAMPTON RD		WALNUT CREEK	CA	94598
PEREL JULIUS	PHRASOR SCIENTIFIC	1536 HIGHLAND AVE		DUARTE	CA	91010
PERRIN RICHARD E	LOS ALAMOS NAT'L LAB	PO BOX 1663, MS 514		LOS ALAMOS	NM	87545
PERRY DONALD L	8155 JEFFERSON HWY	APT 703		BATON ROUGE	LA	70809
PETZINGER G A	9 LAMBERT STREET			WOODBRIDGE	NJ	07095
PIKE ADRIAN	UNIV OF COLORADO	MEDICAL CTR	4200 EAST 9TH AVE	DENVER	CO	80262
PINKSTON J D	MICH STATE UNIV	CHEMISTRY DEPT	BOX250	EAST LANSING	MI	48824
PLASHKO BRUCE E	A E STALEY CO	3200 ELDORADO		DECATUR	IL	62525
PLATTNER R D	NOR REGIONAL LAB	1815 N UNIVERSITY ST		PEORIA	IL	61604
PORTER R F	CORNELL UNIVERSITY	CHEMISTRY DEPT		ITHACA	NY	14853
POWELL LORA J	NBS	BLDG 221, RM A21		WASHINGTON	DC	20234
POWELL MARK L	SCHERING-PLOUGH	DRUG METAB. & PHARMO		BLOOMFIELD	NJ	07003
PRAMANIK B N	SCHERING CORP	60 ORANGE ST		BLOOMFIELD	NJ	07003
PROCTOR B L	UNIV OF TEXAS	ENV SCIENCE	BOX 688	RICHARDSON	TX	75080
PYPER J W	LLL	PO BOX 808, L-365		LIVERMORE	CA	94550
RAFTOGIANIS L	FINNIGAN CORP	845 W MAUDE AVE		SUNNYVALE	CA	94086
RAMJIT HARRI G	MSDRL	DEPT 805	SUMMNEY TPK	WEST POINT	PA	19486
RAPP LARRY A	ARCO, HTC	400 E SIBLEY BLVD		HARVEY	IL	60426
REILLY JIM	INDIANA UNIVERSITY	CHEMISTRY DEPT		BLOOMINGTON	IN	47405
REINHOLD V N	HARVARD MEDICAL SCH	EHRRB	45 SHATTUCK ST	BOSTON	MA	02115
REISER R W	E I DUPONT	EXPERIMENTAL STATION	BIOCHEM, BLDG 324	WILMINGTON	DE	19898
REYNOLDS T P	PO BOX 314			BETHEL	CT	06801
REYNOLDS W E	360 SWETT ROAD			WOODSIDE	CA	94062
RICHIE KRISTY L	NAT'L BUR OF STAN	BLDG 222, RM A113		WASHINGTON	DC	20234
RIDER D M	MICHIGAN STATE UNIV	CHEMISTRY DEPT		EAST LANSING	MI	48824
RIDGE D P	UNIV OF DELAWARE	CHEMISTRY DEPT		NEWARK	DE	19711
RINEHART KENNETH L	UNIV OF ILLINOIS	CHEM,454 ROGER ADAMS	1209 W CALIFORNIA ST	URBANA	IL	61801
ROBBINS RONNY L	TEXAS WOMEN'S UNIV	TWU STATION		DENTON	TX	76204
ROBERTS PETER	10605 UNION TERR WAY			PLYMOUTH	MN	55441
ROBERTSON DONALD H	S.A.T.L.	ANAL CHEM GRP	US ARMY NATICK LABS	NATICK	MA	01760
ROBINSON JAMES D	4 SMOKY LANE			WESTPORT	CT	06880
ROBOZ JOHN	MT SINAI SCH OF MED	1 GUSTAVE LEVY PL		NEW YORK	NY	10029
ROLLER P P	NIH	NCI	BLDG 37, RM 1E22	BETHESDA	MD	20205
ROSELIUS HERBERT A	BALZERS	8 SAGAMORE PARK RD		HUDSON	NH	03051

MEMBER NAME	ADDR1	ADDR2	ADDR3	CITY	STATE	ZIP CODE
ROSEN K T	FMC CORP	PO BOX 8		PRINCETON	NJ	08540
ROSS MARK	CODE 6174	NAVAL RES LAB		WASHINGTON	DC	20375
ROTHBERG J L	RALSTON PURINA CO	3RS CHECKERBOARD SQ		ST LOUIS	MO	63188
RUDAT M A	DUPONT	RES & DEV	EXP STATION 228-101	WILMINGTON	DE	19898
RUSSELL D H	TEXAS A&M UNIV	CHEMISTRY DEPT		COLLEGE STATION	TX	77843
RUSSELL JOHN W	MEAD COMPUCHEM	PO BOX 12652		RES TRI PARK	NC	27709
RYAN PHILIP W	SYSTEMS, SCI & SFTWR	PO BUX 1620		LA JOLLA	CA	92038
SAALFELD F E	NRL	CODE 6100		WASHINGTON	DC	20375
SAMSON P C	112 E BARRETT LANE			SCHAUMBURG	IL	60193
SANDERS K A	1900 WILTSHIRE BLVD			FAIRFIELD	OH	45014
SATKIEWICZ F G	JOHN HOPKINS UNIV	APL	JOHNS HOPKINS RD	LAUREL	MD	20810
SAUTER ANDREW D	2356 AQUA VISTA			HENDERSON	NV	89015
SAVICKAS P J	UNIV OF VIRGINIA	CHEMISTRY DEPT		CHARLOTTESVILLE	VA	22901
SCAMUFFA M D	HEWLETT-PACKARD	5201 TOLLVIEW DR		ROLLING MEADOWS	IL	60008
SCHEPPELE S E	BARTLESVILLE ENERGY	TECHNOLOGY CENTER	PO BOX 1398, DUE	BARTLESVILLE	OK	74003
SCHNUTE W C	FINNIGAN CORP	845 W MAUDE AVE		SUNNYVALE	CA	94086
SCHOELLER DALE A	UNIV OF CHICAGO	BOX 400	950 E 59TH ST	CHICAGO	IL	60637
SCHUEN ALAN E	SCHUEN INSTR	4131 N 24TH ST	SUITE 101	PHOENIX	AZ	85016
SCHOENGOLD D M	2305 EASTON			RICHLAND	WA	99352
SCHRAM K H	UNIV OF ARIZONA	COLLEGE OF PHARMACY		TUCSON	AZ	85721
SCHULZE WILLIAM G	MILLER BREWING CO	3939 W HIGHLAND BLVD		MILWAUKEE	WI	53208
W K SEIFERT	UNIV OF TEXAS HSC	PO BOX 20708		HOUSTON	TX	77030
SENSHARMA DILIP K	UCLA	CHEMISTRY DEPT	405 HILGARD AVENUE	LOS ANGELES	CA	90024
SERUM J W	HP SCIENTIFIC INSTR	1601 CALIFORNIA AVE		PALO ALTO	CA	94304
SETTINE K L	UNIV OF ALABAMA	GCMS CENTER		BIRMINGHAM	AL	35294
SHABANOWITZ J	UNIV OF VIRGINIA	CHEMISTRY DEPT		CHARLOTTESVILLE	VA	22901
SHACKLETON CEDRIC H	UNIV OF CALIFORNIA	PHARMA CHEM DEPT	PARNASSUS AVE	SAN FRANCISCO	CA	94143
SHARMA MANOHAR L	1942 46TH AVE			SAN FRANCISCO	CA	94116
SHERMAN PAUL L	MONSANTO - UIC	800 N LINDBERGH BLVD		ST LOUIS	MO	63167
SHERMAN WILLIAM R	WASHINGTON UNIV	SCHOOL OF MEDICINE	PSYCHIATRY DEPT	ST LOUIS	MO	63110
SHINOHARA Y	1725 FULTON ST	NO 14		SAN FRANCISCO	CA	94117
SHRADER S R	SHRADER ANAL LAB	3450 LOVETT		DETROIT	MI	48210
SIDES G D	1732 TAHITI LANE			ALABASTER	AL	35007
SIECK L W	NBS	A256 CHEMISTRY		WASHINGTON	DC	20234
SIEGEL M M	34 - 24 GRANT ST	F		FAIRLAWN	NJ	07410
SIEVERS ROBERT E	UNIV OF COLORADO	CHEMISTRY DEPT	CAMPUS BOX 215	BOULDER	CO	80309
SILVEIRA E J	SHELL BSRC	PO BOX 4248		MODESTO	CA	95352
SIMONS D S	NBS	BLDG 222, RM A121		WASHINGTON	DC	20234
SINHA M P	JET PROPULSION LAB	MS 11-116	4800 OAK GROVE DR	PASADENA	CA	91103
SKOTNICKI PEGGY A	HOOKER CHEM CO	PO BOX 8		NIAGARA FALLS	NY	14302
SLAYBACK J K	1555 VIA ALEGRIA CT			SAN JOSE	CA	95121
SLIVON L E	BATTELLE LABS	505 KING AVE		COLUMBUS	OH	43201
SMITH DAVID E	960 JUNESONG WAY			SAN JOSE	CA	95133
SMITH D L	UNIV OF UTAH	311 SKAGGS HALL		SALT LAKE CITY	UT	84112
SMITH LARELL K	1155TH TCHOS MCLP			MCCLELLAN AFB	CA	95652
SMITH R D	BATTELLE-NW	BLDG 329, AREA 300		RICHLAND	WA	99352
SOLOMON J J	NEW YORK UNIV	ENVIRON MEDICINE	MEDICAL CENTER	TUXEDO PARK	NY	10987
SPAIN MARK A	5742 HUMMINGBIRD			HOUSTON	TX	77096
SPAKKMAN D D	1657 LUIKA PLACE			CAMPBELL	CA	95008
SPARROW GENE R	ADVANCED R&D, INC	245 E 6TH ST	SUITE 807	ST PAUL	MN	55101
SPHON J A	FDA	HFF-459	200 C ST SW	WASHINGTON	DC	20204
SPINDT C A	SRI INTERNATIONAL	333 RAVENSWOOD AVE		MENLO PARK	CA	94025
STAFFORD G C	1463 ILIKAI AVE			SAN JOSE	CA	95118
STAUFFER J L	ARTHUR D LITTLE INC	ACORN PARK		CAMBRIDGE	MA	02140
STEIN J D	GENERAL ELECTRIC	1334 KATHY CT		LIVERMORE	CA	94550

MEMBER NAME	ADDR1	ADDR2	ADDR3	CITY	STATE	ZIP CODE
STEINER URS	FINNIGAN CORP	355 RIVER OAKS PKWY		SAN JOSE	CA	95134
STEVENSON DAVID A	MATERIALS SCI 5540			STANFORD	CA	94305
STILLWELL R N	BAYLOR COLL MEDICINE	INST LIPID RESEARCH	TEXAS MEDICAL CENTER	HOUSTON	TX	77030
ST JOHN G A	SRI INTERNATIONAL	333 RAVENSWOOD AVE		MENLO PARK	CA	94025
STOFFELS J J	BATTELLE-NW	BLDG 320, AREA 300		RICHLAND	WA	99352
STORMS EDMUND K	893 PINE ST			LOS ALAMOS	NM	87544
STORY M S	15745 WOODACRES RD			LOS GATOS	CA	95030
STOUT S J	AMERICAN CYANIMID	AGRICULTURAL DIV	PO BOX 400	PRINCETON	NJ	08540
STRAUB K M	UNIV OF CALIFORNIA	SPACE SCIENCES LAB		BERKELEY	CA	94720
STULIK DUSAN	1055 EAST 2ND AVE	NO 6		SALT LAKE CITY	UT	84103
STULTS JOHN T	MICH STATE UNIV	CHEMISTRY DEPT		EAST LANSING	MI	48824
SUITER D D	KRATOS	701 E IRVING PARK		ROSELLE	IL	60172
SULLIVAN M R	ELI LILLY CO	PO BOX 618		INDIANAPOLIS	IN	46206
SUN T	USDA-FSQS	PO BOX 6085		ATHENS	GA	30604
SUNDARARAMAN P	1950 COOLEY AVE	NO 6211		E PALO ALTO	CA	94303
SWEELEY C C	MICHIGAN STATE UNIV	BIOCHEMISTRY DEPT		EAST LANSING	MI	48824
SWEETMAN B J	VANDERBILT UNIV	PHARMACOLOGY DEPT		NASHVILLE	TN	37232
SZYBIST J	NUCLIDE CORP	642 E COLLEGE AVE		STATE COLLEGE	PA	16801
TAN Y L	DOE	ENVIRON MEAS LAB	376 HUDSON ST	NEW YORK	NY	10014
TANNENBAUM HARVEY	E I DUPONT	MARSHALL LAB	PO BOX 3886	PHILADELPHIA	PA	19146
TANNER D P	12664 MARKAIRE			ST LOUIS	MO	63141
TECON P	3064 SCOTT BLVD			SANTA CLARA	CA	95050
TENNO KENNETH	1545 LIUNA ST	APT 504		HONOLULU	HI	96814
TERWILLIGER D T	29 CHETWYND RD			PAOLI	PA	19301
THOMAS FAIRWELL T	NIH	BLDG 10, RM 7N115		BETHESDA	MD	20205
THOMPSON J A	UNIV OF COLORADO	SCHOOL OF PHARMACY	CAMPUS BOX 297	BOULDER	CO	80309
THOMSON M L	AMERICAN CYANIMID	AGRICULTURAL DIV	PO BOX 400	PRINCETON	NJ	08540
THORNE LAWRENCE	SANDIA NAT'L LABS			LIVERMORE	CA	94550
THORP J K	3111 WINDMILL			SUGAR LAND	TX	77478
TIERNAN T O	WRIGHT STATE UNIV	BREHM LAB		DAYTON	OH	45431
TODD P J	CORNELL UNIVERSITY	BAKER LABORATORY	PO BOX 380	ITHACA	NY	14853
TOMASSIAN A D	JET PROPULSION LAB	4800 OAK GROVE AVE		PASADENA	CA	91103
TURNER KENNETH B	MIDWEST CTR FOR MASS	CHEMISTRY DEPT	UNIV OF NEBRASKA	LINCOLN	NE	68588
TRUSSELL ALBERT R	JPM ENV RES LAB	555 E WALNUT ST		PASADENA	CA	91101
TSAO CONSTANCE	LINUS PAULING INST	440 PAGE MILL RD		PALO ALTO	CA	94306
TSENG K Y	17006 BEAVER CIRCLE			STRONGSVILLE	OH	44136
TWAY P C	MERCK SHARP & DOHME	RESEARCH LABORATORY	PO BOX 2000	RAHWAY	NJ	07065
UDSETH H R	UNIV OF OF UTAH	CHEMISTRY DEPT	PO BOX 43	SALT LAKE CITY	UT	84112
UPHAM ROGER	TWIN CITY TESTING CO	662 CROMWELL AVE		ST PAUL	MN	55114
VANDER VELDE G	C O M WIERSME	16320 PRINCE DR		SO HOLLAND	IL	60473
VANE F M	HOFFMANN-LAROCHE, INC			NUTLEY	NJ	07110
VAN BREEMEN RICHARD B	JOHNS HOPKINS UNIV	PHARMACOLOGY DEPT	725 N WOLFE ST	BALTIMORE	MD	21205
VAN LANGENHOVE A M	MIT	CHEMISTRY, 56-016		CAMBRIDGE	MA	02139
VAZQUEZ M A	ITT RAYONIER INC	409 E HARVARD		SHELTON	WA	98584
VEILLON CLAUDE	2141 HALLMARK DR			GAMBRILLS	MD	21054
VESTAL M L	UNIV OF HOUSTON	CHEMISTRY DEPT	4800 CALHOUN	HOUSTON	TX	77004
VITEK BRENT	NICOLET INSTRUMENTS	5225-1 VERONA RD		MADISON	WI	53711
VOORHEES K J	COLORADO SCH MINES	CHEMISTRY DEPT		GOLDEN	CO	80401
VOUROS P	NORTHEASTERN UNIV	INST CHEMICAL ANAL		BOSTON	MA	02115
VOYKSNER R D	203-A BRANSON ST			CHAPEL HILL	NC	27514
VRBANAC JAMES	MICHIGAN STATE UNIV	BIOCHEMISTRY DEPT		EAST LANSING	MI	48824
WAHKHAFTIG A L	UNIV OF UTAH	CHEMISTRY DEPT		SALT LAKE CITY	UT	84112
WALKER R W	MERCK SHARP & DOHME	RESEARCH LABORATORY	PO BOX 2000	RAHWAY	NJ	07065
WALLER G R	OKLAHOMA STATE UNIV	BIOCHEMISTRY DEPT		STILLWATER	OK	74074
WALLS F C	UNIV OF CALIFORNIA	SPACE SCIENCES LAB		BERKELEY	CA	94720

MEMBER NAME	ADDR1	ADDR2	ADDR3	CITY	STATE	ZIP CODE
WALTERS DENNIS C	WRIGHT STATE UNIV	BREHM LAB		DAYTON	OH	45435
WANG J S	93 SHADOW RIDGE RD			STAMFORD	CT	06905
WARD MIKE	RESOURCE RECYCLING	11000 MARKET ST		PORTLAND	TN	37148
WATSON J T	DEPT BIOCHEMISTRY	MICHIGAN STATE UNIV		EAST LANSING	MI	48824
WEAVER TONY	SCI GLASS ENGIN	2007 KRAMER LANE		AUSTIN	TX	78758
WEIBEL LEO A	HAZELTON LABS	PO BOX 7545		MADISON	WI	53707
WEINTRAUB SUSAN T	UT HEALTH SCI CTR	7703 FLOYD CURL DR		SAN ANTONIO	TX	78284
WEISS M	124 FOXWOOD			PORTOLA VALLEY	CA	94025
WELCH MICHAEL J	NAT'L BUR OF STANDAR	RM A-113,BLDG 222		WASHINGTON	DC	20234
WELLS G J	VARIAN INSTRUMENT	2700 MITCHELL DR		WALNUT CREEK	CA	94598
WESTON A F	HOOKER CHEMICALS	GRAND ISLAND COMPLEX	LONG ROAD	GRAND ISLAND	NY	14072
WHITAKER TOM J	ATOM SCIENCES INC	114 RIDGEWAY CENTER	PO BOX 138	OAK RIDGE	TN	37830
WHITE E	NBS	A113 CHEMISTRY		WASHINGTON	DC	20234
WHITE EARL L	CHEMICAL INDUSTRY	INSTITUTE OF TOXICOL	PO BOX 12137	RESEARCH TRIANGLE PK	NC	27709
WHITE ROBERT L	UNIV OF CALIFORNIA	CHEMISTRY DEPT		RIVERSIDE	CA	92506
WHITEHOUSE CRAIG	105 BISHOP ST			NEW HAVEN	CT	06511
WILDER J T	UNIV OF CALIFORNIA	1474 FIELDCREST CIR		PLEASANT HILL	CA	94523
WILKINS CHARLES L	UNIV OF CALIFORNIA	CHEMISTRY DEPARTMENT		RIVERSIDE	CA	92521
WILLIAMS PETER	ARIZONA STATE UNIV	CHEMISTRY DEPT		TEMPE	AZ	85287
WILSON CHARLES R	490 OKLAHOMA			GOLDEN	CO	80401
WILSON JAMES	9018 UTE DRIVE			GOLDEN	CO	80403
WINN THOMAS G	HEWLET PACKARD	2000 SOUTH PARK PL		ATLANTA	GA	30339
WISHNOK JOHN S	MIT	NUTRITION & FD SCI	ROOM 56-313	CAMBRIDGE	MA	02139
WITTSTRUCK THOMAS A	NUCLIDE CORP	AGV DIVISION	PO BOX 315	ACTON	MA	01720
WNUK RICHARD J	UPJOHN CO	301 HENRIETTA ST	7255-209-017	KALAMAZOO	MI	49001
WOLFE MARTA M	MASS GENERAL HOSP	MASS SPEC LAB	51 BLOSSOM ST	BOSTON	MA	02114
WOLSTENHOLME W A	13840 W OAK GLEN RD			VALLEY CENTER	CA	92082
WONG C M	LLL	PO BOX 808, L-325		LIVERMORE	CA	94550
WOOD DAVID	150 DAVENPORT DRIVE			STAMFORD	CT	06902
WOOD G M	2 LITTLE BLUFF RD			NEWPORT NEWS	VA	23606
WOOD NEVILLE	BASF WYANDOTTE	140 NEW DUTCH LN		FAIRFIELD	NJ	07006
WOODS J W	8 RICHARDS RD			LYNNFIELD	MA	01940
WU K L	WRIGHT STATE UNIV	BREHM LABORATORY		DAYTON	OH	45431
WYATT J R	NRL	CODE 6110		WASHINGTON	DC	20375
YELLE LAUREN M	JOHNS HOPKINS UNIV	PHARMACOLOGY DEPT	725 N WOLFE ST	BALTIMORE	MD	21205
YELTON R D	116 WALDEN FARM CIR			UNION	OH	45322
YERGEY ALFRED L	NIH	BLDG 6, RM 136		BETHESDA	MD	20205
YERGEY JAMES A	JOHNS HOPKINS UNIV	PHARMACOLOGY DEPT	725 N WOLFE ST	BALTIMORE	MD	21205
YERT L W	CENTER DISEASE CNTRL	RMS TOXICOLOGY	BLDG 31, ROOM 5	ATLANTA	GA	30333
YUST R A	UNIV OF FLORIDA	CHEMISTRY DEPT		GAINESVILLE	FL	32611
YOUNG S E	2455 THADDEUS			MOUNTAIN VIEW	CA	94043
YU K O	AFAMRL-THT			WRIGHT PATT AFB	OH	45433
ZACCHEI A G	MERCK SHARP & DOHME	RESEARCH LABORATORY		WEST POINT	PA	19486
ZARETT DONALD	DOW CHEMICAL CO	ANAL LABS 574 BLDG		MIDLAND	MI	48640
ZUBYK ROSALIE M	230 SUMMIT HOUSE			WEST CHESTER	PA	19380